

Advances in Intelligent Systems and Computing 339

J.K. Mandal

Suresh Chandra Satapathy

Manas Kumar Sanyal

Partha Pratim Sarkar

Anirban Mukhopadhyay *Editors*

# Information Systems Design and Intelligent Applications

Proceedings of Second International  
Conference INDIA 2015, Volume 1

 Springer

# **Advances in Intelligent Systems and Computing**

Volume 339

## **Series editor**

Janusz Kacprzyk, Polish Academy of Sciences, Warsaw, Poland  
e-mail: [kacprzyk@ibspan.waw.pl](mailto:kacprzyk@ibspan.waw.pl)



## *About this Series*

The series “Advances in Intelligent Systems and Computing” contains publications on theory, applications, and design methods of Intelligent Systems and Intelligent Computing. Virtually all disciplines such as engineering, natural sciences, computer and information science, ICT, economics, business, e-commerce, environment, healthcare, life science are covered. The list of topics spans all the areas of modern intelligent systems and computing.

The publications within “Advances in Intelligent Systems and Computing” are primarily textbooks and proceedings of important conferences, symposia and congresses. They cover significant recent developments in the field, both of a foundational and applicable character. An important characteristic feature of the series is the short publication time and world-wide distribution. This permits a rapid and broad dissemination of research results.

## *Advisory Board*

### Chairman

Nikhil R. Pal, Indian Statistical Institute, Kolkata, India  
e-mail: nikhil@isical.ac.in

### Members

Rafael Bello, Universidad Central “Marta Abreu” de Las Villas, Santa Clara, Cuba  
e-mail: rbellop@uclv.edu.cu

Emilio S. Corchado, University of Salamanca, Salamanca, Spain  
e-mail: escorchado@usal.es

Hani Hagrass, University of Essex, Colchester, UK  
e-mail: hani@essex.ac.uk

László T. Kóczy, Széchenyi István University, Győr, Hungary  
e-mail: koczy@sze.hu

Vladik Kreinovich, University of Texas at El Paso, El Paso, USA  
e-mail: vladik@utep.edu

Chin-Teng Lin, National Chiao Tung University, Hsinchu, Taiwan  
e-mail: ctlin@mail.nctu.edu.tw

Jie Lu, University of Technology, Sydney, Australia  
e-mail: Jie.Lu@uts.edu.au

Patricia Melin, Tijuana Institute of Technology, Tijuana, Mexico  
e-mail: epmelin@hafsamx.org

Nadia Nedjah, State University of Rio de Janeiro, Rio de Janeiro, Brazil  
e-mail: nadia@eng.uerj.br

Ngoc Thanh Nguyen, Wroclaw University of Technology, Wroclaw, Poland  
e-mail: Ngoc-Thanh.Nguyen@pwr.edu.pl

Jun Wang, The Chinese University of Hong Kong, Shatin, Hong Kong  
e-mail: jwang@mae.cuhk.edu.hk

More information about this series at <http://www.springer.com/series/11156>

J.K. Mandal · Suresh Chandra Satapathy  
Manas Kumar Sanyal · Partha Pratim Sarkar  
Anirban Mukhopadhyay  
Editors

# Information Systems Design and Intelligent Applications

Proceedings of Second International  
Conference INDIA 2015, Volume 1

*Editors*

J.K. Mandal  
University of Kalyani  
Kalyani, West Bengal  
India

Suresh Chandra Satapathy  
Department of Computer Science  
and Engineering  
Anil Neerukonda Institute of Technology  
and Sciences  
Vishakapatnam  
India

Manas Kumar Sanyal  
Faculty of Engineering, Technology  
and Management  
University of Kalyani  
Kalyani, West Bengal  
India

Partha Pratim Sarkar  
Department of Engineering  
and Technological Studies  
University of Kalyani  
Kalyani, West Bengal  
India

Anirban Mukhopadhyay  
Department of Computer Science  
and Engineering  
University of Kalyani  
Kalyani, West Bengal  
India

ISSN 2194-5357

ISSN 2194-5365 (electronic)

Advances in Intelligent Systems and Computing

ISBN 978-81-322-2249-1

ISBN 978-81-322-2250-7 (eBook)

DOI 10.1007/978-81-322-2250-7

Library of Congress Control Number: 2014958575

Springer New Delhi Heidelberg New York Dordrecht London

© Springer India 2015

This work is subject to copyright. All rights are reserved by the Publisher, whether the whole or part of the material is concerned, specifically the rights of translation, reprinting, reuse of illustrations, recitation, broadcasting, reproduction on microfilms or in any other physical way, and transmission or information storage and retrieval, electronic adaptation, computer software, or by similar or dissimilar methodology now known or hereafter developed.

The use of general descriptive names, registered names, trademarks, service marks, etc. in this publication does not imply, even in the absence of a specific statement, that such names are exempt from the relevant protective laws and regulations and therefore free for general use.

The publisher, the authors and the editors are safe to assume that the advice and information in this book are believed to be true and accurate at the date of publication. Neither the publisher nor the authors or the editors give a warranty, express or implied, with respect to the material contained herein or for any errors or omissions that may have been made.

Printed on acid-free paper

Springer (India) Pvt. Ltd. is part of Springer Science+Business Media ([www.springer.com](http://www.springer.com))

# Preface

The Faculty of Engineering, Technology and Management, University of Kalyani, India is organizing the Second International Conference on INformation Systems Design and Intelligent Applications—2015 (INDIA-2015), during 8–9 January 2015 at the University of Kalyani. This is the First time the Faculty is organizing such a mega event covering all aspects of information system design and applications in Computer Science and Technology, General Science, Educational Research where scopes are not only limited to Computer Science researchers but also include researchers from Mathematics, Chemistry, Biology, Biochemistry, Engineering Statistics, Management and all other related areas where Computer Technologies may assist.

We have received papers from all corners of the world. A huge response has been received by INDIA-2015 in terms of submission of papers and we received 429 submissions across the globe. The Organizing Committee of INDIA-2015 constitutes a strong international programme committee for reviewing papers. A double-blind review process has been adopted. Each paper is reviewed by at least two and at most five reviewers. The decision system adopted by EasyChair has been employed and 210 papers have been selected thorough double-blind review process. The Committee has also checked for plagiarism through the professional software. Finally, 174 registered papers have been included in the two volumes of the proceedings as printed as well as online documents where 87 papers are there in each volume. INDIA-2015 received papers from ten countries outside India, namely Germany, USA, Korea, Portugal, Bangladesh, Nepal, Egypt, Australia, Iran and Vietnam.

Along with the general sessions, INDIA-2015 organizes four special sessions, namely *Multicriteria Decision Analysis and Information Technology (MCDA-IT)* (Chair: Prof. (Dr.) Bijay Baran Pal, Department of Mathematics, University of Kalyani, India), *Wireless Sensor Networks (WSNs)* (Chairs: Prof. Prasanta K. Jana, Department of Computer Science and Engineering, Indian School of Mines,

Dhanbad, India and Dr. Ashok Kumar Turuk, Department of Computer Science and Engineering, National Institute of Technology, Rourkela, India), *Machine Learning and Engineering Application (MLEA)* (Chairs: Dr. B.N. Biswal, Director (A & A), BEC, Bhubaneswar, India and Prof. Pritee Parwekar, ANITS, Visakhapatnam, India), and *Innovations in Pattern Recognition and Image Processing (PRE-IP)* (Chairs: Prof. (Dr.) S.C. Satapathy, Department of Computer Science and Engineering, ANITS, Visakhapatnam, India and Prof. Vikrant Bhateja, Department of Electronics and Communication Engineering, SRMGPC, Lucknow, India). We would like to thank the chairs and associates of the special sessions for all their initiatives to arrange the special sessions.

The proceedings of the conference is published in two volumes in **Advances in Intelligent Systems and Computing** (ISSN: 2194-5357), Springer, indexed by ISI Proceedings, DBLP, EI-Compendex, SCOPUS, Springerlink and will be available at <http://www.springer.com/series/11156>. We convey our sincere gratitude to the authority of Springer for providing the opportunity to publish the proceedings of INDIA-2015.

The first volume of the proceeding contains fields of research like Natural Language Processing, Artificial Intelligence, Virtualization, Intelligent Agent-based Computing, Web Security and Privacy, Service Orient Architecture, Data Engineering, Open Systems, Communications, Smart Wireless and Sensor Networks, Intelligent Computing in Sensor and Ad Hoc Networks, Smart Antennae, VLSI, Microelectronics, Circuit and Systems, Communication Networking and Information Security, Machine Learning, Soft Computing, Intelligent Communication Technology, Mobile Computing and Applications, Cloud Computing.

The second volume contains research topics like Software Engineering, Graphics and Image Processing, Green IT, IT for Rural Engineering, E-Commerce, E-governance, Business Computing, Business Intelligence and Performance Management, ICT for Education, IT for Inclusive Growth, UID and Transparency, Process Reengineering, Molecular Computing, Nano Computing, Chemical Computing, Intelligent Computing for GIS and Remote Sensing, Intelligent Bio-informatics, Bio Computing and Industrial Automation.

We convey our esteemed gratitude to the honourable Vice-Chancellor, Prof. (Dr.) Rattan Lal Hangloo for his extreme enthusiasm for hosting INDIA-2015 at the University of Kalyani. Also, we convey our deep sense of gratitude to the Deans, Faculty of Engineering, Technology and Management, Faculty of Science, Faculty of Arts and Commerce and Faculty of Education for their constant support and association in this big event.

We express our sincere gratitude to UGC New Delhi, India for its financial support and IEEE Kolkata Section for their technical support. We would also like to thank the programme committee members for their efforts, and the reviewers for completing a big reviewing task in a short span of time. Moreover, we would like to

thank all the authors who submitted papers to INDIA-2015 and made a high-quality technical programme possible. Finally, we acknowledge the support received from the faculty members, scholars of Faculty of Engineering, Technology and Management, officers, staffs and the authority of the University of Kalyani.

November 2014

J.K. Mandal  
Suresh Chandra Satapathy  
Manas Kumar Sanyal  
Partha Pratim Sarkar  
Anirban Mukhopadhyay

# Organization

## Chief Patron

Rattan Lal Hangloo                      The Vice-Chancellor, University of Kalyani, India

## Organizing Chair

Manas Kumar Sanyal                      The Dean, Faculty of Engineering, Technology and Management, University of Kalyani, India

## Programme Chair

Jyotsna Kumar Mandal                      Department of Computer Science and Engineering, University of Kalyani, India

## Programme Co-chair

Suresh Chandra Satapathi                      Department of Computer Science and Engineering, ANITS, AU, India

## International Advisory Committee Chair

Partha Pratim Sarkar                      Department of Engineering and Technological Studies, University of Kalyani, India

## Organizing Committee

Anirban Mukhopadhyay	Department of Computer Science and Engineering, University of Kalyani, India
Bijay Baran Pal	Department of Mathematics, University of Kalyani, India
Debabrata Sarddar	Department of Computer Science and Engineering, University of Kalyani, India
Indrajit Lahiri	Department of Mathematics, University of Kalyani, India
Jyotsna Kumar Mandal	Department of Computer Science and Engineering, University of Kalyani, India
Kalyani Mali	Department of Computer Science and Engineering, University of Kalyani, India
Manas Kumar Sanyal	Department of Business Administration, University of Kalyani, India
Partha Pratim Sarkar	Department of Engineering and Technological Studies, University of Kalyani, India
Priya Ranjan Sinha Mahapatra	Department of Computer Science and Engineering, University of Kalyani, India
Susanta Biswas	Department of Engineering and Technological Studies, University of Kalyani, India
Susmita Lahiri	Department of Environmental Engineering, University of Kalyani, India
Udaybhanu Bhattacharyya	Department of Rural Development and Management, University of Kalyani, India
Utpal Biswas	Department of Computer Science and Engineering, University of Kalyani, India

## Local Programme/Publication Committee

Angshuman Bagchi	Department of Biochemistry and Biophysics, Uni- versity of Kalyani, India
Anirban Mukhopadhyay	Department of Computer Science and Engineering, University of Kalyani, India
Bijay Baran Pal	Department of Mathematics, University of Kalyani, India
Jyotsna Kumar Mandal	Department of Computer Science and Engineering, University of Kalyani, India
Manas Kumar Sanyal	Department of Business Administration, University of Kalyani, India



Partha Pratim Sarkar	Department of Engineering and Technological Studies, University of Kalyani, India
Subhash Chandra Sarkar	Department of Commerce, University of Kalyani, India
Suresh Chandra Satapathy	Anil Neerukonda Institute of Technology and Sciences, Vishakapatnam, India
Susanta Biswas	Department of Engineering and Technological Studies, University of Kalyani, India
Susmita Lahiri	Department of Environmental Engineering, University of Kalyani, India
Tuhin Mukherjee	Department of Business Administration, University of Kalyani, India
Udaybhanu Bhattacharyya	Department of Rural Development and Management, University of Kalyani, India
Utpal Biswas	Department of Computer Science and Engineering, University of Kalyani, India

### **Finance Committee**

Anirban Mukhopadhyay	Department of Computer Science and Engineering, University of Kalyani, India
Anjan Kumar Das	The Audit and Account Officer, University of Kalyani, India
Jyotsna Kumar Mandal	Department of Computer Science and Engineering, University of Kalyani, India
Manas Kumar Sanyal	Department of Business Administration, University of Kalyani, India
Tuhin Mukherjee	Department of Business Administration, University of Kalyani, India

### **Editorial Committee**

Anirban Mukhopadhyay	Department of Computer Science and Engineering, University of Kalyani, India
Jyotsna Kumar Mandal	Department of Computer Science and Engineering, University of Kalyani, India
Manas Kumar Sanyal	Department of Business Administration, University of Kalyani, India

Partha Pratim Sarkar	Department of Engineering and Technological Studies, University of Kalyani, India
Suresh Chandra Satapathy	Department of Computer Science and Engineering, ANITS, AU, India

### **Website Committee**

Anirban Mukhopadhyay	Department of Computer Science and Engineering, University of Kalyani, India
Sanjay Das	Department of Engineering and Technological Studies, University of Kalyani, India
Ujjal Marjit	The System-in-Charge, Centre for Information Resource Management, University of Kalyani, India
Utpal Biswas	Department of Computer Science and Engineering, University of Kalyani, India

### **Registration Committee**

Arindam Sarkar	Department of Computer Science and Engineering, University of Kalyani, India
Arup Sarkar	Department of Computer Science and Engineering, University of Kalyani, India
Madhumita Mallick	Department of Computer Science and Engineering, University of Kalyani, India
Madhumita Sengupta	Department of Computer Science and Engineering, University of Kalyani, India
Monalisa Mondal	Department of Computer Science and Engineering, University of Kalyani, India
Priyaranjan Sinha	Department of Computer Science and Engineering, University of Kalyani, India
Mahapatra	Department of Computer Science and Engineering, University of Kalyani, India
Somnath Mulhopadhyay	Department of Computer Science and Engineering, University of Kalyani, India
Sujay Chatterjee	Department of Computer Science and Engineering, University of Kalyani, India
Sushil Kumar Mandal	Department of Environmental Management, University of Kalyani, India

## External Reviewers

A.K. Nayak	IIBM, India
A.K. Tripathi	IIT BHU, India
A. Srinivasan	Chennai, India
A. Ghosal	B.C. Roy Engineering College, India
Anirban Mukhopadhyay	University of Kalyani, India
A.K. Bhattacharya	NIT Durgapur, India
A.K. Mukhopadhyay	BCREC, India
Arpita Chakraborty	Techno India, India
A. Chaudhuri	Jadavpur University, India
A. Dasgupta	Tech Mahindra, India
Arup Sarkar	University of Kalyani, India
Abhik Mukherjee	BESU, India
Amit Kr Mishra	IIT Guwahati, India
Animesh Biswas	University of Kalyani, India
Ashok Kumar Rai	Information and Library Network Centre, India
Ashok Kumar Turuk	NIT Rourkela, India
A.K. Ghosh	Future Institute of Technology, India
Ashish K. Mukhopadhyay	BITM Shantiniketan, India
Asad A.M. AL-Salih	University of Baghdad, Iraq
A. Damodaram	JNTU, Hyderabad, India
A. Roy	BESU, India
Arpan Pal	Tata Consultancy Services, India
Arijit Mukherjee	Tata Consultancy Services, India
Arindam Sarkar	University of Kalyani, India
Aniruddha Sinha	Tata Consultancy Services, India
Avijit Kar	CSE, Jadavpur University, India
Amitabha Nag	Academy of Technology, India
Arindrajit Roy	Academy of Technology, India
Arshad Mohd. Khan	KL University, India
Ashwini B. Abhale	D.Y. Patil College of Engineering, India

B. Basu	OP SIS System, India
B.K. Dey	Tripura University, India
B.B. Choudhuri	ISI Kolkata, India
Bijay Baran Pal	University of Kalyani, India
Biplab Sikdar	BESU, India
B.N. Biswal	BEC, Bhubaneswar, India
Balamurali P.	Tata Consultancy Services, India
Blakrishna Tripathy	VIT University, India
Bhabani P. Sinha	ISI Kolkata, India
Balaram Bhattacharya	Vishva Bharati Shnatiniketan, India
C. Rosen	University of Derby, UK
Chirabrata Bhaumik	Tata Consultancy Services, India
Chandan Bhar	ISM Dhanbad, India
Chiranjeev Kumar	ISM Dhanbad, India
Chirag Arora	KIET, Ghaziabad, India
Dac-Nhuong Le	Hai Phong University, Vietnam
Dileep Kumar Yadav	Jawaharlal Nehru University, New Delhi, India
D. Das	Jadavpur University, India
D. Garg	Thapar University, India
D. Sasmal	BIT Mesra, India
Dambarudhar Seth	KIIT, India
D.D. Sinha	Calcutta University, India
D. Tomar	MNMJEC, India
Debotosh Bhattacharjee	CSE, Jadavpur University, India
Dharmveer Rajppot	JIIT, Noida, India
Debjyoti Mukhopadhyay	Maharashtra Institute of Technology, India
Durgesh Mishra	SAIT, India
E.S. Reddy	ANUCET, India
Foued Melakessou	University of Luxembourg, Luxembourg
Gautam Sen	AS, Jadavpur University, India
Gautam Saha	College of Leather Technology, India
Goutam Sanyal	NIT Durgapur, India
G. Sahoo	BIT Mesra, India
G.N. Singh	ISM, Dhanbad, India
G.R. Sinha	SSG Institue, India
Hari Om	ISM, Dhanbad, India
Harjinder Lallie	University of Warwick, UK
H.R. Vishwakarma	VIT University, India
Indrajit Bhattacharya	CA, KGEC, India
Indrajit Saha	University of Wroclaw, India
Igor N. Belyh	Saint Petersburg State Polytechnical University, Russia
Jagdish Chandra Patni	University of Petroleum and Energy Studies, Dehradun, India
Jyotsna Kumar Mandal	University of Kalyani, India

Jules Raymond Tapamo	UKZN, South Africa
Jimson Matthew	University of Bristol, UK
J.P. Choudhury	KGEC, India
J. Sil	BESU, India
K. Dasgupta	KGEC, India
Kaushik Deb	CUET, Bangladesh
Karthykeyan Subbiah	CUET, Bangladesh
K. Thirupathi Rao	K L University, India
Katricks Chandra Mondal	Jadavpur University, India
Korra Sathya Babu	NIT, Rourkela, India
Krishna Asawa	JIIT, Noida, India
Kavita Choudhary	ITM University, Gurgaon, India
M.N. Gore	MNNIT, Alahabad, India
Madhumita Sengupta	University of Kalyani, India
Malay Bhattacharyya	BESU, India
Manas Kumar Sanyal	University of Kalyani, India
Mihir Narayan Mohanty	SOA University, India
Monalisa Mondal	University of Kalyani, India
Maheswari Senthilkumar	Sambhram Institute of Technology, Bangalore, India
Mihir Narayan Mohanty	Siksha 'O' Anusandhan University, Bhubaneswar, India
Mohammed A.M. Salem	Ain Shams University, Cairo, Egypt
Musheer Ahmad	Jamia Millia Islamia, New Delhi, India
Md. U. Bokhari	AMU, India
M.K. Bhowmik	Tripura University, India
M.K. Naskar	ECE, Jadavpur University, India
Marcus Liwicki	DFKI, Germany
M. Kaykobad	BUET, Bangladesh
M. Sandirigam	University of Peradenia, Sri Lanka
M. Marjit Singh	NERIST, India
N.R. Manna	North Bengal University, India
Nilanjan Dey	Bengal College of Engineering and Technology, Durgapur, India
N. Bhatt	NU, India
Nabendu Chaki	CSE, Calcutta University, India
Narasihmasarma NVS	NIT Warangle, India
P. Dutta	Visva Bharati University, India
P.P. Sarkar	Kalyani University, India
P. Jha	Purbanchal University, Nepal
P.K. Jana	ISM Dhanbad, India
Prateep Misra	Tata Consultancy Services, India
Priya Ranjan Sinha	Kalyani University, India
Mahapatra	
Pritee Parwekar	Anil Neerukonda Institute of Technology and Sciences, India

P.S. Avadhani	Andhra University, India
Parthajit Roy	Burdwan University, India
Prataya Kuila	KIT, Bhubaneswar, India
R.K. Samanta	North Bengal University, India
R.K. Jena	IMT, India
Rituparna Chaki	CSE, WBUT, India
Rabindranath Bera	ECE, SMIT, India
Rajat Pal	Calcutta University, India
Ramesh Babu	Acharya Nagarjuna University, India
Ranjan Maheswari	Rajasthan Technical University, India
R.N. Gupta	BIT Mesra, India
Rashmi Ranjan Rout	IIT, Kharagpur, India
Ratnakar Dash	NIT, Rourkela, India
Rintu Banerjee	IIT, Kharagpur, India
R. Jagadeesh Kannan	SCSE, VIT University, Chennai Campus, India
Sadhana J. Kamatkar	Central Computing Facility, India
Sayan Chakraborty	BCET, Durgapur, India
Shruti Goel	Defence Research and Development Organisation, India
Sourav Samanta	University Institute of Technology, BU, India
Srinivas Aluvala	SR Engineering College, Warangal, India
Srinivas Sethi	Indira Gandhi Institute of Technology, Sarang, India
Steven Lawrence Fernandes	Sahyadri College of Engineering and Management, Mangalore, India
Sumit A. Khandelwal	MIT Academy of Engineering, Pune, India
Suvojit Acharjee	NIT, Agartala, India
Swati Chowdhuri	Seacom Engineering College, Kolkata, India
S.K. Basu	BHU, India
S.K. Nandi	IIT Guwahati, India
Salih Alsalih	UB, Iraq
Sandeep Shukla	Virginia Polytechnic, USA
S. Bhattacharyya	Texas University, USA
S. Neogy	Jadavpur University, India
S. Mal	KGEC, India
S. Dutta	BCREC, India
S. Bhattacharyya	RCCIT, India
S. Mukhopadhyay	Texas University, USA
Sripati Mukhopadhyay	Texas Tech University, USA
S. Shakya	TU, Nepal
S. Samanta	BIT Mesra, India
S. Bandyopadhyay	Calcutta University, India
S. Sarkar	Jadavpur University, India
S. Jha	KEC, Nepal
S. Muttoo	Delhi University, India
S. Satapathy	Andhra University, India

S. Changder	NIT DGP, India
S. Bandyopadhyay	ISI, Kolkata, India
S.K. Mondal	KGEC, India
S. Sen	ITC, India
Sydulu M.	NIT, Warangle, India
Saurav Mallik	ISI, Kolkata, India
Sarika Sharma	ENIAC, Pune, India
Somnath Mukhopadhyay	University of Kalyani, India
Sujoy Chatterjee	University of Kalyani, India
Sudip Misra	IIT, Kharagpur, India
Suresh Chandra Satapathy	ANITS, Vishakapatnam, India
S. Mukherjee	Burdwan University, India
S. Sarkar	NIT Jamshedpur, India
Seema Bawa	Thapar University, India
Subhash Saha	EC, Vidyasagar University, India
Sharad Sinha	CSA, NBU, India
Santanu Sinha	ME, KGEC, India
Santanu Das	ME, KGEC, India
Sunil Karforma	CS, BU, India
S. Roy	NITTTR, Kolkata, India
S.H. Mnene	UKZN, South Africa
Satheesh Kumar Pradhan	Utkal University, India
Seiichi Uchida	Kyushu University, Japan
Sekhar Ranjan Bhadra	BESU, India
S.K. Acharya	BCKV, Kalayani, India
Samar Sen Sarma	Calcutta University, India
Shengping Ren	Illinois Institute of Technology, India
Satchidananda Dehuri	Fakir Mohan University, India
Samir Roy	CSE, NITTTR, India
Swarup Das	CSA, NBU, India
Simon Hollis	University of Derby, UK
Soumen Sarkar	NIT Jamshedpur, India
S. Mukherjee	Burdwan University, India
S.K. Udgata	UOH, India
T.V. Gopal	Anna University, India
T. Som	IIT, BHU, India
T.K.S.Lakshmi Priya	Avinashilingam University, India
Tara Saikumar	JNTU, Hyderabad, India
Utpal Biswas	Kalyani University, India
Utpal Roy	Visva Bharati, India
Uday Kumar R.Y.	NIT Surathkal, India
Udaya Sameer	ANITS, Vishakapatnam, India
Ujjal Maulik	Jadavpur University, India
Utpal Nandy	Vidyasagar University, Midnapore, India
Uttam Kumar Mondal	Vidyasagar University, Midnapore, India

V. Prithiraj	PEC, India
V.S. Despande	MIT College, India
Vaskar Raychoudhury	IIT Roorkee, India
Vikrant Bhateja	SRMGPC, Lucknow, India
Vipin Tyagi	Jaypee University, India
Yu Ye	Hefei University of Technology, China
Zaigham Mahmood	University of Derby, UK



# Contents

<b>Simulation Studies on Distortion of EAS Muons by the Earth's Magnetic Field</b> . . . . .	1
Sandip Dam, Rajat Kumar Dey and Arunava Bhadra	
<b>A Detailed Survey on Misbehavior Node Detection Techniques in Vehicular Ad Hoc Networks.</b> . . . . .	11
Uzma Khan, Shikha Agrawal and Sanjay Silakari	
<b>Detect Mimicry by Enhancing the Speaker Recognition System</b> . . . . .	21
Soumen Kanrar and Prasenjit Kumar Mandal	
<b>SPICE Modeling and Analysis for Metal Island Ternary QCA Logic Device</b> . . . . .	33
Pritam Bhattacharjee, Kunal Das, Mallika De and Debashis De	
<b>Text Independent Speaker and Emotion Independent Speech Recognition in Emotional Environment</b> . . . . .	43
A. Revathi and Y. Venkataramani	
<b>Two-Level Multivariate Fuzzy Logic Based Integrated Model for Monsoon Rainfall Prediction.</b> . . . . .	53
Mahua Bose and Kalyani Mali	
<b>Feed Forward Neural Network Approach for Reversible Logic Circuit Simulation in QCA</b> . . . . .	61
Arijit Dey, Kunal Das, Sanjoy Das and Mallika De	
<b>Large Vocabulary Speech Recognition: Speaker Dependent and Speaker Independent</b> . . . . .	73
G. Hemakumar and P. Punitha	

<b>Optimization of Ultra Wide-Band Printed Monopole Square Antenna Using Differential Evolution Algorithm</b> . . . . .	81
Sharmin Shabnam, Suvrajit Manna, Udit Sharma and Pinaki Mukherjee	
<b>An Efficient Cloud Network Intrusion Detection System</b> . . . . .	91
Partha Ghosh, Abhay Kumar Mandal and Rupesh Kumar	
<b>Mobile WiMAX Physical Layer Optimization and Performance Analysis Towards Sustainability and Ubiquity</b> . . . . .	101
Sajal Saha, Angana Chakraborty, Asish K. Mukhopadhyay and Anup Kumar Bhattacharjee	
<b>Comparison of Classifiers Accuracies from FAVF and NOFI for Categorical Data</b> . . . . .	113
D. Lakshmi Sreenivasa Reddy, B. Raveendra Babu, A. Govardhan, A. Kalpana and Mudimbi Krishna Murthy	
<b>Multi Objective Optimization on Clustered Mobile Networks: An ACO Based Approach</b> . . . . .	123
Sujoy Sett and Parag K. Guha Thakurta	
<b>A Trade-off Analysis of Quality of Service (QoS) Metrics Towards Routing in Mobile Networks: MOGA Based Approach</b> . . . . .	135
Aritra Rudra, Parag Kumar Guha Thakurta and Rajarshi Poddar	
<b>Advanced Bi-directional Home Appliance Communicator with Security System</b> . . . . .	145
Nilava Debabhuti, Sougata Das, Sayantan Dutta, Anusree Sarkar and Apurba Ghosh	
<b>Cyber Attack and Control Techniques</b> . . . . .	157
Apeksha Prajapati and Bimal Kumar Mishra	
<b>Design of Queue-Based Group Key Agreement Protocol Using Elliptic Curve Cryptography</b> . . . . .	167
Priyanka Jaiswal, Abhimanyu Kumar and Sachin Tripathi	
<b>Solving Multi-level Image Thresholding Problem—An Analysis with Cuckoo Search Algorithm</b> . . . . .	177
B. Abhinaya and N. Sri Madhava Raja	

**Comparing Efficiency of Software Fault Prediction Models Developed Through Binary and Multinomial Logistic Regression Techniques** . . . . . 187  
 Dipti Kumari and Kumar Rajnish

**Performance Modeling of Unified TDPC in IEEE 802.16e WiMAX** . . . . . 199  
 Rewa Sharma, C.K. Jha and Meha Sharma

**EmET: Emotion Elicitation and Emotion Transition Model.** . . . . . 209  
 Shikha Jain and Krishna Asawa

**Analysis on Intelligent Based Navigation and Path Finding of Autonomous Mobile Robot.** . . . . . 219  
 Prabin Kumar Panigrahi and Hrudya Kumar Tripathy

**Performance Analysis of Chaotic Lévy Bat Algorithm and Chaotic Cuckoo Search Algorithm for Gray Level Image Enhancement** . . . . . 233  
 Krishna Gopal Dhal, Md. Iqbal Quraishi and Sanjoy Das

**Password Recovery Mechanism Based on Keystroke Dynamics** . . . . . 245  
 Soumen Roy, Utpal Roy and D.D. Sinha

**Performance Analysis of RC4 and Some of Its Variants** . . . . . 259  
 Suman Das, Hemanta Dey and Ranjan Ghosh

**Optimal Image Segmentation of Cancer Cell Images Using Heuristic Algorithms** . . . . . 269  
 A. Atchaya, J.P. Aashiha and R. Vijayarajan

**Improvement of Data Integrity and Data Dynamics for Data Storage Security in Cloud Computing.** . . . . . 279  
 Poonam M. Pardeshi and Bharat Tidke

**An Improvised Extractive Approach to Hindi Text Summarization** . . . . . 291  
 K. Vimal Kumar and Divakar Yadav

**Graph Based Technique for Hindi Text Summarization** . . . . . 301  
 K. Vimal Kumar, Divakar Yadav and Arun Sharma

<b>Generating Empty Convex Polygon Randomly from a Subset of Given Point Set . . . . .</b>	311
Manas Kumar Mohanty, Sanjib Sadhu, Niraj Kumar and Kamaljit Pati	
<b>A Symmetric Key Cryptographic Technique Based on Frame Rotation of an Even Ordered Square Matrix . . . . .</b>	319
Joyita Goswami (Ghosh) and Manas Paul	
<b>A PSO Based Fault Tolerant Routing Algorithm for Wireless Sensor Networks . . . . .</b>	329
Md Azharuddin and Prasanta K. Jana	
<b>Smallest Square Covering <math>k</math> Points for Large Value of <math>k</math> . . . . .</b>	337
Priya Ranjan Sinha Mahapatra	
<b>Connectionist Approach for Emission Probability Estimation in Malayalam Continuous Speech Recognition . . . . .</b>	343
Anuj Mohamed and K.N. Ramachandran Nair	
<b>Design of an Aperture Type Frequency Selective Surface with Sharp Roll -off . . . . .</b>	353
Poulami Samaddar, Sushanta Sarkar, Srija De, Sushanta Biswas, Debasree Chanda Sarkar and Partha Pratim Sarkar	
<b>Effective Classification and Categorization for Categorical Sets: Distance Similarity Measures . . . . .</b>	359
Heba Ayseldeen, Mahmood A. Mahmood and Aboul Ella Hassanien	
<b>Case-Based Reasoning: A Knowledge Extraction Tool to Use . . . . .</b>	369
Heba Ayseldeen, Olfat Shaker, Osman Hegazy and Aboul Ella Hassanien	
<b>Implementation of New Framework for Image Encryption Using Arnold 3D Cat Map . . . . .</b>	379
Kunal Kumar Kabi, Bidyut Jyoti Saha, Arun Chauhan and Chittaranjan Pradhan	
<b>Case Selection Strategy Based on K-Means Clustering . . . . .</b>	385
Heba Ayseldeen, Osman Hegazy and Aboul Ella Hassanien	
<b>Cloud Computing Framework for Solving Virtual College Educations: A Case of Egyptian Virtual University . . . . .</b>	395
Hany Soliman Alnashar, Mohamed Abd Elfattah, M.M. Mosbah and Aboul Ella Hassanien	

**Scheme for Compressing Video Data Employing Wavelets and 2D-PCA** . . . . . 409  
 Manoj K. Mishra and Susanta Mukhopadhyay

**A Hierarchical Optimization Method to Solve Environmental-Economic Power Generation and Dispatch Problem with Fuzzy Data Uncertainty** . . . . . 419  
 Bijay Baran Pal and Mousumi Kumar

**Reverse Logistic Model for Deteriorating Items with Non-instantaneous Deterioration and Learning Effect** . . . . . 435  
 S.R. Singh and Himanshu Rathore

**On the Implementation of a Saliency Based Digital Watermarking** . . . . . 447  
 Abhishek Basu, Susmita Talukdar, Nabanita Sengupta, Avradeeta Kar, Satrajit Lal Chakraborty and Subir Kumar Sarkar

**Interval Goal Programming Approach to Multiobjective Programming Problems with Fuzzy Data Uncertainty** . . . . . 457  
 Shyamal Sen and Bijay Baran Pal

**Modeling Indian General Elections: Sentiment Analysis of Political Twitter Data** . . . . . 469  
 Kartik Singhal, Basant Agrawal and Namita Mittal

**Model Based Test Case Generation and Optimization Using Intelligent Optimization Agent** . . . . . 479  
 Prateeva Mahali, Arup Abhinna Acharya and Durga Prasad Mohapatra

**Automatic Generation of Domain Specific Customized Signatures for an Enterprise Intrusion Detection System Based on Sentimental Analysis** . . . . . 489  
 K.V.S.N. Rama Rao and Sudheer Kumar Battula

**An Efficient Technique for Solving Fully Fuzzified Multiobjective Stochastic Programming Problems** . . . . . 497  
 Animesh Biswas and Arnab Kumar De

**L(4, 3, 2, 1)-Labeling for Simple Graphs** . . . . . 511  
 Soumen Atta and Priya Ranjan Sinha Mahapatra

<b>Compact, Multi-band Microstrip Antenna with High Gain</b> . . . . .	519
Srija De, Poulami Samaddar, Sushanta Sarkar, Sushanta Biswas, Debasree Sarkar and Partha Pratim Sarkar	
<b>Remote Access Control Mechanism Using Rabin Public Key Cryptosystem</b> . . . . .	525
Ruhul Amin and G.P. Biswas	
<b>Intelligent Energy Competency Multipath Routing in WANET</b> . . . . .	535
Santosh Kumar Das, Sachin Tripathi and A.P. Burnwal	
<b>An Improved Swarm Based Hybrid K-Means Clustering for Optimal Cluster Centers</b> . . . . .	545
Janmenjoy Nayak, Bighnaraj Naik, D.P. Kanungo and H.S. Behera	
<b>Some More Properties of Covering Based Pessimistic Multigranular Rough Sets</b> . . . . .	555
B.K. Tripathy and K. Govindarajulu	
<b>Performance Analysis of MC-CDMA in Rayleigh Channel Using Walsh Code with BPSK Modulation</b> . . . . .	565
S. Kuzhaloli and K.S. Shaji	
<b>Dual-Band Microstrip Patch Antenna Loaded with Complementary Split Ring Resonator for WLAN Applications</b> . . . . .	573
Kumaresh Sarmah, Angan Sarma, Kandarpa Kumar Sarma and Sunandan Baruah	
<b>Parallel Implementation of FP Growth Algorithm on XML Data Using Multiple GPU</b> . . . . .	581
Sheetal Rathi and C.A. Dhote	
<b>A Convergence Analysis of The Deterministic Ant System Model.</b> . . . .	591
Abhishek Paul, Swatantra Saha, Suraj Kumar Chaubey and Sumitra Mukhopadhyay	
<b>EAST: Exploitation of Attacks and System Threats in Network.</b> . . . .	601
Sachin Ahuja, Rahul Johari and Chetna Khokhar	
<b>Efficient Set Routing for Continuous Patient Monitoring Wireless Sensor Network with Mobile Sensor Nodes.</b> . . . . .	613
M.S. Godwin Premi, Betty Martin and S. Maflin Shaby	

**Overview of Cluster Based Routing Protocols in Static and Mobile Wireless Sensor Networks** . . . . . 619  
 Sachin R. Jain and Nileshsingh V. Thakur

**A 2 Dot 1 Electron Quantum Cellular Automata Based Parallel Memory** . . . . . 627  
 Mili Ghosh, Debarka Mukhopadhyay and Paramartha Dutta

**Stochastic Simulation Based GA Approach to Solve Chance Constrained Bilevel Programming Problems in Inexact Environment** . . . . . 637  
 Debjani Chakraborti and Bijay Baran Pal

**Highly Discriminative Features for Phishing Email Classification by SVD**. . . . . 649  
 Masoumeh Zareapoor, Pourya Shamsolmoali and M. Afshar Alam

**Signature Based Semantic Intrusion Detection System on Cloud** . . . . . 657  
 S. Sangeetha, B. Gayathri devi, R. Ramya, M.K. Dharani and P. Sathya

**Fuzzy Based Quality of Service Analysis of Scheduler for WiMAX Networks**. . . . . 667  
 Akashdeep

**Color Image Compression Based on Block Truncation Coding Using Clifford Algebra**. . . . . 675  
 Kartik Sau, Ratan Kumar Basak and Amitabha Chanda

**Performance Evaluation of Underground Mine Communication and Monitoring Devices: Case Studies** . . . . . 685  
 Alok Ranjan, H.B. Sahu and Prasant Misra

**Fuzzy Goal Programming Approach for Solving Congestion Management Problem in Electrical Transmission Network Using Genetic Algorithm** . . . . . 695  
 Bijay Baran Pal and Papun Biswas

**A Real-Time Machine Learning Approach for Sentiment Analysis** . . . . . 705  
 Souvik Sarkar, Partho Mallick and Aiswaryya Banerjee

**Benchmark Function Analysis of Cuckoo Search Algorithm** . . . . . 719  
 Joyita Basak, Sangita Roy and Sheli Sinha Chaudhuri

<b>Study of NLFSR and Reasonable Security Improvement on Trivium Cipher</b> . . . . .	731
Subhrajyoti Deb, Bhaskar Biswas and Nirmalya Kar	
<b>A No Reference Image Authentication Scheme Based on Digital Watermark</b> . . . . .	741
Sukalyan Som, Suman Mahapatra and Sayani Sen	
<b>Energy Efficient Routing Approaches in Ad hoc Networks: A Survey</b> . . . . .	751
Jenish Gandhi and Rutvij Jhaveri	
<b>Construction of Co-expression and Co-regulation Network with Differentially Expressed Genes in Bone Marrow Stem Cell Microarray Data</b> . . . . .	761
Paramita Biswas, Bandana Barman and Anirban Mukhopadhyay	
<b>Identifying Two of Tomatoes Leaf Viruses Using Support Vector Machine</b> . . . . .	771
Usama Mokhtar, Mona A.S. Ali, Aboul Ella Hassanien and Hesham Hefny	
<b>A Hierarchical Convex Polygonal Decomposition Framework for Automated Shape Retrieval</b> . . . . .	783
Sourav Saha, Jayanta Basak and Priya Ranjan Sinha Mahapatra	
<b>A Selective Bitplane Based Encryption of Grayscale Images with Tamper Detection, Localization and Recovery Based on Watermark</b> . . . . .	793
Sukalyan Som, Sayani Sen, Suman Mahapatra and Sarbani Palit	
<b>An Incremental Feature Reordering (IFR) Algorithm to Classify Eye State Identification Using EEG</b> . . . . .	803
Mridu Sahu, N.K. Nagwani, Shrish Verma and Saransh Shirke	
<b>Wireless Body Area Networks: A Review with Intelligent Sensor Network-Based Emerging Technology</b> . . . . .	813
Shabana Mehfuz, Shabana Urooj and Shivaji Sinha	
<b>Flow Regime Prediction Using Artificial Neural Networks for Air-Water Flow Through 1–5 mm Tubes in Horizontal Plane</b> . . . .	823
Nirjhar Bar, Manindra Nath Biswas and Sudip Kumar Das	



**Study of Wireless Communication Through Coal Using Dielectric Constant** . . . . . 831  
 Aindrila Bhattacharjee, Sourav Roy, Sayan Chakraborty, Amartya Mukherjee and Soumya Kanti Bhattacharya

**Performance Evaluation of Heuristic Algorithms for Optimal Location of Controllers in Wireless Networks** . . . . . 843  
 Dac-Nhuong Le

**MECAR: Maximal Energy Conserved and Aware Routing in Ad hoc Networks** . . . . . 855  
 Podoli V.S. Sriniva, Maddhi Sunitha and Temberveni Venugopal

**Raga Classification for Carnatic Music** . . . . . 865  
 S.M. Suma and Shashidhar G. Koolagudi

**A Novel Approach for Feature Selection** . . . . . 877  
 Ch. Swetha Swapna, V. Vijaya Kumar and J.V.R. Murthy

**Errata to:  $L(4, 3, 2, 1)$ -Labeling for Simple Graphs** . . . . . E1

**Author Index** . . . . . 887

## About the Editors

**Prof. J.K. Mandal** received his M.Sc. in Physics from Jadavpur University in 1986 and M.Tech. in Computer Science from University of Calcutta. Professor J.K. Mandal was awarded the Ph.D. in Computer Science and Engineering by Jadavpur University in 2000. Presently, he is working as Professor of Computer Science and Engineering and former Dean, Faculty of Engineering, Technology and Management, Kalyani University, Kalyani, Nadia, West Bengal for two consecutive terms. He started his career as lecturer at NERIST, Arunachal Pradesh in September 1988. He has teaching and research experience of 25 years. His areas of research include coding theory, data and network security, remote sensing and GIS-based applications, data compression, error correction, visual cryptography, steganography, security in MANET, wireless networks and unify computing. He has produced nine Ph.D. degrees, one submitted (2013) and eight ongoing. He has supervised 3 M.Phils. and 26 M.Techs. He is life member of the Computer Society of India since 1992, CRSI since 2009, ACM since 2012, IEEE since 2013 and Fellow member of IETE since 2012, Executive member of CSI Kolkata Chapter. He has chaired 17 sessions in various international conferences and delivered 20 expert/invited lectures. He is reviewer of various international journals and conferences. He has over 284 articles and 5 books published to his credit.

**Dr. Suresh Chandra Satapathy** is currently working as Professor and Head, Department of CSE at Anil Neerukonda Institute of Technology and Sciences (ANITS), Andhra Pradesh, India. He obtained his Ph.D. in Computer Science and Engineering from JNTU Hyderabad and M.Tech in CSE from NIT, Rourkela, Odisha, India. He has 26 years of teaching experience. His research interests include data mining, machine intelligence and swarm intelligence. He has acted as program chair of many international conferences and edited six volumes of proceedings from Springer LNCS and AISC series. He is currently guiding eight scholars for PhDs. Dr. Satapathy is also a Sr. Member of IEEE.

**Dr. Manas Kumar Sanyal** obtained his M.Tech. in Computer Science from Calcutta University in 1989. He worked in industries for about four years and joined as Lecturer at BCKV in the year 1994 and obtained his Ph.D. in 2003. Presently he is

working as Dean, Faculty of Engineering, Technology and Management in University of Kalyani, Kalyani, West Bengal. His current research interests include Big Data, e-governance, e-procurement data warehousing and data mining. In addition to presenting his work at numerous international conferences, Dr. Sanyal has also organized and chaired several international and national conferences. He has contributed over 100 research papers in various international journals and proceedings of international conferences.

**Dr. Partha Pratim Sarkar** obtained his Ph.D. in Engineering from Jadavpur University in 2002. He obtained his M.E. from Jadavpur University in 1994 and B.E. in Electronics and Telecommunication Engineering from Bengal Engineering College in 1991. He is presently working as Senior Scientific Officer (professor rank) at D.E.T.S, University of Kalyani, India. His areas of research include microstrip antenna, microstrip filter, frequency selective surfaces and artificial neural network. He has contributed over 210 research articles in various journals and conferences of international repute. He is a life fellow of IETE, and fellow of IE (India).

**Dr. Anirban Mukhopadhyay** is Associate Professor and former Head of the Department of Computer Science and Engineering, University of Kalyani, West Bengal, India. He did his B.E. from National Institute of Technology, Durgapur, India, in 2002 and M.E. from Jadavpur University, Kolkata, India, in 2004, respectively. He obtained his Ph.D. in Computer Science and Engineering from Jadavpur University in 2009. Dr. Mukhopadhyay is a recipient of the University Gold Medal and Amitava Dey Memorial Gold Medal from Jadavpur University in 2004. He also received Erasmus Mundus fellowship in 2009 to carry out post-doctoral research at University of Heidelberg and German Cancer Research Center (DKFZ), Heidelberg, Germany during 2009–2010. Dr. Mukhopadhyay visited I3S laboratory, University of Nice Sophia-Antipolis, Nice, France in 2011 as a Visiting Professor, and University of Goettingen, Germany, as a Visiting Scientist with DAAD scholarship in 2013. He has received Institution of Engineers, India (IEI) Young Engineers Award (2013–2014) and Indian National Academy of Engineering (INAE) Young Engineer Award (2014). He has co-authored one book and more than 100 research papers in various international journals and conferences. He is a senior member of IEEE, USA, and member of Association for Computing Machinery (ACM), USA. His research interests include soft and evolutionary computing, data mining, multiobjective optimization, pattern recognition, bioinformatics and optical networks.

# Simulation Studies on Distortion of EAS Muons by the Earth's Magnetic Field

Sandip Dam, Rajat Kumar Dey and Arunava Bhadra

**Abstract** The distortion of the secondary cosmic ray (CR) muon component triggered by the earth's magnetic field is studied using a Monte Carlo (MC) code dedicated to CR air shower physics. In an inclined shower, a clear separation may be put in evidence by studying the dipole defined by both barycentres of negative and positive muons. The length of this dipole as well as its azimuthal orientation depends on the incidence of the shower characterizing by the angle of the shower axis with the components of the magnetic field and the path of the secondary muons. We observed that the new observable *muonic dipole length* might be useful to determine the nature of primary CR species.

**Keywords** Geomagnetism · Cosmic ray · Muons · EAS modeling · Monte Carlo simulation

## 1 Introduction

To draw any specific conclusions about CRs from their indirect investigation it is very important to know how they interact with the atmosphere and how the shower develops. This knowledge is obtained by comparison of data with MC predictions. Hence air shower simulations are a crucial part of the design of air shower experiments and analysis of their data. But a MC technique relies heavily on high energy

---

S. Dam (✉) · R.K. Dey  
Department of Physics, North Bengal University, Siliguri 734013, West Bengal, India  
e-mail: Sandip-dam@rediffmail.com

R.K. Dey  
e-mail: rkdey2007phy@rediffmail.com

A. Bhadra  
High Energy and Cosmic Ray Research Centre, North Bengal University,  
Siliguri 734013, West Bengal, India  
e-mail: aru-bhadra@yahoo.com

hadronic models which suffer with some degree of uncertainties from one model to another and increasing primary energy. Therefore, we have challenges to develop more accurate hadronic interaction models in place to predict robust results. It is expected that the ongoing LHC experiment will provide new experimental inputs to the interaction models and thereby improving the predictive power of extensive air shower (EAS) simulations significantly in the concerned energy range [1].

The radial distribution of EAS particles is generally assumed to be symmetrical in the plane perpendicular to the shower axis. But presence of intrinsic fluctuations (due to stochastic nature of EAS development) from shower to shower, in addition, zenith angle and geomagnetic effects etc. can perturb this axial symmetry noticeably [2]. Consequent upon, highly inclined showers usually manifest significantly large asymmetries in charged particle distribution.

Apart from geomagnetic effect (GE), asymmetries may arise from azimuthal variation of the charged EAS particles and unequal attenuations accounted from different locations of the EAS in the ground plane (GP) with inclined incidence. These are known as geometrical and atmospheric attenuation effects to azimuthal asymmetries. To retain the GEs on the EAS charged particle distribution alone, geometrical and attenuation effects must be corrected out in the analysis. In our data analysis technique these two sources of azimuthal asymmetries are removed from data.

Here, we address the influence of the geomagnetic field (GF) on secondary muons with zenith angle  $\geq 50^\circ$  at KASCADE site [3] and express the separation between positive and negative muons as muonic dipole moment from the perturbed configuration. This *muonic dipole length* is found quite sensitive to the nature of the primary particle and hence in principle the parameter can be exploited to estimate primary mass. The practical realization of the method in a ground array experiment will be discussed briefly.

The GF effects on the EAS cascade is discussed in Sect. 2. In Sect. 3, we have given the simulation procedure employed here. Data analysis method is described in Sect. 4. In Sect. 5 we report important results obtained from this work. Our main conclusions are pointed out in Sect. 6.

## 2 Effects Due to Earth's Magnetic Field on Muons

The study of CRs with primary energies above  $10^{14}$  eV is usually based on the measurements of EASs, which are essentially cascades of secondary particles produced by interactions of CR particles with atmospheric nuclei. During the development of a CR cascade in the atmosphere, the GF affects the propagation of the secondary charged particles in the shower: the perpendicular component of this field causes the trajectories of secondary charged particles to become curved, with positive and negative charged particles separating to form an electric dipole moment. This aspect was first pointed out by Cocconi nearly sixty years back [4].

He further suggested that the geomagnetic broadening effect can be non-negligible in compare to the Coulomb scattering, particularly for the young showers [4]. For instance, the geomagnetic separation of muons can be used to estimate the height of origin of showers. The positive to negative muons ratio could also evaluate the signature of neutrons emitted from close pulsars or other astrophysical sources (Geminga, Vela, Crab etc.) at few kpc distances [5]. The GF induces an azimuthal modulation of the densities of air shower particles, particularly for large angle incidence [6]. For that reason, the estimated energy of CRs may deviate from the true value up to the  $\sim 2\%$  level at large zenith angles of incidence due to such azimuthal modulation [7].

For the soft component the radiation lengths in atmosphere are very short and electrons and positrons suffer many scatterings and stronger bremsstrahlung effect thereby frequent changing the directions relative to the GF. As a result the lateral spread of the electrons is mainly due to the multiple coulomb scattering and bremsstrahlung, and hence the effect of GF is less pronounced. In contrast after their generation from pion and kaon decays muons travel much longer path without scattering (suffer lesser bremsstrahlung also) and hence come under the influence of GF in a big way. As a result GE should be more pronounced in low momentum muons than very energetic ones, particularly for very large and strongly inclined showers. The work includes more accurate data analysis technique than before by bringing down even the small attenuation contributions from data in order to obtain primary mass information due to GF effects only.

### 3 Simulation Method

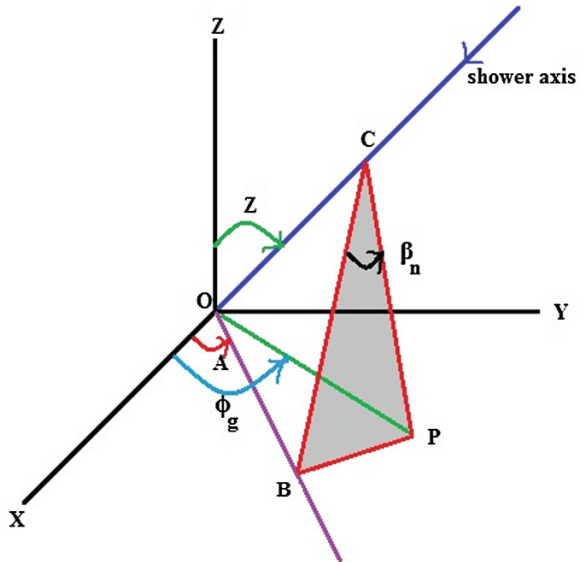
In the framework of the air shower MC simulation program version 6.970 [8], the EAS events are simulated by coupling the high energy (above 80 GeV/n) hadronic interaction models QGSJet 01 version 1c [9] and EPOS 1.99 [10], and the low energy (below 80 GeV/n) hadronic interaction model UrQMD [11]. The EGS4 program library [12] is opted for simulation of the electromagnetic component of shower that incorporates all the major interactions of electrons and photons. We consider the US-standard atmospheric model [13] with planar approximation which works for the zenith angle of the primary particles being less than  $70^\circ$ . The EAS events have been simulated at geographical location corresponds to the experimental site of KASCADE (latitude  $49.1^\circ\text{N}$ , longitude  $8.4^\circ\text{E}$ , 110 m a.s.l.). The EAS events have been generated for Proton (p) Oxygen ( $\text{O}_2$ ) and Iron (Fe) primaries at fixed primary energy  $10^{15}$  eV taking zenith angles of incidence, between  $50^\circ$  and  $68^\circ$  with FLAT option of the atmosphere. About 10,000 EAS events have been generated for this work.

## 4 Data Analysis Method

Secondary charged particles in an EAS are generated maintaining a cylindrical symmetry around the shower axis, which is along the arrival direction of EAS initiating particle. As a result in the absence of GF lateral distribution of EAS charged particles should possess such a symmetry for all radial distances from the axis in a plane normal to the shower axis. In the GP, however, such cylindrical symmetry is distorted for inclined EAS due to geometrical and atmospheric attenuation effects. Since the effect (azimuthal asymmetry) of GF is superimposed with those caused by geometric and attenuation effects, it is convenient to transform the density information of charge particles of air showers in the GP to shower plane (SP) so that the effect of the GF can be isolated out. It should be mentioned, however, that the effect of muon attenuation in the transformation is negligibly small and is ignored here.

An EAS experiment and MC technique both provide information about an EAS initiated by a primary from the GP. To extract the actual variation introduced by the GE in EAS observables, it is necessary to take away the contribution added geometrically from data. In Fig. 1, we have shown the transformation of a point of impact by a cascade particle on the GP to shower front plane in polar coordinates. Here, in the figure  $Z$  and  $A$  denote the primary zenith and azimuth angles respectively, and  $(r_g, \phi_g)$  are polar coordinates of the point of impact (say,  $P$ ) of an EAS charged particle under consideration at the GP while  $(r_n, \beta_n)$  represent the polar coordinates of the point  $P$  at the corresponding SP (plane  $\perp r$  to the shower axis containing  $P$ ), then

**Fig. 1** Geometry for the point of impact  $P$  of a cascade charged particle in polar coordinates in ground and shower front planes respectively



$$r_n = r_g \sqrt{1 - \sin^2 Z \cos^2(\phi_g - A)} \quad (1)$$

Using the figure, the corresponding Cartesian coordinates  $P(x_n, y_n)$  at the SP can be easily obtained as,

$$x_n = r_g \cos(\phi_g - A) \cos Z \quad (2)$$

$$y_n = r_g \sin(\phi_g - A) \quad (3)$$

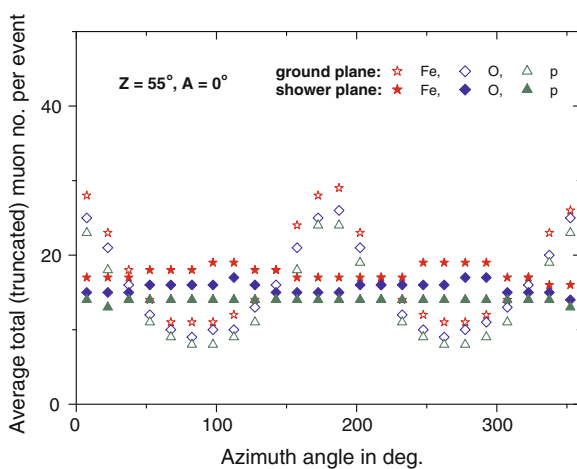
The shaded zone in the diagram ( $APC$ -region) represents the normal plane, where  $OP = r_g$ ,  $CP = r_n$  and  $CB = x_n$ , and  $BP = y_n$ .

We first consider a hypothetical circular full coverage air shower array of radius 300 m taking the shower core as the center of the circle. Employing the Eqs. (2)–(3) we then transform the simulated density or other quantities of interest at GP to the normal plane/SP.

## 5 Results

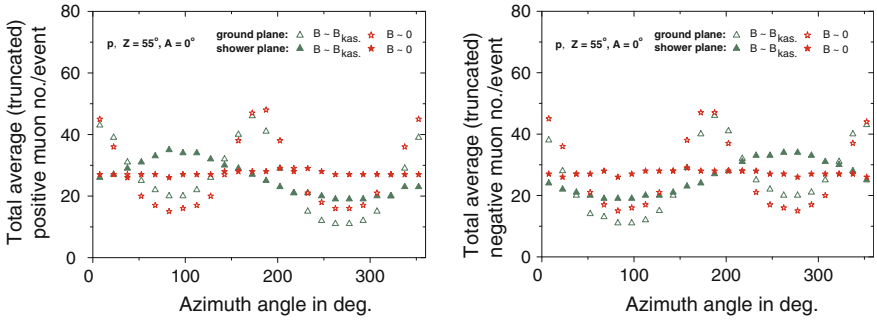
For examining asymmetric characteristics on the azimuthal plane of the charged particle distribution due to GF, we estimated density/total number of charged muons over a small azimuthal angle bin of either  $15^\circ$  or  $10^\circ$  with regard to various situations. The azimuthal variation of total (truncated) muon content at GP and at SP is shown in Fig. 2 for p,  $O_2$  and Fe initiated showers of zenith angle of incidence  $55^\circ$  and arriving from North direction. This figure implies that the azimuthal

**Fig. 2** Azimuthal variation of muon distribution in GP and SP for proton, oxygen and iron primaries in the radial range (0–200 m)

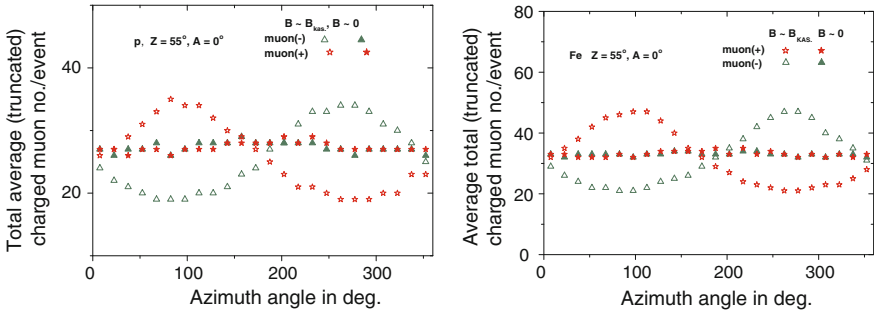




asymmetry in the GP is mainly due to GE while in SP, the observed negligibly small azimuthal asymmetry seems to be due to attenuation effect. It appears that the attenuation effect is small, even at zenith angles of incidence much beyond  $50^\circ$ . Since positive and negative particles behave in an opposite way under GF, the GE is not revealed from the azimuthal variation of the total muon content. To examine GE we draw the angular variation of charged muons in inclined air showers which are shown in Fig. 3 (Left panel— $\mu^+$  and Right panel— $\mu^-$ ) for proton primaries arriving from north direction ( $A = 0^\circ$ ). To understand the influence of GF clearly, we also studied azimuthal variation of charged muons by turning off the GF, which is accomplished in CORSIKA simulation by dividing the components of the geomagnetic field by a factor of ten thousand. Such variations for p are also included in Fig. 3. Azimuthal variations of charged muons for both p and Fe primaries arriving from the North direction are displayed in Left and Right panels of Fig. 4. From Figs. 3 and 4, we have found that the asymmetry in  $\mu^+$  and  $\mu^-$  numbers separately in SPs is nearly zero. To quantify the influence of GF as well as to identify some



**Fig. 3** Azimuthal variation of  $\mu^+$  (left) and  $\mu^-$  (right) for p primary in GP and SP with  $B \approx B_{KAS}$  and  $\approx 0$

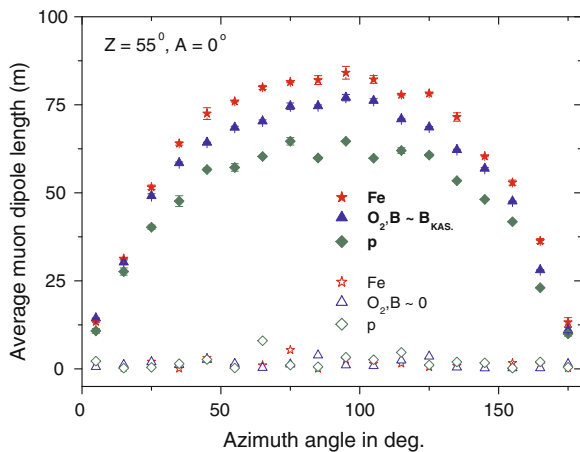


**Fig. 4** Azimuthal variation of charged muons for p (left) and Fe (right) primaries arriving from North direction in SP with  $B \approx B_{KAS}$  and  $B \approx 0$

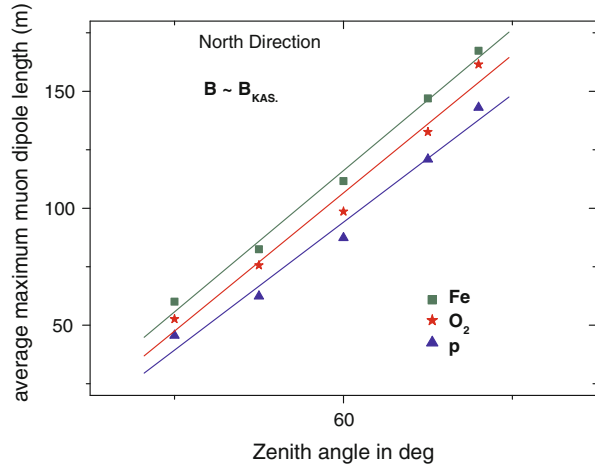
typical signatures of the primary particle we have calculated the coordinates of positive and negative muons barycenters and thereby estimated the average muon dipole length per shower, which is the separation of centre of gravity of negative and positive charged muons in the SP. For this purpose we introduce a procedure of scanning of charged particle density/number with the butterfly (BF) treatment: the BF consists of two opposite wings around the shower core limited by a pair of symmetric arcs corresponding to angle of amount  $15^\circ$  which is called a slim BF. The variation of average muon dipole length/event with azimuthal angle for p,  $O_2$  and Fe initiated EASs of zenith angle of incidence  $55^\circ$  and arriving from North direction is shown in Fig. 5. In this figure the azimuthal variation of average muon dipole length/event is also shown when the GF is switched off. A comparison of the variation of average muon dipole length/event for various primaries is clearly seen from this kind of study. It is found from the Fig. 5 that the average length of the muon dipole increases due to GF up to  $\phi_g = 90^\circ$  and then returns to its initial value at  $\phi_g = 180^\circ$ . The parameter is found sensitive to primary mass; it is largest for Fe and smallest for p at a given primary energy. So the parameter can be used, at least in principle for extracting the nature of primary particles.

The variation of the average maximum value of the muon dipole length against zenith angle is shown in Fig. 6 for p,  $O_2$  and Fe primaries. Here, a maximum value of the parameter is obtained by taking average of all dipole lengths ranging from  $\phi_g = 75^\circ$  to  $\phi_g = 105^\circ$  corresponding to a particular Z and primary species. This parameter might be useful for the measurements of primary mass composition of CRs from the technique adopted in this work.

**Fig. 5** Azimuthal variation of muon dipole length for p,  $O_2$  and Fe primaries arriving from the North direction



**Fig. 6** Variation of average maximum muon dipole length per event with zenith angle for p, O<sub>2</sub> and Fe primaries arriving from North direction



## 6 Conclusions

Our analysis concerning the effects of the GF on positive and negative muon components of inclined EAS reveals several interesting features such as azimuthal asymmetries, sectorial positive-negative muons relative abundances, amplitude of fluctuations among p, O<sub>2</sub> and Fe induced showers. Such effects are found to persist and are of comparable magnitude if we replace the UrQMD code in the simulation by the Fluka/Gheisha code in the treatment of low energy hadron collisions. For very inclined showers the Earth's magnetic field might be used as magnetic separator at least for muons in the GeV energy regime. It seems very interesting to the experimental detection of these features for the understanding of the EAS development under GF.

There are some recent proposals of studying positive and negative muons separately in individual EAS event. In fact few ongoing experiments, such as the WILLI detector [14] in Bucharest, Romania or the Okayama University, Japan EAS installation, have the capability to extract charge information of high energy muons but these experiments do not have large muon detection area, which is needed to extract information about the nature of primaries from the study of geomagnetic influence on EAS muons. If in future these experiments are extended in order to cover larger detection area, or new installation of large muon detection area with capability of charge identification will come up, the present proposal can be exploited to extract the nature of primary CRs.

**Acknowledgments** The authors would like to thank Prof. J. N. Capdevielle of APC, France for many useful suggestions. RKD thanks the University of North Bengal for providing financial support under UGC scheme.

## References

1. Aab, A., et al.: The Pierre Auger Collaboration, arXiv: 1408.1421v1 [astro-ph,HE] (2014)
2. Capdevielle, J.N., Le Gall, C., Sanosyan, Kh.N.: Simulation of extensive air showers at ultra-high-energy using the CORSIKA Monte Carlo Code. *Astropart. Phys.* **13**, 259–275 (2000)
3. Antoni, T., et al.: Astro-ph/0505413. *Astropart. Phys.* **24**, 1–25 (2005)
4. Cocconi, G.: Influence of the Earth's magnetic field on the extensive air showers. *Phys. Rev.* **93**, 646 (1954)
5. Tallai, M.C., Attallah, R., Capdevielle, J.N.: Talk Presented at ISVHECRI 2014, CERN, 18–22 Aug 2014
6. Bowden, C.C.G., et al.: The effect of the geomagnetic field on TeV gamma-ray detection. *J. Phys. G: Nucl. Part. Phys.* **18**, L55 (1992)
7. The effect of the geomagnetic field on cosmic ray energy estimates and large scale anisotropy searches on data from the Pierre Auger Observatory, The Pierre Auger collaboration. *J. Cosmol. Astropart. Phys.* **11**, 022 (2011). doi: [10.1088/1475-7516/2011/11/022](https://doi.org/10.1088/1475-7516/2011/11/022)
8. Heck, D., Knapp, J., Capdevielle, J.N., Schatz, G., Thouw, T.: The CORSIKA air shower simulation program. Forschungszentrum Karlsruhe Report FZK 6019 (Karlsruhe) (1998)
9. Kalmykov, N.N., Ostapchenko, S.S., Pavlov, A.I.: Quark-Gluon\_String model & EAS Simulation problems at ultra-high Energies. *Nucl. Phys. B Proc. Suppl.* **52**, 17 (1997)
10. Werner, K., et al.: Parton ladder splitting and the rapidity dependence of transverse momentum spectra in deuteron-gold collisions at RHIC. *Phys. Rev. C* **74**, 044902 (2006)
11. Bleicher, M., et al.: Relativistic hadron-hadron collisions in the ultra-relativistic quantum molecular dynamics model. *J. Phys. G: Nucl. Part. Phys.* **25**, 1859 (1999)
12. Nelson, W.R., Hiramaya, H., Rogers, D.W.O.: Report SLAC 265 (1985)
13. National Aeronautics and Space Administration (NASA): U.S. Standard Atmosphere Tech. Rep. NASA-TM-X-74335 (1976)
14. Brancus, I.M., et al.: The East-West effect of the muon charge ratio at energies relevant to the atmospheric neutrino anomaly. *Nucl. Phys. A* **721**, 1044c–1047c (2003)

# A Detailed Survey on Misbehavior Node Detection Techniques in Vehicular Ad Hoc Networks

Uzma Khan, Shikha Agrawal and Sanjay Silakari

**Abstract** Communication in Vehicular ad hoc Network relies on exchange of information among different vehicular nodes in the network. This helps to improve the safety, driving efficiency and comfort on the journey for the travellers. In this network, information received from other vehicles is utilized to make majority of the decisions. However, a node may behave malicious or selfish in order to get advantage over other vehicles. A misbehaving node may transmit false alerts, tamper messages, create congestion in the network, drop, delay and duplicate packets. Thus, detecting misbehavior in VANET is very crucial and indispensable as it might have disastrous consequences. This paper presents a detailed survey on some of the important research works proposed on detecting misbehavior and malicious nodes in VANETs. In addition to the details about the techniques used for misbehavior detection, nature of misbehavior, this paper categorizes the schemes for better understanding and also outlines several research scopes to make VANET more reliable and secure.

**Keywords** Vehicular ad-hoc networks (VANETs) · Misbehavior · Detection · Malicious vehicles · Security

---

U. Khan (✉) · S. Agrawal · S. Silakari  
Department of Computer Science and Engineering, University Institute of Technology,  
RGPV, Bhopal, India  
e-mail: uzma.khans@gmail.com

S. Agrawal  
e-mail: shikha@rgtu.net

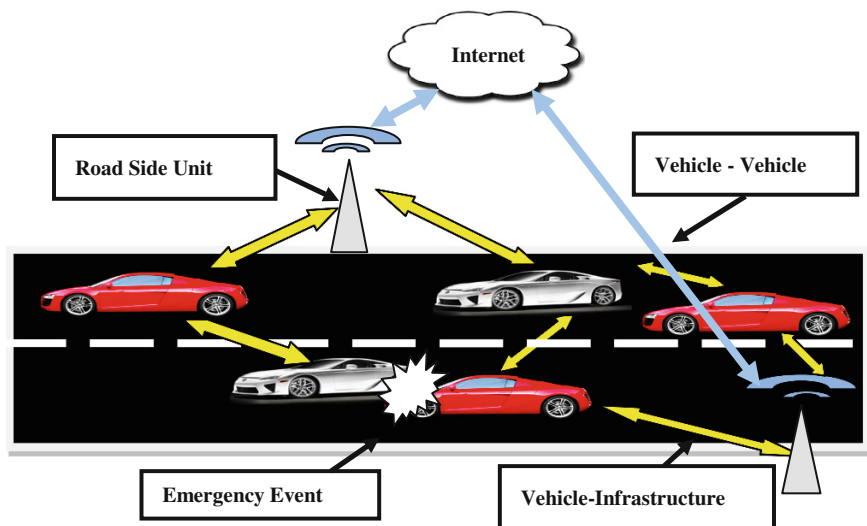
S. Silakari  
e-mail: ssilakari@yahoo.com

## 1 Introduction

Nowadays, Vehicular ad hoc Network has gained much attention to incorporate security on transportation systems. Vehicular ad hoc Network is an ad hoc Network which is considered as a subclass of Mobile ad hoc Network (MANET). VANET exhibits numerous special features such as high mobility, rapidly changing network topology, frequent partitioning etc. As a result of these unique characteristics, many solutions and protocols proposed for MANET might not be suitable or directly applicable to VANETs. Thus VANET needs for its unique solutions [1].

Security of VANETs has been identified as one of the major challenge. VANETs applications support real time communication and deals with life critical information. In order to do it correctly and effectively, it must follow the security requirements such as integrity, confidentiality, privacy, non repudiation and authentication to protect against attackers and malicious vehicular nodes. There are several attacks like black hole, Sybil, DoS, Timing, Illusion etc. which not only affect the driver's and vehicle's privacy but also compromise traffic safety and may lead to loss of life [2]. Thus, in order to become a real technology that assures traffic safety VANETs require appropriate security techniques and mechanisms that will guarantee protection against various misbehaviors and malicious nodes that affects security of VANET. Figure 1 shows the VANET architecture.

In Sect. 1, we have given a brief introduction about VANETs. Section 2 discusses the importance of malicious node detection and classification of misbehavior node detection techniques in VANETs. We present various efforts by researchers under



**Fig. 1** Vehicular ad hoc network architecture

Node-Centric and Data-Centric Misbehavior Detection Techniques in Sects. 3 and 4 respectively. Section 5 concludes the review work with discussion and some future research ideas.

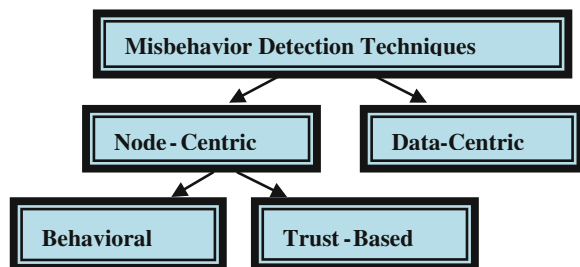
## 2 Misbehavior Nodes Detection in VANETs

Information dissemination in VANETs happens through cooperative behaviour of the vehicular nodes. Messages transmitted in vehicular network carry vital information like traffic jam, emergency brake events, road conditions, accident notifications, bad weather conditions, etc. In such a case, if any vehicle act maliciously and tamper with the messages, the results may be very dangerous. Thus misbehaviors in VANET is a very crucial issue. Misbehavior can be generally referred to as any kind of abnormal behaviour that is deviation from the average behaviour of other vehicular nodes in the VANETs. Hence, detection of misbehaviors and the malicious vehicular nodes involved in such misconducts is extremely imperative, in order to make VANET a secure network. A lot of work has been carried out to detect misbehavior and malicious nodes in Vehicular ad hoc networks. The misbehavior detection schemes can be broadly classified into following types: Node-centric and Data-centric misbehavior detection schemes as shown in Fig. 2. Table 1 differentiates them. Some of the contributions of the researchers under the classification schemes mentioned above are discussed in this section. Considering the numerous advantages of VANETs and hazardous consequences that could result due to misbehavior, security of VANETs has become a prominent area of research.

## 3 Node Centric Misbehavior Detection Schemes

Node-centric techniques need to distinguish among different nodes using authentication. Security credentials, Digital signatures, etc. are used to authenticate the node transferring the message. Such schemes emphasis on the nodes transmitting the messages rather than the data transferred. Depending on the way a node behaves

**Fig. 2** Taxonomy of misbehavior detection techniques in VANETs



**Table 1** Node-centric versus data-centric misbehavior detection techniques

	Based on	Simplicity	Attackers	Additional requirements	Number of misbehavior detected	Overhead
Node centric detection	Authentication of nodes, behavioral and trust analysis	Techniques employed to isolate malicious nodes are simpler	Able to detect insider attackers	Require enhanced OBU's, sensors and radars for monitoring	Limited	Less
Data centric detection	Analyzing the data transmitted among nodes	Complex algorithms and comparisons are used to detect discrepancy in data	Able to detect misbehaviors caused by insiders as well as outsider attackers	Need fast computation capable devices for quick data processing	Many	More



and how reliably it transmits the messages, node-centric techniques can be further categorized as behavioural and trust based node-centric techniques. Behavioural schemes works on the concept of observing a node's behaviour by some trustworthy nodes and uses a metric that helps to identify how effectively a node behaves. Trust based node-centric schemes judge a node by its behaviour in past and present and uses it to obtain the expected future misbehavior. Some of the node centric techniques are discussed below.

In the research work Ghosh et al. [3, 4] have proposed a robust scheme to detect malicious vehicles for Post Crash Notification application. The approach applied, firstly observes a driver's actions post raising a crash alert message. Observed mobility and expected trajectory of the vehicle for the crash mobility model is calculated and if the difference between the two exceeds a certain threshold value, the alert is considered to be false. The approach effectively reduces the false positives and false negatives while effectively detecting misbehavior. In [8] Ghosh et al. improved their previous work [7] by considering the possibility of the fake position information of the vehicle in the PCN along with the false crash alert. The cause-tree representation is used effectively to conjointly accomplish misbehavior detection in addition to identification of its root-cause by employing logical reduction. The scheme proves to be robust and achieves considerable detection of misbehavior.

Kim and Bae [5] have proposed a novel misbehavior based reputation management scheme (MBRMS) which includes three components (a) Misbehavior detection (b) Event rebroadcast and (c) Global eviction algorithms for the detection and filtration of false information in VANETs. Each vehicular node maintains information system of events and corresponding actions for the detection of misbehaving node. The presented mechanism uses outlier detection technique and misbehaving risk value of the bad node to measure the risk level. MBRMS effectively detects and evicts the misbehaving nodes.

In the research work, Daeinabi and Rahbar [6] have proposed the Detection of Malicious Vehicles (DMV) algorithm through observation to discover malicious nodes that drop or duplicate received packets more than a given threshold value. Vehicles are tagged using a distrust value and are monitored by the allocated verifier nodes. Black and white lists are maintained in order to isolate the malicious vehicles from the honest vehicles. It has been observed in simulation that detection of malicious vehicles is faster in case of Constant Speed Motion (CSM) and Smooth Motion Model (SMM) as compared to Fluid Traffic Model (FTM). Performance analysis shows that this misbehavior detection scheme is capable of finding out most existence malicious vehicles even at quite high speeds. Kadam and Limkar [7] have presented an improvement of the DMV algorithm [6]. It not solely detects malicious nodes however additionally their prevention from the VANET. This approach reduced the impact of black hole attack within the VANET and is more efficient and secure compared to DMV.

In the research work, Wahab et al. [8] have used Quality of Service-Optimized Link State Routing (QoS-OLSR) clustering algorithm to detect malicious vehicles in VANET. Certain vehicles may over speed the maximum speed limits or under speed the minimum range, thus may prove to be uncooperative in packet forward

and cluster formation resulting in performance degradation of the network. Authors have proposed a two phase model—incentive and detection. Vehicles are motivated by giving incentives during formation of clusters. After cluster formation, misbehavior is detected by aggregating evidences and cooperative decision using Dempster–Shafer based cooperative watchdog model. Incentives are in the form of reputation where network services are provided depending on reputation value. Watchdogs are appointed from the nodes in the network that monitor behaviour of other nodes in order to ensure vehicles are cooperating with each other. This method maintains stability and Quality of Service with increase in detection probability and decreasing the number of selfish nodes and false negatives.

## 4 Data Centric Misbehavior Detection Schemes

Data-centric approach inspects the data transmitted among nodes to detect misbehavior. It is primarily concerned with linking between messages than identities of the individual nodes. The information disseminated by the nodes in the network is analyzed and compared with the information received by the other nodes, in order to verify the truth about the alert messages received. Thus, any vehicular node which sends some bogus information about different events in the VANETs like fake congestion messages, false location, fake emergency events, accidents, road conditions etc. is considered to be misbehaving. Such misbehaviors are identified through data-centric misbehavior schemes. Few research contributions to the data centric misbehavior detection scheme are as follows.

Vulimiri et al. [9] have proposed a probabilistic misbehaviour detection approach, based on the secondary information or alerts that are created in response to the primary alerts for PCN application. Secondary alerts are thus used to verify the truth and falsity of the primary alerts received by a vehicle. The secondary information received in the form of other causal alerts can be collated to produce a degree of trust for the primary messages. The observed behaviour is compared with the alert sent by the vehicle to verify the conditions for raising the alert. Hence, if the two don't justify one another, it indicates that the alert is fake and hence the vehicle is malicious. Harit et al. [10] have improved [9] in terms of reduced approximation errors. It makes use of a Fox-Hole region which helps to find the safety value of any node on its current location and present speed.

Ruj et al. [11] detected fake alert messages and misbehaving nodes by monitoring the actions of the vehicle after alert messages have been sent. Reported and estimated positions of the vehicle according to the information are matched to make suitable decisions. This scheme imposes fines on the misbehaving node, in place of revoking key/credentials administered by the CA (Certificate Authority) so as to prevent nodes to act maliciously. This results in reduction of the computation and communication cost for the revocation of all the credentials of misbehaving nodes. The result shows that the proposed scheme is better than ECMV [12], LEAVE [13],

Hybrid [14] and PASS [15] schemes in terms of communication overhead involved in sending the CRL (Certificate Revocation List) to RSUs.

Rezgui and Cherkaoui [16] developed a mechanism that collects, at one vehicle, information relating to every neighbour transmission. It then extracts the temporal correlation rules between vehicles concerned in transmissions within the neighbourhood. VANETs Association Rules Mining (VARM) method is proposed to generate association rules which are then utilized to find a faulty or malicious vehicle, i.e., a vehicle that isn't related with vehicles within the neighbourhood following these rules. Ordered structures are constructed depending on precedence relation. It uses itemset-tree concept. The proposed VARM shows superior performance than FP-tree and cats-tree in terms of compactness of the structure and execution time when compared on both sparse and dense data sets.

Grover et al. [17, 18] have presented a security framework based on machine learning approach in order to categorize numerous misbehaviors in VANET. Features are extracted from different attack cases in order to differentiate various types of misbehaviors. The proposed approach efficiently classifies multiple misbehaviors in vehicular network. J-48 and Random Forest classifiers have shown better performance in comparison to other classifiers IBK, Naïve Bayes and AdaBoost1. Majority voting scheme is applied in [18] to improve the accuracy of detection of misbehaviors. This approach is better and efficient in classifying multiple misbehaviors existing in VANET as compared to base classifiers used for classification in [17].

Barnwal and Ghosh [19] have presented a short term MDS which can detect the malicious node that is spreading fake position and speed information through its heartbeat/beacon messages. The observing vehicle uses the information contained in the beacon message for judging a node as honest or malicious. On analysis of the last and present information received, expected and observed position of the reporting vehicle is calculated by the observing node. If it doesn't match, then the suspicion index of the vehicle is increased. Vehicle is considered as malicious if its suspicion index exceeds the threshold value. The advantage of this system is that it does not cause any overload on the VANET communication neither requires any additional sensors as it utilizes periodic transmitted heartbeat message.

In the paper, Huang et al. [20] have proposed a cheater detection protocol which detects malicious vehicles that broadcast fake congestion information for their selfish motives and impersonate non existing vehicle. This approach is based on measurements of local velocity and distance by means of radars to verify the congestion event sent by a vehicular node. It uses kinematic wave detection approach by which a vehicle can make a prediction about the duration of congestion and distance. Thus, it can detect the rogue nodes that sent bogus congestion message. In order to detect and prevent multiple cheaters with forge IDs to fake congestion, the scheme requires the vehicle's signature and certificate to be attached to the wave packet. The presented solution is quite effective as it depends only on communication with neighbouring nodes and does not require a centralized congestion detection system.

## 5 Discussion and Future Work

VANETs have gained a lot of attention as it can greatly improve the safety on roads and driving conditions. Detecting misbehaviors in VANETs is very significant as it can be hazardous. This survey work aims to provide a detailed overview of the various misbehavior detection schemes in VANETs. It is expected that this survey can serve as a helpful guide for the researchers inquisitive about misbehavior detection schemes in VANET and mitigates further research in order to make VANET more secure. Various misbehavior detection techniques have been categorized as Node-Centric and Data Centric Misbehavior Detection Techniques. However, these techniques have certain issues which need to be removed to make VANET more reliable and safe.

The node-centric schemes can be further improved by selecting nodes as observer or verifier after proper authentication. These schemes require good observations and processing the vehicle's actions well to identify the abnormal behaviour, thus there is a need of high speed computation and processing hardware over the OBU to make decisions speedily and accurately. Few misbehavior detection schemes consider the results of the short term misbehavior, however it should be analyzed along with the long term examination for much reliable and better decision making. In Data-centric approach, the detection carried out using the beacon, safety alert messages etc. reduces the extra overhead involved in using sensors and communication of additional messages. But, if the truth parameter value of the information received is not computed speedily, the message may become useless. Hence, efficient processing devices must be equipped in vehicles. Also, inappropriate conclusions drawn from information gathered or overlooking important details could result in poor detection and other misleading decisions. Efficient learning techniques can be used to extract accurate correlation of the events and relationship between vehicular nodes to identify misconducts.

It has been identified that no single MDS can detect all the different types of misbehaviors effectively in VANETs. Thus, hybridization of node-centric and data-centric schemes can be considered in future to integrate the advantages of both the approaches into one. This will help to detect more complicated possible attacks. In VANET, vehicles and drivers have to disclose their identities to the RSUs to establish communication with them. However, privacy and security of such information need to be handled very carefully to avoid misuse by attackers. The resolution of communication pseudonyms is a basic demand for misconduct detection, a well-considered integration is important so as to preserve driver's privacy.

## References

1. Wang, Z., Chigan, C.: Countermeasure uncooperative behaviors with dynamic trust-token in VANETs. In: IEEE International Conference on Communications, ICC'07, pp. 3959–3964 (2007)
2. Al-kahtani, M.S.: Survey on security attacks in vehicular ad hoc networks (VANETs). In: 6th IEEE International Conference on Signal Processing and Communication Systems (ICSPCS), pp. 1–9 (2012)
3. Ghosh, M., Varghese, A., Kherani, A.A., Gupta, A.: Distributed misbehavior detection in VANETs. In: Wireless Communications and Networking Conference, WCNC IEEE, pp. 1–6 (2009)
4. Ghosh, M., Varghese, A., Gupta, A., Kherani, A.A., Muthaiah, S.N.: Detecting misbehaviors in VANET with integrated root-cause analysis. *Ad Hoc Netw.* **8**, 778–790 (2010)
5. Kim, C.H., Bae, I.H.: A misbehavior based reputation management system for VANETS. *LNEE* **181**, 441–450 (2012)
6. Daeinabi, A., Rahbar, A.G.: Detection of malicious vehicles (DMV) through monitoring in vehicular ad-hoc networks. *Multimedia Tools Appl.* **66**(2), 325–338 (2013)
7. Kadam, M., Limkar, S.: D and PMV: new approach for detection and prevention of misbehave/malicious vehicles from VANET. In: Proceedings of the International Conference on Frontiers of Intelligent Computing: Theory and Applications (FICTA) 2013. AISC, vol. 247, pp. 287–295. Springer, Heidelberg (2014)
8. Wahab, O.A., Otok, H., Mourad, A.: A cooperative watchdog model based on Dempster-Shafer for detecting misbehaving vehicles. *Comput. Commun.* **41**, 43–54 (2014). Elsevier
9. Vulimiri, A., Gupta, A., Roy, P., Muthaiah, S.N., Kherani, A.A.: Application of secondary information for misbehavior detection in VANETs. *IFIP. LNCS*, vol. 6091, pp. 385–396. Springer, Berlin (2010)
10. Harit, S.K., Singh, G., Tyagi, N.: Fox-hole model for data-centric misbehavior detection in VANETs. In: 3rd International Conference on Computer and Communication Technology (ICCT), pp. 271–277 (2012)
11. Ruj, S., Cavenaghi, M.A., Huang, Z., Nayak, A., Stojmenovic, I.: On data-centric misbehavior detection in VANETs. In: Vehicular Technology Conference (VTC Fall), IEEE, pp. 1–5 (2011)
12. Wasef, A., Jiang, Y., Shen, X.: Ecmv: efficient certificate management scheme for vehicular networks. In: GLOBECOM, IEEE, pp. 639–643 (2008)
13. Raya, M., Papadimitratos, P., Aad, I., Jungels, D., Hubaux, J.P.: Eviction of misbehaving and faulty nodes in vehicular networks. *IEEE J. Sel. Areas Commun.* **25**(8), 1557–1568 (2007)
14. Calandriello, G., Papadimitratos, P., Hubaux, J.P., Lioy, A.: Efficient and robust pseudonymous authentication in VANET. In: Vehicular ad hoc Networks, pp. 19–28. ACM, New York (2007)
15. Sun, Y., Lu, R., Lin, X., Shen, X., Su, J.: An efficient pseudonymous authentication scheme with strong privacy preservation for vehicular communications. *IEEE Trans. Veh. Technol.* **59** (7), 3589–3603 (2010)
16. Rezgui, J., Cherkaoui, S.: Detecting faulty and malicious vehicles using rule based communications data mining. In: IEEE 36th Conference on Local Computer Networks (LCN), IEEE, pp. 827–834 (2011)
17. Grover J., Prajapati N.K, Laxmi V., Gaur M.S: Machine learning approach for multiple misbehavior detection in VANET. In: CCIS, vol. 192, pp. 644–653. Springer, Berlin (2011)
18. Grover J., Laxmi V., Gaur M.S. Misbehavior detection based on ensemble learning in VANET. In: ADCONS. LNCS, vol. 7135, pp. 602–611. Springer, Berlin (2011)
19. Barnwal, R.P., Ghosh, S.K.: Heartbeat message based misbehavior detection scheme for vehicular ad-hoc networks. In: 2012 International Conference on Connected Vehicles and Expo (ICCVE), pp. 29–34 (2012)
20. Huang D., Williams, S.A., Shere, S.: Cheater detection in vehicular networks. In: IEEE 11th International Conference on Trust, Security and Privacy in Computing and Communications (TrustCom), pp. 193–200 (2012)

# Detect Mimicry by Enhancing the Speaker Recognition System

Soumen Kanrar and Prasenjit Kumar Mandal

**Abstract** Mimicry voice sample is a potential challenge to the speaker verification system. The system performance is highly depended on the equal error rate. If the false accept to reduce, then the equal error rate decrease. The speaker verification process, verifies the claim voice is originally produced by the said speaker or not. The verification process is highly depended upon the biometric features carried out by the acoustic signal. The pitch count, phoneme recognition, cepstral coefficients are the major components to verify the claim voice signal. This paper shows a novel frame work to verify the mimicry voice signal through the two-stage testing. The first stage is GMM based speaker identification. The second stage of testing filters the identification through the various biometric feature's comparisons.

**Keywords** Mimicry voice · Speaker verification · Speaker identification · Acoustic signal · Phonetic · Biometric · Spectrogram pitch · Cepstrogram

## 1 Introduction

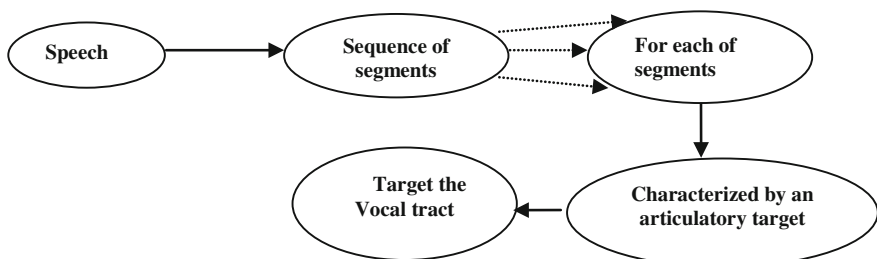
The sensitivity to computer by voice-altered impostor is using trainable speech synthesis technology makes the robustness of a speaker recognition system [1]. Mimicry voice is using synthetic speech against speaker verification based on the spectrum, pitch and cepstrum analysis. Pitch of a particular vocal cord of small duration extracted from the speaker's voice excitation. The same time duration is used to presents the movements of the acoustic signal corresponding to articulation, independent of language. Phonetic event changes significantly, and this is reflected the numbers of segments clearly visualize by spectrogram based on the different

---

S. Kanrar (✉) · P.K. Mandal  
Vehere Interactive Pvt Ltd., Calcutta 700053, West Bengal, India  
e-mail: Soumen.kanrar@vehere.com

P.K. Mandal  
e-mail: prasenjit.mandal@vehere.com

range of frequency bands. Phonetic analysis is based on the important premise that it is possible to describe speech in terms of a sequence of segments. The crucial assumption, that each segment can be characterized by an articulatory target. ‘Articulation’ the activity of the vocal organs in making a speech sounds. The aforesaid biometrics offers greater security than traditional methods in person recognition by GMM based speaker identification [2–6]. In this paper, we present a robust approach to avoid the Mimicry voice that causes the potential security threat to the voice recognition system. We have seen that human tendency to copy the speaking style of some reputed personalities [1]. However, for the security point of view that mimicry voice used as the proxy of some existing voice model for any voice recognition system is a challenging issue. Mimicry voices are very vulnerable for any speaker recognition system [1]. The probable mimicry attack occurs in the domain of Voice dialing, banking over a telephone network, database access services, security control for confidential information and remote access of computers. So verification of the claim speaker is to identify the vocal track of the speaker from a number of existing speaker model present in the system [7]. Vocal cords are producing acoustic energy by vibrating as air passes between them. If the claim speaker voice is very nearer to an existing model in the system or numbers of models, then we proceed for second stage of verification. This is carried out by further speech analysis based on phonetic. Phonetic is concerned with the physical properties of acoustic signal. Phone is a unit of speech sound. Consonants and vowels are classified in terms of its place of articulation. Phonetic describes the place of articulation concentrates on a section through the mid line of vocal tract. Voice is the composition of sequence of discrete sounds or segments (Fig. 1). The segments are composed by consonants and vowels. The vowels and consonants are the fundamental part of the segmentation. The repeated opening and closing of vocal tract are syllables. More closed articulation is consonant, and more open articulation is a vowel. Consonant involve narrowing or restriction at an identifiable place in the vocal tract. The syllables often consider the phonological building blocks of words. All languages have different accent and other varieties of pronunciation, when sound is exemplified by a word in a particular language. If we choose the word for the second stage of verification, then the word should contain at least one vowel and the best chose of the word or words for both the speaker probably from the same language.



**Fig. 1** Speech segmentation

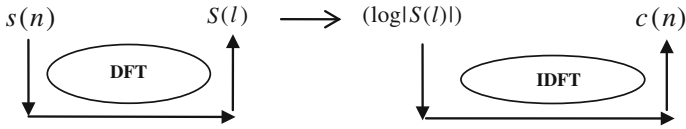


Fig. 2 Cepstral coefficient processing

Neither the movements of the speech organ nor the acoustic signal offers a clear division of speech into successive phonetic units. The segmentation is influenced by knowledge of linguistically significant changes in sound.

Articulation is the mechanical or bio-mechanical process of vocal organ making the speech sound. Articulation is composed of excitation and vocal tract components. To analyze the articulation, these two parts have to be separated. The articulation is the convolution of the respective excitation sequence and vocal tract. Initially, the articulation is in the time domain. Initially,  $s(n)$  is the articulation sequence in time domain, expressed as  $s(n) = e(n) * u(n)$ . Here  $e(n)$  is the excitation sequence and  $u(n)$  is the vocal tract sequence. In the frequency domain, it can be express as  $S(l) = E(l) \cdot U(l)$ .

The cepstral coefficient  $c(n)$  is obtained through the number of process according to Fig. 2.

In the section of ‘target the vocal track’ via (Fig. 1) some types of biometric components used to match the individual’s features. Biometric is associated with a better degree of security and authentication. The stress in the sound and pitch count, excitation in the cepstrogram is the major biometric components used at the second stage of authentication. Acoustic display of a word in the second stage of verification is presented by the spectrogram. The pitch is one of the major constituent parts in the second stage of verification. Pitch presents how high or low, a voice sound seems. Obviously, the pitch count of the two different speakers of a particular word is considered for verification. The pitch depends (approximately) logarithmically on frequency of the acoustic signal. The cepstral analysis gives the excitation of the speaker in the acoustic signal for the particular speaking word by both the speakers. In the second stage of verification, we consider similar and very common words speaking by both speakers. Now by the spectrogram, pitch count and the cepstral analysis verify the claimed speaker voice with the nearest match vocal track present in the voice recognition system. In first stage of the speaker recognition system, the incoming speaker voices submitted to the system, and the second speaker voice is the known speaker voice, of which voice model is presented in the recognition system. Every speaker’s has a number of voice samples of that speaker forming a cluster of that known speaker. The total number of voice models present in the model list of the voice recognition system, which is sum of the number of clusters in the size of individual clusters. The first stage of comparison to the voice recognition system is purely automatic but the second stage of verification purely manually. The decision is based on both stages, first stage identifies the speaker, and second stage verifies the claim. In the first stage,



the identification is done by the statistical hypothesis testing with the existing speaker model in the system. The testing is done by one to many testing where in the second stage of testing, it is one to one testing. The first stage of testing basically drills with the one to many matching, and the numerical score give the best probable prediction about the speaker with the list of the model present in the voice recognition system. The procedure for the first stage of checking is based on the Gaussian mixture model. The Gaussian mixture model is creating through the number of steps. The acoustic feature is extracted from the Mel Frequency Cepstral Coefficient (MFCC). Mel frequency Cepstral coefficients (MFCC) are collective build up the individual Mel frequency Cepstral (MFC). MFC is a physical representation of the short term power spectrum of an acoustic signal in a particular frequency band on a linear cosine transform of the log power spectrum [8]. The extracted acoustic feature from the voice signal after normalize produce various acoustic classes. These acoustic classes belong to an individual speaker voice or a set of speakers. The GMM is the soft representation of the various acoustic classes of an individual person voice or a set of speakers. The probability of a feature vector of being in the acoustic classes is represented by the mixture of different Gaussian probability distribution functions.

## 2 Model Development

Let us consider  $X$  is a random vector i.e.  $X = \{x_1, x_2, x_3, \dots, x_L\}$  be a set of  $L$  vectors, each  $x_i$  is a  $k$ -dimensional feature vectors belong to the one particular acoustic class.  $L$  is the number of acoustic classes and the vector  $x_i$  are statistically independent. So the probability of the set  $X$  for the  $\lambda$  speaker model can be expressed as,  $\log P(X|\lambda) = \sum_{i=1}^L \log P(x_i|\lambda)$ . The distribution of vector  $x_i$  with the  $k$ -dimensional components are unknown. It is approximately modeled by a mixture of Gaussian densities, which is a weighted sum of  $l \leq k$  component's densities, which can be expressed as  $P(x_s|\lambda) = \sum_{i=1}^l w_i N(x_s, \mu_i, \Sigma_i)$ ,  $w_i$  is the mixture weight, where,  $1 \leq i \leq l$  and  $\sum_{i=1}^l w_i = 1$ . Each  $N(x_s, \mu_i, \Sigma_i)$  is a  $k$  variate Gaussian component density presents as

$$N\left(x_s, \mu_i, \Sigma_i\right) = \frac{e^{-\{0.5(x_s - \mu_i)' \Sigma_i^{-1} (x_s - \mu_i)\}}}{(2\pi)^{k/2} |\sqrt{\Sigma_i}|},$$

$\mu_i$  is the mean vector and  $\Sigma_i$  is the covariance matrix.  $(x_s - \mu_i)'$  is the transpose of  $(x_s - \mu_i)$ .

In the speaker identification from the set of speakers  $\{S_i\}$  where  $i$  is countable finite and  $X$  is given utterances, if we claim that the utterance produce by the speaker  $S_k$  from the set of speakers  $\{S_i\}$ . So the basic goal is how it is a valid claim that the speaker  $S_k$  makes the utterance  $X$ . The utterance  $X$  is a random variate that

follows the Gaussian mixture probability distribution. The claim follows the expression  $P(S_k/X)$  present the probability of the utterances  $X$  produce by the speaker  $S_k$ . So  $P(\bar{S}_k/X)$  is the probability that the utterances,  $X$  is not produced by the speaker  $S_k$ . Let,  $\bar{S}_k = \bigcup_i S_i - S_k$  is the collection of large heterogeneous speakers from different linguistics, including both genders and from different zones of the globe.  $\bar{S}_k$  can be better approximated as universal model or world model. It is presented as  $\bar{S}_k \approx \omega$  (say). Now the claim be true according to the rule,

$$\text{if } P(S_k/X) > P(\bar{S}_k/X) \text{ then the utterance produce by } S_k \tag{1}$$

else, the claim is false. So, the utterance produce by other speaker, except  $S_k$ . Since, it is a probabilistic prediction about the claim. However, the process can't predicate the certain events, with values 0 or 1. According to the general definition of probability, produce highest level of prediction about the claimed speaker with the numeric values. It is very often that this predicated score very much depends upon the acoustic classes that obtained from the long step procedure. So the extracted feature largely depends on the digitalization of analogue acoustic signal. There are high chances that the claimed speaker voices, probability comparison values may not be the best or highest value lie in the interval (0, 1).

By the Bayes theorem the expression (1) produce

$$\frac{P(X/S_k)P(S_k)}{P(X)} > \frac{P(X/\omega)P(\omega)}{P(X)},$$

since we assume that  $X$  is not silence clearly,  $P(X) \neq 0$ .

We get,

$$\frac{P(X/S_k)}{P(X/\omega)} > \frac{P(\omega)}{P(S_k)} = \lambda_k \approx \lambda \tag{2}$$

$\lambda$  is a pre assume threshold. To compact the all possible predication we consider the log on the both sides [9].

$$\log \frac{P(X/S_k)}{P(X/\omega)} > \log \lambda_k = \lambda'_k \tag{3}$$

The predicated values indicated how closer the claimed speaker to the existing speaker's voice after comparison. The predicated values are Gaussian in nature so further compactness be done on the predicated values by the statics [10, 11].

$$\frac{\frac{P(X/S_k)}{P(X/\omega)} - \mu}{\sigma} > \lambda \tag{4}$$

### 3 Simulation Results and Discussion

The comparison testing being done in two stages, at the first stage, we consider two speakers voice one of the voice from Indian film actor and personalities Amitabh Bachchan and other voice of the comedian Raju Srivastav. Initial stage, voice models of both the speakers present in the voice recognition system along with the other voice models. In the voice model list, there are 50 voice models present with their model identifier number. The model identifier number of pure Amitabh Bachchan Voice is 1, Model identifier number for Comedian Raju Srivastav pure voice is 2. Model identifier number 3, 4, 5, 6, ..., 50 are the different Bollywood male film star voice models. We have taken two new input voices one of Mr. Amitabh Bachchan and other voice of Comedian Raju Srivastav. Figure 3 shown the predicated test score presented by solid line and dash line for speaker Amitabh Bachchan and Comedian Raju Srivastav. The predicated score for Amitabh Bachchan voice matches with Amitabh Bachchan voice with score value 1.6 and with Raju Srivastav Model with predicated score value 1.65. The given voice of Amitabh Bachchan match with the model identifier 3 and 4 with a score values 0.8 and 0.6. If we consider the accept level of prediction value 1.5, then Mr. Bachchan voice match with both the speakers Mr. Bachchan Model and Raju Srivastav model. The line dash line indicated the Comedian Raju Srivastav new voice. The predicated score of the new voice of Raju Srivastav matched with Mr. Bachchan voice model with score value 1.5 and with Raju Srivastav voice model with predicated score value 2.3. The predicated match score with another model identifier 3 is 0.4. If we consider the accepted range of the prediction is  $[1.5, +\infty)$ , then Amitabh Bachchan voice matches with Amitabh Bachchan voice as well as Raju Srivastav voice.

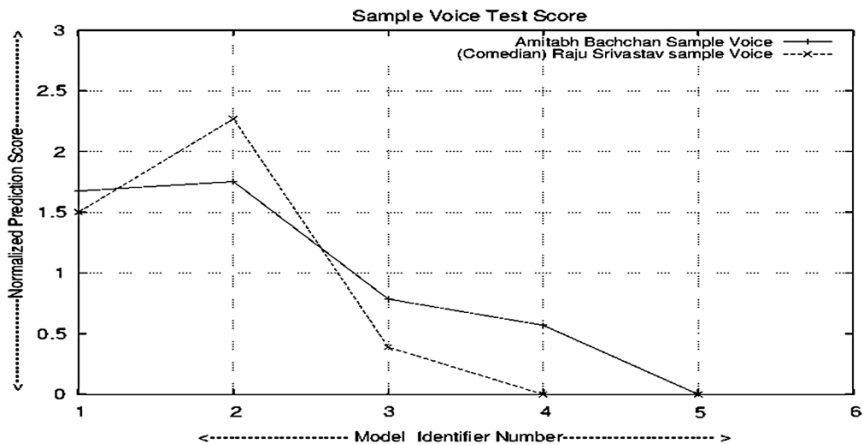


Fig. 3 Simple voice score

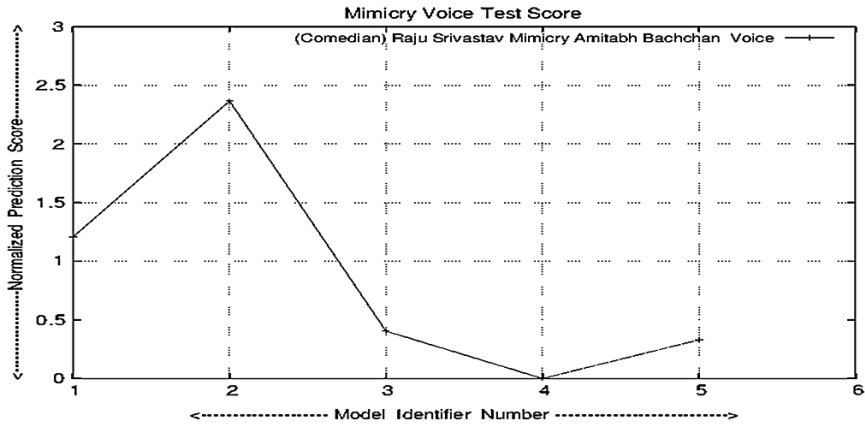


Fig. 4 Mimicry voice score

Figure 4 shows that Raju Srivastav new voice only matches with Raju Srivastav existing model. Other matches with the existing model identifier 3 and model identifier 5 are 0.45 and 0.4 respectively. If we consider the level of acceptance is 1.5 clearly, the Raju Srivastav Mimicry voice matches only with Raju Srivastav existing voice model.

The problem arises, if the level of acceptance is considered as 1.0, then mimicry voice matches with Amitabh Bachchan as well as Raju Srivastav. The above comparative predicated score indicated that mimicry voice is an original voice of Raju Srivastav, not the voice of Amitabh Bachchan. But there is little chance that the voice may be Amitabh Bachchan voice according to the level of acceptance. The Second level of verification results is shown in Figs. 5, 6, 7, and 8. In Figs. 5 and 6 present the wave form, spectrogram and the pitch counts of the two incoming voice in the very compact form. The first row presents the Pitch count, second row presents the spectrogram and the third row presents the acoustic signal of the speaker. We select the word spoken by both the speaker which contains at least one vowel and in the same language. Here we manually selected segment portion of the spoken-word ‘Sign’ of both the speaker. Figures 5 and 6 present the comparison of both the speaker’s pronunciation of the word ‘Sign’. Figure 5 present pronounce of the word ‘Sign’ by Amitabh Bachchan and the Fig. 6 presents pronounce of the word ‘Sign’ by comedian Raju Srivastav. The number of pitch counts for the speaker change, 19 for Amitabh Bachchan spoken word and 15 for Raju Srivastav spoken word. The spectrogram of Amitabh Bachchan spoken word largely changes with the Raju Srivastav spoken word. At the frequency band 3,000–3,500, the harmonics are clearly changes.

Figures 7 and 8 present the Cepstral of the 3,000 ms short term speech segment of the spoken-word ‘sign’. X axis is the time axis, and the Y axis is the cepstral axis. Since cepstral is derived from the log magnitude of the liner spectrum, so it is also symmetrical in the cepstral domain.

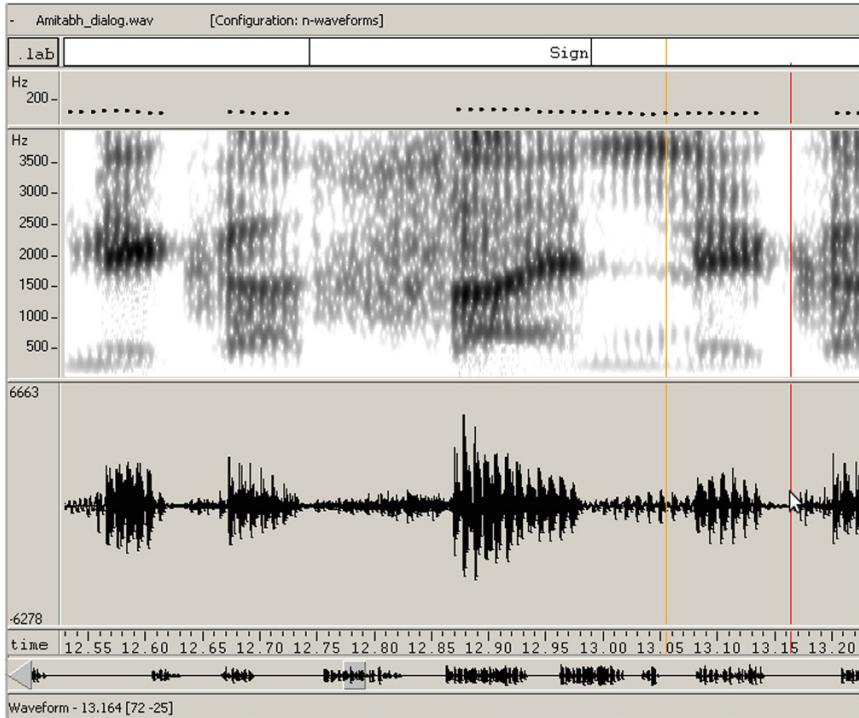


Fig. 5 Spectrogram of word

Figures 7 and 8 present one symmetric part of cepstrum. In the cepstral domain, the vocal tract components are represented by the slowly varying components concentrated near the lower cepstral value area i.e. along the Y-axis. Where the excitation of the speaker's voice is fast varying concentrated near the higher cepstral value area along the Y-axis.

The comparative study of the Figs. 7 and 8 has shown clear difference between them. Figure 7 is the cepstral presentation of the word 'sign' spoken by Amitabh Bachchan and Fig. 8 present cepstral for the word 'sign' spoken by Comedian Raju Srivastav. During the time interval [0, 1,000] the cepstral asset value for Amitabh Bachchan voice is much higher than the Comedian Raju Srivastav voice. Furthermore, we have notice that excitation presents in the interval [1,200, 1,400], [1,550, 1,800], [2,200, 2,500], [2,600, 2,900] for the Amitabh Bachchan voice. In Comedian Raju Srivastav spoken word 'Sign' this many amounts of excitation are not present during the interval [1,200, 3,000]. Further, we have notice that during the interval [750, 3,000] vocal tract present in Comedian Raju Srivastav spoken word 'sign' is much higher than the spoken-word 'sign' by Amitabh Bachchan. Based on the above comparison in the second stage of verification, firmly we can come to the

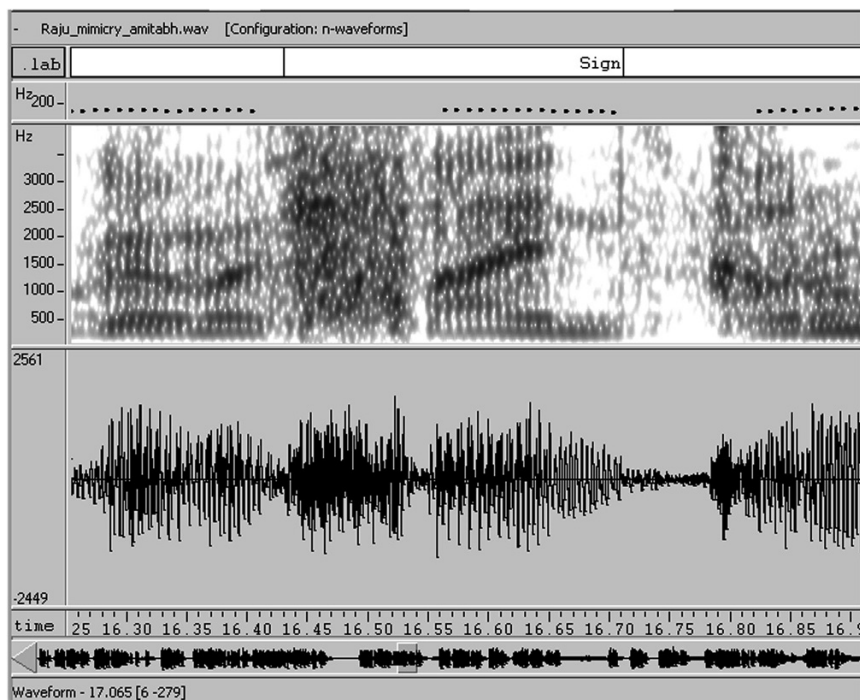


Fig. 6 Spectrogram of word

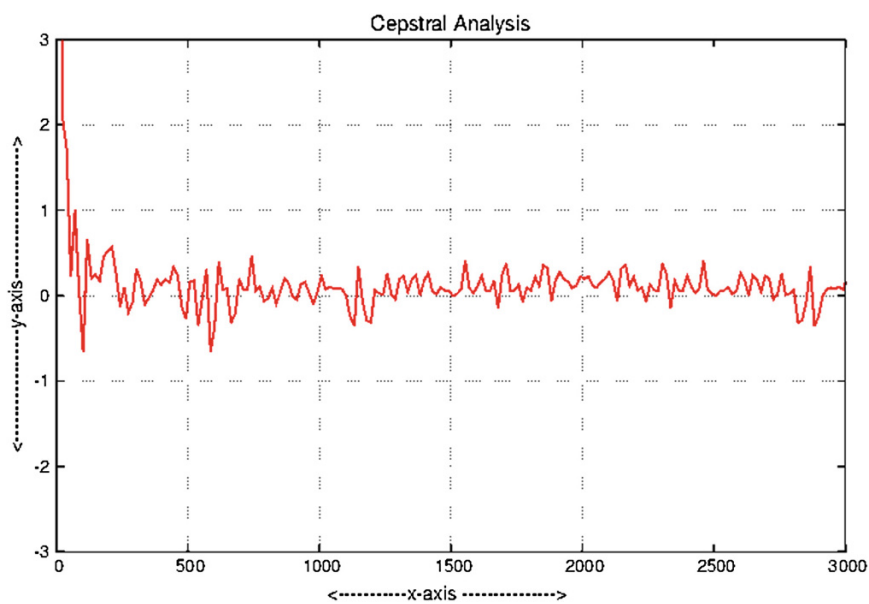


Fig. 7 Cepstrogram of word

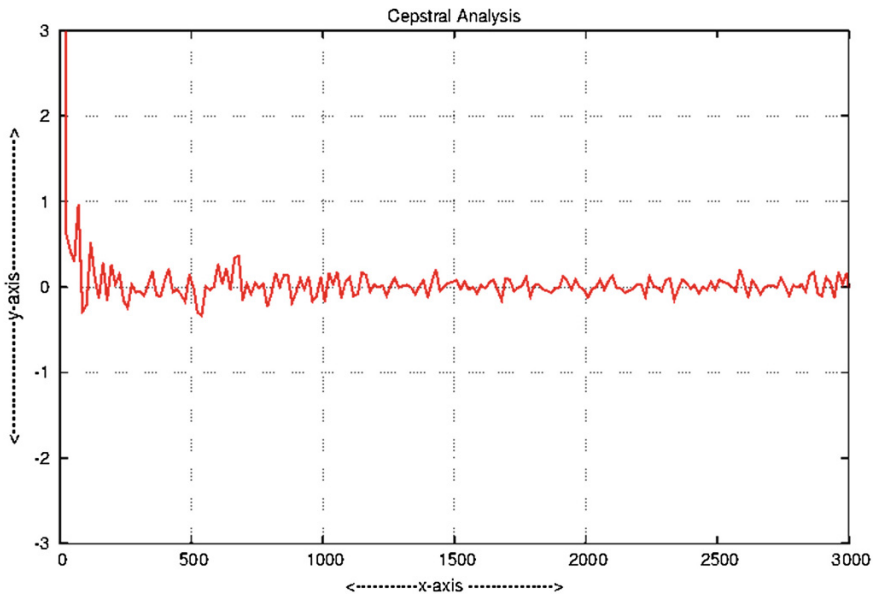


Fig. 8 Cepstrogram of word

conclusion. The articulation comes from different speakers, although the mimicry voice of comedian Raju Srivastav has spoken the same context with same speaking style of Amitabh Bachchan.

## 4 Conclusion

This work presents the work flow of two stages verification for the mimicry voice testing. At the first stage, GMM based speaker identification, which is a one to many identification processes. The second stage is the phonetically based speaker verification for very closer identified speaker. This work to be tested for a large number of collected mimicry voice samples in further extension of this work.

## References

1. Lee L.W., et al.: Vulnerability of speaker verification to voice mimicking. In: Proceeding of International Symposium on Intelligent Multimedia, Video and Speech Processing. Hong Kong, Oct 2004, pp. 145–148
2. Reynolds, D., Quatieri, T., Dunn, R.: Speaker verification using adapted Gaussian mixture models. *Digit. Sig. Process.* **10**, 19–41 (2000)

3. Xiang, B., et al.: Short-time gaussianization for robust speaker verification. In: Proceedings of ICASSP, 2002, vol. 1, pp. 681–684 (2002)
4. Reynolds, D.: Automatic speaker recognition using Gaussian mixture speaker models. *Linciln Lab. J.* **8**(2), 173–191 (1995)
5. Reynolds, D.: Speaker identification and verification using Gaussian mixture speaker models. *Speech Comm.* **17**, 91–108 (1995)
6. Reynolds, D.: Channel robust speaker verification via feature mapping. In: Proceedings of International Conference on Acoustics Speech Signal Process, pp. 53–56. (2003)
7. Apsingeker, V.R., DeLeon, P.: Speaker model clustering for efficient speaker identification in large population applications. *IEEE Trans. Audio Speech Lang. Process.* **17**(4), 848–853 (2009)
8. Bimbot, F., et al.: A tutorial on text-independent speaker verification. *EURASIP J. Appl. Sig. Process.* **4**, 430–451 (2004)
9. Morrison, G.S.: Measuring the validity and reliability of forensic likelihood—ratio system. *Sci. Justice* **5**, 91–98 (2011). doi:[10.1016/j.scijus.2011.03.002](https://doi.org/10.1016/j.scijus.2011.03.002)
10. Auckenthaler, R., Carey, M., Lloyd-Thomas, H.: Score normalizing for text-independent speaker verification system. *Digit. Sig. process.* **10**, 42–52 (2000)
11. Mirghafori, N., Heck, L.: An adaptive speaker verification system with speaker dependent a priori decision thresholds. In: Proceedings of ICSLP, Denver Colorado, Sept 2002



# SPICE Modeling and Analysis for Metal Island Ternary QCA Logic Device

Pritam Bhattacharjee, Kunal Das, Mallika De and Debashis De

**Abstract** The exploration of work ability of the new trend in quantum dot cellular automata (QCA)—the ternary QCA, is the major focus in this paper. Both physically and electrically, our tQCA approach is proving its excellence in comparison to the existing binary QCA (bQCA). We also propose a model description for tQCA that will help in determining its logic performances while operating it in the nano computing regime.

**Keywords** Metal island tQCA · bQCA · tQCA · Capacitive coupling · SPICE modeling

## 1 Introduction

The electronic charge state is being used in very intelligent way to represent the information. In digital electronics, the information representation with binary logic is an innovative idea by means of current switch. The binary ‘1’ and binary ‘0’ are

---

P. Bhattacharjee (✉)  
Bidyandhi Institute of Technology and Management, Durgapur  
West Bengal, India  
e-mail: pritam\_bhattacharjee@live.com

K. Das  
B. P. Poddar Institute of Management and Technology, 137, VIP Road,  
Kolkata 700052, West Bengal, India

M. De  
Department of Computer Science and Engineering, West Bengal University  
of Technology, BF-142, Sector-I, Salt Lake City, Kolkata 700064  
West Bengal, India

D. De  
Sudhir Chandra Sur Degree Engineering College, 540 Dum Dum Road,  
Surermath, Kolkata 700 074, West Bengal, India

represented by means of ‘on’ and ‘off’ respectively in Complementary Metal oxide Semiconductor (CMOS) technology. However, the device size reduction put it into the challenge. It has been noticed that in most promising CMOS technology, charge quantization, power dissipation etc. become problematic in nano scale device design. Now it is an established fact that Quantum dot Cellular Automata (QCA) can be an alternative of promising and empirical CMOS technology [1–8]. Researchers are mostly concentrating on binary logic representation in QCA while it may not be suitable to think all aspects by means of binary logic. Multi-valued logic especially ternary logic has potential advantages like greater data storage capability, faster arithmetic operations, better support for numerical analysis, non-deterministic and heuristic procedures, communication protocol and effective solution for non-binary problems [9–12].

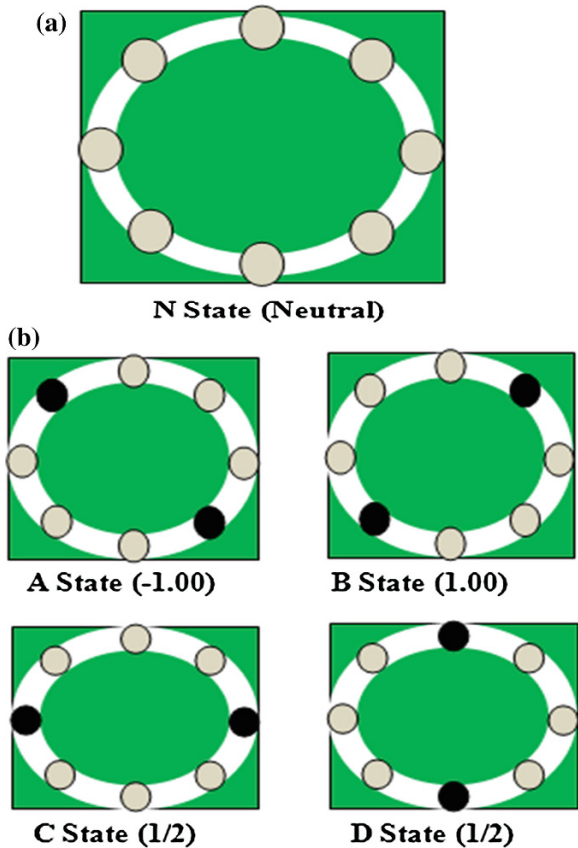
In binary QCA (bQCA), it is considered that a cell consist of four-quantum dot (QD) as charge container at four corner of square shaped cell and two extra electrons confined within the cell. Electrons can tunnel from one QD to another QD through tunnel junction. Now QCA platform is being utilized for ternary logic implementation [9–12]. It is really in infancy stage, several research works need to establish ternary logic implementation. Lebar Bajec et al. introduced ternary QCA (tQCA), reported in [9]. The tQCA can also be classified into semiconductor-based tQCA, Metal Island tQCA like bQCA. The tQCA cell is realized by means of eight QDs confined within a square shaped cell and two extra electrons confined within the cell. Eight QDs are arranged in a ring shape within square cell. The tQCA can have five state polarization ‘ $-1.00$ ’, ‘ $+1.00$ ’, ‘ $1/2$ ’ and No polarization represented by ‘A’, ‘B’, ‘C’, ‘D’ and ‘N’ and are shown in Fig. 1. Details of tQCA have been discussed in Sect. 2. To establish the tQCA as a logic design paradigm, the attention should be given on device performance.

In this paper, the physical properties of tQCA cell are discussed. Focus has been given on time independent steady state behavior of tQCA cell with the help of extended Hubbard model and the empirical studies on metal island tQCA cell with SPICE model is explored. Rest of the paper is organized in the following subsequence; Sect. 2 is dedicated to explore the basic ternary logic and tQCA. The time independent steady state behavior of tQCA cell is explored in Sect. 3. The SPICE model for the realization of metal island tQCA cell is described in Sect. 4. Finally, the conclusion of this work is presented in Sect. 5.

## 2 Ternary Logic and TQCA

The tQCA cell differs from bQCA cell in number of QD present in the cell and polarization state. There are eight numbers of QD arranged in a ring/circular shape within the square shaped cell, shown in Fig. 1. The diameter of ring must be equal to length of a square shape cell. As a result  $R = L/2$ , where ‘R’ is radius of ring/circle and ‘L’ is Length of square shape cell. Therefore, maximum distance of separation between two QD is L. The two extra electrons similar to bQCA are

**Fig. 1** **a** Eight quantum dot arranged in ring within square shape tQCA cell, shows no polarization state and **b** tQCA cell with 'A' state (-1.00), 'B' state (+1.00), 'C' state or 'D' state (1/2)



confined within the cell. The internal circuitry of tQCA cell is made of tunnel junction and junction capacitance. Due to coulomb interaction, the tQCA cell is being polarized. Five possible state of polarity marked as 'A', 'B', 'C' or 'D' and 'N', are shown in Fig. 1.

### 3 Steady State Behavior of TQCA

The previous section has explored the different physical properties and cell architecture in quantum mechanics. Now in this section, an attempt is made to analyze the steady state behavior of tQCA with the help of extended Hubbard model. The Hamiltonian of eight-dot tQCA cell can be expressed as:

$$\begin{aligned}
H^{tQCA} = & \sum_{i,\sigma} (V_0 + V_i) \hat{n}_{i,\sigma} + \sum_{i>j,\sigma} t_{ij} \left( \hat{a}_{i,\sigma}^\dagger \hat{a}_{j,\sigma} + \hat{a}_{i,\sigma}^\dagger \hat{a}_{j,\sigma} \right) \\
& + \sum_i E_Q \hat{n}_{i,\uparrow} \hat{n}_{i,\downarrow} + \sum_{i>j,\sigma,\sigma'} V_Q \frac{\hat{n}_{i,\sigma} \hat{n}_{j,\sigma'}}{|R_i - R_j|}
\end{aligned} \tag{1}$$

Each quantum dot is considered as a site, so tQCA is simply an eight-site system as shown in Fig. 1. For tQCA system, it is considered that the number of extra electrons in the cell is fixed. The overall energy is constant and  $V_0$  is set to zero. The first term  $V_i$  is potential energy of all electrons at site ‘i’ and  $\hat{n}_{i,\sigma} = \hat{a}_{i,\sigma}^\dagger \hat{a}_{i,\sigma}$  is the number operator for the electron spin ‘ $\sigma$ ’.  $\sigma$  is considered to have two states, up-spin ‘ $\uparrow$ ’ and ‘down-spin ‘ $\downarrow$ ’. The charging cost  $E_Q$  defined as

$$E_Q = \frac{V_Q}{(2R/3)} = \frac{3V_Q}{2R},$$

where ‘ $R$ ’ is the radius of quantum dot and  $V_Q$  is the coulomb energy of two electrons separated by two third of the quantum dot’s radius.

For the steady state problem, Hamiltonian equation is solved with time independent Schrödinger equation

$$H^{tQCA} |\psi_i\rangle = E_i |\psi_i\rangle \tag{2}$$

where  $|\psi_i\rangle$  is Eigen state of Hamiltonian and  $E_i$  is the corresponding Eigen value for  $i = 0$ , we have ground state of cell

$$|\psi_0\rangle = \sum_j \psi_j^0 |\phi_j\rangle$$

$|\phi_j\rangle$  is jth basis vector and  $\psi_j^0$  is the coefficient of that basis vector. For eight-site tQCA system, we have  $2^8$  different basis vectors and these are

$$\begin{aligned}
|\phi_1\rangle &= \left| \begin{array}{c} 00000001 \\ 00000001 \end{array} \right\rangle \\
|\phi_2\rangle &= \left| \begin{array}{c} 01000000 \\ 01000000 \end{array} \right\rangle \\
&\dots \\
&\dots \\
|\phi_{256}\rangle &= \left| \begin{array}{c} 10000000 \\ 10000000 \end{array} \right\rangle
\end{aligned}$$

It means that site  $i$  and  $j$  are with up-spin electron state, others are with down-spin electron state. However, the polarization of tQCA cell can be expressed in

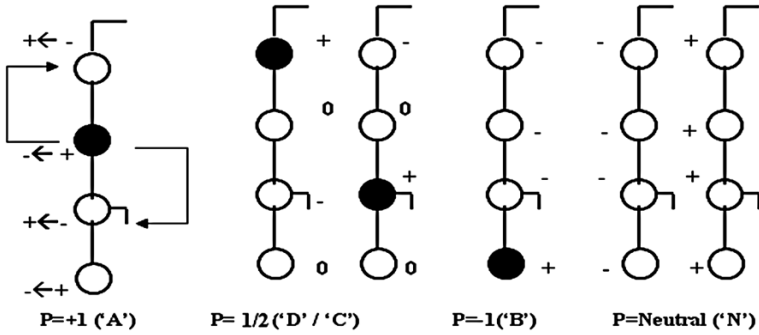


Fig. 2 Logic states in half metal island tQCA cell

terms of  $\sigma_i$ , the expectation value of number operator. The expectation value  $\sigma_i$  is proportional to radius of quantum dot of site 'i'. The polarization P can be expressed as

$$P \equiv \frac{(\sigma_1 + \sigma_5) - (\sigma_2 + \sigma_6) - (\sigma_3 + \sigma_7) - (\sigma_4 + \sigma_8)}{\sum_i \sigma_i} \quad (3)$$

tQCA cell can have four polarization state namely 'A', 'B', 'C' or 'D' and 'N' as shown in Fig. 2. We explore 'A' state ( $p = -1.00$ ) as logic '0', 'B' state ( $p = +1.00$ ) as logic '+1', 'C' and 'D' ( $p = 1/2$ ) represent as logic '1/2' and finally 'N' state is denoted as Neutral state. The tQCA can be compared with existing bQCA counterpart and it has tri-stable or tri-state cell response. Due to its tri-state functionality, it is possible to store a single ternary bit in quantum state.

## 4 Metal Island tQCA Realization

The tQCA can also be manufactured with metal and small capacitance. The principle difference between metal island tQCA and semiconductor-based tQCA, is that in former one device is made with metal capacitive coupled rather than coulomb coupled quantum dot. In case of metal island tQCA, there are several electrons in conduction band, unlike the semiconductor quantum dot QCA device. The metal capacitive coupling cannot be represented with the help of Schrödinger equation. The capacitive model is to be adopted to realize the metal island tQCA. If two metal islands are connected with capacitor, the free charge can be removed and store into the capacitor. However, through the tunneling junction few electrons can tunnel in or out to metal island. The metal island tQCA half-cell architecture can be realized with SPICE model. The parameter considerations are similar with Dolan shadow-evaporation techniques. The schematic diagram of tQCA is shown in Fig. 3. Metal Island is connected with tunnel junction and capacitor, due to capacitive effect the

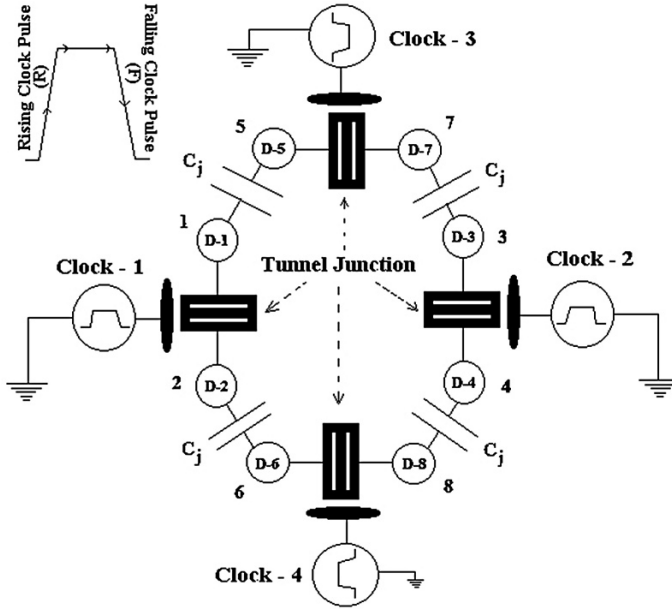


Fig. 3 Schematic of eight-dot tQCA

metal island become charge free. There are eight input bias voltage sources and four controls or clock input sources.

The charge configuration of system is composed of control electrode or clock and Metal Island, coupled by tunnel junctions and capacitance. The electrostatic energy of charge configuration system can be expressed in terms of voltage and charge as

$$E = \frac{1}{2} \begin{bmatrix} q \\ q' \end{bmatrix}^T C^{-1} \begin{bmatrix} q \\ q' \end{bmatrix} - v^T q' \quad (4)$$

where  $C$  is capacitance matrix,  $v$  is column vector of voltage source,  $q$ ,  $q'$  are column vector of island charge and lead charge.

#### 4.1 SPICE Model Description of tQCA

As stated in previous sections, the SPICE model, shown in Fig. 3 has four control knobs or clocks to operate the polarization within its cell. It has eight dot sites (i.e., D-1, D-2, D-3, D-4, D-5, D-6, D-7, D-8) where the free electrons can reside depending on the clock input.  $C_j$  is the junction capacitance between the dots. The tunnel junction provides the potential barrier to the electron transport and is an

**Table 1** Logic configuration of tQCA

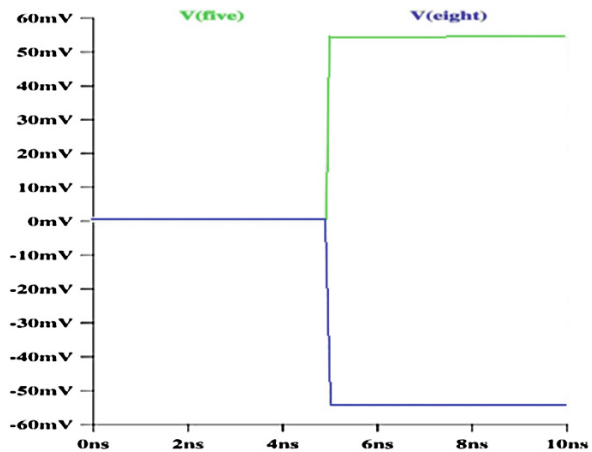
S. No.	Clock-1	Clock-2	Clock-3	Clock-4	Logic state
1.	(F)	(F)	(R)	(F)	“A”
2.	(F)	(F)	(F)	(F)	“Neutral”
3.	(F)	(F)	(F)	(R)	“B”
4.	(F)	(F)	(R)	(R)	“Neutral”
5.	(R)	(F)	(F)	(F)	“C or D”
6.	(R)	(R)	(F)	(F)	“Neutral”
7.	(F)	(R)	(F)	(F)	“D or C”

important criterion in tQCA. The position of the electrons on the dots determines the logic state of the cell. In our previous discussion, we have mentioned the possible logic states, shown in Fig. 2. We have altered the clock inputs (clock-1, clock-2, clock-3, clock-4) issuing them with possible rising pulse (R) and falling pulse (F) combination and obtained the logic states as stated in Fig. 2 and Table 1. The clock implemented triggers at 5 ns.

### 4.2 Determination of the Logic States

Logic ‘A’ states the polarization of the tQCA as ‘+1.00’ and is determined by calculating the potential differences  $V(5 \sim \text{five})$  and  $V(8 \sim \text{eight})$  with respect to the clock inputs. It is seen that  $V(5 \sim \text{five}) > V(8 \sim \text{eight})$  stating the probability of the free electrons to be living at dot D-5 (see Fig. 4). When  $V(5 \sim \text{five}) < V(8 \sim \text{eight})$ , the electrons are likely to be residing at dot D-8, stating the possibility of logic ‘B’ which gives the polarization ‘-1.00’. We report of seeing two unknown logic states

**Fig. 4** SPICE simulation curve stating logic ‘A’



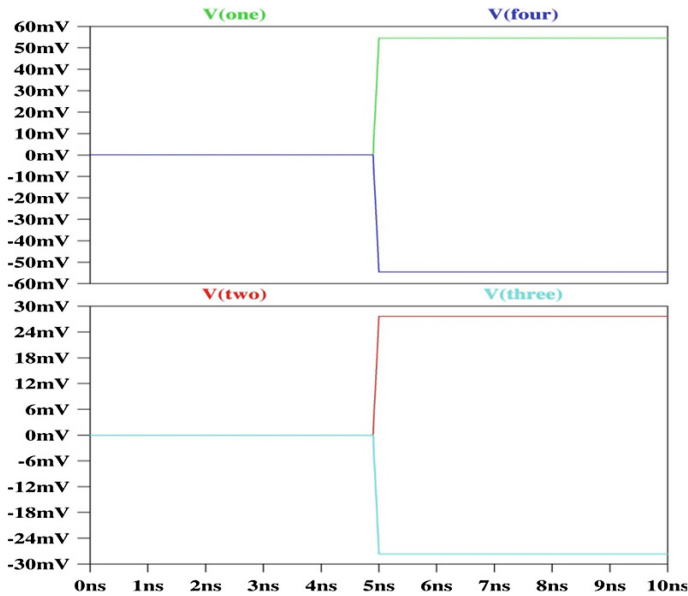


Fig. 5 Voltage curve stating logic ‘C’ or ‘D’

namely ‘C’ and ‘D’ on alternation of the clocks 1 and 2 as talked in Table 1. When clock-1 is high and clock-2 is low, simulation shows that  $V(1 \sim \text{one})$  and  $V(2 \sim \text{two})$  is greater than  $V(3 \sim \text{three})$  and  $V(4 \sim \text{four})$ , depicting free electron can live either in D-1 or D-2 shown in Fig. 5 and again on changing the clock orientation, we see  $V(1 \sim \text{one})$  and  $V(2 \sim \text{two})$  less than  $V(3 \sim \text{three})$  and  $V(4 \sim \text{four})$ , depicting free electron can live either in D-3 or D-4. The neutral state is determined on noticing same voltage level at every diagonal dot site (i.e., D-1, D-4, D-5, and D-8).

## 5 Conclusions

The proposed tQCA has proved its presence in this work. Our work has enabled the path to estimate the performance of tQCA at an extensive level. The approach of SPICE analysis shows that tQCA operates in the milli-volts range ( $\sim 0\text{--}60$  mV), proving its possibility to be used for low power applications in near future. There is no power leakage in tQCA, as in tQCA electronic charge is confined in closed dimension and is also advantageous for static power dissipation since physical movement of electron is not seen here. The excellent steady state behavior of tQCA talks in favor of its ability to operate at room temperature. It will be feasible for fabrication and surely be cost effective in production.



## References

1. Lent, C.S., Taugaw, P.D., Porod, W., Bernstein, G.H.: Quantum cellular automata. *Nanotechnology* **4**, 49–57 (1993)
2. Amlani, I., Orlov, A., Snider, G., Lent, C., Porod, W., Bernstein, G.: Experimental demonstration of electron switching in a quantum-dot cellular automata (QCA) cell. *Superlattices Microstruct.* **25**(1–2), 273–278 (1999)
3. Tougaw, P.D., Lent, C.S.: Dynamic behavior of quantum cellular automata. *J. Appl. Phys.* **80**, 4722–4736 (1996)
4. Lent, C., Tougaw, P.: A device architecture for computing with quantum dots. *Proc. IEEE* **85** (4), 541–557 (1997)
5. Toth, G., Lent, C.: Quasiadiabatic switching for metal-island quantum-dot cellular automata. *J. Appl. Phys.* **85**, 2977–2984 (1999)
6. Das, K., De, D.: Characterization, applicability and defect analysis for tiles nanostructure of quantum dot cellular automata. *J. Mol. Simul. Taylor Francis* **37**(3), 210–225 (2011)
7. Das, K., De, D.: A Study on diverse nanostructure for implementing logic gate design for QCA. *Int. J. Nanosci.* **10**(1–2), 263–269 (2011)
8. Das, K., De, D.: Characterization, test and logic synthesis of novel conservative and reversible logic gates for QCA. *Int. J. Nanosci.* **9**(2), 1–14 (2010)
9. Bajec, I.L., Zimic, N., Mraz, M.: The ternary quantum-dot cell and ternary logic. *IOP Nanotechnology* **17**(8), 1937–1942 (2006)
10. Pecar, P., Mraz, M., Zimic, N., Janez, M., Bajec, I.L.: Solving the ternary QCA logic gate problem by means of adiabatic switching. *Jpn. Appl. Phys.* **47**(6), 5000–5006 (2008)
11. Pecar, P., Ramsak, A., Zimic, N., Mraz, M., Bajec, I.L.: Adiabatic pipelining: a key to ternary computing with quantum dots. *IOP Nanotechnol.* **19**(49), 495401 (2008)
12. Das, K., De, D., De, M.: Realization of semiconductor ternary quantum dot cellular automata. *IET Micro Nano Lett.* **8**(5), 258–263 (2013)

# Text Independent Speaker and Emotion Independent Speech Recognition in Emotional Environment

A. Revathi and Y. Venkataramani

**Abstract** It is well known fact that the accuracy of the speaker identification or speech recognition using the speeches recorded in neutral environment is normally good. It has become a challenging work to improve the accuracy of the recognition system using the speeches recorded in emotional environment. This paper mainly discusses the effectiveness on the use of iterative clustering technique and Gaussian mixture modeling technique (GMM) for recognizing speech and speaker from the emotional speeches using Mel frequency perceptual linear predictive cepstral coefficients (MFPLPC) and MFPLPC concatenated with probability as a feature. For the emotion independent speech recognition, models are created for speeches of archetypal emotions such as boredom, disgust, fear, happy, neutral and sad and testing is done on the speeches of emotion anger. For the text independent speaker recognition, individual models are created for all speakers using speeches of nine utterances and testing is done using the speeches of a tenth utterance. 80 % of the data is used for training and 20 % of the data is used for testing. This system provides the average accuracy of 95 % for text independent speaker recognition and emotion independent speech recognition for the system tested on models developed using MFPLPC and MFPLPC concatenated with probability. Accuracy is increased by 1 %, if the group classification is done prior to speaker classification with reference to the set of male or female speakers forming a group. Text independent speaker recognition is also evaluated by doing group classification using clustering technique and speaker in a group is identified by applying the test vectors on the GMM models corresponding to the small set of speakers in a group and the accuracy obtained is 97 %.

**Keywords** Clustering · GMM · Speech recognition · Probability · MFPLPC · Emotions · Quantization

---

A. Revathi (✉) · Y. Venkataramani  
Saranathan College of Engineering, Tiruchirappalli, India  
e-mail: revathidhanabal@rediffmail.com

© Springer India 2015  
J.K. Mandal et al. (eds.), *Information Systems Design and Intelligent Applications*,  
Advances in Intelligent Systems and Computing 339,  
DOI 10.1007/978-81-322-2250-7\_5

## 1 Introduction

In addition to the linguistic information, the speech signal contains the information regarding age, gender, social status, accent and emotional state of a speaker. It has become a challenging task to recognize a speaker, speech and emotion from emotional speeches. Each speaker expresses different emotions in different ways. Speech recognition on emotional speeches has found applications in call centers. People working in call centers may not behave in same manner when attending calls of the customers. When a customer experiences a negative emotion, the system has to adjust itself to the needs of the customer or pass the control to the human agents for giving alternate convenient reply to the customers. It also has found applications in controlling the hazardous processes where physical presence of humans is not possible. These systems can also be applied in health care systems for which treatments could be extended to the patients with depression and anxiety. Nwe et al. [1] have used short-time log frequency power coefficient as a feature and discrete HMM as a classifier in evaluating the performance of the emotion recognition system. Morrison et al. [2] have compared accuracy of emotion recognition system evaluated by using different classification techniques. Modulation spectral feature is used as a new feature by Wu et al. [3] for emotion recognition. Lee et al. [4] have used hierarchical binary classifier and acoustic & statistical feature for emotion recognition. Vogt and Andr [5] have used combination of pitch, energy and MFCC as feature for emotion recognition and they have done gender detection. Rao et al. [6] have used MFCC and GMM for recognizing emotions. Sapra et al. [7] has used modified MFCC feature and NN classifier for emotion recognition. Speaker identification in emotional environment has been done by Sahini [8] and he has used log frequency power coefficients as feature and evaluated the system using HMM, CHMM and SPHMM. Koolakudi et al. [9] have used MFCC and GMM for speaker recognition in emotional environment. This work is mainly focused on the use of features such as MFPLPC and MFPLPC concatenated with probability and iterative clustering modeling technique for recognizing speech and speaker by using the emotional speech database. Emotion independent speech recognition and text independent speaker recognition systems are evaluated by applying features of the test speeches on the clustering models developed using both features. Recognition rate is computed by considering the test speech being correctly identified for any one of the models corresponding to the feature for both text independent speaker recognition and emotion independent speech recognition and it is better as compared to the testing on individual models.

## 2 Feature Based on Cepstrum

The short-time speech spectrum for voiced speech sound has two components: (1) harmonic peaks due to the periodicity of voiced speech (2) glottal pulse shape. The excitation source decides the periodicity of voiced speech. It reflects the

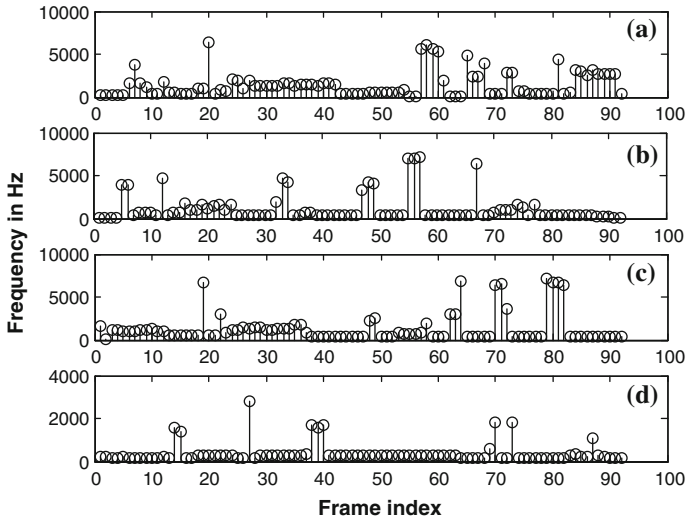
characteristics of speaker. The spectral envelope is shaped by formants which reflect the resonances of vocal tract. The variations among speakers are indicated by formant locations and bandwidth. MFCC is the feature widely used in speech recognition system. It represents the source characteristics of speech signal and based on the known variation of the human ear's critical bandwidth with frequencies, filters spaced linearly at low frequencies and logarithmically at high frequencies preferred to extract phonetically important characteristics of speech. perceptual linear predictive cepstrum (PLP) speech analysis method [10–12] is for modeling the speech auditory spectrum by the spectrum of low order all pole model. This perceptual feature mainly emphasizes the need for critical band analysis which integrates the energy spectral density in the frequency range (0–8) kHz to get the speech auditory spectrum. Loudness equalization is done to emphasize the spectrum in the upper and middle frequencies and cube root compression is performed to reduce the dynamics of the speech spectrum. Then inverse fast Fourier transform is done to get the signal in time domain. Autocorrelation method is used to find linear prediction coefficients. These prediction coefficients are converted into cepstral coefficients by using recursive procedure. Critical band analysis is done using 47 critical bands, when the frequencies are spaced in mel scale. The relationship between frequency in Mel and frequency in Hz is specified as in (1)

$$f(mel) = 2595 * \log(1 + f(Hz)/700) \quad (1)$$

### 3 Characteristics of Emotional Speech—Frequency Domain Analysis

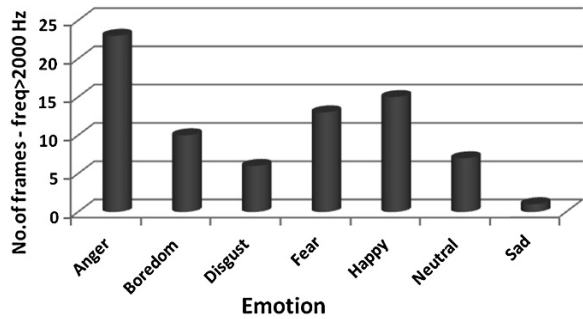
The semantic part of the speech contains linguistic information which reveals the characteristics of the pronunciation of the utterances based on the rules of the language. Paralinguistic information refers to the implicit messages such as emotional state of the speaker. Speeches of the emotions such as anger, fear and happy are displaying the psychological behavior of the speaker such as high blood pressure and high heart rate. These speeches are loud, fast and enunciated with strong high frequency energy. On the other hand, speeches of the emotion sad reveal the characteristics of the speaker such as low blood pressure and low heart rate. These speeches are slow, low volume and possess little high frequency energy. This fact is demonstrated in Fig. 1.

Frequency analysis is done on the emotions of the speaker uttering the same sentence. Speech signals are converted into frames and frequency analysis is done on the frames. Frequencies are calculated on the basis of choosing the frequency bin which has high spectral energy. From the plot shown in Fig. 2, it is indicated that emotions such as anger, fear and happy have more number of frames with high frequency energy and the emotion sadness has very few frames with high frequency energy.



**Fig. 1** Frequency distribution of speech in different emotions—**a** Anger. **b** Fear. **c** Happy. **d** sad

**Fig. 2** Frequency analysis on emotions



Similarly, frequency analysis is done on the speeches uttered by one speaker and the speech uttered by different speakers in the emotion anger.

### 4 Speech/Speaker Recognition Using Clustering Technique and GMM

Emotional speech database considered in this work is a Berlin database which contains about 500 utterances spoken by actors in happy, angry, anxious, fearful, bored and disgusted way as well as in a neutral version. Utterances are chosen from

10 different actors and ten different texts. Ten emotional utterances are collected from five male and female speakers respectively in the age ranging from 21 to 35 years. They are required to utter ten different utterances in Berlin in seven different emotions such as anger, boredom, disgust, fear, happy, neutral and sad. Speech recognition system generally involves the realization of speech signal as the message encoded as the sequence of one or more symbols. This is considered as recognizing the underlying sequence of symbols given a spoken utterance, the continuous speech signal is converted into the sequence of equally spaced discrete parameter vectors. For creating a training model, speech signal is first pre-emphasized using a difference operator. Hamming window is applied on differenced speech frames of 16 ms duration with overlapping of 8 ms. Then the MFPLPC features are extracted. In this work, probability as a feature is extracted by counting the number of samples whose spectral energy is greater than or equal to the average spectral energy of the frame and this feature is concatenated with MFPLPC. For each training model corresponding to continuous speeches, training set of  $K$  utterances are used, where each utterance constitutes an observation sequence of some appropriate spectral or temporal representation. The performance of speech or speaker recognition system based on perceptual features is evaluated by applying test speech vectors to the training models corresponding to the speakers or speeches. MFPLPC feature extraction is dealt in many literatures [10–12]. The usage of Clustering technique [9] for recognizing emotional speeches is depicted in Fig. 3. After the conventional preprocessing, features are extracted. Subsequently, training models are developed using clustering technique. During testing feature vectors are extracted and applied to the training models developed for the speeches. Average of minimum distances is computed for each model. Test speech is identified corresponding to the model which provides minimum of averages. Similarly, feature vectors of test speech are applied to 12 mixture GMM models, and log likelihood values are calculated for each model. Test speech is identified corresponding to the

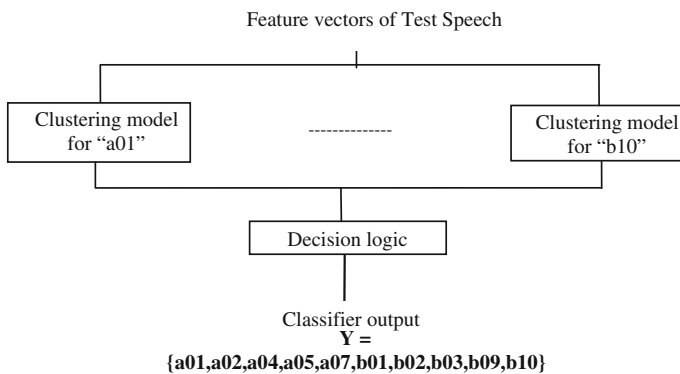


Fig. 3 Speech recognition phase using clustering technique

model which provides the largest log likelihood value. Accuracy can be improved for text independent speaker recognition by creating group models for Female and male speakers and testing is done after group is correctly identified.

### 5 Results and Discussion

The performance of emotion independent speech recognition is evaluated by considering the ten utterances spoken by ten actors. Training models are developed for speeches of emotions such as boredom, disgust, joy, fear, sad and neutral. Testing is done on the speeches of anger emotion. Text independent speaker recognition is done by developing training models for the speeches of nine utterances and testing is done on the speeches of tenth utterance with respect to all emotions. Figure 4 indicates the parallel group classifier for classifying speakers using emotional

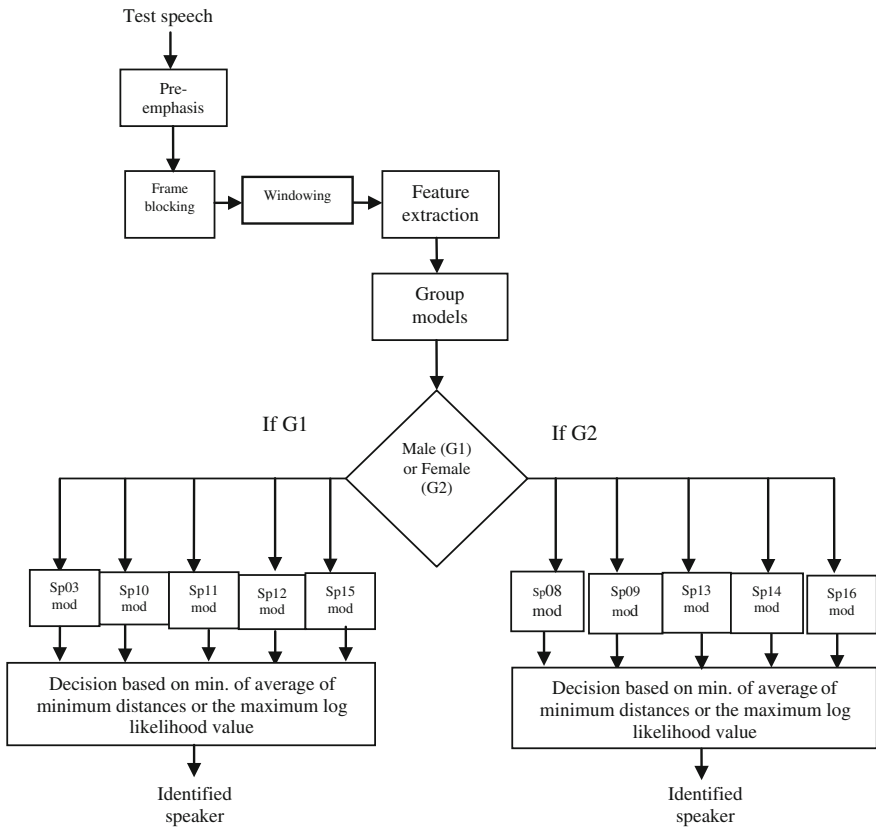


Fig. 4 Parallel group and specific emotional speaker classifier

**Table 1** Accuracy—emotional speech and speaker recognition

Speaker	% RA			Speech		
	MFPLPC	MFPLPC + Prob	MFPLPC, MFPLPC + Prob	MFPLPC	MFPLPC + Prob	MFPLPC, MFPLPC + Prob
Sp03	80.9	82.59	86.52	a01	83.33	85.66
Sp08	91.63	94.42	94.89	a02	96.3	100
Sp09	100	87.88	100	a04	99.2	100
Sp10	98.72	85.9	100	a05	90.17	94.72
Sp11	82.38	82.86	92.86	a07	82.63	88.14
Sp12	100	100	100	b01	93.99	94.27
Sp13	91.86	82.56	95.35	b02	98.27	98.27
Sp14	77.02	79.5	83.85	b03	89.98	94.71
Sp15	99.26	94.03	99.26	b09	91.71	96.19
Sp16	75.69	91.44	94.18	b10	89.11	95.3
% Ave. RA	88.12	88.12	94.7	% Ave. RA	90.986	94.73



**Table 2** Comparison chart—clustering and GMM—group models

Speaker	% RA		Clustering				GMM			
			MFPLPC		MFPLPC + Prob		MFPLPC, MFPLPC + Prob		MFPLPC	
	MFPLPC	MFPLPC + Prob	MFPLPC	MFPLPC + Prob	MFPLPC	MFPLPC + Prob	MFPLPC	MFPLPC + Prob	MFPLPC	MFPLPC + Prob
Sp03	84.27	87.08	91.01	91.01	95.51	95.51	78.65	78.65	98.32	98.32
Sp08	91.63	94.42	94.89	94.89	86.51	86.51	90.7	90.7	93.94	93.94
Sp09	100	89.4	100	90.91	100	100	90.91	90.91	100	100
Sp10	98.72	85.9	100	58.98	100	100	58.98	58.98	100	100
Sp11	84.29	84.76	93.81	93.81	100	100	92.86	92.86	100	100
Sp12	100	100	100	100	94.05	94.05	95.24	95.24	98.81	98.81
Sp13	94.19	83.72	96.51	96.51	95.93	95.93	76.75	76.75	95.93	95.93
Sp14	77.64	82.61	84.47	84.47	78.26	78.26	78.89	78.89	87.58	87.58
Sp15	99.26	94.03	99.26	99.26	100	100	100	100	100	100
Sp16	82.2	92.81	95.81	95.81	86.65	86.65	78.43	78.43	88.02	88.02
% Ave. RA	91.22	89.473	95.576	95.576	93.691	93.691	84.141	84.141	96.56	96.56

database. First, clustering models for the training vectors corresponding to the female speakers and male speakers are developed. Group is correctly identified by first computing average of minimum distances for both the models and group classification is done based on minimum of averages using clustering technique. Subsequently, speaker is identified by applying the test vectors on the clustering models or GMM [10] models developed for the small set of female or male speakers in a group. Speaker is identified by computing the average of minimum distances for the clustering technique and classification is done based on the comparison of all values and identified speaker is the one with minimum of averages. Speaker is identified by first computing the log likelihood values for all the GMM models corresponding to the set of speakers in a group. Then, classification is done with reference to the model whose model log likelihood is the highest. Block diagram of a parallel group classifier and parallel specific emotional speaker classifier is shown in Fig. 4.

Emotion independent speech recognition is performed by creating training models corresponding to the speeches of the speaker of all emotions except anger. Testing is done on the speeches of a speaker concerned with anger emotion. Performance evaluation of emotion independent speech recognition and text independent speaker recognition is shown in Table 1. For some of the speeches or speakers, the accuracy is obtained as 100 %.

Text independent speaker recognition using clustering technique and GMM is evaluated by first doing group classification with reference to the set of female and male speakers. Accuracy is increased by 1 %, if group classification is done prior to respective speaker classification and it is indicated in Table 2.

## 6 Conclusions

We have proposed the use of clustering technique for emotion independent speech recognition and text independent speaker recognition using emotional database in Berlin language. MFPLPC features are extracted from the emotional speeches and clustering models are developed for speeches and speakers. Features of test speeches are applied to the models corresponding to the speech recognition and the accuracy is found to be good. This basic feature is concatenated with probability and models are developed. Overall accuracy is found to be same as that of basic feature. Overall accuracy is further improved by checking the correct identification of the test segment corresponding to any of the feature. Text independent speaker recognition is evaluated by considering the group models corresponding to the set of female and male speakers. Evaluation is done by developing clustering and GMM training models and the accuracy is found to be slightly better for GMM as compared to that of the system tested on clustering models. Accuracy can be further improved by using the database containing the large number of speech samples.

## References

1. Nwe, T.L., Foo, S.W., De Silva, L.C.: Speech emotion recognition using hidden Markov models. *Speech Commun.* **41**, 603–623 (2003)
2. Morrison, D., Wang, R., De Silva, L.C.: Ensemble methods for spoken emotion recognition in call-centres. *Speech Commun.* **49**, 98–112 (2007)
3. Wu, S., Falk, T.H., Chan, W.-Y.: Automatic speech emotion recognition using modulation spectral features. *Speech Commun.* **53**, 768–785 (2011)
4. Lee, C.-C., Mower, E., Busso, C., Lee, S., Narayanan, S.: Emotion recognition using a hierarchical binary decision tree approach. *Speech Commun.* **53**, 1162–1171 (2011)
5. Vogt, T., Andr, E.: Improving automatic emotion recognition from speech via gender differentiation. In: *Proceedings of Language Resources and Evaluation Conference (LREC 2006)*, Genoa (2006)
6. Rao, K.S., Kumar, T.P., Anusha, K., Leela, B., Bhavana, I., Gowtham, S.V.S.K.: Emotion recognition from speech. *Int. J. Comput. Sci. Inf. Technol.* **3**(2), 3603–3607 (2012)
7. Sapra, A., Panwar, N., Panwar, S.: Emotion recognition from speech. *Int. J. Emerg. Technol. Adv. Eng.* **3**(2):341-345 (2013). ISSN 2250-2459, ISO 9001:2008 (Certified Journal)
8. Shahin, I.: Speaker identification in emotional environments. *Iran. J. Electr. Comput. Eng.* **8**(1), 41–46 (2009)
9. Koolagudi, S.G., Sharma, K., Rao, K.S.: Speaker recognition in emotional environment. *Commun. Comput. Inf. Sci.* **305**, 117–124 (2012)
10. Reynolds, D.A., Rose, R.C.: Text independent speaker identification using Gaussian mixture models. *IEEE Trans. Speech Audio Process.* **3**(1), 72–83 (1995)
11. Hermansky, H., Margon, N.: RASTA Processing of Speech. *IEEE Trans. Speech Audio Process.* **2**(4), 578–589 (1994)
12. Revathi, A., Venkataramani, Y.: Use of perceptual features in iterative clustering based Twins Identification System. *Proceedings of International Conference on Computing, Communication and Networking*, pp.1–6, (2008)

# Two-Level Multivariate Fuzzy Logic Based Integrated Model for Monsoon Rainfall Prediction

Mahua Bose and Kalyani Mali

**Abstract** Rainfall prediction is considered as one of the complex tasks in the area of time series forecasting. Timely and accurate forecasting is essential for better decision making. Autoregression based methods have been widely used for rainfall forecasting. But not much works attempted Vector autoregression in this area. This paper presents an integrated multivariate rainfall prediction scheme using Vector autoregression coupled with fuzzy inference and similarity based measure. Proposed method is a two step process where output of first step is fed into the process in the next step. Result shows improved accuracy of the proposed fuzzy logic based model over the individual statistical model.

**Keywords** Feature · Fuzzy · Kernel · Rainfall prediction · Vector autoregression

## 1 Introduction

Time series is a sequence of values or events measured at equal intervals which can be used to predict any future event. Time series analysis identifies hidden pattern in the past data and predicts future pattern. Agriculture, climatology, sales, transport and tourism sector are some examples of different forecasting areas.

Rainfall is a natural phenomenon which varies with time and space and depends on several atmospheric parameters also. South-West Monsoon is the main source of rainfall in India. Flood and Drought are result of fluctuations in the time of onset and withdrawal of monsoon. Rainfall forecasting has great impact on entire population of the country. It provides services to general public as well as farmers,

---

M. Bose (✉) · K. Mali  
Department of Computer Science and Engineering, University of Kalyani, Kalyani  
West Bengal, India  
e-mail: e\_cithi@yahoo.com

K. Mali  
e-mail: kalyanimali1992@gmail.com

fishermen, shipping, air navigation etc. Accurate and timely forecasting of rainfall is a major issue in an agricultural country like India. It not only affects the economic development of a region but also warns people about the possible natural disasters to reduce the loss of life and property.

The objective of this present study is to predict monthly rainfall of a region, in a particular year based on past historical data using integrated forecast models. Vector autoregression is used in the first step in each model and fuzzy rule and kernel based similarity are used in the second step. Performances of Integrated methods are compared with the output of VAR model obtained in the first step.

This paper is organized as follows: Sect. 2 summarizes previous works. Section 3 shows the data used in the experiment. Methodology is explained in Sect. 4. Experimental results are discussed in Sect. 5. In Sect. 6, Conclusion is presented.

## 2 Related Works

Over the decade a lot of techniques using statistical and machine learning methods have been successfully applied for rainfall prediction. Rainfall forecasting based on various statistical techniques namely AR, ARMA, ARIMA, SARIMA have been studied by several authors [1–5]. Hybrid ARNN model [6] has also been proposed. Techniques using fuzzy logic [7–9] has been investigated. Modular Fuzzy Inference System [10], a two layer model [11] using Mamdani-type fuzzy inference together with Bayesian learning and nonlinear programming, a Multivariate model [12] using rule-based fuzzy inference system and a recurrent fuzzy system model with genetic algorithm [13] were also employed. An ensemble method [14] based on ANFIS and ARIMA, has been proposed for forecasting monthly rainfall data. A comparative study [15] showed improved performance of PSO-SVR over the BPNN and ARIMA models. In recent times, pattern similarity-based time-series model [16] has become a very popular method in the area of financial data analysis, weather data forecasting [17], stream data processing etc. The objective of this method is to find those sequences similar to a given pattern.

Above Statistical models are suitable for univariate data. In this experiment two separate models were developed using multiple variables. Vector autoregression is employed in the first step in both of the models. In the second step, fuzzy inference and similarity measure are applied on two models separately.

## 3 Data

Monthly rainfall, maximum temperature and minimum temperature data (1901–2005) of North Central region of India, are collected from the website of Indian Institute Of Tropical Meteorology [18]. Data for 2006 are used for error estimation. Here, Rainfall and temperature have been recorded in mm. and degree- Celsius, respectively.

### 4 Forecast Models

This study presents a two level combined forecast scheme (Fig. 1). Maximum temperature and minimum temperature predicted from level one are used to forecast rainfall in the second step. Before the application of the methods described below, data are normalized using MSN or mean and scale normalization [19].

#### 4.1 Vector Autoregression (VAR) Model

This model [20] is used to study the linear dependencies among multiple time series. Univariate autoregression (AR) model predicts the current value of a time series from its previous values. In VAR Model each variable has an equation which expresses its predicted value based on the past value of its own series and the past values of the other time series. Model order is denoted by the number of past values used.

Let  $X_t = (X_{t1}, X_{t2}, X_{t3})$ , be a vector of dimension 3. Then the first order VAR Model is defined as:

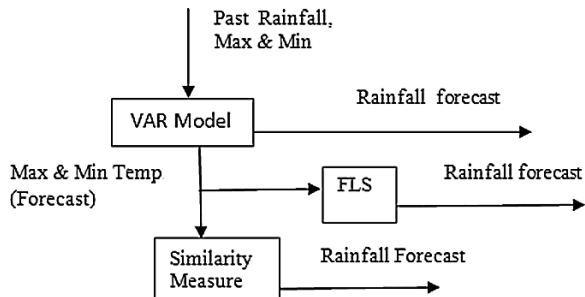
$$X_{t1} = \alpha_1 + \Phi_{11}X_{t-1,1} + \Phi_{12}X_{t-1,2} + \Phi_{13}X_{t-1,3} + \omega_{t1} \tag{1}$$

$$X_{t2} = \alpha_2 + \Phi_{21}X_{t-1,1} + \Phi_{22}X_{t-1,2} + \Phi_{23}X_{t-1,3} + \omega_{t2} \tag{2}$$

$$X_{t3} = \alpha_3 + \Phi_{31}X_{t-1,1} + \Phi_{32}X_{t-1,2} + \Phi_{33} X_{t-1,3} + \omega_{t3} \tag{3}$$

In the above equations  $\omega$  terms represent white noise. Here, Rainfall, Max. Temperature, and Min. temperature are represented by  $X_{t1}, X_{t2}, X_{t3}$ , respectively.

**Fig. 1** Proposed forecasting scheme



## 4.2 Fuzzy Logic System

A FLS has four main parts: fuzzifier, rules, inference engine, and defuzzifier [21]. The functional operations in fuzzy logic system are described by the following steps: A FLS has four main parts: fuzzifier, rules, inference engine, and defuzzifier [20]. The functional operations in fuzzy logic system are described by the following steps: (1) Defining linguistic variables and terms (input or output variables of the system) (2) Defining membership functions (3) Construction of the rule base (4) Fuzzification (5) Fuzzy Inferencing (6) Aggregation of all rules (7) Defuzzification.

The fuzzy set defined here, consists of two input variables: max. temperature and min. temperature and output variable Rainfall. For each input and output, two types of membership function are chosen in this study: trapezoidal and triangular membership functions. The rule base is a set of rules of the IF–THEN form. The IF portion of a rule refers to the degree of membership of input fuzzy sets. The THEN portion refers to the output fuzzy set. Centroid method has been used for defuzzification.

## 4.3 Kernel Based Similarity Approach

The polynomial kernel [22] is generally used with support vector machines and other kernelized models, that represents the similarity of vectors in a feature space over polynomials of the original variables. For degree-2 polynomials, the polynomial kernel is defined as  $K(x, z) = (x^T z + c)^2$ , where  $x$  and  $z$  are vectors in the input space and  $c \geq 0$  is a constant.

Thus, we see  $K(x, z) = \phi(x)^T \phi(z)$ , where, feature mapping  $\phi$  is given by (for  $n = 2$ ). It can also be written as,  $K(x, z) = \sum_{i,j=1}^n (x[i]x[j])(z[i]z[j])$

The Hilbert distance is defined as

$$d(x, z) := \|\phi(x) - \phi(z)\|$$

where,  $\|\phi(x) - \phi(z)\| = \langle \phi(x), \phi(x) \rangle + \langle \phi(z), \phi(z) \rangle - 2\langle \phi(x), \phi(z) \rangle$

$$\text{So, } d(x, z) = \sqrt{K(x, x) + K(z, z) - 2K(x, z)} \quad (4)$$

In our proposed algorithm, maximum and minimum of each (past) year are two elements  $x_1$  and  $x_2$  in vector  $X$ . Predicted Max and Min temp of the next year from step1 using VAR(1) model are two elements  $z_1, z_2$  in input vector  $Z$ . These points are to be mapped into high dimensional space, i.e.,  $\phi(x)$  and  $\phi(z)$  first. Then Distance should be calculated from input vector to all other vectors. First  $n$  shortest distances are taken and corresponding Rainfall values are extracted and their mean is computed. This is forecast for the next year.

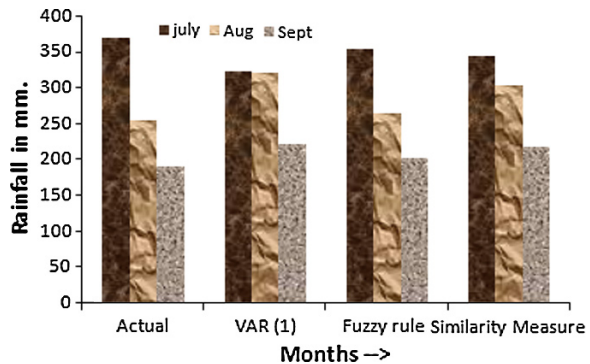
## 5 Experimental Results and Discussion

The experiment is carried out on the datasets namely July, August and September. In VAR(1), current value of rainfall (forecast) for a particular month is a linear combination of its immediate past value and past values of maximum temperature and minimum temperature. Similarly, other two variables are predicted. Predicted maximum temperature and minimum temperature are inputs to the next step.

Instead of measuring similarity using Euclidean distance, kernel based similarity is calculated. Here, forecast value is obtained by taking 3–6 nearest values and best result is obtained taking five nearest values. Based on both the criteria of error estimates, i.e. Root Mean Square Error (RMSE) and Mean Absolute Percentage Error (MAPE), the proposed integrated model using Fuzzy rule produces best result in all cases. Prediction using similarity measure is almost same on July data set but best result for the month of August and September can only be obtained using fuzzy rule.

The error associated with each method depends on several factors such as, choice of kernel, types of membership function, order of VAR model, etc. Performance of the models in step 2 is largely dependent on the accuracy in predicted temperature values in the first step. RMSE values of Max. and Min. temperatures are almost same in first and second order VAR model. But, rainfall forecast using VAR(1) model is better than that of VAR(2). RMSE value in VAR(2) is 66 where as in VAR(1) it is 50. VAR(1) is retained and results are shown in Fig. 2 and Tables 1, 2 and 3.

**Fig. 2** Rainfall: actual versus predicted values using different methods



**Table 1** Rainfall (in mm.)

Month	Actual	Forecast		
		VAR(1)	VAR(1)-Fuzzy rule	VAR(1)-Similarity measure
July	370.4	323.54	355.12	343.9
August	256	321.55	265.31	304.16
September	189.8	221.86	202.03	217.64



**Table 2** Temperature forecast (in degree celsius) using VAR(1)

Month	Maximum temperature		Minimum temperature	
	Actual	Forecast	Actual	Forecast
July	30.7	31.5	24.5	24.2
August	30.3	30.2	23.8	23.6
September	32	30.8	23.1	22.8

**Table 3** Performance evaluation (rainfall forecast)

Error	VAR(1)	VAR(1)-Fuzzy rule	VAR(1)-Similarity measure
RMSE	50.07	12.51	35.57
MAPE	27.57	4.74	20.32

For FLS, each input is sorted into 3 categories and labeled as LOW, MEDIUM, HIGH for each of three data sets. Output (Rainfall) is sorted into 3 categories and labeled as LOW, MEDIUM, HIGH for each of August and September data sets. For July dataset one additional category VERY HIGH has been included. Examples of the rules are:

1. IF Max. Temp. is HIGH AND IF Min. Temp. is HIGH  
THEN rain fall is LOW
2. IF Max. Temp. is LOW AND IF Min. Temp. is MEDIUM  
THEN rain fall is VERY HIGH

## 6 Conclusion

In this paper, two step integrated models have been generated using statistical and soft computing techniques in two different ways and observed that integrated approaches more accurate and effective as compared to single statistical model. In addition to Rainfall forecast, maximum and minimum temperature forecast for the next year are also obtained from this experiment. VAR(1) model produced temperature forecast more accurately than rainfall forecast. For this reason, these temperature values improved the performance of the integrated models. This study has revealed that model using fuzzy inference gives best result. Accuracy of the models can be improved by efficient selection of rules and introducing more input variables such as relative humidity, wind speed, etc. The work discussed in this paper is a preliminary level investigation. In future, it can be extended by merging it with artificial neural network.

## References

1. Burlando, P., Rosso, R., Cadavid, L.G., Salas, J.D.: Forecasting of short-term rainfall using ARMA model. *J. Hydrol.* **144**(1–4), 193–211 (1993)
2. Valipour, M.: Number of required observation data for rainfall forecasting according to climate conditions. *Am. J. Sci. Res.* **74**, 79–86 (2012)
3. Wang, S., Feng, J., Liu, G.: Application of seasonal time series model in the precipitation forecast. *Math. Comput. Model.* **58**(3–4), 677–683 (2013)
4. Narayanan, P., Basistha, A., Sarkar, S., Sachdeva, K.: Trend analysis and ARIMA modelling of pre-monsoon rainfall data for western India. *C. R. Geosci.* **345**(1), 22–27 (2013)
5. Khadar Babu, S.K., Karthikeyan, K., Ramanaiah, M.V., Ramanah, D.: Prediction of rainfall-flow time series using autoregressive models. *Adv. Appl. Sci. Res.* **2**(2), pp. 128–133 (2011)
6. Chattopadhyay, S., Chattopadhyay, G.: Univariate modelling of summer-monsoon rainfall time series: comparison between ARIMA and ARNN. *C. R. Geosci.* **342**(2), 100–107 (2010)
7. Yu, P.-S., Chen, S.T., Wu, C.-C., Lin, S.-C.: Comparison of grey and phase-space rainfall forecasting models using a fuzzy decision method. *Hydrol. Sci.* **49**(4), pp. 655–672 (2004)
8. Annas, S., Kanai, T., Koyama, S.: Neuro-fuzzy approaches for modeling the wet season tropical rainfall. *Agric. Inf. Res.* **15**(3), 331–341 (2006)
9. Fall, G.A., Mohammad, M.-B., Nok, M.H.: Annual rainfall forecasting by using Mamdani fuzzy inference system. *Res. J. Environ. Sci.* **3**(4), pp. 400–413 (2009)
10. Kajornrit, J., Wong, K.W., Fung, C.C.: Rainfall prediction in the northeast region of Thailand using modular fuzzy inference system. In: *IEEE International Conference on Fuzzy Systems*, pp. 1–6, Brisbane, QLD (2012)
11. Kajornrit, J., Wong, K.W., Fung, C.C.: A modular technique for monthly rainfall time series prediction. In: *IEEE Symposium on Computational Intelligence in Dynamic and Uncertain Environments*, pp. 76–83 (2013)
12. Asklany, S.A., Elhelou, K., Youssef, I.K., Abd El-wahab, M.: Rainfall events prediction using rule-based fuzzy inference system. *Atmos. Res.* **101**(1–2), pp. 228–236 (2011)
13. Evsukoff, E., Cataldi, M., de Lima, B.S.L.P.: A multi model approach for long term run-off modeling using rainfall forecast. *Expert Syst. Appl.* **39**(5), 4938–4946 (2012)
14. Suhartono, Faulina, R., Lusua, D.A., Otok, B.W., Sutikno, Kuswanto, H.: Ensemble method based on ANFIS-ARIMA for rainfall prediction. In: *International Conference on Statistics in Science, Business, and Engineering*, pp. 1–4 (2012)
15. Zhao, S., Wang, L.: The model of rainfall forecasting by SVM regression based on PSO algorithm. In: *Proceedings of the 2010 International Conference on Life System Modeling and Simulation and Intelligent Computing, and International Conference on Intelligent Computing for Sustainable Energy and Environment: Part II*, pp. 110–119. Springer, Berlin, Heidelberg (2010)
16. Lvarez, F.M., Troncoso, A., Riquelme, J.C., Ruiz, J.S.A.: Energy time series forecasting based on pattern sequence similarity. *IEEE Trans. Knowl. Data Eng.* **23**(8), 1230–1243 (2011)
17. Sharma, A., Bose, M.: Rainfall prediction using k-NN based similarity measure. In: *The Proceedings of Second International Conference on Recent Advances in Information Technology, ISM, Dhanbad* (2014)
18. Indian Institute of Tropical Meteorology. <http://www.tropmet.res.in>
19. Alam, M.J., Ouellet, P., Kenny, P., O’shaughnessy, D.: Comparative evaluation of feature normalization techniques for speaker verification. In: *Proc. NOLISP, LNAI 7015*, pp. 246–253 (2011)
20. Shumway, R.H., Stoffer, D.S.: *Time Series Analysis and its Application*. Springer Text in Statistics (2000)
21. Mendel, J.: Fuzzy logic systems for engineering: a tutorial. *Proc. IEEE* **83**(3), 345–377 (1995)
22. Vapnik, V.: *The Nature of Statistical Learning Theory*. Springer, New York (1995)

# Feed Forward Neural Network Approach for Reversible Logic Circuit Simulation in QCA

Arijit Dey, Kunal Das, Sanjoy Das and Mallika De

**Abstract** Quantum dot Cellular Automata (QCA) is becoming a new paradigm in nanoscale computing. Artificial Neural Network model is a promising model to design and simulate QCA circuits. This study proposes a new approach to design, model and simulate small circuit as well as large circuit. Feed Forward Neural Network (FFNN) model is used to design and simulate the reversible circuit as well as conservative circuit. The simulation result of this proposed FFNN model gives better result than exhaustive simulation of QCADesigner.

**Keywords** QCA · Artificial neural network · Feed forward neural network (FFNN) · Reversible circuit · Conservative circuit

---

A. Dey (✉)

Department of Computer Application, B.P. Poddar Institute of Management and Technology, Kolkata 700052, West Bengal, India  
e-mail: ad.computerapplication@gmail.com

K. Das

Department of Information Technology, B.P. Poddar Institute of Management and Technology, Kolkata 700052, West Bengal, India  
e-mail: kunaldasqca@gmail.com

S. Das

Department of Engineering and Technological Studies, Kalyani University, Kalyani 741235, West Bengal, India  
e-mail: dassanjoy\_kalyani@yahoo.co.in

M. De

Dr. Sudhir Chandra Sur Degree Engineering College, Kolkata 700052, West Bengal, India  
e-mail: demallika@yahoo.com

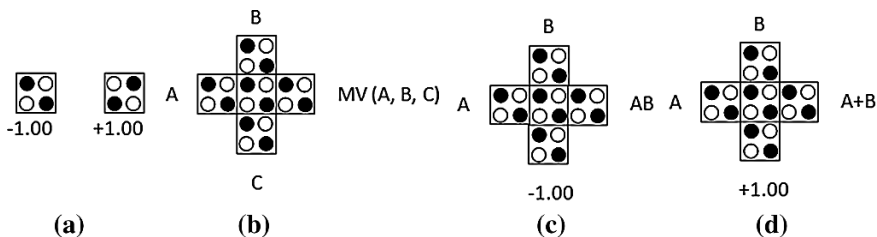
© Springer India 2015

J.K. Mandal et al. (eds.), *Information Systems Design and Intelligent Applications*, Advances in Intelligent Systems and Computing 339, DOI 10.1007/978-81-322-2250-7\_7

# 1 Introduction

The Complementary Metal Oxide Semiconductor (CMOS) technology provides high density and low power Large Scale Integrated Circuit (VLSI) in micro scale computing. Now a days, this technology is facing new challenges like high leakage of current, power dissipation in terms of heat and reaches its limit. Researchers are still finding the alternatives of CMOS technology in nanoscale computing for VLSI design. Semiconductor Industries Association’s International Roadmap for Semiconductors has reported that the circuit size is becoming double in every 18 months [1]. Quantum dot Cellular Automata (QCA) is an emerging technology and an alternative of CMOS technology. QCA was first introduced by Lent et al. [2], Tougaw and Lent [3] in the year 1993. In QCA electrons are confined within the cell so that there is no current and output capacitance in the circuit [4]. The electrons are tunneled through tunnel junction. Each QCA cell consists of four quantum dots and two extra electrons are confined within the cell. These extra electrons are positioned diagonally to hold maximum distance of electrons and these two positions define two states of polarization +1.00 as ‘logic 1’ and -1.00 as ‘logic 0’ respectively as shown in Fig. 1a. The three input majority voter is shown in Fig. 1b. Figure 1c, d shows the basic logic functions AND operation and OR operation by putting one input to fixed polarized -1.00 and +1.00 respectively.

The irreversible computation perform the same way as the conventional computers i.e., once the output is generated from the logic block the input bits are lost, so that the power is retained in the system [5]. Reversible computing computes with almost zero power dissipation. Landauer [6] has proved that each bit information loss produce  $K_B T \ln 2$  J of heat energy for irreversible logic computation where  $K_B$  is Boltzman’s constant and T is the absolute temperature. Bennett [7] has proved zero power dissipation in case of reversible logic computing. Basically, Feynman gate, Fredkin gate and Toffoli gate [8–10] perform as reversible logic gate. In reversible logic computing, the mapping of input vector  $I_V$  and output vector  $O_V$  is bijective i.e., each input yields to a distinct output [8]. In Conservative logic is one type of reversible logic. Conservative logic gate inputs from input vector  $I_V$  and outputs from output vector  $O_V$  are mapped in a way that parity of inputs  $I_V$  and



**Fig. 1** a QCA cell polarization. b Three input majority voter. c AND gate. d OR gate

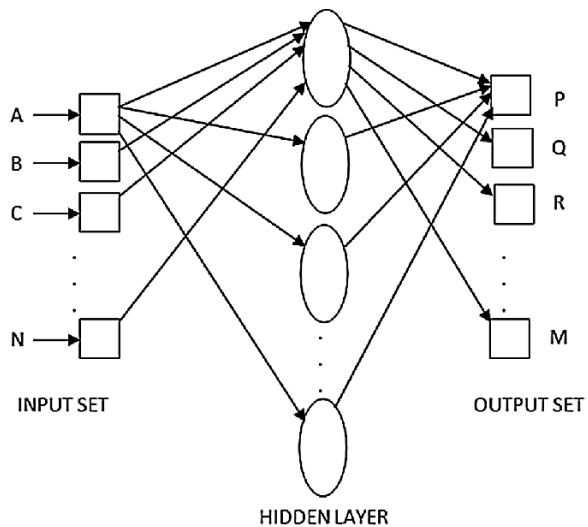
outputs  $O_V$  are preserved i.e., number of 1's present in each input and number of 1's present in output must be same [11]. In earlier works, several tools such as QCADesigner [12] have been used for designing and simulation of small QCA circuits. Recently, VHDL based simulation tools [13, 14], Hopfield neural networks [15, 16] have been introduced for presenting the simulation of QCA circuit. In [17] tansig method has been reported for simulation of QCA circuits.

In this paper, feed forward neural network [18] (FFNN) model is proposed for modeling and simulation of QCA circuit. This method illustrates the modeling and simulation of QCA reversible circuit by means of Knik energy. One cell impresses its neighboring cell due to coulomb interaction, known as Knik energy. The Knik energy is inversely proportional to distance between the charges of two cells  $q_i$  and  $q_j$  and is defined as

$$E_{i,j}^{knik} = \frac{1}{4 \prod \epsilon_0 \epsilon_r} \sum_{n=1}^4 \sum_{m=1}^4 \frac{q_n^i q_m^j}{|r_n^i - r_m^j|} \tag{1}$$

where  $\epsilon_0$  is the permittivity of free space and  $\epsilon_r$  is the relative permittivity. In this approach the polarization of input cells are imposed on the device cell by the effect of Knik energy which calculates the polarization of device cell. This polarization of device cell is transferred to the output cell as resultant polarization. The basic feed forward neural network is shown in Fig. 2. Each input from the input set is connected to each of the process in the hidden layer and the connection of each process of hidden layer is connected to one of the outputs in output set.

**Fig. 2** Feed forward neural network model



## 2 Proposed Feed Forward Neural Network Model

The proposed feed forward neural network (FFNN) model is applied over the reversible logic computing as well as conservative logic computing for modeling and simulation. This FFNN model is very simple to design the reversible logic gate and conservative logic gate. In this study, the reversible logic gate is designed and simulated with few steps. This FFNN model consists of input set, one hidden layer and output set. An artificial feed forward neural network model FFNN is proposed here to demonstrate an experimental study of modeling and simulation of reversible circuits. The FFNN model is illustrated with QCA cell of size 18 nm and distance between a pair of QCA cells of 2 nm. This FFNN model has been tested and simulated by MATLAB 7.7 using a set of training data. The steps involved to design and simulate a reversible logic gate are discussed below:

### Steps of FFNN model

1. Take the number of inputs (NI) of the reversible circuit in the input layer of FFNN model
2. Find the number of process of the hidden layer from the truth table of number of inputs  
Number of Processes (NPr) in the hidden layer =  $2^{NI}$
3. Set number of outputs (NO) in the output layer as the same number as inputs in the input layer.  
Set NO = NI and also Set I = 1.
4. Repeat Step 5 to Step 6 while (I <= NPr)
5. Find the polarization of process P(I)
6. Set I = I + 1
7. The polarization of each process is imposed on the output layer
8. To find a particular output of output layer set the polarization of the processes either the 'imposed polarization' or '0' according to the output function.

### 2.1 Study on Feynman Gate

Feynman Gate is a  $2 \times 2$  reversible logic gate i.e., it has 2 inputs and 2 outputs. The input vector  $I_V$  (A, B) is mapped to output vector  $O_V$  ( $P = A \oplus B$ ,  $Q = A$ ). Figure 3 shows the block diagram of a Feynman gate and the equivalent FFNN model design is shown in Fig. 4. The inputs A and B are put on the processors of input layer. These processors of input layer are connected to each of the process of hidden layer.

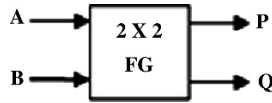


Fig. 3 Block diagram of Feynman gate

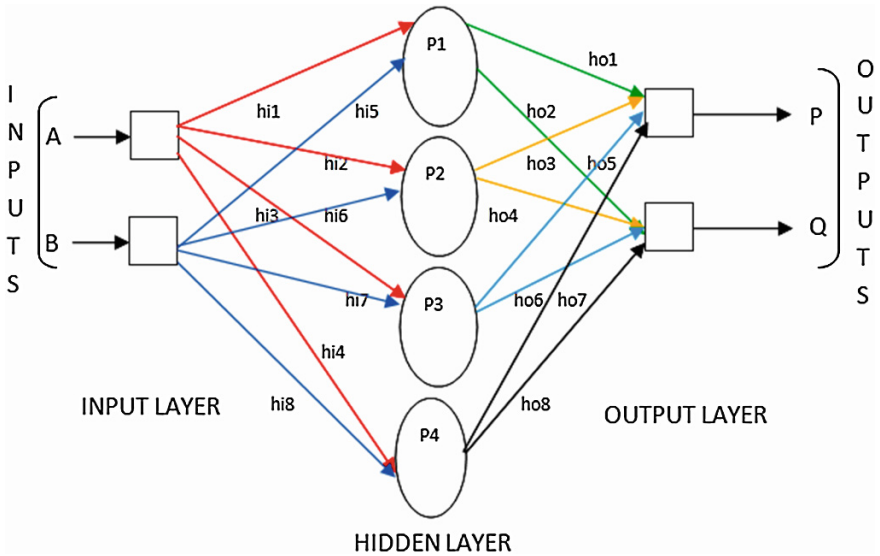


Fig. 4 Feed forward neural network (FFNN) model of Feynman gate

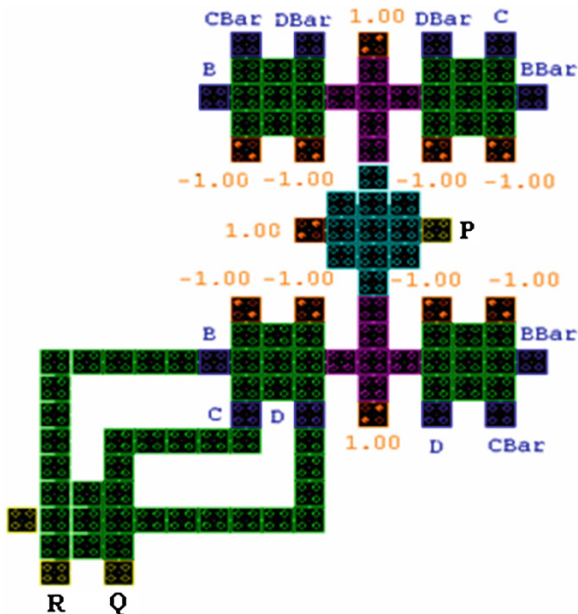
The lines hi1, hi2, hi3, hi4 show the connection between the processes P1, P2, P3, P4 of hidden layer from input A. Similarly, the lines hi5, hi6, hi7, hi8 show the connection to the processes P1, P2, P3, P4 of hidden layer from input B. Now, the polarizations of each connection hi1 to hi8 are imposed on the processes P1–P4 of hidden layer and these polarizations propagate each process to calculate the input combinations. The processes of the hidden layer give all the input combinations that are found from the input set. All these input combinations are connected to each of the input of output layer. The lines ho1, ho2 (input binary combination 00) which are found as outputs from the process P1 of hidden layer, act as inputs to the processors of the output layer. Similarly, ho3, ho4 are the input binary combination 01 produced by the process P2 of hidden layer, ho5, ho6 are the input binary combination 10 produced by the process P3 and the connection ho7, ho8 are the input binary combination 11 produced by the process P4 of the hidden layer. All these processes of hidden layer produce all input combinations from the truth table. All these are connected from hidden layer to each of the output processors of the output layer. The desired results are found by controlling the connections ho1 to ho8 in the processors of output layer. Finally the output processors of output layer drive the outputs P and Q by controlling the polarizations which are found from the

each process of hidden layer. The polarization of the connections  $ho_1, ho_7$  are set to 0, and  $ho_3, ho_5$  are set to 1 to produce the output  $P = \sum (ho_3, ho_5)$  (SOP form) of Feynman gate. The polarization of the connections  $ho_2, ho_4$  are set to 0 and  $ho_6, ho_8$  are set to the polarization that has found from the processes of hidden layer to get the desired result at output  $Q = \sum (ho_6, ho_8)$  (SOP form) of Feynman gate.

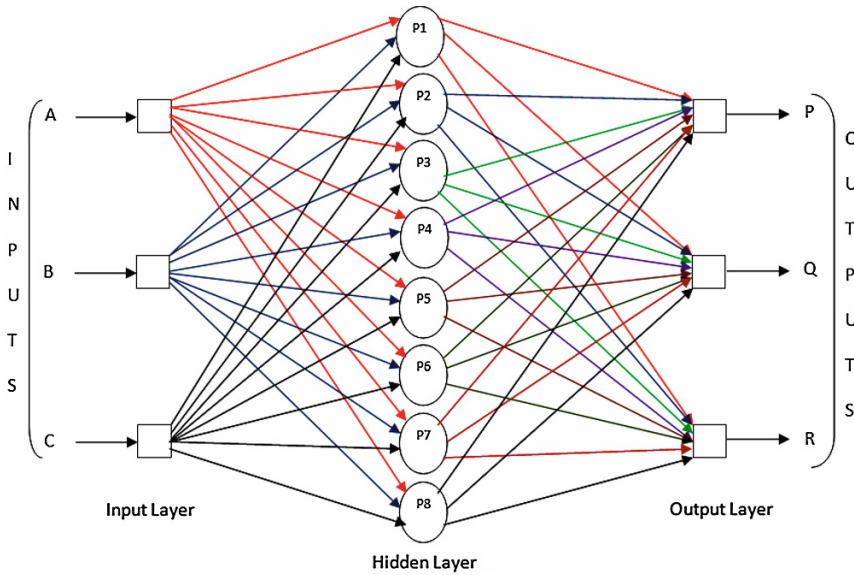
### 3 Feed Forward Neural Network Simulation of Full Adder Circuit

This proposed FFNN model is also applied on QCA circuit design, modeling and simulation. Earlier, one bit conservative, lossless, zero garbage full adder circuit was designed and simulated by exhaustive simulation of QCADesigner [5] as shown in Fig. 5. In this study, the equivalent FFNN model of the conservative, lossless, zero garbage full adder circuit is designed and simulated by a set of training data. The FFNN model simulation is done by MATLAB 7.7. The architecture of the FFNN model of the said full adder circuit design is shown in Fig. 6. In this proposed FFNN model the processes of hidden layer produce all the combinations of inputs that have taken from the input layer i.e., the number of process in the hidden layer is eight as a full adder circuit has 3 inputs. The polarizations of all

Fig. 5 Conservative full adder circuit design by QCADesigner







**Fig. 6** FFNN model of conservative full adder

processes of hidden layer are calculated using Eq. 2, where  $E_K$  is the Knik energy of a QCA cell,  $\Delta E = \hbar/\tau$ , *polarization* gives the polarization of previous cell and  $te$  is the tunneling energy. All these calculated polarizations of the processes of the hidden layer have imposed on the output layer. The weight/polarization of each connection between the processes of hidden layer and output layer control the weight/polarization of each output of the conservative full adder circuit. In this FFNN approach the polarization of the processes are found from the polarization of inputs that are imposed on the process of hidden layer. Once the polarizations of all processes are generated, they are imposed on all the outputs of output layer. Now, the polarization '0' is set to those connections that are not used to find out a particular output. Finally, the proposed FFNN model produces the output of conservative full adder  $P = \sum (1, 2, 4, 7)$ ,  $Q = \sum (3, 5, 6, 7)$ ,  $R = \sum (3, 5, 6, 7)$  (SOP form).

$$Final\ Polarization = \frac{(E_K/2\Delta E) \times polarization}{\sqrt{((1 + Ek)/te) \times polarization}} \tag{2}$$

## 4 Simulation Result Analysis

The design of zero garbage, lossless, conservative full adder circuit is done by QCADesigner as shown in Fig. 5. The exhaustive simulation result by QCADesigner is shown in Fig. 7. The polarization value of P is 0.877, Q is 0.931 and R is 0.930 whereas the proposed FFNN model has given the polarization values of P, Q and R as 0.922, 0.922 and 0.922 respectively. The FFNN model simulation result is given in Table 1. The polarization of the processes of hidden layer is computed and then the polarization of the final output is calculated. In Table 1 the simulation result of FFNN model is given. This simulation result of FFNN model gives a better polarization of output than exhaustive simulation by QCADesigner. The comparison of QCADesigner simulation result (represented by 1) and proposed FFNN model simulation result (represented by 2) for different outputs is shown in Fig. 8.

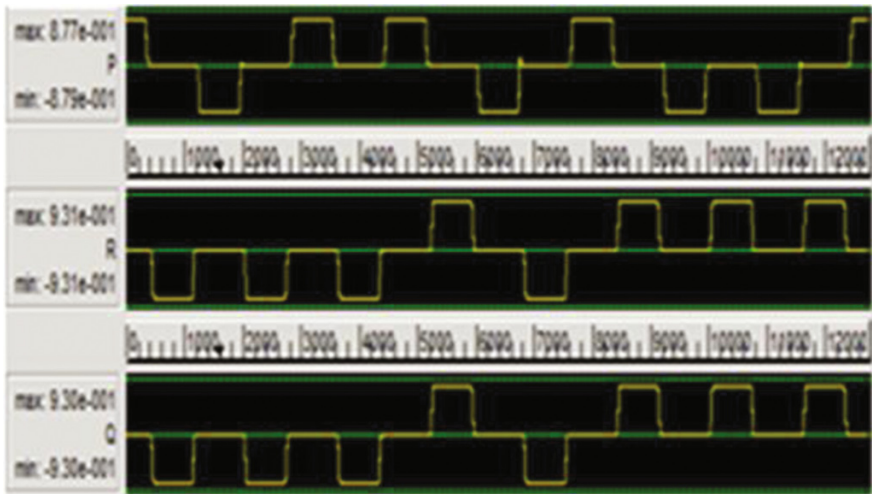
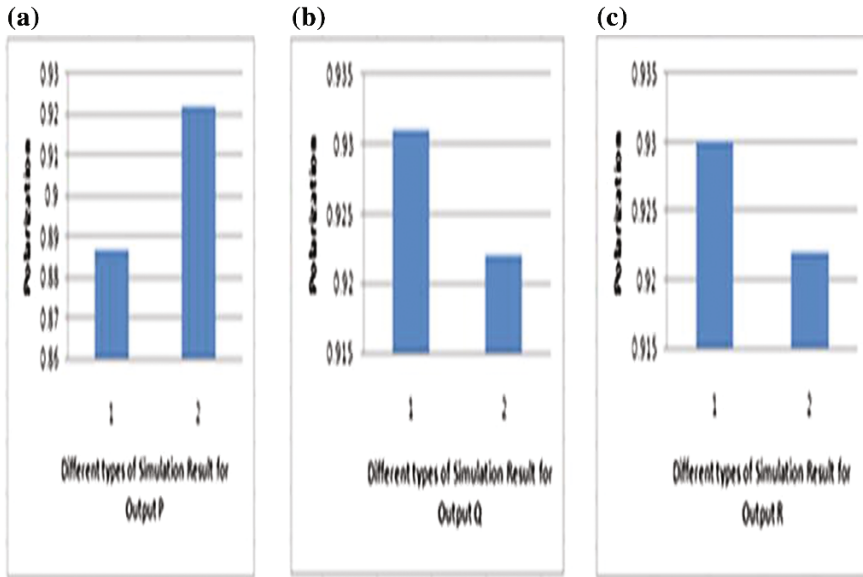


Fig. 7 Simulation result of conservative full adder circuit by QCADesigner

**Table 1** Simulation result of conservative full adder circuit by FFNN model compared with QCADesigner

Initial input polarization of three inputs set for respective min terms	Process No. of hidden layer with calculated polarization of respective processes	Polarization set for output P at output layer	Polarization set for output Q at output layer	Polarization set for output R at output layer	Final polarization at output layer (MAILAB simulation)	Final polarization at output layer (QCADesigner simulation)
A = 1.00 (logic 1) or -1.00 (logic 0)	P1 = 0.943	P1 = 0	P1 = 0	P1 = 0	Output P = 0.922	Output P = 0.877
	P2 = 0.943	P2 = 0.943	P2 = 0	P2 = 0		
	P3 = 0.943	P3 = 0.943	P3 = 0	P3 = 0		
B = 1.00 (logic 1) or -1.00 (logic 0)	P4 = 0.943	P4 = 0	P4 = 0.943	P4 = 0.943	Output Q = 0.922	Output Q = 0.931
	P5 = 0.943	P5 = 0.943	P5 = 0	P5 = 0		
	P6 = 0.943	P6 = 0	P6 = 0.943	P6 = 0.943		
C = 1.00 (logic 1) or -1.00 (logic 0)	P7 = 0.943	P7 = 0	P7 = 0.943	P7 = 0.943	Output R = 0.922	Output R = 0.930
	P8 = 0.943	P8 = 0.943	P8 = 0.943	P8 = 0.943		



**Fig. 8** QCADesigner and proposed FFNN model simulation results **a** for output P, **b** for output Q, **c** for output R

## 5 Conclusion

In this study, the artificial intelligence technology is used to design and simulate QCA reversible as well as conservative circuit. The modeling of QCA circuit using FFNN is very simple and the simulation with an acceptable precision of polarization is done by MATLAB. The accuracy of the polarization at each output is also compared with the exhaustive simulation result of QCADesigner. The result found from MATLAB simulation shows that this FFNN model is efficient and gives an acceptable precision at each output of QCA reversible as well as conservative circuit.

## References

1. International technology roadmap for semiconductors. Semiconductor Industries Association, San Jose, CA. <http://public.itrs.net> (2001)
2. Lent, C.S., Tougaw, P.D., Porod, W., Bernstein, G.H.: Quantum cellular automata. *Nanotechnology* **4**(1), 49 (1993)
3. Tougaw, P.D., Lent, C.S.: Dynamic behavior of quantum cellular automata. *J. Appl. Phys.* **80** (8), 4722–4736 (1996)
4. Smith, C.G.: Computation without current. *Science* **284**(5412), 274 (1999)

5. Dey, A., Das, K., De, D., De, M.: Online testable conservative adder design in quantum dot cellular automata. In: *Emerging Trends in Computing and Communication*, pp. 385–393. Springer India, Berlin (2014)
6. Landauer, R.: Irreversibility and heat generation in the computing process. *IBM J. Res. Dev.* **5** (3), 183–191 (1961)
7. Bennett, C.H.: Logical reversibility of computation. *IBM J. Res. Dev.* **17**(6), 525–532 (1973)
8. Toffoli, T.: *Reversible Computing*, pp. 632–644. Springer, Berlin (1980)
9. Fredkin, E., Toffoli, T.: Conservative Logic, pp. 47–81. Springer, London (2002)
10. Feynman, R.P.: Quantum mechanical computers I. *Found. Phys.* **16**(6), 986 (1985)
11. Das, K., De, D.: Characterization, test and logic synthesis of novel conservative and reversible logic gates for Qca. *Int. J. Nanosci.* **9**(03), 201–214 (2010)
12. Walus, K.: ATIPS laboratory QCADesigner homepage. ATIPS Laboratory, University Calgary. Calgary, Canada (2002)
13. Henderson, S.C., Johnson, E.W., Janulis, J.R., Tougaw, P.D.: Incorporating standard CMOS design process methodologies into the QCA logic design process. *IEEE Trans. Nanotechnol.* **3** (1), 2–9 (2004)
14. Ottavi, M., Schiano, L., Lombardi, F., Tougaw, D.: HDLQ: a HDL environment for QCA design. *ACM J. Emerg. Technol. Comput. Syst. (JETC)* **2**(4), 243–261 (2006)
15. Behrman, E.C., Niemel, J., Steck, J.E., Skinner, S.R.: A quantum dot neural network. In: *Proceedings of the 4th Workshop on Physics of Computation*, pp. 22–24 (1996)
16. Neto, O.P.V., Pacheco, M.A.C., Hall Barbosa, C.R.: Neural network simulation and evolutionary synthesis of QCA circuits. *IEEE Trans. Comput.* **56**(2), 191–201 (2007)
17. Hayati, M., Rezaei, A.: New approaches for modeling and simulation of quantum-dot cellular automata. *J. Comput. Electron.* **13**(2), 537–546 (2014)
18. Bebis, G., Georgiopoulos, M.: Feed-forward neural networks. *Potentials IEEE* **13**(4), 27–31 (1994)

# Large Vocabulary Speech Recognition: Speaker Dependent and Speaker Independent

G. Hemakumar and P. Punitha

**Abstract** This paper addresses the problem of large vocabulary isolated word and continuous Kannada speech recognition using the syllables and combination of Hidden Markov Model (HMM) and Normal fit method. The models designed for speaker dependent and speaker independent mode of working. This experiment has covered 6 million words among the 10 million words from Hampi text corpus. Here 3-state Baum–Welch algorithm is used for training. For the 2 successor outputted  $\lambda(A, B, \pi)$  is combined and passed into normal fit, the outputted normal fit parameter is labeled has syllable or sub-word. In terms of memory requirement and recognition rate the proposed model is compared with Gaussian Mixture Model and HMM (3-state Baum–Welch algorithm). This paper clearly shows that combination of HMM and normal fit technique will reduce the memory size while building and storing the speech models and works with excellent recognition rate. The average WRR is 91.22 % and average WER is 8.78 %. All computations are done using mat lab.

**Keywords** Speaker independent • Speaker dependent • Normal fit • Baum-Welch algorithm

## 1 Introduction

Automatic speech recognition (ASR) is the process by which a computer maps an acoustic speech signal to text. The goal of speech recognition is to develop techniques and systems that enable computers to accept speech input and translate spoken words into text and commands. The problem of speech recognition has been actively studied since 1950s and it is natural to ask why one should continue

---

G. Hemakumar (✉)

Department of Computer Science, Government College for Women, Mandya, India  
e-mail: hemakumar7@yahoo.com

P. Punitha

Department of MCA, PESIT, Bangalore, India  
e-mail: punithaswamy@gmail.com

© Springer India 2015

J.K. Mandal et al. (eds.), *Information Systems Design and Intelligent Applications*,  
Advances in Intelligent Systems and Computing 339,  
DOI 10.1007/978-81-322-2250-7\_8

studying speech recognition. Speech recognition is the primary way for human beings to communicate. Therefore it is only natural to use speech as the primary method to input information into computational device or object needing manual input. Speech recognition is the branch of human-centric computing to make technology as user friendly as possible and to integrate it completely into human life by adapting to humans' specifications. Currently, computers force humans to adapt to computers, which is contrary to the spirit of human-centric computing. Speech recognition has the basic quality to help humans easily communicate with computers and reap maximum benefit from them. The performance of speech recognition has improved dramatically due to recent advances in speech service and computer technology with continually improving algorithms and faster computing.

The speech recognition system may be viewed as working in a five stages namely converting analog speech signal into Digitalization (Normalization part) form, Speech signal segmentation or Voice part detection, Feature extraction part, Speech Model building part, and Testing. In the speech signal, feature extraction is a categorization problem about reducing the dimensionality of the input vector while maintaining the discriminating power of the signal. As we know from fundamental formation of speech recognition system, that the number of training sets and test vector needed for the classification problem grows with the dimension of the given input, so we need feature extraction techniques. In speech processing there are so many methods for feature extraction in speech signal, but still Linear-Predictive coding (LPC) coefficients and Mel-Frequency Cepstral Coefficient (MFCC) are most commonly used technique [1–3].

The objective of modeling technique is to generate speech models using speaker specific feature vector. The speech recognition is divided into two parts that means speaker dependent and speaker independent modes. In the speaker independent mode of the speech recognition the computer should ignore the speaker specific characteristics of the speech signal and extract the intended message. On the other hand in case of speaker dependent recognition machine should extract speaker characteristics in the acoustic signal. To developing speech models there are many techniques namely, Acoustic-Phonetic approach, Pattern Recognition approach, Template based approaches, Dynamic time warping, Knowledge based approaches, Statistical based approaches, Learning based approaches, The artificial intelligence approach, Stochastic Approach [2–4].

This paper discussing the large vocabulary speaker dependent and speaker independent isolated Kannada word recognition using Syllable, HMM and Normal fit technique and compared with HMM and GMM, for the memory size required in storing the speech model and accuracy of recognition. This paper also discuss on large vocabulary continuous Kannada speech recognition for speaker dependent and speaker independent using syllable, combination of HMM and normal fit technique and tri-syllable language model.

The remaining part of the paper is organized into four different sections; Sect. 2 deals with the Text corpus and speech database creation. Section 3 deals with proposed model. Section 4 deals with Experimentation. Section 5 deals with discussion and conclusion.

## 2 Text Corpus and Speech Database Creation

Text corpus of 10 million words has collected from Dr. K. Naryana Murthy, Professor, Department of Computer and Information science, University of Hyderabad, Hyderabad, India in the year 2011. The top 10,000 words most frequently occurred in this corpus are taken. These 10,000 words have occurred 6 million times in Hampi text corpus. Those 10,000 words are record at sampling rate of 8 kHz, 16 bps, mono channel by one adult male speaker by uttering 3 times each word for training and rerecorded each word for testing purpose. These signals were recorded at a little noisy environment, while Gold Wave Software was used to record with the help of mini microphone of frequency response of 50–12,500 Hz.

Secondly Kannada speech corpus is designed for selected 294 words to design the speaker independent recognition model. We have taken age group of 16–60 years native Kannada speakers. Here 5 districts dialects are recorded namely Mysore, Bangalore, Mandya, Chamarajnagar and Ramanagar districts located at southern part of Karnataka state. The signals are recorded at the sampling rate of 8 kHz, 16 bps with mono channel using mini microphone of frequency response of 50–12,500 Hz.

Thirdly, continuous Kannada speech corpus is designed by randomly selecting 250 sentences from Hampi text corpus. The details are shown in Table 1.

Fourthly, continuous Kannada speech designed by IIIT Hyderabad is collected, which consist of 1,000 unique sentences recorded at room environment and pulse code modulation with a frequency of 16,000 Hz/s and 16-bit mono channel.

**Table 1** Continuous Kannada speech corpus designed by us for randomly selected sentences from Hampi text corpus

Language	Kannada
Speech type	Sentence read from documents
Number of sentences used	250 Sentence for minimum length of 2 words, maximum length of 47 words
Number of unique words	2,419 Words
Number of speakers for training	20 Speakers (10 female + 10 male)
Number of speakers for testing	2 (known) + 2 (unknown) = 4 female and 4 male, total = 8 speakers
Speech sampling rate	16 kHz/s, 16 bit mono channel
Recording conditions	Room environment
Number of signals used to training	5,000 Signals
Number of signals used to testing	2,000 Signals
Total signals using in experiment	7,000 Signals
Age categories	19–60 years aged
Total hours of recording	30 h
Total memory size	1.43 GB



### 3 Proposed Method

In this experiment we have designed algorithm in five stages for speaker dependent, speaker independent isolated Kannada word recognition and continuous Kannada speech. The proposed model works in offline mode. So all speech signals are pre-recorded and stored in speech database and then passed on to our algorithm for training or testing the unknown signal.

First stage is Pre-processing stage: In this stage analog speech signal is sampled and quantized at the rate of 8,000 samples/s or 16,000 samples/s.  $S(n)$  is the digitalized value. Then DC component is removed from digitalized sample value using the formula  $S(n) = S(n) - \text{mean}(S)$ . A first order (low-pass) pre-emphasis  $\hat{s}(n) = S(n) - \tilde{a} * S(n - 1)$  network formula is used to compensate for the speech spectral fall-off at higher frequencies and approximates the inverse of the mouth transmission frequency response. Then standardization is done to entire set of values to have standards amplitude. This process will increases or decreases the amplitude of speech signal using the  $S(n) = \hat{s}(n) - \max(|s|)$ . Here we have used the constant value  $\tilde{a} = 0.9955$ .

The second stage is Detection of Voiced/Unvoiced part in speech signal, also called speech signal segmentation. To solve this problem, using dynamic threshold approach, we have designed an algorithm for automatic segmentation of speech signal into sub-word or syllable [5]. Here we have combined the short time energy and magnitude of frame. Dynamic threshold for each frame is detected. Lastly, it is checked for voiced part in that frame using that frame threshold. This is achieved by following these steps

$$Thr_{STE} = \left( \left[ \frac{\sum_{i=1}^n STE}{n} \right] - [\min(STE) * 0.5] \right) + \min(STE) \quad (3.1)$$

$$Thr_{msf} = \left( \left[ \frac{\sum_{i=1}^n msf}{n} \right] - [\min(msf) * 0.6] \right) + \min(msf) \quad (3.2)$$

$$\text{if } (STE \geq Thr_{STE}) \text{ then marked has } Voiced_{STE} = 1 \quad (3.3)$$

$$\text{if } (msf > Thr_{msf}) \text{ then marked has } Voiced_{msf} = 1 \quad (3.4)$$

*if* ( $Voiced_{STE} * Voiced_{msf} = 1$ ) *then*  
*that frame contains voice, otherwise its unvoiced frame*

where STE is Short Time Energy, msf is the Magnitude of Frame, n is number of samples in the frame.

Feature Extraction is the Third stage: Here we have selected the voiced part of signal and then frame blocking was done for N samples with adjacent frames spaced M samples apart. Typical values for N and M correspond to frames of 20 ms duration with adjacent frames overlap by 6.5 ms. A hamming window is applied to each frame using frame same size. Next, the autocorrelation is applied to that part of

signal. LPC method is applied to detect LPC coefficients. The LPC coefficients are converted into Real Cepstrum Coefficients. Here the outputted data will be of the size  $p * L$ , where  $p$  is the LPC order and it will be constant and  $L$  is the number of frames in that voice segmented parts. So it varies. In our experiment we have used LPC order  $p = 24$ .

The Fourth stage is Speech model building: In this stage the real cepstrum coefficients are in dimension of  $p*L$  matrices. This matrix will be passed into k-means algorithm by keeping  $k = 3$  and outputted values are passed into 3 state Baum–Welch algorithm and each syllable or sub-word is trained. The Baum-Welch re-estimation procedure is the stochastic constraints of the HMM parameters

$$\sum_{i=1 \dots N} \bar{\pi}_i = 1 \quad (3.5)$$

$$\sum_{j=1 \dots N} \bar{A}_{ij} = 1, 1 \leq i \leq N \quad (3.6)$$

$$\sum_{k=1 \dots M} \bar{B}_j(k) = 1, 1 \leq j \leq N \quad (3.7)$$

Are automatically incorporated at each iteration. The parameter estimation problem as a constrained optimization of  $P(O|\lambda)$ . Based on a standard Lagrange optimization setup using Lagrange multipliers,  $P$  is maximized by

$$\pi_i = \frac{\pi_i(\partial P / \partial \pi_i)}{\sum_{k=1 \dots N} \pi_k(\partial P / \partial \pi_k)} \quad (3.8)$$

$$A_{ij} = \frac{A_{ij}(\partial P / \partial A_{ij})}{\sum_{k=1 \dots N} A_{ik}(\partial P / \partial A_{ik})} \quad (3.9)$$

$$B_j(k) = \frac{B_j(k)(\partial P / \partial B_j(k))}{\sum_{l=1 \dots M} B_j(l)(\partial P / \partial B_j(l))} \quad (3.10)$$

Normal fit is applied for 2 consecutive HMM parameter  $\lambda(A, B, \pi_i)$  and Normal fit parameters are computed. Her the trained two consecutive  $\lambda(A, B, \pi_i)$  are considered has sample data. So, we will be having a sample  $(x_1 \dots x_n)$ , for this a normal parameter  $(N(\hat{\mu}, \hat{\sigma}^2))$  is computed by using the

$$\hat{\mu} = \bar{x} \equiv \frac{1}{n} \sum_{i=1}^n x_i \quad \text{and} \quad \hat{\sigma}^2 \sim \frac{\sigma^2}{n} \cdot X_{n-1}^2 \quad (3.11)$$

The labeled  $\hat{\mu}$  and  $\hat{\sigma}^2$  value will be classified according to acoustic classes and then stored. Those data have representatives of syllables or sub-words in that particular class. In Language model we have designed bi-syllable language model for each isolated word and tri-syllable language model for continuous speech.

The Fifth stage is Recognition part/Testing Unknown Signal: Initially, for the unknown speech signals HMM parameters are computed and passed into normal fit method. Subsequently, the outputted  $\hat{\mu}$  and  $\hat{\sigma}^2$  value is identified and then matched with trained set of data by retaining threshold values. The outputted syllables or sub-words are matched with the bi-syllable language model. The concatenation of outputted syllables and sub-words are done for word building. On this basis decision is taken has recognized word by checking for top ranked.

## 4 Experimentation

In this paper experimentation are done on recognition of isolated Kannada words and continuous Kannada speech using HMM (3 state Baum-Welch Algorithm alone), GMM and compared with proposed model for same speech database. All experiment programs are written in mat lab and ruined on Intel Core i5 processor speed of 2.67 GHz and RAM of 3 GB. Table 2 shows the details of memory required to storing speech models for different vocabulary size, figures are in Kilo bytes and also shows the average accuracy rate for different size of vocabulary. This shows that our model requires the less memory to store speech models.

The average WRR for IIIT Hyderabad speech corpus is 95.87 % and average WER is 4.13 %. The average WRR for randomly selected 250 sentences from Hampi text corpus is 86.5 % and average WER is 13.5 %. Our model is tested on noised (little) and noiseless signal and the average success rate of noised continuous Kannada speech signals for known speaker and unknown speaker is 81 %.

**Table 2** Shows the average accuracy rate measured with different vocabulary size

Methods / words	HMM		GMM		HMM + Normal fit	
	Accuracy rate (%)	Memory size	Accuracy rate (%)	Memory size	Accuracy rate (%)	Memory size
1,000 Words	83.45	564	91.90	368	92.98	340.92
2,000 Words	82.99	1,128	91.54	736	92.13	681.84
3,000 Words	82.21	1,692	91	1,104	92.02	1,022.76
4,000 Words	82.01	2,259.2	90.78	1,473.6	92.73	1,363.2
5,000 Words	81.90	2,825	90.12	1,843	92.69	1,704.4
6,000 Words	81.77	3,390	90.01	2,211.6	91.11	2,045.28
7,000 Words	81.01	3,954.44	89.05	2,579.64	90.30	2,385.88
8,000 Words	80.32	4,519.36	88.75	2,948.16	89.44	2,726.72
9,000 Words	80.15	5,084.28	88.66	3,316.68	89.42	3,066.84
10,000 Words	80.05	5,648.4	88.45	3,685.6	89.39	3,407.6
Average	81.59		90.03		91.22	

Memory required storing the speech models shown in kilobytes

## 5 Discussion and Conclusion

In this paper, ASR model is designed by combination of HMM and Normal fit method and experimented for recognizing the isolated Kannada words and continuous Kannada speech. Our ASR model is compared with HMM (3-state Baum-Welch Algorithm alone) and GMM for same speech database. The space required to store the model datum has syllable or sub-word representatives in the HMM and GMM required more memory than storing the normal fit parameters. A normal fit method shows the better accuracy rate then the other two methods. This experiment shows that using normal fit (Normal Parameter estimation), ASR model can be designed and it takes less space with good accuracy rate compared to GMM and HMM models. Using our model ASR can be designed for small, medium and large vocabulary. And also ASR can be design for speaker dependent, speaker independent mode of working and isolated word, connected words and continuous speech.

**Acknowledgments** The authors would like to thank for Bharathiar University for giving an opportunity to pursuing part-time Ph.D. degree. Authors would like to thanks for all our friends, reviewers and Editorial staff for their help during preparation of this paper.

## References

1. Swamy, P.P., Guru, D.S. (eds.): Multimedia Processing, Communication and Computing Applications. Lecture Notes in Electrical Engineering, vol. 213, pp. 333–345. Springer, India. doi:10.1007/978-81-322-1143-3\_27 (2013)
2. Hemakumar, G., Punitha, P.: Speech recognition technology: a survey on Indian languages. *Int. J. Inf. Sci. Intell. Syst.* **2**(4), 1–38 (2013)
3. Gaikwad, S.K., et al.: A review on speech recognition technique. *Int. J. Comput. Appl.* (0975–8887) **10**(3), 16–24 (2010)
4. Rabiner, L., Jung, B.-H.: Fundamentals of Speech Recognition. Pearson Education, Singapore (1993)
5. Hemakumar, G., Punitha, P.: Automatic segmentation of Kannada speech signal into syllables and sub-words: noised and noiseless signals. *Int. J. Sci. Eng. Res.* **5**(1), 1707–1711 (2013)
6. Mat lab R2009a help menu on statistics toolbox online: [www.mathworks.com/help/](http://www.mathworks.com/help/)
7. [http://en.wikipedia.org/wiki/normal\\_distribution#cite\\_note-kri127-33](http://en.wikipedia.org/wiki/normal_distribution#cite_note-kri127-33)
8. <http://www.mathworks.in/help/stats/statset.html>
9. David, D.: Expectation-Maximization: Application to Gaussian Mixture Model Parameter Estimation. Lecture Notes Published on April 23 (2009)
10. Rabiner, L.R., et al.: Speaker-independent recognition of isolated words using clustering techniques. *IEEE Trans. Acoust. Speech Sig. Process.* **27**(4), 336–349 (1979)
11. Carlo, T.: Estimating Gaussian Mixture Densities with EM—A Tutorial. Duke University
12. Dimov, D., Azmanov, I.: Experimental specifics of using HMM in isolated word speech recognition. In: International Conference on Computer Systems and Technologies—CompSysTech (2005)
13. Grewal, S.S., Kumar, D.: Isolated word recognition system for English language. *Int. J. Inf. Technol. Knowl. Manag.* **2**(2), 447–450 (2010)

14. Nandyala, S.P., Kishore Kumar, T.: Real time isolated word recognition using adaptive algorithm. In: International Conference on Industrial and Intelligent Information (ICII 2012), IPCSIT, vol. 31 © (2012). IACSIT Press, Singapore (2012)
15. Revathi, A., et al.: Text independent speaker recognition and speaker independent speech recognition using iterative clustering approach. *Int. J. Comput. Sci. Inf. Technol. (IJCSIT)* **1** (2), 30–40 (2009)
16. Das, B.P., Parekh, R.: Recognition of isolated words using features based on LPC, MFCC, ZCR and STE, with neural network classifiers. *Int. J. Mod. Eng. Res. (IJMER)* **2**(3), 854–858 (2012)

# Optimization of Ultra Wide-Band Printed Monopole Square Antenna Using Differential Evolution Algorithm

Sharmin Shabnam, Suvrajit Manna, Udit Sharma  
and Pinaki Mukherjee

**Abstract** A very rapid growth in wireless communication demands antennas with wider bandwidth range to carry out various applications. In this context, ultra wide-band (UWB) technology has gathered a lot of interest because of its substantial bandwidth. In this paper, a novel Differential Evolution (DE) based optimization technique has been proposed to design a UWB printed square monopole antenna. The errors for desired lower band edge frequency and bandwidth are minimized to obtain the parameters of the antenna. These results have been compared with that of Genetic Algorithm (GA) and Particle Swarm Optimization (PSO). Simulation results are given to show the performance of the proposed technique. A 2:1 VSWR bandwidth of 7.2 GHz (4.2–11.4 GHz) is achieved with the help of Differential Evolution (DE).

**Keywords** Differential evolution (DE) · Ultra wide-band (UWB) · Genetic algorithm (GA) · Particle swarm optimization (PSO)

---

S. Shabnam (✉)

Department of Electronics and Communication Engineering, Dumkal Institute of Engineering and Technology, Murshidabad, India

e-mail: sharminshabnam1982@gmail.com

S. Manna · U. Sharma

Department of Electronics and Communication Engineering, Institute of Engineering and Management, Kolkata, India

e-mail: suvrajit.94@gmail.com

U. Sharma

e-mail: uditsharma015@hotmail.com

P. Mukherjee

Department of Electronics and Communication Engineering, Jalpaiguri Government Engineering College, Jalpaiguri 735102, India

e-mail: pinakimail@yahoo.co.in

© Springer India 2015

J.K. Mandal et al. (eds.), *Information Systems Design and Intelligent Applications*,

Advances in Intelligent Systems and Computing 339,

DOI 10.1007/978-81-322-2250-7\_9

## 1 Introduction

Ultra wide-bandwidth (UWB) wireless technology is mostly used for very high-data-rate short-range wireless communication systems with low probability of interception [1, 2]. UWB systems transmit signals across a much wider bandwidth than the conventional systems. According to Federal Communication Commission, UWB should have bandwidth of 7.5 GHz (3.1–10.6). Printed monopole antenna (PMA) is a good candidate for UWB technology. They come in various geometrical shapes like hexagonal, square, circular, rectangular etc. This paper describes the method of optimization of Printed square monopole antenna using Differential Evolution. Differential Evolution (DE) [3, 4] algorithm is a branch of evolutionary programming developed for optimization problems over continuous domains. DE is a variant of Genetic Algorithm (GA). The advantages of DE are its simple structure, ease of use, speed and robustness. The idea is to design an antenna that will have a pre-defined bandwidth with a specific lower and upper band-edge frequency. Parameters like length of the antenna ( $L$ ) and length of the  $50 \Omega$  feed line from the ground surface to the printed patch ( $p$ ) are optimized for the desired bandwidth and lower band-edge frequency. Length, width and feed line length of a printed monopole antenna can be simultaneously varied to obtain optimized dimensions for a given lower band-edge frequency. But that is a computationally tedious and time-consuming process. In the present work optimized values of the parameters are obtained from the optimization program, and the antenna is designed with these parameters. In most of the designs of UWB antennas reported so far, either the patch shape is modified or some modifications are introduced in the ground plane [5–8]. In this paper the ultra wide bandwidth is obtained without incorporating any complex modification in the basic structure of the printed monopole antenna. In this way this work is novel and useful for practicing engineers as compared to other techniques. Results obtained from DE algorithm are compared with that of PSO and GA.

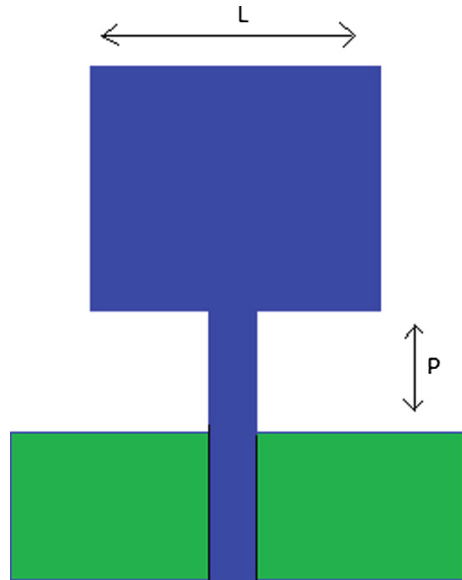
## 2 Printed Monopole Antenna Design

The estimation of lower band-edge frequency of printed monopole antennas is attained using the standard modified formula given for cylindrical monopole antenna [9]. For a PMA lower frequency can be written as

$$f_L = \frac{7.2}{[(L + r + p) \times k]} \text{ GHz} \quad (1)$$

where  $L$  is the height of the planar monopole antenna in cm, which is taken same as that of equivalent cylindrical monopole,  $r$  in cm is the effective radius and  $p$  is the length of the  $50 \Omega$  feed line from the ground surface to the printed patch, whereas  $k$  is

**Fig. 1** A square printed monopole antenna



the empirical constant of the substrate whose value is given by 1.15. The design configuration featuring a printed square monopole antenna (PSMA) is shown in Fig. 1.

For a PSMA, the variables  $L$  and  $r$  are given as

$$L = W(\text{width}) \text{ cm,}$$

$$r = L/2\pi \text{ cm.}$$

Thus the generalised Eq. (1) can be defined as,

$$f_L = \frac{14.4\pi}{[L(2\pi + 1) + 2\pi r]k} \text{ GHz,} \quad (2)$$

### 3 Differential Evolution Algorithm

Differential Evolution is a stochastic, population based optimization algorithm. The advantages of DE are its simplicity, high performance and reliability, few control parameter and low space complexity. This technique has been applied very efficiently to find approximate solutions for problems that are non-differentiable, non-continuous, non-linear, noisy, flat and multi-dimensional or have many local minima. DE is based on real-value operators. It consists of four steps, Initialization, Mutation, Crossover and Selection. The user defined crossover and mutation



parameters has significant impact on the performance of the algorithm [10]. The different steps of Differential Evolution technique are given below:

(a) *Initialization*

Firstly the population is randomly generated within the search space. DE maintains this population of agents which are iteratively combined and updated using the following formula to form new agents.

$$x_{i,G}^j = x_{min}^j + \text{rand}(0, 1) * (x_{max}^j - x_{min}^j) \quad (3)$$

(b) *Mutation*

For a given parameter vector  $x_{i,G}$  three vectors  $x_{r1,G}$ ,  $x_{r2,G}$  and  $x_{r3,G}$  are selected randomly where  $i$ ,  $r_1$ ,  $r_2$  and  $r_3$  are distinct. A mutant vector is generated from three random vectors using the following formula:

$$v_{i,G+1} = x_{r1,G} + F(x_{r2,G} - x_{r3,G}) \quad (4)$$

where  $F$  is a user defined parameter ranging between  $(0, 1)$ .

(c) *Crossover*

In this step, the target vector is mixed with the mutant vector to produce a trial vector. A trial vector  $u_{i,G+1}$  is generated from the elements of the target vector  $x_{i,G}$  and of the mutant vector  $v_{i,G+1}$  using a user defined crossover probability parameter  $CR$ . crossover constant ( $CR$ ), ranging between  $(0, 1)$  actually represents the probability that the trial vector inherits the parameter values from the mutant vector.

$$u_{j_i,G+1} = v_{j_i,G+1}; \quad \text{if } (\text{rand}^j \leq CR) \\ = x_{i,G} \quad \text{otherwise} \quad (5)$$

(d) *Selection*

Lastly, the fitness values of trial vector  $u_{i,G+1}$  and target vector  $x_{i,G}$  is compared and one with better fitness value is retained for the next generation. The process is continued until terminal criterion is satisfied.

## 4 Optimization of Cost Function

The lower band-edge frequency ( $f_L$ ) of printed monopole antennas is a function of antenna dimensions and feed line length above the ground plane. The bandwidth also depends on the ground-plane dimension. The optimization is aimed to minimize two cost functions. These functions are as follows:

$$F(1) = f_{L,desired} - f_{L,calculated} \quad (6)$$

$$F(2) = BW_{\text{desired}} - BW_{\text{calculated}} \tag{7}$$

where  $f_{L_{\text{desired}}}$  is the desired low band-edge frequency and  $BW_{\text{desired}}$  is the desired bandwidth of the antenna. The parameters selected for optimization are square monopole antenna length  $L$  and length of the feed line from ground surface  $p$ .

Parameters chosen for optimization using DE:

1. Population size: 20
2. Crossover constant: 0.6
3. Differential mutation constant (F): 0.4

## 5 Results and Discussion

Table 1 shows optimized geometric dimensions of PSMA for different lower edge frequencies using DE algorithm. Though the UWB range covers from 3.1 to 10.6 GHz, other sets of lower edge frequency, bandwidth, and quality factor are also considered for proving the validity of the optimization technique. For each set, optimized values of  $L$  and  $p$  have been obtained for PSMA. Table 2 shows the comparison of results obtained with GA, PSO and DE algorithm. Figures 2 and 3 show the simulated VSWR plot for PSMA optimized with 3.1 and 4.8 GHz as the

**Table 1** Optimized values of antenna geometric dimensions, lower band-edge frequencies and bandwidth for PSMA using DE algorithm

Desired frequency (GHz)	Calculated frequency (GHz)	Geometric dimensions		Bandwidth	
		L (cm)	P (cm)	Desired (GHz)	Calculated (GHz)
3.1	3.09990076	0.9108	0.3936	7.5	7.500099
4.8	4.7998	0.9179	0.2404	5.8	5.8002
7.4	7.3995	0.7001	0.0346	3.2	3.2005
8.5	8.5001	0.5499	0.0992	2.1	2.0999
10.2	10.19989	0.3386	0.2213	0.4	0.40011

**Table 2** Comparison of results of GA, PSO and DE algorithm

Desired lower frequency (GHz)	Desired band-width (GHz)	Optimized using GA		Optimized using PSO		Optimized using DE	
		Lower frequency (GHz)	Bandwidth (GHz)	Lower frequency (GHz)	Band-width (GHz)	Lower frequency (GHz)	Band-width (GHz)
3.1	7.5	3.3569	7.2431	3.1583	7.4417	3.0999	7.500099
4.8	5.8	4.8205	5.7795	4.8930	5.7070	4.7998	5.8002
7.4	3.2	7.8045	2.7955	7.7008	2.8992	7.3995	3.2005
8.5	2.1	8.7391	1.8609	8.9003	1.6997	8.5001	2.0999
10.2	0.4	10.248	0.352	10.275	0.3250	10.199	0.40011

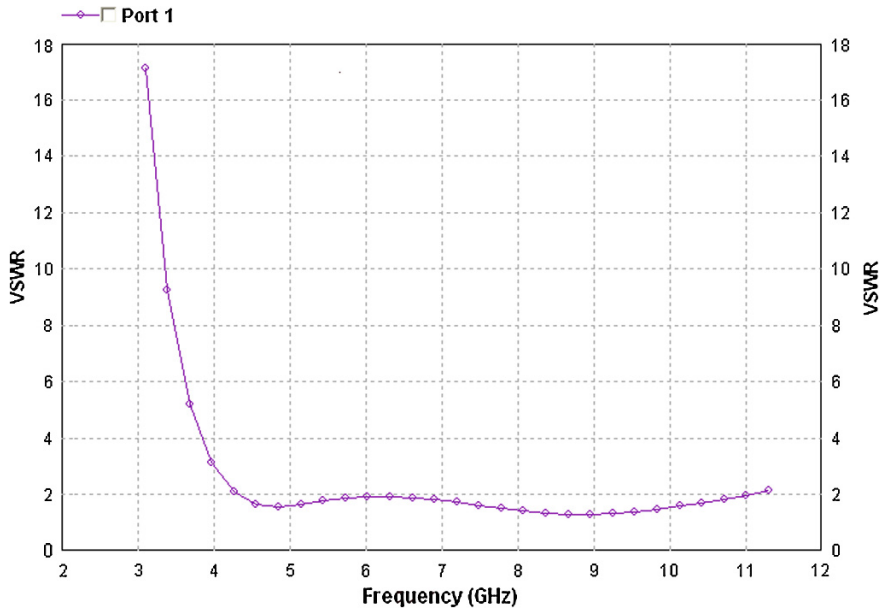


Fig. 2 Simulated VSWR plot for the UWB printed square monopole antenna optimized at 3.1 GHz lower band-edge frequency

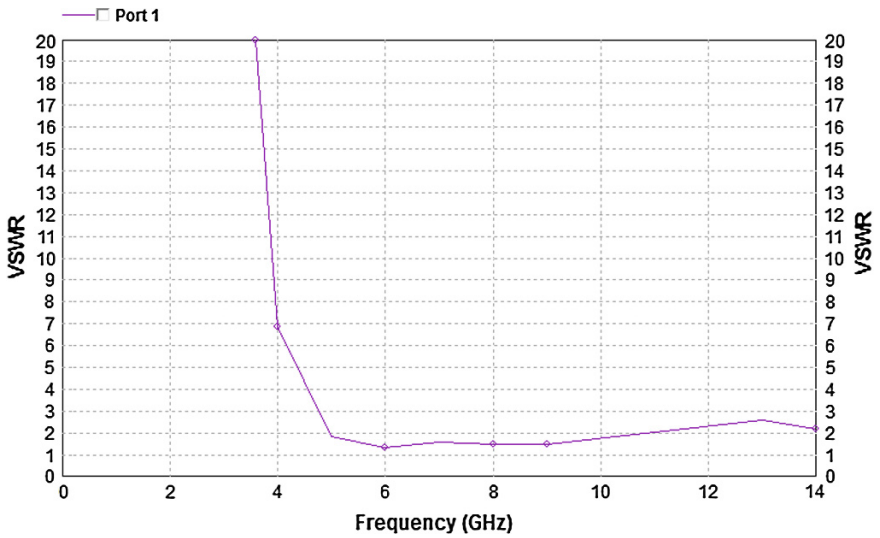
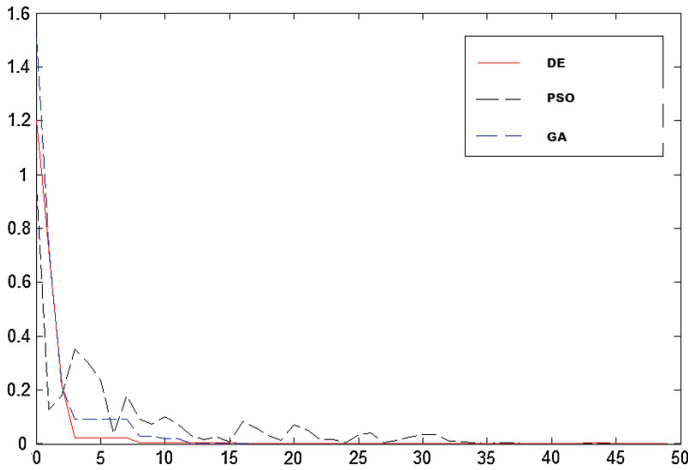


Fig. 3 Simulated VSWR plot for the UWB printed square monopole antenna optimized at 4.8 GHz lower band-edge frequency

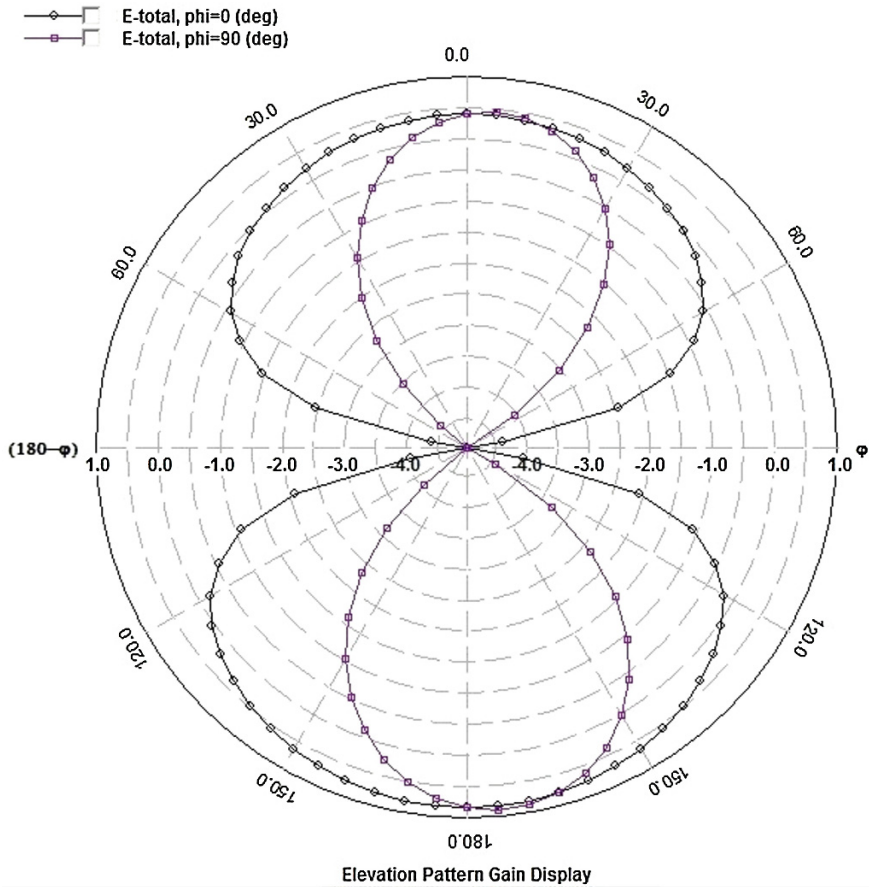


**Fig. 4** Best fitness plots of DE, PSO and GA

lower edge frequency respectively. Simulations are done using ZelandIE3D software. Ground plane dimensions were set at  $10 \text{ mm} \times 2 \text{ mm}$ . In Fig. 4, best fitness plot using DE is compared with that obtained using GA and PSO. Figure 5 shows the radiation pattern for a printed square monopole antenna designed using DE.

## 6 Conclusions

The method of designing UWB printed square monopole antenna using Differential Evolution technique is presented in this paper. The results obtained with DE algorithm are compared with that of PSO and GA. Table 2 shows that the bandwidth achieved with DE algorithm is better than that obtained using GA and PSO. In case of DE, the convergence rate is much better than that obtained with PSO and GA. It can be seen from Fig. 2 that the lower edge frequency has been shifted from the desired value of 3.1 GHz. But it can also be seen that the VSWR is within the value of 2 from 4.2 to 11.4 GHz with an operational bandwidth of 7.2 GHz. On the other hand Fig. 3 shows almost perfect bandwidth ranging from 4.9 to 10.6 GHz. The imperfections in the bandwidth in the first case can be nullified by properly choosing the ground plane dimensions and tuning the optimization parameters. So this computationally efficient method may be extended for design of printed monopole antennas for other ranges of microwave frequencies. The basic structure of the antenna is retained while obtaining the bandwidth. In this way this method is superior as compared to other techniques.



**Fig. 5** Radiation pattern of printed square monopole antenna designed using DE

## References

1. Astanin, L.Y., Kostylev, A.A.: Ultra wideband signals—a new step in radar development. *IEEE AES Syst. Mag.* **7**, 12–15 (1992)
2. FCC report and order on ultra wideband technology. Technical Report FCC02-48. Federal Communications Commission, Washington, DC, USA (2002)
3. Storn, R., Price, K.: Differential Evolution—a simple and efficient heuristic for global optimization over continuous spaces. *J. Global Optim.* **11**, 341–359 (1997). doi:[10.1023/A:1008202821328](https://doi.org/10.1023/A:1008202821328)
4. Qin, A.K., Huang, V.L., Suganthan, P.N.: Differential evolution algorithm with strategy adaptation for global numerical optimization. *IEEE Trans. Evol. Comput.* **13**(2), 398–417 (2009)
5. Khan, S.N., Hu, J., Xiong, J., He, S.: Circular fractal monopole antenna for low VSWR UWB applications. *Prog. Electromagnet. Res. Lett.* **1**, 19–25 (2008)

6. Sim, C.-Y.-D., Chung, W.-T., Lee, C.-H.: Compact slot antenna for UWB applications. *Antenna Wirel. Propag. Lett.* **9**, 63–66 (2010)
7. Gupta, T., Singhal, P.K.: Ultra wideband slotted microstrip patch antenna for downlink and uplink satellite application in C band. *Int. J. Innov. Appl. Stud.* **3**(3), 680–684 (2013)
8. Zhang, X.-Y., Liu, S.-B., Li, C.-Z., Bian, B.-R., Kong X.-K.: A novel fractal patch antenna for UWB applications. In: *Progress in Electromagnetics Research Symposium Proceedings*, pp. 272–275, Suzhou, China, 12–16 Sept 2011
9. Kumar, G., Ray, K.P.: *Broad Band Microstrip Antennas*. Artech House, Boston (2003)
10. Storn, R.: On the usage of differential evolution for function optimization. In: *Biennial Conference of the North American Fuzzy Information Processing Society (NAFIPS)*, pp. 519–523, Berkeley, CA, USA (1996)

# An Efficient Cloud Network Intrusion Detection System

Partha Ghosh, Abhay Kumar Mandal and Rupesh Kumar

**Abstract** Cloud Computing is an Internet based Computing where virtual shared servers provide software, infrastructure, platform and other resources to the customer on pay-as-you-use basis. With the enormous use of Cloud, the probability of occurring intrusion also increases. Intrusion Detection System (IDS) is a stronger strategy to provide security. In this paper, we have proposed an efficient, fast and secure IDS with the collaboration of multi-threaded Network Intrusion Detection System (NIDS) and Host Intrusion Detection System (HIDS). In the existing system, Cloud-IDS capture packets from Network, analyze them and send reports to the Cloud Administrator on the basis of analysis. Analysis of packets is done using K-Nearest Neighbor and Neural Network (KNN-NN) hybrid classifier. For training and testing purpose here we have used NSL-KDD dataset. After getting the report from the Cloud-IDS, Cloud Service Provider (CSP) will generate an alert for the user as well as maintain a loglist for storing the malicious IP addresses. Our proposed model handles large flow of data packets, analyze them and generate reports efficiently integrating anomaly and misuse detection.

**Keywords** IDS · KNN · NN · Multi-threaded NIDS · HIDS · Anomaly detection · Misuse detection

---

P. Ghosh (✉) · A.K. Mandal · R. Kumar  
Information Technology, Netaji Subhash Engineering College, Kolkata, India  
e-mail: partha1812@gmail.com

A.K. Mandal  
e-mail: abhaynsecit@gmail.com

R. Kumar  
e-mail: kumar.rupesh708@gmail.com

## 1 Introduction

Cloud Computing is the next stage in the Internet's evolution. It brings a revolution in IT world by using the Internet services. Cloud Computing provides data and services availability assurance, and quick accessibility and scalability [1]. Cloud Service Providers offer services according to several fundamental models—Infrastructure as a Service (IaaS), Platform as a Service (PaaS) and Software as a Service (SaaS) [2]. IaaS is the most basic Cloud service model in which they provide resources like, physical or virtual machines. In PaaS model, they deliver a Computing platform, typically including Operating System (OS), programming language execution environment, database and web server. In case of SaaS model, they install and operate application software in the Cloud. The Cloud is a virtualization of resources that is managed and maintained by itself. Virtualization provides additional cost-saving benefits as well as enhances speed and flexibility. Most Clouds are built on virtualized infrastructure technology [3]. Virtualization of system and distributed nature makes Cloud infrastructure more effective and as it runs through standard Internet protocol, Cloud are easy targets for intruders due to much vulnerabilities involved in it [4]. So far as security and privacy are concerned, these are the challenging issues for Cloud Computing. The unauthorized access to a system by an intruder is commonly referred to as an intrusion. A Firewall is a crucial component which used as a security guard, placed at the entry point between a private network and the outside Internet network, such that all incoming and outgoing packets have to pass through it. The function of Firewall is to examine every incoming or outgoing packet and decide whether to accept or discard it [5]. In spite of this security maintenance, secured access for Cloud user can't be guaranteed. So to further provide a secure Cloud environment, an IDS model has been proposed in this paper. The Intrusion Detection System (IDS) can be employed as a strong defensive mechanism, as complete security cannot be provided by traditional Firewall [6]. An IDS is a device or software application, which identifies the intrusion and raise alarms for the system administrator [7]. To detect the intrusion, an IDS mainly uses two technique—Misuse (signature based) detection and Anomaly detection. Misuse detection technique is a knowledge based detection system where predefined rules or signature of attacks has already formed that can be used to resolve by pattern matching of known attack. Hence, unknown and variation of known attacks are failed to identify by misuse detection. In case of Anomaly detection, it is a behavior based detection system that defines and characterizes normal behavior of the system. Whenever action deviates from the expected behavior, are considered as anomalies. Therefore, it can be able to detect known as well as unknown attacks [8]. An IDS is basically divided into two types according to its working environment—NIDS and HIDS [9]. A Network based Intrusion Detection System (NIDS) is one that monitor, detect and raises alerts on suspect intrusion to administrative user for network traffic. A Host based Intrusion Detection System (HIDS) is used to monitor and detect the intrusion by keeping the



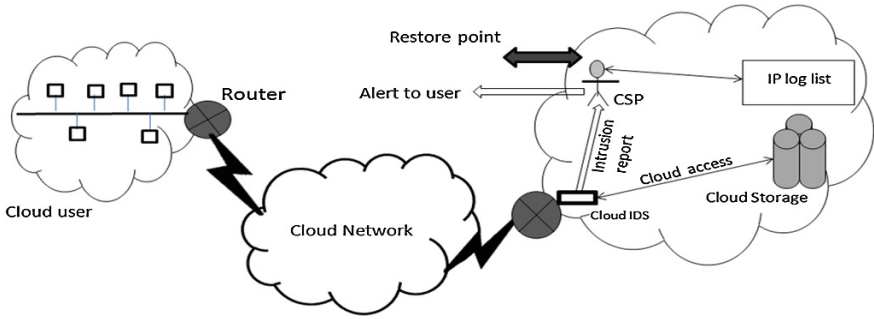
information of a specific host machine and raises alerts to the system administrator. To provide security, here in this paper, we have introduced efficient IDS with the help of Multi-threaded NIDS.

## 2 Related Works

In 2012, Kholidy and Baiardi [10] developed a framework for Cloud based Intrusion Detection System (CIDS) to solve the deficiencies of current Intrusion Detection Systems (IDS). In their system, to increase attacks coverage, CIDS integrates knowledge-based and behavior-based approaches and monitors each node to identify local events. In 2011, Al-Janabi and Saeed [11] developed an anomaly-based Intrusion Detection System which can quickly detect and classify various attacks. They have used Back Propagation Artificial Neural Network to learn system's behavior. KDD'99 data set is used in their experiment and the obtained result satisfies their work objective. In 2010, Mazzariello et al. [12] developed a model, in which the issue of detecting Denial of Service (DoS) attacks are performed by means of resources acquired on demand, on a Cloud Computing platform. The model was used to investigate the consequences of a distributed strategy to detect and block attacks, or other malicious activities, originated by misbehaving customers of a Cloud. In 2010, Bakshi and Yogesh [13] developed an algorithm to secure Cloud from DDOS attacks using Intrusion Detection System in Virtual Machine (VM). That model shows that the IT virtualization strategy can be used to response the Denial of Service attack. In 2009, Ghali [14] has presented a new hybrid algorithm Rough Set Neural Network Algorithm (RSNNA), used to significantly reduce a number of computer resources, both memory and CPU time, and required to detect attacks. The algorithm uses Rough Set Theory in order to reduce features and trained by an Artificial Neural Network to identify any kinds of new attack.

## 3 Proposed Model

The Cloud technology is now widely spread all over and is used frequently with easy access, but with this popularity to maintain security is still an issue of concern. The user requests for the desired data or resources are made through the network. Further approaches are utilized to rescue these requests and respond to those requests. As the Cloud service is truly concerned with the request made by the clients, special arrangements are made to secure these requests from the intruders. The attackers may try to manipulate the user desired request; this process is called an intrusion and is controlled with the help of Intrusion Detection System (IDS). In this regard, our proposed model works fit for the easy and safe execution of the task performed by the Cloud user, shown in Fig. 1.



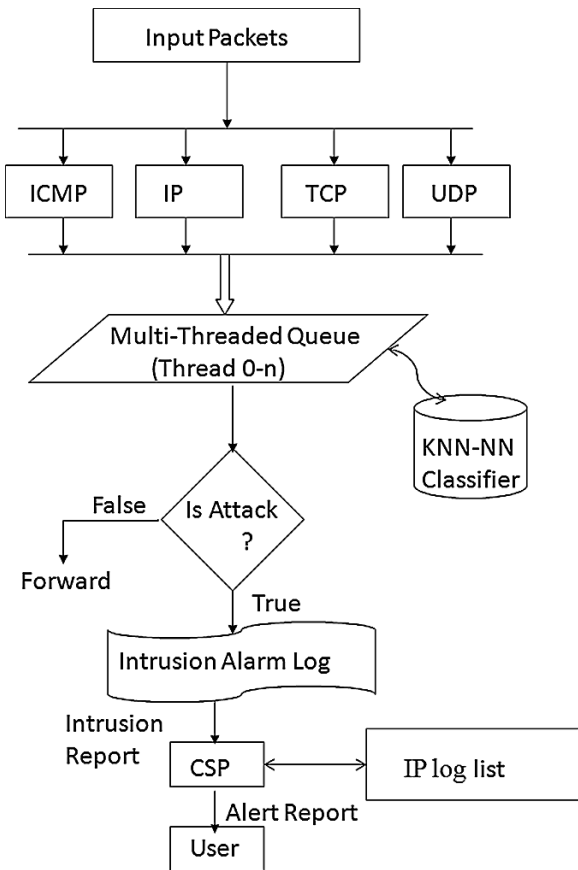
**Fig. 1** Intrusion detection system in cloud environment

In our proposed model, network maintenance or monitoring device called NIDS is used at the bottleneck position of the network. In this model, for intrusion detection, we have used multi-threaded NIDS to monitor the requests send by the user. To overcome the large network traffic and for easy process, the multi-threaded approach is performed. The requests made from the client end are processed with the help of NIDS, incorporated within Cloud-IDS. The Multi-threaded NIDS model for Cloud environment is basically based on three modules—Capture and Query module, Analysis module and Reporting module. The capture module performs the task of capturing and receiving inbound and outbound (ICMP, TCP, IP, UDP) data packets. As large amount of data packets entered into the NIDS, the Capture and Query module first allocates and arrange them in an ordered manner and place them into a shared queue. Further the ordered packets are approached and received as test case for the Analysis part as shown in Fig. 2.

The packets captured from the shared queue are passed to the analysis phase, are finely analyzed with the help of multiple threads concurrently processing there. The Reporting module responds to the analyzed results and notifies the Administrator about the intrusion happened. After capturing all the packets for the analysis purpose, the multiple threads would consistently process and tries to test with the help of KNN-NN classifier. The classifier is already trained by using NSL-KDD data set. The deviated packets from the normal action are further analyzed for Misuse detection. In Misuse detection process, the packets are matched for any of the four attacks DOS, Probe, U2R, and R2L. The analysis process continues in a collaborative manner to enhance the system performance and packet execution.

In our IDS, we have used a Hybrid Multilevel KNN-NN classifier. For any incoming packet, we perform anomaly detection using K-Nearest Neighbor algorithm (KNN). KNN acts as a binary classifier and classifies an action as ‘normal’ or ‘abnormal’. For all the packets classified as ‘abnormal’, an Artificial Neural Network (ANN) is used to perform misuse detection and sub classifies them into specific attack types, shown in Fig. 3. For training our hybrid classifier, we have used the full NSL-KDD training dataset [15]. In order to test our model, we have used the entries of the NSL-KDD testing dataset in the form of network packets. In order to reduce time complexity of the training phase and to improve accuracy of

**Fig. 2** Flowchart of multi-threaded cloud IDS



detection, we have used feature selection on the NSL-KDD dataset. We have selected 25 features of the dataset having the maximum value of Information Gain for training and testing purpose. Using reduced dataset, the learning time and accuracy of our system gets improved instead of full dataset. Our Hybrid Multilevel classifier also performs better than KNN and ANN, when they are used as classifier modules separately.

After analysis, the Administrator gets intrusion reports and works accordingly. The Cloud is having virtualization approach for the resources that are being used. Here a hypervisor server in Cloud hosts a number of clients on one physical machine. As the request passes NIDS for getting access to the Cloud storage, there may introduce another intrusion in the hypervisor server. To overcome this problem, an HIDS is placed in the server to monitor the internal happenings of the hypervisor. So with this deployment, HIDS in hypervisor along with NIDS at bottleneck position, the service made is more secured and reliable. NIDS is confined within the Cloud-IDS and the passed by request for the Cloud storage is again monitored by HIDS. The execution of the request is made using the security

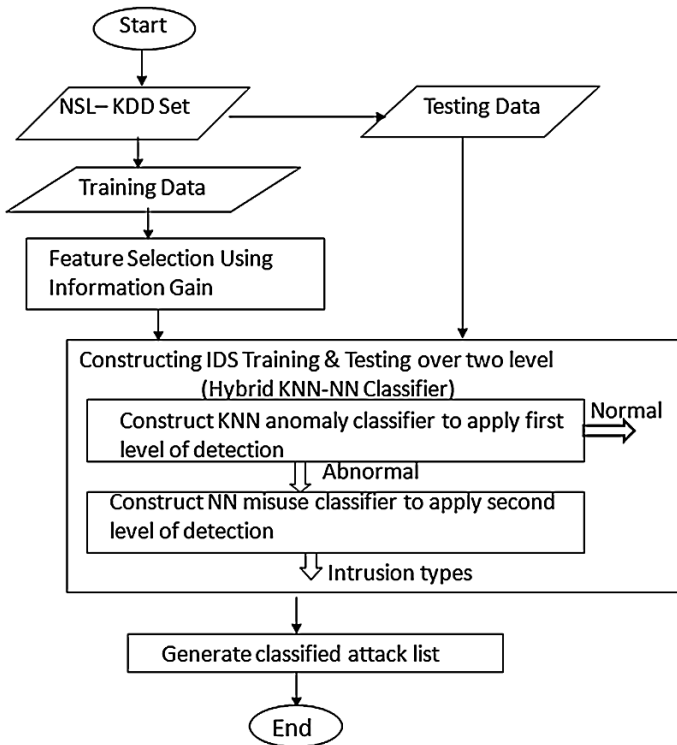


Fig. 3 Flowchart of IDS using KNN-NN classifier

approach proposed in this paper. The CSP (Administrator) is used to maintain an IP log list for the affected client requests. The HIDS and NIDS deployed within the Cloud-IDS are used for the monitoring the user requests. If any request is found of having intrusion by Cloud-IDS, the intrusion report is send to the Administrator for the next process. By getting the intrusion report generated by the Cloud-IDS, the Administrator first alerts the user about the intrusion and with that it also maintains the IP log list. Further the logged intrusion is processed by the Administrator. For each intrusion, the occurrence counter value is incremented by 1. The occurrence counter value is checked with respect to a threshold value. If the counter value doesn't exceed the threshold value, the access is denied for the particular user, shown in Fig. 4.

If the counter value is greater than the threshold value, further IP is made blocked for all operations. This security approach is implemented to get better results in case of different type of attacks performed by the intruder. In the proposed model for data loss or breakdown of system a restore point concept is utilized. The restore point acts as a bookmark to the data file, whenever the packet or data are lost. The task is revised or regained automatically using this restore point whenever the system gets failed due to any sort of reason. The user is served by the facility of

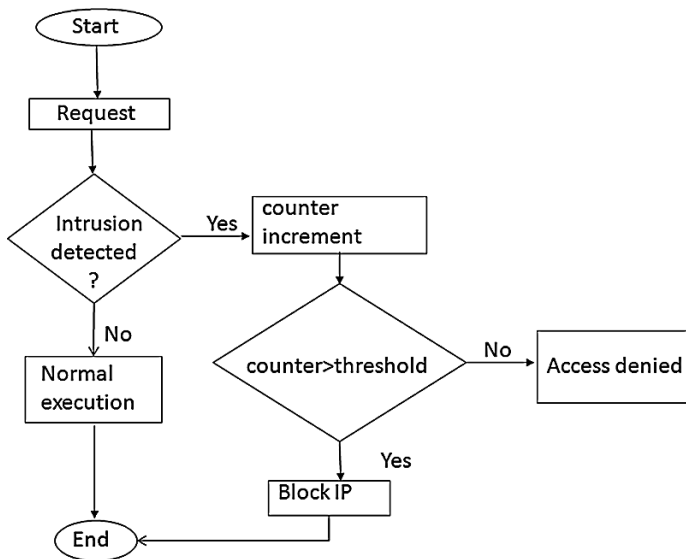


Fig. 4 Intrusion based task of administrator

rollback, without any fuss within a short period of time to the required previous state. This creation and utilization of restore point is provided by a schema associated with the structured data set that can be applied for convenient back up. The format shots of the structured data, taken periodically are used to re-establish services through restore point. In many case the shots are only taken at the time when the structured data set has undergone any change in content, although they may be taken at other tracks as well. The Administrator maintains all the structured data records and also stores the format shots to be used while system breakdown happens. In case of hardware failure or network breakdown, the first and foremost task is to regain the earlier stage after network reoccurrence. With this, organizations are able to respond quickly to take their services back on the network. Switch, Router or firewall configurations may not even provide such an accurate backup to the organization. With this situation further tasks get hampered which results in hours or even days being spent reconstructing a device which can lead to costly processes. Hence for organizations, the proposed automated system concept works as glooming technique and makes easy access for the interrupted task, which makes the organization more profitable. With this easy access technique, the restore point work efficiently with the structured data being provided by the network vendors. This enables them to reduce time, required to analyze for their network configurations. Hence quick access is gained up with the help of restore point and a secure model is created where a Multi-threaded NIDS reports the Administrator to perform future task.

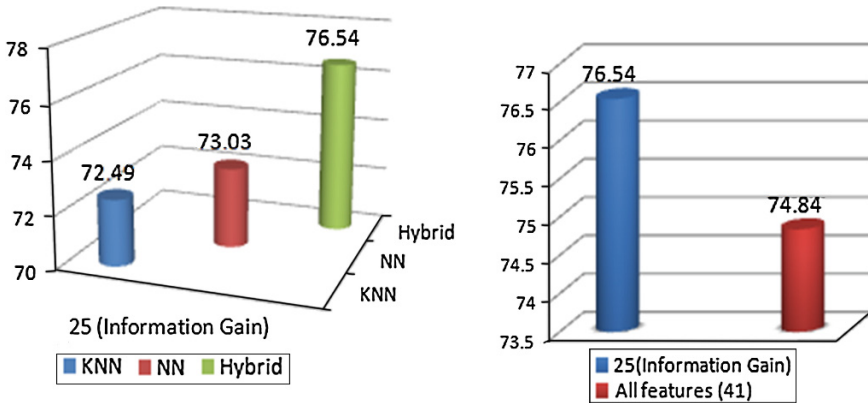


Fig. 5 Detection accuracy

### 4 Experimental Results

For performing our experiment and to evaluate the efficiency of our proposed model, we have used the NSL-KDD benchmark dataset. Relevant feature selection using Information Gain (IG) makes our analysis fast and accurate. It also saves our memory storage. After selecting all the relevant data using Information Gain, hybrid multi level KNN-NN classifier is used for classification. Here KNN is used as a binary classifier for anomaly detection and NN is used for misuse detection to detect all the various attacks. After feature selection, hybrid multilevel KNN-NN classifier makes our system more reliable and secure. Administrator gets the intrusion report after classification and depending upon the occurrence counter value for each intrusion, it takes necessary action. Experimental results show the efficiency and accuracy of our proposed IDS, shown in Fig. 5.

### 5 Conclusion

In this paper, with the collaboration of multi-threaded NIDS and HIDS, a better Intrusion Detection System for securing the Cloud environment has been proposed. In case of proposed NIDS for decreasing memory space and time, a number of relevant features are extracted from the captured data packets. After feature selection, all the packets are classified by a hybrid multi level KNN-NN classifier for getting faster and efficient IDS. Administrator takes suitable action to enhance the system performance after classification. Here a revised restore point is also proposed for quick revival of previous state of the user after network or system reoccurrence. Hence the proposed model serves as an efficient, faster and secure Intrusion Detection System approach in Cloud environment.

## References

1. Mohata, V.B., Dakhane, D.M., Pardhi, R.L.: Cloud based testing: need of testing in cloud platforms. *Int. J. Appl. Innov. Eng. Manage. (IJAIEM)* **2**, 369–373 (2013)
2. Mittal, R., Soni, K.: Analysis of cloud computing architectures. *Int. J. Adv. Res. Comput. Commun. Eng.* **2**, 2087–2091 (2013)
3. Redford, M.: Full virtualization by re-imaging cloud hardware. In: *Computing and Convergence Technology (ICCT)*, pp. 577–583. IEEE Publisher, Seoul (2012)
4. Modi, C., Patel, D., Patel, H., Borisaniya, B., Patel, A., Rajarajan, M.: A survey of intrusion detection techniques in cloud. *J. Netw. Comput. Appl.* **36**, 42–57 (2013)
5. Gouda, M.G., Liu, A.X.: Structured firewall design. *Comput. Netw.* **51**, 1106–1120 (2007)
6. Lei-jun, L., Hong, P.: A defense model study based on IDS and firewall linkage. *Inf. Sci. Manage. Eng. (ISME)* **2**, 91–94 (2010)
7. Karthikeyan, K.R., Indra, A.: Intrusion detection tools and techniques—a survey. *Int. J. Comput. Theory Eng.* **2**, 1793–8201 (2010)
8. Sonawane, S., Pardeshi, S., Prasad, G.: A survey on intrusion detection techniques. *World J. Sci. Technol.* **2**, 127–133 (2012)
9. Ghosh, P., Ghosh, R., Dutta, R.: An alternative model of virtualization based intrusion detection system in cloud computing. *Int. J. Sci. Technol. Res.* **3**, 199–203 (2014)
10. Kholidy, H.A., Baiardi, F.: CIDS: a framework for intrusion detection in cloud system. In: *Ninth International Conference on Information Technology—New Generations*, pp. 379–385. IEEE Computer Society (2012)
11. Al-Janabi, S.T.F., Saeed, H.A.: A neural network based anomaly intrusion detection system. In: *IEEE Computer Society*, pp. 221–226 (2011)
12. Mazzariello, C., Bifulco, R., Canonico, R.: Integrating a network IDS into an open source computing environment. In: *Sixth International Conference on Information Assurance and Security (IAS)*, pp. 265–270. IEEE Publisher, Atlanta, GA (2010)
13. Bakshi, A., Yogesh, B.: Securing cloud from DDOS Attacks using Intrusion detection system in virtual machine. In: *Second International Conference on Communication Software and Networks*, IEEE Computer Society, pp. 260–264 (2010)
14. Ghali, N.I.: Feature selection for effective anomaly-based intrusion detection. *Int. J. Comput. Sci. Netw. Secur. (IJCSNS)* **9**, 285–289 (2009)
15. Tavallaee, M., Bagheri, E., Lu, W., Ghorbani, A.A.: A detailed analysis of the KDD Cup 99 data set. In: *Proceedings of the IEEE Symposium on Computational Intelligence in Security and Defense Application (CISDA)*. pp. 53–58. IEEE Publisher (2009)

# Mobile WiMAX Physical Layer Optimization and Performance Analysis Towards Sustainability and Ubiquity

Sajal Saha, Angana Chakraborty, Asish K. Mukhopadhyay  
and Anup Kumar Bhattacharjee

**Abstract** Mobile WiMAX is emerging as a means for low cost reliable wireless broadband connection compared to traditional DSL cable. The system requirement of next generation mobile WiMAX is supposed to be based on IEEE 802.16 m which is still in letter ballot stage. This paper attempts to make in depth performance evaluation of Mobile WiMAX under various PHY parameters such as modulation and coding schemes (MCS), cyclic prefixes and different path-loss models. Moreover it also present an optimized adaptive modulation scheme that senses the SNR and adaptively switches to required MCS towards achieving the desired level of Quality of Service (QoS) and link stability. Simulation results show that dynamic adaptation of modulation and coding scheme based channel conditions can offer enhanced throughput, load, reduced delay, SNR and BER.

**Keywords** Wimax · Path-loss · Modulation and coding · Load · Throughput

## 1 Introduction

The demand for connectivity and bandwidth is increasing day by day. LTE and WiMAX emerge as promising technology in the market to meet the requirement of the user in a ubiquitous environment. WiMAX became popular worldwide among

---

S. Saha (✉)

Narula Institute of Technology, 81, Nilgunj Road, Kolkata 700109, India  
e-mail: sajalkrsaha@ieee.org

A. Chakraborty

Indian Institute of Engineering Science and Technology (IEST), Howrah 711103, India  
e-mail: angana.chakraborty9@gmail.com

A.K. Mukhopadhyay

SR Group of Institution, Jhansi, India  
e-mail: askm55@gmail.com

A.K. Bhattacharjee

National Institute of Technology, Durgapur, India  
e-mail: anupkumar.bhattacharaya@ece.nitdgp.ac.in

© Springer India 2015

J.K. Mandal et al. (eds.), *Information Systems Design and Intelligent Applications*,  
Advances in Intelligent Systems and Computing 339,  
DOI 10.1007/978-81-322-2250-7\_11

101



them due to simplicity of installation and cost reduction compared with traditional DSL cable.

There are currently three WiMAX systems available

Fixed WiMAX(IEEE 802.16-2004)

Mobile WiMAX(IEEE 802.16e-2005)

Mesh WiMAX(IEEE 802.16-Mesh)

Fixed WiMAX system having coverage area 5–7 km and speed up to 48 Mbps (fixed downlink) and 7 Mbps (fixed uplink). Mobile WiMAX provides speed upto 9.4 Mbps for downlink and 3.3 Mbps for uplink across the coverage area of 3 km. In Mesh WiMAX network WiMAX BS is connected within its coverage area with additional BS with smaller coverage area to relay the connectivity. In this paper various MAC, PHY system design parameters were identified, reviewed and selected on the basis of potential contribution to maximizing performance and minimizing delay and path loss. We identified performance matrices including VoIP packet delay, data packet delay, load, throughput to quantify performances over the optimized mobile WiMAX infrastructure. OPNET modeler and MATLAB are used for simulation. Simulation scenarios were used to observe the impact on the four performance matrices.

## 2 Background Study

In Wireless communication information propagates from transmitted to receiving antenna. During transmission electromagnetic wave faces obstacle causes path loss. Path loss is defined by

$$PL = P_T + G_T + G_R - P_R - L_T - L_R$$

where  $P_T$  and  $P_R$  are transmitted and received power.  $G_T$  and  $G_R$  are the gain of transmitting and receiving antenna.  $L_T$  and  $L_R$  are the feeder losses of the respective antennas. Milanovic et al. [1] compared the accuracy of four different propagation models like SUI model, COST 231 Hata, Macro Model, Model 9999. With received power for 3.5 GHz analysis is made for location with NLOS and LOS propagation conditions separately. Erceg et al. [2] developed a statistical path loss model derived from 1.9 GHz experimental data collected across suburban environments. In [3] a cross layer architecture is developed considering an adaptive MCS scheme in the PHY and a signal and interference to noise ratio (SINR) based call admission control (CAC) scheme is developed in the MAC layer of the WIMAX architecture. Bhunia et al. [4] considered load, jitter, throughput as QoS parameters to analyze the performance of VoIP application in mobile WiMAX. Nevertheless, we made an in depth analysis of the effect of various pathloss models, scheduling algorithm and MCS scheme. It has been shown that AMC scheme enables better QoS while consuming low overall bandwidth of the system.

### 3 Network and System Model

We used OPNET simulator and MATLAB for simulation. Optimized Network Engineering Tool (OPNET) provides a development environment supporting the communication networks. Both behavior and performance of the modeled system can be analyzed through discrete event simulator. OPNET provides graphical editor to enter network model details. It consists four such types of editor names network editor, node editor, process editor and parameterized editor organized in a hierarchical way. We design the optimized network model scenario in OPNET, run the model under different condition, collected data and plot the data in MATLAB. We consider different modulation and coding schemes (MCS) like QPSK1/2, QPSK3/4, 16QAM1/2, 16QAM3/4, 64QAM1/2, 64QAM2/3, 64QAM3/4 as the threshold coverage area of each modulation schemes are different as shown in Fig. 1. Coverage area is determined using the maximum signal to noise ratio (SNR) a MN receive without significant data loss. We introduce an Adaptive Modulation Coding (AMC) that allows the WiMAX system to adjust from higher to lower modulation scheme depending on SNR condition of the radio link. AMC model is discussed elaborately in Sect. 3.1.

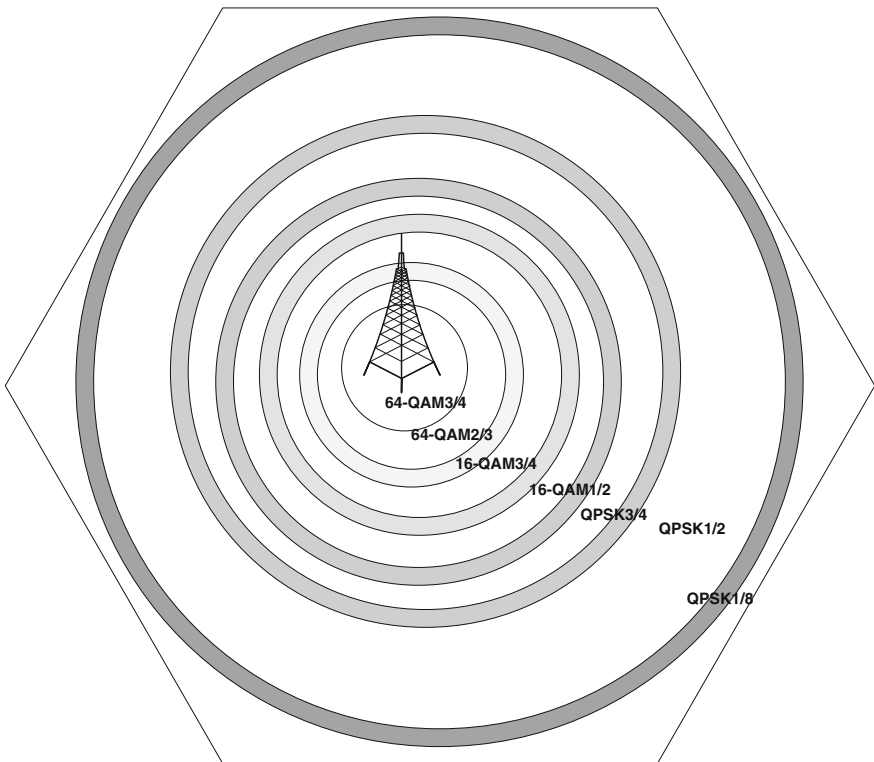


Fig. 1 Cell decomposition into region by each modulation

**Table 1** Parameter taken

Min. MN velocity	60 km/h
Max. MN velocity	100 km/h
Frequency bandwidth used	2.3–2.4 GHz
Channel bandwidth	8.75/10 MHz
FFT size	1,024
RF multiple access mode	OFDMA
Antenna type	Omni directional
MIMO	Matrix 4/4
No. of carriers	2
Transmission power	Max. 20 W
RCV buffer size	64 kB
Antenna gain	23 dBi
<i>Base station parameters</i>	
Maximum number of SS nodes	15
Service class name	Gold (rtPS)
Mac address	Auto assigned
Maximum power transmission	0.5 W
PHY profile	wireless OFDMA 20 MHz
PHY profile type	OFDM
<i>Mobile station parameters</i>	
<i>Handover parameters</i>	
Maximum sustained traffic rate	4 Mbps
Minimum reserved traffic rate	0.5 Mbps

OPNET offers four inbuilt path loss model [5] environment like,

- (i) **Free Space model:** It hardly used in real time environment as it does not consider the multipath fading effect.
- (ii) **Suburban fixed model:** Considering cell with large coverage area and higher antenna height considering MN having low mobility.
- (iii) **Outdoor to indoor pedestrian path loss model:** Small cell size with low antenna height. Pedestrians are located in streets, inside buildings.
- (iv) **Vehicular environment:** Larger cell size and higher antenna height considering MN having mobility (60–180 kmph).

rtPS is taken in MAC sub-layer as initial QoS service class to support real time services with variable bit rates. Other important parameters are shown in Table 1.

### 3.1 AMC Model

The aim of this model is to create a universal machine that can be adapted easily based on MN mobility. Antenna gain of the WiMAX Base Station (BS) is fixed at

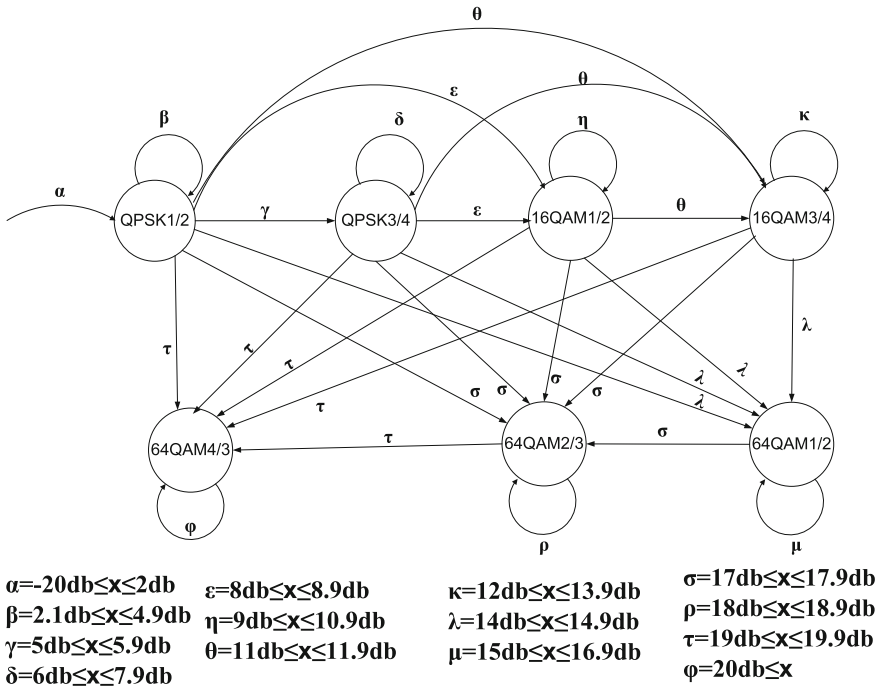


Fig. 2 State diagram of AMC model

15 dbi. When signal strength is high, highest modulation scheme is used (64 QAM) to increase the system capacity. As MN moves out to the periphery of the coverage area causes signal strength fading, our system model moves to lower modulation scheme to maintain QoS and link stability. Change of MCS depends on the threshold SNR received by MN that continuously sense SNR and change MCS according to AMC algorithm.

Working function of AMC model is shown by the state diagram as shown in Fig. 2. Selection of threshold SNR value is a challenging problem. Two techniques to select the threshold SNR are given in [6].

### 4 Simulation Results and Analysis

We set up two mobile nodes Mobile\_1\_1 and Mobile\_2\_1 under base stations BS\_1 and BS\_2 respectively. We gradually increase the traffic to 2, 5, 8, 10 and 15 MNs and analyze the performance of the WiMAX network. Figure 3 shows 15 MNs WiMAX network model under 15 BSs. Although WiMAX standards supports large coverage area but in practice, it supports approximately 3 km.

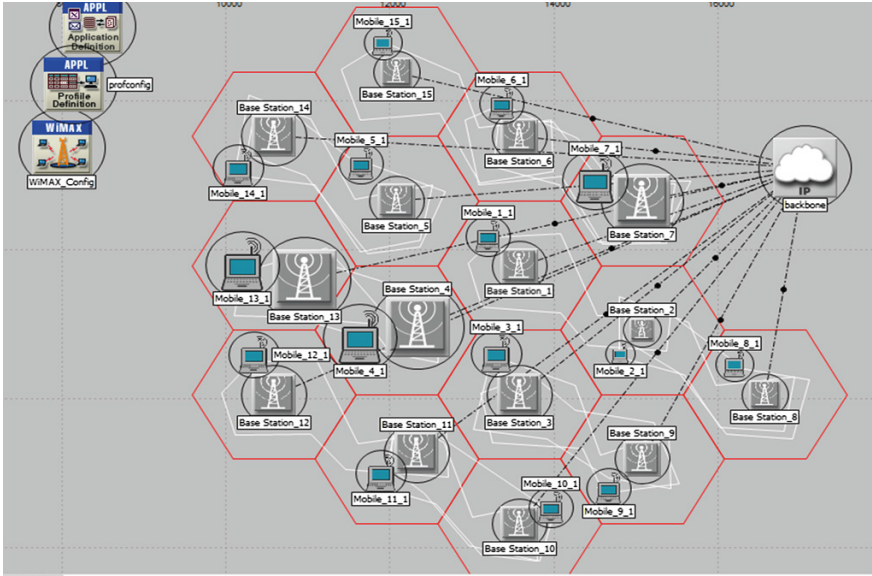
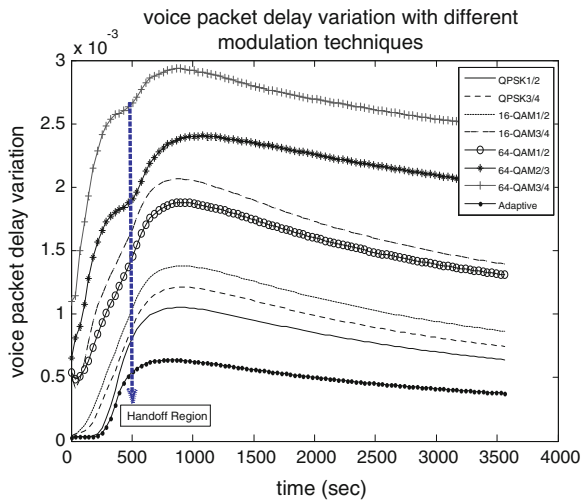


Fig. 3 WiMAX network model considering higher traffic (15 MNs)

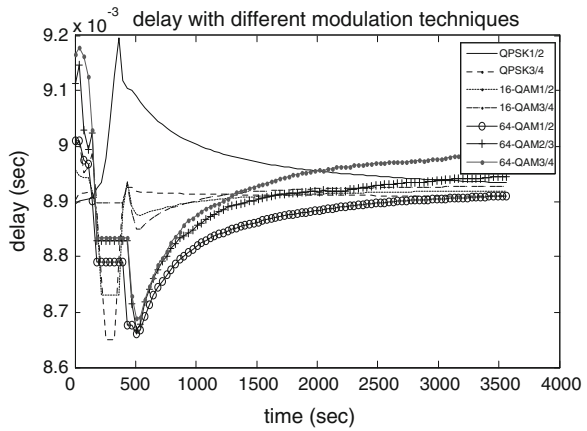
Figures 4 and 5 show delay performance for different fixed type MCS and AMC. Peak VoIP packet delay of AMC is minimum (0.5 ms) among other MCS. Peak delay in Fig. 4 is 3 ms (64QAM3/4) and in Fig. 5 is 9.2 ms (QPSK1/2) that is much below the threshold level of 150 ms as recommended by ITU-T[11].

Variation of load (packets/sec), throughput and SNR have been implemented in Figs. 6, 7 and 8. Initially, the proposed AMC model adapted to higher modulation

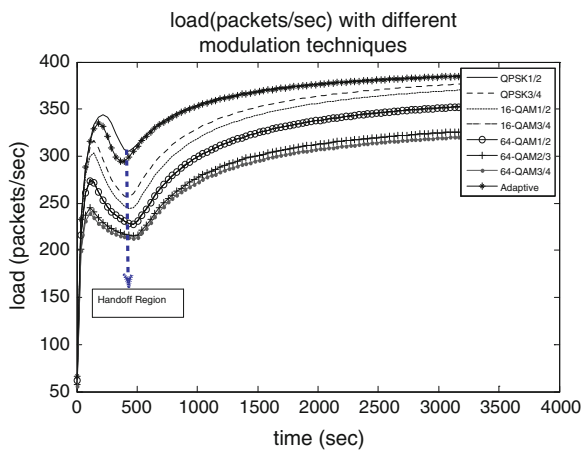
Fig. 4 variation of VoIP delay different MCS



**Fig. 5** Data packet delay at different at MCS

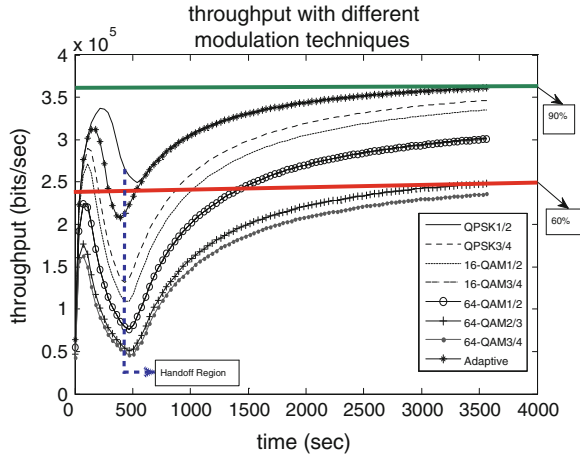


**Fig. 6** Variation of load (packets/sec) different MCS

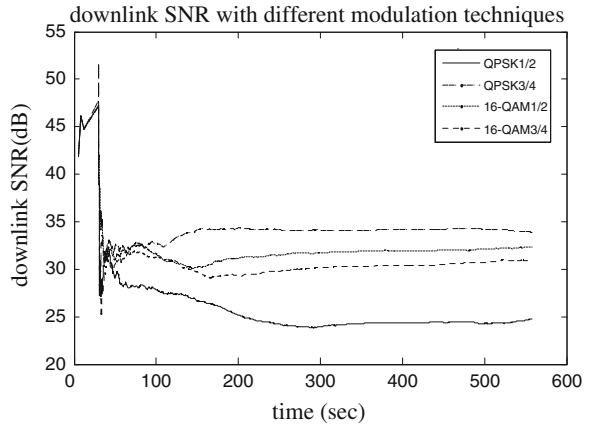


scheme (64 QAM3/4). As MN moves toward the cell boundary, SNR value decreases (Fig. 8) and as it reaches the threshold SNR value, the coding rate changes according to AMC algorithm and the state machine (Fig. 2) keeps different state of lower coding rate (like QPSK1/2) to maintain the quality of the link connection without increasing the signal power (23 dB<sub>i</sub>). In this way, the proposed AMC model adopts a suitable MCS dynamically based on SNR value (Fig. 8) and keeps almost constant throughput (Fig. 7). Empirical analysis also shows that proposed AMC model and QPSK1/2 achieves 90 % throughput (marked by 2 lines in Fig. 7) as maximum sustainable traffic rate of the communication link is 4 Mbps. 64QAM2/3 and 64QAM3/4 fail to achieve the minimum benchmark of 60 % throughput.

**Fig. 7** Throughput performance analysis at different MCS

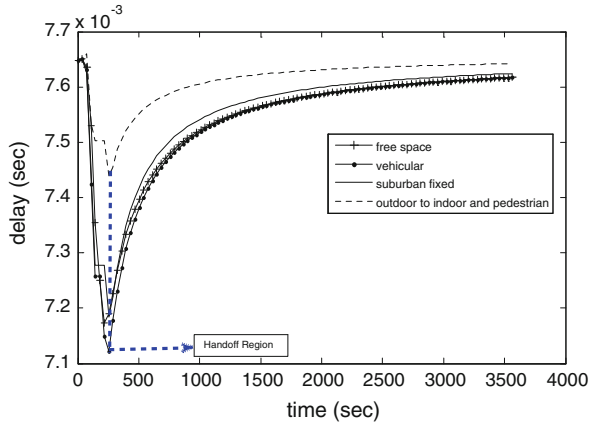


**Fig. 8** Downlink SNR respectively at different MCS

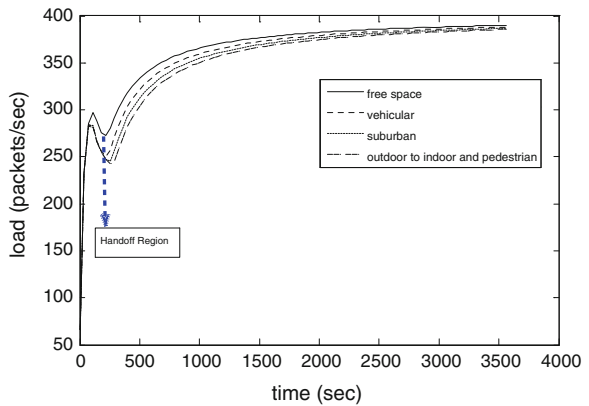


Figures 9, 10 and 11 represent the variation of delay, load (packet/sec) and throughput respectively in different propagation models keeping MN speed constant(100 kmph). Delay for the free space model is minimum and pedestrian moving from outdoor to indoor is maximum, this may be due to the radio wave component reflected and diffracted on building reaching the receiving antenna. Load and throughput is maximum for the free-space propagation model whereas pedestrian moving from outdoor to indoor is minimum. Although all path loss models achieve the minimum throughput benchmark (60 %) in the proposed Wi-MAX system except handoff duration as shown in the Fig. 7. As far as 60 % throughput is concerned, the rate is adequate to support applications like VoIP and video transmission.

**Fig. 9** Variation of delay at different path loss models



**Fig. 10** Variation of load at different path loss Models



**Fig. 11** Variation of throughput at different path loss models

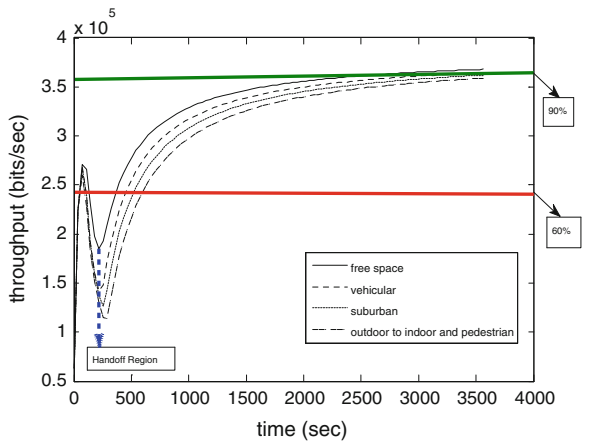




Figure 9 represents delay variation at various path loss models. Figure 10 represents variation of load at different path loss models. Figure 11 represents throughput variation respectively under various path loss models.

## 5 Conclusions

WiMAX is conveniently deployable due to ease of installation and low cost. It is very important to guarantee QoS to the end users to avail and sustain the diversifying applications of WiMAX. An optimized architecture conforming to the recently standardized IEEE 802.16m framework, is needed for integrating both mobility management and QoS to provide broadband service in a ubiquitous environment to end users. In [7], authors analyzed the WiMAX network performance under different service classes in MAC layer. In [8], authors proposed a mobility management model THMIP at network layer to achieve better throughput with minimal handoff latency. In this paper, our analysis on the performance of the WiMAX considered following parameters of the physical layer. (a) Different MCS with constant speed (100 kmph) (b) Different speed with proposed AMC (c) Different path loss models with proposed AMC at a constant speed (90 kmph). Performance matrices considered are delay, load, SNR, throughput. From the empirical studies, it is evident that proposed AMC allows the WiMAX network to yield higher throughput covering longer distance.

## References

1. Milanovic, J., Rimac-Drlje, S., Bejuk, K.: Comparison of propagation models accuracy for WiMAX on 3.5 GHz, electronics, circuits and systems. In: 14th IEEE International Conference on ICECS 2007, pp. 111–114, 11–14 Dec 2007
2. Erceg, V., Greenstein, L.J., Tjandra, S.Y., Parkoff, S.R., Gupta, A., Kulic, B., Julius, A.A., Bianchi, R.: An empirically based path loss model for wireless channels in suburban environments. *IEEE J. Sel. Areas Commun.* **17**(7):1205–1211 (1999)
3. Chowdhury, P., Misra, I.S., Sanyal, S.K.: Cross layer QoS support architecture with integrated CAC and scheduling algorithms for WiMAX BWA Networks. *Int. J. Adv. Comput. Sci. Appl. (IJACSA)* **3**(1), 76–92 (2012)
4. Bhunia, S., Misra, I.S., Sanyal, S.K., Kundu, A.: Performance study of mobile WiMAX network with changing scenarios under different modulation and coding. *Int. J. Commun. Syst.* **24**(8), 1087–1104 (2011)
5. OPNET Technologies Inc: Introduction to WiMAX modeling for network R&D and planning. In: Proceedings of OPNETWORK, Washington, DC, USA (2008)
6. Marabissi, D., Tarchi, D., Fantacci, R., Balleri, F.: Efficient adaptive modulation and coding techniques for WiMAX systems. In: IEEE International conference on Communication (ICC), pp. 3383–3387 (2008)

7. Saha, S. et.al.: Performance analysis of service classes for IEEE 802.16m QoS optimization. In: Proceedings of the 1st International Conference on Emerging Trends and Applications in Computer Science (ICETACS), pp. 149–155 (2013)
8. Saha, S., et al.: QoS and Mobility management issues on next generation mobile WiMAX networks. In: Santos, R., Licea, V., Edwards-Block A. (eds.) Broadband Wireless Access Networks for 4G: Theory, Application, and Experimentation, pp. 298–323. Information Science Reference, Hershey, PA. doi:[10.4018/978-1-4666-4888-3.ch016](https://doi.org/10.4018/978-1-4666-4888-3.ch016)

# Comparison of Classifiers Accuracies from FAVF and NOFI for Categorical Data

D. Lakshmi Sreenivasa Reddy, B. Raveendra Babu, A. Govardhan,  
A. Kalpana and Mudimbi Krishna Murthy

**Abstract** Outlier analysis is an important task in data science. Specifically finding outliers in categorical data is a tough task. To build an accurate Classifier, it is needed to eliminate exact number of outliers from the data. If less number of outliers is found, the obstacles will remain in the original data. An accurate classifier cannot be built on this data. Similarly if more number of outliers is found and eliminated, some original records may be missed. From this data too an accurate classifier cannot be built. So it is needed to eliminate the exact number of outliers while modeling a classifier. Since the data is categorical, in classification modeling, most infrequent records are treated as outliers. These infrequent objects disturb the data in modeling classifier. But how many outliers needed to be found is a problem. This paper presents the new approach normally distributed Outlier factor by infrequency (NOFI) to improve the Classifier accuracy. In modeling a classifier for categorical data, high frequent records are most useful and infrequent records are most useless. So the infrequent records are obstacles in modeling the classifier. There are many effective approaches to detect outliers for numerical data. But for categorical datasets there are few numbers of methods exists. The experiments are conducted for this new method has been applied on bank dataset which is taken from UCI ML Repository. This approach is not needed any input of k, the required number of

---

D. Lakshmi Sreenivasa Reddy (✉)  
Department of CSE, RISE Gandhi Group of Institutions, Ongole, India  
e-mail: urdlsreddy@yahoo.com

B. Raveendra Babu  
Department of CSE, VNRVJIET, Hyderabad, India  
e-mail: rboghpathi@yahoo.com

A. Govardhan  
SIT, JNTUH, Hyderabad, India  
e-mail: govardhan\_cse@yahoo.co.in

A. Kalpana · M. Krishna Murthy  
Department of MCA, RISE Gandhi Group of Institutions, Ongole, India  
e-mail: Kalpana.amiriseti@gmail.com

M. Krishna Murthy  
e-mail: krishnamudimbi@gmail.com

outliers. NOFI would find number of outliers automatically using infrequency of all possible combinations framed from attribute values included in any record.

**Keywords** Outlier analysis • Categorical • AVF score • FAVF score • OFI score • NOFI score

## 1 Introduction

Outlier analysis is an important task in data analysis. Without eliminating these outliers a correct classifier cannot be built. Some of the applications of outlier analysis are like credit card fraud detection, intrusion detection of networks, medical diagnosis analysis, and business decision analysis. In this approach a simple method for classifier accuracy is presented. AVF [1] method is one of the efficient methods to detect outliers in categorical data. In this method, it calculates frequency of each attribute value in each record and finds their average AVF score for each record. But the major problem in this is how many outliers need to be selected from the dataset. In this method we need to give an input for selecting number of outliers. We don't know how these are reliable outliers. This problem is solved by NAVF [2]. By this method the reliable number of outliers is selected automatically. After deleting these outliers automatically by NAVF, the classifier has been built on the remaining data. In another approach FAVF [3] has been built for the same purpose. This method also finds outliers automatically. But the reliability of outliers found by FAVF is less when compared with NAVF. In another approach FPOF [4] for categorical data is also used frequent patterns which are generated from Apriori algorithm [5]. FPOF calculates frequent pattern item sets from each record in data set. From these frequencies it calculates FPOF score and finds k outliers as the least k-FPOF scores. All these methods are used average frequency of each attribute value. This method is so complex because it needs generation of frequent patterns and also needs a threshold value ' $\sigma$ ' and input 'k' as the number of k outliers need to be eliminated. Another method based on frequency is Greedy [6].

## 2 Some of Existing Approaches for Categorical Data

### 2.1 Greedy Algorithm

This method finds the entropy of data set when a record is included in dataset. This method is finds out records from which the datasets give more entropy. Assume that the dataset is denoted by 'D' with 'm' attributes  $A_1, A_2 \dots A_m$  and  $D(A_j)$  is the domain of distinct values in the attribute  $A_j$ , then the entropy of single attribute  $A_j$  is calculated by the  $E(A_j)$ , it is calculated by the below equation.

$$E(A_j) = \sum_{x \in D(A_j)} p(x) \log_2(p(x)) \tag{1}$$

All the attributes are independent to each other by nature, Entropy of the entire dataset  $D = \{A_1, A_2 \dots A_m\}$  is equal to the sum of the entropies of attributes, and is defined as follows.

$$E(A_1, A_2, A_3 \dots A_j) = E(A_1) + E(A_2) + E(A_3) + \dots E(A_j) \tag{2}$$

Entropy of dataset is calculated each time when one record is selected aside. Among all entropies, k-least entropies are selected. The corresponding records for these least entropies are treated as top k-outliers in this dataset. The complexity of Greedy algorithm is  $O(k * n * m * v)$ , where k-is the required number of outliers, n is the number of records in the dataset D, m is the number of attributes in D, and v is the number of distinct attribute values per attribute. The terminology used in this paper is given in Table 1.

**Table 1** Terminology

Term	Description
DB	Database
K	Target number of outliers
N	Number of objects in dataset
M	Number of attributes in dataset
$X_i$	ith object in dataset ranging from 1 to n
$A_j$	jth attribute ranging from 1 to m
$D(A_j)$	Domain of distinct values of jth attribute
$X_{ij}$	Cell value in ith object which takes from domain $d_j$ of jth attribute $A_j$
D	Dataset
V	Set of all distinct values in dataset D
P	Set of all combinations of distinct attribute values, where each attribute occurs only once in any combination
I	Item set
F	Frequent item set
IF	Infrequent item set
$f(x_{ij})$	Frequency of $x_{ij}$ value
FS( $x_i$ )	Set of frequent Item sets of $x_i$ object
IFS( $x_i$ )	Set of infrequent Item sets of $x_i$ object
Minsup	Minimum support of frequent item set
Support(I)	Support of item set I
OFI	Outlier factor by infrequency score
NOFI	Normally distributed outlier factor by infrequency score

## 2.2 Attribute Value Frequency (AVF) Algorithm

AVF approach is simpler and faster approach to find outliers. It needs only one scan of entire database and it does not take more space. The AVF method is defined as below. Let us take “ $x_i$ ” as an object in a dataset. AVF score of this object is defined as below.

$$AVF(x_i) = \sum_{j=1}^m f(x_{ij}) \quad (3)$$

This method also needed input ‘k’ as the number of outliers to be eliminated. This approach gives us more accuracy and low complexity.

## 2.3 Fuzzy Distributed Attribute Value Frequency (FAVF)

This method [3] depends on AVF score. It finds the optimal number of outliers automatically. Outliers found by FAVF are more in number when compared with the number of outliers found by NAVF. FAVF model tried to convert the ambiguity left by NAVF. FAVF uses the S-Fuzzy function and finds three seeds based on AVF scores of the objects. These three seeds are used to distribute the entire dataset. Fuzzy seeds and Fuzzy score are given below. This FAVF method also finds the optimal number of outliers automatically from the original database.

$$b = \text{mean}(f_i) \quad (4)$$

$$a = \begin{cases} b - 3 * \text{STD}(f_i) & \text{if } \max(f_i) > 3 * \text{STD}(f_i) \\ b - 2 * \text{STD}(f_i) & \text{if } \max(f_i) > 2 * \text{STD}(f_i) \\ b - \text{STD}(f_i) & \text{if otherwise} \end{cases} \quad (5)$$

$$c = \begin{cases} b + 3 * \text{STD}(f_i) & \text{if } \max(f_i) > 3 * \text{STD}(f_i) \\ b + 2 * \text{STD}(f_i) & \text{if } \max(f_i) > 2 * \text{STD}(f_i) \\ b & \text{otherwise} \end{cases} \quad (6)$$

$$\text{Fuzzyscore}(x_i) = \begin{cases} 0 & \text{if } f_i < a \\ 2 \left\{ \frac{f_i - a}{c - a} \right\}^2 & \text{if } a \leq f_i \leq b \\ 1 - 2 \left\{ \frac{f_i - a}{c - a} \right\}^2 & \text{if } b \leq f_i \leq c \\ 1 & \text{if } f_i > c \end{cases} \quad (7)$$

where

“ $f_i$ ”  $f(x_i)$  = AVF score of  $i$ th record.

Max ( $f_i$ ) Maximum of AVF scores in the dataset.

- a Mean of AVF scores in the dataset.
- STD (fi) Standard Deviation of all AVF scores in the dataset.

### 2.4 Outlier Factor by Infrequency (OFI)

This approach OFI [7] calculates the outlier factor based on infrequency of each infrequent itemsets involved in a record which is generated by Apriori algorithm [5]. OFI score is calculated by the below formula.

$$= \beta(xi) = \sum_{j=1}^m \frac{|DB|}{1 + f(IFS(xi))} \tag{8}$$

Here,

- Let “xi” is the record of a database DB,
- A<sub>j</sub> = Attribute, where j takes the values from 1 to m,
- IF = Infrequent Itemset,
- IFS (xi) = Set of infrequent Itemsets of “xi”,
- x<sub>ij</sub> = ith value in jth attribute
- |DB| is length of Dataset

OFI score of each record is calculated by the above Eq. (8). The outliers selected by highest OFI score records. This method is also needed an input value “k” to get k-outliers and a threshold value to decide infrequent itemsets. Accuracy of finding outliers is more when compared with BAD score and AVF score methods, but the complexity is more.

### 2.5 Proposed Optimization Method: Normally Distributed Outlier Factor by Infrequency (NOFI)

OFI method finds k-number of outliers based on the input ‘k’. NOFI calculates reliable number of outliers automatically based on the threshold value. This threshold value is calculated as below.

$$\mu_{(\beta)} = \frac{1}{|DB|} \sum_{i=1}^n \sum_{j=1}^m \frac{|DB|}{1 + Frequency(\text{inf frequenc}_t\_Itemsets\_of\_record)} \tag{9}$$

$$= \sum_{i=1}^n \sum_{j=1}^m \frac{1}{1 + \text{Frequency}(\text{infrequent\_Itemsets\_of\_record})} \quad (10)$$

$$\sigma_{(\beta)} = \sum_{i=1}^n \sqrt{(\text{OFI}(xi) - \mu_{(\text{OFI})})^2} \quad (11)$$

$$\text{NOFI score}_{(\beta)} = \tau = \mu_{(\beta)} + 3\sigma_{(\beta)} \quad (12)$$

If  $X_i$  is said to be an outlier in dataset DB, its OFI score must satisfies the below condition.

$$\text{if } \beta(X_i) \begin{cases} \geq \tau, & X_i \text{ is called Outlier } \forall i = 1 \text{ to } n \\ < \tau, & X_i \text{ is called inlier } \forall i = 1 \text{ to } n \end{cases} \quad (13)$$

This proposed optimization method also finds optimal number of outliers automatically in perspective of classifier building.

### 3 Experimental Results and Discussion

The experiments are conducted for this method on bank data with 45221 instances is taken from UCI ML Repository [8]. Only seven categorical attributes are considered for experiments. This method is implemented on PL-SQL. Bank data with 7 attributes and 46 values are considered for experiments. The attributes considered for this experiments are “Job”, “Marital status”, “Education”, “loan”, “housing”, “contact”, ‘Y’ = “Class label attribute”. Bank data has been divided into two parts, first part of data is considered with “Yes” Class label and the number of records are 5,299 in this part and second part with “no” class label has 39,922 records. This partitioning of the Bank dataset has been achieved by using the Clementine tool. The “yes” label records are considered as outliers in this experiment. From the first part, for each 10 records of class “yes” one record is selected by using 10-1 random sampling technique and mixed up with “no” class label records. The mixed up records are 40,427. Both FAVF and NOFI methods have been applied on these mixtures of records to eliminate outliers. After eliminating outliers automatically by NOFI, this method has found 39,899 records as inliers. The total outliers are found by NOFI are 528. Similarly FAVF has been found 332 outliers automatically and eliminated. FAVF has been found 40,095 inliers. After eliminating outliers by both methods classifiers are modeled. Clementine tool has been used to model different classifiers. The classifiers modeled by NOFI show more accuracy than FAVF and direct.

While modeling the classifiers for direct data including outliers the lift values are given in the respective column in Table 2. Each classifier is also used different number of variables. The accuracies of classifiers are also given in Table 2.



**Table 2** Comparison of accuracies of classifiers modeled on original data (including outliers)

Model	Lift	Number of fields used	Accuracy achieved (%)
DL	1.721	4	58.435
LR	2.02	6	98.695
NN	1.931	6	98.695
CHAID	1.954	5	98.695

While modeling the classifiers after deleting outlier by FAVF the lift values are given in the respective column in Table 3. Each classifier is also used different number of variables. The accuracies of classifiers are also given in Table 3.

Similarly the results are given in Table 4 for different classifiers modeled by NOFI (Figs. 1, 2, 3, 4, 5; Table 5) .

The Decision logic (DL) classifier gave 58.435 % of accuracy when tested on test data after trained it on the original data. The same classifier gave 38.001 and 35.559 % accuracy respectively, when the classifier trained on the cleaned data by FAVF and NOFI. When the Neural Networks (NN) classifier is modeled on the original data (without cleaning), it has given 98.685 % accuracy. NN has given 98.873 and 99.068 % accuracy respectively when it is developed on cleaned data cleaned by FAVF and NOFI. Linear Regression (LR) gave the 98.695 % accuracy on the test data when tested it on original data (without cleaned) and 98.873 % accuracy on cleaned data cleaned by FAVF and 99.068 % for NOFI. Similarly CHAID Classifiers gave the same results as LR respectively for original data, cleaned data by FAVF and NOFI.

**Table 3** Comparison of accuracies of classifiers modeled by FAVF

Model	Lift	Number of fields used	Accuracy achieved (%)
DL	1.742	3	38.001
LR	2.094	6	98.873
NN	2.075	6	98.873
CHAID	1.991	5	98.873

**Table 4** Comparison of accuracies of classifiers modeled by NOFI

Model	Lift	Number of fields used	Accuracy achieved
DL	1.788	4	35.559
LR	2.5	6	99.068
NN	2.486	6	99.068
CHAID	2.34	5	99.068

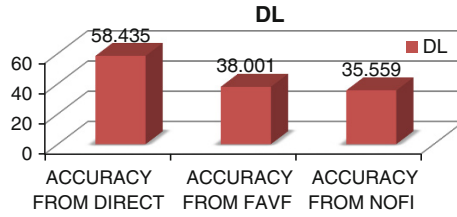


Fig. 1 Comparison of accuracy of classifier DL modeled by direct, FAVF and NOFI

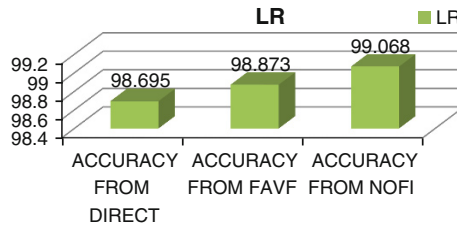


Fig. 2 Comparison of accuracy of classifier LR modeled by direct, FAVF and NOFI

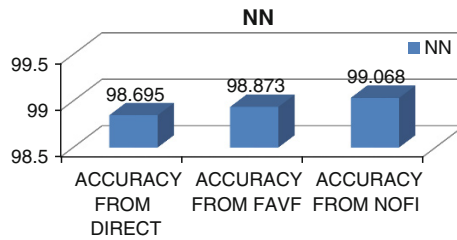


Fig. 3 Comparison of accuracy of classifier NN modeled by direct, FAVF and NOFI

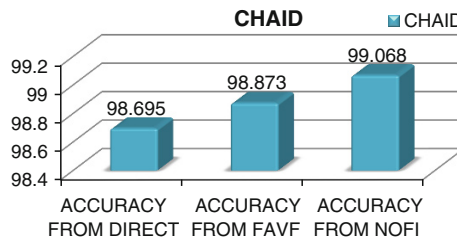
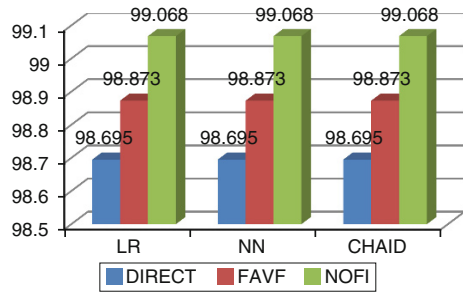


Fig. 4 Comparison of accuracy of classifier CHAID modeled by direct, FAVF and NOFI

**Fig. 5** Comparison of accuracy of classifiers accuracies modeled by direct, FAVF and NOFI



**Table 5** Comparison of accuracy of classifiers accuracies modeled by direct, FAVF and NOFI

9i8Model	Accuracies achieved		
	Direct	FAVF	NOFI
LR	98.695	98.873	99.068
NN	98.695	98.873	99.068
CHAID	98.695	98.873	99.068

### 4 Conclusion and Future Work

This new method has been achieved good results when compared with FAVF method and Direct. NOFI is one of the better methods when compared with others. In future we will compare the precisions and recalls by both methods on different datasets.

### References

1. Koufakou, A., Georgiopoulos, M.: A fast outlier detection strategy for distributed high-dimensional data sets with mixed attributes. *Data Min. Knowl. Disc* **20**, 259–289 (2010)
2. Lakshmi Sreenivasa Reddy, D., Raveendra Babu, B., Govardhan, A.: Outlier analysis of categorical data using NAVF. *Informatica Economica* **17**(1), 5–13 (2013)
3. Lakshmi Sreenivasa Reddy, D., Raveendra Babu, B.: Outlier analysis of categorical data using FuzzyAVF. Presented at IEEE International Conference ICCPCT-2013, pp. 1259–1263
4. He, Z., Xu, X., Huang, J., Deng, S.: FP-Outlier: frequent pattern based outlier detection. *Comput. Sci. Inf. Syst. (ComSIS'05)* **2**(1), 103–118 (2005)
5. Agrawal, R., Srikant, R.: Fast algorithms for mining association rules in large databases. In: *Proceedings International Conference on Very Large Data Bases*, pp. 487–499 (1994)
6. He, Z., Deng, S., Xu, X.: A fast greedy algorithm for outlier mining. In: *Proceedings of PAKDD* (2006)
7. Lakshmi Sreenivasa Reddy, D., Raveendra Babu, B.: Efficient model to find outliers in categorical data using outlier factor by infrequency. Presented at IEEE International Conference ICCPCT-2014, pp. 1324–1328
8. Frank, A., Asuncion, A.: UCI Machine Learning Repository. University of California, School of Information and Computer Science, Irvine, CA. <http://archive.ics.uci.edu/ml> (2010)

# Multi Objective Optimization on Clustered Mobile Networks: An ACO Based Approach

Sujoy Sett and Parag K. Guha Thakurta

**Abstract** Clustering technique transforms a physical network into a virtual one to obtain an improved Quality of service (QoS). Addressing this issue, a multi objective optimization (MOO) on QoS metrics for clustered mobile networks is proposed in this paper. A simultaneous optimization is done by minimizing the number of cluster heads (CHs) to reduce delay in routing call requests as well as maximizing the number of cluster members under a CH such that network coverage is improved. This is obtained through a proposed ant colony optimization (ACO) based routing algorithm followed by a checking procedure on network status to detect emergence of CHs and correctness of subsequent routing. The effectiveness of the proposed approach over existing one is shown with simulation studies.

**Keywords** Routing · Ant colony optimization · Cluster head selection · Clustering · Network coverage · Transmission delay

## 1 Introduction

Mobile networks comprise of different geographic areas known as cells. Each of these is served by a base station (BS), which are linked with neighbors in the network. The task of the BSs is to receive communication from mobile devices scattered in the area. A group of neighboring BSs is considered as a cluster to map the physical network onto a virtual one to reduce the communication overhead. For such reduction, a BS as a node within the cluster is selected as a cluster head (CH). The responsibility of CH is to aggregate communications from its members and act

---

S. Sett (✉) · P.K. Guha Thakurta  
National Institute of Technology, Durgapur, West Bengal, India  
e-mail: sujoysett@gmail.com

P.K. Guha Thakurta  
e-mail: parag.nitdgp@gmail.com

as sole representative for that cluster to establish communication with other clusters. Naturally an objective towards optimization of the number of CHs is required to reduce the transmission delay for a call request.

The reduction of transmission delay is associated with reduction of hop count, which can also lead to reduced energy consumption, provided communication is aggregated between CHs. Low-Energy Adaptive Clustering Hierarchy (LEACH) [1] is a cluster-based protocol using randomized rotation of CHs to achieve even distribution of energy dissipation throughout the network. Further, the HYENAS system [2] selects CHs using model-based processing. Here, the BS determines a node metric for each node in the cluster by considering residual energy and the total sum of squared intra-cluster distance.

The techniques discussed earlier are involved with determination of clusters beforehand and consequently determining the CH corresponding to each cluster. However, several combined model for addressing simultaneous routing and clustering have been studied in the area of dynamic networks [3]. A proposed GEDIR (geographic distance routing) algorithm [4] in this field uses the principle of forwarding the packet to one of its neighbors that are closest to the destination. An extension called Avoidance-GEDIR for clustered networks selects the second closest neighbor to destination for forwarding packets by addressing the higher energy consumption of CH nodes.

The clustering in mobile networks has been extensively studied using the concepts of Evolutionary algorithms. Using these algorithms, an objective function based on network parameters is defined for optimization. Under such scenario, an ant colony optimization (ACO) [5–7] based algorithm is preferably used for determining instantaneous routing over the other alternatives like genetic algorithm [8, 9], due to the reduced execution time of the former. Generally, ACO works upon selection of several initial routes analogous to ant trails. Every successive iteration, these routes are further optimized. For illustration, a chemical known as pheromone is left by ants on their trails which attract other ants. Therefore higher number of ants would travel on an optimal trail towards a food source and deposit more pheromones. Thus optimal routes get reinforced as more requests are being served by the ants. Pheromone slowly evaporates over time, simulating the concept that some routes are nearly abandoned in the long run.

In this paper, the dual objective of maximizing network coverage by CHs and simultaneously reducing the number of CHs in a network, is proposed for optimizing both energy consumption and routing delay. Here, an ACO based routing is developed, so that frequent trails get gradual reinforcement and subsequently CHs emerge naturally from the network. The idle trails loose popularity and are finally abandoned. The terminals corresponding to such reinforced routes are identified as the CHs for the network, the rest being the cluster members. For this trained network, requests are routed by following intermediate CHs thus satisfying the objectives mentioned earlier. Simulation studies highlight the fact that sufficient coverage can be achieved with minimal number of CHs by executing the proposed algorithm. In addition, the threshold value of pheromone above which a route would contribute CHs to the clustered network is identified.

The rest of the paper is organized as follows. Section 2 presents the system model and the problem is described in Sect. 3. Next, the proposed solution is presented in Sect. 4. The simulation results are shown in Sect. 5 followed by conclusions in Sect. 6.

## 2 System Model

The hexagonal cellular layout in mobile networks is transformed into a two dimensional coordinate system in this work as shown in Fig. 1. Every cell is represented as  $(x, y)$  in a 3 axes layout due to the angle  $120^\circ$  [10] covered by a BS in a cell. The next set of cells along axis 1 of the layout is determined by an increment or decrement of  $x$ -values. Similar cells along axis 2 are determined by change of  $y$ -values only, whereas that along axis 3 is done by changes in both the  $x$  and  $y$  values.

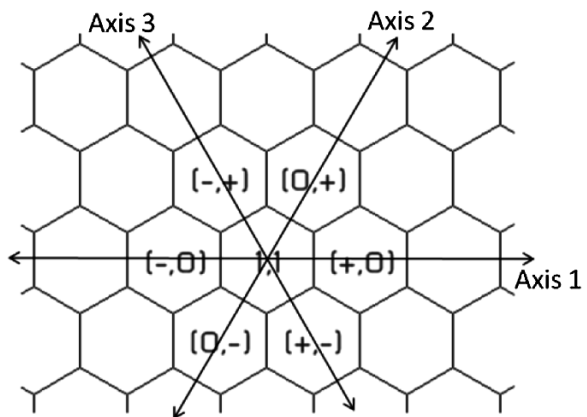
Based upon the layout described in Fig. 1, the neighborhood of every cell is categorized using the physical distance between them. Accordingly, the circles of neighbors around each cell are determined as Node Coordinate Interrelation (NCI) matrix, which is illustrated in Table 1. The model proposed in this work considers up to 5th circle considering the transmission range [11] of every BS.

Two cells  $(x_1, y_1)$  and  $(x_2, y_2)$  are determined as neighbors within transmission range of each other, if the following condition holds.

$$\text{Absolute } (x_1 - y_1 - x_2 + y_2) \leq 3 \tag{1}$$

The value obtained in (1) is used to determine the possible neighborhood of cells while calculating the possibility of forwarding of request through the layout. Thus the members of neighborhood for each cell are populated in this work as the NCI. On the other hand, NCI is populated with an arbitrary high value for the cells beyond

**Fig. 1** Cellular layout represented as coordinate system



**Table 1** Node coordinate interrelation (NCI) matrix

1st Circle	2nd Circle	3rd Circle	4th Circle	5th Circle
$(x, y - 1)$	$(x - 1, y - 2)$	$(x, y - 2)$	$(x - 1, y - 3)$	$(x, y - 3)$
$(x - 1, y - 1)$	$(x - 2, y - 1)$	$(x - 2, y - 2)$	$(x - 2, y - 3)$	$(x - 3, y - 3)$
$(x - 1, y)$	$(x - 1, y + 1)$	$(x - 2, y)$	$(x - 3, y - 2)$	$(x - 3, y)$
$(x, y + 1)$	$(x + 1, y + 2)$	$(x, y + 2)$	$(x - 3, y - 1)$	$(x, y + 3)$
$(x + 1, y + 1)$	$(x + 2, y + 1)$	$(x + 2, y + 2)$	$(x - 2, y + 1)$	$(x + 3, y + 3)$
$(x + 1, y)$	$(x + 1, y - 1)$	$(x + 2, y)$	$(x - 1, y + 2)$	$(x + 3, y)$
			$(x + 1, y + 3)$	
			$(x + 2, y + 3)$	
			$(x + 3, y + 2)$	
			$(x + 3, y + 1)$	
			$(x + 2, y - 1)$	
			$(x + 1, y - 2)$	

transmission range to inhibit direct communication between them. In addition, it is important to mention that  $NCI_{source,destination}$  or  $NCI_{hop}$  is the notation commonly used in this work for removing ambiguity in representation. Identical approach in notation is followed for other essential parameters related with the network.

### 3 Problem Statement

The design of the clustered network in this work is associated with two objectives. The first one is involved with the minimization of the number of CHs such that any request can be routed through minimum number of hops, resulting in reduced delay. Another objective is to simultaneously address the placement of CHs so that maximum coverage can be achieved for the network. Thus the design addressed in this work can be presented by the following multi objective optimization (MOO).

$$\text{Objectives} = \begin{cases} \min(|CH|) \\ \max(\text{coverage}) \end{cases} \quad (2)$$

Subject to:

$$\begin{aligned} \forall \text{ route} \in \text{request} \\ \forall \text{ node} \in \text{route}, \\ NCI_{\text{node,next node}} \leq \text{transmission range} \end{aligned} \quad (3)$$

In (3), the route selected corresponding to a request in the system gets transmitted using hops that are within the transmission range of each other.

## 4 Proposed Model

The model proposed in this work begins with the initialization of the network as discussed earlier. This involves pre-calculation of NCI for the network, along with the resident energy ( $energy_{node}$ ) for BSs and initial pheromone values corresponding to every possible elementary hop ( $pheromone_{hop}$  or  $pheromone_{source,destination}$ ). Next, routing for the incoming set of call requests is attempted by following proposed ACO based algorithm. In addition, the network status is checked after successive intervals of routing to detect emergence of CHs and correctness of subsequent routing by utilizing them.

### 4.1 Proposed ACO Based Algorithm

It is important to introduce the following key terminologies used in the system before presenting the algorithms. Two modulating factors,  $\alpha$  and  $\beta$  has been introduced to normalize the control factors guiding the algorithm discussed later. Another factor  $\lambda$  is applied upon the transmission range for consumption of residual energy at a node. Further, ACO algorithms are characterized by two other factors, pheromone deposit rate ( $Q$ ) and pheromone evaporation rate ( $\rho$ ). By natural observation, value of  $Q$  is selected to be significantly higher than the value of  $\rho$ . The algorithm in this work for determining the routes between the source and destination corresponding to a request while simultaneously using the CHs as intermediate hops is proposed by the following rules.

#### Rule1

The neighbors of a current node residing in the direction of the destination are considered as possible next hop. Among the alternatives, the hop with a higher pheromone value has a greater chance for getting selected. Further, such a hop gradually reinforces the neighbor, which can subsequently emerge as a CH.

#### Rule2

The amount of residual energy of the current node determines the possibility of selecting the next hop as a distant or a near one. Here, if the BSs of a region in the network become low in residual energy, CH density of such regions tends to be higher than the rest of the network. Accordingly transmission delay gets prolonged in such regions.

A request queue is maintained locally at every node, having requests originating from it as well as other neighboring nodes. The queue is derived from the call requests for the entire network, which is characterized by parameters like source node, destination node, call duration and priority of the request. The delay encountered by a request at a specific node depends upon the queue length of that node, having priority equal to or greater than the current request. The selection of the next node to forward the request is determined by the rules introduced earlier.



For all the alternatives lying in the direction of the destination node, a weighted product called ‘taueta’ is derived by obeying the two rules. This ensures that both the factors have sufficient control upon the selection procedure. A roulette wheel selection [12] mechanism upon the cumulative sum of all taueta values determines the next hop. This procedure is described by the following algorithm.

**Algorithm 1.** determine next hop (current node, destination node)

```

 $\forall$  node  $\in$  transmission range of current node
  if node  $\in$  direction(destination)
    nodespossible hop = nodespossible hop  $\cup$  {node};
    tauetanode = ((energysource/NCIsource, node) $\alpha$ ) * (pheromonesource, node) $\beta$ ;
  end if
end for
tauetacumulative = cumulative sum (taueta);
next node = roulette wheel selection (nodespossible hop, tauetacumulative);
trailsource, destination = trailsource, destination  $\cup$  hopcurrent node, next node;

```

Based on Algorithm 1, once a call has been successfully routed from the source to destination, subsequently the residual energy of the initial and intermediate forwarders are reduced by a factor depending on the distance of the transmission hop to the next node. Besides, the pheromone values of the hops used in the current trail is increased, whereas the same for all other possible hops is reduced. This is illustrated by Algorithm 2.

**Algorithm 2.** adjust parameter values (trail)

```

 $\forall$  hop  $\in$  trailsource, destination
  decrease = (1-p) * pheromonehop;
  increase = Q / length(trail);
  pheromonehop = decrease + increase;
  energyhop-source = energyhop-source -  $\lambda$  * length(hop);
end for

```

## 4.2 Evaluation of CH Selection and Network Coverage

The proposed methodology for determining the number of CHs and network coverage is based on the pheromone value of the hops obtained in Algorithm 2. This procedure is executed alongside the routing described in Algorithm 1 to check the emergence of CHs and accuracy of subsequent routing. The pheromone values are initialized to a small fraction uniformly for all the hops. While routing, the pheromone values are updated according to the number occurrence of the hops in the trails. Thus, an important hop has significantly higher probability of getting

selected for future routing. The terminals of such a hop can be treated as CHs, and transmissions are more probable to converge on such a node on later stage as compared to other members. The threshold pheromone for a hop, beyond which CHs emerge, is determined in this phase.

Coverage of the network is defined as the percentage of nodes that finds at least one CH among its neighbors, which undoubtedly, would increase upon decreasing the threshold pheromone. However, decreasing this threshold has the effect of unnecessary increase of CHs in the entire network, which would result in increased delay in subsequent requests. Hence an optimal balance between these two is necessary, which is heuristically determined in this step. The entire procedure is described by Algorithm 3.

**Algorithm 3.** Evaluation of coverage and optimal CH count

```

 $\forall$  threshold  $\in$  {1:0.1 step (-0.05)}
  hopsprominent = {hop | pheromonehop > threshold};
   $\forall$  hop  $\in$  hopsprominent
    CH = CH  $\cup$  {sourcehop}  $\cup$  {destinationhop};
  end for
   $\forall$  node  $\in$  network
    If  $\exists$  neighbornode such that neighbornode  $\in$  CH
      countcoverage = countcoverage + 1;
    end if
  end for
  if countcoverage / count (node  $\in$  network) == 1
    thresholdcoverage = threshold;
    break;
  end if
end for

```

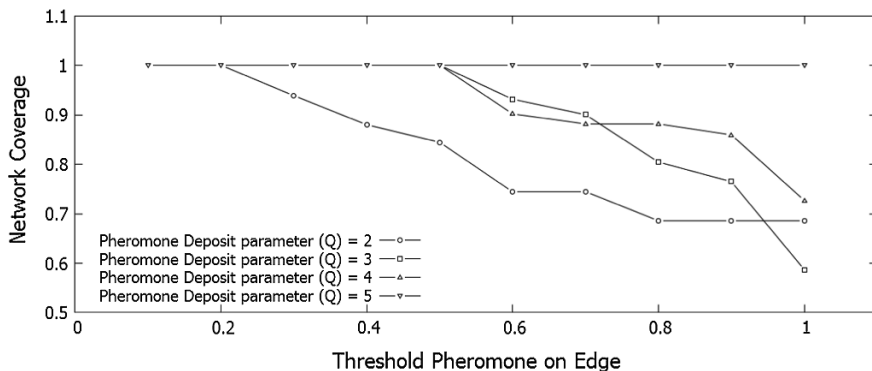
## 5 Simulation Studies

The experimental results for the proposed model have been obtained by simulating a network grid of size  $100 \times 100$ , and simulating random requests between the nodes. The various system parameters are highlighted in Table 2.

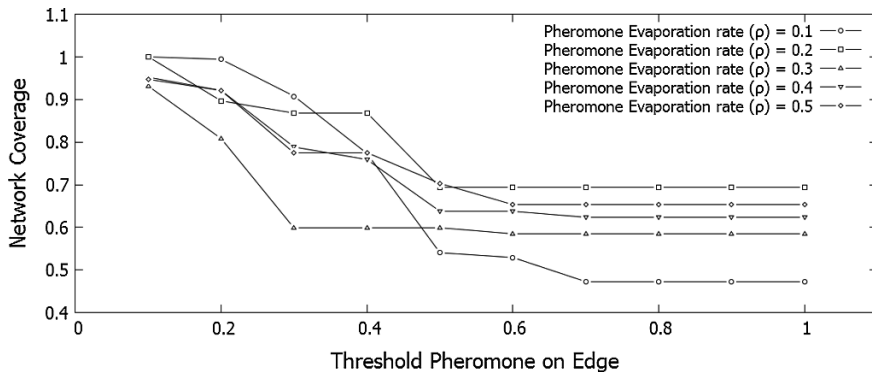
For a randomly generated set of requests, the threshold is varied from 1 to 0.1 with different values of  $Q$  and  $\rho$ . Higher values of  $\rho$  imply more decrease in pheromone value. The increase effect is produced by adding a proportion of the current ant's total trail length, where the proportion is determined by  $Q$ . Higher values of  $Q$  increase the amount of deposited pheromone. Simulation studies show that a high value of  $Q$  leads to identification of high number of CH and total coverage in network. With a low value of  $Q$  ( $=2$ ) we can still achieve total coverage at a low value of threshold. Keeping  $Q$  fixed, next  $\rho$  is varied. With reasonably low value of  $\rho$ , total coverage is achieved, which is illustrated in Figs. 2 and 3.

**Table 2** Simulation parameters

Network grid size	100 × 100
Allowable diversion	Maximum 5 nodes
Objective modulator ( $\alpha$ )	3
Objective modulator ( $\beta$ )	2
Pheromone evaporation rate ( $\rho$ )	0.1
Pheromone deposit rate ( $Q$ )	2.0
Interval for threshold calculation	100 Requests
Energy depletion factor ( $\lambda$ )	0.05



**Fig. 2** Node coverage versus threshold pheromone for different values of Q



**Fig. 3** Node coverage versus threshold pheromone for different values of  $\rho$

Once total coverage in the network is achieved, another objective to minimize the number of CHs is attempted. As we interpret from Fig. 4, a high percentage of CHs (nearly 30 %) can achieve 100 % coverage, whereas only a third of that, i.e. nearly

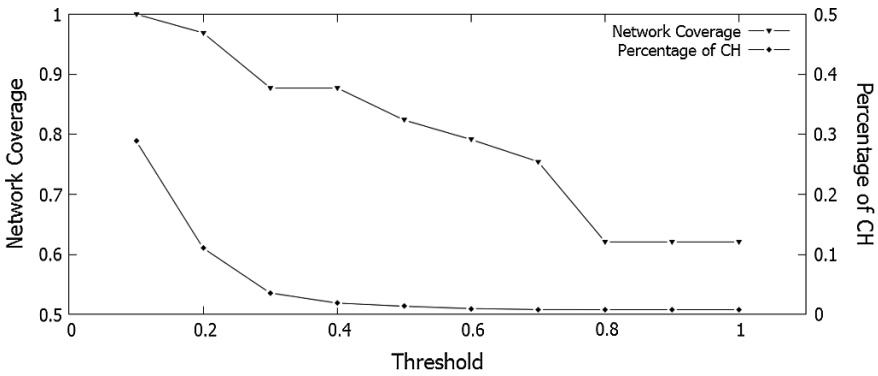


Fig. 4 Node coverage and CH probability versus threshold pheromone

10 % CHs is able to achieve over 95 % coverage in the network. For optimal results, we can target less than 100 % coverage in the network at a reasonably reduced number of CHs, resulting in reduced transmission delay in the network.

Further, a comparison with the iterative approach of CH selection, as attempted in traditional approaches [1, 13–15], is performed. These perform a randomized CH election, based upon the fact that a CH that has been earlier elected has reduced chance of getting elected again. However, the algorithm proposed in current work illustrates a reverse concept, nodes that are elected as CH has higher chance of getting elected in next rounds. The former approaches attempt uniform energy depletion in the network, ignoring the concept of coverage. As seen from Fig. 5, the proposed algorithm selects CHs with stable coverage upon the entire network, which is higher than the average coverage gained by traditional models.

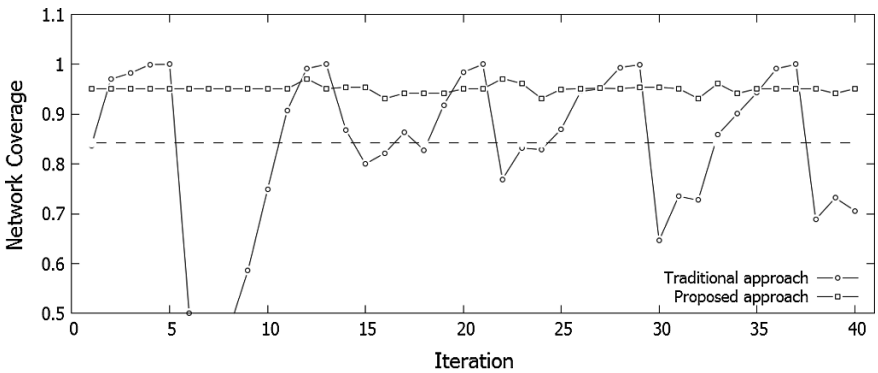


Fig. 5 Comparison of network coverage of the proposed algorithm and traditional approach

## 6 Conclusions

In this work, an ACO based routing algorithm that plays the dual objective of minimizing CHs in the network and increasing coverage is proposed. These objectives are modeled with an attempt to address the granular requirement of reducing the transmission delay and energy consumption in mobile networks. The proposed algorithm is implemented to cluster the routes for call requests in a network. Simulation studies derive the threshold upon the parameters, using which we can achieve maximum network coverage for a minimum assignment of CHs. Improvement by the proposed model over the traditional one is highlighted. Further, subsequent improvements in different network scenarios through similar evolutionary algorithmic approaches are under current investigation.

## References

1. Liao, Q., Zhu, H.: An energy balanced clustering algorithm based on LEACH protocol. In: Proceedings of the 2nd International Conference on Systems Engineering And Modeling (2013)
2. Nghiem, T.P., Kim, J.H., Lee, S.H., Cho, T.H.: A coverage and energy aware cluster-head selection algorithm in wireless sensor networks. In: Emerging Intelligent Computing Technology and Applications. Lecture Notes in Computer Science, vol. 5754, pp. 696–705 (2009)
3. Lee, J., Jung, K., Jung, H., Lee, D.: Improving the energy efficiency of a cluster head election for wireless sensor networks. *Int. J. Distrib. Sens. Netw.* **2014**, Article ID 305037, 6, (2014)
4. Giordano, S., Stojmenovic, I., Blazevic, L.: Position based routing algorithms for Ad Hoc networks: a taxonomy. In: *Ad Hoc Wireless Networking*, pp. 103–136 (2001). ISBN 978-1-4613-7950-8 (Print) 978-1-4613-0223-0 (Online)
5. Bell, J.E., McMullen, P.R.: Ant colony optimization techniques for the vehicle routing problem. *Adv. Eng. Inform* **18**, 41–48 (2004)
6. Gill, N.S., Atri, S., Atri, J.: Clustering approach based on ant colony optimization. *Int. J. Adv. Res. Comput. Sci. Software Eng.* **4**(2), (2014)
7. Pedro, J.M., Pires, J.J.O., Carvalho, J.P.C.: Ant colony optimization for distributed routing path optimization in optical burst-switched networks. *IFSA-EUSFLAT* (2009)
8. Hruschka, E.R., Campello, R.J.G.B., Freitas, A.A., Carvalho, A.C.P.L.F.: A survey of evolutionary algorithms for clustering. *IEEE Trans. Syst. Man Cybern.—Part C: Appl. Rev.* (to appear)
9. Liu, J.L., Ravishankar, C.V.: LEACH-GA: genetic algorithm-based energy-efficient adaptive clustering protocol for wireless sensor networks. *Int. J. Mach. Learn. Comput.* **1**(1), 79–85 (2011)
10. Shakhakarm, N.: Optimization of cellular resources evading intra and inter tier interference in femto cells equipped macro cell networks. *Int. J. Comput. Sci. Issues (IJCSI)* **9**(2), (2012)
11. Wu, Z., Song, H., Jiang, S., Xu, X.: A grid-based stable routing algorithm in mobile Ad Hoc networks. *IEEE First Asia International Conference on Modeling and Simulation*, pp. 181–186, 27–30 (2007)
12. Razali, N.M., Geraghty, J.: Genetic algorithm performance with different selection strategies in solving TSP. In: *Proceedings of the World Congress on Engineering*, vol. II (2011)

13. Cao, T., Wang, Y., Xiong, X., Hao, Y.: Cluster-based routing performance optimization constraint of energy, delay and connectivity metrics in wireless sensor network. *Int. J. Smart Sens. Intell. Sys.* **6**(5), 2103–2118 (2013)
14. Hussain, K., Abdullah, A.H., Iqbal, S., Awan, K.M., Ahsan, F.: Efficient cluster head selection algorithm for MANET. *J. Comput. Netw. Commun.* **2013**, Article ID 723913, 7 (2013)
15. Raghuvanshi, A.S., Tiwari, S., Tripathi, R., Kishor, N.: Optimal number of clusters in wireless sensor networks: an FCM approach. *Int. Conf. Comput. Commun. Technol.* 817–823 (2010)

# A Trade-off Analysis of Quality of Service (QoS) Metrics Towards Routing in Mobile Networks: MOGA Based Approach

Aritra Rudra, Parag Kumar Guha Thakurta and Rajarshi Poddar

**Abstract** The trade-off analysis between two QoS metrics towards efficient routing in mobile networks is proposed in this paper. For such analysis the behavioural natures of end-to-end transmission cost and hop-count as QoS metrics are accounted in discrete domain and subsequently, the probability density functions (*pdf*) of those important factors are determined. The *pdf* of these are transformed into continuous domain to perform mathematical operation and subsequent analysis is presented to obtain the optimal routing path(s). In this context, a multi objective optimization (MOO) on these parameters is proposed and more refined results among all possible solutions are obtained accordingly. The diverse set of possible solutions for such analysis is explored through a Multi Objective Genetic Algorithm (MOGA) based approach.

**Keywords** Trade-off · Optimization · Probability density function · Genetic algorithm · Mobile network

## 1 Introduction

In the past decade, wireless mobile networks have become increasingly popular in the computing domain. This class of network is commonly called mobile cellular networks, which has fixed switching sub-systems known as base stations that synchronize and control all wireless transmissions within their coverage area (or cell) [1]. A mobile node connects to and communicates with the neighbourhood

---

A. Rudra (✉) · P.K.G. Thakurta · R. Poddar

Department of Computer Science and Engineering, National Institute of Technology,  
Durgapur, India

e-mail: aritrarudra@gmail.com

P.K.G. Thakurta

e-mail: parag.nitdgp@gmail.com

R. Poddar

e-mail: rajarshi.poddar@gmail.com

© Springer India 2015

J.K. Mandal et al. (eds.), *Information Systems Design and Intelligent Applications*,

Advances in Intelligent Systems and Computing 339,

DOI 10.1007/978-81-322-2250-7\_14

BSs located within its transmission range [2]. The efficiency of such networks is characterised with different Quality of Service (QoS) metrics like delay, bandwidth, hop-count, transmission cost etc. [3]. The performances of these metrics are interrelated with each other. For example, if the number of hop is reduced, then the distance between two successive hops is increased accordingly. Subsequently, the transmission energy for sending data packet is increased, as it is directly proportional to the distance between hops. In real life application, it is necessary to optimize these QoS parameters to satisfy user requirements. Therefore, a trade-off analysis among these factors needs to be evaluated under such scenario.

The set of works related to the trade-off measurement and its applications spans several distinct areas of literature. The paper presented in [4] studies an optimization scheme for determining the trade-off between two routing cost metrics i.e., delay and bandwidth. Another application on determination of trade-off between the coexisting networks is accounted in [5] which is analysed in terms of transmission capacity. In [6], the fundamental trade-off among delay and infrastructure cost of epidemic routing in mobile networks is studied. The paper in [7] formulates a trade-off policy between energy consumption and other QoS parameters in the mobile grid environment. The performance of the energy QoS trade-off algorithm is compared with other energy and deadline constrained scheduling algorithm.

In [8] the authors discussed the selection of a caching policy by the network administrator based on hop-count and transmission cost with improved QoS. The works in [9, 10] show the trade-off between call arrivals and delay requirements i.e. target delay and delay probability. The trade-offs between two tree based routing strategies with respect to hop count and number of edges are described in [11, 12]. In short, several trade-off analyses of various QoS metrics on different aspects have been carried out. Most of them are resolved using some specific optimization technique. However, a new trade-off analysis for QoS metrics in mobile networks is proposed in this paper to facilitate more refined solutions. This is attempted in this work by proposing a probabilistic model in a comprehensive manner.

The trade-off performance between two QoS metrics in mobile networks namely end-to-end transmission cost ( $t_c$ ) and hop-count ( $h_c$ ) is proposed in this paper. Generally, the behavioural natures of these factors are accounted in discrete domain and subsequently, the probability density functions (pdf) of those important factors are determined. Due to the requirement of mathematical operations, the pdf of these factors are transformed into continuous domain and a trade-off analysis among these is presented to find out the optimal routing path(s). This is formulated using a multi objective optimization (MOO) where a simultaneous optimization on  $t_c$  and  $h_c$  is done. Further, more refined results among all possible solutions are obtained by using a bivariate distribution function involving  $t_c$  and  $h_c$ . Hence, the diverse set of possible solutions for these QoS metrics are explored through a Multi Objective Genetic Algorithm (MOGA) based approach.

The remainder of the paper is organized as follows. The problem addressed in this work is formulated in Sect. 2. The proposed solution for this problem is discussed in Sect. 3. Section 4 shows the simulation results to reflect the performance of the proposed model. Finally, we outline the conclusions of this paper in Sect. 5.



## 2 Problem Formulation

The problem addressed in this work begins with the computation of probability distribution for parameters  $t_c$  and  $h_c$ . Therefore, a two dimensional random walk [13] with random vector is used on cellular structure [1, 14] to determine the distribution function. The pdf of  $t_c$  and  $h_c$  describes the distribution of probability densities of these factors over the sample space. Here, the scatter plot for  $t_c$  and  $h_c$  for a given pair of source ( $s$ ) and destination ( $d$ ) is shown in the following Fig. 1.

Thus  $t_c$  and  $h_c$  are correlated with each other as apparent from Fig. 1. The joint pdf of  $t_c$  and  $h_c$  follows bivariate Gaussian Distribution which is supported by the random walk. To determine such joint pdf, the mean ( $\mu$ ) and standard deviation ( $\sigma$ ) of  $t_c$  and  $h_c$  for all possible routing paths between a pair of  $s$  and  $d$  are computed. Now, (1) expresses the discussed distribution as follows.

$$f(t_c, h_c) = \frac{1}{2 \prod \sigma_{t_c} \sigma_{h_c} \sqrt{1 - \rho^2}} e^{\left[ -\frac{1}{2(1-\rho^2)} \left\{ \left( \frac{t_c - \mu_{t_c}}{\sigma_{t_c}} \right)^2 + \left( \frac{h_c - \mu_{h_c}}{\sigma_{h_c}} \right)^2 - 2\rho \left( \frac{t_c - \mu_{t_c}}{\sigma_{t_c}} \right) \left( \frac{h_c - \mu_{h_c}}{\sigma_{h_c}} \right) \right\} \right]}, \quad (1)$$

$-1 < \rho < 1$

where  $\rho$  denotes the correlation coefficient for bivariate Gaussian Distribution among  $t_c$  and  $h_c$ . The points with minimum probability would support the preference on  $t_c$  and  $h_c$  individually. However, the routing paths with minimum QoS metric values are usually different. Therefore, a path belonging to the set of solutions is selected with optimal values of the corresponding metrics to maintain a successful trade-off between these two. The optimal values of  $t_c$  and  $h_c$  are governed by the following partial differential equations.

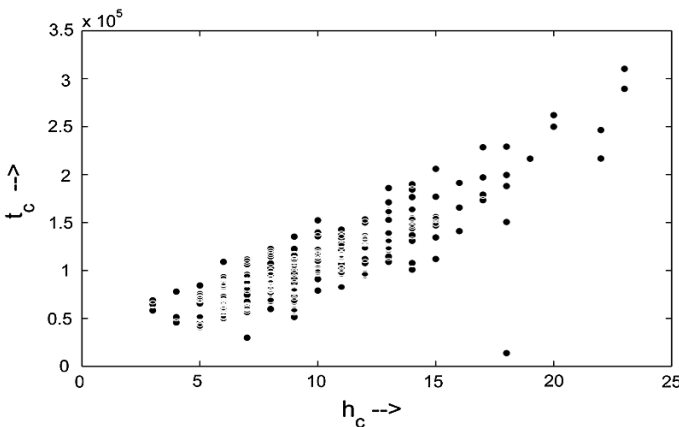


Fig. 1 Scatter plot for  $t_c$  and  $h_c$

$$\frac{\partial f}{\partial Z_c} = \frac{1}{2 \prod \sqrt{1 - \rho^2}} e^{\left[ -\frac{Z_c^2 + Z_{h_c}^2 - 2\rho Z_c Z_{h_c}}{2(1 - \rho^2)} \right]} \left[ -\frac{2Z_c - 2\rho Z_{h_c}}{2(1 - \rho^2)} \right] = 0 \quad (2)$$

$$\frac{\partial f}{\partial Z_{h_c}} = \frac{1}{2 \prod \sqrt{1 - \rho^2}} e^{\left[ -\frac{Z_c^2 + Z_{h_c}^2 - 2\rho Z_c Z_{h_c}}{2(1 - \rho^2)} \right]} \left[ -\frac{2Z_{h_c} - 2\rho Z_c}{2(1 - \rho^2)} \right] = 0 \quad (3)$$

where  $Z_c = \frac{t_c - \mu_{t_c}}{\sigma_{t_c}}$  and  $Z_{h_c} = \frac{h_c - \mu_{h_c}}{\sigma_{h_c}}$ .

The condition for obtaining the trade-off between  $t_c$  and  $h_c$  by solving (2) and (3) is expressed as in the following.

$$Z_c - \rho Z_{h_c} = 0 \quad (4)$$

$$Z_{h_c} - \rho Z_c = 0 \quad (5)$$

Hence, (4) and (5) are combined to provide the required condition for trade-off by the following.

$$\frac{t_c - \mu_{t_c}}{\sigma_{t_c}} = \frac{h_c - \mu_{h_c}}{\sigma_{h_c}} \quad (6)$$

The inter-twining of cost metrics is expressed in terms of  $\rho$  as shown in (1). As the extreme values of pdf would have the lowest probability, minimizing  $f(t_c, h_c)$  would lead to the maximization or minimization. However, for a trade-off in routing metrics, we are interested only with the minima values. Therefore, both  $t_c$  and  $h_c$  needs to be minimized as shown below in (7) respectively. The problem is now formulated as MOO with consideration of the set of all possible routing paths  $P = [\{p_1, p_2, \dots, p_n\} | \forall p_i \in P]$  between  $s$  and  $d$  as follows.

$$\text{objectives} \begin{cases} \min f(t_c, h_c) \\ \min g(p_i) = |p_i|_{t_c} \\ \min h(p_i) = |p_i|_{h_c} \end{cases} \quad (7)$$

$$\text{subject to} \begin{cases} |p_i|_{t_c} \in t_c, \forall p_i \in P \\ |p_i|_{h_c} \in h_c, \forall p_i \in P \end{cases} \quad (8)$$

The constraints in (8) ensure that  $t_c$  and  $h_c$  of a specific path is selected during trade-off analysis.

### 3 Proposed Solution

The model proposed in this work is evaluated with the application of MOGA. The ability of MOGA to search different regions of the solution space makes it suitable to find optimal solutions of multi objective problems in a single run. We use a non-dominated sorting approach NSGA-II [14] to determine the Pareto optimal front. In this context, transformation of network characteristics to GA paradigm and the function of genetic operators for creating offspring population are discussed next.

- **Chromosome encoding:** A chromosome in our proposed MOGA based methodology is a sequence of positive integers corresponding to the IDs of nodes that represent a routing path and each gene of the chromosome provides the order of the nodes in that routing path. The length of the chromosome is variable, but it should not exceed the maximum length  $N$ , where  $N$  denotes the total number of nodes in the network. A chromosome encodes the problem by listing up node IDs from  $s$  to  $d$  based on an information database like routing table of the network. In our work, this information is obtained and managed by using an adjacency matrix.
- **Population Initialization:** There are two ways to generate the initial population such as heuristic initialization and random initialization. Although the mean fitness of the heuristic initialization is already high so that it may help the GAs to find solutions faster, it may explore a small part of the solution space and never find global optimal solutions because of the lack of diversity in the population. Therefore, 80:20 combinations of random initialization and heuristic initialization are effected in this work to take the advantages provided by both methods. The various graph traversal methods are used as heuristics. Thus initial population is now generated with the encoding method described earlier.
- **Selection:** The selection operator is intended to improve the average quality of the population by providing the high-quality chromosomes to get a better chance to be copied into the next generation. As elitism is applied here,  $\xi$  best solutions are forwarded into the next generation where  $\xi$  denotes the elitism count. To fill rest of the population, tournament selection [15] without replacement is perceived in our approach. However, the same chromosome should not be picked twice as a parent. The use of Crowded-Comparison Operator ( $\prec_n$ ) [14] drives the procedure towards a better spread of population in attaining the true Pareto-optimal front.
- **Crossover:** The crossover procedure is used to generate offspring chromosomes from dominant parent chromosomes. In the proposed model, a single point crossover is used to exchange genetic materials between the parent chromosomes. One random site is selected as the crossover site out of the several potential crossing sites. In our problem, the crossover between two paths from  $s$  to  $d$  is shown in Fig. 2.
- **Mutation:** Mutation not only helps to recover any lost gene but also helps to stay away from local optima and head for global optima. The mutation function has the ability to generate a path which has a very different fitness from the

original path, thus preserving diversity in the population. For path with  $s$  and  $d$ , the mutation procedure is shown in Fig. 3.

- **Loop Repair:** The crossover and mutation procedure may give rise to loops in the generated path. The loops are removed from the path with the help of repair function [15].

The procedure to get Pareto optimal solutions is thus described by the following MOGA and subsequently it is discussed in detail.

---

*Algorithm: procedure MOGA* ( $N, t_{max}, p_{crossover}, p_{mutation}$ )

---

*/\*N is the population size,  $t_{max}$  is the desired number of generations,  $p_{crossover}$  and  $p_{mutation}$  denote crossover and mutation probabilities respectively \*/*

```

1.  $t \leftarrow 1$ 
2.  $P_1 \leftarrow$  create a new random population of size  $N$ 
3.  $Q_1 \leftarrow \emptyset$ 
4. while ( $t \leq t_{max}$ ) do
5.    $R_t \leftarrow P_t \cup Q_t$ 
6.    $P_{t+1} \leftarrow \emptyset$ 
7.    $Q_{t+1} \leftarrow \emptyset$ 
8.    $F \leftarrow non\_dominated\_sort(R_t)$ 
9.    $i \leftarrow 1$ 
10.  while( $|P_{t+1}| + |F_i| \leq N$ )do
11.     $assign\_crowding\_distance(F_i)$ 
12.     $P_{t+1} \leftarrow P_{t+1} \cup F_i$ 
13.     $i \leftarrow i + 1$ 
14.  end while
15.  if( $|P_{t+1}| < N$ )
16.     $sort(F_i, <_n)$ 
17.     $P_{t+1} \leftarrow P_{t+1} \cup F_i[1 : (N - |P_{t+1}|)]$ 
18.  end if
19.  while( $|Q_{t+1}| \leq N$ )do
20.     $individual\_A \leftarrow tournament\_selection(P_{t+1})$ 
21.     $individual\_B \leftarrow tournament\_selection(P_{t+1})$ 
22.     $rand\_no \leftarrow$  choose a random number between 0 and 1
23.    if ( $rand\_no \leq p_{crossover}$ )
24.       $Q_{t+1} \leftarrow crossover(individual\_A, individual\_B)$ 
25.    else
26.       $Q_{t+1} \leftarrow individual\_A$  or  $individual\_B$ 
27.    end if
28.     $rand\_no \leftarrow$  choose a random number between 0 and 1
29.    if ( $rand\_no \leq p_{mutation}$ )
30.       $individual\_to\_mutate \leftarrow$  select a random individual from  $Q_{t+1}$ 
31.       $mutated\_individual \leftarrow mutate(individual\_to\_mutate)$ 
32.      replace  $individual\_to\_mutate$  with  $mutated\_individual$  in  $Q_{t+1}$ 
33.    end if
34.  end while
35.   $t \leftarrow t + 1$ 
36. end while
37. end procedure

```

---

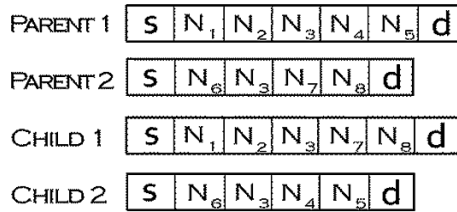


Fig. 2 Crossover used in the proposed work

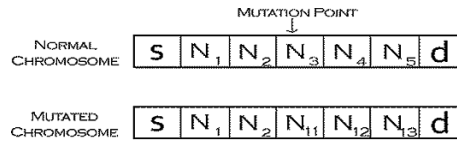


Fig. 3 Mutation used in the proposed work

- Line 1: Generation count (t) is initialized.
- Line 2: Initial population (P<sub>1</sub>) is initialized as discussed previously with N individuals.
- Line 3: Offspring population (Q<sub>1</sub>) is initialized to null.
- Line 4–36: Loop controls the number of generations.
- Line 5: Parent and offspring population are combined into R<sub>t</sub>.
- Line 6–7: Next generation populations are initialized to null.
- Line 8: All non-dominated fronts of the combined population are searched and assigned to F.
- Line 9: Front count i is initialized to 1.
- Line 10–14: Loop is executed until new parent population is filled up.
- Line 11–12: Crowding distance in ith front is computed and included as part of parent population.
- Line 13: The front count is incremented.
- Line 15–18: Check if parent population is filled yet or not.
- Line 16: Sort only the ith front by using Crowded-Comparison Operator (<<sub>n</sub>).
- Line 17: The first (N - |P<sub>t+1</sub>|) elements of the ith front are selected and placed into P<sub>t+1</sub>.
- Line 19–34: The offspring population is generated and filled up using selection, crossover and mutation as discussed earlier.
- Line 35: The generation count is incremented.

### 4 Experimental Results

The simulation of the proposed model has been carried out using MATLAB 7.6 and JAVA on a server with two Intel Xeon processor (2.33 GHz) and 12 GB memory. Now the trade-off analysis is carried out with  $N = 250$  (initial population),  $p_{crossover} = 0.8$  (crossover probability) and  $p_{mutation} = 0.1$  (mutation probability). The Pareto optimal solutions for the optimization of both  $t_c$  and  $h_c$  is obtained through the proposed MOGA and is shown in Fig. 4. Here, it is observed that the transmission cost is increased for reduced hop count and vice versa.

The solution obtained in Fig. 4 is further refined by the expression (1) and are shown with variation against  $t_c$  and  $h_c$  in Figs. 5 and 6 respectively. In these

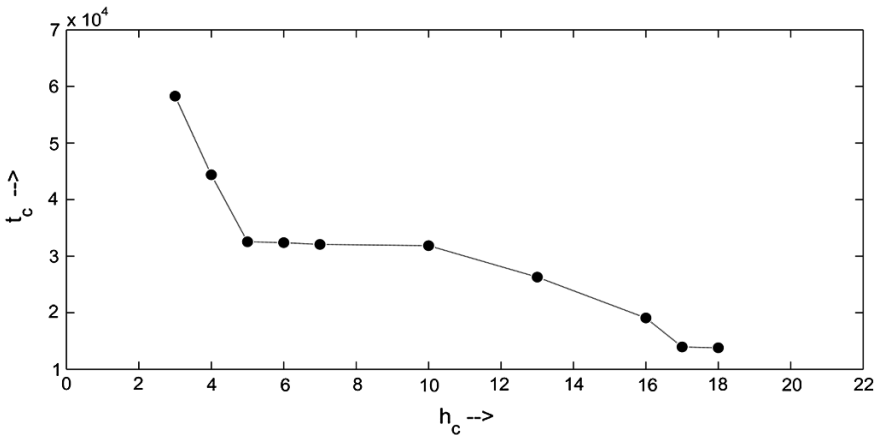


Fig. 4 Pareto optimal solutions for  $t_c$  and  $h_c$

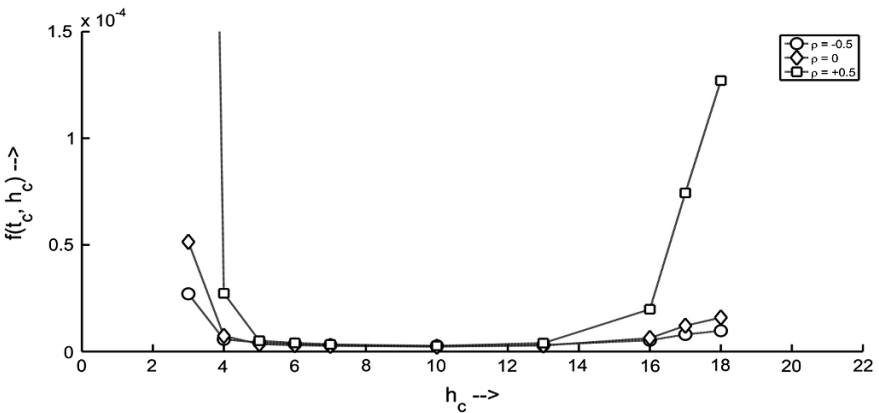


Fig. 5 Refinement for  $h_c$  achieved by varying  $f(t_c, h_c)$

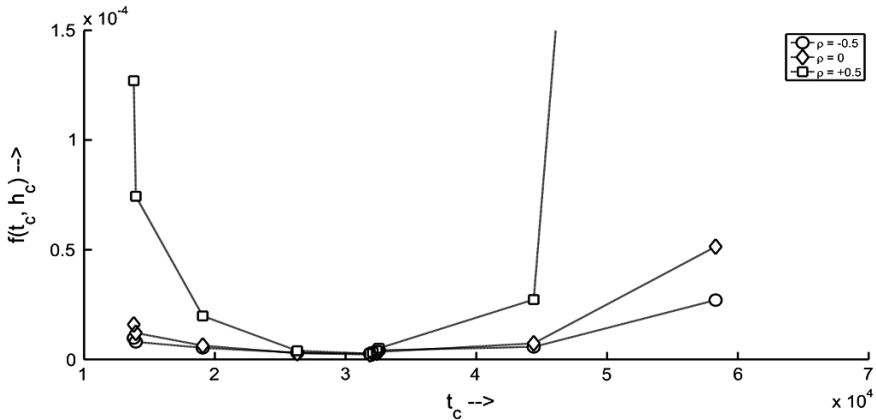


Fig. 6 Refinement for  $t_c$  achieved by varying  $f(t_c, h_c)$

experiments, the refined solutions are obtained for different values of  $\rho$ . It is observed in Fig. 5 that the more perfect solutions for reducing  $h_c$  lie in the lower portion of the curve which was not apparent from Fig. 4. Similarly, Fig. 6 points out the perfect candidates for reducing  $t_c$  and its variation with the same. It is significant that the extreme points in Fig. 4 provide the better results only for any one among  $t_c$  and  $h_c$ , whereas the solutions obtained in both Figs. 5 and 6 provide better trade-off involving both  $t_c$  and  $h_c$ . In addition, resemblance in nature of the curves obtained in Figs. 5 and 6 are apparent from (6). Thus for each route, the deviation of  $t_c$  and  $h_c$  from their mean values are similar which preserves the balance between these QoS metrics from trade-off perspective.

### 5 Conclusions

The efficiency of mobile cellular network is measured with the help of different QoS parameters. The inter-twining of these parameters requires a trade-off performance among these factors. Here, the performance and its effectiveness is established for the metrics end to end transmission cost ( $t_c$ ) and hop-count ( $h_c$ ). In this work, pdf of those factors is determined and subsequently, the analysis on trade-off measurement converges to a MOO problem. Further, the selection of improved solutions is obtained by satisfying another objective after simultaneous minimization of both  $t_c$  and  $h_c$ . The introduction of MOGA based approach is used to obtain the Pareto optimal solutions. In addition, the effectiveness of our proposed model is verified through experimental analysis.

## References

1. Banerjee, S., Roy, S., Thakurta, P.K.G.: Coordinate based directed routing protocol. *Int. J. Inf. Electron. Eng.* **2**(2):170–173 (2012)
2. Wu, Z., Song, H., Jiang, S., Xu X.: A grid-based stable routing algorithm in mobile ad hoc networks. *IEEE First Asia International Conference on Modeling and Simulation*, pp. 181–186, 27–30 Mar 2007
3. Chen, L., Heinzelman, W.B.: A survey of routing protocols that support QoS in mobile ad hoc networks. *IEEE Network* **21**(6):30–38 (2007)
4. Lu, J., Cheng, W.: A genetic-algorithm-based routing optimization scheme for overlay network. In: *Third International Conference on Natural Computation—(ICNC '07)*, vol. 04, pp. 421–425, 24–27 Aug 2007
5. Huang, K., Lau, V.K.N., Chen, V.: Spectrum sharing between cellular and mobile ad hoc networks: transmission-capacity tradeoff. *IEEE J. Sel. Areas Commun. Spec. Issue Stoch. Geom. Random Graphs Anal. Des. Wirel. Netw.* **27**(7):1256–1267 (2009)
6. Zhou, S., Ying, L., Tirthapura, S.: Delay, cost and infrastructure tradeoff of epidemic routing in mobile sensor networks. In: *6th International Wireless Communications and Mobile Computing Conference (IWCMC '10)*, pp. 1242–1246, June 28–July 2, 2010
7. Li, Chunlin, Li, Layuan: Tradeoffs between energy consumption and QoS in mobile grid. *J. Supercomputing* **55**(3), 367–399 (2011)
8. Guha Thakurta, P. K., Mallick, N., Dutta, G., Bandyopadhyay, S.: A new approach on caching based routing for mobile networks. In: *International Conference on Communication, Computing and Security 2011 (ICCCS '11)*, pp. 32–35, 12–14 Feb 2011
9. Soret, B., Torres, M.A., Entrambasaguas, J.T.: analysis of the trade-off between delay and source rate in multiuser wireless systems. *EURASIP J. Wirel. Commun. Networking* **2010**, 12 (2010)
10. Vasef, M.: Effective capacity of a rayleigh fading channel in the presence of interference. *Int. J. Wirel. Mob. Networks* **4**(3):1–19 (2012)
11. Meghanathan, N.: Performance comparison of minimum hop and minimum edge based multicast routing under different mobility models for mobile ad hoc networks. *Int. J. Wirel. Mob. Networks* **4**(3), 1–14 (2011)
12. Meghanathan, N.: Benchmarks and tradeoffs for minimum hop, minimum edge and maximum lifetime per multicast tree in mobile ad hoc networks. *Int. J. Advancements Technol.* **1**(2), 234–251 (2010)
13. Keqin, L.: Performance analysis and evaluation of random walk algorithms on wireless networks parallel and distributed processing. *IEEE international symposium on workshops and Ph.D. forum (IPDPSW)*, 19–23 Apr 2010, pp. 1–8
14. Deb, K., Pratap, A., Agarwal, S., Meyarivan, T.: A fast and elitist multiobjective genetic algorithm: NSGA-II. *IEEE Trans. Evol. Comput.* **6**(2), 182–197 (2002)
15. Poddar, R., Banerjee, S., Thakurta, PKG.: Shortest path routing for co-ordinate based mobile networks: a genetic algorithm approach. In: *International Conference on Advances in Mobile Network, Communication and its Applications (MNCAPPS)*, pp. 50–53, 1–2 Aug 2012



# Advanced Bi-directional Home Appliance Communicator with Security System

Nilava Debabhuti, Sougata Das, Sayantan Dutta, Anusree Sarkar and Apurba Ghosh

**Abstract** The paper is based on an electronic system designed using simple microcontroller to build an intelligent and smart communicator. This communicator builds a wireless communication system between the owner of a house and the appliances which are connected within the house. This system intelligently controls the appliances by taking in decisions from the owner using short messaging system (SMS) and also replying with the correct required decision. The owner can also use this service to ask about the status of the appliances from very far away thus making it a very useful system. The system is efficient and logic based as thus errors has been minimized. It is also cost effective and user friendly.

**Keywords** Microcontroller · Communicator · Mobile · Stepper motor · MODEM · SMS

---

N. Debabhuti (✉) · S. Das · A. Ghosh  
University Institute of Technology, The University of Burdwan, Golapbag (North),  
Burdwan 713104, West Bengal, India  
e-mail: nil4026@gmail.com

S. Das  
e-mail: sougatadas29@gmail.com

A. Ghosh  
e-mail: apurbaghosh123@yahoo.com

S. Dutta  
Uniklinik, RWTH Aachen University, Templergraben 55, 52062 Aachen, Germany  
e-mail: sayantan.dutta@rwth-aachen.de

A. Sarkar  
National Institute of Technology, Durgapur, India  
e-mail: anusree.sarkar1@gmail.com

# 1 Introduction

Short messaging service (SMS) is being used worldwide for sending and receiving small texts. This communication system is used for controlling the home appliances. A wireless communication [1–13] obtained helps people to check status of the appliances and safeguard instruments at home to run unused. This helps to curb the wastage of power and allow the owner to control everything with just a touch of SMS from his or her phone. This small device can be developed further to use voice recognition [7], but it has got its own disadvantages like signal strength needs to be increased and it will add up to the cost of signal from the phone. Using SMS is simple short and very low cost.

The proposed system uses different logically designed programs that have been built into a microcontroller. This module checks the SMS text sent to it which helps it to decide the status of the different appliances to be controlled in the house. A lock system has also been devised along with this system which provides security. This security lock can be opened or closed with a password which can be activated either at the doorstep on a 4 by 3 keypad or through SMS. The proposed device gives a vigilant and clear idea of this low cost effective system. Figure 1 gives the block diagram of the complete system which has been implemented to build this device.

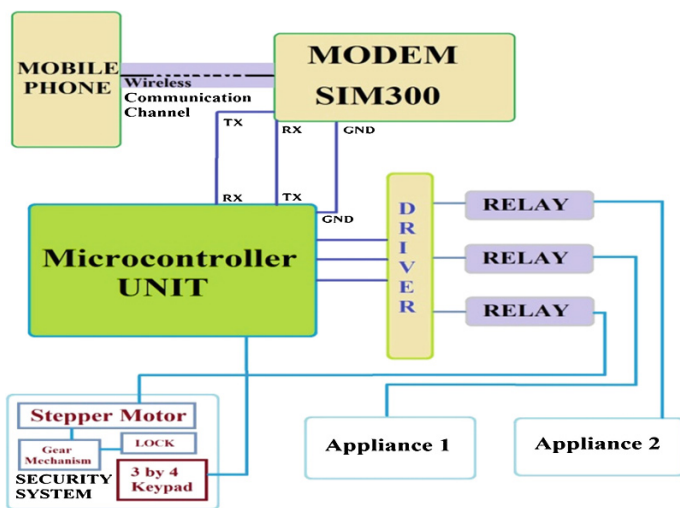


Fig. 1 Block diagram of complete system

## 2 System Description

The Microcontroller is the main operational module of the system. All decisions, sending and receiving is done using logically produced programs burnt into it. Along with that, there are other components used to control and make the device compatible to be used for household purposes.

These components has been divided into the following units or modules and described.

### 2.1 Modulator-Demodulator Device

A modulator-demodulator or usually known as a MODEM is used in this system to send or receive the wireless signals. SIM300D is a all in one chip which helps add data channels and signal modulation demodulation to enhance the communication between two electronic devices [8].

It requires the use of a Subscriber identity Module (SIM) card. This card is just an integrated circuit used to securely store the International Mobile Subscriber Identity (IMSI) and the related key used to identify and authenticate subscribers on mobile telephony. This embedded chip has different contacts just like the legs present in other integrated circuits. Figure 2 shows this SIM card along with its contacts. With the help of this SIM and other connectors, the Global System for Mobile Communication (GSM) module has been developed. Figure 2 shows the image of the GSM module used.

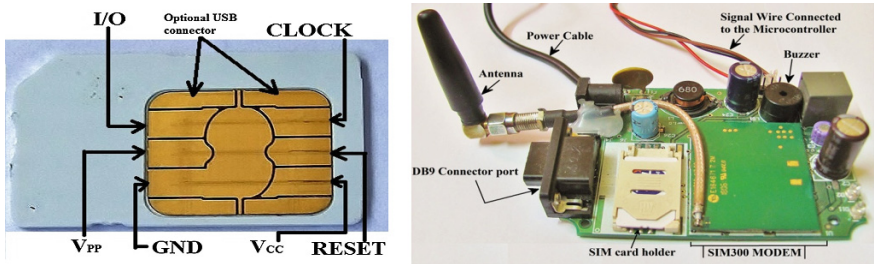


Fig. 2 SIM card and GSM modem

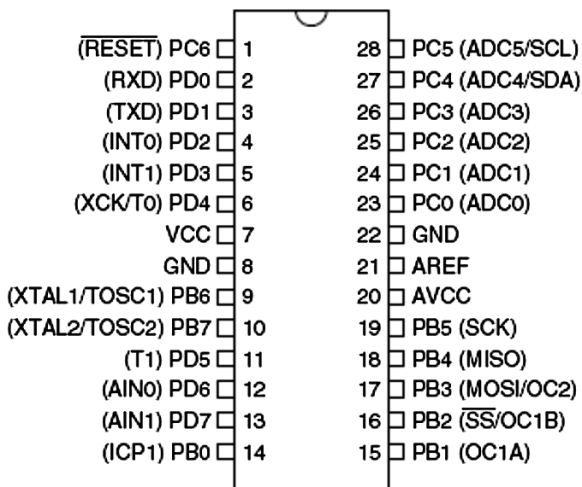
## 2.2 Microcontroller

Microcontroller is the key element in all embedded systems, control and automation processes. It behaves like a single chip microcomputer and is coupled with a processing unit, memory, input output devices, timers, data converters, serial port etc. In this project ATmega8 [9, 10] is used whose pin configuration shown in Fig. 3. It has advanced RISC architecture, 130 powerful instructions and most single-clock cycle execution. It works with  $32 \times 8$  general purpose working registers. It has On-chip 2-cycle multiplier, 8 kB of in-system self-programmable flash program memory, 512 Bytes EEPROM, 1 kB internal SRAM. The GSM modem is connected to ATMEGA8 Microcontroller via serial port using internal UART [6] Module of ATMEGA8.

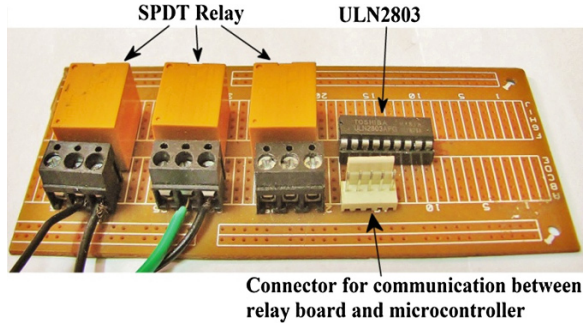
## 2.3 Driver and Relay Unit

This is the unit which changes the status of appliances controlled using the digital signals from the microcontroller. It is just a switch that takes DC signals and closes the current loop of the AC signal so that the appliances can get the required amount of voltage. Relay board consists of three SPDT relay and a relay driver ULN2803. ULN 2803, shown in Fig. 4, is a unipolar motor driver IC with maximum output voltage 50 V and output current 500 mA. It contains eight darlington pair transistors [7], each having a peak rating of 600 mA and can withstand 50 V in off-state. Outputs may be paralleled for higher current capability.

**Fig. 3** Atmega8 pin configuration



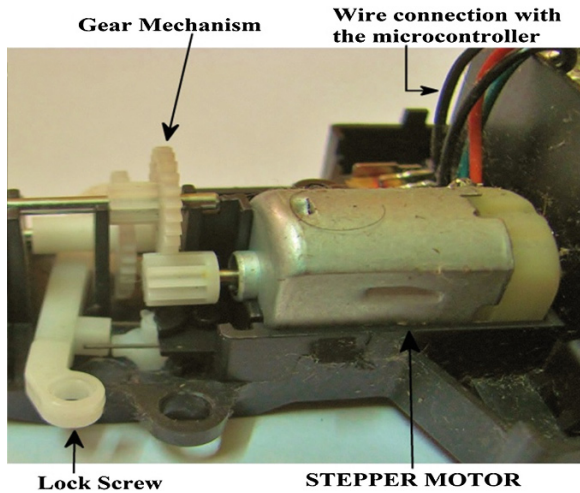
**Fig. 4** Relay board



### 2.4 Security System and Other Appliances

The appliances are correctly controlled via the relay board as per the decisions taken by the microcontroller. There is no restriction to any appliance that can be used. The only extra wiring is the connection of the ULN 2803 port to each of the appliances. The security system on the other hand works using a Stepper Motor. Whenever the motor is turned, a series of gears help the screw to turn and thus locking or unlocking the door, as shown in Fig. 5. A password is used to activate this system and can be Inserted either by using the 3 by 4 keypad provided with the lock or by using an SMS.

**Fig. 5** The security system locks mechanism



### 3 Implementation and Working

This system has the ability to interact with the owner using SMS technology. A simple SMS can convey a decision of either switching OFF an appliance or even controlling the front door of the house. GSM receiver sends the message to the microcontroller. GSM modem and ATMEGA8 communicates through a special command set known as “AT COMMAND SET” [6] these are given in Table 1.

The C program is logically given these commands using which the microcontroller can control the GSM module. The AT commands are used as required and each of the text message received by the microcontroller is checked via loops individually. This checking results in a decision which then sends signals to the relay.

Provisions have been made to check the amount spend in electricity per appliance. It just uses a timer to calculate the last status change. If it was ON then the appliance timer counts until the next OFF. A default amount can be inserted into the program which gives the amount consumed by the appliance per second. The display will show the result of consumption of electricity to the owner and also can send it via SMS.

The password protection has also been made safe so that only the owner can control it. A default six password has been inserted into the program, and it can be changed only if this default password is followed by a new six digit password is send to the system via an SMS. For example “PASSWORD 123456” will unlock the security system and “PASSWORD 123456 270192” will change the password to “270192”. The complete system circuit diagram is given in Fig. 6.

**Table 1** AT commands for SIM300

S. No.	Commands	Description
1	AT+CGMI	Issue manufacturer ID code
2	AT+CGMM	Issue model ID code
3	AT+CSMS	Selection of message service
4	AT+CMGR	Read SMS
5	AT+CMGF	Set the SMS mode to text
6	AT+CMGW	Write SMS
7	AT+CMGS	Send SMS
8	AT+CMGD	Delete an SMS in SMS memory

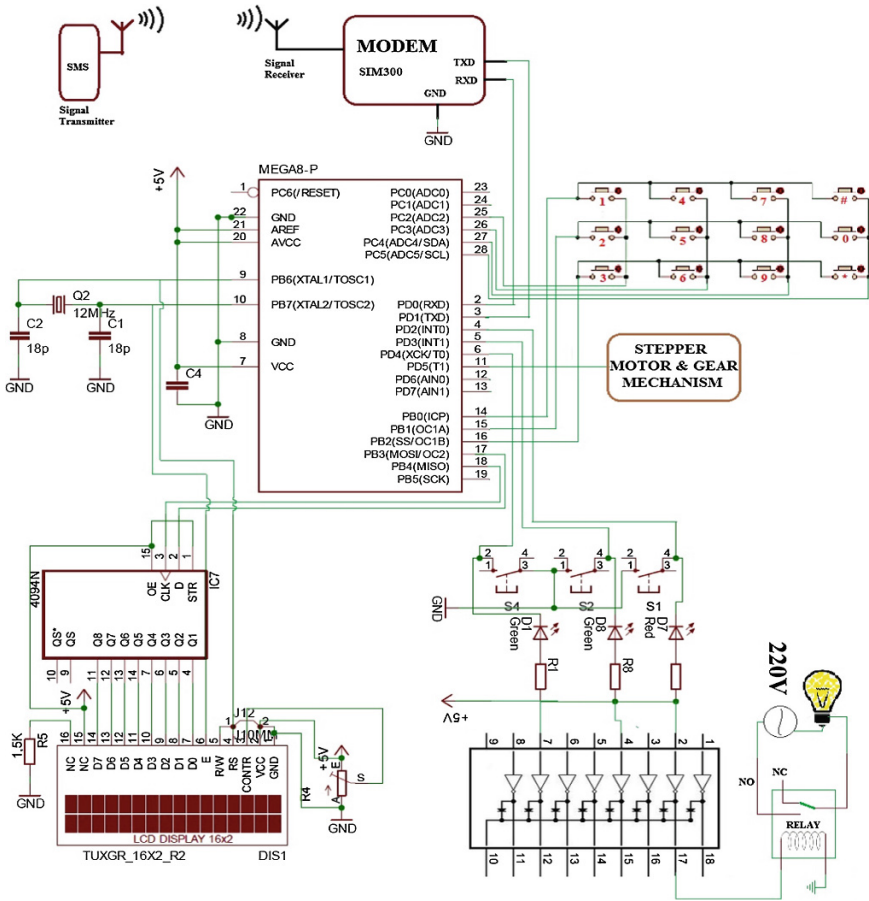


Fig. 6 Circuit diagram of system

### 4 Device Commands and Programming

The developed system uses intrinsic commands as SMS and checks and decides the status of devices. These commands are given in Table 2.

A USART header file has been used and a function is defined which helps the main program to direct the commands to the SIMM300 GSM module. The following code fragment gives the USART write function.

**Table 2** Commands and relay status

S. No.	User commands	Status of relay
1	DEV 1 ON	Device 1 is ON
2	DEV 2 ON	Device 2 is ON
3	DEV 1 OFF	Device 1 OFF
4	DEV 2 OFF	Device 2 OFF
5	PASSWORD XXXXXX	Opens the door lock
6	PASSWORD XXXXXX YYYYYY	Change password
7	STAT DEV 1	Checks status of Device 1
8	STAT DEV 2	Checks Status of Device 2
9	CON HOUSE	Calculates consumption Rs/kWh and sends SMS

```

static int USART_WriteChar(char data)
{
    //Wait untill the transmitter is ready
    if (data == '\n')
        USART_WriteChar('\r');
    while (!(UCSRA & (1<<UDRE)));

    //Now write the data to USART buffer
    UDR=data;
    return 0;
}

```

To initiate a value or a phone number, the code fragment used is given below.

```

void USARTInit(uint16_t ubrr_value)
{
    //Set Baud rate
    UBRRL = ubrr_value;
    UBRRH = (ubrr_value>>8);
    UCSRA=(1<<U2X);
    UCSRC=(1<<URSEL) | (3<<UCSZ0);
    UCSRB=(1<<RXEN) | (1<<TXEN);
}

```

Here, in place of the data, the command is used during the main program. The looping strategy used checks the data each time it has been send. For example, when the main program wants to read a SMS, it will first send the read command to GSM module using the below given code fragment.

```

{
    _delay_ms(200);
    USART_WriteChar('A');
    USART_WriteChar('T');
    USART_WriteChar('+');
    USART_WriteChar('C');
    USART_WriteChar('M');
    USART_WriteChar('G');
    USART_WriteChar('R');
    USART_WriteChar('=');
    USART_WriteChar('1');
    USART_WriteChar('\n');
    while(USARTReadChar()!='\n');
}

```



Now, when an SMS is send, an IF-ELSE case is used to check each character at each space. Taking example of “DEV 1 ON”, the code fragment used is given below.

```

if(ch[0]=='D' && ch[1]=='E' && ch[2]=='V')
{
    if(ch[4]=='1' && ch[7]=='N')
    {
        cbi(PORTD,3);
        printf("Device 1 is ON");
    }
}

```

It checks the first three characters are D, E and V respectively or not. Then it checks whether the character 4 i.e. the number given to the appliance to be controlled and then it checks if the decision is ON or OFF by simply reading the 7th character. In this case the device 1 is ON that means port 3 which is connected to the relay for device 1 is Switched ON.

The security system has been implemented with caution. Only one phone number can be used to open or close or even change the password via SMS. This number is checked using a simple IF-ELSE case and if successful then checks the password.

The status of the device can also be checked by the user. A simple SMS is read by the microcontroller to check and recollect the last status of the device. The port respectively used for the device whose status needs to be determined is given a signal by the microcontroller to check the availability. Then the microcontroller sends the following code to make the GSM module ready to send an SMS to the user.

```

{
    _delay_ms(200);
    USART_WriteChar('A');
    USART_WriteChar('T');
    USART_WriteChar('+');
    USART_WriteChar('C');
    USART_WriteChar('M');
    USART_WriteChar('G');
    USART_WriteChar('W');
    USART_WriteChar('=');
    USART_WriteChar('1');
    USART_WriteChar('\n');
    while(USARTReadChar()!='\n');
}

```

Then it generates the SMS to be send to the users using the following code fragment.

```

Printf (" DEV 1 is ", X);
_delay_ms(200);
USARTInt('9');
USARTInt('9');
USARTInt('0');
USARTInt('3');
USARTInt('9');
USARTInt('9');
USARTInt('5');
USARTInt('4');
USARTInt('6');
USARTInt('0');
while(USARTReadChar()!='\n');

```

Where, X is the status which says either ON or OFF according to the status check that has been implemented before this code. The SMS text is ready and the

mobile number to which it needs to be sent is initialized. This SMS is then send using the this code fragment given below.

```
{
    _delay_ms(200);
    USART_WriteChar('A');
    USART_WriteChar('T');
    USART_WriteChar('+');
    USART_WriteChar('C');
    USART_WriteChar('M');
    USART_WriteChar('G');
    USART_WriteChar('S');
    USART_WriteChar('=');
    USART_WriteChar('1');
    USART_WriteChar('\n');
    while(USARTReadChar()!='\n');
}
```

The user also has the option of checking the consumption of power and the amount spend on it. The unit of currency and the price will be preloaded into the program. The KWH reading will be taken from the electric meter supplied by the electricity service providers. This unit will be multiplied by the price per KWH and stored as a floating value R. This is then send to the user via the following code.

```
_delay_ms(200);
USARTInt('9');
USARTInt ('9');
USARTInt ('0');
USARTInt ('3');
USARTInt ('9');
USARTInt ('9');
USARTInt ('5');
    USARTInt ('4');
USARTInt ('6');
USARTInt ('0');
Printf(" The total cost consumed is ", R);
.....
{
    _delay_ms(200);
    USART_WriteChar('A');
    USART_WriteChar('T');
    USART_WriteChar('+');
    USART_WriteChar('C');
    USART_WriteChar('M');
    USART_WriteChar('G');
    USART_WriteChar('S');
    USART_WriteChar('=');
    USART_WriteChar('1');
    USART_WriteChar('\n');
    while(USARTReadChar()!='\n');
}
```

These program fragments are implemented together and a program is build to work correspondingly to the instrument. The Header files which defines the LCD and the USART are defined outside the main program. The main program only includes the text checking, sending and receiving portions of the system.

## 5 Conclusion

SMS based remote control for home appliances are beneficial for the human generation because mobile is mostly used for communication purposes nowadays. The SMS based remote control for home appliances is easy to implement to make the electrical device ON/OFF. In simple automation system where the internet facilities and even PC are not provided, one can use mobile phone based control system which is simple and cost-effective. In many cases for instance landline phone with extension card could also be used for the system. A Safe security system is provided along with consumer friendliness and the method to check consumption rate of appliances. Moreover, it is interesting to use and user friendly. This system can be developed further in near future and voice signals can be used to implement programs and take decisions at household levels and thus creating a much more intelligent and generic version.

**Acknowledgments** We are thankful to our teacher Dr. Apurba Ghosh for his support and also we acknowledge the effort put into teaching us AVR Atmega8 by the Atmel AVR representatives at a workshop conducted by the University of Burdwan.

## References

1. Chauhan, A., Singh, R.R., Agrawal, S., Kapoor, S., Sharma, S.: SMS based remote control system. *Int. J. Comput. Sci. Manag. Stud.* **11**(02), 19–24 (2011)
2. Wong, E.: A phone-based remote controller for home and office automation. *IEEE Trans. Consum. Electron.* **40**(1), 28–33 (1995)
3. Sriskanthan, N., Tan, F., Karande, A.: Bluetooth based home automation systems. *J. Microprocess. Microsyst.* **26**, 281–289 (2002)
4. Zungeru, A.M., Edu, U.V., Garba, A.J.: Design and implementation of a short message service based remote controller. *Comput. Eng. Intell. Syst.* **3**(4) (2012). ISSN 2222-1719 (paper), ISSN 2222-2863 (online)
5. Yuksekkaya, B., Kayalar, A.A., Tosun, M.B., Ozcan, M.K., Alkar, A.Z.: A GSM, internet and speech controlled wireless interactive home automation system. *IEEE Trans. Consum. Electron.* **52**(3), 837–843 (2006)
6. Das, S., Debabhuti, N., Dutta, S., Das, R., Ghosh, A.: Embedded systems for home appliance control using SMS technology. In: *First International Conference on Automation, Control, Electronic Systems*, IEEE Conference Record: 32377. ISBN 978-1-4799-3894-0 (2014)
7. Mazidi, M.A., Mazidi, J.G.: *The 8051 Microcontroller and Embedded System*. Pearson Education India, Upper Saddle River (2008)
8. Data sheet of Sim300
9. Barnett, R.H., Cox, S., O'cull, L.: *Embedded C Programming and the Atmel AVR*, 2nd edn, pp. 50–51. Cengage Learning, Boston (2006)
10. A workshop on Atmega8 organized by Burdwan University in Sept 2012

11. Boylestad, R.L., Nashelsky, L.: *Electronic Devices and Circuit Theory*, 8th edn, pp. 870–875. Prentice Hall (Pearson Education Inc.), Upper Saddle River (2002)
12. Das, R., Dutta, S., Samanta, K., Sarkar, A., Das, D.: Security based domotics. In: *International Conference on Computational Intelligence: Modeling, Techniques and Applications (CIMTA-2013)*. Elsevier, Amsterdam (ISSN: 2212-0173)
13. Dutta, S., Das, R., Sarkar, A.: Microcontroller based data acquisition system. *Int. J. Eng. Technol.* (2013). Paper Code-IJERTV2IS70678 with ISSN: 2278-0181

# Cyber Attack and Control Techniques

Apeksha Prajapati and Bimal Kumar Mishra

**Abstract** We have developed an Susceptible-Exposed-Infectious-Undetected-Recovered (SEIUR) model. The main feature of this model is the introduction of undetected class. This class is introduced due to the use of un-updated version of antivirus. Optimal control technique is one of the most efficient techniques to plan strategies for better implementation of resources. We have formulated the model and also developed some theoretical results supported by numerical simulation for implementation of control variable in the model.

**Keywords** Cyber attack · Control technique · Undetected class · Antivirus software

## 1 Introduction

Spread of malicious objects in computer network and their control are area of concern for the researcher. Due to advancement of technology various challenges are coming to implement better defense mechanism. To produce better defense mechanism, designing of algorithm, various mathematical model and biological model are suggested by researchers. Epidemic model is biological mathematical models which basically model disease spread and predict its future course. The very similarity between spreading viruses in computer network and spreading malicious codes in biological system motivates researcher to implement various epidemic

---

A. Prajapati (✉) · B.K. Mishra  
Department of Applied Mathematics, Birla Institute of Technology, Mesra,  
Ranchi 835215, India  
e-mail: prajapatiapeksha@gmail.com

B.K. Mishra  
e-mail: drbimalmishra@gmail.com

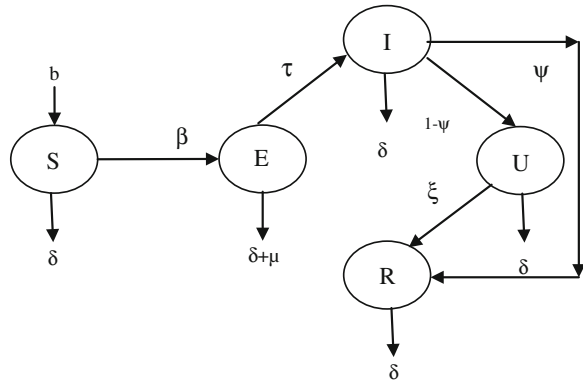
model in cyber attack field. Lots of work has been done in the field of epidemic modeling with spreading malicious codes and its impact in computer network mainly known as e-epidemic modeling. In many places due to lack of technical development and money, the efficiency of supply of hardware/software also has major impact on the transmission of malicious codes. Every organization/states/country has appropriate or limited resources to protect their network from cyber attack. For this purpose we plan strategies by studying implementation of control variable in different form.

Remarkable research has been done in biological epidemics. Most of the models which are developed in computer epidemiology are taken from biological epidemic by changing few compartments or by adding various parameters. Works of Mishra et al. shows diversity in e-epidemic models [1, 2]. The domain of this area is very wide. Fuzzy logic, game theory and difference equations are the various mathematical tools which are implemented in epidemic model. Vaccination plays an important role to reduce the spread of disease or attack in computer network. Wang, et al. [3] presented stability analysis of a Susceptible-Exposed-Infectious-Quarantined-Vaccinated (SEIQV) epidemic model for rapid transmission of worms. This paper presents analysis of vaccinated class. The reproduction rate and stability of the SEIQV model was also discussed. Huang and Sun [4] explained the control mechanism of spread of virus in a scale free network if resources are restricted. He also proposed existence of epidemic tipping point when resources are limited. Optimal control theory provides a valuable tool to begin to assess the trade-offs between vaccination and treatment strategies. Optimal control is a mathematical technique derived from the calculus of variations. A control problem is formulated to control the disease by using an optimal control theory [5]. Epidemic model with non-linear saturated incidence is considered by applying the optimal control techniques to eradicate the infection in the human population. Leptospirosis is the disease which effects human as well as Cattle. Sadiq et al. developed the optimal control techniques for the eradication of leptospira in the host population. For this, three control variables are defined [5]. Next papers concentrate on SI, SEIR epidemic model with different incidence rate and saturated treatment function. This study gives optimal vaccination strategies to minimize the susceptible and infected individuals and to maximize the number of recovered individuals [6, 7].

## 2 Model Formulation

In this section we formulate an epidemic model with various compartments. In this model the total numbers of nodes are divided into five compartments namely, Susceptible, Exposed, Infectious, Undetected and Recovered. The nodes which are vulnerable towards attack are in susceptible class. The nodes which are infectious but not able to transmit infection to other nodes are in Exposed class,  $I$  is the

Fig. 1 SEIUR model



infectious class, the nodes in this class transmit infection to other nodes. *U* is the undetected class. This class has all those nodes which are infected but antivirus failed to detect infection on them due to not regular updation of antivirus. *R* is the recovered class.

*b* is the recruitment rate of new nodes into the network.  $\delta$  is the death rate by natural causes,  $\mu$  is the death rate due to attack.  $\tau$  is the rate of infection in exposed class.  $\beta$  is the infectivity contact rate.  $\Psi$  is the Recovery rate in infectious class.  $\xi$  is recovery rate in undetected class.  $(1 - \Psi)$  is the rate of failure of detection of infection in a node. This rate is implemented because of the use of un-updated antivirus. Due to the use of un-updated antivirus in various nodes the chance of detection of infection in a node is not optimum (Fig. 1).

The governing differential equation of the model is given as

$$\left. \begin{aligned}
 \frac{dS}{dt} &= b - \beta SI - (\delta + \nu)S \\
 \frac{dE}{dt} &= \beta SI - (\delta + \tau)E \\
 \frac{dI}{dt} &= \tau E - (\mu + \delta + 1)I \\
 \frac{dU}{dt} &= (1 - \psi)I - (\mu + \delta + \xi)U \\
 \frac{dR}{dt} &= \xi U + \psi I + \nu S - \delta R
 \end{aligned} \right\} \tag{A}$$

### 3 Equilibrium Points and Reproduction Number

We get the endemic equilibrium point  $(S^*, E^*, I^*, Q^*, R^*)$  as

$$S^* = \frac{1}{R_0}, E^* = \frac{(\mu + \delta + 1)}{\tau} \left( \frac{b}{\beta R_0} - \frac{\delta + \nu}{\beta} \right), I^* = \frac{b}{\beta R_0} - \frac{\delta + \nu}{\beta},$$

$$U^* = \frac{1 - \psi}{\delta + \mu + \xi} \left( \frac{b}{\beta R_0} - \frac{\delta + \nu}{\beta} \right) R^* = \frac{k}{R_0} + \frac{\xi + \delta\psi + \mu\psi}{\delta + \mu + \xi} \left( \frac{b}{\beta R_0} - \frac{\delta + \nu}{\beta} \right)$$

Attack free equilibrium point is  $(b/\delta, 0, 0, 0)$ .

The basic Reproduction number is defined as the expected number of secondary cases that would arise from the introduction of a single primary case into a fully susceptible population.

The basic reproduction number can be obtained by calculating  $V$  and  $F_0$ , where  $V$  and  $F_0$  are given as,

$$V = \begin{pmatrix} \tau + \delta & 0 & 0 \\ -\tau & \delta + \mu + 1 & 0 \\ 0 & \psi - 1 & \delta + \mu + \xi \end{pmatrix} \quad F_0 = \begin{pmatrix} 0 & \beta & 0 \\ 0 & 0 & 0 \\ 0 & 0 & 0 \end{pmatrix}$$

The basic reproduction number  $R_0$  is defined as the dominant Eigen value of  $FV^{-1}$ , that is,  $R_0 = \frac{\beta\tau}{(\delta + \tau)(\delta + \mu + 1)}$ .

### 4 Local Stability of the Attack-Free Equilibrium Stage

In this section we analysed the stability of developed model. Generally for many models we have two equilibrium points, attack free equilibrium point and the endemic equilibrium point. We discuss the stability of attack free equilibrium point.

**Theorem** *Attack free equilibrium point and endemic equilibrium points are locally asymptotically stable.*

*Proof* The Jacobian matrix of the system (A) is given as,

$$J(AF) = \begin{pmatrix} -(\delta + \nu) & 0 & -\beta S & 0 & 0 \\ 0 & -(\delta + \tau) & \beta S & 0 & 0 \\ 0 & \tau & -(\delta + \mu + 1) & 0 & 0 \\ 0 & 0 & 1 - \psi & -(\delta + \mu + \xi) & 0 \\ \nu & 0 & \psi & \xi & -\delta \end{pmatrix} \quad (B)$$



Eigen values of (B) are:  $-(\delta + \nu)$ ,  $-(\delta + \tau)$ ,  $-(\delta + \mu + 1)$ ,  $-(\delta + \mu + \xi)$ ,  $-\delta$   $\square$

Which are all negative; hence the system is locally asymptotically stable at attack free state.

## 5 Optimal Vaccination

Let  $v(t) \in V$  represents percentage of vaccinated nodes in susceptible class per unit time.  $V = \{v/v(t) \text{ is measurable, } 0 \leq v(t) \leq v_{\max} < \infty, t \in [0, T]\}$  indicates an admissible control. So we formulate an optimal control problem to minimize the objective functional

$$J(u) = \int_0^T [C_1 S + C_2 E + C_3 I + C_4 U + \frac{1}{2} W v^2(t)] dt \quad (C)$$

Subject to, the system,

$$\begin{aligned} \frac{dS}{dt} &= b - \beta SI - (\delta + k)S, & \frac{dE}{dt} &= \beta SI - (\delta + \tau)E, & \frac{dI}{dt} &= \tau E - (\mu + \delta + 1)I, \\ \frac{dU}{dt} &= (1 - \psi)I - (\mu + \delta + \xi)U, & \frac{dR}{dt} &= \xi U + \psi I + kS - \delta R \end{aligned} \quad (D)$$

With IC  $S(t) \geq 0, E(t) \geq 0, I(t) \geq 0, U(t) \geq 0, R(t) \geq 0$  and  $C_1, C_2, C_3, C_4$  are small positive constants. These constants maintain a balance in the size of  $S(t), E(t), I(t)$  and  $U(t)$  respectively,  $W$  is related with control variable and it is positive weight parameter. The main objective of our work is to minimize the number of susceptible nodes and maximize the recovered nodes by the implementation of control variable  $v(t)$ .

## 6 Existence of an Optimal Control

For the existence we take a control system (C) with initial conditions. Then we express (C) in terms of  $\phi' = B(\phi) + F(\phi)$ .

We set

$$D(\phi) = B(\phi) + F(\phi) \quad (E)$$

where,

$$\phi = \begin{pmatrix} S(t) \\ E(t) \\ I(t) \\ F(t) \\ R(t) \end{pmatrix}$$

$$B = \begin{pmatrix} -(v(t) + \delta) & 0 & 0 & 0 & 0 \\ 0 & -(\delta + \tau) & 0 & 0 & 0 \\ 0 & \tau & -(\delta + \mu + 1) & 0 & 0 \\ 0 & 0 & 1 - \psi & -(\delta + \mu + \zeta) & 0 \\ v(t) & 0 & \psi & \zeta & -\delta \end{pmatrix}$$

$$F = \begin{pmatrix} b - \beta SI \\ \beta SI \\ 0 \\ 0 \\ 0 \end{pmatrix} \text{ and } F(\phi_1) - F(\phi_2) = \begin{pmatrix} \beta(S_2I_2 - S_1I_1) \\ \beta(S_1I_1 - S_2I_2) \\ 0 \\ 0 \\ 0 \end{pmatrix}$$

$$\begin{aligned} |F(\phi_1) - F(\phi_2)| &= \beta|S_2I_2 - S_1I_1| + \beta|S_1I_1 - S_2I_2| \\ &\leq 2\beta|(S_1I_1 - S_2I_2)| \\ &\leq 2\beta|(S_1 - S_2)I_1 + S_2(I_1 - I_2)| \\ &\leq \frac{b}{\delta} 2\beta|(S_1 - S_2) + (I_1 - I_2)| \\ &\leq M|(S_1 - S_2) + (I_1 - I_2)|, \text{ where, } M = \frac{2\beta b}{\delta} \end{aligned}$$

Also we have,

$$|D(\phi_1) - D(\phi_2)| < P|\phi_1 - \phi_2| \text{ where } P = \max(M, \|B\|) < \infty$$

Here the positive constant  $P$  is independent of the state variables  $S(t)$ ,  $E(t)$ ,  $I(t)$ ,  $U(t)$  and  $R(t)$ . It follows that  $D$  is uniformly Lipschitz and continuous. From the definition of the control  $v(t)$  and restriction on  $S(t)$ ,  $E(t)$ ,  $I(t)$ ,  $U(t)$  and  $R(t)$ , we see that a solution of the system (E) exists. For optimal solution, first we find the Lagrangian and Hamiltonian for the optimal control problem (C) and (D). Here the Lagrangian of the problem is,

$$L(S, E, I, U) = C_1S(t) + C_2E(t) + C_3I(t) + C_4U(t) + \frac{1}{2} Wv^2(t)$$

where  $C_1, C_2, C_3, C_4$  and  $W$  are positive weight constants.

We try to find the minimal value of the Lagrangian. We use Pontryagin's maximum principle to derive the Hamiltonian  $H$ . The Hamiltonian  $H$  for the control problem is given as,

$$H = L(S, E, I, U) + \lambda_1(t) \frac{dS}{dt} + \lambda_2(t) \frac{dE}{dt} + \lambda_3(t) \frac{dI}{dt} + \lambda_4(t) \frac{dU}{dt} + \lambda_5(t) \frac{dR}{dt} \quad (F)$$

where,  $\lambda_1(t)$ ,  $\lambda_2(t)$ ,  $\lambda_3(t)$ ,  $\lambda_4(t)$  and  $\lambda_5(t)$  are adjoint function to be determined.

**Theorem** Let  $S^*(t)$ ,  $E^*(t)$ ,  $I^*(t)$ ,  $U^*(t)$  and  $R^*(t)$  be optimal state solutions which is associated with optimal control variable  $v^*(t)$  for the optimal control problem (C) and (D). Then, there exist adjoint variables  $\lambda_1$ ,  $\lambda_2$ ,  $\lambda_3$ ,  $\lambda_4$  and  $\lambda_5$  that satisfy

$$\begin{aligned} \frac{d\lambda_1}{dt} &= -\frac{\partial H}{\partial S} = -[C_1 - \beta I \lambda_1 - \lambda_1 \delta + \beta \lambda_2 I], \\ \frac{d\lambda_2}{dt} &= -\frac{\partial H}{\partial E} = -[C_2 - \lambda_2(\delta + \tau) + \lambda_3 \tau] \\ \frac{d\lambda_3}{dt} &= -\frac{\partial H}{\partial I} = -[C_3 - \beta S \lambda_1 + \beta S \lambda_2 - \lambda_3(1 + \delta + \mu) + \lambda_4(1 - \psi) + \lambda_5 \psi] \\ \frac{d\lambda_4}{dt} &= -\frac{\partial H}{\partial U} = -[C_4 + (\delta + \mu + \xi) \lambda_4 + \lambda_5 \xi], \quad \frac{d\lambda_5}{dt} = -\frac{\partial H}{\partial R} = \delta \lambda_5 \end{aligned}$$

with transversality conditions:  $\lambda_i(T') = 0$ ;  $i = 1, 2, 3, 4, 5$ .

The optimal control  $v^*$  is given by  $v^*(t) = \max \left\{ \min \left\{ \frac{(\lambda_1(t) - \lambda_5(t)) S^*}{W}, V_{\max} \right\}, 0 \right\}$ .

*Proof* To obtain adjoint equations and transversality condition we formulate Hamiltonian (E).

So by using optimality condition we have along with the transversality conditions:  $\lambda_i(T') = 0$ ;  $i = 1, 2, 3, 4, 5$ .

By optimality conditions, we have  $\frac{\partial H}{\partial u} = W v^*(t) - \lambda_1(t) S^* + \lambda_5(t) S^* = 0$  and at  $v^*$ , we can obtain

$$v^*(t) = \frac{S^*(\lambda_1(t) - \lambda_5(t))}{W}$$

where,  $S^*(t)$ ,  $E^*(t)$ ,  $I^*(t)$ ,  $F^*(t)$  and  $R^*(t)$  are optimal state solutions associated with optimal control variable  $v^*(t)$ .  $\square$

By using the property of control space, we obtain

$$\begin{aligned} v^*(t) &= 0; \quad \text{if } \frac{(\lambda_1(t) - \lambda_5(t)) S^*(t)}{W} \leq 0 \\ v^*(t) &= \frac{(\lambda_1(t) - \lambda_5(t)) S^*(t)}{W}; \quad \text{if } 0 < \frac{(\lambda_1(t) - \lambda_5(t)) S^*(t)}{W} < v_{\max} \end{aligned}$$

$$v^*(t) = v_{\max}; \frac{(\lambda_1(t) - \lambda_5(t))S^*(t)}{W} > v_{\max}$$

So the optimal control is characterize by  $v^*(t) = \max\left\{\min\left\{\frac{(\lambda_1(t) - \lambda_5(t))S^*}{W}, v_{\max}\right\}, 0\right\}$ .

## 7 The Optimal System

Now, the optimal points can be obtained after solving the following system of equations with initial condition  $t = 0$

$$\begin{aligned} \frac{dS}{dt} &= b - \left( \delta + \max\left\{\min\left\{\frac{(\lambda_1(t) - \lambda_5(t))S^*}{W}, v_{\max}\right\}, 0\right\} S(t) \right) - \beta SI \\ \frac{dE}{dt} &= \beta SI - (\tau + \delta)E, \quad \frac{dI}{dt} = \tau E - (\delta + \mu + 1)I, \quad \frac{dU}{dt} = (1 - \psi)I - (\delta + \mu + \xi)U \\ \frac{dR^*}{dt} &= \xi U + \psi I - \left( \delta + \max\left\{\min\left\{\frac{(\lambda_1(t) - \lambda_5(t))S^*}{W}, v_{\max}\right\}, 0\right\} S(t) \right) \\ \frac{d\lambda_1}{dt} &= - \left[ C_1 - (\delta + \max\left\{\min\left\{\frac{(\lambda_1(t) - \lambda_5(t))S^*}{W}, v_{\max}\right\}, 0\right\} + \beta I) \lambda_1 \right. \\ &\quad \left. - \lambda_1 \delta + \beta \lambda_2 I + \lambda_5 \max\left\{\min\left\{\frac{(\lambda_1(t) - \lambda_5(t))S^*}{W}, v_{\max}\right\}, 0\right\} \right] \\ \frac{d\lambda_2}{dt} &= - \frac{\partial H}{\partial E} = - [C_2 - \lambda_2(\delta + \tau) + \lambda_3 \tau], \\ \frac{d\lambda_3}{dt} &= - \frac{\partial H}{\partial I} = - [C_3 - \beta S \lambda_1 + \beta S \lambda_2 - \lambda_3(1 + \delta + \mu) + \lambda_4(1 - \psi) + \lambda_5 \psi] \\ \frac{d\lambda_4}{dt} &= - \frac{\partial H}{\partial U} = - [C_4 + (\delta + \mu + \xi) \lambda_4 + \lambda_5 \xi], \quad \frac{d\lambda_5}{dt} = - \frac{\partial H}{\partial R} = \delta \lambda_5 \\ S(0) &= S_0, E(0) = E_0, I(0) = I_0, U(0) = U_0, \lambda_1(T) = 0, \\ \lambda_2(T) &= 0, \lambda_3(T) = 0, \lambda_4(T) = 0, \lambda_5(T) = 0 \end{aligned}$$

## 8 Conclusion

In this paper we have formulated SEIUR model. The aim of this paper is to minimize the infection of malicious codes in a computer network by implementing control techniques. The unavailability of technology or due to high cost of preventive technique it is important to plan a better strategy to minimize the cyber attack with minimum resources. This motivates us to implement control technique.

Antivirus software is also one of the preventive techniques to minimize the impact of malicious code attack in a network. These types of software are mainly effective at least for few months or year, for this constraint with the software it is better to define our control set and the objective function so that we can formulate an optimal condition. Figure 2 shows the phase portrait of susceptible and infectious class. Figures 3 and 4 show the behavior of undetected class with respect to susceptible class and time respectively. Figure 5 shows recovery of the system is high for system with control. This paper also presents the importance of new class i.e.,

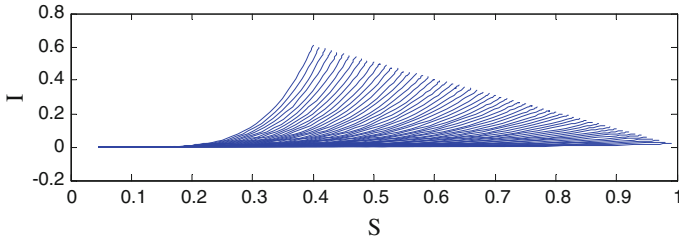


Fig. 2 Infectious class versus susceptible class

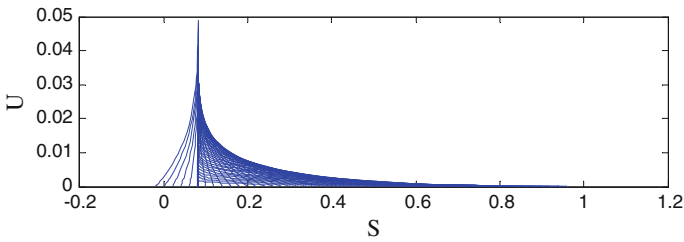


Fig. 3 Undetected class versus susceptible class

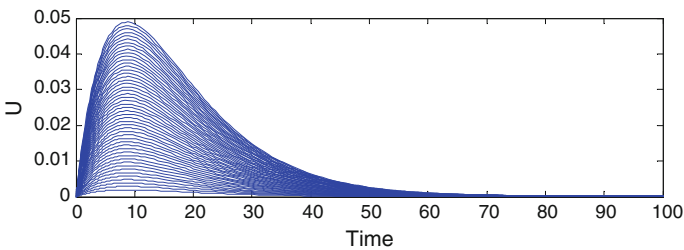


Fig. 4 Undetected class versus time

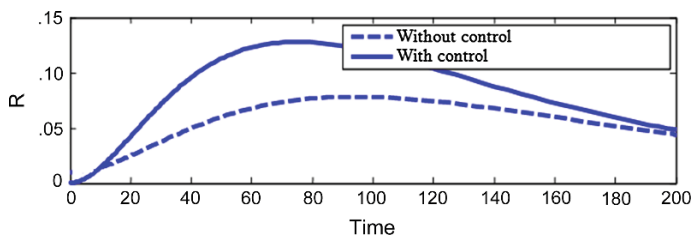


Fig. 5 Recovered class with and without control

undetected class. Optimal antivirus coverage needed to prevent cyber attack. This can be achieved through installing antivirus software on fully susceptible class. It is very valuable and effective technique against cyber attack. The values of the parameters are  $b = 0.01$ ,  $\beta = 0.1$ ,  $\delta = 0.01$ ,  $\mu = 0.02$ ,  $\tau = 0.02$ ,  $\psi = 0.1$ ,  $\xi = 0.002$ .

## References

1. Mishra, B.K., Pandey, K.: Dynamic model of worm propagation in computer network. *Appl. Math. Model.* Elsevier **38**, 2173–2179 (2014)
2. Mishra, B.K., Prajapati, A.: Dynamic model on the transmission of malicious codes in network, *I. J. Comput. Netw. Inf. Secur.* **10**, 17–23 (2013)
3. Wang, F., Zhang, Y., Wang, C., Ma, J., Moon, S.: Stability analysis of SEIQV epidemic model for rapid spreading worms. *Comput. Secur.* **29**(4), 410–418 (2010)
4. Huang, C.Y., Sun, C.T.: Effect of resource limitation and cost influence on computer virus epidemic dynamics and tipping point. Article id-473136, *Hindawi. Interf.* **2**(4), 295–307 (2012)
5. Sadiq, S.F., Khan, M.A., Islam S., Zaman, G., Jung, H., Khan, S.K.: Optimal control of an epidemic model of leptospirosis with nonlinear saturated incidences. *Annu. Res. Rev. Biol.* **4** (3), 560–576 (2014)
6. Laarabi, H., Rachik, M., Kahlaoui, O.E., Labriji, E.H.: Optimal vaccination strategies of an sir epidemic model with a saturated treatment. *Univ. J. Appl. Math.* **1**(3), 185–191 (2013)
7. Ullah, R., Zaman, G., Islam, S., Ahmad, I.: Dynamical features and vaccination strategies in an SEIR epidemic model. *Res. J. Recent Sci. Int. Sci. Congr. Assoc.* **2**(10), 48–56 (2013)

# Design of Queue-Based Group Key Agreement Protocol Using Elliptic Curve Cryptography

Priyanka Jaiswal, Abhimanyu Kumar and Sachin Tripathi

**Abstract** Secure group communication is an important research issue in the field of cryptography and network security, because group applications like online chatting programs, video conferencing, distributed database, online games etc. are expanding rapidly. Group key agreement protocols allow that all the members agree on the same group key, for secure group communication, and the basic security criteria must be hold. The design of secure group communication can be very critical for achieving security goals. Many group key agreement protocols such as Tree-based Group Diffie-Hellman (TGDH) Kim et al. (ACM Trans Inf Syst Secur (TISSEC) 7(1):60–96, (2004)) [1], Group Diffie-Hellman (GDH) Steiner et al. (IEEE Trans Parallel Distrib Syst 11(8):769–780, (2000)) [2], Skinny Tree (STR) Wong et al. (IEEE/ACM Trans Netw 8(1):16–30, (2000)) [3] etc., have been established for secure group communication, but they have suffered from unnecessary delays as well as their communication cost increased due to increased exponentiation. An alternative approach to group key agreement is the queue based group key agreement protocol that reduces unnecessary delays, considers member diversity with filtering out low performance members in group key generation processes. We propose a novel queue based group key agreement protocol that uses the concepts of elliptic curve cryptography. The proposed protocol gives better results than the other existing related protocols and it also reduces computational overheads.

**Keywords** Group diffie hellman · Elliptic curve cryptography (ECC) · Queue based group key agreement

---

P. Jaiswal (✉) · A. Kumar · S. Tripathi  
Department of Computer Science and Engineering, Indian School of Mines,  
Dhanbad 826004, Jharkhand, India  
e-mail: priyanka\_jais4@yahoo.co.in

A. Kumar  
e-mail: abhi\_a1ks@yahoo.co.in

S. Tripathi  
e-mail: var\_1285@yahoo.com

## 1 Introduction

Most of the groupware applications such as video conferencing, online chatting, online game, net gambling, etc. are increasing day by day over internet. Security is the major concern in maintaining such groupware application. Basic security services such as privacy, integrity and authentication, are necessary for groupware application as well as key management is very important in group key agreement protocols for security purpose. Group key can be managed by one of the three ways, as centralized, distributed and contributory group key management [4]. In centralized group key management a single entity or a set of entity is involved in the generation and distribution of group key for group members via a pair-wise secure channel established with each group member. Centralized group key management is a simple group key management as it involves a single (or a set) of the entity. However, Centralized group key management is inappropriate for peer group communication as it involved a trusted third party or online key generation center for supporting the group operation every time. Continuous availability of an entity can be addressed as fault tolerance and replication. However, Centralized group key management work well for one-many multicast network scenarios. Distributed group key management is more suitable in peer group communication as it involved dynamically selecting a group member for distribution of group key. In contrast, in contributory group key management all members equally contribute in generation of group key. This type of protocols is appropriate for dynamic peer groups. This approach avoids the problem of single point of failure.

Group key plays major role in establishing secure group communication. So, key generation is a major task in group key agreement through secure way. Many of group key agreement protocols have been developed earlier for secure group communication [1, 5], but they have some disadvantages. Since the group generation processes takes many modular exponentiations and long time in generation of group key. For achieving higher security, group key protocol should be dynamic, means it should change for each new join or leave member, so that new member have not any knowledge about prior information [6]. Therefore group key management protocol focusing on the group key generation efficiently [1, 7–9]. Modular exponentiation is very expensive in computation of group key [1]. The number of exponentiations for membership depends on group size as when the group size increased the number of exponents will also increase. Tree Based Group Diffie-Hellman (TGDH) uses the concept of Diffie-Hellman key exchange with logical tree structure to achieve efficiency. The efficiency of TGDH is  $O(\log_2 n)$ , where  $n$  is the group size. However, some extra overhead occurred in maintaining a perfect key tree balance. Skinny tree has lower communication overhead, but it increases computation. Burmester–Desmedt (BD) distributes and minimizes computation by using more messages broadcast. All these protocols using similar security properties including group key independence. TGDH, STR, and other key management



are under a homogeneous computing and network environment. However, one of the problems associated with the tree structure is the balancing of the tree, when the members are changing the group.

## 2 Related Work

Groupware application like video conferencing, online gaming, e-chatting, etc. may have different settings. To provide secure group communication, secure key distribution and efficient key management are very necessary to maintain integrity, confidentiality, and authentication. For secure group communication, group key management is responsible for generating the group key and distributing it to all intended recipients in a secure way over an insecure channel [4]. Group key management can be categorized into centralized, distributed and contributory group key management. In a centralized approach, a single entity or a set of entities is involved in generation and distribution of group key. The centralized group key management protocol is not suitable for peer group because it involves a continuous availability of trusted third party (TTP) for generation and distribution of group key, that may cause of single point of failure. However, the Distributed group key management involves dynamically selecting the group key and distributing it to other group member, which is more suitable for dynamic peer group communication. Distributed group key management involves distributing key in a decentralized way. In contrast to centralized approach, contributory group key management involves each group member to equally contribute, to generate the group key. This avoids the problems of single point of failure. Contributory group key management is most suitable for peer group communication, because each member has an equal opportunity to generate a group key. Therefore the proposed protocol, uses the contributory group key management approach to generate the group key. It uses the elliptic curve cryptographic technique to reduce the exponentiation. Some of the other related protocol like Burmester–Desmedt (BD) [10], Group Diffie–Hellman (GDH) [2], Skinny Tree (STR) [3] and Tree Based Group Diffie Hellman (TGDH) [1] and Queue Based Group Diffie Hellman (QGDH) [5], have some limitations. The Burmester–Desmedt (BD), protocol support dynamic operation and uses modular exponentiation to reduce communication overhead, but it requires more message exchange to generate the group key. Group Diffie Hellman (GDH) provides better security, but it requires more computation and communication overhead. The Skinny Tree (STR) Protocol is more suitable for member joining group operation, it has relatively low communication cost, but it does not work well for exclusion of members. The Tree Based group Diffie Hellman (TGDH) provides efficient group key agreement protocol from above related protocols. The Queue Based Group Diffie Hellman (QGDH) uses decentralized group key management and contributory group key distribution mechanism to improve efficiency, however modular exponentiation increases computational overhead. Therefore, we have proposed a new elliptic curve based group key agreement protocol.

### 3 Preliminary

#### 3.1 Elliptic Curve Over Finite Field ( $F_p$ )

Let  $p \geq 3$  be a prime number. Let  $a, b \in F_p$  be such that  $4a^3 + 27b^2 \neq 0$  in  $F_p$ . An elliptic curve  $E$  over  $F_p$  is defined by the equation  $Y^2 \bmod p = (x^3 + ax + b) \bmod p$  where  $(x, y)$ ,  $x, y \in F_p$ , together with an extra point  $O$ , called point identity. The set of points  $E(F_p)$  forms an abelian group with the following addition rules.

- Identity:  $P + O = O + P = P$  for all  $P \in E(F_p)$ .
- Negativity: If  $P(x, y) \in E(F_p)$  then  $(x, y) + (x, -y) = O$ , The point  $(x, -y)$  is defined as  $-P$  called negative of  $P$ .
- Point addition: Let  $P(x_1, y_1), Q(x_2, y_2) \in E(F_p)$ , then  $P + Q = R \in E(F_p)$  and coordinate  $(x_3, y_3)$  of  $R$  is given by  $x_3 = \lambda^2 - x_1 - x_2$  and  $y_3 = \lambda(x_1, x_3) - y_1$  where  $\lambda = \frac{y_2 - y_1}{x_2 - x_1}$ .
- Point doubling: Let  $P(x_1, y_1) \in E(K)$  where  $P \neq -P$  then  $2P = (x_3, y_3)$  where  $x_3 = \left(\frac{3x_1^2 + a}{2y_1}\right)^2 - 2x_1$  and  $y_3 = \left(\frac{3x_1^2 + a}{2y_1}\right)(x_1 - x_3) - y_1$ .

#### 3.2 Elliptic Curve Discrete Logarithm Problem (ECDLP)

Given an elliptic curve  $E$  defined over a finite field  $F_p$ , a point  $P \in E(F_p)$  of order  $n$ , and a point  $Q \in \langle P \rangle$ , find the integer  $l \in [0, n - 1]$  such that  $Q = lP$ . The integer  $L$  is called the discrete logarithm of  $Q$  to base  $P$ , denoted  $L = \log_p Q$ .

#### 3.3 Elliptic Curve Diffie Hellman (ECDH)

Elliptic Curve Diffie Hellman is one of the key exchange protocol used to establishes a shared key between two parties. ECDH protocol is based on the additive elliptic curve group. ECDH selecting the underlying field ( $F_p$ ) or  $GF(2^k)$ , the curve  $E$  with parameters  $a, b$  and the base point  $P$  is equal to  $n$ . The standards often suggest that we select an elliptic curve with prime order and therefore any element of the group would be selected and their order will prime number  $n$ . At the end of the protocol the communicating parties end up with the same value  $K$  which is the point on the curve.

### 4 Proposed Queue Based Group Key Agreement Protocol

In the proposed protocol there are  $(M_1, M_2, M_3, \dots, M_n)$   $n$  number of members in the group, and there is a group controller server (GCS) responsible for every member authentication and key generation. The group controller server (GCS) manages all the consisting group member and contain information about the group members such as current login list of members, information about the registered member, current session key etc. GCS also manages the BKQ according to the arrival of the member. GCS requests all members to generate blind key, then GCS creates a BKQ and stores the blind key in BKQ into the order of the arrival. The highest performance member blind key is always stored on the front end of the BKQ, whereas the low performance member blind key is stored on the rear end of the BKQ. Figure 1 shows an example of structural Blind Key Queue (BKQ), in which the first spot blinded key is computed with the last spot blinded key  $(x_{n1}x_{n2}B)$ , and the member with the second spot is computed key with the member in last second spot  $(x_{n2}x_{n3}B)$ . The proposed algorithm can be categorized into setup phases and key generation phase, in the setup phase KGC initializes public parameters, and in second phase KGC and users are contributed to generate group key.

#### 4.1 Setup

(By KGC) This algorithm takes a security parameter  $k \in Z^*$  and does the following:

KGC chooses a  $k$  bit prime  $p \in Z_p^*$  and determine the tuple  $F_p, E/F_p, B$ .

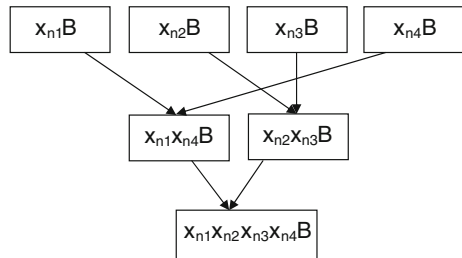
where

$E/F_p$ : Elliptic curve over  $F_p$ .

$B$ : Base point on elliptic curve.

KGC publishes parameters =  $\{F_p, E/F_p, B\}$  as system parameters.

Fig. 1 Blind key queue structure



## 4.2 Key Generation

- Each user select an integer  $x$  where  $x \in Z_p^*$ .
- Each user calculates  $Q_i$  as a product of private key and a base point ( $B$ ).  
 $Q_i = x_i * B$ ,  $Q_i$  is the public key of member  $i$ , where  $1 \leq i \leq n$ .
- Each member sends  $Q_i$  to group controller server (GCS).

When GCS got many requests, GCS arranges those requests in order of their arrival and performs the following operations.

- GCS stores  $Q_i$  in their respective position in queue in order of their arrival from different users.
- GCS arranges each request coming from the group and when a threshold number of members are registered, then GCS says front end and rear end members to generate group key means member with  $A_1$  spot will generate a group key with member in  $A_n$  spot. Member at  $A_2$  spot will generate with member at  $A_{(n-1)}$  and so on.
- After that GCS waits for threshold time, and if any group key arrives, then GCS will recreate public key Queue (PKQ) in order of their arrival. After the threshold time, if group key from certain group is absent, then GCS gives them last chance to generate group key together or independently and send to GCS in the given time. If they still fail then GCS ignore them. They can join later using 'one by one' algorithm.
- The last step is repeated until level  $\log_{2^{n+1}}$  and the session key is generated and stored in current session key (CSK) register. The current session key (CSK) =  $x_1x_2x_3...x_i...x_{(n-1)}x_nB$ .

## 5 Member Join

Join and leave operation is an important part in dynamic group key agreement protocol. Since any time a member or a set of members can join or leave the group.

Whenever a new member wants to join the group, the group controller broadcast a control message to others member to update their public key and then sends back to group controller, then group controller arranges all the keys in order of their arrival as well as with the new member key. It includes the following steps.

- When a new member wants to join the group, it sends their public key to GCS.
- GCS stores member's public key and identity in the database.
- GCS updates, current session key  $CSK = CSK' + Q_i$  (using elliptic curve point addition).
- GCS selects a random number  $N$  between  $[0, p - 1]$ .
- Calculate new current session key  $CSK1 = N * CSK$ .
- GCS broadcasts  $CSK1$  as new session key to all the members including new member and updated  $CSK$ .

## 6 Member Leave/Mass Leave

If a member or set of member wants to leave the group then the group session key of the resulting group must be updated to provide the forward secrecy. The leave operation includes following steps.

- When a member wants to leave the group, it sends leave request to GCS, by sending a public key as  $Q_i$ .
- GCS updates, current session Key  $CSK = CSK - Q_i$ .
- GCS selects a random number  $N$  on  $[0, p - 1]$ .
- Calculate new current session key  $CSK1 = N * CSK$ .
- Update  $CSK$  to  $CSK1$ .
- Broadcast the new  $CSK$  to all members except leaving member.

## 7 Security Analysis and Comparison with Other Protocols

This protocol maintains security due to elliptic curve discrete logarithm problem. Adversary wants to find out the value of  $x$  by the given value of  $B$  and  $Q$  where  $B$  is the base point of the elliptic curve and  $Q = x \cdot B$ , where  $B$  is  $x$  times added to itself to generate  $Q$ . However, it is computationally infeasible to find out the value of  $x$  due to elliptic curve discrete logarithm problem. The responses of the proposed protocol from the various attacks are addressed as follows.

### 7.1 Known Session Key Security

In the proposed protocol, each member  $M_i$  randomly chooses a private key  $x_i \in Z_p^*$  in the session. The session key depends on each member's private key. If an adversary compromise one session key, then it is not an easy task to compromise other's session key. So, it cannot find other's session key. So, this protocol provides known session key security.

### 7.2 No Key Control

The proposed protocol is fully contributive protocol, because the session key of the proposed protocol depends on each members blind key which are computed with each member's private key as  $Q_i = x_i B$ .

### ***7.3 Forward Secrecy***

The coming member does not know about what was the group key earlier because they receive information about the generating point of the elliptic curve. They cannot guess the group key because the group key is computed with each one secrets and generating point of the group key. The secret is a random number, taken privately by each member. Random number is unknown to connecting a member. So, the new member cannot find the previous group key.

### ***7.4 Backward Secrecy***

The leaving member cannot compute the new group key because the share of the leaving member is no longer part of the group key. The group key is updated by GCS using the blind key contribution of all members except the leaving member. So, all the previous group keys are completely unknown to leaving member/s.

### ***7.5 Key Independence***

A member, who knows a set of key, cannot discover previous or future key. So the proposed protocol maintains key independence.

### ***7.6 Comparison with Other Existing Protocols***

This section compares the cost of major group key management operations of the proposed protocol with other existing group key agreement schemes. The comparison Table 1 shows the following notation for comparison.

- n: Number of members in the group
- h: Height of the original key tree
- p: Number of leaving member.

## **8 Conclusion**

We have proposed an efficient queue based group key agreement protocol. We have analyzed many prior group key agreement protocols like TGDH, STR, BD, QBDH etc., they provide better security but they takes more computational overheads. So, we have used elliptic curve cryptographic technique that removes exponentiation to

**Table 1** Comparison with other protocols

Protocols		Messages	Exponentiation
TGDH	Join	3	$3h/2$
	Leave	1	$3h/2$
	Mass leave	$2n$	$3h$
STR	Join	3	4
	Leave	1	$3n/2 + 2$
	Mass leave	1	$3n/2 + 2$
GDH	Join	$n + 3$	$n + 3$
	Leave	1	$n - 1$
	Mass leave	1	$n - p$
BD	Join	$2n + 2$	3
	Leave	$2n - 2$	3
	Mass leave	$2n - 2p$	3
QGDH	Initial setup	$2n - 2$	$3(\log_2 n)/2$
	Join	$2n - 2$	$3(\log_2 n)/2$
	Leave	$2n - 2$	$3(\log_2 n)/2$
	Mass leave	$2n - 2$	$3(\log_2 n)/2$
Proposed protocol	Initial setup	$2n - 2$	0
	Join	2	0
	Leave	2	0
	Mass leave	2	0

reduce computational overheads. The comparison table shows that it provides better results than the other group key agreement protocols.

**Acknowledgment** This work is supported by UGC (University Grant Commission), Govt. of India under project No.—UGC(77)/2012-13/316/CSE. We would like to thank UGC for the support in this research work.

## References

1. Kim, Y., Perring, A., Tsudik, G.: Tree-based group key agreement. *ACM Trans. Inf. Syst. Secur. (TISSEC)*. **7**(1), 60–96 (2004)
2. Steiner, M., Tsudik, G., Waidner, M.: Key agreement in dynamic peer groups. *IEEE Trans. Parallel Distrib. Syst.* **11**(8), 769–780 (2000)
3. Wong, C., Gouda, M., Lam, S.: Secure group communication using key graphs. *IEEE/ACM Trans. Netw.* **8**(1), 16–30. (2000)
4. Amir, Y., Kim, Y., Rotaru, C.N., Tsudik, G.: On the performance of group key agreement protocols. *ACM Trans. Inf. Syst. Secur. (TISSEC)*. **7**(3), 457–488 (2004)
5. Hong, S.: Queue based group key agreement protocol. *Int. J. Netw. Secur.* **9**(2), 135–142 (2009)

6. Diffie, W., Hellman, M. E.: New directions in cryptography. *IEEE Tran. Inf. Theor.* IT **22**(6), 644–654 (1976)
7. Hong, S., Benitez, N.L.: Enhanced group key computation protocol. In: *International Conference on Security and Management-SAM'06*. Las Vegas, USA, 26–29 June 2006
8. Hsu, C.F., Cui, G.H., Cheng, Q., Chen, J.: A novel linear multi-secret sharing scheme for group communication in wireless mesh networks. *J. Netw. Comput. Appl.* **34**(2), 464–468 (2011)
9. Bohli, J.M.: A framework for robust group key agreement. *Comput. Sci. Appl. ICCSA*, 355–364 (2006)
10. Burmester, M., Desmedt, Y.: A secure and efficient conference key distribution system. In: *Advances in cryptology–Eurocrypt'94*, pp. 275–286. Springer, Berlin (1994)



# Solving Multi-level Image Thresholding Problem—An Analysis with Cuckoo Search Algorithm

B. Abhinaya and N. Sri Madhava Raja

**Abstract** In recent years, heuristic algorithms are extensively employed to offer optimal solutions for a class of engineering optimization problems. In this paper, Otsu based bi-level and multi-level image segmentation problem is addressed using Cuckoo Search (CS) algorithm. Optimal thresholds for the gray scale images are attained by analyzing histogram of the image. Maximization of Otsu's between class variance function is chosen as the objective function. In the proposed work, CS algorithm with various search methodologies, such as Lévy Flight (LF), Brownian Distribution (BD), and Chaotic search are analyzed. The proposed work is demonstrated by considering five grey scale benchmark ( $512 \times 512$ ) images. The performance assessment between CS algorithms are carried using established image parameters such as objective function, Root Mean Squared Error (RMSE), Peak to Signal Ratio (PSNR), and Structural Similarity Index Matrix (SSIM). The result shows that BD and chaotic CS provide better objective function, PSNR and SSIM, whereas LF based CS offers faster convergence.

**Keywords** Cuckoo search · Image segmentation · Otsu · Objective function · PSNR · SSIM

## 1 Introduction

Image processing plays a vital role in imaging science. Finding the accurate threshold value to separate an image into desirable object and background remains an extremely significant step in imaging science. In literature, several thresholding procedures have been proposed and implemented by most of the researchers for

---

B. Abhinaya (✉) · N. Sri Madhava Raja  
Department of Electronics and Instrumentation Engineering, St. Joseph's College  
of Engineering, Chennai 600119, Tamil Nadu, India  
e-mail: abhinaya.cse@gmail.com

N. Sri Madhava Raja  
e-mail: nsrimadharaja@stjosephs.ac.in

grey scale and colour images [4–6, 11]. Detailed reviews on existing thresholding techniques can be found in [7, 9, 15]. Among them, global thresholding is considered as the most preferred practice for image segmentation, because of its simplicity, robustness, accuracy and competence [2, 14, 16].

Traditional segmentation scheme offers better result with lesser computation time for a bi-level thresholding problem. When the threshold number increases, complexity of the problem also will increase and the traditional method require more computational time. Hence, in recent years, heuristic algorithm based multi-level image thresholding procedure is widely proposed by the researchers [1, 3, 10, 12].

In this work, bi-level and multi-level image thresholding problem is addressed using the Cuckoo Search (CS) algorithm developed by Yang and Deb in 2009 [17]. The CS algorithm with well known guiding procedures, such as Lévy Flight (LF), Brownian Distribution (BD), and Chaotic search are analyzed. The proposed work is demonstrated by considering five grey scale benchmark ( $512 \times 512$ ) images such as Butterfly, Bridge, Cart, Hill, and House.

## 2 Cuckoo Search Algorithm

In recent years, a considerable number of meta-heuristic algorithms are proposed by the researchers to deal with a class of constrained and unconstrained optimization problems. Cuckoo Search (CS) is one of the successful algorithms, initially proposed by Yang and Deb in 2009 [17]. This algorithm is based on the breeding tricks of parasitic cuckoos [1, 3, 10]. CS algorithm is developed based on the following rules:

- Each cuckoo lays an egg and dumps in a randomly chosen nest
- The nest with high survived egg will be carried over to the next generation. Cuckoo's egg generally hatches several days before than the host's eggs. The cuckoo chick grows faster and expels the host's eggs and chicks.
- In a search universe, the number of host nest is fixed. The host bird discovers the cuckoo's egg with a probability  $p_a \in [0, 1]$ . When the host identifies the egg, it may remove it from nest, or simply abandon the nest and build a new nest.

In most of the heuristic algorithms, the success towards the optimal solution mainly relies on the guiding procedure. Most of the recently developed nature inspired optimization search process is guided by Lévy Flight (LF) strategy [18]. LF is a random walk with a sequence of random steps and is conceptually comparable to the search path of a foraging animal [16]. Along with the LF, in this paper, other related search approach, such as the Brownian Distribution (BD) and Chaotic search (CH) is considered to guide the CS algorithm. BD is a subdiffusive non-markovian process, which obeys a Gaussian distribution with zero mean and time-dependent variance. A detailed description about the LF and BD can be found in [16, 18].

In the literature, a considerable number of chaotic search methods are available [13]. In the proposed work, Ikeda Map (IM) is considered to guide the CS. A complete explanation on IM could be found in [13, 19].

In CS, during the optimization search, the new solution  $(X_i^{(t+1)})$  mainly depends on the old solution  $(X_i^{(t)})$  and the search guiding procedure [16]. In this work, the following expressions are considered to find the new solution;

$$X_i^{(t+1)} = X_i^{(t)} + \alpha \oplus LF \quad (1)$$

$$X_i^{(t+1)} = X_i^{(t)} + \alpha \oplus BD \quad (2)$$

$$X_i^{(t+1)} = X_i^{(t)} + \alpha \times CH \quad (3)$$

where  $\alpha > 0$  is the succeeding step.

### 3 Otsu

Otsu's image thresholding scheme is initially proposed in 1979 [8]. The optimal thresholds for the bi-level and multi-level thresholding process can be attained by maximizing the between-class variance function. A detailed description of Otsu's between-class variance method could be found in [4, 5, 8, 14, 16].

Otsu's bi-level and multi-level thresholding technique is described below.

#### 3.1 Bi-level Thresholding

In this, the image is divided into two classes such as  $C_0$  and  $C_1$  by a threshold at a level 't'. The class  $C_0$  encloses the gray levels in the range 0 to t - 1 and class  $C_1$  encloses the gray levels from t to L - 1.

The probability allocation for  $C_0$  and  $C_1$  can be expressed as;

$$C_0 = \frac{p_0}{\omega_0(t)} \dots \frac{p_{t-1}}{\omega_0(t)} \quad \text{and} \quad C_1 = \frac{p_t}{\omega_1(t)} \dots \frac{p_{L-1}}{\omega_1(t)} \quad (4)$$

where

$$\omega_0(t) = \sum_{i=0}^{t-1} p_i, \quad \text{and} \quad \omega_1(t) = \sum_{i=t}^{L-1} p_i$$

The mean levels  $\mu_0$  and  $\mu_1$  for  $C_0$  and  $C_1$  can be written as;

$$\mu_0 = \sum_{i=0}^{t-1} \frac{ip_i}{\omega_0(t)} \quad \text{and} \quad \mu_1 = \sum_{i=t}^{L-1} \frac{ip_i}{\omega_1(t)} \quad (5)$$

The mean intensity ( $\mu_t$ ) of the entire image can be represented as;

$$\mu_t = \omega_0\mu_0 + \omega_1\mu_1 \quad \text{and} \quad \omega_0 + \omega_1 = 1$$

The objective function for the bi-level thresholding problem can be expressed as;

$$\text{Maximize } J(t) = \sigma_0 + \sigma_1 \quad (6)$$

### 3.2 Multi-level Thresholding

For multi-level thresholding problem, let us consider ‘ $m$ ’ thresholds ( $t_1, t_2, \dots, t_m$ ), which split the image into ‘ $m$ ’ classes:  $C_0$  with gray levels in the range 0 to  $t_1 - 1$ ,  $C_1$  with enclosed gray levels in the range  $t_1$  to  $t_2 - 1$ , ..., and  $C_m$  includes gray levels from  $t_m$  to  $L - 1$ . The objective function for this problem can be expressed as;

$$\text{Maximize } J(t) = \sigma_0 + \sigma_1 + \dots + \sigma_m \quad (7)$$

where  $\sigma_0 = \omega_0(\mu_0 - \mu_t)^2$ ,  $\sigma_1 = \omega_1(\mu_1 - \mu_t)^2$ , ...,  $\sigma_m = \omega_m(\mu_m - \mu_t)^2$ .

\* in this work, objective functions are assigned for  $m = 2$ ,  $m = 3$ ,  $m = 4$ , and  $m = 5$ .

### 3.3 Quality Measures

The well known parameters, such as the Root Mean Square Error (RMSE), the Peak Signal-to-Noise Ratio (PSNR) and Structural Similarity Index Matrix (SSIM) are considered to evaluate the quality of the segmented image.

The mathematical expression is given below:

$$RMSE_{(x,y)} = \sqrt{MSE_{(x,y)}} = \sqrt{\frac{1}{MN} \sum_{i=1}^H \sum_{j=1}^W [x(i,j) - y(i,j)]^2} \quad (8)$$

$$PSNR_{(x,y)} = 20 \log_{10} \left( \frac{255}{\sqrt{MSE_{(x,y)}}} \right); \text{ dB} \quad (9)$$

$$SSIM_{(x,y)} = \frac{(2\mu_x\mu_y + C_1)(2\sigma_{xy} + C_2)}{(\mu_x^2 + \mu_y^2 + C_1)(\sigma_x^2 + \sigma_y^2 + C_2)} \quad (10)$$

where  $x$  and  $y$  are original and segmented images;  $\mu_x$  and  $\mu_y$  are the average values,  $\sigma_x^2$  and  $\sigma_y^2$  are the variance,  $\sigma_{xy}$  is the covariance, and  $C_1 = (k_1L)^2$  and  $C_2 = (k_2L)^2$  stabilize the division with weak denominator, with  $L = 256$ ,  $k_1 = 0.01$ , and  $k_2 = 0.03$  [2].

### 4 Result and Discussions

Otsu guided, CS algorithm based multi-level thresholding techniques have been tested on standard test images ( $512 \times 512$ ), such as Butterfly, Bridge, Cart, Hill, and House. From the grey histogram, it is noted that, the dataset has abruptly changing pixel levels.

The experiments are executed on a work station with a Core i3 2.5 GHz CPU with 2 GB of RAM and equipped with Matlab R2010 software. The CS algorithm parameters are assigned as discussed in [1, 3, 17]; the number of nests ( $n$ ) is 20;  $p_a$  is assigned as 0.25, the dimension ( $D$ ) of the search is chosen as threshold level ‘ $m$ ’, and the total number of run is chosen as 200. The LF and BD parameters are assigned based on the recent work by Raja et al. [16]. In the IM based CS algorithm (CCS), the chaotic attractor parameter ( $u$ ) is assigned with a value of 0.55.

For each image, the segmentation process is repeated 10 times and the average among the trials is chosen as optimal values. Initially, the proposed method is tested on the butterfly image ( $512 \times 512$ ). Figure 1 depicts the 2D Ikeda map (sequential walk strategy) for  $u = 0.55$  and Fig. 2 shows the convergence of the optimization search for  $m = 2$ . From Fig. 2, one can observe that, the LF guided CS (LFCS) offers faster convergence compared to other considered methods. The LFCS converges at 24th iteration, BDCS converges at 85th iteration and CCS converges at 47th iteration.

Fig. 1 IM for  $u = 0.55$

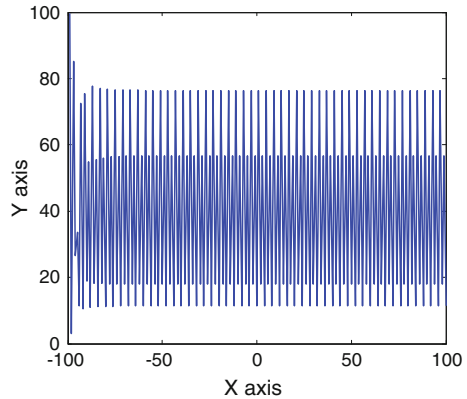
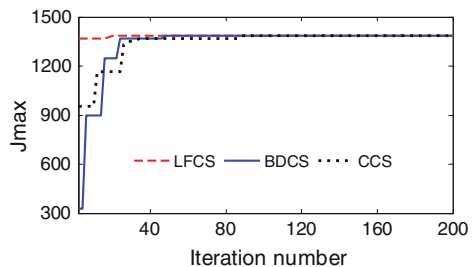


Fig. 2 Convergence of search



Similar thresholding procedure is repeated for all the images in the dataset and the corresponding results are presented in Tables 1, 2, and 3 for  $m = 2, 3, 4,$  and  $5.$

**Table 1** Comparison of objective values and thresholds for the dataset

	m	Objective function			Optimal thresholds		
		LFCS	BDCS	CCS	LFCS	BDCS	CCS
Butterfly	2	1,272.84	<b>1,309.23</b>	1,268.04	93, 158	91, 152	90, 154
	3	1,473.03	1,466.03	<b>1,482.43</b>	76, 122, 176	81, 119, 172	78, 125, 169
	4	1,482.22	1,490.55	<b>1,506.67</b>	70, 99, 137, 183	74, 96, 132, 177	69, 92, 138, 174
	5	1,603.47	1,625.92	<b>1,681.01</b>	66, 84, 133, 162, 186	62, 80, 131, 160, 182	59, 84, 128, 166, 180
Bridge	2	441.09	<b>468.37</b>	455.13	54, 88	62, 86	60, 84
	3	593.02	<b>610.05</b>	608.71	42, 69, 92	58, 71, 88	50, 66, 86
	4	611.74	629.02	<b>645.28</b>	36, 48, 74, 96	42, 64, 78, 93	45, 68, 81, 92
	5	704.37	<b>811.92</b>	798.46	28, 40, 52, 82, 98	22, 38, 59, 77, 102	26, 42, 61, 74, 100
Cart	2	1,729.67	1,783.35	<b>1,790.04</b>	86, 163	78, 172	76, 170
	3	1,784.88	1,791.11	<b>1,805.63</b>	54, 77, 168	48, 86, 180	46, 85, 178
	4	1,818.03	1,808.39	<b>1,825.04</b>	36, 69, 132, 170	32, 72, 138, 182	38, 70, 134, 180
	5	1,865.29	<b>1,874.00</b>	1,865.48	18, 46, 82, 152, 184	22, 48, 103, 150, 192	25, 52, 111, 146, 190
Hill	2	1,689.05	<b>1,703.75</b>	1,694.22	64, 102	62, 107	66, 106
	3	1,705.38	<b>1,729.03</b>	1,711.74	47, 88, 118	42, 93, 114	41, 95, 114
	4	1,793.48	1,803.26	<b>1,821.91</b>	39, 74, 90, 123	28, 70, 102, 126	32, 68, 108, 124
	5	1,826.83	<b>1,864.37</b>	1,855.37	34, 61, 88, 126, 138	25, 60, 84, 115, 134	27, 58, 86, 111, 137
House	2	3,111.64	<b>3,288.18</b>	3,184.27	86, 146	84, 148	81, 136
	3	3,282.19	<b>3,302.37</b>	3,274.03	69, 103, 155	66, 94, 157	68, 98, 148
	4	3,927.27	4,032.18	<b>4,083.33</b>	57, 76, 124, 176	60, 82, 119, 168	58, 89, 125, 154
	5	4,092.28	4,237.00	<b>4,271.56</b>	52, 66, 94, 138, 186	56, 71, 96, 133, 182	51, 74, 90, 132, 178

**Table 2** Original image and segmented images for various 'm' levels


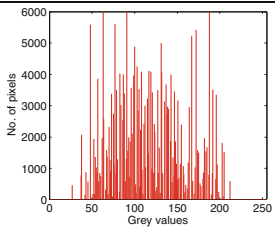
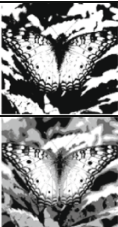
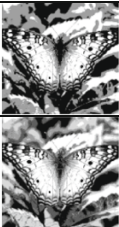

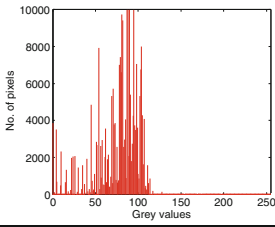



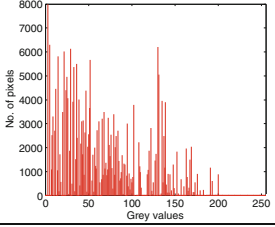



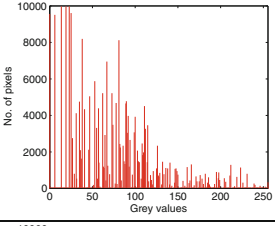
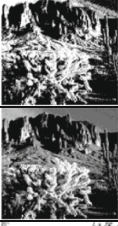
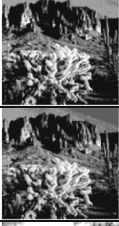

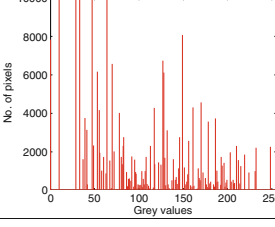


	Image	Grey level histogram	m = 2	m = 3
			m = 4	m = 5
Butterfly				
Bridge				
Cart				
Hill				
House				

Table 3 Comparison of performance measure values

	m	RMSE			PSNR (dB)			SSIM		
		LFCS	BDCS	CCS	LFCS	BDCS	CCS	LFCS	BDCS	CCS
Butterfly	2	71.48	65.95	66.03	11.04	<b>11.74</b>	11.73	0.6758	<b>0.6946</b>	0.6815
	3	57.36	54.12	50.98	12.95	13.46	<b>13.98</b>	0.7038	0.7084	<b>0.7095</b>
	4	43.97	40.36	40.00	15.26	16.01	<b>16.08</b>	0.7846	<b>0.7911</b>	0.7883
	5	38.94	33.05	31.66	16.32	17.74	<b>18.12</b>	0.8035	<b>0.8095</b>	0.8024
	2	31.97	33.14	30.75	18.03	17.72	<b>18.37</b>	0.7046	<b>0.7138</b>	0.7111
Bridge	3	29.56	28.84	27.90	18.71	18.93	<b>19.21</b>	0.7163	0.7224	<b>0.7307</b>
	4	27.33	26.35	26.32	19.39	19.71	<b>19.72</b>	0.7704	<b>0.7802</b>	0.7762
	5	25.93	24.11	24.78	19.72	<b>20.48</b>	20.25	0.7924	0.8035	<b>0.8081</b>
	2	45.43	43.27	44.91	14.98	<b>15.40</b>	15.08	0.7183	<b>0.7188</b>	0.7115
	3	40.01	37.57	36.92	16.08	16.63	<b>16.78</b>	0.7441	<b>0.7490</b>	0.7367
Cart	4	35.35	33.06	32.68	17.16	17.74	<b>17.84</b>	0.7659	0.7618	<b>0.7704</b>
	5	33.85	31.36	30.00	17.54	18.20	<b>18.58</b>	0.8063	0.8099	<b>0.8120</b>
	2	49.47	41.88	41.04	14.24	15.69	<b>15.86</b>	0.6483	<b>0.6749</b>	0.6693
	3	42.24	40.54	40.77	15.61	<b>15.97</b>	15.92	0.6837	0.6796	<b>0.6843</b>
	4	37.46	34.44	33.80	16.65	17.38	<b>17.55</b>	0.7203	<b>0.7457</b>	0.7392
House	5	35.52	32.95	30.35	17.12	17.77	<b>18.48</b>	0.7562	0.7811	<b>0.7905</b>
	2	60.14	54.35	55.94	12.54	<b>13.42</b>	13.17	0.6788	<b>0.6847</b>	0.6822
	3	51.53	50.07	49.99	13.88	14.14	<b>14.15</b>	0.7259	<b>0.7352</b>	0.7310
	4	41.68	38.95	36.55	15.73	16.32	<b>16.87</b>	0.7566	0.7660	<b>0.7694</b>
	5	40.07	37.74	36.02	16.07	16.59	<b>17.00</b>	0.7817	0.7893	<b>0.7912</b>



Table 2 presents the dataset, corresponding grey level histogram, and Otsu based segmented images for  $m = 2, 3, 4, 5$  with Chaotic Cuckoo Search (CCS).

From Tables 1 and 3 outcome, it is noted that, BDCS and CCS offers better objective function, PSNR, and SSIM compared to the LFCS. From this study, it is observed that, LFCS offers faster convergence, where as BDCS and CCS provides superior quality measures for the considered image segmentation problem.

## 5 Conclusions

In this paper, bi-level and multi-level image thresholding problem is addressed using Otsu based Cuckoo Search (CS) algorithm. A comparative study is carried with the most successful guiding procedure, such as Lévy Flight, Brownian Distribution, and Ikeda Map (IM). The simulation result confirms that, Chaotic Cuckoo Search (CCS) offers superior result compared with the LFCS. Due to the nature of sequential walk, the number of iterations taken by the CCS is comparatively larger than LFCS. In future, the implementation with Ikeda map can also be extended with chaotic maps, such as Henon, and Tinkerbell.

## References

1. Agrawal, S., Panda, R., Bhuyan, S., Panigrahi, B.K.: Tsallis entropy based optimal multilevel thresholding using cuckoo search algorithm. *Swarm Evol. Comput.* **11**, 16–30 (2013)
2. Akay, B.: A study on particle swarm optimization and artificial bee colony algorithms for multilevel thresholding. *Appl. Soft Comput.* **13**(6), 3066–3091 (2013)
3. Brajevic, I., Tuba, M., Bacanin, N.: Multilevel image thresholding selection based on the Cuckoo search algorithm. In: *Proceedings of the 5th International Conference on Visualization, Imaging and Simulation (VIS '12)*, pp. 217–222, Sliema, Malta (2012)
4. Ghamisi, P., Couceiro, M.S., Benediktsson, J.A., Ferreira, N.M.F.: An efficient method for segmentation of images based on fractional calculus and natural selection. *Expert Syst. Appl.* **39**(16), 12407–12417 (2012)
5. Ghamisi, P., Couceiro, M.S., Martins, F.M.L., Benediktsson, J.A.: Multilevel image segmentation based on fractional-order Darwinian particle swarm optimization. *IEEE Trans. Geosci. Remote Sens.* **52**(5), 2382–2394 (2014)
6. Hammouche, K., Diaf, M., Siarry, P.: A comparative study of various meta-heuristic techniques applied to the multilevel thresholding problem. *Eng. Appl. Artif. Intell.* **23**(5), 676–688 (2010)
7. Lee, S.U., Chung, S.Y., Park, R.H.: A comparative performance study techniques for segmentation. *Comput. Vis. Graph. Image Process.* **52**(2), 171–190 (1990)
8. Otsu, N.: A threshold selection method from gray-level histograms. *IEEE Trans. Syst. Man Cybern.* **9**(1), 62–66 (1979)
9. Pal, N.R., Pal, S.K.: A review on image segmentation techniques. *Pattern Recogn.* **26**(9), 1277–1294 (1993)
10. Panda, R., Agrawal, S., Bhuyan, S.: Edge magnitude based multilevel thresholding using Cuckoo search technique. *Expert Syst. Appl.* **40**(18), 7617–7628 (2013)

11. Raja, N.S.M., Kavitha, N., Ramakrishnan, S.: Analysis of vasculature in human retinal images using particle swarm optimization based Tsallis multi-level thresholding and similarity measures. In: Panigrahi B.K., et al. (eds.) SEMCCO 2012, vol. 7677, pp. 380–387. LNCS (2012)
12. Rajinikanth, V., Sri Madhava Raja, N., Latha, K.: Optimal multilevel image thresholding: an analysis with PSO and BFO algorithms. *Aust. J. Basic Appl. Sci.* **8**(9), 443–454 (2014)
13. Sanchez, L., Infante, S.: Reconstruction of chaotic dynamic systems using nonlinear filters. *Chil. J. Stat.* **4**(1), 35–54 (2013)
14. Sathya, P.D., Kayalvizhi, R.: Modified bacterial foraging algorithm based multilevel thresholding for image segmentation. *Eng. Appl. Artif. Intell.* **24**, 595–615 (2011)
15. Sezgin, M., Sankar, B.: Survey over image thresholding techniques and quantitative performance evaluation. *J. Electron. Imaging* **13**(1), 146–165 (2004)
16. Sri Madhava Raja, N., Rajinikanth, V., Latha, K.: Otsu based optimal multilevel image thresholding using Firefly algorithm. *Model. Simul. Eng.* **2014**, Article ID 794574, 17 pages (2014)
17. Yang, X.S., Deb, S.: Cuckoo search via Lévy flights. In: *Proceedings of World Congress on Nature and Biologically Inspired Computing (NaBIC 2009)*, pp. 210–214. IEEE Publications, USA (2009)
18. Yang, X.S.: *Nature-Inspired Metaheuristic Algorithms*. Luniver Press, Frome (2008)
19. [http://en.wikipedia.org/wiki/lkeda\\_map](http://en.wikipedia.org/wiki/lkeda_map)

# Comparing Efficiency of Software Fault Prediction Models Developed Through Binary and Multinomial Logistic Regression Techniques

Dipti Kumari and Kumar Rajnish

**Abstract** Software fault prediction method used to improve the quality of software. Defective module leads to decrease the customer satisfaction and improve cost. Software fault prediction technique implies a good investment in better design in future systems to avoid building an error prone modules. The study used software metrics effectiveness in developing models in 2 aspects (binary and multinomial) Logistic Regression. We are developing multivariate (combined effect of object-oriented metrics) models in both aspects for finding the classes in different error categories for the three versions of Eclipse, the Java-based open-source Integrated Development Environment. The distribution of bugs among individual parts of a software system is not uniform, in that case Multinomial aspects helps the tester to prioritize the tests with the knowledge of error range or category and therefore, work more efficiently. Multinomial models are showing better result than Binary models.

**Keywords** OO-metrics · Fault-prone · Prediction · Logistic regression · Multinomial · LR · BMLR · MMLR

## 1 Introduction

Over the past years, software quality has become one of the most important requirements in the development of systems. Fault-proneness estimation could play a key role in quality control of software products [1]. To maintain this quality and develop fault free software, almost in every organization that is involved in the

---

D. Kumari (✉) · K. Rajnish  
Department of Computer Science and Engineering, BIT Mesra, Ranchi 835215,  
Jharkhand, India  
e-mail: Kumari\_dipti0511@yahoo.co.in

K. Rajnish  
e-mail: krajnish@bitmesra.ac.in

software development there are various activities that have to be performed. Such an activity is testing. Software testing is a critical and essential part of software development that consumes maximum resources and effort. Software testing almost takes at least half of the resources and still doesn't assure the 100 % correctness of the system. Also every part of the software seems impossible to test. That's why everyone wants to focus or test only those parts of the software those have high probability to be fault-prone. The aim of various researches is to find such parts of system. Such parts includes classes, methods, inheritance paths etc. Software fault prediction is one of the quality assurance activities in Software Quality Engineering such as formal verification, fault tolerance, inspection, and testing. Software metrics [2, 3] and fault data (faulty or non-faulty information) belonging to a previous software version are used to build the prediction model. The fault prediction process usually includes two consecutive steps: training and prediction. In the training phase, a prediction model is built with previous software metrics (class or method-level metrics) and fault data belonging to each software module. After this phase, this model is used to predict the fault proneness labels of modules that locate in a new software version [4].

Until now, software engineering researchers have used Case-based Reasoning, Neural Networks, Genetic Programming, Fuzzy Logic, Decision Trees, Naive Bayes, Dempster-Shafer Networks, Artificial Immune Systems, and several statistical methods to build a robust software fault prediction model [5–8]. Some researchers have applied different software metrics to build a better prediction model, but recent papers [9] have shown that the prediction technique is much more important than the chosen metric set. In this paper, we attempt to develop binary and Multinomial LR models to estimates the fault-proneness in object oriented environment. We organised this paper as: Sect. 2 provides the Research Background and Research Methodology, Sect. 3 provides Model Evaluation, Sect. 4 provides Analysis of result. Section 5 provides the Conclusion and Sect. 6 provides Future scope.

## 2 Research Background

In this section, we present the selection of data source (Sect. 2.1), selection of metrics in this article (Sect. 2.2), Collection of Fault data and its categorization (Sect. 2.3) and Research methodology (Sect. 2.4).

### 2.1 Selection of Data Source

This study makes use of the data collected from three major releases of Eclipse (Eclipse2.0, Eclipse2.1 and Eclipse3.0). We select Eclipse2.0, 2.1, and 3.0 as the subjects of our study for two reasons: First, their fault data are publicly available

(Therefore, it is easy to externally validate our empirical results by other researchers. Second, they are major releases of Eclipse and have been widely used for several years.

## ***2.2 Selection of Independent Variables***

The selection of software metrics was a difficult task because there are many available metrics. We used two criteria in our selection process:

The set of metrics cover all aspects of OO design.

We have to be able to collect the metrics by using automated tool.

These metrics are characterized into coupling, cohesion, inheritance, class complexity and class-size metrics. We used JHAWK [10] automated tool metric to collect these metrics from the Eclipse source code [11]. JHAWK compiled the source code and give output as each module name and their set of OO metrics. These OO-metrics are independent variables.

## ***2.3 Collection of Dependent Variable***

The binary and multinomial dependent variable in this study is fault proneness. Fault proneness is defined as the probability of fault detection in a class. We collected the fault data from three releases of Eclipse (Versions 2.0, 2.1, and, 3.0) provided by the publicly available data set promise2.0a [12–14]. This data set lists the number of pre-release faults (reported in the first 6 months after release) for each java file in Eclipse2.0, Eclipse2.1 and Eclipse3.0. Pre release bug data are used for study and two types of categorization has been done on the pre release error data:

1. Binary Categorization: In this we only used two values 0 (means no error) and 1 (means with error). If a class contains error in it then we put 1 in error column otherwise 0.
2. Multinomial Categorization: In this we divide the error severity into 4 classes.

For classification our followed steps are as follows:

- We find the descriptive statistics of pre error data. From that we are able to know the min, different number of occurrences of error (nonzero) and max value of error data in all classes of every versions of Eclipse.
- After that, we again find the descriptive statistics of (Min, 25, 50, 75 % and Max) the different occurrences of number of errors (from min (nonzero) to max). Based on that we classified class error data into one of five categories that are defined as follows:
- No Error: class containing zero error

- Nominal: class containing error in the range  $\text{Min} \leq \text{error} < 25\%$
- Low: class containing error in the range  $25\% \leq \text{error} < 50\%$
- Medium: class containing error in the range  $50\% \leq \text{error} < 75\%$
- High: class containing error in the range  $75\% \leq \text{error} < \text{Max}$

More specifically, we attempt to answer the following questions by appropriate statistical analysis technique:

- How accurate do the investigated metrics distinguish between fault-prone and not fault-prone classes (binary categorization)?
- How accurate do the investigated metrics classifies classes into four categories: Nominal, Low, Medium, and High based on the error severity level (multinomial categorization)?

## 2.4 Research Methodology

In this section, we describe logistic regression (LR) analysis in binary and multinomial aspects. LR is the most widely used technique in literature. It is used here to predict dependent variable from a set of independent variables (a detailed description is given by [15, 16]). Binary LR is used to construct models when the dependent variable is binary and Multinomial LR is used to construct models when the dependent variable is not binary but having more than two values.

### 2.4.1 Binary Logistic Regression Model

Binary Logistic regression is a standard statistical modeling method in which the dependent variable  $Y$  can take on only one of two different values [17]. Assume that  $X_1, X_2, \dots, X_n$  represents the independent variables (i.e. the metrics in this study) and  $\Pr(Y = 1|x_1, x_2, \dots, x_n)$  represents the probability that  $Y = 1$  when  $X_1 = x_1, X_2 = x_2, \dots, \text{and } X_n = x_n$ . Then, the logistic regression model assumes that  $\Pr(Y = 1|x_1, x_2, \dots, x_n)$  is related to  $x_1, x_2, \dots, x_n$  by the following equation:

$$\Pr(Y = 1|x_1, x_2, \dots, x_n) = \frac{e^{\alpha + \beta_1 x_1 + \dots + \beta_n x_n}}{1 + e^{\alpha + \beta_1 x_1 + \dots + \beta_n x_n}} \quad (1)$$

where  $\beta$  is are the regression coefficients and can be estimated through the maximization of a log-likelihood.

### 2.4.2 Multinomial Logistic Regression

Multinomial Logistic regression is modified form of binary logistic regression, it is appropriate when the outcome is a polytomous variable (i.e. categorical with more than two categories) and the predictors are of any type.  $Y$  can take on more than two different values depending on the no. of different categories [17]. In the following, let the values be 0, 1, 2, 3 and 4. Here,  $Y = 1, 2, 3$  and  $4$  represents the corresponding class have fault according to the nominal category, low category, mid category and high category and  $Y = 0$  represents the corresponding class have no fault. As in other forms of linear regression, multinomial logistic regression uses a linear predictor function  $f(k, i)$  to predict the probability that observation  $i$  has outcome  $k$ , of the following form:

$$f(k, i) = \beta_{0,k} + \beta_{1,k} \times x_{1,i} + \beta_{2,k} \times x_{2,i} + \dots + \beta_{M,k} \times x_{M,i} \quad (2)$$

where  $\beta_{M,k}$  is a regression coefficient associated with the  $m$ th explanatory variable and the  $k$ th outcome.

## 3 Model Evaluation Criteria

In the literature, many other measures have been proposed for evaluating the predictive effectiveness of classification models such as logistic regression models [18–20]. Accuracy of the model is considered as the comparison factor with the earlier traditional models and may be obtained using Confusion Matrix [21]. A confusion matrix contains information about actual and predicted classifications done by a classification system. TP and TN are the number of correct predictions that an instance is positive and negative respectively. FP and FN are the number of incorrect predictions that an instance is positive and negative respectively.

- Accuracy: the number of classes that are correctly classified divided by the total number of classes. Where TP and TN are the number of correct predictions that an instance is positive and negative respectively. FP and FN are the number of incorrect predictions that an instance is positive and negative respectively. For binary categorization

$$Accuracy = \frac{TP + TN}{TP + TN + FP + FN} \quad (3)$$

For Multinomial categorization

$$Accuracy = \frac{TP + TN_i}{TP + TN_i + FP + FN_i} \quad (4)$$

where  $TP = T_0$ ,  $TN_i = T_1, T_2, T_3$  and  $T_4$ ,  $FP = \sum_{j=1}^4 F_{0j}$   $FN_i = \sum_{i=1}^4 \sum_{j=1}^4 F_{ij}$  where  $i \neq j$ .

Where  $T_0, T_1, T_2, T_3$  and  $T_4$  are the number of correct predictions that an instance is positive, negative in nominal category, low category, mid category and high category. Where  $F_{0i}$  are the number of incorrect predictions that an instance is actually in positive but predicted in nominal category. In  $F_{ij}$  first subscript showing the actual instance and second one is showing the predicted result.

- The general rule to evaluate the classification performance is to find the area under the curve (AUC): AUC = 0.5 means no good classification;  $0.5 < AUC < 0.6$  means poor classification;  $0.6 \leq AUC < 0.7$  means fair classification;  $0.7 \leq AUC < 0.8$  means acceptable classification;  $0.8 \leq AUC < 0.9$  means excellent classification;  $AUC \geq 0.9$  means outstanding classification.

## 4 Experimental Analysis

We have developed binary and multinomial model by taking the combined effect of OO-metrics to identify faulty classes. The model is built using backward elimination in the model and model statistics are shown in Tables 1 and 2 for all 3 versions of Eclipse in binary and multinomial aspects respectively. From table we find that Multinomial categorization are showing good result compare to Binary Categorization.

### 4.1 Validation Result

Tables 3 and 4 summarizes the TP, TN, FP, FN, Sensitivity, (1-Specificity), AUC and Accuracy results from 18-fold cross-validation for the Multivariate models for binary and multinomial aspect respectively for all 3 version of Eclipse. Accuracy result for nominal category is 58–65 % and AUC comes in poor category, but accuracy for low, mid and high category is in 50–60 % and their classification power comes in fair and acceptable classification. PACK is showing best result among all metrics for Eclipse2.0 in MBLR model. Accuracy of nominal category is high compare to other but its discriminating power is in poor class. Other 3 categories have accuracy 69–71 % and low and part of mid comes in acceptable class, but high comes is excellent classification for Eclipse2.1 in MBLR model. PACK is showing the best result among all. Same incidence is found in Eclipse3.0 for MBLR





**Table 2** Multivariate model statistics for multinomial categorization

Eclipse2.0						Eclipse2.1						Eclipse3.0					
Metric	B	S.E	Sig	Metric	B	S.E	Sig	Metric	B	S.E	Sig	Metric	B	S.E	Sig		
NOS	0.003	0.001	0.012	UWCS	-0.007	0.004	0.045	AVCC	0.122	0.02	0	AVCC	0.122	0.02	0		
PACK	0.064	0.004	0	RFC	0.006	0.002	0.004	UWCS	0.011	0.002	0	UWCS	0.011	0.002	0		
CBO	0.019	0.008	0.017	CC	0.01	0.004	0.007	PACK	0.056	0.004	0	PACK	0.056	0.004	0		
FOUT	0.073	0.015	0	MAXCC	0.025	0.007	0	FOUT	0.041	0.013	0.001	FOUT	0.041	0.013	0.001		
AVCC	0.115	0.023	0	NLOC	-0.003	0.001	0.003	TCC	0.007	0.002	0	TCC	0.007	0.002	0		
NLOC	-0.002	0.001	0.011	PACK	0.068	0.004	0	CBO	0.015	0.007	0.023	CBO	0.015	0.007	0.023		
Constant	-1.443	0.057	0	Const	-1.966	0.047	0	Const	-2.085	0.051	0	Const	-2.085	0.051	0		

**Table 3** Evaluation result of the performance of binary multivariate model for all 3 version of eclipse

Version	TP	TN	FP	FN	Sensitivity	1-Specificity	AUC	Accuracy
Eclipse2.0	3,649	879	437	1,683	0.34	0.11	0.62	68.11
Eclipse2.1	5,386	595	309	1,507	0.28	0.05	0.61	76.71
Eclipse3.0	7,250	727	376	2,151	0.25	0.05	0.60	75.94

model. In MMLR model the accuracy of nominal category is 62–66 %,its AUC come in the poor class. But all other 3 categories has accuracy 55 % and AUC for low (in Eclipse2.1 and 3.0) and high (in Eclipse2.0) comes under acceptable class and except high for Eclipse2.1 comes in excellent class. The AUC result for Eclipse2.1 in high category gives the outstanding classification. Binary model is not best way to find the fault-prone and fault-free classes, but Multinomial Logistic regression is the best way to classify the classes in different categories depending on the number of errors in classes and work more efficiently.

## 5 Conclusion

In this paper, we re-examine the ability of metrics (metrics covering all aspects of software's property) for predicting fault-prone classes in OO systems. Our results are summarized as follows:

- When Multivariate logistic regression models built with combined effect of all chosen metrics. This shows better result in prediction. But, among both aspect (i.e. Binary, Multinomial) multivariate model shows better result in multinomial aspect of fault prediction.
- Of the investigated metrics, PACK is the only metric which is used to develop model in both aspects as well as both way bivariate and multivariate. It shows that pack metric has the best discrimination ability.
- We conclude that prioritizing the test on the basis of different number of errors in different error categories is more effective than the category of fault prone and fault free classes in binary categorization for developing fault prediction model.

## 6 Future Work

In the future work, we will replicate this study using these investigated metrics and other modeling techniques to draw stronger conclusion for getting best predictor and model also. In this study we have used all those metric which are capable for giving the significant threshold for differentiating the classes in binary categorization (error-free and error-prone) and also multinomial categorization (nominal, low, mid and high) from our previous study [22].

**Table 4** Evaluation result of the performance of multinomial multivariate model for all 3 version of eclipse

Version	Multinomial multivariate model																						
	True			False			Sensitivity			1-Specificity			AUC			Accuracy							
	Nom	Low	Mid	High	Nom	Low	Mid	High	Nom	Low	Mid	High	Nom	Low	Mid	High	Nom	Low	High				
Eclipse2	694.00	12.00	2.00	2.00	495.00	20.00	2.00	0.00	0.29	0.79	0.75	0.18	0.12	0.17	0.18	0.18	0.59	0.81	0.80	65.91	55.66	55.51	55.51
Eclipse2.1	453.00	5.00	2.00	3.00	368.00	11.00	1.00	1.00	0.26	0.58	0.75	0.11	0.07	0.10	0.11	0.11	0.59	0.74	0.83	62.29	55.55	55.51	55.52
Eclipse3	622.00	7.00	3.00	1.00	409.00	10.00	0.00	0.00	0.23	0.64	0.74	0.10	0.06	0.10	0.10	0.10	0.59	0.78	0.83	64.83	55.58	55.52	55.49

## References

1. Bellini, P., Bruno, I., Nesi, P., Rogai, D.: Comparing fault-proneness estimation models. ICECCS '05 Proceedings of the 10th IEEE International Conference on Engineering of Complex Computer Systems, pp. 205–214 (2005)
2. Misra, S.: Evaluation criteria for object-oriented metrics. *Acta Polytech. Hung.* **8**(5), 109–136 (2011)
3. Pusatli, O.T., Misra, S.: Software measurement activities in small and medium enterprises: an empirical assessment. *Acta Polytech. Hung.* **8**(5), 21–42 (2011)
4. Seliya, N.: Software Quality Analysis with Limited Prior Knowledge of Faults. Wayne State University, Department of Computer Science, Graduate Seminar (2006)
5. Mittal, P., Singh, S., Kahlon, K.S.: Empirical model for fault prediction using object-oriented metrics in mozilla firefox. *Int. J. Comput. Technol. Res.* **1**(6), 151–161 (2013)
6. Kayarvizhy, N., Kanmani, S.: High precision cohesion metric. *WSEAS Trans. Inform. Sci. Appl.* **10**, 79–89 (2013)
7. Zhou, Y., Xu, B., Leung, H.: On the ability of complexity metrics to predict fault-prone classes. *J. Syst. Softw.* **83**, 660–674 (2010)
8. Shatnawi, R., Li, W., Swain, J., Newman, T.: Finding software metrics threshold values using ROC curves. *J. Softw. Maintenance Evol. Res. Pract.* **22**(1), 1–16 (2010)
9. Menzies, T., Greenwald, J., Frank, A.: Data mining static code attributes to learn defect predictors. *IEEE Trans. Softw. Eng.* **32**(1), 2–13 (2007)
10. JHAWK.: Metrics reference. <http://www.virtualmachinery.com/jhawkreferences.html>. Accessed March 2014
11. Eclipse source code (for archived releases): <http://archive.eclipse.org/eclipse/downloads/>. Accessed 3 Dec 2013
12. Eclipse bug data (for archived releases): <http://www.st.cs.uni-sb.de/softevo/bug-data/eclipse>. Accessed 20 Nov 2013
13. Zimmermann, T., Premraj, R., Zeller, A.: Predicting defects for eclipse. In: Proceedings of the Third International Workshop on Predictor models in Software Engineering, 2007
14. Schroter, A., Zimmermann, T., Premraj, R., Zeller, A.: If your bug database could talk. In: Proceedings of the Fifth International Symposium on Empirical Software Eng. **2**, 18–20 2006
15. Hosmer D, Lemeshow S.: Applied Logistic Regression. Wiley, New York (1989)
16. Basili, V., Briand, L., Melo, W.: A validation of object oriented design metrics as quality indicators. *IEEE Trans. Softw. Eng.* **22**(10), 751–761 (1996)
17. George, D., Mallery, P.: SPSS for Windows STEP BY STEP. Pearson Education (2011)
18. Jiang, Y., Cukic, B., Ma, Y.: Techniques for evaluating fault prediction models. *Empirical Softw. Eng.* **13**(5), 561–595 (2008)
19. Bradley, A.P.: The use of the area under the ROC curve in the evaluation of machine learning algorithms. *Pattern Recogn.* **30**(7), 1145–1159 (1997)
20. Hopkins, W.G.: A New View of Statistics. Sport Science, New Zealand (2003)
21. Chidamber, S., Darcy, D., Kemerer, C.: Managerial use of metrics for object-oriented software: an exploratory analysis. *IEEE Trans. Softw. Eng.* **24**(8), 629–639 (1998)
22. Kumari, D., Rajnish, K.: Finding error-prone classes at design time using class based object-oriented metrics threshold through statistical method. *Infocomp J. Comput. Sci.* **12**(1), 49–63 (2013)

# Performance Modeling of Unified TDPC in IEEE 802.16e WiMAX

Rewa Sharma, C.K. Jha and Meha Sharma

**Abstract** One of the major concerns in wireless networks is optimization of power as mobile devices are battery operated. Researchers have been constantly focusing on standard Type I or Type II power saving classes. In our previous work, limitation of standard Type I and Type II power saving classes in IEEE 802.16e was discussed and the idea of TDPC was suggested. In this paper, authors have proposed a new enhanced method of Traffic Dependent Power Conservation, in which each MSS is considered as a single member group initially and then groups are iteratively combined until reasonable sleep schedule is maintained. Authors have successfully modeled the suggested approach, Unified-TDPC to attain desired power optimization. Results clearly illustrates that Unified-TDPC, improve upon TDPC-cum and TDPC-divide and shows better power conservation at the cost of small delay in highly varying load.

**Keywords** WiMAX · TDPC · TDPC-cum · TDPC-divide · Unified-TDPC · AverageDelay · PCE · SF

---

R. Sharma (✉) · C.K. Jha  
Department of Computer Science,  
Banasthali Vidyapeeth, Tonk 304022, Rajasthan, India  
e-mail: rewa10sh@gmail.com

C.K. Jha  
e-mail: ckjha1@gmail.com

M. Sharma  
Department of Electronics and Communication,  
Banasthali Vidyapeeth, Tonk 304022, Rajasthan, India  
e-mail: meha.sharma.25@gmail.com

## 1 Introduction

IEEE 802.16 [1, 2] is a prominent Broadband Wireless Access (BWA) technology that supports high bandwidth and high speed wireless access. IEEE 802.16e [2] is an enhanced version of IEEE 802.16 that facilitate free movement of mobile subscriber stations (MSS) within the range of the network. MSS are no more bound to a particular location. In IEEE 802.16e, MSS depend on battery for providing power. In absence of any power management strategy, the power gets wasted over a long duration of time. Maximum of the power wastage happens when there is no data to receive but MSS keeps on listening to the data on radio channel. IEEE 802.16e defined three power saving classes, which are, Type I, Type II and Type III, which differ from each other in policy of MS availability for data transmission, process of definition, activation, deactivation and the parameters used. Many researchers have focused on performance enhancement based on Type I or II [3–9]. The idea of TDPC has been proposed in our previous work, which uses Type III power saving Class [10]. TDPC models the traffic actively and sleep schedule is determined using traffic situations. Earlier we proposed two approaches, TDPC-cum and TDPC-divide [11] respectively. In this Paper, Previously proposed approaches are improved by proposing a new method, Unified-TDPC to attain optimum power conservation and reduce wastage of energy.

## 2 Related Work

Researchers have been constantly working to improve energy conservation by emphasizing on the significance of sleep mode algorithms. Hwang et al. [12] have proposed power saving mechanism with regular traffic indications where a TRF-IND message is regularly sent at the start of every constant TRF-IND intervals. A statistical sleep window [13] algorithm has also been proposed for improving energy efficiency of MS considering virtual downlink traffic. Huo et al. [14] has proposed a discrete queuing model to calculate the delay of system model and average queue length. In 2008 Alouf et al. [15] investigated queuing models with repetitions in homogeneous environment. Some researchers follow Poisson distribution to study traffic pattern characteristics [16] whereas some others consider other distributions like Erlang distributed inter arrival time [17] and Hyper Erlang distribution interval time [18]. In [19–21] the authors have analyzed energy efficiency and delay of response in PSCI of IEEE 802.16e as a function of relative size of them. Sharma et al. [10, 11] proposed and simulated an algorithm TDPC-cum for reducing energy consumption which treated traffic from all the MSSs as a cumulative flow for deciding sleep window size.

Data accumulation threshold is denoted by  $thresh\_data$  (packets). The probability of exceeding this threshold over  $M$  time frames in a row is given as:

$$\begin{aligned} Pr_{Accum}(M, thresh\_data) &= \sum_{j=thresh\_data+1}^{\infty} \frac{e^{-\lambda MT} (\lambda MT)^j}{j!} \\ &= 1 - \sum_{j=0}^{thresh\_data} \frac{e^{-\lambda MT} (\lambda MT)^j}{j!} \end{aligned} \quad (1)$$

The number of time frames before next awake time frame for an MSS can be computed as the minimum value of  $M$  such that data accumulation probability over  $M$  time frames is higher than a predefined probability threshold,  $Pr\_thresh$ .

$$Length\_awake\_sleepcycle = Min\{M | Pr_{Accum}(M, thresh\_data) \geq Pr\_thresh\} \quad (2)$$

The new value of  $M^*$  is calculated by base station in each awake time frame of Mobile Subscriber Station due to instantly changing network load. Complete network load is considered as cumulative flow while calculating value of  $M^*$ . Awake and sleep cycles of same length may have a different starting time for each MSS. TDPC-divide algorithm proceeds with the assumption of single group ( $M^* = 1$ ), and then we calculate the current load of each MSS. Then divide all the mobile stations into  $M^*$  groups. For each group, calculate  $M_{Grp}^* \equiv AwakeSleepCycleLength(\lambda Grp, thresh\_data)$ .

### 3 Proposed Unified Traffic Dependent Power Conservation Algorithm

The proposed method follows different approach of grouping MSS as compared with TDPC-divide. In this algorithm, we assume each MSS as a single member group, which have their own  $M^*$  values, which varies due to variation in loads. For better power conservation, sleep scheduling method should be able to deal with different values of  $M^*$  as long a viable sleep schedule can be found. And for that, combination of some of the groups becomes necessary. This idea of considering each MSS as a single small group in the beginning and then uniting the groups when required is termed as Unified-TDPC. For the ease of checking schedulability of groups with any possible values of  $M^*$ , the values are converted to newer values, to the closest and smaller power of 2 and is given by  $M^\#$ . For groups having different values of  $M^\#$ , Schedule Feasibility (SF) can be calculated as

$$SF = \sum_i \frac{1}{M_i^\#} \quad (3)$$



If the value of SF is  $\leq 1$  feasible schedule can be found else some groups need to be combined. Value of  $M^*$  should be kept as large as possible after group unification process. The whole process can be defined to have two stages: Non-Degraded Unification and Degraded Unification. If the process of unification of two groups does not result in a smaller value of  $M^\#$ , the process is said to be non-degraded but if it leads to smaller value of  $M^\#$  it is degraded unification process. We always look for a non-degraded unification but if it is not possible then we opt for degraded one.

Stepwise Unified-TDPC Algorithm is as follows:

1. Estimate the current traffic ( $\lambda_i$ ) for each MSSi,  $\lambda_{Grp}$  denotes the total traffic load in the group. In the beginning each MSS lies in a single group.
2. Group load should be sorted. For each group, calculate  $M_{Grp}^*$ , and then convert it to closest and smaller power of 2.
3. If  $SF = \sum \frac{1}{M_{Grp}^\#} \leq 1$ , go to step 4. Else {Try to combine the smallest load group to another group until a non-degraded combination is found. If one is found, repeat step 2 and 3. Else perform degraded unification and merge the two groups having the smallest load and repeat step 2 and 3.}
4. Schedule the groups in accordance with the final set of  $M_{Grp}^\#$ .

## 4 Performance Evaluation

In TDPC-cum, the power conservation efficiency is  $(M^* - 1)/M^*$ . The MSS must remain into awake mode until all of its accumulated data is transmitted completely in a time frame, in this case the power conservation efficiency becomes  $(M^* - 1)/(M^* + N_{ext})$ , where  $N_{ext}$  is the number of extra awake time to transmit the accumulated data. We can calculate PCE (Power Conservation Efficiency) as follows

$$PCE = \sum_{j=0}^{\infty} \left( \frac{M^* - 1}{M^* + j} * \Pr[N_{ext} = j] \right) \quad (4)$$

Assuming the packet arrival time at the base station is distributed uniformly among the time frames in one awake and sleep cycle. Half of the cycle length gives the average access delay for a packet, which can be given as

$$AverageDelay = \sum_{j=0}^{\infty} \left( \frac{M^* + j}{2} * \Pr[N_{ext} = j] \right) \quad (5)$$

We conducted simulation using Network Simulator 2 (NS2) to analyze and compare performance of TDPC-cum and proposed enhancement TDPC-divide, in terms of average access delay and power conservation efficiency. We have also

analyzed power conservation efficiency and delay, in both the algorithms under different load conditions. We have also studied the behavior of proposed algorithm with varying number of MSSs.

Figure 1 shows the PCE comparison between the three algorithms, TDPC-cum, TDPC-divide and Unified-TDPC. Power conservation efficiency of Unified-TDPC and TDPC-divide is significantly better than TDPC-cum.

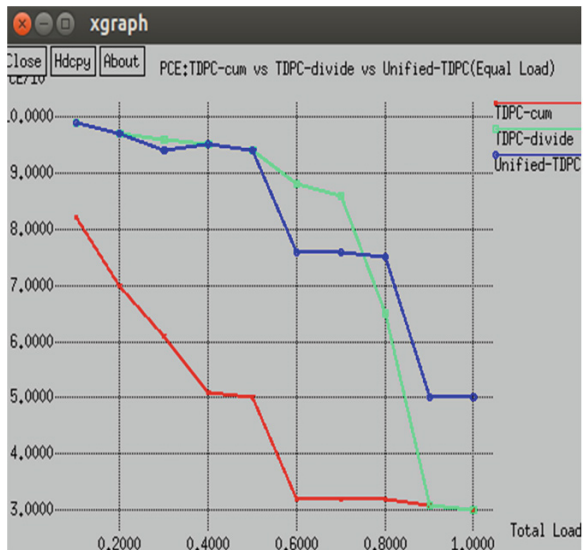
Performance comparison of TDPC-divide and Unified-TDPC shows different outcomes in different traffic conditions. PCE of both the methods is almost similar under lighter load i.e. below 0.5. PCE of TDPC-divide is better than Unified-TDPC when the traffic load is between 0.6 and 0.7 but in case of heavy load conditions (above 0.8) proposed algorithm outperforms TDPC-divide.

It is clearly shown from the Fig. 2 that though the two approaches shows a higher PCE than TDPC-cum but that comes with an increase in their average delays. In moderate and heavy load conditions, TDPC-divide shows lower delay than proposed method. But in case of lighter load Unified TDPC shows lower delay than TDPC-divide.

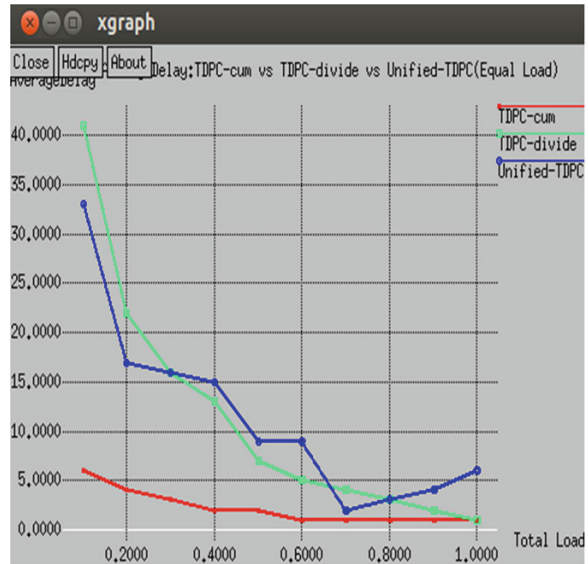
Figures 3 and 4 illustrate the performance result of PCE and Average Delay in case of 8:2 load, which means 80 % of traffic is handled by 20 % of MSS. Unified-TDPC shows better performance than TDPC-divide, when total load is under 0.6 reason for the same is that, PCE of TDPC-divide is constrained by group with the heaviest load. It can also be clearly depicted by the graphs that the performance comes at the cost of slight delay.

Figure 5 displays the result of power saving efficiency of Unified TDPC algorithm under different number of MSSs. Figure 6 shows the PCE of Unified TDPC

**Fig. 1** PCE: comparison (equal load)



**Fig. 2** AverageDelay: comparison (equal load)

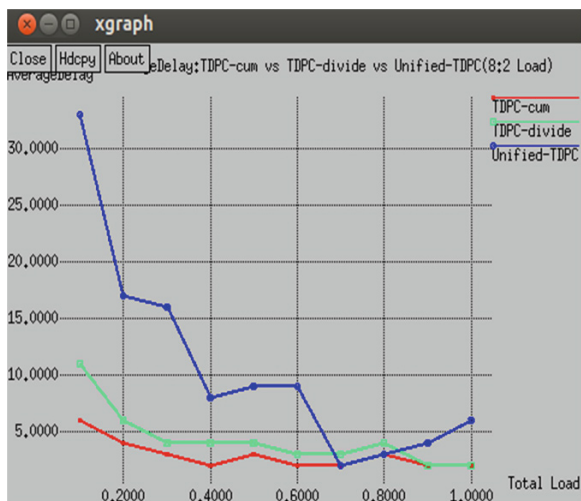


**Fig. 3** PCE: (8:2 load)

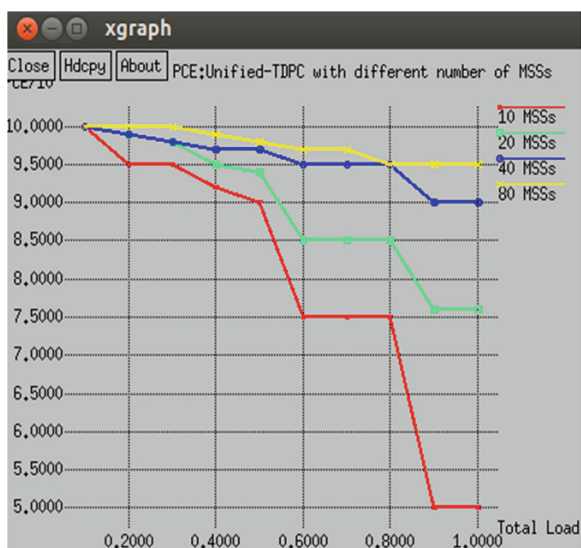


under different load conditions. Higher variation of load, result in lower PCE in TDPC-divide and Unified TDPC, though the impact is more consistent on TDPC-divide.

**Fig. 4** AverageDelay: (8:2 load)



**Fig. 5** PCE with varying number of MSSs



**Fig. 6** PCE comparison in different load conditions



## 5 Conclusion

In our past research, TDPC-cum and TDPC-divide were proposed for power saving in IEEE 802.16e. In this paper, previously proposed methods are revised and improved to present a new approach, Unified-TDPC, for power optimization. The proposed method initially assumes each MSS as a single member group and then the process of combining the groups is repeated until a feasible sleep schedule is determined. Simulation study shows that Unified-TDPC outperforms previously suggested methods, TDPC-cum and TDPC-divide, in terms of better power conservation efficiency. Performance of the algorithm is analyzed with respect to varying number of MSS and varying load distribution. Future work of the research is to extend the idea of TDPC methods and to consider the inputs from base station to further improve power conservation efficiency. Higher PCE results in higher delays. We aim to reduce these delays in our further work, thus maintain a proper balance between power conservation and delays in wireless networks.

**Acknowledgments** I wish to thank Dr. C.K Jha who gave their precious time, knowledge, experience for significant encouragement and support. I would also like to thank anonymous reviewers who gave valuable instructions that has comforted to enhance the quality of the paper.

## References

1. IEEE Std. 802.16-2004: IEEE standard for local and metropolitan area networks—part 16: air interface for fixed broadband wireless access systems (2004)
2. IEEE Std. 802.16e-2006: IEEE standard for local and metropolitan area networks—part 16: air interface for fixed and mobile broadband wireless access systems-amendment for physical and

- medium access control layers for combined fixed and mobile operation in licensed bands (2006)
3. Sheu, S.T., Cheng, Y.C., Chen, L.W.: Listening interval spreading approach (LISA) for handling burst traffic in IEEE 802.16e wireless metropolitan area networks. In: Proceedings IEEE 68th Vehicular Technology Conference (VTC 2008-Fall), pp. 1–5 (2008)
  4. Wu, Y., Le, Y., Zhang, D.: An enhancement of sleep mode operation in IEEE 802.16e systems. In: Proceedings IEEE 69th Vehicular Technology Conference (VTC 2009-Spring), pp. 1–6 (2009)
  5. Chen, J.J., Liang, J.M., Tseng, Y.C.: An energy efficient sleep scheduling considering QoS diversity for IEEE 802.16e wireless networks. In: Proceedings IEEE International Conference on Communications (ICC), pp. 1–5 (2010)
  6. Chen, T.C., Chen, J.C.: Maximizing unavailability interval for energy saving in IEEE 802.16e wireless MANs. *IEEE Trans. Mob. Comput.* **8**(4), 475–487 (2009)
  7. Hwang, E., Kim, K.J., Son, J.J., Choi, B.D.: The power-saving mechanism with periodic traffic indications in the IEEE 802.16e/m. *IEEE Trans. Veh. Technol.* **59**(1), 319–334 (2010)
  8. Cicconetti, C., Lenzini, L., Mingozzi, E., Vallati, C.: Reducing power consumption with QoS constraints in IEEE 802.16e wireless networks. *IEEE Trans. Mob. Comput.* **9**(7), 1008–1021 (2010)
  9. Hsu, C.H., Feng, K.T., Chang, C.J.: Statistical control approach for sleep mode operations in IEEE 802.16 m systems. *IEEE Trans. Veh. Technol.* **59**(9), 4453–4466 (2010)
  10. Sharma, R., Jha, C.K., Sharma, M.: Design and implementation of TDPC sleep scheduling algorithm for energy efficient networks. In: Proceedings of IEEE International Conference on Recent Advances and Innovations in engineering, India (2014)
  11. Sharma, R., Jha, C.K., Sharma, M.: A novel traffic dependent sleep scheduling method for energy conservation. In: Proceedings of IEEE International Conference CONLUENCE, p. 3. India (2014)
  12. Hwang, E., Kim, K.J., Son, J.J., Choi, B.D.: The power-saving mechanism with periodic traffic indications in the IEEE 802.16e/m. *IEEE Trans. Veh. Technol.* **59**, 319–334 (2014)
  13. Hsu, C.H., Feng, K.T., Chang, C.J.: Statistical control approach for sleep-mode operations in IEEE 802.16 m systems. *IEEE Trans. Syst. IEEE Trans. Veh. Technol.* **59**, 4453–4466 (2010)
  14. Huo, Z., Yue, W., Jin, S., Tian, N.: Modeling and performance evaluation for the sleep mode in The IEEE 802.16e wireless networks. In: Proceedings 11th IEEE Singapore International Conference on Communication Systems, pp. 1140–1144, Guangzhou, China (2008)
  15. Alouf, S., Altman, E., Azad, A.P.: Analysis of an M/G/1 queue with repeated inhomogeneous vacations with application to IEEE 802.16e power saving mechanism. Fifth International Conference on Quantitative Evaluation of Systems, pp. 27–36, St Malo, France (2008)
  16. Zhang, Y.: Performance modeling of energy management mechanism in IEEE 802.16e mobile WiMAX. *IEEE Wireless Communications and Networking Conference*, pp. 3205–3209, Kowloon, China (2007)
  17. Nejatian, N.M.P., Nayebi, M.M.: Evaluating the effect of non-poisson traffic patterns on power consumption of sleep mode in the IEEE 802.16e MAC. *IFIP International Conference on Wireless and Optical Communications Networks*, pp. 1–5, Singapore (2007)
  18. Xiao, Y.: Performance analysis of an energy saving mechanism in the IEEE 802.16e wireless MAN. 3rd IEEE Consumer Communications and Networking Conference, pp. 406–410, Las Vegas, NV, USA (2006)
  19. Han, K., Choi, S.: Performance analysis of sleep mode operation in IEEE 802.16e mobile broadband wireless access systems. *IEEE 63rd Vehicular Technology Conference*, pp. 1141–1145, Melbourne, Australia (2006)
  20. Zhu, S., Wang, T.: Enhanced power efficient sleep mode operation for IEEE 802.16e based WiMAX. *IEEE Mobile WiMAX Symposium*, pp. 43–47, Orlando, FL, USA (2007)
  21. Kim, M.G., Choi, J., Kang, M.: Enhanced power-saving mechanism to maximize operational efficiency in IEEE 802.16e systems. *IEEE Trans. Wireless Commun.* 4710–4719 (2009)

# EmET: Emotion Elicitation and Emotion Transition Model

Shikha Jain and Krishna Asawa

**Abstract** Emotion is an important part of human cognition. In one or other way, emotion influences various cognition processes. For the past few decades, researchers are working for the integration of emotions and cognition. In this paper, we are proposing a model for emotion elicitation and emotion transition. The model is based upon the well known appraisal theory of emotions and targets five primary emotions. Since emotions are continuous in nature, they keep on changing either due to another event that occurred in sequence (known as emotion transition) or due to time lapse (called emotion decay). Simultaneous emotion elicitation is also supported by the model. The design of model is using concept of linguistic variables and if-then rules.

**Keywords** Computational emotional model · Emotion modeling · Emotion elicitation · Emotion transition · Emotion decay

## 1 Introduction

In recent studies, it has been shown that emotions play a significant role in human cognitive processes. An agent to be believable, should be able to percept an event, appraise it and make decisions using emotional prospect. Nowadays, research in the field of emotions is attracting the researchers. It has been acknowledged that models of emotion are very useful in the field of counseling, marketing, human assistance application, intelligent games, intelligent user interfaces, tutoring systems, etc. Moreover, in an experiment conducted by Damasio [1], he concluded that emotion

---

S. Jain (✉) · K. Asawa  
Department of Computer Science and Information Technology,  
Jaypee Institute of Information Technology, Noida, India  
e-mail: shi\_81@rediffmail.com

K. Asawa  
e-mail: krishna.asawa@jiit.ac.in

is an essential component for making decision. Person who lacks emotions cannot make small decisions. They cannot distinguish between good and bad.

There is little consensus among psychologists that how to define emotions. In literatures, several definitions exists [2–7]. According to the definition proposed by Hudlicka [4], emotion can be defined as “transient states, lasting for seconds or minutes, typically associated with well-defined triggering cues and characteristic patterns of expressions and behavior”. That means, emotions are triggered because of some event happened in the environment and it keeps on changing with time or with a change in environment.

According to the psychologist, the emotions are categorized into two categories: primary and secondary emotion. Basically, there are six primary emotions [2]: happiness, anger, fear, sadness, disgust, and surprise which clearly represent a distinct action selection. All secondary emotions [7] are derived from mixing of primary emotions.

Over the last decade, various researchers from different fields have proposed formal models that describe the processes related to emotion elicitation and transition [8, 9]. Nevertheless, current emotion models in software agents are much simpler as compared to the human emotional complexity. Although a lot of good work has been carried out in emotion recognition and emotion expression but still lots of research is going on in the field of emotional modeling.

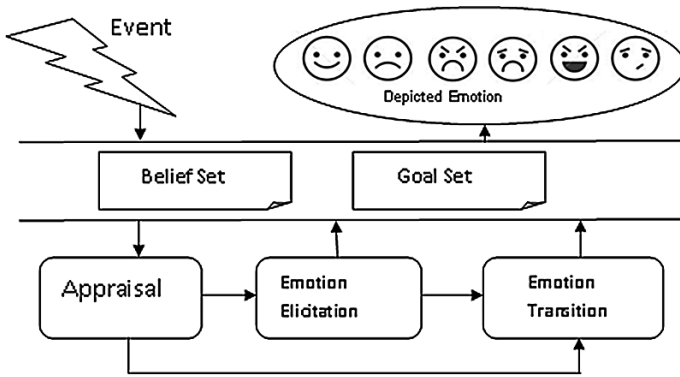
In this paper, we have proposed a domain independent emotion elicitation and emotion transition model called EmET. The model is based upon well known appraisal theories of emotions. Moreover, if no external event occurs, the intensity of emotion decays with time. EmET also allows the simultaneous occurrence of multiple emotions. This model is event based considering the visible happened event only.

Paper is organized as follows: in Sect. 2, we discussed the proposed model in detail. Section 3 shows the simulation of the model in the virtual environment inspired by real scenario. Section 4 discusses some of the existing models. Section 5 compares the proposed model with the existing models. Section 6 concludes the paper with a belief discussion on future scope.

## **2 EmET: Emotion Elicitation and Emotion Transition Model**

Whenever an event occurs, it is sensed by an intended agent to create its own view of the external world. The agent evaluates the event in terms of various parameters, for example, liking/disliking, expectedness/unexpectedness, resources available, its own capability and the goal to be achieved. Depending upon how the agent looks at the event, some emotions are triggered and the intensity values are computed. Since emotions are continuous in nature, they keep on changing either due to another event that occurred in sequence (known as emotion transition) or due to time lapse





**Fig. 1** The proposed model (EmET)

(called emotion decay). At any instance of time, a person can be in multiple emotion state; however, the intensity of one emotion affects the intensity of another emotion. An agent has its own belief set and goal set simulated in a close environment. The belief set stores the facts about objects or events in the memory. The goal set keeps the set of goals need to achieve. The goals are stored in order of priority. The model is shown in Fig. 1.

*Appraisal Variables:* The event appraisal is based upon appraisal variables selected from two appraisal theories: OCC theory [10] and Roseman’s model [11]. The appraisal variables loosely adapted from these theories are: Desirability, Expectedness, OutcomeProbability, Suddenness and CauseHarm. Desirability is associated with each event as a measure of how desirable the event is in pursuit of the goal. Expectedness is the likelihood of that event to occur. OutcomeProbability is the measure of consequences (pleasant/unpleasant) of the event with respect to the goal. If the outcome of the event is not leading us towards the goal then a value N will be assigned to it. Suddenness is if the event has occurred all of a sudden. CauseHarm is whether the current event is threatening or not to agent presently or in the future.

Emotions are uncertain in nature; hence, it is not possible to have a crisp value for emotions. To capture the imprecise and ambiguous nature, the concept of linguistic variables is used. The set of each linguistic variable is defined as:

- D = {UD, N, LowD, MediumD, HighD}
- E = {UE, N, LowE, MediumE, HighE}
- S = {low, medium, high}
- OP = {VUP, UP, N, P, VP}
- CH = {noHarm, causeHarmL, causeHarmH, willcauseHarmL, willcauseHarmH}

The event can be undesirable, low desirable, medium desirable or highly desirable. Similarly, an event can be unexpected, low expected, medium expected or highly expected. The OutcomeProbability can be very unpleasant, unpleasant, pleasant, or very pleasant. It may also possible that we have a neutral feel for an event as far as these appraisal events are concerned.

## 2.1 Emotion Elicitation

Once the event is appraised, emotions are elicited. Agents can express multiple emotions simultaneously for an event. The model targets primary emotions [2]: happy, sad, fear, surprise and anger. These emotions are treated as linguistic variables:

$$\begin{aligned} \text{Happy} &= \{\text{VHighH, HighH, MediumH, LowH, N}\} \\ \text{Sad} &= \{\text{VHighS, HighS, MediumS, LowS, N}\} \\ \text{Anger} &= \{\text{VHighA, HighA, MediumA, LowA, N}\} \\ \text{Fear} &= \{\text{VHighF, HighF, MediumF, LowF, N}\} \\ \text{Surprise(-)} &= \{\text{VHighSr(-), HighSr-, MediumSr-, LowSr-, N}\} \\ \text{Surprise(+)} &= \{\text{VHighSr(+), HighSr+, MediumSr+, LowSr+, N}\} \end{aligned}$$

If-then rules are designed to take care of nondeterministic nature of emotions. It generates the emotion type as well as their intensity (in linguistic terms). For the design of emotion elicitor, a survey was conducted with a number of people from different domains. In the survey, participants were asked to recall two most memorable events of their life, appraise the events on five appraisal variables (as mentioned earlier) and then tell the emotions generated at the time of event occurrence. Based upon OCC theory, Roseman theory and the information gathered from the survey, we concluded that the five appraisal variables selected are closely associated with five primary emotions. In conclusion, exhaustive set of generalized rules is proposed for emotion elicitation.

The generalized form of emotion elicitation fuzzy rules is defined as

$$\begin{aligned} \text{if } \langle D, E, OP, Sud, CH \rangle_{(EV\_ID, TS)} &= \langle A_1, A_2, A_3, A_4, A_5 \rangle_{(EV\_ID, TS)} \\ \text{then} \\ \langle H, S, A, F, Sur(-), Sur(+)} &\rangle_{(EV\_ID, TS)} = \langle E_1, E_2, E_3, E_4, E_5, E_6 \rangle_{(EV\_ID, TS)} \end{aligned}$$

where EV\_ID is event identifier, TS is the timestamp,  $A_{1...5}$  takes the values from the respective sets and  $E_{1...5}$  are the intensities of the elicited emotions (linguistically).

*Example* Suppose an agent is walking in a park where reptiles are expected. While going from one point to another he saw a snake lying in his path. By analyzing the resources, he found that he does not have any stick to hit the snake. So, the agent appraises the event and the following fuzzy rule is fired:

$$\begin{aligned} \text{if } \langle D, E, OP, Sud, CH \rangle_{(EV\_001A, t)} &= \langle UD, MediumE, VUP, Low, willCauseHarm \rangle_{(EV\_001A, t)} \\ \text{then} \\ \langle H, S, A, F, Sur(-), Sur(+)} &\rangle_{(EV\_001A, t)} = \langle N, MediumS, N, VHighF, N, N \rangle_{(EV\_001A, t)} \end{aligned}$$

Upon generating the emotions it updates the belief set of the agent with this information as event id, timestamp, object and elicited emotions along with their intensity.

## 2.2 Emotion Transition

Emotion transition [12] is, basically, the switching from one emotional state to another over the period of time as a series of events occur. Reference [13] has shown how the transition from happy to angry or “becoming angry” has different outcomes from its steady-state counterpart (e.g., steady-state anger, where one begins angry and stays at the same level of anger).

For the first time, it considers the current emotion as  $\langle H, S, A, F, Sur(-), Sur(+)\rangle$ . If-then rules are used to find out the intensity of generated emotions in terms of linguistic variables. Since the transition of an emotion depends upon the current cycle, it takes current emotion along with the values of appraisal variables as input and generates the next emotional state. So, at the next instance of time, the next emotional state becomes a current emotional state and starts the next iteration of the cycle.

For example, at the time  $t_i$ , *Current Emotion(agent)* is *fear* and its intensity is High then based upon the value of the appraised variable as shown below, the emotional state of the agent is changed from {*High Fear*} to {*Medium Anger and VeryHigh Sad*}.

Following examples illustrate how rules are defined linguistically:

Rule 1: *if*  $\langle H, S, A, F, Sur(-), Sur(+)\rangle_{(EV\_002A,t)} = \langle N, N, N, HighF, N, N\rangle_{(EV\_002A,t)}$  *AND*  
 $\langle D, E, OP, Sud, CH \rangle_{(EV\_002A,t)} = \langle UD, MediumE, UP, Low, cause-HarmH\rangle_{(EV\_002A,t)}$  *THEN*  
 $\langle H, S, A, F, Sur(-), Sur(+)\rangle_{(EV\_002A,t+1)} = \langle N, VhighS, MediumS, N, N, N\rangle_{(EV\_002A,t+1)}$

Rule 2: *if*  $\langle H, S, A, F, Sur(-), Sur(+)\rangle_{(EV\_003A,t)} = \langle MediumH, N, N, N, N, N\rangle_{(EV\_003A,t)}$  *AND*  
 $\langle D, E, OP, Sud, CH\rangle_{(EV\_003A,t)} = \langle MediumD, UE, UP, High, noHarm\rangle_{(EV\_003A,t)}$  *THEN*  
 $\langle H, S, A, F, Sur(-), Sur(+)\rangle_{(EV\_003A,t+1)} = \langle N, N, N, N, N, VHighS\rangle_{(EV\_003A,t+1)}$  *AND*  
 $\langle H, S, A, F, Sur(-), Sur(+)\rangle_{(EV\_003A,t+2)} = \langle N, MediumS, HighA, N, N, N\rangle_{(EV\_003A,t+2)}$

In Rule 2, Surprise is the current emotion after appraising the current event. If outcome is pleasant, the emotion at the next instance of time will be positive

otherwise some negative emotions will be generated depending upon the value of appraised variables.

After the emotion elicitation and emotion transition processes, it updates the belief set with the information as event id, timestamp, object and elicited emotions along with their intensity. If the generated emotion is positive, the object will be assigned “GOOD” tag otherwise it will be tagged as “BAD”. The object and/or events are tagged as good or bad so that whenever, in the future, some event associated with that object occurs, the agent can judge the event based upon its past experience.

### 2.3 Emotion Decay

Emotion decay refers to gradual decrease in intensity of emotion with time. According to Velasquez [14], emotions do not disappear once their cause has disappeared, but rather, they decay through time. In literatures, we can find variants of opinion about emotion decay. According to Velasquez, positive emotions decay faster than negative emotions. Following the same, the emotion decay is represented by Poisson distributions in our model. That is,

$$EI\_Dec(e, t) = EI_t(e) = EI_t - 1(e) \times \exp(-0.1 \times d(e) \times t)$$

where  $d(e) = [0.5, 1]$  for +ve emotions and  $d(e) = [0.8, 1]$  for -ve emotions.

## 3 Simulation

This system needs to work in a variety of applications to prove its advanced features; here, we have designed a prototype model for a driver on the road as a driver assisting system which works in closed environment. In this example, we create a driver agent that will assist a driver on the road. The emotion of the driver will be affected by the behavior of others on the road and by the different events.

### 3.1 Scene 1

1. Vehicle is moving with constant speed
2. At crossing, suppose it is green light
3. There is no obstacle/other vehicle nearby
4. Emotion state of driver is neutral
5. Belief Set = {Red light “BAD”; Green Light “GOOD”; Traffic Jam “BAD”; Accident “BAD”; Obstacle “BAD”}
6. Goal = {reach office safely and on time}

Initially, the current emotion of the agent is Neutral. In pursuit of the goal “reach office safely and on time”, desirability of green light is very high. Event expectedness is medium. Since traffic light is green and there is no obstacle in between, the OutcomePropability is also very pleasant. Suddenness is low and the event will not cause any harm. So the triggered rule is:

$$\begin{aligned} & \text{if } \langle D, E, OP, Sud, CH \rangle_{(EV\_004A,t)} = \langle VHighD, MediumE, VP, Low, noHarm \rangle \\ & \quad (EV\_004A,t) \text{ THEN} \\ & \langle H, S, A, F, Sur(-), Sur(+) \rangle_{(EV\_001A,t)} = \langle VhighH, N, N, N, N, N \rangle_{(EV\_001A,t)} \end{aligned}$$

### 3.2 Scene 2

1. It is in continuation of scene 1
2. Vehicle is moving with constant speed to cross the traffic light
3. At crossing, still it is green light
4. There is no obstacle/other vehicle nearby
5. But traffic counter shows that only 5 s to cross the light

Now, the current emotion state of the agent is very happy. In pursuit of the goal “reach office safely and on time”, desirability of green light is very high. Event expectedness is medium. Since, traffic counter shows that only 5 s to cross the light, the OutcomePropability becomes unpleasant. Suddenness is low and the event will not cause any harm. So, the intensity of happiness will get reduced and the agent will feel sad and fear both. The triggered rule is:

$$\begin{aligned} & \text{if } \langle H, S, A, F, Sur(-), Sur(+) \rangle_{(EV\_001A,t)} = \langle VhighH, N, N, N, N, N \rangle_{(EV\_001A,t)} \\ & \quad \text{AND} \\ & \langle D, E, OP, Sud, CH \rangle_{(EV\_004A,t+!)} = \langle VHighD, MediumE, UP, Low, noHarm \rangle \\ & \quad (EV\_004A,t+!) \text{ THEN} \\ & \langle H, S, A, F, Sur(-), Sur(+) \rangle_{(EV\_001A,t+!)} = \langle MediumH, lowS, N, HighF, N, N \rangle \\ & \quad (EV\_001A,t+!) \end{aligned}$$

The EmET model is simulated in many such scenes taken from real scenario. It is observed that the model simulates with high believability. Since we have designed exhaustive set of rules, the model is performing well in any type of given situation generated in a close loop environment.

## 4 Related Work

Several models [15–22] for emotion modeling exist in literatures. Here we have discussed a few that have significant influence. In 2000, El-Nasr et al. [17] proposed a computational and adaptive model of emotions based on event appraisal called

FLAME. It incorporates some learning components to increase the adaptation in modeling emotions. In 2003, Hudlicka [19] proposed a symbolic affective cognitive architecture MAMID that models a number of representative constructs and processes to implement many traits and states based behavioral phenomena. The theory of Emotion and Adaptation of Smith and Lazarus was formalized by Gratch and Marsella [18] in 2004 into EMA, a model to create agents that demonstrate and cope with (negative) affect. In 2008, Dang et al. [15] gave a generic model GRACE to build a computational architecture to express emotions and personality. It defines its emotional process as a physiological emotional response triggered by an internal or external event. Dastani and Meyer [16] and Steunebrink et al. [22] gave the logic representation of four primary emotions and then presented the general structure of the deliberation process for agents with emotional state. The proposal is based upon BDI theory to be incorporated into 2APL, an agent programming language. But they have talked about only emotion triggering.

## 5 Comparative Study

Table 1 summarizes the comparison of the models on some common parameters. In conclusion, we propose a model considering emotion as continuous and hence designed emotion transition module and allowed simultaneous occurrence of multiple emotions.

## 6 Conclusion and Future Work

In this paper we have proposed a domain independent emotion model for emotion generation and emotion transition (EmET). The model is based upon appraisal theories of emotions and OCC elicitation conditions. The fact that emotions are contiguous not discrete lead us to design emotion transition process. Over the

**Table 1** Comparative study

Parameters	FLAME	MAMID	EMA	EBDI	GRACE	EmET
Theory used	OCC and Roseman Th	Scherer theory	Lazarus theory	OCC and PAD	OCC, Lazarus, Scherer Th	OCC, Roseman Th
Emotion (discrete/continuous)	Discrete	Discrete	Discrete	Discrete	Continuous	Continuous
Simultaneous multiple emotion	No	No	No	No	No	Yes

period of time, the intensity of current emotion decreases gradually which is also being taken care as emotion decay. Next, the model can be extended to show the behavioral response of the agent based upon elicited emotion.

## References

1. Damasio, A.: *Descartes' Error: Emotion Reason and the Human Brain*, pp. 127–222. Grosset/ Putnam, New York (1994)
2. Ekman, P.: An argument for basic emotion. *Cogn. Emot.* **6**, 169–200 (1998)
3. Zalta, E.N. (ed.): “Emotion”, *The Stanford Encyclopedia of Philosophy* (Spring 2014 Edition), <http://plato.stanford.edu/archives/spr2014/entries/emotion/>
4. Hudlicka, E.: What are we modeling when we model emotion? In: *AAAI Spring Symposium: Emotion, Personality, and Social Behavior*, pp. 52–59 (2008)
5. Kleinginna, P., Kleinginna, A.: A categorized list of emotion definitions with suggestions for a consensual definition. *Motiv. Emot.* **5**, 345–379 (1981)
6. LeDoux, J.E.: *Emotion, Memory and the Brain*, pp. 50–57. *Scientific American*, USA (1994)
7. Plutchik, R.: *Emotion: Theory, Research, and Experience*. *Theories of Emotion*, p. 1. Academic, New York (1980)
8. Breazeal, C.: Emotion and sociable humanoid robots. *Int. J. Human Comput. Interact.* **59**, 119–155 (2003)
9. Marsella, S., Gratch, J.: EMA: a model of emotional dynamics. *Cogn. Syst. Res.* **10**(1), 70–90 (2009)
10. Ortony, A., Clore, G., Collins, A.: *The Cognitive Structure of Emotions*. Cambridge University Press, Cambridge (1998)
11. Roseman, I.J., Jose, P.E., Spindel, M.S.: Appraisals of emotion—eliciting events: testing a theory of discrete emotions. *J. Pers. Soc. Psychol.* **59**(5), 899–915 (1990)
12. Xiaolan, P., Lun, X., Xin, L. et al.: Emotional state transition model based on stimulus and personality characteristics. *China Commun.* **10**(6), 146–155 (2013)
13. Filipowicz, A., Barsade, S., Melwani, S.: Understanding emotional transitions: the interpersonal consequences of changing emotions in negotiations. *J. Pers. Soc. Psychol.* **101**, 541–556 (2011)
14. Velasquez, J.D.: Modeling emotions and other motivations in synthetic agents. In: *Proceedings of the 14th National Conference on Artificial Intelligence*, pp. 10–15 (1997)
15. Dang, T., Zarshenas, S.L., Duhaut, D.: Grace—generic robotic architecture to create emotions. In: *11th International Conference on Climbing and Walking Robots and the Suort Technologies for Mobile Machines*, Coimbra, Portugal (2008)
16. Dastani, M., Meyer, J.J.: Agents with emotions. *Int. J. Intell. Syst.* **25**(7), 636–654 (2010)
17. El-Nasr, M.S., Yen, J., Ioerger, T.R.: FLAME—a fuzzy logic adaptive model of emotions. *J. Autonomous Agents Multi-agent Syst.* **3**, 219–257 (2000)
18. Gratch, J., Marsella, S.: A domain independent frame-work for modeling emotion. *J. Cogn. Syst. Res.* **5**(4), 269–306 (2004)
19. Hudlicka, E.: Modeling effects of behavior moderators on performance. In *Proceedings of BRIMS-12*, Phoenix, AZ (2003)
20. Jiang, H.: *From rational to emotional agents*. Doctoral Thesis, University of South Carolina (2007)
21. Soleimani, A., Kobti, Z.: Toward a fuzzy approach for emotion generation dynamics based on occ emotion model. *IAENG Int. J. Comput. Sci.* **41**(1) (2014)
22. Steunebrink, B., Dastani, M., Meyer, J.J.: A formal model of emotion triggers: an approach for BDI agents. *Synthese* **185**(1), 83–129 (2012)

# Analysis on Intelligent Based Navigation and Path Finding of Autonomous Mobile Robot

Prabin Kumar Panigrahi and Hrudya Kumar Tripathy

**Abstract** Path-finding is a fundamental problem, which involves for solving a planning problem seeking optimal paths from start state to a goal state. This review paper focused on usage of Radio Frequency Identification (RFID) technology in path-finding and navigation for an autonomous mobile robot. The RFID tags (IC tags) are used for the purpose of tracing the current co-ordinate/location of the Robot. Various searching algorithms are analyzed for the purpose towards navigation of mobile robot. Different soft-computing techniques like Genetic Algorithm, Neural Network, and Fuzzy Logic are considered. This research also focused on some hybrid algorithm for path-finding and navigation of mobile robot. Different methods like cellular automata, Network Simplex Method, Complete Coverage Navigation etc. are also studied.

**Keywords** Mobile robot · Navigation · Localization · Path planning · Shortest path finding · Radio frequency identification (RFID)

## 1 Introduction

One of the first question that many people have in their mind about “Robotics” is “What is a robot”? A robot is an agent which forces the environment. Generally there are two types of robots. First one is the fixed-based robotic manipulators which don’t have any intelligence. These types of robots do not have the mobility. The second category of robots are called mobile robot [1]. A mobile robot is an automatic machine which has the capability of movement in any given environment. Mobile robots have been widely applied in the fields of path patrolling,

---

P.K. Panigrahi (✉) · H.K. Tripathy  
School of Computer Engineering, KIIT University, Patia 751024, Bhubaneswar, India  
e-mail: prabinprakash1@gmail.com

H.K. Tripathy  
e-mail: hktripathyfcs@kiit.ac.in



environmental searching, objects tracking, tour guiding or even house cleaning, etc. These type of robots are intelligent. They perform their task without any intervention of human user. Normally the fixed—base robotic manipulators are programmed to perform repetitive tasks with limited use of sensors, however mobile robots are less structured in their operation and use more sensors. In case of mobile robot the supervisor maintains the current location of the robot. Hence localization plays an important role in mobile robots.

There are various technologies available for mobile robot localization. Many authors have used Radio Frequency Identification (RFID) technology for localization. RFID uses a set of IC tags for getting the current co-ordinate of the robot through the help of antenna.

Navigation is very much essential in mobile robotics. Through navigation, the robot explores the environment. However before navigation another thing should be kept in mind is path-finding. To reach the goal, the robot has to find the shortest path from source to destination. There are various shortest path algorithms available, like BFS, A\*, Dijkstra's algorithm, VGraph algorithms etc. Only the shortest path is not sufficient. The path should be optimal also. For this many authors have used optimization technologies like fuzzy logic, neural network, genetic algorithm etc.

## **2 Discussion on Localization, Path-Finding and Navigation Techniques**

We have analyzed on different technologies and algorithms for finding a path as well as navigating the mobile robot. We have focused on the RFID technology for mobile robot localization. Searching is the fundamental criteria in mobile robot navigation. Hence we have concentrated on different searching algorithms like BFS, A\*, D\*, Dijkstra's, VGRAPH etc. for tracing out the path from source to goal in which the robot will navigate. There are various optimization techniques like Fuzzy Logic Controller (FLC), Artificial Neural Network (ANN), Genetic Algorithm (GA), Genetic Annealing Algorithm, BFO etc. are most helpful in finding the optimal path from source to destination.

One more interesting thing which was found while studying different papers is combining multiple algorithm and developing an efficient one for better result. Many authors have clubbed more than one even two algorithms to optimize the result. Some of them include GA and Fuzzy Logic, GA, Fuzzy Logic and ANN etc. In the following sections we have addressed the use of RFID technology by various authors for localizing the robot (i.e. finding the current co-ordinate position of the robot).

## ***2.1 Mobile Robot Localization Technology***

As previously stated localization plays an important role in mobile robotics. Localization means finding out the current position of the robot i.e. the (x, y) coordinates value. There are various technologies available for localization. One of the popular technology is RFID technology. A set of IC tags are arranged in the grid with equidistance. The robot is equipped with a RFID reader and an antenna which acts as the transponder. When the robot stays over an IC tag its current position is read by the reader and the location is traced out.

The Table 1 addresses the use of RFID technology by various authors in their papers.

## ***2.2 Searching Techniques***

Searching is an essential part in mobile robot navigation. Before navigation, the robot should explore the environment, means it has to search for all possible paths reachable from source to destination. After that it has to search for the shortest path from source to destination. Different shortest path algorithms are analyzed and addressed in the Tables 2 and 3.

## ***2.3 Soft-Computing Analysis***

Soft computing, an innovative approach to constructing computational intelligent systems has just come into the limelight. It is now realized that complex real-world problems require intelligent system that combine knowledge, techniques, and methodologies from various sources. There are various type of soft computing techniques analyzed here for generating an optimal path from source to destination. These techniques are addressed in the Table 4.

## ***2.4 Hybrid Technologies***

While analyzing different algorithms we found that many authors proposed combination of more than one algorithm. These hybrid algorithms found to be more effective than a single algorithm. Some of these hybrid algorithms are addressed on Table 5.

**Table 1** RFID technology

Sl. No.	Paper name	Authors	Description	Mathematical analysis
1	An improved minimum-cost path finding algorithm for mobile robot navigation [2]	Yung-Fu Hsu et al.	The RFID system acquires the location information when the antenna detects an IC tag	$x_{estimate} = (x_1 + x_2 + \dots + x_n)/n$ $y_{estimate} = (y_1 + y_2 + \dots + y_n)/n$ <p>Where n is the detected number by antenna</p> <p>Polar coordinates (r, θ) are defined in terms of Cartesian coordinates (x, y) by</p> $x = r \cos\theta, y = r \sin\theta$ $r = \sqrt{(x^2 + y^2)}, \theta = \tan^{-1}(y/x)$ <p>r: radial distance from origin  θ: counter clockwise angle from the positive X-axis</p>
2	Indoor localization for autonomous mobile robot based on passive RFID. [1]	Sunhong Park et al.	It uses RFID based localization using the concept of polar co-ordinates	$x_{current} = r \cos\theta', y_{current} = r \sin\theta'$ <p>The estimated state of the mobile robot at time k is calculated as follows</p> $\hat{p}(k) = [\hat{x}(k) \hat{y}(k)]^T$ $= [x'(k) + a(k)y'(k) + b(k)]^T$
3	A hierarchical algorithm for indoor mobile robot localization using RFID sensor fusion [3]	Byoung-Suk Choi et al.	Adopts the RFID based localization scheme for indoor mobile robot localization using the sensor fusion technique	<p>The position (P<sub>x</sub>, P<sub>y</sub>) is calculated as follows</p> $P_x = (m - 1) * SecW + (x - 1) * TraW + (TraW/2)$ $P_y = (n - 1) * SecH + (y - 1) * TraH + (TraH/2)$ <p>Where m, n, x, and y are all digits greater than 0. TraW: width of the tag, TraH: height of the tag, SecW: width of the carpet's section, SecH: height of the carpet's section</p>
4	An RFID-based position and orientation measurement system for mobile objects in intelligent environments [4]	Ali Asghar Nazari Shirehjini et al.	A robust indoor positioning system that provides 2-D positioning and orientation information for mobile objects. The system utilizes low-range passive radio frequency identification (RFID) technology	<p>The position (P<sub>x</sub>, P<sub>y</sub>) is calculated as follows</p> $P_x = (m - 1) * SecW + (x - 1) * TraW + (TraW/2)$ $P_y = (n - 1) * SecH + (y - 1) * TraH + (TraH/2)$ <p>Where m, n, x, and y are all digits greater than 0. TraW: width of the tag, TraH: height of the tag, SecW: width of the carpet's section, SecH: height of the carpet's section</p>

(continued)

**Table 1** (continued)

Sl. No.	Paper name	Authors	Description	Mathematical analysis
5	Mapping and localization with RFID technology [5]	Dirk Hihnel et al.	This paper analysis how RFID technology can be enhanced by location information	<p><math>p(x   z_{1:t}, r_{1:t})</math> be the posterior distribution over potential distribution of a RFID tag</p> <p><math>p(y l) = \sum_x p(y x, l)p(x z_{1:t}, r_{1:t})</math></p> <p>According to law of total probability, where <math>p(y   x, l)</math> corresponds to the relative sensor model and <math>l</math> is the position of the robot</p>

**Table 2** Searching algorithms (I)

Sl. No.	Paper name	Authors	Algorithm	Description
1	An improved minimum cost path finding algorithm for mobile robot navigation [2]	Yung-Fu Hsu et al.	A* algorithm	A* algorithm based on the following heuristic function for finding a path from start point to goal point, $f(n) = h(n) + g(n)$ , $g(n)$ calculates the movement cost from starting point to any point $n$ , and $h(n)$ stands for the estimated cost from any given point $n$ to the destination
2	A hierarchical algorithm for indoor mobile robot localization using RFID sensor fusion [3]	Byoung-Suk Choi et al.	Hierarchical algorithm	Discussed the concepts of global position estimation (GPE) and local environment cognition (LPE). Then the hierarchical localization algorithm is used to estimate the position of the mobile robot
3	Using interpolation to improve path planning: the field D* algorithm [6]	Dave Ferguson et al.	Field D* algorithm	Presents an interpolation based planning and re-planning algorithm for generating low-cost paths through uniform and non-uniform resolution grids. This algorithm uses a novel method for computing the path cost of each grid node $s$ given the path costs of its neighboring nodes. The path cost of a node (the cost of the cheapest path from the node to the goal) is computed as: $g(s) = \min_{s' \in nbrs(s)} [c(s, s') + g(s')]$ , where $nbrs(s)$ is the set of all neighboring nodes of $s$ , $c(s, s')$ is the cost of traversing the edge between $s$ and $s'$ , and $g(s)$ is the path cost of node $s'$
4	Roadmap-based path planning using the Voronoi diagram for a clearance-based shortest path [7]	Priyadarshi Bhattacharya et al.	Dijkstra's algorithm	This focuses the utilization of a powerful computational geometry data structure: the Voronoi diagram. First the roadmap is built after that Dijkstra's algorithm is applied to determine the shortest path in the roadmap
5	A Self localization and path planning technique for mobile robot navigation [8]	Jia-Heng Zhou et al.		The previously known map is used for path-planning. For localization of robot a laser range scanner is used which is based on the ICP registration technique. When the robot is in motion, the potential field is used for obstacle avoidance. The visibility graph is created which is mainly based on the current position of the robot for planning the path. Finally to find the shortest path from start to the goal, Dijkstra algorithm is used

**Table 3** Searching algorithms (II)

Sl. No.	Paper name	Authors	Algorithm	Description
1	Optimal path planning for mobile robot navigation [9]	Gene Eu Jan et al.	Higher geometry maze routing algorithm	The approach used in this paper is based on a higher geometry maze routing algorithm. Starting from a top view of a workspace with obstacles called free workspace which is first obtained by virtually expanding the obstacles in the image
2	An algorithm for planning collision free paths among polyhedral obstacles [10]	Tomas Lozano-Perez et al.	VGRAPH algorithm	It describes the collision avoidance algorithm ( <i>VGRAPH algorithm</i> ) for planning a safe path for a polyhedral object moving among known polyhedral objects
3	Mobile robot path planning software and hardware implementations [11]	Lucia Vacariu et al.	BFS algorithm	This is a well-known searching algorithm named BFS algorithm for finding the shortest path from initial node to goal node. This algorithm proved to be more efficient as it finds the shortest distance from source node to each node in the graph
4	Path planning of autonomous mobile robot [12]	O. Hachour	Simple path planning algorithm	The researcher focuses on a simple path planning algorithm for tracing out the path from start to goal position

**Table 4** Soft-computing technologies

Sl. No.	Paper name	Authors	Algorithm	Description
1	Neural networks based path planning and navigation of mobile robots [13]	Valeri Kroumov et al.	Neural Network based algorithm	It presents a fast algorithm for solving the path planning problem for differential drive (holonomic) robots. In general based on the potential field methods
2	An intelligent mobile robot navigation technique using RFID technology [14]	Byoung-Suk Choi et al.	Fuzzy logic controller (FLC) approach	The placement of RFID tags in the 3-D space establish the lines linking with their projections on the ground. It define the "freeways" along which the robot desired to move. It use an extensive use of FLC
3	A prospective fuzzy logic approach to knowledge-based navigation of mobile LEGO-Robot [15]	Hrudaya Ku. Tripathy et al.		Fuzzy logic computation techniques are used for the navigation of mobile robot. This paper also uses the online self-adaptation technique for <i>obstacle avoidance</i>
4	Dynamic path planning algorithm in mobile robot navigation [16]	Soh Chin Yun et al.	Genetic algorithm	In this case genetic algorithm GA is used to assist mobile robot to move, identify the obstacles in the environment, learn the environment and reach the desired goal in an unknown and unrecognized environment
5	Path navigation using computational intelligence [17]	Anupama sharma et al.	(Bacterial foregoing optimization) algorithm	A new method proposed by using BFO algorithms, path navigation is solved by using bacterial foraging optimization algorithm

**Table 5** Hybrid algorithms

Sl. No.	Paper name	Authors	Algorithms	Description
1	Hierarchical path planning approach for mobile robot navigation under the dynamic environment [18]	Zeng Bi et al.	GA + fuzzy theory + genetic annealing algorithm + hierarchical fuzzy coordinated strategy	Adopts a hybrid strategy of GA, fuzzy theory, GA annealing and hierarchical fuzzy to find a collision free optimal path for the mobile robot navigation
2	Evolutionary approach for mobile robot path planning in complex environment [19]	Amir Hosseinzadeh et al.	Hybrid neural network + genetic algorithm + local search method	This uses hybrid neural network, genetic algorithm and local search method for finding an optimal collision free path for the navigation of the mobile robot
3	Efficient path planning algorithm for mobile robot navigation with a local minima problem solving [20]	Jasmin Velagic et al.	Fuzzy logic + genetic algorithm + Dempster-Shafer evidence theory	Integrates genetic algorithm, fuzzy logic and Dempster-Shafer evidence theory for map-building, path-finding and navigation of a mobile robot. The key part is reducing the complexity
4	Path planning and navigation for autonomous mobile robot [21]	Dei-Jeung Huh et al.	Dijkstra's algorithm + fuzzy logic controller (FLC)	This detect the given path and avoid obstacles, the navigation algorithm was composed by using two fuzzy logic control. The shortest path is found by using Dijkstra's algorithm
5	Path planning and navigation for mobile robots in a hybrid sensor network without prior location information [22]	Zheng Zhang et al.	Range and cosine + IMAP algorithm	It focuses on two novel navigation algorithms for outdoor environments, which permit robots to travel from one static node to another along a planned path in the sensor field, namely the RAC and the IMAP algorithms. Using this, the robot can navigate without the help of a map, GPS or extra sensor modules, only using the received signal strength indication (RSSI) and odometry



**Table 6** Additional methods

Sl. No.	Paper name	Authors	Technologies	Description
1	A review paper of navigation and path-finding using mobile cellular automata [23]	Priyata Singhal et al.	Mobile cellular automata	Describes the methods of cellular automata (CA) for the navigation and path-finding of mobile robots. CA is a powerful methods for navigation and path-finding
2	Path planning and navigation of mobile robots in unknown environments [24]	Torvald Ersson et al.	Network simplex method	The re-planning problem is solved using the network simplex method
3	Complete coverage navigation of cleaning robots using triangular cell based map [25]	Joon Seop Oh et al.	Complete coverage navigation	It presents a novel approach for navigation of cleaning robots in an unknown workspace. For doing this, a new map representation method as well as complete coverage navigation method is proposed
4	Path planning system for a mobile robot using self-organizing map [26]	Kazuo ISHII et al.	Self-organizing map	A navigation and a position estimation algorithm based on SOM are introduced into the path planning system
5	Mobile robot navigation using circular path planning algorithm [27]	Sung-Min Han et al.	Circular path planning algorithm	It presents a circular path planning algorithm for a mobile robot using only monocular vision system. A circular path for obstacle avoidance of the mobile robot is calculated by the size and position of obstacles

### 2.5 Additional Supporting Technologies

There exists different technologies found to be more promising in generating an optimal shortest path for mobile robot. Some of these technologies are addressed in Table 6. Our analysis is on various technologies like Mobile Cellular Automata, Network Simplex Method, Complete Coverage navigation, Self-Organizing Map, Circular Path-planning algorithm etc. These are very much powerful tools which can be used for mobile robot path-planning.

## 3 Comparative Analysis

We have gone through different techniques, algorithms, tools for localizing and navigating the mobile robot. The analysis undergoes on the RFID technique for the mobile robot localization. Many searching algorithms for finding the optimal shortest path are being considered. Some other different techniques are found to be more powerful rather than exist one. Based on these studies we prepared the following comparative analysis mentioned in the Tables (7, 8 and 9) and graphs

**Table 7** Analysis on searching algorithms

Sl. No.	Algorithms	No. of papers
1	A* algorithm	2
2	D* algorithm	1
3	Dijkstra's algorithm	3
4	Maze routing approach	1
5	VGraph algorithm	1
6	BFS algorithm	1

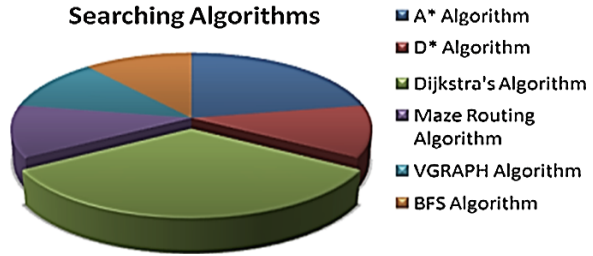
**Table 8** Analysis on optimization algorithms

Sl. No.	Algorithms	No. of papers
1	Genetic algorithm	4
2	Fuzzy logic	5
3	Neural network	2
4	BFO	1

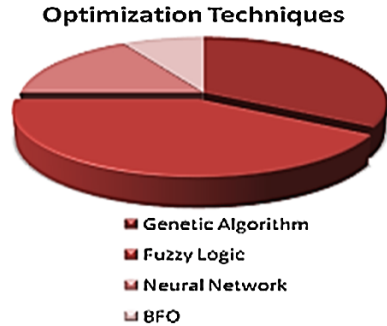
**Table 9** Analysis on supporting algorithms

Sl. No.	Algorithms	No. of papers
1	Mobile cellular automata	1
2	Network simplex method	1
3	Complete coverage navigation	1
4	SOM	1
5	Circular path planning	1

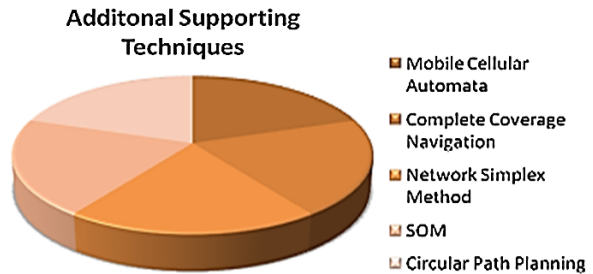
**Fig. 1** Analysis on searching algorithms



**Fig. 2** Analysis on optimization techniques



**Fig. 3** Analysis on various methods



(Figs. 1, 2 and 3) which represents the uses of different technologies and algorithms by various researchers.

From the above analysis we found that **Dijkstra's Algorithm** is used in many papers.

## 4 Conclusion

We have explored different papers on localization, path-finding and navigation of an autonomous mobile robot. Many authors have used different methods and technologies but our analysis shows that RFID technology will provide the optimal

solution for localization of the robot. Hence we are planning to use RFID system for the localization problem of robot in our future work. Also gone through many searching algorithms for path-finding. Many authors have used and suggested different soft-computing techniques for optimizing the generated path. Hence, our further research is going to implement the hybrid algorithm for path-finding of mobile robot.

## References

1. Park, S., Hashimoto, S.: Indoor localization for autonomous mobile robot based on passive RFID. In: Proceedings of the 2008 IEEE International Conference on Robotics and Biomimetics, Bangkok, Thailand, 21–26 Feb (2009)
2. Hsu, Y.-F., Huang, C.-H., Huang, W.-R., Chu, W.-C.: An improved minimum-cost path finding algorithm for mobile robot navigation. *J. Adv. Comput. Netw.* **1**(3) (2013)
3. Choi, B.-S., Lee, J.-W., Lee, J.-J., Park, K.-T.: A hierarchical algorithm for indoor mobile robot localization using RFID sensor fusion. *IEEE Trans. Ind. Electron.* **58**(6), 2226–2235 (2011)
4. Shirehjini, A.A.N., Yassine, A., Shirmohammadi, S.: An RFID-based position and orientation measurement system for mobile objects in intelligent environments. *IEEE Trans. Instrum. Meas.* **61**(6), 1664–1675 (2012)
5. Hihnel, D., Burgard, W., Fox, D., Fishkin, K., Philipose, M.: Mapping and localization with RFID technology. In: Proceedings of the 2004 IEEE International Conference on Robotics and Automation, New Orleans, LA (2004)
6. Ferguson, Dave, Stentz, Anthony: Using interpolation to improve path planning: the field D\* algorithm. *J. Field Robot.* **23**(2), 79–101 (2006)
7. Bhattacharya, P., Gavrilova, M.L.: Roadmap-based path planning using the Voronoi diagram for a clearance-based shortest path. *IEEE Robot. Autom. Mag.* **15**(2), 58–66 (2008)
8. Zhou, J.-H., Lin, H.-Y.: A self-localization and path planning technique for mobile robot navigation. In: Proceedings of the 8th World Congress on Intelligent Control and Automation 21–25 June (2011)
9. Jan, G.E., Chang, K.Y., Parberry, I.: Optimal path planning for mobile robot navigation. *IEEE/ASME Trans. Mechatron.* **13**(4), 451–460 (2008)
10. Lozano-Perez, T., Wesley, M.A.: An algorithm for planning collision-free paths among polyhedral obstacles. *Commun. ACM* **22**(10), 560–570 (1979)
11. Vacariu, L., Roman, F., Timar, M., Stanciu, T., Banabic, R., Cret, O.: Mobile robot path planning software and hardware implementations
12. Hachour, O.: Path planning of autonomous mobile robot. *Int. J. Syst. Appl. Eng. Dev.* **2**(4), 178–190 (2008)
13. Kroumov, V., Yu, J.: Neural networks based path planning and navigation of mobile robots
14. Gueaieb, W., Miah, M.S.: An intelligent mobile robot navigation technique using RFID technology. *IEEE Trans. Instrum. Meas.* **57**(9), 1908–1917 (2008)
15. Tripathy, H.K., Tripathy, B.K., Das, P.K.: A prospective fuzzy logic approach to knowledge-based navigation of mobile lego-robot. *J. Convergence Inf. Technol* **3**(1) (2008)
16. Yun, S.C., Parasuraman, S., Ganapathy, V.: Dynamic path planning algorithm in mobile robot navigation. In: IEEE Symposium on Industrial Electronics and Applications (ISIEA2011), Langkawi, Malaysia, 25–28 Sept 2011
17. Sharma, A., Satav, S.: Path navigation using computational intelligence. *Int. J. Adv. Res. Comput. Sci. Softw. Eng.* **2**(7) 2012

18. Bi, Z., Yimin, Y., Wei, Y.: Hierarchical path planning approach for mobile robot navigation under the dynamic environment
19. Hosseinzadeh, A., Izadkhah, H.: Evolutionary approach for mobile robot path planning in complex environment. *IJCSI Int. J. Comput. Sci. Issues* **7**(4), (2010) (No 8)
20. Velagic, J., Lacevic, B., Osmic, N.: Efficient path planning algorithm for mobile robot navigation with a local minima problem solving. *IEEE* (2006)
21. Huh, D.J., Park, J.H., Huh, U.Y., Kim, H.I.: Path planning and navigation for autonomous mobile robot. *IEEE* (2002)
22. Zhang, Zheng, Li, Zhenbo, Zhang, Dawei, Chen, Jiapin: Path planning and navigation for mobile robots in a hybrid sensor network without prior location information. *Int J Adv Robotic Sy* **10**(172), 2013 (2013)
23. Singhal, P., Kundra, H.: A review paper of navigation and path-finding using mobile cellular automata. *Int. J. Adv. Comput. Sci. Commun. Eng. (IJACSCE)* **2**(I) (2014)
24. Ersson, T., Hu, X.: Path planning and navigation of mobile robots in unknown environments
25. Oh, J.S., Choi, Y.H., Park, J.B., Zheng, Y.F.: Complete coverage navigation of cleaning robots using triangular-cell-based map. *IEEE Trans. Ind Electron* **51**(3), 718–726 2004
26. Ishii, K., Yano, K.: Path planning system for a mobile robot using self-organizing map. *IEEE* (2001)
27. Han, S.M., Lee, K.W.: Mobile robot navigation using circular path planning algorithm. *Int. Conf. Control Autom. Syst.* 14–17 Oct 2008 in COEX, Seoul, Korea (2008)
28. King, J., Likhachev, M.: Efficient cost computation in cost map planning for non-circular robots
29. Pearl, J.: *Heuristics: intelligent search strategies for computer problem solving*. Addison-Wesley Longman Publishing Co. (1984)
30. Barraquand, J., Latombe, J.C.: Robot motion planning: a distributed representation approach. *Int. J. Robot. Res.* **10**(6) (1991)
31. Nakamiya, M., Kishino, Y., Terada, T., Nishio, S.: A route planning method using cost map for mobile sensor nodes. *IEEE* (2007)

# Performance Analysis of Chaotic Lévy Bat Algorithm and Chaotic Cuckoo Search Algorithm for Gray Level Image Enhancement

Krishna Gopal Dhal, Md. Iqbal Quraishi and Sanjoy Das

**Abstract** Dark images can be enhanced in a controlled manner with the help of nature inspired metaheuristic algorithm. In this case image enhancement has been taken as a nonlinear optimization problem. Bat algorithm (BA) and Cuckoo Search (CS) algorithm is one of the most powerful metaheuristic algorithms. In this paper these two algorithms have been modified by chaotic sequence and lévy flight. In BA lévy flight with chaotic step size helps to do intensification. In CS algorithm the random walk has been done via chaotic sequence. Entropy and edge information has been used as objective function. From quantitative and visual analysis it is clear that chaotic lévy BA outperforms the chaotic CS algorithm.

**Keywords** Bat algorithm · Cuckoo search · Particle swarm optimization · Lévy flight · Chaotic sequence · Enhancement factor

## 1 Introduction

The objective of image enhancement is to process an image using some transformation function in such a way that the resultant image is more suitable than the given original image for some specific applications [1]. Enhancement is a pre-processing step in image processing field required for various types of images, such

---

K.G. Dhal (✉) · S. Das  
Department of Engineering and Technological Studies, University of Kalyani,  
Nadia, Kalyani, West Bengal, India  
e-mail: krishnacse42@gmail.com

S. Das  
e-mail: dassanjoy0810@hotmail.com

Md.Iqbal Quraishi  
Kalyani Government Engineering College, Department of Information Technology,  
Nadia, Kalyani, West Bengal, India  
e-mail: iqbalqu@gmail.com

as remote sensing images, medical images and also different real-life images suffering from poor contrast. Applications like contrast enhancement, noise reduction, edge enhancement and edge restoration can be done through Image Enhancement technique. In this paper, contrast enhancement of gray level dark images is taken into contemplation. Along with the gray level, color images can also be enhanced. Color images can be enhanced by separating the image into the chromaticity and intensity components [2, 3]. Histogram transformation is considered as one of the fundamental processes for contrast enhancement of gray level images [4]. Histogram equalization (HE) is a method that has no supremacy over the rate of enhancement. The controlled enhancement is done by putting constraints on the probability density function with the bin underflow and bin overflow [5]. Although based on histogram information different techniques are proposed in literature but enhancement of dark and low contrast images in a controlled manner is still an immense problem. To overcome this setback there is steady rise of soft computing oriented approaches being used nowadays. Recently nature inspired population based metaheuristics have been devised to solve optimization problems [6]. So, they can be also applied in the image processing field where some problems like image enhancement, segmentation etc. has been considered as an optimization problems [7–10]. Differential Evolution and Genetic Algorithm are stochastic and robust metaheuristics in the field of evolutionary computation and also used in image processing field to solve optimization problems [7, 8, 11]. Mutation factor and crossover rate have been modified by chaotic sequence of traditional DE algorithm and experimental result shows that modified DE is far better than traditional DE in image enhancement field with fast convergence rate and maintain also a good diversity property [11]. Swarm optimization algorithms like PSO based on social behavior of organisms such as bird flocking and fish schooling are have been widely applied in image enhancement field where some parameters are optimized [2, 3, 12, 13]. PSO outperforms the GA in image enhancement field [2, 3]. PSO has not only been used for gray scale image enhancement but also was used as a color image enhancement [3]. Newly developed another metaheuristic named ant colony optimization (ACO) is also applied in image enhancement technique and it provides better results than PSO and GA [14]. In this paper image enhancement has been taken as a non-linear optimization problem. Two new nature inspired metaheuristic algorithms are used to optimize the parameters named Bat Algorithm that based on the echolocation behavior of bats [15, 16] and Cuckoo search (CS) algorithm that motivated by the brood parasitism of some cuckoo species [17, 18]. In both algorithm lévy flight has been played a great role. It controls the diversification as well as intensification in these algorithms. But the great disadvantage of lévy flight is to choose the proper value of step size. Lévy flight with fixed step size does not show ergodicity property [19]. To remove this problem chaotic sequence has been used in both algorithms. It has been done because chaotic sequence has ergodicity property [20, 21]. Actually, chaotic sequence has been used in metaheuristic algorithms for the two purposes. One is to generate random numbers and another reason is to enhance the searching feature using chaotic search [22]. In evolutionary computation and swarm based computation chaotic sequence is used

to enhance the capability of the above said algorithms [21, 23, 24]. In this paper it is used to generate random numbers. An algorithm based on the principle of high boost filter is used where low contrast images are being enhanced. Chaotic BA and CS have been used to optimize the parameters needed for enhancement. Experimental results are showing clearly that BA outperforms the CS in terms of image enhancement.

### 1.1 Description of the Proposed Image Enhancement Algorithm

This paper enhance the dark and low contrast images, so the algorithm much depend on the method of high-boost algorithm because principal applications of high-boost filtering is when the input image is darker than desired. By varying the boost coefficient, it generally is possible to obtain an overall increase in average gray level of the image, thus helping to brighten the final result [1].

Maximum generation (MG) is 5.

Step 1 Compute  $\emptyset_1 = \alpha_1 + \left[ \alpha_2 \times \frac{(MG-t)}{MG^2} \right]$

Step 2 For all pixel find the average or mean ( $m(i,j)$ ) of its neighbourhood pixels using  $[3 \times 3]$  window

Step 3 Modify all the pixels by

$$x_1(i,j) = \emptyset_1 \times f(i,j) + (f(i,j) - m(i,j)) \times \emptyset_2 \quad (1)$$

Step 4 IF ( $f(i,j) \leq \emptyset_3$ ) then make  $f(i,j) = 0$

Step 5 While ( $t \leq MG$ ), do step 1 to step 4

From the algorithm it is clear that pixel modifier function used in step 3 is nothing more than a high-boost filter. Functionality of step 4 in this algorithm is to help to maintain a good contrast. In this algorithm there are mainly four parameters, namely  $\alpha_1, \alpha_2, \emptyset_2, \emptyset_3$ .

### 1.2 Enhancement Criterion

The necessity of objective function of optimization algorithms that used for image enhancement is to select a criterion that is associated to a fitness function which will say all about the image feature. In this paper three performance measurement parameters are taken into account. These are Entropy, sum of the edge intensity and the number of edge pixels, or edgels. It can be sure that good contrast enhanced image has more edgels and higher intensity of the edges [2]. If the allotment of the intensities is homogeneous, then histogram is equalized and the entropy of the image will be more. The objective function proposed in this paper is:



$$F(z) = \log_e^{(E(I_e))} \times (n_{edgels(I_e)} / (M \times N)) \times H(z) \tag{2}$$

$F(z)$  is the fitness value of enhanced image,  $E(I_e)$  is the sum of pixel intensities of Sobel edge image  $I_e$ .  $n_{edgels(I_e)}$  is the number of edge-pixels whose intensity value is above a threshold in the Sobel edge image. Based on the histogram, entropy value  $H(z)$  is calculated on the enhanced image  $z$ .  $M, N$  is the number of row and column of the image respectively.

### 1.3 Lévy Flight

Lévy flight has been used here as a random number generator or random walk.

A random walk is a mathematical method of representing a series of consecutive random steps. It can be expressed by the formula

$$S_N = \sum_{i=1}^N X_i \tag{3}$$

where,  $X_i$  is a random step size drawn from a random distribution and  $S_N$  is the sum of each of these consecutive random steps.

Lévy flight is a random walk whose step size is determined from the lévy distribution. It is capable of exploring large amount of search space. Lévy flight is also found in nature as certain species of birds and insects exhibit this type of motion while gathering food [25]. Lévy Flight can be produced using different algorithms which include Rejection algorithm, McCulloch’s algorithm, Mantegna’s algorithm etc. In this study Mantegna’s algorithm has been used. It produces random numbers according to a symmetric lévy stable distribution

$$\sigma = \frac{[\Gamma(1 + \alpha) \sin(\pi\alpha/2)]}{\Gamma((1 + \alpha)/2\alpha_2^{(\alpha-1)/2})]^{1/\alpha}} \tag{3}$$

where,  $\Gamma$  is the gamma function [17, 25],  $0 < \alpha \leq 2$  [25], in this study it is taken as 1.5 which is same as [17].  $\sigma$  is the standard deviation.

As per Mantegna’s algorithm the step length  $v$  can be calculated as,

$$v = \frac{x}{|y|^{1/\alpha}} \tag{4}$$

Here,  $x$  and  $y$  are taken from normal distribution and  $\sigma_x = \sigma, \sigma_y = 1$  [25]. Where  $\sigma$  is the standard deviation.

The resulting distribution has the same behavior of lévy distribution for large values of the random variables [6, 25]. Lévy flight is used for the diversification as well as intensification in stochastic optimization algorithm [17, 25]. For the

diversification the step size has been taken as large and in the case of intensification the step size is small. The repetition of the same position in its space by lévy flight is less likely than that of Brownian motion [6, 25].

### 1.4 Chaotic Sequence

It has been proved that the cooperative behavior of ants and food collection behavior of bees and birds also shows chaotic behavior [22]. The complex behavior of non-linear deterministic system is defined by chaos [20, 21]. Chaos has non-repetition property and for this it searches best solution faster than any searching strategy that depends upon the probability distribution [21]. It also has ergodicity property.

Recently, chaos combined with metaheuristic algorithms and produce good result [21, 23, 24]. Particle swarm Optimization (PSO) used it for enhance the diversification property [21]. Evolutionary optimization algorithms can enhance its capability of searching global best solution using chaotic sequences [23].

There are several chaotic generators like logistic map, tent map, gauss map, sinusoidal iterator, lozi map, chua's oscillator etc. [23]. Among those simple logistic equation that based on logistic map is used in this paper to generate mutation factor. The equation of logistic map is given below:

$$L_{m+1} = aL_m(1 - L_m) \quad (5)$$

$a$  is a control parameter and  $0 < a \leq 4$ ,  $L_m$  is the chaotic value at  $m$ th iteration. Value of  $a$  is 4 and  $L_0$  does not belong to  $\{0, 0.25, 0.5, 0.75, 1\}$  otherwise the logistic equation does not show chaotic behavior [11]. The range of  $L_m$  is transformed to  $[0, 1]$ .

### 1.5 Making of Initial Population

Initially  $n$  numbers of individuals are generated using the equation given below:

$$x_i = low + (up - low) \times \partial \quad (6)$$

$x_i$  is the  $i^{th}$  individual.  $up$  and  $low$  are the upper and lower bound of the search space of objective function.  $\partial$  is the random variable belongs to  $[0, 1]$ . If the initial solutions are generated in this way then the solutions diversely distributed [19].

## 2 Theory and Implementation of BAT Algorithm

One of the most efficient and rigid metaheuristic algorithm for solving computational problems is the BAT Algorithm. Bat algorithm was originally presented by Yang under inspiration of echolocation behavior of bats [15, 16].

### 2.1 Proposed BAT Algorithm

Bat algorithm is composed of global and local search. At first global search is done and then local search is done on those solutions which are found by global search. Local search is done randomly. On which global solution the local search have to apply chosen randomly. The algorithm is given below:

- Step 1: Objective function has been taken as per Eq. (2)
- Step 2: Initialize the population of bats,  $X = \{X_i | i = 1, 2, 3, \dots, n\}$  using Eq. (6). Where,  $\partial$  has been chosen from chaotic sequence. Where,  $n$  is the number of bats or population size
- Step 3: Initialise the Velocity ( $V$ ), Frequency ( $f$ ), Loudness ( $A$ ) and Pulse rate ( $r$ ) to each bat with the help of chaotic sequence
- Step 4: Generate new solutions by adjusting frequency using equations those are given below:

$$f_i = f_{min} + (f_{max} - f_{min}) \times \beta \quad (7)$$

$$V_i^t = w * V_i^{t-1} + (X_i^t - X_*) \times f_i \quad (8)$$

$$X_i^t = X_i^{t-1} + V_i^t \quad (9)$$

Here  $f_i$  controls the pace and range of the movement of every bat.  $X_i$  is the value of the parameter of enhanced image  $i$ ,  $X_*$  is the value of the parameter corresponding to current best enhanced image and  $f_i$  is the frequency of the bat or enhanced image  $i$ .  $w$  is the inertia weight generated using chaotic sequence.

Step 4 is solely the global search part of the algorithm

- Step 5: For selection of best solutions Probability theory is used which is explained below. According to objective function  $f(x)$  of  $X_i$ , probability value  $p_i$  is

$$p_i = \frac{fit_i}{\sum fit_i}$$

where  $fit_i$  is the fitness of the  $i$ th enhanced image and if  $p_i$  is greater than some threshold then the corresponding solution is belong to best solution

- Step 6: *if*( $rand > r_i$ ) where  $rand \in [0, 1]$   
 Select corresponding best solution  $X_i$  and create new solution using equation given below:

$$X_{new_i} = X_{old_i} + L_m \times sign(rand - 0.5) \times A_{avg} \quad (10)$$

Otherwise, remains same

Where,  $A_{avg}$  is the average loudness of all bats,  $\delta$  is a random number belongs to  $[0, 1]$

Step 6 describes the Local Search or intensification part of this algorithm

- Step 7: *if*( $rand < A_i$  &  $fit(X_i) < fit(X_*)$ )  
 Accept solution that derived at local search part,  
 Otherwise Accept solution that derived at global search part

Step 7 is the Simulated Annealing (SA) search

- Step 8: As pulse rate increases and loudness decreases when bat going to reach to its prey, So increase  $r_i$  using

$$r_{i_{new}} = r_{i_{old}} \times (1 - exp(-\alpha t)) \quad (11)$$

where,  $\alpha = 0.3$ ,  $t$  is the current iteration number. Decrease  $A_i$  using

$$\text{Decrease } A_i \text{ using } A_{i_{new}} = A_{i_{old}} \times \gamma \quad (12)$$

where,  $\gamma = 0.9$

- Step 9: Rank the bats and find the current best  $X_*$   
 Step 10: Repeat steps 4–9 equal to the maximum generation  
 Step 11: Post process and visualize the result

## 2.2 Chaotic Cuckoo Search

The aforementioned parasitic behavior among cuckoo birds refers to the aggressive and highly successful reproduction strategy of certain species of cuckoo birds based on an evolutionary predisposition to put down their eggs in the nests of the host birds [17, 18].

### 2.3 Proposed Chaotic Cuckoo Search Algorithm

So depending upon the chaotic random walk the CS algorithm is described below:

1. Objective function has been taken as per Eq. (2)
2. Initialize the population of cuckoos,  $X = \{X_i | i = 1, 2, 3, \dots, n\}$  using Eq. (6). Where  $\vartheta$  has been chosen from chaotic sequence between  $[0, 1]$   $n$  is the number of cuckoo or population size is, and  $X_i$  is the  $i$ th cuckoo.
3. Get a random cuckoo solution means enhanced image by modifying the four enhancement parameters using lévy flight technique.

$$X_i^{t+1} = X_i^t + \vartheta L_m \quad (13)$$

$\vartheta$  is inverse value of golden ratio  $(1 + \sqrt{5})/2$ ,  $L_m \in [0, 0.5]$

4. Evaluate its quality or fitness value ( $fit_i$ ) of  $X_i$
5. Choose a nest with another solution among  $n$  randomly and say this solution is  $j$ .
6. Compare the two fitness values.
7. If  $fit_i > fit_j$  then replace  $X_j$  by  $X_i$  otherwise do nothing.
8. According to fitness  $fit_i$  of each enhanced image  $X_i$  probability value  $p_i$  is

$$p_i = \frac{fit_i}{\sum fit_i}$$

9. Fraction of the worst nests which have the probability values less than some threshold contributing nothing in betterment of solution are abandoned and new solutions ( $X_l$ ) are generated using lévy flight around the abandoned solutions ( $X_k$ ).

$$\text{If } (p_i > T_h) \text{ then } X_i^{t+1} = X_i^t + \vartheta L_m$$

$L_m \in [0, 1]$  and  $T_h = L_m \in [0, 0.5]$

If  $fit_l > fit_k$  then replace  $X_k$  by  $X_l$ , otherwise do nothing.

10. Find the global best solution.
11. Processes 3–9 are repeated until the amount of iterations needed reaches the optimal maximum generation criteria.

In the proposed CS algorithm inverse golden ratio has been used with chaotic sequence. Already it has been proved that inverse value of golden ratio remains better than random fraction [19]. The proposed algorithm is also a simple algorithm with respect to the number of control parameters. Lévy flight with fixed step size does not show ergodicity property [19]. It does not search every point in the search space. But chaotic sequence has ergodicity property. So, it has been used as step size of lévy flight to give the ergodicity capability to lévy flight.











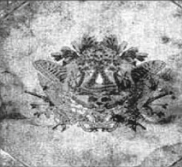

### 2.4 Parameter Selection

The Chaotic BA and CS are applied over have been applied over 100 images with initial population number being varied from 10 to 50 and maximum generations up to 100. In this study, numbers of initial populations have been put to 20, maximum generation for BA is 50, CS is 65 and PSO is 90. The result of CS, BA and PSO are very much parameter dependent. From the experiment value of the parameters are  $\alpha_1 \in [1, 2.5]$ ,  $\alpha_2 \in [0.2, 2]$ ,  $\emptyset_2 \in [0.05, 1]$  and  $\emptyset_3 \in [5, 20]$ .

### 3 Experimental Results

The Chaotic BA and CS are applied over have been applied over 100 images but three of them given below.

**Table 1** Comparison between outputs of different proposed algorithms

Image number	Input image	Image enhanced by chaotic Bat	Image enhanced by Chaotic Cuckoo Search	Image enhanced by PSO
Img 1				
Img 2				
Img 3				

**Table 2** Comparison of among quality parameters

	Image type	No. of edge pixels	Sum of intensities of edge pixels	Fitness value	Enhancement factor
Img 1	Original image	473	109.933	0.1968	
	Output of chaotic bat	3,151	1,634.1	2.6780	6.032
	Output of chaotic cuckoo	3,167	1,648.0	2.4803	5.282
	Output of PSO	3,065	1,652.60	2.4014	4.564
Img 2	Original image	1,782	632.526	1.2356	
	Output of chaotic bat	2,302	1,449.5	1.9689	6.153
	Output of chaotic cuckoo	1,940	1,142.6	1.6070	5.420
	Output of PSO	1,922	1,047.5	1.5718	3.969
Img 3	Original image	511	150.622	0.2208	
	Output of chaotic bat	2,793	1,740.6	2.4843	5.877
	Output of chaotic cuckoo	2,476	1,475.1	2.0678	5.052
	Output of PSO	2,344	1,149	1.6956	3.672

### 3.1 Quality Parameters

Enhancement factor (EF) is calculated using variance and mean of the image [26]. The equation is given below:

$$EF = \frac{\sigma_e^2 / \mu_e}{\sigma_o^2 / \mu_o} \tag{14}$$

where,  $\sigma_e^2$  = variance of the enhanced image,  $\mu_e$  = mean of the enhanced image,

$\sigma_o^2$  = variance of the original image,  $\mu_o$  = mean of the original image

(Tables 1, 2).

## 4 Conclusion

The comparison between chaotic lévy BA and chaotic CS algorithm has been done in this paper. Intensification property of BA is controlled by chaotic lévy flight. In CS algorithm chaotic random walk controls the intensification as well as diversification property. Experimental results prove that chaotic CS algorithm outperforms the PSO algorithm. So, chaotic random walk is also an efficient random walk. In this paper proposed BA outperforms the chaotic CS and PSO. This fact proves the

superiority of chaotic lévy BA over chaotic CS and PSO. These algorithms can be applied in other image processing applications and can be used in multiobjective environment.

**Acknowledgments** This research work is funded by DST-PURSE.

## References

1. Gonzalez, R.C., Woods, R.E.: Digital image processing, 2nd edn. Prentice Hall, New York (2002)
2. Gorai, A., Ghosh, A.: Gray-level image enhancement by particle swarm optimization. In: Proceedings of World Congress on Nature and Biologically Inspired Computing (2009)
3. Gorai, A., Ghosh, A.: Hue preserving color image enhancement by particle swarm optimization, pp. 563–568. IEEE, New York (2011)
4. Garg, R., Mittal, B., Garg, S.: Histogram equalization techniques for image enhancement. *Int. J. Electro. Commun. Technol.* **2**, 107–111 (2011)
5. Yang, S., Oh, J.H., Park, Y.: Contrast enhancement using histogram equalization with bin underflow and bin overflow. *ICIP* (2003)
6. Yang, X.S.: Engineering optimization: an introduction to metaheuristic applications. Wiley, Hoboken (2010)
7. Pal, S.K., Bhandari, D., Kundu, M.K.: Genetic algorithms for optimal image enhancement. *Pattern Recognit. Lett.* **15**, 261–271 (1994)
8. Hashemi, S., Kiani, S., Noroozi, N., Moghaddam, M.E.: An image contrast enhancement method based on genetic algorithm. *Pattern Recogn. Lett.* **31**, 1816–1824 (2010)
9. Yun-Fei, C., Yong-Hao, X., Wei-Yu, Y., Yong-Chang, C.: Multi-level threshold image segmentation based on PSNR using artificial bee colony algorithm. *Res. J. Appl. Sci. Eng. Technol.* **4**, 104–107 (2012)
10. Ma, M., Liang, J., Guo, M., Fan, Y., Yin, Y.: SAR image segmentation based on artificial bee colony algorithm. *Appl. Soft. Comput.* **11**, 5205–5214 (2011)
11. Coelho, L.D.S., Sauer, J.G., Rudek, M.: Differential evolution optimization combined with chaotic sequences for image contrast enhancement. *Chaos, Solitons Fractals* **42**, 522–529 (2009)
12. Braik, M., Sheta, A., Ayesh, A.: Image enhancement using particle swarm optimization. In: Proceedings of the World Congress on Engineering (2007)
13. Shanmugavadivu, P., Balasubramanian, K., Muruganandam, A.: Particle swarm optimized bi-histogram equalization for contrast enhancement and brightness preservation of images. *Vis. Comput.* (2014). doi:[10.1007/s00371-013-0863-8](https://doi.org/10.1007/s00371-013-0863-8)
14. Gupta, K., Gupta, A.: Image enhancement using ant colony optimization. *IOSR J. VLSI Signal Process.* **1**, 38 (2012)
15. Yang, X.S.: A new metaheuristic bat-inspired algorithm. *nature inspired cooperative strategies for optimization. Studies in computational intelligence*, pp. 65–74. Springer, Berlin. (2010)
16. Yang, X.S.: Bat algorithm for multi-objective optimization. *Int. J. Bio-Inspired Comput.* **3**, 267–274 (2011)
17. Yang, X. S., Deb, S.: Engineering optimisation by cuckoo search. *Int. J. Math. Model. Numer. Optim.* **1**, 330–343 (2010)
18. Yang, X.S., Deb, S.: Cuckoo search via lévy flight. In: Proceedings of World Congress on Nature and Biologically Inspired Computing (2009)
19. Jamil, M., Zepernick, H.J.: Lévy flights and global optimization. *Bio-Inspired Comput.* (2013). doi:<http://dx.doi.org/10.1016/B978-0-12-405163-8.00003-X>



20. Boccaletti, S., Grebogi, C., Lai, Y.C., Mancini, H., Maza, D.: The control of chaos: theory and applications. *Phys. Rep.* **329**,103–197 (2000)
21. Leandro, C.S., Viviana, C.M.: A novel particle swarm optimization approach using Henon map and implicit filtering local search for economic load dispatch. *Chaos, Solitons and Fractals* **39**, 510–518 (2009)
22. Sheikholeslami, R., Kaveh, A.: A survey of chaos embedded meta-heuristic algorithms. *Int. J. Optim. Civil Eng.* **3**(4), 617–633 (2013)
23. Caponetto, R., Fortuna, L., Fazzino, S., Xibilia, M.G.: Chaotic sequences to improve the performance of evolutionary algorithms. *IEEE Trans. Evolut. Comput.* **7**, 289–304 (2003)
24. Coelho, L.S., Mariani, V.C.: Use of chaotic sequences in a biologically inspired algorithm for engineering design optimization. *Expert Syst. Appl.* **34**, 1905–1913 (2008)
25. Yang, X.S.: *Nature-inspired metaheuristic algorithms*, 2nd edn. Luniver Press, United Kingdom (2010)
26. Jha, R., K., Chouhan, R.: Noise-induced contrast enhancement using stochastic resonance on singular values. *SIViP* **8**, 339–347. Springer, Berlin (2014). doi:[10.1007/s11760-012-0296-2](https://doi.org/10.1007/s11760-012-0296-2)

# Password Recovery Mechanism Based on Keystroke Dynamics

Soumen Roy, Utpal Roy and D.D. Sinha

**Abstract** Automated password recovery process includes needing the user to response a “secret question” defined as part of the user registration process. The second mechanism in use is having the user offer a “hints” during record-keeping that helps the user remember his password. Here, system may be compromise through the use of brute-force attacks, inherent system weakness or easily guessed secret questions and answers. The third mechanism is One Time Password (OTP), where personal phone or alternative user ID is needed. The fourth mechanism is our proposed, password recovery mechanism based on behavioral biometric characteristics, keystroke dynamics data. Here, users are not only identified by their secret questions answers or hints, but their typing style is also accounted for. It improves the security rank and can be used to identify the real user. In this paper, we have also suggested some future plans that also can be effectively implemented by this technique.

**Keywords** Keystroke dynamics • Password recovery mechanism • Behavioral biometrics • Computer security • Manhattan distance • Euclidean distance • Mahanobolis distance • Z score

---

S. Roy (✉) • D.D. Sinha  
Department of Computer Science and Engineering, University of Calcutta, 92 APC Road,  
Calcutta 700009, India  
e-mail: soumen.roy\_2007@yahoo.co.in

D.D. Sinha  
e-mail: devadatta.sinha@gmail.com

U. Roy  
Department of Computer and System Sciences, Visva-Bharati University, Santiniketan  
731235, India  
e-mail: roy.utpal@gmail.com

## 1 Introduction

Social networking sites, online form fill-up, E-mail ID providers are considered to have user-login mechanism (Knowledge based user authentication technique), where password recovery mechanism is one part. Among all password recovery mechanisms, “secret questions answers” and “password hints” are very popular. But if an attacker collects our personal information and check answer one after another against single question, then attacker may change the password or can get the access of the system. In order to defeat their technique in practice a higher level of security and performance together with low cost version is demanded to an accepted level of error, to be designed.

Now-a-days, Knowledge-based user authentication technique is not limited to password or PIN. Our behavioral biometric properties such as keystroke dynamics: a technology to segregate and distinguish people based on their typing rhythms, is also accounted for. Our proposed system uses personal information of clue for a password or secret question answer at the time of registration, compressing of characters as well takes into account the typing style of depressed characters entered. Here, typing style is a key issue to identify the authentic user, which is stored in the database. It will help recover the password, as strong as biometric properties which are meshed up with personal information that we are habituated to press it daily. It ensures the consistence typing style of a user.

We have collected typing style of three common passwords six times each from 15 different individuals having different age and education level using JAVA language at a fixed keyboard which laboratory made sample password database has been used to train the system. Here system records all the key press and release timing and calculates the duration of depressed characters, latency time between various down and up key sequence latencies for each sample, then found out the actual timing template by applying some statistical methods. Then some features mining mechanism like Euclidean distance, Manhattan distance are used to calculate the score. Minimum score is to be finding out and system decides the corresponding user is valid or not. Thus we can reduce the probability of brute-force or shoulder surfing attacks. The rhythm of the password as it is entered is used to improve the security level and validates the authenticity of the user rather than only Secret question answer or hints. Here, system calculates duration of depressed characters and pause duration between each subsequent characters entered. This timing parameters promise parameters like biometric characteristics that may facilitate non-intrusive, cost-effective and continuous monitoring.

Keystroke Dynamics is not new technique. Bryan and Harter first formally investigated it in 1897 as part of a study on skill gaining in telegraph operators. Spillane suggested in an IBM technical bulletin in 1975 that typing rhythms might be used for identifying the user at a keyboard. Forsen et al. [1] in 1977 conducted first round tests of whether keystroke dynamics could be used to differentiate typists. Gaines et al. [2] produced an extensive report of their investigation with seven typists into keystroke dynamics in 1980. After then, S. Bleha submitted his

Ph.D. thesis on Recognition system based on keystroke dynamics in 1988 [3]. Joyce and Gupta [4] proposed an identity authentication based on keystroke latencies in 1990. Monroe and Rubin [5] proposed keystroke dynamics as a biometric for authentication in 2000. Keystroke dynamics research has been going on for the more than thirty three years. Many methods have been proposed during that time. But all the keystroke dynamics features are not considered in any proposed system. Here, we have considered five effective factors.

Automated password recovery process includes requiring the user to answer a “secret question” defined as part of the user registration process. The second mechanism in use is having the user offer a “password hints” during record-keeping that help the user remember his password. Here, system may be compromised in an attack through the use of brute force, inherent system weakness or easily guessed secret questions and answers. The third mechanism is One Time Password (OTP), where cell phone or alternative user ID is needed.

Keystroke dynamics technique is used in our proposed system where typing style (key pressing and releasing time) will be calculated which is unique [6]. Our system takes all the key pressing and releasing timing and then calculates five timing factors; key hold time and four key latencies of some sequence of key press and release timing and stores it into the database for future purpose. In our system, we have to press any sequence of characters (good to choose some common words like name, address, E-ID, ...) as claimed string, then the system compares with the stored data and decides whether user is authenticated or not and only then the system offers new password or PIN.

## 2 Password Recovery Mechanism

Password recovery mechanism is essential technique in knowledge base user authentication technique, which mechanism provides the facilities to choose a new password once again after verification of the valid user. It is one factor technique where one factor such as “password hints” or “secrete answer” or user’s phone number or email address. But our system takes two factors one is hints or secret answer and keystroke dynamics data.

People are still unimaginable and lazy to choose strong password. Generally, we, as people pick up some words for password from relatively small dictionary which makes easy to break the password for attackers. If we choose stronger password for different access control, it is hard to remember different strong passwords for different systems. Keystroke Dynamics is a technique, which can solve this problem, where we have nothing to remember. Here typing style identifies the user [7–10].

Conventional website authentication method uses the following password recovery method.

## 2.1 Secret Question Answer Method

A System, which asks some selective secret questions to the user as a reference data obtained at the time of registration for comparing purpose in future.

## 2.2 Password Hints Method

It is a clue for password, artificially it is known to the user.

## 2.3 One Time Password (OTP)

Automatically one random password will be generated and it is sent to the user's alternative E-mail ID or Cell phone by the system. This password is valid for one time.

## 3 Keystroke Dynamics

Keystroke dynamics is a behavioral biometrics which is the technique of examining the way a user types on a keyboard and identify him/her based on his/her regular typing pattern [11]. It is the study of whether people can be well-known by their typing pattern, much like handwriting is used to identify the author of a written text.

Our typing style can be easily calculated by simple program which can calculate key pressing and releasing time of each key and then generates key-hold time and keys-latency times of all down up events [7] (Tables 1 and 2).

**Table 1** Key press and release time of fixed-text "kolkata123"

Entered key	Key press time	Key release time
k	0	109
o	172	281
l	375	484
k	609	733
a	749	889
t	1,326	1,451
a	1,482	1,623
1	1,950	2,059
2	2,169	2,278
3	2,387	2,496



## 4 Proposed System

### 4.1 Raw Data Collection

Raw data is a set of personal information and there typing style. Here all the event time will be calculated and that will be stored in the database.

List of the following information are captured when keystroke event happen.

Event	Two events are PRESS and RELEASE of key.
Key code	It is ASCII code of the entered key.
Timestamp	System calculates the time of all the key press and release event occurs. It is usually represented in millisecond (ms).

### 4.2 Data Extraction

After obtaining user's raw keystroke timing information we extracted data in different ways, taking into account the occurrence in time of specific events, number of specific event occurrence in a period of time, simultaneous occurrence of events and others. For the purpose of keystroke dynamics most used measures are user ID, password and their dwell time, flight time, overlapping of specific keys, method of error correcting, cursor navigation-specific keys, key pressure, sequenced combined keys timing (di-graph, tri-graph), typing speed, finger movement style on keyboard etc. In free text authentication fixed password may not be needed but huge data sets are required to identify the valid user.

Our system calculates all key press and release time and generates 5 timing factors (Key Hold time, Down down, up up, up down and down up key latencies) by equations defined in [7].

### 4.3 Features Selection

Some basic features are Di-graph which represents the time information of two consecutive entered keys, Tri-graph which represents the time information of three consecutive entered keys, Dwell time which refers to the key hold time, Flight time which refers to the duration time between pressing and releasing two consecutive entered keys, Error rate which is the occurrence of errors and how to resolve is also a good factor, Shift and Control key: Event of pressing shift or control key and there arrangement of pressing the event also a feature. But in our system we have taken five timing factors and one fixed common words for identifying the valid user.

### 4.4 Decision Making

The capture sample is sent to the conclusion module as soon as its score is considered. This module is answerable for comparing the match score with an identity recognition threshold, determining if the challenge score is valid or not.

Claimant’s keystroke data is presented to the system and equated to the reference stored template via some distance based algorithms. A final decision will be finished based upon the outcome of classification or matching algorithm to govern if a user is genuine or otherwise.

### 4.5 Profile Updating

Characteristics of human may change over time. So update mechanism is needed to update template after acceptable verification or identification. Sometimes, score of different algorithms differs. It would be better if we combined all scores in a single equation like mean value calculation with given weights of all scores.

#### 4.5.1 Overall System Model

Access control system can be accessed by two ways one is normal procedure another is secret question answer or hints. Our system will takes some common strings and rhythm then compares with the stored keystroke data which is generated from normal access. Flow of the control is defined in Fig. 1.

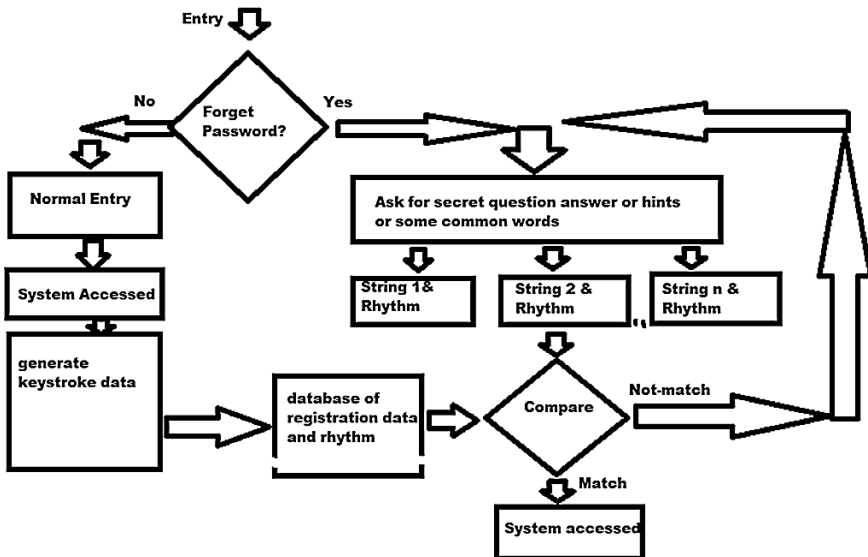


Fig. 1 Total control flow in our system



## 5 Keystroke Dynamics Algorithms

Many classification and distance based or score calculation methods have been applied in keystroke dynamics training over the last three decades [7, 12]. Following are the distance based algorithms were used to evaluate the system.

### 5.1 Manhattan Distance

Manhattan distance is one distance based method which calculates the score and minimum score will be treated as perfect match and corresponding user will be treated as a genuine user. Manhattan distance is formulated below:

$$M = \sum_{i=1}^n (|x_i - y_i|) \quad (1)$$

where  $x = (x_1, x_2, x_3, \dots, x_n)$  represents stored vector and  $y = (y_1, y_2, y_3, \dots, y_n)$  represents the claim vector of the exercise sample.

### 5.2 Manhattan with Standard Deviation Distance

The standard deviation of each feature is calculated as in Eq. 2. Here  $\alpha_i$  represents standard deviation.

$$M_s = \sum_{i=1}^n (|x_i - y_i|) / \alpha_i \quad (2)$$

### 5.3 Euclidean Distance

The score is calculated as the squared Euclidean distance between the stored vector and claim vector as in Eq. 3.

$$E = \sqrt{\sum_i^n (|x_i - y_i|)^2} \quad (3)$$

### 5.4 Mahanobolis Distance

The standard deviation of each feature is calculated, where Mahanobolis distance is presented in Eq. 4.

$$Eh = \sqrt{\sum_i^n ((x_i - y_i)/\alpha_i)^2} \tag{4}$$

### 5.5 Z Score Values

The z score is calculated in Eq. 5:

$$Z = \sum_{i=1}^n (|X_i| - \mu(|X_i|))/\alpha_i \tag{5}$$

where  $\mu(x_i)$  are mean value and  $\alpha$  is standard deviation.

## 6 Evaluation an Analysis

There are some performance measurement parameters that are used to evaluate performance of different biometric system [12].

### 6.1 False Acceptance Rate (FAR)

FAR defined by the following equation:

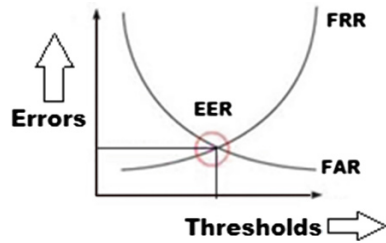
$$FAR = \frac{\text{Number of falsely accepted illegitimate users}}{\text{Total number of imposters}} \% \tag{6}$$

### 6.2 False Rejection Rate (FRR)

FRR defined by the following equation

$$FRR = \frac{\text{Number offalsely denied legitimate users}}{\text{Total number of genuine users}} \% \tag{7}$$

**Fig. 2** Equal error rate or cross error rate



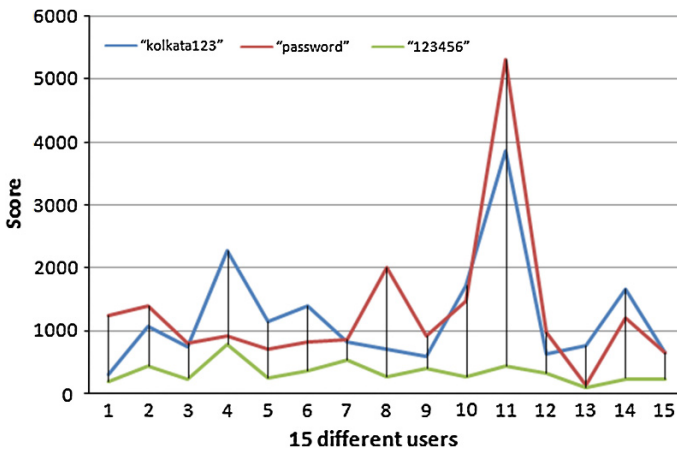
### 6.3 Equal Error Rate (EER)

ERR is the rate at which both ERR and FAR are equal. See the Fig. 2.

In our simulation program in JAVA, we have recoded each key press and release time for six sample of passwords (size of password  $\leq 10$ ) and calculated key hold time and latency time between various down and up key sequence latencies, which are shown in Fig. 3. After then we have calculated score by different algorithms with calculated mean, which are very much similar. Calculated core is defined in the Table 3.

Euclidean distances of the string “123456” of 15 users are very similar. Where “kolkata123” and “password” strings are strong to identify the user which is shown in Fig. 2.

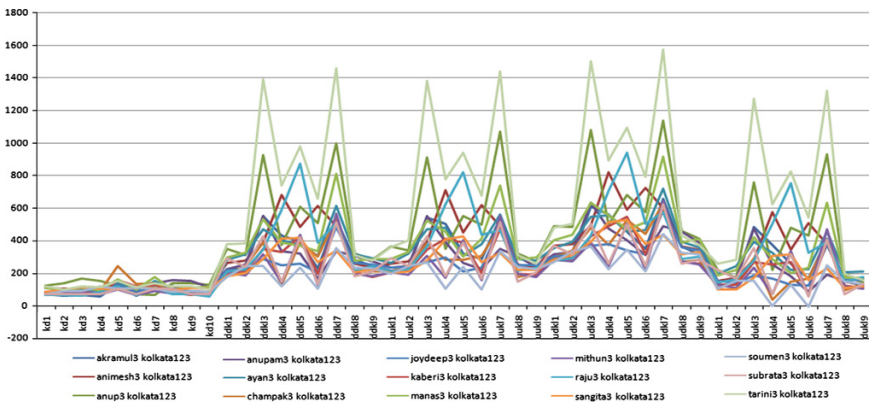
As per the experimental result, we got 0.133 % EER for the string “kolkata123” where 0.4 and 0.53 % EER for the string “password” and string “123456” separately. Size of the string and common used words are best choice to choose secrete question answer or hints where we are habituate to press this type of words daily. We have collected data from the users those are belonging to Kolkata, India, so they



**Fig. 3** Euclidean distances of different set of data for the password “kolkata123”, “password” and “123456”

**Table 3** Score calculation by different algorithms with the fixed-text “kolkata123” for 6 same sample of a user

Samples	Manhattan distance	Manhattan with Sd	Euclidean distance	Mahanabolis distance	Z score
1	758.0	39.5596	161.3877	7.4959	32.8560
2	567.0	28.9450	129.3947	5.7496	24.8224
3	412.0	25.3889	79.6618	4.8356	21.6220
4	525.0	31.8757	98.4937	5.9892	18.8801
5	637.0	36.5833	114.4596	6.3400	28.6692
6	685.0	35.4427	139.2875	6.4269	31.5871



**Fig. 4** 15 same sample of passwords “kolkata123” for 15 different users

are habituated to press string kolkata. We got the better result for the string “kolkata123” because it is a longer size string than other tested strings.

In our experiment, we have collected rhythm of 270 predefined fixed-texts from 15 users from Kolkata and seen that the user’s typing styles are dissimilar as per following line chart generated by the experimental database. Good suggestion is *choose the password what we press daily such as user ID, name, place etc.* Otherwise three factors will affect the system, finger movement time, key searching time and different keyboard (Fig. 4).

## 7 Comparison with Existing Systems

Generally we forget the secret question answer or hints for not frequently using the system. So it would be difficult to access through secret question answer or hints method. OTP would be best probable solution but in OTP, alternative e-mail is required or cell phone. It takes few times. But our system does not need any

alternative e-mail ID or cell phone and no need to remember secret question answer or hints.

Brute-force attacks or shoulder surfing attacks may happen in secret question answer or hints method. But there is no chance in OTP. In our system no one can copy our typing style even if he/she watch our typing style.

## 8 Discussion

Our simulation program, which we have written in JAVA, is working very well and gave promising result. Where all five timing factors are considered to key issue which is unique and cannot be copied or stolen by other users.

Typing style is a behavioural biometric characteristic which may change over time. Person's typing style may vary subsequently during a day or between two days. System needs updating mechanism where each record will be appended by the latest sample to the stored reference data. Size of the stored data may be increased.

Further, improvingly, keystroke dynamics depends upon mental state of the users. In that case keystroke dynamics may change to an extent. Such change yet to be improved so that system can cope with the situation.

In this technique, using different keyboards may affect the way. But if we consider bi-graph (two subsequent keys) or tri-graph (three subsequent keys) or syllable duration, this problem can be resolved or artificial keystroke by general setting [13] is the best solution or keystroke sound which is explained in [14].

If we solve this type of problems, this technique may give best possible solution, which is very easy to implement with the exiting knowledge based authentication technique.

To recognize keystroke dynamics, no extra security apparatus is needed. So this technique is cost effective and can be easily implemented with small alterations.

## 9 Conclusion

Among three password recovery mechanisms there are, secret question answer, password hints and OTP, OTP is the best but we may not have any alternative account or cell phone. In this situation keystroke dynamics is the best possible alternative solution where biometric characteristics are considered to distinguish people. It can be implemented with existing password recovery mechanism with small alterations, which enhances the security level and provides the better performance of the system. This technique can be also effectively implemented in distance-based examination, cyber criminal investigation, identifying back door account etc. But this technique, as of now, suffers from accuracy level and performance. In order to realize this technique in practice a higher level of security and

performance together with low cost version is demanded with an error to an accepted level. Hence, it is highly essential to identify the controlling parameters and optimize the accuracy, performance as well as cost with new algorithms, this is our future job.

**Acknowledgments** Authors acknowledge Mr. Champak Chakraborty, Department of Physics, Bagnan College and Mr. Sourjya Roy, Department of English, Bagnan College for reading the manuscript carefully.

## References

1. Forsen, G., Nelson, M., Raymond Staron, J.: Personal attributes authentication techniques. Technical report RADC-TR-77-333, Rome Air Development Center, Oct 1977
2. Gaines, R., Lisowski, W., Press, S., Shapiro, N.: Authentication by keystroke timing: some preliminary results. Rand Rep. R-2560-NSF, Rand Corporation, California (1980)
3. Bleha, S., Slivinsky, C., Hussien, B.: Computer-access security systems using keystroke dynamics. *IEEE Trans. Pattern Anal. Mach. Intell.* **12**, 1217–1222 (1990)
4. Joyce, R., Gupta, G.: Identity authorization based on keystroke latencies. *Commun. ACM* **33** (2), 168–176 (1990)
5. Monrose, F., Rubin, A.D.: Keystroke dynamics as a biometric for authentication. *Future Gener. Comput. Syst.* **16**(4), 351–359 (2000)
6. Killourhy, K.S.: A scientific understanding of keystroke dynamics. Ph.D. Thesis, Computer Science Department, Carnegie Mellon University, Pittsburgh (2012)
7. Roy, S., Roy, U., Sinha, D.D.: Enhanced knowledge-based user authentication technique via keystroke dynamics. *Int. J. Eng. Sci. Invention (IJESI)* **3**(9), 41–48 (2014)
8. Roy, S., Roy, U., Sinha, D.D.: Rhythmic password-based cryptosystem. In: 2nd International Conference on Computing and System, pp. 303–307. University of Burdwan, West Bengal, India (2013)
9. Roy, S., Roy, U., Sinha, D.D.: Modified knowledge-based user authentication technique. In: 7th International Conference on Mathematical Science for Advancement of Science and Technology, MSAST, vol. 2, p. 236. IMBIC, Kolkata, India (2013)
10. Roy, S., Roy, U., Sinha, D.D.: Combined user authentication technique. In: International Conference on Recent Trends in Science and Technology (ICRTST), pp. 106–113. College of Engineering and Management, Kolaghat, West Bengal, India (2013)
11. Pin, S.T., Andrew, B.J.T., Shigang, Y.: A survey of keystroke dynamics biometrics. *Sci. World J.* **2013** (2013). Article ID: 408280
12. Shima, I.H., Mazen, M.S., Hala, H.: User authentication with adaptive keystroke dynamics. *IJCSI* **10**(4) (2013)
13. Janakiraman, R., Sim, T.: Keystroke dynamics in a general setting. In: *Advances in Biometrics (ICB 2007)*. Lecture Notes in Computer Science, Seoul, Korea, vol. 4642, pp. 584–593. Springer, Berlin
14. Roth, J., Liu, X., Ross, A., Metaxas, D.: Biometric authentication via keystroke sound. *Int. Conf. Biometrics (ICB)* **1**(8), 4–7 (2013)

# Performance Analysis of RC4 and Some of Its Variants

Suman Das, Hemanta Dey and Ranjan Ghosh

**Abstract** RC4 is a simple and fast cipher, which has proved itself as robust enough and it is trusted by many organizations. But a number of researchers claimed that RC4 has some weakness and bias in its internal states. To increase its security, some guidelines recommended discarding the first  $N$  or  $2N$  bytes from the final output stream, where  $N$  is generally 256. In this paper, it has been statistically analyzed whether the outputs of the algorithm really acquire more security by discarding more number of initial bytes, like  $4N$  or  $8N$ . The original and modified algorithms are analyzed with NIST Statistical Test Suite and it has been tried to estimate an optimum quantity of output bytes to be discarded.

**Keywords** Modified RC4 · RC4 security · Stream cipher · Key stream generator · NIST test suite

## 1 Introduction

RC4 is a simple, efficient, fast and easy-to-implement stream cipher. It contains an initialization routine and a random number generator, where random values are selected from an internal state array and two elements are *swapped* in each step. Based on this table-shuffling principle, RC4 is designed for fast software and hardware implementation and widely used in many protocols, standards and commercial products. RC4 cryptanalysis has been mainly devoted to statistical analysis of the output sequence, or to the initialization weaknesses. RC4 contains a secret array of size  $N$  (generally, 256), in which integers  $(0-N-1)$  are swapped,

---

S. Das (✉)

Department of Computer Science and Engineering, University of Calcutta, Kolkata, India  
e-mail: aami.suman@gmail.com

H. Dey · R. Ghosh

Institute of Radio Physics and Electronics, University of Calcutta, Kolkata, India  
e-mail: hemantadey13@gmail.com

© Springer India 2015

J.K. Mandal et al. (eds.), *Information Systems Design and Intelligent Applications*,  
Advances in Intelligent Systems and Computing 339,  
DOI 10.1007/978-81-322-2250-7\_25

259

depending upon two index pointers  $i$  and  $j$  in a deterministic (for  $i$ ) and pseudo-random (for  $j$ ) way. There are two components of RC4: Key-Scheduling Algorithm (KSA) and Pseudo-Random Generation Algorithm (PRGA). KSA performs initializing the S-Box with random-looking permutation of values and PRGA generates the final key-stream bytes [1].

There are several works on strength and weakness of RC4, which shows that there is significant interest in the cryptographic community for it. It has been argued that there are many biases in the PRGA due to propagation of biases in the KSA. Some researchers argued that if the initial  $N$  or  $2N$  bytes from the key-stream are discarded, then these biases can be minimized, hence the security of RC4 increases.

In this paper, the authors have tried to study how the security of RC4 varies if more and more initial bytes from the key-stream are discarded. Firstly  $4N$  (here 1,024) and then  $8N$  (here, 2,048) initial bytes are discarded and the outputs are compared with the original algorithm. These variants of RC4 are analyzed statistically, following the guidelines given by NIST (National Institute of Standards and Technology), USA in their Statistical Test Suite, coded by the authors. It is found that discarding as many numbers of bytes as possible does not actually increase the security of RC4, but there is a certain optimum level, which should be maintained to get more secured outputs.

**Table A.** The RC4 Stream Cipher

<u>KSA</u>	<u>PRGA</u>
<u>Input: Secret Key <math>K</math></u>	<u>Input: S-Box <math>S</math> – The o/p of KSA</u>
for $i = 0, \dots, N - 1$	
$S[i] = i;$	$i = 0; j = 0;$
next $i$	while <i>TRUE</i>
$j = 0;$	{ $i = i + 1$
for $i = 0, \dots, N - 1$	$j = j + S[i]$
{ $j = j + S[i] + K[i]$	swap( $S[i], S[j]$ );
swap( $S[i], S[j]$ );	$z = S[S[i] + S[j]];$
}	}
next $i$	
<u>Output: S-Box <math>S</math> generated by <math>K</math></u>	<u>Output: Random Stream <math>Z</math></u>

## 2 Motivation

RC4 has gone through tremendous analysis since it has become public. Roos [2] showed some weakness in KSA and identified several classes of weak keys for RC4 with some important technical results. He showed strong correlation between the secret key bytes and the final key-stream generated. He suggested discarding *a number of bytes* from the initial key-stream.

Akgün et al. [3] detected a new bias in the KSA and proposed a new algorithm to retrieve the RC4 key in a faster way. Their framework significantly increases the



success rate of key retrieval attack. They showed that KSA leaks information about the secret key if the initial state table is known.

Maitra and Paul [4] revolved the non-uniformity in KSA and proposed for additional layers over the KSA and the PRGA. They named the modified cipher as RC4+, which avoids existing weaknesses of RC4. They presented a three-layer architecture in a scrambling phase after the initialization to remove weaknesses of KSA (KSA+). They also introduced some extra phases to improve the PRGA (PRGA+).

Mironov [5] argued that discarding the initial 12–256 bytes from the output stream of RC4 most likely eliminates the possibility of strong attacks. He estimated the number of bytes to be discarded from the initial key-stream as  $2N$  (here, 512) or  $3N$  (here, 768) to get a more safe output.

Paul and Preneel [6] described a new statistical weakness in the first two output bytes of RC4 key-stream and presented a new statistical bias in the distribution of the first two output bytes of RC4. They recommended to drop at least the initial  $2N$  bytes and argued to introduce more random variables in the PRGA to reduce the correlation between the internal and the external states. They also proposed a new key-stream generator namely RC4A with much less operations per output byte.

Tomasevic and Bojanic [7] used a strategy to favor more promising values that should be assigned to unknown entries in the RC4 table and introduced an abstraction in the form of general conditions about the current state of RC4. They proposed a new technique to improve cryptanalytic attack on RC4, which is based on new information from the tree representation of RC4.

Nawaz et al. [8] introduced a new 32-bit RC4 like faster key-stream generator with a huge internal state, which offers higher resistance against state recovery attacks. This is suitable for high speed software encryption.

Gupta et al. [9] thoroughly studied RC4 designing problem from the view point of throughput. They implemented hardware architecture to generate two key-stream bytes per clock cycle using the idea of loop unrolling and hardware pipelining.

Das et al. [10] eliminated the swap function of KSA by using a mathematical process to fill-up the internal state array of RC4, which has been found giving a better security after statistical analysis.

### 3 Proposed Modifications to RC4

Roos [1] and others strongly discussed about the weakness of KSA and weak keys in RC4. Roos argued that in KSA, only the line of swap directly affects the state table  $S$  while exchanging two elements and hence the previous line  $j = j + S[i] + K[i]$  is responsible for calculating the indexes. Here, the variable  $i$  is deterministic and  $j$  is pseudo-random. Therefore, the swap between two elements may happen once, more than once, or may not happen at all—thus brings a weakness in the KSA. He showed that there is a high probability of about 37 % for an element

not to be swapped at all. He proposed to discard some initial bytes, preferably  $N$  (here, 256), to minimize the effects of these biases.

Mironov [4] used an abstract model to estimate the number of initial bytes that should be dumped from the output stream of RC4. He identified a weakness in the KSA and the PRGA, i.e., the final key-stream of RC4, which appears up to the first  $2N$  or  $3N$  bytes. He blamed the improper *swap* function as a cause of this bias.

In this paper, the authors tried to identify what is the maximum number of bytes that should be discarded from RC4 key-stream before actual encryption starts. They concluded that the number should be more than the previously estimated ones, but it is not that discarding more and more bytes from the output stream really keeps on increasing the security of RC4. Two sets of data (RC4\_1024 and \_2048), generated by discarding  $4N$  and  $8N$  bytes respectively had been analyzed, along with data generated by the original RC4.

Outputs of these variants of RC4 have been tested statistically using the guidance of NIST, by the NIST Statistical Test Suite. For all the algorithms, a same text file has been encrypted 500 times by using 500 same encryption keys, generating 500 ciphertexts for each algorithm, each of which contains at least 1,342,500 bits, as recommended by NIST. The three sets of data are then compared to find out if security varies for these algorithms after the proposed modifications.

## 4 The NIST Statistical Test Suite

NIST developed a Statistical Test Suite, which is an excellent and exhaustive document consisting of 15 tests developed to test various aspects of randomness in binary sequences produced by cryptographic algorithms [11, 12]. The tests are as follows:

1. *Frequency (Monobit) Test*: Number of 1's and 0's in a sequence should be approximately the same, i.e., with probability  $\frac{1}{2}$ .
2. *Frequency Test within a Block*: Whether frequency of 1's in an  $M$ -bit block is approximately  $M/2$ .
3. *Runs Test*: Whether number of runs of 1's and 0's of various lengths is as expected for a random sequence.
4. *Test for Longest-Run-of-Ones in a Block*: Whether the length of the longest run of 1's within the tested sequence ( $M$ -bit blocks) is consistent with the length of the longest run of 1's as expected.
5. *Binary Matrix Rank Test*: Checks for linear dependence among fixed length sub-strings of the sequence, by finding the rank of disjoint sub-matrices of it.
6. *Discrete Fourier Transform Test*: Detects periodic features in the sequence by focusing on the peak heights in the DFT of the sequence.
7. *Non-overlapping Template Matching Test*: Occurrences of a non-periodic pattern in a sequence, using a non-overlapping  $m$ -bit sliding window.

8. *Overlapping Template Matching Test*: Occurrences of a non-periodic pattern in a sequence, using an overlapping  $m$ -bit sliding window.
9. *Maurer's Universal Statistical Test*: Whether or not the sequence can be significantly compressed without loss of information, by focusing on the number of bits between matching patterns.
10. *Linear Complexity Test*: Finds the length of a Linear Feedback Shift Register (LFSR) to generate the sequence—longer LFSRs imply better randomness.
11. *Serial Test*: Determines number of occurrences of the  $2^m$   $m$ -bit overlapping patterns across the entire sequence to find uniformity—every pattern has the same chance of appearing as of others.
12. *Approximate Entropy Test*: Compares the frequency of all possible overlapping blocks of two consecutive/adjacent lengths ( $m$  and  $m + 1$ ).
13. *Cumulative Sums Test*: Finds if the cumulative sum of a sequence is too large or small. Focuses on maximal excursion of random walks, which should be near 0.
14. *Random Excursions Test*: Finds if number of visits to a state within a cycle deviates from expected value, calculates the no. of cycles having exactly  $K$  visits in a cumulative sum random walk.
15. *Random Excursions Variant Test*: Deviations from the expected visits to various states in the random walk, calculates the number of times that a state is visited in a cumulative sum random walk.

In each test, for a bit sequence, NIST adopted different procedures to calculate the  $P$ -values (probability values) for different tests from the observed and expected values under the assumption of randomness. The Test Suite has been coded by us and used to study the randomness features of different variants of RC4.

## 5 Results and Discussions

After analyzing the outputs of the original RC4 and modified ones, using the NIST Statistical Test Suite, as described above, it has been found that though discarding some initial bytes of the key-stream increases the security of RC4, discarding more and more bytes from the outputs do not help to increase the security of RC4—at some point, *the beginning of RC4 ends* [4]. The final analysis and comparison is displayed in Table 1, where the POP (Proportion of Passing) status and Uniformity Distribution of NIST tests for these three algorithms are displayed and compared. The best values of a particular test for each algorithm are shaded (in rows) and then the numbers of shaded cells for each are counted (in columns). The highest count (here, for RC4\_1024) gives the best result, which shows that this one has a better security than the other, at least for this particular data-set.

POPs and uniformity distributions generated by RC4\_1024 and RC4\_2048 for the 15 tests, compared to the expected values [11], are displayed in Tables 2 and 3. Distributions of  $P$ -values generated by the algorithms RC4\_1024 and RC4\_2048 for the 15 tests are displayed in Tables 4 and 5. Here, the interval between 0 and 1 is

**Table 1** Comparison of POP status and uniformity distribution generated by the 15 NIST Tests for RC4 and its variants

Test↓	POP status for NIST tests			Uniformity distribution for NIST tests		
	RC4	RC4 1024	RC4 2048	RC4	RC4 1024	RC4 2048
1	0.988000	0.990000	<b>0.992000</b>	4.154218 <sup>-01</sup>	<b>8.831714<sup>-01</sup></b>	7.981391 <sup>-01</sup>
2	<b>0.992000</b>	0.988000	0.986000	4.904834 <sup>-01</sup>	1.087909 <sup>-01</sup>	<b>6.952004<sup>-01</sup></b>
3	0.992000	<b>0.996000</b>	<b>0.996000</b>	<b>8.920363<sup>-01</sup></b>	5.181061 <sup>-01</sup>	3.537331 <sup>-01</sup>
4	0.982000	<b>0.988000</b>	<b>0.988000</b>	5.790211 <sup>-01</sup>	2.343734 <sup>-01</sup>	<b>5.831447<sup>-01</sup></b>
5	0.984000	0.982000	<b>0.986000</b>	2.492839 <sup>-01</sup>	<b>2.596162<sup>-01</sup></b>	4.788391 <sup>-02</sup>
6	0.980000	0.982000	<b>0.996000</b>	<b>4.170881<sup>-02</sup></b>	1.509358 <sup>-03</sup>	4.901567 <sup>-05</sup>
7	0.990000	<b>0.996000</b>	0.995000	<b>8.272794<sup>-01</sup></b>	4.749856 <sup>-01</sup>	4.446914 <sup>-01</sup>
8	<b>0.992000</b>	<b>0.992000</b>	0.988000	2.224804 <sup>-01</sup>	<b>9.673823<sup>-01</sup></b>	9.093595 <sup>-02</sup>
9	0.982000	<b>0.992000</b>	0.990000	3.856456 <sup>-02</sup>	3.976884 <sup>-01</sup>	<b>8.343083<sup>-01</sup></b>
10	<b>0.992000</b>	0.988000	0.986000	5.462832 <sup>-01</sup>	7.034170 <sup>-01</sup>	<b>7.981391<sup>-01</sup></b>
11	0.982000	<b>0.991000</b>	0.990000	1.699807 <sup>-01</sup>	<b>5.707923<sup>-01</sup></b>	1.916867 <sup>-01</sup>
12	<b>0.992000</b>	0.990000	0.988000	2.953907 <sup>-01</sup>	<b>7.981391<sup>-01</sup></b>	6.204653 <sup>-01</sup>
13	0.995000	<b>0.998000</b>	0.995000	8.201435 <sup>-01</sup>	<b>9.705978<sup>-01</sup></b>	5.030520 <sup>-02</sup>
14	0.983500	<b>0.987500</b>	0.986000	6.729885 <sup>-02</sup>	<b>6.204653<sup>-01</sup></b>	6.291943 <sup>-02</sup>
15	0.985889	<b>0.987667</b>	0.986111	8.386675 <sup>-02</sup>	<b>5.328562<sup>-01</sup></b>	1.503405 <sup>-02</sup>
Total:	4	9	5	3	8	4

**Table 2** POP status and uniformity distribution generated for RC4\_1024

Test↓	Expected POP	Observed POP	Status	Uniformity distribution	Status
1	0.976651	0.990000	Successful	8.831714 <sup>-01</sup>	Uniform
2	0.976651	0.988000	Successful	1.087909 <sup>-01</sup>	Uniform
3	0.976651	0.996000	Successful	5.181061 <sup>-01</sup>	Uniform
4	0.976651	0.988000	Successful	2.343734 <sup>-01</sup>	Uniform
5	0.976651	0.982000	Successful	2.596162 <sup>-01</sup>	Uniform
6	0.976651	0.982000	Successful	1.509358 <sup>-03</sup>	Uniform
7	0.976651	0.996000	Successful	4.749856 <sup>-01</sup>	Uniform
8	0.976651	0.992000	Successful	9.673823 <sup>-01</sup>	Uniform
9	0.976651	0.992000	Successful	3.976884 <sup>-01</sup>	Uniform
10	0.976651	0.988000	Successful	7.034170 <sup>-01</sup>	Uniform
11	0.980561	0.991000	Successful	5.707923 <sup>-01</sup>	Uniform
12	0.976651	0.990000	Successful	7.981391 <sup>-01</sup>	Uniform
13	0.980561	0.998000	Successful	9.705978 <sup>-01</sup>	Uniform
14	0.985280	0.987500	Successful	6.204653 <sup>-01</sup>	Uniform
15	0.986854	0.987667	Successful	5.328562 <sup>-01</sup>	Uniform

**Table 3** POP status and uniformity distribution generated for RC4\_2048

Test↓	Expected POP	Observed POP	Status	Uniformity distribution	Status
1	0.976651	0.992000	Successful	$7.981391^{-01}$	Uniform
2	0.976651	0.986000	Successful	$6.952004^{-01}$	Uniform
3	0.976651	0.996000	Successful	$3.537331^{-01}$	Uniform
4	0.976651	0.988000	Successful	$5.831447^{-01}$	Uniform
5	0.976651	0.986000	Successful	$4.788391^{-02}$	Uniform
6	0.976651	0.996000	Successful	$4.901567^{-05}$	Non-uniform
7	0.976651	0.995000	Successful	$4.446914^{-01}$	Uniform
8	0.976651	0.988000	Successful	$9.093595^{-02}$	Uniform
9	0.976651	0.990000	Successful	$8.343083^{-01}$	Uniform
10	0.976651	0.986000	Successful	$7.981391^{-01}$	Uniform
11	0.980561	0.990000	Successful	$1.916867^{-01}$	Uniform
12	0.976651	0.988000	Successful	$6.204653^{-01}$	Uniform
13	0.980561	0.995000	Successful	$5.030520^{-02}$	Uniform
14	0.985280	0.986000	Successful	$6.291943^{-02}$	Uniform
15	0.986854	0.986111	Successful	$1.503405^{-02}$	Uniform

**Table 4** Distribution of *P*-values generated for RC4\_1024

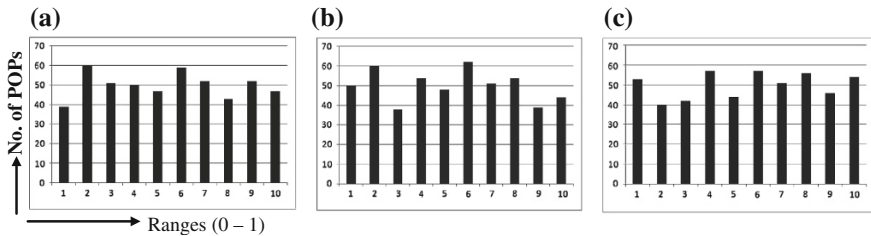
Test↓	1	2	3	4	5	6	7	8	9	10
1	48	45	44	56	50	52	59	46	47	53
2	61	56	39	51	45	44	41	47	67	49
3	51	47	55	51	54	41	43	58	59	41
4	50	60	38	54	48	62	51	54	39	44
5	52	50	51	54	59	47	41	35	62	49
6	48	60	55	26	48	41	62	68	41	51
7	42	44	59	45	57	40	57	53	54	49
8	51	51	59	50	48	43	48	48	51	51
9	41	59	58	38	51	52	53	40	52	54
10	53	47	48	49	58	39	51	44	53	58
11	88	84	97	105	106	95	100	112	102	111
12	41	42	49	53	57	46	51	56	52	53
13	114	84	91	116	93	109	84	82	100	126
14	391	416	424	414	415	393	390	391	402	364
15	902	908	973	894	880	880	907	871	830	955

divided into 10 sub-intervals, and the *P*-values that lie within each sub-interval are counted and displayed. These *P*-values should be uniformly distributed in each sub-interval [11]. Histograms on distribution of *P*-values for two tests (4 and 8) are displayed in Figs. 1a–c and 2a–c respectively.

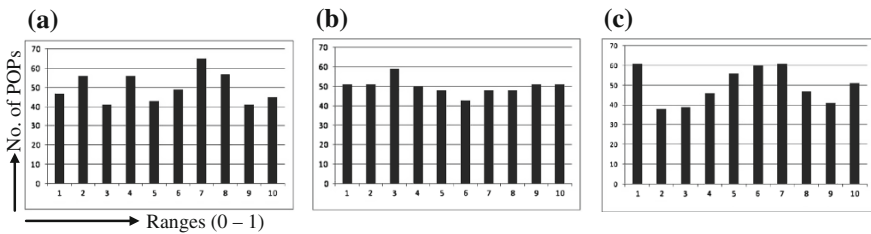
**Table 5** Distribution of *P*-values generated for RC4\_2048

Test↓	1	2	3	4	5	6	7	8	9	10
1	45	52	45	58	47	54	53	53	40	53
2	59	49	45	47	54	44	53	41	50	58
3	47	46	58	57	47	47	48	63	50	37
4	53	40	42	57	44	57	51	56	46	54
5	52	50	47	60	60	46	37	45	52	51
6	43	49	50	40	66	35	47	81	37	52
7	44	52	47	49	46	62	39	55	59	47
8	61	38	39	46	56	60	61	47	41	51
9	54	49	55	44	47	61	50	46	49	45
10	56	46	47	44	54	47	54	46	60	46
11	91	83	91	113	104	88	117	99	101	113
12	45	40	46	49	57	53	62	47	49	52
13	90	73	112	83	111	112	104	105	99	111
14	422	372	425	376	445	402	415	385	397	361
15	872	931	972	889	879	876	938	908	856	879

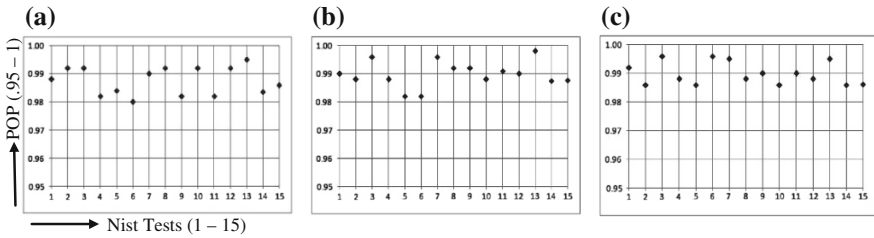
\* Horizontal ranges for Table 4: 1: 0.0–0.1, 2: >0.1–0.2, 3: >0.2–0.3, ..., 10: >0.9–1



**Fig. 1** a–c Histograms for *P*-value distribution of test 4 for RC4, RC4\_1024 and RC4\_2048



**Fig. 2** a–c Histograms for *P*-value distribution of test 8 for RC4, RC4\_1024 and RC4\_2048



**Fig. 3 a–c** Scattered graphs on POP status on 15 NIST tests for RC4, RC4\_1024 and RC4\_2048

Scattered Graphs on the POP Status for the 15 tests are displayed in Figs. 3a–c, which examine the proportion of sequences that pass a test. A threshold value (expected POP) has been calculated following the guidance given by NIST. If the proportion falls outside of (i.e., less than) this expected value, then there is evidence that the data is not random [11]. If most of the values are greater than this expected value, then the data is considered to be random. For a particular algorithm, the more number of POPs tend to 1 for the 15 tests, the more random will be the data sequence.

Finally, it has been observed that discarding so many of the initial key-stream bytes does not actually increase the security—saturation occurs after discarding a certain number of bytes. It is clear, though discarding 1,024 bytes is giving a better result than the original RC4, discarding 2,048 bytes is not that satisfactory. Here, in the current data set, after the statistical analysis, the saturation point has been found as 1,024.

## 6 Conclusion

The RC4\_1024 is found to stand in the better merit list comparing to the standard RC4 and RC4\_2048. It seems that security in RC4 will be enhanced by discarding a certain number of initial bytes (here, 1,024) from the key-stream. It has been observed that to get more secured key-stream bytes from RC4, an optimum level of discarding the initial bytes from the key-stream should be maintained—discarding as many numbers of bytes as possible does not actually increase its security. Rigorous study is required to find more optimum results in this regard.

## References

1. Stinson, D.R.: *Cryptography—Theory and Practice*. Dept. of Combinatorics & Optimization, University of Waterloo, Ontario (2002)
2. Roos, A.: A Class of Weak Keys in the RC4 Stream Cipher. Post in *sci.crypt* (1995)

3. Akgün, M., Kavak, P., Demicri, H.: New results on the key scheduling algorithm of RC4. *INDOCRYPT*, **5365**, 40–52. [http://link.springer.com/content/pdf/10.1007/978-3-540-9754-5\\_4.pdf](http://link.springer.com/content/pdf/10.1007/978-3-540-9754-5_4.pdf) (2008). (Last accessed on 2 July 2014, Lecture Notes in Computer Science, Springer)
4. Maitra, S., Paul, G.: Analysis of RC4 and proposal of additional layers for better security margin. *INDOCRYPT* **5365**, 40–52. <http://eprint.iacr.org/2008/396.pdf> (2008). (Last accessed on 2 July 2014, Lecture Notes in Computer Science, Springer)
5. Mironov, I.: (Not So) Random shuffles of RC4. In: *CRYPTO*, LNCS 2442, pp. 304–319. California (2002) (Last accessed on 18 Aug 2014)
6. Paul, S., Preneel, B.: A new weakness in the RC4 keystream generator and an approach to improve the security of the cipher. In: *FSE 2004*, LNCS, vol. 3017, pp. 245–259. Springer, Heidelberg. <http://www.iacr.org/archive/fse2004/30170244/30170244.pdf> (2004) (Last accessed on 2 July 2014)
7. Tomašević, V., Bojanić, S.: Reducing the state space of RC4 stream cipher. In: Bubak, M. et al. (eds.) *ICCS 2004*, LNCS 3036, pp. 644–647. Springer, Berlin. [http://link.springer.com/chapter/10.1007%2F978-3-540-24685-5\\_110#page-1](http://link.springer.com/chapter/10.1007%2F978-3-540-24685-5_110#page-1) (2004). (Last accessed on 2 July 2014)
8. Nawaz, Y., Gupta, K.C., Gong, G.: A 32-bit RC4-like keystream generator, *IACR Eprint archive*. <http://eprint.iacr.org/2005/175.pdf> (2005). (Last accessed on 2 July 2014)
9. Gupta, S.S., Chattopadhyay, A., Sinha, K., Maitra, S., Sinha, B.P.: High-performance hardware implementation for RC4 stream cipher. *IEEE Trans. Comput.* **82**(4) (2013) (Last accessed on 2 July 2014)
10. Das, S., Dey, H., Ghosh, R.: Comparative study of randomness of RC4 and a modified RC4. *Int. Sci. Technol. Congr. IEMCONG-2014*, 143–149 (2014)
11. National Institute of Standard & Technology (NIST), Tech. Admin., U.S. Dept. of Commerce, A Stat. Test Suite for RNGs & PRNGs for Cryptographic Applications. <http://csrc.nist.gov/publications/nistpubs800/22rec1SP800-22red1.pdf> (2010)
12. Kim, S.J., Umeno, K., Hasegawa, A.: Corrections of the NIST Statistical Test Suite for Randomness. Communications Research Lab., Inc. Admin. Agency, Tokyo (2004)



# Optimal Image Segmentation of Cancer Cell Images Using Heuristic Algorithms

A. Atchaya, J.P. Aashiha and R. Vijayarajan

**Abstract** In this world, protection of health from diseases is quite challenging. Cancer is one of the most harmful diseases which pose a major threat to human. There are two types of cancer tumours developed in human tissues namely benign and malignant. A benign tumour is a mass of cells that lacks the capacity to invade neighbouring tissue or metastasize. A malignant tumour is developed from benign tumour by the process called as tumour progression. This tumour invades neighbouring tissues rapidly and causes organs to get malfunction. In this paper, two benign and malignant images ( $512 \times 512$ ) are taken and evaluated using heuristic algorithms, such as PSO, DPSO, and FODPSO algorithms existing in the literature. The proposed segmentation procedure is executed using the conventional Otsu's between-class variance function. The performances of considered algorithms are analyzed using the popular image parameters, such as objective value, Root Mean Square Error (RMSE), and Peak Signal to Noise Ratio (PSNR), and number of iterations. Results of this study demonstrate that FODPSO offers better result compared to PSO, and DPSO algorithm.

**Keywords** Cancer cell image · Otsu · PSO · DPSO · FODPSO · Performance measure

---

A. Atchaya (✉) · J.P. Aashiha · R. Vijayarajan  
Department of Electronics and Communication Engineering,  
St. Joseph's College of Engineering, Chennai 600119, Tamil Nadu, India  
e-mail: arivaa435@gmail.com

J.P. Aashiha  
e-mail: aashiha.justin@gmail.com

R. Vijayarajan  
e-mail: viraj\_2k@yahoo.com

## 1 Introduction

In recent years, a considerable number of image segmentation methods have been proposed and executed by most of the researchers in the literature [1–3]. Among them, global thresholding is referred as the most efficient procedure for image segmentation, because of its simplicity, robustness, accuracy and competence [4]. In existing parametric thresholding procedures, the geometric constraints of the image are estimated using traditional approach. Most of the classical methods have the following limitations; (i) computational difficulty, (ii) time consuming, and (iii) the overall performance diverge based on the image quality.

The nonparametric segmentation methods such as Otsu, Kapur, and Kittler are very efficient and successful in the case of bi-level thresholding process [5]. When the number of threshold level increases, classical thresholding techniques need extra computational time. Hence, in recent years, heuristic methods based image thresholds has increased the interest of researchers [4–8].

Recent literature illustrates that, the heuristic and meta-heuristic algorithms are widely considered for the segmentation of grey and colour images [6–9]. In this paper, the Particle Swarm Optimization (PSO) algorithm and its recent advancement (DPSO, FODPSO) based methods proposed by Ghamisi et al. [6–8] is considered. The PSO based methods are initially tested on a standard colour image ( $321 \times 481$ ). Further, the PSO based methods are implemented to analyze the cancer cell images ( $512 \times 512$ ).

In human tissues, the cancer tumours developed due to abnormal process of controlled production of cells. The genetic material (DNA) of a cell start producing mutations that affects normal cell growth and division by being damaged. When this happens, sometimes these cells do not die but form a mass of tissue called a tumor. Cancer tumours are of two types namely benign and malignant a benign tumor is a mass of cells (tumor) that lacks the ability to invade neighboring tissue or metastasize. A malignant tumor is developed from benign tumor by process called as tumor progression. This tumor invades neighboring tissues rapidly and causes organs to get malfunction. The benign tumor has slower growth rate and easily curable than malignant tumor.

In this work, PSO, DPSO, and FODPSO algorithms are employed to solve bi-level and multi-level colour image segmentation problem using Otsu's between-class variance method. The parameters such as Mean Squared Error (MSE), Root Mean Squared Error (RMSE), Peak to Signal Ratio (PSNR), and the objective functions are considered as the performance measure values.

## 2 Overview of PSO Algorithms

The traditional PSO algorithm was initially developed by Kennedy and Eberhart in 1995 [10]. PSO is an evolutionary type global optimization technique developed with the inspiration of social activities in flock of birds and school of fish, and is

widely applied in various engineering problems due to its high computational efficiency. Based on the concepts similar to the PSO, recent improvements such as DPSO, FOPSO, and FODPSO [6–8, 11, 12] have been developed. In FODPSO, a group of swarms try to win using Darwin’s theory and the fractional calculus to regulate the convergence rate. Based on this principle, FODPSO enhances the performance of traditional PSO to escape from local optima by running several simultaneous parallel PSO algorithms.

In the proposed work, the heuristic algorithms with the following parameters are considered.

### 3 Methodology

In this paper, Otsu based image thresholding initially proposed in 1979 is considered to segment the colour images [13]. This method offers the optimal threshold by maximizing the between class variance function. A detailed description about this procedure can be found in the articles by Ghamisi et al. [6–8] and this procedure is defined as follows:

For a given RGB image, let there is L intensity levels in the range {0,1,2,..., L-1}. Then, it can be defined as;

$$p_i^C = \frac{h_i^c}{N} \sum_{i=0}^{L-1} p_i^C = 1 \tag{1}$$

The total mean of each component of the image is calculated as:

$$\mu_T^C = \sum_{i=0}^{L-1} ip_i^C = 1 \tag{2}$$

The m-level thresholding presents m – 1 threshold levels  $t_j^c$ , where j = 1,2,..., m – 1, and the operation is performed as;

$$F^C(x, y) = \begin{cases} 0, & f^C(x, y) \leq t_1^C \\ \frac{1}{2}(t_1^C + t_2^C), & t_1^C < f^C(x, y) \leq t_2^C \\ \vdots & \vdots \\ \frac{1}{2}(t_{m-2}^C + t_{m-1}^C), & t_{m-2}^C < f^C(x, y) \leq t_{m-1}^C \\ L - 1, & f^C(x, y) > t_{m-1}^C \end{cases} \tag{3}$$

The probabilities of occurrence  $w_j^C$  of classes  $D_i^c, \dots, D_m^c$  are given by;

$$w_j^C = \begin{cases} \sum_{i=0}^{t_j^C} p_i^C, & j = 1 \\ \sum_{i=t_{j-1}^C}^{t_j^C} +1 p_i^C, & 1 < j < m \\ \sum_{i=t_{j-1}^C}^{L-1} +1 p_i^C, & j = m \end{cases} \quad (4)$$

The mean of each class  $\mu_j^C$  can then be calculated as;

$$\mu_j^C = \begin{cases} \sum_{i=0}^{t_j^C} \frac{p_i^C}{w_j^C}, & j = 1 \\ \sum_{i=t_{j-1}^C}^{t_j^C} +1 \frac{p_i^C}{w_j^C}, & 1 < j < m \\ \sum_{i=t_{j-1}^C}^{L-1} +1 \frac{p_i^C}{w_j^C}, & j = m \end{cases} \quad (5)$$

The Otsu's between class variance of each component can be defined as;

$$\sigma_B^2 = \sum_{j=1}^m w_j^C (\mu_j^C - \mu_T^C)^2 \quad (6)$$

where  $w_j^C$  = probability of occurrence, and  $\mu_j^C$  = mean.

The m-level thresholding is reduced to an optimization problem to search for  $t_j^C$ , that maximize the objective functions of each image component C can be defined as;

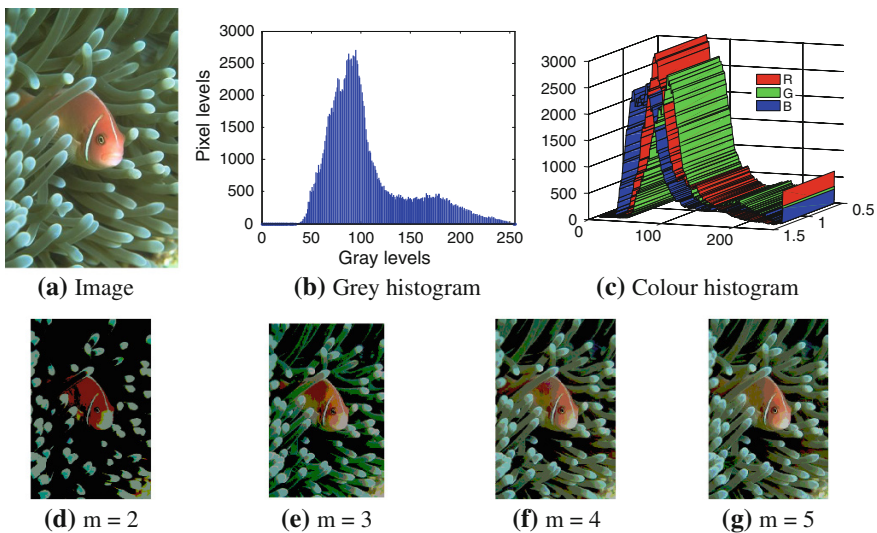
$$\phi^C = \max_{1 < t_j^C < \dots, L-1} \sigma_B^2(t_j^C) \quad (7)$$

The expression for the performance measure values considered in this paper, such as MSE, RMSE, and PSNR can be found in the recent paper by Rajinikanth et al. [4, 5].

### 4 Results and Discussions

Otsu based multi-level segmentation techniques have been implemented on five colour images. Initially, the considered PSO algorithms based method is tested on a Fish image ( $481 \times 321$ ) taken from the Berkeley Segmentation Dataset [14]. Figure 1 shows the original image, grey histogram, colour histogram, and segmented images for  $m = 2, 3, 4, 5$ . From Fig. 1b, c, it can be observed that, the mean value of the R,G,B component of the colour histogram is similar to the grey histogram. Hence, in the proposed work, we presented the optimal thresholds for the segmented colour images. Table 1 presents the performance measure values for the Fish image with PSO, DPSO, and FODPSO algorithms. From this, it is noted that, the FODPSO provides overall best value compared with the PSO and DPSO (Table 2).

The considered segmentation procedure is then used to analyze the cancer cell images ( $512 \times 512$ ) shown in Figs. 2 and 3. The segmented images with the FODPSO are presented in Table 3. Please confirm if the section headings identified are correct. The corresponding performance measure values such as MSE, RMSE, PSNR (dB), maximized objective function values, and the corresponding values are presented in Table 4 (Malignant) and Table 5 (Benign). From these tables, it is noted that, FODPSO algorithm offers better result compared with the PSO and DPSO algorithm.



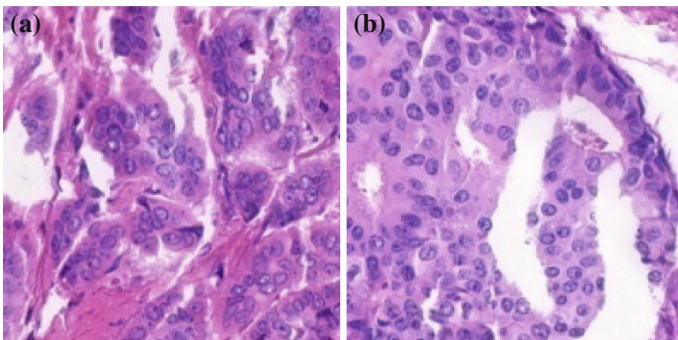
**Fig. 1** Segmented test image using FODPSO algorithm. **a** Image. **b** Grey histogram. **c** Colour histogram. **d**  $m = 2$ . **e**  $m = 3$ . **f**  $m = 4$ . **g**  $m = 5$

**Table 1** Initial parameters of heuristic algorithms

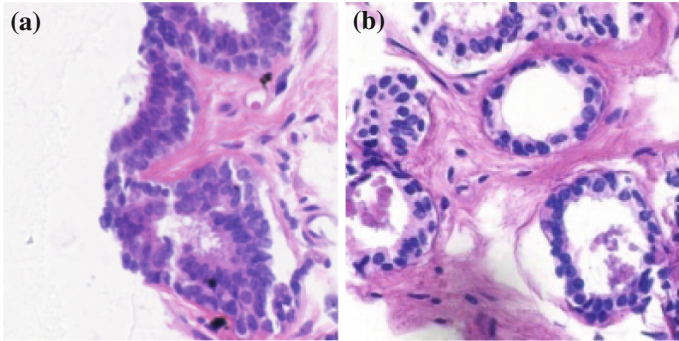
Parameter	PSO	DPSO	FODPSO
Number of iterations	500	500	500
Population	50	50	50
$\rho_1$	1.5	1.5	1.5
$\rho_2$	1.0	1.0	1.0
W	0.8	–	–
$X_{max}$	255	255	255
$X_{min}$	0	0	0
Min population	–	15	15
Max population	–	50	50
Number of swarms	–	4	4
Min swarms	–	2	2
Max swarms	–	6	6
Stagnancy	–	20	20
Fractional coefficient	–	–	0.60

**Table 2** Performance values of fish image

Method	m	MSE	PSNR	DSSIM	Objective function	Optimal threshold
PSO	2	56.1988	13.1363	0.2017	1,247.46	85, 148
	3	40.6867	15.9418	0.1937	1,294.43	72, 126, 162
	4	31.6291	18.1291	0.1725	1,314.38	61, 100, 132, 176
	5	23.4226	20.7381	0.1680	1,391.62	52, 96, 128, 144, 182
DPSO	2	55.2568	13.2831	0.1926	1,244.92	84, 150
	3	41.8543	15.6960	0.1901	1,294.84	71, 124, 164
	4	32.1652	17.9831	0.1788	1,307.72	60, 101, 134, 173
	5	23.9251	20.5537	0.1662	1,384.76	50, 94, 126, 142, 184
FODPSO	2	54.2899	13.4364	0.2085	1,253.03	82, 151
	3	40.0042	16.0887	0.1942	1,287.50	68, 125, 164
	4	31.4545	18.1771	0.1715	1,382.16	57, 104, 138, 174
	5	22.1678	21.2164	0.1635	1,405.27	50, 93, 129, 146, 183



**Fig. 2** Malignant. **a** Image 1. **b** Image 2



**Fig. 3** Benign. **a** Image 3. **b** Image 4

**Table 3** Segmented cancer cell images with FODPSO for  $m = 2-5$

		$m = 2$	$m = 3$	$m = 4$	$m = 5$
Malignant	Image 1				
	Image 2				
Benign	Image 3				
	Image 4				

**Table 4** Performance measures for Malignant cancer cell images

	Method	m	MSE	RMSE	PSNR	Objective function	Optimal threshold
Image 1	PSO	2	1.3597e+04	116.605	6.7964	1.0337e+03	158, 180
		3	5.4785e+03	74.0172	10.7442	1.0303e+03	76, 147, 185
		4	2.6952e+03	51.9153	13.8249	1.0211e+03	48, 105, 133, 191
		5	2.4634e+03	49.6322	14.2155	1.0323e+03	33, 82, 101, 168, 193
	DPSO	2	1.3957e+04	118.170	6.6898	1.0136e+03	154, 182
		3	5.7417e+03	75.7742	10.5404	1.0367e+03	71, 144, 183
		4	2.8924e+03	53.7807	13.5183	1.0673e+03	45, 102, 137, 190
		5	1.6593e+03	40.7347	15.9315	1.0726e+03	34, 85, 107, 162, 194
	FODPSO	2	1.3957e+04	118.140	6.6821	1.1563e+03	150, 184
		3	5.5672e+03	74.6138	10.6744	1.1580e+03	70, 140, 181
		4	2.8380e+03	53.2733	13.6006	1.1638e+03	42, 111, 139, 188
		5	13.601+03	36.3691	16.9161	1.1735e+03	37, 83, 102, 160, 196
Image 2	PSO	2	1.7884e+04	133.731	5.6062	1.2118e+03	94, 148
		3	5.6932e+03	75.4532	75.4532	1.2297e+03	73, 132, 168
		4	2.9181e+03	54.0198	13.4797	1.2287e+03	64, 82, 115, 173
		5	1.6374e+03	40.4644	15.9894	1.2287e+03	51, 94, 128, 159, 184
	DPSO	2	1.2791e+04	113.054	7.0622	1.3668e+03	92, 146
		3	5.9043e+03	76.8396	10.4191	1.3721e+03	70, 131, 169
		4	2.9393e+03	54.2155	13.4483	1.3826e+03	58, 79, 118, 177
		5	1.4580e+03	38.1832	16.4934	1.4023e+03	47, 90, 122, 155, 185
	FODPSO	2	1.2791e+04	123.011	7.0661	1.3827e+03	88, 144
		3	5.9394e+03	77.0673	10.3934	1.4037e+03	67, 136, 166
		4	3.0789e+03	55.4874	13.2469	1.4129e+03	55, 78, 114, 179
		5	1.1083e+03	33.2918	17.6840	1.4141e+03	45, 94, 126, 157, 188



**Table 5** Performance measures for Benign cancer cell images

	Method	m	MSE	RMSE	PSNR	Objective function	Optimal threshold
Image 3	PSO	2	1.3769e+04	117.339	6.7419	1.4421e+03	116, 178
		3	4.1773e+03	64.6322	11.9218	1.4571e+03	89, 144, 193
		4	2.1560e+03	46.4323	14.7944	1.4626e+03	80, 124, 168, 205
		5	2.5163e+03	50.1625	14.1232	1.4640e+03	68, 112, 141, 174, 208
	DPSO	2	9.0604e+03	95.1861	8.5593	1.4376e+03	106, 181
		3	4.2983e+03	65.5618	11.7978	1.4831e+03	82, 147, 190
		4	2.3048e+03	48.0085	14.5044	1.4825e+03	77, 121, 164, 198
		5	1.0024e+03	31.6604	18.1205	1.4903e+03	62, 110, 137, 170, 203
	FODPSO	2	9.0604e+03	95.1861	8.5593	1.4402e+03	111, 178
		3	4.2872e+03	65.4770	11.8090	1.4903e+03	81, 142, 188
		4	2.1691e+03	46.5734	14.7680	1.4926e+03	74, 120, 163, 196
		5	1.1797e+03	34.3474	17.4129	1.4928e+03	60, 115, 138, 175, 205
Image 4	PSO	2	9.0016e+03	94.8769	8.5876	2.4470e+03	86, 166
		3	4.4884e+03	66.9955	11.6099	2.4475e+03	62, 138, 171
		4	2.2276e+03	47.1975	14.6524	2.4488e+03	56, 89, 137, 183
		5	968.4223	31.1195	18.2702	2.4632e+03	46, 76, 150, 177, 203
	DPSO	2	9.6796e+03	98.3851	8.2722	2.4730e+03	82, 168
		3	4.5923e+03	67.7665	11.5105	2.4782e+03	58, 136, 173
		4	2.2276e+03	47.1975	14.6524	2.4802e+03	50, 84, 142, 180
		5	988.0451	31.4332	18.1830	2.4841e+03	48, 73, 156, 172, 191
	FODPSO	2	9.6796e+03	98.3851	8.2722	2.4712e+03	80, 172
		3	4.5923e+03	67.7665	11.5105	2.4501e+03	56, 134, 176
		4	2.2961e+03	47.9174	14.5209	2.4517e+03	48, 81, 147, 183
		5	1.0053e+03	31.7068	18.1077	2.4526e+03	45, 767, 152, 174, 194

## 5 Conclusions

In this paper, an attempt is made to solve the multi-level image segmentation problem using the heuristic algorithms, such as PSO, DPSO, and FODPSO. Maximization of Otsu’s between class variance function is chosen as the objective

function. In order to evaluate the performance of considered heuristic algorithms, five colour test images are examined. This study confirms that, FODPSO offers better performance measure values compared to PSO and DPSO algorithms considered in this study.

## References

1. Lee, S.U., Chung, S.Y., Park, R.H: A comparative performance study techniques for segmentation. *Comput. Vis. Graph. Image Process.* **52**(2), 171–190 (1990)
2. Pal, N.R., Pal, S.K: A review on image segmentation techniques. *Pattern Recogn.* **26**(9), 1277–1294 (1993)
3. Sezgin, M., Sankar, B.: Survey over image thresholding techniques and quantitative performance evaluation. *J. Electron. Imaging* **13**(1), 146–165 (2004)
4. Rajinikanth, V., Aashiha, J.P., Atchaya, A.: Gray-level histogram based multilevel threshold selection with bat algorithm. *Int. J. Comput. Appl.* **93**(16), 1–8 (2014)
5. Rajinikanth, V., Sri Madhava Raja, N., Latha, K.: Optimal multilevel image thresholding: an analysis with PSO and BFO algorithms. *Aust. J. Basic Appl. Sci.* **8**(9), 443–454 (2014)
6. Ghamisi, P., Couceiro, M.S., Benediktsson, J.A.: Extending the fractional order Darwinian particle swarm optimization to segmentation of hyperspectral images. In: *Proceedings SPIE 8537—image signal process. Remote Sens. XVIII*, 85730F, 8 Nov 2012
7. Ghamisi, P., Couceiro, M.S., Benediktsson, J.A., Ferreira, N.M.F.: An efficient method for segmentation of images based on fractional calculus and natural selection. *Expert Syst. Appl.* **39**(16), 12407–12417 (2012)
8. Ghamisi, P., Couceiro, M.S., Martins, F.M.L., Benediktsson, J.A.: Multilevel image segmentation based on fractional-order Darwinian particle swarm optimization. *IEEE Trans. Geosci. Remote Sens.* **52**(5), 2382–2394 (2014)
9. Sarkar, S., Das, S.: Multilevel image thresholding based on 2D histogram and maximum Tsallis entropy—a differential evolution approach. *IEEE Trans. Image Process.* **22**(12), 4788–4797 (2013)
10. Kennedy, J., Eberhart, R.C: Particle swarm optimization. In: *Proceedings of IEEE International Conference on Neural Networks*, pp. 1942–1948 (1995). doi: [10.1109/ICNN.1995.488968](https://doi.org/10.1109/ICNN.1995.488968)
11. Couceiro, M.S., Ferreira, N.M.F., Machado, J.A.T.: Application of fractional algorithms in the control of a robotic bird. *J. Commun. Nonlinear Sci. Numer. Simul. (Special Issue)* **15**(4):895–910 (2010)
12. Couceiro, M.S., Rocha, R.P., Ferreira, N.M.F., Machado, J.A.T.: Introducing the fractional-order Darwinian PSO. *SIViP* **6**(3), 343–350 (2012)
13. Otsu, N: A threshold selection method from gray-level histograms. *IEEE Trans. Syst. Man Cyber.* **9**(1):62–66 (1979)
14. Martin, D., Fowlkes, C., Tal, D., Malik, J.: A database of human segmented natural images and its application to evaluating segmentation algorithms and measuring ecological statistics, in: *Proceedings 8th International Conference on Computer Vision*, vol. 2, pp. 416–423 (2001)

# Improvement of Data Integrity and Data Dynamics for Data Storage Security in Cloud Computing

Poonam M. Pardeshi and Bharat Tidke

**Abstract** Cloud stands today as an emerging standard, however, data outsourcing paradigm is main security concern in cloud. To make sure that the data stored on the cloud is safe, frequent data integrity checking is imperative. This work considers the problem of data integrity in cloud storage and makes use of Dynamic Merkle Hash Tree (DMHT) along with AES and SHA-1 algorithms to solve the same. RSA algorithm has been used by many previously developed systems; the proposed work makes use of AES which leads to performance improvement. The work also makes use of the concept of Third Party Auditor (TPA) to achieve Public Auditing. In case of corruption of data or data loss, the proposed work promises to recover the lost data with the help of a backup system. In order to support dynamic data operations, the Merkle Tree is made dynamic by making use of relative index. Further, to save the communication bandwidth and cost, block level recovery is made instead of recovery of entire file. On comparison with previous systems, the proposed system shows reduction in server computation time. The proposed work thus aims at improving and maintaining data integrity at untrusted server, supports dynamic data operations and makes recovery possible by providing a recovery system.

**Keywords** Advanced encryption standard · Cloud computing · Data dynamics · Merkle hash tree · Public auditability · Recovery system · Secured hash algorithm, third party auditor

---

P.M. Pardeshi (✉) · B. Tidke  
Department of Computer Engineering, Flora Institute of Technology,  
University of Pune, Pune, Maharashtra, India  
e-mail: ppardeshi31@gmail.com

B. Tidke  
e-mail: batidke@gmail.com

## 1 Introduction

Cloud computing has become an emerging and highly appealing trend due to its innumerable benefits. With its massively large storage centers, low cost, high scalability, flexibility in access points and less client system resources utilization, it has successfully diverted many clients towards it. This increase in the number of cloud users along with their sensitive data renders the data outsourcing paradigm in cloud as security demanding area. The dilemma becomes graver when the question arises for the security of confidential data. If the server or Cloud Service Provider (CSP) is untrusted, client may lose important data [1–14, 15–18]. For example, less frequently accessed data can be deleted by server to save storage space on cloud, for personal benefits server may try to hide data errors at the time of Byzantine failures. The cloud thus has many security concerns related to its storage [2–8, 12–14]. Previously, much work has been done on improving the storage security in cloud by verifying the data integrity. All of these works fall under either Private Auditing or Public Auditing. In Private Auditing only client has the right to verify its own data [5, 6] whereas in Public Auditing client can delegate the authority of data verification to a third party on its behalf [4, 9, 11, 13–15, 18]. This third party is referred as a Third Party Auditor (TPA). This paper focuses on improving the data integrity by using DMHT, AES and SHA-1 algorithms. In proposed system, server is assumed to be an untrusted entity, so, the data to be stored on it is encrypted priori using AES-128 algorithm. If the key size of AES is increased from 128 to 192, power and time consumption increases by 8 % and an increase of 16 % is caused by 256 bits key [19, 20], hence, AES-128 has been used in the proposed work both for signing the root of the DMHT and data encryption. The work also assures data availability and recoverability at the time of unpleasant situations at the server such as a server crash in which integrity of data is lost, by providing a backup and recovery system. DMHT has been used to make dynamic operations possible.

## 2 Background Theory

### 2.1 *Third Party Auditor (TPA)*

The TPA is an entity which is equipped with capabilities, knowledge, expertise and skills that client does not possess. It works on behalf of client and is externally allotted by client itself to verify integrity of its data. In other words, it reduces the overhead of client and client no longer needs to do the job of verification on its own.

Cloud Storage Architecture:

Figure 1 shows cloud storage architecture. It has three network entities viz. client, CSP and TPA present in it. Client stores data on cloud server, CSP is the service provider where data is stored and TPA is responsible for auditing the stored data.

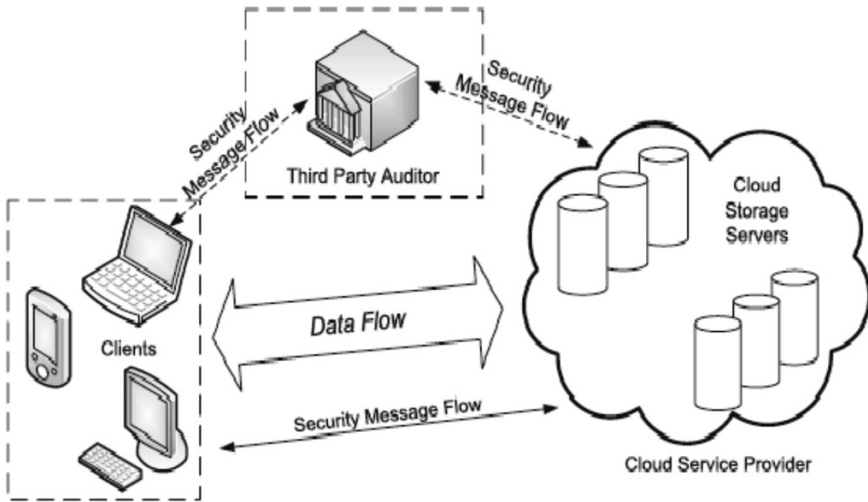


Fig. 1 Cloud storage architecture [1]

## 2.2 Merkle Hash Tree (MHT) and Dynamic Merkle Hash Tree (DMHT)

A Merkle Hash Tree is a used widely for authentication of file blocks by cryptographic structures. Its use greatly reduces server computation time [13]. Its construction takes place in similar fashion as a normal binary tree. However, in this paper, we make use of a DMHT instead of a simple MHT to make dynamic data operations possible. Each node of a DMHT has two auxiliary information viz. a hash value and a relative index unlike a static MHT whose leaf nodes has only hash value [11]. Relative index is a term used for extra data filed carried by each node of DMHT, which is used to indicate number of leaf nodes in the subtree of a node. An example of a MHT is shown in Fig. 2, to make it dynamic, we make use of relative index. So, if there exists a node 'R' with 'a' as left child and 'b' as right child then the information carried by node 'a' will be (ha, na), node 'b' will be (hb, nb) and relative index of root 'R' will be  $nr = na + nb$ . In Fig. 2, relative index of node 'a' is 2, 'b' is also 2 and that of 'r' is 4. To present this concept more clearly, we represent a DMHT in Fig. 3.

**Organization.** Section 3 presents a survey on various systems developed for providing storage security in cloud. Section 4 describes proposed model along with implementation details. Section 5 shows performance analysis and Sect. 6 provides conclusion and future work.

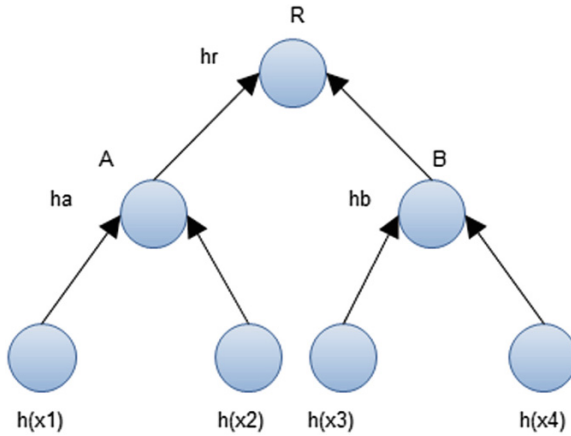


Fig. 2 Merkle hash tree

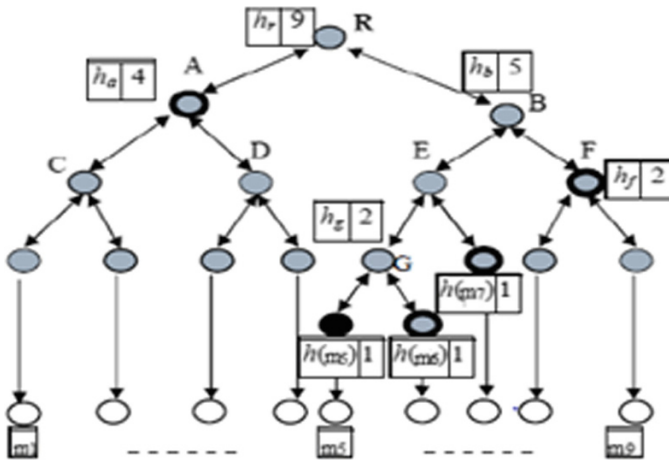


Fig. 3 A dynamic Merkle hash tree [11]

### 3 Literature Review

A lot of work has been done in the storage security area of cloud out of which most work has focused on integrity verification of data stored in cloud. Deswarte et al. [1], makes use of RSA based hash function for file verification. Client can generate multiple challenges using same metadata in this scheme. The computational complexity at the server adds to the limitation of this scheme. A technique proposed by Schwarz and Miller [3] makes use of algebraic signature. In this, a function is used to fingerprint the file block. The computation complexity at client and server side takes place at the cost of linear combination of file blocks, also there are issues related to the security of this

**Table 1** Comparison between different systems

Scheme	Ref. no. attributes					
	[4] G. Ateniese et al	[5] A. Juels et al	[6] G. Ateniese et al	[9] C. Wang et al	[20] S. Zhong et al	Proposed system (AESSS)
Privacy preserving	No	Yes	No	No	Yes	Yes
Unbound No. of queries	Yes	No	No	Yes	Yes	Yes
Public verifiability	Yes	No	No	Yes	Yes	Yes
Use of TPA	No	No	No	Yes	No	Yes
Recoverability	No	Yes	No	No	No	Yes
Dynamic operations	No	No	Yes	Yes	Yes	Yes
Untrusted server	Yes	Yes	Yes	Yes	Yes	Yes

scheme. Ateniese [4] were the first who considered Public Auditing for ensuring possession of files at untrusted servers. The Provable Data Possession (PDP) model supports large data sets in widely-distributed storage systems and is provably-secure for remote data checking. This scheme imposes an overhead of generating metadata on client and provides no support for dynamic auditing. Juels [5], “Proofs of Retrievability” (POR), focuses on static archival of large files. Spot checking and error correcting codes are used in this scheme to ensure data possession and retrievability. Drawback: it cannot be used for public databases and is suitable only for confidential data. Dynamic updation is not possible because of the sentinel nodes, public auditing is not supported by the scheme. Scalable and Efficient Provable Data Possession (S-PDP and E-PDP) protocols [6] makes contribution to the work of Ateniese [4]. It is dynamic version of PDP scheme and relies only on efficient symmetric-key operations. It makes use of less storage space by reducing the size of challenge and response blocks and uses less bandwidth. Shortcomings: number of queries that can be answered are fixed priori, partially dynamic scheme as block insertion is not supported. The scheme proposed by Erway et al. [8] is a dynamic auditing protocol which supports public auditing. It supports data dynamics via general data operation such as block insertion, deletion and block modification. However, the scheme may leak data content to the auditor as it needs linear combination of file blocks to be sent to the auditor for verification. Also, the efficiency of this scheme is not clear. Table 1 shows comparison of different existing systems with proposed one.

## 4 Proposed Work

### Design

Figure 4 represents data flow diagram of AES based Storage Security System which has three network entities viz. client-who stores data on cloud, CSP-generates the proof for data stored in it and TPA-an entity that performs proof verification. Backup server serves the purpose of file recovery.

Notations:  $E_{sk}$ —Secret key encryption,  $F$ —File stored at untrusted cloud server,  $x$ —File block,  $T$ —Tag (signature),  $\Phi$ —Set of tags

### 4.1 The Security Model

The proposed storage security model has two phases: The setup phase and the Integrity verification phase.

#### 4.1.1 The Setup Phase

In this phase, client generates a file  $F = \{x_1, x_2, \dots, x_n\}$  which is a collection on  $n$  number of file blocks. The setup phase has five steps. In first step, for each file block, a signature is generated using secret key, given as  $T_i = E_{sk}(H(x_i))$ , where  $x_i$  is the  $i$ th block of file. In second step all the signatures are collected together to make a signature set called set of tags, represented as  $\Phi = \{T_i\}$ . Then DMHT is constructed and root of tree is signed using secret key as  $sig_{sk}(H(R))$ . In last step, client advertises  $\{F, \Phi, sig_{sk}(H(R))\}$  to the server and deletes  $F$  and  $Sig_{sk}(H(R))$  from local storage Fig. 5.

#### 4.1.2 Integrity Verification Phase

The integrity verification process, in Fig. 6, is initiated by client by sending an auditing request consisting of some metadata such as  $FileId$  and  $ClientId$ , to TPA for a particular file. The TPA then generates a challenge and sends it to the server, for which the server generates a proof. The proof contains the root and signature of the DMHT generated for that particular file. The proof is then sent to the TPA which performs integrity verification. Proof verification is done in two stages; firstly signature of the root is checked for file authentication. For this, the output is true if the signature matches with the one stored during file upload, otherwise false. If true, then the value of the root is checked. If the value of the root is same as that stored

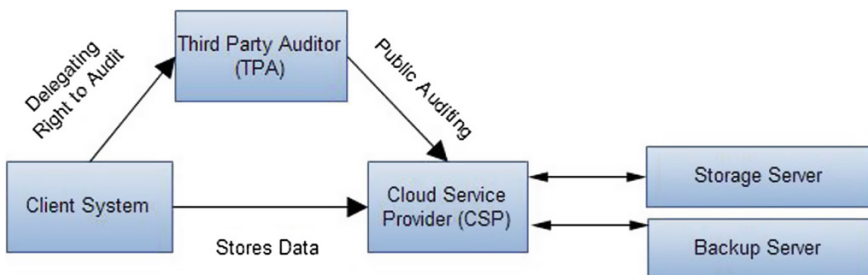


Fig. 4 Data flow in AES based storage security system



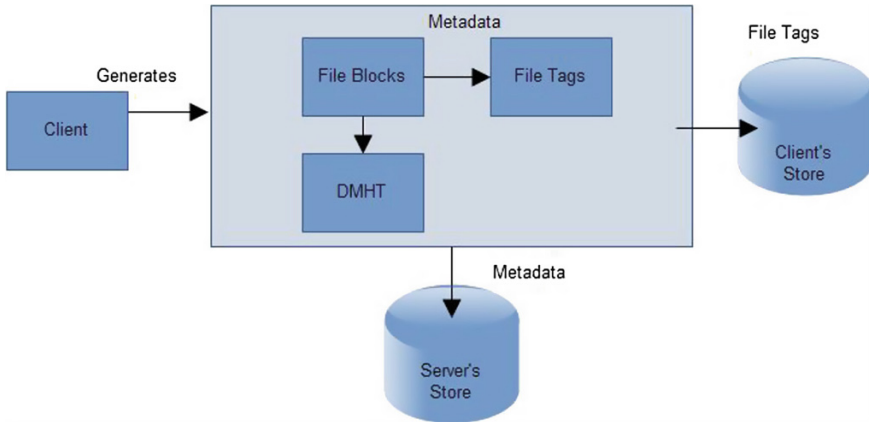


Fig. 5 Pre-processing the file blocks

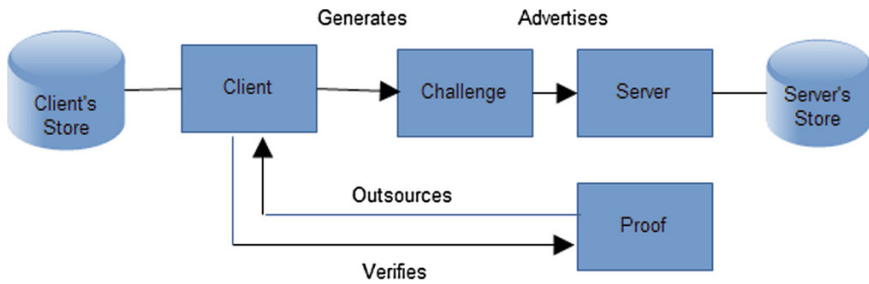


Fig. 6 Integrity checking process flow [14]

previously, then the file is integrated otherwise some part of the file is modified or lost and the file has lost its integrity. Any changes made to any part of the file are reflected in the root of the tree and so for integrity verification, checking only the value of the root is sufficient. Client is notified about the file's condition after verification. The process is Privacy-Preserving as TPA views only the file tags for verification and not the actual data. When a file is found to be infected, block level checking is done to find out particularly which block is infected.

### 4.2 The Recovery System

Users can store a copy of their file in the backup section so that it can be recovered if server undergoes any unpleasant situation such as server crash or link failure or loss or corruption of original file data. Here, block level recovery is done by

fetching exactly the infected block instead of entire file from backup server. This reductions required bandwidth. The recovery system makes data availability possible and hence adds to the plus points of the proposed system.

### 4.3 Dynamic Operations

#### 4.3.1 Method for searching (i-th leaf node)

To perform dynamic operations, searching algorithm is necessary. Firstly  $i$  is compared with index ( $n$ ) of root node. If  $i$  is greater than the root node's index then False is emitted, else, we consider  $k = i$  and  $(h_a, n_a)$  be the left subtree and  $(h_b, n_b)$  is right subtree. We now compare  $k$  with the relative index of the left child. If  $k \leq n_a$  then  $k$  lies in left subtree otherwise in right subtree. If it lies in right subtree, let  $k = k - n_a$  and use this algorithm to find the node right subtree. This procedure is repeated until  $k = 1$  i.e. a leaf node is reached.

##### 1. Insertion

When a block say  $x^*$  has to be inserted after a block  $x_i$ — $i$ th block, signature  $T$  is generated for this block by using secret key. An update request is then constructed as  $\text{update} = (I, i, x^*, T^*)$  and sent to server. Server executes update operation and for this, it follows the steps as: it stores the block  $x^*$  and leaf node  $h(H(x^*))$ . (ii) It finds  $h(H(x_i))$  in DMHT, reserve  $\Omega_i$  and then inserts leaf node  $h(H(x^*))$  after  $i$ -th node. A new internal node is added to the tree with relative index as 2 and information of all nodes which fall between this node and root node are modified by recalculating their hashes and relative index. A new root node is generated based on the changes made.

##### 2. Data Deletion and Modification

Data deletion has similar process and is just the opposite of data insertion operation. Based on node searching algorithm, the required node is searched and then deleted. After deleting it the same procedure is followed as in data insertion. In data modification, the data is replaced and so the structure of the tree remains the same. The procedure followed is same as that in the data insertion.

## 5 Performance Analysis

### 5.1 Verification Time for Different Number of File Blocks

Figure 7 presents a graph for time taken for verification of different number of file blocks. Verification time varies according to variation in number of infected blocks. As observed from Fig. 7, time required for verification of a file when no block is

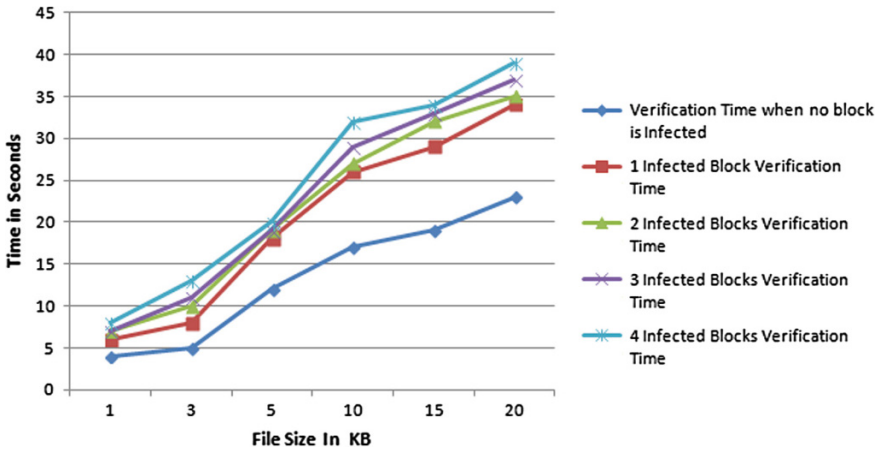


Fig. 7 Comparison of verification time for different number of file blocks

Table 2 Comparison of verification time for different number of file blocks

Sr. No.	File size in MB	Verification time in milliseconds when				
		No block infected	1 Block infected	2 Blocks infected	3 Blocks infected	4 Blocks infected
1	1	4	6	7	7	8
2	3	5	8	10	11	13
3	5	12	18	19	19	20
4	10	17	26	27	29	32
5	15	19	29	32	33	34
6	20	23	34	35	37	39

infected is least while this time increases gradually with the increment in number of infected blocks in a file. For example, for a file size of 3 MB, it takes 5 ms to verify the integrity of file if it is not infected, whereas, when its 1 block is infected it needs 8 ms, for 2 infected blocks 10 ms, for 3 infected blocks 11 ms and for 4 infected blocks it takes 13 ms. Table 2 gives a detailed view of graph represented in Fig. 7.

### 5.2 Server Computation Time

The graph in Fig. 8 shows that server computation time taken by AES based Storage Security System is less as compared to RSA based security system. For example for a file of size 90 kb, AESSS takes 1.3 s while RSA bases system takes nearly 3.8 s for server computation. Thus, the proposed system’s server computation proves to be much less than the other systems.

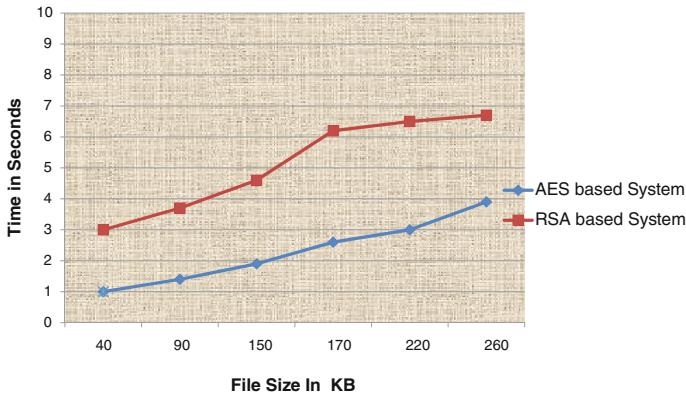


Fig. 8 Server computation time comparison

## 6 Conclusion and Future Scope

The proposed system ensures user data security at untrusted cloud server by frequent integrity checking of stored data. Use of AES algorithm instead of RSA for signature generation and encryption makes the scheme more secured and efficient. The system supports Public Auditing with the help of TPA and relieves its users from the overhead of integrity verification. Use of tags instead of actual data blocks for verification makes the auditing process time efficient and Privacy Preserving. The system supports dynamic data operations by constructing DMHT. The backup and recovery server takes care of availability of data during unpleasant situations at the server. Block level recovery highly reduces the communication cost and time for recovery.

## References

1. Deswarte, Y., Quisquater, J., Saidane, A.: Remote integrity checking. In: Proceedings of Conference on Integrity and Internal Control in Information Systems (IICIS'03), Nov 2003
2. Sebe, F., Domingo-Ferrer, J., Martinez-Balleste, A., Deswarte, Y., Quisquater, J.-J.: Efficient remote data possession checking in critical information infrastructures. *IEEE Trans. Knowl. Data Eng.* **20**(8), 1034–1038 (2008)
3. Schwarz, T., Miller, E.L.: Store, forget and check: using algebraic signatures to check remotely administered storage. In: Proceedings of ICDCS '06. IEEE Computer Society (2006)
4. Ateniese, G.: Provable data possession at untrusted stores. In: Proceedings of the 14th ACM Conference on Computer and Communications Security (CCS'07) (2007)
5. Juels, A.: Pors: proofs of retrievability for large files. In: Proceedings of the 14th ACM Conference on Computer and Communications Security (CCS '07), pp. 584–597 (2007)
6. Ateniese, G.: Scalable and efficient provable data possession. In: Proceedings of the 4th International Conference on Security and Privacy in Communication Networks (SecureComm '08) (2008)

7. Xie, M., Wang, H., Yin, J., Meng, X.: Integrity auditing of outsourced data. In: Proceedings of the 33rd International Conference on Very Large Databases (VLDB), pp. 782–793 (2007)
8. Erway, C., Kuocu, A., Pamanthou, C., R.Tamassia: Dynamic Provable Data Possession. In: Proceedings of the 16th ACM Conference on Computer and Communications Security (CCS'09) (2009)
9. Wang, C.: Enabling public auditability and data dynamics for storage security in cloud computing. *IEEE Trans. Parallel Distrib. Syst.* **22**(5), May 2011
10. Wang, C., Wang, Q., Ren, K., Lou, W.: Ensuring dynamic data storage security in cloud computing. In: Proceedings of the 17th International Workshop Quality of Service (IWQos'09) (2009)
11. Chen, L., Chen, H.: Ensuring dyanmic data integrity with public auditing for cloud storage. In: Proceedins of International Conference on Computer Science and Service System (ICSSS' 2012) (2012)
12. Kufam, L.M.: Data Security in the world of cloud computing. *IEEE Secur. Priv.* **7**(4), 61–64 (2009)
13. Venkatesh, M.: Improving Public Auditability. Data Possession in Data Storage Security for Cloud Computing, ICRTIT-IEEE (2012)
14. Hao, Z., Yu, N.: A multiple-replica remote data possession checking protocol with public verifiability. In: Proceedings of the 2nd International Data, Privacy and E-Com Symposium (ISDPE '10) (2010)
15. Zhou, M., Zhang, R., Xie, W., Qian, W., Zhou, A.: Security and privacy in cloud computing: a survey. In: Sixth International Conference on Semantics, Knowledge and Grids (2010)
16. Sravan Kumar R., Saxena, A.: Data integrity proofs in cloud storage, 978-1-4244-8953-4/11/ \$26.00 ©, 2011 IEEE
17. Varalakshmi, P.: Integrity checking for cloud environment using encryption algorithm, 978-1-4673-1601-9/12/\$31.00 ©, 2012 IEEE
18. Hao, Z., Zhong, S., Yu, N.: A privacy-preserving remote data integrity checking protocol with data dynamics and public verifiability. *IEEE Trans. Knowl. Data Eng.* **23**(9) (2011)
19. Elminaam, D.S.A., Kader, H.M.A., Hadhoud, M.M.: Performance evaluation of symmetric encryption algorithms. *IJCSNS Int. J. Comput. Sci. Netw. Secur.* **8**(12), 280–286 (2008)
20. Singh, S.P., Maini, R.: Comparison of data encryption algorithms. *Int. J. Comput. Sci. Comm. (IJCSC)* **2**(1), 125–127 (2011)

# An Improvised Extractive Approach to Hindi Text Summarization

K. Vimal Kumar and Divakar Yadav

**Abstract** Text summarization is defined as a task of minimizing a text that is produced from one or more texts such that the actual significant information in the texts is not lost. A text summarization tool compresses the text and displays only the important content to the user. Using text summarization, decisions can be made in lesser time and the core of the document be understood. This paper emphasizes on an extractive approach and its implementation on Java. The extractive approach selects the significant sentences based on a thematic approach. Before selecting the thematic words the Hindi stop-words was removed and also the stemming process to retrieve the root words in the sentences under consideration. Stop-word elimination eliminates the semantically null words from the input document and stemming helps in clustering together words with the same radix term. The system is based on an algorithm for scoring the sentences based on occurrence of the radix of thematic words. The sentences with highest score are added to the summary. The generated summary is further processed based on removal of extraneous phrases from the previously selected summary sentences so as to bring the sentences closer to human generated summary. The testing of the accuracy of the system can be made by using a technique called The Expert Game. In expert game, experts underline and extract the most interesting or informative fragments of the text. The recall and precision of the system's summary is measured against the human's extract. Based on the testing, the system is found to be 85 % accurate.

**Keywords** Hindi text summarization · Extractive approach · Thematic approach

---

K. Vimal Kumar (✉) · D. Yadav  
Jaypee Institute of Information Technology, Noida, India  
e-mail: vimalkumar.k@gmail.com

D. Yadav  
e-mail: divakar.yadav@jiit.ac.in

## 1 Introduction

There is need of efficient automatic text summarization as the internet provides the access to a very large amount of data in a particular language. People in today's world invest based on stock market updates and they go to movies, various tourist places on the basis of reviews they've seen. This type of text summarization tool helps them in making decisions in a lesser duration. There is an extensive amount of information available in Hindi as well. There is a growing need to make important decisions in time constrained environments and also understand the gist of a Hindi document in given time without missing out any important information. There are very few summarization systems that target Hindi language. This paper targets the problem of information overload and proposes a system for extractive text summarization which compresses the input document but not losing the important content in the document. As access to data from anywhere has increased so the demand for an automatic text summarization has also increased. Automatic summarization system reduces a text document or a multiple documents into a short set of texts or paragraph that conveys the actual semantics of the text and also should not lose the main meaning described in the text. The compressed text must be able to convey the meaning contained in the original text and not be difficult to comprehend.

Automatic text summarization is the process of shortening a given text, by a computer program, without losing the actual information to be conveyed. There are two widely used methods in text summarization—Extractive and Abstractive. Extractive summarization extracts the texts and creates the summaries by reusing portions (words, sentences, etc.) of the input text, while abstractive summarization is those which create the summaries by re-generating the significant content of the input text. In case of summarization system, there are summarises from single document or multiple documents and these kind of summarization system is called as multi document summarization system.

Majority of the research work carried out so far has been emphasized more on widely used English and other European languages. Indian Languages have been explored little because of the amount of information available in non-English language were less. However, the scenario is now changing and a large amount of information has become available in various languages. The need for text summarization methods that can handle Indian languages appear to be growing. We aim to develop a system for automatic summarization based on extractive summarization techniques for creation of summary of Hindi text documents so that the user can view the summarized form rather than in full. The system would currently produce summary for single text documents and in Hindi. In case of decision making systems based on analysis of large text, Hindi text summarization plays a vital role for the analysis process. Apart from this, Hindi text summarization has various applications in those systems where there is requirement for text analysis and knowledge representation. This system is based on extractive summarization and it attempts to identify the set of significant sentences that are most important for

the understanding of a given document in Hindi. In case of extractive summarization, the identification of significant sentences plays a major role in improving its accuracy.

## 2 Related Work

A lot of summarization approaches exists, but mostly for English and European language. Sentence location based approach works for news articles [1]. Location heuristics used in such a method is: Considering the newswire articles, the first sentence is often taken as the most important sentence and in case of technical articles, last few sentences in the abstract or those from conclusions provide the main details contained in the document. Sentences that are relevant to the title of the text will be extracted from the text and such an approach is called as title keyword approach [2, 3]. Apart from title of the text, the upper case words which contain the acronyms and proper nouns can also be used as a parameter. But such criteria won't work for Indian languages as the proper noun or acronym can't be identified by the upper case letter. In multi document summarization, the system clusters the similar documents and then extracts the important sentences from these clustered documents to form its summary. Such a method is known as Cluster based method. In query based text summarization system, the sentences are scored based on the frequency count of terms (words or phrases). In this type of system, the sentences containing the query phrases are given higher scores than those containing single query words. Based on the sentence scores, the output summary is formed using the high scored sentences.

Universal networking language based approach is basically used for language independent system [4]. This system generates a multi lingual summary by using an Interlingua document representation language called "Universal Networking Language" (UNL). In a graph theoretic approach, each sentence is denoted as a node and two such nodes are connected with an edge if the two sentences corresponding to those nodes share some common words, or similarity. But in all these methods the identification of sentences that has to be extracted is very important. The important sentences or documents can be identified using TF-ISF (Term frequency inverse sentence frequency) method and this method has been adapted from the information retrieval idea of calculating TF-IDF [5].

Since this system focuses on Hindi language, there is a need to bring together different lexical and semantic relations between various words in a system and that system is Hindi WordNet. WordNet organizes the lexical information in terms of word meanings and can be termed as a lexicon based on psycholinguistic principles. The design of the Hindi WordNet is inspired by the famous English WordNet. Hindi WordNet was explored to understand the usage of Hindi WordNet API to make use of the dataset and available synset, hypernyms, hyponyms etc.

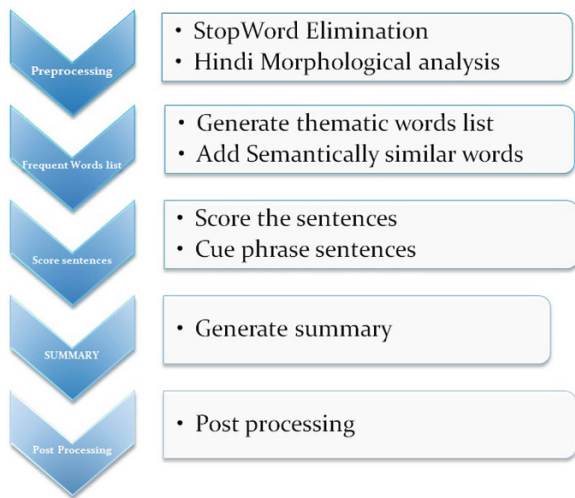


### 3 Proposed Summarization System

Summarization is of two types, abstractive summarization and extractive summarization. Extractive summarization works based on selection of a subset from the existing words, phrases, or sentences in the original text to form the summary. In contrast, an abstractive summarization uses natural language generation techniques to create a summary of a text that is closer to what a human might generate. The task of extractive summarization generates the text summary by concatenating various extracted subset of text segments from the input text [6]. The selection of sentences would be based on single words or multiword expressions. The proposed solution to the summarization system is a thematic term based approach which is based on frequent term based approach [7] for summarization of single Hindi text document. The system is divided into four major steps: pre-processing, thematic word generation, sentence scoring and summary generation. The system architecture for the proposed algorithm is as shown in Fig. 1.

Pre-processing is performed in two steps. First step is stop-word elimination in which semantically null words in Hindi are removed. A list of 170 stop words was used to perform stop-word elimination. The text document after removal of stop-words is input for stemming, in which all the remaining words are converted into their morpheme term. This is performed using longest suffix stripping method [8, 9]. The document thus obtained contains only the radix terms which is used to determine the thematic terms of the document. This is done by recording the occurrence of each term in the document making use of a document-term matrix. The chosen words and their synset are used to score the sentences.

Fig. 1 System architecture



Scoring the sentences is done using the equation given in [1] which is as follows:

$$Sc_j = \sum M[i, j] / |\text{Terms}| \quad (1)$$

where,

$Sc_j$	Score of sentence j
$M[i, j]$	value of the cell [i, j]
$ \text{Terms} $	total number of terms in the document

The top scored words are determined based on the threshold, input by the user. There are sentences which contribute more in the understanding of the document and such sentences have cue phrases like “nishkarsh”, “mahatvapoorna”, “natija”, “parinaam swarup”, “udahran”. These kinds of cue phrases are also included in the summarized version as these sentences contain conclusive remarks and examples [10]. The extracted sentences are output based on their relevance in the input document. Thus the summary is generated for the input document.

The major factor that decides about the efficiency of summarization system is the compression ratio. To achieve the desired compression ratio, the output sentences are further sent for post processing using the local context information [11, 12]. The connector (clause) including connecting words like: कि, जब- तब, अब- तब, तो, पर phrases are identified to select the unimportant text in the summary generated. To reconfirm the selection, the sentence score is also checked for these unimportant clauses and thus would be removed if the score found is less. Also, the words in the extracted sentences are linked with words in its local context. But this may lead to identification of those sentences which are semantically repeated and morphologically related. These sentences are linked through one of the lexical relations based on the morphological relation between sentences.

During this post processing phase, the extraneous phrases are identified on the basis of clauses and connecting words such as “ki” “par” “kintu” “magar” “tab” etc. The phrases are scored based on the relevance to the theme of the main document. The relevance of each word in the phrase is found with the local context and scored based on its relation to the thematic words. An example of removal of extraneous phrases is given below:

#### Original sentence

हैरानी इस बात की है कि अंतर्राष्ट्रीय क्रिकेट मैचों के दौरान हृदय में देशभक्तिका भाव लेकर देखने वाले लोग अब ऐसी स्थानीय स्तर के प्रतियोगिता भी मनोरंजन के लिये देखने लगे है

#### Reduced sentence

अंतर्राष्ट्रीय क्रिकेट मैचों के दौरान हृदय में देशभक्तिका भाव लेकर देखने वाले लोग अब ऐसी स्थानीय स्तर के प्रतियोगिता भी मनोरंजन के लिये देखने लगे है

This process of removing extraneous phrases is done using features of Hindi WorldNet. The identified extraneous phrases are then scored and the phrases having minimum score are removed from the summarized output. By considering the number of links between the words and the type of relation between various words, the system computes the score for each word in the extracted sentence based on the formula provided by Jing [13]:

$$\text{Context Weight}(w) = \sum (L_i \times \text{NUM}_i(w)) \quad (2)$$

where,

$i$	total number of lexical relations types identified
$L_i$	Weights assigned for various types of lexical relation
$\text{NUM}_i(w)$	Number of particular type of lexical relation between $w$ and various words in the input sentence

Extraneous phrases are scored on the basis of following linkages:

- Inflectional Relation to thematic words
- Synset: It is a set of synonymous words. For example, “विद्यालय, पाठशाला, स्कूल”
- Hyponymy and Hyponymy: बेलपत्र is a kind of पत्ता means पत्ता is a hypernym and बेलपत्र is the hyponym.
- Meronymy and Holonymy (Part-whole relation): जड़ (root) is the part of पेड़ (tree), meaning that जड़ (root) is the meronym of पेड़ (tree) and पेड़ (tree) is the holonym of जड़ (root).
- Antonymy: Antonymy is a relation that holds between two words that (in a given context) express opposite meanings

If a phrase or word is found to be strongly related to the local context, it is not removed from the summary sentence. The final summary is thus generated after post-processing.

## 4 Implementation Details

For implementing the above discussed approach, Java version 1.6.18 as programming language and Netbeans 6.9 as platform was used as they supports UTF-8 format, which is necessary for Processing Hindi text. Further Hindi WordNet API is used to determine lexical linkages of the words and phrases with respect to the local context mentioned in the input text and also to determine hypernyms, hyponyms etc.

Screenshots of implementation are given in figures below. In the upper left side window as shown in Fig. 2, user chooses the text document to be summarized.

In the middle left side window the summary is presented to the user along with the identified keywords highlighted in the bottom left side window as shown in Fig. 3.

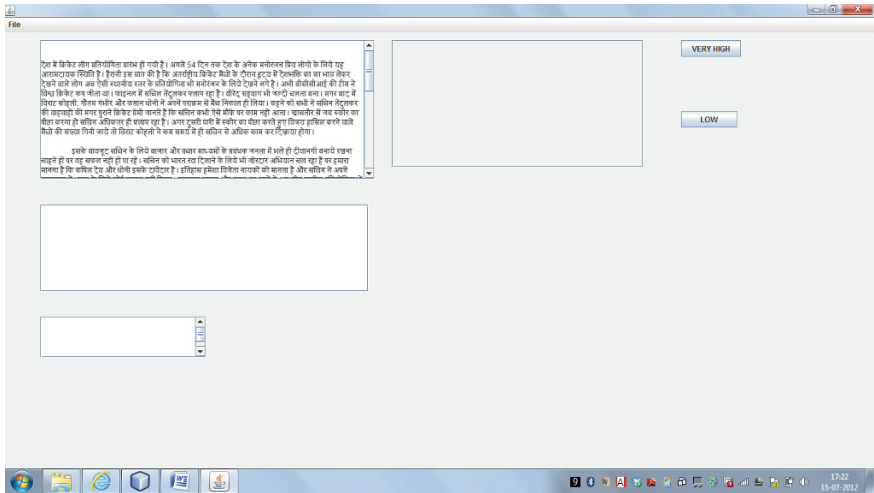


Fig. 2 Test case1-input



Fig. 3 Test case1-output (accuracy: 85.64 %)

Once the input document is chosen, the stop words are eliminated from the document. For the stop word elimination, a list of all the stop words for Hindi language is generated which includes semantically null words. The stop words list consists of 170 words. The list includes sample words like “par”, “inhey”, “jinhey”, “ke”, “pe”, “yeh”, “hain”, “veh”, “ityadi”, “dwara” etc. These words were eliminated before generating frequent words list. Since the stop words and input text

document is in Hindi the entire processing needs to be done in UTF-8 format. The resultant words generated are the semantically important words.

For a sample input sentence “राज्यसभा सचिवालय में नामांकन पत्र की जांच का काम अब मंगलवार तक के लिए टाल दिया गया है।”, the words generated after stop word elimination are “राज्यसभा”, “सचिवालय”, “नामांकन”, “पत्र”, “जांच”, “काम”, “अब”, “मंगलवार”, “टाल”.

The second step of pre-processing which is Hindi morphological analysis is performed using the native method longest suffix matching algorithm. Suffixes are found by clustering the suffixes related to a category. Nouns are inflected based on the case, the number, and the gender. Suffixes are identified to reducing the inflected forms of masculine nouns, feminine nouns, adjective inflections, and verb inflections to a common root.

The root words obtained are the basic keywords and for these words the frequency of occurrence is calculated so as to determine the words which occurs the most in the document. The top most frequent terms generated are then chosen and their semantically similar words are also added to the frequent terms list. The top scored sentences are generated as part of the summary in the order of presence in the original text document.

For evaluation of the summary generated a human analysis technique was used. A gold standard summary was generated by humans and the summary of the system was compared with the system generated summary. The number of lines matching and the total number of lines were used to evaluate the system summary.

During post processing, the tagging system is used to identify the possible adjectives, nouns, verbs and adverbs so that sentences can further be trimmed for a better summary [14]. The score for each phrase is calculated by adding up the score of each word in the phrase. This score indicates how important the phrase is in local context. Based on this score the unimportant phrases can be removed from the extracted sentence.

## 5 Result Evaluation

The generated summary was tested for its accuracy by comparing it with a gold standard summary line by line. The accuracy of the system is tested using an approach called The Expert Game. Ask experts to underline and extract the most interesting or informative fragments of the text. Measure recall and precision of the system’s summary against the human’s extract. The system is found have 85 % match between gold standard summary and system generated summary.

As shown in Table 1, the average accuracy of the system with the expert’s manual summary is found to be 85 % and also the average retention ratio is 81.1 %. This is found to considerably good percentage when compared with the system without the post processing stage. In case of post processing stage the system combines the valuable information by maintaining the same desired compression ratio.

**Table 1** Analysis of system accuracy for various input documents

Document ID	Retention ratio (%)	Accuracy (%)
1	81.08	85.64
2	78.94	85.71
3	83.33	85.15
4	81.08	83.33

## 6 Future Work

The future plan is to develop the multi-document summarization system using this proposed algorithm. For which the extracted summary has to be generated from multiple documents those are related to the context. The enhancement of the system to multiple languages is also a part of the future scope of work involved. The generated summary could be in multiple languages and the system could work on multiple languages to generate summary [15, 16]. This system in combination with a language translation system can be used to generate the summary in a language of the user's choice independent of the source language document. It could involve web mining also to extract the summaries from multiple documents available online.

## References

1. Lloret, E., Palomar, M.: Finding the best approach for multi-lingual text summarisation: a comparative analysis. In: Proceedings of Recent Advances in Natural Language Processing (RANLP), Hissar, Bulgaria (2011)
2. Lloret, E., Palomar, M.: Text summarisation in progress: a literature review. *Artif. Intell. Rev.* **37**(1), pp. 1–41 (2012). ISSN: 0269-2821
3. Alguliev, R.M., Aliguliyev, R.M.: Effective summarization method of text documents. In: Proceedings of IEEE/WIC/ACM International Conference on Web Intelligence (WI'05), pp. 1–8 (2005)
4. Mangairkarasi, S., Gunasundari, S.: Semantic based text summarization using universal networking language. *Int. J. Appl. Inf. Syst.* **3**(8), 18–23 (2012) (Published by Foundation of Computer Science, New York, USA, August 2012)
5. Juneja, V., Germesin, S., Kleinbauer, T.: A learning-based sampling approach to extractive summarization. In: Proceedings of the NAACL HLT 2010 Student Research Workshop, pp. 34–39 (2010)
6. Gupta, V., Lehal, G.S.: Survey of text summarization extractive techniques. *J. Emerg. Technol. Web Intell.* **2**(3), pp. 258–268 (2010)
7. Goldstein, J., Kantrowitz, M., Mittal, V., Carbonell, J.: Summarization text documents: sentence selection and evaluation metrics. In: Proceedings of the 22nd Annual International ACM SIGIR Conference on Research and Development in Information Retrieval (SIGIR'99), Berkeley, USA, 15–19 Aug 1999, pp. 121–128
8. Ramanathan, A., Rao, D.D.: A lightweight stemmer for Hindi. In: Proceedings of EACL (2003)
9. Porter, M.F.: An algorithm for suffix stripping. *Program* **14**(3), 130–137 (1980)

10. Gupta, V., Lehal, G.S.: Features selection and weight learning for Punjabi text summarization. *Int. J. Eng. Trends Technol.* **2**(2), 45–48 (2011)
11. Chen, F., Han, K., Chen, G.: An approach to sentence selection based text summarization. In: *Proceedings of IEEE TENCON02*, pp. 489–493 (2002)
12. Jing, H.: Sentence reduction for automatic text summarization. In: *Proceedings of the 6th Applied Natural Language Processing Conference* (2000)
13. Jing, H.: Cut-and-paste text summarization. Ph.D. thesis, Department of Computer Science, Columbia University, New York (2001)
14. Ray, P.R., Harish, V., Basu, A., Sarkar, S.: Part of speech tagging and local word grouping techniques for natural language processing. *ICON* (2003)
15. Patel, A., Siddiqui, T., Tiwary, U.S.: A language independent approach to multilingual text summarization. *Conference RIAO2007*, Pittsburgh, PA, USA (2007)
16. Mihalcea, R., Tarau, P.: An algorithm for language independent single and multiple document summarization. In: *Proceedings of the International Joint Conference on Natural Language Processing (IJCNLP)*, Korea (2005)

# Graph Based Technique for Hindi Text Summarization

K. Vimal Kumar, Divakar Yadav and Arun Sharma

**Abstract** Automatic Summarization is the process of generating or extracting the important sentences from the given input document. Since there are many such systems for English language so this proposed system is mainly focused on the Hindi language. The basic idea of this summarization system is to identify the important sentences and also to extract them based on its relevance with other sentences. In case of summarization the sentences in the summarized document should be meaningful and relevant to each other, which are achieved using sentential semantic analysis. For finding the relation between each sentence and also to analyze for the importance, the Graph based approach is found to be more appropriate. Based on the frequency of words occurrence in the input document, the sentences are ranked and the ranks are used to identify the important sentences in the document. The relevance between each sentence in the document with other sentences is found using semantic similarity. There may be same information conveyed by two different sentences whose semantic similarity score is very high. Such kind of sentences has to be kept only once in the output. For which an analysis has been performed over various semantically similar sentences. Finally, the identified relevant sentences are merged using the rank and the semantic analysis of the sentences. These identified sentences are rearranged to provide a proper meaningful summarized text to avoid textual continuity in the output text. The system is found to perform well in terms of precision, recall and F-measure with various input documents.

**Keywords** Extractive approach · Graph approach · Hindi language · Summarization · Semantic analysis · Latent semantic analysis

---

K.V. Kumar (✉) · D. Yadav  
Jaypee Institute of Information Technology, Noida, India  
e-mail: vimalkumar.k@gmail.com

D. Yadav  
e-mail: divakar.yadav@jiit.ac.in

A. Sharma  
Gautam Buddha University, Greater Noida, India  
e-mail: arun08sharma@gmail.com



## 1 Introduction

Automatic text summarization system produces a concise about the input document by retaining the most important and relevant text in the output text. Since the information overload on the web has increased the problem of decision making, the need of such a summarization system has increased. These type of summarization systems helps in making decisions as it provides the compressed form of the complete document. There are various other applications which use summarization system and one such application is on search engines to provide abstract information about various links that are searched by the end user. The accuracy of the decision making and search engines depends more on the accuracy of the summarization system being used in it as this is the back bone for those kinds of systems. The summarization system can be designed using two approaches namely Extractive and Abstractive approach. Extractive approach basically extracts out the important and relevant words or phrases or sentences from the input document. Whereas the abstractive generates the output text based on its semantic understanding of the input text. The automatic text summarization system assists in decision making, question answering system and so on. For these kinds of system, there is need for one or more input document to improve the efficiency. There comes the need for multi document summarization system. In case of multi document summarization system, the same extractive and abstractive approach can be used. But, before using these approaches, the system has to identify the relevant documents from the set of input documents. The identification of relevant documents is totally application specific. Considering the descriptive question answering system which requires summarization of the answer based on the input question and these kinds of system also requires a set of documents on different domain so that answers can be retrieved irrespective of the domain. The documents that matches this input question has to be identified and the entire identified documents will be subjected to any of the extractive or abstractive approach to generate the required output text.

This proposed system is designed in such a manner that the summarized text provides the important and relevant information provided in the input text so that there is no loss of information during compression. The graph theoretic approach used in this research makes use of extractive approach to identify important sentences. This extractive approach makes use of normalized TF-IDF to rank the sentences. A TF-IDF matrix has been created between words that are not stop words. To eliminate the stop words, a preprocessing stage is included which makes use of stop words list. After elimination of stop words, the main words are converted to vectors based on the frequency of occurrence of words in each and every sentence of the input document. The TF-IDF values of these words are normalized in the sentential level. Based on the normalized values, the sentences are ranked according to their importance. Now the system has the important sentences but may not be meaningful as there won't be related sentences in the output. So the relevance of extracted important sentences has to be found for which the semantic analysis is carried out between these sentences and edges are created if there is

semantic relevance between the sentences. The semantic analysis gives the similarity between sentences based on its meaning which can provide the information about the relevant text that are required for the summarization system. The semantic analysis used in this system is based on the widely used Latent Semantic Analysis (LSA). These important and relevant sentences have to be put in the output but may not be on the same order of occurrence in the input file. There is need for rearranging the sentences based on their order of occurrence in the input text.

The rest of paper has been organized as: Sect. 2 is about the various relevant works that has been made by various researchers in this particular area. The Sect. 3 describes about the proposed graph based approach in detail with the mathematical explanation. Section 4 describes about the analysis carried over on this system with various input text and also deals about the efficiency of this system. The Sect. 5 deals with the drawbacks of this system and how it can be eradicated in the future.

## 2 Related Work

In recent years, there is vast growth in the number of research works on the automatic text summarization and are focused mainly on the extractive approach. There are systems which make use of hand crafted rules made through various templates that are used to identify the important sentences. This method is confined to the application or on the input document under consideration. For example, the sentences which occur in the abstract and conclusion part of any research document are more important compared to other sections. In the question answering systems, the sentence which matches with the question are more important sentences which has to be retained in the output extracted text. These kinds of rule based system can be improved by unsupervised or supervised algorithms [1–3].

The semantic analysis of sentences can be used to extract out the sentences. For which various algorithms are available such as Latent Semantic Analysis (LSA), Point Mutual Information (PMI), Lesk algorithm. Pal et al. has proposed the Wordnet based method to identify the semantics behind various input text by making use of Lesk algorithm. Based on the semantic analysis, the important sentences are identified and extracted [4].

Devasena et al. has mentioned about a rule based approach for text categorization and summarization. The text categorization is performed using set of pre-classified examples. Once the sentences are classified, the sentences are included in the summarized document if the set of rules are matched. This system has provided good results but may not work in case of sentences not mentioned in the example text and also is limited to the set of rules included in the system [5].

A star map is used in summarization system developed by Kalaiselvan and Kathiravan [6], which constructs a star map between identified important and meaningful sentence based on the linguistic and statistical features of sentences. This system is found to have various applications such as duplicate elimination, exam paper evaluator, lesson planning, Identify Shingling.

Personalized summarization system has improved the conventional summarization system by taking into account the readers preferences. The main source of identifying the reader's preference is through annotation of the documents. Moro and Bielikov' [7] has mentioned that the system performs well by considering the domain in which the text is being used based on the reader's choice. The personalized system may not perform well for all domains as there are words having different interpretation in different domains. For example, the word TABLET has different senses in the electronics and medical domain.

Another approach is to use Universal Networking Language based approach [8]. It is used basically for a language independent application system. A multi lingual summary can be generated with much more ease by using a interlingua document representation language called, "Universal Networking Language" (UNL). This approach can be applied over other languages as well.

### 3 Proposed Method—A Graph Based Approach

Graph based approach is basically designed to provide the summarized text by identifying important, relevant and informative text from the input text for the compression ratio selected by the end user. This approach is broadly divided into three phase—Sentence ranking, Sentential semantic analysis and Sentence extraction (as shown in Fig. 1).

In brief, the sentence ranking algorithm is applied on the input sentences to identify which are important sentences and the relation between each sentence is calculated using the semantic analysis. The following are the description in detail about these phases of the graph based approach,

#### 3.1 Sentence Ranking

In this phase, the system identifies the important sentences based on the sentence ranking method. Sentence ranking is based on the frequency of occurrence of various words mentioned in the text. The TF-IDF method is identified to be well suited to achieve this task. Usually, TF-IDF is applied over a set of document, but since this system is designed over a single input document, the normalized term frequency is considered for sentence ranking. The normalized term frequency is applied over the words mentioned in the texts. So before applying this ranking method, the tokenization has to be made, both at sentence level and word level. With the help of this tokenization process, the input sentence is tokenized to identify each word present in input text [9, 10]. In case if all the input tokenized words are considered for ranking, the rank of sentences will be very biased based on the number of occurrence of various stop words such as Hindi conjunctions. For example, the input sentences may have frequently occurring words such as का, की, etc. and these words may bias the

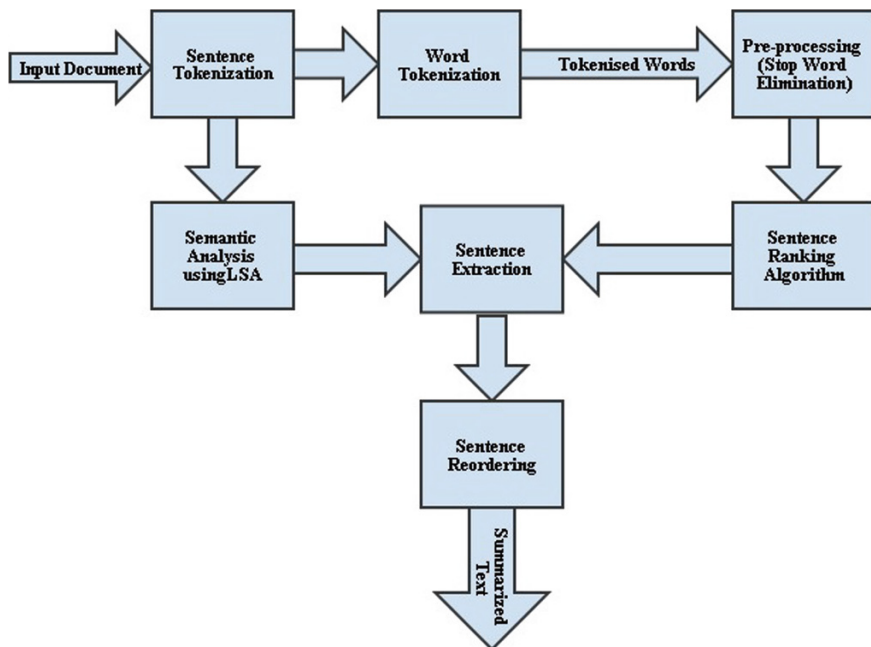


Fig. 1 System architecture

ranking strategy. To avoid such kind of biasing, a preprocessing of the input sentence to eliminate the stop words has to be carried out. A list of Hindi stop words has been made for this preprocessing stage. The term frequency of these preprocessed words is stored in a matrix and the normalized TF is applied over each term mentioned on each sentence to rank the sentences. The normalized term frequency is defined as follows,

$$TF_{norm} = \alpha + (1 - \alpha) * \frac{tf}{tf_{max}} \quad (1)$$

where,  $\alpha$  ranges from 0 to 1 and ideally its set as 0.4.

Based on the sentential value of normalized term frequency, the sentences are ranked and are identified as important sentences in the input text. The system needs to detect the relevant sentences among these important sentences which are identified in the semantic analysis phase.

### 3.2 Sentential Semantic Analysis

The latent semantic analysis (LSA) is used to perform semantic analysis for which the GENSIM tool has been made use of. During sentential semantic analysis the

system should have a grammatically valid sentence so; the system considers the input text as it is by neglecting the preprocessing stage which was used in the previous phase. Then semantic analysis is carried over between every other sentence mentioned in the input document. LSA is basically defined as an application of singular value decomposition over a vector. Initially, each sentence is converted to its corresponding term frequency vectors and these vectors are decomposed into three different matrices—left singular vectors (L), right singular vectors (R) and singular diagonal vector (S) (as shown in Eq. 2),

$$\begin{bmatrix} f_{i1}^1 & f_{i2}^1 & \dots & f_{in}^1 \\ f_{i1}^2 & f_{i2}^2 & \dots & f_{in}^2 \\ \dots & \dots & \dots & \dots \\ f_{i1}^m & f_{i2}^m & \dots & f_{in}^m \end{bmatrix} = L * R * S \quad (2)$$

where  $f_{in}^m$ —indicates the frequency of nth-term in mth-sentence.

The term frequency of words is arranged in the form of a matrix with column as different terms (words) used in the text and row of the matrix as the sentence identification numbers. After the decomposition of this matrix, the product of the right singular matrix and singular diagonal matrix will give the frequency of semantically similar words in different sentences and the similarity between two sentences is found using cosine similarity over the product of right singular vector and singular diagonal vector of the sentence considered. The cosine similarity is calculated using the below mentioned in the equation,

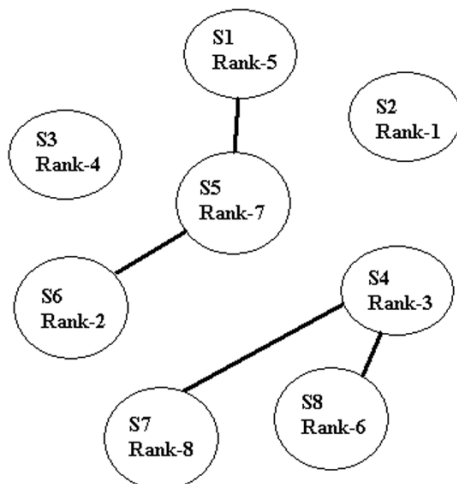
$$\cos \theta = \frac{\sum_{i=1}^n x_i * y_i}{\left( \sqrt{\sum_{i=1}^n x_i^2} * \sqrt{\sum_{i=1}^n y_i^2} \right)} \quad (3)$$

If any of the two sentences is found to be semantically similar, an edge is created between those two sentence nodes. At this phase, the system has identified the relevant sentences and in the previous phase the important sentences are identified, now the system has to extract out the sentences based on the compression ratio mentioned by the end user which is performed in the sentence extraction phase.

### 3.3 Sentence Extraction

The identified sentences are extracted based on the rank and its relevance with other sentences [11, 12]. Visualizing the sentences as nodes in a graph and connecting those nodes which are containing semantically similar sentences. The node which has highest rank is selected and all its relevant sentences are also extracted to the output set of sentences except the sentences which matches above 90 %. Based on

**Fig. 2** Graph representation of sentences



analysis, the sentences whose semantic similarity is more than 90 % are found to convey the same information. To avoid redundant information in the output text, these sentences are not duplicated. In a decreasing order of rank, each of the sentences are considered and extracted to the output text along with its set of semantically related sentences by keeping an eye on the compression ratio.

Considering eight set of sentences, the graph representation according to the analysis performed in previous phase will be as shown in Fig. 2. In Fig. 2, S1 represents sentence-1 and an edge between two nodes denotes that there is semantic relationship between them. Applying the sentence extraction phase over these sentences shown in Fig. 2 will extract the sentence S2 (having rank-1) and there is no semantically similar sentence which is indicated by no connecting edge from this particular node. It'll extract the next highest ranked sentence, i.e., S6. Now, the sentence S6 is connected to S5, it extracts S5 as well. This extraction process is continued until the desired compression is reached. In case a node such as S4 which has two nodes connected with it, then the one which has highest rank among them is considered.

These extracted sentences do not make any proper sense for the final output. So, there is a need for sentence reordering in which the sentences are rearranged to the order of occurrence in the input document. Thus the summarized output will have proper sense without losing the relevant and important information conveyed in the input document.

## 4 Results and Discussion

This system has been tested and analyzed on various documents selected from different domains at different compression ratio. The analysis (mentioned in Table 1) has shown that the system's recall measure is found to decrease with

**Table 1** Precision, recall and F-measure comparison

Compression ratio (%)	Precision (average) (%)	Recall (average) (%)	F-measure (average) (%)
40	76.79	80.53	80
60	79.42	68.78	70
80	82.89	45.27	60

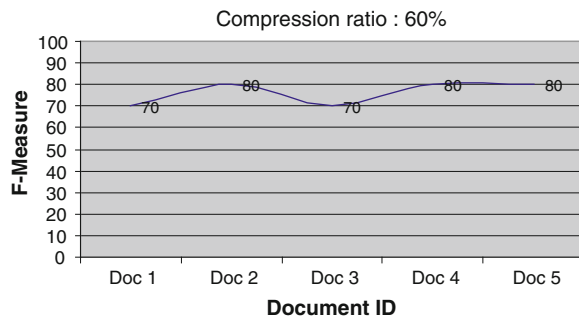
increase in compression ratio. But, the precision of the system is found to improve with increase in compression ratio. On an average the system performs well for the 60 % compression ratio. The systems performance also depends on the input document chosen.

Table 2 and Fig. 3 shows the precision and recall of the system for 60 % compression ratio over five different documents. This analysis shows that the system outperforms in case of 60 % compression ratio and gives an average F-measure as 70 %. The system is also found to perform well with 80 % compression ratio but 60 % compression ratio is considered as an average performance. The degrade in performance at 80 % compression ratio is found to be because of restriction to have less number of output text to convey the same amount of information given in original input text.

**Table 2** Comparison for various documents

Document ID	Precision (%)	Recall (%)	F-measure (%)
1	78.26	56.52	70
2	83.34	77.78	80
3	77.78	66.67	70
4	84.61	76.92	80
5	77.78	77.78	80

**Fig. 3** F-measure comparison of various documents



## 5 Conclusion and Future Work

On average the system's precision, recall, F-measure are calculated as 79, 69 and 70 % respectively. The system gives higher recall which indicates that the system conveys 69 % of the required relevant information from the input text. Also the improvement in precision indicates that the text retrieved by system matches 79 % of with the idle summaries for those documents. So to conclude, this summarization system is found to give improved results in terms of improved precision, recall and F-measure.

The downfall in performance at higher compression ratio in this system can be improved by merging the similar sentences to convey the information on different sentences in a single merged sentence. By including a module to merge those sentences that are found to be more similar or neglecting those sentence those doesn't convey much information can improve this system a lot. Also, this system can be improvised further to increase the precision and recall by applying an abstractive approach over the extractive one. By applying abstractive approach to identify the important sentence and using the semantic analysis to identify the linkages can improve the system. This system can also be used for multi document summarization and can be extended to any of the applications that make use of summarization system.

## References

1. Juneja, V., Germesin, S., Kleinbauer, T.: A learning-based sampling approach to extractive summarization. In: Proceedings of the NAACL HLT 2010 Student Research Workshop, pp. 34–39 (2010)
2. Gupta, V., Lehal, G.S.: A survey of text summarization extractive techniques. *J. Emerg. Technol. Web Intell.* **2**(3), 258–268 (2010)
3. Gupta, V., Lehal, G.S.: Features selection and weight learning for punjabi text summarization. *Int. J. Eng. Trends Technol.* **2**(2) (2011)
4. Pal, A.R., Saha, D.: An approach to automatic text summarization using WordNet. In: Advance Computing Conference (IACC), 2014 IEEE International, pp. 1169, 1173 (2014). doi:[10.1109/IAdCC.2014.6779492](https://doi.org/10.1109/IAdCC.2014.6779492)
5. Devasena, C.L., Hemalatha, M.: Automatic text categorization and summarization using rule reduction. In: Advances in Engineering, Science and Management (ICAESM), 2012 International Conference on, pp. 594, 598, 30–31 Mar 2012
6. Kalaiselvan, M., Kathiravan, A.V.: A pioneering tool for text summarization using star map. In: Pattern Recognition, Informatics and Mobile Engineering (PRIME), 2013 International Conference on, pp. 277, 281, 21–22 Feb 2013
7. Moro, R., Bielikov', M.: Personalized text summarization based on important terms identification. In: Database and Expert Systems Applications (DEXA), 2012 23rd International Workshop on, pp. 131, 135 (2012) doi:[10.1109/DEXA.2012.47](https://doi.org/10.1109/DEXA.2012.47)
8. Mangairkarsi, S., Gunasundari, S.: Article: semantic based text summarization using universal networking language. *Int. J. Appl. Inf. Syst.* **3**(8), 18–23 (2012) (Published by Foundation of Computer Science, New York, USA)
9. Porter, M.F.: An algorithm for suffix stripping. *Program* **14**(3) (1980)



10. Ramanathan, A., Rao, D.D.: A lightweight stemmer for Hindi. In: Proceedings of EACL (2003)
11. Alguliev, R.M., Aliguliyev, R.M.: Effective summarization method of text documents. In: Proceedings of IEEE/WIC/ACM International Conference on Web Intelligence (WI'05), pp. 1–8 (2005)
12. Mihalcea, R., Tarau, P.: An algorithm for language independent single and multiple document summarization. In: Proceedings of the International Joint Conference on Natural Language Processing (IJCNLP), Korea (2005)

# Generating Empty Convex Polygon Randomly from a Subset of Given Point Set

Manas Kumar Mohanty, Sanjib Sadhu, Niraj Kumar  
and Kamaljit Pati

**Abstract** In computational geometry, problem of generating random geometric objects are very interesting and extensively studied problems. In this paper we propose a new algorithm to generate an empty convex polygon from a subset of given point set. Let  $S = \{p_1, p_2, \dots, p_n\}$  be the given point set lying in  $\mathbb{R}^2$ . The proposed algorithm generates a random empty convex polygon consisting of  $k$  vertices in  $S$ . In preprocessing phase we compute Convex Hull Layers  $CL(S)$  in  $O(n \log n)$  time. By using the visibility relationship in Convex Layers, the proposed algorithm generates a random empty convex polygon in  $O(\log n + k)$  time which is improved over the existing solution for this problem.

**Keywords** Polygon · Convex polygon · Convex hull layers · Visibility

## 1 Introduction

In computational geometry, generating random geometric objects like simple polygon, monotone polygon are extensively studied problems. The theoretical applications of geometric objects includes testing of various computational geometry algorithms and verification of the algorithm being tested. There exist a lot of heuristics [1] to generate a random polygon from  $n$  points. Much efforts has also

---

M.K. Mohanty (✉) · S. Sadhu · N. Kumar · K. Pati  
National Institute of Technology, Durgapur, India  
e-mail: munkun41@gmail.com

S. Sadhu  
e-mail: sanjibsadhu411@gmail.com

N. Kumar  
e-mail: nirajcse08@gmail.com

K. Pati  
e-mail: kamaljit.igit@hotmail.com

been applied to generate a specific class of polygons like monotone polygons [2], star shaped polygons [1].

In this paper, our focus is on convex polygons with vertices in  $S$  rather than simple polygons with vertices of  $S$ . Generation of empty convex  $k$ -gons and counting of empty  $k$ -gons in given point set are the problems of this category.

In [3] problem of large convex holes in random point set has been discussed. Counting version of this problem is also quite popular, some of the recent studies includes [4, 5]. A random convex polygon has been generated by Zhu et al. [2]. After  $O(n^3)$  preprocessing on a set  $S$  of  $n$  points, a convex polygon can be generated in  $O(n^2)$  time whose vertices are in  $S$  [2]. In this paper, we compute a  $k$ -gon efficiently than that of existing algorithms. Our algorithm involves two phases. The preprocessing phase involves computing convex layers, which requires  $O(n \log n)$  time. From convex layers we compute visibility information. Visibility information will be used to compute a  $k$ -gon in  $O(\log n + k)$  time. Hence, proposed algorithm computes empty  $k$ -gon in given point set in  $O(\log n + k)$  time after a preprocessing of  $O(n \log n)$ .

Convex layers finds a lot of applications in a variety of fields. Chazelle [6] provides some applications of convex layers. In [7] convex layers has been used to solve TSP problem. In [8] Sadhu et al. applied convex layers to design a heuristic to generate simple polygon from  $S$ .

The outline of the paper is as follows. Section 2 provides some definitions and other concepts required to solve problem. Section 3 describes the algorithm designed to solve the problem along with its complexity analysis. Finally in Sect. 4, we conclude with possible future works.

## 2 Preliminaries

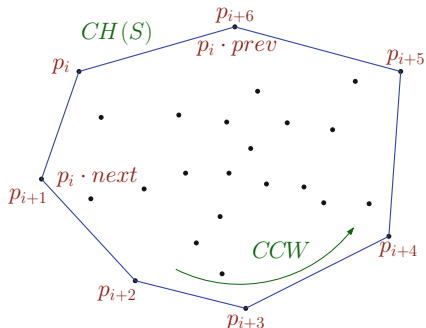
We use the term points and vertices interchangeably throughout the paper. For a pair of point  $p$  and  $q$ , the line segment  $\ell(p, q)$  is defined as directed line segment from point  $p$  to point  $q$ . Henceforth we assume that set  $S = \{p_1, p_2, \dots, p_n\}$  is given point set containing  $n$  points in  $\mathbb{R}^2$ .

**Definition 1** A polygon  $P$  is said to be simple [9] if it consists of straight, non-intersecting line segments, called edges that are joined pair-wise to form a closed path.

An edge connecting two points  $p$  and  $q$  is denoted by  $e(p, q)$ . The  $x$ -coordinate and  $y$ -coordinate of a point  $p$  are denoted by  $x(p)$  and  $y(p)$ , respectively. Here and throughout the paper, unless qualified otherwise, by polygon we mean simple polygon. By empty polygon we mean no point  $p \in S$  lies inside the polygon.

**Definition 2** A subset  $S$  of the plane is called **convex** if and only if for any pair of points  $(p, q) \in S$  the line segment  $\ell(p, q)$  is completely contained in  $S$  [9].

**Fig. 1** Convex hull  $CH(S)$

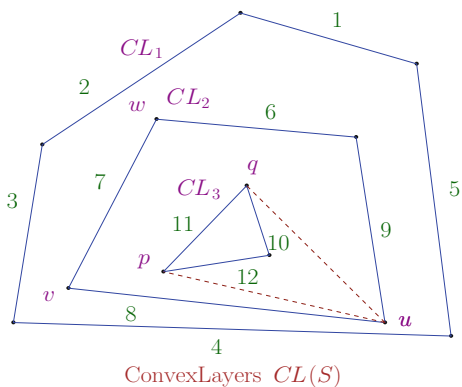


In other terms, a convex hull of given point set is smallest convex set that contains all points of  $S$ . Convex hull of given points is represented by set of vertices, in order, that defines hull edges. The convex hull of point set  $S$ , denoted by  $CH(S)$ , is shown in Fig. 1. The  $CH(S)$  represents a chain of vertices  $\{p_i, p_{i+1}, \dots, p_{j-1}, p_j, p_i\}$  such that  $1 \leq i \leq j \leq n$ . From now on we assume that vertices of convex hull are given in counterclockwise order, as shown in Fig. 1. The lower bound to find  $CH(S)$  of a given point set with  $n$  points, is  $\Omega(n \log n)$  [10].

**Definition 3** A **convex chain** of a polygon is a sequence of consecutive edges where the internal angle between two edges is less than  $180^\circ$ .

Consecutive vertices of convex hull forms a convex chain. Convex layers is the extension to convex hull concept. For the given point set  $S$ , its convex layers set  $CH(S)$  is set of convex layer  $CL_i$  such that each layer  $CL_i \in CL(S)$  is computed by removing points of all previous layers, i.e.  $CL_j$ , where  $j < i$  from point set  $S$ . Hence, convex layers set  $CH(S)$  can be obtained by recursively computing convex hull of point set and removing points lying on computed convex hull, until point set becomes empty. The convex layers of a point set are shown in Fig. 2. In [11] convex layer mentioned to define *depth* of a point as

**Fig. 2** The edge  $e(p, q)$  is not visible to point  $u$ , however it is visible to points  $v$  and  $w$



**Definition 4** The depth of a point  $p$  in a set  $S$  is the number of convex hulls (convex layers) that have to be stripped from  $S$  before  $p$  is removed. The depth of  $S$  is the depth of its deepest point.

For a given point set  $S = \{p_1, p_2, \dots, p_n\}$  we represent its convex hull by  $CH(S)$ , whereas set of convex layers will be represented by  $CL(S)$ . The convex layers set, or simply convex layers,  $CL(S)$  is set of convex layers  $\{CL_1, CL_2, \dots, CL_m\}$ , where  $m$  is the number of convex layers in given point set. In  $CL(S)$ , we follow the inward ordering, hence the outermost layer will be referred as  $CL_1$  and innermost layer as  $CL_m$ , as shown in Fig. 2. Any layer  $CL_i \in CL(S)$  is defined by sequence of vertices. From now on the vertices of convex hull are assumed to be in counterclockwise sequence. Hence, a convex layer  $CL_i$  is represented by counterclockwise circular sequence of vertices.

A point  $p \in S$  is said to be visible [12] from a point  $q \in S$  if the line segment  $\ell(p, q)$  does not intersect any other line segment or does not pass through a third point  $r \in S$ .

**Definition 5** (*Edge Visibility*). An edge  $e(p, q) \in CL_i$  is said to be visible from a point  $u \in CL_{i-1}$ , if  $p, q$  and any point  $r$  (say, midpoint of  $e(p, q)$ ) lying on  $e(p, q)$  is visible from  $u$ .

Consider Fig. 2, the Convex Layer  $CL(S)$  of the point set  $S$  consists of three Convex Layers  $CL_1, CL_2$  and  $CL_3$ . Figure 2 shows that the edge  $e(p, q) \in CL_3$  is “not visible” to the point  $u \in CL_2$ , however edge  $e(p, q)$  is visible to points  $v$  and  $w$  lying on  $CL_2$ .

### 3 Algorithm

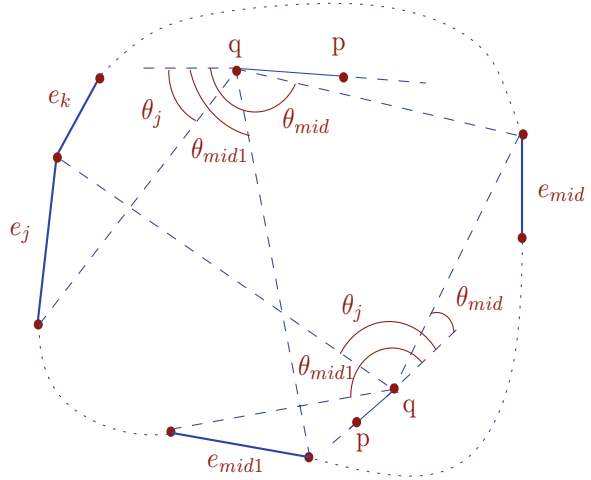
The objective is to generate a random empty convex polygon from a subset of points of  $S$ . Preprocessing phase requires computation of convex layers followed by visibility computation.

The convex layers will be computed using the optimal algorithm proposed in [6]. It is an optimal time algorithm, which computes convex layers in  $O(n \log n)$  time. The lower bound to compute convex hull of a given point set with  $n$  points is  $\Omega(n \log n)$  [10]. Hence, the convex layer algorithm with  $\Omega(n \log n)$  time is an optimal algorithm. The pseudocode in Algorithm 1 describe the preprocessing part before computing a random convex empty polygon from the subset of point set.

**Observation 1** *With respect to an edge  $e(p, q) \in CL_i$ , there must exist at least one vertex  $v \in CL_{i+1}$  visible from the edge  $e(p, q)$ .*

**Lemma 1** *Line number 6 of the Algorithm 1 takes  $O(\log n_{i-1})$  time, where  $n_{i-1}$  is the number of edges in  $CL_{i-1}$ .*

**Fig. 3** The edge  $e(p, q)$  lies inside the convex polygon whose edges  $e_j, e_{mid}, e_{mid1}$  and  $e_k$  are shown. Its other edges are represented by dotted curves



*Proof* Let the edges of the layer  $CL_{i-1}$  be  $\{e_j, e_{j+1}, \dots, e_k\}$ , where  $k = (j + n_{i-1} - 1)$ . Consider Fig. 3. These sequence of edges forms an initial convex chain. Now, the line  $\ell(p, q)$  passing through the edge  $e(p, q) \in CL_i$  must intersect the  $CL_{i-1}$  at two points which are to be found. We compute an index  $mid = (j + k)/2$ . We check in  $O(1)$  time whether the line  $\ell(p, q)$  passes through  $e_j$  and/or  $e_{mid}$ . If yes, we found intersection(s). Otherwise, we test in which side of the line  $\ell(p, q)$ , the edges  $e_j$  and  $e_{mid}$  lies.  $\square$

There are two possible cases:

**Case 1** The edges  $e_j$  and  $e_{mid}$  lie on the same side of  $\ell(p, q)$ . Here,  $\ell(p, q)$  intersect either the convex chain  $\{e_{j+1}, e_{j+2}, \dots, e_{mid-1}\}$  or the convex chain  $\{e_{mid+1}, e_{mid+2}, \dots, e_k\}$  depending on the angles  $\theta_j, \theta_{mid}$  and  $\theta_{mid1}$  (Refer to Fig. 3), where  $mid1$  is the index of the edge  $e_{mid1}$  and is given by  $mid1 = j + (mid - j)/2$ . Find out the angle  $\theta_j$  formed by the edge  $e(p, q)$  and line segment  $\ell(p, r)$  where  $r$  is any one of the end points of the edge  $e_j$ . Similarly find out the angles  $\theta_{mid}$  and  $\theta_{mid1}$  formed by the edge  $e(p, q)$  with the line segments  $\ell(p, s)$  and  $\ell(p, t)$  respectively, where  $s$  and  $t$  are any one of the end points of the edge  $e_{mid}$  and  $e_{mid1}$  respectively. These three angles can be computed in  $O(1)$  time. Now, if the value of  $\theta_{mid1}$  lies in between  $\theta_j$  and  $\theta_{mid}$ , then we have to consider only the convex chain  $\{e_{mid+1}, e_{mid+2}, \dots, e_k\}$ , because the line  $\ell(p, q)$  will pass through this convex chain only. Hence we reject other convex chain. However, if  $\theta_{mid1}$  is either greater than or less than both  $\theta_j$  and  $\theta_{mid}$ , we will consider the convex chain  $\{e_{j+1}, e_{j+2}, \dots, e_{mid-1}\}$  rejecting the other convex chain.

**Case 2** The edges  $e_j$  and  $e_{mid}$  lie on the different sides of  $\ell(p, q)$ . In this case the line  $\ell(p, q)$  will intersect both the convex chains  $\{e_{j+1}, e_{j+2}, \dots, e_{mid-1}\}$  and  $\{e_{mid+1}, e_{mid+2}, \dots, e_k\}$ . Hence both the convex chains are to be considered. We search for intersecting point by recursive procedure by assuming each such convex

chain as the initial convex chain. The intersection points are determined by binary search like procedure and hence, this operation will take  $O(\log n)$  time.

Let  $m$  be the number of convex layers in convex layers set  $CL(S)$ . In step 1 of the Algorithm 1, convex layers set  $CL(S)$  computed using optimal algorithm to compute convex layer proposed in [6].

---

**Algorithm 1:** Preprocessing

---

```

Input: Point Set  $S = \{p_1, p_2, \dots, p_i, \dots, p_n\}$ 
Output: Convex Layers Set  $CL(S) = \{CL_1, CL_2, \dots, CL_m\}$  and
           $ArrayTable[n][n], ArrayB[n]$ 
1 Compute the Convex Layers  $CL(S)$  of  $S$ 
2 Initialize each entry of the array  $B[n]$  to zero
3 for  $i = 2$  to  $m$  do
4   for each edge  $e(p, q) \in CL_i$  do
5     Find the number (say  $t$ ) of vertices  $v \in CL_{i-1}$ , from which the
6     edge  $e(p, q)$  is completely visible
7      $B[t] \leftarrow B[t] + 1$ 
     Store the edge id  $e.id$  of the edge  $e(p, q)$  in  $Table[t][B[t]]$ 

```

---

In Algorithm 1, the  $t$ th row of the  $Table$ , i.e.  $Table[t]$  store the edge-id of those edges  $\in CL(S)$  which are visible from exactly  $t$  number of vertices. The number of edge ids stored in each  $t$ th row of  $Table[][]$  are stored in  $B[t]$ .

**Observation 2** *The Algorithm 1 takes  $O(n \log n)$  time.*

*Proof* Step 1 of the Algorithm 1 requires computation of Convex Layers of  $S$ . To compute convex layers set  $CL(S)$  we use optimal algorithm proposed in [6], which computes  $CL(S)$  in  $O(n \log n)$  time. Then it computes the set of visible vertices for all the edges lying on the Convex Layer, except outermost layer  $CL_1$ . Hence by lemma 2, the time complexity of the Algorithm 1 is  $O(n \log n)$ . □

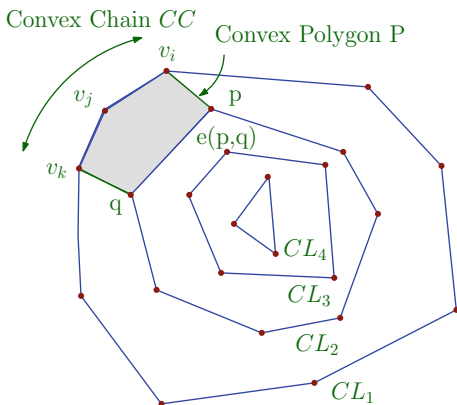
Once the preprocessing part is over, we can generate a random convex (empty) polygon using the Algorithm 2.

**Theorem 3** *The Algorithm 2 computes a random convex polygon (consisting of  $k$  vertices) in  $O(\log n + k)$  time after the preprocessing part is over.*

*Proof* Line number 4 of the Algorithm 2 takes  $O(\log n)$  time as proved in lemma 2. The if-else statement of the Algorithm 2 takes  $O(k)$  time to process the visible vertices. Hence, the overall time complexity of Algorithm 2 is  $O(\log n + k)$ . □

The Fig. 4 shows how an empty Convex Pentagon is randomly generated by the Algorithm 2 after the preprocessing part is over. As shown in Fig. 4, one can generate an empty convex quadrilateral using the edge  $e(p, q)$  and any two vertices

**Fig. 4** The set of vertices visible from the edge  $e(p, q) \in CL_3$  is  $V_e = \{v_i, v_j, v_k\}$  and a convex pentagon (i.e.  $k = 5$ )  $P$  is generated after selecting the random edge  $e$



from the set  $V_e$ . Our algorithm constructs an empty convex polygon using two adjacent Convex Layers  $CL_i$  and  $CL_{i+1}$ .

---

**Algorithm 2: Convex Polygon Generation**

---

**Input:**  $CL(S), Table[n][n], B[n], k$

**Output:** Convex Polygon  $P$  consisting of  $k$  vertices

- 1  $u \leftarrow (k - 2)$  ▷ Since the convex polygon  $P$  will be generated after selecting an edge  $e$  which will be part of the  $P$ , we will consider  $(k - 2)$  points from the  $CL(S)$  (except the two end points of the edge  $e$ )
  - 2 Randomly select an edge  $e$  from the  $t_{th}$  row (where  $t \geq u$  and  $B[t] > 0$ ) of the  $Table[ ][ ]$
  - 3  $V_e \leftarrow$  Set of vertices visible from  $e \in CL_i$ , where  $V_e \in CL_{i+1}$  and  $e \in CL_i$
  - 4 **if**  $(|t| == |u|)$  **then**
  - 5     Connect the vertices  $V_e$  in the order in which they appear in the layer  $CL_i$  to form a convex chain  $CC$
  - 6 **else**
  - 7     Select randomly  $|u|$  number of vertices from the  $V_e$  and connect them in the order in which they appear in the layer  $CL_i$  to form a convex chain  $CC$ ;
  - 8 Connect the two end vertices of  $CC$  with the two end points of  $e$  to get a convex Polygon  $P$
  - 9 **return** Polygon  $P$
- 

**4 Conclusion and Future Works**

Proposed algorithm computes empty convex polygon in given points set. In preprocessing part, convex layers set  $CL(S)$  and the visibility relations among its edges are computed. After  $O(n \log n)$  preprocessing task, a random empty convex



polygon consisting of  $k$  vertices is generated in  $O(\log n + k)$  time which is much faster than the existing algorithm [2].

Proposed algorithm computes empty convex polygon by considering two adjacent convex layers. However, in some cases it may be possible that the empty convex polygon consisting of  $k$  vertices cannot be generated using only two adjacent Convex Layers. Hence, as a future work, we can use more than two neighboring Convex layers of  $CL(S)$  to generate a random empty convex polygon. However, it would be a challenging task to compute empty convex polygon by considering all layers in  $O(\log n + k)$  time.

## References

1. Auer, T., Held, M.: RPG: heuristics for the generation of random polygons. In: Proceedings of 8th Canadian Conference Computational Geometry, pp. 38–44 (1996)
2. Zhu, C., Sundaram, G., Snoeyink, J., Mitchel, J.S.B.: Generating random polygons with given vertices. *Comput. Geom. Theory Appl.* 6:277–290 (1996)
3. Balogh, J., Gonzalez-Aguilar, H., Salazar, G.: Large convex holes in random point sets. *Comput. Geom.* 46(6), 725–733 (2013)
4. Mitchell, J.S., Rote, G., Sundaram, G., Woeginger, G.: Counting convex polygons in planar point sets. *Inf. Process. Lett.* 56(1), 45–49 (1995)
5. Rote, G., Woeginger, G.: Counting convex k-gons in planar point sets. *Inf. Process. Lett.* 41(4), 191–194 (1992)
6. Chazelle, B.: On the convex layers of a planar set. *Trans. Inf. Theory IEEE* 31(4), 509–517 (1985)
7. Liew, S.: Applying convex layers, nearest neighbor and triangle inequality to TSP problem. arXiv preprint arXiv:1204.2350 (2012)
8. Sadhu, S., Kumar, N., Kumar, B.: Random polygon generation through convex layers. *Proc. Technol.* 10, 356–364 (2013)
9. De Berg, M., van Kreveld, M., Overmars, M., Schwarzkopf, O., Overmars, M.H.: *Computational geometry: algorithms and applications*. New York, New York (2000)
10. Yao, A.C.C.: A lower bound to finding convex hulls. *J. ACM* 28(4), 780–787 (1981)
11. Preparatata, F.P., Shamos, M.I.: *Computational Geometry: An Introduction*. Springer, Berlin (1985)
12. Ghosh, S.K.: *Visibility Algorithm in the Plane*. Cambridge University press, Cambridge (2007)

# A Symmetric Key Cryptographic Technique Based on Frame Rotation of an Even Ordered Square Matrix

Joyita Goswami (Ghosh) and Manas Paul

**Abstract** A session based symmetric key cryptographic technique has been proposed in this paper. It considered the plain text as a stream of finite number of binary bits. Using frame rotation technique of square matrix, input bits are oriented to generate cipher text. A session key is generated from the plain text information. Results are generated to compare the proposed technique with Triple-DES (168 bits), AES (128 bits) with respect to different parameters.

**Keywords** FRSM · AES · Triple DES · Session based key · Avalanche · Strict avalanche · Bit independence · Chi-square

## 1 Introduction

In modern era every computer is connected virtually, so data security becomes main concern of modern life. Cryptography is an important aspect for secure communication to protect important data, so network security is the most important topic of researchers [1–5].

The proposed technique is a symmetric key cryptography and it is termed as FRSM where the plain text is considered as a stream of binary bits. The input bit stream chopped dynamically into manageable size of blocks such that bits of each block fitted into an even ordered square matrix. Bit positions are shifted to generate the cipher text using the concept of frame rotation of that square matrix. A session key is generated for one time use in a session of transmission using the information

---

J. Goswami (Ghosh) (✉) · M. Paul  
Department of Computer Application, JIS College of Engineering,  
Kalyani, West Bengal, India  
e-mail: joyitagoswami@gmail.com

M. Paul  
e-mail: manaspaul@rediffmail.com

of block sizes. The plain text can be regenerated from the cipher text using the session key information during decryption.

Section 2 describes the proposed technique along with the algorithms for encryption, decryption and key generation. Section 3 explains FRSM with an example and Sect. 4 contains the results and analysis. Conclusions are drawn in Sect. 5.

## 2 Technique

FRSM consider the plain text as a stream of finite number of binary bits. This bit stream is chopped dynamically into blocks with variable sizes. The block size information of any particular session generates the session key. During encryption the bits of the blocks are taken MSB (Most Significant Bit) to LSB (Least Significant Bit) to fit row-wise into an even order ( $2n \times 2n$ ) square matrix. Any square matrix of order  $2n$  can be imagine as  $n$  number of square frames where inner most frame is denoted as frame 1 and outer most frame as frame  $n$ . Frame  $k$  contains  $4(2k - 1)$  number of cells. Cells of each  $k$ th frame are shifted by circular fashion along clock-wise direction by  $k$  positions. After rotation bits are taken from the square matrix row-wise to form the encrypted block. Cipher text is generated from these encrypted blocks. For decryption the cipher text is considered as a stream of binary bits. Processing the session key the binary bits are sliced into desired sized blocks. The bits of the blocks are taken MSB to LSB to fit row-wise into a square matrix of order  $2n$ . Cells of  $k$ th frame of that matrix are shifted circularly along anti clock-wise direction by  $k$  positions. Now bits are collected from the square matrix row-wise to form decrypted blocks. Plain text is regenerated from decrypted blocks.

Sections 2.1, 2.2 and 2.3 explain encryption algorithm, decryption algorithm and generation of session key respectively.

### 2.1 Encryption Algorithm

*Input: Source stream i.e. plaintext.*

*Output: Encrypted stream i.e. ciphertext.*

*Method: The process takes binary stream and generates encrypted bit stream through a combination of S-Box and P-Box operations.*

STEP 1: *The plain text i.e. the input file is considered as a stream of finite number of binary bits.*

STEP 2: *This binary string chopped dynamically into manageable-sized blocks with different lengths like 4/16/64/144/256/400/...  $[(4n)^2$  for  $n = 1/2, 1, 2, 3, 4, 5, \dots]$  as follows: First  $n_1$  no. of bits is considered as  $x_1$  no. of blocks with block length  $y_1$  where  $n_1 = x_1 * y_1$ . Next  $n_2$  no. of bits is*

considered as  $x_2$  no. of blocks with block length  $y_2$  where  $n_2 = x_2 * y_2$  and so on. Finally  $n_m$  no. of bits is considered as  $x_m$  no. of blocks with block length  $y_m (=4)$  where  $n_m = x_m * y_m$ . So no padding is required.

- STEP 3: Square matrix of order  $\sqrt{y}$  ( $=2n$ ) is generated for each block of length  $y$ . The binary bits of the block are taken from MSB to LSB to fit row-wise into this square matrix.
- STEP 4: Any square matrix of even order (say  $2n \times 2n$ ) can be imagine as  $n$  number of square frames like frame 1, frame 2, frame 3, ....., frame  $n$  where inner most frame is denoted as frame 1 and outer most frame as frame  $n$ . Frame  $k$  contains total  $4(2k - 1)$  number of cells. Cells of frame  $k$  are shifted by circular fashion along clockwise direction by  $k$  positions.
- STEP 5: Bits are taken row-wise from the square matrix to generate the encrypted block of length  $y$ .
- STEP 6: The cipher text is formed converting the encrypted binary string into corresponding characters.

## 2.2 Decryption Algorithm

*Input:* Encrypted stream i.e. ciphertext and session key.

*Output:* Source stream i.e. plaintext.

*Method:* Process takes encrypted binary stream and generates source stream.

- STEP 1: The cipher text is considered as a stream of binary bits.
- STEP 2: Processing the session key information, this binary string breaks into manageable-sized blocks.
- STEP 3: Square matrix of order  $\sqrt{y}$  ( $2n$ ) is generated for each block of length  $y$ . The binary bits of the block are taken from MSB to LSB to fit row-wise into this square matrix.
- STEP 4: Any square matrix of even order (say  $2n \times 2n$ ) can be imagine as  $n$  number of square frames like frame 1, frame 2, frame 3, ..., frame  $n$  where inner most frame is denoted as frame 1 and outer most frame as frame  $n$ . Frame  $k$  contains total  $4(2k-1)$  number of cells. Cells of each frame, say  $k$ th frame, are shifted by circular fashion along anti-clockwise direction by  $k$  positions.
- STEP 5: The decrypted binary string is generated taking the bits row-wise from the square matrix.
- STEP 6: The plain text is regenerated converting the decrypted binary string into corresponding characters.

### 2.3 Generation of Session Key

FRSM generates a session key for one time use in a particular session of transmission to ensure more security. The input binary bit stream is divided into 16 portions where 1st portion contains 20 % of total file size, 2nd portion contains 20 % of remaining file size and so on. Each portion is divided into x no. of blocks with block length y ( $=4n * n$ ). The bits of this block are fitted into an even ordered (2n) square matrix where value of n is selected dynamically for first fifteen portions. Finally last (i.e. 16th) portion is divided into  $x_{16}$  no. of block with block length 4 bits (i.e.  $y_{16} = 4$ ) and we generate  $2 \times 2$  order matrix. So no padding is required. Total length of the input binary string is  $= x_1 * y_1 + x_2 * y_2 + \dots + x_{16} * y_{16}$ . The value of n for each portion is stored as a character in the key file. So the key file contains fifteen characters.

### 3 FRSM with an Example

To illustrate FRSM, let us consider the word “Ma”. The bit representation of the above word is ‘0100110101100001’ which are taken from MSB to LSB into a block of length 16. Bits of the block fit row-wise into an even order ( $=4$ ) square matrix. So matrix is imagined as two square frames, frame 1 and frame 2. Cells of

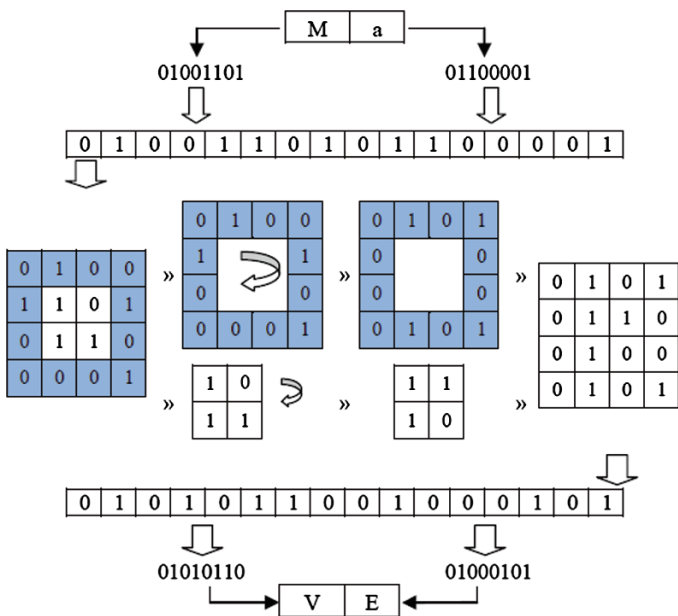


Fig. 1 Flow diagram of FRSM with the input word “Ma”

frame 1 and frame 2 are shifted by circular fashion along clock wise direction by one and two positions respectively. Now bits are taken row-wise to form the encrypted binary string. Two 8 bit binary numbers ‘01010110’ and ‘01000101’ are formed from the above encrypted string. The corresponding equivalent decimal values are 86 ( $\cong$ character ‘V’) and 69 ( $\cong$ character ‘E’) respectively. So the word “Ma” is encrypted as “VE”. Figure 1 shows the flow diagram of FRSM with the input word “Ma”.

## 4 Results and Analysis

The comparative study between Triple-DES (168 bits), AES (128 bits) and the proposed technique FRSM has done on twenty files of twelve different types with file sizes varying from 50 bytes to 137 MB (approx.). Results are generated for analysis and comparison of Encryption and Decryption times (in Sect. 4.1), Avalanche, Strict Avalanche and Bit Independence values (in Sect. 4.2), Chi-square values (in Sect. 4.3) and Character frequencies (in Sect. 4.4).

### 4.1 Analysis of Encryption and Decryption Times

Time taken is the difference between processor clock ticks at the starting and at the end of execution. The lower time indicates the higher speed of execution of the technique. Encryption and decryption times (in milliseconds) of different files calculated for Triple-DES (168 bits), AES (128 bits) and FRSM. Figures 2 and 3 show the graphical representation of encryption and decryption times against the

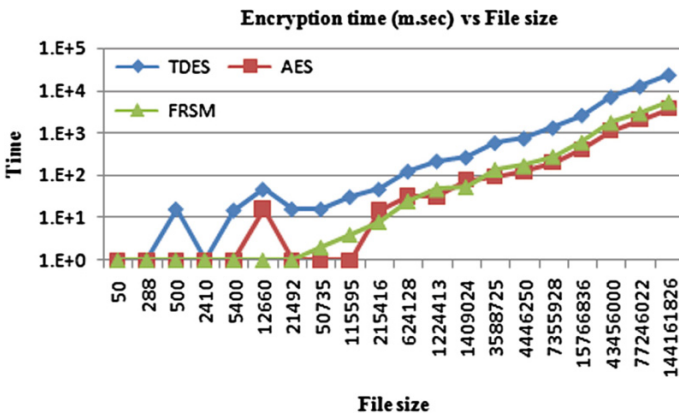
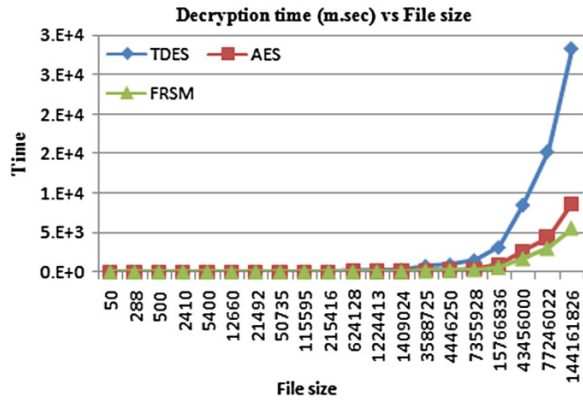


Fig. 2 Graphical representation of encryption times against file sizes in logarithmic scale

**Fig. 3** Graphical representation of decryption times against file sizes in logarithmic scale



input files respectively. Techniques AES and FRSM take near same time to encrypt and decrypt the files where as TDES takes maximum time for both. In both the figures, the slopes of the curves for TDES are higher for larger source files.

### 4.2 Avalanche, Strict Avalanche and Bit Independence Values

Avalanche, Strict Avalanche and Bit Independence are cryptographic tests which measures the degree of security of cryptographic technique. The bit changes among encrypted bytes for a single bit change in the original message sequence for the entire or a relative large number of bytes. The values of Avalanche, Strict Avalanche and Bit Independence closer to 1.0 indicate the high degree of security. Table 1 shows the Avalanche, Strict Avalanche and Bit Independence values for all three techniques. For maximum files, all three measures using TDES, AES and FRSM are very near equal to 1. This analysis may indicate that FRSM provides very good security.

**Table 1** Avalanche and strict avalanche values for TDES, AES and FRSM

Sl. No	File type	Avalanche values			Strict avalanche values			Bit independence values		
		TDES	AES	FRSM	TDES	AES	FRSM	TDES	AES	FRSM
1	Txt	0.990	0.993	0.250	0.903	0.926	0.183	0.156	0.260	0.018
2	Zip	0.986	0.998	0.902	0.944	0.972	0.868	0.394	0.357	0.688
3	Txt	0.996	0.994	0.978	0.989	0.989	0.967	0.412	0.399	0.428
4	Txt	0.999	0.999	0.968	0.997	0.999	0.953	0.480	0.484	0.498
5	Jpg	0.999	0.999	0.992	0.999	0.999	0.990	0.971	0.975	0.983
6	docx	0.999	0.999	0.999	0.999	0.999	0.998	0.976	0.972	0.988
7	Exe	0.999	0.999	0.949	0.999	0.999	0.942	0.634	0.610	0.676
8	Png	0.999	0.999	0.998	0.999	0.999	0.998	0.990	0.991	0.991
9	Rar	0.999	0.999	0.973	0.999	0.999	0.968	0.998	0.997	0.983
10	Dll	0.999	0.999	0.990	0.999	0.999	0.989	0.753	0.755	0.751
11	Exe	0.999	0.999	0.949	0.999	0.999	0.942	0.746	0.740	0.752
12	docx	0.999	0.999	0.997	0.999	0.999	0.997	0.991	0.991	0.990
13	Dll	0.999	0.999	0.972	0.999	0.999	0.970	0.725	0.730	0.791
14	Jpg	0.999	0.999	0.971	0.999	0.999	0.968	0.995	0.995	0.976
15	Pdf	0.999	0.999	0.993	0.999	0.999	0.992	0.975	0.963	0.987
16	Avi	0.999	0.999	0.974	0.999	0.999	0.972	0.993	0.992	0.979
17	Rtf	0.999	0.999	0.991	0.999	0.999	0.986	0.374	0.339	0.356
18	Doc	0.999	0.999	0.996	0.999	0.998	0.993	0.340	0.221	0.415
19	Rar	0.999	0.999	0.995	0.999	0.999	0.994	0.999	0.999	0.996
20	Avi	0.999	0.999	0.768	0.999	0.999	0.737	0.988	0.988	0.631

### 4.3 Chi-square Values for Non-homogeneity Test

The large Chi-square values (compared with tabulated values) may confirm the high degree of non-homogeneity between the source and the encrypted streams. Table 2 shows the Chi-square values using Triple-DES (168 bits), AES (128 bits) and proposed FRSM. Average Chi-square values of all twenty files using TDES, AES and FRSM are 34,143,114,516, 32,603,653,699 and 33,190,935,529 respectively. It may indicates the security of FRSM be good and comparable with that of TDES and AES.

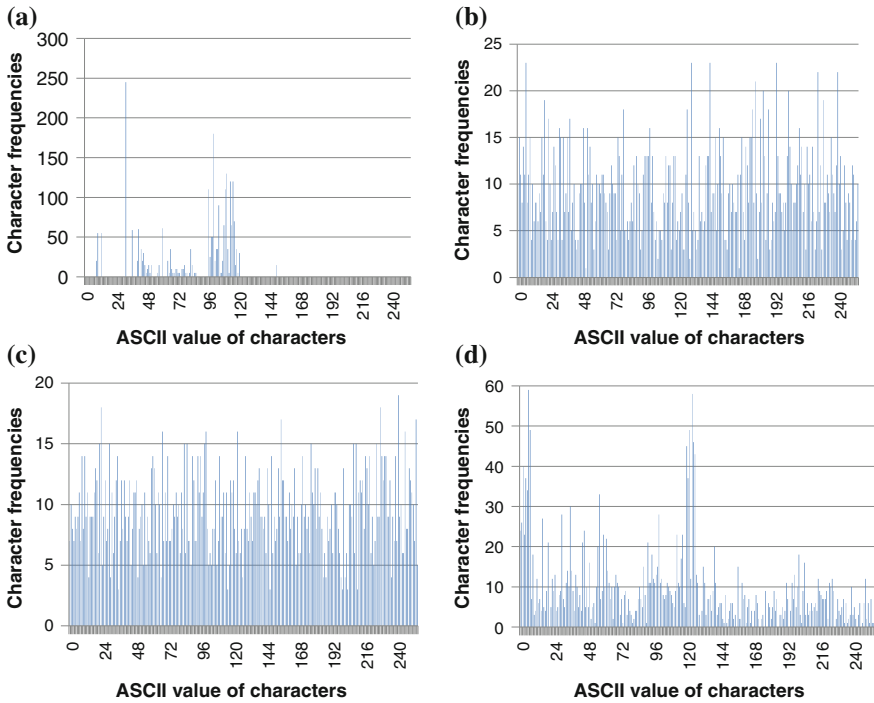


**Table 2** Chi-square values using TDES, AES and FRSM

Sl. No.	File type	File size (Bytes)	Chi-square values		
			TDES	AES	FRSM
1	Txt	50	114	111	141
2	Zip	288	503	529	542
3	Txt	500	1,470	1,546	1,837
4	Txt	2,410	24,059	20,981	51,264
5	Jpg	5,400	936	946	764
6	Docx	12,660	18,333	9,343	1,044
7	Exe	21,492	1,044,334	481,174	61,421
8	Png	50,952	6,085	6,086	4,679
9	Rar	115,595	1,031	1,038	806
10	Dll	215,416	530,985	473,027	275,729
11	Exe	624,128	2,027,106	1,848,171	1,348,006
12	Docx	1,224,413	54,964	55,574	43,742
13	Dll	1,409,024	3,219,751	3,139,562	15,85,202
14	Jpg	3,588,725	78,928	79,292	67,299
15	Pdf	4,446,250	413,610	369,563	652,379
16	Avi	7,355,928	438,208	442,887	225,162
17	Rtf	15,766,836	682,549,634,194	651,782,727,380	663,551,614,764
18	Doc	43,456,000	288,821,670	267,709,342	255,293,527
19	Rar	77,246,022	61,298	61,037	5,265
20	Avi	144,161,826	15,912,744	15,646,387	7,477,006
Average Chi-square values			34,143,114,516	32,603,653,699	33,190,935,529

#### 4.4 Character Frequencies Test

Analysis of Character frequencies for text file (serial number of file is 4) has been performed for TDES, AES and proposed FRSM. Figure 4a shows the spectrum of frequency distribution of characters in the plain text. Figure 4b–d show the spectrums of frequency distribution of encrypted characters in cipher text using TDES, AES and FRSM. In encrypted files, all characters with ASCII values ranging from 0 to 255 appear with certain frequencies. Therefore it is very difficult to detect the actual message for a cryptanalyst. It may indicate that the degree of security of proposed FRSM is very high and is comparable with that of TDES and AES.



**Fig. 4** **a** Graphical representation of the spectrum of frequency distribution of characters for source file. **b** Graphical representation of the spectrum of frequency distribution of characters for encrypted file using TDES. **c** Graphical representation of the spectrum of frequency distribution of characters for encrypted file using AES. **d** Graphical representation of the spectrum of frequency distribution of characters for encrypted file using FRSM

## 5 Conclusion

The proposed FRSM is simple to understand and easy to implement using various high level languages. The performance of FRSM is quite satisfactory because of high processing speed and the degree of security of FRSM may at par with other standard techniques like Triple DES and AES. So the proposed FRSM technique is comparable with the standard available encryption techniques and it is applicable to ensure good security in message transmission of any form through communication network.

## References

1. Navin, A.H., Oskuei, A.R., Khashandarag, A.S., Mirnia, M.: A novel approach cryptography by using residue number system. In: 6th International Conference on Computer Sciences and Convergence Information Technology (ICCIT 2011), pp. 636–639. Seogwipo, 29 Nov–01 Dec 2011
2. Niemiec, M., Machowski, L.: A new symmetric block cipher based on key-dependent S-Boxes. In: 4th International Congress on Ultra Modern Telecommunications and Control Systems and Workshops (ICUMT 2012), pp. 474–478. St. Petersburg, 3–5 Oct 2012
3. Verma, H.K., Singh, R.K.: Enhancement of RC6 block cipher algorithm and comparison with RC5 & RC6. In: 3rd IEEE International Advance Computing Conference (IACC 2013), pp. 556–561. Ghaziabad, 22–23 Feb 2013
4. Mandal, B.K., Bhattacharyya D., Bandyopadhyay, S.K.: Designing and performance analysis of a proposed symmetric cryptography algorithm. In: International Conference on Communication Systems and Network Technologies (CSNT 2013), pp. 453–461. Gwalior, 6–8 Apr 2013
5. Paul, M., Mandal, J.K.: A novel generic session based bit level cryptographic technique based on magic square concepts. In: International Conference on Global Innovations in Technology and Sciences (ICGITS 2013), pp. 156–163. SAINTGITS College of Engineering, Kottayam, 4–6 Apr 2013

# A PSO Based Fault Tolerant Routing Algorithm for Wireless Sensor Networks

Md Azharuddin and Prasanta K. Jana

**Abstract** The main source of energy consumption in the wireless sensor network is due to transmission and receiving of data packets. However the cluster head (CH) near to the base station (BS) in cluster based wireless sensor network depletes energy faster and die quickly due to transmission of heavier data traffic of other CHs to the BS. In this paper we propose a particle swarm optimization (PSO) based approach which construct the routing path and distribute the routing load over the CHs near to the BS and maximize the lifetime of networks. We also consider the fault tolerance issue due to the sudden failure of CHs during data routing phase. The simulation results show the effectiveness of the proposed algorithm over the existing algorithms.

**Keywords** Wireless sensor network · Routing · Lifetime · Fault tolerance · PSO

## 1 Introduction

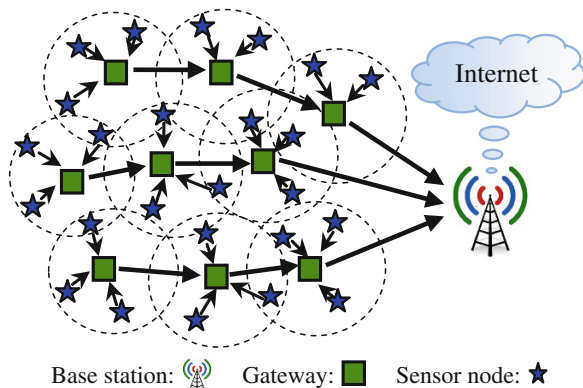
A wireless sensor networks (WSN) become attractive for their wide applications such as environmental monitoring, agriculture, health care, military, domestic and disaster management [1]. In a WSN, sensor nodes sense raw data from their surrounding, process them and finally transmit to a remote location called base station (BS). However unlike traditional networks, WSNs are limited with computation capability, memory and power consumption. Therefore resources should be used wisely to increase the lifetime of the network particularly the energy of the nodes as recharging and replacing the battery power is often infeasible. Many researchers have used the relay node or gateway [2, 3] to maximize the network lifetime as it energy and processing capability is higher than the normal sensor nodes. Moreover

---

M. Azharuddin (✉) · P.K. Jana  
Department of Computer Science and Engineering,  
Indian School of Mines, Dhanbad 826004, India  
e-mail: azhar\_ism@yahoo.in

P.K. Jana  
e-mail: prasantajana@yahoo.com

**Fig. 1** A wireless sensor network model



the relay nodes act as cluster head (CH) in hierarchical WSNs. The CHs in the cluster based WSNs are responsible for performing extra work load such as collecting data from its member sensor nodes, aggregation of this data and transmit it to the BS (see Fig. 1). Therefore high power relay nodes are superior for balancing data gathering and to extend the network lifetime. But the relay nodes are also battery operated and hence energy constraint. Moreover, the relay nodes closer to the BS are heavily loaded for supporting data traffic load of other relay nodes in multi hop communication system and they may die quickly. Failure of relay node has devastating impact to the network operation as the member sensor nodes become inactive and it leaves that portion of the target area uncovered. The relay node also acts as intermediate to forward data in multi hop communication system, therefore some relay nodes become unreachable to the BS due to the failure of a intermediate relay node and creates a network partition. Therefore, load balancing and fault tolerance routing is a challenging issue to the development of WSNs. Note that given  $m$  gateways and an average of  $d$  next hop gateways, there exist  $d^m$  number of valid routes to the BS which may high for a large scale WSN. Therefore, it is an optimization problem to select the best route among them and hence appeals for a metaheuristic approach such as PSO.

In this paper, we present a PSO based approach to construct an appropriate routing schedule for the hierarchical WSNs. We also present a runtime restoration of connectivity of the gateways to the BS in case of their failure during network operation. We perform extensive experiments on the proposed algorithms through simulation run and compare the results with two soft computing based routing algorithms using Genetic Algorithm (GA) as presented by Gupta et al. [4] and Ataul et al. [5]. The results demonstrate that our proposed algorithm performs better than these algorithms. Now onwards, we will be using relay node and gateway interchangeably for the rest of the paper.

The remaining paper is organized as follows. The related works are presented in Sect. 2. Section 3 presents the network model and the terminologies used. The proposed algorithm is presented in Sect. 4. Experimental results are given in Sect. 5 and the Sect. 6 concludes the paper.

## 2 Related Works

A number of routing algorithms have been developed for WSNs [6]. Low energy adaptive cluster hierarchy (LEACH) [7] is a popular clustering and single hop routing algorithm that dynamically rotates the work load of the CHs amongst the sensor nodes which is useful for load balancing. However, the disadvantage of this algorithm is that a node with very low energy may be selected as a CH and thus it can be quickly die. Many algorithms have been designed to improve the performance of LEACH [8]. There are also some routing algorithms which consider the fault tolerant issues [9, 10]. There are some metaheuristic based routing algorithms for WSNs [4, 5]. Ataul et al. [5] proposed a GA-based routing algorithm where selection of individuals is carried out using the Roulette-wheel selection method and the fitness function is defined by network lifetime. Gupta et al. [4] also proposed GA-based routing algorithm called GAR which minimizes the overall communication distance from the gateways to the BS. However, both of the algorithms [4, 5] consider only routing of aggregated data from the gateways to the BS without considering the fault tolerant routing issue. Chakraborty et al. [11] have presented a differential evolution based routing algorithm for more than a thousand relay nodes such that the energy consumption of the maximum energy-consuming relay node is minimized. However, the authors do not take care about the cluster formation and CH failure. Some improper clustering may lead to serious energy inefficiency of the relay nodes. PSO and ant colony optimization (ACO) are used in WSNs for other optimization problems also and they can be found in [12–15]. However, most of algorithms focus on energy efficiency only and none of the above algorithms consider balancing the routing load and fault tolerance issues simultaneously using bio-inspired algorithm.

## 3 Network Model and Terminologies

The model of the WSN assumed here consists of sensor nodes and less energy constraint gateways. All the nodes are deployed manually or randomly into the target region and they are stationary after deployment. A sensor node can communicate to a gateway if they are in the communication range of each other. All the communications are over wireless links and we also assume that wireless links are symmetric, so that, a node can compute the approximate distance to another node based on received signal strength. We use the following terminologies in the proposed algorithm.

1. The set of gateways denoted by  $G = \{g_1, g_2, \dots, g_m\}$  and  $g_{m+1}$  indicates the BS.
2.  $E_r(g_i)$  denotes the remaining residual energy of  $g_i$ .
3.  $R_{max}$  and  $d_{max}$  denote the maximum communication range of the gateways and sensor nodes respectively.
4.  $Next\_Hop(g_i)$  is the gateway  $g_j$  which is selected as next-hop gateway by  $g_i$  towards BS in data routing phase. Here, the next hop gateway may be the BS if the BS is within communication range of  $g_i$ .

## 4 Proposed Algorithm

The operation of the proposed routing algorithm is based on centralized approach and its basic idea is given as follows. At the beginning, each sensor node and gateway undergoes bootstrapping process where the BS assigns unique IDs to all of them. After that the sensor nodes and the gateways broadcast their IDs using CSMA/CA MAC layer protocol. Therefore, each gateway can collect the IDs of the all sensor nodes and the gateways which are within  $d_{max}$  and  $R_{max}$  communication range respectively. Finally, each gateway sends this local network information to the BS for network setup. The network setup consists of a setup phase followed by the steady-state phase. In the set up phase final route setup is done by the BS using the proposed algorithm. When the route setup phase is over, all the CHs are informed about their next hop CH towards the BS. The steady-state phase is divided into some pre-specified rounds, say 50 or 75 rounds. In each round the CHs receives data from its member sensor nodes, aggregate it and finally forward it to the BS. The network setup phase is repeated until there is path from a CH to the BS.

So we adopt an optimization tool like PSO to solve the problem. The basic steps of PSO can be seen in [15, 16]. Now we construct the fitness function for the above problem where our objective is to minimize the energy consumption and maximize the lifetime by distributing the routing load over the gateways in the network.

After receiving the local network information, the BS calculates routing load for each gateway i.e., number of data packets received (say  $P_r$ ) by the each gateway  $g_i$  per round. This can be done as follows.

$$P_r(g_i) = \begin{cases} \sum \{P_r(g_j) | Next\_Hop(g_j) = g_i, g_j \in G\}, & \text{If } Next\_Hop(g_j) = g_i, \forall g_j \in G \\ 0, & \text{Otherwise} \end{cases} \quad (1)$$

Suppose,  $E_R$ ,  $E_T(g_i, Next\_Hop(g_i))$  and  $E_{intra\_clstr}$  is the energy consumption of the gateways due to receiving, transmission of single data packets to its next hop gateway and energy consumption of a gateway  $g_i$  due to intra cluster activity like collection of data from member sensor nodes and aggregation of this data respectively. Therefore, energy consumption of a gateway  $g_i$  (i.e.,  $E_{consmpt}$ ) for supporting data routing in a round can be calculated as follows.

$$E_{consmpt}(g_i) = P_r(g_i) \times E_R + (P_r(g_i) + 1) \times E_T(g_i, Next\_Hop(g_j)) + E_{intra\_clstr}(g_i) \quad (2)$$

Note that we have added one in the data transmission part of the above equation because each gateway has its own data packet after aggregating the data received from its member nodes. Therefore, the lifetime of  $g_i$  with remaining residual energy  $E_r(g_i)$  can be calculated as follows.

$$Lifetime(g_i) = \frac{E_r(g_i)}{E_{consmpt}(g_i)} \quad (3)$$

Since our objective is to maximize the lifetime of gateways by minimizing their energy consumption rate through the balancing of routing load. This can be possible if we maximize the lifetime of the gateway with minimum lifetime by minimizing the routing load over the gateway. Therefore, it can be expressed as follows.

$$\text{Objective: Maximize } Lifetime = \min\{Lifetime(g_i) | \forall g_i \in G\} \quad (4)$$

The PSO based algorithm for the route setup is given in Fig. 2.

**Fault tolerance:** If the next hop gateway of a gateway is failed during the steady phase then the gateway selects another gateway toward the BS to continue its operation. The failure can be detected by a gateway if it does not receive any data

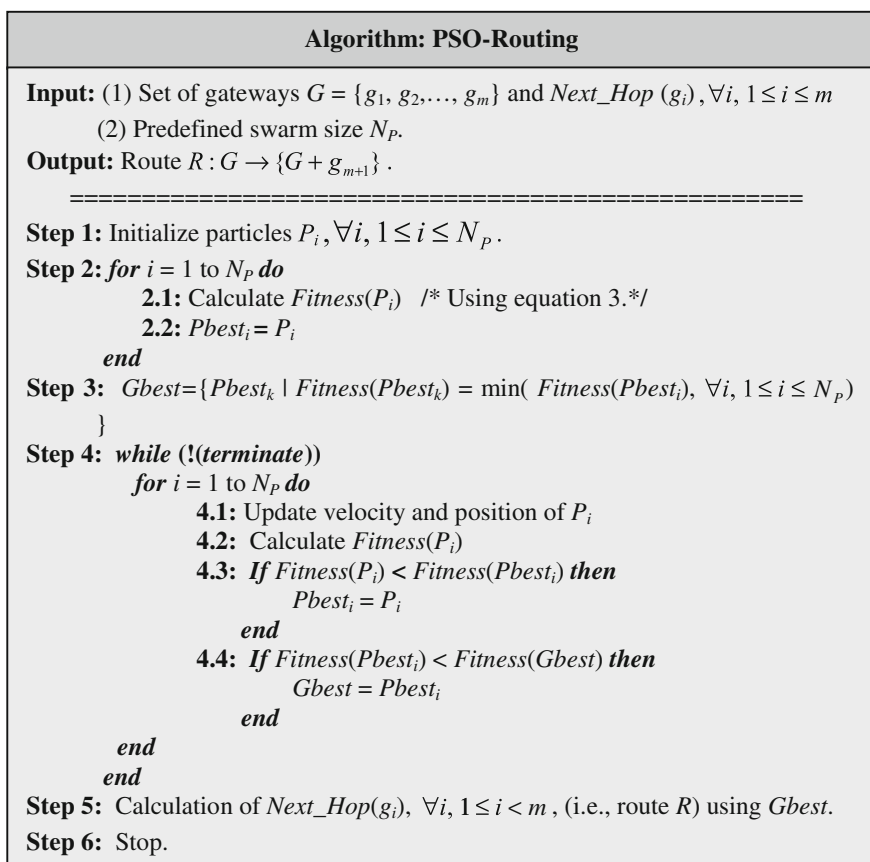


Fig. 2 PSO based routing algorithm

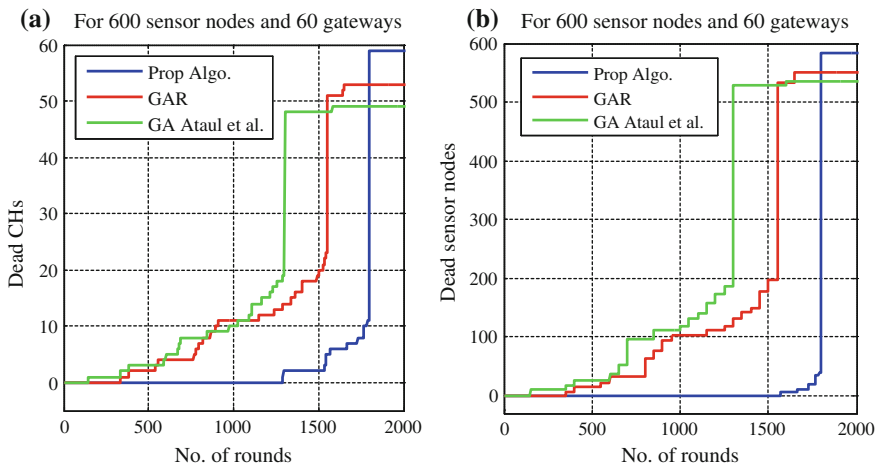


acknowledgement from its next hop gateway [17]. A gateway broadcasts a HELP message when it finds its next hop gateway to be faulty. All the neighbor gateways reply to the HELP message. After that the gateway joins a gateway with maximum lifetime towards the BS if there exists any gateway towards the BS, otherwise the gateway is considered as dead.

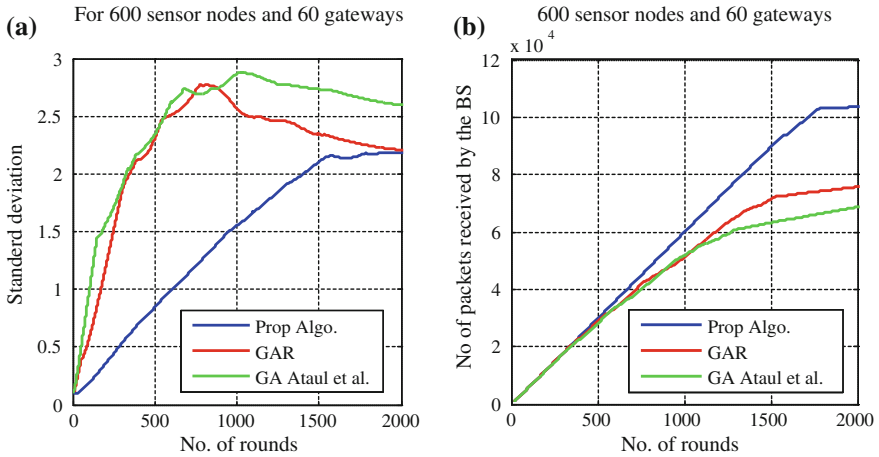
## 5 Simulation Result

We tested the proposed algorithm extensively using C and MATLAB version R2013a. The experiments were run for 600 sensor nodes and 60 gateways deployed in a  $500 \times 500$  square meter area and placing the BS at the coordinates (500, 250) on the boundary using equal scaling. We have also assumed that each sensor node and gateway have initial energy of 2 J and 10 J respectively. A node is considered to be dead if when its energy level reaches to 0 J. In our simulations, the typical energy model and parameters are set same as [7]. Moreover, we also considered an initial population of 60 particles to execute our proposed PSO based algorithms. The values of the PSO parameters were taken same as in [16]. We also executed an existing GA-based routing algorithm (GAR) presented by Gupta et al. [4] and a GA-based multi-hop routing algorithm (GA Ataul et al.) presented by Ataul et al. [5] for the comparison of the proposed algorithm. Note that there is no clustering phase in the proposed and existing algorithm, therefore we ran these algorithm with an existing GA-based clustering algorithm (GALBCA) presented by Kuila et al. [18].

First we compare the algorithms in terms of number of dead CHs. Figure 3(a) shows the number of dead CHs in the proposed algorithm is much lower and first CH is died after long time in the proposed algorithm. This is because we have



**Fig. 3** Comparison in terms of number of **a** dead CHs **b** number of dead sensor nodes



**Fig. 4** Comparison in terms of **a** standard deviation of remaining energy of CHs **b** number of packets received by the BS

distributed the routing load over the CHs specially the CHs near to the BS and thus quick death of CHs is reduced. On the other hand we have also restored the connectivity of the CHs whose next hop CH becomes faulty at any time of the routing phase. As the number of dead CHs is very less, therefore number of dead sensor nodes is also much less than the existing algorithms. This is shown in Fig. 3b.

Figure 4a shows the standard deviation of remaining energy of the CHs and it is much lower than the existing algorithms. This is because we have minimized the energy consumption of the CHs by distributing the routing load over them. Therefore we can claim that proposed algorithm balances the energy consumption in the network. The number of data packets received by the BS is also higher as number of alive CHs in the network is higher and it is shown in Fig. 4b.

## 6 Conclusion

In this paper, we have presented a PSO based routing algorithm which maximizes the lifetime of the network by minimizing the energy consumption of gateways, especially the gateways near to the BS by distributing the routing load over them. The routing algorithm has also considered the fault tolerance issue of the gateways. We have performed various experiments on the proposed algorithm and we have demonstrated that the algorithm performs better than two existing and related algorithms in terms of number of dead CHs, number of dead sensor nodes, standard deviation of remaining energy of CHs and number of data packets received by the BS. In the proposed algorithm, we have considered only routing phase and

permanent failure of the CHs for fault tolerance. In future, our attempt will be made to design energy aware routing and clustering emphasizing on partial and transient failure of the gateways.

## References

1. Akyildiz, I.F., Su, W., Sankarasubramaniam, Y.: A survey on sensor networks. *IEEE Commun. Mag.* **40**(8), 102–114 (2002)
2. Azharuddin, Md., Kuila, P., Jana, P.K.: A distributed fault tolerant clustering algorithm for wireless sensor networks. In: *IEEE ICACCI 2013*, pp. 997–1002 (2013)
3. Azharuddin, Md., Kuila, P., Jana, P.K.: Energy efficient fault tolerant clustering and routing algorithms for wireless sensor networks. *Comput. Electr. Eng.* <http://dx.doi.org/10.1016/j.compeleceng.2014.07.019> (2014)
4. Gupta, S.K., Kuila, P., Jana, P.K.: GAR: An energy efficient ga-based routing for wireless sensor networks. In: *ICDCIT 2013, LNCS 7753*, pp. 267–277 (2013)
5. Ataul, B., et al.: A genetic algorithm based approach for energy efficient routing in two-tiered sensor networks. *Ad Hoc Netw.* **7**, 665–676 (2009)
6. Akkaya, K., Younis, M.: A survey on routing protocols for wireless sensor networks. *Ad Hoc Netw.* **3**, 325–349 (2005)
7. Heinzelman, W., Chandrakasan, A., Balakrishnan, H.: Application specific protocol architecture for wireless microsensor networks. *IEEE Trans. Wireless Commun.* **1**(4), 660–670 (2002)
8. Tyagi, S., Kumar, N.: A systematic review on clustering and routing techniques based upon LEACH protocol for wireless sensor networks. *J. Netw. Comput. Appl.* **36**, 623–645 (2013)
9. Alwan, H., Agarwal, A.: A survey on fault tolerant routing techniques in wireless sensor networks. In: *Proceedings of 3rd International Conference Sensor Technologies and Applications*, Athens, Greece, June 2009, pp. 366–371 (2009)
10. Azharuddin, Md., Jana, P.K.: A distributed algorithm for energy efficient and fault tolerant routing in wireless sensor networks. *Wireless Netw.* <http://dx.doi.org/10.1007/s11276-014-0782-2> (2014)
11. Chakraborty, U.K et al.: Energy-efficient routing in hierarchical wireless sensor networks using differential-evolution-based memetic algorithm. In: *IEEE WCCI 2012*, pp. 1–8 (2012)
12. Saleem, M., et al.: Swarm intelligence based routing protocol for wireless sensor networks: Survey and future directions. *Inf. Sci.* **181**, 4597–4624 (2011)
13. Kulkarni, R.V et al.: Particle swarm optimization in wireless-sensor networks: A brief survey. *IEEE Trans. Syst. Man Cybern. Part C Appl. Rev.* **41**, 262–267 (2011)
14. Kuila, P., Jana, P.K.: A novel differential evolution based clustering algorithm for wireless sensor networks. *Appl. Soft Comput.* <http://dx.doi.org/10.1016/j.asoc.2014.08.064> (2014)
15. Kuila, P., Jana, P.K.: Energy efficient clustering and routing algorithms for wireless sensor networks: Particle swarm optimization approach. *Eng. Appl. Artif. Intell.* **33**, 127–140 (2014)
16. Daniel, B., Kennedy, J.: Defining a standard for particle swarm optimization. In: *Proceedings of the 2007 IEEE Swarm Intelligence Symposium*, pp. 120–127 (2007)
17. Banerjee, I., et al.: Effective fault detection and routing scheme for wireless sensor networks. *Comput. Electr. Eng.* **40**(2), 291–306 (2013)
18. Kuila, P., Gupta, S.K., Jana, P.K.: A novel evolutionary approach for load balanced clustering problem for wireless sensor networks. *Swarm Evol. Comput.*, vol. 12, pp. 48–56 (2013)

# Smallest Square Covering $k$ Points for Large Value of $k$

Priya Ranjan Sinha Mahapatra

**Abstract** Given a set of  $n$  planar points, a positive integer  $k(1 \leq k \leq n)$  and a geometric object, the objective of the  $k$ -cover problem is to find a smallest object such that it covers at least  $k$  input points. A deterministic algorithm is proposed to solve the  $k$ -cover problem when the object is an axis-parallel square and  $k > \frac{n}{2}$ . The time and space complexities of the algorithm are  $O(n + (n - k) \log^2(n - k))$  and  $O(n)$  respectively.

**Keywords** Computational geometry · Facility location · Minimum enclosing square · Matrix search

## 1 Introduction

Let  $S$  be a set of  $n$  planar input points. The points set  $S$  is said to be covered by a geometric object  $C$  if each point of  $S$  lies within the interior of  $C$  or on the boundary of  $C$ . The process of covering a set  $S$  by an object  $C$  is called full covering and the corresponding problem is known as full covering problem. The full covering problem has been well studied in different areas such as facility location, operation research, computational geometry etc. The covering objects used are a circle [1, 2], a rectangle [3], a square [4], a triangle [5], a circular annulus [6], a rectangular annulus [7], a rectilinear annulus [8] etc. Another purpose of covering is to cover the input points partially and corresponding problem is known as partial covering problem. Therefore, one objective of the partial covering problem is to find a smallest object of given type that covers at least  $k$  points of  $S$ . The partial covering problem is also well studied in theoretical computer science and the objects used to cover are a square [9, 10], a rectangle [11–13], and a circle [14]. In this paper we consider the partial covering problem where the covering object is an axis-parallel

---

P.R.S. Mahapatra (✉)

Department of Computer Science and Engineering, University of Kalyani, Kalyani, India  
e-mail: priya@klyuniv.ac.in

© Springer India 2015

J.K. Mandal et al. (eds.), *Information Systems Design and Intelligent Applications*,  
Advances in Intelligent Systems and Computing 339,  
DOI 10.1007/978-81-322-2250-7\_33

337

square. A square is said to be axis-parallel if each of its side is parallel to one of the coordinate axis. This problem is well studied in computational geometry with many variations [15–17]. Interested reader may read these papers [18–21] and the references therein for getting further variation of the partial covering problem. Another motivation of considering this problem comes from classification when the objective is to find a cluster of given shape that contains at least  $k$  points [22–24].

## 2 Preliminaries

The space of all candidate (or potential) solutions of a problem is called the *solution space*, or *search space*. There are some optimization problems for which these solution spaces are known. A well known such optimization problem is the *graph coloring problem* where the task is to find the minimum number of colors to color a graph, say  $G$ , and this number is called the *chromatic number* of  $G$ . Observe that the integral value of the chromatic number will vary between 1 and  $n$  where  $n$  is the number of vertices of the graph  $G$ . This observation implies that the solution space for the graph coloring problem is known. A general approach to solve this problem is as follows. First solve the decision version of such problem and then use the solution of this decision problem to solve the original problem. Observe that the decision version of the graph coloring problem can be expressed as “*is the graph  $G$  is  $k$  colorable?*”. The answer is always “Yes” or “No”. In this case the decision problem is NP-hard [25] and therefore it implies that the original graph coloring problem is also NP-hard.

## 3 Solution for General $k$

In this work we first consider the optimization problem of finding an axis-parallel square for general values of  $k$  that covers at least  $k$  points of  $S$  and the area (perimeter) is minimum. From now onwards a square means an axis-parallel square. Let *size* denote the length of a square. A square  $S_k$  covering  $k$  points of  $S$  is said to be  $k$ -cover square if there does not exist another square having area less than that of  $S_k$  and covering  $k$  points from  $P$  [16]. We have the following result on the characteristics of a  $k$ -cover square.

**Observation 1** Reference [17] *At least one pair of opposite sides of a  $k$ -cover square must contain points from  $P$ .*

This result implies that size of a  $k$ -cover square be determined from the set of horizontal and vertical distances generated from the pair of points in  $S$ . Therefore the solution space for this optimization problem is known. The decision version of this problem can be defined as “*given a length  $\delta$ , does there exist a square of size  $\delta$*

that covers at least  $k$  points of  $S$ ?”. Let  $MaxCover(\delta)$  denote the square of size  $\delta$  that covers the maximum number of points of  $S$ . Note that the decision problem of the original problem is same with the problem of finding a location of  $MaxCover(\delta)$ . The following result in [18] is used to locate  $MaxCover(\delta)$ .

**Result 1** Reference [18] *Given the length  $\delta$ , a location of  $MaxCover(\delta)$  can be computed in  $O(n \log n)$  time using  $O(n)$  space.*

Let  $S = \{p_1, p_2, \dots, p_n\}$  be the set of points on the plane. Without loss of generality let these points of  $S$  be in non-decreasing order on  $x$ - coordinate. Here we use  $(x(p), y(p))$  to denote a point of  $S$ . Note that the result in Observation 1 implies each of two horizontal sides (or two vertical sides) of a  $MaxCover(\delta)$  must contains a point of  $S$ . Thus two types of solutions are required to consider to solve this problem. As these two types are symmetric, the techniques required to find of any one type can be easily extended for other. Therefore, without loss of generality, we assume that each horizontal side of the  $MaxCover(\delta)$  is containing a point of  $S$ . The solution space of the original problem can be viewed as matrix  $M$  given below.

$$\begin{pmatrix} x(p_2) - x(p_1) & x(p_3) - x(p_1) & \dots & x(p_{n-1}) - x(p_1) & x(p_n) - x(p_1) \\ x(p_3) - x(p_2) & x(p_4) - x(p_2) & \dots & x(p_n) - x(p_2) & \\ \dots & \dots & \dots & & \\ \dots & \dots & \dots & & \\ x(p_{n-1}) - x(p_{n-2}) & x(p_n) - x(p_{n-2}) & & & \\ x(p_n) - x(p_{n-1}) & & & & \end{pmatrix}$$

We now conclude that the solution space of the problem can be stored in a lower (upper) triangular matrix of order  $(n - 1) \times (n - 1)$ . The first row of the matrix  $M$  contains  $(n - 1)$  horizontal distances, second row of  $M$  contains  $(n - 2)$  horizontal distances, and so on. This generalization implies that the  $i$ th row of  $M$  has  $(n - i)$  horizontal distances for  $i = 1, 2, \dots, (n - 1)$ . We now compute the number of input points covered by the  $MaxCover(\delta)$  using Result 1 for each value of  $\delta(\in M)$ . Moreover we store the current minimum value of  $\delta$  for which the square  $MaxCover(\delta)$  covers at least  $k$  points of  $S$ . Note that Result 1 can be used to find a placement of  $MaxCover(\delta)$  in  $O(n \log n)$  time and the value of  $\delta$  is one among  $O(n^2)$  values of matrix  $M$ . Thus we can derive the following straight forward result.

**Result 2** *Let  $S$  be the set of  $n$  input points on the plane and  $k(\leq n)$  be an integer constant. A smallest axis-parallel square covering at least  $k$  input points can be found in  $O(n^3 \log n)$  time and  $O(n)$  space.*

### 4 Improvement Using Matrix Search for $k > \frac{n}{2}$

We now improve Result 2 for large values of  $k$  ( $k > \frac{n}{2}$ ). Let  $S_1, S_2, S_3, S_4$  and  $S_5$  be a partition of  $S$  such that  $S = S_1 \cup S_2 \cup S_3 \cup S_4 \cup S_5$  and all the partitions are not required to be pairwise disjoint.  $S_1$  and  $S_2$  are the  $(n - k)$  left most and right most points of  $S$  respectively.  $S_3$  and  $S_4$  are the  $(n - k)$  bottom most and top most points of  $S$  respectively. Moreover  $S_5 = S - S'$  where  $S' = S_1 \cup S_2 \cup S_3 \cup S_4$ . Let the minimum enclosing rectangle (MER)  $R$  contain all points of  $S_5$ . The boundaries of  $R$  is closed in the sense that each side of  $R$  contains at least one point of  $S$ . The following result in [17] is used for  $k > \frac{n}{2}$ .

**Observation 2** Reference [17] *For  $k > n/2, S_k$  must covers all the points of  $R$ .*

The length of the largest side of the minimum enclosing rectangle  $R$  is denoted by  $\Delta$ . The following result is extended in [17] to compute a placement of  $MaxCover(\delta)$  when  $\delta > \Delta$ .

**Result 3** Reference [17] *A placement of  $MaxCover(\delta)$  for a given  $\delta > \Delta$  can be found in  $O((n - k) \log(n - k))$  time using  $O(n)$  space.*

Define  $Q$  be the subset of  $S$  such that  $Q$  is the points of  $S'$  and the points on the boundary of the minimum enclosing rectangle  $R$ . Let  $= \{q_1, q_2, \dots, q_r\}$  denote the non decreasing order of the points in  $Q$  on  $x$ -coordinate. Observe that the number of points in  $Q$  is  $r$  and  $r$  is of  $O(n - k)$ . Moreover the value of  $r$  is at most  $4(n - k)$ . We use  $q_\alpha$  and  $q_\beta$  to denote the points of  $S$  those lie on the right and left side of the minimum enclosing rectangle  $R$  respectively. The results in Observation 2 and Observation 1 imply that the solution space for finding  $S_k$  for  $k > \frac{n}{2}$  is now reduced from the above matrix  $M$  to the following matrix  $N$ .

$$\begin{pmatrix} x(q_\alpha) - x(q_1) & x(q_{\alpha+1}) - x(q_1) & \dots & x(q_r) - x(q_1) \\ x(q_\alpha) - x(q_2) & x(q_{\alpha+1}) - x(q_2) & \dots & x(q_r) - x(q_2) \\ \dots & \dots & \dots & \dots \\ x(q_\alpha) - x(q_i) & x(q_{\alpha+1}) - x(q_i) & \dots & x(q_r) - x(q_i) \\ \dots & \dots & \dots & \dots \\ x(q_\alpha) - x(q_\beta) & x(q_{\alpha+1}) - x(q_\beta) & \dots & x(q_r) - x(q_\beta) \end{pmatrix}$$

Note that the number of elements in the matrix  $N$  is  $O((n - k)^2)$ . We can now use Result 3 for each entry of  $N$ . Thus the following result can be found like earlier.

**Result 4** *Let  $S$  be the set of  $n$  input points on the plane and  $k (> \frac{n}{2})$  be an integer constant. A smallest axis-parallel square covering at least  $k$  points of  $S$  can be found in  $O((n - k)^3 \log(n - k))$  time using  $O(n)$  space.*

It is now shown that the standard *sorted matrices search* by Frederickson and Johnson [26] can be used to improve Result 4. Sorted matrices search is basically a

prune and search technique. The technique has been demonstrated in the last decade in various works dealing with (not only) covering problems and facility location [27]. The idea is to define a decision problem of the original optimization problem and then perform a kind of binary search in order to determine the optimal (in this case, smallest area) value. Recall that in our case, the objective of the decision version of the problem is to find a placement of the square  $MaxCover(\delta)$  where  $\delta \in N$ . Note that elements in each row are in non-increasing order. The same ordering is also true for elements in each column of  $N$ . This implies that  $N$  is a sorted matrix [26, 28]. Using our decision problem we can make a kind of binary search using the sorted matrix  $N$  obtaining running time of  $O(T_d * \log(n - k) + n)$ , where  $T_d$  is the running time of the decision algorithm. Here the task of the decision algorithm is to find a placement of the square  $MaxCover(\delta)$  for  $\delta > \Delta$ . It follows from Result 3 that  $T_d = O((n - k) \log(n - k))$ . In a similar pass we can find another potential solution keeping time and space complexities unchanged. Thus we have the following result.

**Result 5** *Let  $S$  be the set of  $n$  input points on the plane and  $k (> \frac{n}{2})$  be an integer constant. A smallest area square covering at least  $k$  points of  $S$  can be found in  $O(n + (n - k) \log^2(n - k))$  time using  $O(n)$  space.*

## 5 Conclusion

An  $O(n + (n - k) \log^2(n - k))$  time algorithm is proposed to identify a smallest axis-parallel square that covers at least  $k$  points among a set of  $n$  points. It is shown that the search space of the decision problem of the original optimization problem is a sorted matrix when  $k > \frac{n}{2}$ . However, the solution space of the decision problem is not a sorted matrix for general  $k$ . This observation mainly forces the authors in [18] to use another prune and search technique other than matrix search to solve the optimization problem for general  $k$  and their solution requires  $O(n \log^2 n)$  time and  $O(n)$  space. It would be interesting to investigate the possibility of finding an efficient search technique that can reduce the complexity of the optimization problem for general  $k$  other than the method used in [18].

## References

1. Megiddo, N.: Linear-time algorithms for linear programming in  $\mathbb{R}^3$  and related problems. SIAM J. Comput. **12**, 759–776 (1995)
2. Preparata, F.P., Shamos, M.I.: Computational Geometry: An Introduction. Springer, Berlin (1990)
3. Toussaint, G.T.: Solving geometric problems with the rotating calipers. In: Proceedings of IEEE MELECON (1983)
4. Katz, M.J., Kedem, K., Segal, M.: Discrete rectilinear 2-center problems. Comput. Geom. **15**, 203–214 (2000)



5. O'Rourke, J., Aggarwal, A., Maddila, S., Baldwin, M.: An optimal algorithm for finding minimal enclosing triangles. *J. Algorithms* **7**, 258–269 (1986)
6. Agarwal, P.K., Sharir, M., Toledo, S.: Applications of parametric searching in geometric optimization. *J. Algorithms* **17**, 292–318 (1994)
7. Mukherjee, J., Mahapatra, P.R.S., Karmakar, A., Das, S.: Minimum-width rectangular annulus. *Theoret. Comput. Sci.* **508**, 74–80 (2013)
8. Gluchshenko, O., Hamacher, H.W., Tamir, A.: An optimal  $O(n \log n)$  algorithm for finding an enclosing planar rectilinear annulus of minimum width. *Oper. Res. Lett.* **37**, 168–170 (2009)
9. Datta, A., Lenhof, H.E., Schwarz, C., Smid, M.: Static and dynamic algorithms for k-point clustering problems. *J. Algorithms* **19**, 474–503 (1995)
10. Smid, M.: Finding k points with a smallest enclosing square. Report MPI-92-152, Max-Planck-Institute für Informatik, Saarbrücken (1992)
11. Aggarwal, A., Imai, H., Katoh, N., Suri, S.: Finding k points with minimum diameter and related problems. *J. Algorithms* **12**, 38–56 (1991)
12. Ahn, H.K., Bae, S.W., Demaine, E.D., Demaine, M.L., Kim, S.S., Korman, M., Reinbacher, I., Son, W.: Covering points by disjoint boxes with outliers. *Comput. Geom. Theory Appl.* **44**, 178–190 (2011)
13. Segal, M., Kedem, K.: Enclosing k points in the smallest axis parallel rectangle. *Inf. Process. Lett.* **65**, 95–99 (1998)
14. Matoušek, J.: On geometric optimization with few violated constraints. *Discrete Comput. Geom.* **14**, 365–384 (1995)
15. Chan, T.M.: Geometric applications of a randomized optimization technique. *Discrete Comput. Geom.* **22**, 547–567 (1999)
16. Das, S., Goswami, P.P., Nandy, S.C.: Smallest k-point enclosing rectangle and square of arbitrary orientation. *Inf. Process. Lett.* **94**, 259–266 (2005)
17. Mahapatra, P.R.S., Karmakar, A., Das, S., Goswami, P.P.: k-enclosing axis-parallel square. LNCS 6784, pp. 84–93. Springer, New York (2011)
18. Mahapatra, P.R.S., Goswami, P.P., Das, S.: Covering points by isothetic unit squares. In: *Proceeding of the 19th Canadian Conference on Computational Geometry (CCCG 2007)*, pp. 169–172 (2007)
19. Mahapatra, P.R.S., Goswami, P.P., Das, S.: Maximal covering by two isothetic unit squares. In: *Proceeding of the 20th Canadian Conference on Computational Geometry (CCCG 2008)*, pp. 103–106 (2008)
20. Atta, S., Mahapatra, P.R.S.: Genetic Algorithm Based Approach for Serving Maximum Number of Customers Using Limited Resources, vol. 10, pp. 492–497. Elsevier, Amsterdam (2013)
21. Atta, S., Mahapatra, P.R.S.: Genetic Algorithm Based Approaches to Install Different Types of Facilities, vol. 248, pp. 195–203, AISC (Springer) (2014)
22. Andrews, H.C.: *Introduction to Mathematical Techniques in Pattern Recognition*. Wiley-Intersciences, New York (1972)
23. Asano, T., Bhattacharya, B., Keil, M., Yao, F.: Clustering algorithms based on maximum and minimum spanning trees. In: *Proceeding of the 4th Annual Symposium on Computational Geometry*, pp. 252–257 (1988)
24. Hartigan, J.A.: *Clustering Algorithms*. Wiley, New York (1975)
25. Cook, S.: The complexity of theorem proving procedures. In: *Proceeding of the 3rd Annual ACM Symposium on Theory of Computing*, pp. 151–158 (1971)
26. Frederickson, G.N., Johnson, D.B.: Generalized selection and ranking: sorted matrices. *SIAM J. Comput.* **13**, 14–30 (1984)
27. Drezner, Z., Hamacher, H.: *Facility Location: Applications and Theory*. Springer, Berlin (2002)
28. Glzman, A., Kedem, K., Shpitalnik, G.: On some geometric selection and optimization problems via sorted matrices. *Comput. Geom. Theory Appl.* **11**, 17–28 (1998)

# Connectionist Approach for Emission Probability Estimation in Malayalam Continuous Speech Recognition

Anuj Mohamed and K.N. Ramachandran Nair

**Abstract** Automatic speech recognition is one active research area which can exploit the pattern recognition capabilities of artificial neural networks. Several researchers have shown that the outputs of artificial neural networks trained in multi-class classification mode can be interpreted as estimates of a posteriori probabilities of output classes. These probabilities can be used by the state-of-the-art hidden Markov model for speech recognition in estimating the emission probabilities of the states of the hidden Markov model. In this paper, we explore a pairwise neural network system as an alternative approach to multi-class neural network systems to estimate the emission probabilities of the states of a hidden Markov model. Through experimental analysis it is shown that the pairwise recognition system outperforms the multiclass recognition system in terms of the recognition accuracy of spoken sentences.

**Keywords** Continuous speech recognition • Malayalam speech recognition • Multi-class pattern classification • Pairwise pattern classification

## 1 Introduction

Automatic speech recognition (ASR) is a classic pattern recognition problem that aims to produce a text transcription of spoken words automatically. Research in this area attained attention of researchers because of the fast growing demands of ASR systems in versatile applications. The dominant technology for ASR is hidden

---

A. Mohamed (✉)

School of Computer Sciences, Mahatma Gandhi University, Kottayam, Kerala, India  
e-mail: anujmohamed@mgu.ac.in

K.N. Ramachandran Nair

Department of Computer Science and Engineering, Viswa Jyothi College of Engineering and Technology, Vazhakulam, Muvattupuzha, Kerala, India  
e-mail: knrn@hotmail.com

© Springer India 2015

J.K. Mandal et al. (eds.), *Information Systems Design and Intelligent Applications*,  
Advances in Intelligent Systems and Computing 339,  
DOI 10.1007/978-81-322-2250-7\_34

343

Markov model (HMM). An HMM is typically defined and represented as a stochastic finite state automation usually with a left-to-right topology as proposed in [1]. An HMM models an utterance as a succession of discrete stationary states with instantaneous transitions between the states and generates an observation [2]. The sequence of states, which represents the spoken utterance, is “hidden” and the parameters of the probability density functions of each HMM state are needed in order to associate a sequence of states to a sequence of observations. i.e., for any state sequence, the sequence of states can be observed only through the emission/output probability distribution.

State-of-the-art continuous speech recognition (CSR) systems select basic sound units from a limited inventory, like sub-word units, syllables, phonemes, allophones etc. Each basic acoustic unit is modeled by one or more states of an HMM. Being a parametric model, HMM assumes that the underlying speech patterns have Gaussian distribution. Gaussian mixture models (GMM) are often used within each HMM state to model the emission probability of the acoustic patterns associated to that state. Several researchers [3, 4] have shown that the outputs of artificial neural networks (ANNs) trained in classification mode can be interpreted as estimates of a posteriori probabilities of output classes conditioned on the input. Using Bayes’ rule, these state posteriors can be converted to likelihoods required by the HMM framework.

Use of ANN as emission probability estimator has shown good performance for ASR systems for various western languages [5, 6]. Application of multilayer perceptrons (MLP) trained in multi-class classification mode as emission probability estimator in an HMM based CSR system for Malayalam language is proposed in [7]. Many real applications translate into classification problems with a large number of classes and a huge amount of data. ASR falls into this category and the high number of classes to be separated makes the boundaries between classes complex. A multi-class classifier cannot perform at a high level in such cases as the classification algorithm has to learn to construct a large number of separation boundaries. Many studies have demonstrated that an adequate decomposition of such real world problems into sub problems can be favorable to the overall computational complexity. The pairwise classification approach has produced good results when applied to face recognition [8] and cursive handwriting recognition [9]. The efficiency of such pairwise ANN classifiers has not been explored sufficiently in ASR applications. A pairwise classifier for multi-class pattern classification in the context of vowel classification tasks is proposed in [10]. Motivated by this fact, this paper examines the prospect of using a pairwise classification approach for multi-class pattern classification, as a way to improve overall classifier performance. In the present paper, we report on the application of pairwise approach for improving the recognition accuracy of the CSR system for Malayalam language.

This paper is organized as follows. Section 2 gives an overview of ASR system. ANN as phonetic probability estimator of HMM states is explained in Sect. 3. Section 4 details the feature extraction, emission probability estimation using multi-class and pairwise ANN classifiers and the decoding process. Experiments

conducted and the results obtained are given in Sect. 5. Conclusions and future work to enhance the performance of the system are given in Sect. 6.

## 2 Automatic Speech Recognition: Mathematical Formulation

The ASR problem in general can be viewed as a pattern recognition problem. Given an acoustic sequence  $O$  and a sequence of words  $W$ , the goal of the system is to find the most likely word sequence  $W'$  such that

$$W' = \arg \max_w P(W|O). \quad (1)$$

Applying Bayes' rule to this fundamental equation of speech recognition returns

$$W' = \arg \max_w \frac{P(O|W)P(W)}{P(O)}. \quad (2)$$

As  $P(O)$  is equivalent for all complete decodings of  $O$ , this can be ignored, to give the equation

$$W' = \arg \max_w P(O|W)P(W). \quad (3)$$

$P(W)$  is the priori probability of the word sequence  $W$  and is computed using the language model.  $P(O|W)$  is the conditional probability of the acoustic sequence  $O$  given the word sequence  $W$ , and is computed using the acoustic model. A continuous density hidden Markov model which models the real valued vector sequences resulting from acoustic parameter extraction is used as the acoustic model in state-of-the-art continuous speech recognition systems.

## 3 ANN as Phonetic Probability Estimator in HMM

The state-of-the-art HMM framework for ASR uses GMM to estimate the emission probabilities of the HMM states. An important stage in the development of an HMM based ASR system is the accurate estimation of the emission probabilities. The training algorithm for the estimation of the parameters of the GMM is based on likelihood maximization, which assumes correctness of the models and implies poor discrimination. Also, maximizing the likelihood of the training data is not closely related to the typical evaluation criteria of the recognizer: the error rate. These issues with maximum likelihood (ML) estimation motivate an alternative form of estimating model parameters called discriminative training. A model used

for representing a phonetic class is said to be discriminant if it maximizes the probability of producing an associated set of features while minimizing the probability that they have been produced by rival models.

ANNs with its several features, such as their nonlinearity and high classification capability, is a promising field for solving real world problems. Neural network classifiers are easier to apply to real-world problems because they are less sensitive to assumed underlying distributional forms than more conventional probabilistic approaches. ANN by itself has not been shown to be effective for recognition of continuous speech. ASR systems can exploit the pattern classification capabilities of ANNs as it involves development of pattern classification models from speech data. When an ANN is used to solve a classification problem, the network can be trained either to provide the classification directly or to model the posterior probabilities of class membership. Using Bayes' rule, these probabilities can be converted to likelihoods required by the HMM. ANN follows discriminant-based learning. i.e., the network during training maximizes the probability of producing an associated set of features while minimizing the probability that they have been produced by rival models.

ASR falls into the category of classification problems with a large number of classes and a huge amount of data. The large number of classes to be separated makes the boundaries between classes complex. A multi-class classifier cannot perform at a high level in such cases as the classification algorithm has to learn to construct a large number of separation boundaries. Computationally expensive learning algorithms learn many small problems much faster than a few large problems. Therefore, the use of posteriors derived from pairwise classifiers may be helpful to improve the performance. Motivated by this fact, the prospect of pairwise modeling approach for multi-class pattern classification is explored in this paper. The pairwise approach to pattern classification is simple since the binary decision is learned on fewer training examples. It also helps to improve the generalization ability of the network because of the redundancy in the training data.

## **4 Experimental Setup**

### ***4.1 Speech Corpora***

Malayalam is a Dravidian language spoken mainly in the South West of India. Research in Malayalam speech recognition has started recently and the area of CSR is relatively less investigated. The speech corpora developed for training and testing the CSR system described in this paper contains naturally and continuously read Malayalam sentences from both male and female speakers who speak various dialects of Malayalam. Two databases (Dataset1 and Dataset2) for training and one (Dataset3) for testing were developed. The entire corpus consists of 255 sentences with 1,275 words and a total of 7,225 phonemes by 20 (9 male & 11 female) different speakers.

## ***4.2 Acoustic Pre-processing***

The acoustic pre-processor extracts a compact set of features required for speech recognition. The feature vector used in this work is mel-frequency cepstral coefficients (MFCC). The feature vectors are extracted by the following procedure. First the speech signal is digitized at 8 kHz sampling rate with A/D conversion precision of 16 bits. An FFT is performed on every 8 ms on a window of 256 samples which produced 12 dimensional vectors representing the energy in 28 triangular filters spaced according to the mel-frequency scale.

## ***4.3 HMM Emission Probability Estimation Using Multi-Class MLP Classifiers***

In the multi-class classification approach, a single network is used to generate posterior probabilities of all the selected classes. When an input vector,  $x$ , is presented to the network, the activation of each output unit represents the corresponding posterior probability, provided the system has enough parameters and the training does not get stuck at a local minimum. HMMs use likelihoods  $P(O|W)$  where  $O$  is the acoustic observation and  $W$  is the acoustic model. But the neural network estimates the posteriors  $P(W|O)$  and this can be converted to likelihoods by applying the Bayes' rule. This can be achieved by dividing the posterior estimates from the MLP outputs by estimates of corresponding class priors. Supervised training using ANN requires the temporal segmentation of the training sentences and frame labeling. As hand segmentation of the speech corpus is tedious, the baseline CDHMM system described in [11] is used to generate segmented training data by Viterbi-aligning the training reference transcription to the acoustic data.

The multi-class classifier used in this work is a two-layer MLP with a single hidden layer. The input feature vector given to the network is computed from a window of seven speech frames i.e., acoustic vectors from the frame to be classified along with three surrounding frames for the left and right contexts, respectively. A frame is represented by a spectral vector of 12 acoustic features computed every 10 ms. So the input layer of the network has 84 nodes. The hidden layer has 95 nodes all with sigmoid activation function. The output layer has number of nodes corresponding to the context independent phonetic units. The output unit corresponding to the input vectors class has a value "1" while all other outputs have value "0". Network output should sum to one for each input value if outputs accurately estimate the posterior probabilities. This is achieved by using the softmax activation function at the output layer. The cross-entropy error function for multi-class classification problem is used to compute the error between the output of the ANN and the target vector. Back-propagation with batch mode of updating the weights is used for training the network.

#### 4.4 HMM Emission Probability Estimation Using Pairwise MLP Classifiers

In the pairwise approach to  $K$ -class pattern classification there are  $K(K-1)/2$  binary neural networks. The outputs of the pairwise neural network classifiers provide the probabilities  $p_{ij}$  for all pairs of classes  $(i, j)$  with  $i \neq j$ . Let  $p_{ij}(x)$  be the pairwise class probability estimate of the input vector  $x$  to belong to class  $i$ , with  $i \neq j$ . Then the pairwise class probability estimate of the input vector  $x$  to belong to class  $j$ , is given by  $p_{ji}(x) = 1 - p_{ij}(x)$ . Now the multi-class posteriori probabilities are estimated by combining the outputs of the  $K(K-1)/2$  pairwise classifiers using the method described in [9] i.e.,

$$P(c_i|x) = \frac{1}{\sum_{j=1; j \neq i}^K \frac{1}{p_{ij}} - (K - 2)} . \quad (4)$$

For each pair of classes a two layered MLP with a single output unit is created as it is trained on the data of the two classes. The first 12 MFCCs extracted from the input speech signal is used as the input to the network and the MLP has input nodes corresponding to the number of acoustic features. As each of the  $K$  pattern classes is trained against every one of the remaining pattern classes, the redundancy in the training data improves the generalization ability of the network and there is no need to incorporate contextual information. This reduces the dimension of the input feature vector. The output layer consists of a single neuron with sigmoid activation function which has an output range  $[0, 1]$  representing the output phoneme class. The activation function used by the hidden units is sigmoid and the optimal number of hidden units is determined empirically.

The back-propagation algorithm with cross-entropy error criteria is used for training the network. The weights and biases of the network are initialized randomly. In order to make the network training more efficient, the inputs and outputs are normalized to have zero mean and unit standard deviation. In order to improve the generalization capability of the network, performance obtained on a cross-validation set is used as the stopping criterion. The cross-validation set contains the speech utterances that are not used for training. Training continued as long as the performance on the validation set is improved and the training is stopped when the network ceased to improve.

#### 4.5 Decoding and Model Evaluation

Decoding refers to the process of searching for the sub word sequence that may have generated an observation sequence. In CSR, this is achieved by inferring the actual sequence of states that generated the given observation sequence and then

recovering the word sequence from the state sequence. The Viterbi [12] algorithm is widely used for decoding in ASR systems. This algorithm returns a single best state sequence for an unknown input sequence. Trace back through this sequence gives the most likely phone and word sequence. The hypothesized transcription and the reference transcription can then be compared by evaluating their distance according to the Levenshtein metric, in terms of insertions, deletions and substitutions. Using these measures, the word error rate (WER), a common evaluation measure for ASR systems, is computed.

## 5 Results and Discussions

This section compares the recognition performance of the Malayalam CSR system, when the posteriors were estimated using the MLP trained with multi-class and pairwise classification approaches. Table 1 shows the WER of both the systems and the percentage reduction in WER obtained when the pairwise classification approach was used for the emission probability estimation. A strong improvement in recognition performance was observed when the HMM emission probabilities were computed using the pairwise classification approach i.e., a relative improvement of 66.67 % and 57.23 % were obtained when the system was trained with Dataset1 and Dataset2 respectively. This result supports the use of MLPs trained in pairwise classification mode for the estimation of emission probabilities of HMM states.

The pairwise approach yields a more flexible class of models than a multi-class approach, as only one decision boundary requires attention. Number of free parameters to be trained in the case of the two approaches, for the best recognition performance obtained, is shown in Table 2.

**Table 1** Performance of the system with multilayer perceptrons trained with multi-class and pairwise classification approaches for HMM emission probability estimation

Training datasets	WER		% Reduction in WER Multi-class → pairwise
	Multi-class MLP classifier	Pairwise MLP classifier	
Dataset1	2.67	0.89	66.67
Dataset2	3.11	1.33	57.23

**Table 2** Comparison of trainable parameters: HMM with GMM emission probabilities versus HMM/ANN hybrid approaches with MLPs trained in multi-class and pairwise classification modes for emission probability estimation

No. of trainable parameters		% Reduction in Trainable parameters
Multi-class MLP classifier	Pairwise MLP classifier	Multi-class MLP classifier → pairwise MLP classifier
10,475	8,700	16.95



## 6 Conclusions

Recognition accuracy is an important aspect of ASR systems. They must achieve a very high level of performance to be of general interest as a man-machine interface. Enhancing recognition accuracy by way of improving discrimination between pattern classes is one of the fundamentally important research areas for speech recognition. This paper has examined the integration of MLPs trained in pairwise classification mode as emission probability estimators in an HMM based continuous Malayalam speech recognition system. The system with MLPs trained in pairwise classification mode outperforms the system with multiclass classification approach in terms of recognition accuracy of the spoken sentences. The proposed pairwise approach is simple since the binary decision is learned on fewer training examples. It also improves the generalization ability of the network because of the redundancy in the training data and is very useful in the case of very limited training material. Also, adding a new class or modifying the training set of an existing one can be done without retraining all two-class classifiers.

In this work, the a posteriori probabilities obtained from the MLPs trained in multiclass and pairwise classification modes were used as the estimates of emission probabilities of HMM states in an HMM based Malayalam CSR system. Auto associative neural networks and deep neural networks are two emerging alternatives to MLPs as emission probability estimators. The use of these neural network architectures may further improve the performance of the system.

## References

1. Bakis, R.: Continuous speech recognition via centiseconds acoustic states. *J. Acoust. Soc. Am.* **59**, (S1) (1976)
2. Rabiner, L.R.: A tutorial on hidden markov models and selected applications in speech recognition. *Proc. IEEE* **77**, 257–285 (1989)
3. Richard, M.D., Lippmann, R.P.: Neural network classifiers estimate bayesian a posteriori probabilities. *Neural Comput.* **3**, 461–483 (1991)
4. Bourlard, H., Morgan, N.: Continuous speech recognition by connectionist statistical methods. *IEEE Trans. Neural Networks* **4**, 893–909 (1993)
5. Seid, H., Gamback, B.: A speaker independent continuous speech recognizer for amharic, INTERSPEECH, 9th European Conference on Speech Communication and Technology, Lisbon (2005)
6. Meinredo, H., Neto, J.P.: Combination of acoustic models in continuous speech recognition hybrid systems. In: *Proceedings of ICSLP, Beijing* (2000)
7. Anuj, M., Nair, K.N.R.: HMM/ANN hybrid model for continuous malayalam speech recognition. *Procedia Eng.* **30**, 616–622 (2012)
8. Uglov J., Jakaite L., Maple C.: Comparing robustness of pairwise and multiclass neural network systems for face recognition. *EURASIP J. Adv. Signal Proc.* (2008)
9. Price, D., Knerr, S., Personnaz, L., Dreyfus, G.: Pairwise neural network classifiers with probabilistic outputs. In: *Advances in Neural Information Processing Systems*, Tesauro, G., Touretzky, D., Leen, T. (eds.), vol. 7, The MIT Press, Cambridge (1995)

10. Klautau, A., Jevtic, N., Orlitsky, A.: Combined binary classifiers with applications to speech recognition. In: Proceedings of International Conference on Spoken Language Processing, pp. 2469–2472 (2002)
11. Anuj, M., K.N. R. Nair.: Continuous malayalam speech recognition using hidden markov models. In: Proceedings of 1st Amrita-ACM-W Celebration on Women in Computing in India (2010)
12. Viterbi, A.J.: Error bounds for convolutional codes and asymptotically optimum decoding algorithms. *IEEE Trans. Inf. Theory* **13**, 260–269 (1982)

# Design of an Aperture Type Frequency Selective Surface with Sharp Roll -off

Poulami Samaddar, Sushanta Sarkar, Srija De, Sushanta Biswas,  
Debasree Chanda Sarkar and Partha Pratim Sarkar

**Abstract** In this paper effort has been given to design a broad band high roll off aperture type frequency selective surface. To achieve this, different structures like circular, hexagonal, square and tripole are investigated and compared. Tripole is proved to be the best element to achieve high roll off and broad band. The design is modified as double layer to make it even more selective filter. The final design is fabricated and measured to validate. Measured result follows the simulated result closely.

**Keywords** Frequency selective surface · Aperture type · Band pass · Sharp roll off

## 1 Introduction

Frequency selective surface (FSS) is a periodic array of conducting patch type element or dielectric aperture type element [1]. These types of structures show band stop or band pass property for microwave communication. The patch type FSS shows band reject property and aperture type FSS shows band pass property. For

---

P. Samaddar (✉) · S. Sarkar · S. De · S. Biswas · D.C. Sarkar · P.P. Sarkar  
Department of Engineering and Technological Studies, University of Kalyani, Kalyani, India  
e-mail: poulami\_samaddar@rediffmail.com

S. Sarkar  
e-mail: sushantasarkar@aol.com

S. De  
e-mail: srijade@gmail.com

S. Biswas  
e-mail: biswas.su@gmail.com

D.C. Sarkar  
e-mail: dsarkar70@gmail.com

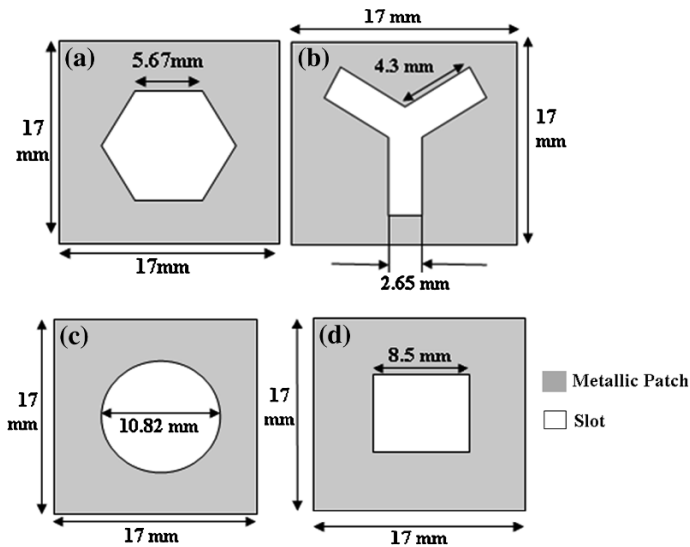
P.P. Sarkar  
e-mail: parthabe91@yahoo.co.in

this nature FSS is used in different devices like antenna radome, frequency sub-reflector system and many other military applications [2, 3]. This type of single layer frequency filters suffers from very poor filtering due to bad roll off. Unwanted frequency band interfere with desired band. To improve this problem different types of processes like cascade technique, microstrip line technique etc. [4, 5] can be adopted. But these kinds of process make the design complicated and very tough for practical implementation.

In this paper different types of basic FSS elements are investigated to achieve maximum roll off. Simulation is done using Method of Moment based software FEKO. The simulated result is compared with practically measured result. Both the results are in good parity.

## 2 Design

This paper deals with aperture type FSS. Different type of shapes (like circular, square, hexagon, tripole etc.) etched out from a metallic sheet in a periodic interval. These FSSs show band pass property [1]. Dielectric constant of the dielectric (acrylic sheet) used for this experiment is 2.8 and width is 1.6 mm. The dimension of the single element of all the four FSS is showed in the Fig. 1. The periodicity and other perimeters of the structures are kept same so that results can be compared properly. At the time of simulation every element is considered as a part of an infinite array. The infinite model excites with plane wave excitation.



**Fig. 1** Single cell of a hexagon, b circular, c square and d tripole aperture type FSS

The four designs are simulated and transmission coefficients of each of them are compared. Tripole type FSS shows best roll off among them. To get even better roll off double layer tripole structure is also investigated. The simulation is done by FEKO software which uses MoM for calculation purpose.

### 3 Result

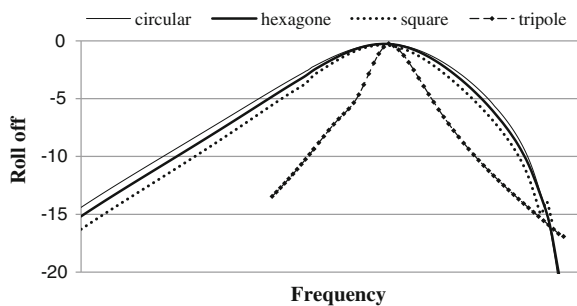
The rolls off for different structures are shown in Table 1. A comparative roll off vs. frequency plot is shown in Fig. 2 for Hexagonal, circular, square and tripole type elements. It is clear from Table 1 and Fig. 2 that tripole type element is best candidate for that. The double layer tripole type FSS provided even better roll off than the one layer tripole FSS.

Double layer tripole is also studied. Tripoles of same dimension printed both side of a dielectric plate. This design shows even better roll off. Comparison between both double layer and single layer tripole is shown in Table 2 and Fig. 3. The final double layer tripole FSS is fabricated using laser cutting technology [6]. Measurement is done in laboratory by standard microwave test bench. The practical result shows good parity with the simulated result as shown in Fig. 4.

**Table 1** Comparison of roll off for different types of elements

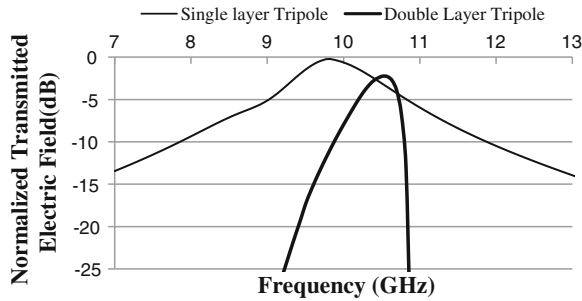
Elements	Upward roll off (dB/ GHz)	Downward roll off (dB/ GHz)
Circular	2	2.67
Hexagon	1.98	2.85
Square	2.2	3.08
Tripole	5	4.63

**Fig. 2** Roll off versus frequency plot for different element to compare roll off

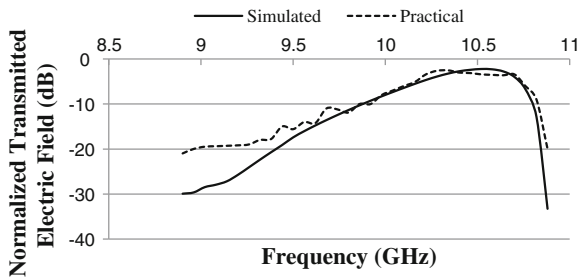


**Table 2** Comparison of roll off for single layer and double layer tripole elements

Type of FSS	Upward roll off (dB/ GHz)	Downward roll off (dB/GHz)
Single layer	5	4.63
Double layer	15	33.33



**Fig. 3** Transmitted electric field versus frequency plot for single and double layer tripole element to compare roll off



**Fig. 4** Simulated and practical transmitted electric field versus frequency plot for double layer tripole FSS

## 4 Conclusion

From the studies it is observed that tripole type FSS is the best selection among circular, hexagonal and square element for high roll off factor. Roll off for tripole FSS increases even more if double layer FSS is used. Although band width is to be sacrificed to achieve sharp roll off, reasonable bandwidth is achieved in the final design. The design may be used in many satellite communications, military etc. applications etc. This work may be further extended to obtain high bandwidth and flat response.

## References

1. Munk, B.A.: Frequency selective surfaces: Theory and design. Wiley, New York (2000)
2. Sarkar, D., Sarkar, P.P., Das, S., Chowdhury, S.K.: An array of stagger-tuned printed dipoles as a broadband frequency selective surface. *Microwave Opt. Technol. Lett.* **35**, 138–140 (2002)
3. Ray, A., Kahar, M., Sarkar, S., Biswas, S., Sarkar, D., Sarkar, P.P.: A novel broad and multiband frequency selective surface. *Microwave Opt. Technol. Lett.* **54**, 1353–1355 (2012)

4. Pelletti, C., Bianconi, G., Mitra, R., Shen, Z.: Frequency selective surface with wideband quasi-elliptic bandpass response. *Electron. Lett.*, vol. 49 (2013)
5. Rashid, A.K., Shen, Z., Li, B.: An elliptical bandpass frequency selective structure based on microstrip lines. *IEEE Trans. Antennas Propag.* **60**, 4661–4669 (2012)
6. Sarkar, P.P.: A novel technique for fabrication of single layer frequency selective surfaces using paper based materials and laser cutting machines, 271/KOL/2012 (pending), 2012

# Effective Classification and Categorization for Categorical Sets: Distance Similarity Measures

Heba Ayseldeen, Mahmood A. Mahmood and Aboul Ella Hassanien

**Abstract** Measuring the similarity between objects is considered one of the main hot topics nowadays and the main core requirement for several data mining and knowledge discovery task. For better performance most organizations are in need on semantic similarity and similarity measures. This article presents different distance metrics used for measuring the similarity between qualitative data within a text. The case study represents a qualitative data of Faculty of medicine Cairo University for theses. The dataset is about 5,000 thesis document with 35 departments and about 16,000 keyword. As a result, we are able to better discover the commonalities between theses data and hence, improve the accuracy of the similarity estimation which in return improves the scientific research sector. The experimental results show that Kulczynski distance yields better with a 92.51 % without normalization that correlate more closely with human assessments compared to other distance measures.

**Keywords** Text clustering · Similarity · Classification

---

H. Ayseldeen (✉) · M.A. Mahmood · A.E. Hassanien  
Scientific Research Group in Egypt (SRGE), Giza, Egypt  
e-mail: heba.ayeldeen@gmail.com

M.A. Mahmood  
e-mail: dr\_mahmoodissr@hotmail.com

A.E. Hassanien  
e-mail: aboitcairo@gmail.com

H. Ayseldeen · A.E. Hassanien  
Faculty of Computers and Information, Cairo University, Cairo, Egypt

M.A. Mahmood  
Institute of Statistical Studies and Research (ISSR), Giza, Egypt



## 1 Introduction

Text classification is important means and methods of text mining, and also a part of data mining. Text classification is a supervised classification of documents, which divides and categorize a text collection into several subsets called sets, the text of each set has greater similarity than the one in different set. Text classification differs from text clustering where labels within the data sets are well known compared to clustering that deals with unsupervised documents [1].

Recently, semantic similarity has been applied in many different applications including the health and medical domain. For better understanding the textual resources, semantic similarity estimation is used [2].

Properly classifying and clustering texts based on certain criteria and trend improves the understanding and relatedness of data. Decision makers find it easy to extract the knowledge based on good classification [3]. Analyzing the relationships between documents based on concepts and terms is one of the semantic analysis methods. The best way to make use of the information retrieved rather than rebuilding it from scratch [4].

Text categorization has recently become a hot topic in the area of information retrieval. The main objective of text categorization is to assign free text documents to one or more predefined categories based on their content. Traditionally this process is performed manually by domain experts. This process is very time-consuming and costly, thus limiting its applicability [5]. The concepts of text similarity and semantic similarity have been extensively developed to tackle this problem in an automatic way. There are many text similarity methods that can be used to ease text categorize, of these methods are: Semantic sequence kin model (SSK), which extracts semantic sequences from a text as its feature strings, and then takes into account both word and word position when 2 semantic sequences are compared [6]. Common semantic sequence model (CSSM), which is similar to semantic sequence kin model, but uses another formula to calculate similarity of semantic sequences, in which the word position is not considered [7]. Word similarity estimation has many direct applications. In word-sense disambiguation, context terms can be semantically compared to discover the most similar sense. In document categorization or clustering, the semantic similarity between words can be compared to group documents according to their subject. In word spelling correction, semantic similarity can assess which is the most appropriate correction for a potential misspelling according to its similarity against context words [3].

The concepts of similarity and distance are crucial in many scientific applications. Similarity and distance measurements are mostly needed to compute the similarities/distances between different objects, an essential requirement in almost all pattern recognition applications including clustering, classification, feature selection, outlier detection, regression, and search. There exist a large number of similarity measurements in the literature; thus, selecting one most appropriate similarity measurement for a particular task is a crucial issue. The success or failure

of any pattern recognition technique largely depends on the choice of the similarity measurement. The similarity measurements vary depending on the data types used [8].

The rest of this paper is organized as follows. Section 2 states brief explanation of different similarity measures types with respect to the distance. Section 3 focus on optimizing documents/texts as by showing mathematically comparisons between the distance based similarity measures. Finally, Sect. 4 addresses conclusions and future work.

## 2 Types of Similarity Measures

Distance based similarity measure is considered as an essential parameter for the classification and measuring the similarity or dissimilarity between two or more vectors/objects (Fig. 1).

Following are distance metric families with 34 different distance metrics used for matching the distance and measuring the similarity between any two or more vectors.

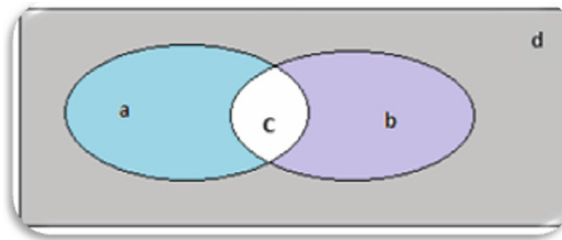
### 2.1 L1 Minkowski Distance Metric Family

In L1 distance metric family all distance metrics are defined for  $p = 1$ .

1. Sorenson distance [9]

$$d_{Sor}(A, B) = \frac{2c}{a + b} \tag{1}$$

We say two points are adjacent if their L1 distance is defined for  $a = 1$ . Eq. 1, is known as Sorenson distance sometimes called or Bray Curtis where difference is normalized by the sum of feature vectors at each dimension.



**Fig. 1** Variables in similarity equations. **a** Set1. **b** Set2. **c** Intersection/common features. **d** Information system/dataset

2. Kulczynski distance [9, 10]

$$d_{Kul}(P, Q) = \frac{\left(\frac{a}{a+b} + \frac{a}{a+c}\right)}{2} \quad (2)$$

While Eq. 2 shows that the Kulczynski distance is measured as the difference of the two vectors A and B normalized by the minimum value between two of the features in A and B.

3. Gower distance [9, 10]

$$d_{Gow}(A, B) = \frac{a + d}{\sqrt{(a - c)(a + c)(b + d)(c + d)}} \quad (3)$$

In 1985, Gower defined a general similarity coefficient to overcome this as in Eq. 3 where A and B for binary variables stands for the presence/absence of that variable.

## 2.2 Inner Product Distance Metrics Family

The inner product distance metrics family deals exclusively with similarity measures which incorporate the inner product of two vectors yields a scalar and is sometimes called the scalar product or dot product.

1. Cosine Similarity [9–16]

$$d_{Cos}(A, B) = \frac{a}{\sqrt{(a + b)(a + c)^2}} \quad (4)$$

Ochiai and Carbo are other names to the cosine co-efficient. As given in Eq. 4, the distance is measured based on the angle between two vectors and is thus often called the angular metric.

2. Jaccard Coefficient [9–11, 13, 15, 17–19]

$$d_{Jack}(A, B) = \frac{a}{a + b + c} \quad (5)$$

Similarly Eqs. 4 and 5 measure the similarity between two vectors as it gives the minimum value for more similar feature vectors.

3. Dice Coefficient [9, 10, 17]

$$d_{Dice}(A, B) = \frac{2a}{2a + b + c} \quad (6)$$

Dice distance is very sensitive to small changes as the numerator is multiplied by factor 2.

### 2.3 Squared Chord Distance Metrics Family

1. Squared Chord [9, 10]

$$d_{Schi}(A, B) = \sqrt{2 \left( 1 - \frac{a}{(a+b)(a+c)} \right)} \quad (7)$$

The sum of geometric means  $\sqrt{AB}$ , where  $A$  referred to as fidelity similarity or squared chord distance metric. Squared chord distance is given by Eq. 7. In squared chord distance, the sum of square of square root difference at each dimension is taken which increases the difference for more dissimilar feature vectors. This distance cannot be used for feature space with negative values.

2. Hellinger distance [9]

$$d_{Heling}(P, Q) = 2 \sqrt{\left( 1 - \frac{a}{(a+b)(a+c)} \right)} \quad (8)$$

The Hellinger distance is another way to measure the distance to check the similarity of even the dissimilarity of two or more points. In 1909 introduced by Ernst Hellinger is the Hellinger distance which is used to quantify the similarity between two probability distributions. Talking about the discrete distribution, for two discrete probability distributions  $A$  and  $B$  their Hellinger distance is defined as in Eq. 8 which is directly related to the Euclidean norm of the difference of the square root vectors.

### 2.4 Other Distance Metrics

1. Average distance [9, 13]

$$d_{Avg}(A, B) = \frac{\sum |a - b| + \max |a - b|}{2} \quad (9)$$

Distance given by Eq. 9 is just the average of city block and Chebyshev distance.

## 2. Sokal and Sneath II [10, 17]

$$S_{SOKAL\&Sneath-II} = \frac{a}{a + 2b + 2c} \quad (10)$$

For the similarity measure as in Eq. 10, this measure has a minimum value of 0, has no upper limit, and is undefined when there are no non matches ( $b = 0$  and  $c = 0$ ).

## 3 Experimental Results

The main target of the study is to increase the scientific research field in the different faculties of Cairo University. To do so, we focused in the theses mining concept for instance for the Faculty of Medicine, Cairo University. Data was collected from the digital library of the Faculty of Medicine and then cleansed for further process. The data collected was theses documents including the title of the theses and the abstract with keywords. The theses documents are classified into Master and doctorate theses. Documents are tracked within the last 10 years separated and categorized based on the departments within the Medicine school. Data collected was 4,878 theses with 15,808 keyword across all departments.

Faculty of Medicine in Cairo University is classified into 35 departments. The aim of the work is to find out the departments that can work together easily to increase the research within the faculty. As well as making it easy for departments to find a way to increase the research within each department.

Different distance measures were applied to get the nearest departments that can work together. Results includes measures of the equations Euclidean distance, City block distance, Sorenson distance, Kulczynski distance, Cosine Similarity, Jaccard Coefficient, Dice Coefficient, Hellinger distance, Sokal and Sneath and Johnson similarity equation.

As previously mentioned, the main objective is to find out the best of departments' combinations that can collaborate easily together. After applying the Cosine similarity on four randomly selected departments (Anatomy, Andrology, Anesthesia and Cardiology), the results shows for instance that the department of Anatomy can work easily with the department of Cardiology with a percentage of 60 %. While the department of Anesthesia with Cardiology by 90 %. While after applying the Dice distance equation the combination of Anatomy with the Cardiology decreased to 40 %. Then the results decreased again with the Jaccard Coefficient, Sokal and Sneath as well as Sorenson; and increased again with the Kulczynski distance equation Tables 1, 2, 3, 4, 5, 6.

After making comparisons between the different distance equations (Cosine similarity distance, Dice Coefficient, Jaccard Coefficient, Sokal and Sneath distance, Kulczynski distance and Sorenson distance), we find out that the Kulczynski

**Table 1** Applying cosine similarity

Departments	Anatomy	Andrology	Anesthesia	Cardiology
Anatomy	1	0.6	0.2	0.5
Andrology	0.6	1	0.3	0.6
Anesthesia	0.2	0.3	1	0.9
Cardiology	0.5	0.6	0.9	1

**Table 2** Applying Dice coefficient

Departments	Anatomy	Andrology	Anesthesia	Cardiology
Anatomy	1	0.6	0.1	0.4
Andrology	0.6	1	0.2	0.5
Anesthesia	0.1	0.2	1	0.9
Cardiology	0.4	0.5	0.9	1

**Table 3** Applying Jaccard coefficient

Departments	Anatomy	Andrology	Anesthesia	Cardiology
Anatomy	1	0.4	0.1	0.3
Andrology	0.4	1	0.1	0.3
Anesthesia	0.1	0.1	1	0.8
Cardiology	0.3	0.3	0.8	1

**Table 4** Applying Kulczynski distance

Departments	Anatomy	Andrology	Anesthesia	Cardiology
Anatomy	1	0.7	0.5	0.6
Andrology	0.7	1	0.5	0.6
Anesthesia	0.5	0.5	1	0.9
Cardiology	0.6	0.6	0.9	1

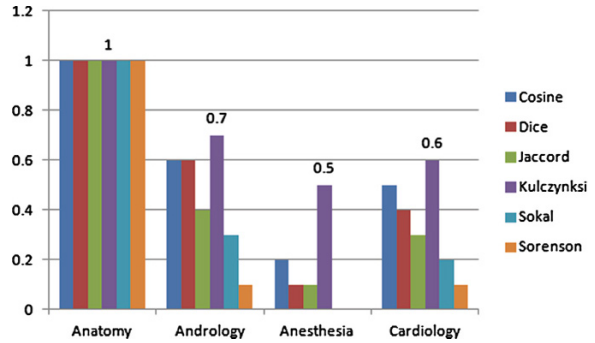
**Table 5** Applying Sokal and Sneath distance

Departments	Anatomy	Andrology	Anesthesia	Cardiology
Anatomy	1	0.3	0	0.2
Andrology	0.3	1	0	0.2
Anesthesia	0	0	1	0.7
Cardiology	0.2	0.2	0.7	1

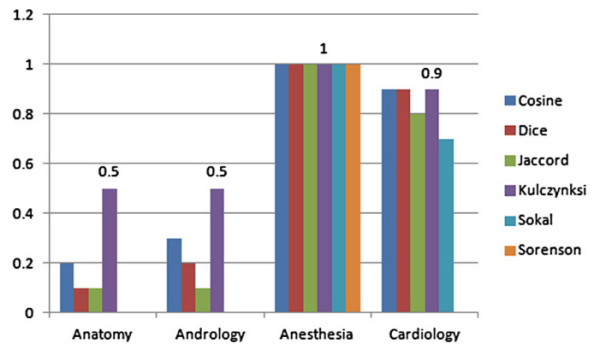
**Table 6** Applying Sorenson distance

Departments	Anatomy	Andrology	Anesthesia	Cardiology
Anatomy	1	0.1	0	0.1
Andrology	0.1	1	0	0.1
Anesthesia	0	0	1	0
Cardiology	0.1	0.1	0	1

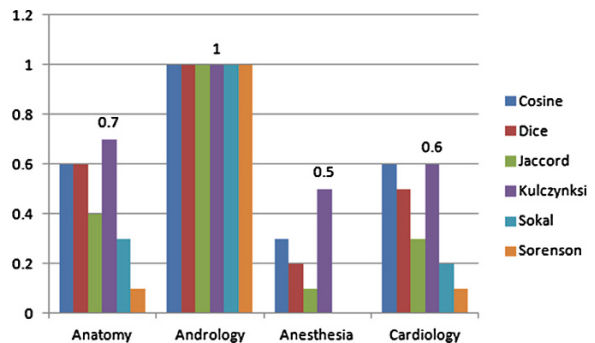
**Fig. 2** Anatomy with others

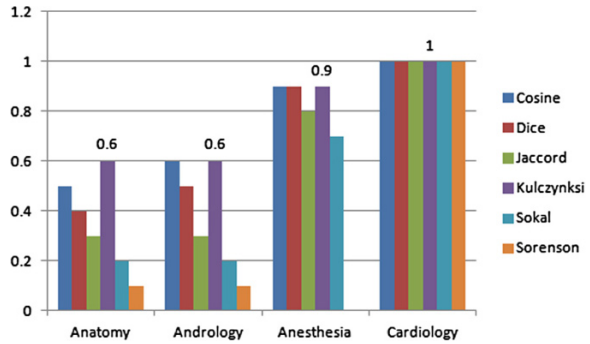


**Fig. 3** Andrology with others



**Fig. 4** Anesthesia with others



**Fig. 5** Cardiology with others

distance is better than any other equations used as shown in the figures below which is more relevant to human assessments (Figs. 2, 3, 4 and 5).

## 4 Conclusion and Future Work

In this paper, we showed mathematically how texts can be clustered by using different similarity distance equations on documents. By taking an example where these documents were clustered and classified better with the Kulczynski distance by 92.51 % directly without applying normalization than other distance measures. Other algorithms can be considered as well for future work, like applying the genetic programming; neural networks and comparing the results simultaneously.

## References

1. Dumais, S., Meek, D., Metzler, D.: Similarity measures for short segments of text. In: Proceeding ECIR'07 Proceedings of the 29th European Conference on IR Research, pp. 16–27 (2007)
2. Hassanien, A.E., Fasmly, A.A., Ayeldeen, H.: Evaluation of semantic similarity across MeSH ontology: A cairo university thesis mining case study. In: 12th Mexican International Conference on Artificial Intelligence, pp. 139–144. Mexico City (2013)
3. Batet, DSaM: Semantic similarity estimation in the biomedical domain: An ontology-based information-theoretic perspective. *J. Biomed. Inf. Arch.* **44**, 749–759 (2011)
4. Kitasuki, T., Aritsugi, M., Rahutomo, F.: Test collection recycling for semantic text similarity. In: Proceeding IIWAS12 Proceedings of the 14th International Conference on Information Integration and Web-based Applications and Services, pp. 286–289 (2012)
5. Liu, T., Guo, J.: Text similarity computing based on standard deviation. In: *Advances in Intelligent Computing*, vol. 1, pp. 23–26. Springer, Berlin (2005)
6. Shen, J.Y., Bao, J.P., Liu, X.D., Liu, H.Y., and Zhang, X.D.: Finding plagiarism based on common semantic sequence model. In: *Proceedings of the 5th International Conference on Advances in Web-Age Information Management*, pp. 640–645 (2004)



7. Lyon, C.M., Bao, J.P., Lane, P.C.R., Ji, W., Malcolm, J.A.: Copy detection in chinese documents using ferret. *Lang. Resour. Eval.* 1–10 (2006, in press)
8. Bandyopadhyay, S., Saha, S.: Unsupervised classification. In: *Unsupervised Classification: Similarity Measures, Classical and Metaheuristic Approaches, and Applications*, pp. 59–73. Springer, Berlin (2013)
9. Bharkad, S.D., Kokare, M.: Performance evaluation of distance metrics: Application to fingerprint recognition. *Int. J. Pattern Recognit. Artif. Intell.* **25** (2011)
10. Choi, S.H., Choi, S.S., Tappert, C.C.: A survey of binary similarity and distance measures. *J. Syst. Cybern. Inf.* **8**(1), 43–48 (2010, Key: citeulike:7358808)
11. Huang, A.: Similarity measures for text document clustering. In: *New Zealand Computer Science Research Student Conference*, pp. 49–56 (2008)
12. McGill, M.J., Salton, G.: *Introduction to Modern Information Retrieval*, McGraw-Hill, New York (1983)
13. Leydesdorff, L.: Similarity measures, author cocitation analysis, and information theory. *J. Am. Soc. Inform. Sci. Technol.* **56**, 769–772 (2005)
14. S. B. a. S. Saha, *Unsupervised Classification: Similarity Measures, Classical and Metaheuristic Approaches, and Applications: Springer Berlin Heidelberg*, 2013
15. Lalitha, Y.S., Sandhya, N., Govardhan, A., Anuradha, K.: Analysis of similarity measures for text clustering. In: *International Conference on Information Systems Design and Intelligent Applications*, p. 976, Vishakhapatnam (2012)
16. Leydesdorff, L., Zaal, R.: Co-words and citations. Relations between document sets and environments. *Informetrics*, vol. 87, pp. 05–119. Elsevier, Amsterdam (1988)
17. De Baets, S.J.B., De Meyer, H.: On the transitivity of a parametric family of cardinality-based similarity measures. *Int. J. Approx. Reason.* **50**, 104–116 (2009)
18. Tang, C., Zhang, A., Jiang, D.: Cluster analysis for gene expression data: a survey. *IEEE Trans. Knowl. Data Eng.* **16**, 1370–1386 (2004)
19. Faria, D., Pesquita, C., Falcao, A.O., Lord, P., Couto, F.M.: Semantic similarity in biomedical ontologies. *PLOS: Comput. Biol.* **5** (2009)

# Case-Based Reasoning: A Knowledge Extraction Tool to Use

Heba Ayeldeen, Olfat Shaker, Osman Hegazy  
and Aboul Ella Hassanien

**Abstract** Case-based reasoning (CBR) is a relative newcomer to AI and is commonly described as an AI as well as KM technology. Case-Based Reasoning is considered as a methodology not a technology to use. Finding the similarities between objects as well as knowledge extraction sometimes is a complicated issue to handle concerning decision makers and executive managers. Learning from previous failures and successes saves plenty of time in understanding the problems and visualizing the data. CBR as a process is one of the most used methods to solve the problem of knowledge capture and data understanding. In this paper we show mathematically the usage of CBR in clustering documents and finding correlations between medical data by using CBR with DB technology as an application. Results yield to an increase in comparison to human assessments and not using CBR methods.

**Keywords** Case-based reasoning · Nearest neighbour · Knowledge discovery · Rough sets algorithm · Problem-solving

## 1 Introduction

The field of AI is widely spread to aid in problem solving and deals with the uncertain information. By the late 1980s and 1990s, AI research had also developed highly successful methods for dealing with uncertain or incomplete information [1].

---

H. Ayeldeen (✉) · A.E. Hassanien  
Scientific Research Group in Egypt (SRGE), Cairo, Egypt  
e-mail: heba.ayeldeen@egyptscience.net

A.E. Hassanien  
e-mail: abo@egyptscience.net

H. Ayeldeen · O. Hegazy · A.E. Hassanien  
Faculty of Computers and Information, Cairo University, Cairo, Egypt  
e-mail: osman.hegazy@gmail.com

O. Shaker  
Department of Molecular Biology, Faculty of Medicine, Cairo University, Cairo, Egypt  
e-mail: olfatshaker@yahoo.com

Many subfields within AI technology appeared that deal with the construction and study of systems that can learn from data, rather than follow only explicitly programmed instructions. With the techniques within Cognitive science, machine learning, support vector machines and others, the problem of finding similarity between objects would be much easier to cope with the environmental and technological changes. Machine learning focuses on prediction, based on known attributes properties learned from the training data [2–5].

Compared to other AI approaches, CBR has several advantages, one of the main added-value is that the training time will be reduced for the solution selection. Case-based Reasoning (CBR) is a problem solving methodology that addresses a new problem by first retrieving a past, already solved similar case, and then reusing that case for solving the current problem. CBR is one of the most used and successful machine learning methodologies that makes the most of a knowledge-rich representation of the different application domains [6–8].

This paper will discuss three different CBR applications, that CBR describes a methodology for problem solving. Section 2 identifies the main characteristics in the life-cycle of a CBR system. While Sects. 3 and 4 discusses CBR using nearest neighbour and CBR using database technology. Section 5 is showing a case study on the usage of DB technology to find the similarity between cases. Section 6 shows the interpreting results and discussion. The last section is the conclusion and future work.

## 2 Knowledge Discovery

As part of knowledge management, knowledge discovery is the process of searching through large volumes of information and extracting subsets of information relevant to a given task. The knowledge discovery process consists of several steps as shown in flowchart 1 [9] (Fig. 1).

### 1. *Understanding the target domain*

Knowledge relevant to a domain must be acquired. Knowledge discovery goals should be identified that benefit the user of a system.

### 2. *Selecting a dataset*

A variety of datasets may contain useful domain knowledge, and the datasets thought to contain the best information should be selected.

### 3. *Data cleaning*

Many datasets include noise. The data cleaning stage is concerned with removing this noise and accounting for missing information.

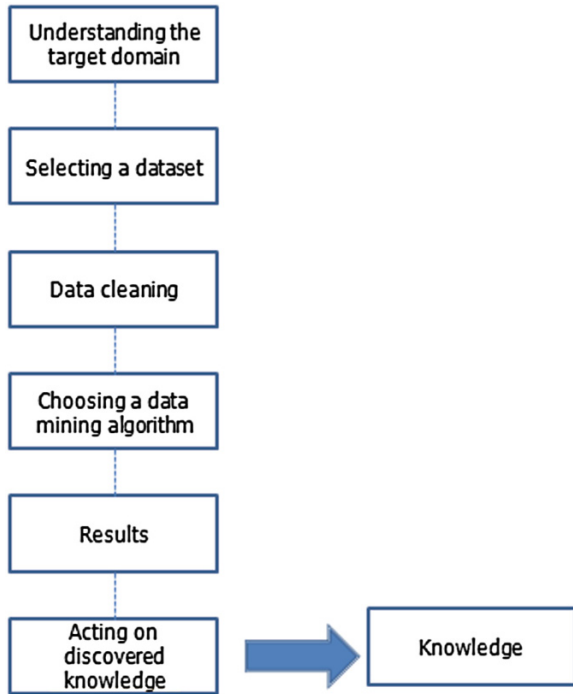
### 4. *Choosing a data mining algorithm*

The knowledge discovery goals from step (1) should be matched with an appropriate data mining strategy.

### 5. *Data mining*

In this step the datasets chosen in step (2) are searched for patterns of interest.

**Fig. 1** Knowledge discovery process



**6. Interpreting results**

This may involve visualization of extracted patterns or a return to any of the previous steps if problems are discovered.

**7. Acting on discovered knowledge**

This may involve reporting knowledge discovered to a user, incorporating the knowledge with a local knowledge base, or checking for inconsistencies with the discovered knowledge and previously acquired knowledge.

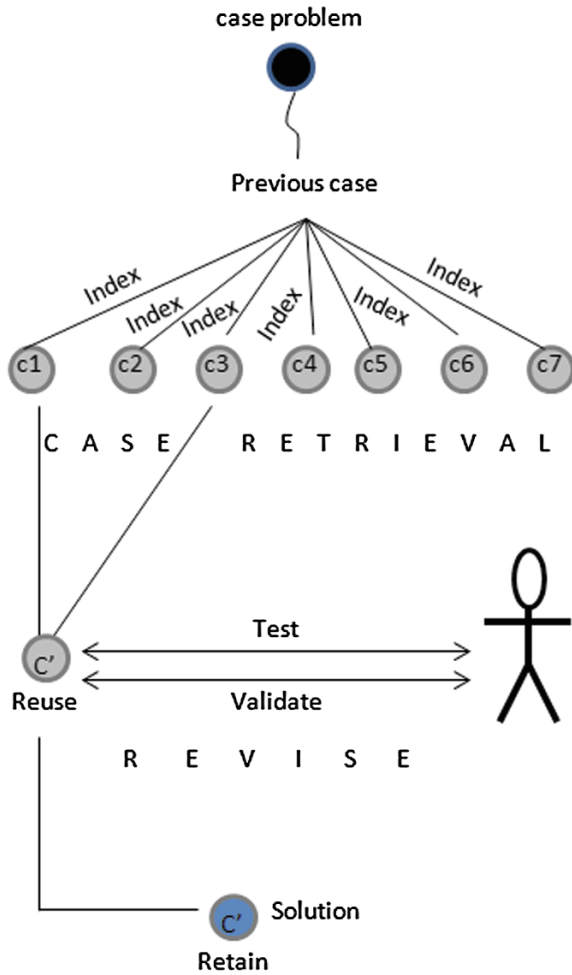
This process is interactive and may be repeated any number of times until useful knowledge has been discovered.

### 3 Case-Based Reasoning

The problem solving life-cycle in CBR system consists mainly of the following four parts: Retrieve cases from previously ones; Reuse the old cases to find the alternative solution needed; Revise the solutions/cases you have got, maybe make some adaptations and Retain the solution after testing and validation [6] (Fig. 2).

Case representation is one of the main tasks within CBR processes [6, 9, 10]. Case indexing refers to assigning indexes to previous cases to ease the process of

**Fig. 2** Problem solving life-cycle in CBR system



retrieval or even making modifications to the cases. It is preferable that these indexes should reflect the important features within the cases like the main attributes affecting the success or the failure of the case, and describe the circumstances in which a case is expected to be retrieved in the future [6, 9].

It is also important to include the measure of success or failure of the case in the case description with stating the different levels of success or failure. Now you have got the completed knowledge required to that case [6].

Case reuse and learning from previous experiences, eliminates the effort and time taken to solve the new coming problem. Different techniques of case selection can be used to retain the best/optimum solution required. Based on the problem you have and the circumstances around it, you start making adaptations on the previous cases near to what you want. So rather than spending so much time of getting the

solution, you make use of the old previous solutions you have in the case warehouse [6, 11, 12].

Before retaining the best or near optimum solution(s), testing and validating with the user or the decision maker is very important task to do. According to the test taken in advance, case is retained [9, 13].

Finally it can be concluded that Case-based reasoning (CBR) is the process of solving new problems based on the solutions of similar past problems [10, 11].

## 4 CBR Using Nearest Neighbour

As mentioned before, there are various CBR techniques used to find the similarities and the correlation between patterns. Nearest neighbour techniques are the most widely used technology in CBR since it is provided by the majority of CBR tools like the Wayland system which is a CBR system that was implemented using a CBR tool called caspian [1, 6].

In nearest neighbour algorithm the similarity of the problem case to a case in the case-library for each case attribute is determined. This measure may be multiplied by a weighting factor. Then the sum of the similarity of all attributes is calculated to provide a measure of the similarity of that case in the library to the target case [1, 6]. This can be represented by Eq. 1:

$$Similarity(T, S) = \sum_{i=1}^n f(T_i, S_i) \times w_i \quad (1)$$

where

T is the target case

S the source case

n the number of attributes in each case

i an individual attribute from 1 to n

f a similarity function for attribute i in cases T and S

and w the importance weighting of attribute i.

This calculation is repeated for every case in the case-library to rank cases by similarity to the target.

## 5 CBR Using Database Technology

CBR could be implemented using database technology as its simplest form. Databases are efficient means of storing and retrieving large volumes of data. Case-based systems make their decisions based on experiences of past situations. They

try to acquire relevant knowledge of past cases and previously used solutions to propose solutions for new problems. If a direct match for an open problem is found in the database, the solution from the matching case is returned. Otherwise, the case is chosen that most closely matches the open problem. Then, the solution applied to the chosen past case is adapted for the open problem. Case-based systems are well suited for learning correlation patterns [1, 14].

The problem with using database technology for CBR is that databases retrieve using exact matches to the queries. This is commonly augmented by using wild cards, such as MAN matching on WOMAN and MANKIND. The use of wildcards, Boolean terms and other operators within queries may make a query more general, and thus more likely to retrieve a suitable case, but it is not a measure of similarity. However, it is possible to use SQL queries and measure similarity [1, 14].

## 6 Applying DB Technology to Find Similarity Between Objects: Case Study

It is not easy to find the similarity between objects and get the correlation between them. Mainly we are concerned with medical data, Breast cancer patients in Egypt. First step is to make use of the DB technology to build the case library.

The structure of the data is as follows: Patient number, Patient type (Control, Fibroadenoma and Cancer patients), Age, Family history, diabetes, hypertension and other proteins parameters like (LAPTM-4B, OPG, RANKL and YKL-40).

These proteins can be used to identify whether the patient has breast cancer or they are considered as control healthy patients.

### 6.1 Subject and Methods

**Subjects** All the breast cancer patients involved in the study were diagnosed at department of Biochemistry and Molecular Biology of Kasr Alainy Hospital of Cairo University. To detect the relationship between LAPTM4B polymorphism and breast cancer vulnerability, one hundred three breast cancer patients and eighty cancer-free healthy controls who were recruited from patients undergoing annual physical examination at Kasr Alainy Hospital of Cairo University were investigated. To analysis the association between LAPTM4B gene polymorphism and OPG gene protein, a long term clinical follow up were enrolled. For all participants in this study, written informed consent was obtained as delineated by the protocol which was approved by the Ethical Committee of Cairo University.

The studied subjects were divided into three groups as follows: Group I: (n = 80) healthy females as a control group. Group II: (n = 40) patients with fibroadenoma. Group III: (n = 88) patients with breast carcinoma, they were classified according to

TNM grading system into 11 cases in stage II, 57 cases in stage III and 20 cases in stage IV. This group included 68 non metastatic breast cancer patients and 20 metastatic subjects.

The Inclusion criteria includes adult females, age ranged from (20–70) years with no previous treatment with chemotherapy or radiotherapy. While the exclusion criteria includes age below 20 and above 70 years, previous treatment with chemotherapy or radiotherapy, other malignancy.

Written consent forms were signed by all participants in this study including the controls. Also, this study was approved by the ethical committee of Kasr Alainy Hospital, Cairo University. All cases were subjected to estimation of LAPT4B protein level in serum. The fibroadenoma and carcinoma biopsies were examined histopathologically.

From each subject, blood sample was taken and separation of serum was made and used for estimation of LAPT4B level by ELISA technique.

**Methods** Detailed history was taken putting in consideration the course of illness, age of onset of the disease, mode of presentation and family history of the cancer.

The protein was extracted from whole blood serum of both patients and control group with QIAamp DNA mini kit (Qiagen, Hilden, Germany), following the manufacturer's instructions.

## 6.2 Tools and Statistical Analysis

All statistical analysis in our study were carried out with WEKA 3.7.9 (WEKA, The university of Waikato). Genotypic frequencies were tested for correlation using the *P*-value test. The presentation software PHP 5.5 was used and by the usage of MySQL tool, We have collected a case warehouse for breast cancer patients.

## 7 Interpreting Results

Spending a lot of time in search as well as finding the symmetry of different sets/article/documents/relations is considered the domain problem for organizations. We take the advantages of KM in our case study, where all data is stored and indexed by the usage of DB technology within case-based tools. The benefits of this CBR tool is to help decision makers and executive managers analyze and take the right decision at the right time.

Tables 1 and 2 show samples of the data used within the case library.

After using DB technology as a storage and indexing tools, PHP tool was used to build the interface of the CBR system. The figures below show the interface of the CBR tool we built where user can easily move from step to another.



**Table 1** Sample data and protein analysis for cancer-free healthy controls

Index	Age	Menst. H	LAPTM4B (pg/ml)	OPG
CC1	44	Pre	202.3	12.5
CC2	45	Pre	613.2	10.6
CC3	47	Pre	646.7	22.1
CC4	44	Pre	613.2	17.4
CC5	53	Post	710	9.7

**Table 2** Sample data and protein analysis for cancer patients

Index	Age	Family. H	LAPTM4B (pg/ml)	OPG
CAN1	52	Yes	518.7	106.5
CAN2	62	Yes	749.8	111.048
CAN3	62	No	829.4	70.068
CAN4	42	Yes	1,033.9	47.976
CAN5	45	Yes	2103	80.25

Making use of the DB technology yield to increase in time saving for case retrieval. For instance we want to retrieve all healthy patients:

```
SELECT *
FROM 'dataset'
WHERE 'PtType' = 0
ORDER BY 'dataset'. 'PtType' DESC.
```

As discussed in Sect. 4 by using patterns, wild cards as well as table joins we can make the query more complicated to achieve/retrieve the targeted case.

```
SELECT ptype.PtType, Age, hypertension, Diabetes, FamHis, LAPTM4B,
RANKL, OPG, YKL40
FROM dataset, ptype
WHERE ptype.ptid = dataset.ptype
AND dataset.PtType = 0
```

Finding correlations between parameters is a good indicator for accuracy. Equation 2 is used to measure the correlation between the proteins used in the data set.

$$r = \frac{1}{n-1} \sum \left( \frac{x-x'}{S_x} \right) \left( \frac{y-y'}{S_y} \right) \quad (2)$$

After different queries selections and joining, results yield that there is a correlation between the two proteins LAPTM-4B and OPG where when new case is added if the LAPTM-4B value is  $\leq 710$  it is 98.1 % to be cancer patient and with the correlation with OPG if OPG value is  $\geq 23.96$  there is a probability that the patient is a healthy one.

## 8 Conclusion and Future Work

No one can deny the importance of databases and database management systems to organizations. Databases technologies aid in the data definition as well as data administration where monitoring users and manipulating data integrity take place. Databases are used to support internal operations of organizations. The database technology has been used in various applications where DB can be used to hold administrative information and more specialized data.

From the study provided in this paper, it can be concluded that by using the CBR techniques with respect to the DB technology results in saving much time in the search and seeking the solutions with a 98.1 % increase in comparison to human assessments and not using CBR applications.

Many other CBR applications maybe used in the future for showing the advantages of using CBR methodologies. Rough sets and the nearest neighbour applications methods are in the future plans as well as similarity measures to find correlation and asymmetry between objects.

## References

1. Watson, I.: Case-based reasoning is a methodology not a technology. *J. Knowl. Based Syst.* **12**, 303–308 (1999)
2. Zawbaa, H.M., El-Bendary, N., Hassanien, A.E., Kim, T.-H.: Machine learning-based soccer video summarization system, Part II. *CCIS*, vol. 263, pp. 19–28. Springer, Heidelberg (2011)
3. Kolodner, J.L.: An introduction to case-based reasoning. *Artif. Intell. Rev.* **6**, 3–34 (1992)
4. Ghany, K.K.A., Hassanien, A.E., Schaefer, G.: Similarity measures for fingerprint matching. In: *International Conference on Image Processing, Computer Vision, and Pattern Recognition*, pp. 21–24, USA (2014)
5. Mouhamed, M.R., Zawbaa, H.M., Al-Shammari, E.T., Hassanien, A.E., Snasel, V.: Blind watermark approach for map authentication using support vector machine. In: *Advances in Security of Information and Communication Networks*, pp. 84–97. Springer, Berlin (2013)
6. Pal, S.K., Shiu, S.C.K.: *Foundations of Soft Case-Based Reasoning* (2004)
7. Jonassen, D.H., Hernandez-Serrano, J.: Case-based reasoning and instructional design: Using stories to support problem solving. *Education Tech. Research Dev.* **2**(50), 65–77 (2002)
8. Davies, J., Goel, A.K.: Visual case-based reasoning II: transfer and adaptation. In: *Proceedings of the 1st Indian International Conference on Artificial Intelligence*, pp. 377–382. Springer, Berlin (2003)
9. Fayyad, U., Piatetsky-Shapiro, G., Smyth, P.: Knowledge discovery and data mining: towards a unifying framework. In: *Proceedings of KDD'96, Second International Conference on Knowledge Discovery and Data Mining*, pp. 82–88 (1996)
10. Park, M.K., Lee, I., Shon, K.M.: Using case based reasoning for problem solving in a complex production process. *Expert Syst. Appl.* **15**, 69–75 (1998)
11. Grupe, F.H., Urwiler, R., Ramarapu, N.K., Owrang, M.: The application of case-based reasoning to the software development process. *Inf. Softw. Technol.* **40**, 493–499 (1998)

12. Rezvana, M.T., Zeinal Hamadania, A., Shalbafzadehb, A.: Case-based reasoning for classification in the mixed data sets employing the compound distance methods. *Eng. Appl. Artif. Intell.* **9**(26), 2001–2009 (2013)
13. Singh, S.K.: *Database Systems: Concepts, Designs and Applications*. Pearson Education India, New Delhi (2006)
14. Lopez De Mantaras, R., Mcsherry, D., et al.: Retrieval, reuse, revision and retention in case-based reasoning. *Knowl. Eng. Rev.* **3**(20), 215–240 (2005)

# Implementation of New Framework for Image Encryption Using Arnold 3D Cat Map

Kunal Kumar Kabi, Bidyut Jyoti Saha, Arun Chauhan  
and Chittaranjan Pradhan

**Abstract** Chaotic map can be used for the image security. Arnold 2D cat map is a common and simple technique out of the different chaotic maps. This technique may be extended to three dimension. Thus, we have proposed a new framework for the image encryption using Arnold 3D cat map. Histogram analysis shows the effectiveness of Arnold 3D cat map as compared to 2D. Also, this framework better resists the differential attacks as compared to the Arnold 2D cat map.

**Keywords** Encryption · Chaotic map · Arnold 2D cat map · Arnold 3D cat map · Image security

## 1 Introduction

Chaotic maps are useful to ensure security because they are easy to generate, are deterministic and are extremely difficult to predict [1–3]. The architecture of these maps is composed of substitution and diffusion. In the substitution stage, chaotic map is employed to shuffle the image pixels. In diffusion stage, pixel values are altered sequentially so that the change made to a particular pixel depends on the previous pixels [1]. These maps are categorized as: 1D, 2D and 3D. 1D chaotic

---

K.K. Kabi (✉) · A. Chauhan · C. Pradhan  
KIIT University, Bhubaneswar, India  
e-mail: kunal.kabi90@gmail.com

A. Chauhan  
e-mail: arunchauhan73@gmail.com

C. Pradhan  
e-mail: chitaprakash@gmail.com

B.J. Saha  
Capgemini, Mumbai, India  
e-mail: bidyutjyotisaha@gmail.com

maps are easy to generate; but, prone to attack due to less number of security keys. 2D maps provide better security due to the increased number of security keys [2].

In 2010, Ding [4] proposed an image encryption algorithm using improved Arnold transform. In 2011, Jin [5] has proposed a digital watermarking algorithm based on Arnold transform. In 2012, Ye and Wong [6] proposed an improved technique using generalized Arnold for the image encryption. In 2012, Pradhan et al. [7] proposed an imperceptible digital watermarking using 2D Arnold map as well as cross chaos map.

When better security is the requirement for the image, higher level of security keys are required. This can be provided by increased dimension. Here, we have extended Arnold 2D technique to Arnold 3D. Section 2 describes Arnold 2D cat map. Section 3 contains our improved Arnold 3D cat map technique and the result analysis of the image encryption using Arnold 3D cat map compared to Arnold 2D cat map.

## 2 Arnold 2D Cat Map

Arnold cat map is a kind of cut-out transformation [8, 9]. It is a type of diffusion cryptosystem [1]. Here, an image is hit with the transformation that apparently randomizes the original organization of its pixels. The number of iterations taken to regenerate the original image is called as Arnold period [7]. We have to choose one number less than the period as the encryption key. The remaining iterations is used as the decryption key. It includes two keys or control parameters [6]:

$$\begin{pmatrix} x' \\ y' \end{pmatrix} = \begin{pmatrix} 1 & a \\ b & ab + 1 \end{pmatrix} * \begin{pmatrix} x \\ y \end{pmatrix} \text{mod } N \quad (1)$$

where,  $a$  and  $b$  are any positive numbers.  $N$  is the size of the square image.  $x, y \in 0, 1, \dots, N - 1$ .

## 3 Proposed Algorithm

### 3.1 Arnold 3D Cat Map

Based on Arnold 2D cat map, a 3D cat map has been developed by using  $c$  and  $d$  as extra parameters.

$$\begin{pmatrix} x' \\ y' \\ z' \end{pmatrix} = \begin{pmatrix} 1 & a & 0 \\ b & ab + 1 & 0 \\ c & d & 1 \end{pmatrix} * \begin{pmatrix} x \\ y \\ z \end{pmatrix} \text{mod } N \quad (2)$$

3D Arnold cat map is chaotic in nature and produces pseudo-random numbers; which can be used for the image encryption. In this method,  $(x, y)$  and  $(x', y')$  are the positions of image pixels before and after mapping,  $z$  and  $z'$  represent the gray scale intensity values of image before and after mapping in Arnold 3D cat map equation. Here, we have changed  $z$  into  $f$  and modify the 3D cat map as:

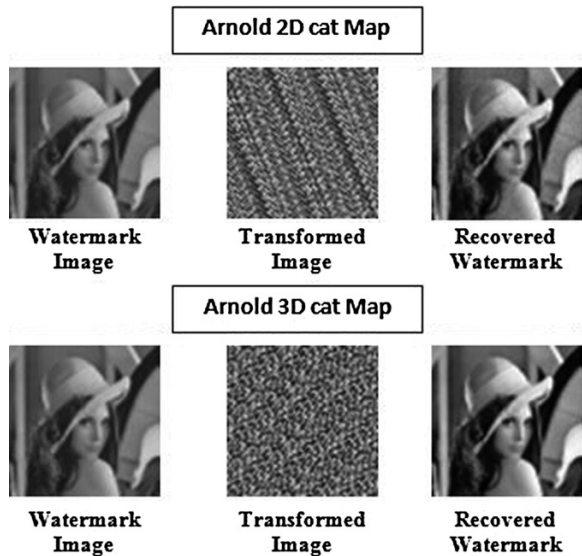
$$\begin{cases} \begin{pmatrix} x' \\ y' \end{pmatrix} = \begin{pmatrix} 1 & a \\ b & ab + 1 \end{pmatrix} * \begin{pmatrix} x \\ y \end{pmatrix} \pmod N \\ f' = (cx + dy + f) \pmod M \end{cases} \quad (3)$$

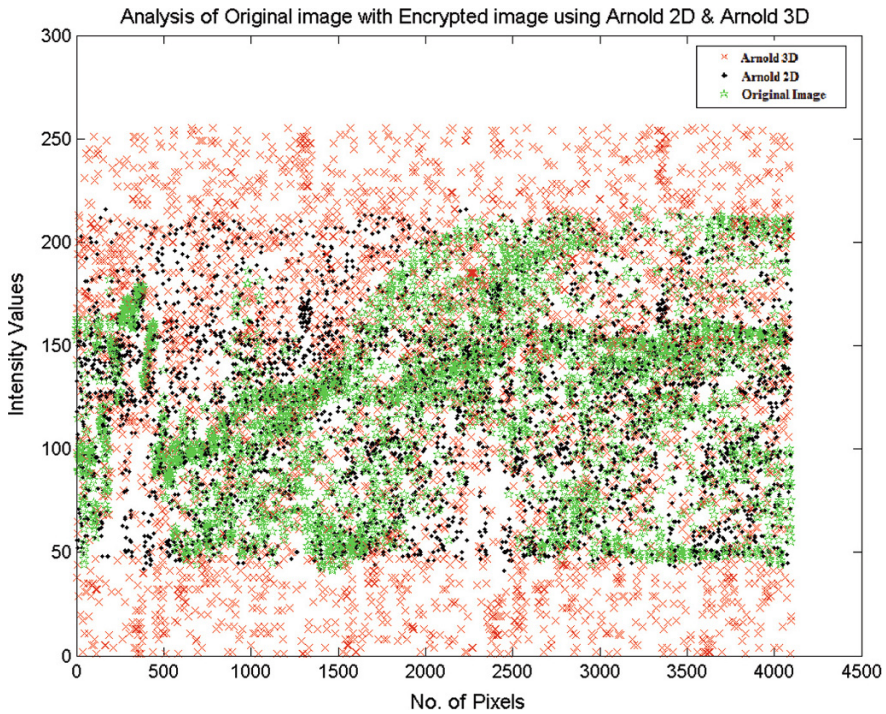
where,  $N$  is image size,  $M$  is the color level. Since we have taken gray scale image,  $M \in [0, 255]$ . Dual encryption is achieved in this 3D cat map since shuffling and substitutions techniques are used. Here, the 3D cat map shuffles the pixel positions with 2D Arnold cat map. Similarly, it substitutes gray values depending on the positions and original gray values of pixels. The results for Arnold 3D cat map for image encryption is shown in Fig. 1.

### 3.2 Result Analysis

This section compares the differences of intensity values of images using histogram analysis. The original image is encrypted using both the techniques Arnold 2D cat map and Arnold 3D cat map.

**Fig. 1** Results for image encryption using Arnold 3D cat map





**Fig. 2** Histogram analysis for Arnold 2D and Arnold 3D map

Figure 2 depicts the histogram analysis for number of pixels versus intensity values for digital image. The Arnold 2D map and Arnold 3D map are applied on a certain image and plotted on a single graph to represent the pixel variations after encryption process. The analysis shows that Arnold 3D cat map is more uniformly distributed than Arnold 2D cat map. Hence, it improves the security and makes it effective to use.

### 3.3 Differential Attack Analysis

Differential attack is also known as chosen plaintext attack, where a pair of cipher text is obtained related to plain text. The resistance to differential attack can be measured with number of pixel change rate (NPCR) and unified average changing intensity (UACI) [10] as:

$$NPCR = \frac{\sum_{i,j} K(i,j)}{a * b} * 100 \% \quad (4)$$

**Table 1** NPCR and UACI values

	Arnold 2D map	Arnold 3D map
NPCR	98.92	99.56
UACI	33.50	33.24

where, a and b are height and width of two pixels. If both pixels contain the same value,  $K(i,j) = 1$ ; otherwise,  $K(i,j) = 0$ . Analysis says higher the NPCR value, greater the resistance to differential attack.

$$UACI = \frac{\left\{ \sum_{i,j} \frac{|B(i,j) - B'(i,j)|}{255} \right\}}{a * b} * 100 \% \tag{5}$$

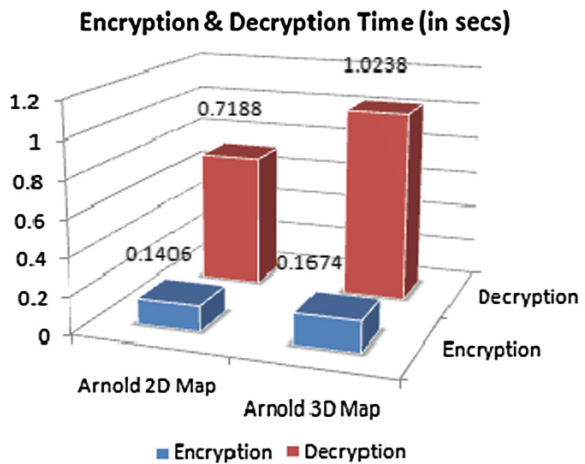
where,  $B(i,j)$  and  $B'(i,j)$  are the pixels of two images.

We have calculated NPCR and UACI under same initial conditions and parameters for Arnold 3D cat map. Further, we have compared our results with the results in Arnold 2D map. Table 1 depicts the simulated results of NPCR and UACI.

From above results, we can see that the NPCR and UACI of Arnold 3D cat map are better than Arnold 2D cat map. It shows that Arnold 3D cat map is more robust against differential attack.

Figure 3 shows that decryption takes more time than encryption in both the cases, which makes it difficult to attack by attackers. As 3D chaotic maps involve more controlling parameters than the 2D chaotic map, these are more secured.

**Fig. 3** Encryption and decryption time





## 4 Conclusion

This paper proposes a new framework of image encryption using Arnold 3D cat map. The effectiveness of this encryption has been verified by the histogram analysis. Also, the security of this technique has been evaluated against the differential attacks using NPCR and UACI values. The result shows that our proposed technique provides better security and resistant to the common differential attacks.

## References

1. Wong, K.W.: Image encryption using chaotic maps. In: *Intelligent Computing Based on Chaos*, vol. 184, pp. 333–354. Springer, Berlin (2009)
2. Abuhaiba, I.S.I., Abuthraya, H.M., Hubboub, H.B., Salamah, R.A.: Image encryption using chaotic map and block chaining. *Int. J. Comp. Netw. Inf. Secur.* **7**, 19–26 (2012)
3. Ahmad, M., Alam, M.S.: A new algorithm of encryption and decryption of images using chaotic mapping. *Int. J. Comp. Sci. Eng.* **2**(1), 46–50 (2009)
4. Ding, M.: Digital image encryption algorithm based on improved Arnold transform. In: *International Forum on Information technology and Applications*, pp. 174–176, IEEE (2010)
5. Jin, X.: A digital watermarking algorithm based on wavelet transform and Arnold. In: *International Conference on Computer Science and Service System*, pp. 3806–3809, IEEE (2011)
6. Ye, G., Wong, K.W.: An efficient chaotic image encryption algorithm based on a generalized arnold map. *Nonlinear Dyn.* **69**(4), 2079–2087 (2012)
7. Pradhan, C., Saxena, V., Bisoi, A.K.: Imperceptible watermarking technique using Arnold's transform and cross chaos map in DCT domain. *Int. J. Comp. Appl.* **55**(15), 50–53 (2012)
8. Liu, H.: A novel image encryption algorithm based on improved 3D chaotic cat map. In: *International Conference for Young Computer Scientists*, pp. 3016–3021, IEEE (2008)
9. Pradhan, C., Mishra, S., Bisoi, A.K.: Non blind digital watermarking technique using DWT and cross chaos. In: *International Conference on Communication, Computing and Security. Procedia Journal*, pp. 897–904 (2012)
10. Wu, Y., Noonam, J.P., Agaian, S.: NPCR and UACI randomness tests for image encryption. *Cyber J. Multi. J. Sci. Technol. J. Sel. Areas Telecommun.* 31–38 (2011)

# Case Selection Strategy Based on K-Means Clustering

Heba Ayeldeen, Osman Hegazy and Aboul Ella Hassanien

**Abstract** Knowledge acquisition is considered as an extraordinary issue concerning organizations and decision makers nowadays. Learning from previous failures and successes saves plenty of time in understanding the problems and visualizing data. Case-based Reasoning (CBR) as a process is one of the most used methods to solve the problem of knowledge capture and data understanding. In this paper we proposed an approach for clustering these documents based on CBR combined with lexical similarity and k-means algorithm for cluster-dependent keyword weighting. The cluster dependent keyword weighting help in partitioning and categorizing the theses documents into more meaningful categories. The proposed approach yield to 91.95 % increase of using CBR in comparison to human assessments.

**Keywords** Knowledge management · Semantic similarity · Case-based reasoning · K-means

## 1 Introduction

Saving a lot of time in finding the optimum solution is considered as a win-win situation. Organizations nowadays, focus on reducing time; effort and resources as well in every single cycle process they do [1]. Case-based Reasoning is con-

---

H. Ayeldeen (✉) · A.E. Hassanien  
Scientific Research Group in Egypt (SRGE), Cairo, Egypt  
e-mail: heba.ayeldeen@gmail.com

A.E. Hassanien  
e-mail: aboitcairo@gmail.com

H. Ayeldeen · O. Hegazy · A.E. Hassanien  
Faculty of Computers and Information, Cairo University, Cairo, Egypt  
e-mail: osmanhegazy@gmail.com

sidered as a full whole integrated system that aid in decision making and planning as well [2].

Case-based Reasoning (CBR) system is a full computational process of discovering patterns in large data sets involving methods at the intersection of artificial intelligence, machine learning, statistics, and database systems. Simply, CBR refers to extracting or “mining” knowledge from large amounts of preexisting data [3–6]. Spending a lot of time in search as well as finding the symmetry of different sets/article/documents and even the relations between objects is considered as the domain problem for organizations. For instance in universities, graduate students take a lot of time in searching, sorting and finding related work for research. On the other hand, staff members spend time in categorizing and classifying related articles based on certain research trend(s) (i.e. year/topic/point of research/results) [5, 7].

Case-based reasoning mainly focuses on overcoming the withdrawals within organization. As a concept, CBR deals with learning from previous experiences to solve new problems. The main advantages of CBR systems are [7–9]:

- *Problem definition and understanding.*  
In situations where insufficient or imprecise data and concepts exists, a case-based reasoner can still be developed using only a small set of cases from the problem domain. As an important step in CBR is the problem representation, where cases are briefly explained and indexed with specific attributes/properties.
- *Reducing the knowledge acquisition.*  
After the case or problem is well represented, the waste of time and the need to extract a solution from scratch would be eliminated. The Knowledge acquisition tasks of CBR consist primarily of the collection of relevant existing experiences/cases/problems and their representation and storage within the data warehouse.
- *Avoiding repeating mistakes made in the past.*  
A system like CBR system where failures are recorded as well as successes, and perhaps the reason for those failures, information about what caused failures in the past can be used to predict potential failures in the future.
- *Making predictions.*  
When information is stored whether success or failure, the case-based reasoner would be able to easily predict the success of the solution suggested for a current problem.
- *Avoiding repeating steps.*  
In problem domains that require significant processes to create a solution from scratch, an earlier solution or maybe modification can be easily found by reusing a previous solution for solving other problems.

Finally it can be concluded that Case-based reasoning (CBR) is the process of solving new problems based on the solutions of similar past problems.

The rest of this paper is organized as follows. Section 2 discusses main fundamentals of CBR used in solving/selecting solutions. Section 3 briefly describes the importance of using lexical similarity to find relatedness of texts and documents.

While Sect. 4 shows a case study and steps involved in selecting the case by lexical similarity with k-means clustering. Section 5 shows the interpreting results of the case study. The last section, presents experimental results and conclusion.

## 2 Case-Based Reasoning: Overview

Case-Based Reasoning is able to utilize the specific knowledge of previously experienced problems situations or cases.

### 2.1 CBR Life-Cycle Processes

In order to ease time taken to find the optimum solutions or even alternative solutions CBR is the answer. CBR is considered as a group of methodologies combined together to predict and make the process of knowledge acquisition easier.

Below are the main processes involved within the problem solving life cycle in a CBR system [7, 9, 10]:

1. Retrieve  
As previously shown in Fig. 1, when we have a new case or problem for instance to solve, similar previously experienced cases can be easily retrieved from the data warehouse of the CBR system.
2. Reuse  
The reusing of the cases would be an option by copying or even integrating the solutions from the cases retrieved.
3. Revise  
Revising or adapting the solution(s) retrieved in an attempt to solve the new ones.
4. Retain  
Retaining the new solution once it has been validated, hence the process of knowledge acquisition and understanding the problem is valid now (Fig. 2).

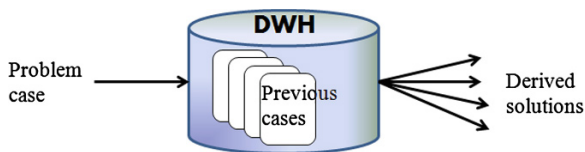
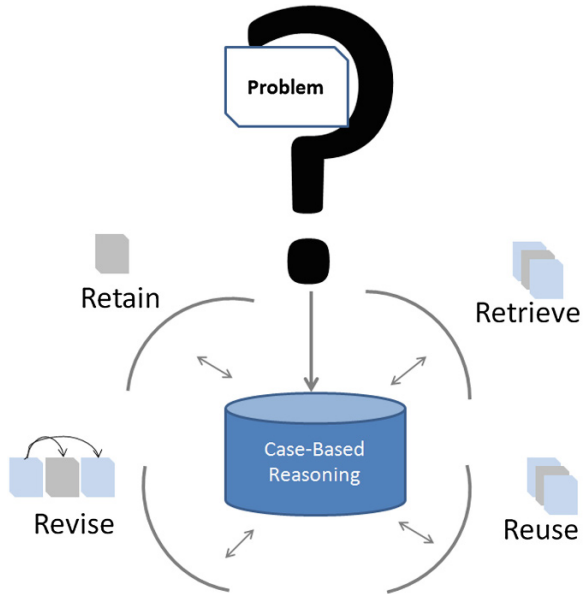


Fig. 1 Case-based reasoning system

**Fig. 2** Case-based reasoning life cycle process



Understanding the problem domain to easily capture the knowledge needed is concerning organizations nowadays. Text representation and data visualizations can be easily accessed by using CBR and make use of every single process within life-cycle of CBR system.

### 3 Lexical Similarity for Text and Document Mining

It is not easy to find the similarity between objects and get the correlation between them. Semantic and lexical similarity as well as text clustering are important means and methods of mining in texts. Text clustering is an unsupervised classification of documents and objects, which divides a text collection into several subsets called clusters, the text of each cluster has greater similarity than the one in different cluster in mean of categorizations of objects [11].

Making predictions and planning concern all decision makers. Properly classifying and clustering texts based on certain criteria and trend improves the understanding and relatedness of data to easily extract the knowledge based on good classification [11, 12]. The processes of retrieving data; reusing; validating and retaining solutions are considered as the best way to make use of the information rather than rebuilding solutions from scratch. Analyzing the relationships between documents based on concepts and terms is one of the semantic analysis methods [11].

The classification and prediction models are two data analysis techniques that are used to describe classes and predict future data classes. Classification is the process of finding a model/function of technique that describes and differentiates data classes or concepts, for the purpose of being able to use the model to predict the class of objects whose class label is unknown [13, 14].

On the other hand, cluster analysis is a method that organizes a large set of unordered text documents into a small number of meaningful and coherent clusters/categories by which similar records are grouped together [5]. A clustering is a collection of data objects that are similar to one another within the same cluster and are dissimilar to the objects in other clusters. An organization can take the hierarchy of classes that group similar events. Text document clustering groups similar documents that to form a coherent cluster, while documents that are different have separated apart into different clusters [4].

### 3.1 K-Mean Clustering Algorithm

K-means clustering is an algorithm to group and categorize objects based on specific features into k number of groups. Clustering is achieved by minimizing the sum of the squares of distances between data and the corresponding centroid of the cluster. The main idea is to assign k-centers for each cluster; however, a better way to select k is to place them as far away from each other as possible and associate each data point in a given data set with the nearest centroid. At this point, k new centroid must be recalculated as bar centers of the clusters resulting from the previous step. Given these new k new centers, a new binding between the same data set points and the nearest new centroid must be performed [4, 6]. The k centers change their location iteratively until no more changes occur. Finally, the k-means algorithm aims to minimize an objective function, in this case a squared error function. The objective function is defined as [15]:

$$J = \sum_{j=1}^x \sum_{i=1}^k ||x_i^j - C_i||^2 \quad (1)$$

where  $||x_i^j - C_i||^2$  is a distance measure between a data point and the cluster center. This is an indicator of the distance between the n data points and their respective cluster centers. Algorithm 1 shows the steps for segmenting images into regions using the k-means clustering algorithm.

## 4 Case Study

### 4.1 Data Collection

Data was collected from the digital library of Faculty of Medicine, Cairo University. Faculty of Medicine in Cairo University is classified into 35 departments. The data collected was these documents including the title of the theses and the abstract with keywords. The theses documents are categorized into Master and doctorate theses. Documents are tracked within the last 10 years separated and categorized based on the departments within the Medicine school. About 4,878 theses data was collected and about 15,808 keyword in the theses data.

**Algorithm 1** K-means clustering algorithm

1. Compute the intensity distribution /\*the histogram of intensities\*/.
2. Initialize the centroids with k random intensities /\*the number of clusters to be found\*/.
3. Initialize  $\mu_i^k = 1$
4. FOR: Each cluster  $C_j$
5. REPEAT:
6. Cluster the points based on distance of their intensities from the centroid intensities.

$$C^{(i)} := \arg \min_i \|x^{(i)} - \mu^i\|^2 \quad (2)$$

7. Compute the new centroid for each of the clusters

$$\mu^i = \frac{\sum_{i=1}^m 1_{C(i)=j} x^i}{\sum_{i=1}^m 1_{C(i)=j}} \quad (3)$$

where i iterates over the all intensities, j iterates over all the centroids, and  $\mu^i$  is the centroid intensity.

8. UNTIL: cluster labels of the image does not change anymore.
9. ENDFOR.

### 4.2 Problem Definition

The aim of the work is to find out the departments that can work together easily to increase the research field in the different faculties of Cairo University. To do so, we focused on the theses mining concept for instance for Faculty of Medicine, Cairo University.

### 4.3 Case Selection by Lexical Similarity and K-Means Algorithm

After refining the keywords within the data sets and removing the stop words, the steps below were used: With the huge amount of data collected, knowledge is then extracted stating that certain departments have potential impact in working together for the purpose of increasing the level of scientific research and helping students in the information retrieval through the theses mining. After calculating the score wait for the tile and the abstract as well, we have (Table 1):

**Algorithm 2** Lexical similarity following K-means

- Iteration 1  
After looping on the keywords, use lexical similarity and start getting all departments in which keyword exists in theses data
- Iteration 2  
Based on combinations from the first iteration, calculate the score weight of keywords over all theses document title
- Iteration 3  
Calculate the score weight of keywords over all theses document abstract
- Iteration 4  
Use k-means algorithm (section 3A) to calculate the distance between all documents
- Iteration 5  
Compare and get highest score for better combinations

To affirm that the combinations are the optimum ones and the best choice that departments can work together in the scientific research iteration was done. By using cluster analysis, making clusters for the results of iteration 2 and comparing it with the new clusters from the last iteration based on the abstract on the theses (Table 2).

**Table 1** Sample of the data: the best combination of departments based on the theses titles

Department 1	Department 2	Weight <sup>a</sup>
Ophthalmology	Orthopedic surgery	8
General surgery	Medical parasitology	8
Otorhinolaryngology	General surgery	1
General surgery	Orthopedic surgery	1
Obstetrics and gynecology	General surgery	2

<sup>a</sup> The weight represents the repetition number of keyword in the theses title



**Table 2** Sample of data: the best combination of departments based on the theses abstracts

Department 1	Department 2	Weight <sup>b</sup>
Ophthalmology	Orthopedic surgery	4
General surgery	Orthopedic surgery	5
Otorhinolaryngology	General surgery	4
General surgery	Medical parasitology	4
Obstetrics and gynecology	General surgery	6

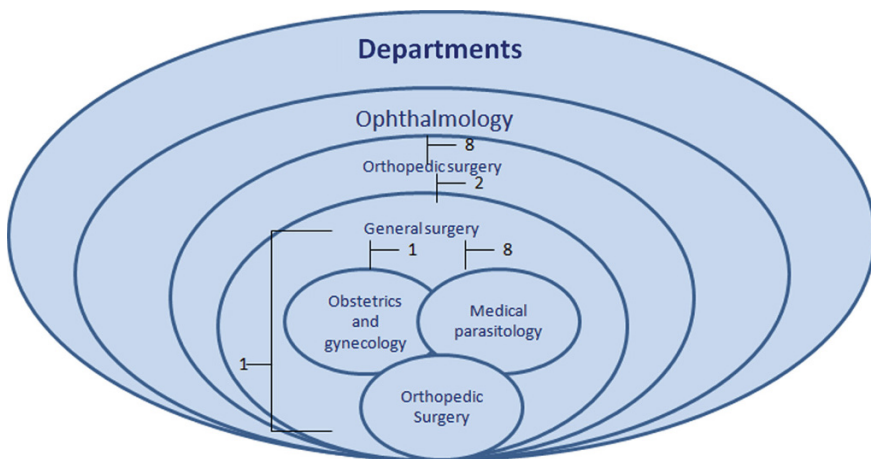
<sup>b</sup> The weight represents the repetition number of keyword in the theses abstracts

### 4.4 Experimental Results

After applying the k-means algorithm, we find out that there is a correlation between the combinations of the abstract with respect to the title. The accuracy percentage of the data affirming that the combination of departments are the optimum based on the objective function defined earlier 93.21, 6.79 % of the data do not affirm that the combinations in the title and keywords match the combination of the abstract (Fig. 3).

Although the documents are classified based on the departments we focused on applying a cluster analysis and then applying the Euclidean distance to get more accurate combination of departments that can potentially work together (Table 3).

Other than a single word, we applied also the use of a phrase (terms) for better results. For example like “Primary care” and “Diabetes mellitus”. So the bag of word can be treated either as a single or a term as a whole. In the case study, we assigned the weights as the number of occurrences of the word in the title of the



**Fig. 3** Using K-means to get the nearest departments based on titles

**Table 3** Bags of words representation of the theses documents (titles)

Word	Occurrences
Ultrasound	87
Biopsy	16
Pacemaker	3
⋮	⋮
Catheters	1
Stents	3

document normalized by the document title length to get the word frequency in each document.

In our case let’s set the threshold change/stopping condition to 0.001 where there is no big change in the values of each documents in the cluster. We continue the steps by calculating the new cluster centers based on K-means algorithm and updated the values.

After several iterations, we see that T1, T3, T5 and T7 are belonging to same cluster 1 which after knowledge extraction can be categorized to easily work together. On the other hand, T2, T4, T6 and T8 are classified to cluster 2 on basis of high membership values in both clusters. Finally it can be concluded that using data warehouse and CBR techniques and methods are much better for human assessment for biomedical data and that applying lexical similarity and K-means clustering algorithm results in better results with 91.95 % than not using CBR.

## 5 Conclusion

Recently, the use of Case-Based Reasoning, semantic similarity measures as well as data mining methods leads to the improvement of many applications. Based on the experimental evaluations it is indicated that the proposed approach yields results that correlate more closely with human assessments than other.

In this paper, we showed mathematically how texts can be clustered and classified by using CBR methods and the lexical similarity k-means algorithm.

Other algorithms can be considered as well for future work, like applying the genetic programming; neural networks and comparing the results simultaneously within the cycle of CBR.

## References

1. Pressman, R.S.: Software Engineering—A Practitioner’s Approach, 5th edn. McGraw-Hill International Edition, New York (chap. 5) (2001)
2. Kolodner, J.L.: An introduction to case-based reasoning. *Artif. Intell. Rev.* **6**, 3–34 (1992)
3. Singh, S. K.: Database Systems: Concepts, Designs and Applications. Pearson Education, India (2006)

4. Han, J., Kamber, M.: *Data Mining: Concepts and Techniques*, 2nd edn. Elsevier Inc., Amsterdam (2006)
5. Rainer, R.K., Snyder C.A. et al.: *Decision Support systems*, pp. 333–341 (1992)
6. Ranjan, J.: *Managing student data: a data mining-based framework for business schools*. *Int. J. Inf. Oper. Manage. Edu.* **4**(1), 83–98 (2011)
7. Pal, S.K., Shiu, S.C.K.: *Foundations of Soft Case-Based Reasoning*. Wiley, Hoboken (2004)
8. Park, M.-K., Lee, I., Shon, K.-M.: *Using case based reasoning for problem solving in a complex production process*. *Expert Syst. Appl.* **15**, 69–75 (1998)
9. Grupe, F.H., Urwiler, R., Ramarapu, N.K., Owrang, M.: *The application of case-based reasoning to the software development process*. *Inf. Softw. Technol.* **40**, 493–499 (1998)
10. Rezvana, M.T., Zeinal Hamadania, A., Shalbafzadehb, A.: *Case-based reasoning for classification in the mixed data sets employing the compound distance methods*. *Eng. Appl. Artif. Intell.* **26**(9), 2001–2009 (2013)
11. Al-Mubaid, H., Nguyen, H.A.: *Measuring semantic similarity between biomedical concepts within multiple ontologies*. *IEEE Trans. Syst. Man Cybern. Part C: Appl. Rev.* **39**, 389–398 (2009)
12. Metzler, D., Dumais, S., Meek, C.: *Similarity measures for short segments of text*. In: *Proceeding ECIR'07. Proceedings of the 29th European Conference on IR Research*, pp. 16–27 (2007)
13. Nelson, S.J., Johnston, W.D., Humphreys, B.L.: *Relationships in medical subject headings. Relationships in the Organization of Knowledge*. K.A. Publishers, New Delhi (2001)
14. Ayeldeen, H., Hassanien, A.E., Fahmy, A.A.: *Evaluation of semantic similarity across MeSH ontology: a Cairo University thesis mining case study*. In: *12th Mexican International Conference on Artificial Intelligence*, pp. 139–144. Mexico City, Mexico (2013)
15. Jain, A.K., Murty, M.N., Flynn, P.J.: *Data clustering: a review*. *ACM Comput. Surv.* **31**, 264–323 (1999)

# Cloud Computing Framework for Solving Virtual College Educations: A Case of Egyptian Virtual University

Hany Soliman Alnashar, Mohamed Abd Elfattah, M.M. Mosbah  
and Aboul Ella Hassanien

**Abstract** Educational institutions across the World rely heavily on information technology (IT) in teaching-learning that accept the services provision and business needs. Whereas buying and preserving a huge number of devices used in educational process whether it is licensed software and/or original hardware require great investment and special skills to support them in the current financial crisis which affect the growing needs while the Higher Education System is facing many obstacles in supplying vital technology support for educational process and its performance measurements. This paper highlights the advantages of cloud computing which is the better mechanism for using ICT to enhance Egyptian Higher Education; such technology provides easy accessibility and scalability, storage and cost minimization. Accordingly, implementing the proposed framework of the hybrid cloud computing for the Egyptian Virtual University will have a significant contribution for enhancing the educational process in the country.

---

H.S. Alnashar (✉)

Computers Engineering Department, Cairo Higher Institute, Cairo, Egypt  
e-mail: nhany73s@gmail.com

M. Abd Elfattah

Faculty of Computers and Information, Mansoura University, Mansoura, Egypt  
e-mail: m\_bdelfatah@ymail.com

M.M. Mosbah

Department of Information System, Arab Academy for Science Technology  
and Maritime Transport, Cairo, Egypt

A.E. Hassanien

Faculty of Computers and Information, Cairo University, Cairo, Egypt  
e-mail: aboitcairo@gmail.com  
URL: <http://www.egyptscience.net>

A.E. Hassanien

Faculty of Computers and Information, Beni Suef, Egypt

H.S. Alnashar · M. Abd Elfattah · A.E. Hassanien  
Scientific Research Group in Egypt (SRGE), Cairo, Egypt

© Springer India 2015

J.K. Mandal et al. (eds.), *Information Systems Design and Intelligent Applications*,  
Advances in Intelligent Systems and Computing 339,  
DOI 10.1007/978-81-322-2250-7\_40

395

**Keywords** Cloud computing · Higher education · Advantages · Virtual university · Framework hybrid cloud

## 1 Introduction

World cannot be considered without technologies. The integration of communication and information technology (ICT) is considered as global trend that occupied a great interest in the world. Nowadays, everything is circulating around development of IT. The role of IT is increasing day after day, every day IT field is growing rapidly, and recently so many innovations have been and still evolved using the IT which made life easier and dynamic than before. In the recent years, educational institutions and universities or even industries contributed in converting the community, many researchers planned to update the current IT in the field of education. Education is often based on internet and ICT to provide educational resources especially from the beginning of the twenty first century, but not as much as in Higher Education (HE) inasmuch the developing countries are often see using IT in HE as luxury.

This concept negatively affects teachers, learners and educational system in such countries due to insufficiency of the infrastructure of ICT and restricted support for providing training for both teachers and learners to make them able to use such technology, while actually most of the information and applications are based on the internet. Every day that goes by, research and educational needs of HE change in line with the development of IT. Egypt has many Universities and educational institutions where many students need to access to computing that have software and hardware which must be renewed in accordance with those changes. As well, every year new versions of software issued to meet the needs of the industry. Naturally, this trend leads to high expenses in providing new software and hardware to be used by learners; however most of the educational institutions budgets are allocated to meet such needs.

Education sector in Egypt is the largest workforce in the Middle East and North Africa that full of investment opportunities. The HE sector in Egypt has 2.5 million served by 20 public universities and 19 private universities while number of students enrolled in private institutes reached 313,931 in June 2012, and about 63,000 staff members, 250,000 post graduate student [1]. No one can decline the necessary role that Cloud computing plays in the development of HE newly. Using Cloud computing in the HE can provides data storage, databases, educational resources, software and applications that can be accessed through Web browser of mobile devices, simply cloud computing provides services anytime anywhere but having in mind the user is not responsible for where the services or the application are located or how it maintained.

The rest of this paper is structured as follows. Section 2 presents implementation of cloud computing technology. In Sect. 3 we present the benefits of cloud computing in EHE-IS. Section 4 presents the related work. In Sect. 5 presents cloud-based egyptian university for information system. Finally, in Sect. 6 conclusions and future work are addressed.

## **2 Implementation of Cloud Computing Technology**

Due to the vital role that cloud computing technology plays in the field of HE systems, whereupon, the implementation of such technology will significantly minimize obstacles that might be faced and get the required results immediately.

The implementation of cloud services at Egyptian Higher Education (EHE) provides various opportunities and benefits for the user (student, instructor, researcher, and etc.). In Egyptian higher education for Information Systems course (EHE-IS).

## **3 Benefits of Cloud Computing in EHE-IS**

According to [2–6] expressed that the following are significant benefits of cloud computing in educational institution and can be divided as follows:

### ***3.1 Technical Part***

- Easily access: allow the students to easily access anywhere, anytime, and browser-based application can also be accessed by different devices (mobile phone, desktop, and etc.).
- Data management: the crash recovery process is nearly unneeded. If the client computer corrupted, there is no need for recovering no lost data because everything is stored in the cloud.
- Multi-tenancy: is a service that provides any application can be used inside or outside the university, while at the same moment this application has its own virtual computing and secure environment. In addition multi-users can use the same operating systems, hardware, software and data storage mechanism but users do not have the ability to see each others data.
- Experience: Students can have a richer and more diverse learning experience, even outside class.

### ***3.2 Economical Part***

The economical part focuses on the post period of the implementation of educational cloud are:

- **Cost Reducing:** it provides low cost solutions for educational process for their students, researchers, and faculty. And also upfront cost to run the systems on the cloud is very low.
- Most of the software applications are free, available, ready-to-use or pay-per-use.

### ***3.3 Non Functional Part***

- **Flexibility:** allow the users to store more data regardless disk space limit and thus users are capable to store their data as much as they can.
- **Reliability:** 24 h without any interruption.
- **Availability:** providing the user with massiveness services regardless any failure is important to give him the ability to establish cloud systems.

### ***3.4 Security Part***

As well as cloud technology provides security benefits for individuals and educational that is using HE system, as the following:

- **Improved incredibility:** anyone can hardly determine where the machines; that store lots of data such as (text, audio/video, image, exams, assignments and also results), are located? In order to avoid any theft case by discovering the physical components.
- **Centralized data storage:** there is no fear to lose any cloud client as the data is stored into the cloud. New client can start from the last point that the previous one has ended, while the task will be easy and very quickly. Suppose that a PC that stores the important data or examination results has stolen.
- **Visualization:** it extends the possibility for the immediate replacement of an exposed cloud server regardless high costs or damages occurred. Creating a clone of a virtual machine is too easy, so any expected cloud outage will be reduced substantially.

## 4 Related Works

The potential and efficiency of using cloud computing in higher education has been recognized by many universities among which we mention university of California, Washington State University's School of Electrical Engineering and Computer Science, higher education institutions from UK, Africa [7], U.S. and others.

In [8] discussed the appropriate cloud application used to constructs a collaborative learning environment. They illustrated benefits of using cloud computing, such as solving the network storage when dealing with huge resources. In Addition, they have focused on reasonable construction of the learning environment to take advantage of all the needed educational tools accessible by cloud computing. Authors in [9] focused on the effectiveness of using services cloud such as IaaS and PaaS in educational fields, especially in teaching advanced Computer Science courses.

The BlueSky cloud framework is presented in [10] an example of a cloud implementation to support scalable and cost efficient services for e-learning systems for basic education in China. By Praveena and Betsy [11] provided a comprehensive introduction to the application of cloud in university. In [12] a framework for Cloud Infrastructure and Application (CloudIA) is presented to build private cloud targeting e-Learning and e-Science applications in university. The CloudIA project is a market-oriented cloud infrastructure, which used different scenarios beside different virtualization technologies that designated the components used in building private cloud. This framework is used to provide PaaS, IaaS and SaaS as services of the cloud to the university.

According to [13] discussed more than ten cloud computing offerings could be delivered in Malaysian universities. Using cloud will enhance the learning environment; thus make the learning process highly reactive and accept the students expectations. Additionally, he claimed that using such cloud technologies evolve cooperation and communication learning environment while he stated clearly that there are some obstacles could hinder the expansion of this technology such as internet connection, privacy of the data and security.

## 5 Cloud Based Egyptian University for Information Systems (CBEU-IS)

### 5.1 Building the Framework

Utilizing Cloud technology in providing multiple services; for example, e-learning environment, will employ vital resource share which help in solving the scalability. Thus, placing Egyptian Virtual University (EVU) services upper cloud technology considered the preferable solution to solve limitations of the current IT (e.g. Department of Information Systems). The general design for Egyptian University



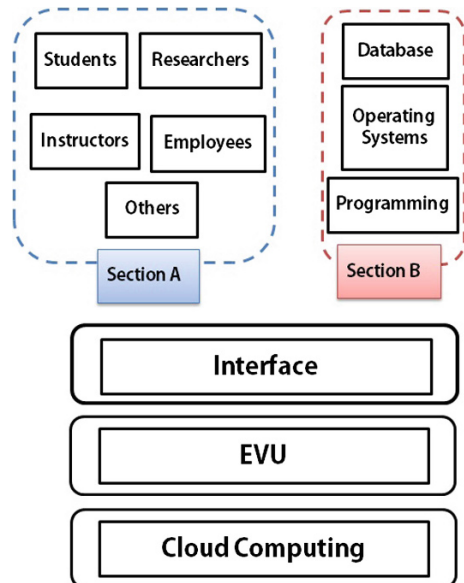
systems depends on the cloud computing technology that has an interface layer which controls the access of users to multiple services.

Effecting cloud based architecture to Information Systems courses will lead in adding the courses content in the suitable layer across the interface by adding the content as shown in Fig. 1. This architecture is responsible for providing more multimedia services for the users. In addition, using videos was a problematic issue in the previous systems while the solution of such problem is to use Cloud infrastructure. Providing cloud-based education for the staff not only portrays the advantages of the attached infrastructure [3] but also using cloud services will gain more solid base in programming and management skills.

Based on the identified courses and selected clouds, the next EVU Ecosystem for Information Systems based on cloud computing (EVUE-IS) framework is offered. The framework focused on how to combine department of information system courses as the process for teaching those courses will base mainly on cloud technology. Figure 2 shows the (EVUE-IS) framework. The presented framework in other words (EVUE-IS) consists of several modules including service management and security and layers including IaaS, PaaS, SaaS and User Interface:

1. **User interface layers:** Is the first layer will be used between the users such as students and instructors etc., and EVU infrastructure through various means such as laptops, mobile devices and desktop. The user interface layer consists of three main components:

Fig. 1 Cloud computing based EVU architecture



*Catalog:* This component has many services; each has detailed information, to determine who can access this service and where the layer is located?

*User portals:* This component provides accessibility to specific web applications or services using internet connection once everything is uploaded

*Store courses:* This component composed for the purpose of sorting the courses by name or access level which can be included in one of the three layers (SaaS, PaaS, and IaaS)

2. **Software as a Service layer:** The second layer helps the user to access to any applications or tools that hosted by the cloud (e.g. Class room management, G-mail and other applications) and the user can use these applications easily. In most cases beginner users will depend on such layer for example students taking introduction to computers course using Microsoft Word to write the report. Also, using Google Apps [14] or SkyDrive [15] is considered as element for this layer.
3. **Platform as a Service layer:** The third layer helps the user to access various platforms according to course level (e.g. database system, software engineering, computer security etc). For example students taking database system course, using this layer give users the ability to build more advanced systems and disseminated database systems through utilizing multiple soft wares to measure and examine the deployed systems and databases such as Amazon [16]. The computer security course, in the PaaS level, student is capable to build inception keys and data encoding mechanisms. Whilst, software needed for engineering course needs a platform to be developed which can be found on the PaaS level.

Various operating systems can be chosen to build particular scheduling algorithm, and distinguish the Central Processing Unit (CPU) utilization to fix the current problem in fast and active way when using different operating systems. Users use PaaS Layer for their own work simply through connecting to the cloud.

4. **Infrastructure as a Service layer:** The forth layer provides flexibility for the user as the same as he dealing with the hardware but as virtualization through using processing, networks, storage and other fundamental computing resources where the user is able to deploy and run sophisticated software, which can include operating systems and applications for example; the advance computer security course, the student does not manage or control the cloud infrastructure but he has control over operating systems, deployed applications, and storage and possibly limited control of select networking components (e.g., host fire-walls, and Amazon's Elastic Compute Cloud (EC2)) are all good examples of IaaS layer services providers.

Furthermore, multi-users have the ability to get the accurate details of the virtualization with some restriction which categorizes the virtualization course set in this layer. This layer can be divided into three levels:

- *Virtual resources maintenance and management*: Resources of EVU infrastructure can be maintained and managed by these components storage, network and power management using open source called Eucalyptus [17].
- *Virtual ingredient Resources*: This level can create any number of VM, each has its own V CPU, V Network V Storage and V Memory while the user can place V OS as guest OS.
- *Physical ingredient*: This level consists of the physical CPU, Storage, Network and Memory acts as hosting machine.

5. **Modules**: The two modules discussed as below:

- *Security*: This module provides authentication process to make the end-users of the EVU logging in and access different layers in the cloud.
- *Service management*: This module based on management and monitoring of the resources, for the purpose of guarantee the Quality OS between layers of the EVU framework.

## 5.2 Implementing the Proposed Framework

The proposed framework utilized the existing IT infrastructure for EVU which would adopt the framework based on cloud computing for (EVU-IS) as illustrated in Fig. 2. Cloud computing consists of four deployment models such as Hybrid cloud [6], that merge public and private cloud together. This mix process makes the user able to gather various services from various cloud service providers [6]. In addition, Hybrid cloud ensures data security for the users and also provides them with important applications to be used in universities by supplying them on the private cloud in spite that such important applications have been hosted from different cloud providers.

Full control considered as the most remarkable feature of the Hybrid cloud, therefore EVU can utilize this feature to control the system once it controlled a part of the infrastructure. Consequently, an open-source named Eucalyptus has been nominated to be used in the proposed framework aiming to manage the repetition of the disseminated data center such as managing large number of connected VMs.

Eucalyptus's main role is to manage the VMs [18]. Using such software accord multiusers the efficiency to run and deploy existing resources which might help the user to experiment the software using its massive features in creating VM infrastructure. Next Fig. 3 shows an overview of hybrid cloud using the Eucalyptus as virtual infrastructure manager between the private and public cloud for (EVU-IS).

This figure shows the eight steps of the authorization process for chosen private cloud. These steps are:

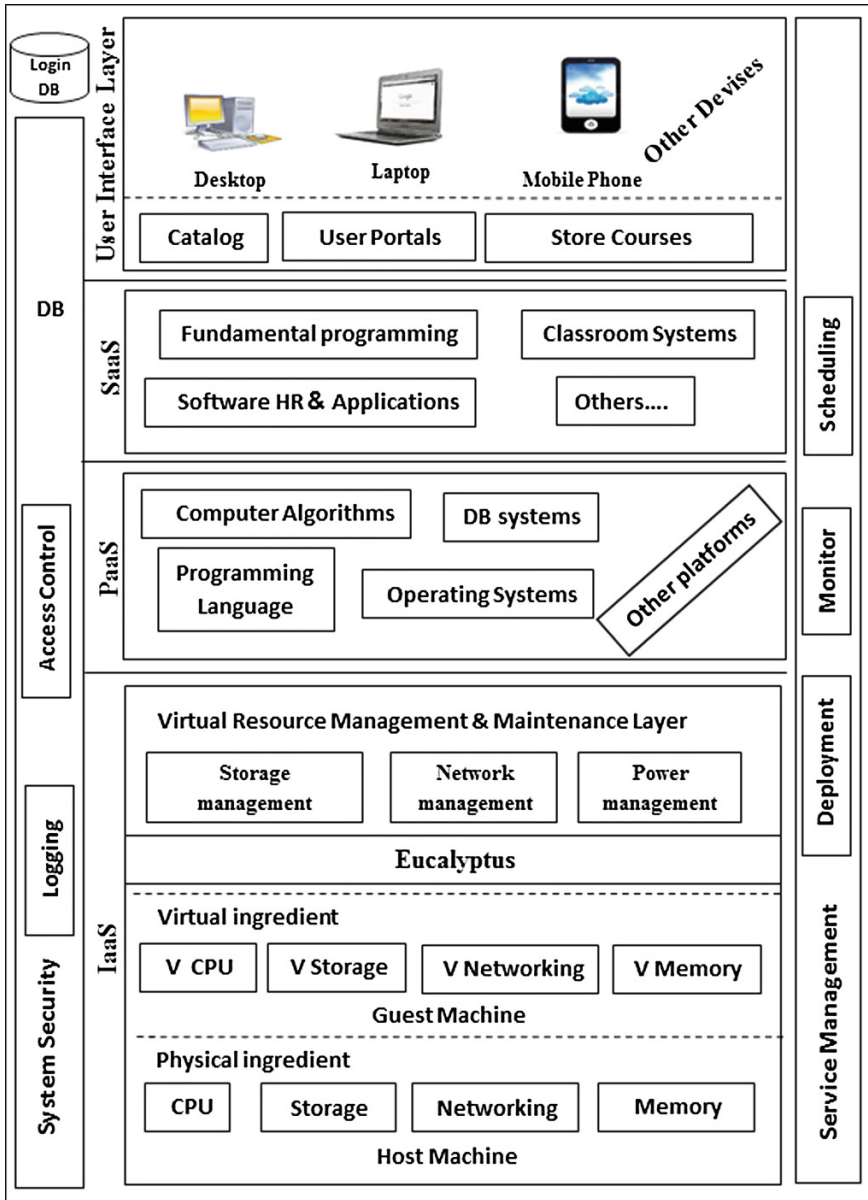
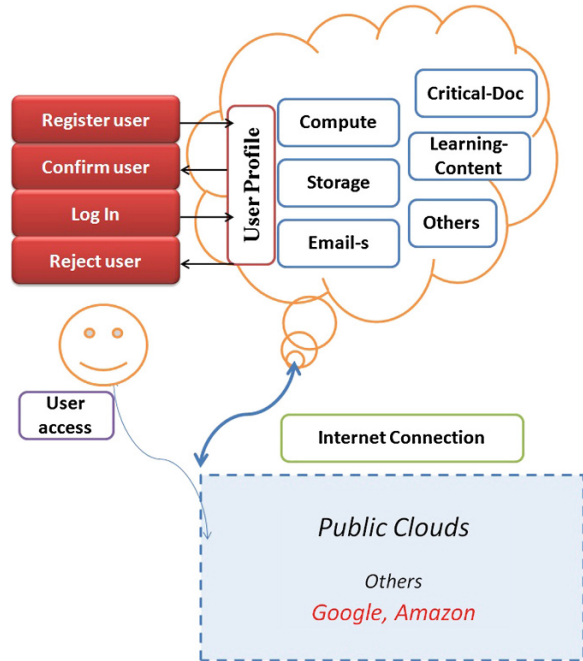


Fig. 2 EVU-IS based on cloud computing

1. The user either he is student, instructor or other, sends a request using EVU hybrid cloud interface to register his User Name and Password.
2. The user profile in private cloud needs to confirm the User Name and Password (Verification level).

**Fig. 3** EVU-IS based on cloud computing



3. Request for any service will be rejected automatically if the user is unauthorized.
4. The request will be redirected to the proper location by Eucalyptus, if the user is authorized to request the service.
5. A connection will be established between the requested service from the cloud and user by the system.
6. The system coincide the service delivery between the user and requested service from the cloud.
7. When the user needs the resource, while he did not exceeded the duration, the system will deliver the service to the resource and user.
8. If the user did not need the requested resource from the cloud. The system will disconnect the user from cloud.

But a very hard task might obstacle the process of transferring the current platform or system to be managed or accessed by the cloud. For example this process needs lots of time to plan and change the present layers and the architecture of the platform to be convenient with the environment of the cloud-based education. Moreover, there is a need for flexibility, accessibility and solutions for developing and deploying the proposed framework. Thus an open-source called Aneka [19] has been nominated for this purpose which will meet the desired requirements and it will be the best solution for this case.

Aneka will be used middleware on top of Eucalyptus to give the ability of supporting multiple programming applications. While integrating various kinds of clouds is the main role of Aneka which allow the developers to run any applications

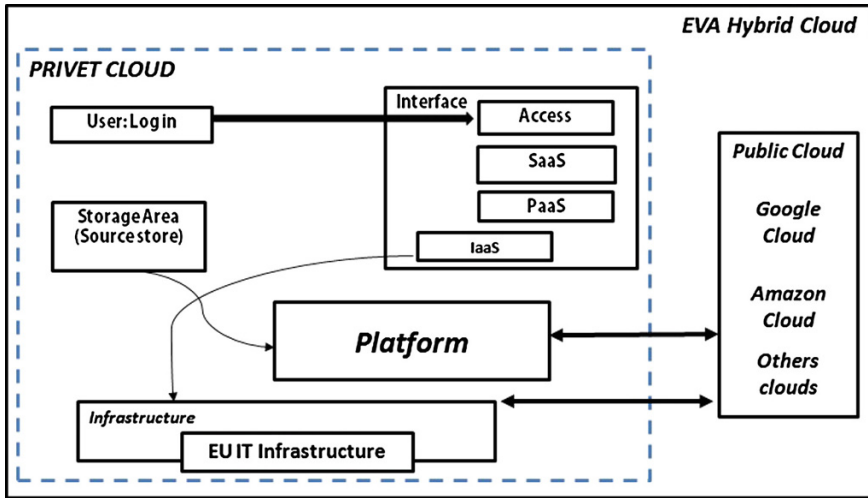


Fig. 4 EVU hybrid cloud

on private cloud however they can easily control or navigate SaaS and PaaS layers from the public cloud directly. Finally, the mentioned features of Aneka [19] is shown in Fig. 4. The private cloud for EVU provides the ability to be connected with public cloud any time for the user can request any service. The components of the EVU hybrid cloud are:

1. *Users Logs*: is the first layer that provides the ability to manage and support the use of resources requirements by user, besides screening the route of the authorizations users and their access to the next layer. Information of Users is stored in the Users Logs such as ID, Password and type.
2. *Use Interface Layer*: This layer is to manage and identify the access type; that could be (student, Instructor, or others), by the systems administrator. This layer consists of three services (SaaS, PaaS, and IaaS).
3. *Platform Layer*: this layer is to develop and deploy any application to access resources of the public clouds, and courses content (learning management system) for EVU and this layer is based on Aneka platform.
4. *Infrastructure Layer*: This layer Contains IT Infrastructure private cloud for EVU and Eucalyptus which plays a vital role in this layer.
5. *Courses store*: This layer consists of deferent services and course content for EVU learning systems, such as database systems, and other data, moreover it contains certain details about the homework and assignments for department of Information Systems students.

## 6 Conclusions and Future Works

Cloud computing offers an infinite number of the potential benefits could be gained to be used in the field of Higher Education to overcome the current system limitations. Accordingly this paper Discusses different cloud topics like cloud deployment types, service delivery models and related concepts. It also discusses the benefits and limitations of cloud computing to higher education institutions. This research investigated the potential benefits of using Cloud Computing in teaching-learning environments to overcome the current learning and service delivery system limitations. The research shows that Hybrid cloud computing is a better choice for deployment in the universities since it gives the combined benefit of private and public clouds. The proposed hybrid Cloud Computing would be used as a road map for further studies on the topic. The proposed framework implemented at departmental level and tested with mutable types of courses. Future work will mainly base on exploring the efficiency of the implementing the framework and its impact on the learners performance.

## References

1. Education sector in Egypt [Online]. <http://opentoexport.com/ar-ticle/education-sector-in-egypt/> (2013)
2. Pocatilu, P., Alecu, F., Vetrici, M.: Measuring the efficiency of cloud computing for e-learning systems. *WSEAS Trans. Comp. J.* **9**, 42–51 (2010)
3. Nasr, M., Ouf, S.: An Ecosystem in e-learning using cloud computing as platform and Web2.0. *ACM* **11**, 134–140 (2011)
4. Shivalingaiah, D., Sheshadri, K.N.: Application of cloud computing for resources sharing in academic libraries. In: *Proceedings of International Conference on Cloud Computing, Technologies, Applications and Management*, pp. 34–37. BITS Pilani, Dubai Campus (2012)
5. Al Noor, S., Mustafa, G., Chowdhury, S.A., Hossain, M.Z., Jaigirdar, F.T.: A proposed architecture of cloud computing for education system in Bangladesh and the impact on current education system. *IJCSNS* **10**, 7–13 (2010)
6. Kwofi, B.: Cloud computing opportunities, risks and challenges with regard to information security in the context of developing countries. M.S. thesis, Department Science in Information Security, Lulea University, Lulea (2013)
7. Sultan, N.: Cloud computing for education: a new dawn? *Int. J. Inf. Manage.* **30**, 109–116 (2010)
8. Mehta, H.K., Chandwani, M., Kanungo, P.: Towards development of a distributed e-learning ecosystem. In: *Proceedings of International Conference on Technologist for Education (T4E)*, pp. 68–71 (2010)
9. Vaquero, L.M.: EduCloud: PaaS versus IaaS cloud usage for an advanced computer science course (2011). doi:[10.1109/TE.2010.2100097](https://doi.org/10.1109/TE.2010.2100097)
10. Dong, B., Zheng, Q., Qiao, M., Shu, J., Yang, J.: BlueSky cloud framework: an e-learning framework embracing cloud computing. In: *Proceedings of International Conference on cloud computing*, pp. 577–582. CloudCom, China (2009)
11. Praveena, K., Betsy, T.: Application of cloud computing in academia. *Int. J. Syst. Manage.* **VII**, 50–54 (2009)

12. Sulistio, A., Reichand, C., Doelitzscher, F.: Cloud infrastructure and applications—CloudIA. In: Cloud Computing, vol. 5931, pp. 583–588. Springer, Berlin (2009)
13. Razak, A.: Cloud computing in Malaysia Universities. In: Proceedings of International Conference on Innovative Technologies in Intelligent Systems and Industrial Applications, pp. 101–106, Malaysia (2009)
14. Google Appengine [Online]. Available: <http://code.google.com/ap-pengine/> (2013)
15. Microsoft, Sky-drive your Cloud [Online]. Available: <http://windows.microsoft.com/en-us/skydrive>. Visited 20 Oct 2013
16. Amazon Web Services [Online]. Available: <http://aws.amazon.com/> (2013)
17. Nurmi, D., Wolski, R., Grzegorzczak, C., Obertelli, G., Soman, S., Youseff, L., Zagorodnov, D.: The eucalyptus open-source cloud-computing system. In: Proceedings of International Conference CCGRID, pp. 124–131. Shanghai (2009)
18. Eucalyptus [Online]. Available: <https://www.eucalyptus.com> (2013)
19. Alrokayan, M., Buyya, R.: A Web Portal for Management of Aneka-Based Multi Cloud Environments (2013)



# Scheme for Compressing Video Data Employing Wavelets and 2D-PCA

Manoj K. Mishra and Susanta Mukhopadhyay

**Abstract** In this paper, we have presented a novel scheme for the compression of video data that employs a combination of wavelets and 2-dimensional principal component analysis. In this method the accordion matrices constructed from group of consecutive video frames are subjected to multi-resolution decomposition using wavelet. Subsequently, *2D-PCA* is applied on the set of decomposed accordion matrices at each level of resolution. The compressed form of the video data finally consists of representative pairs of resolution-specific principal components and projection vectors. The method has been implemented and tested on a set of real video data and the results have been assessed on both qualitative and quantitative basis by measuring parameters like compression ratio (*CR*), peak signal to noise ratio (*PSNR*), structural similarity index measurement (*SSIM*) and the overall performance is found to be satisfactory.

**Keywords** *2D-PCA* · Feature matrix · Projection vector · Video compression · Wavelet structural similarity index

## 1 Introduction

The compression video data of huge size is essentially important for the sake of data archival as well as for communication of video data over public channels with limited channel bandwidth. Video data of natural scenes inherently contains various types of spatial and temporal redundancies which can be exploited to achieving video compression. There is always a trade off between the compression ratio and

---

M.K. Mishra (✉) · S. Mukhopadhyay  
Department of Computer Science and Engineering, Indian School of Mines,  
Dhanbad, Jharkhand 826004, India  
e-mail: manojmishra.ism@gmail.com

S. Mukhopadhyay  
e-mail: msusanta2001@gmail.com

the degradation in the visual quality of the reconstructed video frames in case of lossy compression scheme.

Motion estimation and compensation [1, 2] based encoders are the most widely used in video compression. However, motion estimation and compensation process is computationally intensive which makes it less appropriate for a real-time application. Westwater and Furht [3] have proposed XYZ algorithm which employed 3D DCT in the compression of the video data and the performance is comparable to the MPEG algorithm. Kim and O'Conner [4] have designed a moving edge detection algorithm using DCT coefficients using which, motion estimation can be applied selectively on blocks with a potentially high score of the moving edges. On the other hand, video coder based on 3D accordion transform proposed by Ouni et al. [5] is reported to produce video compression ratio closed to that based on motion estimation based coding but with less complexity in the processing.

The proposed method employs accordion to projects the temporal redundancy of each group of pictures onto spatial domain and combined that with spatial redundancy in one representation. Subsequently, wavelet and 2D-PCA are applied for achieving the compression. The rest of this paper is organized as follows. Next to this introductory section we present a brief review of the tools PCA, wavelet and accordion image in Sect. 2. Section 3 presents the theoretical formulation of the proposed work. The experimental results along with performance analysis are furnished in Sect. 4. Finally, concluding remarks are presented in Sect. 5.

## 2 Preliminaries

### 2.1 Principal Component Analysis

Dimensionality reduction is one of the essential steps commonly used in data compression where a given data in the form of a  $p$ -dimensional variable  $x = (x_1, \dots, x_p)^T$  can be expressed in lower dimensional representation,  $s = (s_1, \dots, s_k)^T$  with  $k \leq p$ , capturing the salient contents in the original data, according to some criterion. Principal component analysis (PCA) [6] achieves this by exploring statistically the similarity and correlation among the data items with an objective to retain the significantly dissimilar parts and simultaneously, removing the similar parts from the data set. The basic idea behind employing PCA is to identify new meaningful underlying variables by mathematically projecting the data variables to an orthogonal subspace for compact representations. Mathematically, it involves procedure that transforms a relatively large number of correlated variables into a comparatively smaller number of uncorrelated variables or principal components. The principal components are generally ranked based on their decreasing importance in expressing the variability in the data set.

### 2.2 Wavelet Decomposition of Image

The concept of multi-resolution decomposition [7–9] of an image originates from sub-band coding [10] which is based on frequency domain analysis of the image. In sub-band coding a bank of band-pass filters are employed to split the image (here, the accordion image). The resulting band-limited image data is sub-sampled to produce sub-images of reduced size and increased sparsity and reduced dynamic range of the intensity of the decomposed sub-images which make them highly useful in coding and compression. Wavelet transforms follow the same principle of sub-band coding but it employs approximation theory [11] in the spatial domain of the image. In DWT [11–13] an image is decomposed into multiple resolution by allowing it to pass through an analysis filter bank followed by decimation operation along both row and column dimension. At each step a better frequency resolution is obtained at the cost of reduced spatial resolution. Widely used wavelets are *Bi-orthogonal* [10], *Daubechies* [13], and *Haar* [14] wavelets.

### 2.3 Accordion Representation

The video data is essentially a temporal sequence of frames with the presence of both intra frame and inter frame redundancies. The accordion matrix [5] is basically a 2D representation of a group of video frames where the column of the accordion matrix come from the column of the frames in a periodic fashion. If  $F(x, y, t)$  represents the video frames with spatial coordinate  $x, y$ , and temporal coordinate  $t$ , the accordion matrix  $A$  is constructed from  $F(x, y, t)$  as illustrated in Fig. 1

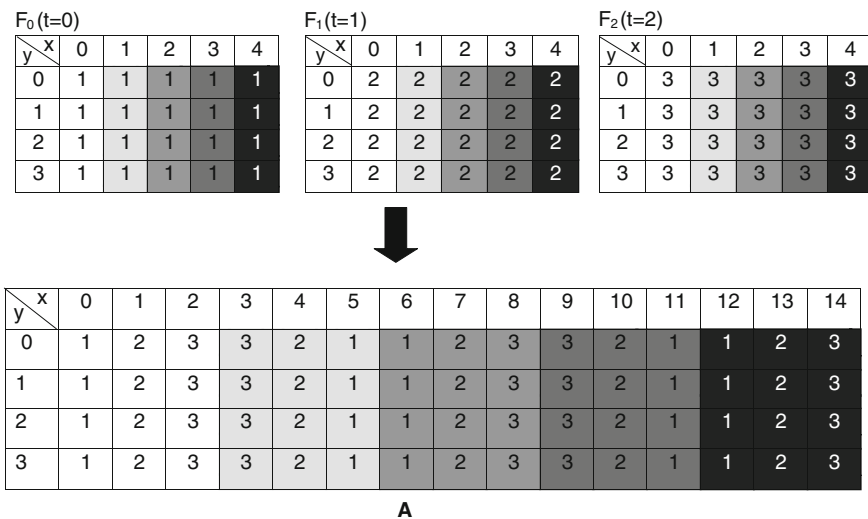


Fig. 1 Accordion image formation

### 3 Proposed Method

Unlike *PCA* [6], the *2D-PCA* [15, 16] is straightaway based on *2D* matrices rather than *1D* vectors constructed from the set of non overlapping blocks or sub-images. Let  $X$  denote an  $n$ -dimensional unitary column vector called as projection vector.  $A$  is  $m \times n$  accordion matrix which is transformed into  $Y$  using  $X$  by following linear transformation:

$$Y = AX \quad (1)$$

The purpose of *2D-PCA* is to select a good projection vector  $X$  by controlling the trace ( $J(X)$ ) of covariance matrix ( $S(X)$ ) constituted by the projected feature vectors as presented below:

$$\begin{aligned} J(X) &= tr(S_X) = tr[E[(Y - EY)(Y - EY)^T]] \\ &= tr[E[(AX - E(AX))(AX - E(AX))^T]] \\ &= tr[X^T E[(A - E(A))^T(A - E(A))]X^T] \end{aligned} \quad (2)$$

Therefore, covariance (scatter) matrix is then defined as:

$$G = E[(A - E(A))^T(A - E(A))] \quad (3)$$

This turns out to be a non-negative definite matrix of size  $n \times n$ , where  $E(\cdot)$  represents the expectation. For ' $L$ ' number of training matrices  $A_k$ , ( $k = 1, 2, \dots, L$ ) each of size  $m \times n$ .

$$E(A) = \frac{1}{L} \sum_{k=1}^L A_k \quad (4)$$

Thus

$$G = \frac{1}{L} \sum_{k=1}^L [(A_k - D)^T(A_k - D)] \quad (5)$$

The set of projection axes ( $X_1, X_2, \dots, X_{d_0}$ ) are the eigenvectors corresponding the  $d_0$  largest eigenvalues of  $G$ . This is known as generalized total scatter criterion, which is further used to extract the projected feature vectors  $Y_i = A_k X_i$ , for  $i = (1, 2, \dots, d_0)$ . Thus feature matrix for an accordion  $A_k$ , is formed as:

$$F = [Y_1, Y_2, \dots, Y_i, \dots, Y_{d_0}]_{m \times d_0} \quad (6)$$

The reduced size of feature matrix for an accordion is the key to video compression. The accordion can be reconstructed from its compressed counterpart as,

$$A_k = [Y_1, Y_2, \dots, Y_i, \dots, Y_{d_0}]_{m \times d_0} [X_1, X_2, \dots, X_{d_0}]_{d_0 \times n}^T \tag{7}$$

Therefore with judicious choice of  $X$  and estimated  $Y$ , the compressed data is formed by a set of  $d_0$  number of  $X$ - $Y$  pairs. For a accordion of size  $m_0 \times n_0$ , the size of the compressed data becomes  $d_0 \times (m_0 + n_0)$  as, each of  $X$  or  $Y$  is having a dimension of  $m_0 \times 1$ . Thus the compression ratio becomes

$$CR = \frac{m_0 \times n_0}{d_0 \times (m_0 + n_0)} \tag{8}$$

As presented in Eq. (7) the compressed accordion matrix is basically ‘ $d_0$ ’ strongest pairs of projection vectors ( $X$ ) and feature vectors ( $Y$ ). The overall compression ratio thus depends on the size of these  $d_0$  vectors.

Application of  $2D$ - $PCA$  on these resolution-specific accordion matrix yields projection and feature vectors of different size and dimension. The resolution-specific features are now more efficiently representable by groups of principal components. Thus there is a considerable reduction in number and size of projection and feature vectors which contributes significantly in improving the compression ratio and  $PSNR$ . This key idea is developed and implemented in this proposed work.

The accordion matrix under study is first decomposed using wavelet transform. At each level of resolution  $k$ ,  $2D$ - $PCA$  is applied on three detail accordion matrices namely  $A_{LH}^k$ ,  $A_{HL}^k$  and  $A_{HH}^k$  and the approximation accordion matrix  $A_{LL}^k$  is left for the next coarse level of resolution ( $k + 1$ ) as illustrated in Fig. 2. If  $s$  represents the resolution level and  $Y_s = A_s \cdot X_s$ , then the size of compressed data set becomes  $\sum_{s=1}^k d_s \times (m_s + n_s)$ ,  $d_s$  being the number of significant principal components at resolution level  $s$ . The compression ratio ( $CR$ ) becomes:

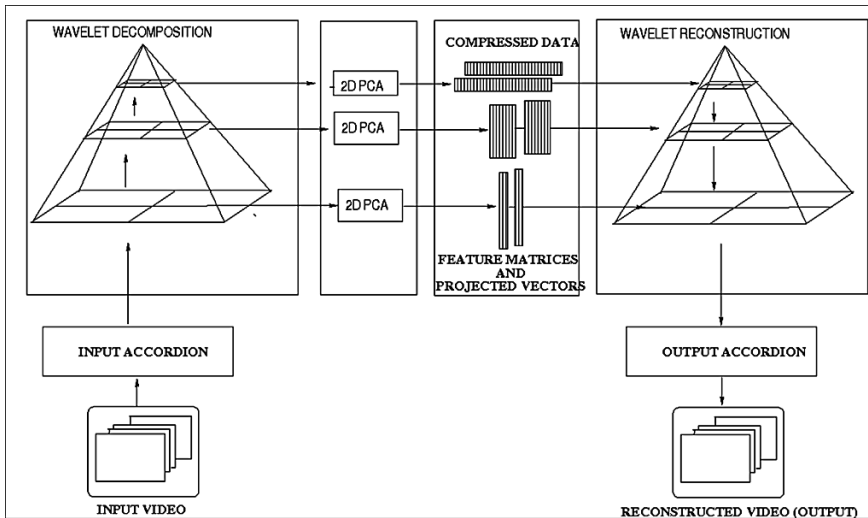


Fig. 2 Schematic diagram of the proposed method

$$CR = \frac{m_0 \times n_0}{\sum_{s=1}^k d_s \times (m_s + n_s)} \tag{9}$$

Since  $s = 0$  represents the original resolution therefore  $m_{s+1} = \frac{m_s}{2}$  and  $n_{s+1} = \frac{n_s}{2}$ . So, compression ratio ( $CR$ ) of our proposed method will become

$$CR = \frac{m_0 \times n_0}{\sum_{i=1}^k \left[\left(\frac{d_i}{2^i}\right)(m_s + n_s)\right]} \tag{10}$$

In our experiments, we have however fixed the compression ratio ( $CR$ ) and determine the number of principal components to be retained to maintain that  $CR$ . In the proposed method, we have considered lesser number of principal components at high resolution.

### 4 Simulation Results

The proposed method for hybrid video compression has been implemented and tested on a source video frames as shown in Fig. 3. It is a clip from a miss America sequence having a frame size of  $144 \times 176$ , which contains same object with relatively slow motion. We are presenting the results on a limited number of frames selected on the basis of their content so as to assess the efficacy of the proposed algorithm. Each of these selected input accordion image (set of 8 frames) is of geometric dimension  $144 \times 1,408$  pixels with 256 intensity levels. In the proposed method, we have employed three different types of wavelets for multi-resolution decomposition, namely: (a) *Bi-orthogonal* [10], (b) *Daubechies* [13], and (c) *Haar* [14] wavelets. In the experimental result we have chosen single values for the overall compression ratio, specifically, 8:1 using three different wavelets. Table 1



Fig. 3 Original miss America sequence

Table 1 Number of principal components selected in different levels

Compression ratio (CR)	Number of principal components to be preserved to maintain the CR			
	Proposed method			
	Level of 256	Level of 128	Level of 64	Level of 32
8:1(bior6.8)	5	33	40	88
8:1(haar)	5	33	40	88
8:1(db9)	5	33	40	88



**Fig. 4** Result of the proposed method (using db9 wavelet)

furnishes the details of the number of resolution-specific principal components we have preserved for maintaining a given value of the overall compression ratio.

The frames reconstructed from the decompressed accordion data are shown in Fig. 4 corresponding to 8:1 compression ratio with using different wavelet. The visual inspection reveals that for a given compression ratio, the quality of the reconstructed images are better in the case of the proposed method in comparison to result obtained by Ouni et al. [5].

### 4.1 Performance Analysis

Natural signals are highly structured. Their pixels exhibit strong dependencies, especially when they are spatially proximate, and these dependencies carry important information about the structure of the objects in the visual scene. The visual quality gives a subjective evaluation of the proposed method and for objective evaluation we furnish a few quantitative measures [17] namely: *Mean Square Error (MSE)*, *Peak Signal to Noise Ratio (PSNR)*, *Structural Similarity Index Measure (SSIM)*. Structural Similarity Index Measure (*SSIM*) computed as:

$$SSIM(A(x, y), A^{-1}(x, y)) = \frac{(2\mu_x\mu_y + c_1)(2\sigma_{xy} + c_2)}{(\mu_x^2 + \mu_y^2 + c_1)(\sigma_x^2 + \sigma_y^2 + c_2)} \tag{11}$$

Here,  $A(x, y)$  is the original image,  $A^{-1}(x, y)$  is the reconstructed image from the compressed data and  $\mu_x$ ,  $\sigma_x^2$  and  $\sigma_{xy}$  be the mean of  $A(x, y)$ , the variance of  $A(x, y)$ , and the covariance of  $A(x, y)$  and  $A^{-1}(x, y)$ , respectively. Approximately,  $\mu_x$  and  $\sigma_x$  can be viewed as estimates of the luminance and contrast of  $A(x, y)$ , and  $\sigma_{xy}$  measures the tendency of  $A(x, y)$  and  $A^{-1}(x, y)$  to vary together.

We have estimated the *MSE*, *PSNR* and *SSIM* of the reconstructed accordion and individual frames corresponding to  $CR = 8:1$ , which are shown in Tables 2 and 3 correspondingly.

**Table 2** PSNR and other parameters for 1st GOP

Proposed method using	CR	MSE	PSNR	SSIM
bior6.8 wavelet	8:1	5.0390	40.9443	0.9983
haar wavelet	8:1	5.8520	39.9859	0.9949
db9 wavelet	8:1	5.5864	40.6557	0.9968

**Table 3** PSNR and other parameters for 8 frames (1st GOP using db9 wavelet)

Frame No.	1	2	3	4	5	6	7	8
MSE	10.8989	6.2065	5.2963	5.3296	5.4749	5.4254	6.8374	10.8427
PSNR	37.7570	40.2024	40.8911	40.8639	40.7470	40.7865	39.7819	37.8427
SSIM	0.9953	0.9973	0.9917	0.9977	0.9972	0.9978	0.9914	0.9935

## 5 Conclusion

In this article, we have proposed a hybrid method of video compression, which employs both wavelet and *2D-PCA*. The accordion image under study is subjected to multi-resolution decomposition using wavelets. Subsequently, *2D-PCA* is applied to the images at each level of resolutions. The set of potential feature vectors and projection vectors are selected at each level of resolution to construct the compressed image data. The method has been formulated, implemented, tested on a set of real *2D* gray-scale images. The method has been evaluated on the basis of *PSNR*, *SSIM* and the overall performance is found to be satisfactory.

## References

1. Agi, I., Gong, L.: An empirical study of secure mpeg video transmission. In: Symposium on Network and Distributed Systems Security. IEEE (1996)
2. MPEG: Motion Picture Expert Group. <http://www.mpeg.org> (1996)
3. Westwater, R., Furht, B.: Real Time Video Compression Techniques and Algorithms. Kluwer Academic Publishers, Boston (1997)
4. Kim, C., O'Connor, N.E.: Low complexity video compression using moving edge detection based on DCT coefficients. In: 15th International Multimedia Modelling Conference (MMM 09) (2009)
5. Ouni, T., Ayedi, W., Abid, M.: New low complexity DCT based video compression method. In: IEEE Telecommunications, ICT '09' (2009)
6. Shlens, J.: A Tutorial on Principal Component Analysis. Center for Neural Science, New York University, New York (2005)
7. Talukder, K.H., Harada, K.: A scheme of wavelet based compression of 2D image. In: Proceedings of IMECS, Hong Kong, pp. 531–536 (2006)
8. Cook, R.L., DeRose, T.: Wavelet noise ACM transactions on graphics. In: Proceedings of ACM SIGGRAPH, vol. 24(3), pp. 803–811
9. Lee, K., Park, S., Suh, W.: Wavelet-based image and video compression. TCOM, pp. 502, April (1997)
10. Vetterli, M., Kovacevic, J.: Wavelets and sub band coding, Prentice Hall, Englewood cliffs (1995)
11. Farge, M.: Wavelet transforms and their applications to turbulence. Ann. Rev. Fluid Mech. **24**, 395–457 (1996)
12. Lau, K.M., Weng, H.-Y.: Climate signal detection using wavelet transform: how to make a time series sing. Bull. Am. Meteor. Soc **76**, 2391–2402 (1995)
13. Torrence, C., Comp, G.P.: A practical guide to wavelet analysis. Bull. Amer. Meteor. Soc. **79**, 61–78 (1998)



14. James, S., Walker, J.: A Primer on Wavelets and Scientific Applications. CRC press, Florida (1999)
15. Wang, K.: Generalized 2D principal component analysis for face image representation and recognition. *Neural Netw.* **18**(5), 585–594 (2005)
16. Dwivedi, A., Prabhanjan, A.: Color image compression using 2-dimensional principal component analysis (2DPCA). In: *Proceeding of ASID*, pp. 8–12 (2006)
17. Wang, Z., Bovik, A.C., Sheikh, H., et al.: Image quality assessment: from error measurement to structural similarity. *IEEE Trans. Image Process.* **13**, 600–612 (2004)

# A Hierarchical Optimization Method to Solve Environmental-Economic Power Generation and Dispatch Problem with Fuzzy Data Uncertainty

Bijay Baran Pal and Mousumi Kumar

**Abstract** This paper presents how the hierarchical decision structure can be effectively used for modeling and solving an environmental-economic thermal power generation and dispatch problems in a fuzzy decision environment. In the proposed approach, minimization of the functions of fuel-cost, environmental-emission and transmission-loss are considered at the three hierarchical levels to solve the problem within a power plant operational system. In the model formulation, a *priority based* linear fuzzy goal programming (LFGP) method is employed to achieve the highest membership value (unity) of the defined fuzzy goals to the extent possible on the basis of priorities in the decision making horizon. To illustrate the effective use of the approach, the problem of standard IEEE 6-Generator 30-Bus System is considered.

**Keywords** Fuzzy goal programming · Goal programming · Hierarchical programming · Power generation and dispatch · Taylor series approximation · Trilevel programming

## 1 Introduction

The thermal power plant operational and planning problems are actually optimization problems that involve various objectives and system constraints for generation of power and dispatch to different destinations. Here, the primary objective is to make a balance for power generation decision and control of emissions discharged to the earth's environment. The mathematical programming (MP) model

---

B.B. Pal

Department of Mathematics, University of Kalyani, Kalyani 741235, West Bengal, India  
e-mail: bbpal18@hotmail.com

M. Kumar (✉)

Department of Mathematics, Alipurduar College, Alipurduar 736122, West Bengal, India  
e-mail: mousumi886@gmail.com

© Springer India 2015

J.K. Mandal et al. (eds.), *Information Systems Design and Intelligent Applications*,  
Advances in Intelligent Systems and Computing 339,  
DOI 10.1007/978-81-322-2250-7\_42

419

for power generation decision was introduced by Dommel and Tinney [1] in 1968. A Comprehensive survey on environmental power dispatch models developed from 1960s to 1970s was first surveyed by Happ [2] in 1977. A comprehensive bibliography works made with consideration of various aspects of economic power dispatch problems during the time period 1977–1988 was prepared by Chowdhury and Rahman [3] in 1990.

Now, since an environmental-economic power generation and dispatch (EE-PGD) problem is multiobjective in nature, the goal programming (GP) approach [4], based on the satisficing philosophy [5] and a robust tool for multiobjective decision analysis, and has been successfully implemented to power generation problems [6] in the past. The other multiobjective approaches like adaptive robust optimization and competitive strategic bidding optimization method to EEPGD problems have also been studied [7, 8] in the recent past.

However, in most of the practical decision situations, it has been realized that decision regarding achievement of objective function(s) is frequently inexact in nature owing to inherent impression in setting parameter values associated with the model of a real-life problem. One of the most prominent approaches for decision analysis in an uncertain environment is fuzzy programming (FP) [9], which is based on the theory of fuzzy sets [10]. The FP approach to EEPGD problems have been studied [11] in the past. Further, fuzzy goal programming (FGP) [12] as an extension of conventional GP to make reasonable decision in fuzzy environment has also been employed to EEPGD problems [13]. But, the deep study on the potential use of such an approach is at an initial stage and yet to be widely circulated in the literature.

Now, in the current context of solving EEPGD problem, it is to be observed that the objectives of minimizing generation-cost, environmental-emission and transmission-loss are highly conflicting in characteristics owing to accelerating rate of demand of thermal power and ever increasing pressure on controlling pollution on the earth. As an essence, optimization of objectives in the framework of hierarchical structure [14], trilevel programming (TLP) [15], as an extension of bilevel programming (BLP) [16] is considered here to solve EEPGD problem with fuzzily described objective functions.

The effective use of the approach is tested on the standard IEEE 6-Generator 30-bus test system. The model solution is also compared with the approaches studied previously to expound the potential use of the approach.

Now, the general model formulation of the PGD problem with three objective functions is discussed in Sect. 2.

## 2 Model Formulation of PGD Problem

The decision variables and objective functions of a PGD problem having  $n$  generators  $G_k$  ( $k = 1, 2, \dots, n$ ) are introduced as follows.

- Definition Decision Variables:  
 $p_k$  = Generation of power (in per unit (p.u.)) from the  $k$ th generator  $G_k$ ,  $k = 1, 2, \dots, n$
- Definition of Objective Functions:

(i) Total fuel-cost function

The total fuel-cost function associated with generation of power from all the generators of the system can be expressed as the sum of a quadratic function and a sin function, where sin function represent the cost incurred for valve-point loading [17] of the PGD problem.

The total fuel-cost (in \$/h) can be expressed as:

$$F_1 = \sum_{k=1}^n [(a_k p_k^2 + b_k p_k + c_k) + |d_k \sin [e_k (p_k^{\min} - p_k)]|] \quad (1)$$

where  $a_k$ ,  $b_k$  and  $c_k$  are the estimated cost-coefficients associated with generation of power from  $k$ th generator,  $d_k$  and  $e_k$  are fuel-cost coefficients involved with valve-point effect during active power generation mode of  $k$ th generator  $G_k$ ,  $k = 1, 2, \dots, n$ .

(ii) Total environmental-emission function

The total emission function can be approximated as a sum of a quadratic function and an *exponential* function, which is associated with active power output from a generator of the system. The total environmental-emission (in ton/h) can be expressed as:

$$F_2 = \sum_{k=1}^n [10^{-2}(\alpha_k p_k^2 + \beta_k p_k + \gamma_k) + \zeta_k e^{\lambda_k p_k}], \quad (2)$$

where  $\alpha_k$ ,  $\beta_k$ ,  $\gamma_k$  and  $\lambda_k$  are emission-coefficients associated with power generation from the  $k$ th generator  $G_k$ ,  $k = 1, 2, \dots, n$ .

(iii) Transmission-loss function

The total transmission-loss (in p.u.) can be modeled as a function of power output from generators. The expression can be presented as:

$$F_3 = \sum_{k=1}^n \sum_{j=1}^n p_k B_{kj} p_k + \sum_{i=1}^n B_{0i} p_k + B_{00} \quad (3)$$

where  $B_{kj}$ ,  $B_{0j}$  and  $B_{00}$  are the *B-coefficients* of the transmission network system, and the matrices  $B_{kj}$ ,  $B_{0j}$  and  $B_{00}$  are of orders  $(n, n)$ ,  $(1, n)$  and  $(1, 1)$  respectively.

- Description of System Constraints

(i) Power Balance Constraint

The total generation of power must cover the sum of the total demand of power.

The power balance constraint appears as:

$$\sum_{k=1}^n p_k = (D_p + F_3) \quad (4)$$

(ii) **Generation Capacity Constraint**

Following the conventional PGD system, the constraints on power generation capacities of individual generators can be defined as:

$$p_k^{\min} \leq p_k \leq p_k^{\max}, \quad k = 1, 2, \dots, n \quad (5)$$

where *min* and *max* stand for minimum and maximum.

Now, TLP problem (TLPP) formulation of the proposed problem in the framework of *priority based* FGP is presented in the following Sect. 3.

### 3 TLPP Formulation

In a TLPP, decision makers (DMs) are located individually at three hierarchical decision levels and each of them independently controls a vector of decision variables for optimizing his/her objective function in the decision making horizon. In TLPP formulation of the proposed EEPGD problem, minimization of total fuel-cost is considered at the first-level problem, and minimization of total environmental-emission and transmission-loss are successively considered at the second-level and third-level problems respectively.

Now, formulation of the model of EEPGD problem within the structure of TLPP is discussed in the following section.

#### 3.1 EEPGD Model Formulation

To design the TLP model of the EEPGD problem, the vector  $\mathbf{P}_G$  of decision variables  $p_k$ ,  $k = 1, 2, \dots, n$  are partitioned into three distinct sets of vectors  $\mathbf{P}_{GL_1}$ ,  $\mathbf{P}_{GL_2}$  and  $\mathbf{P}_{GL_3}$  and introduced them separately to the DMs located at three hierarchical levels depending on the needs and desires of an organisation in the planning context, where  $L_1$ ,  $L_2$  and  $L_3$  indicate first-level, second-level and third-level, respectively.

The generic form of the model can be presented as follows.

Find  $\mathbf{P}_G(\mathbf{P}_{GL_1}, \mathbf{P}_{GL_2}, \mathbf{P}_{GL_3})$  so as to:

$$\underset{\mathbf{P}_{GL_1}}{\text{Minimize}} F_1(\mathbf{P}_G) = \sum_{k=1}^n [(a_k p_k^2 + b_k p_k + c_k) + |d_k \sin[e_k(p_k^{\min} - p_k)]|] \tag{6}$$

(First-level problem)

for given  $\mathbf{P}_{GL_1}; \mathbf{P}_{GL_2}, \mathbf{P}_{GL_3}$  solves

$$\underset{\mathbf{P}_{GL_2}}{\text{Minimize}} F_2(\mathbf{P}_G) = \sum_{k=1}^n [10^{-2}(\alpha_k p_k^2 + \beta_k p_k + \gamma_k) + \zeta_k e^{\lambda_k p_k}] \tag{7}$$

(Second-level problem)

and, for given  $\mathbf{P}_{GL_1}, \mathbf{P}_{GL_2}; \mathbf{P}_{GL_3}$  solves

$$\underset{\mathbf{P}_{GL_3}}{\text{Minimize}} F_3(\mathbf{P}_G) = \sum_{k=1}^n \sum_{j=1}^n p_k B_{kj} p_k + \sum_{i=1}^n B_{0k} p_k + B_{00} \tag{8}$$

(Third-level problem)

subject to the system constraints in (4) and (5),

$$\begin{aligned} &\text{where } \mathbf{P}_{GL_1} \cap \mathbf{P}_{GL_2} \cap \mathbf{P}_{GL_3} = \varphi, \\ &\mathbf{P}_{GL_1} \cup \mathbf{P}_{GL_2} \cup \mathbf{P}_{GL_3} = \mathbf{P}_G \\ &\text{and } \mathbf{P}_G = \{p_1, p_2, \dots, p_n\} \in S(\neq \varphi), \end{aligned} \tag{9}$$

where  $S$  denotes the feasible solution set defined by the system constraints in (4) and (5),  $\cap$  and  $\cup$  stand for the mathematical operations ‘intersection’ and ‘union’, respectively.

Now, FGP formulation of the problem in (9) in a fuzzy environment is presented in the following section.

### 3.2 FGP Problem Formulation

To formulate the FGP model of the TLPP in (9), the objective functions  $F_1(\bullet), F_2(\bullet)$  and  $F_3(\bullet)$  as well as  $\mathbf{P}_{GL_1}$  and  $\mathbf{P}_{GL_2}$  controlled by the first- and second-level DMs are to be defined as fuzzy goals by introducing imprecise aspiration levels to each of them.

### 3.2.1 Fuzzy Goal Description

Let  $(\mathbf{P}_G^B; F_i^B)$  and  $(\mathbf{P}_G^W; F_i^W)$  the independent best and worst decisions, respectively, of the  $i$ th level DM, where  $F_i^B = \text{Min}_{(\mathbf{P}_G) \in S} Z_i(\mathbf{P}_G)$ , and  $F_i^W = \text{Max}_{(\mathbf{P}_G) \in S} Z_i(\mathbf{P}_G)$ , and where  $B$  and  $W$  stand for best and worst, respectively.

Then, from the view point of minimizing the objective functions, the fuzzy objective goals can be expressed as:

$$F_i \lesssim F_i^B, \quad i = 1, 2, 3 \tag{10}$$

where ‘ $\lesssim$ ’ refers the fuzzy version of the symbol  $\leq$  in the sense of Zimmermann [9].

Again, since a higher level DM has the higher power of making decision and the benefit of a lower level DM depends upon the relaxation of decision made by the higher level DMs, the vector of fuzzy decision goals associated with the control vectors  $\mathbf{P}_{GL_i}$  can be defined as:

$$\mathbf{P}_{GL_i} \lesssim \mathbf{P}_{GL_i}^B \tag{11}$$

Further, the increase in the values of aspiration levels of fuzzy decision goals defined in (11) would never be more than  $p_k^{\max}, k = 1, 2, \dots, n$ , defined in (5).

Let  $\mathbf{P}_{GL_1}^t, (\mathbf{P}_{GL_1}^t < \mathbf{P}_{GL_1}^{\max})$  and  $\mathbf{P}_{GL_2}^t, (\mathbf{P}_{GL_2}^t < \mathbf{P}_{GL_2}^{\max})$ , be the vector of upper-tolerance limits of achieving the goal levels of the vector of fuzzy goals defined in (11), where  $t$  means tolerance. Now, the fuzzy goals are to be characterized by the respective membership functions for measuring their degree of achievements in a fuzzy environment.

### 3.2.2 Characterization of Membership Function

The membership functions associated with fuzzy goals in (10) can be expressed as:

$$\mu_{F_i}[F_i(\mathbf{P}_G)] = \begin{cases} 1, & \text{if } F_i(\mathbf{P}_G) \leq F_i^B \\ \frac{F_i^W - F_i(\mathbf{P}_G)}{F_i^W - F_i^B}, & \text{if } F_i^B < F_i(\mathbf{P}_G) \leq F_i^W \\ 0, & \text{if } F_i(\mathbf{P}_G) > F_i^W \end{cases} \tag{12}$$

where  $(F_i^W - F_i^B)$  represents the tolerance range for achievement of  $i$ th level fuzzy goal and  $\mu [\cdot]$  indicates membership function.

Again, the membership functions associated with the vector of fuzzy goals in (11) appears as:

$$\mu_{P_{GL_i}}[P_{GL_i}] = \begin{cases} 1, & \text{if } P_{GL_i} \leq P_{GL_i}^B \\ \frac{P_{GL_i}^t - P_{GL_i}}{P_{GL_i}^t - P_{GL_i}^B}, & \text{if } P_{GL_i}^B < P_{GL_i} \leq P_{GL_i}^t \\ 0, & \text{if } P_{GL_i} > P_{GL_i}^t \end{cases} \quad (13)$$

where  $(P_{GL_i}^t - P_{GL_i}^B)$  is the vector of tolerance ranges for achievement of  $i$ th level fuzzy decision vectors.

Now, the *priority based FGP* [12] formulation of the TLPP in (9) is presented in the following section.

### 3.3 Priority Based FGP Model Formulation

In the process of formulating FGP model of the problem in (9), the membership functions in (12) and (13) are transformed into membership goals by assigning the highest membership value (unity) as the aspiration level and introducing under- and over-deviational variables to each of them.

Then, FGP model under a pre-emptive priority structure can be presented as follows.

Find  $P_G(P_{GL_1}, P_{GL_2}, P_{GL_3})$  so as to:

$$\text{Minimize } Z = P_1(d^-), P_1(d^-), \dots, P_q(d^-), \dots, P_Q(d^-) \quad (14)$$

and satisfy

$$\mu_{F_i} : \frac{F_i^W - F_i(P_G)}{F_i^W - F_i^B} + d_{i1}^- - d_{i1}^+ = 1; \quad i = 1, 2, 3 \quad (15)$$

$$\mu_{P_{GL_i}} : \frac{P_{GL_i}^t - P_{GL_i}}{P_{GL_i}^t - P_{GL_i}^B} + d_{i2}^- - d_{i2}^+ = \mathbf{I}; \quad i = 1, 2 \quad (16)$$

subject to the set of constraints defined in (4) and (5) (16)

where  $Z$  represents the vector of  $Q$  priority achievement functions, and  $d_{i1}^-, d_{i1}^+ \geq 0$ , ( $i = 1, 2, 3$ ), represent under- and over-deviational variables, respectively, and  $d_{i2}^-, d_{i2}^+ \geq 0$ , ( $i = 1, 2$ ) represent vector of under- and over-deviational variables, respectively, and where  $\mathbf{I}$  is a column vector with all elements equal to 1 and dimension of it depends on the dimension of  $P_{GL_1}$ .  $P_q(d^-)$  is a linear function of the weighted under-deviational variables, where  $P_q(d^-)$  is of the form [12]:



$$P_q(d^-) = \sum_{i \in I_q} w_{qi1}^- d_{qi1}^- + \sum_{i \in I'_q} w_{qi2}^- d_{qi2}^- \tag{17}$$

where  $I_q = \{1, 2, 3\}$ ,  $I'_q = \{1, 2\}$  and  $d_{qi1}^- (i = 1, 2, 3)$  and  $d_{qi2}^- (i = 1, 2)$  are renamed for  $d_{i1}^-$  and  $d_{i2}^-$ , respectively, to represent them at the  $q$ -th priority level.  $w_{qi1}^- (i = 1, 2, 3)$  and  $w_{qi2}^- (i = 1, 2)$  are the numerical weights and the vector of numerical weights, respectively, and they are determined as [12]:

$$\left. \begin{aligned} w_{qi1}^- &= \frac{1}{(F_i^W - F_i^B)_q}, \text{ for the defined goals in (14)} \\ w_{qi2}^- &= \frac{1}{(P_{GL_i}^A - P_{GL_i}^B)_q}, \text{ for the defined goals in (15)} \end{aligned} \right\} \tag{18}$$

where the suffix ‘ $q$ ’ in the right hand side of the expressions is used to indicate the weights associated with the goals at  $q$ th priority level.

Also, the priorities have the relationship  $P_1 \ggg P_2 \ggg \dots \ggg P_q \ggg \dots \ggg P_Q$  which implies that the  $q$ th priority level  $P_q$  is preferred to the next priority level  $P_{q+1}$  regardless of any multiplier associated with  $P_{q+1}$  and the symbol ‘ $\ggg$ ’ indicates much greater than.

Now, it is to be followed that the membership functions in (13) are actually nonlinear in characteristics owing to nonlinearity in the associated objective functions. Here, since the objective functions in (6) and (7) are in the form of simple power series [17] in their expanded forms and objective function in (8) is a simple quadratic function, the *Taylor series approximation* technique [18] can be employed here for linearization of nonlinear functions in the process of solving the problem.

### 3.4 Taylor Series Approximation Method

Let  $P_G^* = (P_{GL_1}^*, P_{GL_2}^*, P_{GL_3}^*)$  be the initial approximate solution of the  $F_1(P_G)$  in (6).

Here, the individual best solution obtained in the decision environment could be considered the initial approximate solution.

Using the first order of *Taylor series* expansion, the approximated linear form of  $F_1(P_G)$  can be obtained as:

$$F_1(P_G) = F_1(P_G^*) + \sum_{i=1}^3 \frac{\partial F_1(P_G^*)}{\partial P_{GL_i}} (P_{GL_i} - P_{GL_i}^*) \tag{19}$$

In an analogous way, the linear forms of the expressions in (7) and (8) can be obtained.

Now, formulation of the executable model of the problem is demonstrated via a case example presented in the Sect. 4.

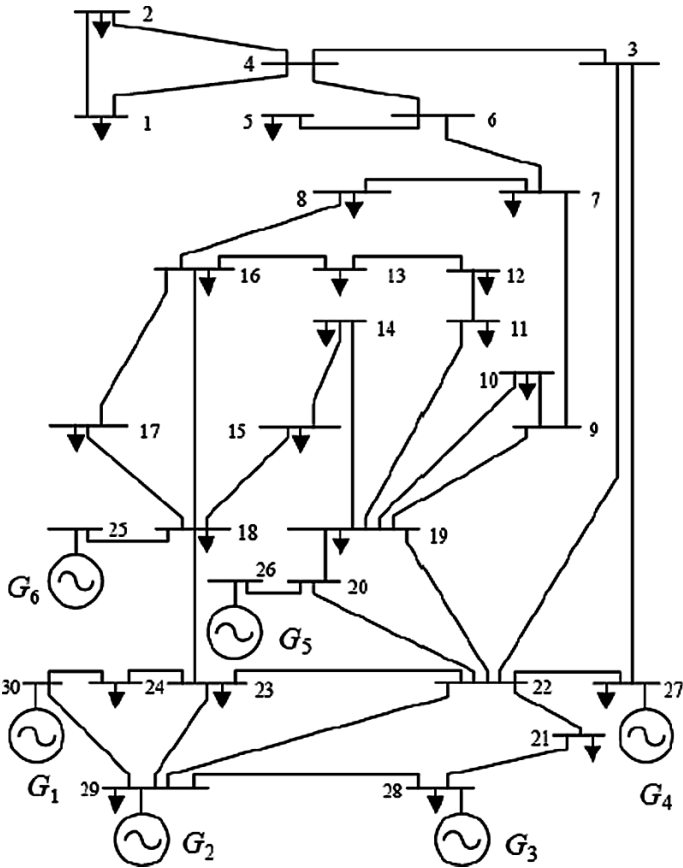


Fig. 1 Single-line diagram of IEEE 30-bus test system

### 4 A Demonstrative Case Example

The standard IEEE 30-bus 6-generator system with 41 interconnected transmission lines [17] is considered as a case example. The total power demand is 2.834 p.u.

The single-line diagram of IEEE 30-bus test system is displayed in Fig. 1.

The parameter values of the fuel-cost function and emission-coefficients are presented in Table 1.

The power generation limits of the generators associated with IEEE 30-Bus system are presented in Table 2.

**Table 1** Data descriptions for cost and emission coefficients of IEEE 30-bus system

Generator	Coefficient									
	Cost coefficients					Emission coefficients				
	a	b	c	d	e	$\alpha$	$\beta$	$\gamma$	$\zeta$	$\lambda$
G <sub>1</sub>	100	200	10	15	6.283	6.490	-5.554	4.091	2.0E-4	2.857
G <sub>2</sub>	120	150	10	10	8.976	5.638	-6.047	2.543	5.0E-4	3.333
G <sub>3</sub>	40	180	20	10	14.784	4.586	-5.094	4.258	1.0E-6	8.000
G <sub>4</sub>	60	100	10	5	20.944	3.380	-3.550	5.326	2.0E-3	2.000
G <sub>5</sub>	40	180	20	5	25.133	4.586	-5.094	4.258	1.0E-6	8.000
G <sub>6</sub>	100	150	10	5	18.48	5.151	-5.555	6.131	1.0E-5	6.667

**Table 2** Power generation limits

Limits	Generator					
	G <sub>1</sub>	G <sub>2</sub>	G <sub>3</sub>	G <sub>4</sub>	G <sub>5</sub>	G <sub>6</sub>
$P_{G_i}^{\min}$	0.05	0.05	0.05	0.05	0.05	0.05
$P_{G_i}^{\max}$	0.50	0.60	1.00	1.20	1.00	0.60

The *B-coefficients* [11] for IEEE 30-bus system are as follows:

$$[B]_{(6,6)} = \begin{bmatrix} 0.1382 & -0.0299 & 0.0044 & -0.0022 & -0.0010 & -0.0008 \\ -0.0299 & 0.0487 & -0.0025 & 0.0004 & 0.0016 & 0.0041 \\ 0.0044 & -0.0025 & 0.0182 & -0.0070 & -0.0066 & -0.0066 \\ -0.0022 & 0.0004 & -0.0070 & 0.0137 & 0.0050 & 0.0033 \\ -0.0010 & 0.0016 & -0.0066 & 0.0050 & 0.0109 & 0.0005 \\ -0.0008 & 0.0041 & -0.0066 & 0.0033 & 0.0005 & 0.0244 \end{bmatrix},$$

$$B_0 = [-0.0107 \quad 0.0060 \quad -0.0017 \quad 0.0009 \quad 0.0002 \quad 0.0030],$$

$$B_{00} = 9.857E-4.$$

Now, without loss of generality, it is assumed that the power generation vector  $\mathbf{P}_G(p_1, p_2, p_3, p_4, p_5, p_6)$  is partitioned into the vectors  $\mathbf{P}_{GL_1} = (p_1, p_5)$ ,  $\mathbf{P}_{GL_2} = (p_2, p_6)$  and  $\mathbf{P}_{GL_3} = (p_3, p_4)$ , which are controlled by the first-, second- and third-level DMs, respectively, in the power generation decision situation.

Then, following the expressions in (6), (7) and (8), and using the data presented in Table 1 and Table 2 as the *B-coefficient* values, the TLP model of the problem can be stated as follows.

Find  $\mathbf{P}_G(p_1, p_2, p_3, p_4, p_5, p_6)$  so as to:

$$\begin{aligned}
\text{Minimize}_{P_{GL_1}} F_1(P_G) &= [100p_1^2 + 120p_2^2 + 40p_3^2 + 60p_4^2 + 40p_5^2 + 100p_6^2 + 200p_1 \\
&+ 150p_2 + 180p_3 + 100p_4 + 180p_5 + 150p_6 + 116.7946 \\
&+ |15\text{Sin}[6.29(0.5 - p_1)]| + |10\text{Sin}[8.98(0.6 - p_2)]| + |10\text{Sin}[14.78(1.0 - p_3)]| \\
&+ |5\text{Sin}[20.94(1.2 - p_4)]| + |5\text{Sin}[25.13(1.0 - p_5)]| + |5\text{Sin}[18.48(0.6 - p_6)]|] \\
&\quad \text{(First-level problem)}
\end{aligned} \tag{20}$$

for given  $P_{GL_1}; P_{GL_2}, P_{GL_3}$  solves

$$\begin{aligned}
\text{Minimize}_{P_{GL_2}} F_2(P_G) &= 10^{-2}(4.091 + 6.49p_1^2 + 5.638p_2^2 + 4.586p_3^2 + 3.38p_4^2 + 4.586p_5^2 \\
&+ 5.151p_6^2 + 26.607) \\
&- 10^{-2}(5.554p_1 + 6.047p_2 + 5.094p_3 + 3.55p_4 + 5.094p_5 + 5.555p_6) \\
&+ (2.0E-4)e^{2.857p_1} (5.0E-4)e^{3.333p_2} + (1.0E-6)e^{8.00p_3} + (2.0E-4)e^{2.00p_4} \\
&+ (1.0E-6)e^{8.00p_5} + (1.0E-4)e^{6.667p_6} \\
&\quad \text{(Second-level problem)}
\end{aligned} \tag{21}$$

and, for given  $P_{GL_1}, P_{GL_2}; P_{GL_3}$  solves

$$\begin{aligned}
\text{Minimize}_{P_{GL_3}} F_3(P_G) &= 0.1328p_1^2 + 0.0487p_2^2 + 0.0182p_3^2 + 0.0137p_4^2 + 0.0109p_5^2 \\
&+ 0.0244p_6^2 - 0.0598p_1p_2 + 0.0080p_1p_3 - 0.0044p_1p_4 \\
&- 0.0020p_1p_5 - 0.0016p_1p_6 - 0.0050p_2p_3 + 0.0008p_2p_4 \\
&+ 0.0032p_2p_5 + 0.0082p_2p_6 - 0.140p_3p_4 - 0.0132p_3p_5 \\
&- 0.0132p_3p_6 + 0.010p_4p_5 + 0.0066p_4p_6 + 0.0010p_5p_6 \\
&- 0.0107p_1 + 0.0060p_2 - 0.0017p_3 + 0.0009p_4 \\
&+ 0.0002p_5 + 0.0030p_6 + (9.857E-4) \\
&\quad \text{(Third-level problem)}
\end{aligned} \tag{22}$$

$$\text{subject to } \sum_{i=1}^6 p_i = F_3 + 2.834 \tag{23}$$

where  $F_3$  can be obtained by (22).

$$\begin{aligned}
&\text{and } 0.05 \leq p_1 \leq 0.50, \quad 0.05 \leq p_2 \leq 0.60, \quad 0.05 \leq p_3 \leq 1.00, \\
&\quad 0.05 \leq p_4 \leq 1.20, \quad 0.05 \leq p_5 \leq 1.00, \quad 0.05 \leq p_6 \leq 0.60.
\end{aligned} \tag{24}$$

Now, in the decision situation, the individual best values of the objective functions in (20), (21) and (22) are successively obtained as:

$$\begin{aligned}(p_1, p_2, p_3, p_4, p_5, p_6; F_1) &= (0.121, 0.286, 0.584, 0.993, 0.524, 0.352; 605.999), \\(p_1, p_2, p_3, p_4, p_5, p_6; F_2) &= (0.050, 0.221, 0.758, 0.050, 0.758, 0.590; 0.1916), \\ \text{and } (p_1, p_2, p_3, p_4, p_5, p_6; F_3) &= (0.086, 0.098, 0.976, 0.500, 0.853, 0.337; 0.0170).\end{aligned}$$

Using *Taylor Series approximation* method, the linear forms of the objective functions in (20), (21) and (22) are obtained as:

$$F_1^*(P_G) = 224.20p_1 + 218.64p_2 + 226.72p_3 + 219.16p_4 + 221.92p_5 + 220.4p_6 - 27.601 \quad (25)$$

$$F_2^*(P_G) = 0.1299 - (0.04883p_1 + 0.0021p_2 - 0.0409p_3 - 0.9075p_4 + 0.0463p_5 + 0.0502p_6) \quad (26)$$

$$F_3^*(P_G) = 0.00255p_1 + 0.00588p_2 + 0.0107p_3 + 0.02503p_4 + 0.01051p_5 + 0.001p_6 - 0.02267 \quad (27)$$

In the sequel of linear transformation, the linear form of the power balance constraint (23) appears as:

$$\begin{aligned}0.99745p_1 + 0.99412p_2 + 0.98930p_3 + 0.97497p_4 + 0.98949p_5 + 0.99900p_6 \\ = 2.76543.\end{aligned} \quad (28)$$

Then, solving the objective functions in (25), (26) and (27) individually subject to the system constraints in (24) and (28), the best values of them are obtained as:

$$\begin{aligned}(p_1, p_2, p_3, p_4, p_5, p_6; F_1^B) &= (0.483, 0.600, 0.050, 0.050, 0.868, 0.600; 616.345), \\(p_1, p_2, p_3, p_4, p_5, p_6; F_2^B) &= (0.4108, 0.4636, 0.5442, 0.3902, 0.5443, 0.5153; 0.1952), \\ \text{and } (p_1, p_2, p_3, p_4, p_5, p_6; F_3^B) &= (0.500, 0.600, 0.050, 0.050, 0.983, 0.60; 0.0211).\end{aligned}$$

Then, the fuzzy objective goals are found as:

$$F_1 \lesssim 616.345 \text{ and } F_2 \lesssim 0.1952 \text{ and } F_3 \lesssim 0.0211 \quad (29)$$

The fuzzy goals associated with power generation decisions, which are under the control of higher level DMs, are obtained as:

$$p_1 \lesssim 0.483, p_2 \lesssim 0.4636, p_3 \lesssim 0.868 \text{ and } p_6 \lesssim 0.5153 \quad (30)$$

Again, in the decision situation, the worst values of the objective functions are found as:

$$(F_1^W, F_2^W, F_3^W) = (617.160, 0.2715, 0.0439), \tag{31}$$

Further, following the procedure, the upper-tolerance limits of the decision variables controlled by the higher level DMs can be considered as

$$(p_1^t, p_2^t, p_3^t, p_6^t) = (0.495, 0.575, 0.982, 0.586).$$

Then, the membership goals of the proposed FGP model are constructed as follows.

$$\begin{aligned} \mu_{F_1} : \frac{645.260 - F_1(\mathbf{P}_G)}{28.815} + d_{11}^- - d_{11}^+ = 1, \quad \mu_{F_2} : \frac{0.2715 - F_2(\mathbf{P}_G)}{0.0763} + d_{12}^- - d_{12}^+ = 1 \\ \mu_{F_3} : \frac{0.0439 - F_3(\mathbf{P}_G)}{0.0228} + d_{13}^- - d_{13}^+ = 1, \quad \mu_{p_1} : \frac{0.495 - p_1}{0.0120} + d_{21}^- - d_{21}^+ = 1, \\ \mu_{p_2} : \frac{0.575 - p_2}{0.1114} + d_{22}^- - d_{22}^+ = 1, \quad \mu_{p_5} : \frac{0.982 - p_4}{0.1140} + d_{23}^- - d_{23}^+ = 1, \\ \mu_{p_6} : \frac{0.586 - p_6}{0.0707} + d_{24}^- - d_{24}^+ = 1 \end{aligned} \tag{32}$$

Then, an executable FGP model of the problem under a given priority structure can be obtained as follows.

Find  $\mathbf{P}_G(p_1, p_2, p_3, p_4, p_5, p_6)$  so as to:

$$\begin{aligned} \text{Minimize } Z = [P_1(0.0114d_{11}^- + 50.505d_{12}^- + 83.33d_{21}^-), P_2(42.918d_{13}^- \\ + 8.978d_{22}^-), P_3(8.772d_{23}^- + 14.144d_{24}^-)] \end{aligned} \tag{33}$$

and satisfy the goal expression in (32) subject to the system constrains in (24) and (28).

The software LINGO (ver. 12.0) is used to solve the problem.

The achieved values of the objectives are

$$\begin{aligned} (F_1, F_2, F_3) = (617.167, 0.19624, 0.02319) \text{ with the membership values} \\ (\mu_{F_1}, \mu_{F_2}, \mu_{F_3}) = (0.975, 0.986, 0.912). \end{aligned}$$

The resultant decision for power generation is

$$(p_1, p_2, p_3, p_4, p_5, p_6) = (0.483, 0.464, 0.050, 0.276, 1.00, 0.515).$$

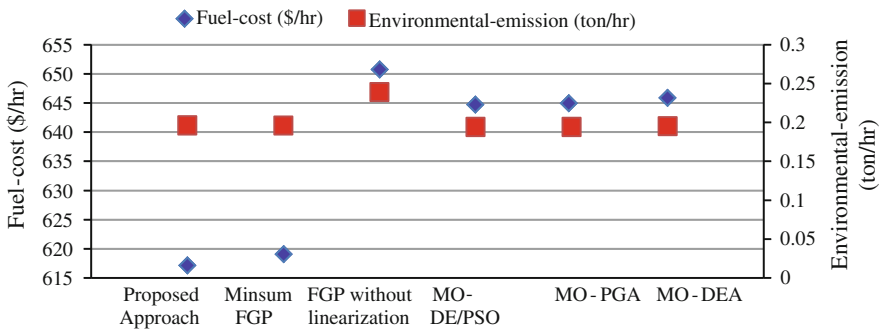
### 4.1 An Illustration for Performance Comparison

To expound the effectiveness of the proposed *priority based* FGP formulation of the EEPGD problem, the model solution is compared with the solutions obtained by using the approaches: conventional linear *minsum* FGP approach [19]; proposed FGP without linearization of objectives functions; Multi-objective optimization algorithm based on particle swarm optimization and differential evolution (MO-DE/PSO) [20], Multi-objective Pareto genetic algorithm (MO-PGA) [21], Multi-objective differential Evolution algorithm (MO-DEA) [22]. The model solution and solutions obtained under the above approaches are presented in Table 3.

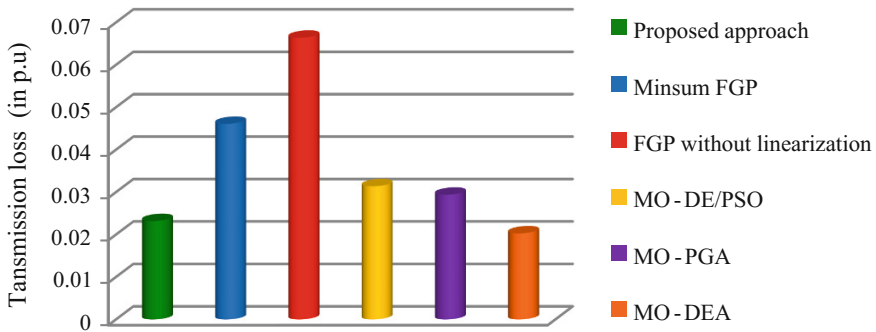
The graphical representations of the results obtained by using the proposed method and the methods studied previously are displayed in Figs. 2 and 3.

**Table 3** Solutions achieved under the proposed approach and other approaches

	Generator	Model					
		<i>Priority based</i> FGP	<i>Minsum</i> FGP	FGP without linearization	MO-DE/PSO	MO-PGA	MO-DEA
Generator output (p.u.)	G <sub>1</sub>	0.4831	0.05	0.1341	0.4191	0.3929	0.3926
	G <sub>2</sub>	0.4642	0.05	0.1283	0.4594	0.3937	0.4625
	G <sub>3</sub>	0.05	0.2811	0.9388	0.5511	0.5815	0.5631
	G <sub>4</sub>	0.2761	1.2	0.4861	0.3919	0.4316	0.4031
	G <sub>5</sub>	1	1	0.8333	0.5413	0.5445	0.5676
	G <sub>6</sub>	0.5147	0.2276	0.2282	0.5111	0.5192	0.4784
Fuel-cost(\$/h)		617.167	619.109	650.711	644.771	644.742	645.879
Environment-emission (ton/h)		0.1962	0.1961	0.239	0.1943	0.1942	0.1952
Transmission-loss (in p.u.)		0.0232	0.0461	0.0664	0.0314	0.0294	0.0203



**Fig. 2** Comparison of fuel-cost (\$/h) and environmental-emission (ton/h) achieved under different approaches



**Fig. 3** Comparison of transmission-loss achieved under different approaches

The graphs show that the proposed approach is more effective in comparison to the others ones from the view point of arriving at the thermal power generation decision with proper control of operational objectives in a thermal power plant operational system.

## 5 Conclusion and Scope for Future Research

The main advantage of using the *priority based FGP* approach to solve the TLP formulation of EEPGD problems is that the computational difficulty with nonlinearity in objective functions does not arise here in the decision search process. Again, an appropriate decision for balancing the achievement of objectives in a hierarchical order on the basis of needs of thermal power demand and reductions of both environmental-emission and transmission-loss can be obtained under the proposed approach. The interval programming approach [23] to PGD problems, where values of model parameter are taken in the form of intervals instead of fuzzy/stochastic description of them may be a problem in future research.

**Acknowledgments** The authors would like to thank the Editors and anonymous Reviewers for their useful suggestions for improving the quality of presentation of the paper.

## References

1. Dommel, H.W., Tinney, W.F.: Optimal power flow solutions. *IEEE Trans. Power Appar. Syst.* **87**, 1866–1876 (1968)
2. Happ, H.H.: Optimal power dispatch—a comprehensive survey. *IEEE Trans. Power Appar. Syst.* **96**, 841–854 (1977)
3. Chowdhury, B.H., Rahman, H.: A review of recent advances in economic dispatch. *IEEE Trans. Power Syst.* **5**, 1248–1258 (1990)



4. Ignizio, J.P.: Goal Programming and Extensions. D.C. Health and Company, Lexington (1976)
5. Simon, H.A.: Administrative behavior. Free Press, New York (1945)
6. Nanda, J., Kothari, D.P., Lingamurthy, K.S.: Economic-emission load dispatch through goal programming techniques. *IEEE Trans. Energy Convers.* **3**, 26–32 (1988)
7. Bertsimas, D., Litvinov, E., Sun, X.A., Zhao, J., Zheng, T.: Adaptive robust optimization for the security constrained unit commitment problem. *IEEE Trans. Power Syst.* **28**, 52–63 (2013)
8. Zhang, G., Zhang, G., Gao, Y., Lu, J.: Competitive strategic bidding optimization in electricity markets using bilevel programming and swarm technique. *IEEE Trans. Ind. Electron.* **58**, 2138–2146 (2011)
9. Zimmermann, H.-J.: Fuzzy Sets, Decision Making and Expert Systems. Kluwer-Nijhoff Publishing, Dordrecht (1987)
10. Zadeh, L.A.: Fuzzy sets. *Inf. Control* **8**, 338–353 (1965)
11. Wang, L.F., Singh, C.: Environmental/economic power dispatch using a fuzzified multi-objective particle swarm optimization algorithm. *Electr. Power Syst. Res.* **77**, 1654–1664 (2007)
12. Pal, B.B., Moitra, B.N., Maulik, U.: A goal programming procedure for fuzzy multiobjective linear fractional programming problem. *Fuzzy Sets Syst.* **139**, 395–405 (2003)
13. Kumar, M., Pal, B.B.: FGP Model for Emission-Economic Power Dispatch, pp. 936–950. *Encyclopedia of Business Analytics and Optimization* (2014)
14. Burton, R.M., Obel, B.: The multilevel approach to organizational issues of the firm-critical review. *Omega* **5**, 395–413 (1977)
15. Zhang, G., Lu, J., Montero, J., Zeng, Y.: Model, solution concept, and Kth-best algorithm for linear trilevel programming. *J. Inf. Sci.* **180**, 481–492 (2010)
16. Pal, B.B., Chakraborti, D.: Using genetic algorithm for solving quadratic bilevel programming problems via fuzzy goal programming. *Int. J. Appl. Manage. Sci.* **5**, 172–195 (2013)
17. Abido, M.A.: Environmental/economic power dispatch using multiobjective evolutionary algorithms. *IEEE Tran. Power Syst.* **18**, 1529–1537 (2003)
18. Odibat, Z.M., Shawagfeh, N.T.: Generalized Taylor's formula. *Appl. Math. Comp.* **186**, 286–293 (2007)
19. Pal, B.B., Moitra, B.N.: A goal programming procedure for solving problems with multiple fuzzy goals using dynamic programming. *Euro. J. Oper. Res.* **144**, 480–491 (2003)
20. Abido, M.A.: Multiobjective evolutionary algorithms for electric power dispatch problem. *IEEE Trans. Evol. Comp.* **10**, 315–329 (2006)
21. Abido, M.A.: A novel multiobjective evolutionary algorithm for environmental/economic power dispatch. *Electr. Power Syst. Res.* **65**, 71–81 (2003)
22. Wua, L.H., Wanga, Y.N., Yuana, X.F., Zhou, S.W.: Environmental/economic power dispatch problem using multi-objective differential evolution algorithm. *Elec. Power Syst. Res.* **80**, 1171–1181 (2011)
23. Inuiyuchi, M., Kume, Y.: Goal programming problems with interval coefficients and target intervals. *Euro. J. Oper. Res.* **52**, 345–360 (1991)

# Reverse Logistic Model for Deteriorating Items with Non-instantaneous Deterioration and Learning Effect

S.R. Singh and Himanshu Rathore

**Abstract** Recycling is the necessary concept for survival of the today's global environment. To encourage this concept, in present article we have developed a reverse logistics model for deteriorating items. The deterioration is treated as non-instantaneous rate with time dependent demand rate. The production rate is directly related with demand rate under the effect of learning. The whole study is done in an inflationary environment. The goal of this study is to find optimum value of total cost function. At the end this article model is numerically illustrated and a sensitivity analysis is performed.

**Keywords** Reverse logistics · Deterioration · Learning · Remanufacturing

## 1 Introduction

Reverse logistics becomes very important in today's global market. It saves our environment as well as human life. In literature the concept of reverse logistics has been studied first by Schrady [1]. Further many authors have extended his work in different aspects. El Saadany and Jaber [2] have studied the reverse logistics model with price and quality dependent return rate. Alamri [3] have developed a reverse logistics inventory model with time dependent production, remanufacturing and demand rates.

Singh and Saxena [4] have developed an optimal return policy for reverse logistics system. In similar manner Singh et al. [5], Yang et al. [6] have considered the reverse logistics concept.

---

S.R. Singh (✉)  
D. N. College, Meerut, India  
e-mail: shivrajpundir@gmail.com

H. Rathore  
Banasthali University, Banasthali, India  
e-mail: rathorehimanshu2003@gmail.com

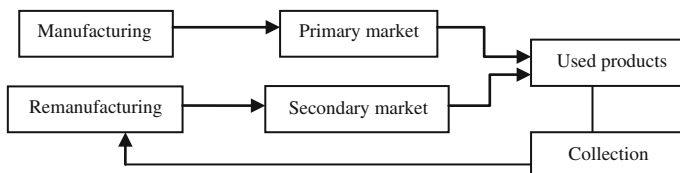
In literature many researchers have assumed that the remanufactured products are as good as manufactured products. But its not always true, means the quality of remanufactured products is low then the quality of fresh products. These low quality products are sold in secondary market at a low price rate whereas fresh products are sold in primary market at high price rate. For literature review we can go through the work of Jaber and El Saadany [7], Konstantaras and Skouri [8], Hasanov et al. [9], Singh and Saxena [10, 11] etc.

In real life it is very common that the customer try to reduce the cost parameters and it is done through experiences of purchasing a particular item. This process is known as learning. In literature Maity et al. [12] have studied the recycling inventory model under the effect of learning. Singh et al. [13] have studied a two-warehouse inventory model with non-instantaneous deterioration rate and effect of learning. Singh et al. [14] have developed an inventory model for non-instantaneously deteriorating items with limited storage capacity.

In this paper we have developed a reverse logistics inventory model for deteriorating items with non-instantaneous deterioration rate. The demand is treated as exponential function of time and production and remanufacturing rates are directly related to the demand rate. Remanufactured products are of low quality then fresh products and sold in secondary market at low price rate. The demands of primary market are satisfied by fresh products at high price rate. The whole study is done under the effect of inflation and learning effect associated with cost of manufacturing and manufacturing. The whole system is represented in Fig. 1.

## 2 Assumptions and Notations

The assumptions and notations which are used in mathematical model formulation are given as follows. The subscript r, m and c are used for remanufacturing, manufacturing and collection cycle respectively.



**Fig. 1** Forward and backward supply chain

## 2.1 Notations

$P_m, P_r$	are the manufacturing and remanufacturing rate respectively
$R_c$	rate of returning items
$D_m(t)$	Time dependent demand rate at primary market
$W: (=D_r(t))$	is the demand rate of customer at secondary market
$\theta_r$	Deterioration rate of remanufactured product
$\theta_m$	Deterioration rate of manufactured product
$\theta_c$	Deterioration rate of the collected items
$t_r$	life time of remanufactured product
$t_m$	life time of manufactured product
$t_c$	Deterioration rate of the collected items
$T$	Total cycle length, $t_i$ : time intervals for $i = 1, 2, 3$
$K_m$	set up cost for manufacturing
$K_r$	set up cost for remanufacturing
$K_c$	set up cost for Collection
$C_c$	unit acquisition cost
$S_m$	unit procurement cost
$C_m$	unit production cost
$C_r$	unit remanufacturing cost
$h_r$	holding cost (per unit per unit time) of owned warehouse
$h_m$	holding cost (per unit per unit time) of rented warehouse
$h_c$	Cost for holing returned items per unit per unit time
$I_{mi}(t)$	inventory level during manufacturing cycle, $i = 1, 2, 3$
$I_{ri}(t)$	inventory level during remanufacturing, $i = 1, 2, 3$
$I_{ci}(t)$	inventory level during collection cycle, $i = 1, 2, 3$ .

## 2.2 Assumptions

- Items are returnable and returned items are remanufactured. In quality both manufactured and remanufacture products are of same quality.
- System is proposed for single item only with constant deterioration rate.
- Items are manufactured/remanufactured at a finite rate of manufacturing and remanufacturing which directly related to the demand rate,  $P_r = k_r D_r(t)$ ;  $P_m = k_m D_m(t)$  where  $k_r$  and  $k_m > 0$ .
- Demand rate is  $D_m(t) = ae^{bt}$  where  $a$  and  $b > 0$  is satisfied by both fresh products of at the primary market. The  $W (=D_r(t) = \alpha e^{\beta t}$ ,  $\alpha$  and  $\beta > 0$ ) is the rate of demand at secondary market which is satisfied by remanufactured products, which are of low quality.
- Cycle length is infinite but we have discussed only a typical cycle of length  $T$ . All other cycles are identical to the cycle  $T$ .

- $C_r + C'_r/n^\lambda$  is the remanufacturing cost under the effect of learning where  $\lambda > 0$  is the learning coefficient.
- $C_m + C'_m/n^\gamma$  is the manufacturing cost under the effect of learning where  $\gamma > 0$  is the learning coefficient.

### 3 Mathematical Model Formulation

The inventory depletion in different cycles is described as follows:

#### 3.1 Remanufacturing Cycle

$$\frac{dI_{r1}(t)}{dt} = P_r - W; \quad I_{r1}(t = 0) = 0, \quad 0 \leq t \leq t_r \tag{1}$$

$$\frac{dI_{r2}(t)}{dt} + \theta_r I_{r2}(t) = P_r - W; \quad I_{r1}(t = t_r) = I_{r2}(t = t_r), \quad t_r \leq t \leq t_1 \tag{2}$$

$$\frac{dI_{r3}(t)}{dt} + \theta_r I_{r3}(t) = -W; \quad I_{r3}(t = t_2) = 0, \quad I_{r2}(t = t_1) = I_{r3}(t = t_1), \tag{3}$$

$$t_1 \leq t \leq t_2$$

Solving (1), (2) and (3) using boundary conditions, we get

$$I_{r1}(t) = \frac{\alpha}{\beta} (k_r - 1) (e^{\beta t} - 1); \tag{4}$$

$$I_{r2}(t) = \alpha (k_r - 1) e^{-\theta_r t} \left( \frac{e^{(\theta_r + \beta)t}}{(\theta_r + \beta)} + \frac{e^{(\theta_r + \beta)t_r} - e^{\theta_r t_r}}{\beta} - \frac{e^{(\theta_r + \beta)t_r}}{(\theta_r + \beta)} \right); \tag{5}$$

$$I_{r3}(t) = \alpha e^{-\theta_r t} \left( \frac{e^{(\theta_r + \beta)t_2}}{(\theta_r + \beta)} - \frac{e^{(\theta_r + \beta)t}}{(\theta_r + \beta)} \right); \tag{6}$$

$$t_2 = \left( \frac{1}{\theta_r + \beta} \right) \log \left\{ \left( k_r e^{(\theta_r + \beta)t_1} + \left( \frac{k_r - 1}{\beta} \right) \left( \theta_r e^{(\theta_r + \beta)t_r} - (\theta_r + \beta) e^{\theta_r t_r} \right) \right) \right\}; \tag{7}$$

### 3.2 Manufacturing Cycle

$$\frac{dI_{m1}(t)}{dt} = P_m - D_m(t); \quad I_{m1}(t = t_2) = 0, \quad t_2 \leq t \leq t_m \tag{8}$$

$$\frac{dI_{m2}(t)}{dt} + \theta_m I_{m2}(t) = P_m - D_m(t); \quad I_{m1}(t = t_m) = I_{m2}(t = t_m), \quad t_m \leq t \leq t_3 \tag{9}$$

$$\frac{dI_{m3}(t)}{dt} + \theta_m I_{m3}(t) = -D_m(t); \quad I_{m3}(t = T) = 0, \quad I_{m2}(t = t_3) = I_{m3}(t = t_3), \\ t_3 \leq t \leq T \tag{10}$$

Solving (8), (9) and (10) using boundary conditions, we get

$$I_{m1}(t) = \frac{a}{b}(k_m - 1)(e^{bt} - e^{bt_2}); \tag{11}$$

$$I_{m2}(t) = a(k_m - 1)e^{-\theta_m t} \left( \frac{e^{(\theta_m + b)t}}{(\theta_m + b)} + \frac{e^{(\theta_m + b)t_m} - e^{\theta_m t_m} e^{bt_2}}{b} - \frac{e^{(\theta_m + b)t_m}}{(\theta_m + b)} \right); \tag{12}$$

$$I_{m3}(t) = a e^{-\theta_m t} \left( \frac{e^{(\theta_m + b)T}}{(\theta_m + b)} - \frac{e^{(\theta_m + b)t}}{(\theta_m + b)} \right); \tag{13}$$

$$T = \left( \frac{1}{\theta_m + b} \right) \log \left\{ \left( k_m e^{(\theta_m + b)t_3} + \left( \frac{k_m - 1}{b} \right) \left( \theta_m e^{(\theta_m + b)t_m} - (\theta_m + b) e^{\theta_m t_m} e^{bt_2} \right) \right) \right\}; \tag{14}$$

### 3.3 Collection Cycle

$$\frac{dI_{c1}(t)}{dt} = R_c - P_r; \quad I_{c1}(t = t_c) = I_{c2}(t = t_c), \quad 0 \leq t \leq t_c \tag{15}$$

$$\frac{dI_{c2}(t)}{dt} + \theta_c I_{c2}(t) = R_c - P_r; \quad I_{c1}(t = t_c) = I_{c2}(t = t_c), I_{c3}(t = t_1) = 0 \quad t_c \leq t \leq t_1 \tag{16}$$

$$\frac{dI_{c3}(t)}{dt} + \theta_c I_{c3}(t) = R_c; \quad I_{c3}(t = t_1) = 0, I_{c1}(t = 0) = I_{c3}(t = T), \quad t_1 \leq t \leq T \tag{17}$$

Solving (15), (16) and (17), using boundary conditions, we get

$$I_{c1}(t) = (R_c t - \frac{\alpha k_r}{\beta} e^{\beta t}); \tag{18}$$

$$I_{c2}(t) = e^{-\theta_c t} \left( \frac{R_c}{\theta_c} (e^{\theta_c t} - e^{\theta_c t_1}) - \frac{\alpha k_r}{(\theta_c + \beta)} (e^{(\theta_c + \beta)t} - e^{(\theta_c + \beta)t_1}) \right); \tag{19}$$

$$I_{c3}(t) = \frac{R_c}{\theta_c} e^{-\theta_c t} (e^{\theta_c t} - e^{\theta_c t_1}); \tag{20}$$

Now acceptable return quantity for used items is  $Q = R_c T$  and the different cost parameters are as follows

1. Present worth of Procurement (POC) and Acquisitions (AC) cost is

$$\begin{aligned} &= S_m \int_{t_2}^{t_3} P_m e^{-Rt} dt + C_c \int_0^T R_c e^{-Rt} dt = a S_m k_m \left( \frac{e^{(b-R)t_3} - e^{(b-R)t_2}}{(b-R)} \right) \\ &\quad + C_c R_c \left( \frac{1 - e^{-RT}}{R} \right) \end{aligned} \tag{21}$$

2. Present worth of Manufacturing cost (MC) and Remanufacturing (RC) cost is

$$\begin{aligned} &= \left( C_m + \frac{C'_m}{n^\gamma} \right) \int_{t_2}^{t_3} P_m e^{-Rt} dt + \left( C_r + \frac{C'_r}{n^\lambda} \right) \int_0^{t_1} P_r e^{-Rt} dt \\ MC + RC &= a k_m \left( C_m + \frac{C'_m}{n^\gamma} \right) \left( \frac{e^{(b-R)t_3} - e^{(b-R)t_2}}{(b-R)} \right) \\ &\quad + \alpha k_r \left( C_r + \frac{C'_r}{n^\lambda} \right) \left( \frac{e^{(\beta-R)t_1} - 1}{(\beta-R)} \right) \end{aligned} \tag{22}$$

3. Present worth of holding Cost is HC

$$\begin{aligned} &= [\text{Holding cost for remanufactured items} + \text{Holding cost for manufactured items} \\ &\quad + \text{Holding cost for collected items}] \end{aligned}$$

$$\begin{aligned}
HC &= \left[ \int_0^{t_r} h_r I_{r1}(t) e^{-Rt} dt + \int_{t_r}^{t_1} h_r I_{r2}(t) e^{-Rt} dt + \int_{t_1}^{t_2} h_r I_{r3}(t) e^{-Rt} dt + \int_{t_2}^{t_m} h_m I_{m1}(t) e^{-Rt} dt \right] \\
&+ \left[ \int_{t_m}^{t_3} h_m I_{m2}(t) e^{-Rt} dt + \int_{t_3}^T h_m I_{m3}(t) e^{-Rt} dt \right. \\
&\left. + \int_0^{t_c} h_c I_{c1}(t) e^{-Rt} dt + \int_{t_c}^{t_1} h_c I_{c2}(t) e^{-Rt} dt + \int_{t_1}^T h_c I_{c3}(t) e^{-Rt} dt \right] \\
HC &= \alpha h_r \left[ \frac{1}{\beta} (k_r - 1) \left( \frac{e^{(\beta-R)t_r} R + (\beta - R) e^{-Rt_r} - \beta}{R(\beta - R)} \right) \right. \\
&+ (k_r - 1) \left( \frac{(\theta_r + \beta) e^{\theta_r t_r} - (\theta_r) e^{(\theta_r + \beta)t_r}}{\beta(\theta_r + \beta)} \right) \left. \right] \\
&+ (k_r - 1) \left( \frac{e^{-(\theta_r + R)t_1} - e^{-(\theta_r + R)t_r}}{(\theta_r + R)} \right) \\
&+ \alpha h_r \left[ (k_r - 1) \left( \frac{e^{(\beta-R)t_1} - e^{(\beta-R)t_r}}{(\beta - R)} \right) \right. \\
&+ \left. \left( \frac{e^{(\theta_r + \beta)t_2}}{(\theta_r + \beta)} \left( \frac{e^{(\theta_r + R)t_1} - e^{(\theta_r + R)t_2}}{(\theta_r + R)} \right) - \left( \frac{e^{(\beta-R)t_1} - e^{(\beta-R)t_2}}{(\beta - R)(\theta_r + \beta)} \right) \right) \right] \\
&+ ah_m \left[ \frac{1}{b} (k_m - 1) \left( \frac{e^{(b-R)t_m} - e^{(b-R)t_2}}{(b - R)} + \frac{(e^{-Rt_m} - e^{-Rt_2}) e^{bt_2}}{R} + \frac{b(e^{(b-R)t_3} - e^{(b-R)t_m})}{(b - R)(\theta_m + b)} \right) \right. \\
&- \left. \left[ \frac{ah_m}{(\theta_m + b)} \left( \frac{e^{(b-R)T} - e^{(b-R)t_3}}{(b - R)} \right) \right] \right. \\
&+ \left. \left[ \frac{ah_m}{(\theta_m + b)} e^{(\theta_m + b)T} \left( \frac{e^{-(\theta_m + R)t_3} - e^{-(\theta_m + R)T}}{(\theta_m + R)} \right) \right] \right. \\
&- \left. \left[ \frac{a(k_m - 1)h_m}{b(\theta_m + b)} \left( \theta_m e^{(\theta_m + b)t_m} - (\theta_m + b) e^{(\theta_m + b)t_2} \right) \right. \right. \\
&\left. \left. \left( \frac{e^{-(\theta_m + R)t_3} - e^{-(\theta_m + R)t_m}}{(\theta_m + R)} \right) \right] \right. \\
&+ h_c \left[ R_c \left( \frac{1}{R^2} - \frac{e^{-Rt_c}}{R^2} - \frac{t_c e^{-Rt_c}}{R} \right) - \frac{\alpha k_r}{\beta} \left( \frac{e^{(\beta-R)t_c} - 1}{(\beta - R)} \right) \right. \\
&+ \left. \frac{R_c}{\theta_c} \left( \frac{e^{-Rt_c} - e^{-RT}}{R} + \frac{(e^{-(R+\theta_c)T} - e^{-(R+\theta_c)t_c}) e^{\theta_c t_1}}{(\theta_c + R)} \right) \right. \\
&- \left. \frac{\alpha k_r h_c}{(\beta + \theta_c)} \left[ \frac{e^{(\beta-R)t_1} - e^{(\beta-R)t_c}}{(\beta - R)} + e^{(\beta + \theta_c)t_1} \left( \frac{e^{-(R+\theta_c)t_1} - e^{-(R+\theta_c)t_c}}{(R + \theta_c)} \right) \right] \right]
\end{aligned}
\tag{23}$$



Now using continuity functions for values of  $t_1, t_2, t_3$  and  $T$  in total cost function. Hence the total cost per unit time is

$$TC(t_1, T) = (1/T)[K_r + K_m + K_c + POC + AC + PC + RC + HC] \quad (24)$$

To minimize total relevant cost, we differentiate  $TC(t_1, T)$  w.r.t to  $t_1$  and  $T$  for optimal value necessary conditions are

$$\frac{\partial TC(t_1, T)}{\partial t_1} = 0; \quad \frac{\partial TC(t_1, T)}{\partial T} = 0;$$

Provided the determinant of principal minor of hessian matrix are positive definite, i.e.  $\det(H1) > 0, \det(H2) > 0$  where  $H1, H2$  is the principal minor of the Hessian-matrix. Hessian Matrix of the total cost function is as follows:

$$\begin{bmatrix} \frac{\partial^2 TC}{\partial t_1^2} & \frac{\partial^2 TC}{\partial t_1 \partial T} \\ \frac{\partial^2 TC}{\partial T \partial t_1} & \frac{\partial^2 TC}{\partial T^2} \end{bmatrix}$$

### 4 Numerical Illustration and Sensitivity Analysis

For the numerical illustration following numerical values are used to calculate optimal value of total cost  $K_m = 150, K_r = 80, K_c = 100, h_r = 1.2, h_m = 1.2, h_3 = 2, h_c = 1, R_c = 60, a = 250, b = 2, \alpha = 100, \beta = 5, k_r = 2, k_m = 2, n = 2, \theta_r = 0.055, \theta_m = 0.05, \theta_c = 0.057, R = 0.01 S_m = 8, C_m = 3, C'_m = 3.2, C_r = 2, C'_r = 2.2, C_c = 2, t_r = 0.3, t_m = 3, t_c = 0.3$  with the help of Mathematical software Mathematica7 optimal values are as follows:  $TC^* = 15,097.9, t_1^* = 0.45299, t_2^* = 1.1063, t_3^* = 5.66352, T^* = 10.4525$ .

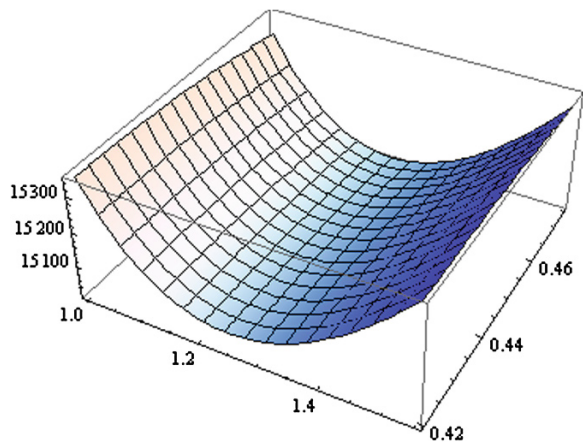
We have performed a sensitivity analysis by changing values of important parameters like demand factors  $a, b, \alpha, \beta$ , learning coefficients  $\lambda, \gamma$  and inflation rate  $R$ . The resultant optimal values of  $t_1^*, t_2^*, t_3^*, T$  and  $TC$  are given in Table 1. The keen observations of Table 1 are as follows:

- Increment in  $a$  and  $b$  results in increment in  $t_1^*, t_2^*, t_3^*, T^*$  and  $TC^*$ .
- Increment in  $\alpha$  results in increment in  $TC^*$  while decrement in  $t_1^*, t_2^*, t_3^*$  and  $T^*$ .
- Increment in  $\beta$  results in increment in  $t_1^*$  and  $TC^*$  while decrement in  $t_2^*, t_3^*$  and  $T^*$ .
- Increment in  $\gamma$  results in decrement in  $t_1^*, t_2^*, t_3^*, T^*$  and  $TC^*$ .
- Increment in  $\lambda$  results in increment in  $t_1^*, t_2^*, t_3^*$  and  $T^*$  while decrement in  $TC^*$ .
- Increment in  $R$  results in decrement in  $t_1^*, t_2^*, t_3^*$  and  $T^*$  while increment in  $TC^*$  (Figs 2 and 3).

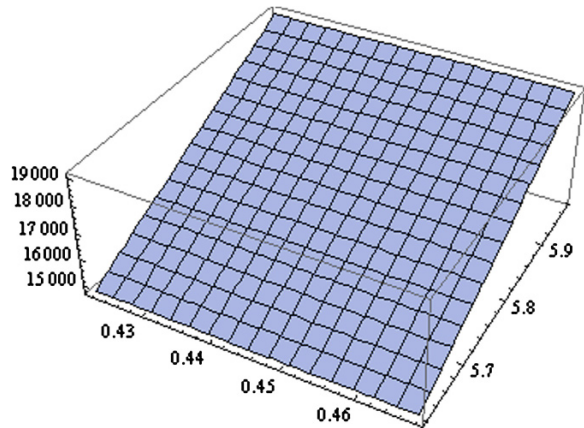
**Table 1** Sensitivity analysis

	$t_1^*$	$t_2^*$	$t_3^*$	$T^*$	$TC^*$
<i>Change in a</i>					
225	0.441224	1.08854	5.64147	10.4261	13,794.7
255	0.45506	1.11042	5.6674	10.4561	15,358.4
275	0.462581	1.12546	5.68151	10.4693	16,400.1
<i>Change in b</i>					
3	0.477475	1.15525	5.80821	10.565	16,113
4	0.492346	1.18499	5.87172	10.6171	16,498.3
5	0.502122	1.20454	5.90696	10.647	16,690.9
<i>Change in <math>\alpha</math></i>					
75	0.481115	1.1626	5.71955	10.5082	15,022.4
125	0.424671	1.04964	5.60711	10.3963	15,168.7
150	0.396159	0.992618	5.55032	10.3397	15,235.1
<i>Change in <math>\beta</math></i>					
4	0.431194	1.11147	5.66889	10.458	15,070.1
6	0.467584	1.1028	5.65992	10.4488	15,116.4
8	0.485903	1.09843	5.65541	10.4441	15,140.5
<i>Change in <math>\gamma</math></i>					
0.03	0.452974	1.10625	5.65622	10.4379	15,097.9
0.04	0.452959	1.10622	5.64898	10.4235	14,998.8
0.05	0.452944	1.10619	5.64178	10.4091	14,950.2
<i>Change in <math>\lambda</math></i>					
0.03	0.453497	1.10729	5.66453	10.4535	15,096.4
0.04	0.454002	1.1083	5.66554	10.4545	15,095.2
0.05	0.454503	1.1093	5.66654	10.4555	15,093.8
<i>Change in R</i>					
0.02	0.452989	1.10628	5.66352	10.4525	15,097.7
0.03	0.452988	1.10627	5.66351	10.4524	15,097.8
0.04	0.452987	1.10626	5.6635	10.4523	15,097.9

**Fig. 2** Convexity of  $TC^*$  w.r.  $t_1^*$  and  $t_2^*$



**Fig. 3** Convexity of  $TC^*$  w.r.  $t_1^*$  and  $t_3^*$



## 5 Conclusion

In this article we have developed a reverse logistics inventory model under the effect of learning and inflation. The items are deteriorating in nature with non-instantaneous deterioration rate. The demand rate is treated as exponential function of time and manufacturing and remanufacturing rates are demand dependent. The remanufactured products which are low in quality than the quality of manufactured product, sold in secondary market whereas fresh products are sold in primary market. The used items are collected from both markets and are remanufacturing unit. The main objective of this study is to find optimal values of total cost function  $TC$  and optimal operating times  $t_1$ ,  $t_2$ ,  $t_3$ ,  $T$ . At the end numerical illustration and sensitivity analysis is elaborated. The whole calculation part is done using Mathematica7. For the future research we can incorporate some other parameters of inventory control system.

## References

1. Schrady, D.A.: A deterministic inventory model for repairable items. *Naval Res. Logistics Q.* **14**, 391–398 (1967)
2. El Saadany, A.M.A., Jaber, M.Y.: A production/remanufacturing inventory model with price and quality dependant return rate. *Comput. Ind. Eng.* **58**(3), 352–362 (2010)
3. Alamri, A.A.: Theory and methodology on the global optimal solution to a general reverse logistics inventory model for deteriorating items and time-varying rates. *Comput. Ind. Eng.* **60**, 236–247 (2010)
4. Singh, S.R., Saxena, N.: An optimal returned policy for a reverse logistics inventory model with backorders. *Adv. Decis. Sci.* 21 (Article ID 386598) (2012)
5. Singh, S.R., Prasher, L., Saxena, N.: A centralized reverse channel structure with flexible manufacturing under the stock out situation. *Int. J. Ind. Eng. Comput.* **4**, 559–570 (2013)

6. Yang, P.C., Chung, S.L., Wee, H.M., Zahara, E., Peng, C.Y.: Collaboration for a closed-loop deteriorating inventory supply chain with multi-retailer and price-sensitive demand. *Int. J. Prod. Econ.* **143**, 557–566 (2013)
7. Jaber, M.Y., El Saadany, A.M.A.: The production, remanufacture and waste disposal model with lost sales. *Int. J. Prod. Econ.* **120**(1), 115–124 (2009)
8. Konstantaras, I., Skouri, K.: Lot sizing for a single product recovery system with variable setup numbers. *Eur. J. Oper. Res.* **203**(2), 326–335 (2010)
9. Hasanov, P., Jaber, M.Y., Zolfaghari, S.: Production, remanufacturing and waste disposal models for the cases of pure and partial backordering. *Appl. Math. Model.* **36**, 5249–5261 (2012)
10. Singh, S.R., Saxena, N.: A closed loop supply chain system with flexible manufacturing and reverse logistics operation under shortages for deteriorating items. *Procedia Technol.* **10**, 330–339 (2013)
11. Singh, S.R., Saxena, N.: An integrated inventory model with remanufacturing of secondary material under shortages. In: *Proceedings of 3rd International Conference on Recent Trends in Engineering and Technology*, Elsevier, Nasik, India pp. 354–359 (2014)
12. Maity, A.K., Maity, K., Mondal, S.K., Maiti, M.: A production-recycling-inventory model with learning effect. *Optim. Eng.* **10**, 427–438 (2009)
13. Singh, S.R., Jain, S., Pareek, S.: An imperfect quality items with learning and inflation under two limited storage capacity. *Int. J. Ind. Eng. Comput.* **4**, 1–12 (2013)
14. Singh, S.R., Rathore, H., Saxena, N.: A two warehouse inventory model for deteriorating items with shortages under inflationary environment. In: *Proceedings of 3rd International Conference on Recent Trends in Engineering and Technology*. Elsevier, India pp. 385–391 (2014)

# On the Implementation of a Saliency Based Digital Watermarking

Abhishek Basu, Susmita Talukdar, Nabanita Sengupta,  
Avradeeta Kar, Satrajit Lal Chakraborty  
and Subir Kumar Sarkar

**Abstract** Digital watermarking at the least significant bit (LSB) for copyright protection is proposed in this paper based on the saliency map. The projected algorithm can embed more information into less perceptive areas within the original image determined by Itti-Koch saliency map. It gives a concept of the areas which has excellent data hiding capacity in an image. The area/region with less perceptibility denotes the most insignificant region from the aspect of visibility in an image, so any modification within these areas will be less evident to any observer. Here the algorithm is being evaluated by means of imperceptibility and robustness. Thus images embed with a watermark will project higher bit capacity.

**Keywords** Digital watermarking · LSB · Copyright protection · Itti-Koch saliency map · Data hiding capacity · Imperceptibility

## 1 Introduction

With the advancement of technology in today's world, new ideas are coming up every day—both constructive and destructive. These days, digital information can be replicated and reproduced with an ease. To prevent this treachery, few methods are implemented to retain the originality and digital watermarking is one of them [1]. It is a proficient mechanism for copyright protection of digitalized information. In this process data is hidden within an object by some unique ways so that others can't reach to the original data and later on the data can be extracted by the owner itself [1, 2].

---

A. Basu (✉) · S. Talukdar · N. Sengupta · A. Kar · S.L. Chakraborty  
RCC Institute of Information Technology, Kolkata 700015, West Bengal, India  
e-mail: idabhishek23@yahoo.com

S.K. Sarkar  
Jadavpur University, Kolkatta 700032, West Bengal, India  
e-mail: su\_sircir@yahoo.co.in

The proposal of this paper is regarding digital image watermarking technique based on Itti-Koch saliency map of an image in which the watermark will be implanted in the less prominent areas of that image. Saliency map signifies visual saliency of a consequent visual sense topographically. It facilitates in evaluating the imperceptibility of an image along with its data embedding capacity. In this proposed technique data hiding is the maximum at those positions where perceptibility is low [3, 4]. By adaptive least significant bit (LSB) substitution technique, the watermark is implanted within the original image [5]. As the bits of watermark are implanted at least significant locations of image, imperceptibility is superior. The data is hidden at numerous places and more than one time to improve the robustness and data hiding capacity [2].

This preliminary introduction about the proposed work is followed by some other sections like description of steps of watermark embedding and the extraction, followed by experimental results and discussions, finally conclusion and reference.

## 2 Watermark Embedding and Extraction

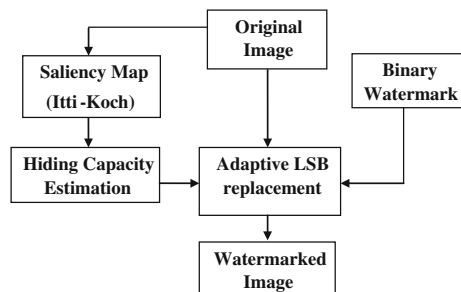
The process of digital image watermarking proposed here aims to attain the trade-off between robustness and imperceptibility of the watermarked image i.e. the original image embedded with the watermark, through increasing the data hiding capacity by embedding multiple copies of the logo in an effective way [5].

Figure 1 shows the process of encrypting a watermark in an image:

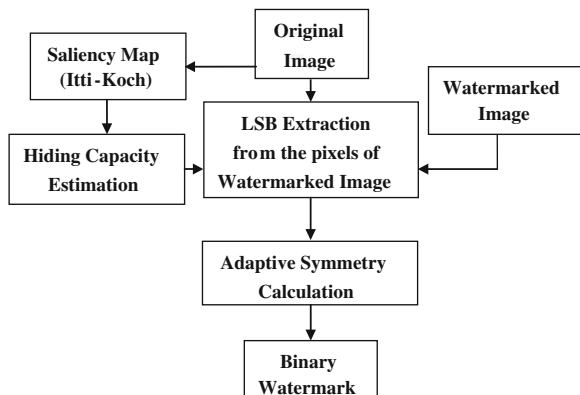
At first the Saliency Map of the original image is produced. Here Itti-Koch algorithm has been followed to produce the map. Hiding capacity estimation is done based on the previous map and main regions where the watermarks can be hidden are approximated. Based on the hiding capacity of the image, the watermark is embedded into it by adaptive LSB replacement process. More bits of the original image are replaced by the bits of the watermark where the original image is more inconspicuous. Thus the Watermarked image is obtained.

Figure 2 provides a scheme of the process of decoding a watermark form a watermarked image.

**Fig. 1** Block diagram of watermark encoder



**Fig. 2** Block diagram of watermark decoder



Saliency map of the original image is produced and hiding capacity estimation of the original image is done as it was done in the encoding process. On the basis of original image & hiding capacity in the original image, LSB is extracted from the pixels of the watermarked image. Adaptive symmetry of the bits of the same order, extracted from different regions of the watermarked image derived from saliency, is computed to retrieve the binary watermark.

## 2.1 Watermark Embedding and Extraction

The architecture for Itti-Koch model [6] is presented in Fig. 3.

The model unites multi-scale image features into a solo topographical saliency map in a bottom-up approach. Visual pre-processing (presented within the marked enclosure), for every pixel in the pyramid, three color channels R, G, B are generated. Four Gaussian pyramids  $R(\sigma)$ ,  $G(\sigma)$ ,  $B(\sigma)$ ,  $I(\sigma)$  are created from these color channels, where  $I = \frac{r+g+b}{3}$ , r, g and b are the colors. The projected approach utilizes grayscale images, to obtain the saliency map. Therefore all the three color channels are assigned as gray channels.

In mammals the sensitivity of intensity and contrast is detected by the neurons that are sensitive either to dark centers on bright surroundings or vice versa, is computed in a set of six maps and the center-surround is implemented here as the difference between center and surround scales.

Orientation feature maps encode local orientation contrast between the centers and surround scales. The feature maps are combined into three conspicuity maps,  $\bar{I}$  for Intensity,  $\bar{C}$  for Color,  $\bar{O}$  for Orientation. This three conspicuity maps are normalized and summed to find out the ultimate output  $S$ , the saliency map.

$$S = \frac{1}{3} (N(\bar{I}) + N(\bar{C}) + N(\bar{O})) \quad (1)$$

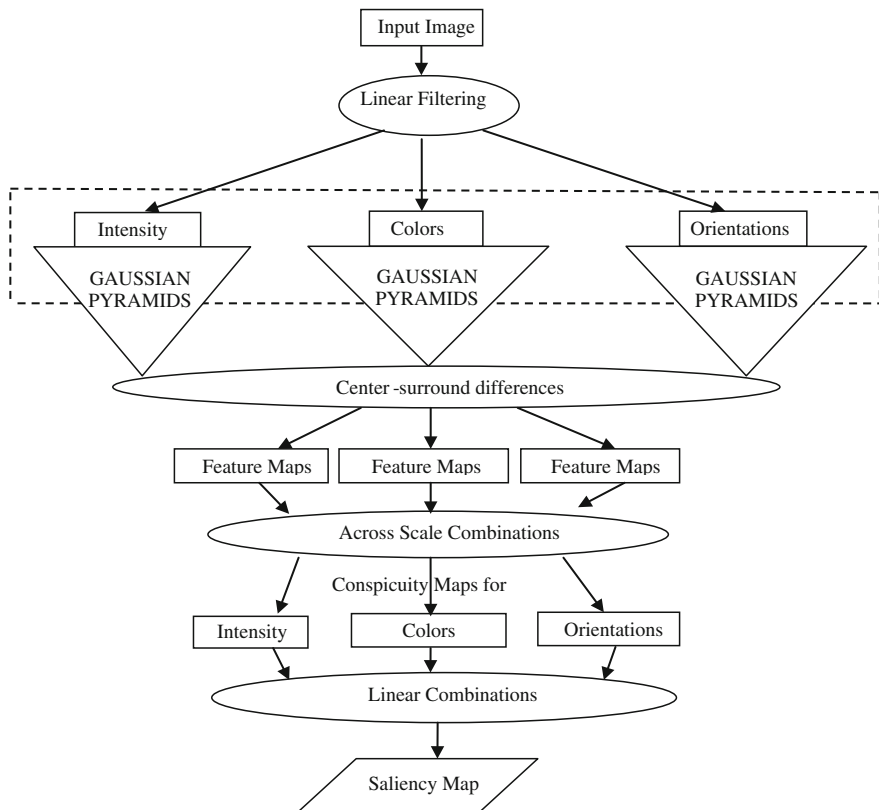


Fig. 3 Architecture of Itti and Koch model

## 2.2 Hiding Capacity Estimation

From the produced saliency map, a hiding capacity estimation map is prepared by using high embedding potency in less perceptible saliency areas and a low embedding potency in areas of more perceptible saliency areas, to acquire enhanced watermark invisibility and to improve the hiding capacity of the embedded watermark.

$$S_{temp_m} = \min(S_m) \quad (2)$$

$$\text{where, } m \leq S_m < (m + 1) \times 0.10; \text{ for } m = 0 \quad (3)$$

$$\text{and } S_{temp_m} = \max(S_m) \quad (4)$$



$$\text{where, } (m \times 0.10) \leq \mathcal{S}_m < (m \times 0.25); \text{ for } m = 1, \quad (5)$$

$$((m - 1) \times 0.25) \leq \mathcal{S}_m < (m \times 0.25); \text{ for } 2 \leq m \leq 3, \quad (6)$$

$$((m - 1) \times 0.25) \leq \mathcal{S}_m \leq (m \times 0.25); \text{ for } m = 4 \quad (7)$$

where  $\mathcal{S}_m$  is the Saliency map of original gray-scale image.  $I_{om}$

### 2.3 Encoder and Decoder

Let the original gray-scale image be  $I_{om}$  of size  $C \times D$  and  $\mathcal{W}_b$  be the binary watermark with size of  $P \times Q$  and illustrated as:

$$I_{om} = \{X(a, b)\}; 0 \leq a < C, 0 \leq b < D, X(a, b) \in \{0, 1, \dots, 255\} \quad (8)$$

$$\mathcal{W}_b = \{Y(i, j)\}; 0 \leq i < P, 0 \leq j < Q, Y(i, j) \in \{0, 1\} \quad (9)$$

$\mathcal{D}_b$  is the function for Decimal to Binary conversion and  $\mathcal{B}_d$  is the function of converting Binary to Decimal.

The adaptive LSB watermarking is defined as functions  $(\mathcal{F}_{enc}, \mathcal{F}_{dec})$ .

$$\mathcal{D}_b\{I_{om}\} = \mathcal{B}I_{om} \quad (10)$$

$$\mathcal{B}I_{om}(0, \mathcal{M}) = \mathcal{W}_b \quad (11)$$

where  $\mathcal{M} \leq 7 - (4 + m)$  and  $\mathcal{M}$  is a positive integer with  $m = \{0, 1, 2, 3\}$

The watermark is implanted only once for every region i.e.  $\mathcal{S}_{temp_m}$ .

So here,

$$\mathcal{F}_{enc} : \mathcal{B}_d\{\mathcal{B}I_{om}, 0, \mathcal{M}\} \rightarrow I_w \quad (12)$$

$I_w$  is the watermarked image of size  $C \times D$ .

Likewise, for decrypting the watermark,  $\mathcal{S}_{temp_m}$ ,  $I_{om}$  and  $I_w$  are compared to get the region where the watermark has been concealed for every value of  $m$ . Let the region be

$$\mathcal{E}_{wm} = \{\mathcal{E}_{wm}(p, q)\}; \text{ where } 0 \leq p < P, 0 \leq q < Q, \mathcal{E}_{wm}(p, q) \in \{0, 1, \dots, 255\} \quad (13)$$

$$\mathcal{D}_b\{\mathcal{E}_{wm}\} = \mathcal{B}\mathcal{E}_m \quad (14)$$

Now if  $\text{Count}_m$  be the function to count binary '0' and '1' in LSBs of each pixel of  $\mathcal{E}_{wm}$  in the following manner and the function returns the value of majority to  $\mathcal{C}_{bit_m}$  where

$$\mathcal{C}_{bit_m} = \{\mathcal{C}_{bit_m}(g, h)\}; \text{Where } 0 \leq g < P, 0 \leq h < Q, \mathcal{C}_{bit_m}(g, h) \in \{0, 1\} \quad (15)$$

Then,

For  $m = 0$  and  $\mathcal{S}_{temp} = 0$ ;

$$\mathcal{C}_{bit_m} = \text{Count}_m\{\mathcal{BE}_m(0, 3), \mathcal{BE}_m(0, 2), \mathcal{BE}_m(0, 1)\} \quad (16)$$

For  $m = 1$  and  $\mathcal{S}_{temp_m} = 0.25$ ;

$$\mathcal{C}_{bit_m} = \text{Count}_m\{\mathcal{BE}_m(0, 2), \mathcal{BE}_m(0, 1), \mathcal{BE}_m(0, 0)\} \quad (17)$$

$$\text{For } m = 2 \text{ and } \mathcal{S}_{temp_m} = 0.50; \mathcal{C}_{bit_m} = \{\mathcal{BE}_m(0, 1)\} \quad (18)$$

$$\text{For } m = 3 \text{ and } \mathcal{S}_{temp_m} = 0.75; \mathcal{C}_{bit_m} = \{\mathcal{BE}_m(0, 0)\} \quad (19)$$

$\text{Count}$  be the function to count binary '0' and '1' for value at the same positions for  $\mathcal{C}_{bit_3}, \mathcal{C}_{bit_2}, \mathcal{C}_{bit_1}$  and the function returns the value of majority to

$$\mathcal{C} = \mathcal{C}(g, h); \text{Where } 0 \leq g < P, 0 \leq h < Q, \mathcal{C}_{bit}(g, h) \in \{0, 1\} \quad (20)$$

Then,

$$\mathcal{C} = \text{Count}\{\mathcal{C}_{bit_3}, \mathcal{C}_{bit_2}, \mathcal{C}_{bit_1}\} \quad (21)$$

where  $\mathcal{C}$  is the decrypted binary watermark.

Hence, following the above processes we get:

$$\mathcal{F}_{dec} : I_w \rightarrow \mathcal{C}; \text{Where } \mathcal{C} \equiv \mathcal{W}_b. \quad (22)$$

### 3 Results and Discussion

The segment reports the experimental outcomes which have been evaluated through comparative study between the earlier methods and the proposed technique. To study the performance of the proposed algorithm by means of imperceptibility, robustness and hiding capacity, four regularly accessible grayscale test images of size  $256 \times 256$  and single binary watermark image of dimension  $16 \times 16$  are used. The binary watermark image is given in Fig. 4 and the test gray scale images are given in Fig. 5. Figure 6 shows the saliency maps for original grayscale images and Fig. 7 stands for hiding capacity estimation based on the saliency maps where different shades represent different hiding capacity. The black region represents the less perceptible saliency region whereas the white region represents the most perceptible saliency region. Figure 8 illustrates the watermarked Images.



Fig. 4 Binary watermark (logo)



(i) Barbara (ii) Cameraman (iii) Lena (iv) Peppers

Fig. 5 Original grayscale images

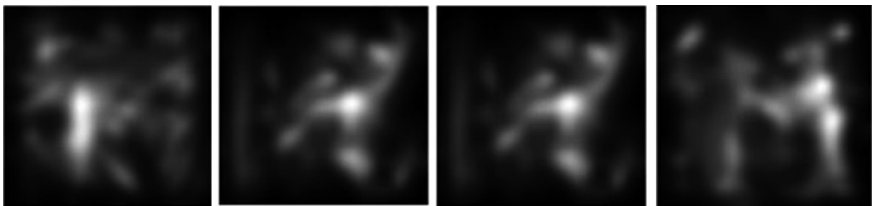


Fig. 6 Itti-Koch saliency maps of original grayscale images

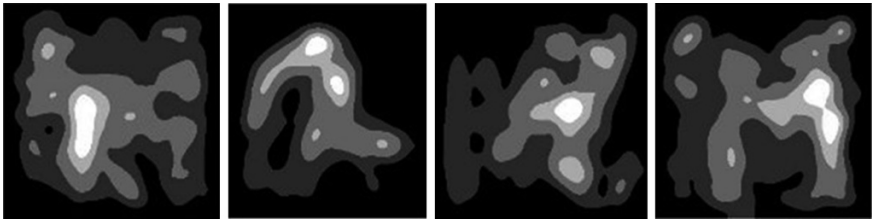


Fig. 7 Hiding capacity estimation based on the saliency maps



Fig. 8 Watermarked images

**Table 1** The performance results of imperceptibility

Original image	SNR	PSNR	MSE	IF	LMSE	UIQI	MSSIM	NQM	AD	MD
Barbara	46.19	52.13	0.398	1	0.0014	0.999	0.9995	46.189	0.0313	15
Cameraman	46.93	52.51	0.365	1	8.5392e-004	1.000	0.9991	46.930	0.0330	15
Lena	46.55	52.15	0.396	1	0.0029	0.999	0.9997	46.550	0.0293	15
Peppers	43.99	49.57	0.718	1	0.0021	0.999	0.9997	43.985	0.0557	15

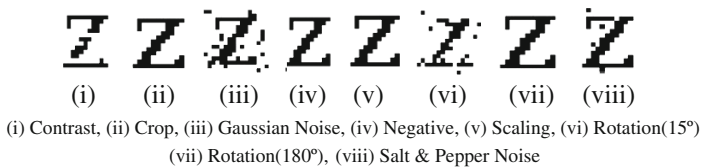
**Table 2** Results for robustness

Name of attacks	NCC	SM	PCC	WDR	WPSNR	MI
Contrast	1	1	0.999	-13.533	26.420	0.0330
Crop	1	1	1	-Inf	Inf	0.0341
Gaussian noise	0.916	1	0.999	-10.065	25.053	0.0329
Negative	1	1	1	-Inf	Inf	0.0341
Scaling	1	1	1	-Inf	Inf	0.0341
Rotation (15°)	0.931	1	0.999	-8.603	24.207	0.0323
Rotation (180°)	1	1	1	-Inf	Inf	0.0341
Salt and pepper noise	0.975	1	0.999	-16.085	32.430	0.0337

Imperceptibility, in this context, refers to the invisibility of the embedded watermark in the test or original images without corrupting the perceptual quality of watermarking [2, 4, 5]. Table 1 tabularizes the number of quality measures required to check the imperceptibility of the watermarks in the watermarked images.

A considerable degradation of quality or information loss will occur if any means of intentional or unintentional processing is applied on the image. Table 2 presents the average results of performance against different attacks comparing the original watermark and the watermark extracted from the watermarked images under attack. Figure 9 provide recovered watermarks after different image impairments.

To validate the performance of the proposed scheme, a comparison among different algorithms is presented in Table 3. The assessment verifies that the projected approach offer improved imperceptibility and better capacity.



**Fig. 9** Recovered watermarks after different image impairments

**Table 3** The performance comparison

Sl. no	Method	PSNR (dB)	Avg. capacity (bpp)
1.	Proposed method	52.51	3.3
2.	Optimal LSB substitution by dynamic prog. [7]	38.34	3
3.	Pair wise LSB matching by immune programming [8]	35.05	2.25
4.	Mielikainen's method [9]	33.05	2.2504
5.	Optimal LSB pixel adjustment process [10]	34.84	4

## 4 Conclusion

In proposed technique saliency map is used as a classifier to distinguish feature of an image based on perceptibility which helps to secure imperceptibility along with robustness of an image. The experimental conclusion implies that the algorithm stand against various attacks with superior hiding capacity. Comparison of the technique with some state of the art technique recommends that projected scheme can be an efficient tool for copyright protection and authentication. Other algorithms may be used in future other than LSB replacement to increase the effectiveness of the watermarking efficiently.

## References

1. Mohanty, S.P.: Digital watermarking: a tutorial review. Report, Department of Electrical Engineering, Indian Institute of Science, Bangalore, India (1999)
2. Basu, A., et al.: Robust visual information hiding framework based on HVS pixel adaptive LSB replacement (HPALR) technique. *Int. J Imaging Robot.* **6**(A11), 71–98 (2011)
3. Itti, L., Koch, C.: A saliency-based search mechanism for overt and covert shifts of visual attention. *Vision. Res.* **40**(10–12), 1489–1506 (2000)
4. Itti, L., Koch, C.: Computational modeling of visual attention. *Nat. Rev. Neurosci.* **2**(3), 194–203 (2001)
5. Basu, A., Sarkar, S.K.: On the implementation of robust copyright protection scheme using visual attention model. *Inf. Secur. J. Global Perspect.* **22**(1), 10–20 (2013)
6. Itti, L., Koch, C., Niebur, E.: A model of saliency-based visual attention for rapid scene analysis. *IEEE Trans. Pattern Anal. Mach. Intell.* **20**(11), 1254–1259 (1998)
7. Chang, C., et al.: Finding optimal least significant-bit substitution in image hiding by dynamic programming strategy. *Pattern Recogn.* **36**, 1583–1595 (2003)
8. Huan, Xu, et al.: Near-optimal solution to pair-wise LSB matching via an immune programming strategy. *Inf. Sci.* **180**, 1201–1217 (2010)
9. Mielikainen, Jarno: LSB matching revisited. *IEEE Signal Process. Lett.* **13**(5), 285–287 (2006)
10. Yang, C.H.: Inverted pattern approach to improve image quality of information hiding by LSB substitution. *Pattern Recogn.* **41**, 2674–2683 (2008)

# Interval Goal Programming Approach to Multiobjective Programming Problems with Fuzzy Data Uncertainty

Shyamal Sen and Bijay Baran Pal

**Abstract** This paper presents interval goal programming approach for solving multiobjective programming problems with fuzzy parameter sets. In the proposed approach, the notion of interval approximation technique to fuzzy numbers is used to transform the objectives with interval parameter sets. In the model formulation, interval arithmetic is employed to convert the problem into the standard goal programming problem. In goal achievement function, both the modelling aspects in goal programming (GP), *minsum* GP and *minmax* GP are taken into account as a convex combination of them to minimize possible deviations from specified target intervals for goal achievements from optimistic point of view of decision maker (DM) in the decision situation. A numerical example is solved to illustrate the proposed approach.

**Keywords** Fuzzy number · Interval approximation · Interval arithmetic · Goal programming · Fuzzy goal programming

## 1 Introduction

The occurrence of inexact data is inherent to most of the real-world decision problems owing to imprecise nature of human judgments. Two prominent techniques, fuzzy programming (FP) and interval programming (IVP) are used to capture such uncertainty. The FP approaches [1], based on fuzzy set theory [2],

---

S. Sen (✉)

Department of Mathematics, Brahmananda Keshab Chandra College,  
Kolkata 700108, West Bengal, India  
e-mail: ssenk@yahoo.co.in

B.B. Pal

Department of Mathematics, University of Kalyani, Kalyani 741235,  
West Bengal, India  
e-mail: bbpal18@hotmail.com

© Springer India 2015

J.K. Mandal et al. (eds.), *Information Systems Design and Intelligent Applications*,  
Advances in Intelligent Systems and Computing 339,  
DOI 10.1007/978-81-322-2250-7\_45

457

concentrate on imprecise data (neither crisp nor random). Interval programming, based on interval arithmetic [3], emphasizes on intrinsic vagueness of estimated model parameters.

Now, in most of the practical decision situations, it is found that problems are with multiplicity of objectives, where objectives often conflict each other to achieve solutions by optimizing objectives in the decision environment. To resolve the crisis, GP approach [4], introduced by Charnes and Cooper to solve problems in crisp environment has been appeared as a robust tool for multiobjective decision analysis. In a fuzzy multiobjective decision environment, fuzzy goal programming (FGP) as an extension of conventional GP has been studied [5], and further extended by pal et al. [6]. Thereafter, FGP has been applied to wide range of real-life problems [7, 8] and widely circulated in the literature [9, 10].

Now, in the real-world decision situation it is to be observed that setting of the imprecise goal values and measuring of tolerance ranges for goal achievement in FGP approaches may not always be possible in a highly sensitive decision environment. To tackle such a situation, IVP [11, 12] has appeared as a flexible tool for solving decision problems with interval parameter sets.

IVP approach in the framework of GP called interval GP (IVGP) has been introduced by Inuiguchi and Kume [13] in 1991. The methodological development on IVP made in the past has been surveyed by Oliveira and Antunes [14] in 2007. However, methodological extension of interval programming is still at an early stage from the viewpoint of its use to different real-life problems.

However, in an uncertain environment, when all the model parameters are represented by sets of fuzzy numbers, the notion of  $\alpha$ -cut in fuzzy sets is used for crisp equivalent formulation of a decision problem. Here, various defuzzification operators [15, 16] are employed to solve  $\alpha$ -level multiobjective programming problem. But, the use of such a traditional approach involves a set of optimization problems, and which leads to involve huge computational load in the solution search process.

To overcome the above situation, the interval approximation approach for decision analysis has been studied [17] in the recent past. But, the constructive solution procure to solve fuzzily described multiobjective decision making (MODM) problems with crisp coefficient interval representations of model parameters is yet to be widely circulated in the literature.

In this paper, IVGP approach to fuzzily described MODM problems is introduced to make a reasonable decision for achievement of objectives within the intervals specified for optimizing them in the fuzzy environment. In the proposed approach, first the intervals within which fuzzy objective coefficients possibly take their values are determined by using the nearest interval approximation method [17] to fuzzy numbers in the decision situation. In IVGP model formulation, the structural constraint sets with fuzzy numbers are transformed into their crisp equivalents by employing the concept of magnitude of a fuzzy number [18] to solve the problem in the framework of IVGP method. In the solution process, minimization of deviational variables associated with objective goals of the formulated

IVGP model is taken into account to arrive at a decision for achievement of goals within the target interval specified for each of them in the decision environment.

Now, the basic definitions related to fuzzy set and fuzzy number are described in the next section.

## 2 Preliminaries on Fuzzy Sets

**Fuzzy Sets:** A fuzzy set  $\tilde{A}$  of a universe  $X$  (relevance in particular context) is characterized by its membership function  $\mu_{\tilde{A}} : X \rightarrow [0, 1]$  and defined as:

$$\tilde{A} = \{ (x, \mu_{\tilde{A}}(x)) \mid x \in X \}.$$

**$\alpha$ -Cut of Fuzzy Sets:**  $\alpha$ -cut of a fuzzy set  $\tilde{A}$  is a subset of  $\tilde{A}$  and defined as  $A_\alpha = \{ x : \mu_{\tilde{A}}(x) \geq \alpha \}$ , for all  $\alpha \in [0, 1]$ .

**Fuzzy Number:** A fuzzy set  $\tilde{A}$  defined on  $\mathfrak{R}$  (a set of real numbers) is said to be fuzzy number if the following conditions are satisfied

- (i)  $\tilde{A}$  is normal, that is height of  $\tilde{A}$  is unity.
- (ii)  $\tilde{A}$  is a convex set.
- (iii) the membership function  $\mu_{\tilde{A}}(x), x \in \mathfrak{R}$ , is at least piecewise continuous.

The membership function  $\mu_{\tilde{A}}(x)$  of is a continuous mapping from  $\mathfrak{R}$  to closed interval  $[0, 1]$  and presented as:

$$\mu_{\tilde{A}}(x) = \begin{cases} 0, & \text{if } x \in (\infty, a_1] \\ f_{\tilde{A}}^L(x), & \text{if } x \in [a_1, a_2] \\ 1, & \text{if } x \in [a_2, a_3] \\ f_{\tilde{A}}^R(x), & \text{if } x \in [a_3, a_4] \\ 0, & \text{if } x \in [a_4, \infty) \end{cases}$$

where  $f_{\tilde{A}}^L(x)$  is strictly increasing and  $f_{\tilde{A}}^R(x)$  a is strictly decreasing function.

If  $f_{\tilde{A}}^L(x)$  and  $f_{\tilde{A}}^R(x)$  linear, then the fuzzy number is called trapezoidal fuzzy number and denoted by  $\langle a_1, a_2, a_3, a_4 \rangle$  and has  $\alpha$ -cut  $A_\alpha = [a_1 + (a_2 - a_1)\alpha, a_4 - (a_4 - a_3)\alpha]$ . In particular, if  $a_2 = a_3$ , then trapezoidal fuzzy number is reduced to triangular fuzzy number and denoted by  $\langle a_1, a_2, a_4 \rangle$  and has  $\alpha$ -cut  $A_\alpha = [a_1 + (a_2 - a_1)\alpha, a_4 - (a_4 - a_2)\alpha]$ .

**Interval Arithmetic Operation:** Let a closed interval  $A$  (named as interval number) is defined as  $A = [a^L, a^U] = \{ a : a^L \leq a \leq a^U \}$ , where  $a^L, a^U$  left and right are limits, respectively of the interval  $A$ .

For a particular case,  $A = [a, a]$  represents only the real number  $a$ .



If  $\xi$  be a scalar then, the scalar multiplication of  $A$  is defined as:

$$\xi A = \begin{cases} [\xi a^L, \xi a^U], & \xi \geq 0 \\ [\xi a^U, \xi a^L], & \xi < 0 \end{cases}$$

The two binary operations, on the two interval numbers  $A_1$  and  $A_2$  are defined as:

$$A_1 + A_2 = [a_1^L + a_2^L, a_1^U + a_2^U]$$

$$A_1 - A_2 = [a_1^L - a_2^U, a_1^U - a_2^L]$$

**Fuzzy Arithmetic Operation:** Let  $\tilde{A}, \tilde{B}$  be two fuzzy numbers and  $\tilde{C}$  be another fuzzy number is defined as  $\tilde{C} = \tilde{A} * \tilde{B}$ . Then  $\alpha$ -cut of fuzzy number  $\tilde{C}$  can be expressed as:

$$C_\alpha = A_\alpha * B_\alpha$$

where ‘\*’ represents a binary operation.

**Interval Approximation of Fuzzy Number:** The fuzzy number can be approximated to an interval number. Uncertainties related to the parameters can be effectively handled by using a suitable approximated interval. The idea of the nearest interval approximation based on the metric ‘D’ (distance function) has been introduced by Grezegorzowski and defined as [17]:

$$N_D(\tilde{A}) = \left[ \int_0^1 A_\alpha^L d\alpha, \int_0^1 A_\alpha^U d\alpha \right]$$

where  $N_D(\tilde{A})$  represents the approximated interval of fuzzy number  $\tilde{A}$  based on the metric ‘D’.

**Ranking of Fuzzy Numbers:** Fuzzy numbers are generally not rank ordered. To establish the order relation between two fuzzy numbers, the ranking function is to be defined. The ranking function  $g : F(\mathfrak{R}) \rightarrow \mathfrak{R}$  where  $F(\mathfrak{R})$  the set of all fuzzy numbers on the real line is  $\mathfrak{R}$ , is defined as:

$$\begin{aligned} g(\tilde{A}_i) < g(\tilde{A}_j) & \text{ implies } \tilde{A}_i < \tilde{A}_j, & i \neq j \\ g(\tilde{A}_i) > g(\tilde{A}_j) & \text{ implies } \tilde{A}_i < \tilde{A}_j, & i \neq j \\ g(\tilde{A}_i) = g(\tilde{A}_j) & \text{ implies } \tilde{A}_i = \tilde{A}_j & \text{ for all } i, j \in I \end{aligned}$$

where  $\tilde{A}_i, \tilde{A}_j \in F(\mathfrak{R})$  and  $I$  is the subset of natural number and it represents the index set.

**Magnitude of a Trapezoidal fuzzy number:** A special type of ranking function, the magnitude of the trapezoidal fuzzy number  $\langle a_0, x_0, y_0, b_0 \rangle$  and defined as [18]:

$$\mathbf{mag}(\tilde{A}) = \frac{1}{2} \left( \int_0^1 (A_\alpha^L + A_\alpha^U + x_0 + y_0) f(\alpha) d\alpha \right)$$

where  $A_\alpha^L = a_0 + (x_0 - a_0)\alpha$ ,  $A_\alpha^U = b_0 - (b_0 - y_0)\alpha$  and  $f(\alpha)$  represents the weight function which is continuous and satisfies the following relations:

$$f(0) = 0, \quad f(1) = 1 \quad \text{and} \quad \int_0^1 f(\alpha) d\alpha = \frac{1}{2}.$$

For the simplicity,  $f(\alpha) = \alpha$  is taken as weight function to define the magnitude of the fuzzy number.

Now, the problem formulation is described in the Sect. 3.

### 3 Problem Formulations

The generic form of a multiobjective programming with fuzzy number involved in the objective function as well as in the constraints can be presented as:

Find  $X (x_1, x_2, \dots, x_n)$  so as to:

$$\text{Maximize} \sum_{j=1}^n \tilde{C}_{kj} x_j, \quad k = 1, 2, \dots, K.$$

so as to satisfy

$$\sum_{j=1}^n \tilde{A}_{ij} x_j \leq \tilde{B}_i, \quad i = 1, 2, \dots, m \tag{1}$$

$$X \geq 0$$

where  $X$  is the vector of decision variables, and the parameters  $\tilde{C}_{kj}$ ,  $\tilde{A}_{ij}$  and  $\tilde{B}_i$  ( $i = 1, 2, \dots, m$ ;  $j = 1, 2, \dots, n$ ) are fuzzy number.

In fuzzy linear programming, fuzzy coefficients are involved in the objective function. To optimize the objective, fuzzy objectives are to be defuzzified by using suitable defuzzification operator. Different defuzzification operators have been circulated in the literature.  $\alpha$ -cut is the widely used operator for the conversion of the objective to its crisps equivalent form. Huge computational loads are involved to solve the  $\alpha$ -level multiobjective programming problems. By using nearest interval approximation of fuzzy number [17], the objective function of the problem can be written as:

$$\begin{aligned}
 \text{Maximize } Z_k(X) &= N_D \left( \sum_{j=1}^n \tilde{C}_{kj} x_j \right) \\
 &= \sum_{j=1}^n N_D(\tilde{C}_{kj}) x_j \\
 &= \sum_{j=1}^n \left[ \int_0^1 C_{kj\alpha}^L d\alpha, \int_0^1 C_{kj\alpha}^U d\alpha \right] x_j \\
 &= \sum_{j=1}^n [c_{kj}^L, c_{kj}^U] x_j
 \end{aligned}$$

where  $[c_{kj}^L, c_{kj}^U]$  represents the nearest interval approximation of the fuzzy number  $\tilde{C}_{kj}$  and the function  $N_D(\tilde{C}_{kj})$  satisfies the linear property and where  $c_{kj}^L = \int_0^1 C_{kj\alpha}^L d\alpha$ ,  $c_{kj}^U = \int_0^1 C_{kj\alpha}^U d\alpha$ .

Now, the parameters involved in the constraints are also fuzzy numbers. It is necessary to transform the constraints into deterministic equivalent according to some point of view defined on the basis of needs and desires of the decision maker (DM). To compare the constraints from both sides with respect to the inequality relation (the symbol ‘ $\leq$ ’ only signifies the relation between the fuzzy numbers from both sides of the relation), a suitable ranking function is to be defined. Using the concept of magnitude of a fuzzy number defined in the Sect. 2, the equivalent crisp form of the constraints in (1) can be presented as [18]:

$$\mathbf{mag} \left( \sum_{j=1}^n \tilde{A}_{ij} x_j \right) \leq \mathbf{mag}(\tilde{B}_i), \quad i = 1, 2, \dots, m \tag{2}$$

where  $\mathbf{mag}(\cdot)$  represents the Magnitude of fuzzy number  $(\cdot)$ .

The interval programming problem formulation is described in the Sect. 3.1.

### 3.1 Interval Programming Problem Formulation

Using interval arithmetic defined in the Sect. 2, the crisp equivalent interval programming problem of fuzzy programming problem in (1) can be formulated as:

$$\begin{aligned}
 \text{Maximize } Z_k(X) &= \left[ \sum_{j=1}^n c_{kj}^L x_j, \sum_{j=1}^n c_{kj}^U x_j \right] \\
 &= [Z_{kL}(X), Z_{kU}(X)] \text{ (say)} \\
 \text{subject to } \sum_{j=1}^n M_{ij} x_j &\leq u_i, \quad i = 1, 2, \dots, m \\
 X &\geq 0
 \end{aligned} \tag{3}$$

where  $\mathbf{mag}(\tilde{A}_{ij}) = M_{ij}$  and  $\mathbf{mag}(\tilde{B}_i) = u_i$ .

In IVP problem, targets have to be set for achieving the objective values in the specified target intervals.

Determination of target intervals is presented in the Sect. 4.

### 4 Determination of Target Intervals

To determine the target intervals, the best and worst solutions of the defined interval valued objectives are to be obtained first.

Let, the individual best and worst solutions of the k-th objective be  $(X_k^b; T_{kU}^*)$  and  $(X_k^w; T_{kL}^*)$ , respectively,

$$\text{where } T_{kU}^* = \text{Max}_{X \in S} Z_{kU}(X), \text{ and } T_{kL}^* = \text{Min}_{X \in S} Z_{kL}(X) \tag{4}$$

where S is the feasible region bounded by the set of constraints in (3).

Now, from the viewpoint of achieving the objective values within the best and worst decisions, the target intervals can be considered as  $[t_k^L, t_k^U]$ ,

$$\text{where } T_{kL}^* \leq t_k^L < t_k^U \leq T_{kU}^*, \quad k = 1, 2, \dots, K \tag{5}$$

Then, incorporating the target intervals, interval valued objectives in (3) can be expressed as [13]:

$$Z_k(X) : [Z_{kL}(X), Z_{kU}(X)] = [t_k^L, t_k^U], \quad k = 1, 2, \dots, K \tag{6}$$

The Goal programming formulation of the problem is described in the Sect. 5.

### 5 Goal Programming Formulation

The interval valued k-th objective with target interval can be restated as:

$$[Z_{kL}(X), Z_{kU}(X)] = [t_k^L, t_k^U], \quad k = 1, 2, \dots, K \tag{7}$$

In the above formulation, it is to be mentioned that a possible solution of the problem exists if the relations

$$Z_{kL}(X) \geq t_k^L$$

$$\text{and } Z_{kU}(X) \leq t_k^U \tag{8}$$

are satisfied simultaneously.

Now, introducing under- and over-deviational variables, the goal expressions in (8) can be presented as:

$$Z_{kL}(X) + \rho_{kL}^- - \rho_{kL}^+ = t_k^L, \quad k = 1, 2, \dots, K \tag{9}$$

$$Z_{kU}(X) + \rho_{kU}^- - \rho_{kU}^+ = t_k^U, \quad k = 1, 2, \dots, K \tag{10}$$

where  $(\rho_{kL}^-, \rho_{kU}^-) \geq 0$  and  $(\rho_{kL}^+, \rho_{kU}^+) \geq 0$  represent the under- and over-deviational variables, respectively.

Now, in a decision making situation, the aim of the DM is to achieve the goal values within the specified ranges by means of minimizing the possible regrets in terms of minimizing the deviational variables involved in the decision situation.

In the field of IVGP, both the aspects of GP, *minsum* GP [6] for minimizing the sum of the weighted unwanted deviational variables as well as *minmax* GP [8] for minimizing the maximum of the deviations, are simultaneously taken into account as a convex combination of them to reach a satisfactory solution within the specified target intervals of the goals.

Then, the regret function appears as:

$$\text{Minimize } Z = \lambda \left\{ \sum_{k=1}^K w_k (\rho_{kL}^- + \rho_{kU}^+) \right\} + (1 - \lambda) \left\{ \max_k (\rho_{kL}^- + \rho_{kU}^+) \right\} \tag{11}$$

Taking  $\max_k (\rho_{kL}^- + \rho_{kU}^+) = V$ , the executable GP model of the problem can be restated as:

$$\begin{aligned} \text{Minimize } & Z = \lambda \sum_{k=1}^K w_k (\rho_{kL}^- + \rho_{kU}^+) + (1 - \lambda)V \\ \text{and satisfy } & \\ & Z_{kL}(X) + \rho_{kL}^- - \rho_{kL}^+ = t_k^L, \quad k = 1, 2, \dots, K \\ & Z_{kU}(X) + \rho_{kU}^- - \rho_{kU}^+ = t_k^U, \quad k = 1, 2, \dots, K \\ \text{subject to } & \sum_{j=1}^n M_{ij}x_j \leq u_i, \quad i = 1, 2, \dots, m \\ & \rho_{kL}^- + \rho_{kU}^+ \leq V, \quad k = 1, 2, \dots, K \\ & X \geq 0 \end{aligned} \tag{12}$$

where  $Z$  represents the regret function for goal achievement, and where  $w_k (> 0)$  with  $\sum_{k=1}^K w_k = 1$  denote the numerical weights of importance of achieving the goals within the respective target intervals, and where  $0 < \lambda < 1$ .

### 6 Illustrative Example

To illustrate the proposed approach the following example is considered.

Find  $X(x_1, x_2)$  so as to:

$$\begin{aligned}
 &\text{Maximize } Z_1(X) = \langle 1, 2, 3 \rangle x_1 + \langle 2, 4, 6 \rangle x_2 \\
 &\text{Maximize } Z_2(X) = \langle 2, 3, 4 \rangle x_1 + \langle 3.5, 5, 6.5 \rangle x_2 \\
 &\text{subject to } \langle 1, 2, 3, 4 \rangle x_1 + \langle 1, 3, 4, 7 \rangle x_2 \leq \langle 10, 11, 12, 14 \rangle \quad (13) \\
 &\qquad \qquad \langle 6, 7, 8, 9 \rangle x_1 + \langle 4, 6, 7, 8 \rangle x_2 \leq \langle 20, 22, 23, 26 \rangle \\
 &\qquad \qquad x_1, x_2 \geq 0.
 \end{aligned}$$

Using the proposed procedure defined in the Sect. 2, the approximated interval of the triangular fuzzy numbers associated with the problem are obtained as:  $N_D(\langle 1, 2, 3 \rangle) = [1.5, 2.5]$ ,  $N_D(\langle 2, 4, 6 \rangle) = [3, 5.5]$ ,  $N_D(\langle 2, 3, 4 \rangle) = [2.5, 3.5]$   $N_D(\langle 3.5, 5, 6.5 \rangle) = [4.25, 5.75]$ ;

Then, magnitudes of the trapezoidal fuzzy numbers of the parameters associated with the constraints in (13) are also obtained as:

$$(M_{11}, M_{12}, M_{21}, M_{22}) = (2.5, 3.417, 7.5, 6.583), \text{ and } (u_1, u_2) = (10.917, 22.417)$$

Using the relation in (4) the best and least solution sets are obtained as:

$$(T_{1L}^*, T_{1U}^*) = (0, 17.57), \text{ and } (T_{2L}^*, T_{2U}^*) = (0, 18.37)$$

Now, taking  $[8, 17.57]$  and  $[12, 18.37]$  as target interval for the objectives, respectively, the executable model can be presented as:

Find  $X(x_1, x_2)$  so as to:

$$\text{Minimize } \vec{Z} = \lambda \sum_{k=1}^{\vec{z}} \vec{w}_k (\vec{\rho}_{kL}^- + \vec{\rho}_{kU}^+) + (1 - \lambda)V$$

and satisfy

$$\begin{aligned}
 1.5x_1 + 3x_2 + \rho_{1L}^- - \rho_{1L}^+ &= 8 \\
 2.5x_1 + 5.5x_2 + \rho_{1U}^- - \rho_{1U}^+ &= 17.57 \\
 2.5x_1 + 4.25x_2 + \rho_{2L}^- - \rho_{2L}^+ &= 12 \\
 3.5x_1 + 5.75x_2 + \rho_{2U}^- - \rho_{2U}^+ &= 18.37 \\
 2.5x_1 + 3.417x_2 &\leq 10.917 \\
 7.5x_1 + 6.583x_2 &\leq 22.417 \\
 \rho_{1L}^- + \rho_{1U}^+ &\leq V, \\
 \rho_{2L}^- + \rho_{2U}^+ &\leq V \\
 0 < \lambda < 1
 \end{aligned}
 \tag{14}$$

For simplicity and without loss of generality, taking  $\lambda = 0.5$  and using the software (LINGO VER 6.0), solution is obtained as  $x_1 = 0, x_2 = 2.823$  with  $Z_1 = [8.47.15.52], Z_2 = [11.99, 16.23]$

*Note.* If the constraints in (13) are defuzzified by using the conventional notion of  $\alpha$ -cut of fuzzy numbers, then the constraints are obtained as:

$$\begin{aligned}
 [1 + \alpha, 4 - \alpha]x_1 + [1 + 2\alpha, 7 - 3\alpha]x_2 &\leq [10 + \alpha, 14 - 2\alpha] \\
 [6 + \alpha, 9 - \alpha]x_1 + [4 + 2\alpha, 8 - \alpha]x_2 &\leq [20 + 2\alpha, 26 - 3\alpha]
 \end{aligned}
 \tag{15}$$

Here, it may be mentioned that, for different values of  $\alpha \in [0, 1]$ , different results can be obtained in the solution search process. It is found that the optimal solution corresponds to  $\alpha = 1$ .

The optimal solution is:  $x_1 = 0, x_2 = 2.823$  with  $Z_1 = [8.47.15.52], Z_2 = [11.99, 16.23]$ , which is the same as that obtained by using the proposed method.

Therefore, it may be said that the proposed approach is computationally more efficient than the conventional method to reach decision in a fuzzy decision environment.

## 7 Conclusion

In this paper, the potential use of IVGP approach to fuzzy MODM problems is presented. The main advantage of the approach presented here is that the computational load for performing sensitivity analysis with variation of level of satisfaction for degree of achievement of fuzzy objectives does not arise in the solution search process.

The proposed method can be extended to solve fractional programming problem as well as multilevel programming problem in hierarchical decision making situations, which may be the problems in future study. However, it is hoped that the proposed method can lead to open up new areas of research for solving real-life problems in uncertain decision environment.

**Acknowledgments** Authors are thankful to the anonymous reviewers and Program Chair of the conference INDIA 2015, for their comments and suggestions to improve the quality of presentation of the paper.

## References

1. Zimmermann, H.-J.: Fuzzy programming and linear programming with several objective functions. *Fuzzy Sets Syst.* **1**, 45–55 (1978)
2. Zadeh, L.A.: The concept of linguistic variable and its application to approximate reasoning. *Inf. Sci.* **8**, 301–352 (1975)
3. Moore, R.E.: *Interval Analysis*. Prentice-Hall, New Jersey (1966)
4. Charnes, A., Cooper, W.W.: *Management Models and Industrial Applications of Linear Programming*, vol. I and II. Wiley, New York (1961)
5. Tiwari, R.N., Dharmar, S., Rao, J.R.: Fuzzy goal programming—an additive model. *Fuzzy Sets Syst.* **24**, 27–34 (1987)
6. Pal, B.B., Moitra, B.N., Maulik, U.: A goal programming procedure for fuzzy multiobjective linear fractional programming problem. *Fuzzy Sets Syst.* **139**, 395–405 (2003)
7. Biswas, A., Pal, B.B.: Application of fuzzy goal programming technique to land use planning in agricultural system. *Omega* **33**, 391–398 (2005)
8. Pal, B.B., Kumar, M., Sen, S.: A priority-based goal programming method for solving academic personnel planning problems with interval valued resource goals in university management system. *Int. J. Appl. Manage. Sci.* **4**, 284–312 (2012)
9. Mehrjerdi, Y.Z.: Solving fractional programming problem through fuzzy goal setting and aspiration. *Appl. Soft Comput.* **11**, 1735–1742 (2011)
10. Jamalnia, A., Soukhakian, M.A.: A hybrid fuzzy goal programming approach with different goal priorities to aggregate production planning. *Comput. Ind. Eng.* **56**, 1474–1486 (2009)
11. Steuer, R.E.: Algorithm for linear programming problems with interval objectives function coefficients. *Manage. Sci.* **26**, 333–348 (1981)
12. Tong, S.: Interval number and fuzzy number linear programming. *Fuzzy Sets Syst.* **66**, 301–306 (1994)
13. Inuiguchi, M., Kume, Y.: Goal programming problems with interval coefficients and target intervals. *Eur. J. Oper. Res.* **52**, 345–361 (1991)
14. Oliveira, C., Antunes, C.H.: Multiple objective linear programming models with interval coefficients—an illustrated overview. *Eur. J. Oper. Res.* **118**, 1434–1463 (2007)
15. Lu, H.W., Huang, G.H., Lin, Y.P., He, L.: A two-step infinite  $\alpha$ -cuts fuzzy linear programming method in determination of optimal allocation strategies in agricultural irrigation systems. *Water Resour. Manage.* **23**, 2249–2269 (2009)
16. Delgado, M., Verdegay, J.L., Vila, M.A.: A general model for fuzzy linear programming. *Fuzzy Sets Syst.* **29**, 21–29 (1989)
17. Grzegorzewski, P.: Nearest interval approximation of a fuzzy number. *Fuzzy Sets Syst.* **130**, 321–330 (2002)
18. Abbasbandy, S., Hajjari, T.: A new approach for ranking of trapezoidal fuzzy numbers. *Comput. Math Appl.* **57**, 413–419 (2009)



# Modeling Indian General Elections: Sentiment Analysis of Political Twitter Data

Kartik Singhal, Basant Agrawal and Namita Mittal

**Abstract** Twitter is a microblogging website where users read and write short messages on various topics every day. Political analysis using social media is getting attention of many researchers to understand the public opinion and trend especially during election time. In this paper, we propose a novel approach based on semantics and context aware rules to detect the public opinion and further predict election results. We crawled the political tweets during the general election in India, and further evaluate our proposed approach against the election results. Experimental results show the effectiveness of the proposed rules in determining the sentiment of the political tweets.

**Keywords** Sentiment analysis · Social media · Political sentiment

## 1 Introduction

Sentiment analysis is a field of natural language processing which focuses on extraction of objective and subjective information from a natural language sentence. With the boom of Online community people are expressing their likes and dislikes towards different subjects in blogs, microblogs and social networking sites like Twitter and Facebook. Analyzing these expressions of short colloquial text [1] can yield vast information about the behavior of the people that can be helpful in many

---

K. Singhal (✉)

The LNM Institute of Information Technology, Jaipur, India  
e-mail: gkkartiks@gmail.com

B. Agrawal · N. Mittal

Malaviya National Institute of Technology, Jaipur, India  
e-mail: thebasant@gmail.com

N. Mittal

e-mail: nmittal.cse@mmit.ac.in

© Springer India 2015

J.K. Mandal et al. (eds.), *Information Systems Design and Intelligent Applications*,  
Advances in Intelligent Systems and Computing 339,  
DOI 10.1007/978-81-322-2250-7\_46

other subjects like Political Science, opinion extraction and Human Computer Interaction (HCI).

With the ever emerging social media, more and more people are expressing their sentiments about current affairs on blogs, microblogs and social networking sites [2]. During the Indian general elections 2014, in the timeframe of 4 months, conversations regarding Indian elections were more than twice the conversations during whole of the 2013 and Indian twitter users also more than doubled.

Early research in this area focuses on adjectives and single word phrases to evaluate sentiments of the sentence like in [3]. An adjective with positive connotation can imply the overall sentiment for the subject positive and an adjective with negative connotation can imply the overall sentiment for the subject negative. However recent studies has showed that verbs and adverbs [4] and two word phrases [5] also contribute significantly to the overall opinion of the sentence. The whole process is depended upon usage of dictionary of words with their ranking (or polarity scores). This has been suggested in [6]. This method is also called lexicon based sentiment analysis. In this a pre-evaluated knowledge base consisting of words and their polarity scores are used like SentiWordNet [7] to determine relation of word phrases and there sentiment score based on classification into positivity and negativity of the subject that signifies the altitude of the author on that particular subject. Recent researches have shifted their focus on Rule Based sentiment analysis [8], Machine Learning approaches [9] and semantic meaning of the sentences [10]. Rule based techniques focuses on set of pre-defined rules which are when detected in a natural language sentence gives a definite output.

In this paper, we proposed an approach for detecting sentiment in political tweets based on our semantic rules. Proposed political sentiment analysis model is unsupervised which don't require any prior training dataset.

This paper organized as follows. Section 2 describes the related works. Section 3 discusses the proposed approach. Section 4 presents the results of the proposed approach with the discussion. Finally, Sect. 5 presents the conclusion.

## 2 Related Work

Previous studies [11–13] show that analyzing these sentiments and patterns can generate useful results which can be handy in determining opinions of public on elections and policies of the government. In [11], authors extract sentiments (positive, negative) as well as emotions (anger, sadness etc.) regarding the major leading party candidates and on the basis of that they calculate a distance measure. The distance measure shows the proximity of the political parties, smaller the distance higher the chances of close political connections between that parties [12] and [13] also shows how twitter data can be helpful in predicting election polls and deriving useful information about public opinions.

Existing problems in analyzing political tweets have been discussed in [14]. Sarcasm tends to reduce the accuracy of the classifier [15] shows how Sarcastic tweets in which a positive sentiment followed by an negative situation is handled. For deep analysis of the sentences, dependency parsing tool should be used which can extract relations among the words that are forming the sentence [16, 17] show the usage of Stanford Dependency Parser [18] (abbreviated from now on as SDP) in extracting these relations.

We also used categorization specified in [16] but modified them a little to suite our approach. Our categorization consists of six entities namely: Modifiers, Intensifiers, Dividers, Negations, Verbs and Objects. We believe that these entities are important as they can significantly affect sentiment of the overall sentences.

### 3 Proposed Approach

In this paper we proposed an approach for sentiment analysis of tweets. We believed in a common system which will be able to solve different problems like Sarcasm, Conjunction and Implicit negation combined. For this we proposed an unsupervised hybrid approach of Lexicon Based and Rule Based Sentiment Analysis which will analyze words related to other words, thus giving overall sentiment of the sentence. For lexicon, SentiWordNet is used which can give us the sentiment scores of a word. A negative score signifies negative connotation and a positive score signifies positive connotation of the word. Tweets were manually downloaded from a time period of 28 February 2014 to 28 March 2014. Our system follows in mainly 4 steps which are explained below.

#### 3.1 *Dependency Extraction*

We used SDP to extract rules from the tweets. The sole reason is to remove extra words that are not related to overall sentiment or contribute very less to the overall sentiment. From these rules, those that are containing verbs, adjectives, adverbs, nouns, conjunctions and negations are extracted and rest are discarded.

When analyzing twitter sentences we found out that due to wrong grammatical formations, efficiency of SDP decreases which will affect our system. When SDP is unable to detect relation between two words, it uses rule 'dep' which shows unknown dependency between those words. To improve this we used Ark twitter POS tagger (abbreviated from now on as ATP) [19]. ATP enables us to determine the part of speech of the two words thus giving us the dependency.

### 3.2 Set Distribution

We approach the problem in set wise manner. It is easier to deal with the problem when it is divided into sets. A natural language sentence is divided into 6 sets according to their part of speech and the polarity of the whole sentence is described by describing polarity of each set in relation to the other sets. Word phrases in the sets contains reference to the words of the previous sets to which they are specifically connected. This helps us in extracting features that will be vital in classifying the sentences according to the rules in next section. The functionality of each set is explained below with the help of example sentence (1).

1. ‘BJP will make good government but still will not remove corruption from India.’
  - Set W0 (Keyword Set)—Includes Subject or Objects containing Keywords Like ‘BJP’. These contain Noun or Noun + Noun. From the above sentence (1) this set will include ‘BJP’.
  - Set W1 (Verb Set)—Includes verbs which describes the action performed by the contents of Set W0 with a reference to the specific noun to which it is connected. From the above example (1), this set includes ‘make’, ‘remove’ because of the extracted rules  $nsubj(make-3, BJP-1)$  and  $nsubj(remove-10, BJP-1)$  from Fig. 1 and we will extract features ‘BJP\_make’, ‘BJP\_remove’.
  - Set W2 (Object/subject set)—Includes objects on which the Set W0 are performing actions. This set also includes Noun and Noun + Noun. From (1) this set includes ‘government’, ‘India’ because of the relations  $dojb(make-3, government-5)$ ,  $dojb(remove-10, corruption-11)$ ,  $prep\_from(remove-10, India-13)$ . We will extract features ‘make\_government’, ‘remove\_corruption’, ‘remove\_India’.
  - Set W3 (Modifier Set)—Includes adjectival and adverbial modifiers that are providing or modifying sentiments from the above sets (W0, W1, W2). From (1) this set includes ‘good’ due to the relation  $amod(government-5, good-4)$ . We will extract features from this as ‘government\_good’.

**Fig. 1** Algorithm for sentiment score calculation

```

Function sentiscore(set(sets)) Begin:
If set is W1(verb Set) then  $S_{new} = 0.0 + S_{set}$ ;
If set is W2(object set) or W3(modifier set) then
  If  $Spre \neq 0$  then  $S_{new} = Spre * \left( \frac{S_{set}}{|S_{set}|} + S_{set} \right)$ ;
  Else  $S_{new} = S_{set}$ ;
If set is W4(intensifier set) then
  If  $Spre \neq 0$  then  $S_{new} = Spre * (1 + S_{set})$ ;
If set is W6(negator set) then  $S_{new} = -S_{prev}$ ;
Return  $S_{new}$ ;
  
```

- Set W4 (Intensifier Set)—Includes adverbial intensifiers that are strengthening or weakening the sentiment scores from the Sets above. From (1) this set includes ‘still’ from the relation *advmod(remove-10, still-7)*. We will extract feature ‘remove\_still.’
- Set W5 (Buffer or Divider Set)—Includes conjunctions like ‘but’ and ‘and’ with references to two words which it is dividing. From (1) this set will include ‘but’ from the relation *conj\_but(make-3, remove-10)*. We will extract feature ‘remove\_make\_but’.
- Set W6 (Negation Set)—includes the negation words like ‘not’, ‘never’ which flips the sentiment score from the sets above. From above example (1) this will include ‘not’ because of the relation *neg(remove-10, not-9)*. We will extract feature ‘remove\_not’.

### 3.3 Context Rules Formation

We developed rules to determine the sentiment of tweets into positive and negative. These rules are presented in Table 1 and each rule is explained with example further. Polarity of the words is determined with the SentiWordNet. We used following abbreviations for the rules.

*Example:* Consider the tweet ‘AAP bhakts r always right, BJP waste time for dharnas. If u don’t trust then see it’ for the above rule. Here keyword is ‘BJP’ and set W1 includes ‘trust’ which is a positive verb in SentiWordNet and W2 includes ‘time’ and ‘waste’ both of these are minor positive and neutral nouns respectively. Notice that negator ‘don’t’ (placed in W6) is attached to trust i.e. we extract feature ‘trust\_don’t’ which will reverse the polarity of Set W1 containing ‘trust’, thus classifying in Rule 1.

**Table 1** Context rules

Rules	Set W1 Verb set	Set W2 Object/Subject set	Set W3 Adjective set	Set W4 Adverb set	Polarity
1	VB-	N+/neutral	*	*	-ve
2	VB-	N-	J-	*	+ve
3	VB+/neutral	N-	*	*	-ve
4	VB+/neutral	N+/neutral	J+/neutral	*	+ve
5	VB+/neutral	N+/neutral	J-	*	-ve
6	VB+/neutral	N+/neutral	J+	RB+	+ve
7	VB+/neutral	N+/neutral	J-	RB+	-ve
8	VB+/neutral	N+/neutral	J+	RB-	+ve
9	VB+/neutral	N+/neutral	J-	RB-	-ve

*VB* verb, *N* noun, *J* adjective, *RB* adverb, \* doesn’t matter, + positive, - negative

### 3.4 Determining Sentiment Scores

Once the rule formation occurs, sentiment scores are calculated using SentiWordNet. We used method similar to specified in [16] in calculating and distributing scores. Let *Spre* be the polarity from the previous sets with which it is connected to, *Sset* be the polarity of particular set and *Snew* be the updated polarity. Figure 1 shows the algorithm used for the sentiment score calculation.

## 4 Results

We prepared a datasets of total 259 tweets from the date of 28 February 2014 to 28 May 2014 just before the time of Indian elections to know the public trend and general opinion about the elections. Among the total tweets 116 are positive, 92 are negative and remaining 51 are objective tweets. We used accuracy as evaluation measure and it is computed by dividing the correctly classified tweets with total number of tweets. Our approach correctly predicted 76 positive tweets and 55 negative tweets. Further, we investigated manually that tweets containing colloquial language (containing Hindi words) is 56 out of which 20 were positive and 17 were negative. We removed these tweets from total tweets. Results are presented in Table 2.

Next, we tried to model elections in National Capital Territory (NCT) Delhi region. For this, we manually downloaded 106 tweets giving sentiments for the Aam Admi Party (AAP) and its party leader Arvind Kejriwal from the same time period by the users of Delhi Region. We investigated tweets with #AamAdmiParty, #AAP and #ArvindKejriwal. Results are presented in Table 3.

**Table 2** Results

Accuracy—positive tweets	$(76/96) \times 100 = 79.17 \%$
Accuracy—negative tweets	$(55/75) \times 100 = 73.33 \%$
Overall accuracy	$(131/171) \times 100 = 76.61 \%$

**Table 3** Results related to modelling elections in NCT Delhi

Number of tweets evaluated containing keyword AAP	106
Tweets containing positive sentiment towards AAP	37
Percentage of users positive about AAP	$(37/106) \times 100 = 34.91 \%$
Tweets containing negative sentiment towards AAP	51
Percentage of users negative about AAP	$(51/106) \times 100 = 48.11 \%$

### 4.1 Discussions and Comparison with Other Approaches

Above results shows that 34.91 % of users were positive towards AAP party in NCT Delhi region. From the Indian General Election results 2014 we know that all the 7 seats of Delhi region were won by Bhartiya Janta Party (BJP). Although AAP was not able to win any seat in NCT Delhi, there voting share in the elections were 32.90 % Ref. [20]. This gives us an error percentage of 6.11 %. So we were able to predict the voting share of AAP with acceptable error percentage.

We compared our proposed approach with the state-of-art approaches. Table 4 presents some cases of where other approaches fails whereas proposed approach performs better than other methods. The example tweets are chosen from the dataset according to the classification type by algorithm.

**Table 4** Handling problems in existing strategies

Type	Example tweets	Di Caro and Grella [16]	Riloff et al. [15]	Blenn et al. [1]	Tan et al. [17]	Our approach
Noun driven sentiment	If AAP comes to power, they will form worst dictators	✗	✗	✗	✓	✓
Verb driven sentiment	AAP bhakts r always right, BJP waste time for dharnas. If u don't trust then see it	✓	✓	✓	✓	✓
Adjective driven sentiment	AAP is worst in forming and managing policies	✓	✓	✓	✓	✓
Adverb driven sentiment	Kejriwal is somewhat less insane then his oppositions	✓	✓	✗	✓	✓
Conjunctions	The IT cell of AAP may be good in photoshop but lack brains in logic when they create crowd	•	•	•	•	✓
Explicit negation	AAP bhakts r always right, BJP waste time for dharnas. If u don't trust then see it	✓	✓	✓	✓	✓
Implicit negation	Meanwhile, Arvind Kejriwal opens AAP's doors to most wanted Maobadi terrorist	✗	•	✗	✗	•
Sarcasm	Wow!!! AAP couldn't be more right in forming the policies	✗	•	✗	✗	•
Sarcasm (positive negative situation)	Absolutely adore it when my bus is late	✗	✓	✗	✗	✓

✓ handled, ✗ not handled, • handled in some cases

## 5 Conclusion

People are increasingly using Social media to express their opinion. And, Twitter is a great source to investigate the public opinion especially during election time. Observing the results has led us to believe that there is a great scope in analyzing Indian political twitter data and considering its sentiment alone can result in giving a general idea about the election results. In this paper, we proposed various rules based on semantic structure of the sentence. Experimental results show the effectiveness of the proposed approach over existing methods.

## References

1. Blenn, N., Charalampidou, K., Doerr, C.: Context-sensitive sentiment classification of short colloquial text. In: Proceedings of IFIP'12, pp. 97–108, Prague, Czech Republic (2012)
2. Mittal, N., Agarwal, B., Agarwal, S., Agarwal, S., Gupta, P.: A hybrid approach for twitter sentiment analysis. In: 10th International Conference on Natural Language Processing (ICON), pp. 116–120 (2013)
3. Agarwal, B., Mittal, N.: Prominent feature extraction for review analysis: an empirical study. *J. Exp. Theor. Artif. Intell.* (2014). doi:[10.1080/0952813X.2014.977830](https://doi.org/10.1080/0952813X.2014.977830)
4. Subrahmanian, V.S., Reforgiato, D.: Ava: adjective-verb-adverb combinations for sentiment analysis. *Intell. Syst.* **23**(4), 43–50 (2008)
5. Turney, P.: Thumbs up or thumbs down? Semantic orientation applied to unsupervised classification of reviews. In: Proceedings of 40th Meeting of the Association for Computational Linguistics, pp. 417–424, Philadelphia, PA (2002)
6. Taboada, M., Brooke, J., Tofiloski, M., Voll, K., Stede, M.: Lexicon-based methods for sentiment analysis. *Comput. Linguis.* **37**(2), 267–307 (2011)
7. Esuli, A., Sebastiani, F.: SentiWordNet: a publicly available lexical resource for opinion mining. In: Proceedings of 5th International Conference on Language Resources and Evaluation (LREC), pp. 417–422 (2006)
8. Romanyshyn, M.: Rule-based sentiment analysis of ukrainian reviews. *Int. J. Artif. Intell. Appl.* **4**(4), 103–111 (2013)
9. Kessler, J.S., Nicolov, N.: Targeting sentiment expressions through supervised ranking of linguistic configurations. In: 3rd International AAAI Conference on Weblogs and Social Media (2009)
10. Bandyopadhyay, S., Mallick, K.: A new path based hybrid measure for gene ontology similarity. *IEEE/ACM Trans. Comput. Biol. Bioinform.* **11**(1), 116–127 (2014). doi:[10.1109/TCBB.2013.149](https://doi.org/10.1109/TCBB.2013.149)
11. Tumasjan, A., Sprenger, T.O., Sandner, P., Welpe, I.: Predicting elections with twitter: what 140 characters reveal about political sentiment. In: Proceedings of ICWSM (2010)
12. O'Connor, B., Balasubramanian, R., Routledge, B.R., Smith, N.A.: From tweets to polls: linking text sentiment to public opinion time series. In: ICWSM (2010)
13. Birmingham, A., Smeaton, A.F.: On using twitter to monitor political sentiment and predict election results. In: Proceedings of the Workshop on Sentiment Analysis Where AI Meets Psychology (SAAIP 2011-IJCNLP), pp. 2–10, Chiang Mai, Thailand (2011)
14. Bakliwal, A., Foster, J., Pui, J.V.D., O'Brien, R., Tounsi, L., Hughes, M.: Sentiment analysis of political tweets: towards an accurate classifier. In: Proceedings of NAACL Workshop on Language Analysis in Social Media, pp. 49–58 (2011)



15. Riloff, E., Qadir, A., Surve, P., De Silva, L., Gilbert, N., Huang, R.: Sarcasm as contrast between a positive sentiment and negative situation. In: EMNLP 2013, pp. 704–714 (2013)
16. Di Caro, L., Grella, M.: Sentiment analysis via dependency parsing. *Comput. Stan. Interfaces* (2012)
17. Tan, L.K.W., Na, J.C., Theng, Y.L., Chang, K.: Phrase-level sentiment polarity classification using rule-based typed dependencies and additional complex phrases consideration. *J. Comput. Sci. Technol.* **27**(3), 650–666 (2012)
18. De Marneffe, M., MacCartney, B., Manning, C.: Generating typed dependency parse from phrase structure parses. *LREC* (2006)
19. Gimpel, K., Schneider, N., O'Connor, B., Das, D., Mills, D., Eisenstein, J., Heilman, M., Yogatama, D., Flanigan, J., Smith, N.A.: Part-of-speech tagging for twitter: annotation, features, and experiments. In: *Proceedings of ACL* (2011)
20. [http://eci.nic.in/eci\\_main1/GE2014/PC\\_WISE\\_TURNOUT.htm](http://eci.nic.in/eci_main1/GE2014/PC_WISE_TURNOUT.htm)

# Model Based Test Case Generation and Optimization Using Intelligent Optimization Agent

Prateeva Mahali, Arup Abhinna Acharya  
and Durga Prasad Mohapatra

**Abstract** Test case optimization is one of the techniques which efficiently manage the exponential growth in time and cost of testing. But in many times the researchers compromise with the code coverage while going for optimization. In this paper, the test suite is optimized using Intelligent Optimization Agent (IOA) while the keeping the percentage of code coverage unchanged. First the System Under Test (SUT) is modelled using UML Activity Diagram (AD) and converted into an Activity Graph (AG). Then the optimized path is found out in AD by using IOA and cost attributes. Then suitable algorithms are proposed to remove the redundant nodes in the optimized path. IOA is an agent based approach as compared to Hybrid Genetic Algorithm (HGA) in Intelligent Test Optimization Agent (ITOA). The proposed approach is found to be effective when compared with other optimization techniques like Genetic Algorithm (GA) and Intelligent Test Optimization Agent (ITOA).

**Keywords** Optimization · IOA · Testing · Code coverage · UML activity diagram

## 1 Introduction

Software maintenance is a challenging and costly activity in **Software Development Life Cycle (SDLC)** [7]. Regression testing is an inherent activity during software maintenance. Regression Testing is the process of retesting of modified system or software using the old test suite to ensure that bug-fixes and functionalities introduced

---

P. Mahali (✉) · A.A. Acharya  
School of Computer Engineering, KIIT University, Bhubaneswar 751024, India  
e-mail: prateevamahali@gmail.com

A.A. Acharya  
e-mail: aacharyafcs@kiit.ac.in

D.P. Mohapatra  
Department of Computer Science Engineering, National Institute of Technology,  
Rourkela 769008, India  
e-mail: durga@nitrkl.ac.in

in the new version of software do not adversely affect the current functionality inherited from previous version [4, 7]. That means if we have a system containing test suite  $T$  and modified program  $P'$  then we have to validate  $P'$  with respect to  $T$  at the time of regression testing [8]. This process is performed due to changes in business logic or addition of new requirements or changes in the existing system. A great percentage of time and cost is spending on re-executing the test suite. Due to this reason, reduction of time and cost are the major challenges. Test case selection, minimization and prioritization [3] are some of the techniques to deal with this problem.

Test case or suite optimization means generating the test cases which should expose undetected faults within minimum time and cost. It also helps to increase the productivity and quality assurance of the system. Simultaneously it reduced testing cost and improved the cycle time. Different techniques for optimization are Genetic Algorithm (GA) [1], Particle Swarm Optimization (PSO) [2], Intelligent Search Engine (ISA) [5], Intelligent Test Case Optimization Agent (ITOA) [6], Artificial Bee Colony (ABC) algorithm etc. [9–11]. Test case or sequence optimization can also be done using Artificial Intelligence (AI) technique.

This paper discusses a model based test case optimization technique to reduce the time and cost of regression testing. Here a utility-based agent is developed called as Intelligent Optimization Agent (IOA) to get an optimized test suite without redundancy node.

The rest of the paper is organized as follows: Section 2 key out the related work done by different researcher. The proposed approach is elaborated in Sect. 3 using a case study of Shopping Mall Management System (SMMS). Section 4 explains the comparison of this approach with the related work and Sect. 5 concludes the paper with a discussion on its future trends.

## 2 Related Work

Mala and Mohan [5, 6] proposed two approaches for test sequence optimization using Intelligent Search Agent (ISA) and Intelligent Test Case Optimization Agent (ITOA). In ITOA, ISA is used for test sequence optimization and Hybrid Genetic Algorithm (HGA) is used for test case optimization. Both proposals are compared with Ant Colony Optimization (ACO) and GA respectively. The advantages of these approaches are it gives optimized test suite without redundancy node.

Mahali and Acharya [4] given a complete different approach for test case prioritization. According to the author's proposal, first the system model is converted into a graph and test cases are generated from the graph. That test cases are used for optimization using Genetic Algorithm (GA) and optimized test sequence is followed for prioritization. The prioritization is done using a priority factor which is based on the comparison of update version of system with the previous version.

The advantages of this approach is it takes less time, effort and cost for regression testing and the prioritize test sequence is much more efficient to detect faults. But it fails to give global optimum fitness value.

### 3 Proposed Approach

In this paper, we have proposed an approach for model based test case optimization using UML activity diagram and intelligent agents. At first system model is converted into an intermediate graph. Test suite optimization is done using an utility-based intelligent agent called as Intelligent Optimization Agent (IOA). Test case optimization is leading for a better test suite in regression testing with respect to time, cost and path coverage. The activities of IOA are:

1. Modulation of Software Under Test (SUT) into UML Activity Diagram (AD).
2. Conversion of AD into Activity Graph (AG) and assigning weight to every nodes and connecting edges.
3. A strategy for generating possible effective test suite and suitable criteria to stop the generation process.
4. An transition rule for addition and deletion of nodes in the execution sequence.
5. Development of optimized test suite/sequences.

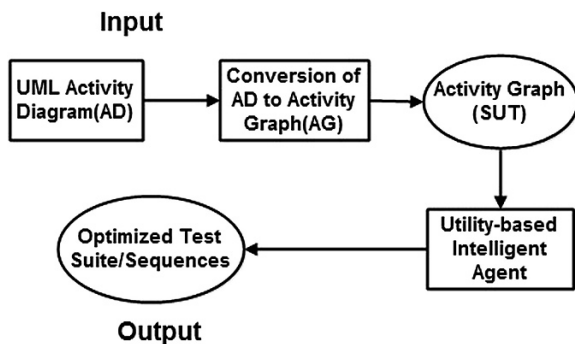
The general framework of the proposed methodology is represented in Fig. 1.

#### 3.1 Internal Design of Intelligent Optimization Agent (IOA)

The internal design of IOA is shown in Fig. 2. IOA has a sensor and state. Sensor is a software code that receives all input required for the agent like nodes, edges, credit value and cost associated with each node and edge respectively. State contains all the states in the system like present state, future state, update state etc.

The main goal of IOA is to find an optimized test sequence or path which covers all nodes of the graph only once. For that reason, first we have to find out all nodes from the directed graph i.e. referred as Software Under Test (SUT). The sensor receives all required input from the graph. Then the nodes are identified by considering the credit value, state, evolution of SUT and action of that node. In the next step, we have to keep continuous observation of each node’s reaction and take

**Fig. 1** General framework for test suite optimization using IOA



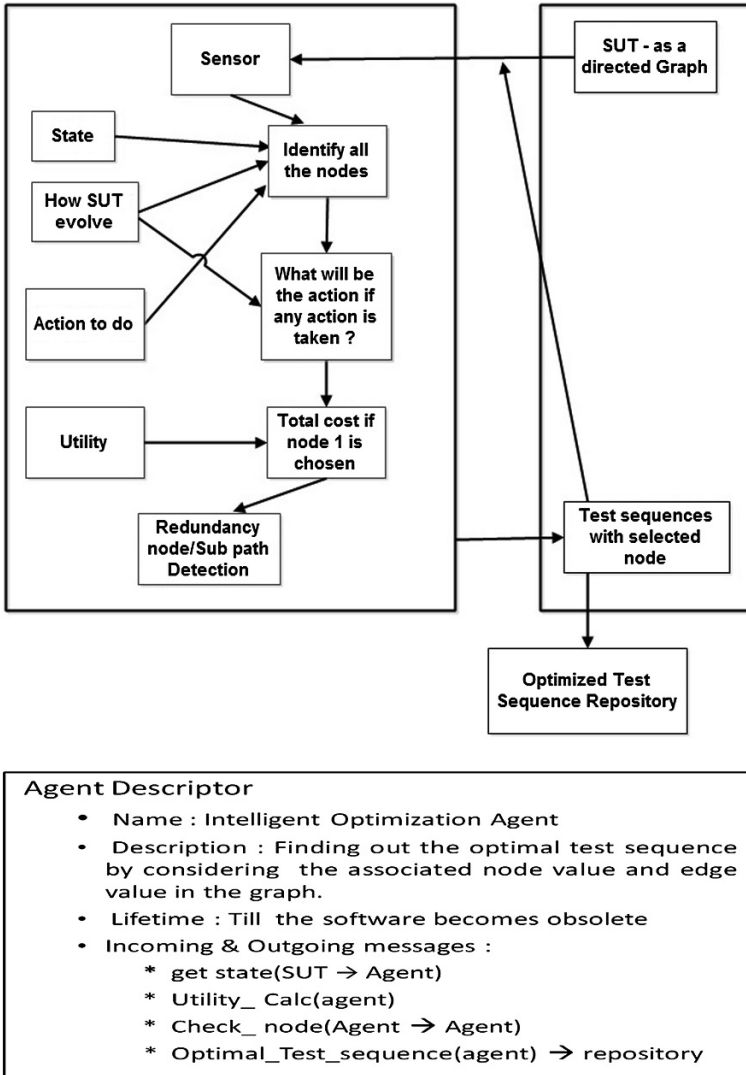


Fig. 2 Internal design of IOA with agent descriptor

decision of further action. The reaction of node may be either the total cost of that node or if there is a subpath in that node, then the total cost of that subpath. For calculating total cost of node, the utilities required to that node is calculated. After finding total cost, redundancy node or subpath is detected. After removing redundancy node/subpath, the generated test sequence is called as optimized test sequence or suite. This is the detail internal architecture and working process of IOA.

### 3.2 IOA Algorithm

Generally intelligent search algorithms are used for path finding and constraint satisfaction problems [6]. Path finding problems are used for finding individual paths from initial or starting state to final or destination state and constraint satisfaction means that path should satisfy limits or controls defined by the agent. In this proposal the goal of path finding means finding an efficient and optimized path from the graph, and constraint satisfaction means the path should not have any redundancy node or subpath which was already covered by other paths and also that path should give maximum coverage within minimum estimated cost. For that reason the algorithm (given in Algorithm 1) is called an Intelligent Optimized Agent algorithm. In order to achieve an effective and efficient optimized algorithm, we need to specify the coverage of test sequences and total integration cost to generate test sequence. This can be achieved by following steps.

1. Finding infeasible test sequences and total integration cost for each test case.
2. Detection and removal of redundancy nodes/sub-paths.
3. Evaluation of maximum path coverage within minimum integration cost.

---

**Algorithm 1** Optimal test case/test path detection algorithm

---

**Input:** SUT (Activity Graph (AG))

**Output:** Optimized test suite-

- 1: Start.
  - 2:  $CV = WN$  //Assign weight of node(WN) to credit value of node(CV ). The weights are assigned according to node type like decision node, control node, normal node etc. Here we have given maximum weight to control node.
  - 3:  $CI=WE$  //Assign weight of node(WE) to integration cost factor(CI ). CI required for joining/integrating the nodes and checking node dependency.
  - 4: Repeat Steps 5 to 8 until getting optimal path. //Optimal path means maximum path coverage of node without redundancy node/subpath.
  - 5: Calculate  $CT = CV + CI$  // CT is the total cost factor required to complete the process.
  - 6: Select the next state based on total cost factor. // State defines the changes of node.
  - 7: If there is any alternative path from the previous node to the next best node, then calculate Total cost(CT can be calculated by adding the total cost of all paths).  

$$CT = CT1 + CT2 + \dots + CTn$$
  - //Total cost factor of next node is the addition of total cost factor of all paths from previous node to next node.
  - 8: If the above path has maximum path coverage then that path is considered as optimal path & from which optimal cost can be calculated.  
 // Maximum path coverage means that path should cover maximum node in the graph.
  - 9: Generate optimized test suite T. //First test case in test suite (T) is the optimal test case.
-

Basically this algorithm describes the detail procedure for generating or detecting an optimal test suite from the directed graph. First the activity diagram is converted into a directed graph representing activities are represented as nodes and edges between two activities as edges between two nodes. Then some weights are assigned to each node and edges. Using top-down approach, total cost factor for each node is calculated by adding the weight of nodes and edges. This process is performed to generate optimal test suite. If redundancy node is present in the optimal test suite then it can be reduced by using Algorithm 2.

As per our proposal, the test case should give maximum path coverage. So a procedure can be defined to calculate path coverage of test cases present in  $T_{update}[]$ .

---

### Algorithm 2 Removal of Redundancy Test Cases

---

**Input:** Optimized test suite (T)

**Output:** Optimized test suite without redundancy node

- 1: Initialize  $R_N[] = \Phi$ . //RN stores the set of redundancy node for each test case.
  - 2: Initialize stack= $\Phi$ .
  - 3: Repeat Steps 4 to 13 until the comparison of all the test cases are not completed.
  - 4: for  $i = N_S$  to  $N_E$  do
  - 5:     //Traverse the path from the starting node and i represent the position of node  $N_S$  and  $N_E$  represent start and end node respectively.
  - 6:     Push the node into a stack and check that node is present in stack previously or not.
  - 7:     if node is already present then
  - 8:          $R_N - N$  //  $R_N$  is a array of redundancy node and N is the node.
  - 9:     else
  - 10:         move to next node.
  - 11:     end if
  - 12: end for
  - 13: Delete the test case which contain redundancy node from T.
  - 14: Update the optimized test suite(T) as  
 $T_{update} = T - T_{RN}$      //  $T_{update}$ = Updated test suite and  $TRN$  = Test case containing redundancy node.
  - 15: Calculate the path coverage and total cost factor of test cases in  $T_{update}$ .
  - 16: Display optimized test suite without redundancy node.
- 

The test case which contains maximum nodes than other test cases, is referred as optimal test case. The resultant test case gives maximum path coverage within minimum total cost and it doesn't contain any redundancy node. Now the new test suite satisfies all defined criteria of our proposed approach. For removing redundancy of subpath, we have to detect and delete the subpath in place of node.

### 3.3 Implementation of IOA Using a Case Study of Shopping Mall Management System (SMMS)

The proposed approach is discussed using a case study of Shopping Mall Management System (SMMS). Here UML Activity Diagram (AD) is used to design the system model. The AD and AG of SMMS is shown in Figs. 3 and 4 respectively. AG of SMMS contains 27 node because 27 activities are present in the AD, where node 1 is the start node and node 27 is the end node. There are one fork and join node (i.e. node 3 and node 5), five control node (i.e. 10, 16, 17, 18 and 19), two decision node (i.e. node 11 and node 22) and others are normal node.

In the next step of proposed approach, the AG of SMMS is used for Intelligent Optimization Agent (IOA) which is a utility-based intelligent agent. IOA is used to find optimized test sequences from the graph. Here each node is assign with some credit value ( $C_V$ ) with respect to importance of node. Highest priority is given to control node i.e. 6 and lowest priority is given to normal node i.e. 1. Each edge is assign with integration cost factor (CI). It can be defined as a cost factor required to integrate the activities (it may be two or more activities or subpath). For example, the integration cost factor of edge 1-2 is 1 due to integration of normal activity and less dependency, but integration cost factor of edge 26-27 is 10 due to integration

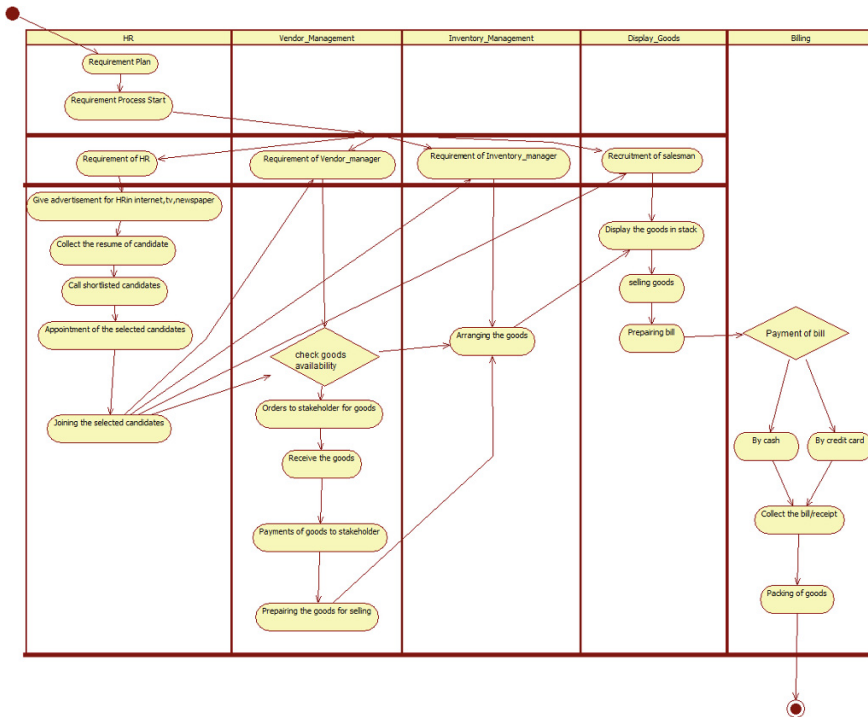
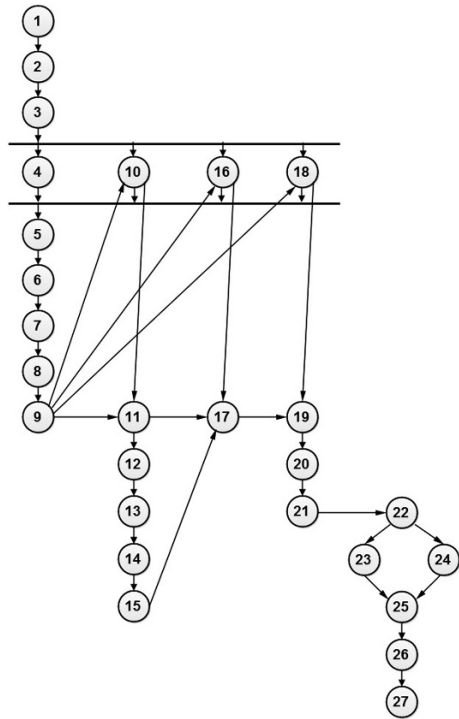


Fig. 3 AD of shopping mall management system (SMMS)



**Fig. 4** AG of shopping mall management system (SMMS)



of all activities (i.e. completion of process) and more dependency than other. The possible test cases of SMMS with the total cost factor ( $C_T$ ) is shown in Table 1. Due to limitation of space we have given only 5 test cases but it gives 38 test cases. Here the sensor receives the inputs like credit value, integration cost factor node and edge number etc.

**Table 1** Independent paths present in AG with total cost

S. No. (path)	Test case name	Independent path	Total Cost
1	T1	1 → 2 → 3 → 4 → 5 → 6 → 7 → 8 → 9 → 11 → 12 → 13 → 14 → 15 → 17 → 19 → 20 → 21 → 22 → 23 → 25 → 26 → 27	177.5
2	T2	1 → 2 → 3 → 4 → 5 → 6 → 7 → 8 → 9 → 11 → 12 → 13 → 14 → 15 → 17 → 19 → 20 → 21 → 22 → 24 → 25 → 26 → 27	177.5
3	T3	1 → 2 → 3 → 4 → 5 → 6 → 7 → 8 → 9 → 11 → 17 → 19 → 20 → 21 → 22 → 23 → 25 → 26 → 27	160.5
.	.	.	
.	.	.	
37	T37	1 → 2 → 3 → 18 → 19 → 20 → 21 → 22 → 23 → 25 → 26 → 27	103
38	T38	1 → 2 → 3 → 18 → 19 → 20 → 21 → 22 → 24 → 25 → 26 → 27	103

**Table 2** Comparison table with related work

Author name	Author’s proposed approach
Mala and Mohan [5]	Test sequence optimization is done using graph based Intelligent Search Agent (ISA). After implementation was compared with ACO
Mala and Mohan [6]	Intelligent test optimization framework includes two types of optimization i.e. test sequence and test case optimization. ISA is used for test sequence optimization and ITOA is used for test case optimization. Here HGA is used for test case optimization
Mahali and Acharya [4]	Test case prioritization was done on optimized test suite. GA is used for test case optimization and test case prioritization was done with respect to cost and time of detecting faults
Our proposed	Test suite or sequence optimization is done using a utility-based intelligent approach agent called Intelligent Optimization Agent (IOA). It gives both local and global optimum of the fitness value and test suite without redundancy node. IOA can give more efficient optimized test suite than GA and ITOA

Further the optimized test suite is generated by implementing algorithms on the test suite (T), generated from AG. This may lead to a problem i.e. redundancy of nodes in the optimal path. After applying these algorithm the optimized test sequence or suite is T5, T6, T31, T32, T11, T12, T23, T24, T1, T2, T33, T34, T25, T26, T14, T15, T7, T8, T3, T4, T19, T20, T9, T10, T21, T22, T29, T30, T37 and T38.

## 4 Comparison with Related Work

Comparison of proposed approach with the related work given in Sect. 2 is discussed in Table 2.

## 5 Conclusion and Future Work

This paper presents a novel approach for test suite optimization using Intelligent Optimization Agent (IOA). IOA is a utility-based intelligent agent which is used for test suite optimization. First the test cases/paths are generated by using optimal test case/test path detecting algorithm and stored in a repository. After completion of the process, a redundancy removing algorithm is applied to remove the redundant node/path. This will lead for reduction of testing effort and cost. Prioritization technique can be applied using concepts like slicing, fault detection capability for different programming scenario like Object Oriented Program (OOP), Aspect Oriented Program (AOP), Component Based System Development (CBSD) etc. This proposal will help us to find efficient test suite as compared to evolutionary technique.

## References

1. Alshraideh, M.A., Mahafzah, B.A., Salman, H.S.E., Salah, I.: Using genetic algorithm as test data generator for stored PL/SQL program units. *J. Softw. Eng. Appl.* **6**, 65–73 (2013)
2. de Souza, L.S., de Miranda, P.B.C., Prudencio, R.B.C., de Barros, F.A.: A multi-objective particle swarm optimization for test case selection based on functional requirements coverage and execution effort. In: 23rd IEEE International Conference on Tools with Artificial Intelligence (2011)
3. Han, X., Zeng, H., Gao, H.: A heuristic model-based test prioritization method for regression testing. In: International Symposium on Computer, Consumer and Control, pp. 886–889. IEEE (2012)
4. Mahali, P., Acharya, A.A.: Model based test case prioritization using UML activity diagram and evolutionary algorithm. *Int. J. Comput. Sci. Inform.* **3**, 42–47 (2013)
5. Mala, D., Mohan, V.: Intelligentester-software test sequence optimization using graph based intelligent search agent. In: International Conference on Computational Intelligence and Multimedia Applications, pp. 22–27 (2007)
6. Mala, D., Mohan, V.: Intelligentester-test sequence optimization framework using multi-agents. *J. Comput.* **3**(6), 39–46 (2008)
7. Mall, R.: *Fundamental of Software Engineering*. PHI Learning Private Limited, New Delhi (2009)
8. Rothermal, G., Untch, R.H., Chu, C., HarRold, M.J.: Prioritizing test cases for regression testing. *IEEE Trans. Softw. Eng.* (2001)
9. Singhal, A., Chandna, S., Bansal, A.: Optimization of test cases using genetic algorithm. *Int. J. Emerg. Technol. Adv. Eng.* **2**, 367–369 (2012)
10. Srikanth, A., Kulkarni, N.J., Naveen, K.V., Singh, P., Srivastava, P.R.: Test case optimization using artificial bee colony algorithm, pp. 570–579. Springer, Berlin (2011)
11. Suman, S.: A genetic algorithm for regression test sequence optimization. *Int. J. Adv. Res. Comput. Commun. Eng.* **1** (2012)

# Automatic Generation of Domain Specific Customized Signatures for an Enterprise Intrusion Detection System Based on Sentimental Analysis

**K.V.S.N. Rama Rao and Sudheer Kumar Battula**

**Abstract** IDS is a powerful tool in monitoring intruders. It detects the intruders based on pre defined patterns known as signatures. But in the context of an enterprise, a single IDS for the whole organization may not function effectively as there will be several business units (domains) such as HR, Finance, Marketing etc. Each business unit will have its own set of activities, business rules and security requirements. It should be possible for the personnel in these enterprise business units to enter their own security business rules. Since many of these personnel do not have expertise in writing signature to IDS, it would be convenient for them to specify the rules in Natural Language statements like English. These natural language statements should be converted to IDS signatures and are supposed to be added to signature database. In this paper, we have provided an interface to enter rules in natural language. Using Sentimental Analysis technique, we processed the natural language statements for conversion to IDS signatures. The converted signatures are added to corresponding business domain signature database. These domain specific customized signatures will certainly enhance the security of an enterprise.

**Keywords** IDS · Enterprise security · Customized signatures · Sentiment analysis · Generation of signatures

## 1 Introduction

Intrusion is an event of successfully exploiting the vulnerability of a system which results in violation of security policy. Intrusion Detection is referred as discovering and revealing such intrusions. Intrusion Detection has two dimensions. The first

---

K.V.S.N. Rama Rao (✉) · S.K. Battula  
Jawaharlal Nehru Institute of Advanced Studies (JNIAS), Hyderabad, India  
e-mail: kvsnramarao@yahoo.co.in

S.K. Battula  
e-mail: sudheer.itdict@gmail.com

K.V.S.N. Rama Rao  
Department of CSE, MLR Institute of Technology, Hyderabad, India

dimension is detection where logs, actions, audit data etc. are observed carefully. The second dimension concentrates on responding and alerting the user who is targeted. Hence an intrusion detection system (IDS) can be developed by collaborated effort of several components. A typical IDS will contain several components such as Audit data processor, knowledge base, decision engine, alarm generation and responses. An IDS having such collaborated components detects intrusion by using primarily two detection methods such as Signature Based detection and Anomaly based Detection. In this paper, we have considered signature based detection Technique for enhancing the enterprise security. Signature based Detection is also known as Misuse Detection, where known patterns of illegal behavior is maintained. These patterns are known as signatures. These signatures are used to detect similar kind of attacks subsequently. Snort [1] is an Open source IDS which maintains signatures of several malwares. A typical snort signature will be as follows:

Ex1: alert tcp *EXTERNAL\_NET*any -> *HOME\_NET* 139

Ex2: drop tcp any any -> 192.168.1.0/24 111 (content: “—00 01 86 a5—”; msg: “mounted access”);

These pre-defined set of signatures holds good for a small organization. But if we consider the case of an enterprise, a single IDS certainly cannot monitor entire organization activities effectively [2]. This is because organization consists of several business units such as HR, Finance, Marketing etc. Each business unit will have its own set of activities, business rules and security policies. For instance, HR dept will have the activities such as Hiring Process, Appraisal, Promotions, Salary determination, position classification, awards review, employees personal data, Immigration details, Health and Life Insurance details, medical reports, training details, employee benefits leaves, Role analysis etc. All these activities and data related to them should be maintained with utmost confidentiality. Hence a single IDS cannot monitor entire organization activities. Each business unit should have its own IDS, such that they can customize their security policies and rules [2, 3]. The personnel working in these business units should be able to enter the security rules. But this requires expertise in writing snort rules. Hence there should be provision for the personnel to enter business rules in a natural language like English. These natural language statements should be converted to snort rules and added to signature database. In this paper, we have addressed this challenge by processing natural language statements using sentimental analysis for converting them to IDS signatures. The remaining paper is organized as follows. In Sect. 2, we discuss about related work. In Sect. 3, we discuss about sentiment analysis technique. In Sect. 4, we present our signature generation methodology. In Sect. 5, we present the pseudo code of our methodology and results. In the last section, we briefly conclude our work.

## 2 Related Work

Yegneswaran [4] has emphasized on modular design framework and developed Nemean system for generation of signatures from honey pot traces. They have generated connection and session aware signatures. Hwang [5] developed a signature

generation scheme. They extracted the signatures from anomalies detected by integration of anomaly detection system with Snort. Newsome et al. [6] generated signatures that contain multiple disjoint content substrings. They have developed with an insight that multiple invariant strings often present in payload. Wang [7] proposed a method to identify worms initial propagation by correlating with payload alerts. This method also enables automatic signature detection. The key principle is correlating multiple alerts which give actual mitigation effect. Portokalidis et al. [8] presented Argos which tracks network data for any invalid usage. If any attack is detected, an intelligent process is run for further processing. In addition, forensic shell code is injected to gather information about attacked process. Further they have generated signatures for the exploits that are immune to payload mutations. Catania and Garino [9] has emphasized that signature based detection is still the most widely used strategy for automatic Intrusion Detection. They reviewed and analyzed several features for deploying each one of the reviewed approaches. Shabtai [10] proposed F-Sign method which analyzes the malicious executables using two approaches and the signature is extracted based on comparison with common repository. Koch [11] gave an over view of up to date security systems latest security related threats and challenges. The requirements for next generation IDS are identified.

### 3 Sentiment Analysis

A sentiment can refer to feelings such as attitudes, emotions or opinions. Sentiment analysis is also known as opinion mining that refers to extract important information from natural language processing. It aims at understanding the opinion of the writer related to an aspect. The opinion can be his judgement or what user wants to say. The main activity in sentiment analysis is to identify the polarity of the given statement i.e. whether the expressed opinion in the statement is positive or negative. For example, assume that a reviewer has expressed his opinion on a movie in an online forum. On such reviews, we can apply sentiment analysis and can determine the ratings for that movie. Sentiment analysis analyzes the statement and categorizes into two types of classes namely positive or negative. For example on a scale of ten, +10 may be assigned for most positive and -10 for most negative. The natural language statements are analyzed critically to find out how they are related to the context. For each word related to context, we assign a score i.e. each contextual word in the statement is associated with a score. Other alternative is to assign positive and negative score strength to determine the sentiment.

Sentiment analysis can be done using any of the three approaches.

- (a) Key word spotting approach involves identifying positive words and negative words in the sentence. Ex: happy, sad, bored etc.
- (b) Lexical affinity approach assigns arbitrary words an probable affinity to particular emotions.
- (c) Statistical methods use machine learning techniques such as support vector machines etc.

Gonaves et al. [12] presented comparisons of popular sentiment analysis methods in terms of coverage and agreement.

In this present study, we have proposed to perform sentimental analysis using key word spotting approach.

## 4 Signature Generation Methodology

Our signature generation methodology is described below.

Step 1: User enters the statement in the interface provided. Input is accepted in natural language.

Step 2: Apply Sentiment analysis for the accepted input as follows:

2.1 Remove the stop words such as is, that, there, the etc. from the statement. For this, we have employed a classic data set to remove the stop words. In addition, we have also taken care of the words that occur more than once.

2.2 After removal of stop words, consider the remaining words in the statement. Parse them into tokens.

2.3 Identify number of positive and number of negative tokens by spotting key words/terms. Match these Key terms with positive and negative words data set.

2.3.1 If the key term under consideration matches with positive data set, it is treated as positive. Similarly we process negative key words. If term do not match with either positive or negative dataset, we will search for synonyms of that key word, then try to judge it as positive or negative.

2.3.2 After this step, we will individually get a count of total positive and negative words.

2.4 Find the difference between identified number of positive and number of negative words.

2.5 If the difference is positive, the sentence is assigned a positive polarity otherwise negative polarity.

Step 3: Based on the polarity obtained using sentiment analysis, we categorize the class to which the snort rule belongs to. The positive class include Alert/log/pass/active prefixes and negative class include drop/reject prefixes. The actual prefix will be decided based on the statement.

Step 4: Generate the snort rule with the prefixes identified in the above step.

Step 5: Add the snort rule to the database of the respective business unit and also to the related business units.

## 5 Implementation Details and Results

The above algorithm is implemented on a Personal Computer with 2.66 GHz Central Processing Unit with Intel Core i5 2450 M CPU @ 2.50 Ghz with 1 TB Hard Disk Drive and 8 GB RAM in WINDOWS 7 Operating System with Dot Net framework and C# Environment.

The pseudo code of our implementation is presented below.

```

1: Class RuleByNLP
2: InputUser NLP Statement
3: Procedure Sentiment(input)
4: /*preprocessing */
5: Input←deletewordsrepeatingmorethanonce(input)
6: /*Associative array */
7: LEXTOKEN←tokenize(input)
8: /*BAG Of STOPWORDS */
9: for each term s ∈ STOPWORDCOLLECTION do
10:  for for each term t ∈ LETOKEN do
11:    if LEXTOKEN[t]=STOPWORDCOLLECTION[s] then
12:      /*new list*/
13:      LEXTOKEN←DeleteWord(LEXTOKEN[t],STOPWORDCOLLECTION[s])
14:    end if
15:  end for
16: end for
17: /*using wordnet */
18: for each term s ∈ POSITIVEWORDBAG do
19:  for each term t ∈ LETOKEN do
20:    if LEXTOKEN[t]= POSITIVEWORDBAG(s) then
21:      possenti←possenti+Value(POSITIVEWORDBAG(s))
22:    end if
23:  end for
24: end for
25: for each term s ∈ NEGATIVEWORDBAG do
26:  for each term t ∈ LETOKEN do
27:    if LEXTOKEN[t]= POSITIVEWORDBAG(s) then
28:      negsenti←negsenti+Value(NEGATIVEWORDBAG(s))
29:    end if
30:  end for
31: end for
32: finalnsenti←possenti-negsenti
33: if finalnsenti >= 0 then
34:  generate positive snort rules like alert log pass etc
35: else
36:  generate negative snort rules like block drop etc
37: end if

```

The figures shown below illustrates the conversion of natural language statements to snort signatures (Figs. 1, 2, 3, 4 and 5).



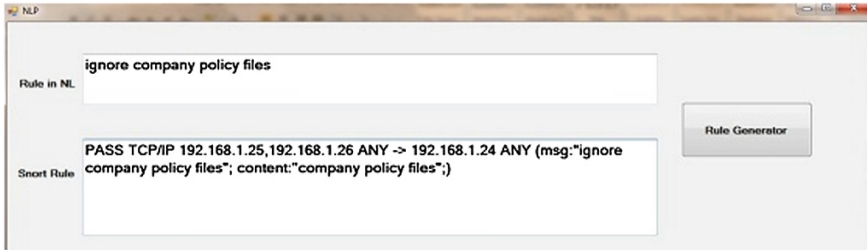


Fig. 1 Generating PASS Snort rule by NLP

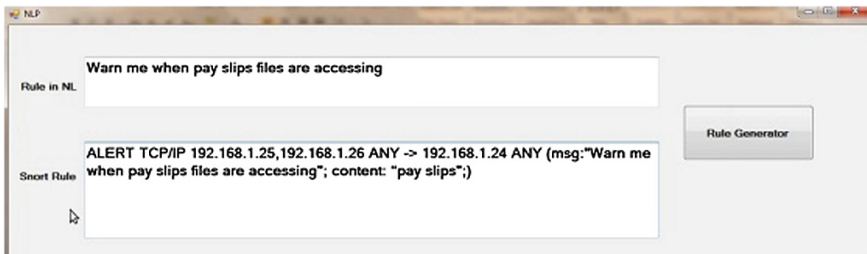


Fig. 2 Generating ALERT Snort rule by NLP



Fig. 3 Generating LOG Snort rule by NLP

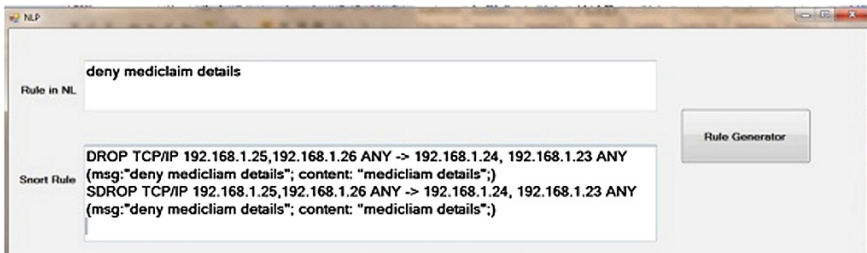


Fig. 4 Generating DROP Snort rule by NLP

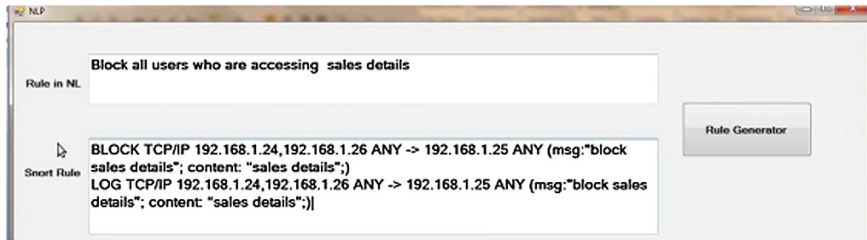


Fig. 5 Generating BLOCK Snort rule by NLP

## 6 Conclusion

Providing security for an enterprise is becoming challenging, as the attack types are increasing. It is a fact that each business unit in an enterprise will have its own activities and business rules which cannot be effectively monitored by a single IDS. Thus there is need for a customized IDS to address the needs of each business unit activities and security policies. Since many personnel in these business units are not expertised in writing snort signatures, we have provided a user interface to enter rules in natural language. These natural language statements are further processed by sentimental analysis and converted to snort signatures. The generated rules will be added to corresponding business unit database. Hence the generation of domain specific signatures will make IDS more robust because it addresses the security policies of business units of an enterprise. Our future work focuses on strengthening the signature generation in big data domain.

**Acknowledgments** We wish to acknowledge the funding for this research project (MRP-4567/14 (SERO/UGC)) from University Grants Commission-South Eastern Regional Office, Hyderabad under Minor Research Projects for the year 2013–2014.

## References

1. Snort Rules. <https://www.snort.org/>
2. McAfee network protection solutions: Next generation intrusion detection system. [http://www.mcafee.com/us/local\\_content/white\\_papers/wp\\_intruvertnextgenerationids.pdf](http://www.mcafee.com/us/local_content/white_papers/wp_intruvertnextgenerationids.pdf). Accessed on May 2009
3. Rama Rao, KVSN, Patra, M.R.: A high level service oriented architectural design for building intrusion detection systems. In: Proceedings in Communication, Network, and Computing (CNC 2010), IEEE, pp. 213–218 (June 2010)
4. Yegneswaran, V., Giffin, J.T., Barford, P., Jha, S.: An architecture for generating semantics-aware signatures. In: USENIX Security, pp. 34–43 (August 2005)
5. Hwang, K., Cai, M., Chen, Y., Qin, M.: Hybrid intrusion detection with weighted signature generation over anomalous internet episodes. *IEEE Trans. Dependable Secure Comput.* **4**(1), 41–55 (2007)

6. Newsome, J., Karp, B., Song, D.: Polygraph: automatically generating signatures for polymorphic worms. In: IEEE Symposium on Security and Privacy, pp. 226–241, IEEE 2005 (May 2005)
7. Wang, K., Cretu, G., Stolfo, S.J.: Anomalous payload-based worm detection and signature generation. In: Recent Advances in Intrusion Detection, pp. 227–246. Springer, Berlin
8. Portokalidis, G., Slowinska, A., Bos, H.: Argos: an emulator for fingerprinting zero-day attacks for advertised honeypots with automatic signature generation. In: ACM SIGOPS Operating Systems Review, vol. 40, no. 4, pp. 15–27. ACM (2006, April)
9. Catania, C.A., Garino, C.G.: Automatic network intrusion detection: current techniques and open issues. *Comput. Electr. Eng.* **38**(5), 1062–1072 (2012)
10. Shabtai, A., Menahem, E., Elovici, Y.: F-sign: automatic, function-based signature generation for malware. *Syst. Man Cybern. Part C IEEE Trans. Appl. Rev.* **41**(4), 494–508 (2011)
11. Koch, R.: Towards next-generation intrusion detection. In: 3rd International Conference on Cyber Conflict (ICCC), IEEE 2011, pp. 1–18. (June 2011)
12. Goncalves, P., Arajo, M., Benevenuto, F., Cha, M.: Comparing and combining sentiment analysis methods. In: Proceedings of the first ACM conference on Online social networks, pp. 27–38, ACM (Oct 2013)

# An Efficient Technique for Solving Fully Fuzzified Multiobjective Stochastic Programming Problems

Animesh Biswas and Arnab Kumar De

**Abstract** This paper develops a fuzzy programming technique for solving multi-objective stochastic programming problems having right side parameters associated with the system constraints follow exponential distribution. In the model formulation process the coefficients of the objectives as well as the system constraints are taken as fuzzy numbers. The variables are also considered as fuzzy variables. In the proposed solution process the probabilistic problem is first converted into an equivalent fuzzy programming model applying chance constrained programming methodology. Then using the concept of ranking function the problem is transferred into an equivalent deterministic model. The individual optimal value of each objective is found in isolation to construct the membership goals of the objectives. Finally fuzzy goal programming approach is used for achieving the best compromise solution to the extent possible in the decision making context. An illustrative numerical example is given to demonstrate the efficiency of the proposed methodology.

**Keywords** Chance constrained programming · Fuzzy random variable · Exponential distribution · Trapezoidal fuzzy number · Ranking function · Fuzzy goal programming

---

A. Biswas (✉)

Department of Mathematics, University of Kalyani, Kalyani 741235, India  
e-mail: abiswaskln@rediffmail.com

A.K. De

Department of Mathematics, Academy of Technology, G.T.Road, Adisaptagram,  
Aedconagar, Hooghly 712121, India  
e-mail: arnab7339@yahoo.co.in

© Springer India 2015

J.K. Mandal et al. (eds.), *Information Systems Design and Intelligent Applications*,  
Advances in Intelligent Systems and Computing 339,  
DOI 10.1007/978-81-322-2250-7\_49

497

## 1 Introduction

In formulation of real life decision making problems it is very much difficult by the experts to articulate the parameters of the model in a precise manner. So it is very much convenient to express those parameters in terms of fuzzy numbers. Bellman and Zadeh [1] first introduced the concept of decision making in fuzzy environment. Tanaka et al. [2] extended this concept for solving mathematical programming problems. Afterwards, Delgado et al. [3] presented a general model for solving fuzzy linear programming (FLP) problems in which constraints are involve with fuzzy inequality and the parameters of the constraints are fuzzy numbers. Rommelfanger [4] has also proposed a general model for solving FLP problems having fuzzy numbers in the coefficients of the objectives. In order to solve those types of FLP problems, different approaches have been presented by several researchers. Ganesan and Veeramani [5] discussed a method for solving FLP problems without converting them to crisp linear programming problems. In recent years, several kinds of approaches for solving fully fuzzified linear programming (FFLP) problems, all the parameters as well as the decision variables of which are expressed by fuzzy numbers are developed [6–10].

In model formulation process it is frequently observed that the occurrences of some system constraints as well as their parameters are uncertain due to conflicting nature of the objectives. Chance constrained programming (CCP) methodology is one of the most useful techniques for dealing with such type of probabilistic uncertainties. Charnes and Cooper [11, 12] first proposed CCP models. The researchers [13, 14] further extend the concept of CCP technique for solving different type of problems. With these advancement in computational resources and scientific computing techniques many complicated optimization models can now be solved efficiently.

Solving fuzzy chance constrained optimization problems has attracted more attention in recent years to the researchers. In fuzzy chance constrained programming, probabilistic and fuzzy aspects are combined together to derive an efficient model to describe real-life planning problems where uncertainty and imprecision of information co-occur. However, this kind of combination creates a great challenge for the researcher [15, 16] to find an efficient solution method for solving decision making models involving both fuzzy and stochastic terms.

Generally, ranking functions are used in the context of finding expected value of a fuzzy number. Thus selection of ranking functions for finding the expected value of fuzzy numbers is an important issue in the decision making process under fuzzy environment. The method for ranking was first proposed by Jain [17]. Later on Yager [18] proposed four indices which may be employed for the purpose of ordering fuzzy quantities in  $[0, 1]$ . In 1998 Cheng [19] developed a method for ranking fuzzy numbers using distance method. For ranking generalised trapezoidal fuzzy numbers Chen and Chen [20] proposed a method in the context of fuzzy risk analysis. Recently Kumar et al. [21] proposed a technique for ranking  $L$ - $R$  type fuzzy numbers.

Most of the problems faced by DMs are multiobjective in nature and they conflict to each other regarding optimization of objectives. To resolve such conflict, the goal programming (GP) approach was introduced by Charnes and Cooper [22] in 1961. The main drawback of classical GP is that the aspiration levels of the goals need to be specified precisely in making a decision. Also the classical GP technique cannot capture directly the uncertainty arises due to the presence of chance constraints associated with the problems. Under this context fuzzy goal programming (FGP) technique [23, 24] is used as an efficient tool for making decision in an imprecisely defined probabilistic multiobjective decision making (MODM) arena. FGP technique for solving CCP problems involving fuzzy random variables (FRVs) have been recently presented by Biswas and Modak [25, 26]. To the best of authors' knowledge an efficient solution technique for solving multiobjective fully fuzzified chance constrained programming (FFCCP) following exponential distribution from the view point of its potential use in different planning problems involving fuzzy parameters is yet to appear in the literature.

In this paper a methodology for solving multiobjective FFCCP problem is developed. The probabilistic constraints are reduced to fuzzy constraints and then deterministic constraints by applying CCP techniques and ranking function respectively. The ranking function is also applied to the objectives to convert them into crisp objectives. Then each objective is solved independently under the modified system constraints to construct the membership goals of each objective. Finally FGP model is used to achieve the most satisfactory solution for the overall benefit of the organization.

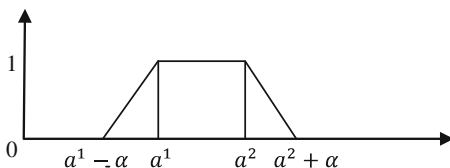
## 2 Preliminaries

In this section brief discussions are made on trapezoidal fuzzy number, ranking functions, arithmetic operations on fuzzy numbers, fuzzy random variables following exponential distribution that are used in model formulation process.

### 2.1 Trapezoidal Fuzzy Number

A fuzzy number  $\tilde{A} = (a^1, a^2, \alpha, \alpha)$  is said to be a symmetric trapezoidal fuzzy number if its membership function  $\mu_{\tilde{A}}$  can be written in the form

$$\mu_{\tilde{A}}(x) = \begin{cases} (x - a^1 + \alpha)/\alpha & \text{if } a^1 - \alpha \leq x \leq a^1 \\ 1 & \text{if } a^1 \leq x \leq a^2 \\ (a^2 + \alpha - x)/\alpha & \text{if } a^2 \leq x \leq a^2 + \alpha \\ 0 & \text{otherwise} \end{cases}$$



**Fig. 1** Trapezoidal fuzzy number

The above fuzzy number can also be expressed as  $\tilde{A} = (a^1 - \alpha, a^1, a^2, a^2 + \alpha)$ . Graphically the trapezoidal fuzzy number can be expressed as Fig. 1.

### 2.2 Ranking Function

A ranking function is a function which maps every fuzzy number into a real number. It is denoted by:  $F(\mathbb{R}) \rightarrow \mathbb{R}$ , where  $F(\mathbb{R})$  denotes the set of all fuzzy numbers defined on  $\mathbb{R}$ .

If  $\tilde{A} = (a^1 - \lambda, a^1, a^2, a^2 + \lambda)$  be a trapezoidal fuzzy number, then its ranking value is defined as [21]

$$R(\tilde{A}) = (c/2)(2a^1 - \lambda) + ((1 - c)/2)(2a^2 + \lambda) \quad 0 \leq c \leq 1$$

### 2.3 Arithmetic Operation on Trapezoidal Fuzzy Number

Let  $\tilde{A} = (a^1, a^2, \alpha, \alpha)$  and  $\tilde{B} = (b^1, b^2, \beta, \beta)$  be two symmetric trapezoidal fuzzy numbers. Then the arithmetic operations on  $\tilde{A} = (a^1, a^2, \alpha, \alpha)$  and  $\tilde{B} = (b^1, b^2, \beta, \beta)$  are defined as [5]

(i) Addition:

$$\begin{aligned} \tilde{A} + \tilde{B} &= (a^1, a^2, \alpha, \alpha) + (b^1, b^2, \beta, \beta) \\ &= (a^1 + b^1, a^2 + b^2, \alpha + \beta, \alpha + \beta) \end{aligned}$$

(ii) Multiplication:

$$\begin{aligned} \tilde{A}\tilde{B} &= (a^1, a^2, \alpha, \alpha)(b^1, b^2, \beta, \beta) = (((a^1 + a^2)/2)((b^1 + b^2)/2) - w, \\ &((a^1 + a^2)/2)(b^1 + b^2)/2 + w, |a^2\beta + b^2\alpha|, |a^2\beta + b^2\alpha|) \end{aligned}$$

where  $w = (k - h)/2$  and  $h = \min\{a^1b^1, a^1b^2, a^2b^1, a^2b^2\}$ ;  $k = \max\{a^1b^1, a^1b^2, a^2b^1, a^2b^2\}$ .

### 2.4 Fuzzy Random Variable Following Exponential Distribution

Let  $X$  be an exponentially distributed random variable. Then the density function of the random variable  $X$  is given by [26]

$$f(x; s) = s \cdot \exp(-sx), \quad 0 \leq x \leq \infty$$

In real life decision making problems, the parameters of the exponentially distributed random variable  $X$  may not be found precisely. Hence the parameters of the random variable  $X$  are considered as fuzzy numbers. Now let  $\tilde{\lambda}$  be considered as a fuzzy number, then the exponential density for the fuzzy number  $\tilde{\lambda}$  is denoted as  $f(x; \tilde{\lambda})$ . The exponential density function for fuzzily described random variable  $\tilde{X}$  is given as:

$$f(x; \tilde{\lambda}) = s \cdot \exp(-sx),$$

where the support of  $\tilde{X}$  is defined on the set of positive real numbers;  $s \in \tilde{\lambda}[\alpha]$ ;  $\tilde{\lambda}[\alpha]$  is the  $\alpha$ -cut of the fuzzy number  $\tilde{\lambda}$ . The fuzzy parameter  $1/\tilde{\lambda}$  is the mean of the random variable  $\tilde{X}$ .

### 3 Formulation of Multiobjective FFCCP Model

A multiobjective FFLP problem under a probabilistic decision making environment is presented as

Find  $\tilde{X}(\tilde{x}_1, \tilde{x}_2, \dots, \tilde{x}_n)$  so as to

$$\begin{aligned} &\text{Maximize } \tilde{Z}_k \approx \sum_{j=1}^n \tilde{c}_{kj} \tilde{x}_j; && k = 1, 2, \dots, K \\ &\text{Subject to } Pr \left( \sum_{j=1}^n \tilde{a}_{ij} \tilde{x}_j \preceq \tilde{b}_i \right) \geq 1 - \gamma_i; && i = 1, 2, \dots, m \\ & && \tilde{x}_j \succeq \tilde{0}; && j = 1, 2, \dots, n \end{aligned} \tag{1}$$

where  $\tilde{b}_i, (i = 1, 2, \dots, m)$  represents exponentially distributed FRV,  $\tilde{c}_{kj} = (c_{kj}^1, c_{kj}^2, \beta_{kj}, \beta_{kj}), \tilde{a}_{ij} = (a_{ij}^1, a_{ij}^2, d_{ij}, d_{ij}), \tilde{x}_j = (x_j^1, x_j^2, \delta_j, \delta_j) (k = 1, 2, \dots, K; j = 1, 2, \dots, n; i = 1, 2, \dots, m)$  are symmetric trapezoidal fuzzy numbers and trapezoidal fuzzy variables respectively and  $\gamma_i$  denotes any real number lies in  $[0,1]$ . Here  $\approx, \succeq, \preceq$  denotes equality, greater than or equal and less than or equal in fuzzy sense.



As  $\tilde{b}_i$  is exponentially distributed FRV, its probability density function can be expressed as

$$f\left(\tilde{b}_i; \tilde{\lambda}_i\right) = s \cdot \exp(-sb_i),$$

where the support of  $\tilde{b}_i$  is defined on the set of positive real numbers,  $s \in \tilde{\lambda}_i[\alpha]$ ;  $\tilde{\lambda}_i[\alpha]$  is the  $\alpha$ -cut of the fuzzy parameter  $\tilde{\lambda}_i$  whose support is also the set of positive real numbers. The mean and variance of the fuzzy random variable  $\tilde{b}_i$  are given by  $E(\tilde{b}_i) = \frac{1}{\lambda_i}$  and  $Var(\tilde{b}_i) = \frac{1}{\lambda_i^2}$ . The mean  $E(\tilde{b}_i)$  is also considered as symmetric trapezoidal fuzzy number which is expressed as  $E(\tilde{b}_i) = (m_i^1, m_i^2, \mu_i, \mu_i), (i = 1, 2, \dots, m)$

### 3.1 FP Model Construction

The technique for converting the multiobjective FFCCP problem into a multiobjective FLP model is discussed in this section. Applying CCP technique the constraints in the multiobjective FFLP problem (1) is transformed into the following form as

$$Pr\left(\sum_{j=1}^n \tilde{a}_{ij}\tilde{x}_j \leq \tilde{b}_i\right) \geq 1 - \gamma_i \text{ or } Pr(\tilde{A}_i \leq \tilde{b}_i) \geq 1 - \gamma_i \text{ (where } \tilde{A}_i = \sum_{j=1}^n \tilde{a}_{ij}\tilde{x}_j; i = 1, 2, \dots, m)$$

$$\text{i.e., } \left\{ \int_t^\infty s \cdot \exp(-sb_i) db_i : t \in \tilde{A}_i[\alpha], s \in \tilde{\lambda}_i[\alpha] \right\} \geq 1 - \gamma_i$$

$$\text{i.e., } \{-\exp(-sb_i)|_t^\infty\} \geq 1 - \gamma_i$$

$$\text{i.e., } t \leq -\frac{1}{s} \ln(1 - \gamma_i); i = 1, 2, \dots, m$$

Since this is true for all  $\alpha \in (0, 1]$ , then the above equation can be written as

$$\tilde{A}_i[\alpha] \leq -\frac{1}{\tilde{\lambda}_i[\alpha]} \ln(1 - \gamma_i) \tag{2}$$

Applying the first decomposition theorem on (2) it becomes

$$\tilde{A}_i \leq -\frac{1}{\tilde{\lambda}_i} \ln(1 - \gamma_i) \quad \text{i.e., } \sum_{j=1}^n \tilde{a}_{ij}\tilde{x}_j \leq -E(\tilde{b}_i) \ln(1 - \gamma_i); \quad i = 1, 2, \dots, m$$

Hence the multiobjective fully fuzzified linear programming model (2) in fuzzy environment is written as

$$\begin{aligned}
 &\text{Maximize } \tilde{Z}_k \approx \sum_{j=1}^n \tilde{c}_{kj} \tilde{x}_j; && k = 1, 2, \dots, K \\
 &\text{Subject to } \sum_{j=1}^n \tilde{a}_{ij} \tilde{x}_j \leq -E(\tilde{b}_i) \ln(1 - \gamma_i); && i = 1, 2, \dots, m \\
 &&& \tilde{x}_j \succcurlyeq \tilde{0}; && j = 1, 2, \dots, n
 \end{aligned} \tag{3}$$

### 3.2 Conversion to Deterministic Model Using Ranking Function

In this section the concept of ranking function is used to convert the FP model into a deterministic form. Using the linearity property of ranking function, the above model (3) is written as

$$\begin{aligned}
 &\text{Maximize } R(\tilde{Z}_k) = \sum_{j=1}^n R(\tilde{c}_{kj})R(\tilde{x}_j); && k = 1, 2, \dots, K \\
 &\text{Subject to } \sum_{j=1}^n R(\tilde{a}_{ij})R(\tilde{x}_j) \leq -R(E(\tilde{b}_i))\ln(1 - \gamma_i); && i = 1, 2, \dots, m \\
 &&& R(\tilde{x}_j) \geq 0; && j = 1, 2, \dots, n
 \end{aligned}$$

Considering the fuzzy numbers and fuzzy variables as trapezoidal type, the problem is expressed as

$$\begin{aligned}
 &\text{Maximize } R(\tilde{Z}_k) = \sum_{j=1}^n R\left(\left(c_{kj}^1, c_{kj}^2, \beta_{kj}, \beta_{kj}\right)\right)R((x_j^1, x_j^2, \delta_j, \delta_j)); && k = 1, 2, \dots, K \\
 &\text{Subject to } \sum_{j=1}^n R\left(\left(a_{ij}^1, a_{ij}^2, d_{ij}, d_{ij}\right)\right)R((x_j^1, x_j^2, \delta_j, \delta_j)) \leq -R((m_i^1, m_i^2, \mu_i, \mu_i))\ln(1 - \gamma_i); && i = 1, 2, \dots, m \\
 &&& R((x_j^1, x_j^2, \delta_j, \delta_j)) \geq 0; && j = 1, 2, \dots, n
 \end{aligned} \tag{4}$$

Alternatively the model can be written as

$$\begin{aligned}
 &\text{Maximize } R(\tilde{Z}_k) = \sum_{j=1}^n R\left(\left(c_{kj}^1 - \beta_{kj}, c_{kj}^1, c_{kj}^2, c_{kj}^2 + \beta_{kj}\right)\right) \\
 &&& R((x_j^1 - \delta_j, x_j^1, x_j^2, x_j^2 + \delta_j)); && k = 1, 2, \dots, K \\
 &\text{Subject to } \sum_{j=1}^n R\left(\left(a_{ij}^1 - d_{ij}, a_{ij}^1, a_{ij}^2, a_{ij}^2 + d_{ij}\right)\right)R((x_j^1 - \delta_j, x_j^1, x_j^2, x_j^2 + \delta_j)) \\
 &&& \leq -R((m_i^1 - \mu_i, m_i^1, m_i^2, m_i^2 + \mu_i))\ln(1 - \gamma_i); && i = 1, 2, \dots, m \\
 &&& R((x_j^1 - \delta_j, x_j^1, x_j^2, x_j^2 + \delta_j)) \geq 0; && j = 1, 2, \dots, n
 \end{aligned} \tag{5}$$

Using the definition of ranking function of trapezoidal fuzzy numbers, the above model (5) is rewritten as

$$\begin{aligned}
 \text{Maximize } R(\tilde{Z}_k) &= \sum_{j=1}^n \left\{ (a/2) \left( 2c_{kj}^1 - \beta_{kj} \right) + ((1-a)/2) \left( 2c_{kj}^2 + \beta_{kj} \right) \right\} \\
 &\quad \left\{ (a/2) \left( 2x_j^1 - \delta_j \right) + ((1-a)/2) \left( 2x_j^2 + \delta_j \right) \right\} \quad k = 1, 2, \dots, K \\
 \text{Subject to } \sum_{j=1}^n &\left\{ (a/2) \left( 2a_{ij}^1 - d_{ij} \right) + ((1-a)/2) \left( 2a_{ij}^2 + d_{ij} \right) \right\} \\
 &\quad \left\{ (a/2) \left( 2x_j^1 - \delta_j \right) + ((1-a)/2) \left( 2x_j^2 + \delta_j \right) \right\} \\
 &\leq \left\{ (a/2) \left( 2m_i^1 - \mu_i \right) + ((1-a)/2) \left( 2m_i^2 + \mu_i \right) \right\}; \quad i = 1, 2, \dots, m \\
 &\quad \left\{ (a/2) \left( 2x_j^1 - \delta_j \right) + ((1-a)/2) \left( 2x_j^2 + \delta_j \right) \right\} \geq 0; \\
 &\quad j = 1, 2, \dots, n, \quad x_j^1 \leq x_j^2, \quad 0 \leq a \leq 1
 \end{aligned} \tag{6}$$

Let  $[\tilde{x}_k^b; R(\tilde{Z}_k)^b] = [(\tilde{x}_{k1}^b, \tilde{x}_{k2}^b, \dots, \tilde{x}_{kn}^b); R(\tilde{Z}_k)^b]$  ( $k = 1, 2, \dots, K$ ) be the best values of the  $k$ th objective obtained by solving each objective independently under the derived set of system constraints. The worst values,  $R(\tilde{Z}_k)^w$  ( $k = 1, 2, \dots, K$ ), of the  $k$ th objective is calculated as

$$R(\tilde{Z}_k)^w = \min \{ R(\tilde{Z}_k) |_{(\tilde{x}_{l1}^b, \tilde{x}_{l2}^b, \dots, \tilde{x}_{ln}^b)}; l = 1, 2, \dots, k : l \neq k \}$$

Hence the fuzzy goal for each objective is expressed as

$$R(\tilde{Z}_k) \succeq R(\tilde{Z}_k)^b; \quad k = 1, 2, \dots, K \tag{7}$$

Thus the membership function for each of the objectives can be written as

$$\mu_{R(\tilde{Z}_k)} = \begin{cases} 0 & \text{if } R(\tilde{Z}_k) \leq R(\tilde{Z}_k)^w \\ (R(\tilde{Z}_k) - R(\tilde{Z}_k)^w) / (R(\tilde{Z}_k)^b - R(\tilde{Z}_k)^w) & \text{if } R(\tilde{Z}_k)^w \leq R(\tilde{Z}_k) \leq R(\tilde{Z}_k)^b \\ 1 & \text{if } R(\tilde{Z}_k) \geq R(\tilde{Z}_k)^b \end{cases} \tag{8}$$

On the basis of above defined membership functions, the FGP model has been framed in the next section.

### 4 Weighted FGP Model Construction

In weighted FGP model formulation process, the membership functions are first converted into flexible membership goals by introducing under- and over- deviational variables to each of them and thereby assigning the highest membership value (unity) as the aspiration level to each of them. Also it is evident that full achievement of all the membership goals is not possible in a MODM context. So the under-deviational variables are minimized to achieve the goal values of objectives in the decision making environment.

Thus a weighted FGP model is formulated as

Find  $\tilde{X}(\tilde{x}_1, \tilde{x}_2, \dots, \tilde{x}_n)$  so as to

$$\text{Minimize } D = \sum_{k=1}^K w_k d_k^-$$

$$\text{Subject to } \mu_{R(\tilde{z}_k)} + d_k^- - d_k^+ = 1; \quad k = 1, 2, \dots, K$$

$$\sum_{j=1}^n \left\{ (a/2) (2a_{ij}^1 - d_{ij}) + ((1-a)/2) (2a_{ij}^2 + d_{ij}) \right\}$$

$$\left\{ (a/2) (2x_j^1 - \delta_j) + ((1-a)/2) (2x_j^2 + \delta_j) \right\}$$

$$\leq \left\{ (a/2) (2m_i^1 - \mu_i) + ((1-a)/2) (2m_i^2 + \mu_i) \right\}; \quad i = 1, 2, \dots, m$$

$$\left\{ (a/2) (2x_j^1 - \delta_j) + ((1-a)/2) (2x_j^2 + \delta_j) \right\} \geq 0; \quad j = 1, 2, \dots, n, x_j^1 \leq x_j^2, \quad 0 \leq a \leq 1$$
(9)

where  $w_k \geq 0$  represents the numerical weights of the goals which are determined as:

$$w_k = \frac{P}{(R(\tilde{Z}_k)^b - R(\tilde{Z}_k)^w)} \quad k = 1, 2, \dots, K; \quad P > 0$$
(10)

The developed model (9) is solved to find the most satisfactory solution in the decision making environment.

### 5 Numerical Example

To illustrate the efficiency of the proposed approach, the following numerical example with exponentially distributed fuzzy random variable is considered.

$$\begin{aligned}
 &\text{Maximize } \tilde{Z}_1 \approx \tilde{3}\tilde{x}_1 + \tilde{7}\tilde{x}_2 \\
 &\text{Maximize } \tilde{Z}_2 \approx \tilde{7}\tilde{x}_1 + \tilde{5}\tilde{x}_2 \\
 &\text{Subject to } \Pr(\tilde{1}\tilde{x}_1 + \tilde{1}\tilde{x}_2 \preceq \tilde{b}_1) \geq 0.36 \\
 &\Pr(\tilde{4}\tilde{x}_1 + \tilde{3}\tilde{x}_2 \preceq \tilde{b}_2) \geq 0.33 \\
 &\Pr(\tilde{2}\tilde{x}_1 + \tilde{5}\tilde{x}_2 \preceq \tilde{b}_3) \geq 0.30 \\
 &\tilde{x}_1, \tilde{x}_2 \succeq \tilde{0}
 \end{aligned}
 \tag{11}$$

Here the coefficients of the objectives as well as system constraints are considered with the following form as

$$\begin{aligned}
 \tilde{7} &= (5, 6, 7, 8); \tilde{5} = (1, 3, 5, 7); \tilde{3} = (1, 2, 5, 6) \\
 \tilde{7} &= (3, 5, 8, 10); \tilde{1} = (0.3, 0.5, 1.5, 1.7); \tilde{2} = (0.5, 1, 4, 4.5); \tilde{4} = (1, 2, 6, 7)
 \end{aligned}$$

The mean of exponentially distributed fuzzy random variables are taken as

$$E(\tilde{b}_1) = \tilde{7} = (3, 5, 7, 9); E(\tilde{b}_2) = \tilde{9} = (4, 7, 10, 13); E(\tilde{b}_3) = \tilde{8} = (3, 6, 9, 12)$$

Also the variables are expressed as

$$\tilde{x}_1 = (x_1^1 - \delta_1, x_1^1, x_1^2, x_1^2 + \delta_1); \tilde{x}_2 = (x_2^1 - \delta_2, x_2^1, x_2^2, x_2^2 + \delta_2)$$

Using the CCP technique and ranking function as described in the model formulation the above model (11) takes the following form

$$\begin{aligned}
 \text{Maximize } R(\tilde{Z}_1) &= (2.75 - 2a)(a(2x_1^1 - \delta_1) + (1 - a)(2x_1^2 + \delta_1)) \\
 &\quad + (2.25 - 1.25a)(a(2x_2^1 - \delta_2) + (1 - a)(2x_2^2 + \delta_2))
 \end{aligned}$$

$$\begin{aligned}
 \text{Maximize } R(\tilde{Z}_2) &= (3.75 - a)(a(2x_1^1 - \delta_1) + (1 - a)(2x_1^2 + \delta_1)) \\
 &\quad + (3 - 2a)(a(2x_2^1 - \delta_2) + (1 - a)(2x_2^2 + \delta_2))
 \end{aligned}$$

Subject to

$$\begin{aligned}
 &(0.8 - 0.6a)(a(2x_1^1 - \delta_1) + (1 - a)(2x_1^2 + \delta_1)) \\
 &\quad + (0.8 - 0.6a)(a(2x_2^1 - \delta_2) + (1 - a)(2x_2^2 + \delta_2)) \leq (4.08 - 2.04a)
 \end{aligned}
 \tag{12}$$

$$\begin{aligned}
 &(3.25 - 2.5a)(a(2x_1^1 - \delta_1) + (1 - a)(2x_1^2 + \delta_1)) \\
 &\quad + (2.75 - 2a)(a(2x_2^1 - \delta_2) + (1 - a)(2x_2^2 + \delta_2)) \leq (6.38 - 3.33a)
 \end{aligned}$$

$$\begin{aligned}
 &(2.12 - 1.75a)(a(2x_1^1 - \delta_1) + (1 - a)(2x_1^2 + \delta_1)) \\
 &\quad + (3 - 2a)(a(2x_2^1 - \delta_2) + (1 - a)(2x_2^2 + \delta_2)) \leq (6.30 - 3.6a)
 \end{aligned}$$

$$(a(2x_1^1 - \delta_1) + (1 - a)(2x_1^2 + \delta_1)) \geq 0$$

$$(a(2x_2^1 - \delta_2) + (1 - a)(2x_2^2 + \delta_2)) \geq 0$$

$$x_1^1 \leq x_1^2; \quad x_2^1 \leq x_2^2; \quad 0 \leq a \leq 1$$

Now each objective is solved independently with respect to the system constraints as described in (12) to find the best values of each objective. The solutions are obtained as

$$[\tilde{x}_{11}^b, \tilde{x}_{12}^b; R(\tilde{Z}_1)^b] = [\tilde{0}, \tilde{2.1}; 18.9] \quad \text{and} \quad [\tilde{x}_{21}^b, \tilde{x}_{22}^b; R(\tilde{Z}_2)^b] = [\tilde{1.96}, \tilde{0}; 14.72]$$

The worst values of the objective are found as  $R(\tilde{Z}_1)^w = 10.78$  and  $R(\tilde{Z}_2)^w = 12.6$ .

From the achieved optimal solutions of the individual objectives the membership goals are found as

$$R(\tilde{Z}_1) \succcurlyeq 18.9 \quad \text{and} \quad R(\tilde{Z}_2) \succcurlyeq 14.72$$

On the basis of the derived aspiration levels of the fuzzy goals, the following membership functions of each of the objectives are derived as

$$\mu_{R(\tilde{Z}_1)} = 0.12R(\tilde{Z}_1) - 1.33 \quad \text{and} \quad \mu_{R(\tilde{Z}_2)} = 0.47R(\tilde{Z}_2) - 5.94.$$

Hence the FGP model is presented by converting the elicited membership functions into membership goals as

Find  $\tilde{X}(\tilde{x}_1, \tilde{x}_2)$  so as to

$$\text{Minimize } D = 0.08d_1^- + 0.12d_2^-$$

$$\text{So as to } 0.12R(\tilde{Z}_1) + d_1^- - d_1^+ = 2.33$$

$$0.47R(\tilde{Z}_2) + d_2^- - d_2^+ = 6.94$$

Subject to

$$\begin{aligned} &(0.8 - 0.6a)(a(2x_1^1 - \delta_1) + (1 - a)(2x_1^2 + \delta_1)) \\ &\quad + (0.8 - 0.6a)(a(2x_2^1 - \delta_2) + (1 - a)(2x_2^2 + \delta_2)) \leq (4.08 - 2.04a) \\ &(3.25 - 2.5a)(a(2x_1^1 - \delta_1) + (1 - a)(2x_1^2 + \delta_1)) \end{aligned} \tag{13}$$

$$\quad + (2.75 - 2a)(a(2x_2^1 - \delta_2) + (1 - a)(2x_2^2 + \delta_2)) \leq (6.38 - 3.33a)$$

$$(2.12 - 1.75a)(a(2x_1^1 - \delta_1) + (1 - a)(2x_1^2 + \delta_1))$$

$$\quad + (3 - 2a)(a(2x_2^1 - \delta_2) + (1 - a)(2x_2^2 + \delta_2)) \leq (6.30 - 3.6a)$$

$$(a(2x_1^1 - \delta_1) + (1 - a)(2x_1^2 + \delta_1)) \geq 0$$

$$(a(2x_2^1 - \delta_2) + (1 - a)(2x_2^2 + \delta_2)) \geq 0$$

$$x_1^1 \leq x_1^2; \quad x_2^1 \leq x_2^2; \quad 0 \leq a \leq 1$$

The software LINGO (Ver. 11.0) is used to solve the problem.

The optimal solution of the problem is obtained as

$$\tilde{x}_1 = (-0.62, 0.065, 0.12, 0.80) \text{ and } \tilde{x}_2 = (-0.55, 0, 1.50, 2.05)$$

The achieved objective values of the given problem is found as  $\tilde{Z}_1 = (-11.96, -1.04, 11.43, 22.35)$  with the ranking value  $R(\tilde{Z}_1) = 16.89$  and  $\tilde{Z}_2 = (-11.02, -0.39, 7.55, 18.18)$  with the ranking value  $R(\tilde{Z}_2) = 14.1$ .

The membership value of each objective is found as  $\mu_{R(\tilde{Z}_1)} = 0.75$  and  $\mu_{R(\tilde{Z}_2)} = 0.71$ .

## 6 Conclusions

This article introduces a new methodology for solving FFMOCPP involving exponentially distributed FRV's. The methodology includes both types of uncertainties like fuzziness and randomness simultaneously. The decision variables are also considered as fuzzy variables. Based on FGP a compromise decision of the multiobjective problem is achieved. The proposed procedure can be extended to solve quadratic fuzzy multiobjective programming problem. The proposed methodology can be applied to different real life problems for obtaining most satisfactory solution in a hierarchical decision making environment. However it is hoped that the proposed methodology may open up new vistas into the way of making decision in a fuzzily defined probabilistic decision making arena.

**Acknowledgments** The authors are thankful to the anonymous reviewers for their valuable comments and suggestions in improving the quality of the paper.

## References

1. Bellman, R.E., Zadeh, L.A.: Decision making in a fuzzy environment. *Manage. Sci.* **17**, 141–164 (1970)
2. Tanaka, H., Okuda, T., Asai, K.: On fuzzy mathematical programming. *J. Cybern. Syst.* **3**, 37–46 (1973)
3. Delgado, M., Verdegay, J.L., Vila, M.A.: A general model for fuzzy linear programming. *Fuzzy sets Syst.* **29**, 21–29 (1989)
4. Rommelfanger, H.: Fuzzy linear programming and applications. *Eur. J. Oper. Res.* **92**, 512–527 (1996)
5. Ganesan, K., Veeramani, P.: Fuzzy linear programs with trapezoidal fuzzy numbers. *Ann. Oper. Res.* **143**, 305–315 (2006)
6. Hashemi, S.M., Modarres, M., Nasrabadi, E., Nasrabadi, M.M.: Fully fuzzified linear programming, solution and duality. *J. Intell. Fuzzy Syst.* **17**, 253–261 (2006)
7. Allahviranloo, T., Lotfi, F.H., Kiasary, M.K., Kiani, N.A., Alizadeh, L.: Solving fully fuzzy linear programming problem by the ranking function. *Appl. Math. Sci.* **2**, 19–32 (2008)

8. Lotfi, F.H., Allahyiranloo, T., Jondabeh, M.A., Alizadeh, L.: Solving a full fuzzy linear programming using lexicography method and fuzzy approximate solution. *Appl. Math. Model.* **35**, 3151–3156 (2009)
9. Kumar, A., Kaur, J., Singh, P.: A new method for solving fully fuzzy linear programming problems. *Appl. Math. Model.* **35**, 817–823 (2011)
10. Guo, X., Shang, D.: Fuzzy approximate solution of positive fully fuzzy linear matrix equations. *J. Appl. Math.* **2013**, 7 (2013)
11. Charnes, A., Cooper, W.W.: Chance-constrained programming. *Manage. Sci.* **6**, 73–79 (1962)
12. Charnes, A., Cooper, W.W.: Deterministic equivalents for optimizing and satisfying under chance constraints. *Oper. Res.* **11**, 18–39 (1963)
13. Kataoka, S.: A stochastic programming model. *Econometrica* **31**, 181–196 (1963)
14. Geoffrion, A.M.: Stochastic programming with aspiration or fractile criteria. *Manage. Sci.* **13**, 672–679 (1967)
15. Iskander, M.G.: Exponential membership function in stochastic fuzzy goal programming. *Appl. Math. Comput.* **173**, 782–791 (2006)
16. Liu, B.: Fuzzy random chance-constrained programming. *IEEE Trans. Fuzzy Syst.* **9**, 713–720 (2001)
17. Jain, R.: Decision-making in the presence of fuzzy variables. *IEEE Trans. Syst. Man Cybern.* **6**, 698–703 (1976)
18. Yager, R.R.: A procedure for ordering fuzzy subsets of the unit interval. *Inf. Sci.* **55**, 2033–2042 (1981)
19. Cheng, C.H.: A new approach for ranking fuzzy numbers by distance method. *Fuzzy Sets Syst.* **95**, 307–317 (1998)
20. Chen, S.J., Chen, S.M.: Fuzzy risk analysis based on the ranking of generalized trapezoidal fuzzy numbers. *Appl. Intell.* **26**, 1–11 (2007)
21. Kumar, A., Singh, P., Kaur, P., Kaur, A.: A new approach for ranking of *L-R* type generalized fuzzy numbers. *Expert Syst. Appl.* **38**, 10906–10910 (2011)
22. Charnes, A., Cooper, W.W.: Goal programming and multiple objective optimizations. *Euro. J. Opl. Res.* **1**, 39–54 (1977)
23. Hannan, E.L.: Linear programming with multiple fuzzy goals. *Fuzzy Sets Syst.* **6**, 235–248 (1980)
24. Narasimhan, R.: On fuzzy goal programming—some comments. *Dec. Sci.* **11**, 532–538 (1980)
25. Biswas, A., Modak, N.: A fuzzy goal programming method for solving chance constrained programming with fuzzy parameters. *Comm. Comp. Inform. Sci.* **140**, 187–196 (2011)
26. Biswas, A., Modak, N.: Using fuzzy goal programming technique to solve multiobjective chance constrained programming problems in a fuzzy environment. *Int. J. Fuzzy Syst. Appl.* **2**, 71–80 (2012)



# Errata to: $L(4, 3, 2, 1)$ -Labeling for Simple Graphs

Soumen Atta and Priya Ranjan Sinha Mahapatra

## Errata to:

Chapter 50 in: J.K. Mandal et al. (eds.), *Information Systems Design and Intelligent Applications, Advances in Intelligent Systems and Computing 339*, DOI [10.1007/978-81-322-2250-7\\_50](https://doi.org/10.1007/978-81-322-2250-7_50)

- Page: 512. The following sentence is required to be added at the end of paragraph 1 in Sect. 1.  
“Some results of simple graphs with  $L(4, 3, 2, 1)$  labeling can be found in [9]”.
- Page: 513. “**Theorem 1**” should be read as “**Theorem 1** [6]”.
- Page: 514. “**Theorem 2**” should be read as “**Theorem 2** [6]”.
- Page: 515. The **Lemma 1** along with its proof in Sect. 3.3 should be read as:

**Lemma 1** For a path  $P_n$  on  $n$  vertices with  $n \geq 7$ , the minimal  $L(4, 3, 2, 1)$ -labeling number  $\lambda(P_n)$  is at most 13.

---

The online version of the original chapter can be found under DOI [10.1007/978-81-322-2250-7\\_50](https://doi.org/10.1007/978-81-322-2250-7_50)

---

S. Atta (✉) · P.R.S. Mahapatra  
Department of Computer Science and Engineering, University of Kalyani, Nadia,  
West Bengal, India  
e-mail: soumen.atta@klyuniv.ac.in

P.R.S. Mahapatra  
e-mail: priya@klyuniv.ac.in

*Proof* A labeling pattern  $\{f(v_1), f(v_2), \dots, f(v_7)\} = \{5, 9, 13, 3, 7, 11, 1\}$  exists for  $n = 7$ . Hence the lemma follows.  $\square$

Page: 515. The Theorem 3 and its proof for Case-IV and Case-V in Sect. 3.3 should be read as:

**Theorem 3** For a path,  $P_n$  on  $n$  vertices, the minimal  $L(4, 3, 2, 1)$ -labeling number  $\lambda(P_n)$  is

$$\lambda(P_n) = \begin{cases} 1 & \text{if } n = 1 \\ 5 & \text{if } n = 2 \\ 8 & \text{if } n = 3 \\ 9 & \text{if } n = 4 \\ 11 & \text{if } n = 5, 6, 7 \end{cases}$$

*Proof*

Case-IV:  $n = 4$ :

The labeling pattern  $\{6, 1, 9, 4\}$  shows that  $\lambda(P_n) \leq 9$  if  $n = 4$ . Let  $V(P_n) = \{v_1, v_2, v_3, v_4\}$ .  $V(P_n)$  has two vertices of degree 2 and other two vertices of degree 1. If either  $f(v_2)$  or  $f(v_3)$  is 1 then either  $f(v_4)$  or  $f(v_1)$  will be at least 12, which is a contradiction. Similar contradiction will arrive if either  $f(v_1)$  or  $f(v_4)$  is set to 1.

Case-V:  $n = 5, 6, 7$ :

Since  $\exists$  a labeling  $\{8, 3, 11, 6, 1, 9, 4\}$ , we can assume that  $\lambda(P_n) \leq 11$  for  $n = 5, 6, 7$ . Let  $f(v_i) = 1$  and either  $v_{i+1}, v_{i+2}$  or  $v_{i-1}, v_{i-2}$  exist. Now  $\lambda(P_3) = 8$  implies that  $f(v_{i+1})$  is either 5, 6, 7 or 8. For  $L(3, 2, 1)$ -labeling [6], note that the possibilities for  $f(v_{i+1})$  is either 5, 6, 7 or 8. Therefore, the similar approach in [6] can be used to handle this case.  $\square$

- Page: 517. The **Claim 1** is not correct and hence the last line of the “**Abstract**” should be read as “This paper also presents an  $L(4, 3, 2, 1)$ -labeling algorithm for path.”

## Reference

9. Sweetly, R.: A study on radio labeling and related concepts in graphs. PhD thesis, Manonmaniam Sundaranar University (2011)

$$|f(x) - f(y)| \geq \begin{cases} 4, & \text{if } d(x, y) = 1 \\ 3, & \text{if } d(x, y) = 2 \\ 2, & \text{if } d(x, y) = 3 \\ 1, & \text{if } d(x, y) = 4. \end{cases}$$

The  $L(4, 3, 2, 1)$ -labeling number  $\lambda(G)$  of a graph  $G$  is the smallest number  $\lambda \in \mathbb{N}$  such that  $G$  has an  $L(4, 3, 2, 1)$ -labeling with  $\lambda$  as its maximum label. An  $L(4, 3, 2, 1)$ -labeling of a graph  $G$  is said to be a minimal  $L(4, 3, 2, 1)$ -labeling of  $G$  if the highest label used in any vertex of  $G$  is  $\lambda$ . An  $L(4, 3, 2, 1)$ -labeling of a graph  $G$  with  $\lambda$  as its maximum label is often denoted as  $\lambda$ - $L(4, 3, 2, 1)$ -labeling.

**Definition 2** A simple connected graph  $G = (V, E)$  with  $|V| = n$  is said to be complete graph if  $\forall x, y \in V, (x, y) \in E$ , i.e. every pair of vertices of the graph are adjacent to each other. This graph is denoted as  $K_n$  [8].

**Definition 3** A simple connected graph  $G = (V, E)$  is said to be a complete bipartite graph if there exists two sets  $A$  and  $B$  such that (i)  $A \cup B = V$  and  $A \cap B = \phi$  with  $|A| = m, |B| = n$  and  $|V| = m + n$ , (ii)  $\forall a_i, a_j \in A, (a_i, a_j) \notin E$  and  $\forall b_i, b_j \in B, (b_i, b_j) \notin E$ , (iii)  $\forall a_i \in A$  and  $b_j \in B, (a_i, b_j) \in E$ . This graph is denoted as  $K_{m,n}$  [8].

**Definition 4** A star graph can be defined as a  $K_{1,n}$  complete bipartite graph. It is generally denoted as  $S_n$  [8].

**Definition 5** A graph  $G = (V, E)$  is said to be a path if  $(v_i, v_{i+1}) \in E, 1 \leq i < n$  where  $|V| = n$  and it is denoted as  $P_n$  [8].

**Definition 6** A graph  $G = (V, E)$  is said to be a cycle if  $(v_i, v_{i+1}) \in E, 1 \leq i < n$  and  $(v_n, v_1) \in E$  where  $|V| = n$  and it is denoted as  $C_n$  [8].

### 3 $L(4, 3, 2, 1)$ -Labeling Numbers for Simple Graphs

#### 3.1 Complete Graphs

In this section we find the minimal  $L(4, 3, 2, 1)$ -labeling number  $\lambda(K_n)$  for complete graphs.

**Theorem 1** For any complete graph,  $K_n$  with  $n$  vertices, the minimal  $L(4, 3, 2, 1)$ -labeling number  $\lambda(K_n)$  is  $4n - 3$ .

*Proof* Let  $K_n = (V, E)$  be a complete graph with vertex set  $V = \{v_1, v_2, \dots, v_n\}$  and also let  $f$  be a minimal  $L(4, 3, 2, 1)$ -labeling of  $K_n$ . Without loss of generality, we can assume that  $f(v_i) < f(v_j)$  when  $i < j$  and  $f(v_1) = 1$ . As  $K_n$  is a complete graph, therefore,  $d(x, y) = 1, \forall x, y \in V, x \neq y$ . This implies that  $|f(x) - f(y)| \geq 4, \forall x, y \in V$ . Again  $f(v_1) = 1$ . Therefore,

$$\begin{aligned}
 f(v_2) &\geq f(v_1) + 4 = 1 + 4 = 5; \\
 f(v_3) &\geq f(v_2) + 4 = 5 + 4 = 9; \\
 &\vdots \\
 f(v_n) &\geq f(v_{n-1}) + 4 = f(v_1) + (n - 1)4 = 1 + (n - 1)4 = 4n - 3.
 \end{aligned}$$

Therefore,  $\lambda(K_n) = 4n - 3$ . □

### 3.2 Complete Bipartite Graphs

In this section we find the minimal  $L(4, 3, 2, 1)$ -labeling number  $\lambda(K_{m,n})$  for complete bipartite graphs.

**Theorem 2** *For any complete bipartite graph,  $K_{m,n}$  with  $(m + n)$  vertices, the minimal  $L(4, 3, 2, 1)$ -labeling number  $\lambda(K_{m,n})$  is  $3(m + n) - 1$ .*

*Proof* Let  $K_{m,n} = (V, E)$  be a complete bipartite graph with  $A = \{a_1, a_2, \dots, a_m\}$  and  $B = \{b_1, b_2, \dots, b_n\}$  such that  $A \cup B = V$  and  $A \cap B = \phi$  and also let  $f$  be a minimal  $L(4, 3, 2, 1)$ -labeling of  $K_{m,n}$ .

Without loss of generality, we can assume that  $f(a_i) < f(a_j)$  when  $i < j$  and  $f(b_i) < f(b_j)$  when  $i < j$  and  $f(a_1) = 1$ . Now  $d(a_i, a_j) = 2, \forall a_i, a_j \in A$  and  $i \neq j$ . Therefore,  $|f(a_i) - f(a_j)| \geq 3, \forall a_i, a_j \in A$  and  $i \neq j$ . Since  $f(a_1) = 1$ , we have

$$\begin{aligned}
 f(a_2) &\geq f(a_1) + 3 = 1 + 3 = 4; \\
 f(a_3) &\geq f(a_2) + 3 = 4 + 3 = 7; \\
 &\vdots \\
 f(a_m) &\geq f(a_{m-1}) + 3 = f(a_1) + (m - 1)3 = 1 + (m - 1)3 = 3m - 2.
 \end{aligned}$$

Again  $d(a_i, b_j) = 1, \forall a_i \in A, b_j \in B$ . Therefore,  $|f(a_i) - f(b_j)| \geq 4$ . Since  $f$  is minimal labeling, we have  $f(b_1) = f(a_m) + 4 = (3m - 2) + 4 = 3m + 2$ .

Moreover,  $d(b_i, b_j) = 2, \forall b_i, b_j \in B$  and  $i \neq j$ . Therefore,  $|f(b_i) - f(b_j)| \geq 3, \forall b_i, b_j \in B$  and  $i \neq j$ . Since  $f(b_1) = 3m + 2$ , we have

$$\begin{aligned}
 f(b_2) &\geq f(b_1) + 3 = (3m + 2) + 3 = 3m + 5; \\
 f(b_3) &\geq f(b_2) + 3 = (3m + 5) + 3 = 3m + 8; \\
 &\vdots \\
 f(b_n) &\geq f(b_{n-1}) + 3 = f(b_1) + (n - 1)3 = (3m + 2) + (n - 1)3 = 3(m + n) - 1.
 \end{aligned}$$

Therefore,  $\lambda(K_{m,n}) = 3(m + n) - 1$ . □

**Corollary 1** *For a star,  $S_n$ , the minimal  $L(4, 3, 2, 1)$ -labeling number  $\lambda(S_n)$  is  $3n + 2$ .*

*Proof* According to the definition of star,  $S_n$  is  $K_{1,n}$ . Therefore, using Theorem 2, we can write  $\lambda(S_n) = 3(1 + n) - 1 = 3n + 2$ . □

### 3.3 Paths

In this section we find the *minimal  $L(4, 3, 2, 1)$ -labeling number  $\lambda(P_n)$*  for paths.

**Lemma 1** *For a path on  $n$  vertices,  $P_n$ , with  $n \geq 7$ , the minimal  $L(4, 3, 2, 1)$ -labeling number  $\lambda(P_n)$  is at least 13.*

*Proof* We prove this lemma using method of contradiction. Let  $f$  be a *minimal  $L(4, 3, 2, 1)$ -labeling* for a path on  $n$  vertices,  $P_n$  and  $v_1$  be the vertex with label 1. Now, suppose that  $\lambda(P_n) < 13$  for  $n \geq 7$ . Obviously keeping  $v_1$  as an end vertex, there exists an induced sub-path of at least three vertices. Let  $\{v_1, v_2, v_3\}$  be this path. Now,  $f(v_2)$  will have the following possibilities.

Case-I:  $f(v_2) = 5$ :

Then  $f(v_3) = 9$  and  $f(v_4) = 13$ , which contradicts our assumption.

Case-II:  $f(v_2) = 6$ :

Then  $f(v_3) = 10$  and  $f(v_4) = 14$ , which contradicts our assumption.

Case-III:  $f(v_2) = 7$ :

Then  $f(v_3) = 11$  and  $f(v_4) = 4, 3$ . Either possibilities of  $f(v_4)$  forces  $f(v_5) \geq 14$ , which contradicts our assumption.

Therefore we can conclude that  $\lambda(P_n)$  is at least 13 for  $n \geq 7$ . □

**Theorem 3** *For a path,  $P_n$  on  $n$  vertices, the minimal  $L(4, 3, 2, 1)$ -labeling number  $\lambda(P_n)$  is*

$$\lambda(P_n) = \begin{cases} 1 & \text{if } n = 1 \\ 5 & \text{if } n = 2 \\ 8 & \text{if } n = 3 \\ 11 & \text{if } n = 4, 5, 6 \\ 13 & \text{if } n \geq 7 \end{cases}$$

*Proof* Here, we prove each of the cases one by one.

Case-I:  $n = 1$ :

For a path,  $P_n$  with  $n = 1$ , the *minimal  $L(4, 3, 2, 1)$ -labeling number  $\lambda(P_n)$*  is 1. This is trivially true. Therefore,  $\lambda(P_1) = 1$ .

Case-II:  $n = 2$ :

For a path,  $P_n$  with  $n = 2$ , the *minimal  $L(4, 3, 2, 1)$ -labeling number  $\lambda(P_n)$*  is 5, as we don't have any other choice of labeling except either  $\{1, 5\}$  or  $\{5, 1\}$ . Therefore,  $\lambda(P_2) = 5$ .

Case-III:  $n = 3$ :

The labeling pattern  $\{5, 1, 8\}$  shows that  $\lambda(P_n) \leq 8$  for  $n = 3$ . Suppose  $\lambda(P_n) < 8$  for  $n = 3$ . If  $f(v_1) = 1$ , then  $f(v_2) \geq 5$  and  $f(v_3) \geq 9$ , which is a contradiction. Again if  $f(v_2) = 1$ , then either  $f(v_1) \geq 5$ ,  $f(v_3) \geq 8$  or  $f(v_1) \geq 8$ ,  $f(v_3) \geq 5$ . In either case we have a contradiction. Therefore,  $\lambda(P_3) = 8$ .

Case-IV:  $n = 4, 5, 6$ :

The labeling pattern  $\{9, 5, 1, 11, 7, 3\}$  shows that  $\lambda(P_n) \leq 11$  for  $n = 4, 5, 6$ . Suppose  $\lambda(P_n) < 11$  for  $n = 4, 5, 6$ . As  $f$  is a minimal  $L(4, 3, 2, 1)$ -labeling, a vertex must have the label 1. If  $f(v_1) = 1$  then  $f(v_4) \geq 13$ , a contradiction. If  $f(v_2) = 1$  then either  $f(v_1) = 5$  or  $f(v_3) = 5$ . When  $f(v_1) = 5$ , then  $f(v_4) = 12$ , a contradiction. When  $f(v_3) = 5$ , then  $f(v_5) = 13$ , a contradiction. Therefore,  $\lambda(P_n) = 11$  for  $n = 4, 5, 6$ .

Case-V:  $n \geq 7$ :

We can find a labeling pattern  $f(\{v_1, v_2, v_3, v_4, v_5, v_6, v_7\}) = \{5, 9, 13, 3, 7, 11, 1\}$ . It can be defined that two vertices with indices  $i$  and  $j$  will get same label if  $i \equiv j \pmod{7}$  and the maximum natural number used to label the first seven vertices starting from index  $i = 1$  to index  $i = 7$  is 13. Therefore, we can conclude that  $\lambda(P_n) \leq 13$  for  $n \geq 7$ . Again using Lemma 3.3 we get  $\lambda(P_n) \geq 13$  for  $n \geq 7$ . So, combining these two results we can finally conclude that  $\lambda(P_n) = 13$  for  $n \geq 7$ .  $\square$

### 3.4 Cycles

**Lemma 2** For a cycle,  $C_n$  on  $n$  vertices, the minimal  $L(4, 3, 2, 1)$ -labeling number  $\lambda(C_n)$  is

$$\lambda(C_n) = \begin{cases} 1 & \text{if } n = 1 \\ 5 & \text{if } n = 2 \\ 9 & \text{if } n = 3 \end{cases}$$

*Proof*

Case-I:  $n = 1$ :

This is trivially true. Therefore,  $\lambda(C_n) = 1$  if  $n = 1$ .

Case-II:  $n = 2$ :

Here we have only two choices for labeling the vertices  $v_1$  and  $v_2$ . The two possibilities of  $\{f(v_1), f(v_2)\}$  is either  $\{1, 5\}$  or  $\{5, 1\}$ . Therefore,  $\lambda(C_n) = 5$  if  $n = 2$ .

Case-III:  $n = 3$ :

Clearly, a cycle with 3 vertices is nothing but a complete graph with 3 vertices. Using Theorem 1 we can compute  $\lambda(K_3) = 9$ . Therefore,  $\lambda(C_n) = 9$  if  $n = 3$ .  $\square$

**Observation 1** For a cycle,  $C_n$  on  $n$  vertices, the distance between any two vertices is at most  $\lfloor \frac{n}{2} \rfloor$ .

**Observation 2**  $\lambda(C_n) \geq \lambda(P_n)$ .

This is true because  $P_n$  is a subgraph of  $C_n$ .

## 4 $L(4, 3, 2, 1)$ -Labeling Algorithm for Path

In this section we present an algorithm of  $L(4, 3, 2, 1)$ -labeling for path,  $P_n$  on  $n$  vertices. The label of any vertex of  $P_n$  obtained from our proposed algorithm depends only on the index of the corresponding vertex.

---

### Algorithm: $L(4, 3, 2, 1)$ -labeling algorithm for Path

---

**Input:** Path,  $P_n$  on  $n$  vertices.

**Output:**  $L(4, 3, 2, 1)$ -labeling for  $P_n$ .

Let the label assigned to the vertex of index  $i$  be denoted as  $L(i)$  where  $1 \leq i \leq n$ .

**begin**

for every vertex of index  $i$

$$L(i) = (4i \bmod 14) + 1$$

**end**

---

An example of label assignment for  $P_n$  with  $n = 20$  using the above algorithm is as follows:  $\{5, 9, 13, 3, 7, 11, 1, 5, 9, 13, 3, 7, 11, 1, 5, 9, 13, 3, 7, 11\}$ .

**Claim 1** The proposed  $L(4, 3, 2, 1)$ -labeling algorithm for Path,  $P_n$  on  $n$  vertices is optimal for  $n \geq 7$ .

*Proof* In Theorem 3 we have already proved that  $\lambda(P_n) = 13$  for  $n \geq 7$ . The label obtained for any vertex with index  $i$  from the proposed algorithm is at most 13. This proves that our proposed algorithm is optimal.  $\square$

## 5 Conclusion

This paper presents  $L(4, 3, 2, 1)$ -labeling for different types of graphs. It may be worthy to find out the *labeling number* for different complex graphs.

## References

1. Hale, W.K.: Frequency assignment: theory and applications. Proc. IEEE **68**(12), 1497–1514 (1980)
2. Roberts, F.S.: T-colorings of graphs: recent results and open problems. Discrete Math. **93**(2), 229–245 (1991)
3. Griggs, J.R., Yeh, R.K.: Labelling graphs with a condition at distance 2. SIAM J. Discrete Math. **5**(4), 586–595 (1992)
4. Yeh, R.K.: A survey on labeling graphs with a condition at distance two. Discrete Math. **306**(12), 1217–1231 (2006)
5. Liu, J., Shao, Z.: The  $L(3, 2, 1)$ -labelling problem on graphs. Math. Appl. **17**(4), 596–602 (2004)
6. Clipperton, J., Gehrtz, J., Szaniszló, Z., Torkornoo, D.:  $L(3, 2, 1)$ -Labeling of Simple Graphs. Valparaiso University, VERUM (2006)
7. Chia, M.L., Kuo, D., Liao, H., Yang, C.H., Yeh, R.K.:  $L(3, 2, 1)$ -labeling of graphs. Taiwan. J. Math. **15**(6), 2439 (2011)
8. Diestel, R.: Graph theory. 2005. Grad. Text. Math. ISBN-13 978-3540261827 (2005)



# Compact, Multi-band Microstrip Antenna with High Gain

Srija De, Poulami Samaddar, Sushanta Sarkar, Sushanta Biswas, Debasree Sarkar and Partha Pratim Sarkar

**Abstract** In this paper, theoretical investigations of a printed microstrip antenna, using coaxial probe feed method is presented. The proposed antenna provides promising enhancement of gain. It also gives triple frequency bands. The high gain with triple band is obtained using E shaped patch and slitted rectangular ground plane. The simulation is carried out using a Method of Moment (MOM) based ANSOFT software. This novel designed antenna of high gain (more than 6dBi) and triple band is described in detail in this study. The proposed antenna is simple in structure compared to the regular stacked or coplanar parasitic patch antennas. It is highly suitable for wireless communications.

**Keywords** Microstrip antenna · Compact · Multi-frequency · High gain

---

S. De (✉) · P. Samaddar · S. Sarkar · S. Biswas · D. Sarkar · P.P. Sarkar  
Department of Engineering and Technological Studies, University of Kalyani,  
Kalyani 741235, West Bengal, India  
e-mail: srijade@gmail.com

P. Samaddar  
e-mail: poulami\_samaddar@rediffmail.com

S. Sarkar  
e-mail: sushantasarkar@aol.com

S. Biswas  
e-mail: biswas.su@gmail.com

D. Sarkar  
e-mail: dsarkar70@gmail.com

P.P. Sarkar  
e-mail: parthabe91@yahoo.co.in

## 1 Introduction

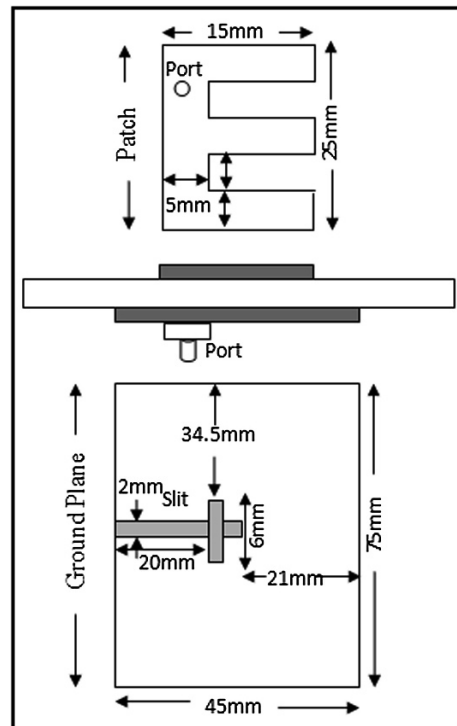
A microstrip patch antenna [1] is one of the most commonly used printed antennas in practice. It enjoys its advantages of low profile, simple structure, low cost, and omnidirectional radiation patterns [1, 2]. Dual-frequency microstrip antennas with a single feed are required in various radar and communications systems, such as synthetic aperture radar (SAR), dual-band GSM/DCS 1800 mobile communications systems, and the Global Positioning System (GPS) [3]. Now a days the optimization of the design and efficiency of printed antennas are most important in communication systems [4–7].

In this study, a simple E shaped patch antenna on a slotted rectangular ground plane has been presented to exhibit multiband operation. This antenna is fed by co axial probe. The proposed design is on regular electrically thin microwave substrate Glass-PTFE.

## 2 Antenna Design

The configuration of the compact triple-band antenna is shown in Fig. 1. The antenna consists of an E shaped microstrip patch, supported on a slitted rectangular ground plane. The patch antenna is printed on a Glass-PTFE substrate with a

**Fig. 1** Design of the antenna



relative permittivity of 2.5 and thickness of 1.6 mm and is fed by coaxial probe feed method.

The feeding point is so positioned to obtain better impedance matching. The dimension of the patch is 15 mm × 25 mm. Each arm of the E shaped patch has equal dimension i.e. 10 mm × 5 mm. A cross shaped slit is embedded on the rectangular ground plane of 45 mm × 75 mm dimension. The patch is embedded at centre position w.r.to the ground plane.

### 3 Results and Discussions

Simulated results have been obtained by ANSOFT based on MOM. The length and width of the microstrip patch antenna, operating at 5.8 GHz are 15 and 25 mm respectively with substrate thickness  $h = 1.6$  mm and dielectric constant  $\epsilon_r = 2.5$  (PTFE). After loading the slit on the ground plane the width (W) and the length (L) of Antenna are calculated from conventional Eqs. 1 and 2 [1].

$$f_r = \frac{C}{2W} \sqrt{\frac{2}{(1 + \epsilon_r)}} \quad (1)$$

$$L = L_{eff} - 2\Delta L \quad (2)$$

where,

$$\frac{\Delta L}{h} = 0.412 \frac{(\epsilon_{reff} + 0.3) \left(\frac{W}{h} + 0.264\right)}{(\epsilon_{reff} - 0.258) \left(\frac{W}{h} + 0.8\right)}$$

$$\epsilon_{reff} = \frac{(\epsilon_r + 1)}{2} + \frac{(\epsilon_r - 1)}{2\sqrt{1 + 12\frac{h}{W}}}$$

$$L_{eff} = \frac{C}{2f_r \sqrt{\epsilon_{reff}}}$$

where

- $L_{eff}$  Effective length of the patch
- $L$  Length of the antenna
- $W$  Width of the antenna
- $f_r$  Resonant frequency of the antenna
- $C$  Velocity of light
- $\Delta L/h$  Normalized extension of the patch length
- $\epsilon_{reff}$  Effective dielectric constant

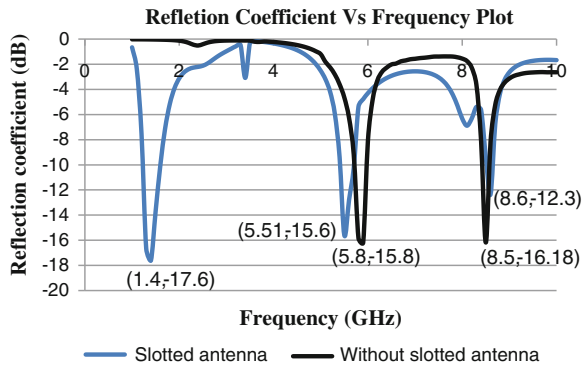
The slotted antenna resonates at 1.4 GHz frequency.

$$\text{Compactness} = \frac{(\text{Area of the slotted antenna} - \text{Area of the without slotted antenna})}{\text{Area of the without slotted antenna}} \times 100\% \tag{3}$$

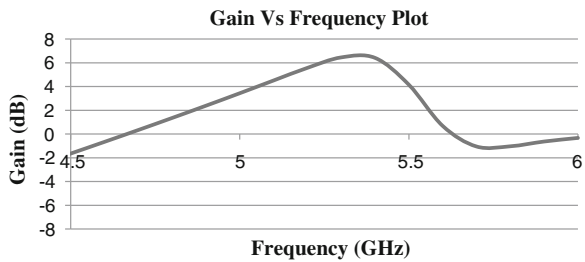
Using the Eq. 3 one gets 94 % size reduction of the designed antenna.

Figure 2 shows the comparative study of the Reflection Coefficient versus Frequency plot for antenna without slot and with slot. The reference antenna resonates at 5.8 GHz at reflection coefficient of -15.8 dB whereas the slitted antenna resonates at 1.4 GHz frequency. From this figure it is shown that the designed antenna resonates at three different resonant frequencies. The frequency ratio of

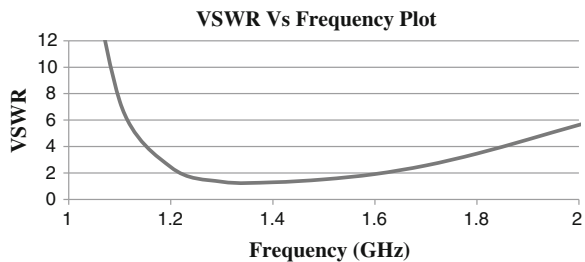
**Fig. 2** Comparative study of the reflection coefficient versus frequency plot of reference and slotted antenna



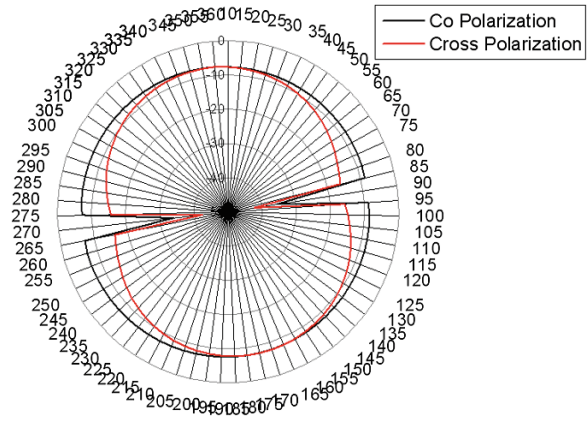
**Fig. 3** Gain versus frequency plot of the slotted antenna



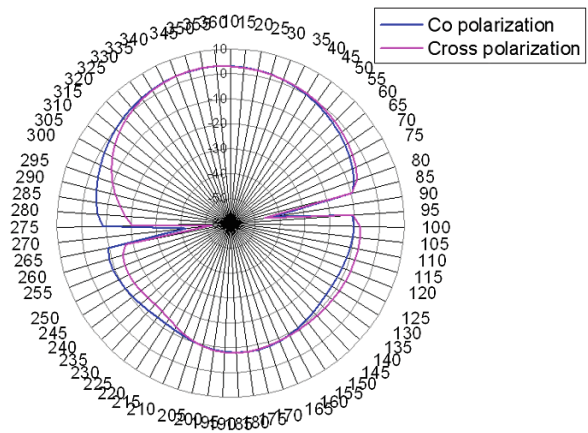
**Fig. 4** VSWR versus frequency plot



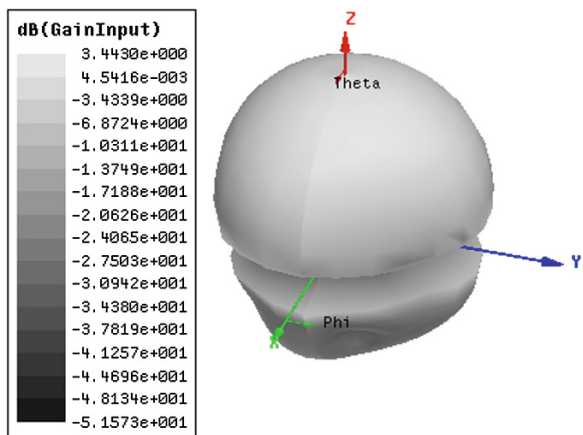
**Fig. 5** Theoretical co and cross radiation pattern at 1.4 GHz frequency



**Fig. 6** Theoretical co and cross radiation pattern at 5.51 GHz frequency



**Fig. 7** Theoretical 3D radiation pattern at 5.5 GHz frequency



3.93 between the two operating frequencies has been obtained. The theoretical gain versus frequency plot is shown in Fig. 3. The gain of this antenna is high which is up to 6.7 dBi. Figure 4 shows the VSWR versus frequency plot. Figures 5 and 6 show the theoretical Co and Cross radiation patterns at 1 and 5 GHz resonant frequencies respectively of the designed antenna. Theoretical 3D radiation pattern at 5.51 GHz is shown in Fig. 7.

## 4 Conclusions

The proposed antenna design makes the reference antenna resonating at three different frequencies. The proposed design also results in size reduction of about 94 %. A gain of 6.7 dBi has also been achieved. The radiation pattern of the antenna is acceptable for use with practical communication designs. Here, the designed antenna may be used in compact wireless communication like compact handheld mobile phone, MRI Instrument etc.

## References

1. Balanis, C.A.: *Advanced Engineering Electromagnetics*. Wiley, New York (1989)
2. Bhunia, S., Biswas, S., Sarkar, D., Sarkar, P.P.: Experimental investigation on dual-frequency broad band microstrip antenna with swastika slot. *Ind. J. Phys.* **81**, 497–499 (2007)
3. Serrano-Vaello, A., Hernandez, S.: Printed antennas for dual-band GSM/DCS 1800 mobile handsets, *Electron Lett.* **34**, 140–141 (1998)
4. Misran, N., Islam, M.T., Shakib M.N., Yatim, B.: Design of Broadband multi-slotted microstrip patch antenna for wireless system. In: *Proceedings of International Conference on Microwave-08*, pp. 23–25 (2008)
5. Bhunia, S., Sarkar, D., Biswas, S., Sarkar, P.P., Gupta, B., Yasumoto, K.: Reduced size small dual and multi-frequency microstrip antenna. *Microwave Opt. Technol. Lett.* **50**(4), 961–965 (2008)
6. Mahmoud, M.N., Baktur, R.: A dual band microstrip fed slot antenna. In: *IEEE Transaction on Antennas and Propagation*, vol. 59, no. 5, pp. 1720–1724, May 2011
7. Chang, T.H., Kiang, J.F.: compact multi\_band h\_shaped slot antenna. In: *IEEE Transactions on Antennas and Propagation*, vol. 61, no.8, pp 4345–4349, August 2013

# Remote Access Control Mechanism Using Rabin Public Key Cryptosystem

Ruhul Amin and G.P. Biswas

**Abstract** There is no efficient algorithm for factoring a large composite number in polynomial time and the security of the Rabin cryptosystem is based on it. As large number of internet users access the web server everyday through insecure channel, therefore, user authentication along with privacy over the world is very important. In this paper, we first proposed Rabin cryptosystem based remote login authentication protocol without using smart card for accessing the web server securely. This paper not only proposed the authentication protocol, but it also applies well popular BAN logic to analyze the security of the proposed protocol. Additionally, we have presented informal security analysis. The proposed protocol not only contributes strong security, but it also achieves others advantages like mutual authentication property, efficient and user-friendly password change phase and an approach which helps to recover the forgot password securely.

**Keywords** Authentication · Rabin cryprosystem · BAN logic · Hash function · Security attacks

## 1 Introduction

In the client-server environment, many password-based user authentication schemes with smart card are widely used to authenticate the user's identity. Smart cards are usually adopted to store the authentication information(s) at the time of registration

---

R. Amin (✉) · G.P. Biswas  
Department of Computer Science and Engineering, Indian School of Mines,  
Dhanbad, Jharkhand, India  
e-mail: amin\_ruhul@live.com

G.P. Biswas  
e-mail: gpbiswas@gmail.com

for the user. Smart card based authentication schemes may suffer from stolen smart card attack. In addition, the cost of the necessary infrastructure for smart card-based schemes, such as the cards and readers add substantially to the cost.

In 1981, it was Lamport [1] who proposed an authentication scheme where the server maintains a verification table which is insecure against stolen verifier attack and then many password with smart card based user authentication schemes [2–11] have been proposed in the literature. However, these schemes are not applicable in such environment because of using the smart card. In 2009, Rhee et al. [12] proposed remote user authentication scheme without smart card and claimed that their protocol achieves mutual authentication property. However, it has been observed that their protocol is insecure against impersonation attack and man-in-the-middle attack. To overcome the above security weaknesses, Chen et al. [13] proposed an improvement of the Rhee et al.'s [12] protocol and also claimed that their protocol is highly secure. After that, He et al. pointed out that Chen et al.'s protocol is vulnerable to privileged insider attack and does not support perfect forward secrecy with no key control. On the other hand, Zhu et al. [14] pointed out that Hwang and Yeh [15] protocol suffers from several kinds of attack and proposed an authentication scheme without smart card based on the ECC cryptosystem. They claimed that the attacker cannot launch any security weakness based on their authentication protocol. However, Islam and Biswas [16] demonstrated that Zhu et al.'s [14] scheme suffers from several security weaknesses such as impersonation attack, clock synchronization problem and no session key agreement. In this paper, we have proposed Rabin cryptosystem based remote access control protocol without smart card for accessing securely the web server.

## *1.1 Road Map of the Paper*

In Sect. 2, we briefly introduce the basic concept of Rabin cryptosystem and related hardness problem. Section 3 addresses our proposed protocol and the security analysis and the discussion are presented in Sect. 5. Finally, the conclusion of this paper is given in Sect. 6.

## **2 Preliminaries**

This section briefly introduces the concept of Rabin cryptosystem and related computationally hardness problem which are presented below:

1. **Rabin Cryptosystem:** It is an asymmetric system, requires a public key and a private key. To generate a key pair, the system chooses two large prime numbers  $p, q$  such that  $p, q \equiv 3 \pmod{4}$  and computes  $n = pq$  and then declares  $n$  is the public key and the private key  $(p, q)$  kept secret.



**Encryption:** Chooses a message  $m$  and then computes  $C = m^2 \bmod n$  is the ciphertext and sends it to the destination location.

**Decryption:** The decryption algorithm is not deterministic function. It applies Chinese Remainder Theorem and private key pairs for obtaining the plaintext and gets four roots as a output. Finally, the original message can be retrieved from the four roots.

2. **Factorization Problem:** It can be stated as the parameter  $n$  is known to anyone where  $n = pq$ , then factoring  $p, q$  is infeasible in polynomial time. The security of the Rabin cryptosystem is based on it.

### 3 Proposed Protocol

This section presents remote access control mechanism without using smart card based on the Rabin cryptosystem for accessing web servers remotely. To achieve mutual authentication and session key agreement, we presented all the process of our proposed protocol in the following as follows:

#### 3.1 System Setup Process

In the system setup phase, the web server chooses two large prime number  $p, q$  such that  $p, q \equiv 3 \bmod 4$  and computes  $n = pq$  and finally publishes  $n$  as a public parameter and keeps  $(p, q)$  as a private key of the system.

#### 3.2 Registration Process

The user initially chooses desired user name  $ID_i$ , password  $PW_i$  and sends  $\langle ID_i, PW_i \rangle$  along with a valid e-mail id/mobile number to the server through secure channel. After receiving it, the web server  $S$  computes  $V_i = h(ID_i || p || q) \oplus PW_i$  and stores  $ID_i, V_i$ , along with e-mail id in the verifier Table 1 and sends an acknowledge message to the user that the registration process has been completed successfully.

**Table 1** Verifier table

Identity	Parameter	E-mail id/mobile number
$ID_1$	$V_1$	abc@gmail.com/9804557
$ID_2$	$V_2$	cba@gmail.com/9868754
$ID_3$	$V_3$	bca@gmail.com/9878712
.	.	.
.	.	.
$ID_n$	$V_n$	bca@gmail.com/9878712

### 3.3 Login and Authentication Process

This process executes several steps which are presented below:

**Step 1:** The user carefully provides the identity and password and press the login button on the web page. Then the user/client-end generates a 128 bits random number  $r_i$  and computes  $L_i = r_i^2 \bmod n$ ,  $G_i = h(ID_i || PW_i || r_i)$ ,  $M_i = h(r_i)$ ,  $K_i = M_i \oplus h(ID_i || PW_i)$  and forwards the login message  $\langle ID_i, L_i, K_i, G_i \rangle$  to the web server through public channel.

**Step 2:** After receiving the login message, the web server first checks the existence of the  $ID_i$  and if it does not exist, terminates the connection; otherwise, retrieves  $PW_i^*$  of the user by computing  $PW_i^* = h(ID_i || p || q) \oplus V_i$ . Then the web server further computes  $A_i^* = h(ID_i || PW_i^*)$ ,  $M_i^* = K_i \oplus A_i^*$  and decrypts the ciphertext  $L_i$  by utilizing the Chinese remainder theorem and finally gets the four roots  $\langle r_1, r_2, r_3, r_4 \rangle$  as a plaintext. After that, the web server takes four consecutive roots as a input  $\langle r_1, r_2, r_3, r_4 \rangle$  and checks the condition whether  $M_i^* = h(r_k)$  or not where  $(k = 1 \text{ to } 4)$  and it is confirmed that one of the conditions must match with the  $M_i^*$ . The web server then checks the condition whether  $G_i^* = G_i$  or not by computing  $G_i^* = h(ID_i || PW_i^* || r)$ . If the condition holds, the web server believes that the  $U_i$  is authentic.

**Step 3:** The web server generates a 128 bits random nonce  $r_j$  and computes  $C_j = h(ID_i || ID_s || r_i || PW_i^* || r_j)$ ,  $D_j = r_i \oplus r_j$  and forwards reply message  $\langle ID_s, C_j, D_j \rangle$  to the user through public channel.

**Step 4:** After receiving the reply message, the user/client-end computes  $r_j^* = D_j \oplus r_i$ ,  $C_j^* = h(ID_i || ID_s || r_i || PW_i || r_j^*)$  and checks the correctness whether  $C_j^* = C_j$  or not. If it does not hold, terminates the connection; otherwise, the user believes that the web server is authentic as well as the protocol achieves mutual authentication property and both the parties computes the session key  $SK = h(ID_i || ID_s || r_i || r_j)$  and starts secure communication.

### 3.4 Password Change Process

This phase is used rarely and should be provided in any password based authentication system. At the time of changing the password, the user provides the old information along with the new desired password  $PW_i^{new}$  and then the web server first authenticates the user based on old informations after executing the step-2 of the authentication process of the proposed protocol. After that, the web server computes  $V_i^{new} = V_i \oplus PW_i \oplus PW_i^{new}$  and replaces the new computed value  $V_i^{new}$  with the old value  $V_i$  of the corresponding  $ID_i$ . Thus, the proposed protocol efficiently change the user's password.

### 3.5 Recovering Forgot Password Process

It is the common problem of many internet users that they forgot their password due to either accessing several number of web server or rarely used. Therefore, it is very important to provide their forgotten password securely. Initially, the user sends the user name and the e-mail id/mobile number to the web server and then checks whether the e-mail id/mobile number is registered or not by using the verification table. If the condition holds, it retrieves the password  $PW_i = h(ID_i || p || q) \oplus V_i$  and sends it to the e-mail id/mobile number through secure channel with an acknowledge message to the user for checking their registered e-mail id/mobile number. Thus, our proposed protocol retrieves the forgot password of the user.

## 4 Authentication Proof Based on BAN Logic

This section addresses the security analysis of our proposed protocol using Burrows-Abadi-Needham logic [17, 18], generally called as BAN logic. The BAN logic is well-known formal model used to analyze the security of authentication and key distribution protocols in the literature. Some preliminaries and notations of the BAN logic are described in Table 2.

In order to prove the proposed protocol secure, the proposed protocol must satisfy the following goals based on the BAN logic which are given as follows:

- **Goal 1:**  $U_i | \equiv U_i \stackrel{SK}{\leftrightarrow} S$
- **Goal 2:**  $U_i | \equiv S | \equiv U_i \stackrel{SK}{\leftrightarrow} S$
- **Goal 3:**  $S | \equiv S \stackrel{SK}{\leftrightarrow} U_i$
- **Goal 4:**  $S | \equiv U_i | \equiv S \stackrel{SK}{\leftrightarrow} U_i$

First the proposed protocol is transformed into idealized form:

$$M_1 : U_i \rightarrow S : ID_i, L_i, K_i, G_i : \langle r_i \rangle_{PW_i}$$

$$M_2 : S \rightarrow U_i : ID_s, D_j, C_j : \langle r_j \rangle_{PW_i}$$

Second, the following assumptions about the initial state of the protocol are made to analyze the proposed protocol:

$$\begin{array}{ll} A_1 : U_i | \equiv \#(r_i) & A_4 : S | \equiv S \stackrel{PW_i}{\leftrightarrow} U_i \\ A_2 : RS | \equiv \#(r_j) & A_5 : S | \equiv U_i \Rightarrow r_i \\ A_3 : U_i | \equiv U_i \stackrel{PW_i}{\leftrightarrow} S & A_6 : U_i | \equiv S \Rightarrow r_j \end{array}$$

**Table 2** List of notations used

Symbol	Description
$U_i$	User/client
$n$	The product of two large prime number $p$ and $q$
$S$	Web server
$ID_i$	Identity of user $U_i$
$PW_i$	User's password
$(p, q)$	The secret key of the server $S$
$r_i$	The random number of generated by the user
$r_j$	The random number selected by the web server
$\oplus$	The bitwise exclusive or operation
$\parallel$	The concatenation operation
$h(\cdot)$	One-way hash function, $h : (0, 1)^* \rightarrow (0, 1)^n$
$P \models X$	$P$ believes $X$
$P \triangleleft X$	$P$ sees $X$
$P \sim X$	$P$ once said $X$
$P \Rightarrow X$	$P$ has jurisdiction over $X$
$\#(X)$	The message $X$ is fresh
$\langle X \rangle_Y$	The formulae $X$ combined with the formulae $Y$
$\{X\}_K$	The formulae $X$ is encrypted under the key $K$
$P \xleftrightarrow{K} Q$	Principals $P$ and $Q$ communicate via shared key $K$
$P \stackrel{X}{\rightleftharpoons} Q$	The formula $X$ is a secret known only to $P$ and $Q$
$SK$	The session key used in the current session
$\frac{P \models P \stackrel{K}{\rightleftharpoons} Q, P \triangleleft \langle X \rangle_K}{P \models Q \mid X}$	Message-meaning rule
$\frac{P \models \langle X \rangle, P \models Y}{P \models \langle X, Y \rangle}$	Belief rule
$\frac{P \models \#(X), P \models Q \mid \sim X}{P \models Q \mid X}$	Nonce-verification rule
$\frac{P \models Q \Rightarrow X, P \models Q \mid X}{P \models X}$	Jurisdiction rule
$\frac{P \models \#(X), P \models Q \mid X}{P \models P \stackrel{K}{\rightleftharpoons} Q}$	Session keys rule

Third, the idealized form of the proposed protocol is analyzed based on the BAN logic rules and the assumptions. The main proofs are stated as follows:

$$M_1 : U_i \rightarrow S : ID_i, L_i, K_i, G_i : \langle r_i \rangle_{PW_i}$$

According to seeing rule, we get  $S1 : S \triangleleft ID_i, L_i, K_i, G_i : \langle r_i \rangle_{PW_i}$ .

According to A3, S1 and message meaning rule, we get  $S2 : S \models U_i \sim r_i$ .

According to A2, S2 and freshness-conjunction rule and nonce verification rule is applied, we get  $S3 : S \models U_i \mid \equiv r_i$ , where  $r_i$  is the necessary parameter of the session key of the proposed protocol.

According to A5, S3 and the jurisdiction rule is applied, we get  $S4 : S | \equiv r_i$ .

According to A2, S3 and the session key rule is applied, we get  $S5 : S | \equiv S \stackrel{SK}{\leftrightarrow} U_i$  (**Goal 3**).

According to A2, S5 and the nonce verification rule is applied, we get  $S6 : S | \equiv U_i | \equiv S \stackrel{SK}{\leftrightarrow} U_i$  (**Goal 4**)

$$M_2 : S \rightarrow U_i : ID_s, D_j, C_j : \langle r_j \rangle_{PW_i}$$

According to seeing rule, we get  $S7 : U_i \triangleleft ID_s, D_j, C_j : \langle r_j \rangle_{PW_i}$ .

According to A4, S7 and the message meaning rule, we get  $S8 : U_i | \equiv S | \sim r_j$ .

According to A1, S8 and freshness-conjunction rule and nonce verification rule is applied, we get  $S9 : U_i | \equiv S | \equiv r_j$ , where  $r_j$  is the necessary parameter of the session key of the proposed protocol.

According to A6, S9 and the jurisdiction rule is applied, we get  $S10 : U_i | \equiv r_j$ .

According to A1, S9 and the session key rule is applied, we get  $S11 : U_i | \equiv U_i \stackrel{SK}{\leftrightarrow} S$  (**Goal 1**).

According to A1, S11 and nonce verification rule is applied, we get  $S12 : U_i | \equiv S | \equiv U_i \stackrel{SK}{\leftrightarrow} S$  (**Goal 2**).

The above discussion proves our objectives mentioned above using BAN logic and it is clear that the  $U_i$  and the  $S$  performs mutual authentication and key agreement property securely.

## 5 Security Analysis and Discussion of the Proposed Protocol

In wireless communication system, it is our assumption that an attacker has maximum power or capabilities over the insecure communication such as (1) the login-reply messages of the proposed protocol passes through the attacker, so the attacker can trap, delete, re-generate, re-route the login-reply message and try to authenticate him/herself to the server or user for retrieving the confidential information(s). The following subsections present the security strength of the proposed protocol:

### 5.1 Strong Security Protection on the Password

It is our assumption that the proposed protocol uses the low entropy password which is guessable in off-line mode in polynomial time, in spite of that the attacker cannot derive or guess the password. We assume that the attacker traps the login-reply message of the protocol and tries to find out the password from the  $\langle G_i, K_i, C_j \rangle$  parameters. It is very clear that the attacker cannot derive the password from the

known parameters, as all the parameters are protected by the non-invertible cryptographic one-way hash function. As mentioned in [19], the probability of guessing the user's password composed of exactly  $n$  character is  $\frac{1}{2^{6n}}$ . Therefore, the probability of guessing the password from the  $G_i$ ,  $K_i$  and  $C_j$  are  $\frac{1}{2^{6n+128}}$  and  $\frac{1}{2^{6n+256}}$  respectively which are enormously negligible and infeasible in polynomial time.

### ***5.2 Strong Security Protection on Login-Reply Message***

In the protocol, the login parameter  $G_i$  is dependent on the user's password, random number and it is possible that an attacker can generate a random number easily. As the login parameters are dependent on the user's password, therefore the attacker fails to forge the valid login message and the same case is also applicable for the reply message. Thus, we can claim that our proposed protocol provides strong security protection on the login-reply message.

### ***5.3 Strong Security Protection on Session Key***

The session key of the authentication protocol must be different for each authentication cycle and if it is disclosed, an attacker can decrypt the ciphertext and will obtain the confidential information. As the attacker cannot retrieve the random numbers from the login-reply messages, he/she fails to compute the session key. If an attacker tries to guess it, the probability of guessing is  $\frac{1}{2^{256}}$ , which is dreadfully hard in polynomial time.

### ***5.4 Strong Security Protection on Stolen-Verifier Attack***

After hacking the verifier table, the attacker tries to extract confidential information (s) from it. As the computation  $h(ID_i || p || q)$  depends upon the secret key of the server, he/she cannot extract the user's password from the  $V_i$  parameter. Therefore, the protocol provides strong security protection on it.

## **6 Conclusion**

This paper contributes an efficient remote access control protocol without using smart card usable for client-server environment and the well popular BAN logic proves that the proposed protocol agreement a session key in each authentication cycle securely. The informal security analysis are also made and it confirms that the

proposed protocol has strong security protection on the user's password, login-reply message, session key and verifier-table. This paper not only provides strong security protection on the authentication protocol, but it also contributes (1) an efficient password change phase, (2) retrieving forgot password procedure, (3) mutual authentication property, and (4) session key agreement etc.

## References

1. Lamport, L.: Password authentication with insecure communication. *Commun ACM* **24**(11), 770–772 (1981)
2. Khan, M.K., Zhang, J.S.: Improving the security of a flexible biometrics remote user authentication scheme. *Comput. Stand. Interface* **29**(1), 82–85 (2007)
3. Liu, J.Y., Zhou, A.M., Gao, M.X.: A new mutual authentication scheme based on nonce and smart cards. *Comput. Commun.* **31**(10), 2205–2209 (2008)
4. Li, C.T., Lee, C.C.: A robust remote user authentication scheme using smart card. *Inf. Technol. Control* **40**(3), 236–245 (2011)
5. Li, X., Qiu, W., Zheng, D., Chen, K., Li, J.: Anonymity enhancement on robust and efficient password authenticated key agreement using smartcards. *IEEE Trans. Industr. Electron.* **57**(2), 43–48 (2010)
6. Amin, R.: Cryptanalysis and an efficient secure ID-based remote user authentication scheme using smart card. *IJCA* **75**(13), 1149–1157 (2013)
7. He, D., Chen, Y., Chen, J.: Cryptanalysis and improvement of an extended chaotic maps based key agreement protocol. *Nonlinear Dyn* **69**(3), 37–42 (2012)
8. Amin, R., Maitra, T., Rana, S.: An improvement of Wang, et. al.'s remote user authentication scheme against smart card security breach. *IJCA* **75**(13), 405–410 (2013)
9. He, D., Chen, J., Hu, J.: Improvement on a smart card based authentication scheme. *J. Internet Technol.* **13**(3), 236–248 (2012)
10. Wu, S., Zhu, Y., Pu, Q.: Robast smart card based user authentication scheme with user anonymity. *Secur. Commun. Netw* **5**(2), 181–185 (2012)
11. Goriparthi, T., Das, M.L., Saxsena, A.: An improved bilinear pairing based remote client authentication protocol. *Comput. Stand. Interface* **31**(1), 181–185 (2009)
12. Rhee, H.S., Kwon, J.O., Lee, D.H.: A remote user authentication scheme without using smart cards. *Comput. Stand. Interface* **31**(1), 6–13 (2009)
13. Chen, B., Kuo, W., Wu, L.: A secure password based remote user authentication scheme without using smart cards. *Inf. Technol. Control* **41**(1), 53–59 (2012)
14. Zhu, L., Yu, S., Zhang, X.: Improvement upon mutual password authentication scheme. *Inter. Semin. Bus. Inf. Manage.* **1**, 400–403 (2008)
15. Hwang, J.J., Yeh, T.C.: Improvement on Peyravian-Zunic's password authentication schemes. *IEICE Trans. Commun.* **E85-B**(4), 823–825 (2002)
16. Islam, S.K., Biswas, G.P.: Improved remote login scheme based on ECC. *IEEE-Inter. Conf. Recent Trends Inf. Technol. ICRTIT*, pp. 6–13 (2011)
17. Burrows, M., Abadi, M., Needham, R.: A logic of authentication. *ACM Trans. Comput. Syst.* **8**(1), 1836 (1990)
18. Tsai, J.-L., Wu, T.-C., Tsai, K.-Y.: New dynamic ID authentication scheme using smart cards. *Int. J. Commun. Syst.* **23**, 1449–1462 (2010)
19. Chang, Y.-F., Yu, S.-H., Shiao, D.-R.: An uniqueness-and anonymity-preserving remote user authentication scheme for connected health care. *J. Med. Syst.* **37**, 9902 (2013)

# Intelligent Energy Competency Multipath Routing in WANET

Santosh Kumar Das, Sachin Tripathi and A.P. Burnwal

**Abstract** In modern era, the use of wireless ad hoc network (WANET) has been increasing rapidly. Every nodes of WANET are directly communicated with each other to share information within the range. This network is dynamic and infrastructure-less, so topology of this network can change very frequently. WANET nodes are powered by battery with limited capacity and due to this reason sometime nodes are fail to transmit data packet from source to destination. The present paper proposes a routing protocol, named Intelligent Energy Competency Multipath routing protocol (IECM) for WANET. The basic idea of IECM is to select energy efficient multipath which reduces energy consumption of ad hoc nodes based on intelligent method. This method is mainly used to extend the lifetime of WANET by specifying a different intelligent scale to each route. This scaling system evaluated by three phase intelligent initiation phase, second path evaluation phase and third multipath route selection phase. Based on the comprehensive simulation of IECM using MATLAB and NS2 and comparative study of same with other existing protocols, it is observed that proposed routing protocol contributes to the performance improvements in terms of energy competency.

**Keywords** WANET · Fuzzy logic · Multipath · Expert system

---

S.K. Das (✉) · S. Tripathi  
Department of CSE, ISM Dhanbad, Jharkhand 826004, India  
e-mail: sunsantosh2007@rediffmail.com

S. Tripathi  
e-mail: var\_1285@yahoo.com

A.P. Burnwal  
Department of Math, GGSESTC Bokaro, Jharkhand 827013, India  
e-mail: apburnwal@yahoo.com



## 1 Introduction

WANET [1–3] is a new paradigm of wireless communication. In this network, there is no fixed infrastructure such as base stations or mobile switching centers. Every nodes that are within each other's radio range communicate directly via wireless links, while those are far apart rely on other nodes to relay messages as routers. These nodes are organized in either homogeneous or heterogeneous manner and typically move in any direction they want due to its dynamic nature. The main role of these nodes is not only responsible for network traffic but also has to forward packets. This features helps to WANET to change network topology frequently. WANET is highly active and distributed in nature as the nodes are powered by batteries with limited capacity. Hence, energy efficient multipath routing is a major challenge. Since these energy sources have a limited lifetime, energy availability is one of the most important constraints for the operation of the WANET. There are different sources of energy consumption in an ad hoc network node. The energy consumption occurred due to sending a packet, receiving a packet, the node when idle mode which occurs when the wireless interface of the node is turned off. Power failure of a node not only affect the node itself but also its ability to forward packets on behalf of others and thus the overall network lifetime. Therefore, energy efficient multipath routing indicates selecting routes that require minimum hops, instead of more no. of hops. Therefore to improve the network performance, the nodes should select the best route in terms of its remaining lifetime. Since the factors impacting the route lifetime are unpredictable, the route of remaining lifetime cannot be systematically derived. Under this situation, battery power, hop count and transmitted packet can be measured by fuzzy intelligent technique.

The framework of proposed routing method in based on two parameter such throughput and energy. These parameters help to determine intelligent scale of each route and help to establish multipath for route discovery and maintenance.

Rest of this paper is organized as follows: Sect. 2 provides related work done in energy efficient routing protocol for ad hoc network. Section 3 addresses the preliminaries related to the proposed method. The details of proposed method describes in Sect. 4. Section 5 illustrates the simulation results of the proposed protocol and compares it with existing protocols. Finally, Sect. 6 concludes the paper.

## 2 Related Works

There have been lot of works are done on energy efficient routing such as Perkins and Royer [4] proposed a method to construct an ad hoc network smart badges in order to acquire information from trapped survivors. Here the authors have shown that smart badges have very limited power sources and very low data rates, which is inadequate in an emergency situation. This problem is formulated as any cast routing problem in which the objective is to maximize the time until the first battery

drains out. Zheng and Kravets [5] proposed an extensible on-demand power management framework for ad hoc networks. It is used for adapting traffic load. In this framework nodes maintain soft-state timers that determine power management transitions. By monitoring routing control messages and data transmission, these timers is set and refreshed on-demand. And nodes that are not involved in data delivery may go to sleep. But it has limitation that this framework does not considered load balancing issues because the correct policy for load balancing is dependent on the communication goals of the network. Su et al. [6] proposed the fuzzy logic modified AODV routing (FMAR) protocol for multicast routing in mobile ad hoc networks. The main aim of this protocol is dynamically evaluate the active routes based on fuzzy logic weighted multi-criteria. It also helps to managing the limited bandwidths of wireless links. But it has some drawback that the proposed protocol does not considered all possible routes as evaluation of route lifetime by fuzzy logic multi-criteria, so it cannot be determine which routes are highly useful. Therefore, routes cannot repair and maintain partially or completely before they crashed. Nayak et al. [7] surveys and classifies the energy-aware routing protocols proposed for MANETs. They minimize either the active communication energy required to transmit or receive packets or the inactive energy consumed when a mobile node stays idle, but listens to wireless medium for any possible communication requests from other nodes. The authors describe two category first is former category that contain transmission power control and load distribution and another is latter category that contain sleep/power-down mode. In many situations, it is not clear that which particular algorithm is the best for this situation; each protocol has its own advantages or disadvantages. So authors facilitate the research efforts in combining the existing solutions to offer a more energy efficient routing mechanism.

### **3 Preliminaries**

#### ***3.1 Fuzzy Logic***

Fuzzy logic is a part of soft computing; it was introduced by Zadeh [8] which became mathematical discipline to express human reasoning in rigorous mathematical notation. It is a multi-valued logic that allows intermediate values to be defined between conventional evaluations like true/false, yes/no etc. Notions like rather long or very long, small or very small can be formulated mathematically and processed. Many authors [9–12] used fuzzy logic in ad hoc network. FL provides a simple way to arrive at a definite conclusion based upon vague, ambiguous, imprecise, noisy, or missing input information.

### ***3.2 Multipath Routing***

Most currently proposed routing protocols for ad hoc networks are unipath routing protocols. In unipath routing, only a single route is used between a source and destination node. Two of the most widely used protocols are the Flooding [13] and the Ad hoc On-demand Distance Vector (AODV) [14] protocols. But these unipath routing protocols has some drawback that these protocols does not handle node failures, link failures, route breakages and maintenance. Therefore multipath [15] routing helps avoid these problems by route discovery and maintenance. It consists of finding multiple routes between a source and destination node. This multipath routing gives up a variety of benefits such as energy efficiency, fault tolerance, load balancing, increased bandwidth, or improved security. These benefits can ease congestion and bottlenecks.

### ***3.3 Expert System***

Expert system [16–20] is computer program that attempts to act like a human expert on a particular subject area to solve particular unpredictable problem. Sometime it is often used to advise non-experts in situations where a human expert in unavailable. Its core elements are knowledge based system and inference engine. The first element knowledge based system is software that uses artificial intelligence techniques to solve any problem in a more efficient way. It includes a database of expert knowledge that helps to retrieve result based on specific queries or conditions. The second element inference engines that process the data by using rule based knowledge representation.

## **4 Proposed Protocol IECM**

The proposed work based on expert system which divides entire system into three phases. These three phases design and evaluated by fuzzy intelligent system. The expert system uses this intelligent system through rule base system and inference engine to solve this energy efficient multipath routing problem. The assumptions and details of these phases will be described as given below:

### ***4.1 Intelligent Initiation Phase***

This is initial phase of the proposed protocol. The main job of this phase to initiated membership function of input variables as throughput and energy and output

variable as intelligent scale and their correspondence base values. In this proposed protocol throughput considered as 500 unit, and energy capacity as 50 joule. Membership functions corresponding to each input variables and output variable are described in Tables 1, 2 and 3.

### 4.2 Path Evaluation Phase

In this phase expert system establish different path for data transmission from source node to destination node. The basic criteria of proposed protocol based on input and output variable is given in Table 4. This criteria helps to evaluate different states and their intelligent scaling which is given in Table 5.

### 4.3 Multipath Route Selection Phase

This phase is specially used to select energy efficient multipath route by the help of fuzzy rule matrix. In this protocol, expert system uses  $3 \times 3$  matrix given in Table 6, where columns are labeled by throughput and rows are labeled by energy and cell are labeled by different intelligent scale to each route. The cell value of this fuzzy rule matrix helps to select multipath for energy efficient routing.

**Table 1** Membership function of throughput

Linguistic values	Notation	Range	Base value
Low	$T_L$	$[T_{La}, T_{Lb}]$	(0, 0, 250)
Medium	$T_M$	$[T_{Ma}, T_{Mb}]$	(0, 250, 500)
High	$T_H$	$[T_{Ha}, T_{Hb}]$	(250, 500, 500)

**Table 2** Membership function of energy

Linguistic values	Notation	Range	Base value
Low	$E_L$	$[E_{La}, E_{Lb}]$	(0, 0, 20)
Medium	$E_M$	$[E_{Ma}, E_{Mb}]$	(5, 25, 45)
High	$E_H$	$[E_{Ha}, E_{Hb}]$	(30, 50, 50)

**Table 3** Linguistic variable of intelligent scale for different routes

Very bad	Bad	Satisfactory	Medium	Less good	Good	Very good	Excellent	Very excellent
$R_{VB}$	$R_B$	$R_S$	$R_M$	$R_{LG}$	$R_G$	$R_{VG}$	$R_E$	$R_{VE}$

**Table 4** Rules for path evaluation

Rule 1: IF (Energy is $E_L$ ) and (Throughput is $T_H$ ) then (Rating of Route is $R_{VB}$ )
Rule 2: IF (Energy is $E_L$ ) and (Throughput is $T_M$ ) then (Rating of Route is $R_B$ )
Rule 3: IF (Energy is $E_L$ ) and (Throughput is $T_L$ ) then (Rating of Route is $R_S$ )
Rule 4: IF (Energy is $E_M$ ) and (Throughput is $T_H$ ) then (Rating of Route is $R_M$ )
Rule 5: IF (Energy is $E_M$ ) and (Throughput is $T_M$ ) then (Rating of Route is $R_{LG}$ )
Rule 6: IF (Energy is $E_M$ ) and (Throughput is $T_L$ ) then (Rating of Route is $R_G$ )
Rule 7: IF (Energy is $E_H$ ) and (Throughput is $T_H$ ) then (Rating of Route is $R_{VG}$ )
Rule 8: IF (Energy is $E_H$ ) and (Throughput is $T_M$ ) then (Rating of Route is $R_E$ )
Rule 9: IF (Energy is $E_H$ ) and (Throughput is $T_L$ ) then (Rating of Route is $R_{VE}$ )

**Table 5** List of different states and their intelligent scale

State	Value	Intelligent scale	Value	State	Value	Intelligent scale	Value
S1	0.08	I1	0.08	S6	0.16	I6	0.067
S2	0.04	I2	0.04	S7	0.08	I7	0.32
S3	0.08	I3	0.027	S8	0.04	I8	0.16
S4	0.16	I4	0.2	S9	0.08	I9	0.107
S5	0.08	I5	0.1				

**Table 6** Fuzzy rule matrix for multipath selection

Energy/Data packet	$T_L$	$T_M$	$T_H$
$E_L$	$R_S$	$R_B$	$R_{VB}$
$E_M$	$R_G$	$R_{LG}$	$R_M$
$E_H$	$R_{VE}$	$R_E$	$R_{VG}$

Thus, each route has a specific intelligent scale in the WANET. In Table 6 demonstrate that source node has established three paths to the destination node such as R7, R8 and R9. If source node sends the same packet along all three paths, as long as at least one of the paths does not fail, destination node will receive the packet. Therefore, multiple paths can provide load balancing and fault-tolerance. Load balancing can be accomplished by scattering the traffic along multiple routes. From a fault tolerance viewpoint, multipath routing can provide route elasticity. Because failure of path not only affect the node itself of this path but also its ability to forward packets on behalf of others and thus the overall network lifetime. Hence, this intelligent scale helps to extend the lifetime of WANET.

## 5 Simulation Results and Analysis

In this section, the performances of this protocol based on energy efficient multipath with respect throughput and energy are simulated using NS2. The functions of IECM and other existing protocol Flooding, AODV and FMAR are coded in fis-files and m-files using MATLAB Fuzzy Toolkit to determine the membership functions of input-output variables and defuzzification output. We evaluate the performance of IECM protocol through simulation and compare it with the state and intelligent scale of different route based on other existing protocols. We consider the ad hoc networks of 100 nodes randomly located in a 1,000 m × 1,000 m region based on grid topology.

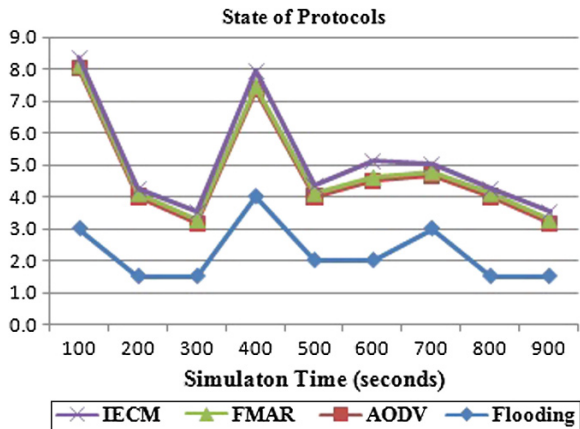
### 5.1 State of Different Protocol

Figure 1 shows the performance of state of different existing protocol with proposed protocol IECM. State of different route evaluated by ratio of throughput with energy. Each and every state has its own linguistic natures.

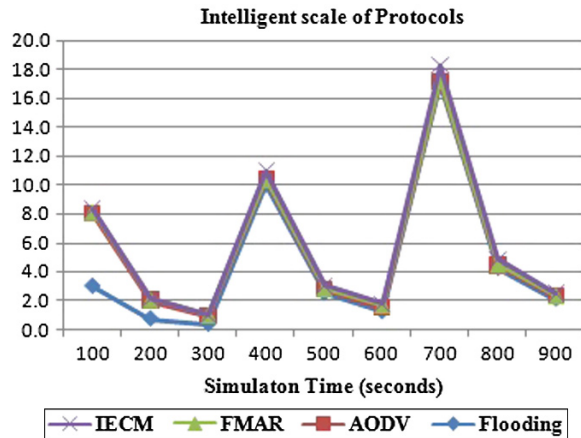
### 5.2 Intelligent Scales of Different Protocol

Figure 2 show the performance of intelligent scale of different existing protocol with proposed protocol IECM. This scales of different route evaluated by mean of throughput and energy. Each and every rating scale has its own linguistic natures.

Fig. 1 State of different route



**Fig. 2** Intelligent scaling of different route



## 6 Conclusion and Future Work

The energy efficient multipath routing is an important issue in wireless ad hoc network. Proposed IECM protocol consumes less energy and saves the network life-time. Thus, IECM provides superior network life durability of the ad hoc nodes. The simulation results shows that proposed protocol is more efficient than others existing protocols in term of multipath routing. In real life all route are not highly useful or acceptable in many situations. So, future work includes identify the statistic of network lifetime based on different parameters and deciding some threshold statistic for rating to each routes. After a certain period review all data for determining that what threshold values are most favorable for energy efficient routing. And finally, choose the optimal energy efficient routes and also next to optimal energy efficient routes according to the network statistic.

## References

1. Ishibashi, B., Boutaba, R.: Topology and mobility considerations in mobile ad hoc networks. *Ad Hoc Netw* **3**(6), 762–776 (2005). doi:10.1016/j.adhoc.2004.03.013. URL <http://www.sciencedirect.com/science/article/pii/S1570870504000289>
2. Agarwal, S., Ahuja, A., Singh, J., Shorey, R.: Route-lifetime assessment based routing (RABR) protocol for mobile ad hoc networks. In: *IEEE International Conference communication*, pp. 1697–1701 (2000)
3. Zhou, L., Haas, Z.J.: Securing ad hoc networks. *Network IEEE* **13**(6), 24–30 (1999)
4. Zussman, G., Segall, A.: Energy efficient routing in ad hoc disaster recovery networks. *Ad Hoc Netw.* **1**(4), 405–421 (2003)
5. Zheng, R., Kravets, R.: On-demand power management for ad hoc networks. *Ad Hoc Netw.* **3** (1), 51–68 (2005)

6. Su, B.-L., Wang, MShi, Huang, Y.-M.: Fuzzy logic weighted multi-criteria of dynamic route lifetime for reliable multicast routing in ad hoc networks. *Expert Syst. Appl.* **35**(1), 476–484 (2008)
7. Yu, C., Lee, B., Yong Youn, H.: Energy efficient routing protocols for mobile ad hoc networks. *Wireless Commun Mob Comput.* **3**(8), 959–973 (2003)
8. Zadeh, L.A.: Fuzzy logic, neural networks and soft computing. *Commun. ACM* **37**(3), 77–84 (1994)
9. Dana, A. et al.: A reliable routing algorithm for mobile adhoc networks based on fuzzy logic. *Int. J. Comput. Sci. Issues (IJCSI)* **8**(3), 128–133 (2011)
10. El-Hajj, W. et al.: A fuzzy-based hierarchical energy efficient routing protocol for large scale mobile ad hoc networks (feer). In: *IEEE International Conference on Communications (ICC'06)*, vol. 8, IEEE (2006)
11. Ghalavand, G. et al.: Reliable routing algorithm based on fuzzy logic for Mobile Ad hoc Network. In: *3rd International Conference on Advanced Computer Theory and Engineering (ICACTE)*, vol. 5, IEEE (2010)
12. Siddesh, G.K., Muralidhara, K.N., Manjula, N. Harihar.: Routing in Ad Hoc Wireless Networks using Soft Computing techniques and performance evaluation using Hypernet simulator. *Int J Soft Comput Eng (IJSCE)* **1**(3), 2231–2307 (2011)
13. Qayyum, A., Viennot, L., Laouiti, A.: Multipoint relaying for flooding broadcast messages in mobile wireless networks. In *Proceedings of the 35th Annual Hawaii International Conference on System Sciences*, pp. 3898–3907 (2002)
14. Perkins, C.E., Royer, E.M.: Ad-hoc on-demand distance vector routing. In: *Proceedings of the 2nd IEEE Workshop on Mobile Computing Systems and Applications* (1999)
15. Mueller, S., Tsang, R.P., Ghosal, D.: Multipath routing in mobile ad hoc networks: issues and challenges. In: *Performance Tools and Applications to Networked Systems*, pp. 209–234. Springer, Heidelberg (2004)
16. Abu, N., Samy, S., Baraka, M.H., AbdulRahman, B.: A proposed expert system for guiding freshman students in selecting a major in AL-AZHAR University, Gaza. *J. Theor. Appl. Inf. Technol.* **4**(9), 889–893 (2008)
17. Buchanan, B.G.: New research on expert systems. *Mach. Intell.* **10**, 269–299 (1982)
18. Henrion, M., Breese, J.S., Horvitz, E.J.: Decision analysis and expert systems. *AI Mag.* **12**(4), 64 (1991)
19. Barzilay, R. et al.: A new approach to expert system explanations. *COGENTEX INC ITHACA NY* (1998)
20. Adebola, O.K., Charles, A.O., Kayode, A.B.: Development of an expert system for message routing in a switched network environment. *Ann. Comput. Sci. Ser.* **10**(2), 61–70 (2012)



# An Improved Swarm Based Hybrid K-Means Clustering for Optimal Cluster Centers

Janmenjoy Nayak, Bighnaraj Naik, D.P. Kanungo and H.S. Behera

**Abstract** Clustering is a frequently used unsupervised pattern recognition technique based on the grouping properties of data. K-means is one of the best known, simple and efficient method of data clustering. But this method is more sensitive to the initial cluster partitioning and suffers in local optimal cluster centers. In this paper, an attempt has been made to hybridize the K-means algorithm with the improved Particle Swarm Optimization (PSO) to improve fitness of cluster centers. The strategy of finding global best solution of IPSO is used to avoid the possibility of falling at local optimal cluster centers. The proposed method IPSO-K-means have been compared with K-means, GA-K-means and PSO-K-means and found better in terms of objective value than the others. Simulation result shows that the proposed method is effective, steady and stable and is more suitable for cluster analysis.

**Keywords** Clustering · K-means · Improved PSO

## 1 Introduction

Clustering is an unsupervised data mining technique and is based on the concept of similarity measures between the cluster groups. The aim of the clustering is to distinguish and reform the clusters of either similar or dissimilar type relying on their distance from the cluster center. K-means clustering is one of the competent clustering

---

J. Nayak (✉) · B. Naik · D.P. Kanungo · H.S. Behera  
Department of Computer Science Engineering and Information Technology,  
Veer Surendra Sai University of Technology Burla, Sambalpur 768018, Odisha, India  
e-mail: mailforjnayak@gmail.com

B. Naik  
e-mail: mailtobnaik@gmail.com

D.P. Kanungo  
e-mail: dpk.vssut@gmail.com

H.S. Behera  
e-mail: mailtohsbehera@gmail.com

techniques for solving large scale non convex optimization problems [1]. This method is useful to reduce the sum of intra cluster distances between the clusters. The algorithm follows a simple concept of classification of a data set into a number of clusters in a dimensional space. The features of the cluster are represented through a data point and relying on the homogeneity condition for which the clusters are separated. The numbers of clusters are considered as ‘k’ (called prior knowledge) helps to group the similar objects in a closer fashion as well as make distance from the dissimilar type. Based on the distance measure from the center, the k sets of clusters are divided into another k sets of subset clusters. Each time the newly formed cluster centers can be iteratively updated by using various optimization techniques. Many researchers have shown their key interest in developing k-means algorithm for diversified application areas. A number of recently proposed k-means clustering algorithms and their applications relevant to the article have been studied in this literature.

To achieve the appropriate cluster centers in the feature space for optimizing the similarity metrics, a no. of GA based clustering algorithm have been developed [2, 3]. The Ahmadyfard and Modares [4] have discussed a hybrid clustering method based on k-means and PSO for better convergence. A novel cat swarm optimized clustering algorithm have been proposed by Santosa and Ningrum [5] for better accuracy as compared to PSO. Kader [6] presented a hybrid two-phase GAI-PSO with k-means data clustering algorithm which performs fast data clustering and can avoid premature convergence to local optima. An improved PSO based k-means algorithm was developed by Zheng and Jia [7] to avoid the local optima problem in normal k-means clustering. Wang et al. [8] introduced a parallel map reduce K-PSO by combining the traditional k-means and PSO algorithm. Naik et al. [9] have proposed a hybrid PSO—K-means clustering algorithm to get optimal cluster centers for cluster analysis. An improved k-means with a hybridized PSO algorithm for web document clustering has been introduced by Jaganathan and Jaiganesh [10]. After the combination of k-means method and mathematical morphology, Yao et al. [11] have developed an improved k-means method for fish image optimization. Monedero et al. [12] presented a modification of the celebrated k-means method for quasi unsupervised learning by controlling the size of the cluster partitions and adjusted by means of the Levenberg–Marquardt algorithm. Shahbaba and Beheshti [13] introduced a novel minimum ACE k-means (MACE) clustering method which has the advantage for the use in synthetic and real data. Tzortzis and Likas [14] developed a minmax k-means algorithm where the cluster weights are set according their variance. To deal with distributed data and overcome the limitations of k-means, Naldi and Campello [15] proposed an evolutionary k-means algorithm for clustering.

Although k-means is a highly influential clustering algorithm used in various real life applications compared to other algorithms, still it has some major limitations like sensitivity to local optimal solutions in which area more works need to be done. By inspiring this, an improved swarm based k-means algorithm has been proposed for more effective and competent real world data clustering. The remaining part of the paper is organized as following manner. Section 2, describes the basic preliminary concepts like k-means, PSO and IPSO. In the Sect. 3, the proposed method (IPSO-k-means)

has been presented. Section 4 presents the experimental set up along with the results obtained. Section 5 gives the conclusion of our work.

## 2 Preliminaries

### 2.1 K-Means Algorithm

The k-means algorithm [16, 17] receives k number of input parameters and performs the partition on a set of n objects in the dimensional space. The method of k-means starts with the random selection of k no of objects and are represented as cluster means. Depending on the distance metric between the object and the cluster mean, for each of the residual objects, a similar object is being assigned which helps to compute a new cluster mean. This process will be continued till the convergence of criterion function. Hence, k-means is able to find the best cluster center points in the space.

#### *Steps of k-means Algorithm*

1. **Select** predefined number of cluster centers randomly from the dataset.
2. **Compute** Euclidian distances of each instance from cluster centers.
3. **Assign** cluster number to each instance based on Euclidian distance. An instance  $i_j$  is assigned to cluster  $c_k$  if Euclidian distance is minimum between  $i_j$  to  $c_k$ .
4. **Find out** new cluster center by computing the mean of all instances in a cluster.
5. If the previous sets of cluster centers are same as new clustering center, then go to step-7.
6. Else go to step-2
7. Exit

### 2.2 PSO Algorithm

Particle Swarm Optimization is bird inspired metaheuristic with random selection of initial populations proposed by Kennedy and Eberhart [18]. Due to lesser parameter settings, the complexity of this population based algorithm is quite less than others. The epitome for the expansion of PSO was to consider a location having no mass or dimension, flying like a bird in multidimensional space, by adjusting its position and exchanging information about the current position in search space according to its own earlier experience and that of its neighbors [19]. While travelling in a group for either food or shelter [20], not only the behavior of various types of swarms indicates a unique indication towards the noncolliding nature between themselves, but also they adjust both their position and velocity. In this mechanism, the swarm members modify their positions as well as the velocities after communicating their group information according to the best position appeared in the current movement of the swarm [21]. The swarm particles would gradually get closer to the specified

position and finally reach the optimal position with the help of interactive cooperation [22]. Each particle has to maintain their local best positions  $lbest$  and the global best position  $gbest$  among all of them.

$$V_i^{(t+1)} = V_i^{(t)} + c_1 * \text{rand}(1) * (l_{best_i}^{(t)} - X_i^{(t)}) + c_2 * \text{rand}(1) * (g_{best}^{(t)} - X_i^{(t)}) \quad (1)$$

$$X_i^{(t+1)} = X_i^{(t)} + V_i^{(t+1)} \quad (2)$$

Equation 1 controls both cognition and social behavior of particles and next position of the particles are updated using Eq. (2),  $V_i(t)$  and  $V_i(t + 1)$  are the velocity of  $i$ th particle at time  $t$  and  $t + 1$  in the population respectively,  $c_1$  and  $c_2$  are acceleration coefficient normally set between 0 and 2 (may be same),  $X_i(t)$  is the position of  $i$ th particle and  $lbest_i(t)$  and  $gbest(t)$  denotes the local best particle of  $i$ th particle and global best particle among local bests at time  $t$ ,  $\text{rand}(1)$  generates a random value between 0 to 1.

### 2.3 Improved PSO Algorithm

In traditional PSO, the basic three steps like calculation of velocity, position and the fitness value will be iterated till the required criteria of convergence are met. The ending criteria may be the maximum change in the best fitness value. However, if the velocity of the swarm will be fixed to zero or nearer to that and the best position will have a fixed value, and then the PSO may lead to be trapped at some of local optima. This happens only due to the swarm's experience on the current and global positions. This experience is to be avoided and should be based on the mutual cooperation among all the swarms in a multidirectional manner [23].

So, in IPSO a new inertia weight factor  $\lambda$  is introduced to control both the local and global search behavior. The value of  $\lambda$  may be decreased quickly [24] during the initial iterations and slowly during the optimal iterations.

The new velocity and position updation can be realized through the Eqs. (3) and (4).

$$V_i^{(t+1)} = \lambda * V_i^{(t)} + c_1 * \text{rand}(1) * (l_{best_i}^{(t)} - X_i^{(t)}) + c_2 * \text{rand}(1) * (g_{best}^{(t)} - X_i^{(t)}) \quad (3)$$

$$X_i^{(t+1)} = X_i^{(t)} + V_i^{(t+1)} \quad (4)$$

## 3 Proposed Algorithm (IPSO-K-Means)

The proposed IPSO-K-means algorithm is a hybrid algorithm based on the combination of improved PSO with K-means algorithm for real world data clustering. Due to the slow convergence speed of basic PSO and easier finding of a local

optimal solution in K-means algorithm, the hybridization of Improved PSO along with K-means algorithm will improve the convergence speed as well as helps to find the global optimal solution. So, the advantages of both the algorithms have been used in this paper, which may lead to achieve an efficient result than the use of any individual algorithms.

**Pseudo Code of IPSO-K-Means Algorithm**

Initialize the position P and velocity V of particles randomly. Each particle is a potential solution for the clustering problem. A single particle represents the centroids of clusters. Hence the population of particles is initialized as follows (Eq. 5):

$$P = \{X_1, X_2, \dots, X_n\} \tag{5}$$

where  $X_i$  represents the centroids of clusters which is a single possible solution (particle) in the search space and can be denoted in Eq. (6).

$$X_i = \{C_{i,1}, C_{i,2}, \dots, C_{i,m}\} \tag{6}$$

where  $C_{i,j}$  represents jth cluster center among m clusters in the datasets.

Iter=1;

**While** (iter<=maxIter)

    Compute fitness of all particles  $X_i$  in population P by using the following objective function in eq. 7:

$$F(X_i) = \frac{k}{\left( \sum_{j=1}^m \sum_{i_k \in C_{i,j}} (i_k - C_{i,j})^2 \right) + d} \tag{7}$$

**If** (iter==1)

        Assign Local best particle lbest=P.

**Else**

        Evaluate fitness of P and P'.

        Compare the fitness of particles based on their fitnesses.

**If** fitness of  $i^{th}$  particle  $X_i$  in P is less than fitness of a particle in P'

            Then assign Lbest (i) = P'(i).

**Else** assign Lbest (i) = P(i).

**End of if**

**End of if**

    Select particles with best fitness value from Lbest as Gbest particle.

    Compute new velocity Vnew of the particle by using P, Lbest and gbest as follows:

$$V_{new_i}^{(t+1)} = \lambda * V_i^{(t)} + c_1 * rand(1) * (l_{best_i}^{(t)} - X_i^{(t)}) + c_2 * rand(1) * (g_{best}^{(t)} - X_i^{(t)})$$

    Generate next positions of particles P' by using P and Vnew as follows:

$$X_i^{(t+1)} = X_i^{(t)} + V_{new_i}^{(t+1)}$$

    Iter = iter+1;

**End of while**

## 4 Experimental Setup and Result Analysis

In this section, the proposed IPSO-K-Means has been implemented in MATLAB and compared with other alternatives (K-Means, GA-K-Means, PSO-K-Means). All the clustering methods are tested with multidimensional real world datasets (Table 1) from UCI repository [25] and have been compared in terms of fitness value of the cluster centers from Eq. (7). The comparison of clustering methods is listed in Table 2. The proposed method has been implemented using MATLAB 9.0 on a system with an Intel Core Duo CPU T5800, 2 GHz processor, 2 GB RAM and Microsoft Windows-2007 OS.

**Table 1** Dataset information

Datasets	No. of pattern	No. of clusters	No. of attributes
Iris	150	3	4
Lenses	24	3	4
Haberman	306	2	3
Balance scale	625	3	4
Wisconsin breast cancer	699	2	10
Contraceptive method choice	1473	3	9
Hayesroth	132	3	5
Robot navigation	5456	4	2
Spect heart	80	2	22

**Table 2** Performance Comparison of IPSO-K-means with the other clustering methods

Datasets	Fitness values of clustering algorithms			
	K-means	GA-K-means	PSO-K-means	IPSO-K-means
Iris	0.012395396	0.013826351	0.014528017	0.014580183
Lenses	0.339904827	0.351735427	0.360239542	0.360282035
Haberman	0.000317745	0.000328364	0.000348162	0.000363902
Balance scale	0.002573387	0.002628475	0.002810827	0.002920182
Wisconsin breast cancer	7.25935E-14	7.26287E-14	7.28928E-14	7.32602E-14
Contraceptive method choice	7.80139E-05	8.03819E-05	8.20198E-05	8.21983E-05
Hayes roth	4.59807E-05	4.70825E-05	4.73918E-05	4.74029E-05
Robot navigation	0.001583094	0.001828362	0.001898018	0.001928362
Spect heart	0.069341756	0.072648917	0.076041565	0.078284661

In the Eq. (7),  $k$  and  $d$  are the parameters used to calculate the fitness of clustering methods along with the proposed method. The simulation has been carried out by setting the values  $k = 50$ ,  $d = 0.1$  and proposed clustering model found better from all existing methods. The acceleration coefficients  $c1$  and  $c2$  are set to 1.4 for early convergence during IPSO iteration. The inertia weight is set between 1.8 and 2 for early convergence. The proposed Improved PSO based technique is able to produce a good cluster center of an object. But there is no certain time to meet the convergence criteria. With the increase in the number of iterations, the cluster center (initially chosen) will be attracted towards its corresponding similar clusters which will lead to obtain the final cluster center with best fitness value. The change in local and global best solution will result the updation in the new position and velocity of the cluster.

## 5 Conclusion

In this paper, a hybrid Improved swarm based K-means algorithm has been designed for the purpose of real world data clustering. The datasets have been considered from the UCI machine learning repository and are tested by various clustering methods like K-means, GA-K-means and PSO-K-means. The fitness value of the clusters obtained by the proposed method helped to get the more nearer and optimal cluster centers. The proposed method not only produces good fitness values but also it improves the cluster accuracy. The procedure to find the optimal cluster center in this paper is quite different and innovative as compared to other existing methods. The results shown in Table 2 from selected data sets indicate that the IPSO-K-means technique is able to find the global optimum solution with small standard deviations as compared to other methods. However, the future work may be planned for optimization of the initial cluster centers of k-means algorithm with the use of any other hybrid techniques.

**Acknowledgments** This work is supported by the Department of Science & Technology (DST), Ministry of Science & Technology, New Delhi, Govt. of India, under grants No. DST/INSPIRE Fellowship/2013/585.

## References

1. Bai, L., Liang, J., Sui, C., Dang, C.: Fast global k-means clustering based on local geometrical information. *Inf. Sci.* **245**, 168–180 (2013)
2. Maulik, U., Bandyopadhyay, S.: Genetic algorithm-based clustering technique. *Pattern Recogn.* **33**, 1455–1465 (2000)

3. Bandyopadhyay, S., Maulik, U., Mukhopadhyay, A.: Multiobjective genetic clustering for pixel classification in remote sensing imagery. *IEEE Trans. Geosci. Remote Sens.* **45**(5), 1506–1511(2007)
4. Ahmadyfard, A., Modares, H.: Combining PSO and k-means to Enhance Data Clustering. In: 2008 International Symposium on Telecommunications, pp. 688–691 (2008). doi:[10.1109/ISTEL.2008.4651388](https://doi.org/10.1109/ISTEL.2008.4651388)
5. Santosa, B., Ningrum, M. K.: Cat swarm optimization for clustering. In: 2009 International Conference of Soft Computing and Pattern Recognition. doi:[10.1109/SoCPaR.2009.23](https://doi.org/10.1109/SoCPaR.2009.23)
6. Kader, A.R.F.: genetically improved pso algorithm for efficient data clustering. In: 2010 Second International Conference on Machine Learning and Computing. doi:[10.1109/ICMLC.2010.19](https://doi.org/10.1109/ICMLC.2010.19)
7. Zheng, X., Jia, Y.: A study on educational data clustering approach based on improved particle swarm optimizer. In: 2011 International Symposium on IT in Medicine and Education (ITME), pp. 442–445 (2011). doi:[10.1109/ITiME.2011.6132144](https://doi.org/10.1109/ITiME.2011.6132144)
8. Wang, J., Yuan, D., Jiang, J.: Parallel K-PSO based on map reduce, pp. 1203–1208 (2012). doi: [10.1109/ICCT.2012.6511380](https://doi.org/10.1109/ICCT.2012.6511380)
9. Naik, B., Swetanisha, S., Behera, D.K., Mahapatra, S., Padhi, B.K.: Cooperative swarm based clustering algorithm based on PSO and k-means to find optimal cluster centroids. In: National Conference on Computing and Communication Systems (NCCCS), pp. 1–5 (2012). doi: [10.1109/NCCCS.2012.6413027](https://doi.org/10.1109/NCCCS.2012.6413027)
10. Jaganathan, P., Jaiganesh, S.: An improved K-means algorithm combined with particle swarm optimization approach for efficient web document clustering, pp. 772–776 (2013). doi: [10.1109/ICGCE.2013.6823538](https://doi.org/10.1109/ICGCE.2013.6823538)
11. Yao, H., Duan, Q., Li, D., Wang, L.: An improved K-means clustering algorithm for fish image segmentation. *Math. Comput. Model.* **58**, 790–798 (2013)
12. Monedero, D.R., Solé, M., Nin, J., Forné, J.: A modification of the k-means method for quasi-supervised learning. *Knowl.-Based Syst.* **37**, 176–185 (2013)
13. Shahbaba, M., Beheshti, S.: MACE-means clustering. *Sig. Process.* **105**, 216–225 (2014)
14. Tzortzis, G., Likas, A.: The min max k-means clustering algorithm. *Pattern Recogn.* **47**, 2505–2516 (2014)
15. Naldi, M.C., Campello, R.J.G.B.: Evolutionary k-means for distributed datasets. *Neurocomputing* **127**, 30–42 (2014)
16. Hartigan, J.A.: *Clustering algorithms*. Wiley, New York (1975)
17. Hartigan, J.A., Wong, M.A.: Algorithm AS 136: a K-means clustering algorithm. *J. R. Statist. Soc. Ser. C* **28**(1), 100–108 (1979). (JSTOR 2346830)
18. Kennedy, J., Eberhart, R.: Particle swarm optimization. In: Proceedings of the 1995 IEEE International Conference on Neural Networks, vol. 4, pp. 1942–1948 (1995)
19. Wei, J., Guangbin, L., Dong, L.: Elite particle swarm optimization with mutation. In: IEEE Asia Simulation Conference— 7th International Conference on System Simulation and Scientific Computing, pp. 800–803 (2008)
20. Khare, A., Rangnekar, S.: A review of particle swarm optimization and its applications in Solar Photovoltaic system. *Appl. Soft Comput.* **13**, 2997–3006 (2013)
21. Babaei, M.: A general approach to approximate solutions of nonlinear differential equations using particle swarm optimization. *Appl. Soft Comput.* **13**, 3354–3365 (2013)
22. Neri, F., Mininno, E., Iacca, G.: Compact particle swarm optimization. *Inf. Sci.* **239**, 96–121 (2013)
23. Yue-bo, M., Jian-hua, Z., Xu-sheng, G., Liang, Z.: Research on WNN aerodynamic modeling from flight data based on improved PSO algorithm. *Neurocomputing* **83**, 212–221 (2012)



24. Dehuri, S., Roy, R., Cho, S.B., Ghosh, A.: An improved swarm optimized functional link artificial neural network (ISO-FLANN) for classification. *J. Syst. Softw.* **85**, 1333–1345 (2012)
25. Bache, K., Lichman, M.: UCI machine learning repository [<http://archive.ics.uci.edu/ml>], Irvine, CA, University of California, School of Information and Computer Science (2013)

# Some More Properties of Covering Based Pessimistic Multigranular Rough Sets

B.K. Tripathy and K. Govindarajulu

**Abstract** Rough sets introduced by Pawlak as a model to capture impreciseness in data is unigranular from the granular computing point of view. In their attempts to introduce multigranulation using rough sets, two models called optimistic multigranular rough sets and pessimistic multigranular rough sets were introduced by Qian et al. in 2006 and 2010 respectively. It is well known that there are several extensions of the basic rough sets to make it more applicable and covering based rough set approach is one among them. Recently, the concept of multigranularity has been extended by Liu et al. to introduce four types of covering based optimistic multigranular rough sets (CBOMGRS). Later, Tripathy et al. introduced the notion of Covering Based Pessimistic Multigranular Rough Sets (CBPMGRS) and proved some of their properties. The important observation is that some of the properties of basic rough sets, which were not true for CBOMGRS, are true for CBPMGRS. So, CBPMGRS seems to be more natural extension of the basic concept than CBOMGRS. Recently Chai has shown that many of the results established by Liu et al. are incorrect, which they rectified. In our results in this paper, we analyse the same for CBPMGRS and incorporate the changes and establish some more properties of CBPMGRS.

**Keywords** Rough sets · Cover · Multigranulation · Optimistic and pessimistic multigranular rough sets

---

B.K. Tripathy (✉)

School of Computing Science and Engineering, VIT University,  
Vellore 632014, Tamil Nadu, India  
e-mail: tripathybk@vit.ac.in

K. Govindarajulu

Vignan Institute of Technology and Management, Mantridi,  
Berhampur 761008, Odisha, India  
e-mail: govinda\_rajulu@rediffmail.com

© Springer India 2015

J.K. Mandal et al. (eds.), *Information Systems Design and Intelligent Applications*,  
Advances in Intelligent Systems and Computing 339,  
DOI 10.1007/978-81-322-2250-7\_55

555

## 1 Introduction

The notion of Rough sets introduced by Pawlak [3] in 1981 is an uncertainty based model, which has proved to be very efficient in many application areas like soft computing, data mining, image processing, pattern recognition and medical diagnosis. The basic mathematical concept used in the definition of a rough set is the notion of equivalence relations. In rough set theory, every crisp set is approximated through a pair of crisp sets, called the lower and upper approximations of the set with respect to an equivalence relation defined over the universe of discourse. The basic notion of rough sets have been extended in many directions to accommodate more areas of application and make the concept more general as equivalence relations are relatively rare [4, 7]. However, the concepts of rough sets developed in the early years are unigranular from the granular computing point of view. In order to handle multiple granulations simultaneously, two types of multigranular rough sets; namely the optimistic multigranular rough sets and the pessimistic multigranular rough sets were introduced by Qian and Liang [5], Qian et al. [6] respectively. Covers are more general concepts than partitions. In an attempt to generalise the notion of rough sets by using covers instead of partitions, several types of covering based rough sets have been introduced in the literature. Following the same trend four types of covering based optimistic multigranular rough sets (CBOMGRS) are introduced in [2]. Several properties of these rough sets have been established there. However, it was observed by Chai [1] that many of the results claimed to be true in this paper are faulty and as a result correct versions of the faulty results have been established. Recently Tripathy et al. defined the related concept of Covering based pessimistic multigranular rough sets (CBPMGRS) and discussed their properties. It was observed in their paper that CBPMGRS seems to be a more natural extension of the basic rough set concept than CBOMGRS. In the case of partition based multigranular rough sets it was established by Tripathy and Raghavan [8, 9] that some of the properties of pessimistic and optimistic versions are different. Also, a comparison of these two types of rough sets and other related rough sets were established. We shall try to establish these properties in the extended cases.

The structure of the rest of this paper is as follows. In Sect. 2 we introduce the different notations and concepts to be used in the paper. In Sect. 3, we shall tabulate the properties of the basic MGRS to be used in the paper.

## 2 Definitions and Notations

In this section we shall introduce the different notations and concepts to be used in the paper. First we start with the definition of rough sets as introduced by Pawlak [3].

Let  $U$  be a universe of discourse and  $R$  be an equivalence relation over  $U$ . By  $U/R$  we denote the family of all equivalence class of  $R$ , referred to as categories or concepts of  $R$  and the equivalence class of an element  $x \in U$ , is denoted by  $[x]_R$ .

By a knowledge base, we understand a relational system  $K = (U, Q)$ , where  $U$  is as above and  $Q$  is a family of equivalence relations over  $U$ . For any subset  $P(\neq \phi) \subseteq Q$ , the intersection of all equivalence relations in  $P$  is denoted by  $IND(P)$  and is called the indiscernibility relation over  $P$ .

**Definition 2.1** Given any  $X \subseteq U$  and  $R \in IND(K)$ , we associate two subsets,  $\underline{R}X = \cup\{Y \in U/R : Y \subseteq X\}$  and  $\overline{R}X = \cup\{Y \in U/R | Y \cap X \neq \phi\}$ , called the R-lower and R-upper approximations of  $X$  respectively.

The R-boundary of  $X$  is denoted by  $BN_R(X)$  and is given by  $BN_R(X) = \overline{R}X - \underline{R}X$ .

The elements of  $\underline{R}X$  are those elements of  $U$ , which can certainly be classified as elements of  $X$ , and the elements of  $\overline{R}X$  are those elements of  $U$ , which can possibly be classified as elements of  $X$ , employing knowledge of  $R$ . We say that  $X$  is rough with respect to  $R$  if and only if  $\underline{R}X \neq \overline{R}X$ , equivalently  $BN_R(X) \neq \phi$ .  $X$  is said to be R-definable if and only if  $\overline{R}Y$ , or  $BN_R(X) = \phi$ .

For basic rough sets, the following properties hold true.

(L1) $\underline{R}X \subseteq X$	(U1) $\underline{R}X \subseteq X$
(L2) $\underline{R}\phi = \phi$	(U2) $\underline{R}\phi = \phi$
(L3) $\underline{R}U = U$	(U3) $\underline{R}U = U$
(L4) $\underline{R}(X \cap Y) = \underline{R}X \cap \underline{R}Y$	(U4) $\underline{R}(X \cap Y) = \underline{R}X \cap \underline{R}Y$
(L5) $X \subseteq Y \Rightarrow \underline{R}X \subseteq \underline{R}Y$	(U5) $X \subseteq Y \Rightarrow \underline{R}X \subseteq \underline{R}Y$
(L6) $\underline{R}(X \cup Y) \supseteq \underline{R}X \cup \underline{R}Y$	(U6) $\underline{R}(X \cup Y) \supseteq \underline{R}X \cup \underline{R}Y$
(L7) $\underline{R}(\sim X) = \sim \overline{R}X$	(U7) $\underline{R}(\sim X) = \sim \overline{R}X$
(L8) $\underline{R}\underline{R}X = \underline{R}X$	(U8) $\underline{R}\underline{R}X = \underline{R}X$
(L9) $\forall X \in U/R, \underline{R}X = X$	(U9) $\forall X \in U/R, \underline{R}X = X$

The optimistic multigranular rough sets were introduced by Qian and Liang [5] as follows. We note that in the beginning there was only one type of Multigranulation and it was not named as optimistic. After the development of a second type of Multigranulation, the first one was called optimistic and the second one was called as pessimistic [5]. We note that we are considering two-granulations only. For granulations of higher order, the definitions and properties are similar. The notations used for the two types of Multigranulations were different in the original papers. But we follow the notations used in a recent paper by Tripathy et al. [7–9]. That is we use  $R + S$  for optimistic Multigranulation and  $R * S$  for pessimistic Multigranulation, where  $R$  and  $S$  are two equivalence relations on  $U$ .

**Definition 2.2** Let  $K = (U, \mathbf{R})$  be a knowledge base,  $\mathbf{R}$  be a family of equivalence relations,  $X \subseteq U$  and  $R, S \in \mathbf{R}$ . We define [7] the optimistic multi-granular lower approximation and optimistic multi-granular upper approximation of  $X$  with respect to  $R$  and  $S$  in  $U$  as

$$\underline{R+S}X = \{x|[x]_R \subseteq X \text{ or } [x]_S \subseteq X\} \tag{2.1}$$

$$\overline{R+S}X = \sim(\underline{R+S}(\sim X)) \tag{2.2}$$

**Definition 2.3** Let  $K = (U, \mathbf{R})$  be a knowledge base,  $\mathbf{R}$  be a family of equivalence relations,  $X \subseteq U$  and  $R, S \in \mathbf{R}$ . We define [6] the pessimistic multi-granular lower approximation and pessimistic multi-granular upper approximation of  $X$  with respect to  $R$  and  $S$  in  $U$  as

$$\underline{R*S}X = \{x|[x]_R \subseteq X \text{ and } [x]_S \subseteq X\} \tag{2.3}$$

$$\overline{R*S}X = \sim(\underline{R*S}(\sim X)) \tag{2.4}$$

Next we present some properties of multigranular rough sets, which shall be used in the proofs of the results of this paper [8, 9].

$$\underline{R+S}(X \cap Y) \subseteq \underline{R+S}(X) \cup \underline{R+S}(Y) \tag{2.5}$$

$$\underline{R+S}(X \cup Y) \supseteq \underline{R+S}(X) \cup \underline{R+S}(Y) \tag{2.6}$$

$$\overline{R+S}(X \cap Y) \subseteq \overline{R+S}(X) \cap \overline{R+S}(Y) \tag{2.7}$$

$$\overline{R+S}(X \cup Y) \supseteq \overline{R+S}(X) \cup \overline{R+S}(Y) \tag{2.8}$$

$$\underline{R*S}(X \cup Y) \supseteq \underline{R*S}(X) \cup \underline{R*S}(Y) \tag{2.9}$$

$$\overline{R*S}(X \cap Y) \supseteq \overline{R*S}(X) \cap \overline{R*S}(Y) \tag{2.10}$$

$$\underline{R*S}(X \cap Y) = \underline{R*S}(X) \cap \underline{R*S}(Y) \tag{2.11}$$

$$\overline{R*S}(X \cup Y) = \overline{R*S}(X) \cup \overline{R*S}(Y) \tag{2.12}$$

### 3 Covering Based Multigranular Rough Sets (CBMGRS)

Four types of covering based multigranular rough sets were introduced by Liu et al. [2] very recently. These four types have been introduced for CBPMGRS by Tripathy et al. very recently. We present the four types of CBPMGRS below. We first present some definitions which are to be used in the sequel.

**Definition 3.1** Let  $(U, C)$  be a covering approximation space, where  $C = \{C_1, C_2, \dots, C_n\}$ . For any  $x \in U$ , we define the sets minimal descriptor and maximal descriptor of  $x$  with respect to  $C$  as

$$md_C(x) = \{K \in C \mid x \in K \text{ and } \forall S \in C \text{ such that } x \in S, S \subseteq K \Rightarrow S = K\} \quad (3.1)$$

and

$$MD_C(x) = \{K \in C \mid x \in K \text{ and } \forall S \in C \text{ such that } x \in S, S \supseteq K \Rightarrow S = K\} \quad (3.2)$$

**Note 3.1** It can be observed that the elements of  $md_C(x)$  are those elements  $K$  of  $C$  which contain  $x$  and there is no other element of  $C$  containing  $x$  which are subsets of  $K$ .

Similarly, the elements of  $MD_C(x)$  are those elements  $K$  of  $C$  which contain  $x$  and there is no other element of  $C$  containing  $x$  which are supersets of  $K$ .

**Definition 3.2** Let  $(U, C)$  be a covering approximation space and  $C_1, C_2 \in C$ . Then for any  $X \subseteq U$ , its type-I pessimistic lower and upper approximations with respect to  $C_1$  and  $C_2$  are defined as

$$\underline{FR}_{C_1 * C_2}(X) = \{x \in U \mid \cap md_{C_1}(x) \subseteq X \text{ and } \cap md_{C_2}(x) \subseteq X\}; \quad (3.3)$$

$$\overline{FR}_{C_1 * C_2}(X) = \{x \in U \mid (\cap md_{C_1}(x)) \cap X \neq \phi \text{ or } (\cap md_{C_2}(x)) \cap X \neq \phi\}; \quad (3.4)$$

If  $\underline{FR}_{C_1 * C_2}(X) \neq \overline{FR}_{C_1 * C_2}(X)$  then  $X$  is called a type-I pessimistic multigranular covering rough set with respect to  $C_1$  and  $C_2$ . Else,  $X$  is said to be type-I pessimistic definable with respect to  $C_1$  and  $C_2$ .

**Definition 3.3** Let  $(U, C)$  be a covering approximation space and  $C_1, C_2 \in C$ . Then for any  $X \subseteq U$ , its type-II pessimistic lower and upper approximations with respect to  $C_1$  and  $C_2$  are defined as

$$\underline{SR}_{C_1 * C_2}(X) = \{x \in U \mid \cup md_{C_1}(x) \subseteq X \text{ and } \cup md_{C_2}(x) \subseteq X\}; \quad (3.5)$$

$$\overline{SR}_{C_1 * C_2}(X) = \{x \in U \mid (\cup md_{C_1}(x)) \cap X \neq \phi \text{ or } (\cup md_{C_2}(x)) \cap X \neq \phi\}; \quad (3.6)$$

If  $\underline{SR}_{C_1 * C_2}(X) \neq \overline{SR}_{C_1 * C_2}(X)$  then  $X$  is called a type-II pessimistic multigranular covering rough set with respect to  $C_1$  and  $C_2$ . Else,  $X$  is said to be type-I pessimistic definable with respect to  $C_1$  and  $C_2$ .

**Definition 3.4** Let  $(U, C)$  be a covering approximation space and  $C_1, C_2 \in C$ . Then for any  $X \subseteq U$ , its type-III lower and upper approximations with respect to  $C_1$  and  $C_2$  are defined as

$$\underline{TR}_{C_1 * C_2}(X) = \{x \in U \mid \cap MD_{C_1}(x) \subseteq X \text{ and } \cap MD_{C_2}(x) \subseteq X\}; \quad (3.7)$$

$$\overline{TR}_{C_1 * C_2}(X) = \{x \in U \mid (\cap MD_{C_1}(x)) \cap X \neq \phi \text{ or } (\cap MD_{C_2}(x)) \cap X \neq \phi\}; \quad (3.8)$$

If  $\underline{TR}_{C_1 * C_2}(X) \neq \overline{TR}_{C_1 * C_2}(X)$  then  $X$  is called a type-III pessimistic multigranular covering rough set with respect to  $C_1$  and  $C_2$ . Else,  $X$  is said to be type-III definable with respect to  $C_1$  and  $C_2$ .

**Definition 3.5** Let  $(U, C)$  be a covering approximation space and  $C_1, C_2 \in C$ . Then for any  $X \subseteq U$ , its type-IV lower and upper approximations with respect to  $C_1$  and  $C_2$  are defined as

$$\underline{LR}_{C_1 * C_2}(X) = \{x \in U \mid \cup MD_{C_1}(x) \subseteq X \text{ and } \cup MD_{C_2}(x) \subseteq X\}; \quad (3.9)$$

$$\overline{LR}_{C_1 * C_2}(X) = \{x \in U \mid (\cup MD_{C_1}(x) \cap X \neq \phi \text{ or } \cup MD_{C_2}(x) \cap X \neq \phi)\}; \quad (3.10)$$

If  $\underline{LR}_{C_1 * C_2}(X) \neq \overline{LR}_{C_1 * C_2}(X)$  then  $X$  is called a type-IV pessimistic multigranular covering rough set with respect to  $C_1$  and  $C_2$ . Else,  $X$  is said to be type-IV definable with respect to  $C_1$  and  $C_2$ .

**Definition 3.6** Let  $C$  be a covering of  $U$  and  $K \in C$ . If  $K$  is the union of some elements in  $C - \{K\}$  then we say  $K$  is a reducible element of  $C$ . Otherwise,  $K$  is said to be an irreducible element of  $C$ .

Removing all the reducible elements from  $C$ , we get the reduct of  $C$  denoted by  $\text{reduct}(C)$ .

**Definition 3.7**  $(U, C)$  be a covering approximation space and  $C_1, C_2 \in C$ . Let  $\text{reduct}(C_1) = \{C_{11}, C_{12}, \dots, C_{1p}\}$  and  $\text{reduct}(C_2) = \{C_{21}, C_{22}, \dots, C_{2q}\}$ . If for each  $C_{1i} \in C_1 \exists C_{2j} \in \text{reduct}(C_2)$  such that  $C_{1i} \subseteq C_{2j}$  then we say  $C_1$  is finer than  $C_2$  and write  $C_1 \prec C_2$ .

**Note 3.2** If  $C_1 \prec C_2$  then for any  $x \in U, md_{C_1}(x) \subseteq md_{C_2}(x)$  and  $MD_{C_1}(x) \subseteq MD_{C_2}(x)$ .

### 4 Properties of CBPMGRS

The following results were established in Tripathy and Govindarajulu [10].

**Theorem 4.1** Let  $(U, C)$  be a covering approximation space and  $C_1, C_2 \in C$ . Then for any  $X \subseteq U$ , we have

$$\underline{FR}_{C_1 * C_2}(\sim X) = \sim \overline{FR}_{C_1 * C_2}(X), \overline{FR}_{C_1 * C_2}(\sim X) = \sim \underline{FR}_{C_1 * C_2}(X) \quad (4.1)$$

$$\underline{SR}_{C_1 * C_2}(\sim X) = \sim \overline{SR}_{C_1 * C_2}(X), \overline{SR}_{C_1 * C_2}(\sim X) = \sim \underline{SR}_{C_1 * C_2}(X) \quad (4.2)$$

$$\underline{TR}_{C_1 * C_2}(\sim X) = \sim \overline{TR}_{C_1 * C_2}(X), \overline{TR}_{C_1 * C_2}(\sim X) = \sim \underline{TR}_{C_1 * C_2}(X) \quad (4.3)$$

$$\underline{LR}_{C_1 * C_2}(\sim X) = \sim \overline{LR}_{C_1 * C_2}(X), \overline{LR}_{C_1 * C_2}(\sim X) = \sim \underline{LR}_{C_1 * C_2}(X) \quad (4.4)$$

### 4.1 Basic Properties of Approximation Operators

It was observed in [2] that out of the nine basic properties of rough set approximation operators three properties do not hold for CBOMGRS. However, it was shown in [10] that. We summarise these properties in the following table.

Lower approximation properties	$\underline{FR}$	$\underline{SR}$	$\underline{TR}$	$\underline{LR}$	Upper approximation properties	$\overline{FR}$	$\overline{SR}$	$\overline{TR}$	$\overline{LR}$
L1	Yes	Yes	Yes	Yes	U1	Yes	Yes	Yes	Yes
L2	Yes	Yes	Yes	Yes	U2	Yes	Yes	Yes	Yes
L3	Yes	Yes	Yes	Yes	U3	Yes	Yes	Yes	Yes
L4	Yes	Yes	Yes	Yes	U4	Yes	Yes	Yes	Yes
L5	Yes	Yes	Yes	Yes	U5	Yes	Yes	Yes	Yes
L6	Yes	Yes	Yes	Yes	U6	Yes	Yes	Yes	Yes
L7	Yes	Yes	Yes	Yes	U7	Yes	Yes	Yes	Yes
L8	Yes	Yes	Yes	Yes	U8	Yes	Yes	Yes	Yes
L9	Yes	Yes	Yes	Yes	U9	No	No	No	No

**Note 4.1** We would like to note that the properties (L4) and (U4) do not hold for CBOMGRS.

**Theorem 4.2** *Let  $(U, C)$  be a covering approximation space and  $C_1, C_2 \in C$ . Then for any  $X, Y \subseteq U$ , the following properties hold true:*

$$X \subseteq Y \Rightarrow \underline{FR}_{C_1 * C_2}(X) \subseteq \underline{FR}_{C_1 * C_2}(Y) \tag{4.5}$$

$$X \subseteq Y \Rightarrow \overline{FR}_{C_1 * C_2}(X) \subseteq \overline{FR}_{C_1 * C_2}(Y) \tag{4.6}$$

$$\underline{FR}_{C_1 * C_2}(X \cap Y) = \underline{FR}_{C_1 * C_2}(X) \cap \underline{FR}_{C_1 * C_2}(Y) \tag{4.7}$$

$$\underline{FR}_{C_1 * C_2}(X \cup Y) \supseteq \underline{FR}_{C_1 * C_2}(X) \cup \underline{FR}_{C_1 * C_2}(Y) \tag{4.8}$$

$$\overline{FR}_{C_1 * C_2}(X \cup Y) = \overline{FR}_{C_1 * C_2}(X) \cup \overline{FR}_{C_1 * C_2}(Y) \tag{4.9}$$

$$\overline{FR}_{C_1 * C_2}(X \cap Y) \subseteq \overline{FR}_{C_1 * C_2}(X) \cap \overline{FR}_{C_1 * C_2}(Y) \tag{4.10}$$

## 5 Some New Properties of CBPMGRS

**Theorem 5.1** *Let  $(U, C)$  be a covering approximation space and  $C_1, C_2 \in C$ . For any  $X \subseteq U$  if  $C_1 \prec C_2$  then  $\underline{FR}_{C_1 * C_2}(X) = \underline{F}_{C_2}(X)$  and  $\overline{FR}_{C_1 * C_2}(X) = \overline{FR}_{C_1}(X)$ .*



*Proof* For any  $X \subseteq U$  we have

$$\begin{aligned} \underline{FR}_{C_1 * C_2}(X) &= \{x \in U \mid \cap md_{C_1}(x) \subseteq X \text{ and } \cap md_{C_2}(x) \subseteq X\} \\ &= \{x \in U \mid \cap md_{C_2}(x) \subseteq X\} \text{ (since } \cap md_{C_1}(x) \subseteq \cap md_{C_2}(x)\text{)} \\ &= \underline{FR}_{C_2}(X) \end{aligned}$$

Again,

$$\begin{aligned} \overline{FR}_{C_1 * C_2}(X) &= \{x \in U \mid (\cap md_{C_1}(x)) \cap X \neq \phi \text{ or } (\cap md_{C_2}(x)) \cap X \neq \phi\} \\ &= \{x \in U \mid (\cap md_{C_1}(x)) \cap X \neq \phi\} \text{ (since } \cap md_{C_1}(x) \subseteq \cap md_{C_2}(x)\text{)} \\ &= \overline{FR}_{C_1}(X) \end{aligned}$$

This completes the proof.  $\square$

**Note 5.1** It may be noted that the lower approximations under multi-covering is same as the second one in and the upper one is same as the first covering. This was not the case for CBOMGRS. It was both the first covering only.

**Theorem 5.2** *Let  $(U, C)$  be a covering approximation space and  $C_1, C_2 \in C$ . Then  $FR_{C_1 * C_2}$  and  $FR_{\text{reduct}(C_1) * \text{reduct}(C_2)}$  and  $SR_{C_1 * C_2}$  and  $SR_{\text{reduct}(C_1) * \text{reduct}(C_2)}$  produce the same multigranulations. That is their lower and upper approximations are the same.*

*Proof* The proof follows as the ‘md’ for both C and reduct(C) are the same.  $\square$

**Note 5.2** The same cannot be said about the other two types of CBOMGRS as ‘MD’ for C and reduct(C) may not be same.

We need the following two definitions for establishing the other results of the paper.

**Definition 5.1** Let C be a covering of U and K be an element of C. If there exists another element K’ of C such that  $K \subset K'$ , we shall say that K is an immured element of covering C.

**Definition 5.2** If we remove all the immured elements of C from C and still we get a covering of U. then the new covering obtained in this way is called the exclusion (C). In [2] sufficient conditions for four coverings from C such that the first two produce the same granulation as the last two was obtained for all four types of covering based optimistic multigranulation were derived. But it was shown in [1] that the result is not true and afresh theorem was proved. We prove the same theorem for PMGRS in the following form.

**Theorem 5.3** *Let  $(U, C)$  be a multigranular covering approximation space and  $C_1, C_2, C_3, C_4 \in C$ . Then  $C_1 * C_2$  and  $C_3 * C_4$  produce the same multigranulations iff either (1) and (4) or (2) and (3) are satisfied from the following.*

1.  $reduct(C_1) = reduct(C_3)$  and  $exclusion(C_1) = exclusion(C_3)$
2.  $reduct(C_1) = reduct(C_4)$  and  $exclusion(C_1) = exclusion(C_4)$
3.  $reduct(C_2) = reduct(C_3)$  and  $exclusion(C_2) = exclusion(C_3)$
4.  $reduct(C_2) = reduct(C_4)$  and  $exclusion(C_2) = exclusion(C_4)$

*Proof* The proofs follows from the fact that C and  $reduct(C)$  produce the same ‘md’ and the definitions of the first type and second type of covering based optimistic multigranulation approximations depend upon ‘md’. □

Similarly, C and  $reduct\textcircled{C}$  produce the same ‘MD’ and the definitions of the third type and fourth type of covering based optimistic multigranulation approximations depend upon ‘MD’.

A result providing sufficient conditions for two different type-1 or type-2 CPMGRS to produce identical lower and upper approximation operators was obtained by using reducts. But it was shown in [1] that the result is again faulty. However, a corrected version was proposed. We provide below a CBPMGRS version of the same result.

**Theorem 5.4** *Let  $(U, C)$  be a multigranular covering approximation space and  $C_1, C_2, C_3, C_4 \in C$ . Then  $FR_{C_1 * C_2}$  and  $FR_{C_3 * C_4}$ ,  $SR_{C_1 * C_2}$  and  $SR_{C_3 * C_4}$  produce identical lower and upper approximations if at least one of the following conditions hold true:*

1.  $exclusion(C_1) = exclusion(C_3)$  and  $exclusion(C_2) = exclusion(C_4)$
2.  $exclusion(C_1) = exclusion(C_4)$  and  $exclusion(C_2) = exclusion(C_3)$

*Proof* We have C and  $exclusion(C)$  produce the same ‘md’. Also, if  $exclusion(C_1) = exclusion(C_3)$  then  $C_1$  and  $C_3$  produce the same ‘md’. Similarly,  $C_2$  and  $C_4$  produce the same ‘md’. So,  $FR_{C_1 * C_2}$  and  $FR_{C_3 * C_4}$  produce the same lower and upper approximations. The other part follows similarly.

A theorem which provides the relationship among the four types of CBOMGRS was provided in [2]. However, the equalities were found to be not true in [1]. However, inclusions hold true. We present below the result which is true for the pessimistic case below. □

**Theorem 5.5** *Let  $(U, C)$  be a multigranular covering approximation space and  $C_1, C_2 \in C$ . Then*

1.  $\underline{SR}_{C_1 * C_2}(X) \cup \underline{TR}_{C_1 * C_2}(X) \subseteq \underline{FR}_{C_1 * C_2}(X)$ ;
2.  $\underline{SR}_{C_1 * C_2}(X) \cap \underline{TR}_{C_1 * C_2}(X) \supseteq \underline{LR}_{C_1 * C_2}(X)$ ;
3.  $\overline{SR}_{C_1 * C_2}(X) \cup \overline{TR}_{C_1 * C_2}(X) \subseteq \overline{LR}_{C_1 * C_2}(X)$ ;
4.  $\overline{SR}_{C_1 * C_2}(X) \cap \overline{TR}_{C_1 * C_2}(X) \supseteq \overline{FR}_{C_1 * C_2}(X)$ ;

*Proof* Follows directly from the definitions of CBPMGRS lower and upper approximations. □

## 6 Conclusion

In this paper we established many properties of Covering Based Pessimistic Multigranular Rough Sets (CBPMGRS) introduced in Tripathy and Govindarajulu [10]. We have analysed the results in [2] and combined it with the remarks on the validity of these results in [1] and synthesized our results accordingly. We observed that many results which hold true for the optimistic case take different shapes in the pessimistic case.

## References

1. Chai, R.: Comments on the paper on multigranulation covering rough sets. Prepublication J. Approximate Reasoning (2014)
2. Liu, C., Miao, D., Qian, J.: On multi-granulation covering sets. *Int. J. Approximate Reasoning* (2014), (Article in press)
3. Pawlak, Z.: Rough Sets. *Int. J. Comput. Inform. Sci.* **11**, 341–356 (1982)
4. Pawlak, Z., Skowron, A.: Rough sets: some extensions. *Inf. Sci.* **177**, 28–40 (2007)
5. Qian, Y.H., Liang, J.Y.: Rough set method based on multi-granulations. In: Proceedings of the 5th IEEE Conference on Cognitive Informatics, vol. 1, pp. 297–303 (2006)
6. Qian, Y.H., Liang, J.Y., Dang, C.Y.: Pessimistic rough decision. In: Proceedings of RST 2010, pp. 440–449. Zhoushan, China (2010)
7. Tripathy, B.K.: Rough sets on fuzzy approximation spaces and intuitionistic fuzzy approximation spaces. Springer international studies in computational intelligence. In: Abraham, A., Falcon, R., Bello, R. (eds.) *Rough Set Theory: A True landmark in Data Analysis*, vol. 174, pp. 3–44 (2009)
8. Tripathy, B.K., Raghavan, R.: Some algebraic properties of multigranulations and an analysis of multigranular approximations of classifications. *Int. J. Inf. Technol. Comput. Sci.* **7**, 63–70 (2013)
9. Tripathy, B.K., Raghavan, R.: On some comparison properties of rough sets based on multigranulations and types of multigranular approximations of classifications. *Int. J. Intell. Syst. Appl.* **06**, 70–77 (2013)
10. Tripathy, B.K., Govindarajulu, K.: On covering based pessimistic multi granular rough sets. Accepted for presentation at ICCICN 2014, Kolkata, India, 2014

# Performance Analysis of MC-CDMA in Rayleigh Channel Using Walsh Code with BPSK Modulation

S. Kuzhaloli and K.S. Shaji

**Abstract** High Speed data rate communication is possible with the help of the Multi Carrier Code Division Multiple Access (MC-CDMA). Inter symbol Interference (ISI) and frequency diversity problems are resolved by MC-CDMA. This paper analyzes the performance of MC-CDMA in the presence of Additive White Gaussian noise using a BPSK modulator in Rayleigh fading channel. The results based on various combining techniques for different users are simulated and compared using MATLAB software.

**Keywords** MC-CDMA · AWGN · BPSK · MRC · ZF

## 1 Introduction

Conventional CDMA multiplexing technique involves many number of users where each user is assigned with a specific code dedicated to it and this is encoded and decoded by the transmitter and the receiver respectively. On the other hand, Orthogonal Frequency Division Multiplexing (OFDMA) also plays a major role in transmission of signal at increased data rates. MC-CDMA referred to as a Frequency domain spreading technique. In this technique each code is transmitted simultaneously with number of subcarriers multiplied by their own spreading code. It is a combination of OFDMA and CDMA and has the benefits of CDMA along with the frequency selectivity of OFDMA. The main contribution of this paper is based on the equalization techniques or the combining techniques like Maximal-

---

S. Kuzhaloli (✉)

Department of ETCE, Sathyabama University, Chennai, Tamil Nadu, India  
e-mail: kuzhal\_oli@yahoo.com

K.S. Shaji

RIITW, Nagercoil, Tamil Nadu, India

© Springer India 2015

J.K. Mandal et al. (eds.), *Information Systems Design and Intelligent Applications*,  
Advances in Intelligent Systems and Computing 339,  
DOI 10.1007/978-81-322-2250-7\_56

565

Ratio Combining and the Zero Forcing is the estimation of the Bit Error Rate (BER) performance using a Binary Phase Shift Keying modulation technique with ordered Hadamard sequence or the Walsh sequence as the spreading codes. This is analyzed for a Rayleigh fading channel conditions of MC-CDMA in the presence of Additive White Gaussian noise (AWGN).

## 2 MC-CDMA System

The main difference between the MC-CDMA and MC-DS CDMA system is that the MC-CDMA is a frequency domain spreading technique and MC-DS-CDMA is a time domain spreading technique. MC-CDMA system is often looked as a combination of CDMA and OFDMA which helps in higher data rates and results in better frequency diversity and has the added advantage of increasing the bandwidth efficiency. It can also be defined as DS-SS-SS-SS modulated again by an OFDMA subcarrier. In this MC-CDMA system a single data symbol is transmitted over a number of narrow band sub-carriers. The spreading technique is carried out in the frequency domain. Both the MC-CDMA transmitter and receiver work with the orthogonal codes.

## 3 Spreading Codes

The spreading codes that are used in CDMA system are Pseudo noise sequence or m-sequence, Gold codes, Walsh codes, Hadamard codes etc. This MC-CDMA is implemented using Walsh Codes [1]. Walsh matrix is a square matrix, derived from Hadamard matrix, where every row is orthogonal to all other rows in the matrix and every column is orthogonal to all other columns in the matrix. User 1 is assigned with code 1 representing the 2nd row of the Walsh code matrix. Similarly User 2 is assigned with the 15th row of the Walsh code matrix. The number of data sub-carriers  $N_c$  is considered to be 16.

The general Hadamard matrix is given by

$$H_{2N} = \begin{array}{|c|c|} \hline H_N & H_N \\ \hline H_N & \overline{H_N} \\ \hline \end{array}$$

The Walsh matrix is obtained from Hadamard matrix with ordered sequencing and the matrix for 16 subcarriers is represented by the  $H_{16}$  matrix.

## 4 BPSK Modulation

Various modulation techniques are involved in modulating the spreaded signal by the carrier signal. But normally some form of Phase shift Keying (PSK) techniques like Binary Phase shift Keying (BPSK), Differential Phase shift Keying (DPSK), Quadrature Phase shift Keying (QPSK) and Minimum Shift Keying (MSK) are involved. Here the modulation technique used is BPSK modulation [2]. Constellation diagram is the most convenient way to represent PSK schemes. Points are plotted in the complex plane wherein the real axis is called the in-phase axes and the imaginary axis is known as the quadrature axes as both the axes are separated by  $90^\circ$ . These constellation points are placed on a circle with uniform angular spacing. Good immunity is achieved by placing the points with maximum plane separation. Any number of phases can be used for the modulation scheme. Here Binary phase Shift keying (BPSK) scheme is considered which uses only two phases separated by  $180^\circ$ . The BPSK equation takes the form  $s_n(t) = \sqrt{(2E_b/T_b)} * \cos(2\pi f_c t + \pi(1 - n))$  yields two phases 0 and  $\pi$ .

## 5 System Channel

The medium which is physically present between the transmitter and the receiver is known as the channel. Noise is present in this physical channel in all the communication systems. Major sources of noises that are generated in the channel are thermal Noise, electrical Noise, Inter-cellular Interference etc. Apart from these noises there are noises that are developed internally like Inter symbol Interference, Inter carrier Interference, Inter Modulation distortion etc. The two channels that are considered in this paper are the Additive White Gaussian Noise (AWGN) and the Rayleigh Channel [3, 4].

### 5.1 AWGN Channel

The very simple environment considered is the Additive white Gaussian Noise (AWGN) channel. The major source is the thermal noise and due to its simplicity manmade noise model as well as multiuser interference is also considered. The general expression to describe an AWGN channel is given by  $g(t) = s(t) + v(t)$ . In

the above expression  $d(t)$  is the transmitted input signal and  $v(t)$  is the additive white noise or disturbance. Spectral density is uniform for this random noise and the amplitude follows Gaussian distribution.

## ***5.2 Rayleigh Channel***

There is large delay in transmitting the signal as there is too much of dispersion when obstacles lie between the transmitting end and receiving end, that is, when they do not lie in the Line-of-sight (LOS). Hence there are several number of transmission paths which leads to superposition. When more number of paths are available they are analyzed using the central limit theorem and they follow the statistical characteristics of the Rayleigh distribution.

## **6 Combining Techniques**

The combining techniques are also referred to as equalizing techniques in which an equalizer is introduced in a network to recover the signal that is badly affected by the Inter symbol Interference and helps in improving the Signal-to-Noise Ratio (SNR) by improving the BER characteristics [5, 6]. The equalizers involved in these techniques are:

### ***6.1 Maximal Ratio Combining (MRC)***

This Maximal-Ratio Combining is also called as ratio-squared or pre detection combining. In this technique every signal is multiplied by a weight factor which is proportional to the signal amplitude. Here signals from every channel is combined together and gain of every channel is made to be inversely proportional to the mean square noise level of that channel and is directly proportional to the root-mean-square value of the signal.

### ***6.2 Zero Forcing (ZF)***

Zero forcing Equalizer is a linear form of equalization algorithm, applies inverse of the frequency channel response to the received signal and hence restores the signal. This zero forcing forces the Inter Symbol Interference to zero. If the channel

frequency response is given by  $F(f)$ , the zero forcing equalization  $E(f)$  is given by  $E(f) = 1/F(f)$ . Hence by combining the channel and the equalizer, the flat frequency response and the linear phase is equal to one i.e.,  $E(f) F(f) = 1$ . The Zero forcing detector has the constraint given by  $W = [H^H \ H]^{-1} \ H^H$ , where  $W$  is the Equalization matrix and  $H$  is the channel matrix. This is known as the pseudo inverse matrix of the general matrix.

### 7 Simulation Results

Simulation is done using MATLAB software. First a random Binary sequence of +1 and -1 is generated and the symbols are multiplied with the channels. Then an Additive White Gaussian noise is added. Finally an equalization procedure is carried out at the receiver and the BER is calculated [7]. Number of users and number of subcarriers considered are 2 and 16 respectively. The modulation technique used is BPSK modulation. Both the sequences are spreaded and IFFT operation is carried out. A cyclic prefix is appended for the users. The number of tappings considered in the Rayleigh channel is 4. Finally Bit Error Rate is calculated for both MRC and ZF Equalization techniques for both the users. The outputs are obtained as shown in Figs. 1, 2, 3 and 4 respectively.

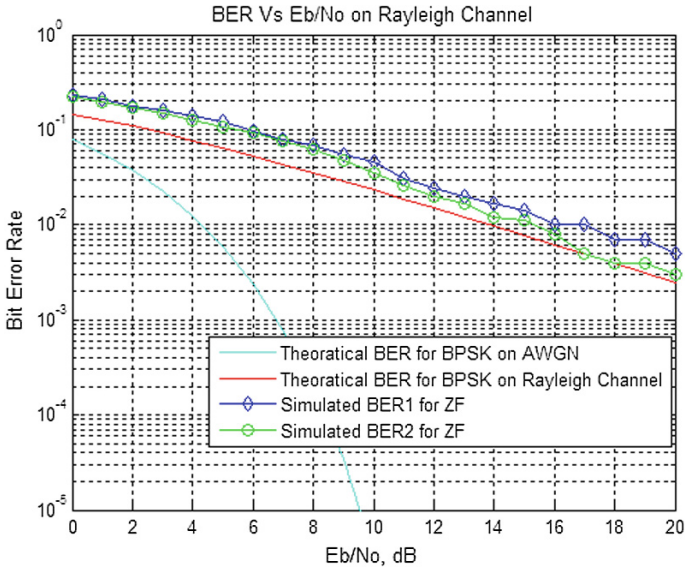


Fig. 1 BER/No for ZF technique for user 1 & 2



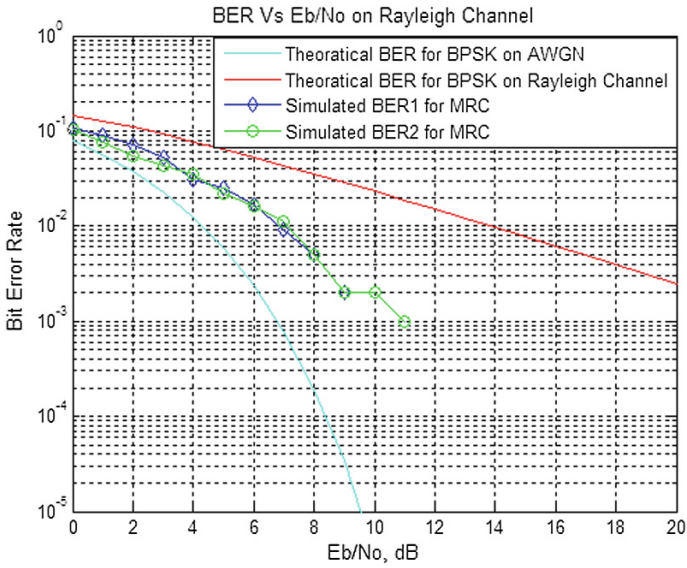


Fig. 2 BER/No for MRC technique for user 1 & 2

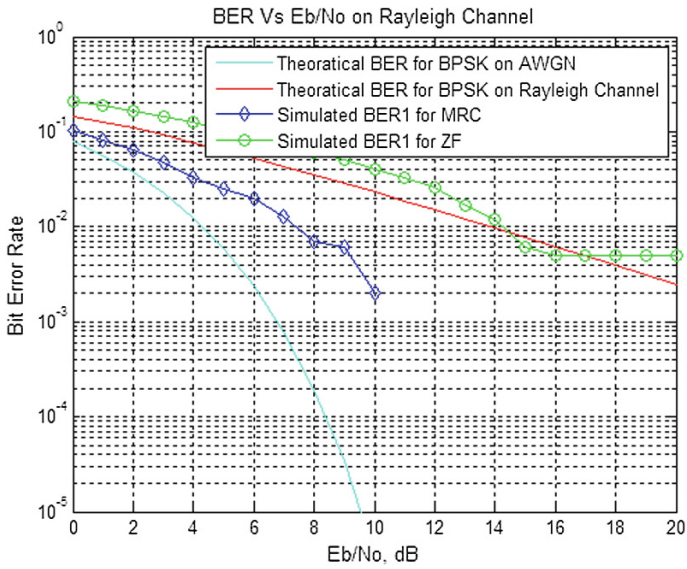


Fig. 3 BER/No for MRC & ZF technique for user 1

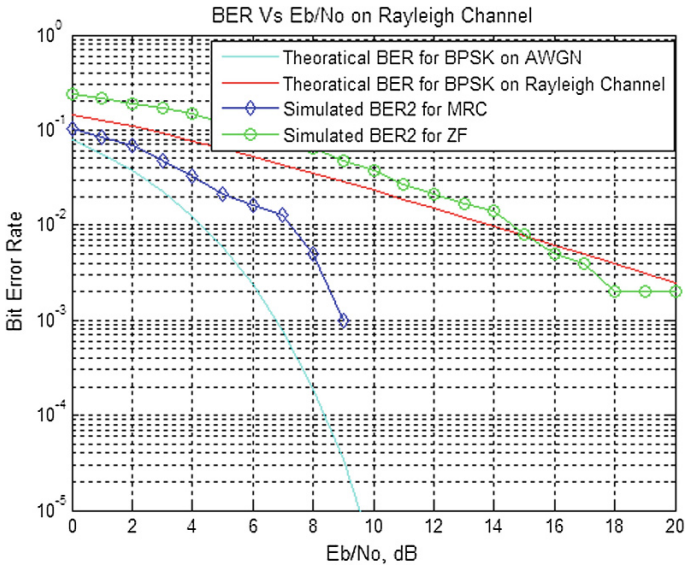


Fig. 4 BER/No for MRC & ZF technique for user 2

## 8 Conclusion

In this paper, the two combining techniques MRC and ZF are implemented on an MC-CDMA system. Performance of an MC-CDMA system using a Rayleigh channel is analyzed with BPSK modulation and Walsh codes for spreading the users. The number of users considered is two. The ratio of  $E_b/N_0$  increases as the value of BER decreases.

## References

1. Singh, M., Kaur, K.: BER performance of MC-CDMA using Walsh code with MSK modulation on AWGN and Rayleigh channel. *Int. J. Eng. Trends Technol. (IJETT)* **4**(7), 3166–3172 (2013)
2. Singh, K., Rajbir Kaur, E.R.: Performance comparison of multi-carrier CDMA using QPSK and BPSK modulation. *IOSR J. Electron. Commun. Eng. (IOSR-JECE)* **7**(3), 61–66 (2013)
3. Satish, V., Suresh, K., Swati, B.: Performance analysis of MCCDMA system in Rayleigh channel and AWGN channel using BPSK modulation technique. *Int. J. Eng. Res. Appl. (IJERA)* **1**(4), 2025–2029. ISSN: 2248-9622 (2012)
4. Ghanim, M.F., Abdullah, M.F.L.: Multi-user MC-CDMA using pseudo noise code for Rayleigh and Gaussian channel. In: *Proceedings of PIERS*, pp. 882–887. Kuala Lumpur, Malaysia (2012)

5. Naveen, V.J, Krishna, K.M., Rajeswari, K.R.: Performance analysis of equalization techniques for MIMO systems in wireless communication. *Int. J. Smart Home* **4**(4), 47–63 (2010)
6. Mahanta, S., Rajauria, A.: Analysis of MIMO system through ZF & MMSE detection scheme. *IJECT* **4**(4), 84–87 (2013). ISSN: 2230-7109 (Online). ISSN: 2230-9543 (Print)
7. Narwal, P., Singh, S., Dr. Prasad, S.V.A.V.: Performance analysis of BER improvement for multi carrier CDMA system. *Int. J. Eng. Innovative Technol. (IJEIT)* **2**(2), 72–74 (2012)

# Dual-Band Microstrip Patch Antenna Loaded with Complementary Split Ring Resonator for WLAN Applications

Kumaresh Sarmah, Angan Sarma, Kandarpa Kumar Sarma and Sunandan Baruah

**Abstract** In this paper, Inset Feed Slotted Rectangular Microstrip patch antenna using a metamaterial based Complementary Split Ring Resonator (CSRR) is designed for operating in dual band frequency range of 2.4–5.8 GHz. The microstrip antenna is designed over a FR4 epoxy substrate with an inset feed microstrip line geometry. To obtain desired dual band and radiation characteristics of the proposed antenna a CSRR is etched in the ground plane. The CSRR structure is used to obtain the dual band characteristics. The resonating frequency of the proposed design is suitable for Wide Local Area Network (WLAN) application. The proposed design is simulated in High Frequency Structural Simulator (HFSS) software. The return loss obtained for both the operating frequency is  $-26$  dB.

**Keywords** Inset feed · Microstrip antenna · WLAN · CSRR

## 1 Introduction

With rapid growth of wireless and mobile communication the need for the design of efficient antenna has received attention. These antennas must be able to operate in different frequency bands. In recent years, researchers have given focus on dual band or multiband antenna for multimode communication system applications [1].

---

K. Sarmah (✉) · A. Sarma · K.K. Sarma  
Electronics and Communication Technology, Gauhati University, Jalukbari,  
Guwahati 781014, India  
e-mail: kumaresh@gauhati.ac.in

K.K. Sarma  
e-mail: kandarpaks@gmail.com

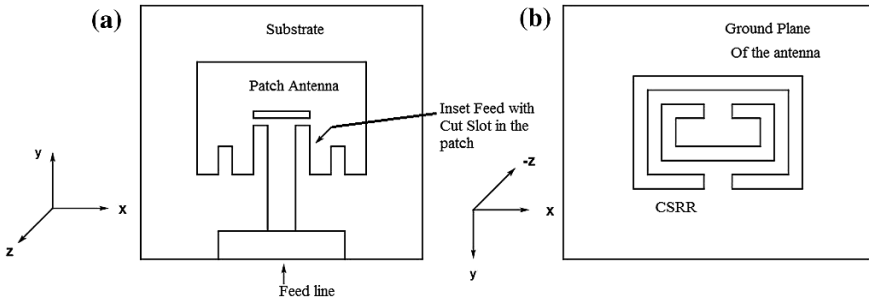
S. Baruah  
Electronics and Communication Engineering, Assam Don Bosco University,  
Azara, Guwahati 781017, India  
e-mail: sunandan.baruah@dbuniversity.ac.in

With the new development of wireless local area network (WLAN), the wireless networks for WLAN will have to be compatible with several standards like as IEEE802.11a, IEEE 802.11b and IEEE 802.11g. Hence, dual band operations in the 2.4 GHz (2.4–2.484 GHz) and 5 GHz (5.15–5.95 GHz) are becoming demanding for practical applications with the rapid development of WLAN. The microstrip patch is currently a popular antenna which is suitable for applications of WLAN and Worldwide Interoperability for Microwave Access (WiMAX) because of its physical properties. These properties are light weight, low profile, low production cost, conformability, reproducibility, reliability and ease of fabrication and integration with solid state devices and wireless technology equipment [2]. Therefore, the design of efficient multi-slot/multi-band microstrip patch antenna for such frequency ranges has become critical for reliable working of upcoming power-aware transceivers.

Although researchers have proposed various topologies to achieve desired multiband operation and radiation characteristics [3–5], metamaterials (MTM) have become popular since they lead to a small resonant antenna [6, 7]. Kuo et al. [8] proposed printed dual-band double-T monopole antenna with certain miniaturization factors. Another reports discussed the working of a novel dual broadband rectangular slot antenna for 2.4 and 5 GHz wireless local area network (WLAN), which achieves impedance bandwidths about 10.6 % for the 2.4 GHz band and 33.8 % for the 5 GHz band [9]. In [10], Malik and Kartikeyan proposed a metamaterial inspired multiband microstrip patch antenna for WiMAX/WLAN applications. Another work reports the working of a small multiband printed antenna for multiple input multiple output (MIMO) using metamaterial structure and introduces whole concepts of miniaturization [11]. In this paper we propose an inset feed rectangular microstrip patch antenna with slotted section loaded with MTM based Complementary Split Ring Resonator (CSRR) ground plane. The designed antenna is found to have operating frequency at 2.4 and 5.8 GHz. The antenna is designed using Finite Element Method (FEM) based software solver i.e. in HFSS. The design methodology of the proposed antenna and the results obtained are discussed in the succeeding sections.

## 2 Proposed Microstrip Antenna Model

In this paper, the design of a dual band rectangular microstrip patch antenna with MTM based CSRR loading at ground plane of the antenna is reported. Here, the “transmission line model” has been used to predict the radiation characteristics of the patch antenna. This model presents an inset feed slotted rectangular microstrip antenna with width ‘W’, height ‘h’ and the length of the transmission line ‘L’. The antenna model consists of three layers namely ground plane, dielectric substrate and metal strip. Figure 1 shows the layout of the proposed inset feed microstrip patch antenna with the CSRR structure. The CSRR structure is used to get the desired resonating frequency at dual band operation at 2.4 and 5.8 GHz.



**Fig. 1** **a** Proposed inset fed slotted rectangular microstrip patch antenna (*top view*). **b** The metamaterial CSRR structure loaded in the ground plane of the microstrip antenna (*bottom view*)

### 2.1 Selection of Dielectric Substrate

There are different substrates materials available with different dielectric constants for antenna design. In our proposed model we used FR4-epoxy substrate to design the microstrip antennas. Dielectric values of the substrate is in the range of  $2.2 \leq \epsilon_r \leq 12$  with a relative permittivity ( $\epsilon_r$ ) value of 4.4. The FR4-epoxy substrate is chosen to get the best resonant behavior of the CSRR structure.

### 2.2 Patch Dimension

The performance of the microstrip antenna depends on its dimension based on which the operating frequency, radiation efficiency, directivity, return loss and other related parameters are fixed. For an efficient radiation, the practical width of the patch and some related terms are given below [12–14]:

- Width of patch ( $W$ ) =  $\frac{c}{2 \times f_r} \times (\frac{\epsilon_r + 1}{2})^{-\frac{1}{2}}$  with Velocity of light  $c = 3 \times 10^8$  m/s
- Effective dielectric constant ( $\epsilon_e$ ) =  $\frac{\epsilon_r + 1}{2} + \frac{\epsilon_r - 1}{2} \times (1 + 12 \times \frac{h}{W})^{-\frac{1}{2}}$  Here  $h = 4$  mm.
- Length of extension ( $\Delta l$ ) =  $0.412 \times \left( \frac{(\epsilon_e + 0.3)(\frac{W}{h} + 0.264)}{(\epsilon_e - 0.258)(\frac{W}{h} + 0.8)} \right)$
- Effective length ( $L_{eff}$ ) =  $\frac{c}{2 \times f_r \times \sqrt{\epsilon_e}}$
- Actual length of patch ( $L$ ) =  $L_{eff} - (2 \times \Delta l)$
- Length of ground ( $L_g$ ) =  $6h + L$
- Width of ground ( $W_g$ ) =  $6h + W$

Using the above expressions, the following dimension of the patch is calculated,  $W = 38.04$  mm,  $\epsilon_e = 3.83$ ,  $\Delta l = 1.81$  mm,  $L = 28.316$  mm. In this geometry, inset feed is used to feed the signals to the antenna.

### 2.3 Design of Strip Line

For a given characteristics impedance  $Z_o$  and dielectric constant  $\epsilon_r$ , the relation between width (W) of strip line and thickness (h) (in our design  $h = 4$  mm) of the dielectric layer is given in [12, 13]. For the present design, the characteristics impedance of port1 is  $Z_o = 50 \Omega$ . Therefore, the width of port 1 is 7.64 mm. Again the length of strip is  $\frac{\lambda_g}{4}$ , where  $\lambda_g = \frac{\lambda_o}{\sqrt{\epsilon_r}}$ . In our design,  $\epsilon_r = 4.4$ . Therefore, the length of the strip is 14.8975 mm. The base model is modified with further improvements to increase the gain by incorporating three slots as shown in Fig. 1

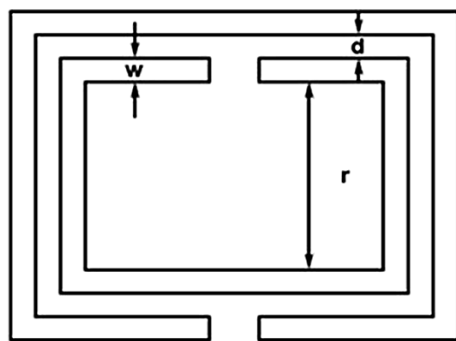
### 2.4 Design of CSRR

A CSRR is a negative image of the metaresonator split-ring resonator (SRR). It is made up of two concentric copper rings with a slit in each ring. The CSRR is made by removing the copper in the shape of the SRR from ground plane of microstrip antenna. The various considerations to design CSRR are discussed in the following sections [15].

- Gap between the rings (**d**): Gap between the rings is usually in the range of 0.1–1 mm.
- Width of the rings (**w**): Width of the rings is usually in the range of 0.011–0.134 mm.
- Inner spacing of the ring (**r**): Inner spacing of the ring is in the range of 1.2–10.3 mm.

In our design, a square CSRR structure is etched in the ground plane which is shown in Fig. 2. The design parameters of the CSRR are presented in the Table 1.

**Fig. 2** Metamaterial complementary split ring resonator structure (CSRR) loaded in the ground plane of the microstrip antenna



**Table 1** Dimensional parameters of the loaded metamaterial CSRR

Dimensional parameters	Dimensions in (mm)
d	0.12
w	1
r	6.69

### 2.5 Feeding Techniques

Patch feeding can broadly be classified as either contacting or non-contacting. In the contacting method, either a microstrip line or coaxial cable is used to directly excite the radiating patch. This makes this techniques easy to fabricate and simple to model. The main advantage of these techniques is that impedance matching is relatively easy since the probe or microstrip line can be placed at any desired position [14, 16]. In this geometry, inset feed is used to feed the antenna. The length of the inset feed of microstrip patch antenna is given by [12–14, 16],

microstrip patch antenna (not to scale)

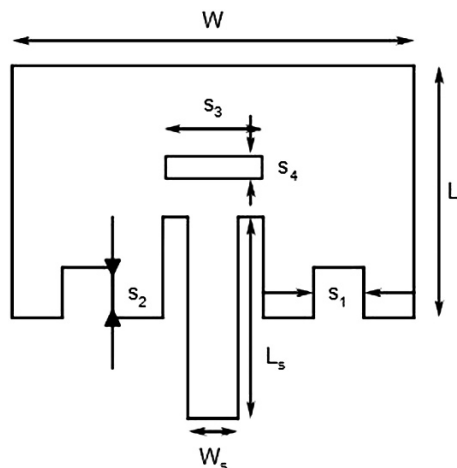
$$l = 10^{-4} (0.001699\epsilon_r^7 + 0.13761\epsilon_r^6 - 6.1783\epsilon_r^5 + 93.187\epsilon_r^4 - 682.69\epsilon_r^3 + 2561.9\epsilon_r^2 - 4043\epsilon_r + 6697) \frac{L}{2}$$

where  $\epsilon_r$  the permittivity of the dielectric and L is the length of the microstrip patch. The design parameters of the proposed microstrip patch antenna are summarized in the Table 2. Figure 3 shows the basic geometry of the patch structure.

**Table 2** Geometrical parameters of microstrip patch antenna

Dimension parameters	Value in (mm)
L	28.316
W	38.04
$L_g$	52.316
$W_g$	62.04
$W_s$	7.64
$L_s$	14.8975
$s_1$	4.2
$s_2$	4.5
$s_3$	10
$s_4$	1

**Fig. 3** Geometrical dimension of rectangular microstrip patch antenna (not to scale)





### 3 Results and Discussion

The  $S_{11}$  parameters of the simulated result, which shows an efficient approximation, are shown in Fig. 4. From the results shown in Fig. 4 we can observe that there are two operating frequencies of the designed antenna. One is at 2.4 GHz and another at 5.8 GHz. Both the frequencies are suitable for lower ISM band and WiMAX/WLAN applications. The dual band frequency of the proposed model is obtained due to the presence of the metaresonator CSRR at the ground plane of the microstrip antenna. The first resonating frequency at 2.4 GHz is obtained from the slotted microstrip antenna and second at 5.8 GHz due to the CSRR structure. The simulated impedance bandwidth at the 2.4 GHz is about 200 MHz with corresponding return loss as  $-25.5$  dB and for 5.8 GHz the bandwidth is about 200 MHz with the corresponding value of return loss as  $-26.5$  dB which is enough for impedance matching. The resonating frequency is close enough to the specified frequency band feasible for WiMax/WLAN applications. Figure 5 shows the

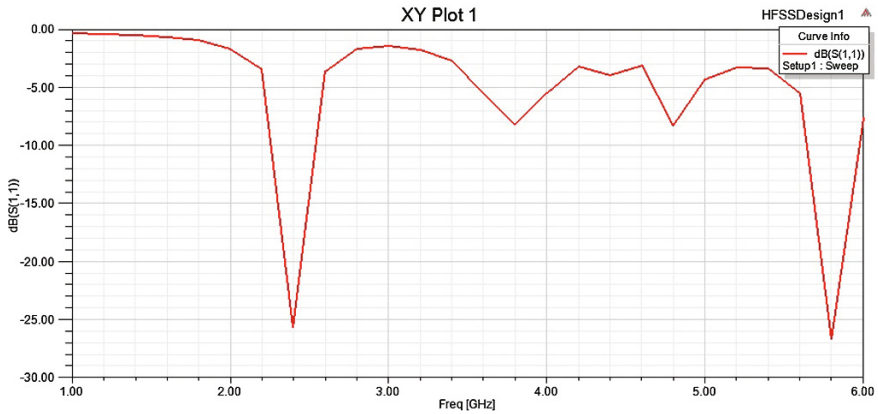


Fig. 4 Return loss  $S_{11}$  plot of the designed antenna shows the operating frequencies at 2.4 and 5.8 GHz

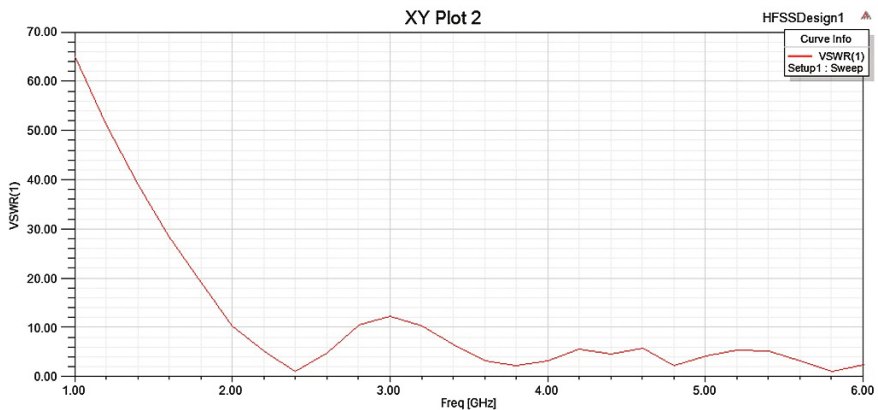
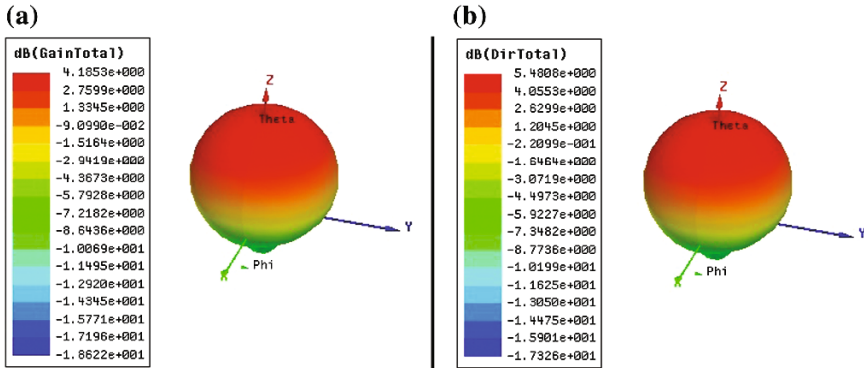


Fig. 5 VSWR plot of antenna at 1.2 at 2.4 GHz and 1.1 at 5.8 GHz



**Fig. 6** a Gain plot of proposed antenna. b Directivity plot of proposed antenna

VSWR plot of the designed antenna. The VSWR of the proposed model is found to be almost 1.2 at 2.4 GHz and about 1.1 at 5.8 GHz. The obtained VSWR is less than ( $<2$ ) which can be accepted as good approximation compared to the results reported in [17]. The gain of the proposed antenna is also simulated using HFSS and it is found to be around 4.2 dB for the far field pattern. Figure 6a shows the gain plot and Fig. 6b shows the directivity plot of the proposed antenna. The directivity is found to be nearly 5.5 dB along the elevation plane. The proposed design shows a return loss of  $-26$  dB which is marginally higher than that reported in [10]. However, the bandwidth in this case is much high at 200 MHz than that reported in [18]. Due to the use of the metaresonator CSRR the performance in terms of bandwidth has been improved by around 100 MHz compared to the work in [10, 18]. The significance of the work is that it is a simplistic design which supports up to two bands at which simultaneous communication can be maintained. The dual band characteristics, high bandwidth provision and low return loss make it a short range, high data rate radiating system.

## 4 Conclusions

In this paper, a dual band slotted microstrip patch antenna employing a metamaterial resonator (CSRR) is proposed. The dual band characteristics of the antenna are achieved due to the CSRR. The experimental results obtained show efficient radiation characteristics for WLAN frequency bands. The proposed design can be easily integrated to microwave circuits and it is also suitable for ISM band and WiMax/WLAN applications.

**Acknowledgment** The authors are thankful to the Ministry of Communication and Information Technology (MCIT), Govt. of India.

## References

1. Ge, Y., Esselle, K., Bird T.: Compact triple-arm multi-band monopole antenna. In: Proceedings of IEEE International Conference Workshop: Antenna Technology Small Antennas and Novel Metamaterials, pp. 172–175 (2006)
2. Gupta, R., Gupta, N.: Two compact microstrip patch antennas for 2.4 GHz band—a comparison. *Microwave Rev.* **12**(2), 29–31 (2006)
3. Lee, Y.C., Sun, J.-S.: A new printed antenna for multiband wireless applications. *IEEE Antennas Wirel. Propag. Lett.* **8**, 402–404(2009)
4. Eshtiaghi, R., Shayesteh, M.G., Zad-Shakooian, N.: Multicircular monopole antenna for multiband applications. *IEEE Antennas Wirel. Propag. Lett.* **10**, 1205–1207 (2011)
5. Naser-Moghadasi, M., Sadeghzadeh, R.A., Fakheri, M., Aribi, T., Sedghi, T., Virdee, B.S.: Miniature hook-shaped multiband antenna for mobile applications. *IEEE Antennas Wirel. Propag. Lett.* **11**, 1096–1099 (2012)
6. Eleftheriades, G.V., Grbic, A., Antoniades, M.: Negative-refractive index transmission-line metamaterials and enabling electromagnetic applications. *IEEE Antennas Propag. Soc. Int. Symp. Digest*, 1399–1402 (2004)
7. Erentok, A., Ziolkowski, R.W.: Metamaterial-inspired efficient electrically small antennas. *IEEE Trans. Antennas Propag.* **56**(3), 691–707 (2008)
8. Kuo, Y.L., Wong, L.: Printed double-t monopole antenna for 2.4/5.4 GHz dual-band WLAN operations. *IEEE Trans. Antennas Propag.* **51**(9), 2187–2192 (2003)
9. Wu, J.-W., Hsiao, H.-M., Lu, J.-H., Chang, S.-H.: Dual broadband design of rectangular slot antenna for 2.4 and 5 GHz wireless communication. *Electron. Lett.* **40**(23), 1461–1463 (2004)
10. Malik, J., Kartikeyan, V.: Metamaterial inspired patch antenna with L-Shape slot loaded ground plane for dual band (WiMAX/WLAN) applications. *Prog. Electromagn. Res. Lett.* **31**, 35–43 (2012)
11. Yem, V.V., Chi, P.V., Journet, B.: Novel MIMO antenna using complementary split ring resonator(CSRR) for LTE applications. In: International Conference on Advance Technologies for Communications (ATC), pp. 222–226, Hanoi (2012)
12. Singh, Y.K., Ghosh, S., Prathyush, K., Ranjan, S., Suthram, S., Chakrabarty, A., Sanyal, S.: Design of a microstrip patch antenna array using IE3D software. In: Proceedings of National Conference on Communication (NCC 2003), pp. 611–615 (2003)
13. Pozar, D.M.: *Microwave Engineering*, 4th edn. Wiley, USA (1998)
14. Balanis, C.A.: *Antenna Theory, Analysis and Design*, 3rd edn. Wiley, USA (2005)
15. Pendry, J.B., Holden, A.J., Robbins, D.J., Stewart, W.J.: Magnetism from conductors and enhanced nonlinear phenomena. *IEEE Trans. Microwave Theory Tech.* **47**(11), 2075–2084 (1999)
16. Ali, A., Dheyab, A.S., Karim, A.H.: Improving bandwidth rectangular patch antenna using different thickness of dielectric substrate. *ARNP J. Eng. Appl. Sci.* **6**(4), 16–21 (2011)
17. Kang, L., Yin, Y.Z., Fan, S.T., Wei, S.J.: A novel rectangular slot antenna with embedded self-similar T shaped strips for WLAN applications. *Prog. Electromagnetics Res. Lett.* **15**, 19–26 (2010)
18. Sarkar, D., Saurav, K., Srivastava, K.V.: Design of a novel dual band microstrip patch antenna for WLAN/WiMax applications using complementary split ring resonator and partially defected ground structure. In: Proceedings of Progress in Electromagnetics Research, pp. 821–825. Taipei, 25–28 March 2013

# Parallel Implementation of FP Growth Algorithm on XML Data Using Multiple GPU

Sheetal Rathi and C.A. Dhote

**Abstract** The FP Growth algorithm is inherently faster than Apriori as it has less number of combinations to be considered. However, the gap here is that the tree building task is a strenuous process in terms of time and memory. Several attempts have been made to improvise the algorithm. In this paper, a model is proposed to implement a parallel FP Growth algorithm that makes use of the elimination process employed by FP Growth algorithm without generating the actual tree (or multiple smaller trees). This not only improves performance of the algorithm but also results in more efficient memory usage. The proposed algorithm Accelerated Frequent Itemset Mining (AFIM) makes use of multiple Graphics Processing Unit (GPU) system.

**Keywords** Parallel computing · FP growth · Frequent itemset mining · High performance computing · Graphics processing unit

## 1 Introduction

Data Mining and Knowledge Discovery in Databases (KDD) is a rapidly growing interdisciplinary field. It can also be stated as the process of automated extraction of hidden, previously unknown and potentially useful information from large databases [1]. Association rule mining is an integral task of data mining research domain and it is the process to help find the relationship between the itemset in a large number of databases.

---

S. Rathi (✉)  
SGBAU, Amravati, Maharashtra, India  
e-mail: sheetal.rathi@thakureducation.org

C.A. Dhote  
PRMITR, Badnera, Maharashtra, India  
e-mail: vikas.dhote@rediffmail.com

Apriori [2], Eclat [3] and FP Growth [4] are the major vital algorithms used for association rule mining. Research suggest that the methodologies mainly used rely heavily on an Apriori-like [5] candidate set generation-and test approach. However, the approach fails when the dataset is very large. Another important methodology is EClat [3] that proved a substantial milestone in the development of association rule mining process. The third approach towards association rule mining is using FP Growth method proposed by Han and Pei [4]. The frequent pattern (FP) growth uses only 2 database scans irrespective of the length of longest transaction, whereas the Apriori needs  $n + 1$  scans ( $n$ : length of the longest pattern).This significantly reduces computation time and cost especially when the number of candidate itemsets are more. However, because of its flat tree like structure, the basic FP growth algorithm fails miserably when it comes to storage space. To speed up the process, many researchers have directed their research in developing parallelized variants of the method [6–10].

In this paper, we propose a highly parallel FIM algorithm that is optimized for a platform consisting of GPUs and CPU. The key idea is to use the trimming feature of the FP-Growth Algorithm used after the tree generation before even the tree is generated. All the transactions are kept separately and not combined into a tree.

## 2 Related Work

Literature suggests that to mine association rules efficiently, the frequent itemset mining step has to be accelerated effectively because this is the most time consuming step. Enormous amount of work has been done to speed up this process.

### 2.1 *Parallel Approach*

High-performance parallel and distributed computing environment is becoming increasingly important, as data continues to grow inexorably in size and complexity. Several efforts have been applied to parallelize the mining process such as shared-memory systems (SMPs), distributed-memory systems, hybrid systems consisting of a cluster of SMPs and geographically distributed systems [11, 12].

In [10], the authors designed a parallel algorithm to work in distributed data framework. It does not need to create the overall FP tree because of which it can handle scalable data. A modern multi core processor is used to implement parallel FP tree algorithm [13]. Two techniques were used: a cache-conscious FP-array and a lock-free dataset tiling parallelization mechanism. Zang et al. [14] presented two parallel FIM algorithms, Apriori and Eclat on shared memory platform. The strategy was to implement three different vertical data representations; vertical transaction id set, vertical bitvector, and diffset. They concluded that Apriori is only scalable when used with diffset while Eclat is generally scalable but achieves its best scalability with diffset.

## 2.2 GPU Acceleration

Bakos et al. [15] developed a new parallel Frequent Itemset Mining algorithm called “Frontier Expansion” developed from Eclat. High performance is achieved by using a heterogeneous platform consisting of a shared memory multiprocessor and GPU coprocessors. Here a partial breadth-first search is utilized to make use of extreme parallelism while being controlled by the accessible memory capacity. Authors concentrate on the task of scaling a MapReduce application using the CPU and GPU together in a combined architecture [16]. Different methods like map-dividing scheme and pipelining were developed for dividing the work. Dynamic work distribution schemes were devised for both the approaches. Their implementation of MapReduce is based on an endless reduction method, which avoids the memory overheads of storing key-value pairs. Huang et al. [9] utilizes the computing power offered by GPUs and extend CPU-based data mining algorithms for mapping to CPU-GPU hybrid and scalable architecture for speeding up the computing process.

## 3 Preliminaries

### 3.1 Problem Definition

The association rule mining is a two-step process:

1. Find all frequent itemset having minimum support.
2. Generate strong rules having minimum confidence, from the frequent itemset.

### 3.2 Basic FP Growth Algorithm

Frequent patterns are mined from an FP-tree using a method called FP-growth. All the node-links from the header table are traversed to generate complete frequent patterns. The general idea is to create conditional pattern bases depending on the support threshold and in turn generate rules based on minimum confidence.

- 1) IF Tree contains a single path P THEN
- 2) FOR all each  $\beta =$  nodes combination in P, DO
- 3) generate pattern  $= \beta U \alpha$  with  
Support = minsup of nodes in  $\beta$ ; ELSE
- 4) FOR all  $\alpha_i$  in the header of Tree DO  
BEGIN
- 5) generate pattern  $\beta = \alpha_i U \alpha$  with support  $= \alpha_i$ .support;
- 6) Construct conditional pattern base of  $\beta$

```

Tree $\beta$  = construct conditional FP-tree of  $\beta$ ;
7) IF Tree $\beta \neq \emptyset$  THEN
8) CALL FP-growth (Tree $\beta$ ,  $\beta$ );
9) END;

```

### 3.3 Graphics Processing Unit

In this paper we exploit the highly parallel computation power of GPU for frequent itemset mining process. Unlike multi-core CPUs, the cores on the GPU are virtualized, and GPU threads are executed in Single Instruction, Multiple Data (SIMD) which are in turn managed by the hardware. Because of the embedded hardware based design, the GPU programming is cut down and also improves program scalability and portability. The main reason behind this is that programs are unaware about physical cores and rely on hardware for thread management (Fig. 1).

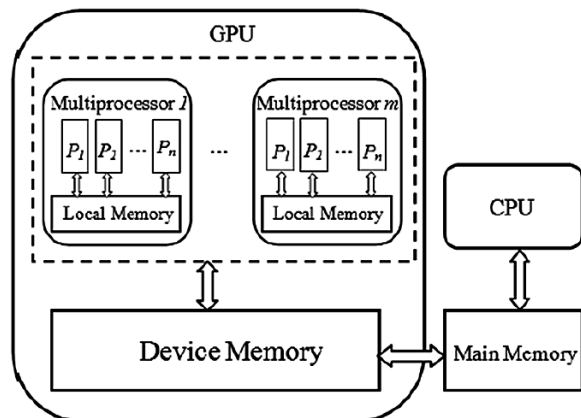
The inspiration behind using General purpose graphical processing unit (GPGPU) is its cost effectiveness as compared to the distributed and parallel approaches implemented so far [10, 14, 17].

## 4 Framework Architecture of AFIM

Scalable GPU-based parallel model for speeding up the frequent itemset mining (FIM) process is implemented in this paper. The purpose of doing this is to best exploit the computing resources obtained by GPUs and extend traditional, CPU-based data mining algorithms for mapping to CPU-GPU hybrid architecture,.

The idea to be implemented in this algorithm is to apply Accelerated Frequent Itemset Mining (AFIM) algorithm and use the trimming feature of the FP-Growth

**Fig. 1** The many core architecture of GPU (Source [18])



Algorithm used after the tree generation before even the tree is generated. All the transactions are kept separately and not combined into a tree. The entire process can be summarized as follows:

1. The arrays of individual transactions are grouped into different sections based on the initial item in each transaction i.e. all transactions with the same item at the start are grouped together in one section. Thus, multiple such sections are formed based on the occurrence of the most frequently occurring items in most transactions. Once grouped, that item is considered the first part of the pattern. The next part is thus identified by repeating the same process over the new section formed. The items of the subsection are then appended to the original first item of the given section.  
Here, each section of the transaction basically represents 1 level of the tree. The 0th partition i.e. no partition represents all the transactions. The 1st partition represents the items formed at level 1 of the FP tree i.e. it identifies those transactions which have most frequent item in the first place of each transaction. It is to be noted that each partition may result in multiple sections based on the variance in the transaction set.
2. Elimination takes place in this step by discarding those item patterns/transactions which do not have sufficient count to meet the threshold criteria.
3. Each section then undergoes the same process of partitioning and identifying the different items that occur after the dominant item of that given section.
4. At this point, the CPU forces the GPU for synchronizing all threads.
5. The above process is iteratively repeated for every subsection as GPUs are not suited for recursion. This ends up locating the most frequent and obvious patterns in the transactions. In the GPU implementation, we assign different section to different blocks in a GPU. Each block then individually assesses its own section and identifies recurring patterns in its section.

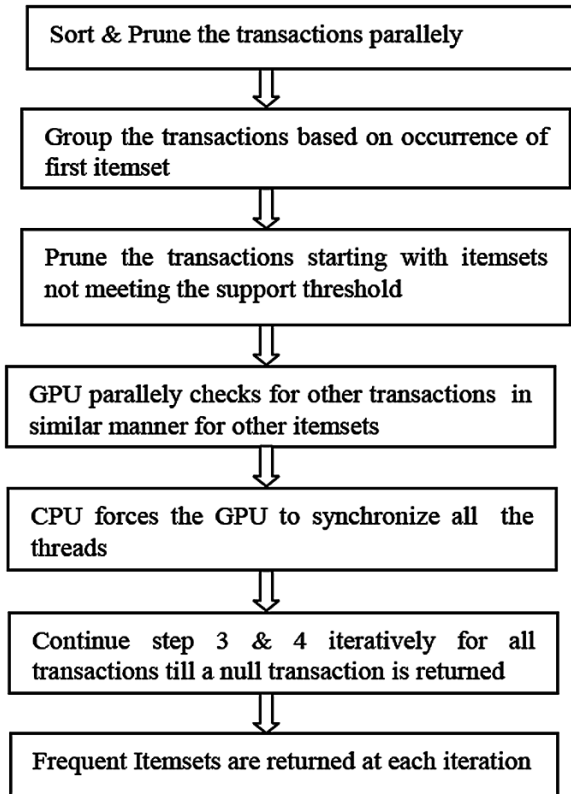
Each section when formed has two roles to play;

1. The dominant item i.e. the item in the 1st position of all the transactions in that given section is identified. The remaining part of each transaction in the section is then subjected to further partitioning and
2. On receiving the frequent pattern found by the subsections of a section, the section merges it with the frequent item that it has identified and passes it on up to the section of which it is a subsection.

As can be seen, the entire process appears very tree like but the actual FP tree is not generated. The process flow diagram is as shown in Fig. 2.



**Fig. 2** Proposed AFIM model



## 5 Experimental Result and Analysis

Various synthetic data sets were generated using Python script for testing the AFIM algorithm. Again a fully optimized CPU is used for serial computation and a GPU-CPU model is used for the parallel part.

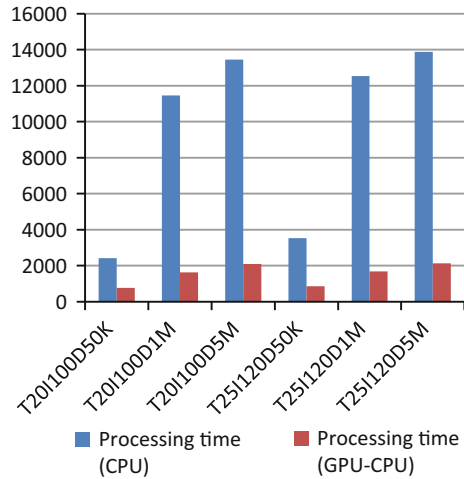
The system configuration used is Intel Xeon E5-2620 (6 cores, 12 threads, and clock speed of 2 GHz), RAM: 15 GB GPU: Tesla K40c (GDDR5 SDRAM). The characteristics of the dataset were varied in such a way that for first three datasets, i.e. T20I100D50K, T20I100D1M, and T20I100D5M only the dataset size is increased and the performance is evaluated. In the next three datasets, T25I120D50K, T25I120D1M and T25I120D5M, the itemset count and transaction length is differed. The driver used was the NVIDIA driver for Ubuntu 10.04 (CUDA compilation tools, release 5.0, VO.2.1221) with CUDA support driver version NVIDIA-SMI 331.67. Table 1 elaborates the speed up of CPU-GPU implementation with respect to the CPU based implementation.

It is evident that there is considerable speed up for AFIM model as compared to core CPU implementation which is clearly depicted in Fig. 3. However, even if the

**Table 1** Performance evaluation of CPU and GPU-CPU

Synthetic dataset	Processing time (CPU)	Processing time (GPU-CPU)	Speed up
T20I100D50K	2,425	769	3.15
T20I100D1M	11,453	1,635	7.00
T20I100D5M	13,452	2,089	6.43
T25I120D50K	3,524	854	4.12
T25I120D1M	12,539	1,687	7.43
T25I120D5M	13,869	2,135	6.49

**Fig. 3** Performance evaluation of CPU and CPU-GPU architecture



characteristics of datasets are changed, there is no considerable difference in the amount of processing time take, both by CPU and GPU for the same size of dataset.

In above figure, we have compared the AFIM algorithm with the fully optimized CPU on the same machine configuration. Synthetic datasets with varying characteristics were tested on the two processors, CPU and CPU-GPU architecture.

## 6 Conclusion

Association Rule mining has been parallelized for a long time with expensive system setup. This paper has aimed to perform Association Rule mining using parallel processing with the help of Graphic processors, which have in-built hardware capability of multi-threading and that has been leveraged for our algorithm.

Previous work does not prevail the use of GPU for FP-growth algorithm. Instead literature speaks about the various approaches exploited to achieve parallelism in FP-growth using shared and distributed processors. In this paper we have

parallelized FP-growth approach on multi-threaded Graphic Processor. There was considerable speed up on different synthetically generated datasets with different characteristics. In addition to the speed boost, the dataset size also progressed. Initially starting from 100 transactions it succeeded in achieving scale up in data size of up to 5 million transactions.

**Acknowledgments** This project is based upon work supported by the CUDA Centre of Excellence (CCOE), IIT Bombay.

## References

1. Kamber, M., Han, J.: *Data Mining: Concepts and Techniques*, 2nd edn. Morgan Kaufmann Publishers, Burlington (2006)
2. Agrawal, R., Srikant, R.: Fast algorithms for mining association rules. In: *Proceedings of 20th International Conference on Very Large Data Bases*, pp. 487–499. Morgan Kaufmann Publishers Inc., San Francisco, CA, USA (1994)
3. Pei, J., Han, J., Mortazavi-Asl, B., Wang, J., Pinto, H., Chen, Q., Hsu, M.-C.: Mining sequential patterns by pattern-growth: the prefix span approach. *IEEE Trans. Knowl. Data Eng.* **16**(10), 1–17 (2004)
4. Han, J., Pei, J.: Mining frequent patterns by pattern-growth: methodology and implications. *SIGKDD* **2**(2), 30–36 (2000)
5. Zaiane, O.R., El-Hajj, M., Lu, P.: Fast parallel association rule mining without candidacy generation. In: *Proceedings of IEEE International Conference on Data Mining ICDM*, pp. 665–668 (2001)
6. Hu, J., Yang-Li, X.: A fast parallel association rules mining algorithm based on FP-forest. In: *Part II LNCS*, pp. 40–49. Springer, Berlin (2008)
7. Chen, M., Gao, X.D., Li, H.F.: An efficient parallel FP-growth algorithm. In: *Proceedings of International Conference on Cyber-Enabled Distributed Computing and Knowledge Discovery*, pp. 283–286 (2009)
8. Orlando, S., Palmerini, P., Perego, R., Silvestri, F.: *5th International Conference Porto, Portugal* (2002)
9. Huang, Y.-S., Yu, K.-M., Zhou, L.-W., Hsu, C.-H., Liu, S.-H.: Accelerating parallel frequent itemset mining on graphics processors with sorting LNCS vol. 8147, pp. 245–256. IFIP International Federation for Information, Springer, Berlin (2013)
10. Wang, Z., Wang, C.: A parallel association-rule mining algorithm. In: *WISM'12 Proceedings of the 2012 International Conference on Web Information Systems and Mining*, pp. 125–129. Springer, Berlin (2012)
11. Vikram singh, T., Robil, V.: Data mining by parallelization of FP-growth algorithm. *Int. J. Eng. Res. Dev.* **5**(9), 0–35 (ISSN: 2278-067X) (2013)
12. Zaki, M.J.: Parallel and distributed association mining: a survey. *IEEE Concurrency* **7**(4), 14–25 (1999)
13. Liu, L., Li, E., Zhang, Y., Tang, Z.: Optimization of frequent itemset mining on multiple-core processor. In: *Proceedings of VLDB 07.acm*, pp. 1275–1285, 23–28 Sept 2007
14. Zhang, Y., Zhang, F., Bakos, J.: Frequent itemset mining on large-scale shared memory machines. In: *Proceedings of IEEE International Conference on Cluster Computing*, pp. 585–589 (2011)
15. Bakos, J.D., Zhang, F., Zhang, Y.: Accelerating frequent itemset mining on graphics processing unit. *J. Supercomput.* **66**(1), 94–117 (2013). doi:[10.1007/s11227-013-0887-x](https://doi.org/10.1007/s11227-013-0887-x)

16. Agrawal, G., Chen, L., Huo, X.: Accelerating MapReduce on a coupled CPU-GPU architecture. IEEE SC12. Salt Lake City, Utah, USA (2012). 978-1-4673-0806-9/12
17. Böhm, C., Noll, R., Plant, C., Wackersreuther, B., Zherdin, A.: Data mining using graphics processing units. In: Transactions on Large-Scale Data-and Knowledge-Centered Systems I LNCS, vol. 5740, pp. 63–90. Springer, Berlin (2009)
18. Fang, W., Lau, K.K., Lu, M., Xiao, X., Lam, C.K., Yang, P.Y.: Parallel data mining on graphics processors. Technical Report HKUSTCS0807 (Oct 2008)

# A Convergence Analysis of The Deterministic Ant System Model

Abhishek Paul, Swatantra Saha, Suraj Kumar Chaubey  
and Sumitra Mukhopadhyay

**Abstract** Ant System (AS) is the first algorithm in the Ant Colony Optimization (ACO) domain to have successfully implemented. But, a little have been put forward about the mathematical analysis of the stochastic model based AS. In this paper, a deterministic solution of the classical Ant dynamics is introduced. A transfer function model is developed and the system characterization is done in frequency domain. It is helpful to explore the system behavior that gives the supportive analysis on the stability of the Ant System. Also we deduce the necessary bounds of the trail persistence  $\rho$  which will control the ant dynamics to avoid over accumulation of pheromone and search for good optimal solution using Region of Convergence (ROC) criterion. Simulation results also present supportive evidence of the analysis.

**Keywords** Ant system · Transfer function · Frequency domain analysis · Stability · Region of convergence · Travelling salesman problem (TSP)

---

A. Paul (✉) · S. Saha · S.K. Chaubey  
Department of Electronics and Communication Engineering,  
Camellia Institute of Technology, Madhyamgram, Kolkata, India  
e-mail: mr.abhishekpaul@gmail.com

S. Saha  
e-mail: swatantrasaha@yahoo.in

S.K. Chaubey  
e-mail: surajkumarchaubey14@gmail.com

S. Mukhopadhyay  
Radio Physics and Electronics, University of Calcutta, Kolkata, India  
e-mail: sumitra.mu@gmail.com

## 1 Introduction

Ant Colony Optimization (ACO) [1] is an important bio-inspired optimizations technique that has notified its presence over the decade for solving different complex problems. Ant System (AS) [2] is the first of its kind in this domain. It models the ant foraging behavior and also, optimizes globally. It posses' features like robustness, positive feedback, distributed computing and can be easily implemented with other algorithms. A lot of simulation work has been carried out on the Ant algorithms and their variants in different application domain. However, not much of related work on the theoretical analysis of ant dynamics has been explored in literature. Graph-based Ant System [3] was framed by Gutjahr where an analytical analysis on convergence has been studied. Also the author carried out a meticulous analysis on the finite-time dynamics of ACO and its convergence speed [4]. A convergence analysis has been established by Stutzle and Dorigo [5] for ACO algorithm. A differential equation approach using extended difference operator has been used by Abraham et al. [6] to study deterministic Ant System dynamics and ensure its stability and convergence.

Ant System dynamics is governed by the pheromone trail intensity update rule given in (1). The performance of the Ant System depends on the choice of values determined by the trail persistence,  $\rho$  in (1) and the values in general lie within  $0 < \rho < 1$  [2]. The values proposed in literature for the trail persistence are random in nature that suits the algorithm with best optimal result. So, there is a need to corroborate the range of values taken by the trail persistence and establish stability of the Ant dynamics. This article presents a deterministic model of basic AS based on transfer function model. Henceforth, frequency domain analysis helps us to find out the range of values taken by the trail persistence that ensure the stability of this linear ant system model. Also this paper focuses on the substantiation made to the consolidated range of trail persistence,  $\rho$  which establishes the effectiveness in characterization of the Ant dynamics. Also it is conformed in this paper that for a stable ant dynamics, the uncontrolled pheromone deposition growth is not seen and the explosion of pheromone concentration is resolved. Moreover, the study does not violate the stochastic behavior of the ant dynamics, as the selection process of ants' path is based on probability. Results of computer simulation have been provided in order to support the analytical claims made in this paper.

This paper is further organized as: Sect. 2 gives the deterministic modeling of the Ant Dynamics and its transfer function. Stability and convergence criterion of the Ant System using ROC is established in Sect. 3. Section 4 depicts the simulation results on TSP that validates the stability of the Ant System using ROC. Also the Frequency domain analysis is used to validate the range of values of the pheromone trail persistence,  $\rho$  that ensure stability of the Ant System. And finally the paper concludes in Sect. 5.

## 2 Modeling the Deterministic Framework of the Ant System

Ant System being stochastic in nature, it is hard to establish the nature of the system and to derive its stability. On such a ground, this paper is a humble effort towards the development of transfer function based model of ant dynamics and subsequently frequency domain analysis is made to establish the convergence of this system. The consolidated range of the trail persistence factor,  $\rho$  is validated in this paper which pledge in finding the optimal solution.

### 2.1 Basic Ant System

Ant-System (AS) [2] is the first successful technique to emphasize the swarm nature of the real ants. The pheromone updation formula of the system in any path segment is defined as,

$$\tau(t+1) = (1 - \rho)\tau(t) + \Delta\tau(t+1) \quad (1)$$

where,  $\tau(t)$  is the intensity of trail in any path segment at time  $t$  and  $\Delta\tau$  is the incremental contribution in intensity of trail in that path segment.

$\rho$  ( $0 \leq \rho < 1$ ) is the pheromone evaporation (decay) parameter;  $(1 - \rho)$  is the pheromone residual parameter. Also the path selection of the ant system is governed by a probability factor which is again controlled by  $\tau(t)$ .

### 2.2 Formulation of Transfer Function

In this section we will try to model the ant dynamics using transfer function based approach by linearization method. This approach is helpful to find out the local stability around equilibrium point of a system as the local behavior of the system can be approximated using linear model.

Let us consider the pheromone updation equation of basic Ant System given in (1) as a first order linear closed loop system and we try to recast the equation as follows.

$$\begin{aligned} \tau(t+1) &= (1 - \rho)\tau(t) + \Delta\tau(t+1) \quad (2) \\ \Rightarrow \tau(t) - \tau(t-1) &= -\rho\tau(t-1) + \Delta\tau(t); \end{aligned}$$

$$\Rightarrow \frac{d\tau}{dt} = -\rho\tau(t-1) + \Delta\tau(t); \quad (3)$$

Taking Laplace Transform of the above equation we get,

$$sT(s) - \tau(0) = -\rho e^{-s}T(s) + \Delta T(s); \quad (4)$$

where,  $T(s)$  and  $\Delta T(s)$  are the Laplace transform of  $\tau(t)$  and  $\Delta\tau(t)$  respectively.

Now, to study the system response and establish its stability, we further simplify and consider the system as a causal system, i.e.,  $\tau(0) = 0$  and for  $t < 0$ . Here, we expand  $e^{-s}$ , and taking up to first order term the Eq. (4) is represented as,

$$sT(s) + \rho(1-s)T(s) = \Delta T(s);$$

$$\Rightarrow (s(1-\rho) + \rho)T(s) = \Delta T(s);$$

$$\begin{aligned} \Rightarrow \frac{T(s)}{\Delta T(s)} &= \frac{1}{s(1-\rho) + \rho} = F(s) \\ &= \text{Transfer Function of the deterministic Ant System.} \end{aligned} \quad (5)$$

The characteristics equation of the deterministic ant system is given by,

$$s(1-\rho) + \rho = 0 \quad (6)$$

$$\Rightarrow s = \frac{-\rho}{(1-\rho)} \quad (7)$$

In the next section we perform the characteristics analysis of the system using ROC.

### 3 ROC Analysis of Ant Dynamics

In this section we analyze the ant dynamics given in (7) using ROC, and establish the stable operating zone. In this paper, we take the help of Region of Convergence (ROC) to study the characteristics of the ant system and further explore the stability of the system. The stability of the system is ensured from different range of values of ROC which also validates the range of value of the pheromone factor,  $\rho$  for ants' successful operation.



**Table 1** Characterization of the deterministic Ant System for  $0 < \rho < 1$  using ROC

Rho ( $\rho$ )	$s = \frac{-\rho}{(1-\rho)}$	ROC ( $\sigma$ )	Poles	Comments	System stability
0.1	-0.11	$\sigma > -0.11$	-0.11	Pole lies on left half of s-plane. ROC include imaginary axis	Stable
0.3	-0.43	$\sigma > -0.43$	-0.43	Pole lies on left half of s-plane. ROC include imaginary axis	Stable
0.5	-1	$\sigma > -1$	-1	Pole lies on left half of s-plane. ROC include imaginary axis	Stable
0.7	-2.33	$\sigma > -2.33$	-2.33	Pole lies on left half of s-plane. ROC include imaginary axis	Stable
0.9	-9	$\sigma > -9$	-9	Pole lies on left half of s-plane. ROC include imaginary axis	Stable

### 3.1 ROC and Stability Analysis of Ant System Dynamics

The range of values for which, ‘s’ converges for a given signal is known as *Region of Convergence* (ROC). The ROC gives an idea of the stability of a system and by property it does not contain any poles. The stability of a close loop system can be easily analyzed from its characteristic equation using ROC. Tables 1 and 2 shows the characterization of the Ant system for different values of  $\rho$ .

Table 1 shows the Region of Convergence for  $0 < \rho < 1$ . It is seen that the values of pheromone trail within this range give favorable results by including the

**Table 2** Characterization of the deterministic Ant System for  $0 < \rho, \rho > 1$ , and  $\rho = 0, 1$  using ROC

Rho ( $\rho$ )	$s = \frac{-\rho}{(1-\rho)}$	ROC ( $\sigma$ )	Poles	Comments	System stability
-0.2	0.16	$\sigma > 0.16$	+0.16	Pole lies on right half of s-plane. ROC does not include imaginary axis	Unstable
-0.4	0.28	$\sigma > 0.28$	+0.28	Pole lies on right half of s-plane. ROC does not include imaginary axis	Unstable
-0.8	0.44	$\sigma > 0.44$	+0.44	Pole lies on right half of s-plane. ROC does not include imaginary axis	Unstable
1.2	6	$\sigma > 6$	+6	Pole lies on right half of s-plane. ROC does not include imaginary axis	Unstable
1.4	3.5	$\sigma > 3.5$	+3.5	Pole lies on right half of s-plane. ROC does not include imaginary axis	Unstable
1.8	2.25	$\sigma > 2.25$	+2.25	Pole lies on right half of s-plane. ROC does not include imaginary axis	Unstable
0	0	$\sigma > 0$	0	Pole lies on the imaginary axis. ROC does not include imaginary axis	Unstable
1	$\infty$	$\sigma > \infty$	$\infty$	Pole lies on the exterior of the s-plane. ROC does not include imaginary axis	Unstable

imaginary axis in its area of convergence. Whereas, for  $\rho < 0$  and  $\rho > 1$ , system does not include the imaginary axis and this make the system unstable. The supportive results are present in Table 2. Again for  $\rho = 0$ , the pole lie on the origin. Hence ROC does not include the imaginary axis, and it leads to unstable system. But for  $\rho = 1$ , the poles are located at infinity. Hence the system behavior is unstable. It is clear from Tables 1 and 2 that the value of pheromone trail  $\rho$  within  $0 < \rho < 1$  will give successful modeling of the ant system.

So, it is proved that the Ant System is stable for  $0 < \rho < 1$  using ROC. In the next section, we simulate the Ant System on TSP for various values of  $\rho$  to validate the range of parameters which will ensure the stability of ant system.

## 4 Simulation Results and Analysis of the Ant System Dynamics

The simulation study is done on TSP to prove the effectiveness of our deterministic modeling of the Ant System, and validates the range of value of the pheromone factor,  $\rho$  for ants' successful operation. The simulation is made in MATLAB-R2010a, ver. 7.10.0.499, in a Windows 7 environment, running on INTEL CORE 2DUO, 2.20 GHz processor, and 3 GB RAM. The efficacy of our proposed algorithm has been tested using Ulysses16.tsp, Ulysses22.tsp and Oliver30.tsp problems (Euclidean 2D distance TSP problems). For simplicity, we have adopted number of ants equal to number of cities (here, the number of ants = 30, for a 30-city problem). Experiments were carried out for 6,000 iterations and were averaged over 20 successive trials for different values of pheromone trail,  $\rho$ .

Table 3 analyses the outcome of the Ulysses16.tsp for different values of pheromone trail. Similarly Tables 4 and 5 gives the same outcome for Ulysses22.tsp and Oliver30.tsp problems. From Tables 1, 2 and 3 we find that ant system algorithm behaves successfully when the pheromone trail is  $0 < \rho < 1$ . This is the best fit range of  $\rho$  for Ant System. This is also been proved from the below figures of simulation. Figure 1a shows the iterative best cost and average node branching of Ulysses16.tsp problem for  $\rho > 0$ . Figure 1b shows the same of Oliver30.tsp for  $\rho < 0$ , and Fig. 1c of Ulysses22.tsp for  $\rho = 1$ . It is found that the system shows premature convergence for all the above values of rho,  $\rho$ . Hence, the ant system is unstable for the values of rho,  $\rho$  depicted in figures. But, the system converges at high value for  $\rho = 0$  (in Fig. 1d) for Ulysses16.tsp problem.

Hence it is proved that trail persistence,  $\rho$  should be  $0 \leq \rho \leq 1$  for successful operation of Ant System algorithm. The algorithm is unstable for  $\rho < 0$ ,  $\rho > 1$ . So, we have proved and validated the consolidate range of trail persistence,  $\rho$  where the Ant System will be stable and will find its optimal solution more effectively.

**Table 3** Analysis of Ant System for different values of  $\rho$  for ULYSSES16 problem

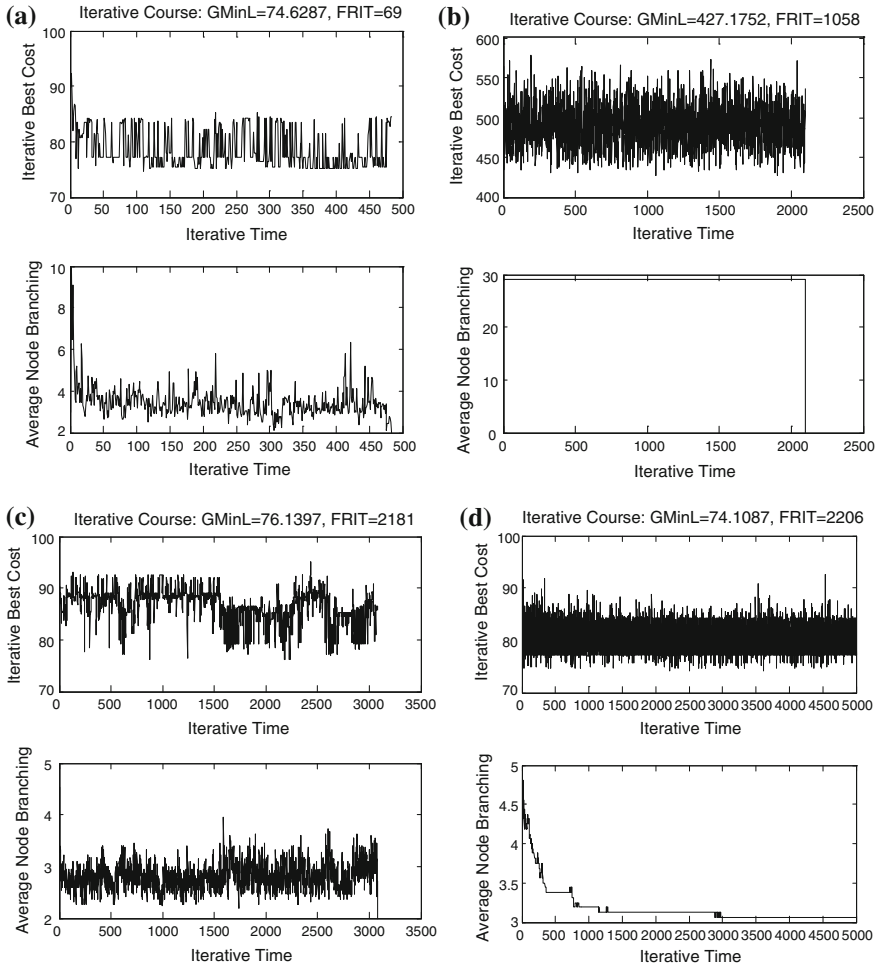
TSP	RHO ( $\rho$ )	Best	Worst	Average	Relative deviation (%)	Optimal iteration
ULYSSES16 (73.9876)	$\rho = 0.1$	73.9998	74.6287	74.1721	0.016487	816
	$\rho = 0.3$	73.9998	74.2473	74.1007	0.01647	1,161
	$\rho = 0.5$	73.9998	74.6148	74.1315	0.016487	458
	$\rho = 0.7$	73.9998	74.2348	75.9836	0.016487	1,267
	$\rho = 1$	73.9998	–	–	0.016487	<b>148</b>
	$\rho = -0.2$	28.27	–	–	-161.7177	3,862
	$\rho = -0.4$	15.1111	–	–	-389.6242	2,096
	$\rho = 1.2$	75.182	–	–	0.016489	224
	$\rho = 1.4$	74.6287	–	–	0.859053	63

**Table 4** Analysis of Ant System for different values of  $\rho$  for ULYSSES22 problem

TSP	RHO ( $\rho$ )	Best	Worst	Average	Relative deviation (%)	Optimal iteration
ULYSSES22 (75.3)	$\rho = 0.1$	75.3984	76.6287	76.1721	0.130677	816
	$\rho = 0.3$	75.3984	76.9243	76.1007	0.130677	61
	$\rho = 0.5$	75.3984	75.9648	75.5615	0.130677	458
	$\rho = 0.7$	75.3984	76.2103	75.9836	0.130677	1,267
	$\rho = 1$	76.1397	–	–	1.10284	2,181
	$\rho = -0.2$	22.5068	–	–	-234.5656	3,865
	$\rho = -0.4$	26.4169	–	–	-185.0448	2,090
	$\rho = 1.2$	76.2751	–	–	1.2784	1,369
		$\rho = 1.4$	76.057	–	–	0.99531

**Table 5** Analysis of Ant System for different values of  $\rho$  for OLIVER30 problem

TSP	RHO ( $\rho$ )	Best	Worst	Average	Relative deviation (%)	Optimal iteration
OLIVER30 (423.7406)	$\rho = 0.1$	423.7406	424.6717	423.9121	0	2,681
	$\rho = 0.3$	423.7406	423.9117	423.9173	0	621
	$\rho = 0.5$	423.7406	423.9117	423.8676	0	458
	$\rho = 0.7$	423.7406	423.9117	423.8996	0	2,267
	$\rho = 1$	423.9117	–	–	0.04036	1,348
	$\rho = -0.2$	425.2667	–	–	0.35886	1,106
	$\rho = -0.4$	427.1752	–	–	0.80403	1,058
	$\rho = 1.2$	426.5438	–	–	0.657189	1,727
		$\rho = 1.4$	442.3633	–	–	4.20982



**Fig. 1** The iterative best cost and average node branching of **a** Ulysses16.tsp problem for  $\rho = 1.4$  ( $\rho > 1$ ), **b** Oliver30.tsp problem for  $\rho = -0.4$  ( $\rho < 1$ ), **c** Ulysses22.tsp problem for  $\rho = 1$  and **d** Ulysses16.tsp for  $\rho = 0$ . The figures show premature convergence except Fig. 1d

## 5 Conclusion

This paper satisfactorily depicts a novel deterministic framework of the linear model of the Ant System and also validated the effective range of trail persistence,  $\rho$  where the Ant System will optimize better. This article is the first step in modeling deterministic platform of the ant system. The stability of this closed loop Ant dynamics is confirmed using Region of convergence for an effectual range of pheromone persistence and that is validated with the theoretical values as proposed in literature.

## References

1. Dorigo, M., Di Caro, G.: The ant colony optimization meta-heuristics. *IEEE Trans. Syst. Man Cybern. Part B* **34**(2), 1161–1172 (2004)
2. Dorigo, M., Maniezzo, V., Coloni, A.: The ant system: optimization by a colony of cooperating agents. *IEEE Trans. Syst. Man Cybern. Part B* **26**, 29–41 (1996)
3. Gutjahr, W.J.: A graph-based ant system and its convergence. *Future Gener. Comput. Syst.* **16** (9), 873–888 (2000)
4. Gutjahr, W.J.: On the finite-time dynamics of ant colony optimization. *Methodol. Comput. Appl. Probab.* **8**(1), 105–133 (2006)
5. Stützle, T., Dorigo, M.: A short convergence proof for a class of ACO algorithms. *IEEE Trans. Evol. Comput.* **6**(4), 358–365 (2002)
6. Abraham, A., Konar, A., Samal, N.R., Das, S.: Stability analysis of the ant system dynamics with non-uniform pheromone deposition rules. In: *Proceedings of International Conference on 2007 IEEE Congress on Evolutionary Computation (CEC 2007)*, pp. 1103–1108. IEEE (2007)

# EAST: Exploitation of Attacks and System Threats in Network

Sachin Ahuja, Rahul Johari and Chetna Khokhar

**Abstract** In modern era, computer network is an emerging field. With the invention of powerful computer network concepts today we are able to share information with each other. We build complex systems so that user can use these systems with ease. But with this comes the question of security. There comes a question, is the data that we share safe? Complex systems built with the intent to use shared data for example such as social networking sites certainly have some security loopholes. The most important as well as the most difficult task of a developer is to ensure that whatever the situation be, the system is consistent. But, as a matter of fact, no developer can guarantee that. Systems do possess some vulnerabilities. In the work that follows, we have tried to explore some prevalent system vulnerabilities and network attacks. Using JAVA as a programming language we have shown the flaws/shinks in the Web Programming and successfully simulated the vulnerabilities and attacks and demonstrated encouraging results.

**Keywords** Dictionary attack · DoS attack · Brute force attack · Threat

## 1 Introduction

To begin with, System/Network security is a critical area which has become a hot buzz in the recent years owing to the enormous number of the web site/applications getting developed and hosted on the web server (both real and rogue). Some of these sites are poorly coded by the programmers as a result they become easy fish

---

S. Ahuja (✉) · R. Johari · C. Khokhar  
USICT, GGSIP University, Dwarka, Delhi, India  
e-mail: sachin.ahuja1992@gmail.com

R. Johari  
e-mail: rahuljohari@gmail.com

C. Khokhar  
e-mail: chetnakhokhar92@gmail.com

for millions of hackers and crackers looking for the vulnerabilities in the Web Sites, so that they can launch massive attacks and take over the control of these sites hosting millions of Apps. We have worked on various system vulnerabilities (password ageing, empty string password, empty catch block problem etc.) and on the network attacks (Denial of Services, Dictionary attack and Brute force attack). With the help of programming we have tried to explore these attacks and vulnerabilities. For better understanding we have carried out the mathematical modeling of the network. We have also discussed the problems that a system may face if it is not safe against these loopholes. For completeness and clarity the paper is organized as follows: Sect. 2 discusses about Objectives, Sect. 3 discusses about the related work, Sect. 4 discusses about the Simulation performed, Sect. 5 discusses about the methodology adopted, Sect. 6 discusses about the mathematical modeling of network attacks, Sect. 7 discusses about the result, Sect. 8 discuss about conclusion and future work. Section 9 contains all the figures followed by acknowledgement and references section.

## 2 Objective

The Open Web Application Security Project (OWASP) [1, 2] is a worldwide not-for-profit charitable organization focused on improving the security of software. The same has listed various vulnerabilities and network attacks. We through our work have tried to explore these vulnerabilities and attacks. We have tried to explore different security loopholes that a system may possess. A developer while developing any system should ensure that system is safe against these vulnerabilities. The system should also protect itself against an attack made by an attacker with the intent to gain control of the system.

## 3 Related Work

Huluka and Popov use Root Cause Analysis (RCA) in session management and broken authentication Vulnerabilities and identify the way to improve different aspects of security of web applications. Through RCA they found 9 root causes that lead to broken authentication vulnerability and 11 root causes that lead to session management vulnerability and they also provide deep detailed view of vulnerabilities, which results in effective solutions. These solutions are used to minimize the recurrence of attacks on web applications [3]. Fonseca et al. present a prototype tool and methodology for the evaluation of security mechanism of web applications. The idea behind their methodology is that they assess the existing mechanisms of security and tools in different scenarios by injecting realistic vulnerabilities in an application and attacking them. They also propose the Vulnerability and Attack Injector Tool (VAIT) which automates the entire process. They have shown

the effectiveness of proposed methodology by running the tool on set of experiments. The results of their research proved that the methodology proposed by them is an effective way not only for the evaluation of weakness of security mechanism but also helps in identifying the ways of its improvement [4]. Sadeghian et al. presents a comprehensive review of different types of SQL injection detection and prevention techniques. They made the detailed analysis of all the techniques and provided the strengths and weaknesses of each technique. The structural classification of the SQL injection detection and prevention techniques assists other researchers in the adoption of correct technique for their studies [5]. In [6] author(s) demonstrate the comparative performance analysis of MD5, DES and AES encryption algorithms [1] on the basis of execution time, LOC (Lines of Code) over a web application. In [7] author(s) discusses and analyzes the current developments in online authentication procedures including one-time-password systems, biometrics and Public Switched Telephone Network for cardholder authentication. The author(s) proposes a complete new framework for both onsite and online (Internet shopping) credit card transactions. In [8, 9] author(s) presents a detailed review on various types of vulnerabilities, Structured Query Language Injection attacks, Cross Site Scripting Attack, and prevention techniques. The Author(s), also proposes future expectations and possible developments of countermeasures against Structured Query Language Injection attacks. In [10] author(s) presents an integrated model to prevent reflected cross site scripting attack and SQL Injection attacks in applications which are made in PHP. These models work in two modes which are production and safe mode environment. They create sanitizer model for reflected cross site scripting attack and security query model for SQL Injection attack in safe mode. They validate user input text against sanitizer model and input entries which create SQL queries are validated against security query model in production mode. In [11] author(s) demonstrates the exploitation of web vulnerabilities in a credit card validation web application using brute force and dictionary attack. In [12] author(s) also proposes a similar technique to handle the security of the alphabets and numbers but without any detailed comparison. In [13] author(s) proposes a technique to encrypt and decrypt the Alphabets, Numbers and Alphanumeric data in minimum span of time with minimum lines of code, designed logic of which has been coded in JAVA. In [14] Scholte et al. represents IPAAS, a novel technique. This technique is based on automated detection of data type of input parameters which successfully prevents the exploitation of XSS and SQL injection vulnerabilities [15]. They implemented this technique for PHP applications and also analyzed the performance of this technique by running this technique on five real-world web applications. Their technique successfully prevented 65 % of XSS vulnerabilities and 83 % of SQL injection vulnerabilities. In [16] author(s) have designed a Java based tool to show the exploitation of Injection using SQL Injection attack [1] and Broken Authentication [2] using Brute Force Attack and Dictionary Attack and the prevention of all these attacks by storing the data in our database in encrypted form using AES algorithm [17].



## 4 Simulation Performed

We have used java programming paradigm as a tool for exploring the above discussed attacks and vulnerabilities. We have used JAVA DEVELOPMENT TOOLKIT as a tool for stimulating the same. The results along with the outputs are discussed above. We have used Microsoft Access to build our own database and used Microsoft Excel to draw the plots that we have shown in our work.

## 5 Our Methodology

We have divided our methodology into two parts:

### 5.1 Methodology for Exploring Vulnerabilities

#### 5.1.1 Vulnerability

Although many definitions of vulnerabilities exist. But, simply speaking it is a 'flaw' or a Programming bug committed by a novice programmer. If a system has a flaw, the attacker can access that flaw and will take advantage of this flaw to reduce system assurance and reliability. The different vulnerabilities are explained below:

#### Password Ageing

Password ageing can result in the possibility of diminished password integrity. If a user does not change his/her password for a long period of time, his/her user account can be tracked by any person and make his account insecure. If no mechanism is in place for managing password aging, users will have no incentive to update passwords in a timely manner. Therefore, support for password ageing mechanisms must be added in the design phase of development.

#### Empty String Password

Using an empty string as a password can make an account insecure. It is never a good idea to assign an empty string to a password variable. If the empty password is used to successfully authenticate against another system, then the corresponding account's security is likely to be compromised because it accepts an empty password. Thus, a constraint should be imposed that the user should not make empty string as password and if he does there should be an error 'empty string password...'.

## Empty Catch Block Problem

It is usually a bad idea having an empty catch block. When an exception is thrown and not caught, the process has given up an opportunity to decide if a given failure or event is worth a change in execution. Instead, one should catch the exact exception types that he expects because these are the types the program code is prepared to handle. For example, concept of dangling pointers can be a consequence of empty catch block problem.

## 5.2 Methodology for Exploring Network Attacks

### 5.2.1 Network Attacks

In computers, a network attack is any attempt to destroy, expose, alter, disable, steal or gain unauthorized access to or make unauthorized use of a resource (say data). The attacker tries to invade into the system to destroy it. Any attempt made for such intent is called as a network attack. Various network attacks are explained below:

#### Denial of Service

DOS stands as an acronym for “Denial of Service”. This is caused due to the massive traffic at the server end. The large amount of traffic causes the throughput of the server to reduce. The large amount of requests causes the server to go busy. The high amount of traffic causes the server to respond abnormally. At the end the server will not be able to respond to the clients properly. As a result of which the following two scenarios can occur:

- (i) The response time of server for client reduces drastically due to which system throughput and efficiency decreases.
- (ii) The system hangs due to increased traffic as a result of which the system crashes.

Figures 1 and 2 show a client server architecture. Figure 1 represents server window which is ready to receive request from clients. Clients in turn try to request to server. As a client is connected to server, a “Hello Client” message is sent on client window by server as a confirmation. It has been found that in DOS, the Server is bombarded by millions of requests, some genuine and the rest bogus/fake, resulting in collapse of the Services provided by the Server.

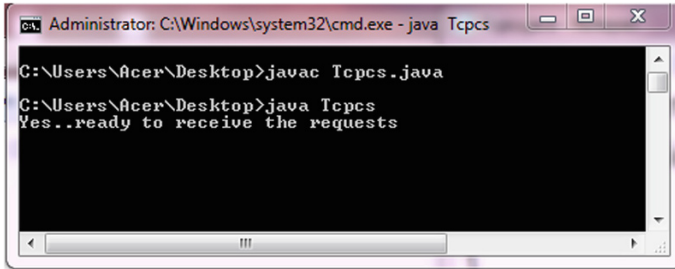
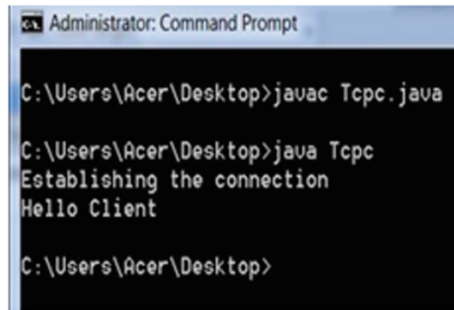


Fig. 1 Server side window for denial of service attack

Fig. 2 Client side window for denial of service attack



### Dictionary Attack

The dictionary attack is a type of attack in which a hacker can spy on the system by using a pre designed list of probable passwords. The programmer can develop a database consisting of these probable passwords. These passwords can be formed by reviewing the profile of the person. A Database was created in MS Access and populated with hundreds of ID's bearing Username and Password. The above formed list of passwords can be compared against the password entered by the programmer. If the password entered by the user matches any of the password in the list then the system is at risk and it can easily be attacked by an experienced hacker. We have implemented dictionary attack using a Microsoft Access database which is connected to a Java program using jdbc-odbc drivers. Figure 3 shows the simulation of Dictionary Attack being successful. The username and password entered by the user in a java form is matched in the usernames and passwords present in the database. The program of "Dictionary Attack" has been executed and the "number of iterations" versus "length of the password" has been plotted as shown in Fig. 4. It can be seen from the plot that the number of iterations to find a given password does not depend on the length of the string entered. Rather, it depends on the number of

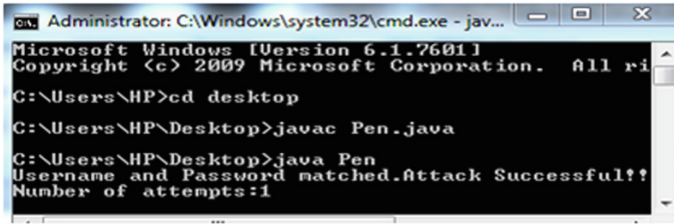
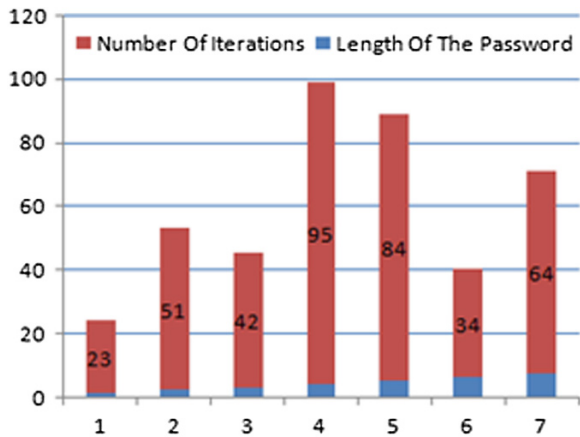


Fig. 3 Execution of dictionary attack showing the attack being successful

Fig. 4 Histogram for dictionary attack showing number of iterations versus length of the password



records that the database contains. We have executed this program by taking a small database of about 100 records where each record consists of characters (a-z) from UNICODE character set. If the entered password is not there in the database we have to iterate a maximum of iterations equal to the number of records in the database.

### Brute Force Attack

The brute force attack is one of the best attacks if one wants to analyze the password sensitivity of a system. In this attack we have built a character set and the program tests all the possible combinations of characters present in the character set against the password entered by the user. If the password entered by the user matches with any of the combinations as discussed above the password is said to be cracked and the system is at risk. The simulation of same has been shown in Fig. 5. The program of “Brute Force Attack” has been executed and the “number of iterations\*0.0001” versus “length of the password” has been plotted as shown in Fig. 6. It can be seen from the plot that the number of iterations to find a given

Fig. 5 Execution of brute force attack being successful

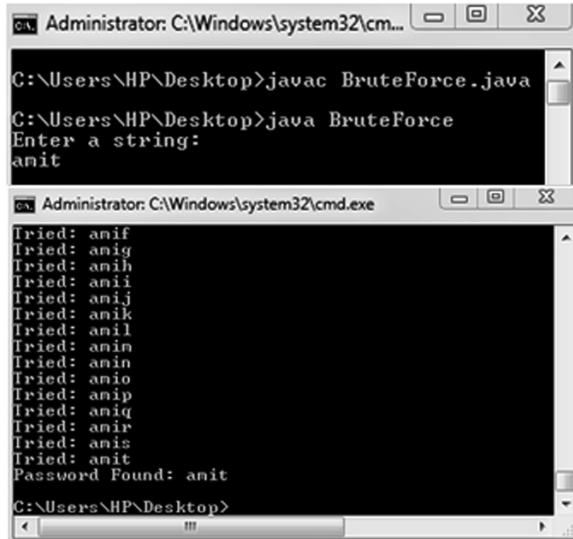
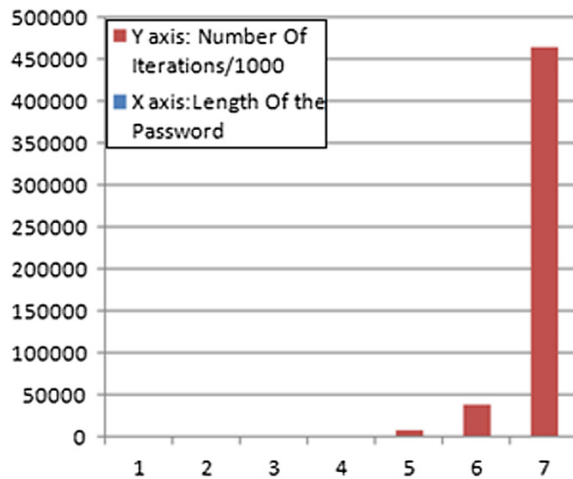


Fig. 6 Histogram showing number of iterations versus length of the password for brute force attack



password depends on the length of the string entered. The password entered by user is checked against all the possible combinations of characters (a-z) from UNICODE character set. Brute force is a stronger attack than Dictionary attack because it has a very high probability of cracking the password. It can be seen that as the length of the entered password increases, the number of iterations required to break the password also increases. The security of a system can be increased if we put some password restrictions and make the length of the password greater than or equal to 7 characters. This is so because it will hinder the attacker from cracking the password in that transient amount of time when the system is momentarily at rest.

## 6 Mathematical Modeling of Network Attacks

### 6.1 DoS

$l \leftarrow$  Number of legitimate requests.;  $q \leftarrow$  Number of bogus requests  
 $r \leftarrow$  Total number of requests generated;  $s \leftarrow$  Total number of requests being received at the server.;  $P \leftarrow$  Performance of the server at time (t).

DOS()

{if  $q \gg l$ {P dips, affecting throughput due to the success of DOS attack} else if  $l \gg q$ {The attack was un successful, P and throughput increases} else{Server works at maximum speed and delivers at consistent throughput.} end if; end if}.

$D \leftarrow$  Difference between number of legitimate requests and number of bogus requests.  $D = l - q$ . As the number of fake requests ( $q$ ) increases the system throughput decreases. Simply put, as  $q$  increases the number of legitimate requests handled by the server decreases per unit time. Therefore the difference between the number of legitimate and bogus requests is the key parameter to represent the time complexity of the algorithm discussed above.  $P$  (Performance of server) =  $\Theta(D) = \Theta(l - q)$ .

### 6.2 Brute Force Attack

Note: Our character set contains characters a-z.

$P \leftarrow$  Plain text string to be searched.

$S \leftarrow$  String which is compared with the pattern to be searched.

$n \leftarrow$  Length of the string P

flag  $\leftarrow$  true, if attack is successful, otherwise false

Brute\_Force\_Attack()

{ for  $i = 1$  to  $n$

    Compare all the combinations of S of length  $i$  with P

        if( $S==P$ ){ flag = true } //Attack Successful

        else{flag = false} //Attack not successful

end for }

Time Complexity: Suppose, if the length of the string P is 1 the number of maximum attempts will be 26 because the size of character set is 26. Now if size of P is 2 the number of possible combinations will be  $(26 + 26^2)$ . Similarly, when the size of the P to be searched is “n” the number of combinations will be:  $(26 + 26^2 + 26^3 + \dots + 26^n)$ . If we use the rules of asymptotic notations  $26^n$  will be the dominant factor. Therefore in our case: Time Complexity =  $\Theta(26^n)$ . Now it is logical to say that because the size of character set was 26 in our case, there complexity of the algorithm comes out to be  $26^n$ . However if the number of characters in the character set is  $m$ , then: **Time complexity:**  $\Theta(m^n)$ ; **Space complexity:**  $\text{num} * n$ . Here: num are the number of bytes per symbol by the encoding scheme being employed according to the architecture.

### 6.3 Dictionary Attack

$P \leftarrow$  Plaintext to be searched ;  $N \leftarrow$  Number of records in dictionary  
 $i \leftarrow$  Number of iterations.

Assumptions : Threshold value for number of attempts to search  $N$ .

Dictionary\_Attack()

```
{ for i=1 to N
  R  $\leftarrow$  ith record in the dictionary
  if ( R is equal toP){Record matched. Search successful}
  else if (i>n){Record not matched. Search unsuccessful}
  end if ; end if; end for }
```

**Time Complexity:**  $O(N)$ . The time taken to search for the plaintext will be a linear search (according to our algorithm) in the dictionary and will be of order  $N$ .

## 7 Result

Various attacks and vulnerabilities given by OWASP such as Denial of service (DOS) Attack, Brute Force Attack, and Dictionary Attack have been executed using Java programming platform. The results of various simulations have been shown wherever necessary and different graphs have been plotted.

## 8 Conclusion and Future Work

Various vulnerabilities and attacks have been explored. We suggest that for developing a secure and a reliable system the developer while writing code should take care of these vulnerabilities during the development phase of SDLC (software development life cycle). Otherwise system and data integrity may be at risk and the system will have some loopholes which an attacker can use to invade into the system. These are not the only vulnerabilities or attacks. There are many. In our future work, we will be exploring other vulnerabilities and attacks and will also be giving the solutions for the vulnerabilities and attacks discussed in this paper.

## 9 Figures

See Figs. [1](#), [2](#), [3](#), [4](#), [5](#) and [6](#).

## References

1. [https://www.owasp.org/index.php/Top\\_10\\_2013-A1-Injection](https://www.owasp.org/index.php/Top_10_2013-A1-Injection)
2. [https://www.owasp.org/index.php/Top\\_10\\_2013-A2-Broken\\_Authentication\\_and\\_Session\\_Management](https://www.owasp.org/index.php/Top_10_2013-A2-Broken_Authentication_and_Session_Management)
3. Huluka, D., Popov, O.: Root cause analysis of session management and broken authentication vulnerabilities. In: IEEE, pp. 82–86 (2012)
4. Fonseca, J., Vieira, M., Madeira, H.: Evaluation of web security mechanisms using vulnerability and attack injection. In: IEEE (2013)
5. Sadeghian, A., Zamani, M., Manaf, A.A.: A taxonomy of SQL injection detection and prevention techniques. In: IEEE, pp. 53–56 (2013)
6. Johari, R., Jain, I., Ujjwal, R.L.: Performance analysis of MD5, DES and AES encryption algorithms for credit card application. In: International Conference on Modeling and Computing, ICMC (2014)
7. Gupta, S., Johari, R.: A new framework for credit card transactions involving mutual authentication between cardholder and merchant. In: 2011 International Conference on Communication Systems and Network Technologies (CSNT), pp. 22–26. IEEE (2011)
8. Johari, R., Sharma, P.: A survey on web application vulnerabilities (SQLIA, XSS) exploitation and security engine for SQL injection. In: 2012 International Conference on Communication Systems and Network Technologies (CSNT), pp. 453–458. IEEE (2012)
9. Johari, R., Gupta, N.: Secure query processing in delay tolerant network using java cryptography architecture. In: International Conference on Computational Intelligence and Communication Networks (CICN), pp. 653–657. IEEE (2011)
10. Sharma, P., Johari, R., Sarma, S.S.: Integrated approach to prevent SQL injection attack and reflected cross site scripting attack. In: International Journal of System Assurance Engineering and Management, pp. 343–351. Springer, Berlin (2012)
11. Jain, I., Johari, R., Ujjwal, R.L.: Web vulnerability exploitation using brute force attack and dictionary attack. In: Proceedings of 9th National Conference on Smarter Approaches in Computing Technologies and Applications (2014)
12. Ruby, L., Johari, R.: Designing a secure encryption technique for web based application. Int. J. Adv. Res. Sci. Eng. (IJARSE) **3**(7), 159–163 (2014)
13. Ruby, L., Johari, R.: SANE : secure encryption technique for alphamumeric data over web based applications. Int. J. Eng. Res. Technol. (IJERT) **3**(8), (2014)
14. Scholte, T., Robertson, W., Balzarotti, D., Kirida, E.: Preventing input validation vulnerabilities in web applications through automated type analysis. In: IEEE 36th International Conference on Computer Software and Applications, pp. 233–243 (2012)
15. [https://www.owasp.org/index.php/SQL\\_Injection](https://www.owasp.org/index.php/SQL_Injection)
16. Jain, I., Johari, R., Ujjwal, R.L.: CAVEAT: credit card vulnerability exhibition and authentication tool. In: Second International Symposium on Security in Computing and Communications (SSCC'14), pp. 391–399. Springer, Berlin (2014)
17. [http://en.wikipedia.org/wiki/Advanced\\_Encryption\\_Standard](http://en.wikipedia.org/wiki/Advanced_Encryption_Standard)



# Efficient Set Routing for Continuous Patient Monitoring Wireless Sensor Network with Mobile Sensor Nodes

M.S. Godwin Premi, Betty Martin and S. Maflin Shaby

**Abstract** Static sensor nodes are effectively and efficiently replaced by mobile sensor nodes in WSN applications like tracking, periodic weather monitoring, etc. In this paper, challenges in WSN routing are focused with mobile nodes. A new routing protocol called as set routing is proposed for wireless sensor networks with mobile nodes. In set routing, the sets of nodes are constructed after deployment. Routing overhead is fully given to static sink node or base station. Direction based linear mobility pattern is chosen for its greater coverage area with low energy spent and is used in set routing. Set routing is simulated using Omnet++ and Matlab and the performance is studied. The results are compared with cluster based routing and mobile leach protocols and found that delivery ratio is higher in our set routing.

**Keywords** Direction based linear mobility · Master nodes · Neighbouring sets · Sink node

## 1 Introduction

The wireless sensor network is a data centric multi-hop network [1]. Motes are playing vital role in wireless sensor networks to collect the data as well as to transmit the same to the sink node. These motes sense the data or receive the data from neighbors, process and store the same, and at last transmit/forward to the sink node. After deployment, all the sensor nodes or motes self organize them and start sense the data. Then all these data are transmitted to the sink [2–4]. There are many advantages of mobile wireless sensor networks when compared to static wireless sensor networks like increased coverage area and highly improved target tracking. When mobility is introduced in the motes generally the energy will drop. But this can be avoided by using solar power harvesting. With respect to applications the

---

M.S. Godwin Premi (✉) · B. Martin · S. Maflin Shaby  
Faculty of Electrical and Electronics, Sathyabama University, Chennai, India  
e-mail: msgodwinpremi@gmail.com

number of mobile nodes required may vary. Also depend on the scenario all the nodes can be mobile or only few nodes can be mobile. In order to reduce the propagation delay, energy and path loss new routing schemes are developed based on different conditions for the third logical layer.

## 2 Related Work

Jonathan Henderson introduced a hierarchical clustering algorithm for sensor networks, called Low Energy Adaptive Clustering Hierarchy (LEACH) [5]. The extension of LEACH protocol is the solar-aware LEACH (sLEACH) protocol [6]. To enhance the network lifetime solar powered nodes are introduced. However, in simulation both sLEACH and the original LEACH used the same algorithm and so both protocols are affected in the same manner. The Cluster Based Routing (CBR Mobile) protocol [7–11] for WSN is proposed by Awwad (2009) [12] to avoid that packet loss. The proposed protocol is implemented in two phases similar to LEACH. They are setup phase or registration phase and steady state phase. Like LEACH, the stages of setup phase are cluster head election, advertisement, decision, schedule creation. In this protocol, always a cluster head is made free to receive the data from unconnected sensor nodes. Each cluster head takes turn to be free for this operation. Since the unconnected nodes are joined in the newly formed cluster with a free cluster head as the cluster head, the data loss is very much reduced. In normal situation the protocol works as proactive, and sends data to cluster head in advance. If the sensor nodes did not receive data request message from its cluster head, it will send the message to a free cluster head. In LEACH-Mobile, sensor nodes wait for the request message for two consecutive failure frames. But CBR mobile protocol immediately sets up the registration phase to avoid accumulation of packet losses.

## 3 System Description

In this paper, a scenario is considered in such a way that the mobile sensor nodes are deployed in one end of hospital. The sink node or the base station is present in the centre of the hospital. The mobile sensor nodes are static until they receive START message from the sink node. The sink node sends the sample REQ message to all nodes. All mobile nodes send the REPLY message with their identity. Based on the time of arrival, using low cost localization algorithm sink node calculates the initial location of all the mobile nodes. After the initial locations of all the mobile nodes are determined, different sets are formed by sink node. For the initial position, master node(s) for each set is determined by the sink node. Moreover the nearby sets are noted by the sink node. After the set formation the sink node send the START message. START message contains the next stop position for all the mobile nodes.

Route information in every position is given to individual sets by the sink node. After receiving the START message from sink node they start moving in the prescribed direction. In order to cover all eight directions the direction of movement of sensor nodes should be as below (NW → N → NE → E → SE → S → SW → W): Left → Left → Down → Down → Right → Right → Up → Up. At regular intervals of time all the nodes are static in order to forward or transmit the data. The data are sensed by the sensor nodes when they are mobile and the data are transmitted or forwarded to the sink node when they are static. It is considered that there are no collisions during the movement and the entire nodes are free to move with equal speed. Also, the sink node initially calculates the location of the nodes using low cost localization algorithm and the nodes are named/addressed. Entire network is controlled by the sink node i.e.; when to move, when to stop, which direction to choose, whom to forward the data, speed, etc. For a mobile node the sink node selects minimum of eight stop positions around the sink. At every stop position, route and the next stop position are informed to all nodes via master node. Route discovery message flow is shown in Fig. 1. In this technique as the computing overhead is taken by sink node, route computing overhead is reduced at individual sensor nodes. As the sink node computes the route for each stop point and informs about the new route, energy spent for controlled mobility is partially compensated at individual sensor node. Thus patients in each room are monitored regularly by the sensor node and the data is transmitted to the base station. Patients in each room in every block will be monitored by same set of nodes in the next rounds providing the continuous measurement.

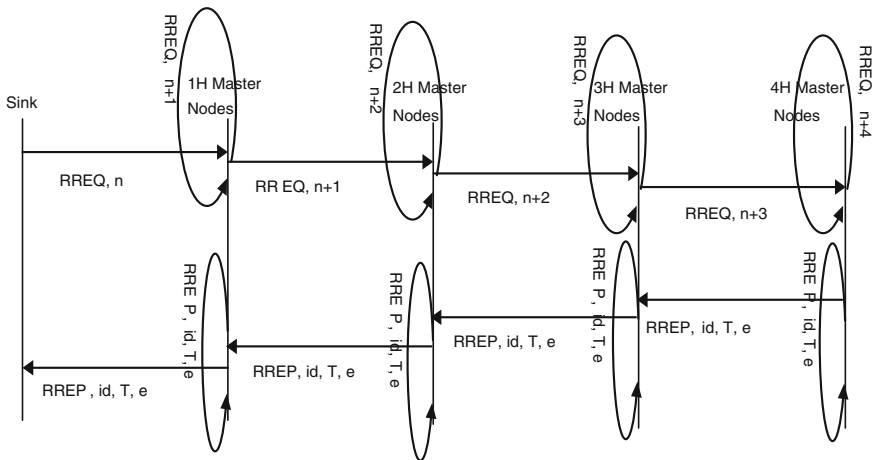


Fig. 1 Route discovery message flow

### 4 Simulation Results

Simulations are carried out in OMNeT++ 4.1 IDE with MiXiM Framework. Each sensor node is designed by understanding the logical layers of WSN and is developed as a NED using the supporting files. Results obtained using OMNet++ and Matlab are shown in Figs. 2, 3 and 4. It is found from the results that the

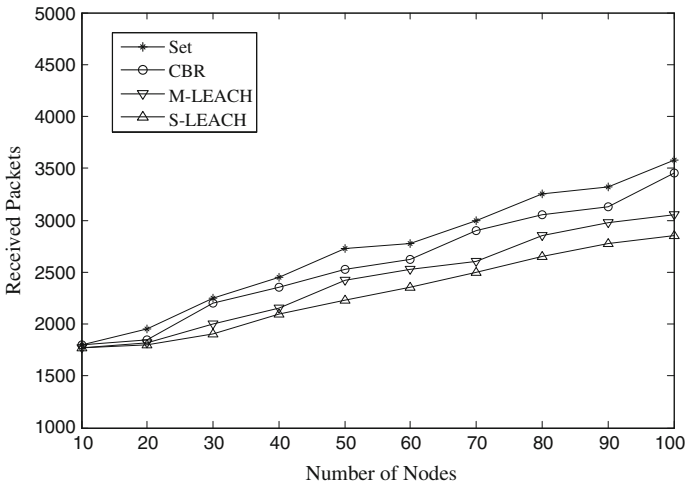


Fig. 2 Received packets

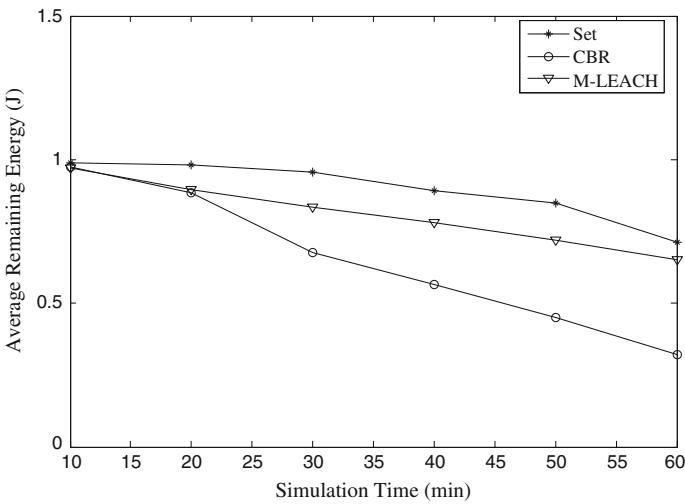
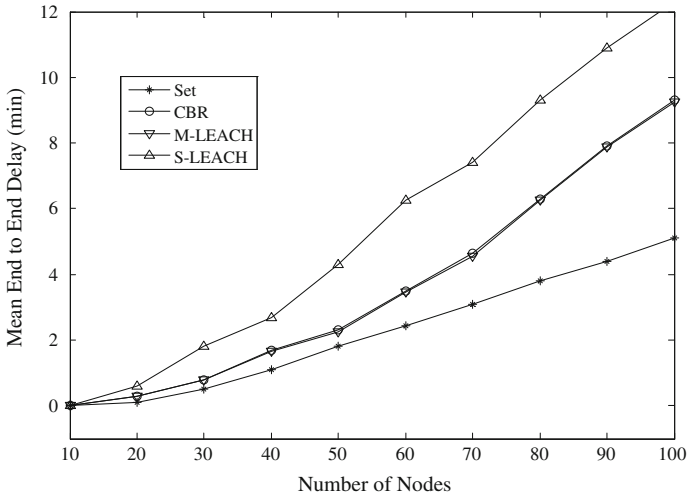


Fig. 3 Average remaining energy



**Fig. 4** Mean end to end delay

number of packets received and the remaining energy are high in set routing compared to existing cluster based routing, mobile LEACH and solar LEACH. Also the mean end to end delay is reduced in set routing. It is observed that received packets are more in set routing compared with other protocols. Moreover from Fig. 3 it is proved that energy spent is minimized in set routing. Also from Fig. 4 it is clear that mean end to end delay is minimized in set routing.

## 5 Conclusion

It is observed that set routing is the best suitable routing protocol for the continuous patient monitoring in the hospital. It is also observed that minimum number of nodes is required for maximum efficiency. Thus rather than spending for lot of sensor nodes, the required data can be gathered with a minimum number of mobile nodes. From the setup suggested in the study, it is observed that the network is energy efficient for the required amount of data collection.

## References

1. Al-Karaki, J.N., Kamal, A.E.: Routing techniques in wireless sensor networks. *IEEE Wirel. Commun.* (2004)
2. Godwin Premi, M.S., Shaji, K.S.: MMS routing for wireless sensor networks. In: *IEEE Computer Society* (2010)

3. Godwin Premi, M.S., Shaji, K.S.: MMS routing to enhance lifetime in wireless sensor networks. In: *Proceedings of Conference Wireless Communication and Sensor Networks (2009)*
4. Godwin Premi, M.S., Shaji, K.S.: Router performance with AoI and RoI routing for wireless sensor networks. In: *2010 IEEE International Conference on Communication Control and Computing Technologies (2010)*
5. Henderson, J.: *A study of the LEACH protocol for wireless sensor networks—implementing LEACH*. Mississippi Valley State University (2009)
6. Voigt, T., Ritter, H., Schiller, J.: Solar aware Routing in Wireless Sensor Networks. In: *Personal Wireless Communications*, pp. 847–852. Springer, Berlin (2003)
7. Ibriq, J., Mahgoub, I.: Cluster-based routing in wireless sensor networks: issues and challenges. In: *SPECTS'04*, pp. 759–766 (2004)
8. Zhang, L., Hu, Z., Li, Y., Tang, X.: Grouping based clustering routing protocol in wireless sensor networks. In: *International Conference on Wireless Communications, Networking and Mobile Computing (2007)*
9. Liliana, M., Arboleda, C., Nasser, N.: Cluster-based routing protocol for mobile sensor networks. In: *Qshine'06 (2006)*
10. Hussain, S., Matin, A.W.: Hierarchical cluster-based routing in wireless sensor networks. In: *Proceedings of IPSN (Poster) (2006)*
11. Kang, T., Yun, J., Lee, H., Lee, I.: A clustering method for energy efficient routing in wireless sensor networks. In: *Proceedings of the 6th WSEAS (2007)*
12. Awwad, S.A.B., Ng, C.K., Noordin, N.K., Rasid, M.F.A.: Cluster Based Routing protocol for Mobile Nodes in Wireless Sensor Network. In: *International Symposium on Collaborative Technologies and Systems, May 2009*, pp. 233–241

# Overview of Cluster Based Routing Protocols in Static and Mobile Wireless Sensor Networks

Sachin R. Jain and Nileshsingh V. Thakur

**Abstract** Wireless Sensor Network (WSN) is one of the hottest research areas now days. WSNs can be used to monitor environmental conditions like light, sound, temperature, pollution, humidity, wind speed and direction, pressure, and many more. Also WSNs are used in industrial process monitoring and control, machine health monitoring, traffic monitoring, space exploration, disaster management etc. Cluster based WSN provide much better support, functionality, advantages and results in ample variety of applications, because of this, many cluster based routing protocols have been developed for WSN. This paper focus on concise study of the clustering based routing protocols. In this paper, brief overview of the cluster based routing techniques for Static WSN where, the sensor nodes are fixed, i.e. not moveable, and for Mobile WSN, where the sensor nodes are fixed and/or mobile in nature, i.e. they can move from one location to another, is presented.

**Keywords** Cluster based routing • Wireless sensor networks • Static nodes • Mobile nodes

## 1 Introduction

Wireless Sensor Network [1–3] is one of the hot areas in research now days. It is consist of a group of spatially distributed and dedicated autonomous cooperative tiny, low cost, small battery powered static and/or mobile sensor nodes which have

---

S.R. Jain (✉)

Department of Computer Science and Engineering, Priyadarshini Institute of Engineering and Technology, Nagpur, India  
e-mail: sachinjain98440@rediffmail.com

N.V. Thakur

Department of Computer Science and Engineering, Ram Meghe College of Engineering and Management, Badnera, Amravati, India  
e-mail: thakurnisvis@rediffmail.com

capability to sense, actuate, compute, move from one location to another and communicate with each other. WSNs can be used to monitor environmental conditions like light, sound, temperature, pressure, pollution levels, humidity, and many more. Development of WSN was motivated by military applications but, nowadays, WSNs applications has been extended to traffic monitoring, health monitoring, industrial process monitoring and control, machine monitoring, etc.

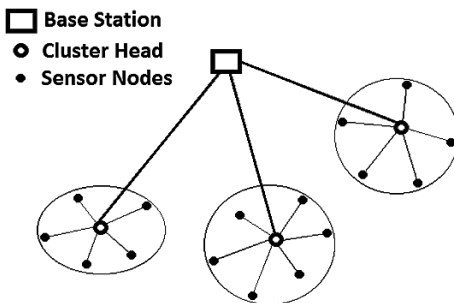
Sensor nodes are deployed densely in the region of interest for monitoring of any desired data, where there is no network infrastructure, so the nodes must cooperate to accomplish communication, global control and information aggregation. WSN aims to collect data from a desired region of interest and sometimes control an environment. Generally in the basic operations performed in WSN, like sensing, computing, communication, moving from one location to another and routing the sensed data, carried out during the lifetime of the wireless sensor network, battery of the sensor nodes may ruin quickly, due which the desired operations may not be completed and the network may fail. To avoid such situations and to prolong the lifetime of the operation and the network, the battery life of the sensor nodes is considered as one of the key issues. It is must to find out the factors affecting the battery life of the sensors and ways to reduce the energy consumption of sensor nodes and that is one of the main challenges in Wireless Sensor Networks.

Cluster Based Routing (CBR) [4] is one of the most popular routing schemes used in static as well as mobile WSN. In this type of routing protocols the sensors are grouped into different clusters, in each cluster there is a Cluster Head (CH) which collects data from each of the member nodes in its cluster. The CH may collect data from the sensors periodically or TDMA scheduling may be done for collecting the data from the sensors. Figure 1 illustrates the cluster based routing in WSN.

Cluster based routing protocols have a variety of advantages compared with flat routing protocols [5, 6], such as more scalability, less load, less energy consumption, Data Aggregation/Fusion, Collision Avoidance, more robustness, Load Balancing, Maximizing of the Network Lifetime, Quality of Service etc.

In this paper we are classifying the WSN into two categories i.e. Static Wireless Sensor Network (SWSN) and Mobile Wireless Sensor Network (MWSN). The SWSN generally consist of the sensor nodes, which are static in nature i.e. once the nodes are deployed in the field their position is fixed, they do not have the

Fig. 1 Cluster based routing in wireless sensor networks





capability to move from one location to another. Whereas MWSN consist of sensor nodes which are static and/or mobile in nature i.e. once the nodes are deployed in the field, they can move from one location to other [7]. The routing of data from the sensor to the BS in MWSN is more complicated than that of SWSN, as because of the mobility of the sensor nodes, the topology changes rapidly in MWSN.

## 2 Cluster Based Routing Protocols in SWSN

This section presents the discussion on routing protocols in Static Wireless Sensor Networks (SWSN), which works only on static sensor nodes. Summary of studied protocols is presented in tabular manner.

Low Energy Adaptive Clustering Hierarchy (LEACH) protocol [8] is a self organizing, adaptive clustering protocol for Wireless Sensor Networks (WSNs) which uses the concept of randomization to distribute load among the nodes in WSN. Operation of LEACH protocol is alienated into rounds where each round composed of two phases: set-up phase in which clusters are formed and CH is selected for each cluster using the residual energy of the nodes and steady phase in which using TDMA the nodes sends data to their CH during time slots allocated to them.

Hussain and Matin [9] have discussed Hierarchical Cluster based Routing protocol (HCR) in which each cluster is managed by a set of associates known as head-set and uses round-robin technique. Cluster Head (CH) receives messages from the cluster members, aggregates the message and transmits it to the Base Station (BS). All the transmissions are single-hope and CHs transmit long range broadcast messages and the Cluster Members (CM) transmits short range broadcast messages. After a specific number of transmissions cluster reformation is done, called as a round. The simulation is performed on versions of HCR (HCR-1, HCR-2) and LEACH and found that HCR-1 shows a minor improvement over LEACH but for HCR-2 the improvement is enhanced.

Another cluster-based routing protocol for sensor networks is discussed in [10] by Lee et al., where the sensor nodes do not know their location. According to the conditions of the network, it uses the remaining energy of sensor networks and wanted number of CHs. For the proposed protocol simulation was carried out with two initial energy levels and it was found that the protocol improves the data rate and lifetime of the sensor networks compared to LEACH.

WSNs are similar as that of a Neural Network of human beings, which is a cluster of firmly related individual units and carry outs a special function, discussed by Guo et al. [11]. The authors have proposed Dynamic Clustering Reactive Routing (DCRR) algorithm based on the architecture and principle of neural network in which the sensor nodes are event driven. The performance of DCRR is compared with TEEN, and found that DCRR algorithm attains significantly better balance in battery power distribution and increases the energy efficiency and the lifetime of the network.

Threshold sensitive Energy Efficient sensor Network (TEEN) [12] is LEACH based hierarchical routing protocol used for time critical application domains in WSN. It uses LEACH's method to form the cluster. It has simple nodes with first-level CHs which are formed away from BS and second-level CHs which are formed near to BS. The CH sends two types of data to neighbor nodes, one is Hard Threshold (HT) mode where the nodes transmit data if sensed data attributes are of interest, second is Soft Threshold (ST) mode where any minor change in the sensed value of the attribute is transmitted further.

TEEN has main assumptions [13, 14]: BS can transmit data to all nodes directly, it uses two-tier architecture for CHs and BS with all sensor nodes has same initial energy. TEEN has weakness too: Node has to wait for time slot for data transmission, if node has no data to transmit the time slot is wasted and CH has to keep its transmission on always for data from nodes.

The comparative analysis of some of the cluster based routing algorithm in Static Wireless Sensor Network is summarized in Table 1.

### 3 Cluster Based Routing Protocols in MWSN

This section presents the discussion on routing protocols in Mobile Wireless Sensor Networks (MWSN), which works on both, static and mobile sensor nodes. Summary of studied protocols is presented in tabular manner.

One of the main challenges in MWSN is Packet loss due to the mobility of the sensor nodes and it comes in parallel with energy consumption. In paper [15], authors propose adaptive TDMA scheduling and round free cluster head protocol called Cluster Based Routing (CBR) protocol for Mobile Nodes in WSN. The performance of the proposed protocol is evaluated using MATLAB and it is found that it reduces the packet loss by around 25 % compared to LEACH Mobile protocol. It is seen that the protocol is also energy aware, shows significant improvement in the data transfer success rate in the mobility environment compared to LEACH-Mobile protocol.

To reduce the complexity of sensors and the cost of construction of WSN, Duan et al. [16] have designed three-layer mobile node architecture. They proposed a Shortest Path (SP) routing protocol to save energy of nodes. The simulation results show that Shortest Path routing protocol outperforms LEACH by redefining the function of nodes, keeping most of the time some nodes in sleeping mode and transmitting data packets through the shortest path to the sink.

A routing protocol is proposed by Ying and Yang [17] for MWSN. It has both fixed and mobile sensor nodes in the same network. It is called as Energy-efficient Chain-cluster Routing protocol (ECRM). The static nodes whose battery are difficult to be recharged, are set into the communication backbone to maintain the basic connectivity of network, and the mobile nodes, whose battery can be recharged, are set as CH to prolong the fixed node's lifetime and improves the energy efficiency.

**Table 1** Comparative analysis of various routing algorithm in SWSN

Refs.	Concept	Assumptions	Phases	Working	Remark
[8]	Self organizing, adaptive clustering Uses randomization to distribute load Round Robin cluster head selection	BS is fixed and far away Nodes have enough power to communicate with BS directly Single hop transmission	Set-up Steady Election	CH is selected using residual energy of nodes Using TDMA nodes sends data to CH Nodes self-organized into new set of cluster, and cluster contains a head-set	Uses data fusion at CH Improves lifetime of network
[9]	Clusters are maintained for short duration called round BS changes desirable no. of CHs	Members perform short range, CH performs long range broadcasting Sensor nodes do not-necessarily know their own position	Data transfer Construction Communication	Head-set members performs long range transmission to BS Uses remaining energy of sensor networks and desired number of CHs	HCR-1 shows minor improvement over LEACH but for HCR-2 improvement is enhanced Improves data rate and lifetime of networks compared to LEACH
[10]	LEACH based hierarchical routing protocol Used for time critical application	BS and all sensor nodes have same initial energy Uses two-tier architecture for CHs	Set-up Steady	CH selected using residual energy of nodes Using TDMA nodes sends data to CH	Uses data fusion at CH Improves network lifetime compared to LEACH
[11]	TEEN based hierarchical routing protocol Uses hybrid network Selects temporary CH according to similarity and isochronisms of local on-the-spot data	BS and all nodes have different initial energy Uses two-tier architecture for CHs Based on architecture and principle of neural network Nodes are event driven Self-organizing multi-hop network	Set-up Steady Excite Transmit Receive	CH is selected using residual energy of nodes Using TDMA nodes sends data to CH Node monitors sudden change in environment Transmits excitement info. to other nodes Node receives excitement information from other nodes	Uses data fusion at CH Improves lifetime compared to TEEN Performance of DCRR is remarkably better compared with TEEN
[12]	TEEN based hierarchical routing protocol Uses hybrid network	BS and all nodes have different initial energy Uses two-tier architecture for CHs	Set-up Steady	CH is selected using residual energy of nodes Using TDMA nodes sends data to CH	Uses data fusion at CH Improves network lifetime compared to LEACH
[13]	TEEN based hierarchical routing protocol Uses hybrid network	BS and all nodes have different initial energy Uses two-tier architecture for CHs	Set-up Steady	CH is selected using residual energy of nodes Using TDMA nodes sends data to CH	Uses data fusion at CH Improves network lifetime compared to LEACH

**Table 2** Comparative analysis of various routing algorithm in MWSN

Refs.	Concept	Assumptions	Phases	Working	Remark
[4]	Zone based information	Homogeneous and location aware Nodes	Route creation	Combined updating mechanism including periodic and event based	Acts as a hybrid routing protocol
	Cluster like communication between nodes	BS is stationary, mobile nodes	Route prevention		
[15]	Cluster based routing	Mobile nodes	Cluster and CH formation	Sends data to CH in efficiently	Energy aware
	TDMA scheduling concept	BS is far away	TDMA scheduling, data routing	Based on received signals	Adaptive scheduling, improved data rate
[16]	Multi-layer	Mobile nodes are of 3 types	Neighbor discovery	Data collection, routing table maintenance	Reduces complexity and construction cost
	Cluster based	Sensor, fusion, control nodes	Shortest path construction	Data processing placed in different nodes	Save energy of nodes
[17]	Energy efficient chain-cluster routing (ECRM)	Fixed mixed with mobile homogeneous nodes	Backbone setup, cluster formation	Fixed nodes considered, CH at each layer is chosen	Save energy consumption and overheads produced
	Uses efficient CH selection criteria	Nodes transmit data to BS continuously, BS is far away	Steady communication	Data flow to BS via communication link	Robust to network size and energy efficient
[18]	Based on LEACH	Homogeneous nodes, communicate directly to BS	Set-Up	Randomly rotates CH, activities are equally shared	Reduces energy dissipation, doubling lifetime
	Randomization for distributing energy load	BS is fixed and far away, One CH work as local BS	Steady	Compression at CH, divides operation into rounds	Distribute energy evenly
[19]	Data centric braided multipath algorithm	Nodes are homogeneous	Path establishment, data forwarding	Uses previous information, detecting loops and dismantling	Good performance in high data delivery rate
	Uses multipath inter-leaving routing	Nodes are mobile	Route maintenance, localized path refresh	Monitoring data delivery	Low overhead,
	Reverse path based forwarding algorithm	BS is far away	Loop handling	Maintaining braided multiple paths	Loop avoidance

An Energy-Efficient Communication Protocol for Wireless Micro-sensor Networks is discussed by Heinzelman et al. [18]. It uses the concept of LEACH and randomization for distributing energy load among sensor nodes in the network. Simulation results show that the algorithm is better as it reduces the energy dissipation doubles the lifetime for networks and it is able to distribute energy dissipation evenly throughout the sensors.

In [19] the Multipath Algorithm for MWSN is discussed by A. Aronsky and A. Segall. It uses Data Centric Braided Multipath (DCBM) algorithm with multipath interleaving routing and Reverse Path Based Forwarding algorithm. The algorithm achieves good performance in terms of high data delivery rate and low overhead, it also helps in avoiding loop formation in the network.

Cluster Based Routing Protocol for MSN is discussed in [4], which is based on Zone Based Information and there is cluster like communication between nodes. The basic assumptions are: all nodes are homogeneous, all nodes are location aware, BS is stationary and sensor nodes are mobile. It uses a combined updating mechanism, including periodic and event based updates. It acts as a hybrid routing protocol.

The comparative analysis of various cluster based routing algorithm in Mobile Wireless Sensor Network is summarized in Table 2.

## 4 Conclusion and Discussion

WSN consist of a set of spatially distributed and dedicated autonomous cooperative tiny, low cost, limited battery powered static and/or mobile sensor nodes deployed densely in a region of interest. The sensor nodes have the capability to sense, actuate, compute, move from one location to another, communicate with each other and send data to sink or base station using single hop or multi hop communication with the help of various routing protocols available for WSN. Cluster based routing is one of the best approaches for routing of data to the sink or BS, it has many advantages over a direct communication or a flat WSN. In this paper various clusters based routing protocols for Static and Mobile WSNs are discussed and analyzed. The basic assumptions, working environment, advantages, limitations, and working style of various clusters based routing protocols for Static and Mobile Wireless Sensor Networks is also discussed in this paper.

## References

1. Buratti, C., Conti, A., Dardari, D., Verdone, R.: An overview on wireless sensor networks technology and evolution. *Sensors*, pp. 6869–6896 (2009)
2. Yick, J., Mukherjee, B., Ghosal, D.: Wireless sensor network survey. *Comput. Netw.* **52**, 2292–2330 (2008)

3. Akyildiz, I.F., Melodia, T., Chowdhury, K.R.: A survey on wireless multimedia sensor networks. *Comput. Netw.* **51**, 921–960 (2007)
4. Arboleda, L.M., Nasser, N.: Cluster-based routing protocol for mobile sensor networks. In: *Proceeding of the 3rd International Conference on Quality of Service in Heterogeneous Wired/Wireless Networks*, Article No. 24, pp. 474–480. ACM (2006)
5. Wajgi, D., Thakur, N.V.: Load balancing based approach to improve lifetime of wireless sensor networks. *Int. J. Wirel. Mobile Netw.* **4**(4), 155–167 (2012)
6. Wajgi, D., Thakur N.V.: Load balancing algorithms in wireless sensor networks: a survey. *Int. J. Comput. Netw. Wirel. Commun.* **2**(4), 456–460 (2012)
7. Akewar, M.C., Thakur, N.V.: A study of wireless mobile sensor network deployment. *Int. J. Comput. Netw. Wirel. Commun.* **2**(4), 533–541 (2012)
8. Heinzelman, W., Chandrakasan, A., Balakrishnan, H.: Energy-efficient communication protocol for wireless micro sensor networks. In: *Proceedings of the 33rd Annual Hawaii International Conference on System Sciences*, pp. 3005–3014. HICSS (2000)
9. Hussain, S., Matin, A.W.: Hierarchical cluster-based routing in wireless sensor networks. In: *Proceeding of 5th International Conference on Information Processing in Sensor Network*, pp. 1–2. IPSN06, USA (2006)
10. Lee, G., Kong, J., Lee, M., Byeon, O.: A cluster-based energy-efficient routing protocol without location information for sensor networks. *Int. J. Inf. Process. Syst.* **1**(1), 49–54 (2005)
11. Guo, B., Li, Z.: A dynamic-clustering reactive routing algorithm for wireless sensor networks. *Wirel. Netw.* **15**(4), 423–430 (2009)
12. Manjeswar, A., Agrawal, D.P.: TEEN: A protocol for enhanced efficiency in wireless sensor networks. In: *Proceedings 15th International Parallel and Distributed Processing Symposium*, pp. 2009–2015. IEEE (2001)
13. Bhattacharyya, D., Kim, T., Pal, S.: A comparative study of wireless sensor networks and their routing protocols. *Sensors*, 10506–10523 (2010)
14. Maimour M., Zeghilet, H., Lepage, F.: Cluster-based routing protocols for energy efficiency in wireless sensor networks, pp. 167–188. CRAN laboratory, France (2010)
15. Awwad, S.A.B., Ng, C.K., Noordin, N.K., Rasid, M.F.A.: Cluster based routing protocol for mobile nodes in wireless sensor network, pp. 233–241. IEEE (2009)
16. Duan, Z., Guo, F., Deng, M., Yu, M.: Shortest path routing protocol for multi-layer mobile wireless sensor networks. In: *International Conference on Networks Security, Wireless Communications and Trusted Computing*, pp. 106–110. IEEE (2009)
17. Ying, T., Yang, O.: A novel chain-cluster based routing protocol for mobile wireless sensor networks. In: *6th International Conference on Wireless Communications Networking and Mobile Computing (WiCOM)*, pp. 1–4. IEEE (2010)
18. Heinzelman, W.R., Chandrakasan, A., Balakrishnan, H.: Energy-efficient communication protocol for wireless micro-sensor networks. In: *Proceedings of the 33rd Annual Hawaii International Conference on System Sciences*, pp. 1–10. IEEE (2000)
19. Aronsky, A., Segall, A.: A multipath routing algorithm for mobile wireless sensor networks. In: *Third Joint IFIP Wireless and Mobile Networking Conference*, pp. 1–6 (2010)

# A 2 Dot 1 Electron Quantum Cellular Automata Based Parallel Memory

Mili Ghosh, Debarka Mukhopadhyay and Paramartha Dutta

**Abstract** In the present scope, a new design methodology of parallel memory is offered. It is designed using 2 dot 1 electron Quantum-Dot Cellular Automata (QCA) paradigm. This methodology ensures better efficiency and high degree of compactness. One bit design methodology can be extended to design multiple bit parallel memory. Here we present 2 bit memory using 2 dot 1 electron QCA.

**Keywords** Parallel memory · 2 dot 1 electron QCA · Loop · n bit memory

## 1 Introduction

High speed and integrated circuitry are treated as the major requirement of digital industry. CMOS technology provides all these features with some added benefits. Thus it rules the digital industry from a past few decades. But the recent advancement in the digital industry due to the emergence of nanotechnology and nano scale devices threatens the existence of CMOS technology in the world of nano scale devices. CMOS technology is going to achieve its scaling limits in the near future. CMOS technology possesses some limitations in nano scale designs. Some of these limitations are off state leakage current, dimensional restriction, degraded switching performance etc. This leads to an urge of highly efficient nanotechnology offering cost optimum designs. QCA is one of the most promising

---

M. Ghosh (✉) · P. Dutta

Department of Computer and System Sciences, Visva Bharati University, Santiniketan, India  
e-mail: ghosh.mili90@gmail.com

P. Dutta

e-mail: paramartha.dutta@gmail.com

D. Mukhopadhyay

Department of Computer Science and Engineering, Bengal Institute of Technology and Management, Santiniketan, India  
e-mail: debarka.mukhopadhyay@gmail.com

© Springer India 2015

J.K. Mandal et al. (eds.), *Information Systems Design and Intelligent Applications*,  
Advances in Intelligent Systems and Computing 339,  
DOI 10.1007/978-81-322-2250-7\_63

627

alternative to the CMOS technology. The design methodology of the memory unit is based on the design proposed in [1]. This paper supplements implementation of the design proposed in it. But in the present scope we implemented this using 2 Dot 1 electron QCA. The rest of the paper is organized in the following manner. Section 2 presents the basics of 2 Dot 1 electron QCA. Section 3 proposes the advantages of 2 Dot 1 electron QCA designs. In Sect. 4, the previous reportings in this domain has been briefly discussed. Section 5 presents the 2 Dot 1 electron QCA implementation of the design and Sect. 6 determines the output states of the proposed design. In Sect. 7 the stability and compactness of the proposed design have been analysed. The design methodology of the memory is then compared with the existing designs in Sect. 8. Conclusion is drawn in Sect. 9.

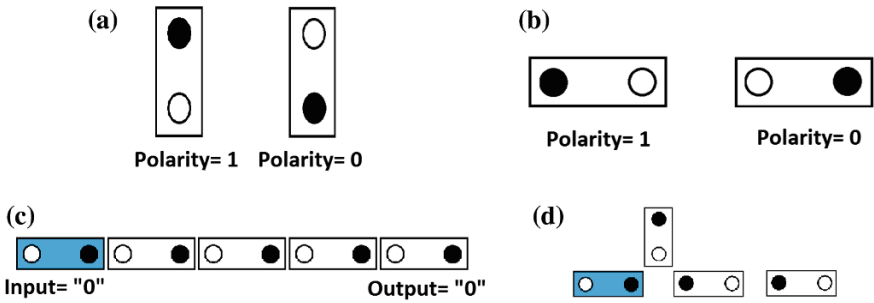
## 2 Basics of 2 Dot 1 Electron QCA

QCA concept is based on the concepts of cells and quantum dots. Quantum dots are capable of containing free electrons which can tunnel between the quantum dots. The cell configuration is used to represent the binary information. The most common form of QCA is 4 Dot 2 electron QCA and it has been well explored in [2, 3]. 2 Dot QCA cells can align either vertically or horizontally as shown in Fig. 1. The basic constructs of 2 Dot 1 electron QCA consists of binary wire, inverter, majority voter gate and planar wire crossing as shown in Figs. 1c, d, 2 and 4 respectively (Fig. 3).

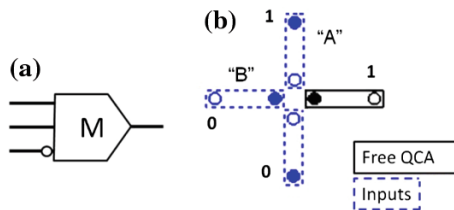
### 2.1 Clocking Mechanism

The QCA clocking is a bit different from conventional CMOS clocking. It is basically a quasi adiabatic four phase clocking mechanism. This type of clock is used in QCA to control the movement of channel electron and to supply energy to weak input signals. QCA clock consists of four phases: switch, hold, release and relax [4, 5]. At the beginning of switch phase the electrons are latched into dots with minimum energy. During the switch phase electrons gain extra energy from applied clock. During hold phase electrons obtain enough energy to surpass the capacitive barrier. During release phase electrons dissipate energy to the environment and at the end of this phase the electrons will latch at the other dots. During relax phase electrons will be confined into the dots with minimum energy. So, during this relax phase the cells in a clock zone will act as input for the next zone cells. Each and every QCA architecture is in general divided into four clocking zones and each clocking zone is  $\pi/2$  out of phase with its previous zone as shown in Fig. 5a.

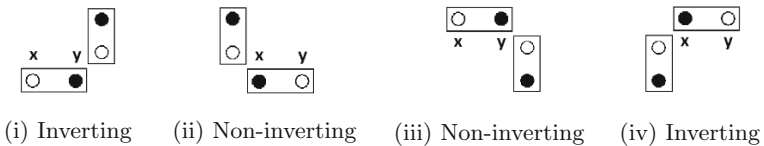




**Fig. 1** Binary encoding in 2 dot QCA cell **a** with vertical alignment and **b** with horizontal alignment and **c** 2 Dot 1 electron QCA wire and **d** inversion by oppositely aligned cell

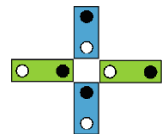


**Fig. 2** Majority voter gate **a** schematic representation and **b** QCA implementation



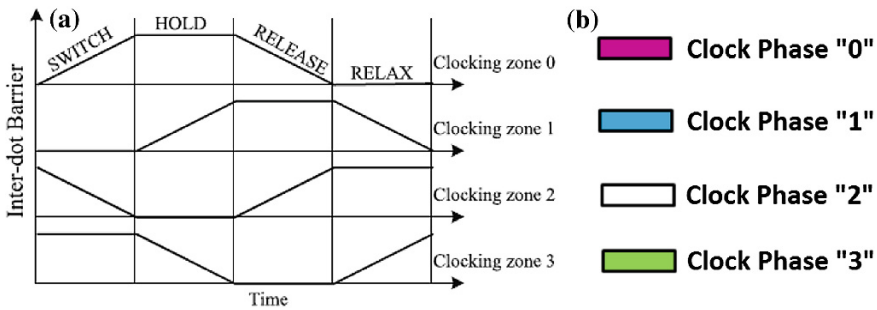
**Fig. 3** Inversion by corner cell placement

**Fig. 4** Planar crossing of wires



### 3 Advantages of 2 Dot 1 Electron QCA

2 Dot 1 electron QCA provides all the benefits of QCA structures over conventional CMOS technology along with advantages over the 4 Dot 2 electron QCA counterpart. The advantages of 2 Dot 1 electron QCA over the 4 Dot 2 electron QCA are enlisted as following:



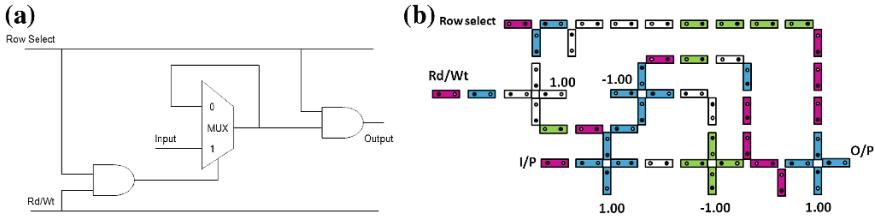
**Fig. 5** a 2 dot QCA clocking and b colour code of different clock phases

1. The 4 Dot 2 electron QCA consists of 4 quantum dots and 2 electrons. Thus there are six possible configurations among which four are ambiguous [6]. But as the name suggests, 2 Dot 1 electron QCA cell consists of 2 quantum dots and 1 free electron. Thus there are exactly two cell configurations both being valid.
2. For any logic circuitry the number of quantum dots and free electron in 2 Dot 1 electron QCA is halved from that of the 4 Dot 2 electron QCA.

## 4 Previous Reportings in this Domain

This domain has been vastly explored using 4 Dot 2 electron QCA. Design of memory unit using 4 Dot 2 electron has been reported in [7–10]. H-memory structure, line based memory, loop based memory and parallel memory units have reported. But all of the said reportings are done in the field of 4 Dot 2 electron QCA. Here we will discuss one of the previous work reported in [10] which is the base of our present work.

In [10], a parallel memory unit design along with 1 bit and 2 bit serial memory designs. Our prime focus is on the parallel memory unit. As shown in Fig. 6a the design consists of two AND gates and one  $2 \times 1$  multiplexer. The major signals used by the memory unit are *RowSelect*,  $\overline{Rd/Wt}$ , *Input*. The *Rowselect* input behaves as a memory chip selector and the  $\overline{Rd/Wt}$  is used to signify whether the memory unit will be used for either *Read* or *Write* operation. If the desired operation is a read operation then the previous data is retained using a feedback loop and if the desired operation is a write operation then the new data input is stored in the memory unit. It is well defined using Fig. 6a.

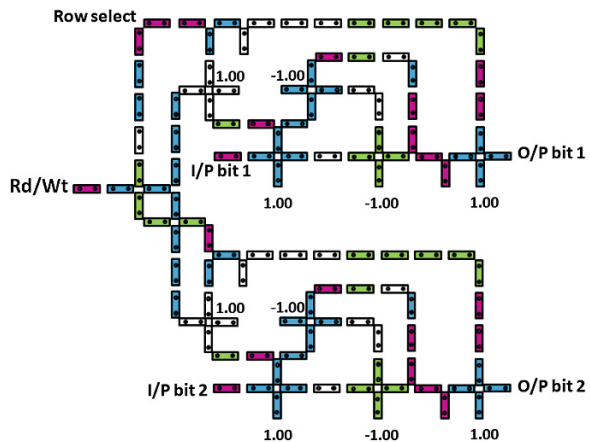


**Fig. 6** **a** Schematic diagram of the parallel memory unit and **b** parallel memory implementation in 2 dot 1 electron QCA

### 5 Proposed Design

The proposed design is based on the block diagram as indicated in Fig. 6a. The design has been implemented using 2 Dot 1 electron QCA. 2 Dot 1 electron QCA has some basic advantages over the 4 Dot 2 electron QCA as discussed in Sect. 3. The design consists of two AND gates and one  $2 \times 1$  MUX. The AND gates are implemented in 2 Dot 1 electron QCA architecture using two majority voter gates and the MUX is implemented using three majority voter gates. At first a one bit parallel memory design has been implemented using 2 Dot 1 electron QCA as shown in Fig. 6b. The memory unit design shown in Fig. 6b can be used to design higher order parallel memory in 2 Dot 1 electron QCA architecture. To design  $n$ -bit parallel memory in 2 Dot 1 electron QCA, we need to use  $n$  such parallel memory unit as shown in Fig. 6b. The *RowSelect* and  $\overline{Rd/Wt}$  must be common for all the  $n$  units. In Fig. 7 a 2-bit parallel memory unit design using the said principle is shown.

**Fig. 7** 2-bit parallel memory implementation in 2 dot 1 electron QCA



### 6 Determination of Output State of the Proposed Design

The field of 2 Dot 1 electron QCA is emerging comparatively with a slow speed as there is no open source simulator of 2 Dot 1 electron QCA available such as QCA Designer [11] of 4 Dot 2 electron QCA. Thus, the proposed design in 2 Dot 1 electron QCA is verified using potential energy calculations as available in [3]. The potential energy between two point charges is

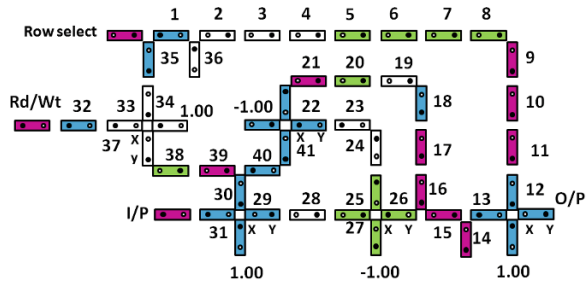
$$U = Kq_1q_2/r \tag{1}$$

$$Kq_1q_2 = 9 \times 10^{-9} \times (1.6)^2 \times 10^{-20} \tag{2}$$

$$U_T = \sum_{t=1}^n U_t \tag{3}$$

where  $U$  is the potential energy,  $q_1, q_2$  are the point charges,  $K$  is the Boltzman constant and  $r$  is the distance between the two point charges.  $U_T$  is the total potential energy for a particular electron position for all of its neighbour electrons. Quantum dots contains induced positive charge. Electrons always latch at a position with minimum potential energy. Thus potential energy at each possible electron position is evaluated. Figure 8 presents the cell numbering of the proposed parallel memory design with 2 Dot 1 electron QCA. The potential energy calculations are shown in Table 1. In Fig. 9, it is shown that the 2-bit parallel memory consists of two parallel memory units as justified in Table 1. Both the units can be justified in the similar manner. The polarity of the long array of likely oriented cells are determined by the property of binary wire.

Fig. 8 A parallel memory unit design with cell positions



**Table 1** Output state of parallel memory unit design

Cell	Electron position	Total potential energy	Comments
1	–	–	Input cell with polarity <i>RowSelect</i>
35, 34	–	–	Attains the polarity of cell input <i>RowSelect</i> according to corner placement shown in Fig. 3(iii)
36	–	–	Attains the inverse polarity of cell 1
32, 33	–	–	Attains the inverse polarity of cell <i>Rd/Wr</i>
2	–	–	Attains the inverse polarity of cell 36
3, 4, 5, 6, 7, 8	–	–	Attains the polarity of cell 2
9, 10, 11, 12	–	–	Attains the polarity of cell 8 according to corner placement shown in Fig. 3(iii)
37	x	$3.33 \times 10^{-20}$ J	Electron will latch at position y due to less energy
37	y	$0.54 \times 10^{-20}$ J	
38, 39, 30	–	–	Attains the polarity of cell 37
29	x	$6.75 \times 10^{-20}$ J	Electron will latch at position y due to less energy
29	y	$0.3 \times 10^{-20}$ J	
28, 27	–	–	Attains the polarity of cell 29
22	x	$-13.41 \times 10^{-20}$ J	Electron will latch at position x due to less energy
22	y	$-1.38 \times 10^{-20}$ J	
23	–	–	Attains the polarity of cell 22
24, 25	–	–	Attains the polarity of cell 23 according to corner placement shown in Fig. 3(iii)
26	x	$-13.41 \times 10^{-20}$ J	Electron will latch at position x due to less energy
26	y	$-1.38 \times 10^{-20}$ J	
16, 17, 18	–	–	Attains the inverse polarity of cell 26 according to corner placement shown in Fig. 3(i)
19, 20, 21	–	–	Attains the polarity of cell 18 according to corner placement shown in Fig. 3(iii)
15	–	–	Attains the polarity of cell 16 according to corner placement shown in Fig. 3(ii)
14	–	–	Attains the polarity of cell 15 according to corner placement shown in Fig. 3(iii)
13	–	–	Attains the inverse polarity of cell 14 according to corner placement shown in Fig. 3(iv)
O/P	x	$6.75 \times 10^{-20}$ J	Electron will latch at position y due to less energy
O/P	y	$0.3 \times 10^{-20}$ J	

## 7 Analysis of Proposed Design

Two important measures of any design in 2 Dot 1 electron QCA are the effective area of the design and the stability of the design.

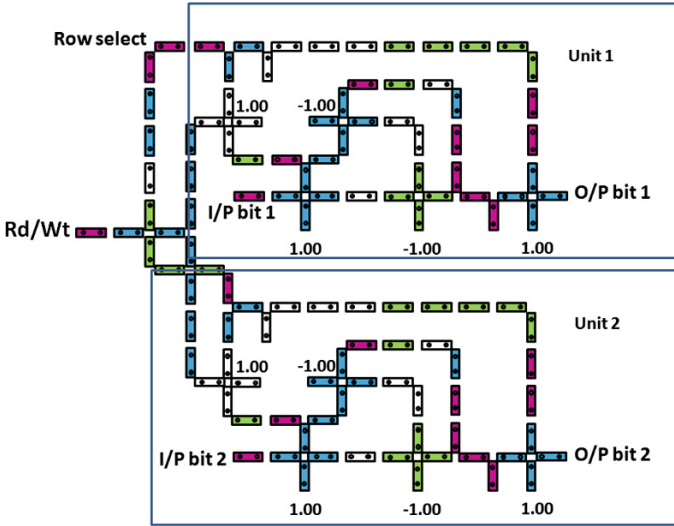


Fig. 9 2-bit parallel memory design with cell positions

## 7.1 Effective Area

The 2 Dot 1 electron QCA cells are rectangular in shape. Let us say the size of a 2 Dot 1 electron QCA is of size  $a \times b$ . As shown in Fig. 6b the parallel memory unit in 2 Dot 1 electron QCA is constructed using 48 such cells. So, the effective area of the design is  $48ab$  and the area covered by the design is  $60ab$ . So, the area utilization ratio of the design is 4:5. Similarly the effective area ratio of the 2-bit parallel memory design is 113:156.

## 7.2 Stability Measure

Stability of any design has a significant contribution in judging the acceptance of that particular design. The stability of any design in 2 Dot 1 electron QCA can be ensured if the following conditions are met:

1. Each and every input signal of a majority voter gate must reach the gate at the same time with same strength.
2. The output of a majority voter gate must be taken off at the same clock phase or at the next clock phase.
3. Every cell of a majority voter gate must be at the same clock.

As we can see in Fig. 6b, the design satisfies all the constraints and hence ensures stability.

**Table 2** Comparison of existing parallel memory unit design in 4 dot QCA with the proposed design in 2 dot QCA

	Parallel memory unit design in [10]	Proposed parallel memory unit design
Number of cells	104	48
Compactness of design (%)	34	80
Energy required to run	Relatively higher amount of energy needed as there are 208 number of electrons	Lesser amount of energy required as there are 96 number of electrons

## 8 Comparative Study

This section will give a comparative analysis of the proposed design in 2 Dot 1 electron QCA with the existing 4 Dot 2 electron QCA design as proposed in [10]. As seen in Sect. 3, the 2 Dot 1 electron QCA exhibits some beneficiary properties which minimizes the energy requirement as well as the energy dissipation of a logic construct. The comparative study is explained in Table 2.

## 9 Conclusion

In this article, a design methodology of parallel memory has been proposed using 2 Dot 1 electron QCA. Further, it is shown that how this memory unit can be used to construct  $n$ -bit parallel memory and an implementation of 2-bit parallel memory is given. Each of the designs are justified using potential energy calculations. Here, also we gave a brief analysis of the proposed design with respect to stability and effective area.

## References

1. Walus, K., Vetteth, A., Jullien, G.A., Dimitrov, V.: RAM design using quantum-dot cellular automata. In: Proceedings of Nanotechnology Conference, vol. 2 pp. 160–163 (2003)
2. Dutta, P., Mukhopadhyay, D.: New architecture for flip flops using quantum-dot cellular automata. In: Proceedings of the 48th Annual Convention of Computer Society of India Vol II Advances in Intelligent Systems and Computing, vol. 249, pp. 707–714. Springer, Berlin (2013)
3. Mukhopadhyay, D., Dutta, P.: QCA based novel unit reversible multiplexer. Adv. Sci. Lett. **16**, 163–168 (2012)
4. Mukhopadhyay, D., Dinda, S., Dutta, P.: Designing and implementation of quantum cellular automata 2:1 multiplexer circuit. Int. J. Comput. Appl. **25**, 21–24 (2011)

5. Mukhopadhyay, D., Dutta, P.: Quantum cellular automata based novel unit 2:1 multiplexer. *Int. J. Comput. Appl.* **43**, 22–25 (2012)
6. Hook IV, L.R., Lee, S.C.: Design and simulation of 2-d 2-dot quantum-dot cellular automata logic. *IEEE Trans. Nanotechnol.* **10**, 996–1003 (2011)
7. Vankamamidi, V., Ottavi, M., Lombardi, F.: A Line-based parallel memory for QCA implementation. *IEEE Trans. Nanotechnol.* **4**, 690–698 (2005)
8. Frost, S.E., Rodrigues, A.F., Janiszewski, A.W., Rausch, R.T., Kogge, P.M.: Memory in motion: a study of storage structures in QCA. In: *Proceedings 1st Workshop on Non-Silicon Computing* (2002)
9. Berzon, D., Fountain, T.J.: A memory design in QCAs using the squares formalism. In: *Proceedings of the Great Lakes Symposium on VLSI*, pp. 166–169. IEEE (1999)
10. Agrawal, D., Ghosh, B.: Quantum dot cellular automata memories. *Int. J. Comput. Appl.* **46**, 27–30 (2012)
11. Walus, K., Dysart, T., Jullien, G.A., Budiman, R.A.: QCA designer: a rapid design and simulation tool for quantum-dot cellular automata. *IEEE Trans. Nanotechnol.* **3**, 26–31 (2004)



# Stochastic Simulation Based GA Approach to Solve Chance Constrained Bilevel Programming Problems in Inexact Environment

Debjani Chakraborti and Bijay Baran Pal

**Abstract** This article presents how the genetic algorithm (GA) based stochastic simulation can be used for solving fuzzy goal programming (FGP) model of a chance constrained bilevel programming problem (BLPP). A numerical example is solved to illustrate the proposed approach.

**Keywords** Chance constrained programming · Stochastic simulation · Fuzzy goal programming · Bilevel programming · Genetic algorithm

## 1 Introduction

Bilevel programming (BLP) problem is a special case of multiobjective decision making (MODM) problem in a hierarchical decision system. It is actually the most widely used and primitive version of a multilevel programming problem (MLPP) [1] having multiple Decision Makers (DMs) with multiplicity of objectives in a large hierarchical decision making organization.

In an BLPP, two DMs are located at two hierarchical decision levels. Each of them independently control a vector of decision variables for optimizing the individual objective functions which often conflict each other in the decision making situation. Although, the execution of decision power is sequential from the upper-level DM (leader) to lower-level DM (follower), the decision of the leader having higher power of making decision is often affected by the reaction of the follower owing to his/her dissatisfaction with the decision of the leader. As a consequence, decision deadlock often arises and the problem of distribution of proper decision

---

D. Chakraborti (✉)

Department of Mathematics, Narula Institute of Technology, Kolkata 700109, WB, India  
e-mail: debjani\_333@yahoo.co.in

B.B. Pal

Department of Mathematics, University of Kalyani, Kalyani 741235, WB, India  
e-mail: bbpal18@hotmail.com

© Springer India 2015

J.K. Mandal et al. (eds.), *Information Systems Design and Intelligent Applications*,  
Advances in Intelligent Systems and Computing 339,  
DOI 10.1007/978-81-322-2250-7\_64

637

powers to the DMs is encountered in most of the hierarchical decision situations. So, it is a challenge to the hierarchical decision organizations to make a proper balance of the decision powers of the DMs.

Most of the classical approaches for solving hierarchical problems developed so far in the past often lead to the paradox that the leader's decision power is dominated by the follower. In a hierarchical decision structure of a decentralized system, however, it is essential that the DMs need to be cooperative with each other for a minimum level of satisfaction of each of them for survival and sustainable growth of an organization.

The real-world decision environment involves high level of complexity and uncertainty. The DMs are frequently faced with three types of uncertainties, viz. stochastic, fuzzy and interval valued, for setting of the parameter values of the decision problems due to imprecision of human judgments. The stochastic programming (SP) is based on the probability theory, which was initially introduced by Charnes and Cooper [2].

The idea of fuzzy programming (FP) [3] based on the concept of fuzzy set theory [4] has been introduced to overcome the shortcomings of the classical approaches for solving complex hierarchical optimization problems.

However, in the real-world decision situations, it has been recognized that the combination of any two or all three types uncertainties are increasingly involved in introducing the parameter values of the problems. The modelling aspects of MODM problems under randomness and fuzziness were first studied by Luhandjula [5] in 1983.

But, in most of the previous studies, the chance constraints having independent normally distributed random parameters are converted into their deterministic equivalent to solve the problems by using conventional deterministic tools. But, in an uncertain decision environment, different types of discrete as well as continuous random parameters are frequently involved, and computational difficulty often arises in converting them to deterministic equivalent. To overcome the difficulty, the chance constrained programming (CCP) [6] with the stochastic simulation [7] has been studied [8] deeply in the past.

Most of the conventional hierarchical decision problems were solved using traditional linear approximation approaches [9] which involve huge computational load and inherent approximation errors in the decision search process.

To overcome the computational difficulties arising out of the use of these traditional (single-point based) solution search approaches, the GAs [10, 11] as prominent tools to optimization of MODM problems has been introduced to solve BLPPs [12]. However, the extensive study in this area is at an early stage. Although, FP approaches to chance constrained BLPPs have been investigated in the past, the use of FGP method to BLPPs with chance constraints is yet to widely circulate in the literature.

In this article, the FGP approach to stochastic simulation based chance constrained BLPPs having random parameters with lognormal probability distribution is presented.

In the solution process, the GA method is efficiently used to solve the BLPP in an interactive manner with regard to fitting of the parameter values to reach an acceptable decision as a most satisfactory one in the decision environment.

To illustrate the proposed approach, a numerical example is solved.

## 2 Problem Formulation

Let  $X = (x_1, x_2, \dots, x_n)$  be the vector of deterministic decision variables involved with the two hierarchical decision levels. Then, let  $F_k$  and  $X_k$  be the objective function and the decision vector, respectively, of the leader and follower  $k = 1, 2$ ; where  $\bigcup_k \{X_k | k = 1, 2\} = X$ .

Then, the BLPP in the hierarchical decision structure can be presented as:

Find  $X(X_1, X_2)$  so as to:

$$\text{Max}_{X_1} F_1(X_1, X_2) = c_{11}X_1 + c_{12}X_2 \quad (\text{leader's problem})$$

where, for given  $X_1, X_2$  solves

$$\text{Max}_{X_2} F_2(X_1, X_2) = c_{21}X_1 + c_{22}X_2 \quad (\text{follower's problem}) \tag{1}$$

Subject to

$$X \in S = \{ X \in R^n | \text{Pr} [AX \leq b] \geq p, X \geq 0, b \in R^m \}$$

where, ‘Pr’ indicates the probabilistically defined constraints,  $A$  is a coefficient matrix and  $b$  is a resource vector and  $p(0 < p < 1)$  is the vector of satisficing probability levels defined for the randomness of the parameters in the constraints set. Again, it is assumed that the feasible region  $S (\neq \Phi)$  is bounded.

In the present decision situation, it is assumed that the elements of the coefficient matrix  $A$  and the resource vector  $b$  are independent continuous normally distributed random variables. Now, the stochastic simulation approach to the chance constraints for estimation of random parameters in the solution search process is described in the following Sect. 2.1.

### 2.1 Stochastic Simulation for Parameter Estimation

The generation of random numbers during the simulation run for constraint satisfying has been well documented in [8] and widely used in for solving CCP problems.

In the present decision situation, without loss of generality, it is assumed that random parameters follow lognormal probability distributions.

Now, the simulation process adopted in the decision system can be defined as follows: The probabilistic constraints in (1) can be explicitly presented as:

$$\Pr \left[ \sum_{j=1}^n a_{ij}x_j \leq b_i \right] \geq p_i, \quad i = 1, 2, \dots, m \tag{2}$$

$$\text{Let } g_i(X, v) = \left( \sum_{j=1}^n a_{ij}x_j - b_i \right) \tag{3}$$

$$\text{Then, } \Pr[g_i(X, v) \leq 0] \geq p_i, \quad i = 1, 2, \dots, m. \tag{4}$$

where  $v = (v_1, v_2, \dots, v_{n+1})$  is the  $(n + 1)$  component vector of random elements, where the dimension of each of which is  $(m + 1)$ , and where  $v_j^T = (a_{1j}, a_{2j}, \dots, a_{mj})$ ,  $j = 1, 2, \dots, n$ , and  $v_{n+1}^T = (b_1, b_2, \dots, b_m)$ ,  $T$  means transpose.

Then, for a given vector  $X$ , let  $R$  independent random vectors be generated in such a way that  $v^{(r)} = (v_1^{(r)}, v_2^{(r)}, \dots, v_{n+1}^{(r)})$ ,  $r = 1, 2, \dots, R$  for the given probability distributions of the defined vectors of random variables.

Let,  $R'$  be the number of occasion of  $R$  trials for which the expression  $g_i(X, v) \leq 0$ ,  $i = 1, 2, \dots, m$ , in (3) is satisfied.

Then, probability of satisfying the constraints appears as:  $P = \frac{R'}{R}$ .

Here, if  $P \geq p_i \quad \forall i$ , is satisfied,  $X$  is reported as the feasible solution for optimizing the defined objectives.

Now, the process of simulation run is summarized in the following steps:

**Simulation Algorithm:**

- Step 1. Initialize  $R' = 0$ .
- Step 2. Generate vectors of random numbers  $(v^{(r)}, r = 1, 2, \dots, R)$  according to the given distribution of the random parameters.
- Step 3. If the constraints  $g_i(X, v) \leq 0, \quad i = 1, 2, \dots, m$ , is satisfied, then set  $R' = R' + 1$ .
- Step 4. Repeat Step 2 and Step 3 ‘P’ times,
- Step 5. Compute  $P = \frac{R'}{R}$
- Step 6. Report the solution  $X$  as a feasible solution, where the constraints set are satisfied with the prescribed probabilities  $(P \geq p_i, \quad \forall i)$ .

Now, how the proposed simulation process works for feasibility verification of a candidate solution (a chromosome) in a genetic search process is briefly described as follows.

## 2.2 Use of Stochastic Simulation for GA Scheme

- Determine the initial candidate solutions (the chromosome).
- Verify the feasibility criteria using the stochastic simulation and determine the fitness scores (the objective function values).
- Use the sampling mechanism in GA for parent selections and update the chromosomes (offspring) using the genetic operators.
- Repeat the process through the feasibility testing until the stopping criteria (termination condition for GA search process) is reached.

Now, in the solution search process, a GA scheme through the use of the defined simulation technique is presented in the following Sect. 3.

## 3 Design of the GA Scheme

In the literature of the GAs, there are a number of schemes in [10, 11] for generation of new populations with the use of the different operators: selection, crossover and mutation. Here, the binary coded representation of a candidate solution called chromosome is considered to perform genetic operations in the solution search process. The conventional Roulette wheel selection scheme in [10], single-point crossover [11] and bit-by-bit mutation operations are adopted to generate offspring in new population in search domain defined in the decision making environment. The fitness score of a chromosome  $v$  (say) in evaluating a function, say  $eval(Ev)$ , based on maximization or minimization of an objective function defined on the basis of DMs needs and desires in the decision making context.

## 4 FGP Problem Formulation

In FGP formulation of the problems, both the objectives  $F_1$  and  $F_2$  and the control vectors  $X_1$  are to be transformed into fuzzy goals by means of assigning an imprecise aspiration level to each of them. Then, the defined fuzzy goals are characterized by the membership functions to measure the degree of goal achievement in terms of membership values.

In the present decision situation, the individual best decisions of the DMs are taken into consideration and they are evaluated by using the proposed GA scheme.

Let,  $(X_1^l, X_2^l; F_1^l)$  and  $(X_1^f, X_2^f; F_2^f)$  be the optimal solutions of the leader and follower, respectively, when calculated in isolation over the feasible solution space  $S$ , where

$$F_1^l = \max_{(X_1, X_2)} F_1(X_1, X_2) \text{ and } F_2^f = \max_{(X_1, X_2)} F_2(X_1, X_2)$$

Then, the fuzzy objective goals appear as

$$F_1 \gtrsim F_1^l, F_2 \gtrsim F_2^f$$

Also the fuzzy goal for the control vector  $X_1$  is obtained as

$$X_1 \gtrsim X_1^l.$$

where ‘ $\gtrsim$ ’ refers to the fuzziness of an aspiration level and it is to be understood as ‘essentially greater than’ in the sense of Zimmermann [13].

Now, in the decision situation, it is assumed that both the DMs have a motivation to cooperate with each other to make a balance of decision powers, and they agree to give a possible relaxation of their individual optimal decision. Then, lower-tolerance limits of the respective fuzzy objective goals for the leader and follower can be determined as  $F_1^l [= F_1(X_1^l, X_2^f)]$  and  $F_2^f [= F_2(X_1^l, X_2^f)]$ , respectively.

Further, since the leader has a higher power of making decision, a certain relaxation of  $X_1^l$  as a lower-tolerance limit should be given for searching a better decision by the follower.

Let,  $X_1^p (X_1^f < X_1^p < X_1^l)$  be the lower tolerance limit of  $X_1^l$ .

Then, characterization of membership functions of the defined fuzzy goals are presented in the following Sect. 4.1.

### 4.1 Characterization of Membership Function

The membership function for the fuzzy objective goal of the leader appears as [12]:

$$\mu_{F_1} [F_1(X_1, X_2)] = \begin{cases} 1 & \text{if } F_1(X_1, X_2) \geq F_1^l, \\ \frac{F_1(X_1, X_2) - F_1^f}{F_1^l - F_1^f} & \text{if } F_1^f \leq F_1(X_1, X_2) < F_1^l, \\ 0 & \text{if } F_1(X_1, X_2) < F_1^f \end{cases}$$

Similarly, the membership function for the fuzzy objective goal of the follower takes the form:

$$\mu_{F_2} [F_2(X_1, X_2)] = \begin{cases} 1 & \text{if } F_2(X_1, X_2) \geq F_2^f, \\ \frac{F_2(X_1, X_2) - F_2^l}{F_2^f - F_2^l} & \text{if } F_2^l \leq F_2(X_1, X_2) < F_2^f, \\ 0 & \text{if } F_2(X_1, X_2) < F_2^l \end{cases} \tag{6}$$

The membership function for the fuzzy decision of the leader appears as

$$\mu_{X_1}[X_1] = \begin{cases} 1 & \text{if } X_1 \geq X_1^l, \\ \frac{X_1 - X_1^p}{X_1^l - X_1^p} & \text{if } X_1^p \leq X_1 < X_1^l, \\ 0 & \text{if } X_1 < X_1^p \end{cases} \tag{7}$$

Now, the FGP model formulation is presented in the following Sect. 4.2.

### 4.2 FGP Model Formulation

In the fuzzy goal achievement function, minimization of the sum of the under deviatational variables on the basis of the relative weights of importance of achieving the goals is taken into consideration. The *minsum* FGP model can be presented as:

$$\begin{aligned} &\text{Find } X(X_1, X_2) \text{ so as to} \\ &\text{Minimize: } Z = \sum_{k=1}^2 w_k^- d_k^- + w_3^- d_3^- \\ &\text{and satisfy } \frac{F_1(X_1, X_2) - F_1^f}{F_1^l - F_1^f} + d_1^- - d_1^+ = 1, \\ &\frac{F_2(X_1, X_2) - F_2^f}{F_2^l - F_2^f} + d_2^- - d_2^+ = 1, \\ &\frac{X_1 - X_1^p}{X_1^l - X_1^p} + d_3^- - d_3^+ = I \end{aligned} \tag{8}$$

subject to the system constraints (1).

Here,  $d_k^-, d_k^+ \geq 0$ , with  $d_k^- \cdot d_k^+ = 0$  ( $k = 1, 2$ ) represent the under- and over-deviatational variables, respectively, associated with the k-th membership goals and  $d_3^-, d_3^+ \geq 0$  with  $d_3^- \cdot d_3^+ = 0$  represent the vector of under- and over-deviatational variables associated with the membership goals defined for the decision vector  $X_1$ , and  $I$  is a column vector with all elements equal to 1 and the dimension of it depends on the decision vector  $X_1$ ,  $Z$  represents the goal achievement function consisting of the weighted under-deviatational variables and vectors of weighted under-deviatational variables, where the numerical weights  $w_k^- (> 0)$ ,  $k = 1, 2$  and the vector of the numerical weights  $w_3^- (> 0)$ , represent the relative weights of importance of achieving the goals to their aspired levels, and they are determined as [12]:

$$w_1^- = \frac{1}{F_1^l - F_1^f}, \quad w_2^- = \frac{1}{F_2^l - F_2^f}, \quad \text{and } w_3^- = \frac{1}{X_1^l - X_1^p}$$

Now, the GA method as a decision satisficer [14] rather than optimizer can be employed in the solution search process of the problem to find a satisfactory solution for the DMs.

The fitness function under the GA scheme appears as:

$$\text{Eval}(E_v) = (Z)_v = \left( \sum_{k=1}^2 w_k^- d_k^- + w_3^- d_3^- \right)_v, \quad v = 1, 2, \dots, \text{pop\_size}$$

In the decision search process, the best chromosome  $E^*$  with the highest score at a generation is determined as

$$E^* = \min\{\text{eval}(E_v) | v = 1, 2, \dots, \text{pop\_size}\}$$

in the genetic search process.

The efficient use of the proposed approach is illustrated by a numerical example presented in the Sect. 5.

### 5 Numerical Illustration

Let  $x_1, x_2$  be the decision variables under the control of the leader and  $x_3$  be the decision variable under the control of the follower.

Then, the BLPP is of the form:

$$\text{Maximize } F_1(x_1, x_2, x_3) = 5x_1 + 6x_2 + 3x_3 \quad (\text{the leader's problem})$$

and, for given  $x_1, x_2; x_3$  solves

$$\text{Maximize } F_2(x_1, x_2, x_3) = 2x_1 + 3x_2 + 8x_3 \quad (\text{the follower's problem})$$

subject to

$$\begin{aligned} \text{Pr } [a_{11}x_1 + a_{12}x_2 + a_{13}x_3 + a_{14}x_4 \leq b_1] &\geq 0.99, \\ \text{Pr } [a_{21}x_1 + a_{22}x_2 + a_{23}x_3 + a_{24}x_4 \leq b_2] &\geq 0.90, \\ \text{Pr } [a_{31}x_1 + a_{32}x_2 + a_{33}x_3 + a_{34}x_4 \leq b_3] &\geq 0.95, \\ 1 \leq X_j \leq 3, \quad j = 1, 2, 3, 4. \end{aligned} \tag{9}$$

In the decision making environment, let it be assumed that the parameters  $a_{ij}$  ( $i = 1, 2, 3; j = 1, 2, 3, 4$ ) and  $b_i$  ( $i = 1, 2, 3$ ) are independent random variables having the characteristics of lognormal distribution.

Now, it is to be followed that a lognormal random variable is actually the exponential of a normal random variable [15]. Here, following the notion of distribution of random variables, the characteristics of a lognormal random variable can be defined as follows.



Let  $y$  be lognormal random variable with known mean and variance. Then,  $\ln(y)$  would be normally distributed, and  $\frac{\ln(y) - \mu}{\sigma}$  follows conventional standard normal distribution, where  $\mu$  and  $\sigma^2$  represent the mean and variance of the normally distributed random variables  $\ln(y)$ , and where ‘ln’ means natural logarithm.

The values of  $\mu$  and  $\sigma^2$  in terms of the known mean,  $E(y)$  and variance  $Var(y)$ , can be defined as [15]:

$$\begin{aligned} \mu &= \ln(E(y) - \frac{1}{2}\sigma^2), \\ \text{and } \sigma^2 &= \ln\left(1 + \frac{Var(y)}{[E(y)]^2}\right). \end{aligned} \tag{10}$$

Now, the means and variances of  $a_{ij}$  and  $b_i$ ,  $\forall i$  and  $j$ , are presented in Table 1 and Table 2, respectively.

Now, using the data in Table 1 and Table 2,  $\mu$  and  $\sigma^2$  can easily be computed by following the expressions in (10). Then, the proposed stochastic simulation for lognormal distribution of the defined random parameters can be employed to estimate the values in the solution search process.

The GA is implemented using the Optimization Toolbox (MATLAB R 2010a). It is employed at different stages for evaluation of the problem. The execution is made in Intel Pentium IV with 2.66 GHz. Clock-pulse and 3 GB RAM.

Now, following the procedure and employing the proposed GA scheme, the individual best (maximum) and least (minimum) values of the objectives are successively obtained as:

$$\begin{aligned} (x_1^l, x_2^l, x_3^l; F_1^l) &= (0.4360, 0.6541, 0; 6.1042) \\ (x_1^f, x_2^f, x_3^f; F_2^f) &= (0.0717, 0.0904, 0.6094; 5.2896), \text{ respectively.} \end{aligned}$$

**Table 1** Means of lognormal variables

$E(a_{11}) = 3$	$E(a_{12}) = 2$	$E(a_{13}) = 6$	$E(a_{14}) = 4$	$E(b_1) = 50$
$E(a_{21}) = 5$	$E(a_{22}) = 7$	$E(a_{23}) = 9$	$E(a_{24}) = 8$	$E(b_2) = 80$
$E(a_{31}) = 10$	$E(a_{32}) = 12$	$E(a_{33}) = 5$	$E(a_{34}) = 3$	$E(b_3) = 60$

**Table 2** Variances of lognormal variables

$Var(a_{11}) = 8$	$Var(a_{12}) = 5$	$Var(a_{13}) = 25$	$Var(a_{14}) = 15$	$Var(b_1) = 10$
$Var(a_{21}) = 20$	$Var(a_{22}) = 30$	$Var(a_{23}) = 40$	$Var(a_{24}) = 32$	$Var(b_2) = 15$
$Var(a_{31}) = 45$	$Var(a_{32}) = 50$	$Var(a_{33}) = 20$	$Var(a_{34}) = 8$	$Var(b_3) = 12$

Then, the fuzzy goals can be defined as:

$$F_1 \gtrsim 6.1042, F_2 \gtrsim 5.2896, \text{ and } x_1 \gtrsim 0.4360, x_2 \gtrsim 0.6541$$

The lower-tolerance limits of the objective goals are determined as:

$$F_1^f = 2.7291, F_2^l = 2.8343$$

The leader feels that his/her control variables  $x_1$  and  $x_2$  can be relaxed up to 0.2 and 0.1, respectively, for the benefit of the follower, and not beyond of them. So,  $x_1^p = 0.2$  ( $x_1^f < 0.2 < x_1^l$ ) and  $x_2^p = 0.1$  ( $x_2^f < 0.1 < x_2^l$ ) act as lower-tolerance limits of the decisions  $x_1$  and  $x_2$ , respectively.

Following the procedure and using the above numerical values, the membership functions of the defined fuzzy goals can be constructed by using (5), (6) and (7). Then, the resultant FGP model appears as: Find  $(x_1, x_2, x_3)$  so as to

$$\text{Minimize } Z = \frac{1}{3.3751} d_1^- + \frac{1}{2.4553} d_2^- + \frac{1}{0.2360} d_3^- + \frac{1}{0.5541} d_4^-$$

and satisfy:

$$\begin{aligned} \mu_{F_1} &: \frac{5x_1 + 6x_2 + 3x_3 - 2.7291}{3.3751} + d_1^- - d_1^+ = 1, \\ \mu_{F_2} &: \frac{2x_1 + 3x_2 + 8x_3 - 2.8343}{2.4553} + d_2^- - d_2^+ = 1, \\ \mu_{x_1} &: \frac{x_1 - 0.2}{0.2360} + d_3^- - d_3^+ = 1, \\ \mu_{x_2} &: \frac{x_2 - 0.1}{0.5541} + d_4^- - d_4^+ = 1, \\ d_q^+, d_q^- &\geq 0, q = 1, 2, 3, 4 \end{aligned} \tag{11}$$

subject to the system constraints in (9)

The obtained solution of the problem in (11) is

$$\begin{aligned} (x_1, x_2, x_3) &= (0.4360, 0.6530, 0.0009) \text{ with} \\ (F_1, F_2) &= (6.1007, 2.8382) \end{aligned}$$

The achieved membership values are

$$\mu_{F_1} = 0.9990, \mu_{F_2} = 0.0016, \mu_{x_1} = 1 \text{ and } \mu_{x_2} = 0.9980.$$

The result shows that a most satisfactory decision is achieved here from the point of view of hierarchical execution of decision powers of the DMs in the decision making context.

**Note 1:** If the conventional fuzzy min-max approach [13] is used to solve the problem in the same decision making environment, where maximization of  $\lambda$  subject to  $\lambda$  'less than equal to' for all the defined membership functions with  $0 \leq \lambda \leq 1$  is considered, then the solution using the Software LINGO (version 11.0) is found as

$$\begin{aligned}(x_1, x_2, x_3) &= (0.3327, 0.4116, 0.2753) \text{ with} \\ (F_1, F_2) &= (4.9590, 4.1026)\end{aligned}$$

The achieved membership values are

$$\mu_{F_1} = 0.6607, \mu_{F_2} = 0.5166, \mu_{x_1} = 0.5623 \text{ and } \mu_{x_2} = 0.5624.$$

The result indicates that, although the hierarchical order of the decision powers of the DMs is preserved here, the solution is inferior in comparison to the solution obtained by using the proposed GA based FGP approach in terms of obtaining a better decision of the leader by using the proposed approach.

Also, under the proposed approach, the leader's higher power of making decision in the hierarchical decision system is preserved and a satisfactory solution for the follower within the specified tolerance range is achieved here in the decision situation.

As such, a comparison of the model solution shows that the solution under the proposed model is superior over the conventional FP approach in the decision making environment.

## 6 Conclusion

In this article, how the stochastic simulation based GA method can be efficiently used to solve the chance constrained BLP problems is presented. The main advantage of using the stochastic simulation technique to the chance constraints is that the computational complexity for transforming the constraints to the deterministic equivalent does not arise here.

The main advantage of the proposed approach is that a compromise decision for achievement of the aspired goal levels of the objectives defined individually for each of them can be made on the basis of their weights of importance and the admissible tolerance values of the aspired goal levels of the objectives. Further, the proposed FGP model is flexible enough to accommodate different other aspiration levels and associated tolerance ranges defined in the decision situation and that depends on the DMs' needs and desires in the decision making context.

In future study, the proposed method can be extended to solve MLPPs as well as other decentralized planning problems from the view point of their potential use to real-life problems.

However, it is hoped that the approach presented here may open up many new vistas of future works in the field of large-scale hierarchical decentralized decision problems.

## References

1. Sakawa, M., Nishizaki, I.: Cooperative and Non-cooperative Multi-Level Programming. Springer, New York (2009)
2. Charnes, A., Cooper, W.W.: Chance constrained programming. *Manage. Sci.* **6**, 73–79 (1959)
3. Zimmermann, H.-J.: Fuzzy mathematical programming. *Comput. Oper. Res.* **10**, 291–298 (1983)
4. Zadeh, L.A.: Fuzzy Sets. *Inf. Control* **8**(3), 338–353 (1965)
5. Luhandjula, M.K.: Linear programming under randomness and fuzziness. *Fuzzy Sets Syst.* **10**, 45–55 (1983)
6. Miller, L.B., Wagner, H.: Chance-constrained programming with joint constraints. *Oper. Res.* **13**, 930–945 (1965)
7. Liu, B.: Theory and practice of uncertain programming. Physica- Verlag, Heidelberg (2002)
8. Jana, R.K., Biswal, M.P.: Stochastic simulation-based genetic algorithm for chance constraint programming problems with discrete random variables. *Int. J. Comput. Math.* **81**(12), 1455–1463 (2004)
9. Kornbluth, J.S.H., Steuer, R.E.: Goal Programming with Linear Fractional Criteria. *Eur. J. Oper. Res.* **8**, 58–65 (1981)
10. Holland, J.H.: Adaptation in natural and artificial systems. University of Michigan Press, Ann Arbor, MI (1975)
11. Goldberg, D.E.: Genetic Algorithms in Search. Optimization & Machine Learning. Addison-Wesley, Reading, MA (1989)
12. Pal, B.B., Chakraborti, D.: Using genetic algorithm for solving quadratic bilevel programming problems via fuzzy goal programming. *Int. J. Appl. Manag. Sci. (IJAMS)* **5**(2), 172–195 (2013)
13. Zimmermann, H.-J.: Fuzzy programming and linear programming with several objective functions. *Fuzzy Sets Syst.* **1**, 45–55 (1978)
14. Deb, K.: Multi-objective Optimization using Evolutionary Algorithms. Wiley, New York (2002)
15. Blumenfeld, D.: Operations Research Calculations Handbook, 2nd edn. CRC Press, Boca Raton (2010)

# Highly Discriminative Features for Phishing Email Classification by SVD

Masoumeh Zareapoor, Pourya Shamsolmoali and M. Afshar Alam

**Abstract** Unstructured text documents have drawn recently more attention, because with growing amount of text documents, there is a need to classify them automatically. But an important problem in field of text categorization is the huge dimensional and very sparse dataset which hurts generalization performance of classifiers. This paper presents a Singular Value Decomposition (SVD) technique to email classification, in order to compress optimally only the kind of documents (in our experiments email classes) and to retain the most informative and discriminate features from an email document. The performance evaluation is performed on email dataset which is publicly available to demonstrate the benefit of the LSA.

**Keywords** Data mining · Dimension reduction · Email classification · Feature extraction

## 1 Introduction

In data mining technique, where the aim is to “find unknown and potentially interesting patterns in large databases a common task is automatic classification” [1]. Text classification has been an important application due to the very large amount of text documents that we have to deal with daily. Several popular techniques have been used for text categorization. These techniques are based on the “vector space” model for representing each document as vector [2]. One of the important examples of text which most of people deal with it is email. In recent

---

M. Zareapoor · P. Shamsolmoali (✉) · M. Afshar Alam  
Department of Computer Science, Jamia Hamdard University, New Delhi, India  
e-mail: pshams@jamiyahamdard.ac.in

M. Zareapoor  
e-mail: mzarea@jamiyahamdard.ac.in

M. Afshar Alam  
e-mail: aalam@jamiyahamdard.ac.in

years, e-mails have become a common medium of communication for most internet users. When classifying the emails, often the data contained in emails are very complex, multidimensional [3]. Then, the uses of dimensionality reduction techniques are useful in the “classification task in order to avoid the curse of dimensionality”. Generally an e-mails can be categorized into three [4]—“Ham, Spam and Phishing”. Ham is legitimate e-mail while spam is “an unsolicited email”. On the other hand phishing is an unsolicited, deceitful, and potentially harmful email. Generally phishing emails, “depend on forged email that pretence from a legitimate company or financial institution”. Then, through a link within the email, the phisher attempts to forward users to fake Websites. These fake Web sites are designed to “deceptively obtain financial data (usernames, passwords, credit card numbers, and personal information, etc.) from genuine users” [5]. Victims of e-banking phishing email expose their bank account number, password, credit card number, and other important information needed for financial transaction to the attacker. “The attacker then misuses this information to make transactions from the victims account. This issue not only affects normal users of the internet, but also causes a big problem for companies and organizations those are misused by the attackers”. In our experiments, we use 10-fold cross validation technique. In order to have a better overview of the performance of the PCAI and LSAI, we present a comparison with the SMO classifier, a popular Support Vector Machine (SVM) with good behavior in text document classification.

## 2 Related Work

Numerous techniques have been developed “to overcome the phishing attack problem”. They include “black listing and white listing [6], network and content based filtering [7], client and server side tool bars [3, 7]”. The first technique consists of lists of “malicious phishing websites (the black list) and lists of legitimate non-malicious websites (white list), where each link in a message must be checked in both lists”. PhishTank [1] is a corpus of “URLs of suspected websites that has been reported as phishing attack which is commonly used by the researchers”. Email providers block phishing emails if the message body contains of PhishTank URLs. Network level protection is usually achieved by blocking a series of IP addresses or set of domains from entering the network [8]. In all these research works, one of the main problem of email classification is highly dimensionality of features, because texts are often represented by a large vocabulary of individual terms. Thus dimensionality reduction has been popular since the early 90 s in text processing tasks [2, 9] like, the technique of latent semantic analysis (LSA) [10]. LSA is an application of “principal component analysis” (PCA) where a document is represented along its “semantic axes”. In a text categorization task, documents are represented by a LSA vector model both when training and testing the categorization system. The computation of the latent components that represent correlated features is very valuable.

### 3 Dimensionality Reduction Techniques

In text classification tasks, the documents or examples are represented by thousands of tokens, which make the classification problem very hard for many classifiers. Dimensionality reduction is a typical step in many data mining problems, which transform our data representation into a “shorter”, more compact, and more predictive one [2, 11]. The new space is easier to handle because of “its size”, and also to carry the most important part of the information needed to distinguish between emails, allowing for the “creation of profiles that describe the data set”. In this paper, we are concentrating on binary classification problem, where we want to distinguish phishing emails from legitimate. Our long vector data are represented in “highly discriminative features, which can deal with an amount of noise and heterogeneity” in the data. For these reasons we used two well-known approaches: Principal Component Analysis (PCA) [2, 12] and Latent Semantic Analysis (LSA) [10], which “involves obtaining the principal components into the term-to-document sparse matrix”.

#### 3.1 Principal Components Analysis (PCA)

PCA is a well known technique that can reduce the dimensionality of data by “transforming the original attribute space into smaller space”. In the other word, the purpose of principle components analysis is to “derive new variables” that are combinations of the original variables and are uncorrelated. This is achieved by transforming the “original variables”  $Y = [y_1, y_2, \dots, y_p]$  (where  $p$  is number of original variable) to a “new set of variables”,  $T = [t_1, t_2, \dots, t_q]$  (where  $q$  is number of new variables), which are combinations of the original variables. Transformed attributes are framed by first; “computing the mean ( $\mathcal{M}$ ) of the dataset, then covariance matrix” of the original attributes is calculated as follow [2, 9]:

$$Covariance = \frac{1}{n(Y - \mathcal{M})^T(Y - \mathcal{M})}$$

And the second step is, “extracting its eigenvectors”. The eigenvectors [13] (principal components) introduce as a “linear transformation from the original attribute space to a new space in which attributes are uncorrelated”. Afterward, the obtained eigenvectors can be sorted “according to the amount of variation in the original data”. The best “ $n$  eigenvectors” (those one with highest eigenvalues) are selected as new features while the rest are discarded. A principal component is the “unsupervised method” that is mean it is no use of the class attribute. One of the main pitfalls of standard Principal Components Analysis (PCA) is the “expensive time” which it requires to perform an “eigenvalue decomposition” to find the PCs. But in this paper we use a relation of the covariance matrix with the Singular Value

Decomposition (SVD) [14] instead of compute the eigenvectors directly from Co, since “SVD is less restrictive”.

### 3.2 Latent Semantic Analysis (LSA)

Generally, LSA analyzes “relationships between a term and concepts” which is contained in an unstructured collection of text. It is called Latent Semantic Analysis, because of “its ability to correlate semantically related terms that are latent in a text”. LSA produces a set of concepts, “which is smaller in size than the original set, related to documents and terms” [10]. LSA are computed by using “SVD (Singular Value Decomposing)” to identify pattern between the “terms and concepts contained in the text, and find the relationships between documents”. The method commonly referred as “concept searches”. It has ability to “extract the conceptual content of a body” of text by “establishing associations between those terms that occur in similar contexts”. LSA is mostly used for “page retrieval systems and text clustering purposes”. LSA overcomes two of the most problematic keyword queries: “multiple words that have similar meanings and words that have more than one meaning”.

## 4 The Classic SVD Method

In this Section, we provide the basic methodology, which is usually followed for text categorization. We defined a dictionary which contains all the unique words of all documents (emails) in the dataset. The value of each dimension in a document’s vector is the frequency of a specific word in that document. The words are also called “terms”; the dimensions’ values are called “term frequencies”. In the following, we show how vector space model is applied in the following three documents [14]: A: “Sun is a star”. B: “Earth is a planet”. C: “Earth is smaller than the Sun”.

So, the dictionary is defined as: “D = [a, Earth, is, planet, smaller, star, Sun, than, the]”. As is clear, the length of the vector in above documents is 9. The frequency vectors are:

$$\begin{array}{l}
 A = [1, 0, 1, 0, 0, 1, 1, 0, 0] \\
 B = [1, 1, 1, 1, 0, 0, 0, 0, 0] \\
 C = [0, 1, 1, 0, 1, 0, 1, 1, 1]
 \end{array}
 \quad \Rightarrow \quad
 \begin{bmatrix}
 1 & 0 & 1 & 0 & 0 & 1 & 1 & 0 & 0 \\
 1 & 1 & 1 & 1 & 0 & 0 & 0 & 0 & 0 \\
 0 & 1 & 1 & 0 & 1 & 0 & 1 & 1 & 1
 \end{bmatrix}_{3 \times 9}$$

Frequency values are 0 or 1 because the size of our document is very small. Some words or terms, like “a and is, are found not that much useful information that helps the document categorization”. If we can remove them from matrix then the categorization will be done more effectively. For this purpose, stop words technique can be used, “which is a list of words that will be ignored during the creation of the dictionary”. All the previous methods, they used “stop word removal technique, for



eliminating the noise and redundancy”. But in this paper, instead of using stop words, we applied direct, “dimensionality reduction technique” for removing the noise through SVD (Singular Value Decomposition). If applying the SVD technique to “an  $[r \times c]$  matrix  $M$ ” [14], it will be analyzed to a “product of three matrices” like: an  $[r \times r]$  “orthogonal matrix  $U$ ”, a  $[r \times c]$  “diagonal matrix  $W$ ” and the transpose of a  $[c \times c]$  “orthogonal matrix  $V$ ”. The “SVD formula is:  $M_{r \times c} = U_{r \times r} W_{r \times c} V_{c \times c}^T$ ”.

Next, we will use SVD to “compress the size of dataset to convert to the small space vector as well as compact one”. Each row of the table is a documents or emails. Each column is the unique words or terms. Each cell of this matrix is frequency vector. Based on SVD, we calculate a score from 0 to 100 for each term or word. The lower “the score is the more similar to noise and can be removed from the dataset”.

## 5 Experiments and Results

### 5.1 Corpora

The public email corpora which we used for performing our tests are (Table 1): SpamAssassin (SA),<sup>1</sup> and the Phishing Corpus (PC).<sup>2</sup>

### 5.2 Preprocessing

An email consists of two parts, header and body message. The header contains information about the message such as, sender, receiver, subject, servers, etc. The body contains the message and usually is one of two forms: HTML or plain-text [15]. The HTML emails contain a “set of tags to format the text to be displayed on screen”. For building the dictionary of the email messages as we explained in Sect. 3, we used SVD technique (instead of stop word removal technique) for removing the words which do not have significant importance in “building the classifiers”. Meanwhile, we use the well-known Term Frequency-Inverse Document Frequency (TF-IDF) scheme [9] for creating TDF matrix. At the end we obtain the message matrices  $X_{2750 \times 2173}$ , where each row in the matrix corresponds to a document (e-mail) and each column corresponds to a term (word) in the document. Each cell represents the frequency (number of occurrence) of the corresponding word in the corresponding document. The obtained matrix ( $X$ ) is the ones used to perform the PCA and LSA based on SVD. The vector that is generated

<sup>1</sup> Available at: <http://spamassassin.apache.org/publiccorpus>.

<sup>2</sup> Available at: <http://monkey.org/~jose/wiki/doku.php?id=PhishingCorpus>.

**Table 1** Number of emails for per corpus

Corpus	Phishing	Ham	Total
SA		1,800	
PC	950		
			2,750

**Table 2** Performance of the different methods over the 10-folds

Methods	Number of features				
PCA I	50	170	500	1,500	2,750
LSA I	50	170	500	1,500	2,750
PCA	50	170	500	1,500	2,750
LSA	50	170	500	1,500	2,750

in this stage is considered as long vector, and decreasing the size of these vectors to short vector with dimensional reduction techniques.

### 5.3 Classification Model

In this stage, we want to build the suitable classifier, in order to compare the performance of the PCA and LSA techniques which are based on SVD. After several comparison and trail we choose to use SMO classifier [16], a linear SVM which has very good performance in sparse data and which is well suited for text classification. For building SMO implementation we used following settings: a lineal kernel (polynomial with exponent 1); complexity constant equal to 100 (Table 2).

### 5.4 Evaluation Matrices

In this paper for better overview, the results are presented in the form of the area under the Receiver Operating Characteristic (ROC) curve, which aims at a “high true-positive rate and a low false-positive rate”. We also provide results in terms of accuracy of the classification for better understanding. As we can see from the Figs. 1 and 2 the PCA and LSA obtain the good result in detecting phishing email while only using a large numbers of features. In the other hand, they have a good performance only with more features. When we applying the PCA for reducing the dimension in dataset, then the new feature space which are obtained are not that much discriminative for classes. But if we use SVD eigenvalues for both technique (LSAI, PCAI), they need commonly much less features to obtain a good classification. It means that for these proposed techniques choosing more features does not

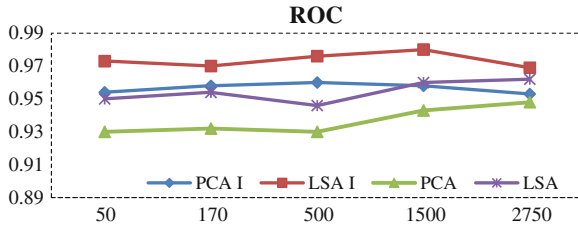
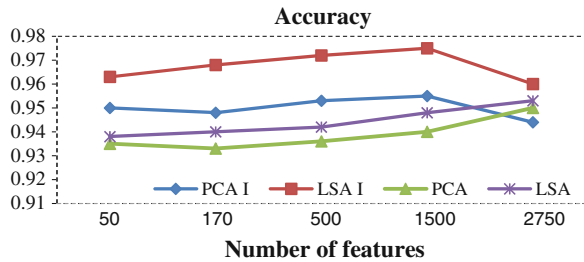


Fig. 1 Performance of LSA and PCA in term of ROC

Fig. 2 Performance of LSA and PCA in term of accuracy



have effect or might degrade the performance of the classifiers. Also from these results, we can observe that the LSAI features extracted techniques are well suited to discriminate between ham and phishing emails.

## 6 Conclusion

In this paper we presented and evaluated a novel technique based on PCA and LSA which are two well known dimensional reduction technique, and better known in text classification. In our proposed technique, we did not use any traditional technique for removing the useless information from the dataset like stop world removal technique. We used SVD technique for reducing the noise and dimension from original dataset. And from the results, found that PCAI and LSAI are having good performance when the number of feature is less. It means that, the SVD technique can find the very discriminative features from dataset. The results show good classification performance when using the PCA based on SVD techniques 10-fold cross-validation.

## References

1. PhishTank: Available from: <http://www.phishtank.com> (2014). Accessed 14 Jan 2014
2. Gomez, J.C., Moens, M.F.: PCA document reconstruction for email classification. *Comput. Stat. Data Anal.* **56**, 741–751 (2012)
3. Verbeek, J.J.: Supervised feature extraction for text categorization
4. Basnet, R., Sung, A.H.: classifying phishing emails using confidence-weighted linear classifiers. In: *Proceedings of the International Conference on Information Security and Artificial Intelligence (ISAI)*, pp. 108–112. (2010)
5. Zareapoor, M., Seeja K.R.: Text mining for phishing email classification. In: *Intelligent Computing, Communication and Devices*, pp. 65–71. Springer, Heidelberg (2015)
6. Huillier, G.L., Weber, R., Figueroa, N.: Online phishing classification using adversarial data mining and signaling games. In: *Proceedings of the ACM SIGKDD* (2009)
7. Ramanathan, V., Wechsler, H.: Phishing detection and impersonated entity discovery using conditional random field and latent dirichlet allocation. *J. Comput. Secur.* **34**, 123–139 (2013)
8. Snort: Network intrusion prevention and detection system. Available from: <http://www.snort.org/> (2014). Accessed 03 Feb 2014
9. Gomez, J.C., Boiy, E., Moens, M.F.: Highly discriminative statistical features for email classification. *Knowl. Inf. Syst.* **31**, 23–53 (2012)
10. Huillier, G.L., Hevia, A., Weber, R., Rios, S.: Latent semantic analysis and keyword extraction for phishing classification. Department of Computer Science, University of Chile (2010)
11. Kim, H., Howland, P., Park, H.: Dimension reduction in text classification with support vector machine. *J. Mach. Learn. Res.* **6**, 37–53 (2005)
12. Biricik, G., Diri, B., Sonmez, A.C.: Abstract feature extraction for text classification. *Turk. J. Elec. Eng. Comp. Sci.* **20**, 1137–1159 (2012)
13. Tsymbal, A., Puuronen, S., Pechenizkiy, M., Baumgarten, M., Patterson, D.W.: Eigenvector-based feature extraction for classification. In: Haller, S.M., Simmons, G. (eds.) Paper presented at the FLAIRS conference, pp. 354–358. AAAI Press, Menlo Park (2002)
14. Symeonidis, P., Kehayov, I., Manolopoulos, Y.: Text classification by aggregation of SVD eigenvectors. In: *Proceedings of the 16th East European Conference on Advances in Databases and Information Systems*, pp. 385–398. Springer, Heidelberg (2012)
15. Akinyelu, A.A., Adewumi, A.O.: Classification of phishing email using random forest machine learning technique. *J. Appl. Math.* (2014)
16. Platt, J.C.: Fast training of support vector machines using sequential minimal optimization, pp. 185–208. MIT Press, Cambridge (1998)

# Signature Based Semantic Intrusion Detection System on Cloud

S. Sangeetha, B. Gayathri devi, R. Ramya, M.K. Dharani  
and P. Sathya

**Abstract** Now a days, many enterprise applications are using cloud platform. Security is the most sensitive issue in cloud platform. Intrusion detection System is used to protect the Virtual machine from threats. This paper proposes Application level Signature based Semantic Intrusion Detection System, which concentrates on the application level to detect application specific attacks. A packet sniffer is placed between cloud user and Virtual cloud provider. The packets of various protocols are captured by packet sniffer and dispatch it to its corresponding parser. The parser translates a sequence of packets into protocol messages and dispatches the packet to the corresponding state machine which consists of message parsing grammar. The message parsing grammar analyses the messages and checks with the semantic rules. If any signature does not matches with the rule-base and found to be malicious. The IDS interpreter generates alert to the cloud provider. The Signature based semantic Intrusion Detection System reduces the false alarm rate. So, the accuracy of the detection rate gets increased.

**Keywords** Signature based detection · Network based intrusion detection system · HTTP · FTP · HTML attacks

## 1 Introduction

Cloud Computing is an emerging technology in the recent years. It provides basic services such as Software as a Service, Platform as a Service, Infrastructure as a service, Security as a Service etc. While providing these services, there exist several issues such as data issues [1, 2]: Data Lock-in, Data Transfer Bottlenecks, Traffic Management, Reputation sharing, security issue: availability of Service, Data

---

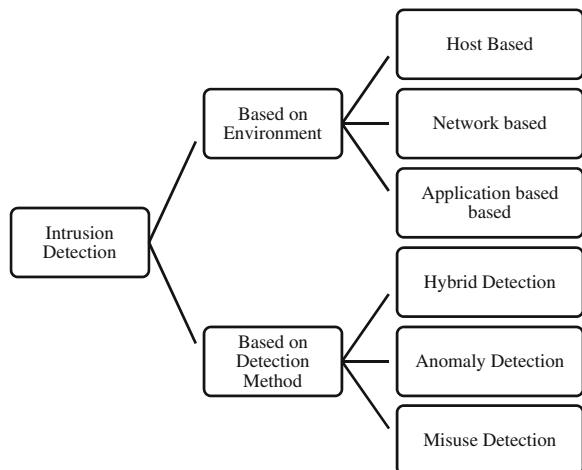
S. Sangeetha (✉) · B. Gayathri devi · R. Ramya · M.K. Dharani · P. Sathya  
Department of Computer Science and Engineering, Faculty of Engineering,  
Avinashilingam University, Coimbatore, India  
e-mail: Visual.sangi@gmail.com

Security, performance issues and energy issue since cloud services are stipulated through Internet. In this, cloud security has gained more importance over the past years with the increase in the number of threats targeting network for information and misuse. Cloud virtualizations runs through standard protocols and are vulnerable to intruders for cyber attacks [3]. Intrusion Detection System plays vital tool for cloud security to prevent outside attacks rather than inside attacks. Attacks are of two types: (1) Active Attacks—likely to change the content. (2) Passive attacks —does not change the content but monitors/listens [4, 5]. The existing IDS works in the network layer which makes the intruder to intrude at application level. Some of the authorized port such as HTTP (80) is kept always open for providing the web services to the cloud user. Other protocols at application layer, such as FTP (21) is not opened always but can be opened when needed. The attack that goes undetected by network layer can be detected by Application level IDS. The efficient IDS technique is incorporated in cloud infrastructure to predict these attacks which works at application level. The classification of IDS and its detection techniques are discussed in the following chapter.

## 2 Classification of IDS

The Intrusion Detection System has been classified based on the following factors (i) Based on environment and (ii) based on detection techniques. Figure 1 shows the Classification of IDS [1, 6].

Fig. 1 Classification of IDS



**Table 1** Comparison of host based IDS and network based IDS

	HIDS	NIDS
Pros	No extra hardware required	Can monitor multiple system at a time
Cons	Need to install on each machine	It helps only for detecting external intrusions
Deployment	On virtual machine	In virtual cloud provider

## 2.1 Based on the Environment

IDS has been classified into 3 types [7].

**Network based IDS (NIDS):** It monitors the network traffic and analyses the network for any maliciousness.

**Host based IDS (HIDS):** It monitors the activity of a system and detects the intrusive behavior through monitoring and analyzing log file.

**Application based IDS:** It analyses the particular application for vulnerability.

The Table 1 shows the comparison of Host based IDS and Network Based IDS.

## 2.2 Based on Detection Method

**Signature based Detection:** This method uses signature based pattern matching by comparing the captured patterns with the existing historical data in knowledge base to detect intrusions. It is used to detect known attacks.

**Anomaly Detection:** In this method, the legitimate users behavior are collected over a period of time and the statistical test will applied on observed behavior to detect any abnormalities. It is used to detect unknown attacks. Apart from statistical test, machine learning based and data mining technique can be used to detect anomalies.

**Hybrid Detection:** This method enhances the detection rate by combining both misuse and anomaly detection. The misuse detection detects only known attacks and the unknown attacks not detected by the misuse will be detected by anomaly method.

## 3 Semantic Versus Non-semantic

The packets transferred between cloud users and servers are captured and analyzed for any intrusion. Based on the detection techniques discussed, a signature based intrusion detection system is built to analyze the packets that are expected to be delivered to the network service or application. The intrusions can be detected either semantically or non-semantically.

### ***3.1 Non-semantics Based IDS***

Non-semantics based IDS hunted for the patterns in the input traffic and if the pattern matches with some predefined pattern then a intrusion alert will be displayed. An intelligent hacker may intrude the system by simply not using the patterns hunted by the non-semantics based IDS. So, a non-semantics based intrusion detection system fails miserably.

### ***3.2 Semantic Based IDS***

A semantics based IDS will define a rule such that the occurrence of some sort of patterns in the network traffic definitely indicates a malicious activity. So there are no false positives (false alarm of an attack) in semantic based IDS. Moreover, the time taken for detecting an attempt is very lesser than non-semantic based IDS since the search space is reduced.

## **4 Architecture of Cloud IDS**

The packets transferred between cloud users and servers are captured by packet sniffer and analyzed for any maliciousness by Cloud IDS Engine [8]. The architecture of the Cloud IDS is shown in Fig. 2. Ethereal is used for protocol analyzer/packet capturing. The Protocol analyzer recognizes the protocol type and dispatches the packet to the corresponding state machine. A protocol analyzer will need to parse messages according to a protocol-specific message format and it reduce the number of false positive and false negative. This needs parsing to be done incrementally, since application-layer messages can be split among several packets. Correct parsing state must be maintained between packets, else partial messages will be analyzed incorrectly. The messages are then analyzed by the message parsing grammar. Semantic Classification tree is constructed by analyzing the specification of the protocol [9]. The specification gives the Rules and the individual patterns which will be matched in the corresponding fields of the protocol [10]. The tree is formed in the top-down format. As each node on the path from the root to a leaf node checks with the input, if any signature does not matches with the rule base then it raises alerts to the cloud IDS Interpreter which in turn alerts the Virtual Cloud Provider. The traffic is continuously monitored and analyzed for any malicious behavior and is reported to the administrator.



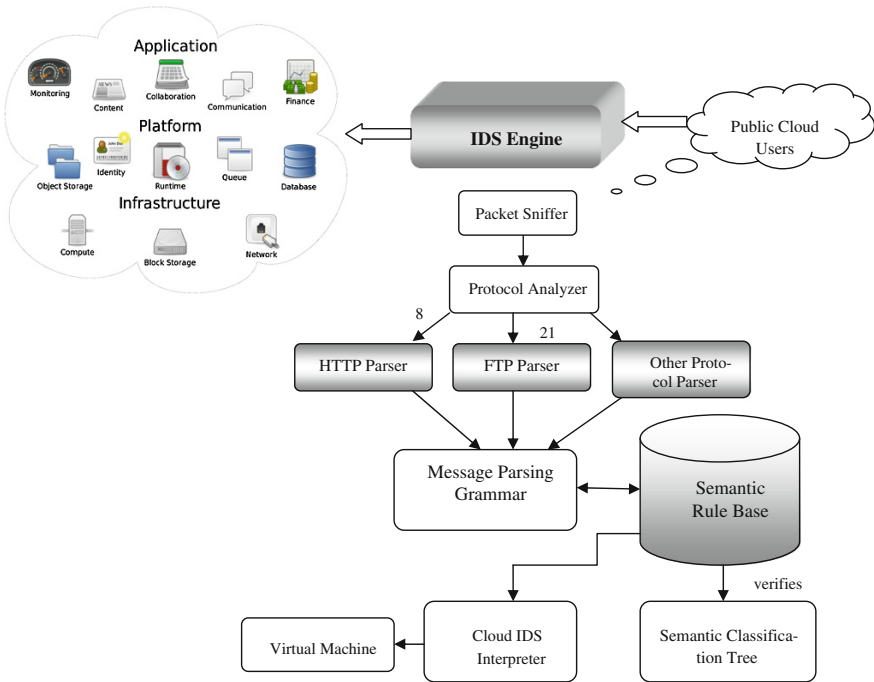


Fig. 2 Architecture of cloud IDS

## 5 Vulnerabilities at Application Level Protocol

The attackers make the system to be compromised by hacking the protocols such as HTTP, FTP etc.... at application layer. The semantic Classification tree has been generated for the following vulnerabilities if any malicious code matches with the semantic rule base then it raises alerts to the cloud IDS Interpreter which in turn generates alert to the Virtual Machine.

### 5.1 HTTP Vulnerabilities

The HTTP protocol is application level protocol and is based on the pattern of request/response [11]. A client establishes a connection with a server and sends a request to the server in the form of a request method, URI, and version, followed by a MIME-like message containing request modifiers, client information, and possible body content. The server responds with a status line, including the message’s protocol version and a success or error code, followed by a MIME-like message containing server information, entity meta information, and possible body content. Most HTTP communication is initiated by a cloud user agent and consists of a

request to be applied to a resource on server. The HTTP Grammar is constructed. Based on this Grammar, Semantic classification tree is generated and analyses the message for any intrusions.

The following table gives an overview of various HTTP attacks and the extent to which the intruders can compromise the system by gaining information about the system. The HTTP Request syntax: Method/URI/Version. The method can be GET, POST etc. The attacks can be analyzed by looking at the GET method and the corresponding response. The signatures by which the intruders can compromise the system through HTTP Request is shown in Table 2. The HTTP responses are identified by the status codes associated with it and are shown in Table 3.

**Table 2** Vulnerabilities at HTTP request

Attack	Impact of the attack
NASM attack	The attacker can make a standard HTTP request that contains 'nasm' in the URI to compiling a variety of sources on various platforms into executable binary files
XTERM	An attacker uses a "xterm" command to open an interactive session then uses that session to move a root kit to the system
CHSH	The attacker can make a standard HTTP request that contains '/bin/chsh' in the URI to change the shell of a user present on the host
"ID"	HTTP request containaig '/usr/bin/id' in the URL can return sensitive information on groups and users present on the host
"NETCAT"	An attacker uses a "netcat" command to gain elevated privileges on the server by using netcat to open another connection
"~" Requests	Using '~' attackers determine a valid user on the target system. Once an attacker has a valid username, they may try guessing passwords, or brute forcing until they get a valid password
"gcc"	Using 'gcc' in the URI, the attacker can compile a program needed for other attacks on the system or install a binary program of his choosing
"ps"	Using '/bin/ps' in the URI, the attackers can check for various services running on a system to exploit or for the presence of security software, such as host IDS or monitoring scripts
"CHOWN"	Using '/bin/chown' in the URI, attacker can change file permissions of files present on the host
"+" Requests	An attacker or worm will copy cmd.exe to a file inside the web root. Once this file is copied, an attacker has full control over the windows machine
"Requests"	This character shows that there is someone trying a SQL injection attack against the software. Allows an attacker to insert SQL commands into the script
"uname"	Using 'uname' in the URI, attacker gains information on the host operating system

**Table 3** Vulnerabilities at HTTP response

Attack	Impact of the attack
OK 200	The request is satisfied
Created 201	The request is success, but the textual part of the response line indicates the URI by which the newly created document should be known
Accepted 202	The request has been accepted for processing, but not completed
Partial information 203	The meta information returned from the server is not a definitive set of object, but is from a private web
No response 204	Server has received the request but no response and the client stay
Error 4xx, 5xx	The 4xx—the client seems to have erred, and the 5xx codes—the server seems to have erred. It is impossible to distinguish these cases
Bad request 400	The request has bad syntax or inherently impossible to be satisfied
Unauthorized 401	This message gives a specification of acceptable authorization schemes
Forbidden 403	The request is prohibited for something. Authorization will not help
Not found 404	The server has not found the URI specified
Internal Error 500	The server encountered an unexpected condition which prevented it from fulfilling the request
Not implemented 501	The server does not support the required facility
Service temporarily overloaded 502	The server cannot process the request due to a high load (whether HTTP servicing or other requests)
Gateway timeout 503	This is equivalent to internal error 500, this shows that the response from the other service has not returned within a time
Redirection 3xx	It indicates action to be taken by the client in order to fulfill the request
Found 302	The data requested actually resides under a different URL, the redirection may be altered on occasion as for “Forward”

## 5.2 FTP Vulnerabilities

FTP URL Syntax ftp://user:password@host:port/path

(By RFC 1738)

USER

A user name (user id) on the host

PASSWORD

The password corresponding to the user name

HOST

The fully qualified domain name of a network host, or its IP address

PORT

The port number 21

Table 4 shows the vulnerabilities at FTP.

**Table 4** Vulnerabilities at FTP

Attack	Impact of the attack
FTP tar attack	This event is generated when an attempt is made to access roots home directory in an ftp session
FTP CWD ~ root attempt	This event is generated when an attempt to abuse an FTP servers functionality and configuration weaknesses is attempted

**Table 5** Scripting vulnerabilities

Attack	Impact of the attack
Cross site scripting	The attacker insert malicious script or HTML into a web page, that redirects the user to its own website
SQL injection attack	An intruder to send crafted user name and/or password field that will modify the SQL query. Eg) 'or 1 = 1
Denial of service attack	It denies normal access to legitimate users. This attack can also be in the form of an infinite loop that gets executed in the client's browser [15]
Brute force attack	A brute force attack is a method of defeating a cryptographic scheme by trying a large number of possibilities

### 5.3 Scripting Vulnerabilities

There are several applications vulnerable to the HTML scripting attacks. The scripting attacks can be found in HyperText Markup Language (HTML). The malicious HTML-based content will be embedded by the attackers within cloud user web requests. Many of the browsers are enabled in default and has the capability to interpret the scripts embedded within HTML content. The attacker can successfully inject the script embedded in HTML, it will be executed by Cloud user [12]. By executing the injected malicious code, the attacker can modify the content or can hack the username and password. The code can be written in any scripting languages. Scripting tags which are used to insert malicious content are <SCRIPT>, <OBJECT>, <APPLET> and <EMBED>. Cross Site Scripting (CSS), SQL Injection, Denial of Service and Brute force are the most common of all attacks in HTML [11] shown in Table 5.

The vulnerabilities mentioned above can be detected by IDS engine. The semantic classification tree will be generated for these vulnerabilities by analyzing the features of request and its corresponding response sequence. The signature that does not matches with the semantic rule base checks for any maliciousness and report to the virtual cloud provider [13, 14]. The complete semantics of the HTTP, FTP transferred (request-response) between cloud user and cloud provider are maintained. The IDS engine checks the pattern of each incoming packet individually for attack.

## 6 Conclusion

The proposed architecture of cloud IDS at application level protects the vulnerabilities at levels since it protects the below layers. The semantic Classification tree plays vital role by parsing the various protocol message to the IDS Interpreter and has an efficient memory usage since the amount of memory needed for working of the IDS depends on the rule size. The signatures and rules are updated automatically and can be expandable with more semantic parameters. The false alarm rate gets reduced by using Signature based Intrusion Detection System. Hence the vulnerabilities can be detected more accurately.

## References

1. Modi, C., Patel, D., Borisaniya, B., Patel, H., Patel, A., Rajarajan, M.: A survey of intrusion detection techniques in cloud. *J. Netw. Comput. Appl.* **36**, 42–57 (2013)
2. Reddy, V.K., Rao, B.T., Reddy, L.S.S., Kiran, P.S.: Research issues in cloud computing. *Glob. J. Comput. Sci. Technol.* **11**(11), 1–8 (2011)
3. Subashini, S., Kavitha, V.: A survey on security issues in service delivery models of cloud computing. *J. Netw. Comput. Appl.* **34**, 1–11 (2011)
4. Qaisar, S., Khawaja, K.F.: Cloud computing: network/security threats and countermeasures. *Interdisc. J. Contemp. Res. Bus.* **3**(9), 1323–1329 (2012)
5. Oktay, U., Sahingoz, O.K.: Attack types and intrusion detection systems in cloud computing. In: *Proceedings of the 6th International Information Security and Cryptology Conference*, Sept 2013
6. Scarfone, K., Mell, P.: Guide to intrusion detection and prevention systems (IDPS). NIST special publication, vol. 800, p. 94 (2007)
7. Mazzariello, C., Bifulco, R., Canonoco, R.: Integrating a network IDS into an open source cloud computing. In: *Proceedings of the 6th International Conference on Information Assurance and Security (IAS)*, pp. 265–70 (2010)
8. Roschke, S., Feng, C., Meinel, C.: An extensible and virtualization compatible IDS management architecture. In: *Proceedings of the 5th International Conference on Information Assurance and Security*, pp. 130–140 (2009)
9. Abbes, T., Bouhoula, A., Rusinowitch, M.: Protocol analysis in intrusion detection using decision tree. In: *Proceedings of the International Conference on Information Technology: Coding and Computing (ITCC'04) IEEE* (2004)
10. Sangeetha S., Vaidehi V.: Fuzzy aided application layer semantic intrusion detection system-FASIDS. In: *Proceedings of International Journal of Network Security and its Application (IJNSA April 2010)*, vol. 2, pp. 39–56 (2010)
11. Bellamy Jr, W.: TCP Port 80—HyperText transfer protocol (HTTP) header exploitation. *Cgsecurity.com* (2002)
12. Hallaraker, O., Vigna, G.: Detecting malicious javaScript code in mozilla. In: *Proceedings of the 10th International Conference on Engineering of Complex Computer Systems (ICECCS 2005)*, pp. 85–94 (2005)
13. Krugel, C., Toth, T.: Using decision trees to improve signature-based intrusion detection. In: *Proceedings of the 6th International Workshop on the Recent Advances in Intrusion Detection (RAID'2003)*, LNCS, vol. 2820, pp. 173–191 (2003)

14. Vieira, K., Schuler, A., westphall, C.: Intrusion detection techniques in grid and cloud computing environment. In: Proceedings of the IEEE IT Professional Magazine (2010)
15. Bakshi, A.,yogesh, B.: Securing cloud from DDoS attacks using intrusion detection system in virtual machine. In: Proceedings of the 2nd International Conference on Communication Software and Networks, pp. 260–264. (2010)

# Fuzzy Based Quality of Service Analysis of Scheduler for WiMAX Networks

Akashdeep

**Abstract** WiMAX is an upcoming technology gaining grounds day by day that has inherent support for real and non real applications. The rise in number of real time application with popularity of mobile phones always tests scheduler performance of broadband wireless systems like WiMAX. Distribution of resources in such networks has always been a challenging phenomenon. This problem can be solved if scheduling decision is based on traffic conditions of incoming traffic. This paper proposes an application of fuzzy logic by virtue of which an intelligent system for distribution of resources has been defined. The system works as adaptive approach in granting bandwidth to those traffic classes that has relatively higher share of incoming traffic in its queues. The results demonstrate significance of the proposed method.

**Keywords** Fuzzy logic · WiMAX · Quality of service

## 1 Introduction

Worldwide Interoperability for microwave access is IEEE 802.16 standard popularized by WiMAX forum under the name WiMAX [1]. It is broadband wireless technology which by virtue of its technical specification is gaining popularity among end users as it provides support for number of real time applications. The popularity of mobile phones has put lot of pressure on today's wireless networks to provide required quality of service. The demand for number of applications is increasing day by day while amount of resources remains limited. Distribution of resources in such networks is always a challenging task as growing quality of service demands of real time applications are always difficult to met. The increase in

---

Akashdeep (✉)  
UIET, Panjab University, Chandigarh, India  
e-mail: akashdeep@pu.ac.in

number of real time applications sometimes makes low priority non real time classes starve for resources.

Traffic in WiMAX network is categorized into five different service classes namely unsolicited grant service (UGS), extended real time polling service (ertPS), real time polling service (rtPS), non real time polling service (nrtPS) and best effort (BE). IEEE 802.16 standard specifies only priority to these classes and does not specify any fixed mechanism for allocation of resources to these. Equipment manufacturers are free to design and implement their own algorithms [2]. Increasing number of multimedia applications makes resource allocation a very complex and tedious process as real time applications are always hungry for more and more resources. It becomes very intricate to maintain relatively good quality of service levels for all sorts of traffic classes and situation gets more complex with rise in number of packets in network. In order to maintain good quality of system performance, allocation of resources shall be immediate and dynamic. This requires scheduling system to be intelligent and powerful so that it can adapt itself to incoming traffic pattern of various applications. This paper discusses performance of one such system developed using fuzzy logic. The fuzzy logic system works according to changes in traffic patterns of incoming traffic and adapts itself to these changes so that appreciable performance level can be maintained for all service classes.

Fuzzy logic is useful where information is vague and unclear and resource allocation process in WiMAX suits application of fuzzy logic to it. Design of intelligent systems for WiMAX networks has started gaining popularity very shortly as number of papers in this direction is still limited. Few of these studies are available at [3–11]. Fuzzy logic has been employed by Bchini et al. [12] and Simon et al. [3] in handover algorithms. Use of fuzzy logic for implementing inter-class scheduler for 802.16 networks had been done by Sadri and Mohamadi [5]. Authors had defined fuzzy term sets according to two variables  $dq_{rt}$  which means latency for real time applications and  $tq_{nrt}$  meaning throughput for non real time applications. Shuaibu et al. [4] has developed intelligent call admission control (CAC) in admitting traffics into WiMAX. Alsahag et al. [6] had utilized uncertainty principles of fuzzy logic to modify deficit round robin algorithm to work dynamically on the basis of approaching deadlines. The Fuzzy based scheduler dynamically updates bandwidth requirement by different service classes according to their priorities, latency and throughput by adjusting the weights of respective flows. Similar studies were also given by Hedayati et al. [7], Seo et al. [8] and Akashdeep and Kahlon [9]. Authors of current study has already implemented such study that works on fuzzy logic [9] and neural network [10]. The study works on two input parameters and outputs a weight value to be used for bandwidth allocation. This paper presents an extension of that approach that utilizes values of instantaneous queue length as an additional variable.



## 2 Working of System

WiMAX implement a request grant mechanism for resource allocation. Different SS connected to BS request resources from BS and these requests are classified into different queues by classifier of IEEE 8021.6. The scheduler at BS listens to these request and serves these queues by performing two different functions:- allocating resources to different request made by SS and transmission of data to different destinations. BS scheduler component serves these requests on per connection ID basis by taking into consideration available resources and request made by that particular connection. Presently IEEE 802.16 specify priority order for various traffic classes and does not specify any algorithms for resource allocation among these classes. Real time classes have high priority as a result of which low priority non real time classes tend to suffer increased delays in resource allocation process and may sometimes be malnourished. This can be improved by devising strategy that could adapt itself to changing requirements of incoming traffic.

The proposed system is motivated by theories of fuzzy logic where fuzzy logic can work to serves queues belonging to different scheduling services using its uncertainty principles. The designed system works as component of base station and works on three input and one output variables. The input variables are taken as:

Latency for real time applications, throughput for non real time applications and queue length share of real and non real time applications considered together. The output of fuzzy system is taken as weight of queues serving real time traffic. Membership functions for these variables have been defined utilizing knowledge of domain expert as shown in Fig. 1. Five different linguistic levels are defined for first input variable and output variables. The membership function are defined as Negative Big (NB), negative small (NS), Zero (Z), Positive small (PS) and positive big (PB). Three membership functions are considered for second and third input variable. The dynamism of variables is taken in range between 0 and 1. The rule base consists of 45 rules which have been framed considering qualities of input variables into consideration. The rule base has been defined considering the nature and dynamism of input traffic and is considered to be sufficiently large.

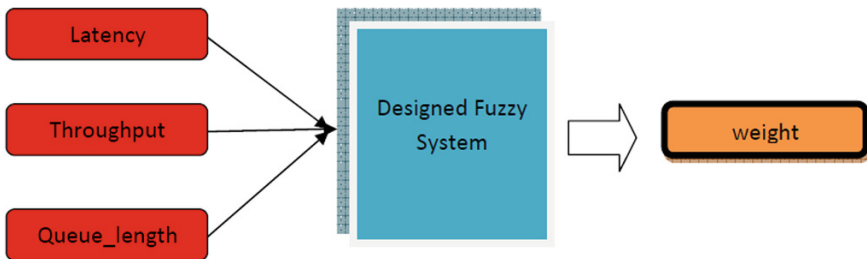


Fig. 1 Structure of fuzzy logic based system for resource allocation

The initial weight for any flow (i) is calculated from the following equation

$$w_i = \frac{R_{\min(i)}}{\sum_{i=0}^n R_{\min(i)}} \quad (1)$$

where  $R_{\min(i)}$  is the minimum reserved rate for flow (i).

$$\sum_{i=0}^n w_i = 1 \quad 0.001 \leq w_i \leq 1 \quad (2)$$

All flows shall satisfy the constraint of Eq. (2). Equation (2) enables system to allocate minimum value of bandwidth to all flows as weights of queues cannot be zero. Whenever new bandwidth request is received by BS, BS calls fuzzy inference system. The fuzzy system reads values of three input variables, fuzzifies these values and inputs it to the fuzzy scheduler component at BS. Fuzzy reasoning is thereafter applied using fuzzy rulebase and a value in terms of linguistic levels is outputted. At last, de-fuzzification of output value is done to get final crisp value for weight. De-fuzzification is performed using centre of gravity method and inference is applied using Mamdani's method. The outputted value is taken as weight for real time traffic. The bandwidth allocation to different queues is made on basis of weight assigned to that queue on the basis of equation

$$B_{real} = S_i \times \left( \frac{w_i}{\sum_{i=1}^n w_i} \right) \times \left( \frac{FrameDuration}{Maximum Latency} \right) \quad (3)$$

where  $S_i$  is the number of slots requested for that flow.

### 3 Performance Analysis of Fuzzy Adaptive Method

The proposed solution has been tested on Qualnet Developer 5.2. The proposed scheme is tested by designing a network consisting of one BS and a number of SS. Experiments are conducted to check whether proposed system was able to provide desired quality of service levels to traffic classes. Analysis of performance is done on basis of parameters like delay, throughput and jitter. Simulation is aimed at making sure that proposed scheme is able to provide a relative good QoS levels to all traffic classes. Performance is measured by varying number of SS in ratio of 1:1:1:3:4 for example when total number of SS was 60, the number of UGS, ertPS and rtPS was taken as 6 while number of nrtPS connections was 18 and number of BE connections was 24. Results presented in this section justifies that proposed system was able to provide enough bandwidth opportunities to satisfy increasing requirements of different types of traffic.

**Fig. 2** Delay of various service classes

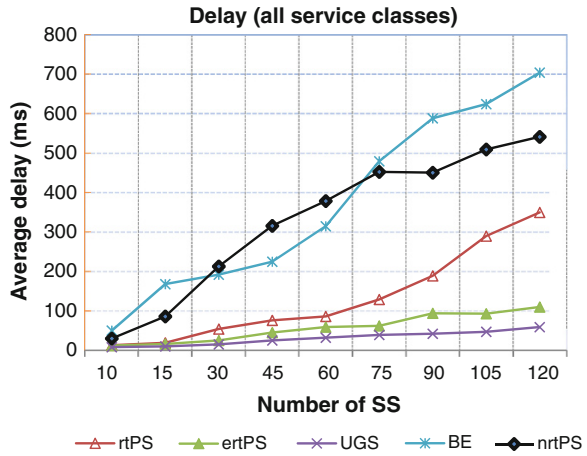
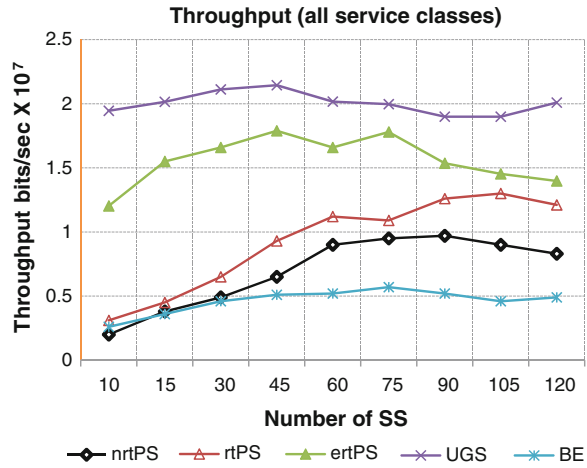


Figure 2 shows average delay incurred by various services in our fuzzy based inference system. It is evident from figure that delay of UGS and ertPS classes is almost bounded as required by IEEE 802.16 standard. This comes from the fact that scheduler offers higher precedence to UGS and ertPS classes and makes periodic allocations to these classes. Delay of rtPS class shows linear increase till number of SS is about 65 and thereafter growth is almost exponential. This may be attributed to increase in traffic of UGS and ertPS classes which are more prioritized. Delays for nrtPS and BE service classes shows an increasing trend as number of SS increases this is because real time service flows are being offered more share of bandwidth. The delay for BE is better as compared to delay for nrtPS class till a limited number of SS, this is because scheduler was able to provide residual bandwidth opportunities to BE connections. Delay for nrtPS eventually outperforms BE service class as number of connections increases. Nevertheless scheduler was able to avoid starvation of BE flows.

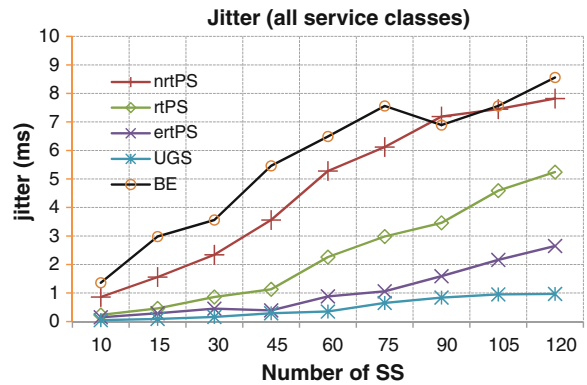
Figure 3 shows throughput of different service classes with an increase in number of SS. Throughput increases as number of connections increase which is expected. Higher throughput for UGS and ertPS is evident as their increasing demand forces system to allocate more amount of bandwidth. Throughput for UGS is almost constant as BS allocates slots to UGS class after fixed interval. Throughput for ertPS shows a small decline as number of SS increase beyond 75, this may be attributed to an increase in number of UGS connections which has high priority. Throughput for rtPS, nrtPS and BE remains almost neck to neck till number of SS are limited(30) as requirements for all classes are getting met thereafter scheduler starts to assign more priority to rtPS as compared to nrtPS and BE in order to satisfy its latency requirements. The throughput for BE class is minimum as there are no QoS requirement for BE class.

Figure 4 shows plot of average jitter for our fuzzy based method as function of number of SS. The average jitter for UGS is very small and shows a marginal rise with increase in number of SS. This is because of increase in amount of over all

**Fig. 3** Throughput of various service classes



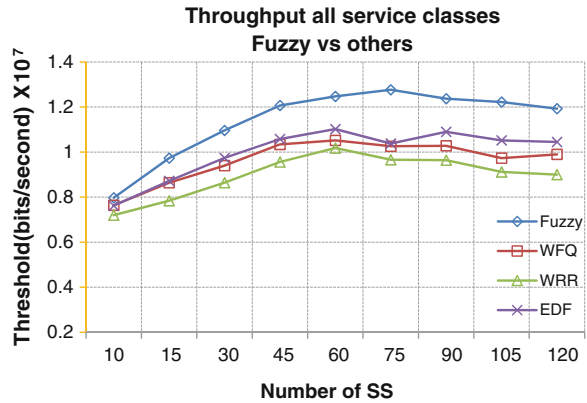
**Fig. 4** Jitter observed by various service classes



traffic in network and it shows that even UGS class may have packet losses. Jitter of ertPS and rtPS is relatively good considering amount of load being handled by system. Jitter in case of nrtPS and BE is high as expected because of dual reason of increase in overall traffic and their low priorities. However it is tolerable as both these classes are independent of delay variations.

The fuzzy system was also compared with number of algorithms like WFQ, WRR and EDF. Figure 5 shows that fuzzy system exhibits a significant improvement in terms of throughput observed for various service classes followed by EDF. The reason was that fuzzy system shows a quick response for real time traffic and is also able to provide increasing number of scheduling opportunities for non real time traffic when there are not stringent requirements from real time traffic. It results in overall throughput increase for the system which is not the case with other algorithms. These algorithms tend to starve low priority nrtPS and BE traffic classes and degrade their performance levels.

**Fig. 5** Throughput comparison of fuzzy system with WFQ, EDF and WRR



### 4 Conclusion and Future Scope

The above study proposed an application of fuzzy logic for allocation of resources in WiMAX networks. The approach is adaptive and resource allocation decision is taken by considering values of three input variables extracted from incoming traffic. Results indicate that system was able to provide desired quality of service levels to all traffic classes. The approach was tested under conditions of heavy load but performance of network was still quite appreciable. As future scope, the performance of the system needs to be justified by comparing with set practices in related field. The system shall also be tested for performance by deliberately increasing effects of higher priority traffic and observing responses of low order traffic classes.

### References

1. IEEE, Draft: IEEE standard for local and metropolitan area networks. 727 Corrigendum to IEEE standard for local and metropolitan area networks—Part 16: 728 air interface for fixed broadband wireless access systems (Corrigendum to IEEE Std 729 802.16-2004). IEEE Std P80216/Cor1/D2, 730 (2005)
2. IEEE, Draft: IEEE standard for local and metropolitan area networks. 731 Corrigendum to IEEE standard for local and metropolitan area networks—732 advanced air interface. IEEE P80216m/D10, 1–1132 (2010)
3. Simon, J., Maria, D., Juan, A., Gomez, P., Miguel, A., Rodriguez, A.: Embedded intelligence for fast QoS-based vertical handoff in heterogeneous wireless access networks. *J. Per Comp.* <http://dx.doi.org/10.1016/j.pmcj.2014.01.009> (2014)
4. Shuaibu, D.S., Yusof, S.K., Fiscal, N., Ariffin, S.H.S., Rashid, R.A., Latiff, N.M., Baguda, Y.S.: Fuzzy logic partition-based call admission control for mobile WiMAX. *ISRN Commun. Netw.* **171760**, 1–9 (2010)
5. Sadri, Y., Mohamadi, S.K.: An intelligent scheduling system using fuzzy logic controller for management of services in WiMAX networks. *J. SuperComput.* **64**, 849–861 (2013)

6. Alsahag, A.M., Ali, B.M., Noordin, N.K., Mohamad, H.: Fair uplink bandwidth allocation and latency guarantee for mobile WiMAX using fuzzy adaptive deficit round robin. *J. Net. Com. Appl.* <http://dx.doi.org/10.1016/j.jnca.2013.04.004i> (2013)
7. Hedayati, F.K., Masoumzadeh, S.S., Khorsandi, S.: SAFS: a self adaptive fuzzy based scheduler for real time services in WiMAX system. In: 2012 9th International Conference on Communications (COMM), 21–23 June 2012, pp. 247–250
8. Seo, S.S., Kang, J.M., Agoulmine, N., Strassner, J., Hong, J.W.-K.: FAST: a fuzzy-based adaptive scheduling technique for IEEE 802.16 networks. In: 2011 IFIP/IEEE International Symposium on Integrated Network Management (IM), 23–27 May 2011, pp. 201–208
9. Akashdeep, Kahlon K.S.: An adaptive weight calculation based bandwidth allocation scheme for IEEE 802.16 Networks. *J. Emerg. Technol. Web Intell.* **6**(1), 142–147 (2014)
10. Akashdeep, Kahlon, K.S.: A neural based proposal for scheduling of IEEE 802.16 networks. *Int. J. Eng. Technol.* **4**(5), 328–332 (2012)
11. Frantti, T.: Multiphase transfer of control signal for adaptive power control in CDMA systems. *J. Control Eng. Practice* **14**(5), 489–501 (2006)
12. Bchini, T., Tabbane, N., Tabbane, S., Chaput, E., Beylot, A.: Fuzzy logic based layers 2 and 3 handovers in IEEE 802.16e network. *J. Comput. Commun.* **33**, 2224–2245 (2010)

# Color Image Compression Based on Block Truncation Coding Using Clifford Algebra

Kartik Sau, Ratan Kumar Basak and Amitabha Chanda

**Abstract** Block Truncation Coding (BTC) is one of the most moment preserving (arithmetic mean and standard deviation) methods for compressing an image. Absolute Moment Block Truncation Coding (AMBTC) is an improved version of BTC, preserves only arithmetic mean. The present work deals with image compression based on Absolute Moment Block Truncation Coding (AMBTC) and Clifford Algebra for color images. A color image is divided into three distinct planes, Red (R), Green (G) and Blue (B) and the proposed method applied on these three planes separately. Each element of pixel is represented into a sum of largest perfect square of positive integers. Experimental results of proposed method give satisfactory result in terms of different parameters such as Peak Signal to Noise Ratio (PSNR), Bit Rate (BR), and Structural SIMilarity Index (SSIM).

**Keywords** Image compression · Clifford algebra · BTC · AMBTC · PSNR · SSIM

## 1 Introduction

Data compression is the art of reducing the size or electronic space or data bits of a data file in order to save space or transmission time. As data size is increasing day by day and it becomes more complex, more storage space is required to keep it.

---

K. Sau (✉) · R.K. Basak  
Department of Computer Science and Engineering,  
Budge Budge Institute of Technology, Kolkata 700137, West Bengal, India  
e-mail: kartik\_sau2001@yahoo.co.in

R.K. Basak  
e-mail: ratan.iww@gmail.com

A. Chanda  
Department of Computer Science and Engineering,  
University of Calcutta, Kolkata 700 009, West Bengal, India  
e-mail: amitabha39@gmail.com

It is used to overcome this limited storage capacity problem and reduces the transmission cost. Image is also a kind of data. Image compression techniques are also required for the same reason. It controls data in such a way so that the visual clarity does not affect to the viewer. The aim of image compression technique is to represent an image with shortened number of bits without introducing substantial degeneration of visual clarity of compressed image. Image compression can be classified into two broad categories one is lossy compression and another is lossless compression [1, 2–4]. For lossless compression technique there is no difference between original image and regenerated image, on the other hand lossy compression makes some difference. The nature and characteristics of regenerated image using lossless compression is satisfactory but compression ratio is poor but lossy compression delivers less image quality with higher compression ratio. Block Truncation Coding (BTC) and Absolute Block Truncation Coding (AMBTC) are lossy image compression which compresses monochrome image information introduced by Delp and Mitchell [5, 6]. It brings out 2 bits per pixel and low computational complexity. The objective of BTC was to achieve moment preserving quantization for each non overlapping block of pixels and therefore the clarity of image remains satisfactory and the intension of reducing storage space was also achieved. The quantizers of the Delp and Mitchell's BTC were arithmetic mean and standard deviation and it provides one bit quantized output. Each block needs to preserve mean and standard deviation; this is the overhead of this method. Another lossy compression method is absolute moment block truncation coding (AMBTC) [6] which keeps the higher mean and lower mean of each non-overlapping block. In this paper we proposed a method based on absolute moment block truncation coding and Clifford Algebra [7–9] to compress a color image. Proposed method delivers satisfactory image clarity and also gives a good parametric result in terms of PSNR and SSIM [10, 11]. This paper is organized as follows. Section 2 explains of different image quality parameters. Section 3 describes our proposed method in the form of algorithm and flowchart. Experimental results introduce to show the feasibility of the proposed method in Sect. 4 and finally some conclusions are made in Sect. 5.

## 2 Image Quality Parameters

Let  $g = (g_0, g_1, g_2, \dots, g_{M-1})^T$  be a vector having  $n$  elements. Let each element is coded by  $b$  bits. Therefore, total bits required for representing  $g$  is  $Mb$  bits. Now the vector  $g$  is transmitted to another vector  $G$  i.e.  $G = Tg$  by a transformation  $T$ . Let the vector  $G$  is represented by  $k$  bits. Three relations are possible between  $Mb$  and  $k$ .

$$1. Mb \gg k \quad 2. Mb = k \quad 3. Mb < k$$

Relation 2 and 3 are not efficient for data compression. Relation 1 may be achieved either by retaining only  $M' (< M)$  elements of  $G$  or by encoding the elements of  $G$  in such a way that the average number of bits per element is  $b' (< b)$ .



Therefore,  $k = M'b$  or  $k = Mb'$ . The amount of data reduction is given by  $C = \frac{Mb-k}{Mb} \times 100$ . The major steps of data compression procedure are transformation  $\rightarrow$  feature selection  $\rightarrow$  encoding.



Now we reconstruct the digital image from  $G'$  and obtain  $\bar{g}$ . Hence there may be some discrepancy between  $g$  and  $\bar{g}$ . This Discrepancy is considered as error. So error can be defined as follows.  $error = \|g - \bar{g}\|$  So the objective compression technique is to achieve the maximum amount of data reduction (C) without introducing objectionable error. This errors may be signifies in terms of PSNR and SSIM [1, 2, 4, 12].

### 2.1 Peak Signal to Noise Ratio (PSNR)

Thus PSNR is defined as follows:

$$PSNR = 10 \log \left( \frac{L^2}{MSE} \right) \text{ dB} \tag{1}$$

$$MSE = \frac{1}{MN} \sum_{i=1}^M \sum_{j=1}^N [y(i,j) - x(i,j)]^2 \tag{2}$$

### 2.2 Structural SIMilarity (SSIM) Index

SSIM index [13] is calculated as follows:

$$SSIM(x, y) = \frac{(2\mu_x\mu_y + C_1)(2\sigma_{xy} + C_2)}{(\mu_x^2 + \mu_y^2 + C_1)(\sigma_x^2 + \sigma_y^2 + C_2)} \tag{3}$$

where

$$\mu_x = \frac{1}{N} \sum_{i=1}^N x_i \tag{4}$$

$$\sigma_x = \left( \frac{1}{N} \sum_{i=1}^N (x_i - \mu_x)^2 \right)^{1/2} \quad (5)$$

$$\sigma_{xy} = \frac{1}{N} \sum_{i=1}^N (x_i - \mu_x)(y_i - \mu_y) \quad (6)$$

$$C_1 = (k_1 L)^2, k_1 \ll 1 \text{ and } C_2 = (k_2 L)^2, k_2 \ll 1$$

Here all symbols infers it usual meaning.

### 3 Proposed Method

The proposed method (abbreviated as CICBTCCA) for color image compression using AMBTC, introduced by Lema and Mitchell [6] and Clifford Algebra [7–9], is described as follows. In this approach we represent a positive integer as a sum of largest perfect square of positive integers. The largest square is figure out from the given integer, and then the same process is repeated from the residual part of the integer successively. The steps of the proposed method are given below:

- Step 1: A color image of size  $M \times N$  is split into three planes (R, G, and B) of size  $M \times N$ .
- Step 2: Each plane of size  $M \times N$  is split into non-overlapping blocks of the size  $m \times m$  (normally  $4 \times 4$  pixels).
- Step 3: Determine the arithmetic mean ( $\bar{x}$ ) of each block i.e.  $\bar{x} = \frac{1}{m} \sum_{i=1}^m x_i$ . In this method we modify the arithmetic mean with the help of Clifford algebra which generalize the real numbers, complex numbers, quaternion and several other hyper-complex number systems. The theory of Clifford algebras is informally associated with the theory of quadratic forms and orthogonal transformations. The following steps are involved to describe the calculation of new mean for a block [12].
  - Step 3.1: Consider an integer number  $n$  ranges from 0 to 255. Generate a set (s) of largest possible integers (duplication allowed) so that the square of summation of all those integers is equal to  $n$  and with lowest possible cardinality of s.
  - Step 3.2: Generate a vector using s in descending order so that components of vector must belongs to 15 to 0.
  - Step 3.3: Continue step 3.1 and 3.2 for all elements for a block.
  - Step 3.4: Determine the element which has maximum frequency from  $m * m$  vectors index-wise and if the of frequency of each vector element is same then choose the element which is minimum valued integer. Continue this process for all indices of vectors.

- Step 3.5: Generate a resultant vector ( $v$ ) by the elements returned from step 3.4.
- Step 3.6: Find sum of square of each element of resultant vector.
- Step 3.7: The new mean named as C-mean represented by  $\mu$  is calculating using arithmetic mean and the result from step 3.6. The definition of C-mean is defined as follows (Fig. 1):

$$\mu = \bar{x} + \alpha(\bar{x} - vs)$$

$$\text{where, } \bar{x} = \frac{1}{n} \sum_{i=1}^n x_i \text{ and } vs = \sum (v_i)^2, \alpha = 0.267$$

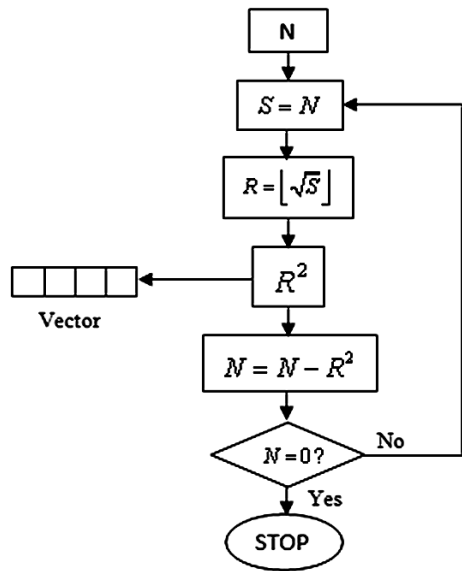
Step 4: Two quantization levels higher c-mean ( $x_H$ ) and lower c-mean ( $x_L$ ) are calculated. C-mean of those values ( $C_H$ ) which are greater than arithmetic mean of a block is higher c-mean and c-mean of rest of the values ( $C_L$ ) of that block is lower c-mean.  $C = C_H \cup C_L$  and  $C_H \cap C_L = \phi$

$$x_H = cmean(\{f(x_i) : f(x_i) \geq \Psi; f(x_i) \in C\}) \tag{7}$$

$$x_L = cmean(\{f(x_i) : f(x_i) < \Psi; f(x_i) \in C\}) \tag{8}$$

$$\text{where } \Psi = cmean(\{f(x_i) : f(x_i) \in C\}) \tag{9}$$

**Fig. 1** Block diagram to generate vectors for c-mean



Step 5: To encode a binary block represented by  $B$  assume a threshold  $\Psi$ . Elements of  $B$  are quantized as 1 if the element  $f(x_i)$  in the block is greater than quantized threshold  $\Psi$  otherwise 0. i.e.

$$B = \begin{cases} 1 & f(x_i) \geq \Psi \\ 0 & f(x_i) < \Psi \end{cases} \quad (10)$$

$x_H$ ,  $x_L$  and  $B$  these three are needed to reconstruct the image. During transmission sender only send this three

Step 6: During reconstruction the decoder will replace “1” in place of  $x_H$  and “0” in place of  $x_L$

$$Z = \begin{cases} x_L & \text{if } B = 0 \\ x_H & \text{if } B = 1 \end{cases} \quad (11)$$

Step 7: Merge three plane to produce compressed image.

## 4 Experimental Result

Our proposed method is tested on more than hundred color images of size  $512 \times 512$ , 8 bpp. For the sake of simplicity we are showing here only six color images namely Airplane, Lena, Girl, Splash, Pepper and Sparsha. The proposed method is also compared with color absolute moment block truncation coding which is first order moment preserving technique. The comparisons are based on

**Table 1** Comparative study among AMBTC and CICBTCCA

Images	Parameters	AMBTC	CICBTCCA
Airplane	PSNR	31.278437	31.476641
	SSIM	0.986557	0.987114
Lena	PSNR	31.986589	32.073399
	SSIM	0.994937	0.995348
Girl	PSNR	09.235195	33.849670
	SSIM	0.026791	0.991850
Splash	PSNR	34.910271	34.779186
	SSIM	0.997406	0.997057
Pepper	PSNR	31.464678	31.607178
	SSIM	0.994786	0.994903
Sparsha	PSNR	30.940117	31.013016
	SSIM	0.99079	0.991158

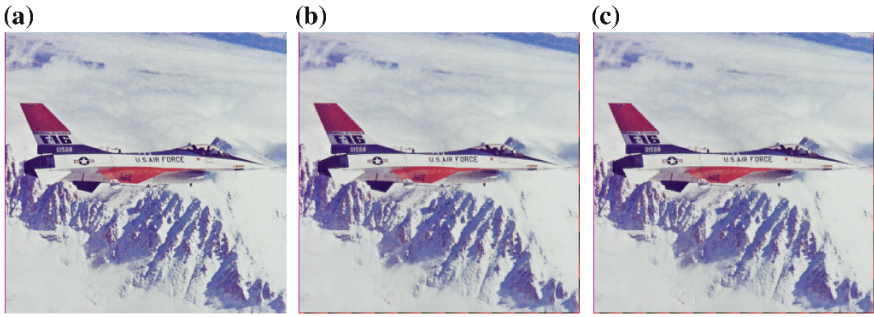


Fig. 2 Airplane a reference image; output of b AMBTC; c CICBTCCA



Fig. 3 Lena a reference image; output of b AMBTC; c CICBTCCA

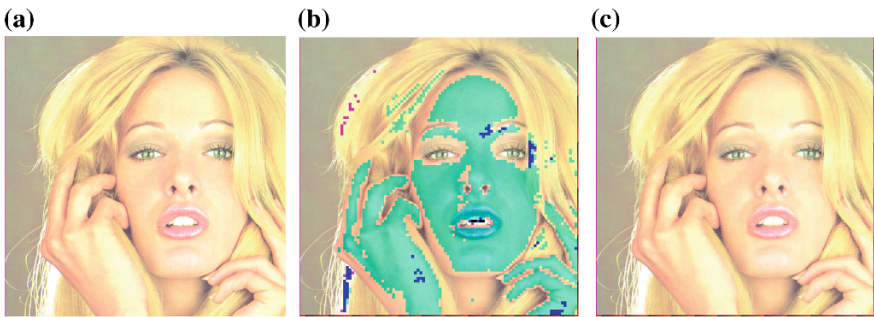


Fig. 4 Girl a reference image; output of b AMBTC; c CICBTCCA

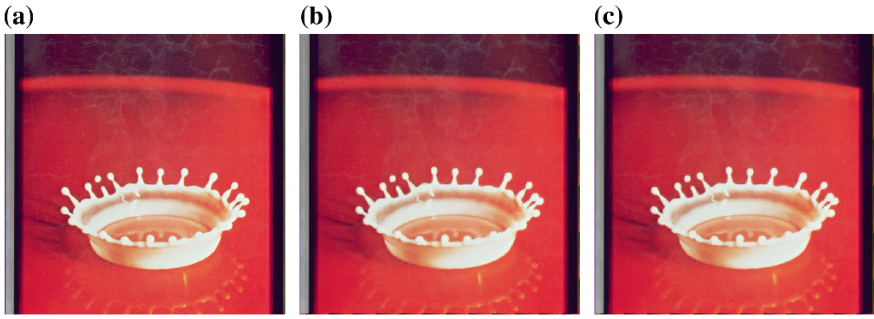


Fig. 5 Splash a Reference image; output of b AMBTC; c CICBTCCA

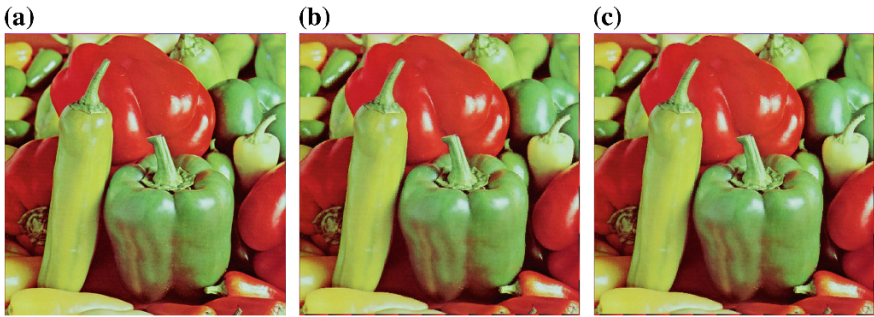


Fig. 6 Pepper a reference Image; output of b AMBTC; c CICBTCCA



Fig. 7 Sparsha a reference image; output of b AMBTC; c CICBTCCA

two parametric measures like PSNR and SSIM [1, 2, 12] for the clarity of image and the structure of the image. The experimental results are tabulated in the Table 1 (Figs. 2, 3, 4, 5, 6, and 7).

## 5 Conclusion

The experimental result of our proposed method for color image compression based on absolute block truncation coding and Clifford algebra has been shown in the Table 1. Proposed method splits the color image into three color plane viz. red, green and black. Each plane is divided into non-overlapping blocks of size  $4 \times 4$ . We are using  $512 \times 512$  color image where each pixel consist of three values ranges from 0 to 255. We found that using our proposed method we have got better PSNR and SSIM value rather than AMBTC method. The performance of our proposed method has been compared with color AMBTC and is found better than this method. The value of alpha is chosen so cleverly so that PSNR of the reconstructed images give promising results. Using Clifford algebra in our method the pixel value can reach more close to the original one.

**Acknowledgment** The author wishes to thanks the reviewer, whose comments have helped improving the presentation of the paper.

## References

1. Gonzalez, R.C., Eugene, R.: Digital Image Processing, edn. 3. Pearson, London (2012)
2. Chanda, B., Majumder, D.D.: Digital Image processing and Analysis, edn. 2. PHI, India (2011)
3. Jayaraman, S., Esakkirajan, S., Veerakumar, T.: Digital Image Processing, edn. 1. Tata McGraw Hill, Noida (2009)
4. Jain, A.K., Fundal of Digital Image Processing, edn. 2. PHI, India (2010)
5. Delp, E.J., Mitchell, O.R.: Image compression using block truncation coding. *IEEE Trans. Commun.* **27**, 1335–1342 (1979)
6. Lema, M.D., Mitchell, O.R.: Absolute moment block truncation coding and its application to color images. *IEEE Trans. Commun.* **COM-32**(10), 1148–1157 (1984)
7. Lounesto, P.: Clifford Algebras and Spinors. Cambridge University Press, Cambridge (1997)
8. Snygg, J.: Clifford Algebra: A Computational Tool for Physicists. Oxford University press, Oxford (1997)
9. Hestenes, D., Sobczyk, G.: Clifford algebra to Geometric Calculus. D. Riedel publishing Co., Holland (1984)
10. Eskicioglu, A.M., Fisher, P.S.: Image quality measures and their performance. *IEEE Trans. Commun.* **34**, 2959–2965 (1995)
11. Yamsang, N., Udomhunsakul, S.: Image quality scale (IQS) for compressed images quality measurement. In: Proceedings of the International Multiconference of Engineers and Computer Scientists, vol. 1, pp. 789–794 (2009)
12. Sau, K., Basak, R.K., Chanda, A.: Image compression based on block truncation coding using clifford algebra. *Procedia Technol.* **10**, 699–706 (2013)

13. Wang, Z., Bovik, A.C., Sheikh, R., Simoncelli, E.P.: Image quality assessment: from error measurement to structural similarity. *IEEE Trans. Image Process.* **13**(1), 600–612 (2004)
14. Franti, P., Nevalainen, O., Kaukoranta, T.: Compression of digital images by block truncation coding: a survey. *Compu. J.* **37**(4), 308–332 (1994)
15. Chanda, A.: A new signal processing tool developed with the help of the clifford algebra. In: *Proceedings of the 22nd IASTED International Conference on Modelling and Simulation*. Calgary, Canada, pp. 314–321 (2011)
16. Voloshynovskiy, S., Pereira, S., Herrigel, A., Baumgartner, N., Pun, T.: A stochastic approach to content adaptive digital image water marking .In: *Proceedings of the Third International Workshop on Information Hiding*, pp. 211–236 (1999)



# Performance Evaluation of Underground Mine Communication and Monitoring Devices: Case Studies

Alok Ranjan, H.B. Sahu and Prasant Misra

**Abstract** Communication and environmental monitoring play a major role in underground mining both from production and safety point of view. However, underground mining communication as well as monitoring devices encounter several challenges because of the nature of underground features and characteristics. Lack of real time information from underground workings may hamper production and create serious safety risks. Proper communication and monitoring devices are inevitable requirements for better production and improved safety. Communication and environmental monitoring devices are basic element of underground mine infrastructure. This paper describes the performance of communication and monitoring devices being used in underground mines. An attempt has been made to assess the safety risks by these devices which may dictate future research directions.

**Keywords** Mine communications · Monitoring · Wireless communication · Tracking · Safety · Ventilation on demand

## 1 Introduction

Mining has been considered as one of the oldest endeavours along with agriculture. The mining industry is always considered to be very critical that sustain civilization of any country. India is enriched with a number of mineral reserves and ranks

---

A. Ranjan (✉) · H.B. Sahu  
National Institute of Technology, Rourkela 769008, India  
e-mail: alokranjan007@hotmail.com

H.B. Sahu  
e-mail: hbsahu@nitrrkl.ac.in

P. Misra  
Robert Bosch Center for Cyber Physical Systems, Indian Institute of Science,  
Bangalore, India  
e-mail: prasant.misra@rbccps.org

among the top producers of coal, chromite, iron, etc. There are two types of mining operation commonly practiced, viz. opencast and underground. Opencast operation is involved in the mining of ore at surface level, whereas underground mining is for minerals that occur at greater depth. In underground mining, mainly there are two types of mining methods widely practiced to extract the ore body. These are board and pillar also known as room and pillar, and longwall mining methods. In India, majority of coal mines are practicing board and pillar mining method. However, the percentage of ore extraction is lower than the longwall mining method. In underground metal mines however, a number of methods are practiced, the common methods being cut and fill, shrinkage and sub-level stopping. It is easier to communicate and carry out monitoring in opencast mines, since access to different locations is comparatively easier and there is less hindrance in communications. In a particular shift of operation, large numbers of miners are present inside a mine for production and other activities. To this high number of mine personnel; safety is a prime and critical concern for every mining industry [1]. Underground mine environment poses a variety of challenges, because of the typical constructional features and environmental conditions. The key hazardous parameters, viz. toxic gases, humidity, dust, noise, temperature and vibrations are required to be monitored. Among all hazardous parameters; toxic gases, humidity, noise, dusts and temperature are major key parameters and need to be monitored continuously [2]. For coal mines, methane is a prime concern because of its explosive nature and Carbon monoxide (CO) is also found occasionally which is a acutely poisonous gas. In metal mines, noxious gases like SO<sub>2</sub> and H<sub>2</sub>S are needed to be monitored for better working environment. Therefore, continuous mine monitoring is very much crucial and critical need for the mining industries. Apart from these hazardous parameters, there is another unique set of characteristics in underground mines. These are mainly discontinuities in ore body, water seepage, poor visibility, narrow pathway, noise and rough surfaces. These set of unique features add additional challenges to mining professionals and researchers. Risks and their mitigation efforts to minimize the risks and improved safety in underground mines differs perceptibility from normal industries. Communication and monitoring of mine environment is very much required for any underground mine. It plays a significant role for both safety and production. Communication is the only source inside the mine working which uniquely contributes in emotional support among the miners. Also, it is used for better work coordination among miners to manage the mining operation efficiently. Presently, safe working operation is a prime concern for all mining industries. In the past, a numbers of accidents have occurred due to different hostile conditions present in underground mines. Any accident in underground mine brings loss of not only human lives, but also damage to infrastructure and causes problems in rescue and recovery work. On such occasions two way reliable communication may help to save lives and properties through planned rescue and escape operations [3]. There are mainly three kinds of communication techniques used in underground mines namely through the earth (TTE), through the wire (TTW), through the air (TTA). However, hybrid system is also in used and is reliable. Hybrid system includes both the features of TTW and TTA [2]. In India,

wired based infrastructure is mainly used for both communication and monitoring purposes. However, recently few underground mines have attempted to install TTA communication and monitoring systems. In this paper, an attempt has been made to assess the safety and risks through present communication and monitoring devices. The experiences gained from the visit of two underground metal mines and one coal mines have been presented here. These studies have been carried out during the month of February–March in the year of 2014. We studied the newly installed communication and monitoring devices presently working in the visited mines. This paper targets current researchers which are working and developing solutions for the mining industries. Also, this paper will help researchers to understand and formulation of problems in a better manner for future research. The paper has been divided into four sections. In Sect. 2, we briefly share information about the visited underground mines. Section 3, deals with the studies on the present communication and monitoring devices. We have done performance assessment of the present communication systems based on different considerations mainly the basic operation, coverage and survivability for each studied mine. The concluding remarks and future research discussion is presented in Sect. 4. In Sect. 5 we ended up our studies with conclusions.

## 2 Background of Studied Underground Mines

For our studies, we have selected both underground coal and metal mines. This is because, we wanted to carry out analysis and assessment of both types of mines which are mainly involved in underground mine operations. However, there are other types of mines also there such as iron ore, manganese, limestone, etc. but most of them are involved in open pit operations. We have given name to our studied mine as Site A and Site B for the metal mines and Site C for the underground coal mines. In the following paragraph, we briefly present the information related to the studied mine site, i.e. A, B and C.

*Site A:* Site A, is a metal mines. This mine is involved in extraction of uranium ore. The extracted ore is utilized in the power plant for India. This mine is one of the most modernized mines of India and uses shaft sinking to access the ore body. At present, the wired telephone system is mainly used for two way voice communication purpose. There are approximately 650 mine personnel working per day. In this site, we studied the present communication and tracking devices installed and working inside mine tunnel. We further examined the operation and architecture of the installed system. Although wired based telephone system is working well, but with the vision of modernization in mining operation and improvement in mine safety and production; hybrid system based communication and tracking devices had been installed by the mine management. Therefore, we primarily focused on our studies about the newly installed wireless based communication and tracking devices for this mine.

*Site B:* Site B, is also a metal mine and is involved in uranium productions for India. This mine involves approximately 550 mine personnel per day. Entry to this mine is with an inclined driven at  $8^\circ$  to the horizontal. Here also TTW communication technique is used for daily communications. We examined the ventilation on demand system which is currently installed and working in the mines. This system is also used for monitoring noxious gas concentration, i.e. CO and SO<sub>2</sub>. The other objective of the ventilation management system than better ventilation support is to save the energy consumptions by the ventilation fans.

*Site C:* Site C, is an underground coal mine. This mine uses board and pillar method to extract the ores. Presently, only wired telephone system is used for communication purposes. Communication is achieved with the help of central dispatch centre (CDC) which is at the surface. This CDC works as an interface for communication from surface to underground and vice versa.

### 3 Assessment of Present Communication and Monitoring Devices

#### 3.1 *Site A: Communication and Tracking Systems*

**Basic Operation:** Presently, the installed system targets to track the mine personnel and mining equipment. The installed system is based on wireless local area network architecture (WLAN) and is shown in Fig. 1. Internet protocol (IP) phones are used for voice communication among mine personnel. Every IP phone is registered to the access points. There are total nine phones working currently and registered to the different access points. One person can have communication with the other who is in the range of an access point to whom those IP phones are registered. Ethernet is used as the backbone network. The access point is installed at different working locations inside the mine workings. The data are transmitted over the Ethernet cable to the server, which is installed in the underground control room. In the installed network, Radio frequency identification (RFID) readers are used for reading the passive tags mounted over the mine trucks and mine equipment. RFID readers are installed at different locations and is connected through radio frequency cables. When the tag comes under the range of RFID readers then it reads the tag id and that information is passed through the RF cable to the control room. At control room, the authorized person can see the location of mine trucks and equipment. This help to manage the resources efficiently.

**Coverage:** Mining operations in an underground mine is carried out in a number of levels occurring at different depths from the surface. The working area in each level is again divided into a number of blocks or sections. These blocks or sections are connected with the main access through drivers, cross-cuts and raises. Limited line of sight is there for communication devices due to discontinuities in coal seams. The overall coverage of the installed WLAN architecture was limited to those areas

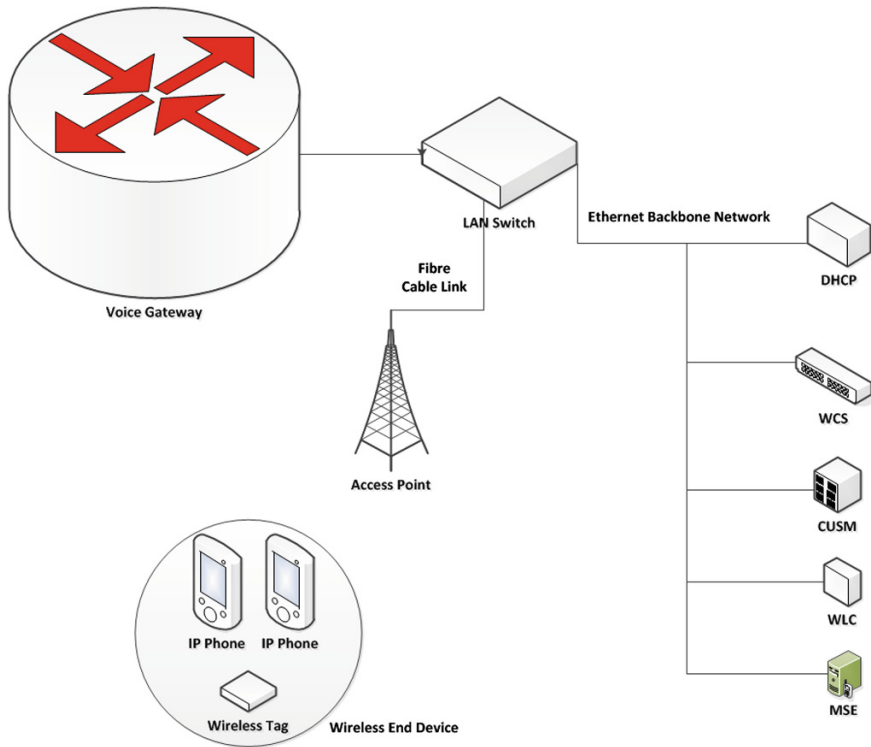


Fig. 1 Installed WLAN architecture

where access points were installed and the particular IP phone registered was coming under the range of that particular installed access point. Furthermore, the IP phone configuration to the access point was not dynamic means restricted to accessibility to which it is associated. To expand coverage area additional infrastructure would be required. The coverage of the present system installed is up to a length of 100 m as pointed out by the mine management. But during our studies 40 m distance was achieved for two way voice communication. The mobility support is limited to coverage area. Also dynamic configuration of the IP phone is not available.

**Survivability:** Post-accident communication is one of the most demanded features of communication and tracking devices to be installed in underground mines [4]. Therefore, the survivability of communication and monitoring devices even after catastrophic events, for example roof-falls, gas explosion, fire, collapse of the side walls and inundation are very much critical. The communication device can get damaged due to any of these events. This kind of uncertain condition present inside mines, need a full proof component design that must be rigid and immune enough to sustain in such environment. The current tracking and communication system is using ethernet as a backbone network. The chances of damages in the network is

still there. However, the system is cased and immune to dusts and humidity, the ruggedness and shock resistivity is still have to be checked. In case any roof-falls or collapse of side wall occurs then the network will get affected and may lead to failure of communication. The system should be designed in such a way that the survivability of installed device is maximum after any accident.

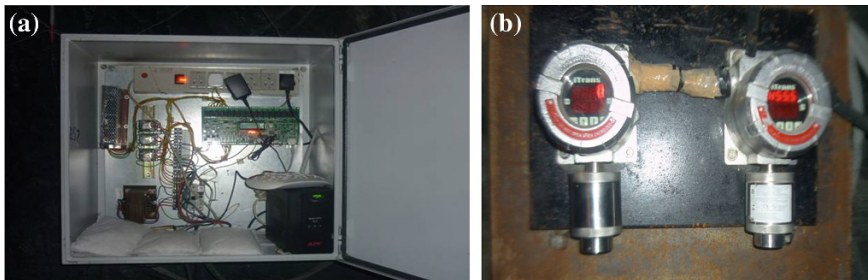
### 3.2 Site B: Ventilation Management

**Basic Operation:** The installed architecture is based on the wired infrastructure. In the installed system, there are two major components; detector (transmitter) and controller which work as receiver. Detector is responsible for sensing the noxious gas concentration at working areas. The detectors are connected through fibre cable to the controller. The sensed data from the detector is transmitted over the cable to the controller. The controller further processes the sensed data on its own. The controller is further connected to the switch using relay cable for on/off operation for the ventilation fan. The maximum statutory limits for detector are 100 ppm for CO and 5 ppm for SO<sub>2</sub>. After receiving the readings from transmitter i.e. detector, the controller worked with the following algorithms;

- i. Switched on the fan if any or both conditions CO > 30 ppm, SO<sub>2</sub> > 1.5 ppm exist.
- ii. Switch off the fan if both conditions CO < 10 ppm and SO<sub>2</sub> < 0.5 ppm exist.

The distance between a detector and the controller was 600 m (Fig. 2).

**Coverage:** To support better work environment, ventilation is vital inside underground mines. The coverage of the installed ventilation management system is limited to working areas where extraction of minerals is going on. To cover new area with time, there is an obvious need of additional infrastructure support. This may lead to chances of vulnerability in safety because the wired infrastructure may get damaged. Also additional detectors and additional sink controllers will have to be installed. Currently only one controller is there. To ensure reliability additional or back up controller is still required.



**Fig. 2** Ventilation management system at site B. **a** Controller. **b** Gas detectors

**Survivability:** Environmental knowledge helps to improve the security measure to minimize the risks. The mining industry now feels the need to adopt a reliable and flexible communication technology to address different daily purposes. The ventilation management system is well cased and immune enough to dusts, humidity and explosions. The controller case is rugged and shock proof. Since, the wired connection is very complex, the chances of damages can't be avoided. The chances of damage may be caused due to movement of transportation systems, drilling operation and general maintenance works. At present scenario, Indian mines have mainly the wired infrastructure based monitoring devices. The disadvantage of having such infrastructure is that once the wired network has any technical issues or is damaged due to any of the incidents like roof-falls, fire, inundation and gas explosion then the entire system is affected and sometimes leads to collapse of overall communication system. This can create havoc among miners about their safety. At the very same time if any emergency occurs, then that may lead to serious accidents. In addition, this may further affect the overall mine production.

### ***3.3 Site C: Present Communication System***

**Basic Operation:** The studied site C, is currently using wired based infrastructure for two way voice communication from surface to underground and vice versa. The installed system is based on code system. There is one board at the CDC centre and that board is connected through the twisted co-axial cable. The telephone set is installed at prefixed known locations decided by the mine management at different working levels. Communication takes place with the help of an operator at the surface only. When a person working underground wants to talk with other mine personnel either on the surface or underground, then the first call he has to make is to the CDC. After receiving a call from underground working, the operator at the surface first identifies that from which working level the call is. He then switches the connection to the desired location demanded by the initial caller. The installed and working system is shown in Fig. 3.

**Coverage:** Wired communication inside mine works in fixed point communication fashion because of poor mobility support. In the mine, the telephone sets have been kept at prefixed locations. These locations are decided by the mine management. This limited position of telephone systems restricts the accessibility of the communication system. A person has to walk out for communicating to other working levels or to the surface. Furthermore, the sound quality is not so good due to additional noise in the network. Reliability of the overall network is adversely affecting due to the additional noise in the transmitted signals.

**Survivability:** The mine layout can vary considerably from mine to mine. The numbers of miners are grouped together in working section where ore is extracted. Whereas, different group of mine personnel is present inside mine for daily activities like drilling, blasting, transportation, maintenance, safety check, constructional





**Fig. 3** Communication system at site C. **a** Chord based communication board at surface. **b** Telephone set

work and general maintenance. Every mine is involved in safety assessment on its own level to maximize the efficiency of installed systems and survivability. The communication system installed and working currently at site C, is a legacy system which is functioning since decades. It needs a regular check. Since, the wired connection is only the source of connection to different workings, the chances of network failure is high. The telephone set installed is having issue. Wired connection is done with the stitching in the side walls of the mine galleries. If any wire cut occurs then that working level will go for obvious communication failure. In such situation, the chances of risks can not be avoided. Also, the main circuit board at surface is having complex topology arrangement and is very old. To provide a secured environment for underground miners, it is also recommended that there should be a redundant communication path for backup in case any emergency occurs or the primary link fails.

## 4 Discussion

Operations involved in mining industries have been considered as a most hazardous production activity due to various risks parameters like humidity, poor visibility, toxic gas concentration, poor ventilation, potential rock falls, water seepage and dusts [5]. The summarized studies of the studied communication systems presently working in different mines is given in Table 1. The studied underground mines have communication systems based on WLAN and TTW architecture. It was being noted that however the communication system is working fine, but risks of failure of devices are still a concern. The performance of the communication devices in surface area found to be good but in case of underground mine workings their performance was poor. Additional noise in the transmitted signal degrades the signal quality at the receiver end. Scalability and accessibility of the devices are



**Table 1** Summarized studies on present communication and monitoring devices

Mine site	Architecture	Coverage	Survivability	Type	Performance	Maintenance
Site A	WLAN	Limited	Poor	Hybrid	Good	Complex
Site B	Wired	Moderate	Poor	Through the wire (TTW)	Good	Complex
Site C	Wired	Limited accessibility	Very poor	Through the wire (TTW)	Poor	Complex

found poor and needs to be researched in future. Wired based system is inconvenient to dispose in areas like narrow pathways and the area to be exploited. Also, the coverage and maintenance problem is there with wired communication devices. In view of the deployment cost, wired infrastructure is expensive and needs a regular performance check. It can be analysed that post-accident, two way reliable communication may help to save lives and properties through planned rescue and escape operations [3]. In the current scenario in Indian mines, communication and monitoring devices is limited to wired infrastructures, which is further restricted to coverage, flexibility, reliability and scalability. Normally the mines have separate communication and monitoring technologies. However, there may be some mines which are satisfied with only one installed communication system, which can be used for both monitoring and communication purposes, since, the installed devices are packaged with proprietary protocols. Therefore, interoperability, and further scalability of the network is another issue to be resolved. The opportunities with wireless communication and tracking devices to be deployed in underground mines are totally different than traditional wireless communication in normal industries. Underground mines are highly prone to risks and continuous monitoring of mine environment is complex and needs interdisciplinary research efforts. An improved safety working environment not only boosts the confidence in miners, but also indirectly helps in enhanced productivity. To support mobility, ease deployment, easy maintenance and scalability; a robust and reliable wireless communication technology may be best suited to such a hostile and dynamic environment. Wireless infrastructure is very much capable to minimize these limitations moderately. Having a wireless infrastructure inside mines, gives a number of advantages over traditional wired network [6]. The necessity of wireless communication in underground mines has evolved from maximization of productivity, tracking and monitoring and also communication between miners for better coordination as well. The complexity in maintenance and network scalability of wired infrastructure is giving opportunities for new wireless technology to be deployed in underground mines in the near future.

## 5 Conclusion

Most of the underground mines in India have wired systems for monitoring mine environment and two way voice communications. It may be noted from the mines studied in the paper that the communication devices had a limited to moderate coverage area and their survivability is poor. It is also noted that the performance is poor to satisfactory under normal conditions. However, in emergency situation failure of these systems may lead to disastrous consequences. It is also noted from studies that the maintenance of the systems are complex. As the mines are becoming larger, the communication devices must have extended coverage area which may require interoperability efforts by the researchers. A number of research opportunities are available which can be achieved by means of new emerging wireless communication technologies. However, one has to carry out research on characteristics of the wireless channel inside underground mines. The present communication scenario of the Indian mines implies that to enhance the safety goals; research on reliable communication and monitoring system is still needed. Since, the underground mine workings pose various safety risks; one has to ensure that the developed system is intrinsically safe to avoid any dangerous occurrences.

**Acknowledgment** The authors would like to thank the officials of Uranium Corporation of India Limited (UCIL) and official of different underground collieries. Authors also extend their gratitude to Shri Ajay Ghade, General Manager (Technical Services & Planning, UCIL) and Mr. P.K. Parhi (Dy. General Manager, Mines). We are also sincerely thankful to Mr. Rajeev Kumar (Safety officer, MCL).

## References

1. Bandyopadhyay, L., Chaulya, S., Mishra, P.: Wireless communication in underground mines. RFID-Based Sens. Netw. (2010)
2. Misra, P., Kanhere, S., Ostry, D., Jha, S.: Safety assurance and rescue communication systems in high-stress environments: a mining case study. *IEEE Commun. Mag.* **48**(4), 66–73 (2010)
3. Wang, X., Zhao, X., Liang, Z., Tan, M.: Deploying a wireless sensor network on the coal mines. In: *IEEE International Conference on Networking, Sensing and Control*, pp. 324–328. IEEE, New Jersey (2007)
4. Yarkan, S., Guzelgoz, S., Arslan, H., Murphy, R.R.: Underground mine communications: a survey. *IEEE Commun. Surv. Tutorials* **11**(3), 125–142 (2009)
5. Ranjan, A., Sahu, H.: Advancements in communication and safety systems in underground mines: present status and future prospects. In: *Proceedings of the Zaytoonah University International Engineering Conference on Sustainability: Design and Innovation (ZEC Sustainability 2014) (CD-ROM)*, Amman, Jordan, May 13–15 (2014)
6. Yang, W., Huang, Y.: Wireless sensor network based coal mine wireless and integrated security monitoring information system. In: *ICN'07 6th International Conference on Networking*, pp. 13–13. IEEE, New Jersey (2007)

# Fuzzy Goal Programming Approach for Solving Congestion Management Problem in Electrical Transmission Network Using Genetic Algorithm

Bijay Baran Pal and Papun Biswas

**Abstract** This article presents an efficient genetic algorithm (GA) based fuzzy goal programming (FGP) approach to solve Congestion Management (CM) problem in electrical power transmission network by generation rescheduling or load shedding of participating generators and loads. In the proposed approach, FGP and GA are applied at two stages for model formulation and solving the problem of CM. The proposed approach is tested on the standard IEEE 6-Generator 30-Bus System and the model solution is compared with the solution obtained in a previous study.

**Keywords** Congestion management · Fuzzy goal programming · Genetic algorithm · Load shedding · Membership function · Optimal power flow

## 1 Introduction

Demand of electric power has increased in an alarming rate in the recent years. The demand is increasing at a faster rate as compared to the increase in transmission line capacity. Congestion or overload [1] in transmission lines generally occur due to the generation outages, sudden increase in load demand, or failure of some equipments.

The mathematical programming approach for estimation of voltage drops and line loadings for each network element out of service was first introduced in [2]. Thereafter, different classical optimization models based on load flow has been developed in the past century for CM problem in [3, 4]. Congestion management in

---

B.B. Pal (✉)

Department of Mathematics, University of Kalyani, Kalyani, West Bengal, India  
e-mail: bbpal18@hotmail.com

P. Biswas

Department of Electrical Engineering, JIS College of Engineering, Kalyani,  
West Bengal, India  
e-mail: papun.biswas.2008@ieee.org

© Springer India 2015

J.K. Mandal et al. (eds.), *Information Systems Design and Intelligent Applications*,  
Advances in Intelligent Systems and Computing 339,  
DOI 10.1007/978-81-322-2250-7\_70

695

a real time operational environment is proposed in [5]. The AC-Optimal Power Flow (OPF) based approach to congestion along with congestion cost allocation is proposed by Rau [6]. The efficient model for location of unified power flow controller (UPFC) for congestion management is proposed by Verma et al. [7]. Rodrigues and DaSilva proposed a minimum load curtailment problem, to manage congestion problem is presented in [8]. A multiobjective OPF with voltage security constraints considering transmission congestion using location marginal price is presented in [9]. By using rescheduling of generation and loads for congestion management with voltage security constraints is presented in [10]. A simple and cost efficient method of generation rescheduling and load shedding for congestion management is proposed in [11].

Recently, global optimization techniques with the use of heuristic methods have been applied to solve the optimal CM problem [12, 13] with impressive success. The approach based on fuzzy estimation for identification of collapse sequences is used in CM problem in [14].

In this paper, a GA-based FGP approach is proposed to solve the CM problem. The problem is formulated as an optimization problem with constraint functions. In this study, the fuzzy representation of different objectives is considered such as minimizing the overload alleviation and operation cost in the problem formulation stage. The problem is solved with different selection and crossover function. The proposed approach has been tested on the standard IEEE 6-Generator 30-bus test system. The model solution is also compared with the approach studied in [12] previously to expound the potential use of the approach.

Now, a CM problem is discussed in the Sect. 2.

## 2 CM Problem Description

In the case of a CM problem with transmission constraints and load characteristics, two conflicting objective functions, alleviation of overload and cost of operation, are generally involved [12] in the environment of making decision.

Now, the objectives and system constraints are introduced as follows:

### 2.1 Definitions of Objective Functions

**Overload Alleviation Function** The alleviation of overload in electric power transmission system appears as:

$$F_1 = \sum_{i=1}^{nl} (S_i - S_i^{\max})^2 \quad (1)$$

where,  $F_1$  is the cumulative overload,  $nl$  is number of overloaded line, and where  $S_i$  and  $S_i^{max}$  are the MVA flow and MVA capacity of line  $i$ , respectively.

**Operation Cost Function** The total operational cost of a power plant in CM problem is expressed as the sum of fuel cost and the cost of load shedding.

The total operation cost function can be expressed as:

$$F_2 = \sum_{i=1}^{ng} (a_i + b_i P_{gi} + c_i P_{gi}^2) + \sum_{k=1}^{pl} (a'_k + b'_k L_{shd,k} + c'_k L_{shd,k}^2) \tag{2}$$

where  $F_2$  is the total operating cost,  $ng$  is the number of participating generators,  $pl$  represents number of participating loads,  $P_{gi}$  is the power generation from  $i$ -th generator,  $L_{shd,k}$  is amount of load shedding at bus  $k$ , and where  $a_i, b_i, c_i$  are the cost coefficients associated with generation of power from generator  $g_i$ , and  $a'_k, b'_k, c'_k$  are the cost coefficients of load shedding at bus  $k$ .

## 2.2 Description of System Constraints

The system constraints associated with generation of power are defined as follows:

### Equality Constraints

*Power Balance Constraint* The power balance constraint can be express as

$$P_{gi} - P_{di} = \sum_{j=1}^{nb} |V_i||V_j||Y_{ij}| \cos(\delta_i - \delta_j - \theta_{ij})$$

$$Q_{gi} - Q_{di} = \sum_{j=1}^{nb} |V_i||V_j||Y_{ij}| \sin(\delta_i - \delta_j - \theta_{ij}) \tag{3}$$

where

- $P_{gi}, Q_{gi}$  real and reactive power generation at bus  $i$ ;
- $P_{di}, Q_{di}$  real and reactive power demand at bus  $i$ ;
- $nb$  number of buses;
- $Y_{ij}$  self-admittance of node  $i$ ;
- $\delta_i, \delta_j$  bus voltage angle of bus  $i$  and bus  $j$ , respectively;
- $\theta_{ij}$  impedance angle of line between buses  $i$  and  $j$ .

### Inequality Constraints

*Generation Capacity and Voltage Constraint* Following the conventional power generation and dispatch system, the constraints on the generator outputs can be considered as:

$$\begin{aligned}
 P_{g_i}^{\min} &\leq P_{g_i} \leq P_{g_i}^{\max}, \\
 Q_{g_i}^{\min} &\leq Q_{g_i} \leq Q_{g_i}^{\max}, \quad i = 1, 2, \dots, N \\
 V_i^{\min} &\leq V_i \leq V_i^{\max}, \quad i = 1, 2, \dots, N
 \end{aligned}
 \tag{4}$$

where min and max stand for minimum and maximum values, respectively.

Now, the FGP model of the proposed CM problem is described in the Sect. 3.

### 3 FGP Model Formulation of the CM Problem

In the decision situation, the objectives in (1) and (2) can be defined as the fuzzy goals by assigning imprecise aspiration levels to each of them.

The fuzzy goals of the objective functions take the form:

$$F_1 = \sum_{i=1}^{nl} (S_i - S_i^{\max})^2 < F_1^A, \tag{5}$$

$$F_2 = \sum_{i=1}^{ng} (a_i + b_i P_{g_i} + c_i P_{g_i}^2) + \sum_{k=1}^{pl} (a'_k + b'_k L_{\text{shd},k} + c'_k L_{\text{shd},k}^2) < F_2^A, \tag{6}$$

where  $F_1^A$  and  $F_2^A$  are the aspiration levels of the defined objective functions.

Now, considering  $F_1^U$  and  $F_2^U$  as the upper-tolerance limits of achieving the respective fuzzy goals and where ‘<’ refers to the fuzziness of an aspiration level and it is to be understood as ‘essentially less than’ [15].

Now, the fuzzy goals are characterized by the respective membership functions for measuring their degree of achievements in a fuzzy decision environment.

#### 3.1 Membership Function

The membership function representation of the fuzzy objective goals appear as:

$$\mu_{F_1}[F_1] = \begin{cases} 1, & \text{if } F_1 \leq F_1^A \\ \frac{F_1^U - F_1}{F_1^U - F_1^A}, & \text{if } F_1^A < F_1 \leq F_1^U \\ 0, & \text{if } F_1 > F_1^U \end{cases} \tag{7}$$

where  $(F_1^U - F_1^A)$  is the tolerance range for achievement of the overload alleviation goal.

$$\mu_{F_2}[F_2] = \begin{cases} 1, & \text{if } F_2 \leq F_2^A \\ \frac{F_2^U - F_2}{F_2^U - F_2^A}, & \text{if } F_2^A < F_2 \leq F_2^U \\ 0, & \text{if } F_2 > F_2^U \end{cases} \quad (8)$$

where  $(F_2^U - F_2^A)$  is the tolerance range for achievement of total operation cost goal.

**Note:**  $\mu[\cdot]$  represents membership function.

Then, the *minsum* FGP model formulation for the defined membership functions is presented in the Sect. 3.2.

### 3.2 Minsum FGP Model

In the process of formulating FGP model of the problem, the membership functions are transformed into membership goals.

The *minsum* FGP model can be presented as [16]:

Find  $(S_i, P_g, L_{shd})$  so as to:

Minimize:  $Z = \sum_{k=1}^2 w_k^- d_k^-$

and satisfy

$$\begin{aligned} \mu_{F_1} : \frac{F_1^U - F_1}{F_1^U - F_1^A} + d_1^- - d_1^+ &= 1, \\ \mu_{F_2} : \frac{F_2^U - F_2}{F_2^U - F_2^A} + d_2^- - d_2^+ &= 1, \end{aligned} \quad (9)$$

subject to the constraints defined in (3)–(4),

where  $d_k^-, d_k^+ \geq 0$ ,  $(k = 1, 2)$  represent the under- and over-deviational variables, respectively, associated with the respective membership goals.  $Z$  represents goal achievement function,  $w_k^- > 0$ ,  $k = 1, 2$  denote the relative numerical weights of importance of achieving the aspired goal levels and can be determined as in [16]:

$$w_k^- = \begin{cases} \frac{1}{F_1^U - F_1^A} & \text{for membership function in (7)} \\ \frac{1}{F_2^U - F_2^A} & \text{for membership function in (8)} \end{cases}$$

The GA scheme employed in the process of solving the problem is presented in the Sect. 4.

## 4 GA Scheme for CM Problem

In the literature of GAs, there are a number of schemes [17] for generation of new populations. The fitness score of a chromosome  $v$  (say) in evaluating a function, say  $eval(E_v)$ , based on maximization or minimization of an objective function defined on the basis of DM's needs and desires in the decision making context.

The fitness function can be defined as:

$$eval(E_v) = (Z)_v = \sum_{k=1}^K \{w_k^- d_k^-\}_v, \quad (10)$$

where the subscript ' $v$ ' refers to the fitness value of the selected  $v$ -th chromosome,  $v = 1, 2, \dots, \text{pop\_size}$ . The best chromosome with largest fitness value at each generation is determined as:

$$E^* = \max\{eval(E_v) | v = 1, 2, \dots, \text{pop\_size}\}$$

or

$$E^* = \min\{eval(E_v) | v = 1, 2, \dots, \text{pop\_size}\}, \quad (11)$$

which depends on searching of the maximum or minimum value of an objective function, respectively.

Now, the executable model of the problem is demonstrated via a case example in the Sect. 5.

## 5 A Demonstrative Case Example

The standard IEEE 30-bus 6-generator test system [11] is considered to illustrate the potential use of the approach. The total system demand for the 21 load buses is 283.4 MW. The detailing of the simulation runs carried out in the test system is given in Table 1. The data description of different types of power generation cost-coefficients and load shedding cost-coefficients are presented in Tables 2 and 3, respectively.

**Table 1** Simulation runs

Run	Different simulation cases
1	Overload simulation by reducing capacity of line 1–2 from 130 to 50 MW
2	Overload simulation by reducing capacity of line 1–3 and 2–4 from 130 to 50 MW and 65–15 MW
3	Overload simulation for outage of unit 3 at bus 5 and by reducing capacity of line 2–5 from 130 to 50 MW



**Table 2** Data description of power generation costs-coefficients

Type	Max gen capacity (MW)	a	b	c
T <sub>1</sub>	<25	0.0	2,025.00	1.500
T <sub>2</sub>	50	0.0	1,875.00	1.425
T <sub>3</sub>	100	0.0	1,800.00	1.350
T <sub>4</sub>	200	0.0	1,650.00	1.250
T <sub>5</sub>	250	0.0	1,575.00	1.500
T <sub>6</sub>	300	0.0	1,575.00	1.250
T <sub>7</sub>	350	0.0	1,500.00	1.350
T <sub>8</sub>	400	0.0	1,500.00	1.250
T <sub>9</sub>	500	0.0	1,200.00	1.500
T <sub>10</sub>	>500	0.0	1,200.00	1.000

**Table 3** Data description of load shedding cost-coefficients

Amount of load in a bus (MW)	$a'_k$	$b'_k$	$c'_k$
≤10	0.0	1,200	1.00
≤20	0.0	1,200	1.50
≤30	0.0	1,500	1.25
≤40	0.0	1,500	1.35
≤50	0.0	1,575	1.25
≤60	0.0	1,575	1.5
≤75	0.0	1,650	1.25
≤100	0.0	1,800	1.35
≤125	0.0	1,875	1.425
>125	0.0	2,025	1.5

The GA is implemented using the Optimization Toolbox under MATLAB (MATLAB R 2010a) at different stages for evaluation of the problem. The parameter values with Roulette Wheel selection and Single Point crossover are taken as follows:

Crossover probability = 0.8, Mutation Probability = 0.07, and Maximum Generation Number = 100.

The goal achievement function  $Z$  in (9) appears as the evaluation function in the GA search process for solving the problem.

The simulated results of the Runs in the test system under smooth cost curves are presented in Table 4.

Now, to show the potential use of the approach, the model solution is compared with the solution obtained by using the Particle Swarm Optimization (PSO) method in [12]. The solution achievement is presented in Table 5.

A comparison shows that the solution obtained by using the proposed GA based FGP approach is superior over the PSO based method from the view point of achieving a better decision for optimizing the objectives of the CM problem.

**Table 4** Simulation runs for the test system under proposed method

Run	Overloaded condition			Solution		
	Line/unit	MVA flow	MVA capacity	MVA flow	$P_{ng}$ ( $ng = 1, 2, 5, 8, 11, 13$ )	Cost (Rs/h)
1	1–2	63.08	50	49.98	(84.99, 63.47, 57.08, 46.83, 0.00, 35.13)	539,166.93
2	1–3 and 2–4	38.94 23.72	50 15	30.89 14.78	(92.51, 33.92, 50.06, 53.59, 8.56, 48.87)	540,433.35
3	2–5 and out of unit 3	40.33	50	<b>55.04</b> (5.04 MVA Extra Flow)	(83.07, 14.55, 0.00, 68.17, 60.71, 63.38)	559,643.46
				<b>47.36</b>	(79.06, 4.69, 0.00, 68.16, 61.86, 63.05) (12.2 MW load-shaded)	536,047.13

**Table 5** Simulated results of the runs in the test system under PSO method

Run	Overloaded condition		Solution	
	Line/unit	MVA capacity	MVA flow	Cost (Rs/h)
1	1–2	50	49.16	541,171
2	1–3 and 2–4	50 15	12.31 14.99	542,465
3	2–5 and out of unit 3	50	49.88	565,979

## 6 Conclusions

In this paper, a GA based FGP approach is presented to solve the CM problem. The main advantage of the proposed method is that a multiobjective optimization problem can be converted into a goal oriented single objective optimization problem, which leads to achieve a compromise solution of the problem with multiplicity of conflicting objectives. Further, the computational load and approximation error inherent to the use of conventional linearization approaches can be avoided here with the use of the GA based solution method. Furthermore, the proposed approach is flexible enough to accommodate different other restrictions as and when needed in the decision making context. However, within the framework of the proposed model, consideration of other objectives and constraints that are concerned with power plant operations may be a problem in future study.

Finally, it is hoped that the solution approach presented here may lead to future research for proper management of congestion problem in electric power transmission environment.

**Acknowledgments** The authors are thankful to the anonymous Reviewers and Program Chair of INDIA-2015, for their valuable comments and suggestions to improve the quality of presentation of the paper.

## References

1. Bhattacharya, K., Bollen, Math H.J., Daalder, Jaap E.: Operation of Restructured Power Systems. Kluwer Academic Publishers, The Netherlands (2001)
2. Abiad, A.H.El., Stagg, G.S.: Automatic evaluation of power system performance-effect of line and transformer outages. *AIEE Trans.* **PAS-81**, 712–716 (1963)
3. Mamandur, K.R.C., Berg, G.J.: Economic shift in electric power generation with line flow constraints. *IEEE Trans. Power App. Syst.* **PAS-97**(7), 1618–1626 (1978)
4. Medicherla, T.K.P., Billinton, R., Sachdev, M.S.: Generation rescheduling and load shedding to alleviate line overload—analysis. *IEEE Trans. Power App. Syst.* **PAS-98**(6), 1876–1884 (1979)
5. Fang, R.S., David, A.K.: An integrated congestion management strategy for real time system operation. *IEEE Power Eng. Rev.* **19**(5), 52–53 (1999)
6. Rau, N.S.: Transmission loss and congestion cost allocation: an approach based on responsibility. *IEEE Trans. Power Syst.* **15**(4), 1401–1409 (2000)
7. Verma, K.S., Singh, S.N., Gupta, H.O.: Location of unified power flow controller for congestion management. *Electr. Power Syst. Res.* **58**, 89–96 (2001)
8. Rodrigues, A.B., DaSilva, M.G.: Impact of multilateral congestion management on the reliability of power transactions. *Electr. Power Energy Syst.* **25**, 113–132 (2003)
9. Milano, F., Canizares, C.A., Invernizzi, M.: Multi-objective optimization for pricing system security in electricity markets. *IEEE Trans. Power Syst.* **18**(2), 596–604 (2003)
10. Yamin, H.Y., Shahidepour, S.M.: Transmission congestion and voltage profile management coordination in competitive electricity markets. *Electr. Power Energy Syst.* **25**, 849–861 (2003)
11. Talukdar, B.K., Sinha, A.K., Mukhopadhyay, S., Bose, A.: A computationally simple method for cost-efficient generation rescheduling and load shedding for congestion management. *Electr. Power Energy Syst.* **27**(5–6), 379–388 (2005)
12. Hazra, J., Sinha, K.A.: Congestion management using multi objective particle swarm optimization. *IEEE Trans. Power Syst.* **22**(4), 1726–1734 (2007)
13. Balaraman, S., Kamaraj, N.: Congestion management using hybrid particle swarm optimization technique. *Int. J. Swarm Intell. Res.* **1**(3), 51–66 (2010)
14. Hazra, J., Sinha, A.K.: Identification of catastrophic failures in power system using pattern recognition and fuzzy estimation. *IEEE Trans. Power Syst.* **24**(1), 378–387 (2009)
15. Zimmermann, H.-J.: *Fuzzy Sets, Decision Making and Expert Systems*. Kluwer Academic Publisher, Boston (1987)
16. Pal, B.B., Moitra, B.N., Maulik, U.: A goal programming procedure for fuzzy multiobjective linear fractional programming problem. *Fuzzy Sets Syst.* **139**(2), 395–405 (2003)
17. Goldberg, D.E.: *Genetic Algorithms in Search, Optimization, and Machine Learning*. Addison-Wesley, Reading (1989)

# A Real-Time Machine Learning Approach for Sentiment Analysis

Souvik Sarkar, Partho Mallick and Aiswaryya Banerjee

**Abstract** The rapid increase in data volume and human concern about quick information mount the need for knowledge discovery with meager time span. Discover facts (data) about real entity and derive conclusions (information) from those facts and storing them for future use and reference (knowledge), is an art to get the true feeling and sentiment. In recent trend, knowledge discovery and knowledge management has been highly influenced by Sentiment Analysis. Sentiment Analysis provides contextual polarity of a document with respect to some issues or some topic. This paper contributes a new approach of deploying Artificial Neural Network and k-Mean algorithm for Sentiment Analysis. The approach incorporate the linguistic analysis of different components of a sentence(Adverb, Adjective, Noun, Verb) into a artificial neural network for supervised learning and k-Mean algorithm for unsupervised learning and the output (five cluster representing strong like, weak like, doubtful, weak dislike and strong dislike) from the network will not only simplify e-Discovery(rapid identification of potentially relevant data) solutions and opinion analysis system but also shown significant advancement from the previous research on this domain. The system not only classify documents and provide a relevant information but also optimizes steps of different techniques used for Sentiment Analysis and increases the performance (reducing memory and processor utilization) by modifying the deployed algorithms.

**Keywords** Knowledge discovery · Knowledge management · Sentiment analysis · Artificial neural network · K-mean · E-discovery · Opinion analysis system

---

S. Sarkar (✉)

Ibm India Pvt. Ltd., Kolkata, India  
e-mail: souviksarkar@in.ibm.com

P. Mallick · A. Banerjee

Techno India University, Kolkata, India  
e-mail: partho.mallick@gmail.com

A. Banerjee

e-mail: banerjee.aiswaryya@gmail.com

© Springer India 2015

J.K. Mandal et al. (eds.), *Information Systems Design and Intelligent Applications*,  
Advances in Intelligent Systems and Computing 339,  
DOI 10.1007/978-81-322-2250-7\_71

705

## 1 Introduction

E-Discovery or Electronic discovery is a process of retrieving and securing a transparent view of the content of digital forensic evidence. The field of automatic information extraction from existing documents is a part of the E-Discovery Reference Model [1]. E-Discovery includes data either in structured or unstructured form. The utmost difficulty is faced in extracting information from unstructured data which opened up new fields of mapping upon the clean semantics of structured database. This process includes high expenses incurred over domain specific expert analyzer and lead to introduction of sentiment analysis in the field of e-Discovery. It is a field of computer science which deploys different machine learning and Natural Language Processing Technique for deriving useful patterns from existing data volume about various entities which is considered to be knowledge. This knowledge is iteratively input for further knowledge discoveries. The concept deals with the process of reverse engineering and is a vital step of software mining where existing software can be studied to establish models like entity-relationship diagrams. So, it is of utmost importance to devise a mechanism, where the true sentiment of any sentence be correctly and efficiently evaluated, because knowledge itself is based solely on evaluations from data. The basic task is automatically extracting target text and classifying the polarity of the text, that is whether the expressed opinion is positive, negative or neutral and also, by what extent. The proposed system aims to determine the attitude of the document with near optimal, processor and memory, utilization for each steps involved.

## 2 Previous Work

Some prior studies have been made on Sentiment Analysis to focus on the document-level classification of sentiment [2, 3] where documents are incorporated with single sentiment. Some other workers [4, 5] trusted on quantitative information such as the frequencies of word associations or statistical predictions of favorability to provide sentiment to words. In 1997, Hatzivassiloglou and McKeown come up with an automatic acquisition of sentiment expressions, but they confined to adjectives and only one sentiment could be assigned to every word. Kanayama Hiroshi, Nasukawa Tetsuya And Watanabe Hideo introduces a method for translation from text documents to a set of sentiment units and remove two types of errors out of the four claimed by Nasukawa and Yi (2003). In order to predict the orientation of a document [2, 3] or the positive/negative/neutral polarity of an opinion sentence within a document, Sentiment Analysis through light on assigning a polarity or a strength to subjective expressions (words and phrases that express opinions, emotions, sentiments, etc.) [6–8]. Subsequent work has been done to focus on the strength of an opinion expression where each clause within a sentence can have a neutral, low, medium or a high strength [9]. Adverbs are used for

opinion mining in [10] where adjective phrases such as “excessively affluent” were used to extract opinion carrying sentences. Yu and Hatzivassiloglou [8] uses sum based scoring with manually scored adjectives and adverbs, while Chklovski [11] uses a template based methods to map expressions of degree such as “sometimes”, “very”, “not too”, “extremely very” to a [-2, 10] scale. Benamara et al. [12] shows that using adverbs and Adverb Adjective Combination produces significantly higher Pearson correlations (of opinion analysis algorithms vs. human subjects) than these previously developed algorithms that did not use adverbs or Adverb Adjective Combination. V.S. Subrahmaniam and Diego Reforgiato shows another way to identify intensity of opinion on any topic by analyzing the sentiments expressed by combinations of adjective, verb and Adverb [13]. Adverb-Adjective Combination is very much important for opinion analysis but for achieving better result we must take in consideration domain categorization of adverb and Adverb-Adjective-Noun (AAN) combination [14] instead of only Adverb-Adjective Combination. After this Adverb-Adjective-Noun-Verb [15] combination is proposed for sentiment analysis merging previous research [14, 13]. But working with real-time huge dataset, processor and memory utilization for those implementation, absence of some parameter while decision making, instead of clustering of sentences of a document for final decision just only depend on some score are some of the issues that remain untouched till now. This paper has taken its initiative to bridge these gaps.

### 3 SentiWordNet

WordNet is a large lexical database of English. Nouns, verbs, adjectives and adverbs are grouped into sets of cognitive synonyms (synset), each expressing a distinct concept. Synsets are interlinked by means of conceptual-semantic and lexical relations [16]. WordNet structure makes it a useful tool for computational linguistics and natural language processing. A WordNet with subjectivity annotation will be referred to as a SentiWordNet [17], a lexical resource in which each synsets of WORDNET is associated to three numerical scores Obj, Pos and Neg describing how Objective, Positive and Negative the terms contained in the synset are Each of the three scores ranges from 0.0 to 1.0, and their sum is 1.0 for each synset.

#### 3.1 Adverb Scoring

Adverbs in a sentence determine the intensity of an adjective. The adverb classification shown below is highly influenced by Benamara and her colleagues’ research [12]:

**Adverbs of affirmation:** such as absolutely, certainly, exactly, totally, and so on.

**Adverbs of doubt:** such as possibly, probably, roughly, apparently, seemingly and so on.

**Strong intensifying adverbs:** such as astronomically, exceedingly, extremely, immensely, and so on.

**Weak intensifying adverbs:** such as barely, scarcely, weakly, slightly, and so on.

**Negation and Minimizers:** such as not, hardly -these somewhat different than the preceding four categories as they usually negate sentiments.

The adverb scoring methodology takes the help of SentiWordNet for scoring these adverbs between 0 and 1 depending upon its intensity of modifying adjective. Assigning a score of 1 to an adverb indicate that it completely affirms an adjective, whereas a -1 score signifies that the adverb has opposite impact on an adjective. For example “He is not a good boy”. The word “not” just reverses the meaning of the adjective “good”.

$$\text{Scoring}(\text{adverb}) = \frac{\sum(\text{P}_{\text{Score}}) - \sum(\text{N}_{\text{Score}})}{n} \quad (1)$$

$\text{P}_{\text{Score}}$  Positive Score of a sense of a word obtained from SentiWordnet  
 $\text{N}_{\text{Score}}$  Negative Score of a sense of a word obtained from SentiWordnet  
 $n$  is the no. of Sense obtained for that word in Adverb domain of SentiWordNet.

### 3.2 Adjective Scoring

An adjective is a part of a sentence that quantifies a noun. As discussed in previous section we can deduce the scoring of adjective of a sentence with the help of SentiWordNet in a similar manner. The scoring of adjective lies in the range from +1 to -1.

$$\text{Scoring}(\text{adjective}) = \frac{\sum(\text{P}_{\text{Score}}) - \sum(\text{N}_{\text{Score}})}{n} \quad (2)$$

$\text{P}_{\text{Score}}$  Positive Score of a sense of a word obtained from SentiWordnet  
 $\text{N}_{\text{Score}}$  Negative Score of a sense of a word obtained from SentiWordnet  
 $n$  is the no. of Sense obtained for that word in Adjective domain of SentiWordNet.

### 3.3 Noun Scoring

Only abstract class of noun are useful in opinion analysis. Abstract noun can be classified into two sets:

- Positive Abstract Noun such as joy, victory, faith and so on. Positively reinforce an opinion.
- Negative Abstract Noun such as destruction, sorrow, stupidity, pain, failure, hatred, sadness and so on. Negatively reinforce an opinion.

Since a noun just makes a 180° change of the sentence, scoring of Noun will be either +1 or -1 depending upon SentiWordnet positive and negative polarity decision. For example “acute pain”, the adjective “acute” have some intensity may be positive or negative. But the noun “pain” is negative means it will have a score of -1. If “acute” is positive the noun “pain” will reverse the polarity of the sentence with same intensity as that of the adjective “acute”. Similarly, if “acute” is negative the noun “pain” will reverse the polarity of the sentence to positive with same intensity as that of the adjective “acute”.

$$aScore(noun) = \frac{\sum(P_{Score}) - \sum(N_{Score})}{n} \tag{3}$$

$P_{Score}$  Positive Score of a sense of a word obtained from SentiWordnet  
 $N_{Score}$  Negative Score of a sense of a word obtained from SentiWordnet  
 $n$  is the no of Sense obtained for that word in Noun domain of SentiWordNet

Since we are considering abstract noun, it cannot have a neutral score i.e. 0. So we have not considered that condition in the final scoring of noun as follow:

$$Scoring(noun) = \begin{cases} 1 & Score(noun) > 0 \\ -1 & Score(noun) < 0 \end{cases} \tag{4}$$

### 3.4 Verb Scoring

Verb can be categorized in two, Auxiliary Verb (can, could, may, must, should, will, be, have, do, etc.) and Main Verb (it conveys a real meaning and doesn't depend on another verb) of which only Main Verb are useful in opinion analysis. Scoring of verb of a sentence with the help of SentiWordNet is workout in a similar manner. The scoring of Verb lies in the range from +1 to -1.



$$\text{Scoring(Verb)} = \frac{\sum(\text{P}_{\text{Score}}) - \sum(\text{N}_{\text{Score}})}{n} \quad (5)$$

$\text{P}_{\text{Score}}$  Positive Score of a sense of a word obtained from SentiWordnet  
 $\text{N}_{\text{Score}}$  Negative Score of a sense of a word obtained from SentiWordnet  
 $n$  is the no of Sense obtained for that word in Verb domain of SentiWordNet.

#### 4 AANV Axioms

Assuming AFF, DOUBT, WEAK, STRONG and MIN respectively be the sets of adverbs of affirmation, adverbs of doubt, adverbs of weak intensity, adverbs of strong intensity and minimizers. Suppose fSense is AANV(Adverb-Adjective-Noun-Verb) [15] scoring function that takes as input, one adverb, one adjective, one noun and one verb and returns a number between  $-1$  and  $+1$ . After bringing modification in the process of scoring different parts of the sentences (Adverb, Adjective, Noun and Verb) the axioms are as follows:

1. If  $\text{adv} \in \text{AFF} \cup \text{STRONG}$  &  $\text{scoring}(\text{adj}) < 0$ , then

$$\begin{aligned} f\text{Sense}(\text{adv}, \text{adj}, \text{noun}, \text{verb}) \\ = (\text{sc}(\text{verb}) + \text{sc}(\text{adj}) - (1 - \text{sc}(\text{adj})) * (1 - \text{sc}(\text{verb})) * \text{sc}(\text{adv})) \\ * \text{sc}(\text{noun}) \end{aligned} \quad (6)$$

- If  $\text{adv} \in \text{AFF} \cup \text{STRONG}$  &  $\text{scoring}(\text{adj}) > 0$ , then

$$\begin{aligned} f\text{Sense}(\text{adv}, \text{adj}, \text{noun}, \text{verb}) \\ = (\text{Scoring}(\text{verb}) + \text{Scoring}(\text{adj}) + (1 - \text{Scoring}(\text{adj})) \\ * (1 - \text{Scoring}(\text{verb})) * \text{Scoring}(\text{adv})) * \text{Scoring}(\text{noun}) \end{aligned} \quad (7)$$

2. If  $\text{adv} \in \text{WEAK} \cup \text{DOUBT}$  &  $\text{sc}(\text{adj}) > 0$ , then:

$$\begin{aligned} f\text{Sense}(\text{adv}, \text{adj}, \text{noun}, \text{verb}) \\ = (\text{Scoring}(\text{verb}) + \text{Scoring}(\text{adj}) - (1 - \text{Scoring}(\text{adj})) * (1 - \text{Scoring}(\text{verb})) \\ * \text{Scoring}(\text{noun})) \end{aligned} \quad (8)$$

If  $\text{adv} \in \text{WEAK U DOUBT}$  &  $\text{Scoring}(\text{adj}) < 0$ , then:

$$\begin{aligned} fSense(\text{adv}, \text{adj}, \text{noun}, \text{verb}) & \\ &= (\text{Scoring}(\text{verb}) + \text{Scoring}(\text{adj}) + (1 - \text{Scoring}(\text{adj})) \\ &\quad * (1 - \text{Scoring}(\text{verb})) * \text{Scoring}(\text{adv})) * \text{Scoring}(\text{noun}) \end{aligned} \quad (9)$$

3. If  $\text{adv} \in \text{MIN}$ , then:

$$fSense(\text{adv}, \text{adj}, \text{noun}, \text{verb}) = -\text{Scoring}(\text{adj}) * \text{Scoring}(\text{verb}) * \text{Scoring}(\text{noun}) \quad (10)$$

In case a blog or an article consist of more than one sentence we consider two cases

- Case 1 If Standard Deviation of fSense scores for all these sentences is above a certain threshold value. Then, Geometric Mean of fSense scores for all these sentences is taken as final Sentiment scoring of that blog or article.
- Case 2 If Standard Deviation of fSense scores for all these sentences is below that threshold value. Then, Arithmetic Mean of fSense scores for all these sentences is taken as final Sentiment scoring of that blog or article.

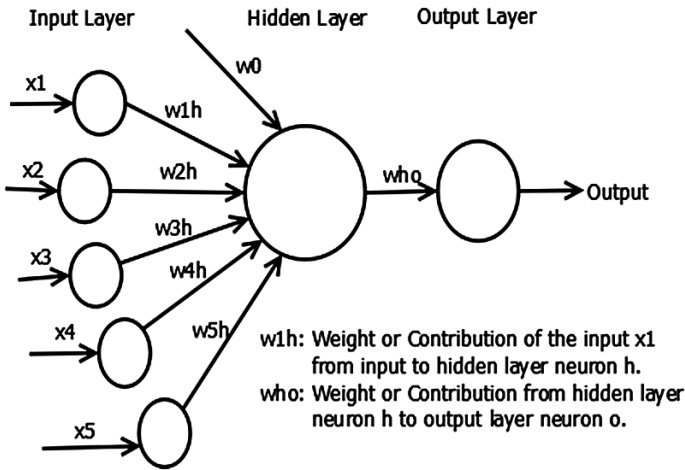
## 5 Deploying Artificial Neural Network

Artificial Neural Network is a mathematical model inspired by biological neural network to work on complex dataset, perform non-linear task and failure of one element does not hampers the total network. All these features are needed while working in Sentiment Analysis field. All the dataset in this field will be very complex and also huge in volume. Since this paper takes its focus on different parts of a sentence (Adverb, Adjective, Noun and Verb), the dataset will contain data with missing part of sentence (a sentence may not contain an adverb or an adjective or a noun or even a verb also especially while working with blogs data). So absence of anyone will not hamper the system to deduce a decision. Also we have the benefits of non-linear programming while clustering, since there will be different non-linear constraints. Generalized parameters for Artificial Neural Network are denoted in the Table 1 and overview of the system in the Fig. 1.

In our problem statement (Fig. 1) we will have four input neurons, one hidden neuron and one output neuron. Four input neuron will be representing Adverb, Adjective, Noun and Verb. Activation signal  $\delta(x_i)$  is representing the presence (1) or absence (0) of any one of Adverb, Adjective, Noun and Verb in the sentence.

**Table 1** Parameters for artificial neural network

	Input	Hidden	Output
Number of neuron	$n + 1$	$q + 1$	$p$
Neuron index range	$i = 0 \dots 4$	$h = 0 \dots q$	$j = 1 \dots p$
Activation	$x_i$	$z_h$	$y_j$
Signal	$\delta(x_i)$	$\delta(z_h)$	$\delta(y_j)$
Weights	$\rightarrow w_{ih} \rightarrow$	$\rightarrow w_{hj} \rightarrow$	



**Fig. 1** Artificial neural network representing our sentiment analysis system

$$\delta(x_i) = \begin{cases} 1 & \text{for presence} \\ 0 & \text{for absence} \end{cases}$$

where  $i = 1, 2, 3, 4$  and  $x_1 = \text{adverb}, x_2 = \text{adjective}, x_3 = \text{noun}, x_4 = \text{verb}$ .

(11)

The weight or the contribution of anyone of the part of sentence  $w_{ih}$  for making the final decision is given by their individual scoring obtained in the previous sections (Sects. IV, V, VI, and VII).

$$w_{1h} = \text{Scoring}(\text{adv}), \quad w_{2h}$$

$$w_{3h} = \text{Scoring}(\text{verb}), \quad w_{4h}$$

The activation  $z_h$  for the one hidden neuron is given by

$$z_h = \sum_{i=0}^n w_{ih} \delta(x_i)$$

(12)

and its activation signal  $\delta(z_h)$  is calculated using the help of the fSense Axioms defined in Sect. VIII.

$$\delta(z_h) = \left\{ \begin{array}{l} fSense(adv, adj, noun, verb) \\ \end{array} \right\} \begin{array}{l} Axiom1 \\ Axiom2 \\ Axiom3 \\ Axiom4 \end{array} \tag{13}$$

The activation  $y_j$  for the one output neuron is given by

$$y_j = \sum_{h=0}^q w_{ho} \delta(z_h) \quad \text{where } w_{ho} = 1 \tag{14}$$

$w_{ho}$  is the weight from hidden to output neuron and is always equals 1 for the proposed application. The activation signal  $\delta(y_j)$  is represented by

$$\delta(y_j) = \left\{ \begin{array}{l} 1, \quad 1 \geq y_j > 0.6 \\ 2, \quad 0.6 \geq y_j > 0.2 \\ 3, \quad 0.2 \geq y_j > -0.2 \\ 4, \quad -0.2 \geq y_j > -0.6 \\ 5, \quad -0.6 \geq y_j \geq -1 \end{array} \right. \tag{15}$$

The output will cluster all the dataset into five clusters strong Like(1), weak Like (2), doubtful(3), weak dislike(4), strong Dislike(5).

## 6 Deploying K-Mean

Clustering, an unsupervised learning problem, deals with organizing objects into groups by finding a structure in a collection of unlabeled data. The k-mean algorithm is known to be the most efficient of converging to numerous local minima depends upon selection of initial seeds since selecting an outlier (they are away from normal samples) as initial seed will increases the number of iterations for convergence and also lead to bad solutions. While working in the field of sentiment analysis we cannot effort such dependency (clustering algorithm for a large data set. But its efficiency high CPU and memory utilization) since in each iteration of the algorithm the system may deal with more than lakhs of data points(sentences in a blog or report). Before going through this problem the basic steps of k-Mean algorithm is shown in Fig. 2.

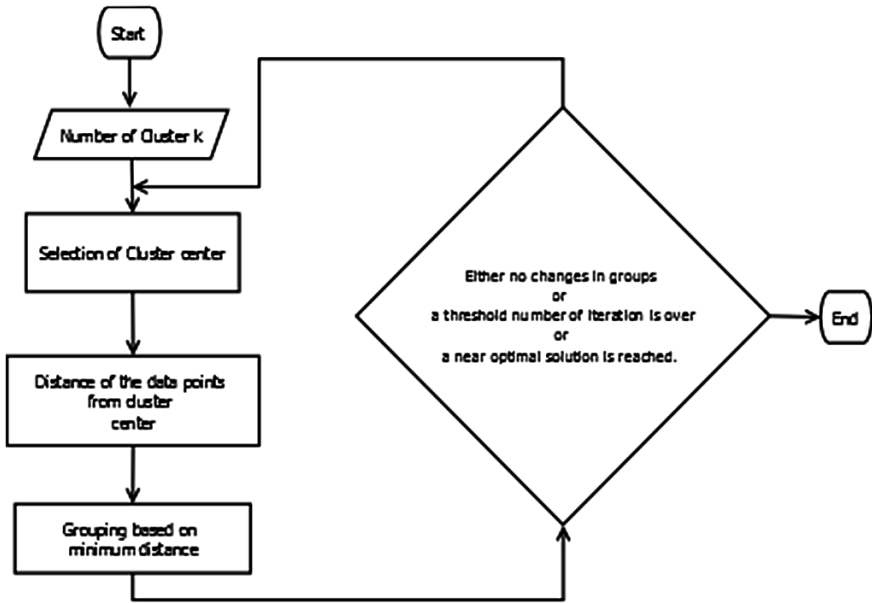


Fig. 2 K-mean algorithm flowchart

**6.1 Problem Definition: Cluster a Set X of N Points in D Dimensional Space into C Clusters**

X: set of n points

$$X = \{x_1, x_2, \dots, x_n\}$$

$$x_i = \{x_{i1}, x_{i2}, \dots, x_{id}\} \text{ for } i = 1, 2, \dots, n. \tag{16.1}$$

V: set of c cluster centers

$$V = \{v_1, v_2, \dots, v_c\}$$

$$v_j = \{v_{j1}, v_{j2}, \dots, v_{jd}\} \text{ for } j = 1, 2, \dots, c \tag{16.2}$$

**Initialization:** Select randomly chosen c points from the data as the initial centers.

$$v_j = x_k \text{ where } k = \text{rand}([1..n]) \text{ for } j = 1, 2, \dots, c. \tag{17}$$

**Clustering:** Assign  $x_k \rightarrow \text{Cluster } j \text{ such that } x_k \text{ is closest to } v_j$

$$d(x_k, v_j) = \min d(x_k, v_j) \text{ for } j = 1, 2, \dots, c.$$

$$d(x_k, v_j) = \|x_k - v_j\|. \text{ (EuclidianDistance)}$$

**Output:**  $n_i$  = number of points in cluster  $i = 1, 2, \dots, c$ .

$x_j^i$  = the  $j$ th point in cluster  $i, i = 1, 2, \dots, c$ .

**Update:** Compute new cluster center as the centroid of the points assigned to the cluster.

$$v_i^* = (1/n_i) \sum x_j^i \text{ for } i = 1, 2, \dots, c \quad (18)$$

**Loop or Terminate:** Terminate if there is no/negligible change in centroids.

If  $v_i^* = v_i$  for  $i = 1, 2, \dots, c \rightarrow$  terminate

Otherwise go to Clustering Step.

**Objective Function:** Minimizes J, the mean squared error

$$J = \sum \sum d^2(x_k^j, v_j), \quad j = 1, 2, \dots, c \text{ and } k = 1, 2, \dots, n_j \quad (19)$$

For avoiding selection of initial seed as outlier, we start with multiple starting point sets as initial seed. After first iteration depending upon the outcomes, on polling basis we will decide one of the processes to complete the clustering. And also a near optimal solution is far more cost effective than an optimal solution so we also modified the termination conditions as explained below:

## 6.2 Problem Definition: Cluster a Set X of n Points in d Dimensional Space into c Clusters

X: set of n points with each point representing each sentence of a document or a blog.

$$X = \{x_1, x_2, \dots, x_n\}$$

d: Four features or attributes are identified for clustering the data points or sentences: scoring of adverb, scoring of adjective, scoring of noun and scoring of verb.

$$x_i = \{x_{i1}, x_{i2}, \dots, x_{id}\} \text{ for } i = 1, 2, \dots, n \text{ and } d = 1, 2, 3, 4. \quad (20)$$

V: set of c cluster centers.

c: Five clusters are identified as Strong Like, Weak Like, Doubtful, Weak Dislike, Strong Dislike.

$$v = \{v_1, v_2, \dots, v_c\} \text{ where } c = 5$$

$$v_j = \{v_{j1}, v_{j2}, \dots, v_{jd}\} \text{ for } j = 1, 2, \dots, c \quad (21)$$

**Initialization:** Select randomly seven sets (denoted by  $t$ ) of  $c$  points from the data as the initial centers.

$$v_j^t = x_k \quad \text{where } k = r \text{ and } ([1..n]) \text{ for } j = 1, 2, \dots, c \text{ and } t = 1, 2, \dots, 7. \quad (21)$$

**Clustering:** Start with seven parallel clustering:

Assign  $x_k \rightarrow$  Cluster  $j$  such that  $x_k$  is closest to  $v_j^t$

$$d(x_k, v_j^t) = \min d(x_k, v_j^t) \quad \text{for } j = 1, 2, \dots, c.$$

$$d(x_k, v_j^t) = \|x_k - v_j^t\|. \quad (\text{Euclidian Distance})$$

**Output:**  $n_{it}$  = number of points in cluster  $i$  for set  $t$ , where  $i = 1, 2, \dots, c$  and  $t = 1, 2, 3, \dots, 7$ .  $x_j^i$  = the  $j$ th point in cluster  $i$ ,  $i = 1, 2, \dots, c$ .

**Update:** Compute new cluster center as the centroid of the points assigned to the cluster

$$v_i^{t*} = (1/n_{it}) \sum x_j^{it} \quad \text{for } i = 1, 2, \dots, c. \quad (22)$$

Now all these 35 centroids is taken as input for AANV axioms and fSense score is calculated. Now Euclidian distance of all the fSense score is calculated from midpoint of different threshold defined for Strong Like ( $1 \diamond 0.6$ ), Weak Like ( $0.6 \diamond 0.2$ ), Doubtful ( $0.2 \diamond -0.2$ ), Weak Dislike ( $-0.2 \diamond -0.6$ ), Strong Dislike ( $-0.6 \diamond -1$ ) i.e. Strong Like (0.8), Weak Like (0.4), Doubtful (0), Weak Dislike (-0.4), Strong Dislike (-0.8). Now five centroids are selected whichever a closest fSense score with respect to the five threshold values has defined. Now with these five centroids as initial seed for k-Mean algorithm, the clustering process is completed with modified termination conditions as follows:

- no changes in groups
- a threshold number of iteration is over (a threshold value is obtained by statistical analysis on k-mean algorithm)
- a near optimal solution is reached or a negligible changes of groups.

## References

1. EDRM: Electronic Discovery Reference model. <http://www.edrm.net/>
2. Turney, P.: Thumbs up or thumbs down? Semantic orientation applied to unsupervised classification of reviews. In: Proceedings of 2006 International Conference on Intelligent User Interfaces (IUI06) (2002)
3. Pang, B., Lee, L., Vaithyanathan, S.: Thumbs up? Sentiment classification using machine learning techniques. In: Proceedings of the Conference on Empirical Methods in Natural Language Processing (EMNLP), pp. 79–86 (2002)

4. Subasic, P., Huettner, A.: Affect analysis of text using fuzzy semantic typing. *IEEE Trans. Fussy Syst.* (2001)
5. Morinaga, S., Yamanishi, K., Tateishi, K., Fukushima, T.: Mining product reputations on the web. In: *Proceedings of the 8th ACM SIGKDD* (2002)
6. Kim, S.O., Hovy, E.: Determining the sentiment of opinions. In: *Coling04* (2004)
7. Hatzivassiloglou, V., McKeown, K.: Predicting the semantic orientation of adjectives. In: *ACL-97* (1997)
8. Yu, H., Hatzivassiloglou, V.: Towards answering opinion questions: separating facts from opinions and identifying the polarity of opinion sentences. In: *Proceedings of EMNLP-03* (2003)
9. Wilson, T., Wiebe, J., Hwa, R.: Just how mad are you? Finding strong and weak opinion clauses. In: *AAAI-04* (2004)
10. Bethard, S., Yu, H., Thornton, A., Hatzivassiloglou, V., Jurafsky, D.: Automatic extraction of opinion propositions and their holders. In: *Proceedings of AAAI Spring Symposium on Exploring Attitude and Affect in Text* (2004)
11. Chklovski, T.: Deriving quantitative overviews of free text assessments on the web. In: *Proceedings of 2006 International Conference on Intelligent User Interfaces (IUI06)*, Sydney, Australia, 29 Jan–1 Feb 2006
12. Benamara, F., et al.: Sentiment analysis: adverbs and adjectives are better than adverbs alone. In: *Proceedings of 2007 International Conference on Weblogs and Social Media (ICWSM 07)* (2007)
13. Subrahmanian, V.S., Reforgiato, D.: *Adjective-Verb-Adverb Combinations for Sentiment Analysis*. Published by the IEEE Computer Society (2008)
14. Sing, J.K., Sarkar, S., Mitra, T.K.: Development of a novel algorithm for sentiment analysis based on adverb-adjective-noun combinations. In: *NCETACS-2012, National Conference on Emerging Trends and Applications in Computer Science* (2012)
15. Sarkar, S., Mallick, P., Mitra, T.K.: A novel machine learning approach for sentiment analysis based on Adverb-Adjective-Noun-Verb (AANV) combinations. *Int. J. Recent Trends Eng. Technol.* 7(1) (2012)
16. <http://wordnet.princeton.edu/>
17. Esuli, A., Sebastiani, F.: SENTIWORDNET: A Publicly Available Lexical Resource for Opinion Mining?



# Benchmark Function Analysis of Cuckoo Search Algorithm

Joyita Basak, Sangita Roy and Sheli Sinha Chaudhuri

**Abstract** Cuckoo Search (CS), has been developed by Yang and Deb [1] is one of the newly added bio inspired algorithm which is mostly used to solve optimization problems. This is based on metaheuristic search algorithm. Cuckoo Search is named as its principle is based on reproduction strategy of Cuckoo bird. In this paper a comparative analysis is implemented on the algorithm with using five standard benchmark functions and experiment results can be used for better performances on optimization.

**Keywords** Cuckoo search · Metaheuristic optimization · Levy flight · Benchmark function

## 1 Introduction

### 1.1 Cuckoo Breeding Behavior

Cuckoo birds attract attention not only for their beautiful voice but their engagement in brood parasitism. This aggressive reproduction strategy is followed by different species of Cuckoos.

Cuckoo birds cannot build their nests but they lay eggs in the nest of other host birds. Firstly, here two instances may be occurred. (i) Host birds egg may be

---

J. Basak (✉)

CSE Department, Narula Institute of Technology, Kolkata, India  
e-mail: joyitabasak@gmail.com

S. Roy

ECE Department, Narula Institute of Technology, Kolkata, India  
e-mail: roysangita@gmail.com

S.S. Chaudhuri

ETCE Department, Jadavpur University, Kolkata, India  
e-mail: shelism@rediffmail.com

© Springer India 2015

J.K. Mandal et al. (eds.), *Information Systems Design and Intelligent Applications*,  
Advances in Intelligent Systems and Computing 339,  
DOI 10.1007/978-81-322-2250-7\_72

719

destroyed by the parasitic cuckoo bird to increase hatching probability of its own egg, (ii) Host birds, which may be of different species, when discover that those eggs are not their own, then they either destroy the eggs or leave the nest all together. So get an identical look, genetically evolution make a mimic look to the cuckoo eggs with host eggs. So that most host birds cannot identify the parasitic eggs.

Secondly, cuckoo chicks are hatched slightly earlier than host chicks. When the first cuckoo chick is hatched, they blindly propelled the host eggs out of the nest. As a result they can be offered more food by host birds.

Thirdly, it has been observed that the cuckoo chicks can mimic the voice of host chicks; as a result they can get same feeding opportunity with host chicks.

## 2 Metaheuristic Optimization

A metaheuristic [2] is a method that guides to find, generate and also to select a lower-level procedure i.e. heuristic which may gives a better solution for optimization [3] problems, especially with limited information or incomplete computation capacity. Metaheuristics also make some assumptions about the optimization problem being solved, and so this can be useful for solving a variety of problem.

The properties that characterize most metaheuristics:

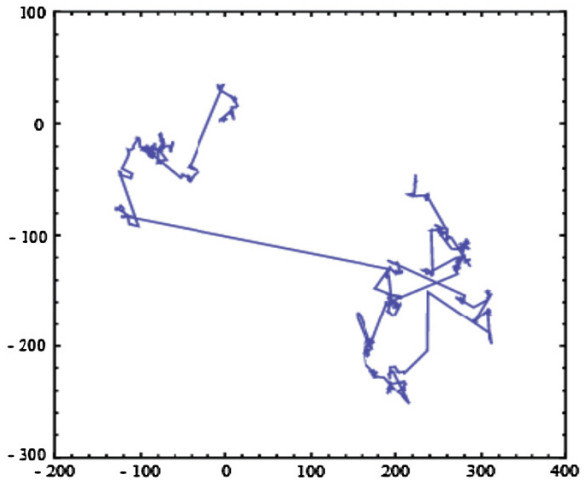
- Metaheuristics are such a method that guides the search process.
- The objective is to efficiently explore the search space in order to find near-optimal solutions.
- Metaheuristic algorithms constitute some techniques which are used for simple local search procedures to complex learning procedures.
- These are usually non-deterministic and hold approximate value.
- This procedure is not problem-specific.

## 3 Levy Flight

Levy flight named [4] according to the name of French Mathematician Paul Pierre Levy. Levy flight [5, 6] is one type of random walk which can be observed as an optimal search technique, it is adapted by many animals and insects. While moving or flying, they follow the path of long trajectories with sudden right angle turns combined with random, short movements. It describes foraging patterns in natural systems, such as systems of ants, bees, zooplanktons, bumbles etc.

Mathematical formulation of Levy flight is widely used in simulations of random and pseudo-random phenomena which is observed nature. These flights can also be noticed in the movements of turbulent fluids. Levy-style search behavior [7] and random search in general has been applied to optimization and implemented in many search algorithms [8, 9]. One of such algorithms is Cuckoo Search Algorithm [10].

**Fig. 1** Example of Levy Flight starting at (0,0) [13]



A new solution  $x(t + 1)$ , can be generated using a Levy flight for cuckoo  $i$ , according to the following equation (Fig. 1):

$$x_i(t + 1) = x_i(t) + \alpha^{Leavy(\lambda)} \tag{1}$$

According to [11] the power law behavior of the Levy distribution has some advantage due to:

- (i) Reduced probability of returning to previously visited sites in the problem search space;
- (ii) Effective and efficient exploration of the far-off regions of the function landscape.

The second property helps an optimization algorithm to escape from a local minimum or minima when the function has deep and wide basins.

### 4 Levy Flight Based Cuckoo Search Algorithm

Cuckoo Search Algorithm is proposed [1, 10] to solve stochastic global optimization problems which is based on breeding behavior of certain species of cuckoos.

There are following three idealized rules:

1. Each Cuckoo lays one egg and dumps it in a randomly selected nest. Here eggs represent a set of solution coordinates, at a time.
2. A fraction of the nests containing the best eggs, represents as solutions, will be carried over to the next generation.

3. The number of nests is fixed but there is a probability that a host can discover an alien egg. If this occurs, the host can either destroy the egg or the nest and these results in building a new nest in a new location.

### Algorithm for Cuckoo Search

Begin

Objectivefunction  $f(x), x=(x_1, x_2, \dots, x_d)^T$

Generate initialpopulationof

A hostnests  $x_i (i=1, 2, 3, \dots, n)$

While( $l < \text{Maxgeneration}$ ) or ( $\text{stopcriterion}$ ) Get a cuckoo randomlybyLevy

Flights

Evaluate itsquality/fitness  $F_i$ ; Choose a nestamong

$n(\text{say}, j)$ randomly **if** ( $F_i > F_j$ ),

Replace  $j$  by thenewsolution;

End.

Afunction( $p_a$ )of worse nests

Areabandoned and new onesarebuilt;

Keep the best solutions

(ornestswithquality solutions);

Rank the solutions and findthecurrent best

Endwhile

Post process results and visualization

End

In real world, this is to point out that if a cuckoo's egg is very similar to a host's eggs, then this cuckoo's egg is very difficult to be discovered by the host bird, thus the fitness should be related to the difference in solutions. Therefore, it is a better idea to do a random walk in such a way with some random step sizes [1].

## 5 Benchmark Functions

These test functions [12] which are used here as the fitness functions for solving global optimization problems.

Here are some functions, which are helpful to evaluate characteristics of optimization algorithms,

- (a) Velocity of convergence.
- (b) Robustness.
- (c) Precision.

Benchmark functions are mostly used in evaluating performance of popular benchmark methods. There are two types of benchmark functions:

- (i) Unimodal and
- (ii) Multimodal

Unimodal functions are those which have only one optimum position and multimodal functions have two or more local optima. Here, we used the following functions:

- Ackley
- Griewank
- Beale
- Rosenbrock
- Booth.

## 6 Experiments

For testing the performance of Cuckoo Search algorithm, five well known benchmark functions are used here and compared with the optimal value.

### Pseudo-code for Cuckoo Search

1. Initialize  $n$  nests
2. Repeat till stopping criteria is met
  - (a) Randomly select a cuckoo using levy flight
  - (b) Calculate its fitness
  - (c) Randomly select a nest
  - (d) Calculate its fitness
  - (e) If  $(F_c < F_n)$  then Replace the nest with the cuckoo
  - (f) A fraction  $p_a$  of nest are replaced by new nests

(g)

- (i) Calculate fitness
- (ii) Calculate best nests by Standard Benchmark function [(1) Ackley, (2) Griewank, (3) Beale, (4) Roosenbrock, (5) Booth]

(h) Store the best nest as optimal fitness value

3. Post process will be the best nest position

Authors use following functions to observe our algorithm performance.

### 6.1 Ackley Function

- (i) Ackley function is a multimodal continuous function with a cosine wave of moderate amplitude.
- (ii) This function is widely used for testing optimization algorithms.
- (iii) In its two-dimensional form, (shown in below) it is characterized by a large hole at the centre and nearly smooth outer region.
- (iv) It has a large number of local minima but only one global minimum.
- (v) The function poses a risk for optimization algorithms, particularly hill-climbing algorithms, to be trapped in one of its many local minima.

Ackley function is defined by

$$f(x) = -a \exp\left(-b \sqrt{\frac{1}{d} \sum_{i=1}^d x_i^2}\right) - \exp\left(\frac{1}{d} \sum_{i=1}^d \cos(cx_i)\right) + a + \exp(1) \quad (2)$$

Search domain:  $-15 \leq x_i \leq 30$ ,  $i = 1, 2, \dots, n$ .

Here, X is in interval of  $[-15, 30]$ . For this function, the global minimum value is 0 and the corresponding global optimum solution is  $x_{opt} = (x_1, x_2, \dots, x_n) = (0, 0, \dots, 0)$  (Fig. 2).

### 6.2 Griewank Function

- (i) The Griewank function comprehensively used to test the convergence of optimization functions.
- (ii) It has many widespread local minima. However, the location of the minima is regularly distributed.
- (iii) When its number of dimensions increases, it can be observed that its number of minima grows exponentially.

Griewank function is defined by

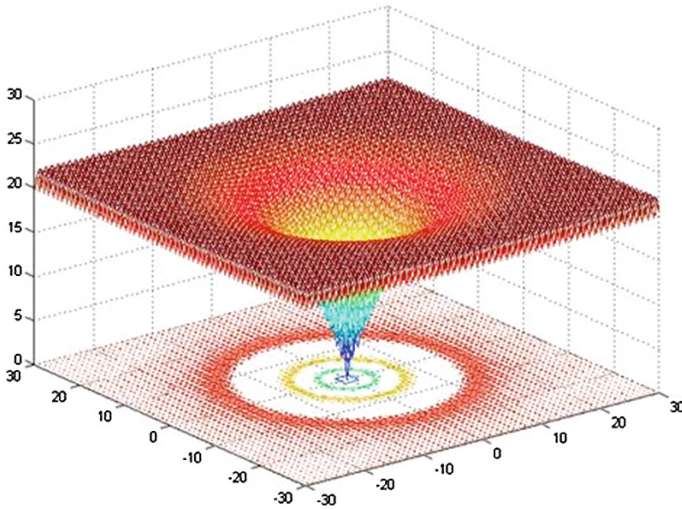


Fig. 2 Surface plot for Ackley function [13]

$$f_n(x_1, \dots, x_n) = 1 + \frac{1}{4,000} \sum_{i=1}^n x_i^2 - \prod_{i=1}^n \cos\left(\frac{x_i}{\sqrt{i}}\right) \tag{3}$$

Search domain:  $-600 \leq x_i \leq 600, i = 1, 2, \dots, n$ .

Here, X is in the interval of  $[-600, 600]$ . For this function, the global minimum value is 0 and the corresponding global optimum solution is  $x_{opt} = (x_1, x_2, \dots, x_n) = (100, 100, \dots, 100)$  (Fig. 3).

### 6.3 Beale Function

- (i) The Beale function is multimodal.
- (ii) It has sharp peaks at the corners of the input domain.
- (iii) This test function is used to evaluate the performance of optimization algorithms.
- (iv) The function is usually evaluated on the square  $x_i \in [-4.5, 4.5]$ , for all  $i = 1, 2$ .

Beale function definition:

$$f(x, y) = (1.5 - x + xy)^2 + (2.25 - x + xy^2)^2 + (2.625 - x + xy^3)^2 \tag{4}$$

Search domain:  $-4.5 \leq x_i \leq 4.5, i = 1, 2$ .

For this function, there is a global minimum at (3,0.5) (Fig. 4).

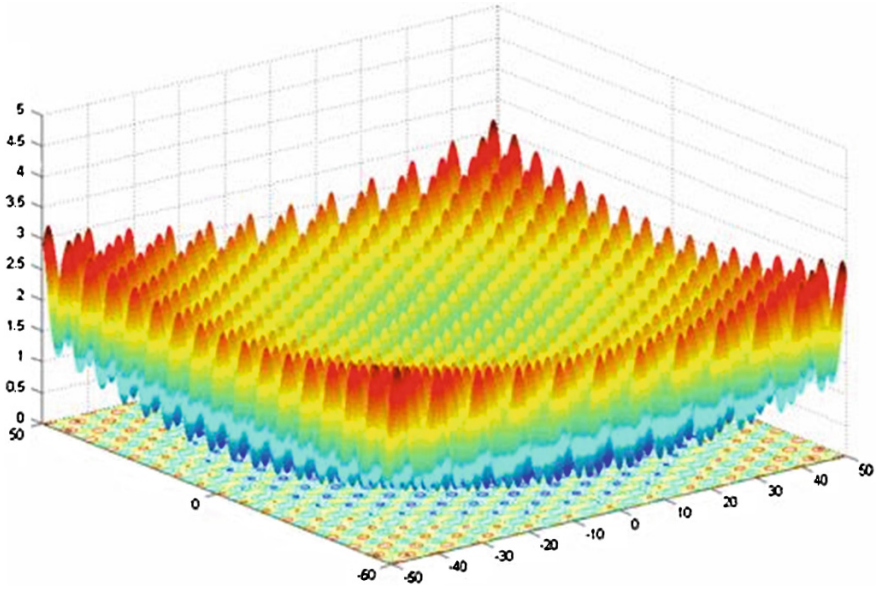


Fig. 3 Surface plot for Griewank function [13]

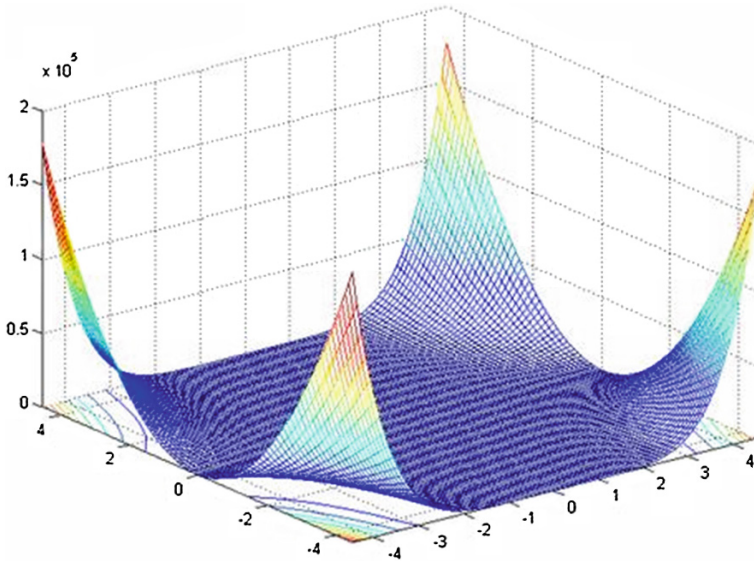


Fig. 4 Surface plot for Beale function [13]



### 6.4 Rosenbrock Function

- (i) Rosenbrock function is used for gradient-based optimization algorithms.
- (ii) This function is unimodal, and non-convex.
- (iii) The global optimum is inside a parabolic shaped flat valley.
- (iv) In 1960, Howard H. Rosenbrock introduce with this function.
- (v) It is also known as Rosenbrock’s valley, is a classic optimization problem, also known as Banana function.

Rosenbrock function definition:

$$f(x) = \sum_{i=1}^{n-1} [100(x_{i+1} - x_i^2)^2 + (x_i - 1)^2] \tag{5}$$

Search domain:  $-5 \leq x_i \leq 10, i = 1, 2, \dots, n$ .

For this function, a unique global minimum value is 0 which lies at (1, 1) (Fig. 5).

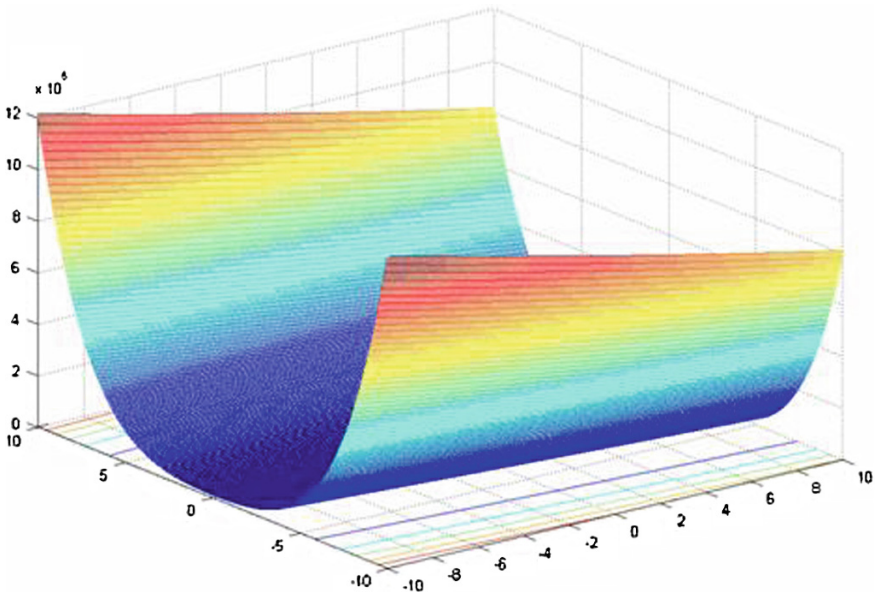


Fig. 5 Surface plot for Rosenbrock function [13]

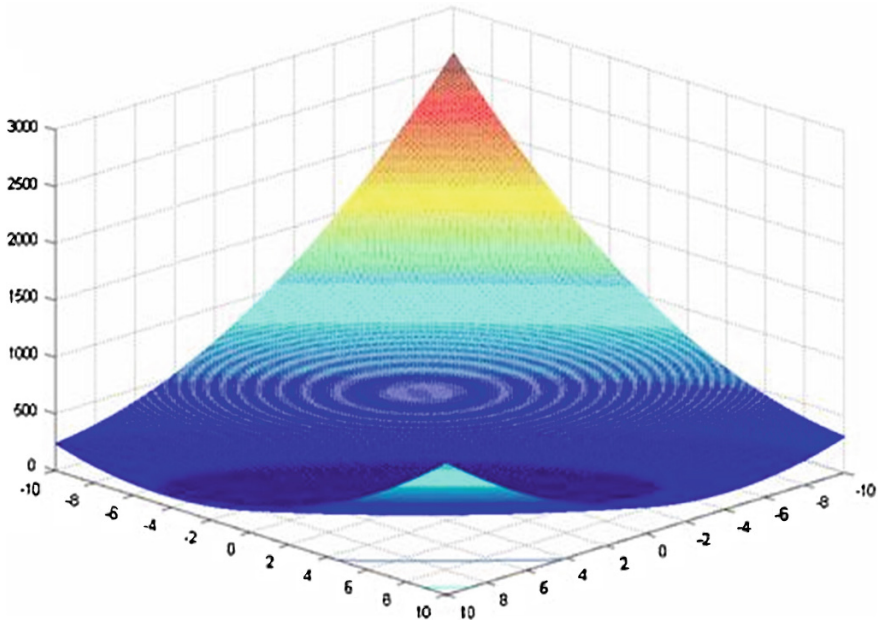


Fig. 6 Surface plot for Booth function [13]

### 6.5 Booth Function

- (i) This function is continuous and unimodal.
- (ii) Booth function is usually evaluated on the square  $x_i \in [-10, 10]$ , for all  $i = 1, 2$ .
- (iii) This is used to evaluate the performance of optimization algorithms.

Function definition:

$$f(x, y) = (x + 2y - 7)^2 + (2x + y - 5)^2. \quad (6)$$

Search domain:  $-10 \leq x_i \leq 10$ ,  $i = 1, 2$  (Fig. 6).

## 7 Output

Each function is simulated twenty times. Maximum, minimum, mean and standard deviation of each function is evaluated. Here for a finite set of numbers, the Standard Deviation (SD) is found, by taking the square root of the mean (i.e. average) of the squared differences of the values from their average value. SD indicated the amount of deviation from the mean value. The above SDs show that Ackley is least deviated and Beale is the widely diverged (Table 1).

**Table 1** Implementing cuckoo search with different object function and getting result for maximum, minimum, mean and standard deviation value

Function name	Max	Min	Mean	SD
Ackley	9.8361e-006	4.0312e-006	7.26e-06	1.94263e-06
Beale	9.9720e-006	9.5635e-009	4.47e-06	3.28496e-06
Booth	9.8495e-06	1.5403e-07	4.38e-06	2.64461e-06
Rosenbrock	9.5491e-006	2.2715e-006	5.84287e-06	2.82941e-06
Griewank	9.9968e-006	3.6002e-006	7.11e-06	2.08487e-06

**System Support:** These evaluation processes of each test function are practically instantaneous with a 1 GB RAM, Pentium 4 processor and 3 GHz desktop (personal) computer.

## 8 Conclusion

In this paper authors have make a survey on several well known benchmark object functions applied on the cuckoo search algorithm. Maximum, minimum, mean and SD of five well known benchmark functions are simulated. These results demonstrate the efficiency for optimizing complex multimodal problems. Here authors observed that CS performs best using Ackley among five standard Benchmark functions.

## References

1. Yang, X.-S., Deb, S.: Cuckoo search via Lévy flights. In: World Congress on Nature and Biologically Inspired Computing, Coimbatore, India, pp. 210–214 (2009)
2. Yang, X.S.: Nature-Inspired Metaheuristic Algorithms. Luniver Press (2008)
3. Bulm, C., Roli, A.: Metaheuristics in combinatorial optimization: overview and conceptual comparison. *ACM Comput. Surv.* **35**, 268–308 (2003)
4. Roy, S., Chaudhuri, S.S.: Cuckoo search algorithm using Lévy flight: a review. *IJ. Mod. Educ. Comput. Sci.* **12**, 10–15 (2013)
5. Pavlyukevich, I.: Lévy flights, non-local search and simulated annealing. *Comput. Phys.* **226**, 1830–1844 (2007)
6. Pavlyukevich, I.: Cooling down Lévy flights. *J. Phys. A Math. Theor.* **40**, 12299–12313 (2007)
7. Viswanathan, G.M., Raposo, E.P., da Luz, M.G.E.: Lévy flights and super diffusion in the context of biological encounters and random searches. *Phys. Life Rev.* **5**(3), 133–150 (2008)
8. Chen, T.Y., Cheng, Y.L.: Global optimization using hybrid approach. *WSEAS Trans. Math.* **7** (6), 254–262 (2008)
9. Ozdamar, L.: A dual sequence simulated annealing algorithm for constrained optimization. In: Proceedings of the 10th WSEAS International Conference on applied mathematics, pp. 557–564 (2006)

10. Yang, X.S., Deb, S.: Engineering optimization by cuckoo search. *Int. J. Math. Model. Numer. Optim.* **1**(4), 330–343 (2010)
11. Jamil, M., Zepernick, H.-J., Yang, X.-S.: Lévy flight based cuckoo search algorithm for synthesizing cross-ambiguity functions. In: 2013 IEEE Military Communications Conference
12. Andrei, N.: An unconstrained optimization test functions collection. *Adv. Model. Optim.* **10** (1) (2008)
13. Object functions. [http://www-optima.amp.i.kyoto-u.ac.jp/member/student/hedar/Hedar\\_files/TestGO\\_files/Page364.htm](http://www-optima.amp.i.kyoto-u.ac.jp/member/student/hedar/Hedar_files/TestGO_files/Page364.htm)

# Study of NLFSR and Reasonable Security Improvement on Trivium Cipher

Subhrajyoti Deb, Bhaskar Biswas and Nirmalya Kar

**Abstract** The decision regarding widely acceptable stream cipher for hardware security is one of the challenging assignment. Trivium cipher is ironed out most of the weakness of the other stream ciphers. Beside this, our paper presents the security analysis of Trivium and some modification of cipher which gives better security level. Our primary focus is finding some particular biases of output and reasonable algebraic attack with some guessing approach. More specifically, we show some modifications which can increase its security level without changing its internal structure. For this cipher finally we obtain some new cryptanalytic result and the next part of the paper we study some algebraic analysis of Trivium cipher and we try to show that it is vulnerable to different types of attacks and try to recover the overall internal state of the stream cipher.

**Keywords** Cryptanalysis · Trivium cipher · Stream cipher · Algebraic attack · Non-linear feedback shift register · Linear equation

## 1 Introduction

In the literature review of symmetric key cryptology, the stream ciphers are observe that to be one of the most important primitives. So far, stream cipher that has some kind of internal state which is regularly updated [1]. For instance there length is  $n$  bits, then the function [2]  $f$  can be defined as

---

S. Deb (✉) · B. Biswas · N. Kar  
Computer Science and Engineering Department,  
National Institute of Technology, Agartala, India  
e-mail: subhrajyoti.cse@nita.ac.in

B. Biswas  
e-mail: bhaskar.cse@nita.ac.in

N. Kar  
e-mail: nirmalya@nita.ac.in

$$f : \mathbb{GF}(2)^n \rightarrow \mathbb{GF}(2)$$

The Trivium stream cipher was originally proposed by De Canniere and Preneel [1]. In data encryption primitives Trivium stream cipher is widely applicable both in hardware and in software level. This stream cipher is a hardware-oriented synchronous stream cipher, which claimed a key size of 80 bits and an initialization vector (IV) size of 80 bits and it remain consistent when it was submitted. In that approach, it presented in [3], Trivium stream cipher is algebraic in nature. Attacking on Trivium are propose by Babbage in [3], that evidence is given that internal state bits of Trivium can be protect with a time complexity  $c^{283.5}$ . The study and analysis of Trivium literature proposed mainly the algebraic structure of the cipher which has the propensity basis on guess and determine types of attack or it may recover the internal state bits of the Trivium cipher which can be mounted and resist by algebraic attack [4]. We try to modify the literature structure of Trivium so that its appropriate structure can be used to provide a improve security. This modified version of Trivium relay the better security to the internal state recovery of that cipher attack.

### 1.1 Description of the Cipher

Trivium consists two processes that concentrate the values of 15 specific state bits and uses them both to update 3 bits of the internal state. Let  $s_1, s_2, \dots, s_{288}$  be the 288 internal bits and the key stream generated at a particular time  $i$  ( $i = 0, 1, \dots, n$ ). This process is repeated for  $4 * 288 = 1,152$  times. So it can be summarized by the following generation of pseudo code [5] represent in Algorithm 1.

---

**Algorithm 1** Key and IV Setup Generation Process of Trivium

---

```

for  $t = 1$  to  $n$  do
    ( $s_1, s_2, \dots, s_{93}$ ):= ( $K_1, K_2, \dots, K_{80}, 0, \dots, 0$ )
    ( $s_{94}, s_{95}, \dots, s_{177}$ ):= ( $IV_1, IV_2, \dots, IV_{80}, 0, 0, 0, 0$ )
    ( $s_{178}, s_{179}, \dots, s_{288}$ ):= ( $0, \dots, 0, 1, 1, 1$ )
     $t_1$ :=  $s_{66} \oplus s_{93}$ 
     $t_2$ :=  $s_{162} \oplus s_{177}$ 
     $t_3$ :=  $s_{243} \oplus s_{288}$ 
     $z_i$ :=  $t_1 \oplus t_2 \oplus t_3$ 
     $t_1$ :=  $t_1 \oplus s_{91} \cdot s_{92} \oplus s_{171}$ 
     $t_2$ :=  $t_2 \oplus s_{175} \cdot s_{176} \oplus s_{264}$ 
     $t_3$ :=  $t_3 \oplus s_{286} \cdot s_{287} \oplus s_{69}$ 
    ( $s_1, s_2, \dots, s_{93}$ ):= ( $t_3, s_1, \dots, s_{92}$ )
    ( $s_{94}, s_{95}, \dots, s_{177}$ ):= ( $t_1, s_{94}, \dots, s_{176}$ )
    ( $s_{178}, s_{179}, \dots, s_{288}$ ):= ( $t_2, s_{178}, \dots, s_{176}$ )
end for
    
```

---

In each round of Trivium cipher a single bit include linear function of six state bits. Generally this key-stream process repeated until  $N \leq 2^{64}$  bits of key-stream generated. Each state bits are rotated, and as well as the process is repeats in the same manner. The generation of key stream is described by the following pseudo-code [5] represent in Algorithm 2.

---

**Algorithm 2** Key Stream Generation Process of Trivium

---

```

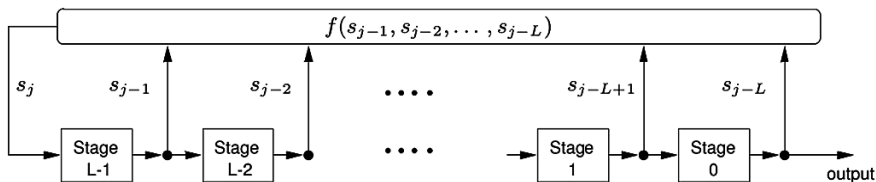
for  $t = 1$  to  $n$  do
     $t_1 := s_{66} \oplus s_{93}$ 
     $t_2 := s_{162} \oplus s_{177}$ 
     $t_3 := s_{243} \oplus s_{288}$ 
     $z_i := t_1 \oplus t_2 \oplus t_3$ 
     $t_1 := t_1 \oplus s_{91} \cdot s_{92} \oplus s_{171}$ 
     $t_2 := t_2 \oplus s_{175} \cdot s_{176} \oplus s_{264}$ 
     $t_3 := t_3 \oplus s_{286} \cdot s_{287} \oplus s_{69}$ 
     $(s_1, s_2, \dots, s_{93}) := (t_3, s_1, \dots, s_{92})$ 
     $(s_{94}, s_{95}, \dots, s_{177}) := (t_1, s_{94}, \dots, s_{176})$ 
     $(s_{178}, s_{179}, \dots, s_{288}) := (t_2, s_{178}, \dots, s_{176})$ 
end for
    
```

---

## 2 Study of Non-linear Feedback Shift Register

### 2.1 Structure of Non-linear Feedback Shift Register

A non-linear feedback shift register (NLFSR) works as same as a linear feedback shift register (LFSR) but there is some difference between them, in linear feedback shift register the feedback function is linear, that is it is only the combination of contents of L stages for a L length linear feedback shift register [4]. In non-linear feedback shift register feedback function is not linear, a non-linear feedback shift register is a combination of L stages of a L-length NLFSR [2, 6–8]. In non-linear contents are produced by adding a stage content to feedback (Fig. 1).



**Fig. 1** A NLFSR structure of length L

The feedback function of NLFSR can be defined as

$$s_j = f(s_{L-1}, s_{L-2}, \dots, s_0) \text{ where } j = (L, L+1, L+2, \dots).$$

## 2.2 Non-linear Combination Generator

Non-linear combination generator is another type of a linear feedback shift register. More than one linear feedback shift register is used and each linear feedback shift register where output is a key bit. Output of these linear feedback shift register are combined for producing a final output bit [4, 7, 8]. Each output bit of each linear feedback shift register are combined non-linearly for producing a non-linear output bit.

A Non-linear feedback shift register state variables can be represented as  $x = (x_0, x_1, \dots, x_{l-1})$  which denote the state variable  $s = (s_0, s_1, \dots, s_{l-1}) \in (0, 1)^l$ .

## 3 Implementation Details on Trivium Cipher

The linear correlations between key stream bits and internal state recovery bits are simple to compute due to the reason of  $\mathbb{Z}_2$  is simply describe to be equal to  $s_{66} \oplus s_{93} \oplus s_{162} \oplus s_{177} \oplus s_{243} \oplus s_{288}$ . Trivium stream cipher state evolves in a non linear way i.e. not easy for an attacker to add these equations in order to efficiently recover the internal state [9]. 288-bit nonlinear feedback shift register are uses in Trivium. Trivium cipher uses nonlinear state-update three bits of the internal state and keystream bits are represented as a linear combination of the contents of six stages of its internal state.

This paper we try to describe the algebraic representation of Trivium. In that section we briefly explain some differential fault analysis of Trivium stream cipher and try to generate some the polynomial equation system that represent the inner state of Trivium cipher. Our attack description and the results are presented in next section respectively.

### 3.1 Proposed Work

In this paper we analyse the biases of Trivium cipher. As a case-study of Trivium cipher, we present a new method of finding linear feedback bits and the linear combination of keystream bits of the cipher. Our approach is to change some



**Table 1** Testing key and IV setup speed

No. of keys	Total time	Key setup speed
9,000	202.67 usec	45.10 cycles/byte
700	223.14 usec	638.50 cycles/byte

**Table 2** Testing stream encryption speed

No. of encrypted blocks	Total time	Encryption speed
22 blocks	242.15 usec	5.38 cycles/byte

particular state bits without changing the elegant structure of stream cipher and compare the output with the original one. So far, our proposed method confined that some modification of statebits increases security level without changing internal structure of the cipher. We are able to show that statebit stream and generated new bit stream variables has a significant impact on the success of our algebraic attack on Trivium cipher.

### 3.2 Performance Analysis

The hardware testing eStream framework determined five conditions of performance based on power consumption, area compactness, throughput, simplicity and flexibility. Trivium cipher feedback can be allowing more than one bit to be per cycle processed. Our implemented testing key and IV performance result are described in Table 1 and testing stream encryption speed performance result described in Table 2.

## 4 Analysis of Different Attacks on Trivium Cipher

Out of two variants of attacks state recovering attack is the first variant which tries to guess some state bits value. In that case it reduces the linear equations which can be implemented based on the elimination process. Another form of attack is known as distinguishing attack. This attack procedure collects information on keystream generation process and creates a distinguisher. Main focus stays only on state recovery attack [2]. As a polynomial expression  $F(K, IV) = Y$ , where K is the secret key of n bits  $(x_1, x_2, \dots, x_n)$  and IV is known publicly initialization vector (IV) of m bits  $(v_1, v_2, \dots, v_m)$ .

We use the expression  $F_i(K, IV) = Y_i$  is to represent the polynomial expression for the *i*th output bit of Trivium cipher [10]. Our main approach of this attack is to combine the equations in K but randomly representation of IV in such a manner which is low degree equations in the variable K [11]. The chosen IV s can be

chosen in such a way that linear equations of unknowing bits in  $K$  can be obtained. In fact internal statebits of Trivium consists of 288 bits which are set in 3 shift registers respectively [11]. In generally some primitive polynomials can be determined to use to create an LFSR. This LFSR has the degree of the polynomial that will cycle over all non-zero states in Trivium [10, 12, 13]. The pseudo number generation in  $n$  bit shift registers are randomly scrolls between  $(2n - 1)$  values. This process quickly computes using less number of combinational logic. So basically when it reaches its final state, it tries to traverse the sequence exactly as before [9]. This External LFSR is one way of implementing i.e. all XOR gates are sequentially into one another and ends up as the input to the least or most significant bit of the LFSR [11]. So XORs are external form of the shift register and in internal structure of LFSR XOR gates are not sequential [11]. Recall that if  $f(X) \in \mathbb{F}_p[X]$  is a polynomial of  $n$  degree such that  $f(0) \neq 0$ , then there is positive integer  $\phi \leq q^n - 1$  such that  $f(X)$  divides  $X^\phi - 1$ . The least such  $\phi$  is called the order of  $f(X)$  and is denoted by  $\text{ord}(f(X))$ . If  $f(X)$  is any nonzero polynomial in  $\mathbb{F}_p[X]$ , then we can write  $f(X) = X^\zeta g(X)$ , where  $\zeta \geq 0$  and  $g(X) \in \mathbb{F}_p[X]$ .

In Raddum's approach the key stream generation procedure of Trivium takes one linear combination of 6 sequence bits and 2 sequence bits from A, B and C registers. The key stream bits are represented in following way [14, 15].

$$\begin{aligned} z_{66} &= A_{93} \oplus A_{66} \oplus B_{81} \oplus B_{66} \oplus C_{111} \oplus C_{66} \\ z_{69} &= A_{96} \oplus A_{69} \oplus B_{84} \oplus B_{69} \oplus C_{113} \oplus C_{68} \end{aligned}$$

#### 4.1 Reasonable Degree Changes in Trivium Cipher

In our paper, Trivium reasonable modification is easy and elegant structure. The proposed modification is minimizing the number of linear equations that appears during the previous clock bits [12, 13]. In Trivium, our proposed modified equations forms a higher degree than the original structure. In our paper we try to compare with original algebraic structure of Trivium and modified structure of Trivium. In linear equations and other lower degree polynomial equations can be guessed and finally the remaining secret bits can be recovered. The proposed idea of modification tries to discard this simple recovery of bits even some bits which are guessing bit position [10–12]. So this approach may be determined if feedback of the product term comes in the output bits in prior manner. This modify key generation process is described by the following Algorithm 3.

**Algorithm 3** Reasonable modification of Key and IV Set up Generation Process of Trivium

```

for  $t = 1$  to  $n$  do
     $t_1 := s_{33} \oplus s_{93}$ 
     $t_2 := s_{173} \oplus s_{177}$ 
     $t_3 := s_{209} \oplus s_{288}$ 
     $z_i := t_1 \oplus t_2 \oplus t_3$ 
     $t_1 := t_1 \oplus s_{91} \cdot s_{92} \oplus s_{143}$ 
     $t_2 := t_2 \oplus s_{175} \cdot s_{176} \oplus s_{243}$ 
     $t_3 := t_3 \oplus s_{286} \cdot s_{287} \oplus s_{67}$ 
     $(s_1, s_2, \dots, s_{93}) := (t_3, s_1, \dots, s_{92})$ 
     $(s_{94}, s_{95}, \dots, s_{177}) := (t_1, s_{94}, \dots, s_{176})$ 
     $(s_{178}, s_{179}, \dots, s_{288}) := (t_2, s_{178}, \dots, s_{287})$ 
end for
    
```

In that section we try to get linear equations comparison with of the original structure and of Trivium cipher [9]. As we mentioned previously, the feedback product of the cipher comes first in output prior to the original structure [11, 13]. Consequently  $s_1, s_{94}$  and  $s_{178}$  are replaced by  $t_3, t_1$ , and  $t_2$  respectively. After 65 clocks with update of  $s_1, s_{94}$  or  $s_{178}$  in such a manner. The Trivium cipher modification approach does not induced any extra logic gate except a reasonable change in the position of the feedback function. This procedure is to reduce the number of linear equations of the cipher. The difference between the degrees of algebraic structure of cipher with the original version of the cipher is described in Fig. 2.

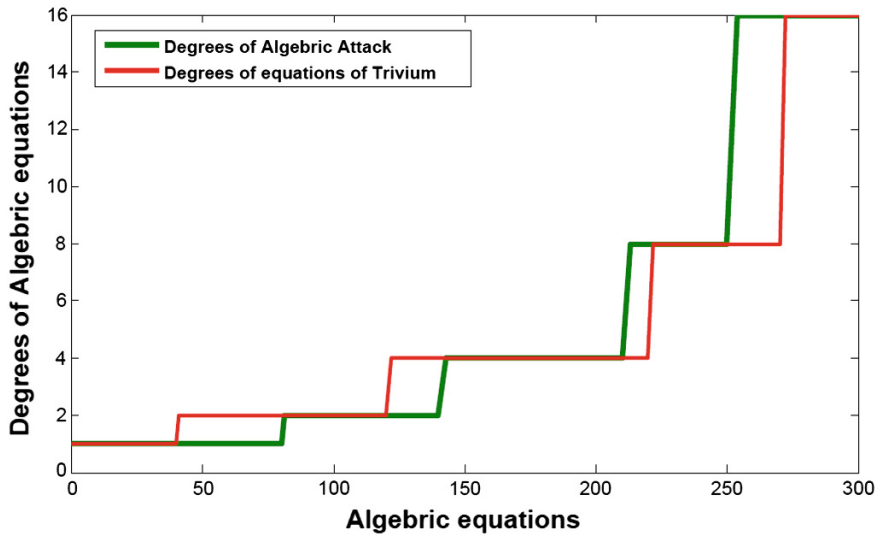
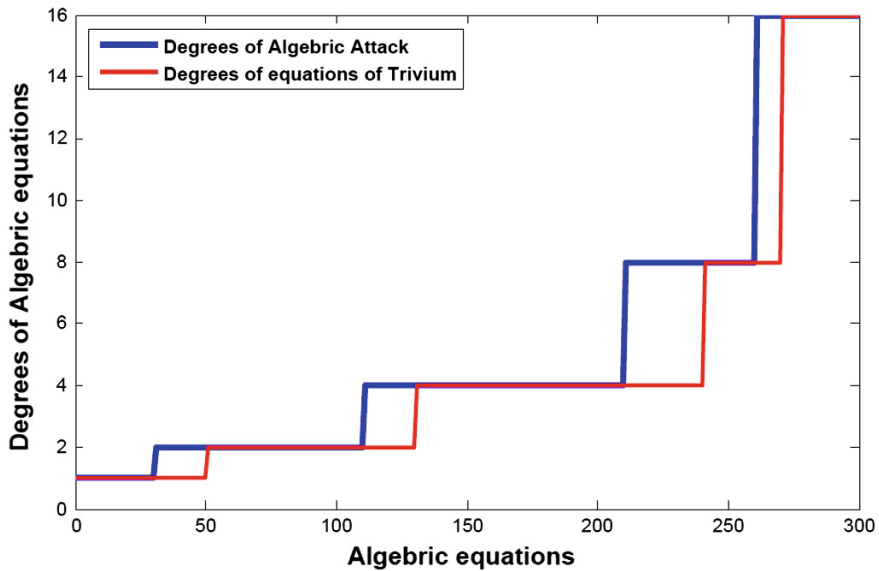


Fig. 2 Comparison of degree of trivium equation with algebraic attack



**Fig. 3** Comparison between modified structure of trivium with algebraic attack

After the reasonable changes we get first 33 linear equations which is same as original cipher. As we compare with 66 linear equations of the original cipher, some degrees are reasonably changed step by step. Finally we compare our version with the original one, we get some reasonable high degrees rather than the original version is described in Fig. 3. The sequential guessing bits are not ideal only the reason of product terms of sequential bits [13, 16]. Trivium structure has three registers which is updating the feedback variables of the three registers and it becomes mutually dependent based on the degrees of equations.

## 5 Conclusion and Future Work

In this paper we try to present some weakness of Trivium stream cipher which provide random sequence generators through non-linear shift registers. Several research problems on Trivium is till remain unanswered like patterns of behavior, algebraic attack, lengths, weak keys etc. So questions arises basis on its bits security level which can be rapidly increase with equal number of statebits. Under this design paradigm, we present reduced variant sized modifications of that stream generator, which increases the bit security level of Trivium cipher. We speculate the properties identified in the reduced sized model would remain invariant in the original ones and it would be worthwhile to innovate a new framework of Trivium cipher.

## References

1. De Canniere, C., Preneel, B.: Trivium Specifications. eSTREAM, ECRYPT Stream Cipher Project, Report (2008)
2. Khoo, K., Gong, G., Lee, H.K.: The rainbow attack on stream ciphers based on Maiorana-McFarland functions :ACNS 2006, LNCS 3989, pp. 194–209 (2006)
3. Babbage, S.: Some thoughts on Trivium. <http://www.ecrypt.eu.org/stream/papersdir/2007/007.pdf>
4. Berbain, C., Gilbert, H., Joux, A.: Algebraic and correlation attacks against linearly filtered non linear feedback shift registers. In: Avanzi, R.M., Keliher, L., Sica, F. (eds.) Selected Areas in Cryptography (SAC 2008). Lecture Notes in Computer Science, vol. 5381, pp. 184–198. Springer, Berlin (2009)
5. Turan, M.S., Kara, O.: Linear Approximations for 2-round Trivium. <http://www.ecrypt.eu.org/stream/papersdir/2007/008.pdf>
6. Dubrova, E.: A List of Maximum-Period NLFSRs, Cryptology ePrint Archive, Report 2012/166, March 2012, <http://eprint.iacr.org/2012/166> (2012)
7. Dubrova, E.: A scalable method for constructing Galois NLFSRs with period  $2^n-1$  using cross-join pairs. Technical Report 2011/632, Cryptology ePrint Archive, November 2011. <http://eprint.iacr.org/2011/632> (2011)
8. Dutta, A., Paul, G.: Deterministic hard fault attack on trivium. In: Advances in Information and Computer Security. Lecture Notes in Computer Science, vol. 8639, pp 134–145. Springer, Berlin (2014)
9. Maximov, A., Biryukov, A.: Two trivial attacks on trivium. <https://eprint.iacr.org/2007/021.pdf> (2007)
10. Teo, S.G., Wong, K.K.H., Bartlett, H., Simpson, L., Dawson, E.: Algebraic analysis of Trivium-like ciphers <http://www.eprint.iacr.org/2013/240.pdf>
11. Gierlichs, B. et al.: Susceptibility of eSTREAM Candidates towards Side Channel Analysis. SASC 2008—The State of the Art of Stream Ciphers, Workshop Record, pp. 123–150. <http://www.ecrypt.eu.org/stream> (2008)
12. Mohamed, M.S.E., Bulygin, S., Buchmann, J.: Improved differential fault analysis of trivium. COSADE 2011—Second International Workshop on Constructive Side-Channel Analysis and Secure Design. [http://cosade2011.casede.de/files/2011/cosade2011\\_talk15\\_paper.pdf](http://cosade2011.casede.de/files/2011/cosade2011_talk15_paper.pdf) (2011)
13. Modifications in the Design of Trivium to Increase its Security Level Afzal, M., Masood, A. <https://eprint.iacr.org/2009/250>
14. Raddum, H.: Cryptanalytic results on trivium, eSTREAM, ECRYPT Stream Cipher Project, Report 2006/039 (2006)
15. Schilling, T.E., Raddum, H.: Solving compressed right hand side equation systems with linear absorption. In: Hellesteth, T., Jedwab, J. (eds.) Sequences and Their Applications (SETA 2012). Lecture Notes in Computer Science, vol. 7280, pp. 291–302. Springer, Berlin (2012)
16. Borgho, J., Knudsen, L.R., Matusiewicz, K.: Hill climbing algorithms and trivium. In: Biryukov, A., Gong, G., Stinson, D.R. (eds.) Selected Areas in Cryptography (SAC 2010). Lecture Notes in Computer Science, vol. 6544, pp. 57–73. Springer, Berlin (2011)

# A No Reference Image Authentication Scheme Based on Digital Watermark

Sukalyan Som, Suman Mahapatra and Sayani Sen

**Abstract** A no reference approach based on digital watermarking is proposed for the authentication purpose of images undergoing some malicious or non-malicious attacks. It is no reference in the sense that it neither requires a reference image nor an external watermark. This feature makes the scheme attractive for situations where authentication of an image must be done without having an access to the original image or the reference watermark. The watermark is constructed from the image itself and is embedded as a robust signature in the image. The Discrete Wavelet Transform (DWT) is used to separate the approximation and detail regions of the image. The watermark is constructed from the low frequency region and embedded into the spatial domain by modifying the Least Significant Bits (LSBs) of each pixel. Upon comparison, based on metrics like Peak Signal to Noise Ratio (PSNR) and Structural Similarity Index (SSIM), authentication is ensured. Exhaustive simulations on the images from a well-known image database have been carried out to demonstrate the performance of the proposed approach.

**Keywords** Discrete wavelet transform (DWT) · Peak signal to noise ratio (PSNR) · Structural similarity index (SSIM)

---

S. Som (✉)

Department of Computer Science, Barrackpore Rastraguru Surendranath College,  
Barrackpore, Kolkata, India  
e-mail: sukalyan.s@gmail.com

S. Mahapatra · S. Sen

Department of Computer Science and Engineering, University of Kalyani,  
Kalyani, Nadia, India  
e-mail: sumancse19@gmail.com

S. Sen

e-mail: sayani.sen@gmail.com

© Springer India 2015

J.K. Mandal et al. (eds.), *Information Systems Design and Intelligent Applications*,  
Advances in Intelligent Systems and Computing 339,  
DOI 10.1007/978-81-322-2250-7\_74

# 1 Introduction

Presently we are breathing in an age where we are exposed to a remarkable explosion of visual imagery. Although we had confidence in the integrity of such visual imagery in the days of yore, today's emergence of the digital technology has begun to erode this confidence. Overwhelming growth in the frequency and sophistication of image processing softwares are becoming the concern behind the security, authentication and integrity of digital images and videos. Over the past few years, digital watermarking based approaches have become a popular means to facilitate authentication and content-integrity verification of multimedia contents. Blind or no-reference image authentication techniques, where the receiver has neither the original image nor the tracer watermark, forms an important field of current research [1–3]. On the contrary, with-reference approaches relies on the fact that embedding of an extraneous, imperceptible or perceptible watermark, known as the tracer watermark, in the original image is done and the tracer watermark is made available to the receiver. Extraction of embedded watermark is made from the received image by the receiver and he then estimates the extent of degradation with reference to the tracer one [4]. A major pitfall of such with-reference approaches is that the tracer watermark must be known to the user and hence must be sent through a secure channel separately. An important contribution of the proposed scheme is that it eliminates such dependence by generating the watermark from the image itself and further still, forming a reliable estimate of the reference watermark from the received image.

In the proposed scheme, generation of watermark is done using Discrete Wavelet Transform (DWT) coefficients of an image. Choice of DWT can be justified by the useful properties. Firstly, it has multiresolution capability. Secondly, it has better space frequency localization over their counterparts like Discrete Cosine Transform (DCT). Thirdly, wavelet transform decomposes an image into three spatial directions, like horizontal, vertical and diagonal that reflect the anisotropic properties of Human Visual System (HVS) based image representation. Finally, blocking artifacts are not observable in DWT based image modifications. The watermark is constructed from the image itself and is embedded as a robust signature in the image. The Discrete Wavelet Transform (DWT) is used to separate the approximation and detail regions of the image. The watermark is constructed from the low frequency region by applying Canny edge detector. The binary watermark is embedded into the LSBs of each of the pixels of the image. To authenticate a received image the watermark is generated from the image itself and compared with the extracted one.

The rest of the paper is organized as follows. In Sect. 2 proposed scheme has been stated. Performance of the proposed method is evaluated in Sect. 3. To prove the superiority of the scheme, comparison with existing state-of-the-art is stated in Sect. 4. Conclusions and scope for future directions of work are drawn in Sect. 5.

## 2 Proposed Scheme

### 2.1 Image Feature Extraction

A two-level Wavelet Transform (WT) of the grayscale image is performed. For the sake of simplicity, the most common form of DWT, Haar Wavelet is adopted for the said purpose in the literature. More specifically, a single WT of an image  $A$  of size  $M \times N$  yields the matrices  $cA_1$  (corresponding to the first level approximation of  $A$ ) and  $cH_1, cV_1, cD_1$  corresponding to the horizontal, vertical and diagonal details of  $A$ , each of size  $M/2 \times N/2$ . The edges of an image represent the boundaries between the areas having uniform intensity and texture. This edgemap is used to form the feature map of the image that has to be embedded as the watermark. In this literature, binary edge image is computed by using Canny edge detector from the coefficients in  $cA_1$ .

### 2.2 Watermark Embedding

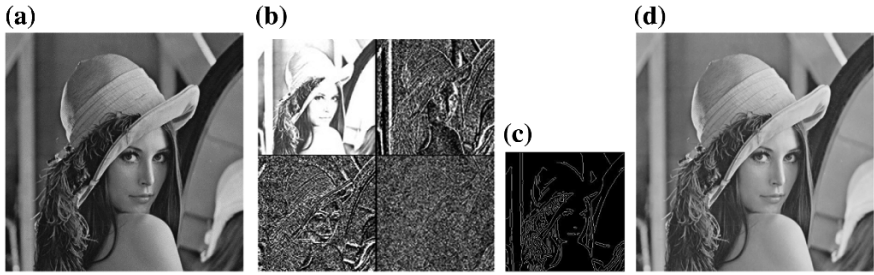
The watermark is embedded in the spatial domain directly by modifying the LSBs of the image pixels. The procedure to embed the watermark is as follows:

- A two-level DWT is applied on the original image, say  $I_{org}$  of size  $2^n \times 2^n$ ;  $n \in \mathbb{N}$ ;  $n > 0$ . It divides the image into 4 sub-bands  $cA_1, cH_1, cV_1$  and  $cD_1$ .
- A binary edge map is generated by applying Canny edge detector on the coefficients of  $cA_1$  which has to be embedded as the binary watermark. The binary watermark  $W_{Gen}$  is of size  $2^{n-1} \times 2^{n-1}$ .
- To embed the watermark in  $I_{org}$ , it is sub-divided into 4 equal and disjoint blocks of size  $2^{n-1} \times 2^{n-1}$ , say  $B_1, B_2, B_3, B_4$ .
- Each watermark bit is substituted in the LSBs of the binary values of each of the pixels of the sub-images  $B_i, i = 1, 2, 3, 4$  simultaneously.
- The watermarked image  $I_{org}^W$  is formed by concatenating each of the watermarked blocks  $B_i, i = 1, 2, 3, 4$ .

### 2.3 Watermark Extraction

The watermarked image  $I_{org}^W$  may encounter degradation due to malicious (intentional) or non-malicious (unintentional) attacks. Let the received watermarked image be denoted by  $I_{rec}^W$ . To extract the watermark from the received image, it is first sub-divided in 4 equal and disjoint blocks as done during watermark embedding. A watermark of size  $2^{n-1} \times 2^{n-1}$ , say  $W_{Ex}$  is extracted from either one of the 4 blocks chosen randomly. To authenticate an image extracted watermark, say  $W_{Ex}$  is compared with the generated watermark, say  $W_{Gen}$  afresh from the received image by using the watermark generation technique already stated above.



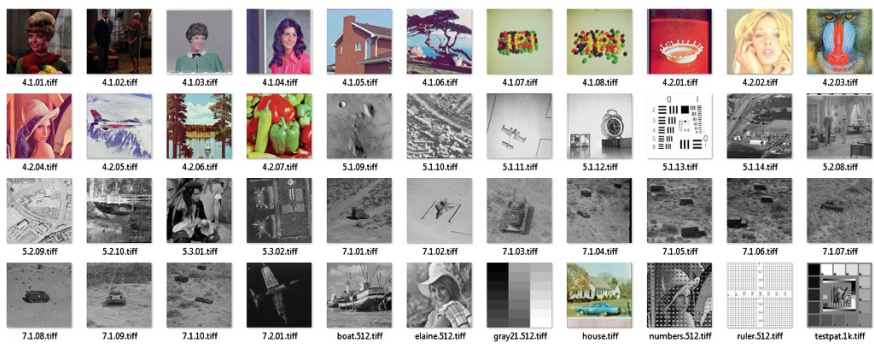


**Fig. 1** a A grayscale image Lena, b 2D DWT using Haar Wavelet on image (a), Watermark generated from  $cA_1$  of (b) using Canny edge detector, d Watermarked image of Lena in (a)

In Fig. 1a we present a grayscale image of Lena of size  $512 \times 512$  on which 2D DWT using Haar wavelet is applied. We consider approximation coefficients in  $cA_1$  to generate binary watermark of size  $256 \times 256$  by applying Canny edge detection algorithm. The generated binary watermark is shown is Fig. 1c and the watermarked image is shown in Fig. 1d.

### 3 Experimental Results

The proposed algorithm has been exhaustively simulated and their performance has been tested over commonly used and widely accepted USC-SIPI [5] image database, maintained by Signal and Image Processing Institute, University of Southern California. The *misc* volume of the database has been chosen in this literature to prove the efficacy of the proposed scheme. The proposed scheme and the existing state-of-the-art, considered for comparison, have been implemented using Matlab 7.10.0.4(R2010a) on a system running with Windows 7 (32 bit) with Intel Core i5 CPU and 4 GB DDR3 RAM. In Fig. 2 a thumbnail view of the images considered from the *misc* volume of the database is shown.



**Fig. 2** A thumbnail view of the *misc* volume of USC-SIPI image database

The performance of the proposed method is measured by the Peak Signal-to-Noise Ratio (PSNR) and Structural SIMilarity (SSIM) index [6]. Let  $I_1(i, j)$  and  $I_2(i, j)$  be the gray level intensities of the pixels at the  $i$ th row and  $j$ th column of two images of size  $M \times N$  respectively. The MSE between these two images is defined in Eq. (1), PSNR is defined in Eq. (2).

$$MSE = \frac{1}{M \times N} \sum_{i=0}^{M-1} \sum_{j=0}^{N-1} |I_1(i, j) - I_2(i, j)|^2 \tag{1}$$

$$PSNR = 20 * \log_{10} \left( \frac{255}{\text{sqrt}(MSE)} \right) \tag{2}$$

The SSIM index between two images  $I_1$  and  $I_2$  as described in [6] is computed using Eq. (3).

$$SSIM(I_1, I_2) = \frac{(2\mu_{I_1}\mu_{I_2} + C_1)(2\sigma_{I_1I_2} + C_2)}{(\mu_{I_1}^2 + \mu_{I_2}^2 + C_1)(\sigma_{I_1}^2 + \sigma_{I_2}^2 + C_2)} \tag{3}$$

where  $\mu, \sigma, \sigma^2$  denote average, variance, covariance respectively and  $C_1$  and  $C_2$  are constants as described in detail in [6]. An image with a PSNR value of 35 dB or more and SSIM close to unity is widely accepted as an image of good quality.

### 3.1 Imperceptibility of Watermark

A digital watermark is called imperceptible if the original cover signal and the marked signal are perceptually indistinguishable. Relatively high value of PSNR (in dB) and SSIM indicate that better imperceptibility of watermark is achieved by the proposed technique. In the proposed scheme, the average PSNR between the original and their watermarked versions over the images in the database considered is 51.1201 dB and SSIM evaluated for the same is 0.9980 which indicates that the robustness of the method is preserved. In Table 1, the MSE, PSNR, SD and SSIM

**Table 1** Imperceptibility of the watermark: MSE, PSNR, SD and SSIM of original and watermarked images

Image	MSE	PSNR	SD	SSIM
Baboon	0.4996	51.1448	42.3215	0.9991
Lena	0.5012	51.1305	47.8619	0.9975
Airplane	0.4981	51.1580	46.4165	0.9973
Sailboat	0.4988	51.1519	65.5884	0.9981
Peppers	0.4983	51.1560	53.8834	0.9976
Boat	0.5146	51.0163	46.6800	0.9983
Elaine	0.5067	51.0832	46.0663	0.9981
Average	0.5025	51.1201	49.8311	0.9980

between some sample images, chosen from the database, and their watermarked versions are presented.

### 3.2 Watermark Payload

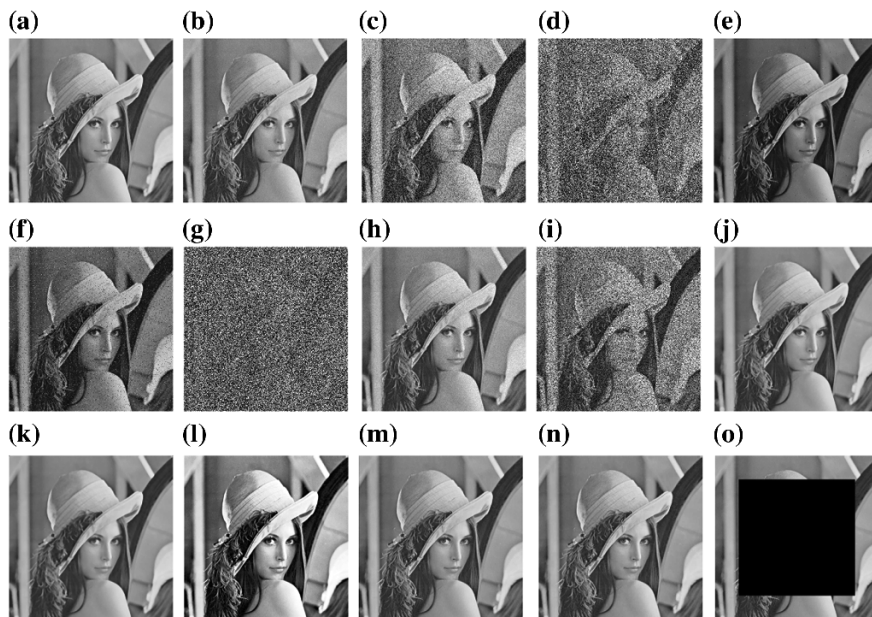
A watermark of size  $2^{n-1} \times 2^{n-1}$  is embedded in an image of size  $2^n \times 2^n$  by subdividing the image into four equal and disjoint blocks by substituting the LSBs of each pixel. Therefore, the payload of the proposed scheme is  $2^{n-1} \times 2^{n-1}$  bits per byte.

### 3.3 Performance Under Various Attacks

To evaluate the effectiveness of the proposed scheme against tampering, various types of malicious and non-malicious attacks are applied viz. (1) Salt-and-Pepper noise, (2) Average white gaussian noise, (3) Speckle noise, (4) JPEG compression, (5) Median filtering, (6) Histogram Equalization and (7) Cropping pixel values. In Table 2, a summary of the results obtained in terms of PSNR and SSIM between the

**Table 2** Quality evaluation of proposed scheme under various attacks

Attacks		PSNR (dB)	SSIM
Adding noise	Salt and pepper 0.001	69.4962	0.9998
	Salt and pepper 0.05	58.5938	0.9978
	Salt and pepper 0.9	51.3267	0.9849
	AWGN 0.001	51.1336	0.9665
	AWGN 0.05	51.0639	0.9685
	AWGN 0.9	51.0681	0.9786
	Speckle noise 0.001	51.1580	0.9667
	Speckle noise 0.01	51.1332	0.9665
	Speckle noise 0.5	50.8934	0.9702
JPEG compression	90 %	51.1472	0.9665
	70 %	51.1420	0.9663
	50 %	51.5194	0.9704
	20 %	51.1424	0.9599
	10 %	54.0263	0.9850
Median filtering	3 × 3 mask	58.1272	0.9977
	5 × 5 mask	57.4660	0.9971
Histogram equalization		50.7641	0.9469
Cropping	10 %	63.8284	0.9989
	20 %	61.9723	0.9982
	50 %	61.4323	0.9979
	90 %	64.7389	0.9994



**Fig. 3** Effect of applying different attacks: **a** watermarked image of Lena, applying AWGN with  $\mu = 0$  and  $\sigma =$  **b** 0.001, **c** 0.05, **d** 0.9, Applying Salt and Pepper noise with  $\mu = 0$  and  $\sigma =$  **e** 0.001, **f** 0.05, **g** 0.9, applying speckle noise with **h** 0.01, **i** 0.5, Applying median filtering with masks **j**  $3 \times 3$ , **k**  $5 \times 5$ , **l** Applying histogram equalization, Applying JPEG compression with QF **m** 70, **n** 50, **o** Applying cropping attack of 50 at center

extracted and the generated watermark from the received watermarked image is presented. From the results we observe the following:

Simulation results against JPEG compression attack show that a decrease in quality factor decreases the imperceptibility of watermarked image but increases the robustness of watermark. The high value of Similarity Ratio indicates that the proposed method is able to withstand such kind of attacks. The watermarked image is attacked with salt and pepper noise, AWGN and Speckle noise with different mean and standard deviation and/or densities and observed a moderate PNSR value, with a high similarity ratio. Experimental results against cropping attacks disclose that the robustness of watermark is high with an acceptable PSNR value.

In Fig. 3 we present the watermarked image of Lena and some of the attacks and their effects on the watermarked image.

## 4 Comparison with Existing State-of-the-Art

To prove the superiority of the algorithm, we compare the results with some of the existing state-of-the-art. From Table 3 we can conclude that proposed scheme

**Table 3** Comparison of average PSNR (in dB) and SSIM of watermarked images

Metric	Proposed scheme	Ref. [1]	Ref. [2]	Ref. [3]	Ref. [7]
PSNR	51.1201	59.1168	58.3421	59.2328	56.2083
SSIM	0.9980	0.8496	0.8767	0.8885	0.9933

provides moderate imperceptibility as compared to the related ones already available in terms of PSNR and offers highest similarity index measured in terms of SSIM.

## 5 Conclusion

A No Reference Image Authentication Scheme based on DWT based digital watermark has been proposed that embeds and extracts the watermark information effectively. In this method, the low frequency subband of wavelet domain is used to construct the content based watermark and the watermark pattern is embedded in the spatial domain, by sub-dividing the image into four equal and disjoint blocks, by substituting the LSBs. This watermarking scheme deals with the extraction of the watermark information in the absence of original image and authenticates an image in absence of the tracer watermark, hence the no reference scheme was obtained. The performance of the watermarking scheme is evaluated with content preserving common image processing attacks and content altering intentional attacks. Experimental results demonstrate that the proposed scheme guarantee the safety of the watermark, and identifies malicious attacks while tolerating Filtering operations, JPEG compression, Geometric distortions, Image adjustment and histogram equalization. Hence the proposed technique is effective for image authentication. Improve the performance of the proposed scheme for the situations where very small areas are tampered and developing a threshold to determine whether the tamper is malicious or non-malicious would be of future concern.

**Acknowledgments** The authors would like to convey their sincere respect and thankfulness to Dr Sarbani Palit, Asst. Professor, CVPRU, ISI, Kolkata and Sri Kashi Nath Dey, Department of Computer Science and Engineering, University of Calcutta, West Bengal, India for being the constant source of inspiration and motivation for pursuing their research work.

## References

1. Sathik, M.M., Sujatha, S.S.: An improved invisible watermarking technique for image authentication. *Int. J. Adv. Sci. Technol.* **24**, 61–73 (2010)
2. Sathik, M.M., Sujatha, S.S.: A novel DWT based blind watermarking for image authentication. *Int. J. Netw. Secur.* **14**(4), 223–228 (2012)

3. Sathik, M.M., Sujatha, S.S.: Authentication of digital images by using a semi-fragile watermarking technique. *Int. J. Adv. Res. Comput. Sci. Softw. Eng.* **2**(11), 39–44 (2012)
4. Chamlawi, R., Khan, A., Ushman, I.: Authentication and recovery of images using multiple watermarks. *Comput. Electr. Eng.* **36**(3), 578–584 (2010)
5. USC-SIPI image database. Available at <http://sipi.usc.edu/database>. (Accessed on 27 Feb 2014)
6. Wang, Z., Bovik, A.C., Sheikh, H.R., Simoncelli, E.P.: Image quality assessment: from error visibility to structural similarity. *IEEE Trans. Image Proc.* **13**(4), 600–612 (2004)
7. Sujatha, S.S., Sathik, M.M.: Feature based blind approach for robust watermarking. In: *International Conference on Communication, Control and Computing Technologies*, pp. 182–185 (2010)

# Energy Efficient Routing Approaches in Ad hoc Networks: A Survey

Jenish Gandhi and Rutvij Jhaveri

**Abstract** Mobile Ad hoc Network (MANET) is a form of short term based network that contains multidimensional nodes having major concern such as battery power resources. Energy is playing as consequential undertakings in MANET. Limited power of network causes many effects on the performance of the networks. Lack of energy factor may break the connection which can mess the network or routing process. Routing process requires efficient utilization of battery power or energy to maintain the network condition so that packet can be transferred without any obstacle in the performance. As well as, network life or life of node is proportional to battery life which is powered by limited capacity. The meaning of energy-efficient is not about consuming less energy but to increase the time duration to maintain the network performance level. Routing performances can differ depending upon the network parameters. In order to reduce the usage of energy and to increase the life span of battery, several others Ad hoc routing protocols are reviewed with their novel conceptions and optimization techniques over the main routing protocols.

**Keywords** Mobile Ad hoc network · Energy efficiency · Network lifetime · Energy-efficient routing approaches

## 1 Introduction

Networking is the process of sharing the resources or communication between two or more parties {source, destination}. Infrastructure network (i.e. Cellular Network) and infrastructureless network (i.e. MANET, VANET and so on.) is the type of

---

J. Gandhi (✉) · R. Jhaveri  
SVM Institute of Technology, Bharuch 392001, Gujarat, India  
e-mail: jenish.r.gandhi@gmail.com

R. Jhaveri  
e-mail: rhj\_svmit@gmail.com

wireless network [1]. Infrastructure based network is not a “peer-to-peer” connection similar to Ad hoc network. It is roundabout connection between two or more network points which is able to get to be through fixed wireless access point called as central administrator. While in infrastructureless network, all nodes in network act as a router.

Meaning of Ad hoc is “for this” and “for this situation” comes from Latin. American uses word “Ad hoc” for immediate and special purpose. It means Ad hoc word use for temporary basis. Same thing, Mobile Ad hoc network (MANET) is temporary based network in which physical network layout will change frequently as network point is moving. Due to this dynamic topology, MANET has need of more system resources such as efficient power supply or energy, network throughput, network lifetime. MANET have a many key challenges [2, 3] such as limited power support, limited bandwidth, network lifetime, end-to-end delay, Quality of Service (QoS), network security.

The Major end, purpose of the MANET is to maximize the throughput, improve the life span of the network and minimize the delay time. Throughput can be measured through Packet Delivery Ratio (PDR). Routing is the process of selecting the best path through which it forwards the traffic over a network. All network points in MANET are dependent on battery power, in other words, network points are battery driven. Flooding the packet often may cause connection failure. Reason for connection failure is:

- Energy exhaustion by single dead node
- Node is moving out-of range of its close-by node

The rest of this paper is organized as follows. The energy-efficient issue is presented in Sect. 2. In Sect. 3, we provides summary of literature available on traditional routing protocols. Finally we conclude the paper in Sect. 4 with future research opportunities on energy-efficient.

## 2 Energy Efficiency Issues

The energy-efficient routing is voluminous concern in the MANET. All nodes are battery-driven, powered by constrained battery capacity. Due to the lack of energy, Node cannot communicate efficiently with another node. It is obligatory to take action to ameliorate the energy of node. This paper defines sundry efficiency routing protocol to solve the energy related problem. The parameters or process define as below in which node consuming more Energy.

- During transmit the packets
- On receiving the packets
- In a idle mode
- In a slumber mode



The various energy challenges are define as below:

1. **Limited Bandwidth:** Basically, Limited bandwidth in wireless network refers to packet connection's capacity and round-trip delay time (RTD) or round-trip time (RTT). It means Circumscribed bandwidth affects the network during the traversal of packets because of length of time taken for a request and reply.
2. **Battery Constraint:** Battery power is paramount concern into the Ad hoc network. Each node in wireless Ad hoc network is operates on battery potency. Less energy can affect the communication of the network.
3. **Packet losses due to transmission errors:** Certain connection may break due to the dynamic deopment of the node. The physical network topology often changes when node moves. In an astronomically immense network, a dead node exhausts all energy can cause the transmission error.
4. **Security threats:** Security is big challenge in terms of secure communication in Ad hoc network. The several security threats affect the network due to limited cryptographic measure, node traverse without adequate protection and static topology which is not adequate in dynamic comporment. As a result node grabs more battery power which affects the overall performance of the network.
5. **Mobility-induced route changes:** Ad hoc wireless network is dynamic topology. Certain connection may be break frequently due to the node movement during perpetual session of the network.
6. **Routing Overhead:** In wireless network, nodes are changing its location frequently. As a result, stale entry in obtained in routing table that increase the routing overhead.

### 3 Related Work

Energy saving is big concern in wireless Ad hoc network. In recent past years, many researchers have addressed energy-efficiency related issue and innovate incipient conceptions and novel techniques. Below shows few algorithm based on Energy efficiency mechanism.

Zhao and Tong [4] proposed EAGER protocol which includes proactive and reactive approaches based on traffic and mobility conditions. EAGER divides the network into equipollent size cell. It works based on two routing protocol: Intra-cell proactive routing and another Inter-cell reactive routing protocol. EAGER culls the optimal peripheral area that can be used to minimize the node in a traversal process.

Kim et al. [5], in this, LRCA is utilized to change the route if a node is dead or have a less-battery life by broadcasting the HELP and OK message.

Shin et al. [6], modified the conventional routing protocol with the avail of K-hop PRREQ message. K-hop PRREQ message used to reduce the number of broadcasting of route request (RREQ) message. K-hop PRREQ is use by sender to broadcast with hope with the use of Time To Live (TTL) field.

Loganathan and Ramamoorthy [7], describe comparison between the pristine DSDV and modified DSDV with the use of cost parameter assign for link and path of the Ad hoc network. The cost parameter include parameters such as hop count (h), total inference (I), Node link delay (d), Residual energy of a node (R), node transmission power (T). The cost parameter is cummulate with different optimization function and for optimal path MAX/MIN Energy-Half-Interference Hop multicast algorithm in utilization.

Karuppanan and Mahalaksmi [8], in this, MANET is a subset of VANET. OLSR include data such as broken link information which leads the vagueness. Fuzzy Rough-OLSR (FR-OLSR) reduces the force of uncertainty in the dataset and produces the optimal path for packet traversal. FR-OLSR based on Fussy Rough set theory. FR based theory obviate the problem that is incapable to defense. FR defines the degree of kindred attribute between two objects which measured in 0–1 interval.

Kim et al. [9], proposed, TEES is based on DSR, use to reduce the control packet overhead and increase the amount of packet delivery ratio. TEES find the optimal path based on two levels LB (Lower Bound) and UB (Upper Bound). The energy value is compared with LB and UB to compute the case LC (Low Case), MC (Middle Case) and HC (High Case).

Shivashankar et al. [10], Described conventional the power aware algorithm. In DSR, the routing packet load increases the time for a multipath. DSR cull the path which have minimum number of hops. EPAR (Efficient Power Routing Protocol) select the path with the maximum lowest hop energy. DSR performance is inefficient in terms of medium and large size networks. For this, EPAR, MTPR is proved to be preponderant. EPAR in terms of throughput provide a preponderant result.

De Rango et al. [11], proposed EE-OLSR which is the modification of OLSR protocol to reduce the battery consumption. EE-OLSR is work on two methodologies, one is, EA-Willingness Setting and another one is Overhearing Exclusion. The willingness of node can be described by two steps or metrics: (1) Battery capacity and, (2) Predicted lifetime.

Sheng et al. [12], an energy-efficient protocol NCE-DSR (Number of times nodes send Constraint Energy DSR) based on DSR. NCE-DSR considers the two domain value MAX and AVE value that is added to datagram to record the mean value and the maximum value of the number of times node sending messages are protected or chosen for route selection.

Vazifehdan et al. [13], In this, two novel energy aware routing algorithm is proposed in which Reliable Minimum Energy Cost Routing (RMECR) is used to elongating the operational lifetime of the network while RMER reducing the consuming energy during end-to end packet traversal.

Fahrnv et al. [14], proposed, Predictive Energy Efficient Bee Routing (PEEBR) is a swarm based optimization algorithm that work on two phases: (a) node level and (b) network level.

Rekha et al. [15], GFSR is a grid based protocol used to exchange the control message and data packet by selecting the good candidate called the gateway. Grid includes the gateway and gateway is the node that used to forward the packet. GFSR chooses the best path by observing the node during transmission and checks whether it's gateway or not. Nearest node to the virtual grids is good candidate call gateway.

Ur Rahman Khan et al. [16], in this, the higher rate of mobility degrade the performance of network and maximize the packet delivery ratio. As a result, stale routes are updated into the routing table. DSDV uses stale route it signifies not a valid route to destination. Eff-DSDV utilizes the stale routes in case of broken link. In case of broken link, Eff-DSDV engenders the temporary link by sending one-hop packet to the destination.

Chettibi and Chikhi [17], the paper utilizes the Zero-order Sugeno Fuzzy Logic System adjust the willingness parameter into the OLSR protocol. FLS check the willingness of node by considering two parameters such as RE (Remaining Energy) and ERL (Expected Residual Lifetime).

Roy et al. [18], SEEC (Signal and Energy Efficient Clustering) play consequential role while cluster dies. It considers the second node as a cluster head while cluster head's power level goes below to the certain threshold value.

Mangai and Tamilarasi [19], the ILCRP (Improved Location aided Cluster based Routing Protocol) used to maintain the nodes location by utilizing the GPS. Due to the advantages of system, ILCRP used to reduce the control overhead. ILCRP works on three phases: cluster formation, route maintenance, route discovery.

Sharma et al. [20], proposed, new algorithm MCGCR (Modified Cluster Head Gateway Switch Routing Protocol) combining the two approaches: proactive and reactive approach. MCGCR ameliorate the routing performance by utilizing the cluster heads and gateways.

Verma [21], the main three areas that consume more power, namely, radio frequency, nodes processing unit and energy consume by nodes. To calculate the energy consumption by node, ZRP with anycast is use. Anycast is use while node is consuming more energy in receiving and sending the packet. The total energy calculated by sum of receiving and sending packet process.

SreeRangaRaju and Mungara [22], ZRP utilizes the query methodology targeting the peripheral nodes which is more efficient than the flooding process. It is possible that the neighbour receive the packet multiple times. It is obligatory to reduce the control overhead. The query control mechanism used to reduce the delay in which detection mechanism include source node's id and query id pair. In this, node sends the packet to the peripheral node. It may transpire that packet may receive multiple times through peripheral node. At this time, query bordercasting approach is use.

Table 1 describes the survey on various traditional routing protocols with their novel conception and optimization techniques.

**Table 1** A survey on traditional routing protocol

Topic name	Protocol	Description	Mechanism/ algorithm	Methodology	Performance/QoS
Energy-efficient adaptive routing for Ad hoc networks with time-varying heterogeneous traffic [4]	EAGER	Eager protocol works based on two routing protocol: Intra-cell proactive routing and Inter-cell reactive protocol	Energy aware geo-location aided routing	Partitioning the network into equal sized cells	Large-scale energy, Overhead, difficult to maintain the location of nodes
LRCA: enhanced energy-aware routing protocol in MANET [5]	LRCA	LRCA is utilized to transmute the route if a node is dead or have a less battery life	Local route change algorithm	Route change with the help of HELP, OK, RCRQ message	Packet loss rate, route recovery, power consumption
Energy efficient route discovery for mobile HCI in Ad hoc networks [6]	DSR, AODV	K-hop PRREQ message use to reduce the number of broadcasting of route request message	K-hop pre-route request message	Message broadcast with the use of Time To Live (TTL) value	Energy consumption, route discovery
Performance analysis of enhanced DSDV protocol for efficient routing in wireless Ad hoc networks [7]	MPB-DSDV	Newly protocol assign the cost parameter like hop count, total inference, node link delay, residual energy, transmission power	MAX/MIN energy-half-hop multicoast algorithm	By assigning the cost parameter for link and path	Network energy, network lifetime
Enhanced optimized link state routing protocol for VANET using fuzzy rough set [8]	FR-OLSR	FR-OLSR based on fuzzy rough set theory which is obviate the problem that is incapable to defense	Fuzzy rough set theory	FR is used to define the similarity between objects to remove the uncertainty	Uncertainty in routing information, vagueness due to broken link in OLSR
A routing protocol for throughput enhancement and energy saving in MANETs [9]	TEES based on DSR	TEES find the optimal path based on two levels Lower Bound and Upper Bound	Throughput enhancement and energy saving	Choose path by comparing three cases (LC, MC, HC) with two energy level UB and LB	Throughput, control packet overhead
Designing energy routing protocol with power consumption optimization in MANET [10]	EPAR, MTPR, DSR	EPAR calculate the lowest hop energy which is given battery power for each path	Conventional power aware algorithm	Path selection based on energy	Network lifetime, energy consumption, PDR, throughput

(continued)

**Table 1** (continued)

Topic name	Protocol	Description	Mechanism/ algorithm	Methodology	Performance/QoS
EE-OLSR: energy efficient OLSR routing protocol for mobile Ad hoc networks [11]	EE-OLSR	Modified OLSR works on two method such as Willingness setting and Overhearing exclusion	EA-willingness setting mechanism	Node willingness can quantified by battery capacity and predicted life time	Battery consumption, network lifetime, network performance
A novel energy-efficient approach to DSR based routing protocol for Ad hoc network [12]	NCE-DSR	NCE-DSR calculate the cost function by considering two values Mean and Max for elongate the duration of network lifetime	Number of times send constraint energy DSR	Route selection using cost function	Energy consumption, hardware overhead, network lifetime
Energy-efficient reliable routing considering residual energy in wireless Ad hoc networks [13]	RMECR, RMER	New routing protocol use genetic routing algorithm which calculate the MECP between every two nodes of the network	Genetic routing algorithm	Energy reduction using Minimum Energy Cost Path (MECP)	Energy efficiency, reliability, network lifetime, end-to-end delivery
PEEBR: predictive energy efficient bee routing algorithm for Ad hoc wireless mobile networks [14]	PEEBR	PEEBR is a swarm based optimization algorithm that work on two phases, Node level and Network-level	Swarm intelligent routing algorithm	Potential path selection based on integrity ratio	Optimal path, energy consumption, battery power saving
Efficient routing algorithm for MANET using grid FSR [15]	Grid FSR	GFSR partitioning the network in two dimensional virtual grid and select the best gateway through minimum distance between virtual grid and node	Fisheye state routing algorithm	Path selection by choosing alternative gateway in grid	Bandwidth
An efficient DSDV routing protocol for MANET and its usefulness for providing internet access to Ad hoc hosts [16]	Eif-DSDV	Eif-DSDV utilizes the temporary routes in case of broken link	Efficient DSDV	Route establish by creating the temporary link.	End-to-end delay, PDR, Mobile-IP overhead
FEA-OLSR: adaptive energy aware routing protocol for MANETs using zero-order sugeno fuzzy system [17]	FEA-OLSR	The paper utilizes the FLS to adjust the willingness parameter to check the willingness of node	Zero-order Sugeno fuzzy logic system	Node willingness computes by the use of FLS	Energy-efficient routing

(continued)

**Table 1** (continued)

Topic name	Protocol	Description	Mechanism/ algorithm	Methodology	Performance/QoS
Energy efficient cluster based routing in MANET [18]	CBRP	SEEC consider the alternative node as a cluster head (CH) while previous CH's power level fall down to the certain threshold value	Signal and Energy Efficient Clustering (SEEC)	Minimize the energy cost by selecting the other node as a cluster head (CH)	Energy level, signal strength, battery power level
A new approach to geographic routing for location aided cluster based MANETs [19]	ILCRP	ILCRP (Improved Location aided Cluster based Routing Protocol) used to maintain the nodes location using GPS. Due to advantages of GPS, it reduce the control overhead	Cluster based routing algorithm	Providing location information of nodes by utilizing the GPS	Performance metrics (end-to-end delay, control overhead, PDR)
An efficient cluster based routing protocol for MANET [20]	MCGSR	MCGSR amalgamate the two approaches, proactive and reactive, to improve the routing performance by utilizing the cluster head and good candidate	Modified cluster head gateway switch routing protocol	By utilizing the cluster heads and gateways	Performance metrics
Energy efficient routing in MANET with ZRP and anycast [21]	ZRP	ZRP with anycast is utilized to calculate the total energy consuming by node, as well as, check the total active nodes of network	ZRP with anycast addressing	By applying anycast in ZRP	Energy-efficient
Tuning ZRP framework for CR networks and MANETs [22]	ZRP	Bordercasting use IERP to broadcast the packet to node in zone boundary to control the overhead packet	Query control mechanism, selective bordercasting procedure	By utilizing IERP mechanism which is differ from IERP in ZRP	Delay in route acquisition, congestion, throughput

## 4 Conclusion and Future Scope

To evaluate the energy consumption, this paper surveys various routing protocols with their novel conceptions and optimization techniques over the pristine routing protocols. Paper also describes the erudition of conventional routing protocol briefly. Maintaining the energy level and network life is voluminous concern in Ad hoc network. For that, efficient routing protocols are required to discover the routes which facilitate the secure and reliable communication.

It is infeasible to compare the routing protocols with one another because protocols are dependent on network parameters or each protocol has a different goal with different postulation. The network parameters affect the overall performance of the protocol in the network. As well as, each modified routing protocols perform independently in case of energy cognate issue. Due to this reasons, Results cannot be compared with one another.

We surveys several routing protocols utilizing a single-hop and multi-hop routing process. But there are many open questions in case of maintaining the energy level such as QoS guarantees, adaptability, and security. QoS and adaptability is most crucial during communication process in Ad hoc network which are found missing in most of the routing protocol being proposed. Therefore, new optimization techniques or energy-efficient routing protocol that address QoS and adaptability need to be developed.

## References

1. Saxena, N., Chaudhari, N.S.: Message Security in Wireless Networks: Infrastructure based vs. Infrastructureless Networks. IEEE, New Jersey (2012)
2. Singh, Y., Siwach, M.V.: Quality of service in MANET. Int. J. Innov. Eng. Technol. 2012
3. Yang, H., Luo, H., Ye, F., Songwu, L., Zhang, L.: Security in mobile Ad hoc networks: challenges and solutions. Wirel Commun IEEE **11**(1), 38–47 (2004)
4. Zhao, Q., Tong, L.: Energy-efficient adaptive routing for Ad hoc networks with time-varying heterogeneous traffic. In: ICASSP, IEEE International Conference, vol. 5, pp. v-801 (2005)
5. Kim, K.W., Lee, J.S., Hwang, K.J., Kim, Y.K., Lee, M.M., Chung, K.T., Chon, B.S.: LRCA: enhanced energy-aware routing protocol in MANETs. Adv. Artif. Intell. 897–901 (2006)
6. Shin, K., Park, K., Chung, M.Y., Choo, H.: Energy efficient route discovery for mobile HCI in ad-hoc networks. In: Human Interface and the Management of Information, Interacting in Information Environments, pp. 635–644. Springer, Berlin (2007)
7. Loganathan, D., Ramamoorthy, P.: Performance analysis of enhanced DSDV protocol for efficient routing in wireless Ad hoc networks. Int. J. Eng. Sci. **2**(10), 01–08 (2013)
8. Karuppanan, K., Mahalaksmi, S.: Enhanced optimized link state routing protocol for VANET using fuzzy rough set. Int. J. Electr. Comput. Sci. Eng. **04**, 2333–2343 (2012). ISSN: 2277-1956
9. Kim, H., Han, S., Song, J.: A routing protocol for throughput enhancement and energy saving in mobile Ad hoc networks. In: Computational Science and Its Applications—ICCSA 2006, pp. 359–368, Springer, Berlin (2006)
10. Shivashankar, S.H.N., Golla, V., Jayanthi, G.: Designing Energy Routing Protocol with Power Consumption Optimization in MANET. IEEE, New Jersey (2013)

11. De Rango, F., Fotino, M., Marano, S.: EE-OLSR: energy efficient OLSR routing protocol for mobile ad-hoc networks. In: Military Communications Conference, IEEE, pp. 1–7 (2008)
12. Sheng, L., Shao, J., Ding, J.: A novel energy-efficient approach to DSR based routing protocol for Ad hoc network. In: International Conference on Electrical and Control Engineering, International Conference, pp. 2618–2620. IEEE (2010)
13. Vazifehdan, J., Venkatesha Prasad, R., Niemegeers, I.: Energy-efficient reliable routing considering residual energy in wireless Ad hoc networks. *IEEE Trans. Mobile Comput.* **13**(2) (2014)
14. Fahrnv, I.M.A., Hefny, H.A., Nassef, L.: PEEBR: predictive energy efficient bee routing algorithm for ad-hoc wireless mobile networks. In: The 8th International Conference on INFormatics and Systems (INFOS2012), pp. NW-18. IEEE, 14–16 May 2012
15. Rekha, S.N., Chandrasekar, C., Kaniezhil, R.: Efficient routing algorithm for MANET using Grid FSR. In: The International Proceedings of Computer Science and Advancement in Information (IPCSIT), vol. 20, pp. 86–92. Singapore (2011)
16. Ur Rahman Khan, K., Reddy, A.V., Zaman, R.U., Reddy, K.A., Harsha, T.S.: An efficient DSDV routing protocol for MANET and its usefulness for providing Internet access to Ad hoc hosts. In: TENCON 2008-2008, IEEE Region 10 Conference, pp. 1–6 (2008)
17. Chettibi, S., Chikhi, S.: FEA-OLSR: an adaptive energy aware routing OLSR: an adaptive energy aware routing OLSR: an adaptive energy aware routing protocol for MANETs using zero-order sugeno fuzzy system. *Int. J. Comput. Sci. Issues* **10**(2), 1 (2013)
18. Roy, A., Hazarika, M., Debbarma, M.K.: Energy efficient cluster based routing in manet. In: International Conference on Communication, Information and Computing Technology (ICCICT), pp. 1–5. IEEE (2012)
19. Mangai, S.V., Tamilarasi, A.: A new approach to geographic routing for location aided cluster based MANETs. *EURASIP J. Wirel. Commun. Netw.* **1**, 1–10 (2011)
20. Kumar, S.D., Kumar, C., Mandal, S.: An efficient cluster based routing protocol for MANET. In: Advance Computing Conference (IACC), IEEE 3rd International, pp. 224–229 (2013)
21. Verma, S.B.: Energy efficient routing in MANET with ZRP and anycast. *Int. J. Comput. Sci. Mobile Comput.* **2**(7), 296–301 (2013)
22. SreeRangaRaju, M.N., Mungara, J.: Tuning ZRP framework for CR networks and MANETs. In: Performance Computing and Communications Conference (IPCCC), 2010 IEEE 29th International, pp. 289–293 (2010)



# Construction of Co-expression and Co-regulation Network with Differentially Expressed Genes in Bone Marrow Stem Cell Microarray Data

Paramita Biswas, Bandana Barman and Anirban Mukhopadhyay

**Abstract** It is important to understand the interaction mechanism among co-expressed and co-regulated genes in stem cell to restrict the abnormal growth of cell tissues (tumor) which may lead to cancer. In this article, differentially co-expressed and co-regulated genes exist in normal stem cells and stem cell derived tumors are identified from sample Bone Marrow microarray data. By performing statistical t-test between sample groups, first we have identified differentially expressed genes (DEG). Then up-regulated (UR) and down-regulated (DR) genes are separated by setting a  $p$ -value cutoff at 0.001. After identifying the differentially expressed genes, distinguished co-expressed up-regulated and down-regulated genes are found. Subsequently, we have constructed pair-wise co-expression networks with the co-expressed genes. Finally, we have studied the significance of co-expressed genes with gene ontology (GO) and we have found significant GO-ids. This study is expected to lead to finding of pathways for diseases.

**Keywords** Stem cell · Differentially expressed genes · t-test · Gene ontology · Co-regulated and co-expressed genes

---

P. Biswas · A. Mukhopadhyay (✉)  
Department of Computer Science and Engineering, University of Kalyani,  
Kalyani 741235, West Bengal, India  
e-mail: anirban@klyuniv.ac.in

P. Biswas  
e-mail: paramita.biswas1991@gmail.com

B. Barman  
Department of Electronics and Communication Engineering, Kalyani Government  
Engineering College, Kalyani 741235, West Bengal, India  
e-mail: bandanabarman@gmail.com

## 1 Introduction

Stem cells [1] have remarkable potential i.e. atypical characteristics to develop into many different cell types in the body during growth of early life. Sometimes, the unrestricted growth of stem cells or the abnormal growth of cell tissue causes cancer. Stem cells are distinguished from other cell types by two important characteristics. First, they are unspecialized cells capable of renewing themselves through cell division or sometimes after long periods of inactivity. Second, under certain physiologic or experimental conditions, they can be induced to become tissue or organ-specific cells with special functions. Researchers primarily worked with two kinds of stem cells: embryonic stem cells and non-embryonic “somatic” or “adult” stem cells. The induced pluripotent stem cells (iPSCs) [2–4] are some specialized adult cells which “reprogrammed” genetically to assume a stem cell like state in special condition. This property is unique property of stem cell it can be explored by gene expression analysis. Microarray gene expression data to predict and analysis of cancer disease becomes very important. These data can be characterized by genome variables and with their corresponding observations (experiments) in a experimental limitations [5]. To discover co-regulated genes, analysis of gene expression data [6] is required. Previously, it has been assumed that similar patterns in gene expression profiles usually suggest relationships between the genes. Now it is proved genes targeted by same transcription factors, tend to show similar expression patterns along time. Analyzing expression profiles of genes, targeted by same transcription factors revealed complex relationships between co-regulated gene pairs and it also includes co-expression relationships. In this article, we developed a simple algorithm to find differentially co-expressed and co-regulated genes, and then, to construct pairwise co-expression network. We applied the algorithm on sample gene expression microarray data of normal stem cells (*nscr*), stem cells derive tumors cells (*scdtr*) and patch tumor cells (*ptr*).

## 2 Materials and Methods

For finding and analyzing the relationship between differentially co-expressed genes (DCEG), many techniques have been developed in the literature. Here, we applied statistical t-test [7, 8] and Benjamini Hochberg method [9] to identify differentially expressed genes (DEG) [10] within sample groups of *nscr* and *scdtr*, *nscr* and *ptr* (<http://www.ncbi.nlm.nih.gov/GSE20948>). In addition to this, we have studied the significance of up-regulated and down-regulated genes. We code the algorithms with using Matlab. The main steps of proposed algorithms are discussed in the following subsections.

## 2.1 Preprocessing of the Dataset

Our sample Bon Marrow microarray gene expression data is in normalized form. Normalized data for each gene is typically known as an ‘expression ratio’ or as the logarithm of expression ratio. We have done data preprocessing with filtered out low expressed values and null values from the datasets.

## 2.2 Identification of Differentially Co-expressed Genes

In this section, we discuss the steps to identify DEG. First, a standard statistical t-test is performed for detecting significant changes between measurements of genes in sample microarray groups. It may occur two types of errors, 1: a false positive by declaring that a gene is differentially expressed when it is not, and 2: a false negative when the test fails to identify a truly differentially expressed gene. Second, Benjamini Hochberg method [9] is used for choosing significantly differentially expressed genes. It is done by the following equation:

$$P \leq y * \frac{\alpha}{m}, \quad (1)$$

where  $P$  is the largest  $p$ -value called significant,  $y$  is the number of genes called significant and  $m$  is the total number of genes tested,  $\alpha$  is false discovery rate (FDR) [11, 12], defined as the expected ratio of the number of false positives to the total number of positive calls in a differential expression analysis between two sample groups [11]. FDR can be measured [11] as,

$$FDR = Err \left[ \frac{F}{F + T} \right] = Err \left[ \frac{n_0 \cdot [1 - specificity]}{n_0 \cdot [1 - specificity] + n_1 \cdot sensitivity} \right], \quad (2)$$

where  $F$  is the number of false positives,  $T$  is the number of true positives, and  $S$  is the total number of features called significant. Also,  $n$ , number of  $p$ -values is seen more clearly,  $n_0$  is the number of truly null features in the study, and  $n_1 = n - n_0$  is the number of truly alternative features. Regardless of whether the  $p$ -value threshold is fixed or data-dependent, the quantities  $F$ ,  $T$  and  $S$  are random variables. Therefore, it is common statistical practice to write the overall error measure in terms of an expected value, which we denote by  $Err$  [11].

## 2.3 Proposed Algorithm

**Input:** phenotype1: gene expression values of normal stem cell (*nscr*),  
 phenotype2: gene expression values of stem cell derive tumor (*scdtr*),  
 phenotype3: gene expression values of patched tumor (*ptr*).

- Output:** All differentially expressed genes.
- Step1:** Perform two-sample t-test to evaluate differential expression of genes from phenotype1 and phenotype2. Their  $p$ -values and t-scores are stored.
- Step2:** Perform a permutation t-test to compute the  $p$ -values of 10,000 permutations by permuting the columns of the gene expression data matrix of phenotype1 and phenotype2.
- Step3:** Determine the number of genes considered to have statistical significance at the  $p$ -value 'cutoff' of 0.001.
- Step4:** Estimate FDR for the genes with statistically significant  $p$ -values.
- Step5:** Create a scatter plot of gene expression data, plotting significance versus fold change of gene expression ratios of phenotype1 and phenotype2.

## ***2.4 Separation of Up-regulated and Down-regulated Genes***

We plot the volcano plot of identified all differentially expressed genes as volcano plot (Fig. 4) of two phenotypes returns a structure containing information for genes that are considered to be both statistically significant and significantly differentially expressed. This information helps us to identify co-regulated genes, specially up-regulated and down-regulated genes. Now based on cutoff value (0.001), up-regulated and down-regulated genes are separated from the total set of differentially co-expressed genes.

## ***2.5 Extraction of Co-expressed and Co-regulated Genes***

To separate co-expressed and co-regulated genes from the identified DEG, we generate an algorithm and code the algorithm with using Matlab. DEGs which have the same  $p$ -value are called co-expressed genes. Up-regulated and down-regulated genes with similar  $p$ -values are known as co-expressed and co-regulated genes. Our proposed algorithm is as follows:

### **Algorithm**

- Input:** Exp: differentially expressed genes or up-regulated or down-regulated genes.
- Output:** All Co-expressed and Co-regulated genes.
- Step1:** Each distinct  $p$ -value of Exp and its respective position are stored in separate data vector and index vector.

**Step2:** These data vector  $p$ -values are compared with the  $p$ -values of the original data, and if they match then their corresponding information is extracted from Exp with the help of the index vectors.

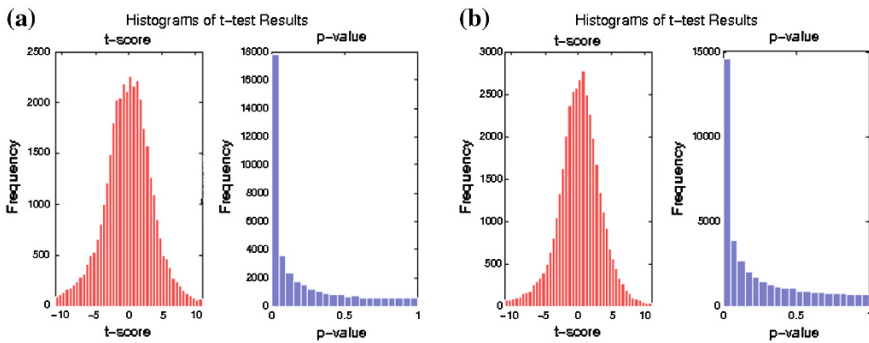
**Step3:** The process is repeated until all distinct data vector  $p$ -values are compared.

### 2.6 Visualization of Differentially Co-expression and Co-regulation Network

We constructed pair-wise co-expression network to understand the relationship among co-expressed and co-regulated genes. Co-expression networks are built depending on their corresponding  $p$ -values. We have used cytoscape software to visualize the pair-wise network. The genes having same  $p$ -value construct a paired structure.

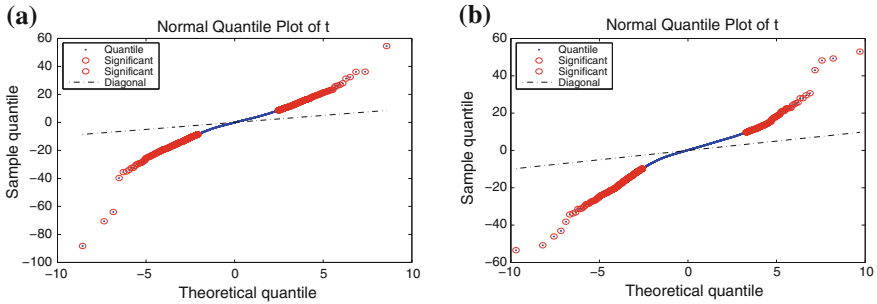
## 3 Results and Discussion

The Bon Marrow microarray data consists of 45,101 genes with having normal stem cell tissue ( $nscr$ ) responses (5no.), stem cell derived tumor tissue ( $scdtr$ ) responses (5no.) and patched tumor cell tissue ( $ptr$ ) responses (4no.) are taken for the study. After analysis, we considered only the genes having  $p$ -value  $\leq 0.001$  as significant genes (Figs. 1 and 2). Out of 45,101 genes from the dataset, 2,325 genes for sample first group ( $nscr$ – $scdtr$ ), 2,056 genes for sample second group ( $nscr$ – $ptr$ ) of data have been extracted on the basis of  $p$ -value which is approximately 5 % of total number of genes. Now, estimated false discovery rate (FDR) for statistically significant  $p$ -values are computed by using Eq. 2. As a result, we get 1,110, 792

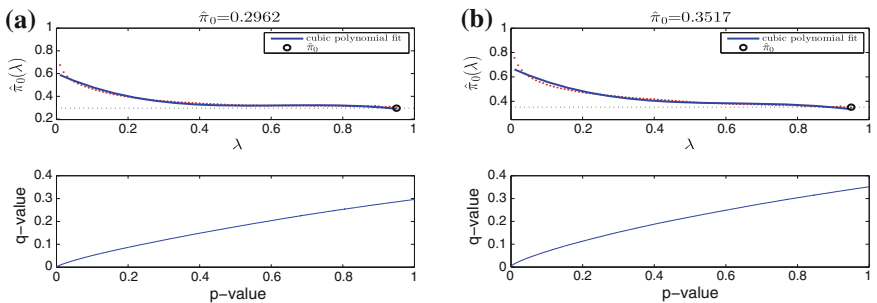


**Fig. 1** a Histogram plot of sample group  $nscr$  and  $scdtr$ . b Histogram plot of sample group  $nscr$  and  $ptr$

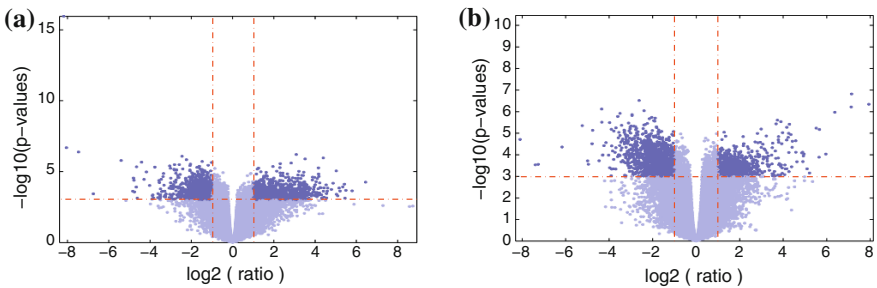
up-regulated and 1,215, 1,264 down-regulated genes for two sample groups (Figs. 3 and 4) respectively. It implies that 2–3 % genes of total 45,101 genes are up-regulated and down-regulated.



**Fig. 2** a Quantile plot of sample group *nscr* and *scdtr*. b Quantile plot of sample group *nscr* and *ptr*



**Fig. 3** a Fold change plot of sample group *nscr* and *scdtr*. b Fold change plot of sample group *nscr* and *ptr*

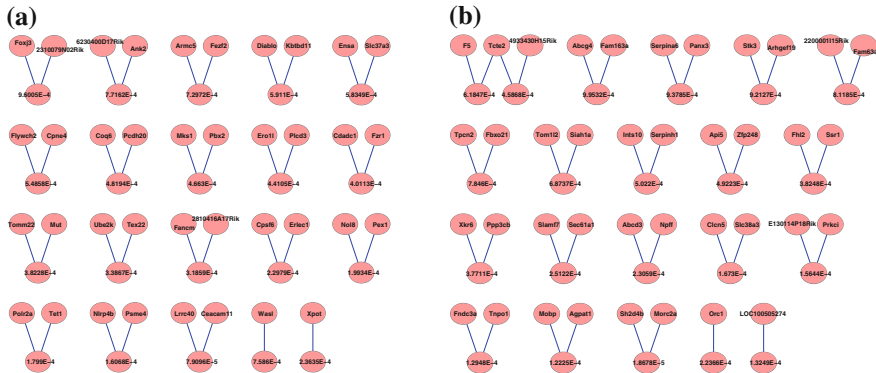


**Fig. 4** a Volcano plot of sample group *nscr* and *scdtr*. b Volcano plot of sample group *nscr* and *ptr*

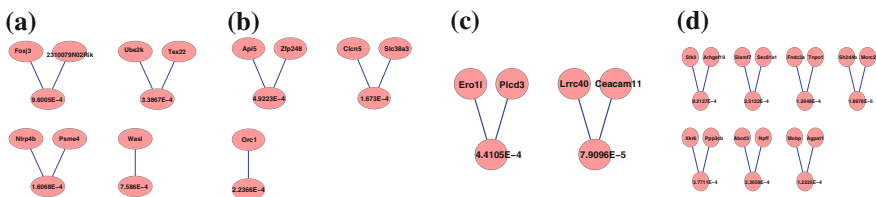
Further, with finding similar *p*-values co-expressed and co-regulated genes are extracted from all differentially co-expressed genes (DCEG), up-regulated (UR) and down-regulated (DR) genes. We get 8, 4 numbers of up-regulated and down-regulated genes for group1 i.e. approximately 0.01 and 0.008 % of total 45,401 genes. Again we get 6, 14 numbers of up-regulated and down-regulated genes for group2 i.e. approximately 0.01 and 0.03 % of the total 45,101 genes. It is shown in the Table 1. The interaction among co-expressed and co-regulated genes depending on corresponding *p*-values, 6 paired networks are developed (Figs. 5 and 6).

**Table 1** The table shows resulting differentially expressed and co-expressed genes of all sample groups

Samples	DEG	DCEG	UR-DEG	UR-DCEG	DR-DEG	DR-DCEG
<i>nscr</i> and <i>scdtr</i>	2,326	20 pairs	1,110	4 pairs	1,215	2 pairs
<i>nscr</i> and <i>ptr</i>	2,056	21 pairs	792	3 pairs	1,264	7 pairs



**Fig. 5** a Pairwise network of differentially co-expressed genes of sample group *nscr* and *scdtr*. b Pairwise network of differentially co-expressed genes of sample group *nscr* and *ptr*



**Fig. 6** a Pairwise network of differentially co-expressed up-regulated genes of sample group *nscr* and *scdtr*. b Pairwise network of differentially co-expressed up-regulated genes of sample group *nscr* and *ptr*. c Pairwise network of differentially co-expressed down-regulated genes of sample group *nscr* and *scdtr*. d Pairwise network of differentially co-expressed down-regulated genes of sample group *nscr* and *ptr*

Significance analysis for sample groups(nscr-scdtr)		
GO in BP	GO Term	Genes
GO in CC	GO:0000166~nucleotide binding	1447935_AT, 1434527_AT, 1426902_AT, 1417779_AT, 1419029_AT, 1428950_S_AT, 1417188_S_AT, 1428716_AT, 1437372_AT (P_Value=1.4E-3)
	GO:0030554~adenyl nucleotide binding	1447935_AT, 1434527_AT, 1426902_AT, 1417779_AT, 1419029_AT, 1417188_S_AT, 1428716_AT (P_Value=2.8E-3)
GO in MF	GO:0031974~membrane-enclosed lumen	1424693_AT, 1428950_S_AT, 1418893_AT, 1448486_AT, 1426242_AT, 1443116_AT, 1425768_AT(P_Value=2.4E-4)
	GO:0070013~intracellular organelle lumen	1424693_AT, 1428950_S_AT, 1418893_AT, 1448486_AT, 1443116_AT(P_Value=1.1E-3)
Significance analysis for sample groups(nscr-ptr)		
GO in BP	GO Term	Genes
GO in CC	GO:0046907~intracellular transport	1448695_AT, 1455043_AT, 1416190_A_AT, 1437915_AT (P_Value=3.5E-3)
	GO:0006915~apoptosis	1443112_AT, 1457590_AT, 1423390_AT, 1418512_AT(P_Value=4.2E-3)
GO in MF	GO:0005768~endosome	1427732_S_AT, 1448695_AT, 1429400_AT (P_Value=6.1E-3)
	GO:0016021~integral to membrane	1427732_S_AT, 1417764_AT, 1443863_AT, 1454387_AT, 1455043_AT, 1421025_AT, 1457590_AT, 1457112_AT, 1416190_A_AT, 1424304_AT, 1416679_AT, 1446013_AT, 1453472_A_AT, 1429400_AT (P_Value=6.5E-3)
GO in MF	GO:0005524~ATP binding	1427732_S_AT, 1448695_AT, 1416679_AT, 1443172_AT, 1457590_AT, 1418512_AT, 1429532_AT, 1429400_AT. (P_Value=1.2E-3)
	GO:0032559~adenyl ribonucleotide binding	1427732_S_AT, 1448695_AT, 1416679_AT, 1443172_AT, 1457590_AT, 1418512_AT, 1429532_AT, 1429400_AT (P_Value=1.2E-3)

Fig. 7 Significant genes analyzed with gene ontology

The significance of the identified DEG are studied and analyzed with Gene Ontology (GO). We have listed it in Fig. 7.

### 4 Conclusion

In this paper, we first found DEG and then found correlations between gene-pairs for construction of co-expressed and co-regulated networks under diseased conditions that assist the interpretability of network. We also generated pairwise differentially co-expression network and constructed the same for differentially co-expressed and co-regulated genes of Bone Marrow stem cell microarray data. We also analyze the significance of DEG for the same microarray data. From our



sample data we found 82 significantly co-expressed genes and 30 co-expressed and co-regulated genes. In future study, we can apply artificial intelligence based sophisticated techniques (fuzzy logic, neural networks, evolutionary computation) for better construction of cancer-specific regulatory networks.

## References

1. William, et al, J.B.: Functional recovery of spinal cord injury following application of intraslesional bone marrow mononuclear cells embedded in polymer scaffold-two year follow-up in a canine. *J. Stem Cell Res. Ther.* **1**(3) 2011
2. Hanna, J., et al.: Treatment of sickle cell anemia mouse model with iPS cells generated from autologous skin. *Science* **318**(5858), 1920–1923 (2007)
3. Saha, K., Jaenisch, R.: Technical challenges in using human induced pluripotent stem cells to model disease. *Cell Stem Cell* **5**(6), 584–595 (2009)
4. Jiang, Y., et al.: Pluripotency of mesenchymal stem cells derived from adult marrow. *Nature* **418**(6893), 41–49 (2002)
5. Vaishali, K., Vinayababu, A.: Application of microarray technology and soft computing in cancer biology: a review. *Int. J. Biometr. Bioinform.* **5**(4), 225–233 (2011)
6. Chen, J.J.: Key aspects of analyzing microarray gene-expression data. *Pharmacogenomics* **8**(5), 473–482 (2007)
7. Allen, et al. J.D.: Comparing statistical methods for constructing large scale gene networks. *PLoS ONE* **7**(1) (2012)
8. Vardhanabhuti, S., et al.: A comparison of statistical tests for detecting differential expression using affymetrix oligonucleotide microarrays. *OMICS* **10**(4), 555–566 (2006)
9. Benjamini, Y., Hochberg, Y.: Controlling the false discovery rate: a practical and powerful approach to multiple testing. *J. Roy. Stat. Soc.* **57**(1), 289–300 (1995)
10. Bandyopadhyay, S., Mallik, S., Mukhopadhyay, A.: A survey and comparative study of statistical tests for identifying differential expression from microarray data. *IEEE/ACM Trans. Comput. Biol. Bioinform.* **11**(1), 95–115 (2014)
11. Storey, J.D., Tibshirani, R.: Statistical significance for genome-wide studies. *Proc. Natl. Acad. Sci.* **100**(16), 9440–9445 (2003)
12. Storey, J.D., Taylor, J.E., Siegmund, D.: Strong control conservative point estimation and simultaneous conservative consistency of false discovery rates: a unified approach. *J. Roy. Stat. Soc.* **66**(1), 187–205 (2004)

# Identifying Two of Tomatoes Leaf Viruses Using Support Vector Machine

Usama Mokhtar, Mona A.S. Ali, Aboul Ella Hassanien  
and Hesham Hefny

**Abstract** One of the most harmful viruses is Tomato yellow leaf curl virus (TYLCV), which is widespread over the world with tomato yellow leaf curl disease (TYLCD). It causes some symptoms to tomato leaf such as upward curling and yellowing. This paper introduces an efficient approach to detect and identify infected tomato leaves with these two viruses. The proposed approach consists of four main phases, namely pre-processing, image segmentation, feature extraction, and classification phases. Each input image is segmented and descriptor created for each segment. Some geometric measurements are employed to identify an optimal feature subset. Support vector machine (SVM) algorithm with different kernel functions is used for classification. The datasets of a total of 200 infected tomato leaf images with TSWV and TYLCV were used for both training and testing phase. N-fold cross-validation technique is used to evaluate the performance of the presented approach. Experimental results showed that the proposed classification approach obtained accuracy of 90 % in average and 92 % based on the quadratic kernel function.

**Keywords** Image processing · K-Mean clustering algorithm geometric features · Support vector machine (SVM)

---

U. Mokhtar (✉) · H. Hefny  
Inst. of Stat. Studies and Res. (ISSR), Cairo University, Cairo, Egypt  
e-mail: usamamokhtar@yahoo.com

H. Hefny  
e-mail: hehefny@hotmail.com

M.A.S. Ali  
Faculty of Computers and Information, Minia University, Minya, Egypt  
e-mail: mony\_4it@yahoo.com

A.E. Hassanien  
Faculty of Computers and Information, Cairo University, Cairo, Egypt  
e-mail: aboitcairo@gmail.com

## 1 Introduction

Agriculture is one of the most serious for national income for most countries. Tomatoes are one of the most widely cultivated food crops throughout the world due to its high nutritive value. It contains a lot of vitamins and nutrients such that vitamin C. It occupies the fourth level between word vegetables. Egypt is one of the famous countries that interested in tomatoes cultivation. It ranked fifth among leader countries in the world [1].

Although farmers do great effort in selecting good seeds of plants and creating suitable environment for plants growing, there are a lot of diseases that effect on plants. There are many factors that cause plant diseases: Plant pathogens such as (fungi, Bacteria, and Virus diseases) are the principal reasons for plant disease. Also, there are some insect that feed on the parts of plant such as (sucking insect pests), and plant nutrition such as (lack of micro elements) also, have critical effect on plant growing [2]. Viral diseases are the most common diseases of tomatoes. The amount of damage they cause varies, depending on the particular virus or combination of viruses present, the virulence of the virus strains, the susceptibility of the variety, the timing of infection, the abundance of insect vectors, and environmental conditions [3].

Now a days, Automatic detection of plant diseases attracts a lot of researcher in different domains because of there great benefits in monitoring large fields of crops, and thus automatically detect the symptoms of diseases as soon as they appear on plant leaves [4, 5]. Several approaches have been already introduced for image segmentation. K-means algorithm [6–8] is the most popular method for image segmentation because of its ability to cluster huge data points very quickly [9].

In [10], a new hybrid approach for image segmentation proposed for the automatic classification of leaf diseases based on high resolution multispectral and stereo images. They used Leaves of sugar beet for evaluating their approach. In [11], authors used computer image processing technique to introduce fast and accurate new method for grading of plant diseases. At the beginning, leaf region was segmented by using Otsu method [12, 13]. To detect the disease spot edges the disease spot regions were segmented by using Sobel operator. Finally, plant diseases are graded by calculating the quotient of disease spot and leaf areas.

Machine learning methods can successfully be applied as an efficient approach for disease detection. Many of these methods have been applied in agricultural researches. For example: Artificial Neural Networks (ANNs), Decision Trees, K-means, k-nearest neighbors. Support Vector Machines (SVMs) one of these approach that have been used extensively in this field. For example, in [14] authors used SVMs to identify visual symptoms of cotton diseases. In [6] authors presented an image recognition approach for wheat diseases detection using multi-class support vector machines (SVMs) after calculating features of diseased image regions of wheat disease was proposed. After calculating leaf image, image samples are trained and recognized using multi-class RBF SVM. In [15] authors employed

the same classifier that trained and tested with some texture statistics features that have been computed for the useful segments.

In [1], an automated system has been developed to classify the leaf brown spot and the leaf blast diseases of rice plant based on the morphological changes of the plants caused by the diseases. Radial distribution of the hue from the center to the boundary of the spot images has been used as features to classify the diseases by Bayes' and SVM Classifier. In [16] author try to solve the difficulty of parameter determination in the original support vector machine (SVM) by using the genetic algorithm (GA) to select the parameters of the SVM automatically and the orthogonal method is utilized to determine the best GA parameters. In [17] Automated detection using vision system and pattern recognition are implemented to detect the symptoms of nutrient diseases and also to classify the disease group. In this paper, Support Vector Machine (SVM) is evaluated as classifier with four different kernels namely linear kernel, polynomial kernel with soft margin and polynomial kernel with hard margin.

This research aimed to develop a method that detect and identify type of virus that has infected tomato leaves. In order to decide if the infected tomatoes leaf is with TSWV or TYLCV image processing techniques have been used. The proposed approach is consisted of three main stages, image clustering, feature extraction and feature classification. To evaluate these results N-fold cross-validation has been used.

The remainder of this paper is ordered as follows. Section 2 review the basic conc algorithm. Section 3 shows the proposed new neutrosophic set. Section 3 describes the different phases of the proposed identifying two of tomatoes leaf viruses. Section 4 shows the experimental results and analysis. Finally, Conclusion and future work are discussed in Sect. 5.

## 2 Preliminaries

### 2.1 *K-Means Clustering Algorithm*

Image Segmentation is considered as one of the most important techniques for image analysis as well as in high-level image understanding images and extracting the information from them that can be used for different tasks such that robot vision, object recognition, and medical imaging. The goal of image segmentation is to partition an image into a set of disjoint regions with uniform and homogeneous attributes such as intensity, colour, tone or texture, etc. The image segmentation approaches can be divided into four categories: thresholding, clustering, edge detection and region extraction [18]. K-means clustering algorithm is the most popular method for image segmentation. K-Means algorithm is an unsupervised clustering algorithm that can use for classifying the input data into K groups that

called clusters. These clusters are non-hierarchical and they do not overlap. Every member of a cluster is closer to its cluster than any other cluster.

## 2.2 The Support Vector Machine

The support vector machine (SVM) is a type of classifier that is originally a binary Classification method developed by Vapnik and colleagues at Bell laboratories [19, 20]. The main advantages of SVM are: It can obtain current optimal solution under finite samples; it can obtain the global optimal solution without falling into local optimums that normal algorithms have; it transforms nonlinear problems into linear problems in a higher dimension space, and the algorithm complexity is unrelated with space dimension [21]. To explain idea of SVM we will discuss the following two cases.

### The Separable Case

*Fully Linearly Separable* For a binary classification problem with input space  $X$  and binary class  $Y$  where  $y \in \{-1, 1\}$ . There may exist many separating hyper-planes that correctly classify the data. The goal of SVM is selecting between them the one that maximizes the distance between the separating hyper-planes. The goal of SVM is to search for the optimal

$$w \cdot x + b = 0 \quad (1)$$

where  $w$  is normal to the hyperplane. Since SVM search for the separating hyperplane with largest margin. This can be formulated as follows:

$$y_i(x_i \cdot w + b) - 1 \geq 0 \quad \forall i \quad (2)$$

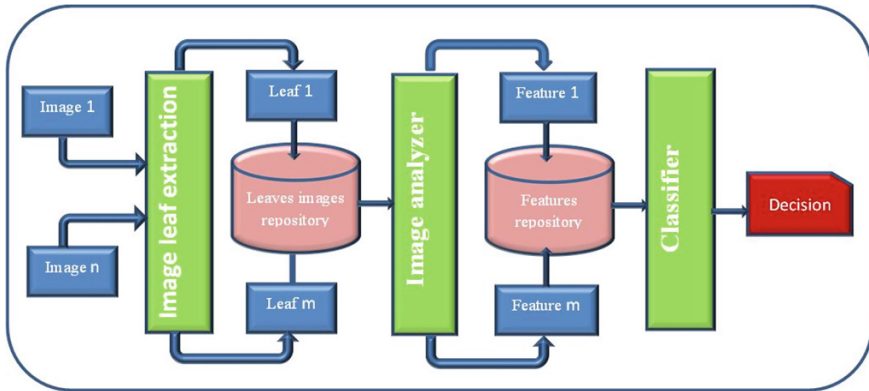
### Not Fully Linearly Separable

In order to extend the SVM methodology to handle data that is not fully linearly separable, we relax the constraint 2 slightly to allow for misclassified points as follow:

$$y_i(x_i \cdot w + b) - 1 \geq 0 + \epsilon_i \quad \text{where } \epsilon_i \geq 0 \quad \forall i \quad (3)$$

## 3 The proposed identifying of tomatoes leaf viruses

In general, most computer vision algorithms share a common Framework. Figure 1 depicts the layout structure of a common image processing-based disease detection algorithm.



**Fig. 1** Over all system structure

The algorithm begins with acquiring and collecting digital images from suitable environment. To prepare the acquired images to next step, image-processing techniques are applied such that image transformation, image resizing, image filtering etc. the next step is to segment image using a suitable image segmentation technique such that Clustering, edge detection, region growing to extract the infected part of leaf image. Then we extract useful features that are necessary for further analysis using suitable feature extraction techniques. These features may be color, shape texture features. After that, several analytical discriminating techniques are used to classify the images according to the specific problem. Figure 2 shows the overall architecture of the proposed identifying two of tomatoes leaf viruses using Support Vector Machine.

### 3.1 Image Acquisition

The first stage of this approach is the image acquisition stage. This phase plays an important role in any image classification system. We must select these images carefully to achieve the intended task in this approach. Science, the aim of this article is to distinguish between two types of virus, TSWV and TYLCV that infect tomatoes leaves, for this work we collected different specimens of infected tomatoes leaves for each type of virus from the internet [22]. Since, some of these images contain more than one tomato leaves, therefore we addressed this issue in the preprocessing stage, for more details see the next section at the end of this phase we have 200 image of infected tomato leaves 100 for each virus type.

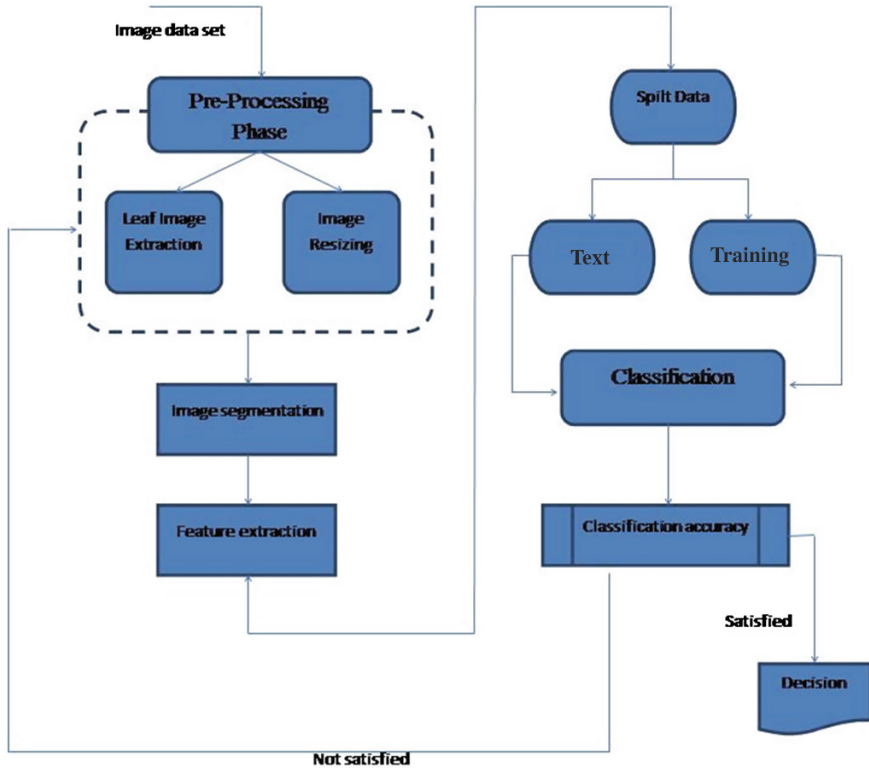


Fig. 2 The layout structure of the proposed system

### 3.2 Pre-processing

To increase the efficiency of the classification and prediction process, a pre-processing phase should be considered to enhance the quality of the input tomato leaves images and to make the feature extraction phase more reliable. It can be decomposed into the following two steps:

#### Extracting image of tomato leaves from the acquired images

As we mention before, most of acquired images have more than one leaf image and may be other things, since the aim of this research is to identify type of virus that affect tomato leaf, we need to deal with single tomato leaf at a time. In order to achieve that, these images have been manually cropped to extract a single leaf that is saved in jpeg format.

#### Image Resizing

In this work, all images must be with the same size and equal dimensions. So, the gray image should be resized to equal dimensions.

### 3.3 Image segmentation phase

In this paper, in order to extract regions of interest, we have selected the most frequently used K-Mean clustering algorithm. Since it is challenging to visually distinguish between colors of leaf images, we have been used The  $L^* a^* b$  color space that also known as CIELAB or CIE  $L^* a^* b$  hence, it enables us to quantify these visual differences. The  $L^* a^* b$  color space is derived from the CIE XYZ tristimulus values. The  $L^* a^* b$  space consists of a luminosity  $L^*$  or brightness layer, chromaticity layer  $a^*$  indicating where color falls along the red-green axis, and chromaticity layer  $b^*$  indicating where the color falls along the blue-yellow axis [23].

### 3.4 Feature Extraction Phase

After the leaf image has been segmented and isolated the infected parts of leaf, the next step is to extract some useful features. The purpose of feature extraction is to reduce the original dataset by measuring certain features or properties of each image such as texture, color and shape. In the proposed approach, we measure two types of features, geometric features and histogram feature to be later use for classification.

#### Geometric Features

At this stage, we need to calculate some geometric features (refer to [24]).

- Image Length: The total length of infected part of leaf is calculated.
- Image Area: Compute area of infected part of leaf.
- Image Area Estimate: Compute area of infected part of leaf with respect to edges and corners.
- Image Perimeter: Compute perimeter of infected part of leaf.
- Euler number: In this stage, we compute the Euler number, or Euler Poincare characteristic, of a infected part of image that correspond to the number of connected components in the image.

#### Histogram Feature

In this step we calculate histogram to image in HSV color space. So we first convert image from RGB color V color space. Then image must be quantized in  $8 * 2 * 2$  equal bins.



### 3.5 Classification Phase

The final step of this work is a classification phase, in this approach, SVM technique has been applied for classification of tomato leaf image to any of the following states, infected with TSWV or with TYLCV. The inputs of this stage are training dataset feature vectors and their corresponding classes, whereas the outputs are the decision that determines type of virus that infected tomato leaf. To achieve good results, SVM was trained and tested using different kernel functions that are: Linear kernel, radial basis function (RBF) kernel, QP kernel, Multi-Layer Perceptron (MLP) kernel and Polynomial kernel [25, 26].

For the process of evaluating the results, we used N-fold cross-validation technique [27] with  $N = 10$ , firstly, dataset is divided into equally (or nearly equally) N-subsets. Then the cross-validation process is performed N times with each sub-set being once the test dataset and all the others being the training dataset. This process is repeated N times. Hence we take the average of performance of N runs. The algorithm performance measure can be calculated as the average of the performances of 50 runs.

## 4 Experimental Results

As we mention before the aim of this work is to detect and identify type of virus that infected tomato leaves. here we focus on two types of virus TSWV and TYLCV. Tomato spotted wilt is caused by a virus that is usually spread by thrips. Tomato plants that infected with spotted wilt become stunted and often die. Initially, leaves in the terminal part of the plant stop growing, become distorted, and turn pale green. In young leaves, veins thicken and turn purple, causing the leaves to appear bronze. Necrotic spots, or ring spots, are frequently present on infected leaves and stems often have purplish-brown streaks [28]. Figure 3 illustrates an example of tomato plant image infected with TSWV.

Tomato yellow leaf curl disease (TYLCV) caused by the whitey-transmitted begomovirus (genus Begomovirus, family Geminiviridae) is one of the most damaging diseases of tomato. [29] If virus infected tomato plants at a young stage, tomato plants can be severely stunted and will not produce fruit. Foliage shows an upright or erect growth habit, leaves curl upwards and may be crumpled. Interveinal chlorosis is also observed in the leaves. Figure 4 illustrates an example of tomato plant image infected with TYLCV.

After we collected some prototypes of infected tomato leaves for each type of virus, we cropped them to extract single tomato leaf for each image. K-mean clustering algorithm has been employed to extract regions of interest. Figure 5 demonstrates sample resultant images before and after the segmentation.

**Fig. 3** Leaf lesions due to Tomato spotted wilt virus on tomato

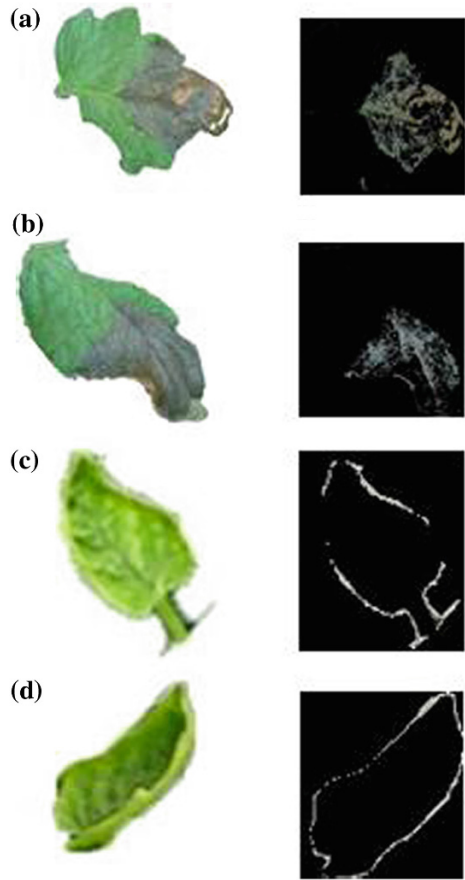


**Fig. 4** Yellow, distorted tomato foliage caused by Tomato yellow leaf curl virus



After preprocessing phase is done, we calculated some geometric features and histogram as we mention before that constrict feature vectors. The last phase is the classification and prediction of new objects, it is dependent on the support vector machine (SVM). SVM was trained and tested using different kernel functions that are: (Linear kernel, (RBF) kernel, QP kernel, (MLP) kernel and Polynomial kernel). Figure 6 shows the overall accuracy of the classification based on different SVM kernel functions. The Quadratic (QP) kernel function shows the better accuracy classification accuracy.

**Fig. 5** 9-a, 9-b are samples of Leaf infected with TSWV before and after clustering, 9-c, 9-d are samples of Leaf infected with TYLCV before and after clustering



**Fig. 6** Results for different SVM kernel functions



## 5 Conclusions and Future Works

Support vector machine (SVM) algorithm with different kernel functions is used for classification and identifying two of tomatoes leaf viruses. The datasets of total 200 infected tomato leaf images with TSWV and TYLCV were used for both training and testing phase. N-fold cross-validation technique is used to evaluate the performance of the presented approach. Experimental results showed that the proposed classification approach has obtained with accuracy of 90 % in general and the highest classification accuracy of 91.5 % has been achieved using Quadratic kernel function. Our future works will focus on detection and identification other types of virus that infect tomato plants.

## References

1. Peralta, I.E., Spooner, M.D., Razdan, M.K. Mattoo, A.K.: History, origin and early cultivation of tomato (Solanaceae). *Genet Improv Solanaceous Crops Tomato* **2** (2007)
2. Agrios, G.N.: *Plant Pathology*, 4th edn. Academic Press (1997)
3. Sikora, E.J.: *Virus diseases of tomato*. ANR-0836 (2011)
4. Rumpf T., Mahlein, A.K., Steiner, U., Oerke, E.C., Dehne, H.W., Plümer L.: Early detection and classification of plant diseases with support vector machines based on hyperspectral reflectance. *Comput. Electron. Agric.* **47**(1), 91–99 (2010)
5. Hillnhuetter, C., Mahlein, A.K.: Early detection and localisation of sugar beet diseases: new approaches. *Gesunde Pflanzen* **60**(4), 143–149 (2008)
6. Lin, W.T., Lin, C.H., Wu, T.H., Chan, Y.K.: Image segmentation using the k-means algorithm for texture features. *World Acad. Sci. Eng. Technol.* **65** (2010)
7. Goclawski, J., Sekulska-Nalewajko, J., Gajewska, E., Wielanek, M.: An automatic segmentation method for scanned images of wheat root systems with dark discolourations. *Int. J. Appl. Math. Comput. Sci.* **19**(4), 679–689 (2009)
8. ISA, N.A.M.: Automated edge detection technique for Pap smear images using moving K-means clustering and modified seed based region growing algorithm. *Int. J. Comput. Internet Manage.* **13**(3), 45–59 (2005)
9. Gonzales, R.C., Richard, E.W.: *Digital image processing*, 2nd edn. (2002)
10. Valliammal, N., Geethalakshmi, S.N.: Plant leaf segmentation using non linear K means clustering. *Int. J. Comput. Sci. Issues (IJCSI)* **9**(3), 212–217 (2012)
11. Weizheng, S., Yachun, W., Zhanliang, C., Hongda, W.: Grading method of leaf spot disease based on image processing. In: *Proceedings of IEEE International Conference on Computer Science and Software Engineering*, vol. 6, pp. 491–494 (2008)
12. Sezgin, M.: Survey over image thresholding techniques and quantitative performance evaluation. *J. Electron. Imaging* **13**(1), 146–168 (2004)
13. Otsu, N.: A threshold selection method from gray level histograms. *IEEE Trans. Syst. Man Cybern* **9**(1), 62–66 (1979)
14. Camargo, A., Smith, J.S.: An image-processing based algorithm to automatically identify plant disease visual symptoms. *Biosyst. Eng.* **102**(1), 9–21 (2009)
15. Arivazhagan, S., Shebiah, R.N., Ananthi, S., Varthini, S.V.: Detection of un-healthy region of plant leaves and classification of plant leaf diseases using texture features. *Agric. Eng. Int. CIGR J.* **15**(1), 211–217 (2013)
16. Tian, J., Hu, Q., Ma, X.X., and Han, M.: An improved kpca/ga-svm classification model for plant leaf disease recognition. *J. Comput. Inf. Syst.* **8**(18), 7737–7745 (2012)

17. Asraf, H.M., Nooritawati, M.T., Rizam, M.S.B.: A comparative study in kernel-based support vector machine of oil palm leaves nutrient disease. *Procedia Eng.* **41**, 1353–1359 (2012)
18. Fu, K.S., Mui, J.K.: A survey on image segmentation. *Pattern Recogn.* **13**(1), 3–16 (1981)
19. Vapnik, V.: *The nature of statistical learning theory*. Springer (2000)
20. Burges, C.J.C.: A tutorial on support vector machines for pattern recognition. *Data Min. Knowl. Disc.* **2**(2), 121–167 (1998)
21. Zhang, W., Jin, X.: Image recognition of wheat disease based on RBF support vector machine. In: *Proceedings of the International Conference on Advanced Computer Science and Electronics Information (ICACSEI 2013)*. Atlantis Press (2013)
22. <http://www.ipmimages.org>
23. Subbaiah, V., Aparna, G.S., Gopal, D.V.R.S.: Computer aided molecular modeling approach of H & E (Haematoxylin & Eosin) images of colon cancer. *Int. J. Comput. Appl.* **44**(9), 5–8 (2012)
24. Legland, D., Kiêu, K., Devaux, M.F.: Computation of minkowski measures on 2d and 3d binary images. *Image Anal. Stereology* **26**(2), 83–92 (2011)
25. Vanschoenwinkel, B., Manderick, B.: Appropriate kernel functions for support vector machine learning with sequences of symbolic data. *Deterministic Stat. Methods Machine Learn.* 256–280 (2005)
26. Boolchandani, D., Sahula, V.: Exploring efficient kernel functions for support vector machine based feasibility models for analog circuits. *Int. J. Des. Anal. Tools Circuits Syst.* **1**(1) (2011)
27. Prekopcsák, Z., Henk, T., Gáspár-Papanek, C.: Cross-validation: the illusion of reliable performance estimation. In: *RCOMM RapidMiner Community Meeting and Convergence* (2010)
28. Sikora, E.J., Gazaway, W.S.: *Wilt Diseases of Tomatoes*. Published by the Alabama Cooperative extension system. Reviewed for web June 2009, Anr-0797
29. Rojas, M.R., Kon, T.: First report of tomato yellow leaf curl virus associated with tomato yellow leaf curl disease in California. *Am. Phytopathol. Soc.* **91**(8), 1056 (2007)
30. Al Bashish, D., Braik, M., Sulieman B.A.: Detection and classification of leaf diseases using K-means-based segmentation and neural-networks-based classification. *Inf. Technol. J.* **10**(2), 267–275 (2011)
31. Phadikar, S., Sil, J., Das, A.K.: Classification of rice leaf diseases based on morphological changes. *Int. J. Inf. Electron. Eng.* **2**, 460–463 (2012)

# A Hierarchical Convex Polygonal Decomposition Framework for Automated Shape Retrieval

Sourav Saha, Jayanta Basak and Priya Ranjan Sinha Mahapatra

**Abstract** With the increasing number of images generated every day, textual annotation of images becomes impractical and inefficient. Thus, content-based image retrieval (CBIR) has received considerable interest in recent years. Keeping it as the primary motivational focus, we propose a method which exploits different degrees of convexity of an object's contour using a multi-level tree structured representation called Hierarchical Convex Polygonal Decomposition (HCPD) tree and the method also uses a special spiral-chain-code to encode the polygonal representation of decomposed shape at every node. The performance of the proposed scheme is reasonably good and comparable with existing state-of-the-art algorithms.

**Keywords** Convex polygon · Content based shape retrieval · Shape representation

## 1 Introduction

Due to the recent developments in digital imaging technologies, an increasing number of images are generated every day. In today's tech-savvy world, internet boom is continually driving interest in people to retrieve images of their interest from large data-pool. In order to achieve this task, images have to be represented by

---

S. Saha (✉) · J. Basak

Department of Computer Science and Engineering, Institute of Engineering and Management, Kolkata, India  
e-mail: souravsaha1977@gmail.com

J. Basak

e-mail: lettertojayanta@gmail.com

P.R.S. Mahapatra

Department of Computer Science and Engineering, University of Kalyani, Kalyani, West Bengal, India  
e-mail: priya\_cksly@yahoo.co.in

© Springer India 2015

J.K. Mandal et al. (eds.), *Information Systems Design and Intelligent Applications*, Advances in Intelligent Systems and Computing 339, DOI 10.1007/978-81-322-2250-7\_78

783

specific features. Early attempts tried to use textual annotation of images and then search images using their annotations. Clearly, this method is not practical for large databases. In addition, the textual annotation of image content by itself is a difficult and subjective process. Therefore, searching images using generic features has received considerable attention in recent years. Shape is considered the most promising for the identification of entities in an image. It can be argued that most real subjects are easily identified using only their silhouettes. A user survey in [1] indicated that 71 % of the users were interested in retrieval by shape. Shape is a concept which is widely understood yet difficult to define formally. The human perception of shapes is a high-level concept whereas mathematical definitions tend to describe shape with low-level features. However, for 2-D objects, Marshall [2] tried to define shape as a function of position and direction of simply connected curves within the two-dimensional field. Shape is important visual information that has received much attention from researchers in pattern recognition and computer vision in the past few decades. Most existing techniques for shape analysis and recognition are concerned with single-object shapes, i.e. the silhouette of an object. The main motivation of this research work is to focus on the geometric information, including shape and topology, for content-based image retrieval.

### ***1.1 Related Work***

In the past, contour and skeleton were usually used to analyze and represent the shape of objects. Contour-based is an important aspect of human visual perception. Polygonal approximation has been a very popular shape representation technique. It not only satisfactorily represents a shape, but also significantly reduces the amount of processing data for further applications. Therefore, many shape recognition (matching) methods through polygonal approximation [3] have been proposed. However, some conventional methods are somewhat sensitive to non-consistent results of polygonal approximation. Latrcki and Lakamper [4] proposed a convexity rule for shape decomposition based on discrete contour evolution. They concentrate some of decomposition of 2D objects into meaningful visual parts and proposed a contour evaluation method for identifying the visual part whether it is a significant convex part or not. The skeleton is another important method for object representation and recognition. Skeleton-based representations are the abstractions of objects, which contains both shape features and topological structures of original objects. Many researchers have made efforts to recognize the generic shape by matching skeleton structures represented by graphs or trees [5]. Unfortunately, these approaches have only demonstrated the applicability to objects with simple and distinctive shapes, and therefore, cannot be applied to more complex shapes like shapes in a MPEG-7 data set [6]. In this paper, we propose a method which exploits the different degrees of convex properties of contour curvature using multi-level tree structured representation called Hierarchical Convex Polygonal Decomposition (HCPD).

## 2 Proposed Scheme

The main objective of this research is to develop, implement and evaluate a prototype system for multi-level shape matching and retrieval. We model shape of image objects using a tree structured representation called Hierarchical Convex Polygonal Decomposition (HCPD). The hierarchy of the HCPD reflects the inclusion relationships between the objects' various curvatures along the boundary. To facilitate shape-based matching, a new spiral-chain code for each convex polygon is stored at the corresponding node in the HCPD. The similarity between two HCPD s is measured based on the maximum similarity at every level of the HCPD-tree, where a one-to-one correspondence is established between the nodes of the two trees. An effective string matching algorithm, called Fuzzy Levenshtein edit distance [7], is used to measure the similarity between the shape-attributed nodes' spiral-chain code representation of a polygon (Fig. 1).

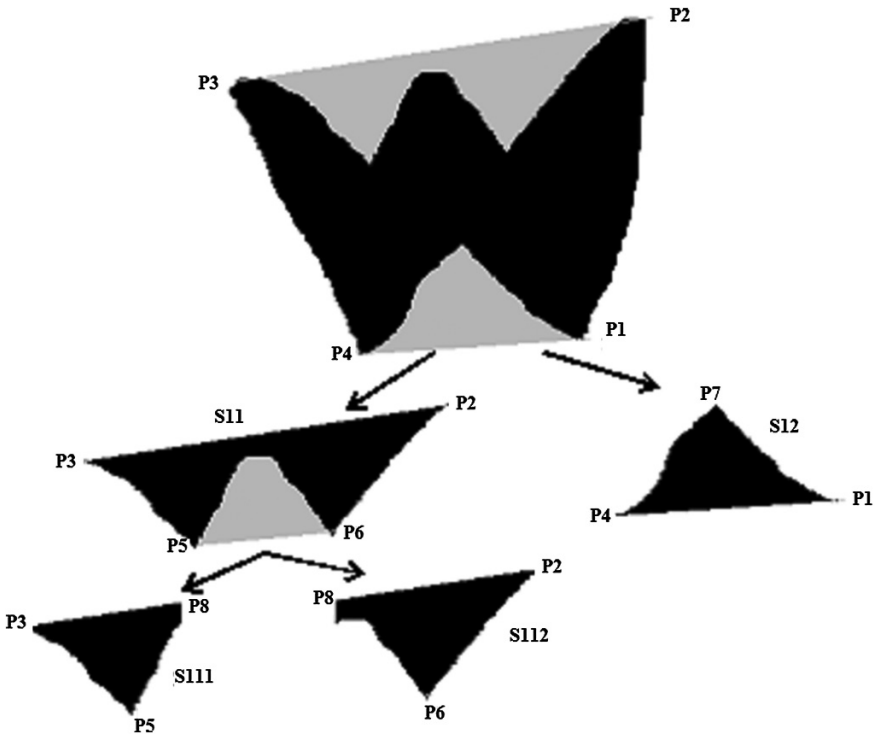


Fig. 1 Hierarchical convex polygonal decomposition



## 2.1 Hierarchical Convex Polygonal Decomposition

Given a binary image, our proposed method hierarchically decomposes the shape into several disconnected convex and non-convex sub-shapes by forming convex-polygon of the input shape. As shown in figure, shaded regions represent decomposed sub-shapes which are further decomposed at next lower levels. At first level, the convex polygon  $\langle P1, P2, P3, P4 \rangle$  results in two sub-shapes, namely S11 and S12. At second level, S11 is further decomposed into S111 and S112 based on convex polygon  $\langle P2, P3, P5, P6 \rangle$ . As long as convex-polygonal boundary of a shape results in significant non-convex regions, the decomposition operation continues down the tree levels. Therefore, we have not decomposed S12, S111 and S112 further. Notably, we obtain convex-polygon for every decomposed shape generated as child node during hierarchical-tree structured decomposition process as shown in figure and encode each of them with a unique spiral chain directional encoding scheme as illustrated in subsequent section. The formal algorithm is presented below.

```

Algorithm: DecomposeShape(Shape S){
Input: Binary Object Shape S
Output: Hierarchical Tree of convex-polygons and their
corresponding spiral-chain-code
1 L <-FindBoundaryPoint(S);
2 FindConvexPolygon(L);
3 Determine & save Spiral-chain code of the polygon for
respective tree-node.
4 Determine non-convex regions;
5 for(each non-convex region:  $S_i$ ) do{
6     DecomposeShape( $S_i$ ) }
7 }

```

## 2.2 Boundary Point Tracing

Boundary point tracing is one of many preprocessing techniques performed on digital images in order to extract information about their general shape. In our proposed work, we followed Moore's neighborhood contour tracing strategy [8] to extract boundary points in a specific order (counter-clockwise) to decide which of them form convex-polygon of the object. The boundary point selection criteria examines eight-neighborhood of a point, P, namely locations P1, P2, P3, P4, P5, P6, P7 and P8 as shown in Fig. 2 in counter-clockwise direction. The general idea of Moore's neighborhood contour tracing technique is that every time the counter-clockwise scanning hits an object pixel-point, P, backtrack i.e. trace back to the

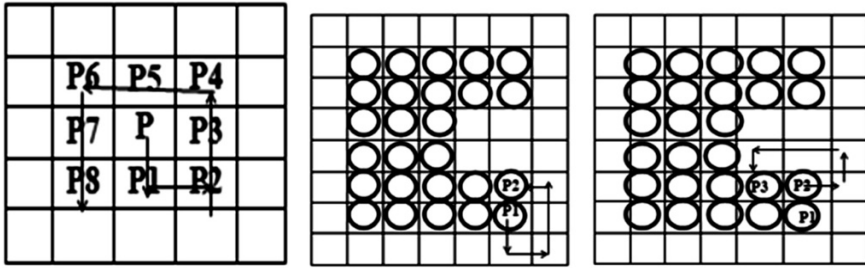
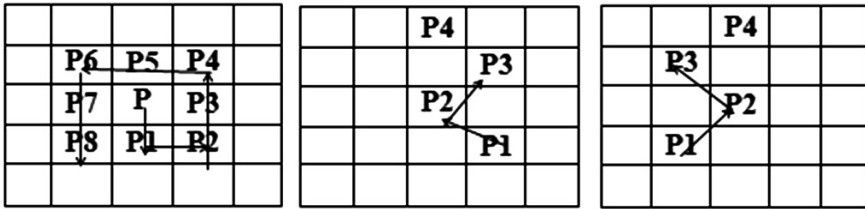


Fig. 2 Boundary point tracing

neighbor pixel from where the object pixel-point P’s location was entered and go around pixel P in anti-clockwise direction, visiting each pixel in its 8-neighborhood, until a new object pixel-point is encountered. The algorithm terminates when the start pixel is visited for a second time.

### 2.3 Convex Polygonal Approximation

Our convex polygonal covering of a shape is primarily inspired by Graham’s scan algorithm [9] for determining convex hull of an object. Given a digital object, the idea is to detect three successive boundary points in counter-clockwise direction to form an ordered triplet-points  $\langle p_1, p_2, p_3 \rangle$  as a candidate and attempt to single out a point from the ordered triplet that needs either to be discarded or picked up for the convex-polygon. The point selection or elimination is based on whether these three points make a left turn or right at position  $p_2$ . The equation as stated below helps us in deciding the turn-direction as it yields non-negative value for left turn but a right turn produces negative value. In case  $p_1, p_2, p_3$  forms a left turn, we may consider boundary point  $p_1$  as convex-polygonal point and the remaining points  $p_2, p_3$  are set as first and second element for the next candidate triplet-points. On the other hand, a right turn implies that  $p_2$  cannot be on convex-polygon of the object and in that case  $p_1, p_3$  are set as first and second element for our next candidate triplet-points. Subsequently, another boundary point ( $P_4$ ) in counter-clockwise direction is detected and added as the last point of our next candidate triplet-points. Once again we repeat the same procedure to find out the point from the ordered triplet that needs either to be discarded or picked up based on the above mentioned convexity analysis of point  $p_2$ . Our approach deviates from Gram’s scan algorithm with regards to that fact that it considers only boundary points in counter-clockwise direction instead of every object points and discards inclusion of a point if the triangular area generated by the triplet  $\langle p_1, p_2, p_3 \rangle$  falls below an empirically selected threshold value. Thus the modified algorithm basically results in an approximated convex-polygon covering the boundary of the input object (Fig. 3).



**Fig. 3** Convex polygon vertex selection

$$f(p_1, p_2, p_3) = (p_2.x - p_1.x) * (p_3.y - p_1.y) - (p_3.x - p_1.x) * (p_2.y - p_1.y) \quad (1)$$

```

Algorithm: FindApproximateConvexPolygon {
Input: Boundary point-list: L
Output: Convex Polygonal Approximation

1 p1 <- first point in Boundary point-list: L;
2 p2 <- second point in Boundary point-list: L;
3 p3 <- third point in Boundary point-list: L;
4 while(p3 != first point of Boundary point-list: L){
5   if( p1, p2, p3 form a left turn){
6     if(the triangular area generated with p1, p2, p3
7       > AreaThreshold){
8       add p1 to convex polygon point list.}
9     p1<-p2;
10    p2<-p3;
11    p3 <- next point in Boundary point-list: L;}
12  else {
13    p2<-p3;
14    p3 <- next point in Boundary point-list: L;}
15  }}

```

## 2.4 Convex Polygon Spiral-Chain-Code

In our proposed scheme, we have developed a new spiral chain-code to encode a convex polygon. The idea behind the scheme is to arrange the sides in descending order of their length and consider the largest side as the first reference base. Subsequently, repeatedly we pick up the next available largest un-encoded side from the ordered list and the chain code for the newly chosen side is determined based on the direction of the vector drawn from the mid-point of the last chosen side to the

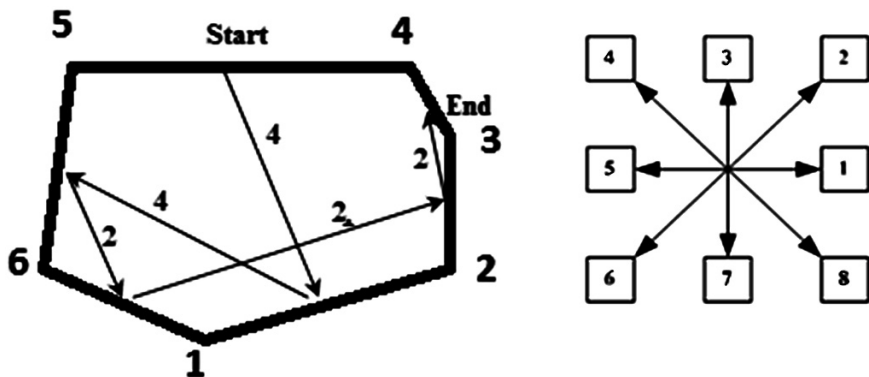


Fig. 4 Convex polygon spiral-chain-coding

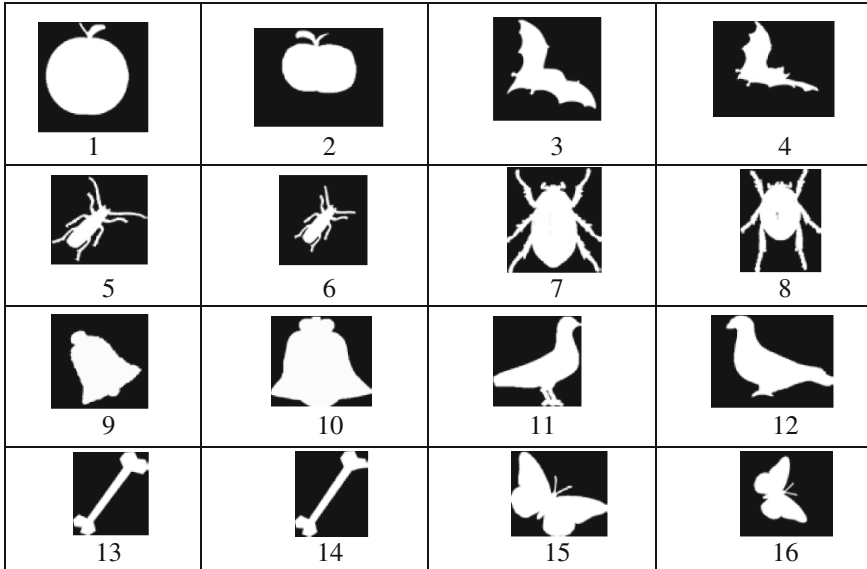
mid-point of the newly chosen side. The chain code as shown in Fig. 4 which is used to encode the direction assumes last selected side as X-axis with its counter-clockwise direction (i.e. from node  $i$  to node  $i + 1$ ) as positive direction. For example, the sides of the convex polygon shown in Fig. 4 are assumed to be ordered as  $\{(4, 5), (1, 2), (5, 6), (6, 1), (2, 3), (3, 4)\}$  based on their length arranged from largest to shortest. The spiral-chain code for the polygon is  $\{4, 4, 2, 2, 2\}$ .

### 3 Experimental Results

To evaluate the performance of the proposed shape retrieval system, experiments have been conducted based on the MPEG-7 test database [6]. The dataset consists of 1,400 shapes grouped into 70 classes, each class containing 20 similar objects. Some of the shapes have experienced a number of transformations, such as scales, cuts and rotations and also the image resolution is not constant among them. Figure 5 presents a set of sample images from MPEG-7 test database.

#### 3.1 Performance Evaluation Metric

Evaluation of retrieval performance is a crucial problem in content-based image retrieval, mainly due to the subjectivity of the human similarity judgment. The evaluation of a shape retrieval system depends on the application domain. However, many different methods for measuring the performance of a system have been created and used by researchers. Perhaps the most widely used measure, for retrieval effectiveness; in the literature is the “Bull’s eyes test” [6]. This frequently



**Fig. 5** Image sample data set (MPEG-7 database)

used test in shape retrieval enables the comparison of our approach against other performing shape retrieval techniques. Every shape in the dataset is compared to all other shapes, and the number of shapes retrieved from the same class among the top 40 retrieved similar shapes based on the applied algorithm is reported. Ideally the bull's eye retrieval rate for a query image is the ratio of the total number of retrieved shapes from the same class to the highest possible number which is 20 on MPEG-7. Thus the overall Bulls Eye Percentage (BEP) can be calculated taking average over individual BEP score for every query image from the data set.

### 3.2 Results

The following table presents the performance of our proposed algorithm for the sample data set shown in Fig. 2 as compared to popular Rammer's Polygonal Shape Chain-Code [3]. As described in previous section, every class of image data set contains 20 samples and relevant retrievals are the images belonging to the class to which the query image is ideally included. One of the interesting observations during experimentation is that as the number of sides in the polygonal shape-representation of an image increases, the performance of retrieval rate falls down. However, on the average the new proposed algorithm resulted in 83.5 % on Bull's eyes test, which seems reasonably good and comparable with existing 7 state-of-the-art algorithms (Table 1).

**Table 1** Performance comparison table for the sample data set

Sample no.	Rammer's polygon-chain-code		Proposed algorithm	
	Relevant retrieval	BEP score (%)	Relevant retrieval	BEP score (%)
1	17	85	17	85
2	14	70	15	75
3	15	75	16	80
4	14	70	16	80
5	11	55	14	70
6	11	55	15	75
7	12	60	15	75
8	13	65	15	75
9	17	85	18	90
10	16	80	19	95
11	15	75	17	85
12	14	70	18	90
13	17	85	19	95
14	17	85	19	95
15	13	65	18	90
16	14	70	17	85

## 4 Conclusion

A novel framework is proposed for CBIR which exploits different degrees of convexity of an object's contour using a multi-level tree structured representation and the method also uses a special spiral-chain-code to encode the polygonal representation of decomposed shape at every node. The performance of the proposed scheme is reasonably good and comparable with existing state-of-the-art algorithms. However, we need to further investigate the performance issues based on complexity of contour curvature as well as various effective shape decomposition tree matching schemes.

## References

1. Lambert, S., de Leau, E., Vuurpijl, L.: Using pen-based outlines for object-based annotation and image-based queries. In: 3rd International Conference on Visual Information and Information Systems, pp. 585–592. Amsterdam, The Netherlands (June 1999)
2. Marshall, S.: Review of shape coding techniques. *Image Vis. Comput.* **7**(4), 281–294 (1989)
3. Ramer, U.: An iterative procedure for the polygonal approximation of plane curves. *Comput. Graph. Image Process.* **1**(3), 244–256 (1972)
4. Latecki, L.J., Lakamper, R.: Convexity rule for shape decomposition based on discrete contour evolution. *Comput. Vis. Image Underst.* **73**(3), 441–454 (1999)

5. Ruberto, C.D.: Recognition of shape by attributed skeletal graphs. *Pattern Recogn.* **37**, 21–31 (2004)
6. <http://www.dabi.temple.edu/~shape/MPEG7/dataset.html>
7. Navarro, G.: A guided tour to approximate string matching. *ACM Comput. Surv.* **33**(1), 31–88 (2001)
8. [http://www.imageprocessingplace.com/downloads\\_V3/root\\_downloads/tutorials/contour\\_tracing\\_Abeer\\_George\\_Ghuneim/moore.html](http://www.imageprocessingplace.com/downloads_V3/root_downloads/tutorials/contour_tracing_Abeer_George_Ghuneim/moore.html)
9. Graham, R.L.: An efficient algorithm for determining the convex hull of a finite planar set. *Inf. Process. Lett.* **1**, 132–133 (1972)

# A Selective Bitplane Based Encryption of Grayscale Images with Tamper Detection, Localization and Recovery Based on Watermark

Sukalyan Som, Sayani Sen, Suman Mahapatra and Sarbani Palit

**Abstract** Ciphred data need an additional level of protection in order to safeguard them from being tampered after the decryption phase. Ciphred data, upon being deciphered by the intended receiver, is unprotected and it can be easily doctored by ever-developing, sophisticated image processing softwares. In the proposed scheme, we introduce a selective bitplane based encryption of grayscale images coupled with the facility of tamper detection, localization and restoration based on DWT based digital watermark. The original image is first sub-divided into blocks where Discrete Wavelet Transform (DWT) is applied to generate the watermark. This is embedded in four disjoint portions of the image to increase the probability of restoration of the tampered image from tampers. To add another level of security to the transmission of the watermarked image a selective bitplane based encryption based on chaos is applied. The watermarked image is first partitioned into its constituent bitplanes and then first four bitplanes from Most Significant Bitplane (MSB) is encrypted by a chaos based pseudorandom binary number generator (PRBG). The enciphered bitplanes are concatenated with unencrypted ones to produce the cipher watermarked image. The validity and novelty of the proposed scheme is verified through exhaustive simulations using different images of two well-known image databases.

---

S. Som (✉)

Department of Computer Science, Barrackpore Rastraguru Surendranath College,  
Barrackpore, Kolkata, India  
e-mail: sukalyan.s@gmail.com

S. Sen · S. Mahapatra

Department of Computer Science and Engineering, University of Kalyani, Kalyani, India  
e-mail: sumancse19@gmail.com

S. Mahapatra

e-mail: sayani.sen@gmail.com

S. Palit

CVPR Unit, Indian Statistical Institute, Kolkata, India  
e-mail: sarbanip@isical.ac.in

© Springer India 2015

J.K. Mandal et al. (eds.), *Information Systems Design and Intelligent Applications*,  
Advances in Intelligent Systems and Computing 339,  
DOI 10.1007/978-81-322-2250-7\_79

793



**Keywords** Discrete wavelet transform · Chaos · Cryptography · 1D logistic map · Information entropy · Peak-signal-to-noise-ratio (PSNR)

## 1 Introduction

Visual information in the form of images and videos has become an inevitable part of modern civilization with the advent of sophistications in transmission of them through internet. Transmitted images may have different applications viz. commercial, military and medical applications. So it is necessary to encrypt image data before transmission over the network to preserve its security and prevent unauthorized access. In recent years number of different image encryption schemes has been proposed in order to overcome image encryption problems. The chaos-based encryption has suggested a new and efficient way to deal with the intractable problem of fast and highly secure image encryption [1–5]. Since the last decade a different approach for content protection has gained attention of researchers. To overcome the computational complexity, reduce the cost of encrypting digital images and to facilitate real time transmission with lesser bandwidth requirement the idea of encrypting only portion of data, termed as partial encryption in many occasions, is preferred. Selective bitplane based encryption of digital images may refer to partial encryption where only some bitplanes are encrypted depending their relevance and significance. In [6] an analysis of the security of the selective bitplanes based encryption is performed. It has been demonstrated that, when more than the MSB is selected for the ciphering procedure, the reconstructed image, obtained by replacement attack, is severely affected. While cryptographic measures are employed to protect the privacy of the information during transmission, watermarking techniques are suitable for copyright protection. Tampering of digital media and its detection has been an interesting problem since long. Digital watermarks are used not only to protect authentication of digital data but also to provide means to localize the tamper made and attempt to restore as close as possible to the original one. Recent research has started focusing on the possibility of providing both the security services simultaneously as encrypted data becomes vulnerable for being tampered by the fraudulent receiver after decrypting it. Despite the difficulties of realizing effective algorithm that combine simultaneously watermarking and selective bitplane based encryption, some solutions have been proposed [7–10].

In this communication, an attempt is made to propose a selective bitplane based encryption of grayscale images coupled with the facility of tamper detection, tamper localization and restoration by DWT based digital watermark. The original image is first sub-divided into non-overlapping blocks of size  $2 \times 2$  where 1 level 2D DWT is applied to generate the watermark which is then embedded in four disjoint portions of the image to increase the probability of restoration of the tampered image. To add another level of security to the transmission of the

watermarked image a symmetric key selective bitplane driven encryption based on chaos is applied. The watermarked image is first partitioned into its constituent binary bitplanes and then first four bitplanes from Most Significant Bitplane (MSB) is encrypted by a chaotic PRBG formed by the use of 1D Logistic maps. The enciphered bitplanes are concatenated with unencrypted ones to produce the cipher watermarked image.

The rest of the paper is organized as follows: In Sect. 2, the proposed scheme is explained with experimental results and their analysis being done in Sect. 3. Section 3 presents the comparison of the scheme with existing State-of-art. Finally, conclusions are drawn in Sect. 4 where future directions of work is also mentioned.

## 2 Proposed Scheme

An encrypted image becomes vulnerable for being tampered after being decrypted at the receiver end. Thus to preserve the authenticity of an image being transmitted in encrypted form is preserved by embedding a watermark, generated from the image itself, before encryption. The watermark is used for tamper detection, localization and restoration up to a great extent. Thus the proposed scheme consists of two parts—watermark embedding and encryption (sender), decryption and watermark extraction: tamper detection, localization and restoration (receiver).

### 2.1 Watermark Generation and Embedding

- An image  $I_{org}$  of size  $2^n \times 2^n$ ,  $n \in N$  and  $n \geq 2$  is sub-divided into non-overlapping  $2 \times 2$  sized blocks.
- A look-up table constructed using Eq. (1) that holds the mapping address of each block in  $I_{org}$ .

$$X' = [f(x) = (k \times X) \bmod N] + 1 \quad (1)$$

where  $X, X' (\in [0, N - 1])$  the block number,  $k$  (a prime and  $\in Z - \{\text{factors of } N\}$ ) a secret key and  $N (\in Z - \{0\})$  the total number of blocks in the image.

- A push-aside operation modifies the lookup table by pushing right the columns belonging to the left half and viceversa.
- 2-D DWT is applied on each block using the Haar wavelet. The approximation coefficient matrix  $LL_1$  and detail matrices  $HL_1$ ,  $LH_1$  and  $HH_1$  are produced. The watermark is generated from  $LL_1$  sub-band coefficient.
- $I_{org}$  is divided horizontally and vertically into four disjoint and equal parts. A block (say,  $A$ ) and its partner block (say,  $C$ ) can be located at the same positions of two parts situated at opposite angles.

- The 12-bit watermark for block  $A$  and its partner block  $C$  is constructed by combining five MSBs of  $LL_1$  sub-band coefficient of the block  $A$ , five MSBs of  $LL_1$  sub-band coefficient of its partner block  $C$ , in-block parity-check bit  $p$  and its complementary bit  $v$ .
- The 12-bit watermark generated from a block ( $A$ ) and its partner block ( $C$ ) is embedded into their mapping blocks ( $\bar{A}$  and  $\bar{C}$ ). The 3 LSBs of each of the 4 pixels of a mapping block are replaced by the 12-bit watermark.

## 2.2 Image Encryption

- Each pixel of watermarked image  $I_{org}^W$  is decomposed into its corresponding 8 bit binary equivalent and thus 8 bit-planes  $BP_i(x, y) \forall i = 1, 2, \dots, 8$  are formed.
- Keys for diffusing the significant bitplanes are generated using 1D Logistic map based PRNG with chosen values of the triplet  $(x_0, y_0, \mu)$ . The PRBG is based on two 1D Logistic maps stated in Eq. (2)

$$x_{n+1} = \mu x_n(1 - x_n) \text{ and } y_{n+1} = \mu y_n(1 - y_n) \quad (2)$$

where  $x \in [0, 1]$  and  $\mu \in (3.57, 4]$ . The bit sequence is generated by comparing the outputs of both the maps as in Eq. (3)

$$\begin{aligned} g(x_{n+1}, y_{n+1}) &= 1; \text{ if } x_{n+1} \geq y_{n+1} \\ &= 0; \text{ if } x_{n+1} < y_{n+1} \end{aligned} \quad (3)$$

- The first four bitplanes considered as the significant ones, are encrypted as  $CBP_j = BP_j \oplus K_j \forall j = 1, \dots, 4$ . The cipher bit planes  $CBP_j$  and the unencrypted bitplanes  $BP_i$  are combined together to form the cipher image as  $C_i(x, y) = CBP_j + BP_k \forall i = 1, 2, \dots, 8, j = 1, \dots, 4$  and  $k = 5, \dots, 8$  where  $+$  is used to denote concatenation.

## 2.3 Image Decryption

Upon receiving the encrypted image along with the key  $(x_0, y_0, \mu)$  one will perform decryption in a manner reverse to that outlined in Sect. 2.2 to get the decrypted image.

## 2.4 Watermark Extraction: Tamper Localization and Restoration

The embedded watermark has to be extracted in order to detect and localize tamper and restore from it. Three types of tamper has been considered in this literature—Direct Cropping, Object Insertion and Object manipulation. The procedure is stated below. A 3-level hierarchical tamper detection and localization is performed, the algorithm for which is described below.

**Tamper detection and localization** In level 1, for each block B

- Retrieve the 12-bit watermark from B.
- Get the parity-check bits  $p$  and  $v$  respectively from the 11th and 12th bits of the watermark.
- Perform XOR operation on the 10 LSBs of the 12-bit watermark, resulting in  $p'$ .
- If  $p = p'$  and  $p \neq v$ , mark block B valid, else invalid.

In Level 2, for each block B marked valid after Level 1 detection

- If at least one of the four triples (N, NE, E), (E, SE, S), (S, SW, W), (W, NW, N) of the  $3 \times 3$  neighborhood of block B has all of its blocks marked invalid, mark block B invalid.

In Level 3, for each block B marked valid after level 2 detection

- If at least five of the  $3 \times 3$  neighboring blocks of block B are marked invalid, mark block B invalid.

**Restoration of image from tamper** A two-stage restoration scheme is applied for recovering the invalid blocks.

In Stage 1: For each nonoverlapping block B of size  $2 \times 2$  pixels marked invalid

- Find the mapping block  $B'$  of B from the look-up table.
- If  $B'$  is valid then  $B'$  is the candidate block, go to the last step here.
- Find the mapping block of  $B'$ 's partner-block  $B''$ .
- If  $B''$  is valid then  $B''$  is the candidate block; otherwise stop, leave block B alone.
- Retrieve the 12-bit watermark from the candidate block.
- If block B is located in the upper left or lower right quarter of the image, the 5-bit representative information of block B starts from the 1st bit (MSB) of the 12-bit watermark; otherwise, it starts from the 6th bit.
- Pad four 0s (as LSBs) to the 5-bit representative information to form a new 9-bit coefficient.
- Perform the inverse DWT operation based on this coefficient as the approximation coefficient resulting in a new block of size  $2 \times 2$ .
- Replace block B with this new block and mark block B as valid.

In stage 2 After stage 1 recovery

- Recover the remaining invalid blocks from the pixels of the neighboring blocks represented as directional triples (N, NE, E), (E, SE, S), (S, SW, W) and (W, NW, N) surrounding them.
- Finally, the lost blocks are generated by interpolating pixel values.

### 3 Experimental Results, Tests and Analysis

The proposed algorithm has been exhaustively simulated and its performance has been tested over commonly used and widely accepted USC-SIPI [11] image database, maintained by Signal and Image Processing Institute, University of Southern California. The *misc* volume of the database has been chosen in this literature to prove the efficacy of the proposed scheme. The proposed scheme and the existing state-of-the-art, considered for comparison, have been implemented using Matlab 7.10.0.4 (R2010a) on a system running with Windows 7 (32 bit) with Intel Core i5 CPU and 4 GB DDR3 RAM. In Fig. 1 a thumbnail view of the images considered from the *misc* volume of the database is shown. In Fig. 2 an original image of Lena, its watermarked image, the ciphered watermarked image, and the decrypted image are shown. To prove the efficacy of the proposed algorithm tests has been performed on the encrypted image and the decrypted image (watermarked) separately.

#### 3.1 Tests on Encryption

**Histogram Analysis** In order to have a perfect ciphered image the histogram of the image must exhibit uniformity of distribution of pixels against the intensity values.

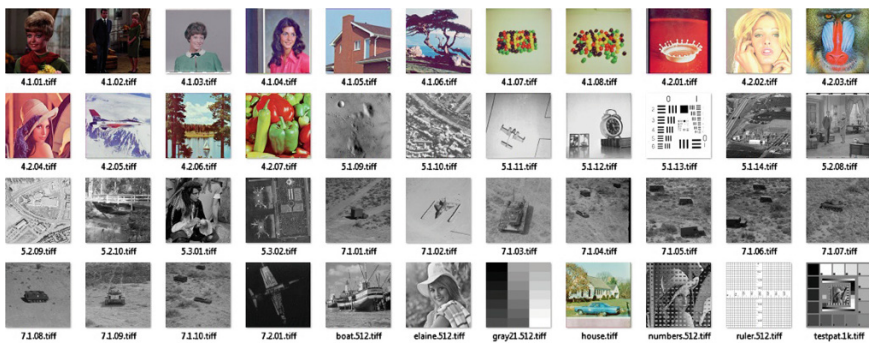
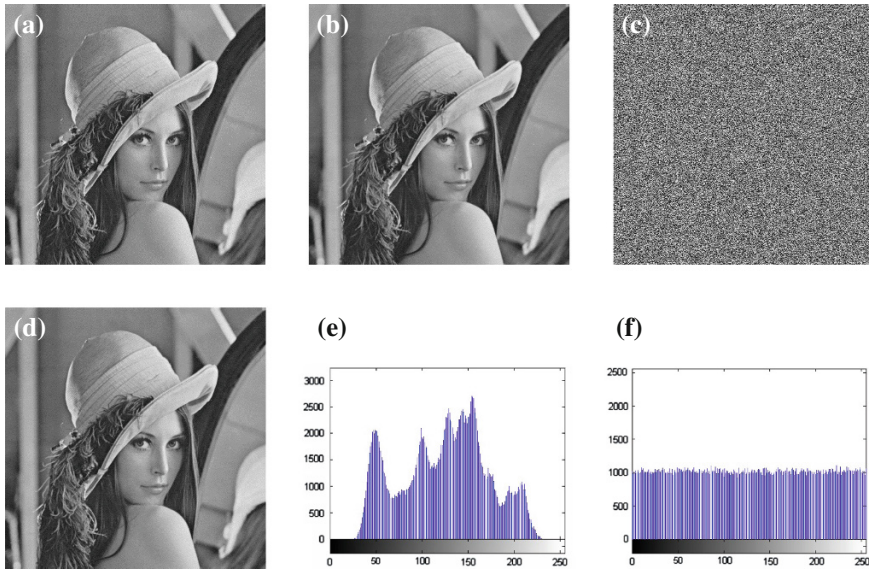


Fig. 1 A thumbnail view of the *misc* volume of USC-SIPI image database



**Fig. 2** a Original image, b watermarked image, c encrypted watermarked image, d decrypted image, e Histogram of (b), f histogram of (c)

The histograms of original and encrypted images have been analysed. In Fig. 2e, f the histograms of the watermarked image of Lena of size  $512 \times 512$  and corresponding cipher image has been presented which depicts that the histograms of plain image has certain pattern where as that of the cipher image are uniformly distributed.

**Correlation Coefficient Analysis** It is observed that there exists high correlation among adjacent pixels in an original image but poor correlation between the neighbouring pixels of corresponding cipher image. Karl Pearson’s Product Moment correlation coefficient is used to find the correlation of horizontally, vertically and diagonally adjacent pixels of both the plain and cipher image and the correlation between the plain image and cipher image pixels. The average values of correlation coefficient of the horizontally adjacent pixels in watermarked and cipher image are 0.9804 and 0.0018 where as that the same in vertically adjacent pixels are 0.9725 and 0.0008 respectively. The correlation coefficient between the watermarked image and their ciphered image is 0.0008.

**Key sensitivity and key space analysis** A good cryptosystem should be sensitive to a small change in secret keys i.e. a small change in secret keys in encryption process results into a completely different encrypted image and in the decryption process original image is not found. A good encryption scheme must have a large key space to make brute force attack infeasible. In the proposed algorithm, the initial conditions and the system parameters of the chaotic maps i.e. the triplet  $(x_0, y_0, \mu)$  forms the symmetric key. Considering the precision of

calculation as  $10^{-14}$  the key space for the proposed scheme is  $10^{14} \times 10^{14} \times 10^{14} = 10^{42}$  which is reasonably large enough to resist the exhaustive attack.

**Information Entropy Test** It is well known that the entropy  $H(s)$  of a message source  $s$  can be calculated as:

$$H(s) = \sum_{i=1}^{2^N-1} p(S_i) \cdot \log_2 \frac{1}{p(S_i)} \quad (4)$$

where  $p(S_i)$  is the probability of symbol  $S_i$  and the entropy is expressed in bits. When the messages are encrypted, their entropy should ideally be 8. If the output of such a cipher emits symbols with entropy less than 8, there exists certain degree of predictability, which threatens its security. In our algorithm the average of entropy of the cipher images is 7.9997 which is close to ideal value.

### 3.2 Use of Watermark: Tamper Detection, Localization and Recovery

**Measurement of watermark and encryption Quality** To measure the imperceptibility of watermark and encryption quality well known metrics viz. PSNR and SSIM is used. For an encrypted image smaller PSNR and SSIM is expected where as for the watermarked image to be imperceptible a PSNR greater than 35 dB and SSIM close to unity exhibits better image quality. The average PSNR and SSIM of the watermarked image is 41.5 and 0.97 dB respectively where as the PSNR for encrypted version of the watermarked image is dB.

**Performance against tampering** To evaluate the effectiveness of the proposed scheme against tampering, localize the tampers, and restore them back as close as possible to the original, the decrypted watermarked images went through different types of tampers—Direct Cropping, Object Insertion and Object manipulation. An watermarked image cropped at different positions ranging from as small as 5 % to as large as 95 % with the PSNR of restored image from 42.05 to 19.87 dB. The average PSNR of restored image is 31.5 dB. One of the most common image tampering attack is insertion of objects is by copying regions of the watermarked image and pasting them into somewhere else in that image. The proposed watermarking system detects, localizes, and recovers the tampered regions of the images tampered by inserting small, medium, and large objects. The proposed scheme is capable of restoring an attacked image by removing, destroying, or changing specific regions or objects in it. In Fig. 3 the results of tamper detection, localization and restoration is presented.



**Fig. 3** The results of different tampers and their restored versions

## 4 Conclusion and Future Scope

Our results show that encrypting only a part of the image is sufficient to conceal significant information while reducing the complexity of encrypting the entire image. Embedding a DWT based watermark, generated from the image itself provides a solution to detect and localize tampers done in the decrypted image while providing the option to restore it as close as possible to the original one. Further research will be carried out to improve the performance for situations where very small areas are tampered.

## References

1. Lian, S., Sun, J., Wang, Z.: A block cipher based on a suitable use of chaotic standard map. *Chaos Solitons Fractals* **26**(1), 117–129 (2005)
2. Pisarchik, A.N., Flores-Carmona, N.J., Carpio-Valadez, M.: Encryption and decryption of images with chaotic map lattices. *CHAOS J.* **16**(3), 033118-033118-6. American Institute of Physics (2006)
3. Pareek, N.K., Patidar, V., Sud, K.K.: Image encryption using chaotic logistic map. *Image Vis. Comput.* **24**(9), 926–934 (2006)
4. Dongming, C., Zhiliang, Z., Guangming, Y.: An improved image encryption algorithm based on chaos. In: *Proceedings of IEEE International Conference for Young Computer Scientists*, pp. 2792–2796 (2008)
5. Som, S., Kotal, A.: Confusion and diffusion of grayscale images using multiple chaotic maps. In: *National Conference on Computing and Communication Systems (NCCCS)* (2012)
6. Podesser, M., Schmidt, H.-P., Uhl, A.: Selective bitplane encryption for secure transmission of image data in mobile environments. In: *5th Nordic Signal Processing Symposium in Mobile Environments*
7. Lian, S., Liu, Z., Wang, H.: Commutative watermarking and encryption of media data. *Optical Eng. Lett.* **45**(8), 080510 (2006)
8. Lian, S., Liu, Z., Ren, Z., Wang, H.: Commutative encryption and watermarking in video compression. *IEEE Trans. Circuits Syst. Video Technol.* **17**(6), 774–778 (2007)



9. Schmitz, R., Li, S., Grecos, C., Zhang, X.: A new approach to commutative watermarking-encryption. In: CMS 2012, LNCS 7394, pp. 117–130 (2012)
10. Schmitz, R., Li, S., Grecos, C., Zhang, X.: Towards more robust commutative watermarking-encryption of images, In: IEEE International Symposium on Multimedia, pp. 283–286 (2013)
11. USC-SIPI image database available at <http://sipi.usc.edu/database>. Accessed 27 Feb 2014

# An Incremental Feature Reordering (IFR) Algorithm to Classify Eye State Identification Using EEG

Mridu Sahu, N.K. Nagwani, Shrish Verma and Saransh Shirke

**Abstract** In this work investigation of eye state identification is performed using EEG system. Binary classifications developed to categories the eye state in the classes open and closed. Feature subset selection is one of the important steps in classification. The present work is for finding feature subset selection named as Incremental Feature Reordering (IFR), it gives most non dominant feature (MND) for Electroencephalography (EEG) signal corpus and create reorder set. The removal of MND gives optimal subset feature and it increases the classifier accuracy and efficiency. The data structure used here is a two way doubly linked list, it creates dynamic environment for reordering the ordered set.

**Keywords** EEG · Binary classification · Incremental feature reordering · MND

## 1 Introduction

Feature ordering is a process of ordering the feature based on their correlation found in feature vector. Various methods present for feature ordering in different area of Bio-Medical, Bio-Informatics, and Bio-Science etc. The proposed method is based

---

M. Sahu (✉) · N.K. Nagwani  
Department of Computer Science and Engineering, NIT Raipur, Raipur 492010,  
Chhattisgarh, India  
e-mail: mrisahu.it@nitrr.ac.in

N.K. Nagwani  
e-mail: nknagwani.cs@nitrr.ac.in

S. Verma  
Department of Electronics and Telecommunication, NIT Raipur, Raipur, Chhattisgarh, India  
e-mail: shrishverma@nitrr.ac.in

S. Shirke  
Department of Electrical Engineering, NIT Raipur, Raipur 492010, Chhattisgarh, India  
e-mail: saransh.shirke@gmail.com

on Incremental Feature Reordering (IFR), which is suitable for finding most non dominant (MND) features from large features set. The literatures show that “the m best features are not the best m features” [1–4], and reversal of this is “the m worst features are not the worst m features”, so the proposed work is applicable for finding which features are more non dominant then others. In Machine learning literature is says that minimum feature subset selection is NP-Hard problem [5], IFR is a method which will remove the MND features from feature set and removal of those from feature set increase the accuracy and decreases the memory requirement of feature space. This method is applied in Electroencephalography (EEG) system.

EEG is a device for measuring the brain waves. A German scientist named Hans Berger, who invented EEG about more than 80 years ago. EEG signals are applicables in computer game [6], track emotion [7], for handicapped person to control devices [8], for military scenario [9]. EEG signals also used in stress features identification [10]. In proposed work EEG signals are used as input for eye state classification.

Classification is one of the major tasks of data mining tool, which place similar patterns in similar group. For classification, a feature subset selection is used as a pre-processing step in machine learning [11], where relevant features are identified and selected. IFR is a preprocessed state for eye state identification whether it is open or closed. Different approaches to feature subset selections [12–15] found that the subset of individually good features does not necessarily lead to good classification accuracy. The proposed method is using greedy paradigm for finding the reordered set, it is a method for creating a MND feature header linked list, for feature subset selection. Many classification algorithms is proposed in the area of Bio-Medical device [16], the literature shows that instance based classifier is performing well as compare to others like tree based, SVM based etc. [17]. K\* classifier which is a kind of instance based classifier is used in presented work [18].

## 2 K-Star Instance Based Classifier (K\*)

The K-Star algorithm is an instance based classifier like IBL (Instance Based Learner); an instance based classifier is a type of classifier that it works with unknown to the known according to some proximity based measures such as similarity or distance functions [19]. It uses the entropy distance measure for selecting value for the classifier parameters. Entropy is a measure of uncertainty of a random variable [20]. The performance of K-star classifier on EEG signal classification is compared with different classifier shown in Fig. 1.

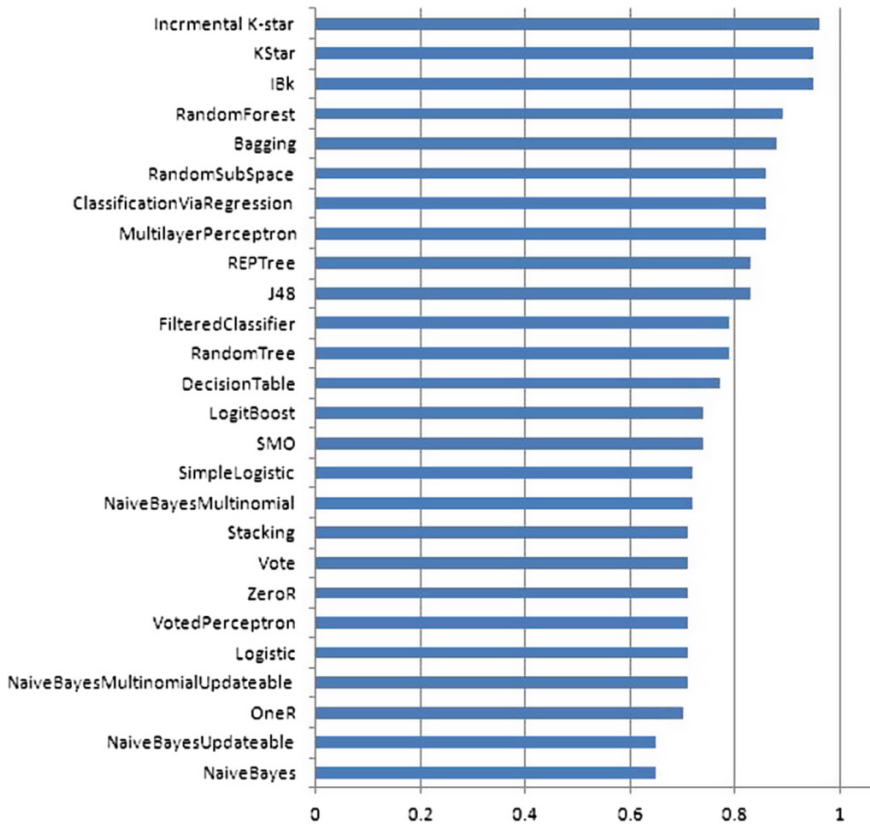
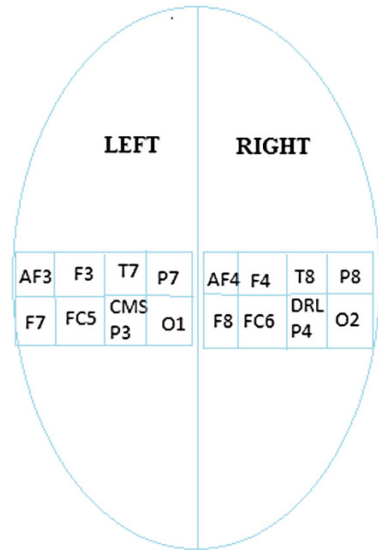


Fig. 1 Classifiers accuracy graph

### 3 Electroencephalography System (EEG)

The EEG is the kind of Bio-Medical device it is measurable by connecting electrodes known as Electroencephalography [21]. The system having 16 (F7, F3, F4, FC6, T8, P8, O2, CMS as eye open state and AF3, AF4, FC5, F8, T7, P7, O1, DRL as eye closed state), shown in Fig. 2. Eye state identification is applicable in the area of infant sleep walking state identification [22], driving drowsiness detection [23], epileptic seizure detection [24], classification of bipolar mood disorder (BMD) and attention deficit hyperactivity disorder (ADHD) patients [25], stress features identification [10], human eye blinking detection [26].

**Fig. 2** Emotive device

## 4 Corpus (EEG)

The Corpus consists of 14,980 instances with 15 features each (14 features representing the values of Electrodes and one as eye state (Boolean Variable)). Statistical Evaluation finds outlier detections in the present corpus because three instances (899, 10,387, and 11,510) declared as extreme values in this, removal of it makes new corpus and it is having 14,977 instances. The corpus is taken from the link [http://suendermann.com/corpus/EEG\\_Eyes.arff.gz](http://suendermann.com/corpus/EEG_Eyes.arff.gz). EEG eye state dataset was donated by Rosler and Suendermann from Baden-Wuerttemberg Cooperative State University (DHBW), Stuttgart, Germany [17]. The output of the corpus “1” indicates the eye-closed and “0” indicates the eye-open state.

## 5 Proposed Method

The proposed method is named as Incremental Feature Reordering (IFR) its input is a corpus of EEG sensor data set then step by step procedure is performed for pre-processing then dividing the preprocessed corpus into training, testing and validation (60, 20 and 20 %) datasets. The corpus having the class labels as  $C = \{0, 1\}$  and it is kind of binary class labels. The output of the algorithm is MND feature set; the removal of it from feature set could not affect the accuracy of instance based classifier.

**Algorithm for Finding MND Feature from Feature Set**

- Step 1 Take input as corpus.
- Step 2 Find outliers present in corpus and removal of this from corpus.
- Step 3 Create three sets training, testing, validation.
- Step 4 Create Feature ordered set from different Feature ordering Algorithm:
  - 4.1 BestFirst and CfsSubsetEval
  - 4.2 Ranker and CorrelationAttributeEval
  - 4.3 Ranker and GainRatioAttributeEval
  - 4.4 Ranker and InfoGainAttributeEval
  - 4.5 Ranker and OneRAttributeEval
  - 4.6 Ranker and ReliefFAttributeEval
  - 4.7 Ranker and SymmetricalUncertAttributeEval
  - 4.8 GreedyStepwise and CfsSubsetEval
  - 4.9 RerankingSearch and CfsSubsetEval
- Step 5 Create an N number of Two Way Header Linked list.
- Step 6 Apply searching for last most element from each header node.
- Step 7 Push it into stack.
- Step 8 Repeat Step 6 and 7 until last two way header linked list.
- Step 9 Pop one by one element from stack until stack is empty.
- Step 10 Apply K-star classification technique after popping one element.
- Step 11 Store accuracy and popped element in two dimensional arrays.
- Step 12 Repeat Step 10 and 11 for node until N header node is not obtained.
- Step 13 Search maximum accuracy from two dimensional array.
- Step 14 Declare this feature as MND feature.
- Step 15 Create new corpus which does not have MND features.

The Algorithm steps shows, getting of most non dominant feature set. These are pre-processing stapes for K\* classifier. The data structure two way header linked list is used in proposed methodology it is better choice for storing the reordered set, it gives dynamic memory allocation for allocating the header node with specified ordered list generated from various ordering algorithms shown in Table 1.

**6 Result Analysis**

During the Experiment nine different ordering algorithms taken. Then K\* classification accuracy measures shown in Table 1, it is ordered set have minimal features giving very less accuracy in EEG corpus. Method selects only those ordered set giving more accuracy, 95.01 % accuracy is highest and it is present in six different set obtained by different ordering algorithm, but the ordered set is different from each others. Each algorithm declared MND different from others but this is an observation that MND must be present in all last valued dataset from different algorithm. Hear it is {T7, F7, F3, F7, P8, F3} the set having repetitive MNDs so

**Table 1** Classification accuracy of K-star with feature ordering

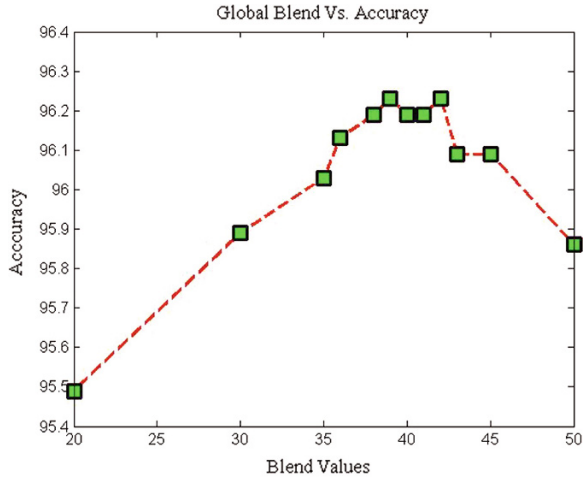
Serial Number	Feature ordering algorithm	OrderedFeatureVector	K* (%) accuracy
1.	BestFirst and CfsSubsetEval	AF3, P7, O1, P8, AF4.	77.40
2.	Ranker and CorrelationAttributeEval	AF4, F7, F8, F4, T8, AF3, FC6, P7, P8, FC5, F3, O2, O1, T7	95.01
3.	Ranker and GainRatioAttributeEval	P8, AF3, O1, FC6, P7, AF4, F8, T8, T7, F4, FC5, O2, F3, F7	95.01
4.	Ranker and InfoGainAttributeEval	O1, P7, AF3, AF4, F8, F4, P8, FC6, T8, O2, T7, FC5, F7, F3	95.01
5.	Ranker and OneRAttributeEval	O1, P7, AF3, AF4, F8, P8, F3, T7, T8, FC5, O2, F4, FC6, F7	95.01
6.	Ranker and ReliefFAttributeEval	F7, O1, P7, F8, FC6, AF4, AF3, T7, FC5, T8, F3, O2, F4, P8.	95.01
7.	Ranker and SymmetricalUncertAttributeEval	AF3, O1, P7, AF4, P8, F8, FC6, F4, T8, T7, FC5, O2, F7, F3.	95.01
8.	GreedyStepwise and CfsSubsetEval	AF3, P7, O1, P8, AF4.	77.40
9.	RerankingSearch and CfsSubsetEval	AF3, P7, O1, P8, AF4	77.40

eliminate this, then the new set obtained by this is {T7, F7, F3, P8}. It is an optimal set which gives MND for the corpus. The removal of one feature from two way header list and classification accuracy is mapped in Table 2, it is showing that removal of P8, gives more accuracy then others and it is also present in MND set.

**Table 2** Classification accuracy of K-star after feature removal with global blend value = 20

Attributes removal	TPR	FPR	Precision	Recall	FMeasure	MCC	ROC Area	PRC Area	Accuracy	ER
Attributes selected(14)	0.95	0.051	0.95	0.95	0.95	0.899	0.989	0.989	95.26	4.74
F3	0.95	0.053	0.95	0.95	0.95	0.898	0.991	0.991	94.96	5.04
F7	0.942	0.063	0.942	0.942	0.942	0.883	0.987	0.987	94.19	5.81
FC5	0.946	0.057	0.946	0.946	0.946	0.891	0.989	0.989	94.59	5.41
T7	0.942	0.061	0.942	0.942	0.942	0.882	0.988	0.989	94.16	5.84
O2	0.948	0.056	0.948	0.948	0.948	0.895	0.99	0.991	94.79	5.21
T8	0.942	0.061	0.942	0.942	0.942	0.882	0.988	0.989	94.16	5.84
FC6	0.938	0.065	0.938	0.938	0.938	0.875	0.986	0.987	93.83	6.17
P8	0.955	0.047	0.955	0.955	0.955	0.909	0.991	0.991	95.49	4.51
F4	0.944	0.059	0.944	0.944	0.944	0.886	0.989	0.989	94.39	5.61
F8	0.94	0.063	0.94	0.94	0.94	0.878	0.988	0.988	93.99	6.01
AF4	0.943	0.061	0.943	0.943	0.943	0.884	0.988	0.989	94.26	5.74
AF3	0.944	0.058	0.944	0.944	0.944	0.887	0.988	0.988	94.43	5.57
P7	0.942	0.061	0.942	0.942	0.942	0.882	0.988	0.988	94.19	5.81
O1	0.935	0.069	0.935	0.935	0.935	0.869	0.982	0.983	93.52	6.48

**Fig. 3** Accuracy rate versus global blend value



Classification accuracy is measured by using K\* classifier with global blend as default value 20.

The best MND comes with “Ranker and ReliefFAttributeEval” and for proposed work it is declared as best ordering algorithm for EEG corpus to classify of eye states. Performance of IFR algorithm is compared with 26 different well known classification algorithms and it is shows in Fig. 1.

Then Experiment is to find which global blend is most appropriate for proposed work because the default blend (20) in weka is not global blend for EEG eye state classification. It is evaluated in different values of blend ranging from 20 to 50, and then calculates accuracy of K\* classifier, the best result comes with 42 and 39 shown in Fig. 3. Here 39 is declared as global blend for EEG corpus. Classification accuracy is increased by 0.74 % which is a relative to when blend value is default setting with 20.

## 7 Conclusion

In this proposed work, an IFR approach based K-star classification is applicable in area of EEG eye state identification. The approach is unique in a way that it firstly find the order set generated from different algorithms and then it will stored in a new order set for selecting the feature which is most non dominant feature, and removal of this improves the efficiency of classifier with minimum error rate. The experiment result shows many ordering algorithms are not giving a proper order set for EEG eye state identification. The proposed approach performing well and it is compared with well known classifiers and found that it require less space and less time to identify the eye state, it uses greedy paradigms to create a set of optimal non dominant feature order. The data structure used in proposed approach is two way



header linked list. It provides dynamic environment for node creations and giving runtime memory management for reorder set. In future, some issues remain as open topic for further research, is any algorithm for creating an optimal algorithm with polynomial time complexity to find MND set for high dimensional datasets and those dataset having variable dimensionality.

**Acknowledgments** This research is supported by the National Institute of Technology, Raipur and many thanks to WEKA machine learning group as well as Rosler and Suendermann from Baden-Wuerttemberg cooperative state university (DHBW), Stuttgart, Germany for providing EEG corpus.

## References

1. Webb, A.: Statistical pattern recognition. Arnold (1999)
2. Cover, T., Thomas, J.: Elements of Information Theory. Wiley, New York (1991)
3. Cover, T.M.: The best two independent measurements are not the two best. *IEEE Trans. Syst. Man. Cybern.* **4**, 116–117 (1974)
4. Jain, A.K., Duin, R.P.W., Mao, J.: Statistical pattern recognition. A review. *IEEE Trans. Pattern Anal. Mach. Intell.* **22**(1), 4–37 (2000)
5. Mondal, M., Mukopadhyay, A.: An improved minimum redundancy maximum relevance approach for feature selection in gene expression data CIMTA (2013)
6. Pour, P.A., Gulrez, T., AlZoubi, O., Gargiulo, G., Calvo, R.: Brain-computer interface: next generation thought controlled distributed video game development platform. In: Proceedings of the CIG, Perth, Australia (2008)
7. Pham, T.D., Tran, D.: Emotion recognition using the emotiv EPOC device. *Lecture Notes in Computer Science*, vol. 7667 (2012)
8. Ossmy, O., Tam, O., Puzis, R., Rokach, L., Inbar, O., Elovici, Y.: MindDesktop—computer accessibility for severely handicapped. In: Proceedings of the ICEIS, Beijing, China (2011)
9. van Erp, J., Reschke, S., Groojen, M., Brouwer, A.-M.: Brain performance enhancement for military operators. In: Proceedings of the HFM, Sofia, Bulgaria (2009)
10. Sulaiman, N., Taib, M.N., Lias, S., Murat, Z.H., Aris, S.A.M., Hamid, N.H.A.: Novel methods for stress features identification using EEG signals. *Int. J. Simul. Syst. Sci. Technol.* **12**(1), 27–33 (2011)
11. Yu, L., Liu, H.: Feature selection for high-dimensional data: a fast correlation-based filter solution. In: Proceedings of International Conference on Machine Learning, vol. 3, p. 856 (2003)
12. Kwak, N., Choi, C.H.: Input feature selection by mutual information based on Parzen window. *IEEE Trans. Pattern Anal. Mach. Intell.* **24**(12), 1667–1671 (2002)
13. Langley, P.: Selection of relevant features in machine learning. In: Proceedings of AAAI Fall Symposium on Relevance (1994)
14. Jaeger, J., Sengupta, R., Ruzzo, W.L.: Improved gene selection for classification of microarrays. In: Proceedings of Pacific Symposium Biocomputing, pp. 53–64 (2003)
15. Kohavi, R., John, G.: Wrapper for feature subset selection. *Artif. Intell.* **97**(1–2), 273–324 (1997)
16. Wang T., Guan, S.U., Man, K.L., Ting, T.O.: EEG eye state identification using incremental attribute learning with time-series classification. *Math. Probl. Eng.* **2014** (2014)
17. Rösler, O., Suendermann, D.: First step towards eye state prediction using EEG. In: Proceedings of the International Conference on Applied Informatics for Health and Life Sciences. Istanbul, Turkey (2013)

18. Leary, J.G., Tigg, L.E.: K\*: an instance-based learner using an entropic distance measure. In: Proceedings of International Conference on Machine Learning (1995)
19. <http://www.fon.hum.uva.nl/praat/manual>
20. Cover, T.M., Thomas, J.A.: Elements of information theory chapter 2. Wiley, New York (1991). Print ISBN 0-471-06259-6, Online ISBN 0-471-20061-1
21. <http://electronics.howstuffworks.com/emotiv-epoc1.html>
22. Estévez, P.A., Held, C.M., Holzmam, C.A. et al.: Polysomnographic pattern recognition for automated classification of sleep-waking states in infants. *Med. Biol. Eng. Comput.* **40**(1), 105–113 (2002)
23. Yeo, M.V.M., Li, X., Shen K., Wilder-Smith, E.P.V.: Can SVM be used for automatic EEG detection of drowsiness during car driving. *Saf. Sci.* **47**(1), 115–124 (2009)
24. Polat, K., Günes, S.: Classification of epileptiform EEG using a hybrid system based on decision tree classifier and fast Fourier transform. *Appl. Math. Comput.* **187**(2), 1017–1026 (2007)
25. Sadatnezhad, K., Boostani, R., Ghanizadeh, A.: Classification of BMD and ADHD patients using their EEG signals. *Expert Syst. Appl.* **38**(3), 1956–1963 (2011)
26. Nguyen, T., Nguyen, T.H., Truong, K.Q.D., van Vo, T.: A mean threshold algorithm for human eye blinking detection using EEG. In: Proceedings of the 4th International Conference on the Development of Biomedical Engineering in Vietnam, pp. 275–279. Ho Chi Minh City, Vietnam (2013)

# Wireless Body Area Networks: A Review with Intelligent Sensor Network-Based Emerging Technology

Shabana Mehfuz, Shabana Urooj and Shivaji Sinha

**Abstract** The increasing interest and the constant miniaturization of intelligent wireless sensor based devices have empowered the development of Wireless Body Area Networks (WBANs). Recent evolution in wearable and implantable sensors and rapid growth in the low power, energy efficient and short range wireless communication technologies are enabling the implementation of WBANs. The design of these networks requires the new protocols with respect to those used in general purpose wireless sensor networks. This survey paper aims at reporting an overview of the concept of WBANs with applications, characteristics, hardware design issues and supporting short range radio technologies and standards. A brief overview of the existing and past projects is also discussed. Finally, this article highlights some of the design challenges and open research issues that still need to be addressed to make WBANs truly ubiquitous for a wide range of applications.

**Keywords** Body sensors · Health care · On body communication · Propagation channel · Ultra wide band (UWB) · Wireless body area networks

## 1 Introduction

Body area networks (BANs) are a new kind of personal area communication networks consists of smart sensors placed inside, on or around the human body, typically consists of a collection of low-power, miniaturized, lightweight devices

---

S. Mehfuz (✉) · S. Sinha  
Jamia Millia Islamia University, Delhi, India  
e-mail: shabana\_mehfuz@yahoo.com

S. Sinha  
e-mail: shivaji2006@gmail.com

S. Urooj  
Gautam Buddha University, Greater Noida, India  
e-mail: shabanaurooj@ieee.org

with wireless communication capabilities. WBANs enable different applications, especially in healthcare monitoring and hence new possible market with respect to Wireless Sensor Networks (WSNs). On the other hand, their design issues are affected by several challenges for new paradigms and protocols in the proximity of a human body [1].

Body Area Network is formally defined by IEEE 802.15 as, “a communication standard, optimized for low power devices and operation in the vicinity of or inside a human body to serve a variety of applications including medical, consumer electronics or personal entertainment and other”. It focuses on communication in the human body area that is the immediate environment around the human body which includes the nearest objects that may be part of the body [2]. Basic requirements of a WBAN are listed below

- Limited coverage range (<0.01–2 m).
- Extremely low power consumption in sleep mode.
- Support of dynamic data rate ranging from 1 Kb/s to several Mb/s.
- QoS support for critical physiological data.
- Low latency over multi-hop network architecture.

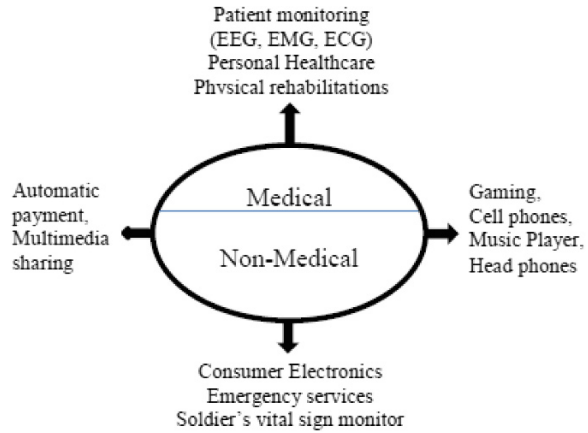
## 2 Application of WBAN in Health Care

There are different categorizations for application and usage models of body area networks. WBANs will play an important role in real time monitoring enabling ubiquitous:

- Medical health care services, e.g. Medical check-up
- Physical rehabilitations
- Physiological monitoring of vital parameters.

The tiny biosensors can collect various real time vital health parameters including blood pressure, SpO<sub>2</sub>, electroencephalogram (EEG), electrocardiogram (ECG), carotid pulse, glucose rate, body temperature. The BAN is also used in other non-medical areas such as military, sport, and entertainment. IEEE 802.15.6 categorizes WBAN applications in medical and non-medical (Consumer Electronics) as can be seen in Fig. 1. The WBAN can also be used in entertainment applications such as microphones, MP3-players, cameras, head-mounted displays and advanced computer appliances. They can be used in virtual reality and gaming purposes, personal item tracking, exchanging digital profile or business card and consumer electronics [3].

**Fig. 1** BAN application categorization



### 3 Characteristics of WBAN

Unlike conventional wireless sensor networks (WSNs) and Adhoc networks, WBANs have their own typical characteristics. The following points distinguish WBANs from Wireless Sensor Networks (WSNs) and also create new technical challenges [3].

#### 3.1 Architecture

A WBAN consists of only two categories of nodes; sensors in or on a human body and router nodes around WBAN wearers or second tier radio devices equipped on the wearers, functioning as an infrastructure for relaying data [4].

#### 3.2 Density

When more nodes are required for a specific application, they are added accordingly in Body Area Networks. So the density of nodes is low in WBAN as compared to Wireless Sensor Networks (WSN).

#### 3.3 Data Rate

Since WBAN is a heterogeneous network, which requires monitoring of periodical physiological activities, so require relatively stable data rate.

### ***3.4 Power Supply and Demand***

For the data acquiring, processing, and further transmission, WBAN requires suitable energy supplies. Implanted body sensor devices in the human body are powered by batteries, which are sometimes not possible to replace; thus, techniques like Wireless RF energy harvesting or body motion based energy harvesting must be required.

### ***3.5 Latency, Reliability and Security***

Because the medical information possesses confidential character, high reliability, low delay and stringent security mechanisms are required in WBANs mechanisms are required in WBAN to protect patient information.

### ***3.6 Network Topology***

In WBAN, it is more variable due to body motion, while very likely to be static in WSN.

## **4 Wireless Body Area Networks Architecture**

The Body Area Network (WBAN) is a human centered communication network as shown in Fig. 2. The network consists of three types of nodes. The Sensor nodes consist of implanted and body surface nodes. These nodes collect vital parameters of the human body, such as ECG, EEG and EMG [5].

This information is transmitted to either intermediate router node or to an external coordinator node. The intermediate router node exchanges the data and control messages between the sensor and coordinator node. The Coordinator node is an external node which acts as a gateway for higher layer applications [3].

## **5 Hardware and Devices**

A body sensor node consists of two parts; the physiological sensor and the radio platform as shown in Fig. 3.

The function of body sensor is to convert human's physiological energy to analog signals. Sensors are in direct contact with the human body surface or even

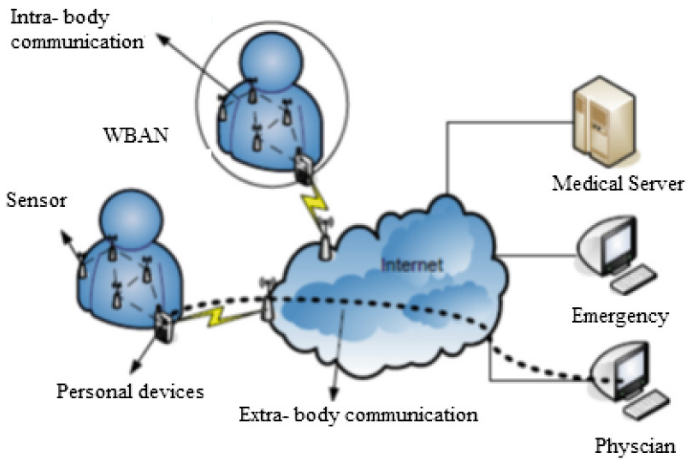


Fig. 2 WBAN application architecture of medical healthcare

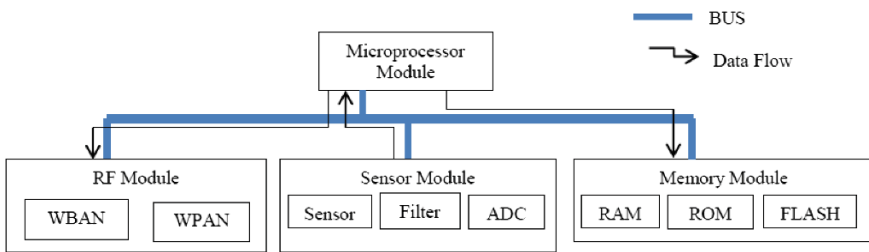


Fig. 3 Modules of sensor node platform

implanted inside the body, their size, quality of materials and physical compatibility is very important to human tissues. Short range radio technologies transmit the sensed data. The Table 1 compares the different radio interfaces in which overall IEEE 802.15.4 is widely adopted [2].

Table 1 Comparison of body sensor wireless platforms

Model	Wireless standard	Frequency (GHz)	Data rate (Kbps)	Outdoor range (m)
UWB	IEEE 802.15.6	3.1–10.6	10,000	<30
MicAz	IEEE 802.15.4	2.4	250	75–100
Imote2	Bluetooth	2.4–2.4835	250	30
ZigBit	IEEE 802.15.4	2.4–2.4835	250	3,700
BT node	Bluetooth	2.4	300	50
Mica2	IEEE 802.15.4	0.868/0.916	38.4	>100

## 6 Frequency Dependent Characteristics of Body

When the human body is exposed to an electromagnetic field, its characteristics are treated at the tissue level. Electrical properties of the human body are characterized by the cell membrane and the conductive intracellular fluid at the tissue level. When the human body is exposed to an electromagnetic field, its characteristics are treated at the tissue level. The human body has very unusual electromagnetic property values. The properties, electric permittivity and electric conductivity are not well known and depend on the activity of the person. These properties have been extensively studied in the last fifty years from 10 Hz to almost 10 GHz [6]. Since biological tissues, mainly consist of water, they behave neither as a conductor nor a dielectric, but as a dielectric with losses. The attenuation of transmitting power in the human body is due to absorption by body tissue, which is frequency dependent. At low frequency, the skin depth is large and therefore the electromagnetic wave can go into the depth of the human body.

Figure 4 shows the variation of electromagnetic properties for three representative tissues in the range 10 kHz to 1 GHz, blood (very high water content), muscle (high water content) and fat (low water content). Compared to classical dielectrical materials, the dielectric permittivity is high. It is found that at 1 kHz, the relative permittivity of the blood is 435,000. With an increase in frequency, relative permittivity decreases. In the same way, the conductivity of the muscle varies from 0.3211 to 0.9982 in the 1 kHz to 1 GHz frequency band. The wetter a tissue is, the lossy it is; the drier it is, the less lossy it is. On the other hand, the permeability of biological tissues is that of free space [7].

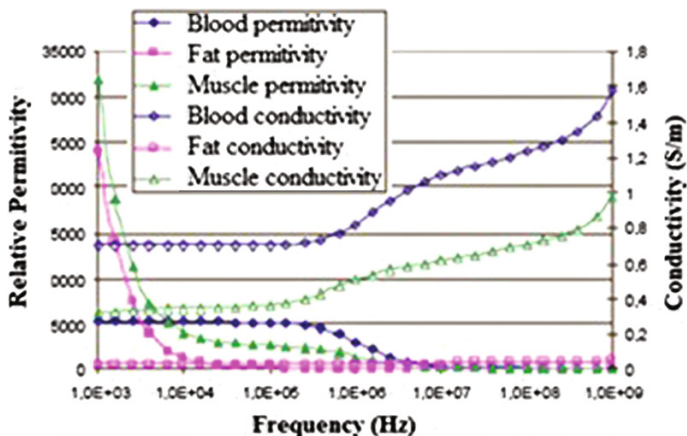


Fig. 4 Variation of electric properties with frequency for blood, fat and muscle tissues



## 7 Channel Modelling and IEEE 802.15.6 Physical Layer

In the past few years, researchers have characterized and model the propagation channel inside and on the body surface both through the measurement and simulation. Channel model is important for the development of

- More effective antenna with Low SAR with efficient coupling for to the dominant mode propagation
- Prediction of link performance for PHY layer.

WBAN is greatly affected by the amount of path loss that occurs due to different body channel impairments. It was found that the path loss depends on the separation between transmitter and receiver, location and height of antennas, propagation medium such as moist or dry air [12]. Equation (1) Suggests the path loss (PL) in [4, 8]

$$PL(d) = PL(d_o) + 10n \log_{10} \left( \frac{d}{d_o} \right) + \sigma_s \quad (1)$$

where,  $d_o$  is the path loss at a reference distance  $d_o$ ,  $n$  is the path loss exponent, ( $n = 2$  for free space) and  $\sigma_s$  is the standard deviation. Equation (2) gives the dependence of path loss of distance do as well as frequency f.

$$PL = 20 \log_{10} \left( \frac{4\pi df}{c} \right) \quad (2)$$

where c is the light velocity.

The propagation of electromagnetic (EM) energy on the surface of the body or inside the human body has been investigated in [7]. The propagation around the human body is divided into

- Direct line of sight (LOS)
- Indirect or non-line of sight (NLOS).

In the former, the curvature effects on the body are not taken into account. While in the later, the effects of propagation from the front of the body to the side or the back of the body are evaluated. The simulation and experimental conclusions for propagation along the human body in the line of sight (LOS) channel model was studied in [7]. The studies were done for both narrowband and UWB signals. The path loss exponent  $n$  is calculated between 3 and 4, depending on the position of the nodes. The study in [9] shows that the antenna height impact on the path loss. The closer the antenna is to the body, the higher the path loss and a difference of more than 20 dB is observed for an antenna placed at 5 mm and 5 cm. The small size sensors and antennas will be close to the body which will result in a higher path loss [10, 11].

According to the Federal Communications Commission (FCC), Ultra Wide Band (UWB) technology has emerged as a solution for the wireless BANs. UWB refers to any radio technology having a transmission bandwidth exceeding the lesser of 500 MHz or 20 % of the center frequency. Due to low power spectral density emission and license free use in the 3.1–10.6 GHz frequency band, UWB is suitable for short range, RF emissions sensitive (e.g., in a hospital) indoor environment [13]. UWB transmitters are designed using simple techniques, although UWB receivers require complex hardware design techniques. It also consumes comparatively higher power. In order to achieve reliable, low power radio communication, a sensor node can be constructed using a UWB transmitter and a narrow band receiver.

Narrowband UWB pulses do not cause significant interference to other systems operating in the vicinity and do not represent a threat to patients' safety.

## 8 Research Challenges and Conclusion

In this survey paper, a comprehensive review of WBANs in terms of its applications, characteristics, network architecture, hardware requirement, physical layer modeling and recent low power, short range technologies is presented. As a complement to existing wireless technologies, the WBAN plays a very important role in interdisciplinary research and development. We truly believe that this survey can be considered as a source of inspiration for future research directions. Several open issues like Physical characteristics of sensors and effect of RF circuits, Bio-compatibility, Security, Authentication and Privacy, Routing protocols still need to be addressed. In particular, for life-saving applications, thorough studies and tests should be conducted before WBANs can be widely applied to humans.

## References

1. Cavallari, R., Martelli, F., Rosini, R., Buratti, C., Verdone, R.: A survey on wireless body area networks: technologies and design challenges. In: Proceedings of the Communications Surveys and Tutorials IEEE, vol. 99, pp. 1–23 (2014)
2. Thotaheva, K.M.S., Khan, J.Y., Yuce, M.R.: Power efficient ultra wide band based wireless body area networks with narrowband feedback path. *IEEE Trans. Mob. Comput.* **13**, 1829–1842 (2013)
3. Movassaghi, S., Abolhasan, M., Lipman, J., Smith, D., Jamalipour, A.: Wireless body area networks: a survey. In: Proceedings of the Communications Surveys and Tutorials IEEE, vol. 99, pp. 1–29 (2014)
4. Smith, D.B., Miniutti, D., Lamaheva, T.A., Hanlen, L.W.: Propagation models for body-area networks: a survey and new outlook. *IEEE Antennas Propag. Mag.* **55**(5), 97–117 (2013)
5. Cotton, S.L., D'Errico, R., Oestges, C.: A review of radio channel models for body centric communications. *Radio Sci.* **49**(6), 371–388 (2014)

6. Zhang, M., Lim, E.G., Wang, Z., Tillo, T., Man, K.L., Wang, J.C.: RF characteristics of wireless capsule endoscopy in human body. In: Proceedings of the Grid and Pervasive Computing, vol. 7861, pp. 700–706 (2013)
7. Smith, D.B., Miniutti, D., Hanlen, L.W.: Characterization of the body-area propagation channel for monitoring a subject sleeping. *IEEE Trans Antennas Propag.* **59**(11), 4388–4392 (2011)
8. Reusens, E., Joseph, W., Vermeeren, G., Martens, L., Latre, B., Braem, B., et al.: Path-loss models for wireless communication channel along arm and torso. In: Proceedings of the IEEE APSIS, pp. 336–339 (2007)
9. Gianluigi, T., Ghavam, N., Edwards, D.J., Monorchio, A.: UWB body area network channel modeling: an analytical approach. *Int. J. Electron. Commun. (AEU)* **66**(11), 913–919 (2012)
10. Cotton, S.L.: A statistical model for shadowed body-centric communications channels: theory and validation. *IEEE Antennas Propag.* **62**(3), 1416–1424 (2014)
11. Naganawa, J., Wangchuk, K., Kim, M., Aoyagi, T., Takada, J.: Simulation-based Scenario-Specific Channel Modeling for WBAN Cooperative Transmission Schemes. *IEEE J. Biomed. Health Inform.* **99**, 1 (2014)
12. Wang, L., Sodhro, A.H., Qiao, D., Zhou, Y., Li, Y.: Power-aware wireless communication system design for body area networks. *J. E-Health Telecommun. Syst. Netw. (ETSN)* **2**, 23–28 (2013)
13. Khaleghi, A., Chavez-Santiago, R., Balasingham, I.: An improved ultra wideband channel model, including the frequency-dependent attenuation for in-body communications. In: IEEE Annual International Conference of the Engineering in Medicine and Biology Society (EMBC), pp. 1631–1634 (2012)

# Flow Regime Prediction Using Artificial Neural Networks for Air-Water Flow Through 1–5 mm Tubes in Horizontal Plane

Nirjhar Bar, Manindra Nath Biswas and Sudip Kumar Das

**Abstract** Artificial Neural Network (ANN) based techniques for the classifications of flow regimes in air-water flow through 1–5 mm tubes are presented. 218 data points are based on the experimental investigation in 3 and 4 mm tubes and 2114 data points from various experimental results from the published literature for air-water two-phase flow in small diameter tubes have been used. Five different well known artificial neural network models have been used to predict the flow regime. The ANN model based on Radial Basis Function and Principal Component Analysis gives better predictability over the other networks used.

**Keywords** Flow regime · Multilayer perceptron (MLP) · Radial basis function · Support vector machine · Principal component analysis

## Nomenclature

N      Number of data points  
 $x$       Input value  
 $y$       Output value  
MSE    Mean Square Error,  $\frac{1}{N} \sum_{i=1}^N (x_i - y_i)^2$

---

N. Bar (✉) · M.N. Biswas  
Government College of Engineering and Leather Technology, LB Block,  
Sector III, Salt Lake City 700 098, Kolkata, India  
e-mail: nirjhar@hotmail.com

M.N. Biswas  
e-mail: profmnbiswas@yahoo.co.in

S.K. Das  
Chemical Engineering Department, University of Calcutta,  
92 A. P. C. Road, Kolkata 700 009, India  
e-mail: drskdaspapers@hotmail.com

## 1 Introduction

Gas-liquid two-phase flow widely exists in industrial processes, such as, power generation, thermal engineering, chemical processes, petroleum refineries and petrochemical industries, nuclear industry and many other heat transfer equipment with phase change. In the two-phase gas-liquid flow the hydrodynamics, heat transfer and mass transfer characteristics are largely influenced by the flow regimes. In many industrial systems like power generation, nuclear reactors, petroleum and biochemical processing systems, it is necessary to monitor the flow regimes during normal and also transient operation conditions for the safety and overall performance. So the accurate prediction of the flow regime is an important task.

Gas-liquid two-phase flow patterns in small channels have been investigated extensively in the past [1–14]. Definitions of flow regime are generally based on the description and graphical illustrations. The visual flow pattern classification is based on visual observation, which probably varies for different viewers, particularly in the transition from one flow regime to another. Many literatures are available on the development of different techniques, such as conductivity probe, radiation attenuation, hot wire anemometer etc. for flow regime identification. Early work on the empirical flow regime map developed by Baker [15] and other researchers [16–19] attempts to develop a generalized flow regime map. Taitel and Dukler [17] proposed a flow regime map containing predominant four flow regimes namely, stratified, intermittent, bubble and annular with superficial gas velocity and superficial liquid velocity as co-ordinates and also propose physical based criteria for the transition from one regime to the next. Taitel [19] proposed a unified model for the prediction of flow regime transitions in channels of any orientation based on simple physical criteria using the well known two-phase dimensionless group, Froude number ( $Fr$ ), the parameter  $T$  which relates the liquid pressure drop to buoyancy, and Lockhart-Martinelli parameter,  $X$ . They also developed the regime transition criteria that gives the distinction between the flow regimes that are driven by surface tension, e.g., bubble and intermittent flow and the flow regimes that are driven by shear force, e.g., stratified and annular flow.

The present study aims to develop an objective flow pattern indicator for air-water flow in small diameter horizontal tubes. This indicator should be capable of predicting the flow regimes as well as the transition zones and also the uses of easily measurable input parameters such as velocities of gas and liquid, physical properties of fluids and tube diameters. The artificial neural network (ANN) approach can solve this problem. Himmelblau [20] and Cong et al. [21] reported some ANN applications in the multiphase flow system and it has also been proved to be able to solve complex tasks in a number of practical applications. Cai et al. [22] used self Kohonen self-organizing feature map model to classify the flow regimes of air-water two-phase horizontal flow. Recently Bar and Das [14] successfully predicted flow regimes related to air-water flow in micro channels using three different ANN structures i.e., two types of Multilayer Perceptrons (MLP) trained with Back-propagation (BP) algorithm and Levenberg Marquardt (LM) algorithm respectively

and Support Vector Machine (SVM) of diameters ranging from 0.05–0.6 mm in horizontal plane.

The present study deals with the creation of data bank from the flow regime studies conducted by various researchers [2, 7–9, 11–13] and our own experimental data [23]. Five different ANN structures are used for the flow pattern prediction and these are two types of Multilayer Perceptrons (MLP) trained with Backpropagation (BP) algorithm and Levenberg Marquardt (LM) algorithm, Radial Basis Function (RBF), Support Vector Machine (SVM) and Principal Component Analysis (PCA).

## 2 The Neural Network

The following neural network models are used for this analysis,

- (i) Multilayer Perceptron with Backpropagation algorithm (MLP BP)
- (ii) Multilayer Perceptron with Levenberg-Marquardt algorithm (MLP LM)
- (iii) Radial Basis Function (RBF)
- (iv) Principal Component Analysis (PCA)
- (v) Support Vector Machines (SVM)

All the models of neural network used for this analysis had been discussed thoroughly in our previous publications [14, 23–27].

## 3 Data Collection

The total 2,332 data are collected from the experimental investigation [23] and also from the literature [2, 7–9, 11–13] to predict the different flow regimes for air-water gas-liquid flow through 1–5 mm diameter horizontal tubes through ANN. Given below are the inputs parameters and their range:

1. Gas flow rate,  $U_g$  varies from a minimum of 0.016 m/s to a maximum of 98.3 m/s;
2. Liquid flow rate  $U_l$  varies from a minimum of 0.00155 m/s to a maximum of 9.64 m/s;
3. Diameter of the tube,  $D$  varies from a minimum of 0.001 m to a maximum of 0.005 m.

Table 1 summarizes the data used for ANN studies. Table 1 consists of the 15 different types of flow regimes presented by the various authors. The flow regimes such as Annular (A), Slug-Annular (SA) and Wavy Annular (WA) as described by various authors in their individual papers are taken as Annular flow regime (A) for this study. The Bubble or Bubbly flow regime (B), Dispersed Bubbly flow regime (DB or DiB) and Bubble-train Slug flow regime (BTS) as described by various authors in their individual papers are taken as Bubbly flow regime (B) for this study. Intermittent flow regime (I), Slug flow regime (SI), Plug flow regime (P) and

**Table 1** Description of data collected from literature for air-water flow

Authors	Diameters used (mm)	Number of data points	Flow regimes (as per authors)	Flow Regimes (as per present study)
Barnea et al. [2]	4	171	DB, EB, SI, WA, SW, SS, A	B, I, A, S,
Triplett et al. [7]	1.097, 1.45	480	B, SI, C, SA, A	B, C, I, A
Coleman and Garimella [8]	1.3, 1.75, 2.6	295	B, Di, A, WA, P, SI	B, Di, A, I,
Yang and Shieh [9]	1, 2, 3	355	B, Di, A, SA, W, SI, P	B, Di, A, I, W
Chen et al. [11]	1	125	C, BTS, SI, A	B, C, I, A
Ide et al. [12]	1, 2.4, 4.9	179	B, I, A,	B, I, A,
Venkatesan et al. [13]	1.2, 1.7, 2.6, 3.4	509	B, DiB, SA, SI, A, S, WA	B, I, A, S,
Bar et al. [23]	3, 4	218	I, A, Di, W	I, A, Di, W

Elongated Bubble flow regime (EB) as described by various authors in their individual papers are taken as Intermittent flow regime (I) for this study. Stratified Wavy flow regime (SW) and Stratified Smooth flow regime (SS) as described by various authors in their individual papers are taken as Stratified flow regime (S) for this study. The Churn flow regime (C), Dispersed flow regime (Di) and Wavy flow regime (W) are left as it is without any change for this study. Therefore for this study the 15 types of flow regimes are modified to 7 to reduce the complexity, i.e., duration of training for the ANN analysis.

In general, researchers use either normalized data or raw data for ANN analysis. From our previous experience here only the raw data is used for ANN analysis [23–27]. All the data is first randomized into five different samples to eliminate any sampling error that may arise. Then they are individually analyzed (training, cross-validation and final prediction) using all the networks separately. The output is presented with 7 columns corresponding to 7 flow regimes. The output is then translated into numerical data from symbolic data, i.e., into 7 columns consisting of 0 and 1, where each row of the input corresponding to a unique set of air velocity, water velocity and tube diameter is represented in the output by 6 values of numeric 0 and one value of numeric 1. The row having number 1 indicates a flow regime associated with that unique set of inputs.

A Neurosolution 5.07 software is used for this analysis.

For the analysis of the ANN the following are considered,

1. Air-water flow only
2. Circular tubes having diameter ranging from 1–5 mm kept horizontally
3. Normalization of the data is not consider
4. MLPs, RBF and PCA having only one hidden layer
5. Hyperbolic tangent function used in all the hidden and output layers of respective ANNs

6. The processing element numbers vary from 1 to 25 in all analysis
7. Similar percentage of data for training, cross-validation and prediction are used for all cases

## 4 ANN Methodology

2,332 data points are used for ANN analysis, out of which 1,981 data points for training, 234 data points for cross-validation and 117 data points are used for final prediction.

The total data was first randomized for five different samples to eliminate sampling error. Then each of these five samples was analyzed (training, cross-validation and final prediction) for all five different neural networks, i.e., two Multilayer Perceptrons, Radial Basis Function, Support Vector Machine and Principal Component Analysis network.

The minimum value of Mean Squared Error (MSE) for all the networks are shown in Table 2. The criterion to stop training was MSE value of 0.01 and Table 2 clearly indicated that it never reached throughout the training for all algorithm. The network model having the number of processing elements in the hidden layer for which the minimum value of cross-validation MSE is reached, are then used to get the final result related to prediction. This procedure of training and cross-validation is followed for all the five different samples.

The optimum number of processing elements that are used in the hidden layer for Multilayer Perceptrons, Radial Basis Function and Principal Component Analysis network during training are shown in Table 3.

Maximum of 32,000 epochs, learning rate 1 and momentum coefficient 0.7 for hidden layer, learning rate 0.1 and momentum coefficient 0.7 for output layer are used for training of MLP network with BP algorithm. However, the training has been set to stop after 10,000 consecutive epochs when no improvement is observed for cross-validation MSE. It took a minimum of 16 h 28 min to a maximum of 18 h 32 min to train the five samples using MLP network trained with BP algorithm.

The MLP network with LM algorithm is trained with a maximum of 1,000 epochs. The initial value of damping factor ( $\lambda$ ) was 0.01. However, the training has

**Table 2** Minimum value of MSE for cross-validation reached during training for all five different ANNs

Sample number	Minimum value of MSE for cross-validation				
	MLP		RBF	PCA	SVM
	BP	LM			
1	0.0823	0.0961	0.0561	0.0555	0.0929
2	0.0789	0.0913	0.0621	0.0559	0.0939
3	0.0662	0.0807	0.0448	0.0371	0.0791
4	0.0817	0.0877	0.0551	0.0547	0.0797
5	0.0887	0.0978	0.0611	0.0609	0.0908



**Table 3** Optimum number of processing elements in the hidden layer during training for four different ANNs

Sample number	MLP		RBF	PCA
	BP	LM		
1	24	25	20	25
2	23	21	22	24
3	25	20	23	22
4	24	18	24	24
5	24	20	23	25

been set to stop after 100 consecutive epochs when no improvement is observed for cross-validation MSE. It took a minimum of 11 h to a maximum of 12 h 7 min to train the five samples using MLP network trained with LM algorithm.

For the training of RBF network 1,000 epochs for unsupervised learning and maximum of 1,000 epochs for supervised learning were used. The numbers of clusters were kept at 15. However the training has been set to stop after 100 consecutive epochs during supervised learning phase when no improvement is observed for cross-validation MSE. It took a minimum of 77 h 51 min to a maximum of 89 h 19 min to train the five samples using RBF network.

There are 3 principal components kept for this analysis. For training of PCA network with three principal components, 1,000 epochs have been used for unsupervised learning and also 1,000 epochs for supervised learning. However the training has been set to stop after 100 consecutive epochs during supervised learning phase when no improvement is observed for cross-validation MSE. For the supervised learning LM algorithm was used for updating the weights. It took a minimum of 21 h 57 min to a maximum of 31 h 15 min to train the five samples using PCA network.

For the training with SVM network 1,000 epochs are used. However, the training has been set to stop after 100 consecutive epochs when no improvement is observed for cross-validation MSE. It took a minimum of 34 min to a maximum of 2 h 15 min to train the five samples using SVM network.

## 5 Results and Discussion

The final result related to flow regime was identified by observing the predicted value which is closest to 1. Table 4 presents the final performance of the predicted flow patterns.

The perfection of final result may be due to the following reasons:

1. Overlapping of data points as indicated by the experimental observations outside the region marked by the boundary lines.
2. Some data points that lay on the boundary lines of the different flow regimes as observed by the researchers and represented in the graph.

**Table 4** Comparison of ANN predictions with experimental flow regime data with five different ANN used

Sample number	ANN analysis with 1981 data used for training, 234 data for cross-validation and 117 data for prediction				
	Number of data predicted accurately				
	MLP		RBF	PCA	SVM
BP	LM				
1	91	84	105	98	92
2	93	86	98	104	98
3	93	89	105	106	93
4	94	93	100	97	93
5	90	87	101	101	100
Mean	92.2	87.8	101.8	101.2	95.2

From the mean calculated in Table 4, it is clear that the Radial Basis Function gives slightly better predictability over the other networks. But time may be a factor as it is clearly seen that for the prediction using PCA network time is approximately 3 times lesser than that of the training with RBF network, which is an advantage where the analysis is done in a computer with lesser speed.

## 6 Conclusions

Experimental data of flow regime for two-phase air-water flow through 1–5 mm horizontal tubes are collected from literature and ANN predictability is tested using five well known different models using Neurosolution 5.07 software. The ANN model based Radial Basis Function and Principal Component Analysis gives good predictability over the other networks.

## References

1. Suo, M., Griffith, P.: Two-phase flow in capillary tubes. *J. Basic Eng.* **86**, 576–582 (1964)
2. Barnea, D., Luninski, Y., Taitel, Y.: Flow pattern in horizontal and vertical two phase flow in small diameter pipes. *Can. J. Chem. Eng.* **61**, 617–620 (1983)
3. Barajas, A.M., Panton, R.L.: The effect of contact angle on two-phase flow in capillary tubes. *Int. J. Multiph. Flow.* **19**, 337–346 (1993)
4. Fukano, T., Kariyasaki, A.: Characteristics of gas–liquid two-phase flow in a capillary. *Nucl. Eng. Design.* **141**, 59–68 (1993)
5. Mishima, K., Hibiki, T., Nishihara, H: Some characteristics of air–water two-phase flow in small diameter tubes. In: *Proceedings of the 2nd International Conference of Multiphase Flow*, vol. 4, 3–7, pp. 39–46, Tokyo, Japan (1995)
6. Mishima, K., Hibiki, T.: Some characteristics of air–water two-phase flow in small diameter vertical tubes. *Int. J. Multiph. Flow.* **22**, 703–712 (1996)
7. Triplett, K.A., Ghiaasiaan, S.M., Abdel-Khalik, S.I., Sadowski, D.L.: Gas–liquid two-phase flow in microchannels. Part I: two-phase flow patterns. *Int. J. Multiph. Flow* **25**, 377–394 (1999)

8. Coleman, J.W., Garimella, S.: Characteristics of two-phase patterns in small diameter round and rectangular tubes. *Int. J. Heat Mass Trans.* **42**, 2869–2881 (1999)
9. Yang, C.Y., Shieh, C.C.: Flow pattern of air–water and two-phase R-134a in small circular tubes. *Int. J. Multiph. Flow.* **27**, 1163–1177 (2001)
10. Zhao, T.S., Bi, Q.C.: Co-current air–water two-phase flow patterns in vertical triangular microchannels. *Int. J. Multiph. Flow.* **27**, 765–782 (2001)
11. Chen, W.L., Twu, M.C., Pan, C.: Gas-liquid two-phase flow in micro-channel. *Int. J. Multiph. Flow.* **28**, 1235–1247 (2002)
12. Ide, H., Kariyasaki, A., Fukano, T.: Fundamental data on gas–liquid two-phase flow in microchannels. *Int. J. Therm. Sci.* **46**, 519–530 (2007)
13. Venkatesan, M., Das, S.K., Balakrishnan, A.R.: Effect of tube diameter on two-phase flow patterns in mini tubes. *Can. J. Chem. Eng.* **88**, 936–944 (2010)
14. Bar, N., Das, S.K.: Prediction of flow regime for air-water flow in circular micro channels using ANN. *Procedia Technol.* **10**, 242–252 (2013)
15. Baker, O.: Simultaneous flow of oil and gas. *Oil and Gas J.* **53**, 185–195 (1954)
16. Mandhane, J.M., George, G.A., Aziz, K.A.: Flow pattern map for gas–liquid flow in horizontal pipes. *Int. J. Multiph. Flow.* **1**, 537–553 (1974)
17. Taitel, Y., Dukler, A.E.: A model for predicting flow regime transitions in horizontal and near horizontal gas–liquid flow. *AIChE J.* **22**, 47–55 (1976)
18. Weisman, J., Duncan, D., Gibson, J., Crawford, T.: Effects of fluid properties and pipe diameter on two-phase flow patterns in horizontal lines. *Int. J. Multiph. Flow.* **5**, 437–462 (1979)
19. Taitel, Y.: Flow pattern transition in two phase flow, keynote lecture. In: *Proceedings of the 9th International Heat Transaction Conference 19–24 August, No. KN-14*, pp. 237–254, Jerusalem, Israel (1990)
20. Himmelblau, D.M.: Application of artificial neural network in chemical engineering. *Korean J. Chem. Eng.* **17**, 373–392 (2000)
21. Cong, T., Su, G., Qiu, S., Tian, W.: Applications of ANNs in flow and heat transfer problems in engineering: a review work. *Prog. Nucl. Energy* **62**, 54–71 (2013)
22. Cai, S., Toral, H., Qiu, J., Archer, J.S.: Neural network based objective flow regime Identification in air-water two phase flow. *Can. J. Chem. Eng.* **72**, 440–445 (1994)
23. Bar, N., Ghosh, T.K., Das, S.K., Biswas, M.N.: Air-water flow through 3 mm and 4 mm Tubes—experiment and ANN prediction. *Artif. Intell. Syst. Machine Learn.* **3**(8), 531–537 (2011)
24. Bar, N., Biswas, M.N., Das, S.K.: Prediction of pressure drop using artificial neural network for gas non-newtonian liquid flow through piping components. *Ind. Eng. Chem. Res.* **49**, 9423–9429 (2010)
25. Bar, N., Das, S.K.: Comparative study of friction factor by prediction of frictional pressure drop per unit length using empirical correlation and ANN for gas-non-newtonian liquid flow through 180° circular bend. *Int. Rev. Chem. Eng.* **3**(6), 628–643 (2011)
26. Bar, N., Das, S.K.: Gas-non-newtonian liquid flow through horizontal pipe—gas holdup and frictional pressure drop prediction using multilayer perceptron. *Am. J. Fluid Dyn.* **2**(3), 7–16 (2012)
27. Bar, N., Das, S.K.: Frictional pressure drop for gas-non-newtonian liquid flow through 90° and 135° circular bend: prediction using empirical correlation and ANN. *Int. J. Fluid Mech. Res.* **39**(5), 416–437 (2013)

# Study of Wireless Communication Through Coal Using Dielectric Constant

Aindrila Bhattacharjee, Sourav Roy, Sayan Chakraborty, Amartya Mukherjee and Soumya Kanti Bhattacharya

**Abstract** Dielectric constant is an important parameter having a wide range of applications in satellite and terrestrial communication, wireless communication especially for GPS, environmental monitoring and ground penetrating radar (GPR) surveys. It controls vertical and horizontal imaging, resolution, propagation velocity of electromagnetic waves through material, and reflection coefficients across interfaces of different materials. Although the communication process gets disrupted due to lower penetration ability of Electromagnetic Wave. High dielectric constant of the medium, low frequency and attenuation constant of EM wave etc. are main culprits of this disruption. Hence, in order to find a solution to this problem, four modeled coal samples of variable porosity, mineralogy, and saturation are taken. It is observed that the bulk dielectric constant generally varies from 2 to 38 in the materials modeled. The decrease in dielectric constant with increase in frequency is mainly due to polarization of polar molecule and non-polar molecule of coal under the influence of extra electric field. Hence, in order to receive the reflected EM waves above background noise, the dielectric constant of the material medium must be greater than 2.

**Keywords** Dielectric constant · Electromagnetic waves · Ground penetrating radar (GPR) · Electric field · Polarization

---

A. Bhattacharjee (✉) · S. Roy  
Department of ECE, Bengal College of Engineering and Technology, Durgapur, India  
e-mail: abaindrila5@gmail.com

S. Roy  
e-mail: sourav.roy12@rediffmail.com

S. Chakraborty · A. Mukherjee · S.K. Bhattacharya  
Department of CSE, Bengal College of Engineering and Technology, Durgapur, India  
e-mail: sayan.cb@gmail.com

A. Mukherjee  
e-mail: mamartyacse1@gmail.com

S.K. Bhattacharya  
e-mail: soumyakanti.bhattacharya@gmail.com

## 1 Introduction

Dielectric permittivity refers to a complex function [1] that has both real and imaginary components. The imaginary component of dielectric permittivity [2–4] is generally expressed as dielectric loss, which represents dispersion and attenuation. The real component of dielectric permittivity is generally denoted by dielectric constant ( $\epsilon_r$ ), which is the ratio of the capacity of a material to store electric-field in any medium to that of free space. Dielectric loss is insignificant [2] if the conductivity of a material is lesser than 10 milliSiemens/meter (mS/m). Thus, dielectric constant [5, 6] is naturally the main component of dielectric permittivity. Magnetic permeability is generally represented by the product of the permeability of free space ( $m_0$ ) and relative magnetic permeability ( $m_r$ ). The effect of magnetic permeability on Ground Penetrating Radar (GPR) response is insignificant for materials having unity relative magnetic permeability ( $m_r = 1$ ). Dielectric constant [3] usually decreases with increasing frequency, while dielectric loss and conductivity increase with increasing frequency. The relative permittivity of a material is the ratio of its dielectric permittivity and vacuum permittivity which [7] can be expressed as the property of the material which defines the force between two point charges in the material. When the material is placed between two conducting plates, permittivity is the amount of energy stored in the material per unit voltage applied to the electrodes. Relative permittivity is typically denoted by  $\epsilon_r(w)$  (sometimes  $\kappa$  or  $K$ ) and is defined as:

$$\epsilon_r(w) = \frac{\epsilon(w)}{\epsilon_0} \quad (1)$$

where,  $\epsilon(w)$  is the complex frequency-reliant absolute permittivity [8] of the material, and  $\epsilon_0$  is the vacuum permittivity. The relative static permittivity,  $\epsilon_r$  can be calculated:

$$\epsilon_r = \frac{C_r}{C_0} \quad (2)$$

Earlier, various research works have been done to study the importance of dielectric constant in the field of Wireless Communication [4]. The role of skin depth in communication has also been discussed in detail which will help in getting a brief idea of the material which must be chosen for establishing a better communication network.

## 2 Methodology

Dielectric constant [9] is calculated by the use of an LCR meter. The model of LCR meter used is Agilent E4980A. 16451B is also used in the measurement. The 16451B is a test fixture for measuring disc and film dielectric materials when connected to Agilent's LCR meters or impedance analyzers, and is usable up to 15 MHz. The 16451B provides the fixture assembly, four interchangeable Guarded/Guard electrodes and accessories. The name and description of the fixture assembly are listed in the following table.

- (a) Unguarded electrode—This electrode is connected to the  $H_C$  (High current) and  $H_p$  (High potential) terminal of the instrument.
- (b) Guarded/Guard Electrode—This electrode is combined by a Guarded electrode and a Guard electrode. The guarded electrode is connected to the  $L_C$  (Low current) and  $L_p$  (Low potential) terminals of the instrument. The guard electrode is connected to the guard terminal. This electrode is interchangeable and is movable using the knobs on the micrometer.
- (c) Guarded/Guard Electrode attachment Screw—This screw secures the Guarded/Guard electrode.
- (d) Micrometer—The micrometer is used to adjust the distance between electrodes. Do not use this to measure thickness the of test material.
- (e) Adjustment knob—This knob should be used for coarse adjustment of electrode distance. Do not use the large knob to bring the Guarded/Guard electrode into contact with the Unguarded electrode or test material.

The dielectric constant [10], a fundamental parameter of insulating or dielectric materials, is calculated from the capacitance value when the material is used as the dielectric. A practical measurement procedure is described in "Typical Measurement Procedure by the Measurement Methods". For the dielectric constant calculation, a solid material is considered which is shaped into a disc. The dielectric constant can be obtained using the following equation:

$$\varepsilon = \varepsilon_r \times \varepsilon_0 = \frac{t}{A} C_p \quad (3)$$

where,  $\varepsilon$  = Dielectric constant (permittivity) [F/m]  $\varepsilon_0$  = Space permittivity =  $8.854 \times 10^{-12}$  [F/m];  $\varepsilon_r$  = Relative dielectric constant (Relative permittivity) of test material;  $C_p$  = Equivalent parallel capacitance value [F];  $t$  = Thickness of test material [m];  $A$  = Area of electrode [m<sup>2</sup>]. Thus, the relative dielectric constant [11, 12] (generally called the dielectric constant) of the test material,  $\varepsilon_r$  was obtained by measuring the capacitance value and calculating using the following equation:

$$\varepsilon_r = \frac{t \times C_p}{A \times \varepsilon_0} = \frac{t \times C_p}{\pi \times \left(\frac{d}{2}\right)^2 \times \varepsilon_0} \quad (4)$$

where,  $d$  = Diameter of electrode[m]. The dielectric dissipation factor ( $=\tan \delta$ ; loss tangent) of test material  $D_r$  can be obtained directly by measuring the dissipation factor.

### 3 Proposed Method

#### 3.1 Electrode Method

This method uses rigid electrodes which make contact directly with the surface of the test material. This method is applicable for thick, smoother, slightly compressible materials. The merits of this method are (i) procedure to measure capacitance is simple, (ii) it is not necessary to apply thin film electrodes, (iii) equations to obtain dielectric constant are simple. The main disadvantage or demerits of this method is air film (error caused by air gap between electrodes and surface of the test material) causes error.

#### 3.2 Procedure

The following algorithm has been developed for this work.

**begin**

**prepare** test material so that 16451B can measure it.

**connect** the 16451B to the Agilent E4980A.

**set** up Agilent E4980A to measure capacitance ( $C_p$ ).

**set** the test material between the electrodes.

**measure** the capacitance ( $C_p$ ) and calculating the dielectric constant.

**end**

### 4 Electromagnetic Waves in Dielectric Media

In a “simple” material, the electric field satisfies equation

$$\nabla^2 \vec{E} - \mu\epsilon\vec{E} = 0 \quad (5)$$

Similarly, the magnetic field satisfies equation:

$$\nabla^2 \vec{B} - \mu\epsilon \vec{B} = 0 \quad (6)$$

These are the equations for wave traveling with speed  $v$ , given by:

$$v = \frac{1}{\sqrt{\mu\epsilon}} \quad (7)$$

Experimentally, it has been found that  $v$  is the speed of light in the material. In a vacuum, the speed of wave is  $c$ , is given by:

$$c = \frac{1}{\sqrt{\mu_0\epsilon_0}} \quad (8)$$

Light is an electromagnetic wave. The wave equation is solved by:

$$\vec{E}(\vec{r}, t) = \vec{E}_0 \cos(\omega t - \vec{k} \cdot \vec{r} + \phi_0) \quad (9)$$

where  $\vec{E}_0$  and  $\vec{k}$  are constant vectors, and  $\omega$  and  $\phi_0$  are constant scalars. The fact that only a single frequency is present in the wave means that the wave is monochromatic [6]. This field equation is the valid solution of the wave equation if  $\vec{k}$  and  $\omega$  satisfies:

$$\frac{\omega^2}{k^2} = v^2 = \frac{1}{\mu\epsilon} \quad (10)$$

This equation is known as Dispersion relation: it relates the frequency of the wave  $\omega$  to the wave factor  $\vec{k}$ . The behavior of the wave at the boundary between two media depends on the ratio of the electric field  $\vec{E}$  to the magnetic intensity  $\vec{H}$ . The ratio of the amplitudes of the electric field to the amplitude of the magnetic intensity is called the impedance  $Z$  of the medium. In free space,

$$Z_0 = \frac{E_0}{H_0} = \sqrt{\frac{\mu_0}{\epsilon_0}} \quad (11)$$

where,  $[B_0 = \mu_0 H_0]$ .

The impedance of free space  $Z_0$ , is a physical constant with value:  $Z_0 \approx 376.7 \Omega$ . The refractive index  $n$  of a material is defined as the ratio of the speed of electromagnetic waves in vacuum to the speed of electromagnetic waves in the material:

$$n = \frac{c}{v} = \frac{\sqrt{\mu\epsilon}}{\sqrt{\mu_0\epsilon_0}} = \sqrt{\mu_r\epsilon_r} \quad (12)$$



For most transparent materials,  $\mu_r \approx 1$ . Now in this case:

$$n \approx \sqrt{\epsilon_r} \quad (13)$$

Electromagnetic waves carry energy. The energy density in electric field is given by:

$$U_E = \frac{1}{2} \epsilon \overrightarrow{E^2} \quad (14)$$

The energy density in magnetic field is given by:

$$U_H = \frac{1}{2} \mu \overrightarrow{H^2} \quad (15)$$

The energy flux (energy crossing unit area per unit time) is given by the Pointing vector:

$$\vec{S} = \vec{E} \times \vec{H} \quad (16)$$

The propagation velocity of electromagnetic waves through a material and reflection coefficients is controlled by Dielectric constant. In the infinite homogeneous semi-conductive medium, the propagation of electro-magnetic waves is

$$\vec{E} = \vec{E}_0 e^{-\beta r} e^{-j\omega r} \quad (17)$$

where,  $E_0$  is a constant vector. The  $r$  is propagation direction of the radius vector. As shown in Eq. (17) the amplitude is attenuated along the propagation direction of electromagnetic waves by  $e$  the exponential, in which

$$\alpha = \omega \sqrt{\frac{\mu\epsilon}{2} \left( \sqrt{1 + \left(\frac{\sigma}{\omega\epsilon}\right)^2} + 1 \right)} \quad (18)$$

and

$$\beta = \omega \sqrt{\frac{\mu\epsilon}{2} \left( \sqrt{1 + \left(\frac{\sigma}{\omega\epsilon}\right)^2} - 1 \right)} \quad (19)$$

$\mu(H/m)$  for the magnetic permeability,  $\epsilon(F/m)$  as the dielectric constant,  $\sigma(S/m)$  for the conductivity,  $\omega(\text{rad/s})$  sent waves of angular frequency. The depth at which the amplitude of the wave is reduced to about 0.37 compared to the amplitude at the surface is called the “skin depth”. Skin depth and wavelength will

depend on frequency and coal parameters,  $\sigma$  = soil conductivity and  $\varepsilon$  = permittivity or dielectric constant. Skin depth in an arbitrary material is given by:

$$\delta = \left( \frac{\sqrt{2}}{\omega\sqrt{\mu\varepsilon}} \right) \left[ \sqrt{1 + \left( \frac{\sigma}{\omega\varepsilon} \right)^2} - 1 \right]^{-1/2} \quad (20)$$

where,  $\delta$  = skin or penetration depth,  $\omega = 2\pi f$ ,  $f$  = frequency,  $\sigma$  = conductivity [Siemens/meter, S/m],  $\mu = \mu_r \times \mu_0$  = permeability,  $\mu_0$  = permeability of vacuum =  $4\pi \times 10^{-7}$  [H/m],  $\mu_r$  = relative permeability,  $\varepsilon = \varepsilon_r \times \varepsilon_0$  = permittivity,  $\varepsilon_0$  = permittivity of vacuum =  $8.854 \times 10^{-12}$  [F/m],  $\varepsilon_r$  = relative permittivity. In coal mine communication medium is semi conductive. Hence, in order to decrease the attenuation of electromagnetic waves in their transmittance, lower frequency should be used. In the large semi-conductive medium, to meet the  $\sigma \gg \omega\varepsilon$ ,  $\sigma/\omega\varepsilon \gg 1$ ,  $\alpha$ ,  $\beta$  expression can be simplified as:

$$\alpha \approx \beta \approx \sqrt{\pi\mu\sigma f} \quad (21)$$

At a distance, and if the fields decay to the original  $e^{-1}$ , then the distance called the penetration depth of field  $\delta$ .

$$\delta \approx \frac{1}{\beta} \approx \frac{1}{\sqrt{\pi\mu\sigma f}} \quad (22)$$

## 5 Results and Discussion

The resistivity and conductivity can be calculated using the following formulae:

$$\rho = R \frac{l}{A} \quad (23)$$

and

$$\sigma = \frac{1}{\rho} \quad (24)$$

The dielectric constant, resistance, resistivity and conductivity of the four samples has been calculated using the thickness and capacitance of the material, displayed in Agilent E4980A. The dielectric constant [12–14] of the samples has been calculated for a frequency ranging from 1 to 300 kHz which is shown in Table 1.

Table 1 shows dielectric constant at different frequencies. At 50–100 kHz, the resistance and resistivity of the coal samples have decreased effectively whereas

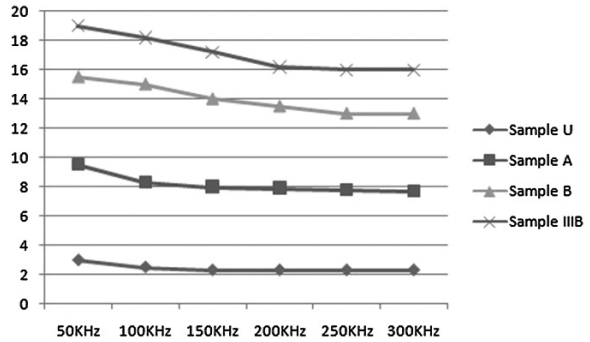
**Table 1** Dielectric constant at different frequencies

Sample name	Thickness (in mm)	C <sub>p</sub> (in pF)	$\epsilon_r$	Resistance (R)	Resistivity ( $\rho$ )	Conductivity ( $\sigma$ )
<i>Dielectric constant at 1 kHz</i>						
U	10	17.25	7.91	4.98 M $\Omega$	1,148,781.42	$8.70 \times 10^{-7}$
A	8.1425	70.8	26.46	1.47 M $\Omega$	398,704.19	$2.50 \times 10^{-6}$
B	7.1	50.38	16.42	736.7 K $\Omega$	137,558.5	$7.26 \times 10^{-6}$
III B	9.185	23.4	9.86	3.56 M $\Omega$	861,539.38	$1.16 \times 10^{-6}$
<i>Dielectric constant at 50 kHz</i>						
U	10	6.49	2.9789	97.14	22,408.15	$4.46 \times 10^{-5}$
A	8.1425	16.73	6.2526	55.85	15,241.06	$6.56 \times 10^{-5}$
B	7.1	19.41	6.3255	38.9	7,263.5	$1.37 \times 10^{-4}$
III B	9.185	8.01	3.3765	86.87	21,011.56	$4.75 \times 10^{-5}$
<i>Dielectric constant at 100 kHz</i>						
U	10	6.07	2.7861	42.45	9,792.32	$1.02 \times 10^{-4}$
A	8.1425	14.97	5.5948	27.61	7,534.57	$1.32 \times 10^{-4}$
B	7.1	20.55	6.6970	21.6	4,033.2	$2.47 \times 10^{-4}$
III B	9.185	7.42	3.1282	40.06	9,689.46	$1.03 \times 10^{-4}$
<i>Dielectric constant at 150 kHz</i>						
U	10	5.87	2.6943	26.16	1,354.08	$7.38 \times 10^{-4}$
A	8.1425	13.91	5.1987	18.10	3,795.93	$2.63 \times 10^{-4}$
B	7.1	19.04	6.2049	15.23	3,555.19	$2.81 \times 10^{-4}$
III B	9.185	7.16	3.0185	25.31	1,731.8	$5.77 \times 10^{-4}$
<i>Dielectric constant at 200 kHz</i>						
U	10	5.74	2.6346	18.60	1,324.09	$7.55 \times 10^{-4}$
A	8.1425	13.62	5.09	13.37	3,716.80	$2.69 \times 10^{-4}$
B	7.1	18.13	5.9083	11.79	3,385.27	$2.95 \times 10^{-4}$
III B	9.185	6.91	2.91	18.25	1,671.3	$5.98 \times 10^{-4}$
<i>Dielectric constant at 250 kHz</i>						
U	10	5.641	2.5892	14.3	3,298.7	$3.03 \times 10^{-4}$
A	8.1425	13.15	4.9146	10.56	2,881.74	$3.47 \times 10^{-4}$
B	7.1	17.191	5.6023	9.64	1,808.80	$5.55 \times 10^{-4}$
III B	9.185	6.8	2.866	14.15	3,422.51	$2.92 \times 10^{-4}$
<i>Dielectric constant at 300 kHz</i>						
U	10	5.59	2.5658	11.54	2,662.03	$3.75 \times 10^{-4}$
A	8.1425	12.92	4.8287	8.7	2,374.16	$4.21 \times 10^{-4}$
B	7.1	17.3	5.6378	8.17	1,525.52	$6.55 \times 10^{-4}$
III B	9.185	6.64	2.7990	11.5	2,781.54	$3.59 \times 10^{-4}$

their conductivity has increased. From 200 kHz onwards, the dielectric constant decreases slowly with the increase in frequency.

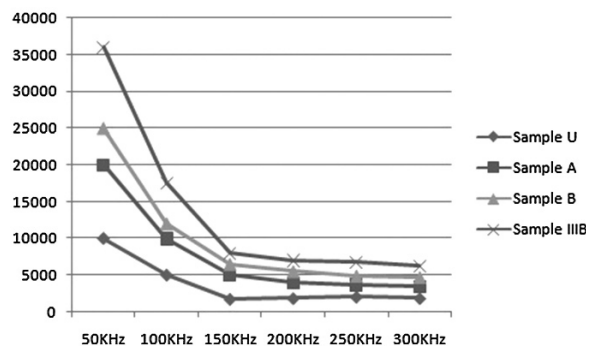
Figure 2 illustrates that the skin depth decreases exponentially with the increase in frequency. At higher frequency the media conductivity becomes higher which

**Fig. 1** Dielectric constant versus frequency



results in severe attenuation and hence causes a weaker penetration effect. Hence, it is better to reduce the operating frequency to Very Low Frequency (VLF). Finally, Table 1 also shows that the dielectric constant is the lowest at the highest frequency. The skin depth, resistance and resistivity of the material also decrease with sudden increase in frequency. But the conductivity increases in parallel to the increase in frequency. Figure 1 shows the relation between the dielectric constant and

**Fig. 2** Skin depth versus frequency



frequency of four coal samples. It is clearly seen that the dielectric constant decreases with the increase in frequency and hence causes a better penetration effect for the communication purpose. The graph shown in Fig. 1 deals with the relation between dielectric constant and frequency of the four coal samples. Visual observation of Fig. 2 proves that the skin depth decreases exponentially with the increase in frequency and hence results in establishment of a better communication network.

## 6 Conclusion

The work presented in this paper and the results shown previously, describes that dielectric constant decreases with increase in frequency and tend to attain stability at higher test frequency. The changes happened mainly due to polarization of polar molecule and non-polar molecule of coal under the influence of extra electric field. The action time of alternative electric field on coal lasted for a comparatively short period in the same direction under circumstances of high test frequency. Hence, it is hard to change direction for polar molecule. Therefore, the dielectric constant measured at higher test frequency was smaller than the value measured at lower frequency. The increase in attenuation constant ( $\alpha$ ) may cause lower penetration ability of Electromagnetic Wave. Skin depth got decreased exponentially with increase in frequency. The higher the frequency  $f$ , or the greater the media conductivity  $\sigma$ , the more severe attenuation of radio waves occurs because the medium more readily absorbs the higher energies of the upper harmonics. This might be related to the stiffness or elasticity of the medium, and hence results in weaker penetration ability. Therefore, the operating frequency will be reduced to Very Low Frequency (VLF) to a certain degree of penetration. This played an important role while choosing VLF for this work. This work can be further extended in near future overcoming the weaknesses of this method.

## References

1. Martinez, A., Byrnes, A.P.: Modeling dielectric-constant values of geologic materials: an aid to ground-penetrating radar data collection and interpretation. *Kansas Geol. Surv. Curr. Res. Earth Sci. Bull.* **247**(1), 1–16 (2001)
2. Cai, M.: *Rock mechanics: achievements and ambitions*. CRC Press, Boca Raton (2011)
3. Tao, J.: Research on electromagnetic wave through-the-earth wireless communication for coal mine disaster. In: *Web Information Systems and Mining, Lecture Notes in Computer Science*, vol. 6987, pp. 1–10 (2011)
4. Weir, W.B.: Automatic measurement of complex dielectric constant and permeability at microwave frequencies. *Proc. IEEE* **62**(1), 33–36 (1974)
5. Das, N.K., Voda, S., Pozar, D.M.: Two methods for the measurement of substrate dielectric constant. *IEEE Trans. Microw. Theory Tech.* **35**(7), 636–642 (1987)

6. Shebani, N.M., Surman, L., Khamoudi, B.M., Abul-kassem, A.S.: Measurement of dielectric constant of some materials using planar technology. In: Second International Conference on Computer and Electrical Engineering, ICCEE '09, pp. 352–356 (2009)
7. Du, P., Lin, X., Xin, Z.: Dielectric constants of PDMS nanocomposites using conducting polymer nanowires. In: 2011 16th International Solid-State Sensors, Actuators and Microsystems Conference (TRANSDUCERS), pp. 645–648 (2011)
8. Peterlin, A., Elwell, J.H.: Dielectric constant of rolled polyvinylidene fluoride. *J. Mater. Sci.* **2** (1), 1–6 (1967)
9. Treichel, H.: Low dielectric constant materials. *J. Electron. Mater.* **30**(4), 290–298 (2001)
10. Vodák, F.: Dielectric constant of ann-element moist capillary-porous material. *Czechoslovak J. Phys. B* **23**(10), 1093–1101 (1973)
11. Pontes, F.M., Lee, E.J.H., Leite, E.R., Longo, E., Varela, J.A.: High dielectric constant of SrTiO<sub>3</sub> thin films prepared by chemical process. *J. Mater. Sci.* **35**(19), 4783–4787 (2000)
12. Rao, D.A.A.S.N.: Dielectric constants of crystals. *Proc. Indian Acad. Sci. Sect. A* **27**(3), 177–183 (1948)
13. Elworthy, P.H., McIntosh, D.S.: The effect of solvent dielectric constant on micellisation by lecithin. *Kolloid-Zeitschrift und Zeitschrift für Polymer* **195**(1), 27–34 (1964)
14. Ahamed, M.M., Bhowmik, K., Shahidulla, M., Islam, M.S., Rahman, M.S.: Rectangular microstrip patch antenna at 2 GHz on different dielectric constant for pervasive wireless communication. *Int. J. Electr. Comput. Eng. (IJECE)* **2**(3), 417–424 (2012)

# Performance Evaluation of Heuristic Algorithms for Optimal Location of Controllers in Wireless Networks

Dac-Nhuong Le

**Abstract** In this paper, we have presented the new Ant Colony Optimization scheme for the optimal location of controllers in wireless networks, which is an important problem in the process of designing cellular mobile networks. Our objective functions are determined by the total distance based on pheromone matrix of ants satisfies capacity constraints to find good approximate solutions. Our proposed algorithms may give feasible solutions to this problem based on the global search for high quality feasible solutions. The experimental results show that our pro-posed algorithm has achieved a much better performance than the previous approaches based on heuristic and evolution algorithms.

**Keywords** Base station controller · Wireless networks · Heuristic · Ant colony optimization

## 1 Introduction

The size and complexity of computer networks have been growing very fast in the last decade. In the past, a computer network usually only served a small number of devices. Nowadays, it is common to find a computer network that serves hundreds of even thousands of devices. It seems they this incredible growth will continue as the customers needs and the telecommunication technology keep growing. As the size and complexity of computer networks grow, so too does the need for good design strategies. Optimal the placement of base stations in the designing of a wireless network is very important for a cheaper and better customer service. This issue is related to the problems of location of devices [1, 2]. The objective of *Terminal Assignment* (TA) problem [3] involves with determining minimum cost links to form a network by connecting a given collection of terminals to a given

---

D.-N. Le (✉)

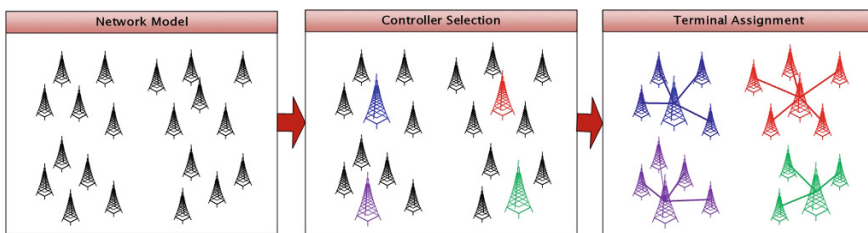
Haiphong University, Haiphong, Vietnam  
e-mail: Nhuongld@hus.edu.vn

collection of concentrators. The capacity requirement of each terminal is known and may vary from one terminal to another. The capacity of concentrators is known. The cost of the link from each terminal to each concentrator is also known. The problem is now to identify for each terminal the concentrator to which it should be assigned, under two constraints: Each terminal must be connected to one and only one of the concentrators, and the aggregate capacity requirement of the terminals connected to any concentrator must not exceed the capacity of that concentrator. The assignment of BTSs to switches problem introduced in [4]. In which it is considered that both the BTSs and controllers of the network are already positioned, and its objective is to assign each BTSs to a controller, in such a way that a capacity constraint has to be fulfilled. The objective function in this case is then formed by two terms: the sum of the distances from BTSs to the switches must be minimized, and also there is another term related to *handovers*, between cells assigned to different switches which must be minimized.

## 2 Problem Formulation

Let us consider a mobile communication network formed by  $N$  nodes (*BTSs*), where a set of  $M$  controllers must be positioning in order to manage the network traffic. It is always fulfilled that  $M \ll N$ , and in the majority of cases. We start from the premise that the existing *BTSs* infrastructure must be used to locate the switches, since it saves costs. The complete *optimal location of controller problem* (OLCP) has to deal with two issues in Fig. 1. First, the selection of the  $N$  controllers in  $M$  nodes, second for each selection, an associated TA problem [5].

Let  $l_1, l_2, \dots, l_N$  is set of  $N$  *Base Stations* (BTSs),  $w_1, w_2, \dots, w_N$  is the weight requirement of BTS,  $(l_{j1}, l_{j2})$  is the coordinates of BTS  $l_j \forall j = 1 \dots N$  on the Euclidean grid; Let  $r_1, r_2, \dots, r_M$  is set of *Base Station Controllers* (BSCs) should be established,  $p_1, p_2, \dots, p_M$  is the capacity can satisfy of BSC  $r_i$ ,  $(r_{i1}, r_{i2})$  is the coordinates of BSC  $r_i, \forall i = 1 \dots M$  on the Euclidean grid. The weights and capacity are positive integers and  $w_i < \min\{p_1, p_2, \dots, p_M\}, \forall i = 1, 2, \dots, N$ . Assign each BTS to one of BSC such that no BSC exceeds its capacity. Let  $\tilde{x} = \{\tilde{x}_1, \tilde{x}_2, \dots, \tilde{x}_M\}$  be a vector such that means that BTS  $l_j$  has been assigned to BSC  $r_i$ , with  $i$  is an integer such that  $\tilde{x}_j = i$ .



**Fig. 1** Optimal location of controller problem model



Capacity of each BSC must be satisfied  $\sum_{j \in R_i} w_j < p_i, i = 1..M$  where,  $R_i = \{j | \tilde{x}_j = i\}$ , i.e.,  $R_i$  represents the BTSs that are assigned to BSC  $r_i$ . Let  $X = \{x_{ij}\}_{M \times (N-M)}$  is a binary matrix describes the connection between the BTS  $l_j$  to BSC  $r_i$ . Such that,  $x_{ij} = 1$  means that BTS  $l_j$  has been connected to BSC  $r_i$ , and otherwise. The objective of optimal location of controller problem is minimize the total connectivity costs between  $(N - M)$  BTSs to  $M$  BSCs. The cost of connection from BTS  $l_j$  to BSC  $r_i$  is calculated by  $cost\ t_{ij} = \sqrt{(l_{j1} - r_{i1})^2 + (l_{j2} - r_{i2})^2}$ . The problem can be defined as follows:

$$f(\tilde{x}) = \sum_{i=1}^M \sum_{j=1}^{N-M} cost\ t_{ij} x_{ij} \rightarrow \min \tag{1}$$

Subject to:

$$\sum_{i=1}^M x_{ij} = 1, \quad \forall j = \overline{1..N-M} \tag{2}$$

$$\sum_{i=j}^{N-M} w_j x_{ij} \leq p_i, \quad \forall i = \overline{1..M} \tag{3}$$

### 3 Related Works and Our Works

Both TA and OCLP are *NP-complete* combinatorial optimization problems [1, 6, 7], so heuristic approach is a good choice [8]. All the previous work on the TA provides powerful approaches when the cost of assigning a single terminal to a given concentrator is known before running the algorithms. The cost function is the Euclidean distance between a terminal and its associated concentrator [1]. A *Greedy* is the first algorithm proposed by Abuali et al. in [3] for solving the TA. Khuri and Chui proposed a GA (*Genetic Algorithm*) with a penalty function as an alternative method for solving the TA [4]. They showed its performance by means of the comparison with the greedy algorithm *GA-Greedy* proposed in [3]. The improved GA is proposed include: GENEsYs (*Genetic Search*) [7], LibGA [9], and GGA (*Group Genetic Algorithm*) [10]. In [5], Sanz et al. introduced a hybrid heuristic consisting of SA (*Simulated Annealing*) and a Greedy algorithm for solving the OLCF problem is called by SA-Greedy algorithm. An improvement of *SA-Greedy* is *LB-Greedy* algorithm [11], the lower bound comes from the solution obtained by assigning each BTS  $l_j$  to the nearest BSC  $r_i$ . A hybrid neural-GA in which a *Hopfield neural network* [12] manages the problems constraints and a GA searches for high quality solutions with the minimum possible cost called by *Hybrid I, Hybrid II* proposed in [5, 13].

In the latest works on the OCLP, we proposed GA-BSC [14], *Particle Swarm Optimization* (PSO-BSC) [15] and *Ant Colony Optimization* (ACO-BSC1) [16] algorithms.

## 4 Our Proposed

In this section, we propose a new ACO algorithm combined *Local search* to improve the speed and quality of solution. The ACO algorithm is originated from ant behavior in the food searching. When an ant travels through paths, from nest food location, it drops pheromone. According to the pheromone concentration the other ants choose appropriate path. The paths with the greatest pheromone concentration are the shortest ways to the food [17].

**Ant Encoding:** We consider that configurations are sets of  $M$  nodes which will be evaluated as BSCs for the network. The encoding of the ant  $k$  configuration is by means of binary string of length  $N$ , say  $k = \{x_1, x_2, \dots, x_N\}$  where  $x_i = 1$  in the binary string means that the corresponding node has been selected to be a controller, whereas a 0 in the binary string means that the corresponding node is not a BSC, but serve as BTS. We must select  $N$  nodes to be the controllers of the network. We use fully random initialization in order to initialize the ant population. After that, the ant  $k$  will have  $p$  1s, we use *Ant\_Repair* function to ensure that all binary strings of ants have exactly  $M$  1s.

---

### Algorithm 1 Ant\_repair

---

*Input:* The ant  $k = \{x_1, x_2, \dots, x_N\}$  has  $p$  1s

*Output:* The ant  $k$  will have exactly  $M$  1s

**BEGIN**

**IF**  $p < M$  **THEN** Adds  $(M - p)$  1s in random positions;

**ELSE** Select  $(p - M)$  1s randomly and removes them from the binary string;

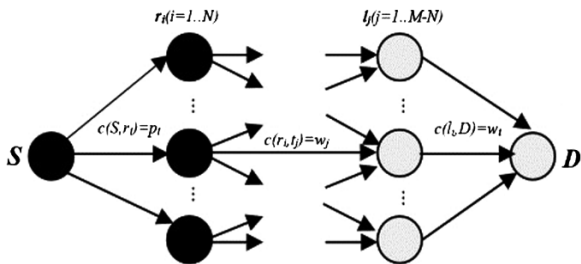
**END.**

---

The pheromone matrix is generated with matrix elements that represent a location for ant movement, and in the same time it is possible receiver location. Each ant  $k$  has exactly  $M$  1s representing  $M$  BSCs is associated to one matrix. We use real encoding to express an element of matrix  $A_{M \times N}$  (where  $N, M$  are the number of BTSs, and BSCs). We construct a transport network  $G = (I, J, E)$  where  $I = \{1, 2, \dots, M\}$  is the set of BSCs,  $J = \{1, 2, \dots, N - M\}$  is the set of BTSs and  $E$  is the set of edge connections between BSC  $r_i$  and the BTS  $l_j$ . We adding two vertices  $S$  (*Source*) and  $D$  (*Destination*) is shown in Fig. 2.

**Construct Ant Solutions:** Each ant can move to any location according to the transition probability defined by:

**Fig. 2** The transport network  
 $G = (I, J, E)$



$$P_{ij}^k = \frac{[\tau_{ij}]^\alpha [\eta_{ij}]^\beta}{\sum_{l \in N_i^k} [\tau_{il}]^\alpha [\eta_{il}]^\beta} \tag{4}$$

in which,  $\tau_{ij}$  is the pheromone content of the path from BSC  $r_i$  to BTS  $l_j$ ,  $N_i^k$  is the neighborhood includes only locations that have not been visited by ant  $k$  when it is at BSC  $r_i$ ,  $\eta_{ij}$  is the desirability of BTS  $l_j$ , and it depends of optimization goal so it can be our cost function. The influence of the pheromone concentration to the probability value is presented by the constant  $\alpha$ , while constant  $\beta$  do the same for the desirability. These constants are determined empirically and our values are  $\alpha = 1$ ,  $\beta = 10$ . The ants deposit pheromone on the locations they visited according to the relation.

$$\tau_j^{new} = \tau_j^{current} + \Delta\tau_j^k \quad \text{or} \quad \tau_{ij} = (1 - \rho)\tau_{ij} + \rho\Delta\tau_{ij} \tag{5}$$

where  $\Delta\tau_j^k = \frac{1}{\sqrt{(r_{i1}-l_{j1})^2 + (r_{i2}-l_{j2})^2}}$  is the amount of pheromone that ant  $k$  exudes to the BTS  $l_j$  when it is going from BSC  $r_i$  to BTS  $l_j$ . The cost function for the ant  $k$  is the total distance between BSCs to BTSs is given by (1). The stop condition we used in this paper is defined as the maximum number of interaction  $N_{max}$ . The pseudo-code of ACO-BSC1 algorithm to solving OCLP as follows:

---

**Algorithm 2** MMAS algorithm to optimizing QoS for multimedia services

---

```

BEGIN
  Generating the pheromone matrix for the Ant  $k$ ;
  Update the pheromone values and set  $x^* = k$ ;  $i = 1$  ;
  REPEAT
    FOR  $k = 1$  TO  $K$  DO
      Computing the cost function for the ant  $k$  by the formula (1);
      Computing probability move of ant individual by the formula (4);
      IF  $f(k) < f(x^*)$  THEN
        Update the pheromone values by the formula (5);
        Set  $x^* = k$ ;
      ENDFOR
    UNTIL ( $i > N_{Max}$ ) or (an acceptable solution is found);
  END.
  
```

---

ACO-BSC1 algorithm combined with local search is called by ACO-BSC2. The local search algorithm described as follows:

---

**Algorithm 3** Local Search

---

```

BEGIN
  c1 = randomly select a BSC in solutions;
  c2 = randomly select a BSC in solutions;
  S = {candidatei} by swapping a BTS between BSC c1 and BSC c2;
  CurentSolution = candidate1;
  FOR EACH candidatei in S DO
    IF f(CurentSolution) > f(candidatei) THEN CurentSolution = candidatei;
  END.

```

---

## 5 Experiments and Results

In our experiments, we have already defined parameters for our algorithms: ant population size  $K = 100$ , Maximum number of interaction  $N_{Max} = 500$ , parameter  $\alpha = 1$ ,  $\beta = 10$ . In order to test the performance of our algorithm, we tackle a set of TA and OCLP instances of different difficulties in 3 case studies. We present the results we have obtained followed by an analysis.

**Case study 1:** We experiment on 13 test cases in [3]. The coordinates of terminals and concentrators have been randomly obtained in a 100 grid, whereas the weights associated with each terminal were randomly generated  $w_j \in [1, 6], \forall j = 1..N$ . The capacities of each concentrator assigned fixed  $p_i = 12, \forall i = 1..M$ . Table 1 shows the comparison of the best objective function of *ACO-BSC1*, *ACO-BSC2*, *Greedy*, *GENEsYs*, *LibGA*, *GGA* algorithms. The results listed under the *Greedy* algorithm are

**Table 1** Performance evaluation of the best solution of algorithms in Case study 1

Test	N	M	Greedy	GENEsYs	LibGA	GGA	ACO-BSC1	ACO-BSC2	Improved (%)
#1	100	32	1203	1153	1138	<b>1115</b>	<b>1115</b>	<b>1115</b>	0.88
#2	100	32	1253	1180	<b>1159</b>	1166	1166	<b>1159</b>	0.94
#3	100	31	1274	1216	1181	<b>1170</b>	<b>1170</b>	<b>1170</b>	1.04
#4	100	33	1438	1394	1344	1359	1344	<b>1303</b>	1.35
#5	100	27	1600	1540	1500	1469	1469	<b>1423</b>	1.77
#6	100	27	1446	1393	<b>1373</b>	1388	1388	<b>1373</b>	0.73
#7	100	31	1961	1917	1838	1863	1838	<b>1725</b>	2.36
#8	100	27	1865	1803	1702	1781	1630	<b>1615</b>	2.50
#9	100	31	1564	1492	1425	1412	1412	<b>1394</b>	1.70
#10	100	31	1367	1251	1216	1225	1225	<b>1182</b>	1.85
#11	200	93	2002	1939	1898	1919	1769	<b>1721</b>	2.81
#12	300	96	2673	2607	2579	2595	2369	<b>2213</b>	4.60
#13	400	128	3432	3327	3282	3316	3168	<b>2775</b>	6.57

the best solutions yielded by the implementation after 100 executions in each case. We force *Greedy* algorithm to stop after 10,000 iterations in order to make a comparison with the *GENEsYs*, *LibGA*, *GGA* algorithms which also iterate for 10,000 generations. We use the same population size is 500 and the same crossover rate is 0.6 in the three genetic algorithms. The experiment results show that our approach are useful to reach the feasible regions very fast more than the three genetic algorithms. The *GENEsYs*, *LibGA*, *GGA* algorithms may have to wander for a large of generations in the search space before the feasible regions can be identified. The *Greedy* algorithm is the fast algorithm, but it does not always produce near optimal solutions, and the *GENEsYs* does not perform as well as the *LibGA*, *GGA* algorithms in all cases. While, our proposed algorithms run very efficiently and yields feasible solutions consistently based on the heuristic information.

**Case study 2:** Table 2 summarize the results of executing the *Hybrid I*, *Hybrid II*, *ACO-BSC1* and *ACO-BSC2* algorithms in the best and average cases on 15 test cases after 100 executions in each case. The 15 TA test cases of different sizes, the difficulty increases with the problem size in [5]. The coordinates of terminals and concentrators have been randomly obtained in a 100 grid, whereas the weights associated with each terminal were randomly generated. The capacities of each concentrator vary from one problem to another, being in a range. Experimental results show that the proposed algorithms are found to be optimal solution in the best case similar to the *Hybrid II* algorithm. However, the performance of *ACO-BSC1*, *ACO-BSC2* algorithms equally or better than the *Hybrid I* and *Hybrid II* algorithms in all cases. The discovery of the *ACO-BSC2* algorithm are better demonstrated in the average objective function.

**Case study 3:** We experiment on 10 OCLP instances of different sizes, the difficulty increases with the problem size. The coordinates of terminals and concentrators have been randomly obtained in Table 3, whereas the weights associated with each terminal were randomly generated  $w_j \in [1, 30], \forall j = 1..N$ . The capacities of each concentrator vary from one problem to another, being in a range  $p_i \in [50, 150], \forall i = 1..M$ . We compare the results obtained by the objective function of the *SA*, *SA-Greedy*, *LB-Greedy*, *GA-Greedy*, *GA-BSC*, *PSO-BSC*, *ACO-BSC1* and *ACO-BSC2* algorithms in the best and average cases. All experiment are independent of all others, the results listed in Table 4 is the best solutions and average solutions after 100 executions in each case. The experimental results show that the objective function of our algorithms has achieved a much better performance than other algorithms. In the small grid size and small number of nodes such as problem #29, #30 and #31, all algorithms has approximate results both the best solutions and the average solutions. However, when the problem size is large, the experimental results are considerable different such as problem #34, #35, #36, #37 and #38. In some cases, all algorithms choose the same set of nodes to be BSCs, but the objective function results of the *ACO-BSC2* algorithm are much better.

Table 5 shows the computational time of the seven algorithms. The computation time of the *GA-BSC*, *PSO-BSC* is smaller than the *SA*, *SA-Greedy* and *LB-Greedy* algorithm, however it is larger than the *ACO-BSC1* and *ACO-BSC2* algorithms

**Table 2** Performance evaluation of the solutions of algorithms in Case study 2

Test	N	M	$\sum w_j$ ( $j = 1 \dots N$ )	$\sum p_i$ ( $i = 1 \dots M$ )	Hybrid I		Hybrid II		ACO-BSC1		ACO-BSC2	
					Best	Average	Best	Average	Best	Average	Best	Average
#14	10	3	35	39	<b>73.8</b>	<b>73.8</b>	<b>73.8</b>	<b>73.8</b>	<b>73.8</b>	<b>73.8</b>	<b>73.8</b>	<b>73.8</b>
#15	10	3	39	42	<b>86.9</b>	<b>86.9</b>	<b>86.9</b>	<b>86.9</b>	<b>86.9</b>	<b>86.9</b>	<b>86.9</b>	<b>86.9</b>
#16	10	3	34	37	<b>96.6</b>	<b>96.6</b>	<b>96.6</b>	<b>96.6</b>	<b>96.6</b>	<b>96.6</b>	<b>96.6</b>	<b>96.6</b>
#17	20	6	77	83	<b>151.1</b>	152.6	<b>151.1</b>	152.8	<b>151.1</b>	152.6	<b>151.1</b>	<b>152.3</b>
#18	20	6	61	68	<b>164.6</b>	166.8	<b>164.6</b>	168.3	<b>164.6</b>	166.8	<b>164.6</b>	<b>165.9</b>
#19	20	6	72	79	<b>165.7</b>	167.1	<b>165.7</b>	167.3	<b>165.7</b>	167.1	<b>165.7</b>	<b>167.1</b>
#20	30	10	117	127	295.8	303.4	<b>295.4</b>	307.2	<b>295.4</b>	303.5	<b>295.4</b>	<b>301.3</b>
#21	30	10	98	120	<b>303.1</b>	318.5	<b>309.8</b>	322.1	<b>303.1</b>	319.9	<b>303.1</b>	<b>316.9</b>
#22	30	10	94	120	311.6	321.9	<b>304.8</b>	325.9	<b>304.8</b>	320.8	<b>304.8</b>	<b>316.1</b>
#23	50	17	182	204	496.6	517.2	<b>490.3</b>	521.8	<b>490.3</b>	514.5	<b>490.3</b>	<b>501.8</b>
#24	50	17	174	193	<b>516.6</b>	538.8	521.7	541.5	<b>516.6</b>	536.1	<b>516.6</b>	<b>529.9</b>
#25	50	17	173	204	546.4	571.4	<b>542.6</b>	572.2	<b>542.6</b>	561.6	<b>542.6</b>	<b>550.2</b>
#26	100	30	292	360	884.1	925.6	<b>881.3</b>	924.4	<b>881.3</b>	915.9	<b>881.3</b>	<b>914.4</b>
#27	100	30	334	360	<b>815.4</b>	883.6	823.4	878.9	<b>815.4</b>	878.3	<b>815.4</b>	<b>871.8</b>
#28	100	30	342	360	<b>849.4</b>	898.8	862.8	907.4	<b>849.4</b>	893.4	<b>849.4</b>	<b>878.3</b>

**Table 3** Main features of OCLP problems tackled

Test	Number of BTSs (N)	Number of BSCs (M)	Grid size	$\Sigma w_j(j = 1 \dots N)$	$\Sigma p_i(i = 1 \dots M)$
#29	10	2	100 × 100	174	195
#30	15	3	100 × 100	298	324
#31	20	4	100 × 100	381	413
#32	40	6	200 × 200	527	638
#33	60	8	200 × 200	962	1150
#34	80	10	400 × 400	1258	1435
#35	100	15	600 × 600	1479	1612
#36	120	20	800 × 800	1581	1835
#37	150	25	1000 × 1000	1793	1908
#38	200	50	1500 × 1500	2384	2571

**Table 4** Comparison of the results obtained by the difference algorithms considered

Test	SA		SA-Greedy		LB-Greedy		ACO-BSC1	
	Best	Average	Best	Average	Best	Average	Best	Average
#29	<b>187.4</b>	196.3	<b>187.4</b>	192.6	<b>187.4</b>	189.1	<b>187.4</b>	<b>187.4</b>
#30	<b>315.0</b>	347.6	<b>315.0</b>	328.5	<b>315.0</b>	335.4	<b>315.0</b>	<b>315.0</b>
#31	428.3	431.5	427.2	429.8	419.6	428.7	<b>418.7</b>	<b>419.1</b>
#32	1784.7	1826.3	1798.5	1818.9	1658.2	1735.4	<b>1615.3</b>	<b>1631.5</b>
#33	2091.3	2135.9	1996.7	2215.1	1954.7	1976.3	<b>1916.6</b>	<b>1945.2</b>
#34	4625.6	4863.2	4612.4	4863.2	4531.8	4627.5	<b>4518.1</b>	<b>4557.4</b>
#35	7346.4	7955.6	7536.5	8027.2	7213.7	7371.9	<b>7136.5</b>	<b>7182.9</b>
#36	12863.7	14769.6	13753.8	14176.8	10863.7	11325.7	<b>9578.4</b>	<b>9621.7</b>
#37	23638.6	24518.2	26624.3	26875.1	19569.2	18423.6	<b>16874.7</b>	<b>17934.5</b>
#38	157894.2	167452.1	168253.7	172147.5	143665.4	151763.9	<b>141257.2</b>	<b>14855.8</b>
Test	GA-BSC		GA-Greedy		PSO-BSC		ACO-BSC2	
	Best	Average	Best	Average	Best	Average	Best	Average
#29	<b>187.4</b>	191.4	<b>187.4</b>	190.7	<b>187.4</b>	188.5	<b>187.4</b>	<b>188.2</b>
#30	<b>315.0</b>	328.3	<b>315.0</b>	329.1	<b>315.0</b>	327.6	<b>315.0</b>	<b>323.4</b>
#31	415.4	425.6	417.3	428.5	<b>412.7</b>	<b>416.8</b>	<b>412.7</b>	<b>416.8</b>
#32	<b>1615.3</b>	1637.2	<b>1615.3</b>	1639.5	<b>1615.3</b>	1631.9	<b>1615.3</b>	<b>1628.7</b>
#33	<b>1910.6</b>	2027.4	1927.3	2105.8	1911.9	2012.7	<b>1910.6</b>	<b>1934.1</b>
#34	4507.8	4623.9	4539.3	4681.7	<b>4503.4</b>	4572.8	<b>4503.4</b>	<b>4543.9</b>
#35	7144.1	7352.4	7156.3	7320.2	7137.1	7217.3	<b>7136.5</b>	<b>7161.8</b>
#36	9584.3	10625.1	9632.5	11150.5	<b>9563.6</b>	97121.4	<b>9563.6</b>	<b>9611.2</b>
#37	16896.7	16912.5	<b>16861.3</b>	16894.8	<b>16861.3</b>	16878.1	<b>16861.3</b>	<b>16872.2</b>
#38	141276.9	141362.8	141335.2	141374.1	<b>141235.8</b>	141272.8	<b>141235.8</b>	<b>141257.7</b>

**Table 5** Computation time (in seconds) of compared difference algorithms

Test	SA	SA-Greedy	LB-Greedy	GA-Greedy	GA-BSC	PSO-BSC	ACO_BSC1	ACO_BSC2
#29	0.4528	0.4278	0.3912	0.3986	0.3979	0.3858	0.3711	<b>0.3681</b>
#30	0.5793	0.5284	0.4837	0.4695	0.4788	0.4672	<b>0.4629</b>	0.4756
#31	1.1547	1.2719	1.1956	1.1967	1.1859	1.1753	<b>1.1467</b>	1.1491
#32	1.9561	1.8260	1.7978	1.8153	1.7547	1.7193	1.6836	<b>1.6173</b>
#33	2.3934	2.1868	2.1329	2.1411	2.0972	2.0448	<b>2.0423</b>	2.0426
#34	3.0284	2.9525	2.9851	2.8772	2.8561	2.7923	2.7568	<b>2.6331</b>
#35	3.6874	3.7356	3.5647	3.5626	3.5723	3.5539	3.5482	<b>3.5072</b>
#36	4.2693	4.1388	4.0522	3.9784	3.9841	3.9311	3.9269	<b>3.6851</b>
#37	5.1932	5.2191	5.2326	5.2167	5.1871	5.1589	5.1251	<b>5.0775</b>
#38	6.5471	6.2833	6.1972	6.1523	6.1365	6.0921	6.0343	<b>6.0148</b>

compared. The *ACO-BSC2* algorithm is able to obtain much better solutions than the *ACO-BSC1* algorithm, which is a reasonable computation time. The *ACO-BSC2* is the fastest algorithm, as expected in almost cases.

## 6 Conclusion and Future Works

In this paper, we have presented the new ACO scheme for the optimal location of controllers in wireless networks. The proposed algorithms overcomes the disadvantages of previous approaches based on Greedy heuristics are no longer valid, and *blind* algorithms are necessary for achieving high quality solutions to the problem. Our algorithms may give feasible solutions to this problem based on the global search for high quality feasible solutions. The experimental results show that our proposed algorithms have achieved a much better performance than previous heuristic algorithms. Optimizing location of controllers in wireless networks with profit, coverage area and throughput maximization is our next research goal.

## References

1. Krishnamachari, B., et al.: Base station location optimization in cellular wireless networks using heuristic search algorithms. In: Wang, L. (ed.) *Soft Computing in Communications*. Springer, Berlin (2003)
2. Menon, S., et al.: Assigning cells to switches in cellular networks by incorporating a pricing mechanism into simulated annealing. *IEEE Trans. Syst. Man Cybern.* **34**(1), 558–565 (2004)
3. Abuali, F.N., et al.: Terminal assignment in a communications network using genetic algorithms. In: *Proceedings of the 22nd Annual ACM Computer Science Conference*, pp. 74–81. ACM press (1994)
4. Merchant, A., Sengupta, B.: Assignment of cells to switches in PCS networks. *IEEE/ACM Trans. Netw.* **3**(5), 521–521 (1995)



5. Sanz, S.S., et al.: A Hybrid Greedy-Simulated Annealing algorithm for the optimal location of controllers in wireless networks. In: Proceedings of the 5th WSEAS Madrid, pp. 159–164 (2006)
6. Glaer, C., Reith, S., Vollmer, H.: The complexity of base station positioning in cellular networks. *Discrete Appl. Math.* **148**(1), 112 (2005)
7. Back, T.: GENEYs 1.0 Software distribution and installation notes, Systems Analysis Research Group, LSXI, University of Dortmund, Germany (1992)
8. Gendreau, M., Potvin, J.Y.: *Handbook of Meta-heuristics*. Springer, Berlin (2010)
9. Corcoran, A.L., Wainwright, R.L.: LibGA: A User-Friendly Workbench for Order-Based Genetic Algorithm Research. In: Proceeding of the 1993 ACM/SIGAPP, pp. 111–117. ACM Press, New York
10. Jong, D., Kenneth, A.: *An Analysis of the Behavior of a Class of Genetic Adaptive Systems*. Dissertation Abstracts International, University of Michigan (1975)
11. Bernardino, E.M.: A hybrid differential evolution algorithm for solving the terminal assignment problem. *Lecture Notes in Computer Science*, vol. 5517, p. 179186. Springer, Berlin (2007)
12. Hopfield, J.J., Tank, D.W.: Neural computation of decisions in optimization problems. *Biol. Cybern.* **52**, 141152 (2007)
13. Sanz, S.S., et al.: Optimal switch location in mobile communication networks using hybrid genetic algorithms. *Appl. Soft Comput.* **8**(4), 14861497 (2008)
14. Le, D.-N., et al.: A New Evolutionary Approach for the Optimal Location of Controllers in Wireless Networks. In: Proceeding of 2nd ICICM 2012, pp. 81–86. Hongkong, 26–27 Oct 2012
15. Le, D.-N., et al.: A novel PSO-based algorithm for the optimal location of controllers in wireless networks. *Int. J. Comput. Sci. Netw. Secur.* **12**(8), 23–27 (2012)
16. Le, D.-N.: PSO and ACO algorithms applied to optimizing location of controllers in wireless networks. *Int. J. Comput. Sci. Telecommun.* **3**(10), 1–7 (2012)
17. Sttzle, T., Ibanez, M.L., Dorigo, M.: *A Concise Overview of Application of Ant Colony Optimization*. Wiley, Hoboken (2010)

# MECAR: Maximal Energy Conserved and Aware Routing in Ad hoc Networks

Podoli V.S. Sriniva, Maddhi Sunitha and Temberveni Venugopal

**Abstract** Ad hoc wireless networks are power constrained since nodes operate with limited battery energy. To maximize the lifetime of these networks, network-related transactions through each mobile node must be controlled such that the power dissipation rates of all nodes are nearly the same. Assuming that all nodes start with a finite amount of battery capacity and that the energy dissipation per bit of data and control packet transmission or reception is known, in this regard our earlier work devised a novel routing protocol referred as Maximal Power Conserved and Battery Life Aware Routing (MPC-BLAR). The other significant QoS factor in route selection is that establishing a route by nodes with sufficient battery life. This paper explored a novel hop level energy availability measurement and applied on MPC-BLAR. Simulation results show that the proposed power aware source routing protocol called Maximal Energy Conserved and Aware Routing (MECAR) has a higher performance Power preservation in wireless ad hoc networks is a decisive factor as energy resources are inadequate at the electronic devices in use. Power-aware routing strategies are fundamentally route selection strategies built on accessible ad hoc routing protocols. This paper proposed a new Maximal Power Conserved and Battery Life Aware Routing (MPC-BLAR) topology for mobile ad hoc networks that enhances the network life span. Simulation results prove that the projected protocol has a higher performance other

---

P.V.S. Sriniva (✉)

TKR College of Engineering and Technology, Medbowli, Saroornagar,  
Meerpet 500079, Hyderabad, India  
e-mail: pvssrinivas23@gmail.com

M. Sunitha

Department of Computer Science and Engineering, CVR College of Engineering,  
Mangalpalli, Ibrahimpatnam, R.R.Dist 501510, India  
e-mail: palemonisunitha@gmail.com

T. Venugopal

Department of Computer Science and Engineering, JNTUHCEJ, Jagityal,  
Karimnagar Dist 505327, India  
e-mail: t\_vgopal@rediffmail.com

© Springer India 2015

J.K. Mandal et al. (eds.), *Information Systems Design and Intelligent Applications*,  
Advances in Intelligent Systems and Computing 339,  
DOI 10.1007/978-81-322-2250-7\_85

855

minimal energy usage, energy level aware and energy conserving routing protocols such as MTPR, MMBCR and CMMBCR.

**Keywords** Mobile ad hoc network · Power-aware · Overhearing · Battery capacity aware · Minimum total transmission power

## 1 Introduction

Networks are shaped in a dynamic manner of computer or communication nodes loosely connected to assist the forwarding of information between nodes by relaying packets through hop level nodes are referred as ad hoc networks. Each node under ad hoc networks connects to their hop level nodes and maintain connection to any other node by discovering multi hop level connectivity. Building an ad hoc network is a base requirement in situations like military and rescue operations. Hence the ad hoc network augments in situations like, transmitting data/message between any two nodes of the network with no base station support. Due to constrained infrastructure, dynamic connectivity and multi hop level relay based communication, achieving quality of service in an ad hoc network is a noteworthy practical confront, especially in ensuring the lifespan of the network, since the resources and energy levels of the nodes are constrained to finite level, wireless connectivity and mobility are other factors. These distinctiveness [1] oblige restrictions on connectivity and packet transmissions between nodes of the ad hoc network. Out of all these issues the limited lifetime of the battery that provides energy to nodes can be considered as a critical and significant issue since if battery with no energy levels downs the node that partitions the network. Hence the energy conservation techniques are in need to enhance the battery lifetime. It is apparent that energy competent routing topologies should be implemented in place of the traditional routing strategies. All of these conventional routing strategies establish routing paths in the aim of shortest path and neglects the desired proportionality between energy levels required and available, consequently fallout in a quick exhaustion of the battery capacity of the nodes due to routes that are used extremely high in the network. In this regard, to preserve battery lifespan of the nodes, a variety of routing schemes labeled as power aware routing protocols have been designed to select substitute routes. These power aware routing strategies selects routes such that packet routes through paths that justify the proportionality between energy levels required to route and energy levels available at nodes. The underlying process of route discovery and optimal path selection in power-conscious routing protocols are capable of the absorption of the emerging routing topologies such as DSR [2], TORA [3], and AODV [4].

## 2 Related Work

The superior degree of power consumption at hop level nodes in a shortest path based routing is the severe topic that attracts current research. In this regard several power aware routing solutions proposed. The superior degree of power consumption is proportionate to distance between nodes. In this regard Wu et al. [5] anticipated a new mechanism to lessen power consumption while escalating channel use. The approach is considered the RTS/CTS packet transmissions to measure the battery lifespan used to forward data packets by a node to its target hop level neighbor node, considering this and attempted to generalize the proportionality between battery lifespan is used and relative distance to the target node. Singh and Raghavendra [6] projected the PAMAS protocol, a new channel admission topology for ad hoc networks that aims to avoid the wastage of the battery lifespan during idle time of the node. In this regard the PAMAS uses two distinct data and signaling channels. The signaling channel observes the idle time of the nodes and alerts them such that they shut down their RF devices. In addition, Wan et al. [7] proposed a routing solution for lowest energy usage broadcasting that committed to fixed MANETs. Laura Feeney offered in [8] a blend of simulation and experimental outcomes showing that energy and bandwidth are considerably divergent metrics and that resource usage in routing protocols is not completely addressed by bandwidth-centric investigation. In recent times, a few routing protocols boarding proficient power consumption have been projected. Our proposed routing model called MECAR concerned with power-aware route selection mechanisms for MANET routing protocols.

The Minimum Total Transmission Power Routing (MTPR) [9] was originally developed to reduce the total transmission power use of the nodes contributing in the attained route. According to Rappaport [10], the obligatory transmission power is proportional to  $d^\alpha$ , where ' $d$ ' represents the distance between any two consecutive hop level nodes and ' $\alpha$ ' value is in the range of 2–4. This concludes that the route discovery process of the MTPR opts more hop level nodes with low transmission distances compared to fewer hops with high transmission distances. But in contrast to the advantage of minimum total transmission power usage, increase in the hop level node count of selected routing paths can augment the end-to-end delay. Moreover MTPR is not considering the proportionality between the power available at the nodes and the power required, hence the selected routing path often experience the breakage due to nodes with no energy. In the context of the limits observed in power aware routing models such as MTPR, Singh et al. [11] introduced routing model labeled “Min-Max Battery Cost Routing (MMBCR)” that considers proportionality between battery levels available at nodes and battery levels required as a metric and discovers the routing paths with extended lifetime. In the aim of selecting routing paths with extended lifetime, the MMBCR is not considering the objective of energy levels saving with minimum total transmission power. This limits the performance of MMBCR in cases such as all nodes with maximum battery capacities. In this regard Toh [12] introduced a hybrid protocol called “Conditional Min-Max Battery Capacity Routing” that adapts to MTPR if all

nodes with maximal battery levels otherwise to MMBCR. Apart from transmission distance and battery aware routing strategies [9, 11, 12], the energy conservation based techniques such as (i) Scheduling the node to sleep during idle time and scheduling awake when required, (ii) Proportioning the transmission power and distance between nodes. Due to the difficulties and implementation issues these models are impractical. The sleep/awake scheduling models required additional hardware with transmission scheduling requirements loaded [13]. Scheduling transmission power that based on distance between nodes is inaccurate due to the issues in determining the distances between nodes, in particular if the nodes are having mobility then additional hardware like GPS receivers required or distance measuring algorithm must be location aware [14].

In regard to overcome the limits explored about routing strategies [9–14] cited most frequently in literature, we devised a novel routing strategy called Maximal Power Conserved and Aware Routing (MPC-BLAR) [15] in our earlier work.

Research in this arena of power aware routing has been focusing on explaining routing protocols that works on less battery resource usage techniques. The energy estimation of the selected route is impractical since they do not take into consideration the amount of power needed and the power level that is available, which is the main drawback in all these models. All these protocols only consider the highest power level that exists and quantity, which is needed to perform the routing. The actual consumption of energy in the context of conflict nodes and coding awareness is not considered during the process of measuring a node lifetime. A model devised in [15] details that the left over energy in the nodes taking part in path involving the start and end is piled and sent to RREQ message-making use of a novel field added to the RREQ message. In this scenario a RREP reply will not be given by the destination node for the RREQ to come in first. In turn it will wait for  $3 * \text{NODE\_TRAVERSAL\_TIME}$  and gets RREQ meant for the node and appends energy of those nodes taking part in the path. The mean energy of the network that takes part on the path is got by separating the entire energy separated into the number of nodes taking part in the network.

Here in this paper, our proposed routing Strategy called Maximal Energy Conserved and Aware Routing (MECAR) devised an effective hop level available energy measuring strategy (AEMS).

### **3 MECAR: Maximal Energy Conserved and Aware Routing**

The available energy at hop level node is a significant metric of QoS. Henceforth an optimal mechanism is essential to determine the hop level node energy resources in regard to transmit the data. The existing models are finding the energy required to transmit the data is available at each hop level node or not. This measuring process is suboptimal since none of the existing models are considering the energy consumption rate in regard to conflict nodes. Here we devise a routing strategy

called MECAR, which is an extension to MPC-BLAR [15]. The MECAR explores the actual energy levels possible to utilize at a hop level node, which become practical due to considering the energy sharing between conflict nodes.

### 3.1 Route Request

The Route Request Strategy that we devised under MPC-BLAR [15] is the same, which we adapt for MECAR.

### 3.2 Route Response Process

Route response process, as like as MPC-BLAR [15] here also RREP carries the hop level distances and signal to noise ratio of the current response path, and also carries the conflict nodes and their energy requirements at every hop level node of the current response path. The conflict nodes can be defined as follows:

Let  $h_{i+1}$  found to be hop level node to  $h_i$  in the path towards target node. Then the other nodes that are connected to  $h_{i+1}$  and using it for transmission services are referred as conflict nodes.

The route response strategy is as like as that opted for MPC-BLAR, but the packet structure is revised and the structure of RREP at a hop level node  $h_i$  revised and is as follows:

$$\begin{aligned}
 hl &= \{h_1, h_2, \dots, h_{i-3}, h_{i-2}, h_{i-1}, h_i, h_{i+1}, h_{i+2} \dots, h_m, n_d\} \\
 dl &= \{d_{(h_m \rightarrow n_d)}, d_{(h_{m-1} \rightarrow h_m)}, \dots, d_{(h_i \rightarrow h_{i+1})}\} \\
 sl &= \{snr_{(h_m \rightarrow n_d)}, snr_{(h_{m-1} \rightarrow h_m)}, \dots, snr_{(h_i \rightarrow h_{i+1})}\} \\
 cner &= \langle c_1, er_1 \rangle, \langle c_2, er_2 \rangle \dots \langle c_n, er_n \rangle \\
 cnl &= \{cner_{(h_m \rightarrow n_d)}, cner_{(h_{m-1} \rightarrow h_m)}, \dots, cner_{(h_i \rightarrow h_{i+1})}\} \\
 RREP &= \langle id(n_d), id(n_s), hl, dl, sl, cnl \rangle
 \end{aligned}$$

Here

‘hl’ Is a list of nodes used by RREQ to reach the destination node  $n_d$  from the source node ‘ $n_s$ ’.

‘dl’ Is a list of distances between each two consecutive hop level neighbor nodes that belongs to ‘hl’.

‘sl’ Is a list of signal to noise ratios between each two consecutive hop level neighbor nodes that belongs to ‘hl’ and measured using the approach discussed in MPC-BLAR.

‘cner’ Is the list of conflict nodes and their energy requirements at hop level node.

‘cni’ Is the list of ‘cner’ of all hop level nodes of the current response path.

Once RREP reaches the source node  $n_s$ , then the source node registers the path used by RREP into the optimal paths list.

### 3.3 Route Selection Process

The Route Selection process is also similar to that opted by MPC-BLAR [15]. In addition here in MECAR we use hop level available energy measuring strategy (AEMS) to filter optimal paths that described below.

Step 1: For each path  $\{p \forall p \in rpl\}$

BEGIN

Step2: For each node  $\{n \forall n \in p\}$  find actual energy possible at hop level node  $\{n+1 \exists n+1 \in p \ \& \ n \rightarrow n+1\}$

BEGIN

Let  $cner_{(n \rightarrow n+1)} = \langle (c_1, er_1), (c_2, er_2), \dots, (c_m, er_m) \rangle$  and find the actual energy available as follows:

$$aep_{(n \rightarrow n+1)} = \left( \frac{1}{er_1} + \frac{1}{er_2} + \frac{1}{er_3} + \dots + \frac{1}{er_m} \right)^{-1}$$

Step 3: If  $aep_{n \rightarrow n+1} < \tau_h$  then

BEGIN

Discard path  $P$  from  $rpl$

Continue to Step 1;

END

Else Continue to step2

END

END

Further the optimal path can be choose from the ‘rpl’. MECAR adopts the similar strategy that opted by MPC-BLAR [15] .

Each path  $P_i$  will be ranked based on ‘ $snr_{\delta}(p_i)$ ’ such that the path with lowest ‘ $snr_{\delta}(p_i)$ ’ value will be ranked as high. If more than one path is conflicting on same rank then those paths will be ranked based on ‘ $d_{\tau}(p_i)$ ’ such that the path with lowest ‘ $d_{\tau}(p_i)$ ’ value will be ranked as high.

## 4 Simulations and Results Discussion

### 4.1 Experimental Setup

The experiments were conducted using NS 2. We build a simulation network with hops under mobility and count of 50–200. The simulation parameters described in Table 1. The simulation model aimed to compare MPC-BLAR [15] and MECAR. The performance check of these two protocols carried out against to the QOS metrics describe in following section.

### 4.2 Results Discussion

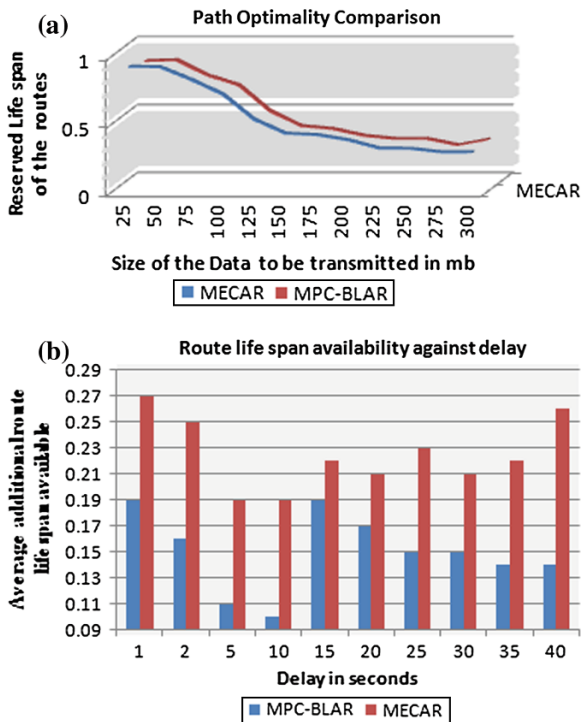
Figure 1a indicates a MECAR advantage over MPC-BLAR in Path optimality in the context of route lifespan. The average additional 15 % of route survivability has been observed for MECAR than MPC-BLAR, it has happened since MECAR is considering the leap nodes with higher energy, but in the case of MPC-BLAR, it considers average signal-to-noise ratio required and minimum battery capacity of

**Table 1** Simulation parameters that we considered for experiments

Node count	Range of 50–200
Network area	1,500 × 300 m dimensions
Radio frequency	Range of 250 m
Number of source and destination node sets	20
Data pattern for each source node per second	4 packets
Payload of the data per packet	512 bytes
Data-load used	In the range of 128–512 kbps
Bandwidth used at physical link	2 Mbps
Timeout set for the primary route request in seconds	2
Utmost timeout set for the route request in seconds	40
Maximum number of routes can be cached	32
Caching policy	First-In-First-Out



**Fig. 1** Evaluation report on MECAR performance over MPC-BLAR. **a** Path optimality of MPC-BLAR and MECAR. **b** Comparison between MECAR and MPC-BLAR as a function of the delay time and additional lifespan of route



the hop level nodes between the source and destination nodes as metrics during route discovery.

MECAR is found similar to MPC-BLAR in packet overhead during route discovery and data transmission. The observed overhead is due to conditional broadcasting used in route discovery phase of both routing topologies and the process of path selection that selects the path with fewer signal-to-noise ratios. The proposed MECAR protocol is indicating the slightly high MAC load overhead as like as MPC-BLAR, which is due to the process of determining the signal-to-noise ratio required between any two consecutive hop level nodes.

The impact of average route survivability against increased end-to-end delay observed in MECAR is significantly high that compared to the survivability of the route against end-to-end delay in MPC-BLAR. This is due to the consideration of leap node life span during optimal path selection in MECAR. The minimal hop count is not playing any role in optimal path selection process of the both routing protocols MECAR and MPC-BLAR. The high hop count leads to the higher value of ‘ $snr_{\delta}$ ’ that indicates the low optimality of the path. Hence the optimal path that selected in MECAR is possible with less number of hop.

## 5 Conclusion

This paper was presented an evaluation of power aware routing protocols [5–14], and described their limits that can be subtle and difficult to discover by informal reasoning about the properties of the protocols. In this regard we devised a novel power aware routing strategy that referred as MPC-BLAR [15]. With motivation gained from empirical analysis and simulation studies conducted on MPC-BLAR, here we proposed a novel Maximal Energy Conserved and aware routing (MECAR) strategy that is an extension to our earlier work [15]. The proposed MECAR protocol applies conditional broadcasting to avoid the verification of battery capacity while choosing the optimal path from the paths selected by route discovery phase, which similar to MPC-BLAR. Unlike MPC-BLAR [15], the MECAR explores leap node level energy availability measurement in addition to MPC-BLAR strategy. Simulation results show that the proposed power aware source routing protocol called Maximal Energy Conserved and Aware Routing (MECAR) has a higher optimality towards the survivability of the routes than state of the art power aware routing protocols, which includes MPC-BLAR.

## References

1. Perkins, C.E., Bhagwat, P.: Highly dynamic destination-sequenced distance-vector routing (DSDV) for mobile computers. In: Proceedings of SIGCOMM'94 Conference on Communications Architectures, Protocols and Applications, August 1994, pp. 234–244 (1994) Available at <http://www.cs.umd.edu/projects/mcml/papers/Sigcomm94.ps>
2. Johnson, D.B., Maltz, D.A.: Dynamic source routing in ad hoc wireless networks. In: Imielinski, T., Korth, H. (eds.) *Mobile Computing*, Chap. 5, pp.153–181. Kluwer Academic Publishers, Dordrecht (1996)
3. Park, V., Corson, S.: Temporally-ordered routing algorithm (TORA) version 1: functional specification. draft-ietf-manet-tora-spec-04.txt, IETF, Work in Progress, July 2001
4. Perkins, C., Royer, E., Das, S.: Ad hoc on demand distance vector (AODV) routing. draft-manet-ietf-aodv-8.txt, IETF, Work in Progress, March (2001)
5. Wu, S.-L., Tseng, Y.-C., Sheu, J.-P.: Intelligent medium access for mobile ad hoc networks with busy tones and power control. In: Proceedings of the International Conference on Computer Communications and Networks (1999)
6. Singh, S., Raghavendra, C.S.: PAMAS—power aware multi-access protocol with signalling for ad hoc networks ACM SIGCOMM Comput. Commun. Rev. **28**, 5–26 (1998)
7. Wan, P.-J., Calinescu, G., Li, X.Y., Frieder, O.: Minimum-energy broadcast routing in static ad hoc wireless networks. In: Proceedings of IEEE INFOCOMM 2001 (Apr 2001)
8. Feeney, L., Nilsson, M.: Investigating the energy consumption of a wireless network interface in an ad hoc networking environment. In: Proceedings of IEEE INFOCOM, Anchorage, AK (2001)
9. Scott, K., Bambos, N.: Routing and channel assignment for low power transmission in PCS. In: ICUPC'96 (Oct 1996)
10. Rappaport, T.S.: *Wireless Communications: Principles and Practice*, Prentice Hall, Upper Saddle River (1996)
11. Singh, S., Woo, M., Raghavendra, C.S.: Power-aware with routing in mobile ad hoc networks. In: Proceedings of Mobicom 1998, Dallas, TX (1998)

12. Toh, C.-K.: Maximum battery life routing to support ubiquitous mobile computing in wireless ad hoc networks. In: IEEE Communications Magazine (June 2001)
13. Wentzloff, D.D., Calhoun, B.H., Min, R. Wang, A., Ickes, N., Chandrakasan, A.P.: Design considerations for next generation wireless power-aware micro sensor nodes. In: Proceedings of 17th International Conference on VLSI Design, Jan 2004, pp. 361–367 (2004)
14. Tseng, Y.-C., Hsieh, T.-Y.: Fully power-aware and location-aware protocols for wireless multi-hop ad hoc networks. In: Proceedings of 11th International Conference on Computer Communications and Networks, Oct'02, pp. 608–613
15. Sunitha, M., Venugopal, T., Srinivas, P.V.S.: MPC-BLAR: maximal power conserved and battery life aware routing in ad hoc networks. In: Fifth International Conference on Computational Intelligence, Modelling and Simulation (CIMSIm), pp. 345, 350. 24–25 (Sep 2013). doi: [10.1109/CIMSIm](https://doi.org/10.1109/CIMSIm)

# Raga Classification for Carnatic Music

S.M. Suma and Shashidhar G. Koolagudi

**Abstract** In this work, an effort has been made to identify *raga* of given piece of Carnatic music. In the proposed method, direct *raga* classification without the use of note sequence has been performed using pitch as the primary feature. The primitive features that are extracted from the probability density function (pdf) of the pitch contour are used for classification. A feature vector of 36 dimension is obtained by extracting some parameters from the pdf. Since non-sequential features are extracted from the signal, artificial neural network (ANN) is used as a classifier. The database used for validating the system consists of 162 songs from 12 *ragas*. The average classification accuracy is found to be 89.5 %.

**Keywords** Carnatic music · *Raga* · Machine learning · Artificial neural network · Pitch

## 1 Introduction

Computational Musicology is an emerging field that includes the study of techniques for analyzing various kinds of music. It helps to study science behind music and develops a scientific framework for this art. The analysis of music helps to understand the culture and the heritage of the society the music is evolved in. Most of the studies in this area are dedicated to Western Music whereas very fewer studies have tried to explore Indian Classical Music (ICM) [1, 2]. ICM is broadly classified into Hindustani and Carnatic music. Though these two music types have same base and similar framework, they differ in many factors. ICM is characterized by two basic elements—it should follow a specific note sequence known as *raga* and a specific

---

S.M. Suma (✉) · S.G. Koolagudi  
National Institute of Technology Karnataka, Surathkal, Karnataka, India  
e-mail: suma.cs13f02@nitk.edu.in

S.G. Koolagudi  
e-mail: koolagudi@nitk.edu.in

rhythm known as *Taal* [3]. *Raga* is considered to be the backbone of ICM. In a broader sense, *raga* can be understood as the framework that tells all the protocols that should be followed while rendering the piece of music. Since *raga* is the crucial element in the melodic framework of ICM, automatic *raga* identification is one of the important steps in Computational Musicology as far as ICM is considered. Some of the applications of automatic *raga* identification are: development of music recommendation systems, automatic note transcription, music indexing, on-line teaching and learning of music and so on. It may be considered as the first logical step in the process of creating computational methods for ICM.

Some of the characteristics of *raga* are *swara* (notes), *arohana-avarohana* pattern and characteristic phrases. Technically, a note can be defined as an identifiable fundamental frequency component (pitch) of a singer with a beginning and an ending time, of a duration determined by these [2]. The ratio of the fundamental frequencies of two notes is referred to as an interval [2]. The notes are categorised as *Shadja* (*Sa*), *Rishaba* (*Ri*), *Gandhara* (*Ga*), *Madhyama* (*Ma*), *Panchama* (*Pa*), *Dhaivatha* (*Da*) and *Nishadha* (*Ni*). These seven notes are further classified into different types based on the interval system (scale) used. There are three kinds of scales that are generally used in Carnatic and Hindustani music theory: a 12-note scale, a 16-note scale and the scale which contains 22 microtones. Each *raga* is defined using unique sequence of notes that is used in rendering the music clip. Few *ragas* share same set of notes, but they differ in the melody because of different *arohana-avarohana* pattern and characteristic phrases. *Arohana-avarohana* pattern refers to ascending and descending progression of notes. This tells about the transition between the notes that can occur in a given *raga*. Characteristic phrase is defined as a condensed version of the characteristic arrangement of notes, peculiar to each *raga*, which when repeated in a recital enables a listener to identify the *raga* being played [3]. Other than these important features, *raga* is also characterised by the relative position, strength and duration of notes and also *gamakas*. *Gamakas* are the beautification elements that tell about the dynamics of the pitch contour.

Unlike western music where the frequency of notes is fixed, ICM gives liberty of choosing the frequency of base note to the artists while performing. Western classical music uses equal tempered notes whereas just-intoned notes are used in ICM. In equal tempered scale all notes are equally spaced i.e. all notes have the same frequency ratio with respect to its previous note. But in just-intonation scale the notes are not equally spaced. In ICM, no two performances of the same *raga* by the same singer would be same. ICM is relatively unexplored because of its complicated grammars, extensive use of *gamaka* and the liberty given to singer for improvising while performing. All these complexities in analysing ICM, left it as relatively less explored computational musicology. In ICM, the sequential note information plays an important role in construction of melody unlike chords and rhythm which play an important role in western music. Hence, many of the methods proposed in the past [3–5] have used Hidden Markov Model (HMM) for identification of *ragas*.

In this work, an effort has been made to identify *raga* without the knowledge of the scale using low-level features. Pitch and its derivatives are used as features for

identification of the *raga*. Various kinds of musical clips from both *Janaka* (*ragas* with all 7 notes) and *Janya ragas* (*ragas* having 5 or 6 notes) are used for the study.

The paper is organised as follows. A review of related work is given in Sect. 2. Section 3 explains the proposed method. Experimentation and results along with explanation of database are given in Sects. 4 and 5 concludes the work with some further research directions.

## 2 Literature Review

Since *raga* gives melodic framework attained through pitch manipulation, many research contributions use pitch and its derivatives as the major features for the task of *raga* identification. Some of the works [6, 7] have also used timbre and other features along with pitch derivatives. The literature can be broadly classified into two categories. The first, the works that have used note information explicitly for identification of *raga* and the second, the works that have not used note information. We discuss both kinds of work in this section. One of the main challenges in reviewing the works is lack of standard corpora of ICM. The works that have been carried out are evaluated using different databases collected by the researchers. Hence while reviewing the work the databases considered are also discussed.

In the work [3], HMM is used for the identification of Hindustani *ragas*. The method proposed in this work uses note sequence as a feature. Two heuristics namely Hillpeak heuristics and Note duration heuristics are proposed for note transcription. Many micro-tonal variations present in the ICM makes the note transcription a challenging task even for a monophonic piece of music. The heuristics proposed in this method tries to overcome these variations. Hillpeak heuristics considers the changes in the sign of the slope of the pitch contour for identification of presence of a note. Note duration heuristics assumes that a note sustains for the period of at least 25 ms and estimates the note for every 25 ms. Another main contribution of this work is characteristic phrase analysis. A n-gram model is proposed for identification of repetitive sequence of notes and based on this *raga* is identified. The overall *raga* identification accuracy is claimed to be 77 %. The main drawback of the work is limited data set and accuracy of note transcription. Only two *ragas* are used for validating the system. The database has many limitations such as the musical notes in *arohana-avarohana* sequence are sung externally, the piece of music should be in G-sharp scale. The accuracy of note transcription is not appreciably high even after lot of constraints on the dataset. Similar work has been carried out by Arindam et al. [4]. The note transcription of the given musical piece is manually performed and this sequence is used for evaluating HMM. It is observed that HMM is 100 % accurate in identifying *ragas* if correct note sequence is given as input. However, it is difficult to achieve high accuracy in ICM transcription because of the micro-tonal variations and improvisations. Rajeswari et al. [8] have used *tala* information to identify the number of notes in the given musical piece, further this is used for identification of *ragas*.

Surendra et al. [9] have used similar method of identifying the *raga* in Carnatic music using the note sequence information. Since the data set is restricted to single scale identifying the notes is simpler task. The features extracted are the notes present, number of notes present and type of *arohana-avarohana* sequence. *Arohana-avarohana* patterns are classified as linear or nonlinear based on the pair of notes present in the sequence. They have used ANN as a classifier. The system is tested using 20 *ragas* with 3–5 songs in each *raga*. The paper has claimed 95 % of accuracy in *raga* identification. Ranjani et al. [10] have proposed a method for identification of tonic and other notes which leads to identification of *raga* from the Carnatic music. The property of the tonic note with pitch of highest mean and least variation shown in pitch histogram, is used for identification of tonic pitch value. This method estimates the probability density function (pdf) from the pitch contour. Using Semi-Continuous Gaussian Mixture Model (SC-GMM), tonic frequency and *raga* of the musical piece are identified. The data set used for this experiment consisted of 5 *Sampurna ragas* which is the major limitation. This paper has claimed 86.3 % of accuracy in *raga* identification. However, the experiments conducted were limited only to *arohana-avarohana* sequences. The main drawback of the method that use note information explicitly is that any error in identification of notes, contributes to the error in identification of *raga* as well.

The works that do not consider note information, mainly concentrate on variations in pitch histogram for *raga* classification. The pitch histograms give better results for stable regions of smaller input clips compared to longer duration inputs. In [11], spectrally derived tone profiles are used as features. A tone profile is a histogram of note values weighted by duration [11]. The tone profile is obtained by taking the DFT of the segment and summing up the energies of the bins surrounding the note centers. It is further normalised using tonic frequency. The music clips were classified using k-NN algorithm. This paper has claimed 100 % of accuracy in Hindustani *raga* identification. However this method cannot be generalised because the data set consisted of very few *ragas* and the music clips were rendered by single artist. Parag et al. in [12] have used Pitch Class Distribution (PCD) and Pitch Class Dyad Distribution (PCDD) as features. PCD is obtained directly from the pitch histograms, that is normalised using the input tonic value and folded into one octave. PCDD is a note bi-gram which is called dyads in musical terms. Dyads are calculated from rough estimation of notes using pitch onsets. This paper has claimed 97 % *raga* recognition accuracy. The system is tested using the data set consisting of instrumental music clips played by a single artist in 17 *ragas*. In the work of Koduri et al. [13], the predominant pitch from vocal region of polyphonic music is used for identification of *ragas* from Carnatic music. The *raga* classification is performed using pitch histogram weighted by duration and frequency of occurrence as the features. The *raga* classification is performed using k-NN classifier. The experiment is performed on the data set consisting of 176 tunes from 10 *ragas* consisting of both vocal and instrumental music. This method is claimed to give 75.6 % accuracy. Pranay et al. [6] have used the concept of *vadi swara* (the dominant note for the *raga*) for identification of *raga* in Hindustani music. From the studies, it is shown that Hindustani note intervals are

closer to equal tempered than just intonation intervals [14]. In [6], ICM notes are associated with Western note intervals for extracting features. This method uses chromagram features along with MFCCs and timbre features for identification of *raga*. A chromagram is a visual representation of energies in the 12 semitones (or chromas). The most repeating frequency component or semitone is assumed as the *vadi*. The classification is performed using HMM and GMM. 97 % accuracy is claimed using this method. Even though the results are promising, it cannot be generalised since the system is evaluated using only 4 *ragas*. The *vadi swara* for different *ragas* cannot be unique when a larger data set with more than 20 *ragas* is considered.

In this work, an effort has been made to overcome some of the limitations that exist in the past methods. The proposed method considers a comprehensive data set consisting of variety of music clips from different kinds of *ragas*. We try to eliminate the explicit note identification and scale dependency (tonic identification).

### 3 Proposed Method

In the proposed method pitch and its derivatives are used as features for identification of *raga* since melody is the result of variations in the pitch. From [7], it is evident that the pitch histogram for different *ragas* differ. Hence in this study we use some of the parameters obtained from the pdf of pitch contour for identification of *raga*. The flow diagram of the proposed system is shown in Fig. 1. In training phase, the extracted features and corresponding *raga* labels are used to construct a ANN model for classification. In testing phase, the feature vectors are fed to trained ANN model for obtaining the *raga* labels. The accuracy of the system is obtained by comparing them against the actual *raga* labels.

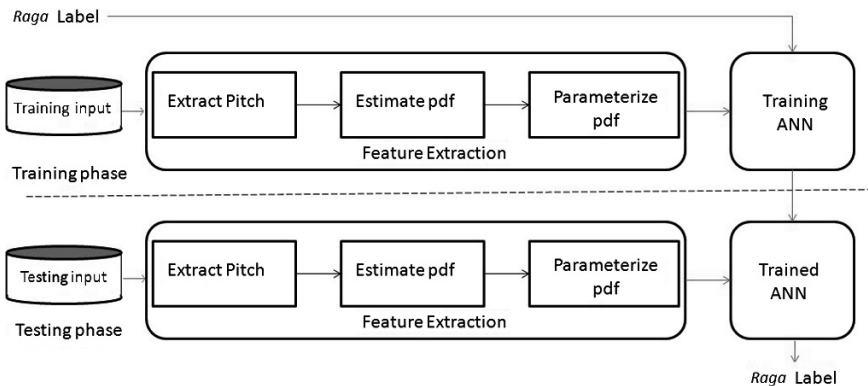
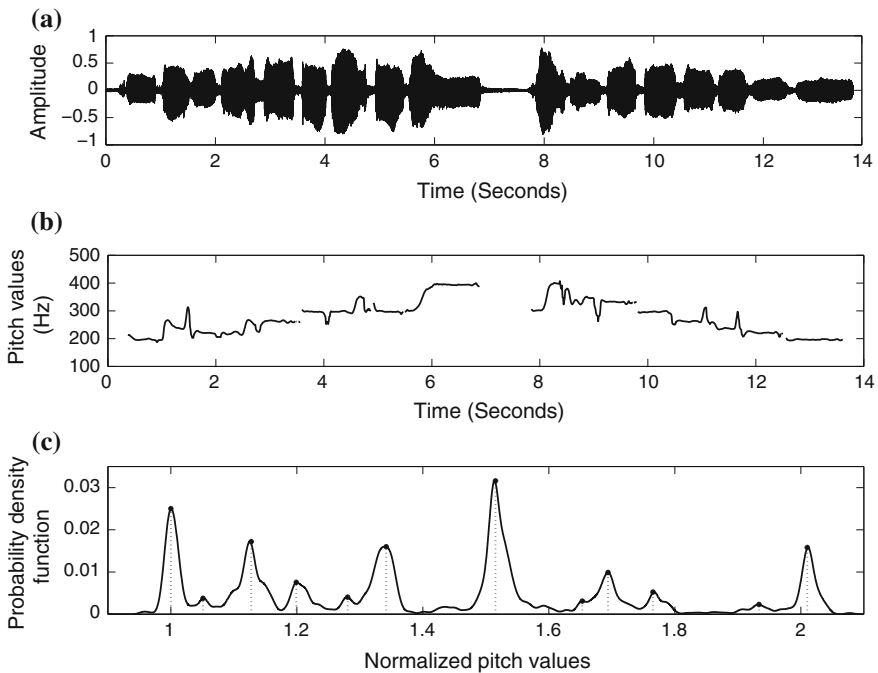


Fig. 1 Flow diagram of the proposed system



### 3.1 Feature Extraction

The pitch contour is extracted from the input signal (piece of music) using auto-correlation method [15]. The average pitch values are obtained for the frame of every 50 ms with 50 % overlapping to avoid transition cliques. The pitch contour of *arohana-avarohana* sequence is shown in Fig. 2b. Different pitch values corresponding to different notes are rendered in the piece of music. A sharp rise and fall in the contour is observed when the transition from a note to another takes place. From the pitch values, pdf is obtained using kernel density estimation method (Gaussian kernel is assumed). Bandwidth range is taken into account from minimum and maximum pitch values. The pdf obtained is shown in Fig. 2c. One can observe that the prominent peaks correspond to the notes present in the *raga*. Even though Carnatic music is defined using 16-note interval system, only 12 distinct frequency components are present [14]. Each *raga* is defined using 5, 6 or 7 note combination. Hence from the pdf curve, parameters of the 12 prominent peaks are considered for characterizing the *raga*. From the pdf, frequency of 12 peaks are obtained and their mean (height of the peaks in pdf) and variances are calculated. Variance of the peak is calculated by considering 20 frequency values on both side of the peak frequency. Since the database consists of clips rendered by different



**Fig. 2** Feature extraction for *raga Ananda Bhairavi*. **a** A music piece rendered in *raga Ananda Bhairavi*. **b** Pitch contour of the input music clip. **c** Peak selection from the pdf of pitch contour

singers in different scale, there is a need to normalise the frequencies of peaks. The frequency that lies in between 100 and 200 Hz having the highest mean is used as a normalising factor. For some clips played by instruments, all the frequency components lie above 200 Hz. In such cases, the frequency having highest mean is used as a normalising factor. All 12 prominent frequencies are divided by the normalising frequency. The peaks and mean values extracted are illustrated in Fig. 2c.

The feature vector obtained using the above procedure is of 36 dimensions (12 normalised frequency values, 12 mean values of the peak frequency and 12 variances). Features 1–12 are the normalised prominent pitch values, features 13–24 are the height of the corresponding peaks and the features 25–36 are the variance of the corresponding peaks. This is illustrated in the Fig. 2c.

### 3.2 Raga Identification Model

ANN consists of number of simple processing elements, called neurons, that are interconnected to each other [16]. A typical multilayer network, consists of a number of layers namely input layer, output layer. One single neuron makes the simple operation of a weighted sum of the incoming signals and a bias term (or threshold), fed through an activation function resulting in the output value of the neuron [16].

In the proposed system, ANN with feed-forward backdrop learning algorithm is used as a classifier (shown in Fig. 3a). It consists of 1 hidden layer. The input layer consists of 36 neurons which is equals to the size of feature vector. The number of neurons in the hidden layer is taken as 40. This number is chosen after experimenting with various number of neurons ranging from 20 to 50. The accuracy of the system is maximum when the number is 40. The number of neurons in the

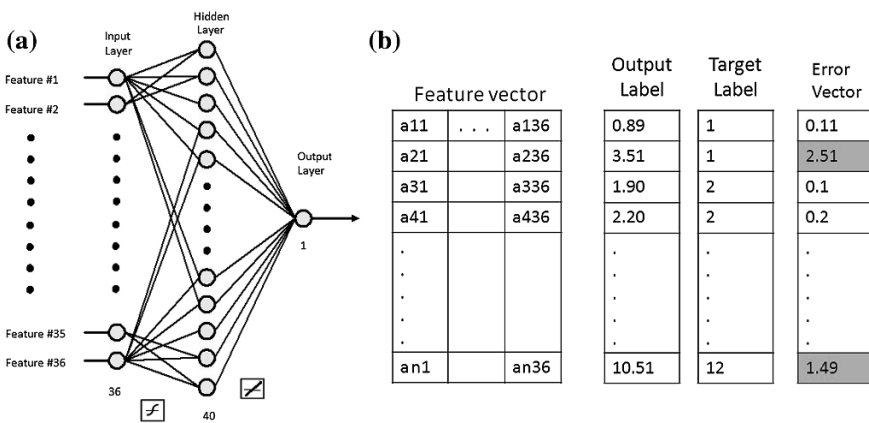


Fig. 3 Raga classification model. a Architecture of ANN. b Error vector calculation and validation

output layer is fixed as 1. Activation function for hidden and output layers is chosen as tan-sigmoid and pure-line respectively. For each *raga* different value is expected as an output. For example, if 2 *ragas* are considered for classification, if input is *raga* 1, then 1 is expected as outcome and if input is *raga* 2, then 2 is expected as output value. ANN is trained accordingly with different labels for different *ragas*. During testing, the *raga* label obtained from the system (output label) is validated using the actual *raga* labels (target labels refer Fig. 3b). The difference between system output and actual output is calculated resulting in the error vector. If the error value is strictly less than 0.5, then the input is considered to be correctly classified. This process is illustrated in Fig. 3b. The gray marked values in error vector indicates mis-classification.

## 4 Result and Analysis

### 4.1 Database

Monophonic and polyphonic clips from 12 *ragas* listed in the Table 1 are considered to form a database. *Ragas* are chosen in such a way that database includes all notes that are present in Carnatic Music. Particularly, *Kalyani* and *Shankarabharanam* both *ragas* are included because *Kalyani* when perceived in a different tonic becomes *Shankarabharanam*. There is high chance of mutual mis-classification between these two *ragas* if the identification is highly tonic dependent. The proposed method is tonic independent and hence the classification of *Kalyani* and *Shankarabharanam* is crucial aspect of this work. In the same way, we also include the *ragas* which share the same set of notes such as *Ananda Bhairavi* and *Reethigowlai* (These two *ragas* share same set of notes), as there is high level of mis-classification between them if set of notes is used for classification. The

**Table 1** Database: *Ragas* used and number of clips

S. No.	<i>Raga</i> name	Number of clips
1	Abhogi	16
2	Harikhambojhi	11
3	Kalyani	13
4	Malayamarutha	10
5	Mayamalavagowla	14
6	Hindolam	17
7	Mohanam	12
8	Hamsadwani	12
9	Nattai	13
10	Shankarabharanam	13
11	Ananda Bhairavi	16
12	Reethigowlai	15

polyphonic music clips consist of vocals accompanied by Tambura or Tabla. The database is made rich in variety by including *arohana-avarohana*, *krutis*, *alapanas* from different *ragas* rendered by instruments and different singers including both male and female. We have also included both *Janaka* and *Janya ragas* in our database. *Janaka ragas (Sampurna ragas)* contain all seven notes whereas *Janya ragas* contain fewer than seven notes.

## 4.2 Performance Evaluation

The experiment is performed using different number of neurons in the hidden layer. Considering 40 number of neurons in the hidden layer yielded the best results. The system is validated using three experiments. Initially the *raga identification* system is developed with 131 music clips from the first 10 ragas of the Table 1, using 70 % of them for training and 30 % for testing. The average *raga* recognition accuracy is found to be 91.5 %. The accuracy of recognition for each *raga* in this experiment is given in Table 2. In the second experiment, the system is tested to verify if the features are able to distinguish between *ragas* that are composed using the same set of notes (*Ananda Bhairavi* and *Reethigowlai*). The system is validated using only these two *ragas*. Using 21 clips for training and 10 clips for testing the accuracy of classification in this experiment is found to be 80 %. This can be justified using the normalisation performed using the pitch value having highest mean and the other parameters such as mean and variances. This either corresponds to tonic or highly repeating note which is called *Jeeva Swara* in Carnatic music. *Jeeva Swara* is different for different *ragas* when they are composed of same notes. If normalisation

**Table 2** Accuracy of the *raga* classification

S.No.	Raga name	Classification accuracy (in percentage)	
		Training and testing with first ten <i>ragas</i>	Training and testing with twelve <i>ragas</i>
1	Abhogi	100.0	100.00
2	Harikhambojhi	100.0	100.00
3	Kalyani	80.00	92.30
4	Malayamarutha	100.00	90.00
5	Mayamalavagowla	80.00	85.71
6	Hindolam	100.00	100.00
7	Mohanam	100.0	91.67
8	Hamsadwani	100.0	91.67
9	Nattai	80.00	84.61
10	Shankarabharanam	80.00	84.61
11	Ananda Bhairavi	NA	80.00
12	Reethigowlai	NA	80.00

factor is tonic, then the means and variances of the peaks differ because the importance given for various notes is different in different *ragas*. Hence classification of *raga* becomes efficient using the proposed features.

In the third experiment, the *raga* recognition system is validated using 5-fold validation method. Complete database consisting of 162 clips from 12 *ragas* is divided into 5 sets, each set consisted of songs from all *ragas*. From these sets, 4 are used for training the network and the remaining one is used for testing. The experiment is repeated for 5 times so that the system is validated against each set. The average result of 5 experiment for each *raga* is listed in Table 2. The average classification accuracy is 89.51 %.

## 5 Conclusion and Future Scope

In this work, a system for direct *raga* classification without use of explicit note sequence is proposed. Set of low-level features obtained from the signal are used as features. A comprehensive data set consisting of variety of music clips is used for validating the proposed method. An effort has been made to come up with a *raga* classification system that is independent of tonic note information. From the study, it is evident that pdf and primitive features give good accuracy even for *ragas* composed of same set of notes. The accuracy of the system clearly demonstrates that the features capture more details about *raga* rather than just the set of notes.

As a future work, the system shall be tested with larger database having hetero-phonous music clips (composed of more than one melody such as vocal accompanied by violin) and also film songs that are composed based on *ragas*. The proposed features shall be tested with other classifiers as well. Further, the *raga* information shall be used for developing systems for transcription of notes, music recommendation based on *raga* information and so on.

## References

1. Bello, J.P., Daudet, L., Abdallah, S., Duxbury, C., Davies, M., Sandler, M.B.: A tutorial on onset detection in music signals. *IEEE Trans. Speech Audio Process.* **13**(5), 1035–1047 (2005)
2. Klapuri, A., Davy, M.: *Signal processing methods for music transcription*. Springer, New York Inc., Secaucus NJ USA (2006)
3. Pandey, G., Mishra, C., Ipe, P.: Tansen: A system for automatic raga identification. In: *Proceedings of Indian International Conference on Artificial Intelligence*, pp. 1350–1363 (2003)
4. Bhattacharjee, A., Srinivasan, N.: Hindustani raga representation and identification: a transition probability based approach. *IJMBC* **2**(1–2), 66–91 (2011)
5. Sinith, M., Rajeev, K.: Hidden markov model based recognition of musical pattern in South Indian classical music. In: *IEEE International Conference on Signal and Image Processing* (2006)

6. Dighe, P., Agrawal, P., Karnick, H., Thota, S., Raj, B.: Scale independent raga identification using chromogram patterns and swara based features. In: IEEE International Conference on Multimedia and Expo Workshops (ICMEW), pp. 1–4 (2013)
7. Koduri, G.K., Serra, J., Serra, X.: Characterization of intonation in carnatic music by parametrizing pitch histograms. In: International Society for Music Information Retrieval, pp. 199–204 (2012)
8. Sridhar, R., Geetha, T.: Swara identification for South Indian classical music. In: 9th International Conference on Information Technology (IEEE) (2006)
9. Shetty, S., Achary, K.K.: Raga mining of indian music by extracting arohana-avarohana pattern. *Int. J. Recent Trends Eng.* **1**(1), 362–366 (2009)
10. Ranjani, H.G., Arthi, S., Sreenivas, T.V.: Carnatic music analysis: Shadja, swara identification and raga verification in alapana using stochastic models. In: IEEE Workshop on Applications of Signal Processing to Audio and Acoustics, pp. 29–32 (2011)
11. Chordia, P.: Automatic rag classification using spectrally derived tone profiles. *Int. Comput. Music Conf.* **2004**, 1–4 (2004)
12. Chordia, P., Rae, A.: Raag recognition using pitch-class and pitch-class dyad distributions. In: Proceedings of International Conference on Music Information Retrieval (2007)
13. G.Koduri, Gulati, S., Rao, P.: A survey of raaga recognition techniques and improvements to the state-of-the-art. *SMC* (2011)
14. Krishnaswamy, A.: On the twelve basic intervals in south Indian classical music. In: 115th AES Convention, New York (2003)
15. Rabiner, L.R.: On the use of autocorrelation analysis for pitch detection. *IEEE Trans. Acoust. Speech Signal Process.* **25**(1), 24–33 (1977)
16. Suykens, J.A.K., Vandewalle, J.P.L., Moor, B.L.R.D.: *Artificial Neural Networks for Modelling and Control of Non-Linear Systems*. Springer, US (1996)

# A Novel Approach for Feature Selection

Ch. Swetha Swapna, V. Vijaya Kumar and J.V.R. Murthy

**Abstract** Clustering problem suffers from the curse of dimensionality. Dimensionality reduction of a feature set refers to the problem of selecting relevant features which produce the most predictive outcome and similarity functions that use all input features with equal relevance may not be effective. We introduce an algorithm that discovers clusters by different combinations of dimensions via local weightings of features. This approach avoids the risk of loss of information encountered in global dimensionality reduction techniques, and does not assume any data distribution model. Our method associates to each cluster a weight vector, whose values capture the relevance of features within the corresponding cluster. To judge the efficiency of the proposed method the results are experimentally compared with other optimization methods such as Genetic Algorithm (GA), Particle Swarm Optimization (PSO) and Differential Evolution (DE) for feature selection.

**Keywords** Feature selection · DE · PSO · GA

## 1 Introduction

The main goal of feature selection is to find a minimal feature subset from a problem domain with high accuracy in representing the original features [1]. In real world problems feature selection is an important process must due to the abundance of noisy, irrelevant or misleading features. An extensive method may be used for this purpose, it is quite impractical for most datasets. Usually feature selection

---

Ch. Swetha Swapna (✉) · V. Vijaya Kumar · J.V.R. Murthy  
Computer Science Department, JNTU Kakinada, Kakinada, Andhra Pradesh, India  
e-mail: swetha\_swapna@yahoo.com

V. Vijaya Kumar  
e-mail: vijayvakula@yahoo.com

J.V.R. Murthy  
e-mail: mjonnalagedda@gmail.com

algorithms involve heuristic or random search strategies in an attempt to avoid this prohibitive complexity. However, the degree of optimality of the final feature subset is often reduced.

The problem of feature selection has been widely investigated due to its importance to a number of disciplines such as pattern recognition and knowledge discovery. Feature selection allows the reduction of feature space, which is crucial in reducing the training time and improving the prediction accuracy. This is achieved by removing irrelevant, redundant, and noisy features (i.e., selecting the subset of features that can achieve the best performance in terms of accuracy and computational time). As described in paper [1] the most existing feature selection algorithms consist of the following four components:

- **Starting point in the feature space.** The search for feature subsets could start with (i) no features, (ii) all features, or (iii) random subset of features.
- **Search procedure.** Ideally, the best subset of features can be found by evaluating all the possible subsets, which is known as exhaustive search. However, this becomes prohibitive as the number of features increases, where there are  $2^N$  possible combinations for  $N$  features. Accordingly, several search procedures have been developed that are more practical to implement, but they are not guaranteed to find the optimal subset of features. These search procedures differ in their computational cost and the optimality of the subsets they find.
- **Evaluation function.** The existing feature selection evaluation functions can be divided into two main groups: filters and wrappers. Filters operate independently of any learning algorithm, where undesirable features are filtered out of the data before learning begins [2]. On the other hand, performance of classification algorithms is used to select features for wrapper methods [3].
- **Criterion for stopping the search.** Feature selection methods must decide when to stop searching through the space of feature subsets. Some of the methods ask the user to predefine the number of selected features. Other methods are based on the evaluation function, like whether addition/deletion of any feature does not produce a better subset.

These limitations of dimensionality reduction techniques suggest that, to capture the local correlations of data, a proper feature selection procedure should operate locally in the input space. Local feature selection allows different distance measures to be embedded in different regions of the input space such distance metrics reflect local correlations of data. In this paper we propose a soft feature selection procedure that assigns (local) weights to features according to the local correlations of data along each dimension. Dimensions along which data are loosely correlated receive a small weight that has the effect of elongating distances along that dimension. Features that correlate strongly with data receive a large weight, which has the effect of constricting distances along that dimension. The rest of this paper is structured as follows. Section 2 presents the K-means clustering algorithm. Section 3 presents the Concepts of proposed novel method for feature selection. Section 4 details the experimentation carried out and presents the discovered results. The paper concludes with a discussion on the observations and highlights the scope for future work in this area in Sect. 5.



## 2 K-Means Clustering Algorithm

One of the most important components of a clustering algorithm is the measure of similarity used to determine how close two patterns are to one another. K-means clustering groups data vectors into a predefined number of clusters, based on Euclidean distance as similarity measure. Data vectors within a cluster have small Euclidean distances from one another, and are associated with one centroid vector, which represents the “midpoint” of that cluster. The centroid vector is the mean of the data vectors that belong to the corresponding cluster.

For the purpose of this paper, the following symbols are defined:

- $N_d$  denotes the input dimension, i.e. the number of parameters of each data vector
- $N_0$  denotes the number of data vectors to be clustered
- $N_c$  denotes the number of cluster centroids (as provided by the user), i.e. the number of clusters to be formed
- $z_p$  denotes the p-th data vector
- $m_j$  denotes the centroid vector of cluster j
- $n_j$ , is the number of data vectors in cluster j
- $C_j$ , is the subset of data vectors that form cluster

Using the above notation the standard K-means algorithm is summarized as

1. Randomly initialize the  $N_c$  cluster centroid vectors
2. Repeat
  - (a) For each data vector, assign the vector to the class with the closest centroid vector, where the distance to the centroid is determined using

$$d(z_p - m_j) = \sqrt{\sum_{k=1}^{N_d} (z_{pk} - m_{jk})^2}. \tag{1}$$

where k subscripts the dimension.

- (b) Recalculate the cluster centroid vectors, using

$$m_j = \frac{1}{n_j} \sum_{z_p \in C_j} z_p. \tag{2}$$

until a stopping criterion is satisfied.

The K-means clustering process can be stopped when any one of the following criteria are satisfied: when the maximum number of iterations has been exceeded, when there is little change in the centroid vectors over a number of iterations or when there are no cluster membership changes.

### 3 Proposed Method for Feature Selection

Consider a set  $S$  of  $N$  data points in some space of dimension  $D$ . Here cluster  $C$  is a subset of data points, together with a vector of weights  $W = (w_1, w_2, \dots, w_D)$ , such that the points in  $C$  are closely clustered according to the weighted Euclidean distance measure using  $w$ . The component  $w_j$  measures the degree of correlation of points in  $C$  along feature  $j$ . Depending upon the degree of correlation of points in  $C$  along feature, we calculate more relevant feature corresponding to that cluster. After finding relevant features corresponding to each cluster we can find all relevant features of data set for clustering. Now our problem is how to estimate the weight vector  $W$  for each cluster in the data set.

**Definition** Given a set  $S$  of  $N$  points  $x$  in the  $D$ -dimensional Euclidean space, a set of  $k$  centers  $\{c_1, c_2, \dots, c_k\}$ ,  $c_j \in R^D$ ,  $j = 1, 2, \dots, k$ , coupled with a set of corresponding weight vectors  $\{w_1, w_2, \dots, w_k\}$ ,  $w_j \in R^D$ ,  $j = 1, 2, \dots, k$ , partition  $S$  into  $k$  sets  $\{A_1, A_2, \dots, A_k\} : A_j = \left\{ x \mid \left( \sum_{i=1}^D w_{ji}(x_i - c_{ji})^2 \right)^{1/2} < \left( \sum_{i=1}^D w_{li}(x_i - c_{li})^2 \right)^{1/2}, \forall l \neq j \right\}$  where  $w_{ji}$  and  $c_{ji}$  represent the  $i$ th components of vectors  $w_j$  and  $c_j$  respectively. The set of centers and weights is optimal with respect to the Euclidean norm, if they minimize the error measure:  $E_1(C, W) = \sum_{j=1}^k \sum_{i=1}^D w_{ji} e^{-X_{ji}}$  subject to constraints  $\sum_{i=1}^D w_{ji}^2 = 1 \neq j$ .  $C$  and  $W$  are  $(D \times k)$  matrices whose column vectors are  $c_j$  and  $w_j$  respectively, i.e.  $C = [c_1 \dots c_k]$  and  $W = [w_1 \dots w_k]$ .  $X_{ji}$  represents the average distance from the centroid  $c_j$  of points in cluster  $j$  along dimension  $i$ , and is defined as  $X_{ji} = \frac{1}{|A_j|} \sum_{x \in A_j} (c_{ji} - x_i)^2$ , where  $|A_j|$  is the cardinality of set  $A_j$ . The exponential function  $E_1$  has the effect of making the weights  $w_{ji}$  more sensitive to changes in  $X_{ji}$  and therefore to changes in local feature relevance.

**Algorithm** We start with well-scattered points in  $S$  as the  $k$  centroids: we choose the first centroids in such a way that they are far from one another. This can be done either in random or using any clustering algorithm. Here we have used K-means clustering for finding cluster center for clusters. We initially set all weights to  $\frac{1}{\sqrt{D}}$ . Given the initial centroids  $c_j$ , for  $j = 1, \dots, k$ , we compute the corresponding sets  $A_j$  as given in the definition above. We then compute the average distance along each dimension from the points in  $A_j$  to  $c_j$ . Let  $X_{ji}$  denote this average distance along dimension  $i$ . The smaller  $X_{ji}$  is, the larger is the correlation of points along dimensions  $i$ . We use the value  $X_{ji}$  in an exponential weighting scheme to credit weights to features (and to clusters):  $w_{ji} = \exp(-h \times X_{ji}) / (\sum_{l=1}^D (\exp(-h \times 2 \times X_{jl})))^{1/2}$  where  $h$  is a parameter that can be chosen to maximize (minimize) the influence of  $X_{ji}$  on  $w_{ji}$ . We empirically determine the value of  $h$  through cross-validation in our experiments with simulated data. The exponential weighting is more sensitive to changes in local feature relevance [4] and gives rise to better performance

improvement. Note that the technique is centroid-based because weightings depend on the centroid. The computed weights are used to update the sets  $A_j$ , and therefore the centroids' coordinates. The procedure is iterated until convergence is reached, i.e. no change in centers' coordinates is observed. After convergence we will check weight vectors  $\{w_1, w_2, \dots, w_k\}$  and determine relevant features corresponding to each cluster and then relevant features of dataset for clustering. The resulting algorithm is summarized in the following

Input: N points  $x \in R^N$ , k and h

1. Using K-Means clustering algorithm determine k initial centroids  $c_1, c_2, \dots, c_k$ ;
2. Set  $w_{ji} = \frac{1}{\sqrt{D}}$ , for each centroid  $c_j$ ,  $j = 1, \dots, k$  and each feature  $i = 1, 2, 3, \dots, D$ .
3. For each centroid  $c_j$ , for each point x set  $A_j = \left\{ x \mid \left( \sum_{i=1}^D w_{ji}(x_i - c_{ji})^2 \right)^{1/2} < \left( \sum_{i=1}^D w_{li}(x_i - c_{li})^2 \right)^{1/2}, \forall l \neq j. \right\}$
4. For each centroid  $c_j$ , and for each feature i:
  - Set  $X_{ji} = \frac{1}{|S_j|} \sum_{x \in S_j} (c_{ji} - x_i)^2$
  - Set  $w_{ji} = \exp(-h \times X_{ji}) / \left( \sum_{l=1}^D (\exp(-h \times 2 \times X_{jl})) \right)^{1/2}$
5. For each centroid  $c_j$ , and for each point x:
  - Recompute  $A_j = \left\{ x \mid \left( \sum_{i=1}^D w_{ji}(x_i - c_{ji})^2 \right)^{1/2} < \left( \sum_{i=1}^D w_{li}(x_i - c_{li})^2 \right)^{1/2}, \forall l \neq j \right\}$
6. Set  $c_j = \frac{\sum_x x 1_{A_j(x)}}{\sum_x 1_{A_j(x)}}$ , for each  $j = 1, 2, \dots, k$  where  $1_{A_j(\cdot)}$  is the indicator function of set A
7. Iterate 3, 4, 5, 6 until convergence
8. Determine relevant feature corresponding to each cluster:
  - ith feature is more relevant to jth cluster if  $w_{ji} > \frac{1}{\sqrt{D}}$
9. Determine relevant features of data set for clustering:
  - ith feature is more relevant to dataset for clustering if ith feature shows for more period of its relevance with clusters.

## 4 Experiment and Results

We run the RoughGA, RoughPSO, RoughDE and the proposed novel dimensionality reduction technique to reduce the dataset as lower dimensional dataset. The detailed description of RoughGA, RoughPSO and RoughDE algorithm are given in paper [5].

### 4.1 Experimental Setup

The parameters of the algorithms RoughGA, RoughPSO and RoughDE are defined and taken from [5]. The size of the population in GA, swarm size in PSO and particle size in DE are set to  $(\text{int})(10 + 2 * \sqrt{D})$ , where  $D$  is the dimension of the position, i.e., the number of condition attributes. Each experiment (for each algorithm) was repeated 3 times with different random seeds with number of fitness function evaluation is 600. The proposed algorithm is run 10 times and taken mean for solution as a result.

### 4.2 Datasets Used

The following real-life data sets are used in this paper which is taken from UCI Machine Repository and from websites <http://www.ailab.si/orange/datasets.asp>. Here,  $N$  is the number of data points,  $D$  is the number of features, and  $K$  is the number of clusters.

- **Iris** plants database ( $N = 150$ ,  $D = 4$ ,  $K = 3$ ): This is a well-known database with 4 inputs, 3 classes, and 150 data vectors. The data set consists of three different species of iris flower: Iris setosa, Iris virginica, and Iris versicolour. For each species, 50 samples with four features each (sepal length, sepal width, petal length, and petal width) were collected. The number of objects that belong to each cluster is 50.
- **Glass** ( $N = 214$ ,  $D = 9$ ,  $K = 6$ ): The data were sampled from six different types of glass: (1) building windows float processed (70 objects); (2) building windows nonfloat processed (76 objects); (3) vehicle windows float processed (17 objects); (4) containers (13 objects); (5) tableware (9 objects); and (6) headlamps (29 objects). Each type has nine features: (1) refractive index; (2) sodium; (3) magnesium; (4) aluminum; (5) silicon; (6) potassium; (7) calcium; (8) barium; and (9) iron.
- **Wisconsin breast cancer data set** ( $N = 683$ ,  $D = 9$ ,  $K = 2$ ): The Wisconsin breast cancer database contains nine relevant features: (1) clump thickness; (2) cell size uniformity; (3) cell shape uniformity; (4) marginal adhesion; (5) single epithelial cell size; (6) bare nuclei; (7) bland chromatin; (8) normal nucleoli; and

- (9) mitoses. The data set has two classes. The objective is to classify each data vector into benign (239 objects) or malignant tumors (444 objects).
- **Wine** (N = 178, D = 13, K = 3): This is a classification problem with “well-behaved” class structures. There are 13 features, three classes, and 178 data vectors.
  - **Vowel data set** (N = 871, D = 3, K = 6): This data set consists of 871 Indian Telugu vowel sounds. The data set has three features, namely F1, F2, and F3, corresponding to the first, second and, third vowel frequencies, and six overlapping classes {d (72 objects), a (89 objects), i (172 objects), u (151 objects), e (207 objects), o (180 objects)}.
  - **Pima Diabates data** (N = 768, D = 8, K = 2): This data set consists of 768 data vectors, 8 features and 2 classes.
  - **Haberman’s Survival Data Set** (N = 306, D = 3, K = 2): This data set consists of 306 data vectors, 3 features and 2 classes.
  - **Zoo** (N = 100, D = 13, K = 7).
  - **Shuttle-landing control** (N = 253, D = 6, K = 2).
  - **Monks** (N = 432, D = 6, K = 2).
  - **Lung cancer** (N = 32, D = 56, K = 3).
  - **Hayes roth** (N = 160, D = 4, K = 3).
  - **Ionosphere** (N = 351, D = 32, K = 2).
  - **Balance scale** (N = 625, D = 4, K = 2).
  - **E. coli** (N = 336, D = 7, K = 8).
  - **Vehicle** (N = 846, D = 18, K = 4).

### 4.3 Simulation Strategy

All the experiment codes are implemented in MATLAB 7. The experiments are conducted on a Pentium 4, 1 GB RAM, and the system is Windows XP Professional.

### 4.4 Experimental Results

To judge the accuracy of the proposed algorithm, the algorithm runs for 10 times and then taken the mean of number of features found. For other algorithms the results are directly taken from paper [5] and given in Table 1.

It is clearly evident from the Table that the proposed method performs equally well with other methods in all investigated datasets except Zoo dataset. Particularly with Lung cancer data and Hayes roth dataset it excels in finding optimal number of features compared to other three methods.

**Table 1** Datasets used in the experiments

Sl. No.	Datasets	No. of instances	No. of features	No. of clusters	RoughGA	RoughPSO	RoughDE	Proposed method
1	Iris	150	04	03	02-03	02-03	02	02
2	Glass	214	09	06	03	03	03	03
3	Wine	178	13	03	03	02-03	02-03	03
4	Vowel	462	10	11	3	02-04	02	02-03
5	Breast cancer Wisconsin	683	9	2	4	4	2	02
6	Zoo	101	16	7	5	5	5	07
7	Pima Indian diabetes	768	8	2	2	2	2	02
8	Shuttle landing control	253	6	2	6	6	4-6	4-6
9	Monk1	432	6	2	3	3	3	3
10	Lung cancer	32	56	3	21	21	19	17
11	Hayes Roth	160	4	3	3	3	3	2
12	Ionosphere	351	32	2	12	12	12	12
13	Balance scale	625	4	2	4	4	2-4	3-4
14	<i>E. coli</i>	336	7	8	3	3	3	3
15	Haberman's survival	306	3	2	3	3	3	2
16	Vehicle	846	18	4	6	6	4	4

## 5 Conclusion

In this paper, we have investigated the problem of finding optimal number of features using a novel feature selection technique. The proposed approach discovered the best feature combinations in an efficient way. We evaluated the performance of the proposed algorithm with RoughGA, RoughPSO and RoughDE. The results indicate that proposed technique gives equally and better results than RoughGA, RoughPSO and RoughDE, specially for large scale problems, although its stability needs to be improved in further research. The proposed algorithm could be an ideal approach for solving the reduction problem when other algorithms failed to give a better solution.

## References

1. Blum, A.L., Langley, P.: Selection of relevant features and examples in machine learning. *Artif. Intell.* **97**, 245–271 (1997)
2. Hall, M.A.: Correlation-based feature selection for machine learning. Ph.D. thesis, The University of Waikato (1999)
3. Kohavi, R.: Wrappers for performance enhancement and oblivious decision graphs. Ph.D. thesis, Stanford University (1995)
4. Bottou, L., Vapnik, V.: Local learning algorithms. *Neural Comput.* **4**(6), 888–900 (1992)
5. Satapathy, S.C., Naik, A.: Hybridization of Rough Set and Differential Evolution Technique for Optimal Features Selection, vol. 132, pp. 453–460. Springer-AISC, Heidelberg (2012)

# Errata to: $L(4, 3, 2, 1)$ -Labeling for Simple Graphs

Soumen Atta and Priya Ranjan Sinha Mahapatra

## Errata to:

Chapter 50 in: J.K. Mandal et al. (eds.), *Information Systems Design and Intelligent Applications, Advances in Intelligent Systems and Computing 339*, DOI [10.1007/978-81-322-2250-7\\_50](https://doi.org/10.1007/978-81-322-2250-7_50)

- Page: 512. The following sentence is required to be added at the end of paragraph 1 in Sect. 1.  
“Some results of simple graphs with  $L(4, 3, 2, 1)$  labeling can be found in [9]”.
- Page: 513. “**Theorem 1**” should be read as “**Theorem 1** [6]”.
- Page: 514. “**Theorem 2**” should be read as “**Theorem 2** [6]”.
- Page: 515. The **Lemma 1** along with its proof in Sect. 3.3 should be read as:

**Lemma 1** For a path  $P_n$  on  $n$  vertices with  $n \geq 7$ , the minimal  $L(4, 3, 2, 1)$ -labeling number  $\lambda(P_n)$  is at most 13.

---

The online version of the original chapter can be found under DOI [10.1007/978-81-322-2250-7\\_50](https://doi.org/10.1007/978-81-322-2250-7_50)

---

S. Atta (✉) · P.R.S. Mahapatra  
Department of Computer Science and Engineering, University of Kalyani, Nadia,  
West Bengal, India  
e-mail: soumen.atta@klyuniv.ac.in

P.R.S. Mahapatra  
e-mail: priya@klyuniv.ac.in



*Proof* A labeling pattern  $\{f(v_1), f(v_2), \dots, f(v_7)\} = \{5, 9, 13, 3, 7, 11, 1\}$  exists for  $n = 7$ . Hence the lemma follows.  $\square$

Page: 515. The Theorem 3 and its proof for Case-IV and Case-V in Sect. 3.3 should be read as:

**Theorem 3** For a path,  $P_n$  on  $n$  vertices, the minimal  $L(4, 3, 2, 1)$ -labeling number  $\lambda(P_n)$  is

$$\lambda(P_n) = \begin{cases} 1 & \text{if } n = 1 \\ 5 & \text{if } n = 2 \\ 8 & \text{if } n = 3 \\ 9 & \text{if } n = 4 \\ 11 & \text{if } n = 5, 6, 7 \end{cases}$$

*Proof*

Case-IV:  $n = 4$ :

The labeling pattern  $\{6, 1, 9, 4\}$  shows that  $\lambda(P_n) \leq 9$  if  $n = 4$ . Let  $V(P_n) = \{v_1, v_2, v_3, v_4\}$ .  $V(P_n)$  has two vertices of degree 2 and other two vertices of degree 1. If either  $f(v_2)$  or  $f(v_3)$  is 1 then either  $f(v_4)$  or  $f(v_1)$  will be at least 12, which is a contradiction. Similar contradiction will arrive if either  $f(v_1)$  or  $f(v_4)$  is set to 1.

Case-V:  $n = 5, 6, 7$ :

Since  $\exists$  a labeling  $\{8, 3, 11, 6, 1, 9, 4\}$ , we can assume that  $\lambda(P_n) \leq 11$  for  $n = 5, 6, 7$ . Let  $f(v_i) = 1$  and either  $v_{i+1}, v_{i+2}$  or  $v_{i-1}, v_{i-2}$  exist. Now  $\lambda(P_3) = 8$  implies that  $f(v_{i+1})$  is either 5, 6, 7 or 8. For  $L(3, 2, 1)$ -labeling [6], note that the possibilities for  $f(v_{i+1})$  is either 5, 6, 7 or 8. Therefore, the similar approach in [6] can be used to handle this case.  $\square$

- Page: 517. The **Claim 1** is not correct and hence the last line of the “**Abstract**” should be read as “This paper also presents an  $L(4, 3, 2, 1)$ -labeling algorithm for path.”

## Reference

9. Sweetly, R.: A study on radio labeling and related concepts in graphs. PhD thesis, Manonmaniam Sundaranar University (2011)

# Author Index

## A

Aashiha, J.P., 269  
Abd Elfattah, Mohamed, 395  
Abhinaya, B., 177  
Acharya, Arup Abhinna, 479  
Afshar Alam, M., 649  
Agrawal, Basant, 469  
Agrawal, Shikha, 11  
Ahuja, Sachin, 601  
Akashdeep, 667  
Ali, Mona A.S., 771  
Alnashar, Hany Soliman, 395  
Amin, Ruhul, 525  
Asawa, Krishna, 209  
Atchaya, A., 269  
Atta, Soumen, 511  
Ayeldeen, Heba, 369, 385  
Azharuddin, Md, 329

## B

Banerjee, Aiswaryya, 705  
Bar, Nirjhar, 823  
Barman, Bandana, 761  
Baruah, Sunandan, 573  
Basak, Jayanta, 783  
Basak, Joyita, 719  
Basak, Ratan Kumar, 675  
Basu, Abhishek, 447  
Battula, Sudheer Kumar, 489  
Behera, H.S., 545  
Bhadra, Arunava, 1  
Bhattacharjee, Anup Kumar, 101  
Bhattacharjee, Pritam, 33  
Bhattacharya, Soumya Kanti, 831  
Bhattacharjee, Aindrila, 831  
Biswas, Animesh, 497  
Biswas, Bhaskar, 731  
Biswas, G.P., 525  
Biswas, Manindra Nath, 823

Biswas, Papun, 695  
Biswas, Paramita, 761  
Biswas, Sushanta, 353, 519  
Bose, Mahua, 53  
Burnwal, A.P., 535

## C

Chakraborti, Debjani, 637  
Chakraborty, Angana, 101  
Chakraborty, Satrajit Lal, 447  
Chakraborty, Sayan, 831  
Chanda, Amitabha, 675  
Chaubey, Suraj Kumar, 591  
Chaudhuri, Sheli Sinha, 719  
Chauhan, Arun, 379

## D

Dam, Sandip, 1  
Das, Kunal, 33, 61  
Das, Sanjoy, 61, 233  
Das, Santosh Kumar, 535  
Das, Sougata, 145  
Das, Sudip Kumar, 823  
Das, Suman, 259  
De, Arnab Kumar, 497  
De, Debashis, 33  
De, Mallika, 33, 61  
De, Srija, 353, 519  
Deb, Subhrajyoti, 731  
Debabhuti, Nilava, 145  
Dey, Arijit, 61  
Dey, Hemanta, 259  
Dey, Rajat Kumar, 1  
Dhal, Krishna Gopal, 233  
Dharani, M. K., 657  
Dhote, C. A., 581  
Dutta, Paramartha, 627  
Dutta, Sayantan, 145

**E**

Ella, Aboul, 771

**G**

Gandhi, Jenish, 751  
 Gayathri devi, B., 657  
 Ghosh, Apurba, 145  
 Ghosh, Mili, 627  
 Ghosh, Partha, 91  
 Ghosh, Ranjan, 259  
 Godwin Premi, M. S., 613  
 Goswami (Ghosh), Joyita, 319  
 Govardhan, A., 113  
 Govindarajulu, K., 555  
 Guha Thakurta, Parag K., 123

**H**

Hassan, Usama Mokhtar, 771  
 Hassanien, Aboul Ella, 369, 385, 395  
 Hefny, Hesham, 771  
 Hegazy, Osman, 369, 385  
 Hemakumar, G., 73

**I**

Iqbal Quraishi, Md., 233

**J**

Jain, Sachin R., 619  
 Jain, Shikha, 209  
 Jaiswal, Priyanka, 167  
 Jana, Prasanta K., 329  
 Jha, C.K., 199  
 Jhaveri, Rutvij, 751  
 Johari, Rahul, 601

**K**

Kabi, Kunal Kumar, 379  
 Kalpana, A., 113  
 Kanrar, Soumen, 21  
 Kanungo, D.P., 545  
 Kar, Avradeeta, 447  
 Kar, Nirmalya, 731  
 Khan, Uzma, 11  
 Khokhar, Chetna, 601  
 Koolagudi, Shashidhar G., 865  
 Krishna Murthy, Mudimbi, 113  
 Kumar, Abhimanyu, 167  
 Kumar, K Vimal, 301  
 Kumar, Mousumi, 419  
 Kumar, Niraj, 311  
 Kumar, Rupesh, 91

Kumari, Dipti, 187

Kuzhaloli, S., 565

**L**

Lakshmi Sreenivasa Reddy, D., 113  
 Le, Dac-Nhuong, 843

**M**

Maflin Shaby, S., 613  
 Mahali, Prateeva, 479  
 Mahapatra, Priya Ranjan Sinha, 337, 511, 783  
 Mahapatra, Suman, 741, 793  
 Mali, Kalyani, 53  
 Mallick, Partho, 705  
 Mandal, Abhay Kumar, 91  
 Mandal, Prasenjit Kumar, 21  
 Manna, Suvrajit, 81  
 Martin, Betty, 613  
 Mehfuz, Shabana, 813  
 Mishra, Bimal Kumar, 157  
 Mishra, Manoj K., 409  
 Misra, Prasant, 685  
 Mittal, Namita, 469  
 Mohamed, Anuj, 343  
 Mohanty, Manas Kumar, 311  
 Mohapatra, Durga Prasad, 479  
 Mosbah, M.M., 395  
 Mukherjee, Amartya, 831  
 Mukherjee, Pinaki, 81  
 Mukhopadhyay, Anirban, 761  
 Mukhopadhyay, Asish K., 101  
 Mukhopadhyay, Debarka, 627  
 Mukhopadhyay, Sumitra, 591  
 Mukhopadhyay, Susanta, 409  
 Murthy, J.V.R., 877

**N**

Nagwani, N. K., 803  
 Naik, Bighnaraj, 545  
 Nayak, Janmenjoy, 545

**P**

Pal, Bijay Baran, 419, 457, 637, 695  
 Palit, Sarbani, 793  
 Panigrahi, Prabin Kumar, 219  
 Pardeshi, Poonam M., 279  
 Pati, Kamaljit, 311  
 Paul, Abhishek, 591  
 Paul, Manas, 319  
 Poddar, Rajarshi, 135  
 Pradhan, Chittaranjan, 379

Prajapati, Apeksha, 157  
Punitha, P., 73

**R**

Rajnish, Kumar, 187  
Rama Rao, K.V.S.N., 489  
Ramachandran Nair, K.N., 343  
Ramya, R., 657  
Ranjan, Alok, 685  
Rathi, Sheetal, 581  
Rathore, Himanshu, 435  
Raveendra Babu, B., 113  
Revathi, A., 43  
Roy, Sangita, 719  
Roy, Soumen, 245  
Roy, Sourav, 831  
Roy, Utpal, 245  
Rudra, Aritra, 135

**S**

Sadhu, Sanjib, 311  
Saha, Bidyut Jyoti, 379  
Saha, Sajal, 101  
Saha, Sourav, 783  
Saha, Swatantra, 591  
Sahu, H.B., 685  
Sahu, Mridu, 803  
Samaddar, Poulami, 353, 519  
Sangeetha, S., 657  
Sarkar, Anusree, 145  
Sarkar, Debasree Chanda, 353, 519  
Sarkar, Partha Pratim, 353, 519  
Sarkar, Souvik, 705  
Sarkar, Subir Kumar, 447  
Sarkar, Sushanta, 353, 519  
Sarma, Angan, 573  
Sarma, Kandarpa Kumar, 573  
Sarmah, Kumaresh, 573  
Sathya, P., 657  
Sau, Kartik, 675  
Sen, Sayani, 741, 793  
Sen, Shyamal, 457  
Sengupta, Nabanita, 447  
Sett, Sujoy, 123  
Shabnam, Sharmin, 81  
Shaji, K.S., 565

Shaker, Olfat, 369  
Shamsolmoali, Pourya, 649  
Sharma, Arun, 301  
Sharma, Meha, 199  
Sharma, Rewa, 199  
Sharma, Udit, 81  
Shirke, Saransh, 803  
Silakari, Sanjay, 11  
Singh, S.R., 435  
Singhal, Kartik, 469  
Sinha, D.D., 245  
Sinha, Shivaji, 813  
Som, Sukalyan, 741, 793  
Sri Madhava Raja, N., 177  
Sriniva, Podoli V.S., 855  
Suma, S.M., 865  
Sunitha, Maddhi, 855  
Swetha Swapna, Ch., 877

**T**

Talukdar, Susmita, 447  
Thakur, Nileshsingh V., 619  
Thakurta, Parag Kumar Guha, 135  
Tidke, Bharat, 279  
Tripathi, Sachin, 167, 535  
Tripathy, B.K., 555  
Tripathy, Hrudya Kumar, 219

**U**

Urooj, Shabana, 813

**V**

Venkataramani, Y., 43  
Venugopal, Temberveni, 855  
Verma, Shrish, 803  
Vijaya Kumar, V., 877  
Vijayarajan, R., 269  
Vimal Kumar, K., 291

**Y**

Yadav, Divakar, 291, 301

**Z**

Zareapoor, Masoumeh, 649